68 number 3 | may 2011

NEUROSURGERY

THE REGISTER OF THE NEUROSURGICAL MIND

WWW.NEUROSURGERY-ONLINE.COM

SEA-SEA (1970) BY GERHARD RICHTER (b. 1932)

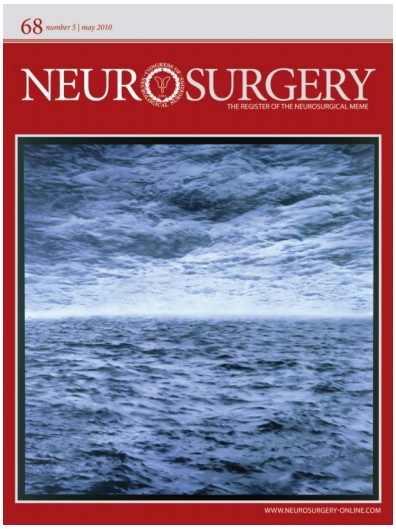

The invention of photography in 1837 changed the form and function of painting forever. No longer the optimal medium for portraiture, scientific documentation or for the production of a verisimilitude of nature and outer reality, painting was freed to become increasingly abstract, to become a medium like music or poetry, an explorer of psychological or philosophical truths and inner verities. The supposed advantages of photography, its portability, its scientific objectivity and its reproducibility, came with certain artistic losses: a physically flat surface, easily multiplied in endless copies, that cut the cord or autographic connection between the audience and the author of the work. In short, the small black and white photographs of the later nineteenth and early twentieth centuries did not seem to share "the aura" and uniqueness of a masterpiece created on canvas. To some degree, the endless multiplication and easy availability of images of Leonardo's *Mona Lisa* also damaged the magic of the original; one no longer needed to visit the Louvre in order to commune with La Giaconda but could easily turn to a magazine or newspaper. The power of the mass media and the world's drowning in a flood of images only became worse with the invention of moving pictures, the subject of Walter Benjamin's essential essay, "The Work of Art in the Age of Mechanical Reproduction" (1936), the brilliant exegesis in which the concept of "aura" was first bruited and the fascistic use of mass media predicted. Benjamin also foresaw a time when everyone would become a writer rather than a reader (ie, the development of "blogs") and all the arts would become "mass" in nature and somewhat debased.[1] What he could not foresee was the invention of the hand-held video camera around 1970 and the use of computer programs to "edit" or fictionalize photography through colorization, massive enlargement and other types of manipulation. In a manner similar to the way in which painting and drawing were changed by photography, sculpture and installation have been jolted and altered by motion pictures, video and computer-generated effects. Paradoxically, the impact of these changes has been greatest on photography itself; a medium that once reveled in its differences from painting became, in the 1980s and 1990s, a substitute or "simulacrum" of painting, aping the coloristic effects and grand scale of the older medium, taking upon itself the functions of nineteenth century history painting and twentieth century surrealism and fantasy. Along the way, art photography lost its role in social documentation and much of its scientific reliability. The generation of German photographers trained in Dusseldorf by Bernd and Hilla Becher, Thomas Ruff, Candida Hofer, Thomas Struth and Andreas Gursky, as well as that American master of self-disguise Cindy Sherman, produced photographs that commented on painting by directly imitating its most classical (ie, non-tactile) effects, photographs that successfully competed for visual impact and dollars in the marketplace of ideas and artistic success. For the umpteenth time in the course of the 20th century, painting appeared to be well and truly "dead."

Into this debate on the role of photography in late Modernism and the relative importance of painting stepped Gerhard Richter (b. 1932), also once a professor in Dusseldorf, who has spent fifty years utilizing painting to comment on photography rather than the other way around. Richter has the ability to meld the technical virtuosity of a Vermeer with the conceptual brilliance of a Duchamp; in this way he has managed to recuperate all of the classical tropes of painting, its usefulness in scientific documentation, portraiture and history, its ability to fool the eye, the concept of the masterpiece and the uniqueness of the author while, at the same time, eschewing all evidence of emotion, and denying the possibility of a "signature style." By signature style I mean all those elements of a picture like paint handling, color palette and range of subject matter, that make any authentic Monet or Rembrandt self-evidently look like a "Monet" or a "Rembrandt" whether or not the painting is signed. How and why has Richter done this? Is the chameleon-like appearance of his work simply a joke, a kind of braggadocio to prove that he can do anything he wants to do really well or a serious commentary on our largely image-mediated world? Are the cool surfaces of his paintings simply further evidence of his bloody-minded nature or are even paintings such as these susceptible to real emotions and philosophical inquiry?

To begin with, Richter paints photographs, that is to say, photorealist paintings that look like photographs (he even smears his immaculate surfaces to give a hint of the optical blur produced by the lens), many of which are based on photographs he has taken or travel souvenirs and postcards or found snapshots in the meaning that Duchamp gave to his "ready-made" objects. Further, Richter often paints *on* photographs thereby expunging the physical separation of the two media, the photographic ground contributing the representational (ie, figurative) component of the picture while his brushstrokes add the abstract portion. In Richter's hall of mirrors, it is possible to buy an original photograph he's recently made of a painting that he once painted, a painting originally based on a photograph taken or found by Richter. At times Richter has even painted wholly abstract paintings based on photographs of brushstrokes randomly made and smeared on specimen cards kept in his files and documented in his on-going project, *Atlas*.[2] In this way and others, Richter eliminates the conceptual difference between photography and painting since all of his

Copyright © Congress of Neurological Surgeons. Unauthorized reproduction of this article is prohibited.

early work, whether wholly abstract or wholly figurative in nature is based on an image-mediated world (ie, photographs) rather than any actual experience of the real world. Richter believes in the essential equivalency of abstraction and representation; he has painted hundreds of works in each mode but rarely combines the two. His more recent abstractions have been "spontaneously" made but share the cool photographic surfaces of the earlier photo-based abstractions. His photo-realist portraits and landscapes are clearly recognizable as "Richters," so too his classic abstract paintings in acid reds, greens and blues, his color chart paintings made of random assortments of paint samples, his mirror paintings in which the viewer sees himself and his environment. In this way, Richter has put an end to the concept of the signature style and has helped inaugurate Post-Modernism, the pluralistic and self-referential artistic period in which we live. A Richter retrospective looks like a group show put on by a half-dozen emotionally cool geniuses from several different artistic schools; simply put, he is the most important painter in the contemporary world.

Politics helped form him. He was fortunate to be born in Dresden, while it was still "in" East Germany; there he was forced to learn classical artistic skills in order to produce bland Soviet-style art. Like Picasso and Matisse before him, Richter draws like an angel and his color sense is acute. Eventually his repressive education would make him develop an artistic practice in which he might use his formidable talents. For a while the only work he could find was the painting of stage sets. Stultified by his environment, he escaped to the West in 1962 and, with his artistic partner Sigmar Polke (1943-2010), became greatly influenced by American Pop Art and Andy Warhol in particular. For a brief time, Richter and Polke formed one of the great artistic dyads, like Picasso and Braque, and laughingly invented a new movement called "Capitalist Realism," a short-lived style in which paintings based on commercial products and ads were combined with a kind of "living sculpture" or performance art. As if the gallery functioned like a furniture showroom, Polke and Richter hung out on the couches all the time their pictures were shown. And Richter destroyed all of the art he had made prior to moving to the West. Almost all of his earliest surviving paintings are photorealist in nature and painted in gray tonalities, en grisaille, so as to better imitate their sources in black and white photographs. Richter invented a series of cardboard and plastic "combs" with which he could smear his perfectly made photographic copies and introduce the optical distortion of the camera lens thereby tipping off the viewer that the real subject of the painting was the physical photograph itself and not merely the object contained within it. Of course, not all photographic subjects are of equal weight; Richter is old enough to have lived through the Second World War and has close family members who belonged to the Nazi Party and served as German soldiers. One of his most famous early paintings is "Uncle Rudi" (1965), based on a family snapshot of his father's brother proudly posed and smiling in his Wehrmacht uniform. After painting a series of black and white mountains, Richter turned to the sea and produced a stunning group of canvases intended to function as seascapes (1969-1970). These are at once the most abstract and the most powerful seascapes painted since the nineteenth century, the majority of them greater than six feet on a side. They are composed of pure water and sky without evidence of ships, humans or animals. The even tonalities of white, gray and black compacted into clouds and waves above and below the horizon line increase the sense of brooding menace and produce an abstract effect like that of Rothko's exactly contemporaneous late paintings in which a single rectangle of dark color floats on either side of a horizontal line. Although all of these seascapes are beautiful and stupendous to behold, I believe that "Sea-Sea" (1970) is the most impressive of them all. The key to Richter's subterfuge is in the title, the two "seas", and his trickery revealed in plate 194 of *Atlas*; the source for the painting is actually a photo-collage in which Richter has glued together the ocean from one snap to serve as the sea in his painting and the sea from another snap to serve as the sky.[2] Before computer manipulated pictures became possible, Richter knew that the modern photograph could lie and so could one of his painted photographs.

Of course, we want to see a stormy sky above a wave-swept sea. When visual input is inconclusive, the visual system adjusts the processing of current input on the basis of past experience; this effect can be demonstrated in both short-term and long-term situations.[3] Our brains are hard-wired to make sense of the world based on incomplete information; it's a wonder that we are so often correct in our conclusions. The visual system, in particular, obeys the biological imperative to keep us safe in a world of environmental dangers and fleeing prey; its fleeting glimpses conveyed by the two optic nerves represent one third of the entire input (6 million afferent fibers) to the brain's CPU, and the brain must often complete the incomplete information it receives. Stimuli without a clear structure, like Rorschach inkblots, allow multiple interpretations, some of which depend on which visual field (ie, hemisphere) receives the information.[4] Richter makes the processing of his image as difficult as possible by eliminating our expectation of a figure/ground relationship. Confronted by a visual image we seem to need a dominant shape or figure, with a definite contour, set against a background; the figure-ground relationship is one of the great discoveries of Gestalt psychology. In addition, we prefer figures that obey the gestalt law of Prägnanz, the tendency towards meaning, simplicity and completeness. In "Sea-Sea" there is uniformity above and below the horizon line with no definite figure, everything is "ground" and everything appears to be water. The hundreds of wavelets are too numerous for us to properly analyze; furthermore we expect them to move. Matisse commented that "movement thus understood corresponds to nothing in nature: when we capture it by surprise in a snapshot, the resulting image reminds us of nothing that we have seen"[5]; Richter has painted just such a snapshot. Spatial ambiguity in such a picture is further increased when color effects are removed and the eye must depend on the gray scale alone. In the Renaissance, wall paintings of statues situated in architectural niches were often painted in whites and grays so as to

Copyright © Congress of Neurological Surgeons. Unauthorized reproduction of this article is prohibited.

better create the illusion of shallow depth when deep shadows were not realistic or physically possible. The spatial recession in Richter's painting is similarly shallow and ambiguous; this image of "sky" and ocean hovers in its uniform treatment of "object" between the real world and the empyrean of an abstract universe, between something we know and something we're not quite sure of, like the photograph real and not-real, like the modern painting too, an object in our world and yet not completely of it.

Michael Salcman, MD
Baltimore, Maryland

REFERENCES

1. Benjamin W. The Work of Art In The Age of Mechanical Reproduction. In: Benjamin W, ed. *Illuminations, Essays and Reflections*. New York, NY: Schocken Books; 1969:217-251.
2. Richter G. *Atlas of the photographs, collages and sketches*. New York, NY: D.A.P.; 1997, plate 194.
3. Brascamp JW, Knapen THJ, Kanai R, Noest AJ, van Ee R, van den Berg AV. Multi-timescale perceptual history resolves visual ambiguity. *PLoS ONE*. 2008;3(1):e1497 (published online).
4. Regard M, Landis T. Beauty may differ in each half of the eye of the beholder. In: Rentschler I, Herzberger B, Epstein D, eds. *Beauty and the Brain, Biological Aspects of Aesthetics*. Boston, MA: Birkhäuser Basel; 1988:251-253.
5. Livingstone M. *Vision and Art. The Biology of Seeing*. New York, NY: Abrams; 2002:76-77.

Copyright © Congress of Neurological Surgeons. Unauthorized reproduction of this article is prohibited.

Relationship of Growth to Aneurysm Rupture in Asymptomatic Aneurysms ≤ 7 mm: A Systematic Analysis of the Literature

Mohamad Chmayssani, MD*
Jean G. Rebeiz, MD‡
Tania J. Rebeiz, MD‡
H. Hunt Batjer, MD§
Bernard R. Bendok, MD§

*Department of Neurology, Baylor College of Medicine, Houston, Texas; ‡Department of Neurology, American University of Beirut, Beirut, Lebanon; §Department of Neurosurgery, Northwestern University, Chicago, Illinois

Correspondence:
Bernard R. Bendok, MD,
Department of Neurological Surgery,
Northwestern University Feinberg School of Medicine,
676 N St. Clair St,
Ste 2210,
Chicago, IL 60611.
E-mail: bbendok@nmff.org

Received, March 23, 2010.
Accepted, October 1, 2010.

Copyright © 2011 by the
Congress of Neurological Surgeons

BACKGROUND: The apparent paradox of natural history data suggesting low rupture risk of small asymptomatic aneurysms and the median size of aneurysm rupture remains unexplained. Aneurysm growth rates and their potential relationship with rupture risk have not been well examined in natural history studies.

OBJECTIVE: To examine the question of whether small asymptomatic aneurysms ≤ 7 mm that are followed up over time rupture and to determine the relationship between aneurysm growth and rupture.

METHODS: We reviewed all publications on unruptured aneurysms published from 1966 to 2009. We then selected all aneurysms ≤ 7 mm for which measurements were reported for at least 2 time points and for which initial asymptomatic status and ultimate outcome (rupture vs unruptured) were reported. Using the Mann-Whitney *U* test, we compared absolute diameter annual growth rate.

RESULTS: Our search retrieved 64 aneurysms. Thirty aneurysms ruptured during follow-up, of which 27 were enlarged before rupture (90%). Thirty-four aneurysms did not rupture, of which 24 enlarged during follow-up (71%). There was a statistically significant trend toward larger absolute diameter growth for ruptured aneurysms vs unruptured aneurysms (3.89 ± 2.34 vs 1.79 ± 1.02 mm; $P < .001$), respectively. Annual growth rates for aneurysms for the 2 groups, however, were not statistically different (27.46 ± 18.76 vs 32.00 ± 29.30; $P = .92$).

CONCLUSION: Small aneurysms are prone to growth and rupture. Aneurysm rupture is more likely to occur in aneurysms with larger absolute diameter growth, but rupture can also occur in the absence of growth. The annual growth rate in both groups suggests that rate of growth of aneurysms is highly variable and unpredictable, justifying treatment or close diagnostic follow-up.

KEY WORDS: Aneurysm growth, Aneurysm rupture, Small aneurysms

Neurosurgery 68:1164–1171, 2011 DOI: 10.1227/NEU.0b013e31820edbd3 www.neurosurgery-online.com

With the advent of new imaging techniques, intracranial aneurysms are diagnosed with greater frequency. Based on radiographic and autopsy studies, the prevalence of intracranial aneurysms is approximately 0.4% to 6.0%. It has been suggested that 2% of adults without risk factors harbor asymptomatic intracranial aneurysms.[1] Of patients with cerebral aneurysms, 20% to 30% have multiple aneurysms.[2] Aneurysm rupture is a major threat, accounting for 0.4% to 0.6% of all deaths.[3]

ABBREVIATIONS: CTA, computed tomographic angiography; **ISUIA,** International Study of Unruptured Intracranial Aneurysms; **MRA,** magnetic resonance angiography; **SAH,** subarachnoid hemorrhage

The bleeding rate of unruptured aneurysms has been a subject of significant investigation and has been found to vary depending on study design and study population.[4-8] The management of unruptured cerebral aneurysms remains controversial because of the uncertainty and seeming unpredictability of the natural history. The International Study of Unruptured Intracranial

Copyright © Congress of Neurological Surgeons. Unauthorized reproduction of this article is prohibited.

Aneurysms (ISUIA)[9,10] suggested low rupture risk for asymptomatic anterior circulation aneurysms ≤ 7 mm in diameter; consequently, the number of conservatively treated, unruptured small aneurysms ≤ 7 mm has likely increased. The apparent paradox of natural history data suggesting low rupture risk of small asymptomatic aneurysms and the small median size of aneurysm rupture[11,12] remains unexplained and perplexing. Major limitations of available natural history studies include absent data on aneurysm growth rates and their potential relationship to rupture, selection bias, and short follow-up time intervals.

Aneurysm growth is likely associated with rupture, but this relationship has not been well characterized in the literature. Hence, follow-up imaging to screen for growth or change in morphology of asymptomatic aneurysms remains controversial.[13,14] Therefore, an important question to answer is whether close follow-up helps to establish or refute a relationship between aneurysmal behavior and growth. We therefore aimed to examine the literature regarding the relationship between aneurysm growth and rupture. We specifically examined the question of whether small asymptomatic aneurysms ≤ 7 mm that are followed up over time rupture and whether aneurysm growth affects rupture risk.

METHODS

Using the following key words, combined with the word aneurysms, in different combinations, we reviewed all publications on unruptured aneurysms published from 1966 to 2010: untreated, incidental, symptomatic, risk of rupture, subarachnoid hemorrhage (SAH), intracranial/intracerebral aneurysms, growth, and follow-up. We searched the reference lists of all relevant citations for additional studies.

We then selected all ≤ 7-mm aneurysm cases for which measurements were reported for at least 2 time points and for which initial asymptomatic status and ultimate outcome were reported. When available, we noted whether patients had single or multiple aneurysms, family history of SAH, previous history of SAH, smoking, and hypertension.

We excluded cases of (1) patients < 18 years of age, (2) mycotic intracranial aneurysms, (3) traumatic aneurysms, (4) aneurysmal growth or rupture after carotid endarterectomy, (5) aneurysms for which information regarding size and duration of follow up was not available (ie, we excluded pooled data because we could not determine the fate of an aneurysm on an individual basis), (6) de novo aneurysms, and (7) aneurysms that exist as a part of a genetic syndrome, eg, Alagille syndrome and polycystic kidney disease.

Aneurysmal growth was defined on the basis of the imaging modality used. With computed tomographic angiography, aneurysm growth was defined as an increase in size of > 0.5 mm during the follow-up period.[14] Using magnetic resonance angiography (MRA), we defined aneurysmal growth as any difference in maximal diameter, but for aneurysms < 5 mm, only a change in size of ≥ 1 mm on follow-up examination was noted as significant growth.[13] Finally, when angiography was used, at least at the follow-up scan, aneurysmal growth was defined as any change in maximal diameter during follow-up.[15] For each of the selected cases, we computed absolute growth (where T1 is time 1 and T 2 is time 2): size (T2) − size (T1); percent growth: {[size (T2) − size (T1)] / size (T1)} × 100; and annual growth rate (percent yearly increase): [size(T2) − size (T1)] / duration of follow-up, ie, (absolute growth / duration of follow-up).[15] We used the Mann-Whitney test for 2 reasons: An outlier can derive a *t* test, especially with a small data set, and the *t* test could not be used because data are not necessarily normally distributed. All statistical tests were 2 sided. A value of $P < .05$ was considered significant.

RESULTS

Our search retrieved 51 patients 34 to 81 years of age (mean ± SD, 58.00 ± 12.68 years) harboring a total of 64 asymptomatic aneurysms ≤ 7 mm; 30 of 64 aneurysms (47%) had subsequent rupture.[13-24] The aneurysms were localized as depicted in Figure 1 and Tables 1 and 2.

Of the total cases, 11% of the aneurysms were in the posterior circulation and 89% in the anterior circulation, mirroring the normal anatomic distribution of cerebral aneurysms.[21] For the aneurysms retrieved, with vs without subsequent rupture, a history of hypertension was noted in 6 of 9 (21 not applicable) vs 14 of 28 (6 not applicable), smoking in 1 of 1 (29 not applicable) vs 5 of 19 (15 not applicable), family history of SAH in 0 of 0 (30 not applicable) vs 9 of 191 (5 not applicable), history of previous SAH in 4 of 6 (24 not applicable) vs 8 of 9 (25 not applicable), and multiple aneurysms in 10 of 151 (5 not applicable) vs 23 of 28 (6 not applicable), respectively (not applicable means information was not provided).

The size of aneurysms ranged between 1.00 and 7.00 mm (2.99 ± 1.25 mm); 81% of the aneurysms (52 of 64) were < 5 mm. The follow-up period ranged between 6 months and 20 years (5.85 ± 4.75 years). Among the aneurysms that ruptured, 3 had no growth and 27 grew before rupture (90%), whereas

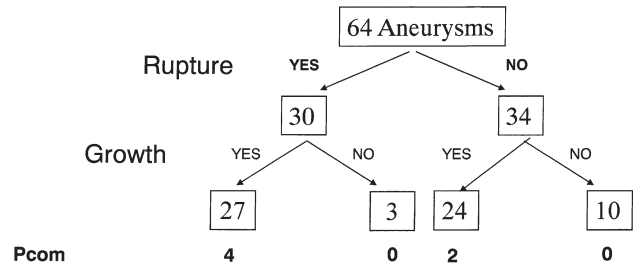

Pcom	4	0	2	0
Acom	6	0	4	1
ACA	2	0	1	1
IC	6	0	5	3
MCA	3	2	8	2
BA	2	0	1	1
PICA	1	0	0	0
ICPC	3	0	2	1
PCA	0	0	1	0
SCA	0	0	0	1
Pericallosal	0	1	0	0

FIGURE 1. *Breakdown of cases with respect rupture, growth, and anatomic location. ACA, anterior cerebral artery; Acom, anterior communicating artery; BA, basilar artery; IC, internal carotid artery; ICPC, internal carotid-posterior communicating artery; MCA, middle cerebral artery; PCA, posterior cerebral artery; Pcom, posterior communicating artery; PICA, posterior inferior cerebellar artery; SCA, superior cerebellar artery.*

Copyright © Congress of Neurological Surgeons. Unauthorized reproduction of this article is prohibited.

TABLE 1. Ruptured Aneurysms[a]

No.	Reference	Age, y	Size at Time 1 (Enlarged), mm	Follow-up, y	Location	Imaging
1	Stuntz et al[16]	38	3 (9)	9	Pcom	Angio → Angio
2	Misra et al[18]	34	3 (6)	11	Pcom	Angio → Angio
3	Schievink[21]	70	4	2.5	MCA	Angio → Angio
4	Schievink[21]	57	4	9.5	Pericallosal	Angio → Angio
5	Schievink[21]	41	2 (4.5)	4	Pcom	Angio → Angio
6	Vanninen[21]	45	2.5 (7)	3	MCA	MRA → Angio
7	Yasui et al[20]	47	1 (3)	3.2	ICA	Angio → Angio
8	Yasui et al[20]	38	2 (3)	11	AcomA	Angio → Angio
9	Yasui et al[20]	74	2 (3.5)	2.25	ACA	Angio → Angio
10	Yasui et al[20]	57	2 (5)	2.58	ICA	Angio → Angio
11	Yasui et al[20]	73	2 (8)	20	ICA	Angio → Angio
12	Yasui et al[20]	62	3 (5)	3	AcomA	Angio → Angio
13	Yasui et al[20]	54	3 (7)	12	AcomA	Angio → Angio
14	Yasui et al[20]	60	3 (7)	7	PICA	Angio → Angio
15	Yasui et al[20]	59	3 (10)	10	AcomA	Angio → Angio
16	Yasui et al[20]	54	3 (15)	6	ICA	Angio → Angio
17	Yasui et al[20]	79	5 (8)	2	BA	Angio → Angio
18	Yasui et al[20]	46	5 (9)	2	MCA	Angio → Angio
19	Yasui et al[20]	56	5 (10)	7	ICA	Angio → Angio
20	Yasui et al[20]	50	5 (10)	10	AcomA	Angio → Angio
21	Kamitani et al[15]	58	1.6 (7.1)	16	ICPC	Angio → Angio
22	Kamitani et al[15]	52	1.30 (3.5)	20	ICPC	Angio → Angio
23	Kamitani et al[15]	57	2.5 (7)	9	ACA	Angio → Angio
24	Suga et al[22]	75	4.5 (5.5)	1.67	Basilar	MRA → MRA(Angio)
25	Suga et al[22]	66	7 (13)	9.25	ICA, PcomA	CTA → Angio
26	Yonekura[23]	53	2.9 (5.7)	2.25	ICA	Unspecified
27	Yonekura[23]	71	4.9 (5.9)	0.58	AcomA	Unspecified
28	Yonekura[23]	77	4.5 (4.5)	0.58	MCA	Unspecified
29	Yonekura[23]	42	4 (7)	1.5	MCA	Unspecified
30	Burns et al[13]	NA	6 (9.4)	8.3	Pcom	MRA → MRA

[a]Acom, anterior communicating artery; Angio, angiography; BA, basilar artery; IC, internal carotid artery; ICPC, internal carotid-posterior communicating artery; MCA, middle cerebral artery; MRA magnetic resonance angiography; PCA, posterior cerebral artery; Pcom, posterior communicating artery; PICA, posterior inferior cerebellar artery; SCA, superior cerebellar artery.

among the aneurysms without subsequent rupture, 24 of 34 (71%) enlarged during follow-up. There was a trend toward larger absolute diameter growth for ruptured aneurysms vs unruptured aneurysms (3.89 ± 2.34 mm vs 1.79 ± 1.02 mm, respectively). This trend was statistically significant ($P < .001$; Figure 2). Similar results were reached when growth percentage for aneurysms with and without rupture was computed (138.38 ± 94.40 vs 76.40 ± 53.66; $P < .001$). For the 2 groups, the size of aneurysms at the end of follow-up was 7.19 ± 2.90 vs 4.44 ± 1.46 mm; $P < .001$). The same findings also apply for anterior circulation aneurysms; aneurysms with subsequent rupture had significantly larger absolute diameter growth compared with the unruptured group (4.00 ± 2.59 vs 1.69 ± 0.95 mm; $P < .001$). We compared size of aneurysms at diagnosis, time 1, in each of the 2 groups (with and without rupture) to rule out the possibility that ruptured aneurysms had larger mean size at diagnosis (time 1) that could account for increased risk for enlargement and subsequent rupture (3.30 ± 1.52 vs 2.65 ± 0.97 mm; $P = .14$). Along the same lines, there was no statistical significance when age at time 1 was compared for the 2 groups (56.42 ± 12.35 vs 59.04 ± 12.73 years; $P = .31$). On the other hand, annual growth rates, percent yearly increase, for aneurysms with growth and subsequent rupture were not statistically different (27.46 ± 18.76 vs 32.00 ± 29.30; $P = .92$; Figure 3). This finding can be attributed to the highly variable annual growth rate of aneurysms and is discussed below.

DISCUSSION

Understanding the natural history of unruptured aneurysms is critical to patient management. There has been debate regarding the appropriate management of unruptured intracranial aneurysms because of the discrepancy in outcomes between older and more recent natural history studies. Because unruptured aneurysms were not treated before 1979 in Helsinki, Juvela et al[5,25,26] were able to retrospectively examine the long-term

Copyright © Congress of Neurological Surgeons. Unauthorized reproduction of this article is prohibited.

TABLE 2. Unruptured Aneurysms[a]

No.	Reference	Age, y	Size at Time 1 (Enlarged), mm	Follow-up, y	Location	Imaging
1	Yoshimoto[34]	64	3 (7)	7	Pcom	Angio → Angio
2	Misra et al[18]	34	1.5(4)	11	Pcom	Angio → Angio
3	Schievink[21]	70	4	2.5	MCA	Angio → Angio
4	Kamitani et al[15]	49	1.5 (2.5)	10.00	ICPC	Angio → Angio
5	Kamitani et al[15]	52	2 (3.4)	11.00	MCA	Angio → Angio
6	Kamitani et al[15]	54	2.5 (3.00)	8.00	MCA	Angio → Angio
7	Kamitani et al[15]	54	2.60 (3.30)	8.00	ACA	Angio → Angio
8	Kamitani et al[15]	34	1.8 (2.0)	5.00	IC	Angio → Angio
9	Kamitani et al[15]	56	2.44 (3.20)	9.00	ICPC	Angio → Angio
10	Kamitani et al[15]	58	2.40	2.00	ICPC	Angio → Angio
11	Suga et al[22]	71	3.0 (4.0)	10.00	AcomA	MRA → MRA(Angio)
12	Wermer et al[33]	56	2.8 (3.5)	1.00	MCA	CTA → CTA
13	Wermer et al[33]	38	1.0 (3.0)	5.00	MCA	CTA → CTA
14	Wermer et al[33]	58	2.5 (4.0)	2.00	Acom	CTA → CTA
15	Miyazawa et al[24]	61	4.0 (6.0)	3.25	ICA	MRA → MRA
16	Miyazawa et al[24]	61	3.0 (5.0)	3.25	MCA	MRA → MRA
17	Miyazawa et al[24]	71	3.0 (5.0)	0.83	ICA	MRA → MRA
18	Miyazawa et al[24]	71	2.00	0.83	SCA	MRA → MRA
19	Miyazawa et al[24]	70	3.0 (5.0)	1.08	ICA	MRA → MRA
20	Miyazawa et al[24]	70	2.00	1.08	ICA	MRA → MRA
21	Miyazawa et al[24]	72	3.0 (5.0)	1.25	ICA	MRA → MRA
22	Miyazawa et al[24]	72	3.00	1.25	ICA	MRA → MRA
23	Miyazawa et al[24]	72	2.00	1.25	MCA	MRA → MRA
24	Miyazawa et al[24]	81	2.0 (6.0)	3.92	AcomA	MRA → MRA
25	Miyazawa et al[24]	72	2.0 (4.0)	1.58	MCA	MRA → MRA
26	Miyazawa et al[24]	72	2.00	1.58	ACA	MRA → MRA
27	Miyazawa et al[24]	61	2.0 (4.0)	4.25	MCA	MRA → MRA
28	Miyazawa et al[24]	61	3.00	4.25	ICA	MRA → MRA
29	Miyazawa et al[24]	61	4.00	4.25	BA	MRA → MRA
30	Miyazawa et al[24]	56	2.0 (4.0)	1.33	BA	MRA → MRA
31	Miyazawa et al[24]	55	3.0 (6.0)	1.67	AcomA	MRA → MRA
32	Miyazawa et al[24]	78	5.0 (8.0)	1.50	MCA	MRA → MRA
33	Miyazawa et al[24]	78	2.00	1.50	AcomA	MRA → MRA
34	Burns et al[13]	NA	4.9 (5.6)	5.20	PCA	MRA → MRA

[a]Acom, anterior communicating artery; Angio, angiography; BA, basilar artery; IC, internal carotid artery; ICPC, internal carotid-posterior communicating artery; MCA, middle cerebral artery; MRA magnetic resonance angiography; PCA, posterior cerebral artery; Pcom, posterior communicating artery; PICA, posterior inferior cerebellar artery; SCA, superior cerebellar artery.

natural history of unruptured aneurysms in 142 patients. During 2575 person-years, 23% of patients suffered a SAH, resulting in an incidence of 1.3%. Comparable findings were reported by Tsutsumi etal[7,27] in a smaller study of 62 patients with saccular unruptured aneurysms detected by cerebral angiography between 1976 and 1997. Likewise, Winn et al[28] reviewed 3684 cerebral angiography studies obtained at the University of Virginia between April 1969 and January 1980. Using a prevalence rate of 0.65% and mathematical reasoning on the frequency of SAH during that time period in the North American population, they computed a 0.72% to 1.36% annual rupture rate for aneurysms < 10 mm. However, the ISUIA suggested a drastically lower risk of SAH, by a factor of 10 to 20, for aneurysms < 10 mm. Study investigators concluded that the size of intracranial aneurysms is the key factor in determining the risk of rupture and raised new controversy regarding the threshold aneurysm size recommended for treatment. The retrospective arm of the ISUIA indicated a critical risk of rupture for a diameter of 10 mm. A 0.05% annual rupture rate was identified in small anterior-circulation aneurysms < 10 mm in patients who had no previous history of SAH.[10] Although its prospective arm found this critical limit to be 7 mm, ISUIA reported zero rupture risk for anterior circulation asymptomatic aneurysms < 7 mm in patients without history of SAH over a 5-year follow-up period.[9]

As a consequence of the ISUIA findings, many small aneurysms are now followed up with serial imaging with very few data to support this approach. Although aneurysm growth has been suggested as a risk factor for rupture,[15] it has not been well studied in natural history studies. Scant and conflicting data exist on aneurysm growth, which leaves clinicians with little guidance

Copyright © Congress of Neurological Surgeons. Unauthorized reproduction of this article is prohibited.

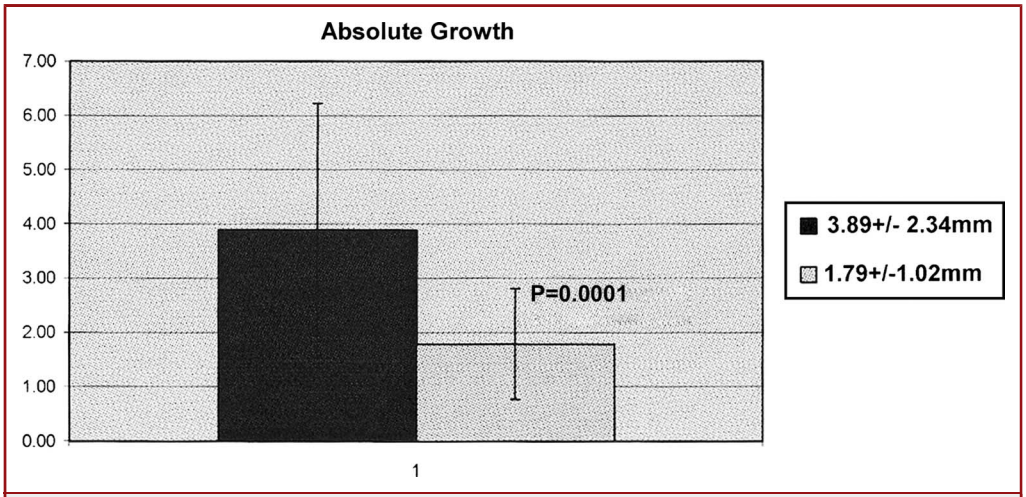

FIGURE 2. *Left, ruptured. Right, unruptured.*

in determining the optimal surveillance strategy for unruptured aneurysms. Over a mean follow-up period of 47 months, Burns et al[13] showed that aneurysmal growth was detected in 6.9% of aneurysms (12 of 173) < 8 mm, whereas Phan et al[29] found that aneurysmal growth is limited to larger aneurysms (> 9 mm). Over a shorter median follow-up period of 29.3 months, Miyazawa et al[24] detected aneurysmal growth in 7.9% of aneurysms with an original diameter of ≤ 8 mm. Matsubara et al[30] documented 2.5% (3 of 123) aneurysmal growth in very small aneurysms ranging from 2 to 4 mm. However, no clear consensus exists as to whether aneurysm growth affects aneurysmal behavior. Kamitani et al[15] concluded that aneurysms growing faster than 8%/y resulted in subsequent bleeding, whereas lower growth rates did not correlate with subsequent rupture. On the contrary, Asari and Ohmoto[4] found that changes in aneurysm size did not correlate with later SAH. One explanation for this discrepancy is the relatively small number of growing aneurysms in the studies, which does not allow definitive conclusions. Only 3.2% (3 of 92) grew over the mean 1.3-year follow-up period, and only 2 aneurysms subsequently ruptured.[14] A second potential explanation for the discrepancy is the short-term follow-up in aneurysm growth studies.[14,30]

To better comprehend the relationship between aneurysm growth and rupture in small aneurysms, we reviewed all case analyses reported in the literature of well-documented aneurysm growth. We selected all ≤ 7-mm aneurysms for which there were

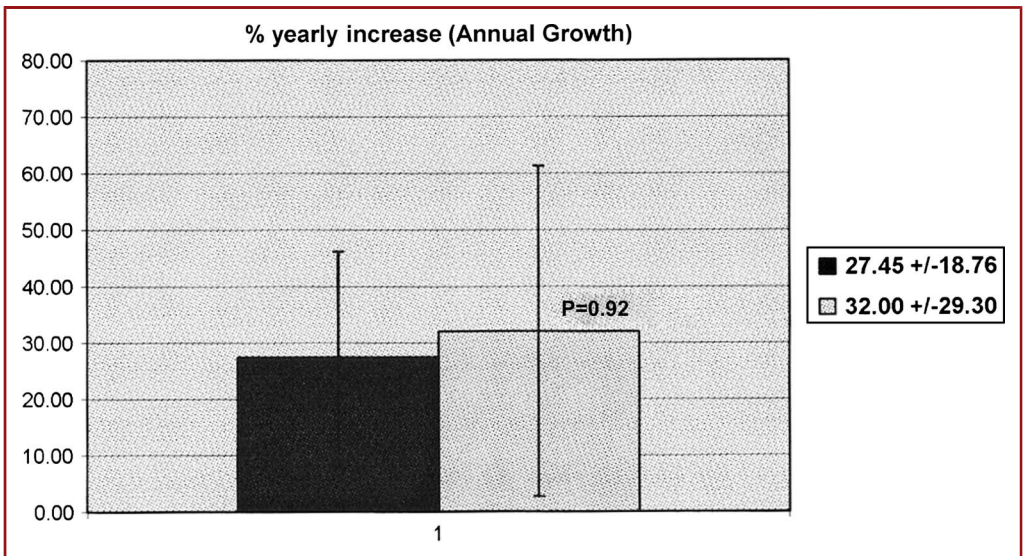

FIGURE 3. *Left: ruptured. Right, unruptured.*

Copyright © Congress of Neurological Surgeons. Unauthorized reproduction of this article is prohibited.

reported measurements for at least 2 time points and for which initial asymptomatic status and ultimate outcome were reported.

The majority of cases identified with our strict selection criteria were < 5 mm in diameter (2.99 ± 1.25 mm) and were studied over a mean follow-up period of 5.85 ± 4.75 years, similar to the ISUIA follow-up period. Nearly half (46.8%, 30 of 64) of the aneurysms were noted to be ruptured, which raises questions regarding the suggested benign course of small asymptomatic anterior circulation aneurysms.[9,10] In our study, the size of aneurysms at rupture was 7.19 ± 2.90, which is consistent with a recent publication reporting its findings in which 627 of 889 aneurysms had ruptured at a small size.[12] Of these ruptured cases, 71.8% were < 7 mm in diameter, and the mean diameter of the aneurysms was 6.28 mm.[12] Our findings add to the paradox of recent natural history data[9,10] that suggest a low rupture risk of small asymptomatic aneurysms and small median size of aneurysm rupture.[12]

In our analysis, aneurysms with larger absolute diameter growth or percent growth were more likely to rupture, but rupture still occurred in the absence of growth. Of the ruptured cases, 90% (27 of 30) were preceded by growth. On average, ruptured aneurysms grew twice as much in size compared with the unruptured cases (3.89 ± 2.34 vs 1.79 ± 1.02 mm, respectively; $P < .001$). As discussed earlier, those findings were not confounded by initial size or by pooling data from anterior and posterior circulations. Our results are consistent with a noteworthy long-term study that observed that ruptured aneurysms had more often increased significantly in size (≥ 1 mm) than the largest aneurysms in patients with no rupture.[26] Because risk factors were not consistently reported in the cases we identified, our analysis was restricted to the relationship between aneurysm growth and aneurysm rupture.

Given that growth rate is directly proportional to absolute growth, it was intriguing that aneurysms with larger absolute diameter growth, destined to rupture, did not have statistically significantly larger annual growth rates compared with aneurysms that did not rupture. From a mathematical standpoint, growth rate equals absolute growth divided by duration of follow-up (time). Because the data showed no significance in growth rates between ruptured and unruptured aneurysms, the time variable is suggested to be the source of variation.

Two possible patterns of aneurysm growth have been postulated: linear (constant growth) and episodic with periods of growth alternating with periods of no growth.[31,32] In principle, the former would be coupled with a constant predictable risk based on the growth rate and initial size. On the other hand, episodic growth could be associated with periods of high and low risk of rupture.[32] Unfortunately, scant data are available on growth rate profiles over time because conducting such a study would be formidable in that it requires scanning and monitoring of massive groups of healthy individuals and patients harboring unruptured intracranial aneurysms frequently over prolonged periods of time. Frequent follow-up is costly, may have psychosocial consequences,[33] and in the case of CTA might be harmful because of radiation exposure, contrast allergic reactions, or contrast-induced nephropathy. However, information about the change in or consistency of aneurysm growth rates has been attained through mathematical modeling, as illustrated by Koffijberg et al[31] and previous studies,[34,35] demonstrating irregular growth rates for intracranial aneurysms. Those findings are consistent with clinical studies. In their long-term study, Juvela et al[5] showed that the growth rate of aneurysms varied significantly. Similar results were reported 3 decades earlier by Allcock and Canham[36] in their angiography-based study. During our literature search, we encountered a number of cases that could support the sporadic growth (Figure 4).[15,23] The notion that growth rate is irregular is at least proven mathematically through simulation models and at best supported by sporadic clinical data. Therefore, clinical data tailored to monitoring aneurysms frequently for extended periods of time are needed to delineate the details of growth patterns of aneurysms.

The limitations of our study include the fact that referenced data that met our strict inclusion criteria did not consistently provide information regarding the presence or absence of cerebrovascular risk factors, history of SAH, family history SAH, or the presence of single vs multiple aneurysms. Thus, our analysis was restricted only to the impact of aneurysm growth on aneurysm behavior. Furthermore, we had strict inclusion criteria, which resulted in the omission of a significant number of cases from our analysis. Thus, our conclusions stem from cases that met our inclusion criteria but certainly not from all reported small aneurysmal cases in the literature. Our research question and methods required availability of the size of the aneurysm at 2 time points and duration of follow-up for each individual aneurysm. Either most of the studies did not provide all 3 pieces of information, or if they did,[5] their data were reported as group data with the size range exceeding our cutoff criteria of 7 mm, which rendered inclusion in our analysis impossible because we could not determine the fate of aneurysms on an individual basis. On the other hand, the majority of cases extracted were from series

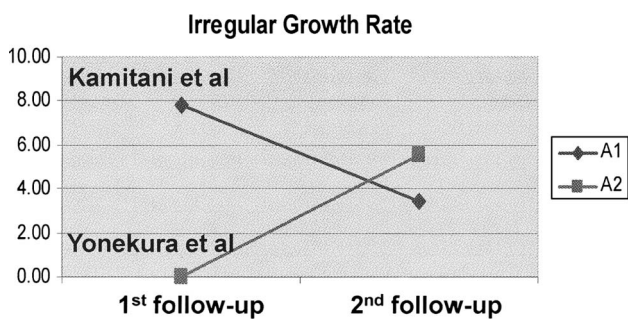

FIGURE 4. *Case 1: at the first follow-up, the annual growth rate was approximately 8%; at the second follow-up, annual growth rate was approximately 3.6%, which confirms that growth is not linear. Case 2: at first follow-up, no growth was noted (0%); at the second follow-up, the annual growth rate was calculated at approximately 6%, which validated that aneurysm growth is episodic and erratic.*

Copyright © Congress of Neurological Surgeons. Unauthorized reproduction of this article is prohibited.

and not individual case reports focused on the question we asked. Publication bias hence did not likely bias our results.

Additionally, the study conclusions may be compromised by the introduction of diagnostic error when acquiring and interpreting the image scans taken at the 2 references time periods using different imaging modalities. However, 91% of cases (58 of 64) were scanned with the same imaging modality at both time points, suggesting that this is not a major source of error. Half of the aneurysm cases (32 of 64) were directly comparable at both time reference periods with angiography, the gold standard for the diagnosis and analysis of cerebral aneurysms. Of the remaining 32 cases, 23 were imaged at both time periods with MRA, with 2 cases further confirmed by additional angiography obtained at time 2. MRA is considered an effective tool for following up cerebral aneurysms; interobserver agreement in 1 study was excellent ($\kappa = 0.942$).[5] Two other cases had initial and second scans taken with different modalities. For these 2 cases, angiography was used at the second time period, but in 1 case, the initial scan used MRA and the other used CTA. Finally, 1 case comparison used CTA for both initial and final scans.

Our knowledge regarding aneurysm growth rate is far from complete. It is clearly misleading to rely on annual growth rate for stratification of rupture risk. Growth rate of aneurysms appears highly variable, episodic, and unpredictable. Unfortunately, from the available data, it is not possible to determine the most appropriate time interval between diagnostic follow-up studies in patients with unruptured aneurysms.[37] Although variable growth rates of cerebral aneurysms may rationalize more frequent screening, scheduled surveillance may become less effective because aneurysmal growth is erratic.

The risk of lifetime rupture is underestimated if we extrapolate remaining lifetime events solely on initial aneurysm size. Aneurysm growth when identified is a potential predictor of subsequent aneurysm rupture. Lack of growth is not a guarantee of benign aneurysm behavior. Rupture of aneurysms remains unpredictable, and enlargement is only 1 factor that can influence aneurysmal behavior. Novel epidemiological, morphological, and ultimately biological hypotheses need to be examined and assimilated into 1 model that allows better selection of patients who would benefit from aggressive treatment. Unfortunately, despite decades of research, aneurysm behavior remains predictably unpredictable even in small asymptomatic aneurysms.

CONCLUSION

Our review suggests that small asymptomatic aneurysms ≤ 7 mm in diameter pose risk for SAH. The benign label suggested by ISUIA for these aneurysms may not be warranted. Aneurysm growth seems to correlate with higher risk of rupture, but rupture can occur without growth. For aneurysms that are not treated, surveillance imaging appears warranted, but the frequency of surveillance remains difficult to determine because of the erratic nature of aneurysm growth and behavior. Future studies should better examine this issue. Future natural history studies should take aneurysm growth into account.

Disclosure

The authors have no personal financial or institutional interest in any of the drugs, materials, or devices described in this article.

REFERENCES

1. Vernooij MW, Ikram MA, Tanghe HL, et al. Incidental findings on brain MRI in the general population. *N Engl J Med*. 2007;357(18):1821-1828.
2. Stehbens WE. Aneurysms and anatomical variation of cerebral arteries. *Arch Pathol*. 1963;75:45-64.
3. Tidswell P, Dias PS, Sagar HJ, Mayes AR, Battersby RD. Cognitive outcome after aneurysm rupture: relationship to aneurysm site and perioperative complications. *Neurology*. 1995;45(5):875-882.
4. Asari S, Ohmoto T. Natural history and risk factors of unruptured cerebral aneurysms. *Clin Neurol Neurosurg*. 1993;95(3):205-214.
5. Juvela S, Porras M, Heiskanen O. Natural history of unruptured intracranial aneurysms: a long-term follow-up study. *J Neurosurg*. 1993;79(2):174-182.
6. Rinkel GJ, Djibuti M, Algra A, van Gijn J. Prevalence and risk of rupture of intracranial aneurysms: a systematic review. *Stroke*. 1998;29(1):251-256.
7. Tsutsumi K, Ueki K, Morita A, Kirino T. Risk of rupture from incidental cerebral aneurysms. *J Neurosurg*. 2000;93(4):550-553.
8. Yasui N, Suzuki A, Nishimura H, Suzuki K, Abe T. Long-term follow-up study of unruptured intracranial aneurysms. *Neurosurgery*. 1997;40(6):1155-1159.
9. Wiebers DO, Whisnant JP, Huston J III, et al. Unruptured intracranial aneurysms: natural history, clinical outcome, and risks of surgical and endovascular treatment. *Lancet*. 2003;362(9378):103-110.
10. Unruptured intracranial aneurysms: risk of rupture and risks of surgical intervention: International Study of Unruptured Intracranial Aneurysms Investigators. *N Engl J Med*. 1998;339(24):1725- 1733.
11. Wiebers DO, Whisnant JP, Sundt TM Jr, O'Fallon WM. The significance of unruptured intracranial saccular aneurysms. *J Neurosurg*. 1987;66(1):23-29.
12. Joo SW, Lee SI, Noh SJ, Jeong YG, Kim MS, Jeong YT. What is the significance of a large number of ruptured aneurysms smaller than 7 mm in diameter? *J Korean Neurosurg Soc*. 2009;45(2):85-89.
13. Burns JD, Huston J III, Layton KF, Piepgras DG, Brown RD Jr. Intracranial aneurysm enlargement on serial magnetic resonance angiography: frequency and risk factors. *Stroke*. 2009;40(2):406-411.
14. Wermer MJ, van der Schaaf IC, Velthuis BK, Majoie CB, Albrecht KW, Rinkel GJ. Yield of short-term follow-up CT/MR angiography for small aneurysms detected at screening. *Stroke*. 2006;37(2):414-418.
15. Kamitani H, Masuzawa H, Kanazawa I, Kubo T. Bleeding risk in unruptured and residual cerebral aneurysms: angiographic annual growth rate in nineteen patients. *Acta Neurochir (Wien)*. 1999;141(2):153-159.
16. Stuntz JT, Ojemann GA, Alvord EC, Jr. Radiographic and histologic demonstration of an aneurysm developing on the infundibulum of the posterior communicating artery: case report. *J Neurosurg*. 1970;33(5):591-595.
17. Yoshimoto T, Suzuki J. Surgical treatment of an aneurysm on the funnel-shaped bulge of the posterior communicating artery: case report. *J Neurosurg*. 1974;41(3):377-379.
18. Misra BK, Whittle IR, Steers AJ, Sellar RJ. De novo saccular aneurysms. *Neurosurgery*. 1988;23(1):10-15.
19. Vanninen RL, Hernesniemi JA, Puranen MI, Ronkainen A. Magnetic resonance angiographic screening for asymptomatic intracranial aneurysms: the problem of false negatives: technical case report. *Neurosurgery*. 1996;38(4):838-840.
20. Yasui N, Magarisawa S, Suzuki A, Nishimura H, Okudera T, Abe T. Subarachnoid hemorrhage caused by previously diagnosed, previously unruptured intracranial aneurysms: a retrospective analysis of 25 cases. *Neurosurgery*. 1996; 39(6):1096-1100.
21. Schievink WI. Intracranial aneurysms. *N Engl J Med*. 1997;336(1):28-40.
22. Suga M, Yamamoto Y, Sunami N, Abe T, Kondo A. Growth of asymptomatic unruptured aneurysms in follow-up study: report of three cases [in Japanese]. *No Shinkei Geka*. 2003;31(3):303-308.
23. Yonekura M. Small unruptured aneurysm verification (SUAVe Study, Japan): interim report. *Neurol Med Chir (Tokyo)*. 2004;44(4):213-214.

Copyright © Congress of Neurological Surgeons. Unauthorized reproduction of this article is prohibited.

24. Miyazawa N, Akiyama I, Yamagata Z. Risk factors for growth of unruptured intracranial aneurysms: follow-up study by serial 0.5-T magnetic resonance angiography. *Neurosurgery*. 2006;58(6):1047-1053.
25. Juvela S. Natural history of unruptured intracranial aneurysms: risks for aneurysm formation, growth, and rupture. *Acta Neurochir Suppl*. 2002;82:27-30.
26. Juvela S, Porras M, Poussa K. Natural history of unruptured intracranial aneurysms: probability of and risk factors for aneurysm rupture. *J Neurosurg*. 2000;93(3):379-387.
27. Tsutsumi K, Ueki K, Morita A, Usui M, Kirino T. Risk of aneurysm recurrence in patients with clipped cerebral aneurysms: results of long-term follow-up angiography. *Stroke*. 2001;32(5):1191-1194.
28. Winn HR, Jane JA Sr, Taylor J, Kaiser D, Britz GW. Prevalence of asymptomatic incidental aneurysms: review of 4568 arteriograms. *J Neurosurg*. 2002;96(1):43-49.
29. Phan TG, Huston J III, Brown RD Jr, Wiebers DO, Piepgras DG. Intracranial saccular aneurysm enlargement determined using serial magnetic resonance angiography. *J Neurosurg*. 2002;97(5):1023-1028.
30. Matsubara S, Hadeishi H, Suzuki A, Yasui N, Nishimura H. Incidence and risk factors for the growth of unruptured cerebral aneurysms: observation using serial computerized tomography angiography. *J Neurosurg*. 2004;101(6):908-914.
31. Koffijberg H, Buskens E, Algra A, Wermer MJ, Rinkel GJ. Growth rates of intracranial aneurysms: exploring constancy. *J Neurosurg*. 2008;109(2):176-185.
32. Britz G, Winn HR. Assessing the constancy of intracranial aneurysm growth rates. *J Neurosurg*. 2008;109(2):173-174.
33. Wermer MJ, van der Schaaf IC, Van Nunen P, Bossuyt PM, Anderson CS, Rinkel GJ. Psychosocial impact of screening for intracranial aneurysms in relatives with familial subarachnoid hemorrhage. *Stroke*. 2005;36(4):836-840.
34. Yoshimoto Y. A mathematical model of the natural history of intracranial aneurysms: quantification of the benefit of prophylactic treatment. *J Neurosurg*. 2006;104(2):195-200.
35. Chang HS. Simulation of the natural history of cerebral aneurysms based on data from the International Study of Unruptured Intracranial Aneurysms. *J Neurosurg*. 2006;104(2):188-194.
36. Allcock JM, Canham PB. Angiographic study of the growth of intracranial aneurysms. *J Neurosurg*. 1976;45(6):617-621.
37. Weir B. Unruptured aneurysms. *J Neurosurg*. 2002;97(5):1011-1012.

COMMENTS

Small aneurysms < 7 mm in diameter have a low risk of rupture on the basis of the results of International Study of Unruptured Intracranial Aneurysms (ISUIA) and other studies. However, the majority of ruptured aneurysms observed clinically are small. This paradox has never been resolved. In this study, 64 small aneurysms were identified in the literature with anatomic measurements at multiple time points. Fifty-one aneurysms enlarged over time, and nearly half of all aneurysms went on to rupture. These findings challenge the conservative management posture that resulted from ISUIA, suggesting that small aneurysms that are supposed to be safe to observe are indeed prone to growth and rupture. This article will not change this accepted management option in selected patients, but it emphasizes the importance of meticulous follow-up. Aneurysm growth and rupture are clearly related, and enlargement should indicate intervention. Better imaging methods are needed to detect growth, and we have found that contrast-enhanced magnetic resonance imaging will measure changes in aneurysm volume over time that might be imperceptible visually.[1] Changes in aneurysm size are only a surrogate for analyzing the complex interactions between hemodynamic forces and aneurysmal tissues. Ultimately, direct measurements of these biological factors will offer meaningful guidance in selecting unruptured aneurysms for treatment.

Michael T. Lawton
San Francisco, California

1. Dispensa BP, Saloner DA, Acevedo-Bolton G, et al. Estimation of fusiform intracranial aneurysm growth by serial magnetic resonance imaging. *J Magn Reson Imaging*. 2007;26(1):177-183.

This study asks the question, Are we really safe not recommending treatment for unruptured aneurysms < 7 mm? Although this is a retrospective literature review, a group of patients were identified who were followed up for growth and rupture. A fairly large number of aneurysms demonstrated growth, and a very high percentage of those that bled demonstrated growth. Although it is difficult to draw any definitive conclusions from these data, the study reinforces the fact that many aneurysms are dynamic, and making recommendations based solely on maximal aneurysm diameter is likely an oversimplification of the situation. We hope that in the future, advanced imaging and biological markers will help us understand which patients should undergo treatment of unruptured cerebral aneurysms.

Sean D. Lavine
New York, New York

Copyright © Congress of Neurological Surgeons. Unauthorized reproduction of this article is prohibited.

A Review of Laboratory and Clinical Data Supporting the Safety and Efficacy of Cyclosporin A in Traumatic Brain Injury

Dzenan Lulic, MD
Jack Burns, MS
Eunkyung Cate Bae, MS
Harry van Loveren, MD
Cesar V. Borlongan, PhD

Center of Excellence in Aging and Brain Repair, Department of Neurosurgery and Brain Repair, University of South Florida College of Medicine, Tampa, Florida

Correspondence:
Cesar V. Borlongan, PhD,
Center of Excellence in Aging and Brain Repair,
Department of Neurosurgery and Brain Repair,
University of South Florida College of Medicine,
12901 Bruce B. Downs Blvd.,
MDC 78, Tampa, FL 33612.
E-mail: cborlong@health.usf.edu

Received, June 24, 2010.
Accepted, October 2, 2010.

Copyright © 2011 by the Congress of Neurological Surgeons

For decades, cyclosporin A (CsA) has proved to be safe and effective for use in transplantation. In the past 10 years, this agent has shown neuroprotective effects in animal models of traumatic brain injury (TBI). This review article provides a critical overview of the literature on CsA neuroprotective effects in animal studies and current findings of clinical trials in the treatment of TBI with an emphasis on the possible CsA molecular mechanism of action. Animal data provide compelling evidence of the therapeutic benefits of CsA in TBI, but the outcome indices are heterogeneous with respect to the animal model of TBI as well as the route, dose, and timing of CsA administration. Similarly, clinical studies (phase II trials) adapting almost identical patient inclusion criteria have demonstrated the safety of CsA use in TBI, but the clinical trials are also heterogeneous based on study design, especially with regard to the variable timing of CsA administration after TBI. In view of the translational shortcomings of the preclinical studies and the rather pilot nature of the limited clinical trials that recently reached phase III, we offer guidance on the future directions of laboratory investigations on CsA that could improve the safety and efficacy of this agent in subsequent larger clinical trials.

KEY WORDS: Central nervous system, Cyclosporin A, Immunosuppressant, Neuroprotection, Neurotrauma

Neurosurgery 68:1172–1186, 2011 DOI: 10.1227/NEU.0b013e31820c6cdc www.neurosurgery-online.com

Traumatic brain injury (TBI) is a complex disease, with a high prevalence among the young population[1,2] and significant socioeconomic burden[3] associated with the disease. There has been intensive research on different agents that would aid in treatment of this complex disease process. Because the initial injury is often devastating, it requires immediate treatment, suggesting that aggressive therapy is indicated.[4] Although there are no unified indication guidelines for surgical treatment, in some cases with focal injury, the most appropriate option seems to be surgical. However, in cases of isolated diffuse axonal injury with no significant increase in intracranial pressure, surgical decompression is usually not indicated.[5,6] Pharmacological intervention with neuroprotective agents either to aid with surgical decompression or to prevent secondary damage triggered by primary insult and enhance repair has been postulated as one of the future modalities of treatment.

There have been a number of neuroprotective agents that were effective in animal models of TBI, all of which target a number of different processes involved in the pathophysiology of TBI. They included bradykinin inhibitors, calcium channel blockers, *N*-methyl-d-aspartate receptor antagonists, free radical scavengers, and agents preventing lipid peroxidation, as well as corticosteroids, magnesium, and canbinols as agents with multiple actions.[7-9] Unfortunately, all of the clinical trials using these agents had disappointing results.[7] Moreover, erythropoietin, progesterone,

ABBREVIATIONS: APP, amyloid precursor protein; **ATP**, adenosine triphosphate; **BBB**, blood-brain barrier; **CsA**, cyclosporine A; **CypD**, cyclophilin D; **FF-AT**, nuclear factor of activated cells; **FPI**, fluid percussion of injury; **GCS**, Glasgow Coma Scale; **LTP**, long-term potentiation; **mPTP**, mitochondrial permeability transition pore; **NAA**, *N*-acetyl aspartate; **NO**, nitric oxide; **NOS**, nitric oxide synthase; **TBI**, traumatic brain injury

Copyright © Congress of Neurological Surgeons. Unauthorized reproduction of this article is prohibited.

and bradykinin agonists are currently under investigation in phase III trials, but the results are pending.

Nevertheless, disappointing results in clinical trials for a number of potential candidates for use in neuroprotection in TBI did not stop the search for new agents that would reduce mortality and morbidity in TBI. Encouraging animal data have pointed to CsA as one of the neuroprotectants that showed benefits in animal models of TBI. Of great clinical relevance is CsA's safety profile and promising benefits in small-scale phase II clinical trials. Phase III clinical trials on CsA have recently commenced. In our effort to further advance the scientific and clinical application of CsA with a keen interest in enhancing the successful translation of this drug discovery, we review current literature supporting CsA's therapeutic benefits and its postulated mechanism of action in TBI.

As seen in Figure 1, TBI is a complex and multifaceted pathophysiological problem that involves a dysregulation of calcium homeostasis as its central element.[10-12] This process includes breakdown of cell membrane[13,14] and cytoskeletal elements,[14,15] mitochondrial membrane potential dysregulation[11,16] and mitochondrial permeability transition pore (mPTP) formation[17-21] as well as glutamate toxicity,[10] edema formation, release of matrix metalloproteinases,[22,23] oxidative stress,[24,25] and release of inflammatory cytokines.[26,27] The cascade of these events ultimately leads to cell death and necrosis of brain parenchyma. Each of the mentioned processes is a potential target for pharmacological intervention, and the agent that targets multiple cell death pathways theoretically should offer the best protection against secondary injury in TBI. To this end, CsA has been shown to possess novel, multipronged neuroprotective features that may block the numerous TBI-mediated cell death processes.

CsA, AN IMMUNOSUPPRESSANT AND NEUROPROTECTANT

CsA is an undecapeptide isolated from the fungus *Tolypocladium inflatum Gams,* which is grown from a soil specimen in Norway. Its immunosuppressive properties were initially discovered by Borel et al,[28] which showed that CsA was able to suppress the activity of T-lymphocytes. Since this discovery, CsA clinical use was initially reserved as an immunosuppressant in transplant medicine because of its ability to alter T-lymphocyte activity. It has also been used to reduce the incidence of transplant rejection by the host.

The neuroprotective properties of CsA were not known until the mid-1990s because of its inability to cross the blood-brain barrier (BBB). Although CsA was an immunosuppressant that had been discovered earlier than others, the first neuroprotective effects were noticed with FK506 (tacrolimus, Prograf; Fujisawa Healthcare, Osaka, Japan).[29] FK506, like CsA, inhibits calcineurin. FK506 showed neuroprotection from glutamate toxicity in neural cultures through the inhibition of nitric oxide synthase (NOS) via upstream inhibition of calcineurin. Evidence of the neuroregenerative effects of CsA was not illustrated until a few years later when Palladini et al[30] found that CsA promoted axonal sprouting in the rat spinal cord transection model.

MECHANISM OF ACTION OF CsA

Recent insights into the pathophysiology of TBI have implicated mitochondrial damage and bioenergetic failure, cysteine protease activation, and calcineurin modulation, most of which have been the target of many immunosuppressants, including CsA.[31,32]

CsA binds a number of proteins including cytoplasmic high-affinity receptor cyclophilin A. CsA and cyclophilin A create a binary complex that binds calcineurin, a calcium-calmodulin–dependent phosphoserine-phosphothreonine protein phosphatase with numerous cellular targets (Figure 2).[33] In T lymphocytes, calcineurin causes dephosphorylation of cytoplasmic nuclear factor of activated T cells (NF-AT), which induces production of interleukin-2 necessary for T-lymphocyte activation.[34] Several cyclophilins have been discovered such as cyclophilins B, C, and D. Cyclophilin D (CypD) is located in mitochondria and, unlike A, B, and C, it is involved in neuroprotection.[35]

Cyclophilins belong to a group of molecules also known as immunophilins that bind immunosuppressant agents such as CsA. Because many of the immunophilins have neurotrophic and neuroprotective effects, they are also referred to as neuroimmunophilins. Neuroimmunophilins not only inhibit calcineurin, but they also block mitochondrial permeability transition and mitochondrial mega pore formation (Figure 2).

Although the protective effects of CsA were first discovered in T lymphocytes, the brain has about 20-fold greater tropism for CsA than for the T cells.[36] The benefits with CsA as a neuroprotective agent are achieved only with a high dose (ie, >10 mg/kg) and long-term administration of the drug. However, such a high dose and long-term administration of CsA produce negative side effects such as nephrotoxicity and hepatotoxicity. Thus, a major limiting factor in producing the therapeutic effects of CsA is its ability to cross the BBB. It has been demonstrated that CsA's protective effects may be enhanced by mechanical disruption of the brain parenchyma.[20,37,38] One novel approach involves the administration of endogenous ligands or their analogues to increase the permeability of the BBB by activation of receptors on the endothelial cells comprising the BBB.[39,40] The selective B_2 bradykinin receptor agonist Cereport (RMP-7; Alkermes Inc., Waltham, Massachusetts) has been shown to transiently increase the permeability of the BBB.[41] However, the BBB is inherently disrupted in the case of TBI, and systemic delivery of CsA does not represent a formidable challenge.

Another target of calcineurin that is blocked by CsA is NOS. Activated calcineurin dephosphorylates NOS, which induces production of nitric oxide. Nitric oxide (NO) is an intracellular messenger when synthesized in moderate amounts; however, excessive levels can be toxic. NO is a well-known neurotoxin induced in the case of glutamate neurotoxicity and is a free radical that can inactivate proteins and enzymes.[24] It can also interact

Copyright © Congress of Neurological Surgeons. Unauthorized reproduction of this article is prohibited.

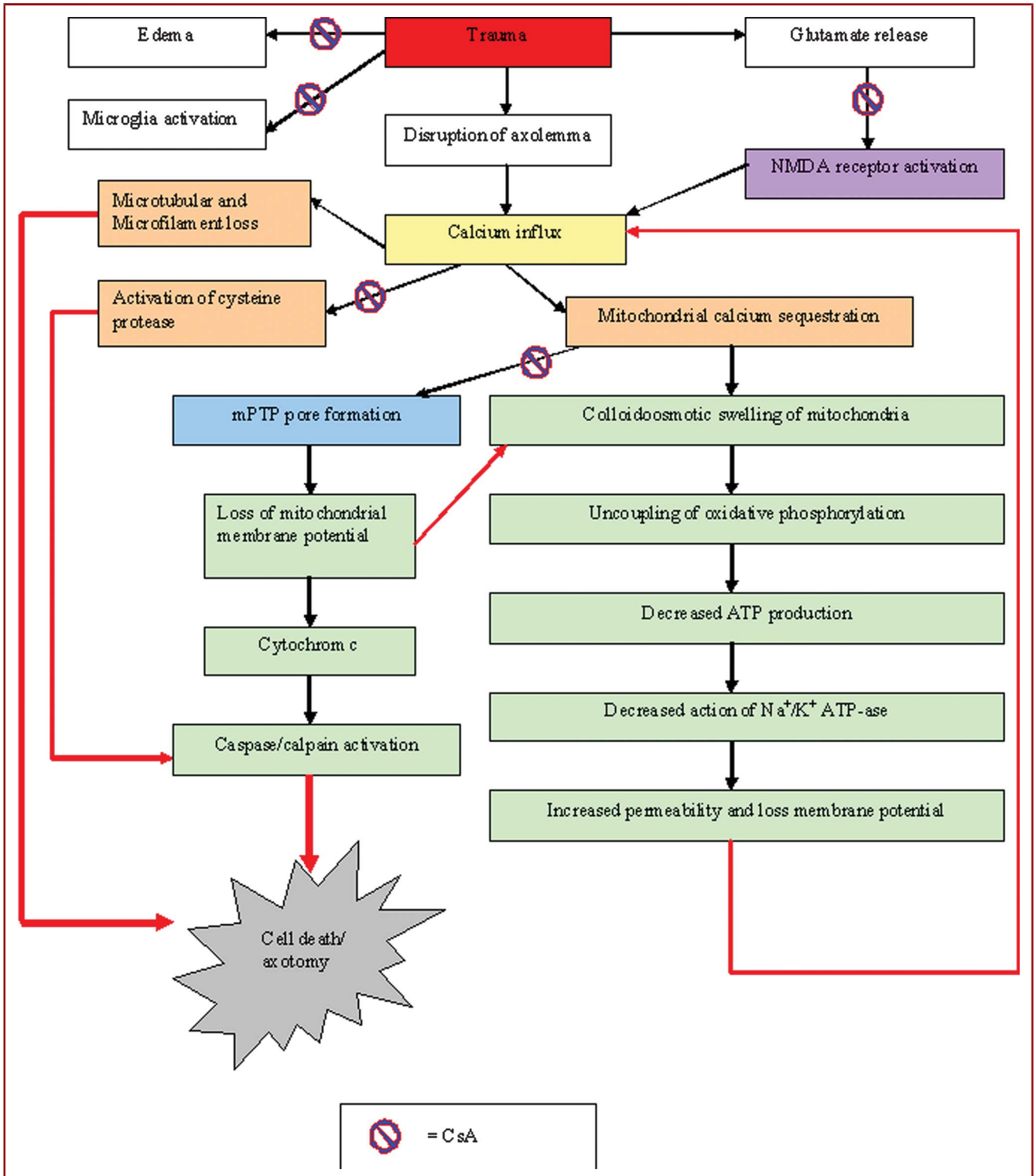

FIGURE 1. *Schematic diagram highlighting different cellular and molecular processes involved in secondary brain injury, which usually occur simultaneously after traumatic brain injury (TBI). This figure also shows putative neuroprotective pathways targeted by cyclosporin A (CsA) in abrogating TBI. ATP, adenosine triphosphatase; mPTP, mitochondrial permeability transition pore; Na^+/K^+ ATP-ase, sodium-potassium adenosine triphosphatase; NMDA, N-methyl D-aspartate.*

Copyright © Congress of Neurological Surgeons. Unauthorized reproduction of this article is prohibited.

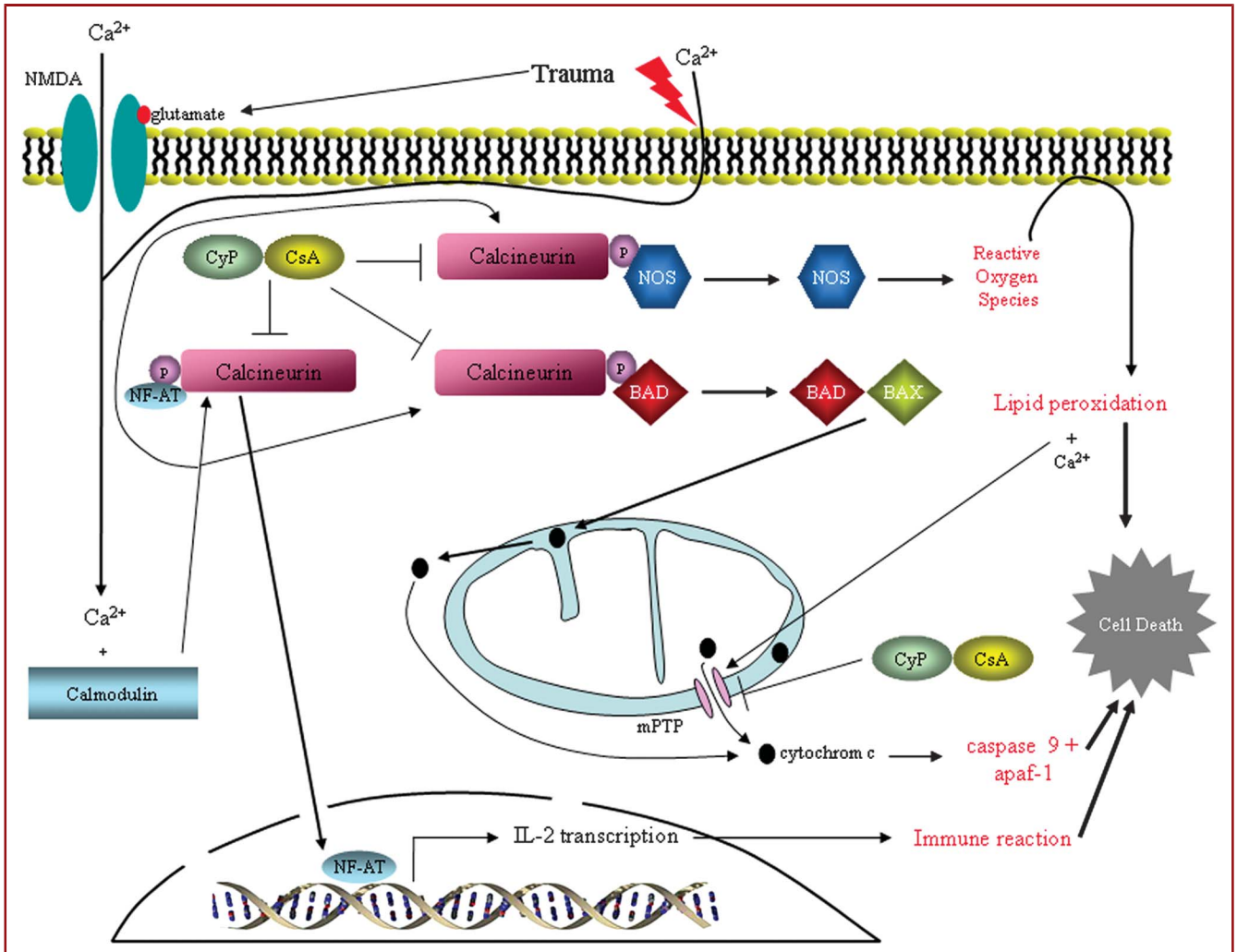

FIGURE 2. *An overview of the molecular mechanisms of action of cyclosporin A (CsA). Trauma causes membrane damage, which allows the influx of extracellular calcium. Calcium also penetrates the cell via* N*-methyl-*D*-aspartate (NMDA) channels, which are activated by trauma-induced glutamate excitotoxicity. Calcium has 2 main actions. It activates calmodulin and is sequestered in mitochondria. Calmodulin phosphorylates and activates calcineurin. Further downstream, this enzyme dephosphorylates nitric oxide synthase (NOS), nuclear factor of activated T cells (NF-AT), and Bcl-2–associated death promoter (BAD), all of which triggers specific pathways that induce cell death. On the other hand, calcium accumulation in mitochondria contributes to the creation of mitochondrial permeability transition pore (mPTP) to induce another pathway that leads to cell death initiation. CsA, by binding cyclophilin (CyP), blocks the action of calcineurin and blocks mPTP formation. P, phosphate; IL-2, interleukin-2, BAX, Bcl-2–associated X protein; ATP, adenosine triphosphate; caspase 9 and apaf-1, apoptosis-initiating proteins.*

with O_2^- and create peroxynitrite ($ONOO^-$), which is a highly neurotoxic molecule.[25]

Oxygen free radical species can induce lipid peroxidation, which plays a significant role in spinal cord injury models. Because lipids are fundamental blocks of biological membranes, destruction of lipids leads to decreased fluidity of membranes and inhibits enzyme function.[21,25,42] Lipid peroxidation is inhibited even 12 hours after the administration of CsA in spinal cord injury models in rats.[43]

Reactive oxygen species formed under oxidative stress, such as the activation of NOS, attach to membrane protein thiols and produce cross-linkage reactions that may open membrane pores on Ca^{2+} binding.[44] It seems that toxic concentrations of Ca^{2+}, together with oxidative stress, might be related to mPTP opening, which leads to mitochondrial dysfunction and triggers the cell death cascade by the release of cytochrome c, procaspase-9, and apoptosis-inducing factor (Figure 2).[21] However, the exact mechanism through which calcium can trigger mPTP opening is

Copyright © Congress of Neurological Surgeons. Unauthorized reproduction of this article is prohibited.

still unclear and may involve CypD and possibly voltage-dependent anion channels.

Recent evidence by Baines et al,[45] however, raises a question about the role of voltage-dependent anion channels in mPTP opening and cell death. mPTP is a protein complex that spans both the outer and inner mitochondrial membranes. It is hypothesized that mPTP minimally consists of the voltage-dependent anion channel, the adenine-nucleotide translocase in the inner membrane, and CypD in the matrix.[45,46] CypD appears to be a critical component of the mPTP because there is evidence that CypD translocates to the mPTP where it can interact with adenine-nucleotide translocase, inducing the pore formation.[21,47] By binding to CypD, CsA inhibits crucial steps in mPTP formation, which subsequently will prevent the activation of apoptotic cascade events in TBI. In support of this model is the current evidence that CypD has a major role in energy failure, but not in glutamate excitotoxicity; therefore, CypD is tied to the mitochondrial dysfunction rather than increased intracellular calcium levles.[48,49] According to this study, CypD-deficient mice displayed a reduction in brain infarct size after acute middle cerebral artery occlusion and reperfusion.[48,50,51] This finding is reinforcing the evidence that CsA inhibits activation of mitochondrial permeability transition and pore formation[52] by inhibiting matrix CypD interaction with pore proteins.[53] Additionally, this is in concordance with the findings that peripherally administered CsA attenuates mitochondrial dysfunction and neuronal damage in an experimental rodent model of TBI in a dose-dependent manner.[42]

CsA has been demonstrated to produce neuroprotective effects in both in vivo and in vitro models of excitotoxicity.[35,54] Protective effects of CsA in the case of glutamate excitotoxicity are evident at multiple levels. As previously mentioned, CsA prevents mPTP opening and preserves normal mitochondrial function (Figure 2). However, in the case of glutamate excitotoxicity, it also acts through inhibition of calcineurin-mediated release of synaptic vesicles.[31] By inhibiting calcineurin, CsA prevents phosphorylation and subsequent activation of dynamin I and synapsin I, both of which both been implicated in regulation of neurotransmitter release.[31,55] Additionally, it also blocks calcineurin-mediated dephosphorylation of NOS subsequently blocking NOS activation. Activated NOS is responsible for the production of NO release, which plays an important role in neurotransmitter release from synaptic vesicles.[24,31,56]

An equally critical cell death pathway that is blocked by CsA entails the apoptosis signaling mechanism, which involves Ca^{2+}-induced activation of Bcl-2–associated death promoter. Bcl-2–associated death promoter is a Ca^{2+}-calcineurin sensitive proapoptotic Bcl-2 protein, which on activation translocates from cytosol to mitochondria to initiate cytochrome c release and the apoptotic cascade.[57,58] Calcineurin inhibitors like CsA block the apoptotic response linking calcineurin activation and the subsequent translocation of Bcl-2–associated death promoter to cell death.[58]

The full extent of action and neuroprotective effects of CsA are still being elucidated. There is emerging evidence that CsA could induce neuroprotective effects through other pathways and stimulate the production of neurotrophic factors.[59-61]

EVIDENCE OF CsA NEUROPROTECTION IN TBI IN ANIMAL MODELS

There are a number of studies that have shown the efficacy and safety of CsA in animal models of TBI. They are briefly summarized in the Table. These studies demonstrated that CsA had neuroprotective effects measured by various indicators of TBI using different doses of CsA.

The first use of CsA in animal models of TBI was reported by Okonkwo et al[62,63] in 1999. They showed that pre- and 30 minutes post-treatment intrathecal CsA administration in the rat cortical impact model was protective against secondary axotomy and also preserved mitochondrial integrity. The same year Scheff and Sullivan[64] were able to show that systemic administration of CsA 15 minutes before cortical impact in a similar rat model of TBI exhibited neuroprotective effects.

The most promising evidence that CsA could have a direct human application in TBI was demonstrated in the case report of a 14-year-old German girl who was an orthotopic liver transplant recipient on chronic CsA therapy.[65] She incidentally had a severe TBI and made a remarkable, unexpected recovery that has been attributed to the neuroprotective effects of CsA.

One of the indicators of the early events in TBI is manifested by change in mitochondrial morphology. Okonkwo and Povlishock[63] were the first to show that intrathecal administration (10 mg/kg CsA) in the impact acceleration rat model of TBI was beneficial in reducing changes in mitochondrial morphology. They used horseradish peroxidase to achieve mitochondrial visualization via electron microscopy in damaged axons. The mean percentage of damaged mitochondria in horseradish peroxidase–containing axons of untreated animals was 72%, whereas the mean percentage of damaged mitochondria in horseradish peroxidase–containing axonal segments of CsA-treated animals was 28%. This was a significant difference between the groups. Only about one third of total mitochondria were dysfunctional in axons of CsA-treated animals, which represented promising evidence that CsA could protect against secondary axotomy by preserving normal mitochondrial function. Additionally, amyloid precursor protein (APP) accumulation, an indicator of axonal damage, was significantly decreased in axons of animals treated with CsA.[63]

Further evidence that CsA has protective effects against axonal damage was presented by the same group using the previously mentioned model of TBI. They looked at axonal damage caused by calcium-induced calpain activation, which targets spectrin as one of the cytoskeletal proteins, and calcium-induced neurofilament compaction.[14] Pretreatment with CsA was able to significantly reduce immunoreactivity of damaged axons to calpain-induced spectrin degradation compared with axons in vehicle-treated animals. CsA also reduced immunoreactivity in neurofilament compaction marker RMO14.[62]

Copyright © Congress of Neurological Surgeons. Unauthorized reproduction of this article is prohibited.

TABLE. Overview of Animal Studies Demonstrating Efficacy of Cyclosporin A in Traumatic Brain Injury[a]

Study	TBI Model/ Animal	Route	CsA Dose	Outcome
Okonkwo and Povlishock, 1999[63]	IA/rat	i.t.	10 mg/kg 30 min before injury	Preserves mitochondrial morphology and prevents axonal failure in 1 and 24 h after diffuse axonal injury
Okonkwo at al., 1999[62]	IA/ rat	i.t.	10 mg/kg 30 min before injury	Decreased calcium-calpain–induced neurofilament compaction and cytoskeletal damage 1 h after injury
Buki et al, 1999[13]	IA/rat	i.t.	10 mg/kg 30 min post-injury	Decrease in neurofilament compaction, calpain-induced axonal injury and decrease in APP accumulation in damage axons 24 h post-injury
Scheff and Sullivan, 1999[64]	CCI/rat and mice	i.p.	1. Immediately post-injury + 1 dose 24 h post-injury 40 mg/kg or 20 mg/kg (mice and rats) 2. 150 mg/kg, 40 mg/kg, or 20 mg/kg dose 5 min before injury (mice)	Significant reduction in volume of cortex damage 7 days post-injury. No significant benefit of FK506.
Sullivan et al, 1999[71]	CCI	i.p.	20 mg/kg 15 min post-injury	Preservation of mitochondrial transmembrane potential, decrease in mPTP opening, decrease in mitochondrial Ca^{2+} and decrease in ROS generation 30 min and 1 h post-injury
Sullivan et al, 2000[78]	CCI/rat	s.c.	1. Pump 4.5 mg/kg/day + single loading dose 20 mg/kg 15 min post-injury 2. Pump 10 mg/kg/day + single loading dose 20 mg/kg 15 min post-injury 3. Vehicle loaded pump + 2 boluses of 20 mg/kg 15 min and 24 h post-injury	Volume of cortex damaged was significant at 7 days. The best result evident with s high dose of CsA 10 mg/kg/day.
Albensi et al, 2000[73]	CCI/rat	i.p.	20 mg/kg 15 min post-injury	Prevention of LTP impairment and complete prevention of LTD in CA1-CA3 at 48 h post-injury
Riess et al, 2001[75]	CCI/rat	i.p.	10 mg/kg 15 min post-injury and daily administration of the same dose for the next 28 days	Improvement in composite neuroscore 4 wk post-injury, and recovery of motor and sensory-motor function, but no benefits in cognitive testing
Suehiro and Povlishock, 2001[66]	IA + hypothermia/ rat	i.t.	20-min period (rapid rewarming) or over a 90-min period (slow rewarming) and 10 mg/kg CsA at the beginning of rewarming	24-h APP (an indicator of axonal injury) was measured and was significantly reduced in CsA + rapid rewarming group
Alessandri et al, 2002[74]	FPI/rat	i.v.	1. Infusion 0.125 mg/kg for 3 h post-injury 2. Infusion 18.75 mg/kg for 3 h post-injury	CsA at both concentrations abolished the 25% decrease in O_2 consumption (Vo_2) 5 h post-injury. Lower dose of CsA ameliorated acute motor deficits (days 1-5 post-injury) and learning and memory impairments in a Morris water maze test on days 11-15 post-injury
Fukui et al, 2003[83]	CCI/rat	i.v.	1. 20 mg/kg 1-h infusion 30 min post-injury 2. 20 mg/kg 1-h infusion 30 min post-injury	24 h post-injury there was no significant change in brain water content and no exacerbation of brain edema encountered with i.t. administration of CsA

(Continues)

Copyright © Congress of Neurological Surgeons. Unauthorized reproduction of this article is prohibited.

TABLE. ***Continued***

Study	TBI Model/ Animal	Route	CsA Dose	Outcome
Fee at al, 2003[26]	ACI/mice-recombinase activating gene knockout	i.p.	1. 0.05 mg/g 2 h pre-injury 2. 0.05 mg/g during injury 3. 0.05 mg/g 2 h post-injury	There is a decrease in density of apoptotic cells and a decrease size of injury evident on MRI, but no change in neutrophil infiltration
Van Den Heuvel et al, 2004[67]	IA/sheep	i.t.	10 mg/kg 30 min post-injury	Reduction in APP mRNA 2 and 6 h post-injury
Signoretti et al, 2004[72]	IA/rat	i.t. and i.v.	1. i.t. 10 mg/kg 30 min post-injury 2. i.v. 20 mg/kg 30 min post-injury, continuous 1-h infusion 3. i.v. 35 mg/kg 30 min post-injury, continuous 1-h infusion	6 h post-injury for levels of NAA significantly reduced and ATP levels restored in i.t. and 35 mg/kg i.v. CsA administration groups
Gabbita et al, 2005[69]	CCI/rat	i.p.	20 mg/kg 15 min post-injury and 24 h post-injury	168 h post-injury, cleaved tau protein was significantly decreased only in hippocampus
Redell et al, 2007[82]	CCI/rat	i.p.	20 mg/kg 30 min post-injury	24 h post-Evans blue extravasation was decreased to assess for permeability BBB

[a]TBI, traumatic brain injury; CsA, cyclosporin A; I/A, impact acceleration; i.t., intrathecal; APP, amyloid precursor protein; CCI, cortical contusion injury; i.p., intraperitoneal; mPTP, mitochondrial permeability transition pore; ROS, reactive oxygen species; s.c., subcutaneous; LTP, long-term potentiation; LTD, long-term depression; FPI, fluid percussion injury; i.v., intravenous; ACI, aseptic cerebral injury; MRI, magnetic resonance imaging; NAA, *N*-acetyl aspartate; ATP, adenosine triphosphate; BBB, blood-brain barrier.

These 2 studies have shed more light on the importance of mitochondrial function and prevention of mPTP formation by CsA as the main mechanism that preserves mitochondrial and cellular integrity. These studies also presented evidence that Ca^{2+} load as a central intracellular messenger is able to trigger an irreversible and detrimental cascade of events in TBI resulting in the loss of axonal function and secondary axotomy.

Suehiro and Povlishock[66] studied the damaging effects of rewarming after induced hypothermia, and they further investigated the ability of CsA to attenuate axonal changes after injury. Although hypothermia has been proven to be neuroprotective when followed by rapid rewarming, it exacerbated effects of TBI and axonal damage, most likely by inducing mPTP formation. Suehiro and Povlishock[66] were able to show that administration of 10 mg/kg CsA was able to attenuate axonal damage in animals with TBI after rapid rewarming compared with a control group.

Another study by the Povlishock group reported that intrathecal administration of 10 mg/kg CsA 30 minutes after injury was also neuroprotective. Buki et al[13] reported that in an impact acceleration rat model of TBI, CsA-treated animals had significant preservation of axonal structure with decreases in neurofilament compaction calcium-induced calpain activation and immunoreactivity of APP in damaged axons. These protective effects were measured 24 hours after the injury. Thus, CsA was able to decrease the effects of Ca^{2+}-induced axonal failure and axonal disconnection even 24 hours after the administration of CsA.

A group from South Australia also looked at APP expression, but this time in a sheep model of TBI. Their data supported the Povlishock group findings. The Australian group evaluated APP mRNA expression after TBI.[67] In CsA-treated animals, APP mRNA expression was significantly reduced 2 and 6 hours after drug administration. These findings suggested that there is likely down-regulation of APP in TBI.[67] Although APP has some beneficial effects, it still remains unclear how this down-regulation of APP can be of benefit. APP is cleaved by β-secretase and by gamma-secretase to produce Aβ, which is neurotoxic and one of the central players in the pathogenesis of Alzheimer disease.[67,68]

In addition to APP, there is another protein that has been investigated as a potential marker of neuronal damage after TBI. It is a proteolytic product of intracellular microtubule-associated protein tau, known as cleaved tau. This protein is elevated in the brain and in the serum after mild, moderate, or severe TBI.[69,70] However, CsA significantly attenuated TBI-induced cleaved tau elevation only in the hippocampus.[69] Authors of this study attributed such findings to a sample size that failed to yield significant difference in cleaved expression in other regions of the brain.

Another study by Sullivan et al[71] from the University of Kentucky was able to directly implicate the role of mitochondria in TBI and also demonstrate potential benefits of CsA by preserving mitochondrial function. They offered elegant evidence that mitochondrial dysfunction and calcium play a major role in TBI. They used a slightly different treatment paradigm and

Copyright © Congress of Neurological Surgeons. Unauthorized reproduction of this article is prohibited.

a different model of TBI than the studies cited previously. Fifteen minutes after cortical contusion treatment groups received a CsA dose of 20 mg/kg. They used a number of biochemical markers of mitochondrial function to show that 30 minutes and 1 hour post-injury in the CsA-treated group there was significant attenuation of mitochondrial dysfunction in terms of preservation of mitochondrial membrane potential. CsA was able to prevent mitochondrial permeability transition opening, which was measured by the loss of absorbance (540 nm) after the addition of Ca^{2+}. Additionally, there was a decrease in reactive oxygen species production.[71] This study was able to directly link mPTP blockage by CsA to the neuroprotective effects of CsA observed in other studies.

Signoretti et al[72] attempted to assess the effect of CsA on mitochondrial dysfunction after TBI by measuring the level of reduced *N*-acetyl aspartate (NAA) and adenosine triphosphate (ATP) loss to evaluate the degree of bioenergetic failure. The most important function of mitochondria is to produce ATP. ATP levels are related to the synthesis and catabolism of NAA.[72] Because an elevation of NAA levels was seen in TBI, the authors not only tried to see the effects of CsA on NAA levels and total ATP content, but they also compared the efficacy of intrathecal and intravenous CsA administration. In CsA-treated animals, they found that 6 hours after injury NAA levels were significantly reduced and ATP levels were restored compared with controls. These effects appeared to be most significant in the intrathecal and the 35-mg/kg intravenous delivery groups.[72] Thus, CsA was able to restore and maintain normal mitochondrial function and safe ATP levels necessary for maintenance of cellular ionic homeostasis.

TBI not only affects and destroys brain parenchyma, it also has a devastating effect on many aspects of neurological functioning. Some patients have permanent motor deficits, and other patients often have memory and learning deficits.[73] Albensi et al[73] were looking at hippocampal slices of the CA3-CA1 regions after controlled cortical impact. Recordings from hippocampal neurons were obtained 48 hours after injury. The group of animals receiving the intraperitoneal bolus of CsA at 20 mg/kg 15 minutes post-injury had significant reduction in long-term potentiation (LTP) impairment, whereas long-term depression was prevented. It seems that inhibition of calcineurin was able to preserve LTP. Preservation of LTP could be attributed to CsA preventing cell death and preserving synapses.

LTP has been confirmed as one of the main synaptic mechanisms that is implicated in learning and memory. However, another group from the Medical College of Virginia was able to demonstrate behavioral outcomes that support the findings by Albensi et al.[73] Alessandri et al[74] showed that 0.125 mg/kg CsA infused for 3 hours significantly prevented learning and memory deficits and was confirmed by Morris water maze testing 11 to 15 days after fluid percussion injury (FPI). The same dose ameliorated motor deficits after injury, and CsA improved the depression of oxygen consumption (Vo_2) after FPI in cortical and hippocampal tissue. A higher CsA dose (18.75 mg/kg) previously known to be neuroprotective improved cognitive performance after FPI, but unexpectedly worsened motor deficit outcomes.[74]

There have been other studies that looked at how much CsA would affect motor and sensory functioning after TBI. Reiss et al[75] used a number of tests to evaluate such an outcome. All animals initially had significant motor impairment, but 4 weeks after daily 10 mg/kg CsA administered 15 minutes after the injury, the treated group demonstrated significant improvement. They also performed better on sensory-motor function testing. Investigators did not see any benefits in cognitive functioning in CsA-treated groups.[75]

Thus, these 2 studies examining motor outcomes have conflicting results. They both use different CsA dosing, regimens of administration, and time endpoints when animals were tested for motor function, all of which might contribute to the discrepancy in the findings. Additionally, such discrepancies can also be attributed to neurotoxic effects produced by high CsA doses, which were previously addressed in different animal studies[76-78] and human case reports.[79,80]

Cerebral edema represents one of the most dangerous complications after TBI. Cytotoxic edema appears early in TBI, and there have been few studies looking at the effect of CsA on cerebral edema. One in vitro study on cultured astrocytes subjected to FPI showed an increase in swelling 1 to 24 hours after injury with the peak occurring at 3 hours post-injury.[81] They also demonstrated an increase in NO production, mPTP opening, loss of mitochondrial membrane potential, and reduction of ATP levels. They also demonstrated induction of mitogen-activated protein kinases such as JNK1, ERK1/2, and p38, all of which function as intracellular signaling kinases. Pretreatment with CsA 10 minutes after injury significantly reduced swelling in cultured astrocytes and blocked the loss of mitochondrial membrane potential. CsA was also able to significantly reduce trauma-induced phosphorylation of JNK1, ERK1/2, and p38.[81] Thus, Jayakumar et al[81] demonstrated that CsA is able to inhibit cytotoxic edema by acting on different cellular components involved in edema formation.

On the other hand, vasogenic edema is an important component in the pathophysiology of TBI. The BBB is compromised in TBI either focally or diffusely. Redell et al[82] looked at cyclophilin A expression in early TBI and its role on BBB permeability. The researchers found that a CsA dose of 20 mg/kg 30 minutes post-injury was able to significantly reduce Evans blue extravasation 24 hours after cortical contusion injury. These findings were consistent with those of Sullivan's group, which also showed that the same dose of CsA 15 minutes after the injury decreased extravasation of IgG 1 and 2 hours after FPI.[77]

The Fukui et al[83] study aimed to assess whether intravascular CsA administration may also influence brain edema formation, as in the case of intrathecal CsA administration. Animals were exposed to focal brain injury after which they received 20 mg/kg or 35 mg/kg intravenous CsA by continuous infusion over 1 hour. The infusion was initiated 30 minutes after the insult. The brain water content using the gravimetric method was assessed 24 hours

Copyright © Congress of Neurological Surgeons. Unauthorized reproduction of this article is prohibited.

post-injury. Intravenously administered CsA of either 20 or 35 mg/kg did not significantly change the brain water content.[83]

Another factor that is implicated in TBI is activation of immune cells and microglia after TBI, which can contribute to secondary neuronal damage. In the aseptic cerebral injury model in wild-type mice, intraperitoneal CsA administration of 0.05 mg/g 2 hours before or simultaneously with injury had significantly decreased the size of injury, the density of apoptotic cells, and neutrophil infiltration 24 hours after treatment.[26] They also used magnetic resonance imaging to evaluate tissue destruction and BBB dysfunction and showed attenuation in the size of the brain lesion after aseptic cerebral injury. Because CsA inhibits T cells, they concluded that the aforementioned effects might be caused by the inhibition of T-cell activation in aseptic cerebral injury.[26]

As previously mentioned, most of the studies used different models of TBI with different doses of CsA and various routes of administration and timing. There have been several studies that examined dose-response curves and dosing regimens in animal models of TBI.[42,77,78] Sullivan et al[77] showed that intraperitoneal administration of CsA at a dose of 20 mg/kg was the most beneficial in providing neuroprotective effects. They also showed that the same dose offered better protection after TBI when administered 15 minutes and 1 hour after injury with subsequent repeated doses of 20 mg/kg 24 hours after injury. It was interesting that there were no neuroprotective effects when CsA was used 6 hours after injury. Moreover, the treatment 1 hour post-injury was as effective as treatment 24 hours after injury.[77] They concluded that there was a 24-hour period in which CsA administration offers neuroprotective effects.

A study of continuous subcutaneous infusion of CsA conducted by Sullivan et al[78] showed neuroprotection at the highest dose of 10 mg/kg/day with about 74% cortical preservation 7 days after cortical contusion injury. Although continuous infusion showed to be protective after 7 days, it still remains unclear what would be the exact therapeutic window for delivery of CsA because the previous dose-response study showed neuroprotection when administered 24 hours post-injury. It is possible that mechanisms of secondary brain injury caused by TBI might remain active even 24 hours after injury and that prolonged administration of CsA could be of benefit. That said, there remains the risk of CsA toxicity, in terms of neurotoxicity, nephrotoxicity, or immunosuppression, which have all been well documented in previous studies.[76-79,84]

Furthermore, Okonkwo et al[42] showed that CsA produces effects in a dose-dependent fashion on APP 4 hours post-injury. They also confirmed that 10 mg/kg administered intravenously with slow infusion over 1 hour was the most neuroprotective compared with other doses or intrathecal administration. Additionally, a 50-mg/kg intravenous dose was toxic and ineffective in attenuating axonal injury.[42]

There has been only 1 animal study to date that has raised the question of the neuroprotective effects of CsA. Setkowicz and Guzik[85] tried to assess whether CsA or FK506 will offer neuroprotection in the developing rat brain after brain injury on postnatal days 6 and 30. The injury was caused by drilling through the skull and passing the drill 2 to 3 mm into the cerebral hemisphere. CsA or FK506 was administered intraperitoneally 30 minutes post-injury with repeat injection 24 hours post-injury. The brains were examined at postnatal day 60. They found that CsA had a negative effect on the brain mass in the CsA-treated group and did not demonstrate better neuroprotective effects compared with the vehicle alone.[85] Because this study was done in the developing brain, the negative effect of CsA might be explained by the neurotoxicity of CsA on the developing nervous system.[76,78-80,84] Also, it is known that even adult animals can recover after central nervous system injury[86-88]; however, potential for young animals to recover significantly after brain injury is likely to be far greater, especially after the prolonged time period when they chose to evaluate animals for central nervous system injury. Thus, failure to find any significant effect of CsA by this group of researchers might be attributed to the inherent ability for central nervous system recovery in young animals.[89-93]

Thus far, neuroprotective effects have been proven in TBI in a large number of animal studies in the past decade, but CsA use does not come without side effects. Its use has been associated with immunosuppression, neurotoxicity, and nephrotoxicity. Successes of CsA in neuroprotection have prompted a search for other CsA analogues that might have neuroprotective effects without the CsA-like side effect profile. It was postulated that the immunosuppressive effects of CsA have been mainly mediated by calcineurin inhibition. Other agents such as NIM811, which inhibit mPTP but not calcineurin, were good candidates for testing for neuroprotection.[47] So far, NIM811 was able to significantly inhibit free radical production in spinal cord contusion models in rats and maintain better mitochondrial function.[94] NIM811 produced results comparable to those of CsA with respect to the reduction in lipid peroxidation, prevention of mitochondrial failure, and reduction of protein damage, specifically reduction of cytoskeletal protein alpha-specrtin damage in the mouse model of controlled cortical TBI.[95,96]

Although the cited studies vary in experimental design and the doses of CsA used, most of them showed the benefits of CsA in animal models of TBI. Equally important to note is that most of these studies explored the efficacy of CsA in models of severe traumatic injury. However, many patients have moderate and mild TBI, indicating the need to comparatively explore CsA effects in animal models that correlate with mild, moderate, and severe TBI in humans. The plausibility of creating such models has already been proven.[97] Additionally, all animals used in the studies were adult males. We believe that it would be necessary to examine the effects of CsA in neonatal and young animal models of TBI. There has been only 1 study so far that examined the model of brain injury in the developing brain, and it found no therapeutic benefit of CsA.[85] In our opinion, this study had some questionable findings that led to premature conclusions about CsA efficacy in the developing brain in that there was no control treatment to delineate the confounding effects of the robust

Copyright © Congress of Neurological Surgeons. Unauthorized reproduction of this article is prohibited.

neuroplasticity inherent in neonates. Although the findings of such a study raise controversy about the neuroprotective role of CsA in the developing brain, it also prompts further investigations to shed more light on the influence of age (neonatal vs adult) on both disease pathology and therapeutic intervention. Along with same line, determining the effects of CsA in TBI in females should also be investigated because it has been shown that female sex hormones such as estrogens and progesterone are also neuroprotective.[8,98,99] It is unkown whether this female "hormonal advantage" in neuroprotection could have synergistic effects with CsA treatment.

Moreover, CsA success in TBI models has prompted new research and testing on analogues of CsA, such as NIM118, that do not have nephrotoxic side effects. Despite the absence of full characterization of CsA efficacy and the mechanism of action as presented here, the overall preclinical data strongly supported initiation of small clinical trials.

HUMAN STUDIES ON THE USE OF CsA IN TRAUMATIC BRAIN INJURY

Most of the human studies on CsA were on efficacy and safety as part of phase II trials. Multicenter phase III trials are still in progress, but there have been some promising data coming from phase II trials already. All 4 phase II trials showed safety of CsA for neuroprotection after TBI.

One of the first studies on human subjects by Empey et al[100] from the University of Kentucky explored pharmacokinetics and CsA disposition in TBI. This was a phase II, randomized, dose-escalation, placebo-controlled trial with 30 patients enrolled and divided into 3 different cohorts. Inclusion criteria for this study were the following: TBI patients aged 16 to 65 years old, Glasgow Coma Scale (GCS) score of 4 to 8, at least 1 reactive pupil, systolic blood pressure greater than 90 mm Hg, oxygen saturation greater than 85%, no major systemic injury or organ dysfunction, and no serious chronic illness, systemic infection, or renal disease (serum creatinine >2.0 mg/dL). Within 8 hours of injury, cohort I received a 0.625-mg/kg dose; cohort II, a 1.25-mg/kg dose; cohort III, a 2.5-mg/kg of CsA or placebo intravenously every 12 hours for 72 hours. Their data showed that the pharmacokinetics in the TBI population is different from that in populations in previous studies that focused on healthy individuals or the transplant patient population. The TBI population had whole blood clearance, steady-state volume of distribution, and a half-life higher than in other published reports.[100]

TBI is followed by a significant decrease in cellular immune response and T-cell activation.[101,102] CsA, being an immunosuppressant itself by blocking T-cell activation and proliferation, could present a serious problem in already immunosuppressed patients with TBI. Mazzeo et al[102] conducted a randomized, placebo-controlled study to evaluate the safety and tolerability of CsA and its effect on cell-mediated immunity in severe head injury patients. Their study included 59 patients. Inclusion criteria were a GCS score of 8 or less and age older than 16 years, whereas exclusion criteria were applied to patients with both pupils fixed and dilated, a history of immunosuppression, and a lack of family consent. Exactly 36 patients received an infusion of 5 mg/kg of CsA over 24 hours within 12 hours after injury. Another 8 patients from this cohort received an additional 5 mg/kg 24-hour infusion of CsA with 200 mg ketoconazole via a feeding tube to enhance the bioavailability of CsA. Twelve patients received a placebo within 12 hours after injury. Although more than 60% of all patients had a decreased baseline lymphocyte count, it alone was associated with an increase in pulmonary infections rather than treatment with CsA. Baseline, 48-hour, and 72-hour lymphocyte counts; CD3, $CD4^+$, and $CD8^+$ count; and CD4/CD8 ratio did not differ between the CsA-treated group and the placebo group. They also documented T-cell infiltration in brain parenchyma in 4 patients undergoing craniotomy for decompression.[102]

In summary, this study concluded that CsA administration was not associated with a decrease in T-cell immunity. Instead, compromised immunity was related to severe head injury itself, as previously documented in other studies. It still is unclear why a potent immunosuppressant like CsA had a paradoxical effect on the cellular immunity and did not further lower immune competence in patients with TBI. Nevertheless, the study conducted by Mazzeo et al[102] did indicate the possibility of the safe use of CsA in TBI patents. Further investigation is still necessary with a larger sample size for more definitive conclusions. Another drawback of this study is that it was not blinded, and the placebo group had a significantly better GCS score than the CsA cohort, which suggests a possible selection bias. Perhaps phase III trials will offer some more insight into the nature of CsA interaction with cell-mediated immunity in patients with TBI.

As part of ongoing research in safety and efficacy of CsA, there was another clinical study by Mazzeo et al[103] conducted at Virginia Commonwealth University and the University of Florida. This was a randomized, double-blind, microdialysis and cerebral hemodynamics study in patients with severe TBI. Fifty patients were enrolled in the study. Inclusion criteria for this study were age older than 16 years, GCS score of 3 to 8, ventriculostomy, and microdialysis catheter placement. Exclusion criteria were the following: both pupils fixed and dilated; blood urea nitrogen greater than 20 mg/dL and serum creatinine greater than 1.3 mg/dL; and a history of impaired renal or hepatic function, cancer, immunosuppression, coagulopathy, and pregnancy or inability to exclude pregnancy. Within 12 hours post-injury, patients randomly received a placebo or an infusion of CsA in a dose of 5 mg/kg over 24 hours. Two patients were excluded from the study because of microdialysis catheter dysfunction. The CsA-treated group had significantly higher glucose, lactate, and pyruvate levels in microdialysate, whereas glutamate levels and the lactate/pyruvate ratio were significantly lower than in the placebo group. The CsA-treated group also had significantly higher mean arterial pressure, cerebral perfusion pressure, and intracranial pressure.[103]

Copyright © Congress of Neurological Surgeons. Unauthorized reproduction of this article is prohibited.

It has been established that low glucose and pyruvate in most microdialysis studies after TBI were associated with poor outcomes after TBI[104-106]; therefore, the results of this study by Mazzeo et al[103] are promising. Moreover, low extracellular glutamate levels in the CsA-treated group were encouraging because high glutamate levels are associated with poor outcomes.[107] However, it is difficult to find an explanation for high lactate levels in the CsA group because it too has been an indicator of poor outcomes. Although the results of this study are encouraging, it also raised many questions about the effects of CsA on biochemical processes in the injured brain that we still do not completely understand such as the previously mentioned increase in lactate levels in the CsA-treated group. The latter indicates that more research in this area is still needed to aid in understanding the meaning of the results obtained by this study.

An additional study that directly evaluated the safety and efficacy of CsA was performed by Hatton et al.[108] The study was a phase II, randomized, double-blind, dose-escalation trial with 40 patients enrolled. Patients included in this trial were aged 16 to 65 years old with a GCS score of 4 to 8, a motor score of 2 to 5, and within 8 hours of injury. Patients eligible for this study had to have at least 1 reactive pupil, hemodynamic stability, placement of an intraventricular catheter, and additional positive computed tomography findings of brain trauma. Exclusion criteria were similar to previously mentioned studies and included chronic disease, renal disease, previous neurological disease, and immunosuppression. Patients were divided into 4 cohorts. Within 8 hours of injury, cohort I received a 0.625-mg/kg dose; cohort II, a 1.25-mg/kg dose; cohort III, a 2.5-mg/kg dose of CsA or placebo intravenously delivered every 12 hours for 72 hours. Cohort IV received a 2.5-mg/kg loading dose and then a 5-mg/kg/day continuous infusion for 72 hours. There was no statistical difference in mortality rates between cohorts or the CsA and placebo groups, and no difference in risk of infection, renal dysfunction, seizures, or liver function test results. The most common infection encountered in the CsA and placebo groups was pneumonia. Additionally, investigators did not notice a statistical difference in conjunctivitis, corneal deposits, or cortical blindness at 3- and 6-month follow-up between the placebo and CsA-treated groups. At 3- and 6-month follow-up, there was no significant difference between placebo or CsA groups when evaluated by the Glasgow Outcome Scale or the Extended Glasgow Outcome Scale, but the probability of favorable outcomes varied by CsA dose, with a significant difference in better outcomes with continuous infusion of CsA in cohort IV.[108]

This was a well-conducted phase II trial that showed that CsA administration was safe in patients with TBI, including better outcomes seen with a continuous infusion of 5 mg/kg CsA with an initial CsA loading dose of 2.5 mg/kg. Such information should be very useful for phase III trials in progress because it offered the most effective administered dose associated with better outcomes. Such dosing might yield statistical significance because of the much larger sample size used in phase III trials.

The most recent dual-center study from National Institutes of Health–National Institute of Neurological Disorders and Stroke and Virginia Commonwealth University assessed the safety and tolerability of a single infusion of 5 mg/kg CsA within the first 12 hours after injury.[109] Infusion of CsA was administered over 24 hours. This double-blind, placebo-controlled trial had initially 50 patients enrolled. Inclusion and exclusion criteria in this Mazzeo et al[102] study were identical to the 2006 study by the same group discussed previously. One patient was excluded because of the severity of multiple traumatic injuries and multiple organ dysfunction, whereas the remaining 49 patients were randomly assigned to placebo (n = 13) and CsA treatment groups (n = 36). This study demonstrated that CsA is safe for use within the first 12 hours of injury as a single infusion of 5 mg/kg. However, the authors found a transient increase in the blood urea nitrogen levels at 24 and 48 hours and a transient increase in the white blood cell count 24 hours after the infusion of CsA with no adverse outcomes associated with these findings. There was no significant difference in levels of creatinine, aspartate aminotransferase, and alanine aminotransferase, alkaline phosphatase, hemoglobin, or platelets between the groups. Additionally, infusion of CsA was associated with an increase in mean arterial pressure and cerebral perfusion pressure for 3 days after the infusion, but none of these increases required therapeutic intervention because the mean arterial pressure and cerebral perfusion pressure were still within the normal range. There were 11 deaths in this trial ranging 8 to 27 days after admission, with a higher rate of mortality in the CsA treatment group (n = 9). The causes of death were mostly withdrawal of care by the families of the patients. The authors attributed this higher mortality rate to more severe systemic sequelae in the treatment group patients and not to the drug effect.[109]

Neurological outcome was assessed using the Glasgow Outcome Scale at 3 and 6 months after injury. There was no significant difference between the treatment and placebo groups, most likely because of the classification of severe injury in the treatment groups.[109]

In summary, all studies have similar inclusion criteria and all of them confirmed the safety of CsA for use in TBI patients. As in animal studies, clinical trials vary with respect to the study design, timing, and length of administration of CsA after TBI.

FUTURE DIRECTIONS

Because of the absence of phase III trials, it is difficult to foresee the future of CsA in TBI, but it is necessary to continue work on its safety and efficacy of CsA in TBI. Regardless of the results of large-scale clinical trials, it is difficult to believe that CsA will be a ''magic bullet'' for treating TBI because it affects many, but not all, pathophysiological processes triggered by trauma to the brain. It is expected, however, that CsA will be one of the weapons in the arsenal of neurosurgeons and neurocritical care specialists to aid in the treatment of this devastating and complex disease process. One can hypothesize that the use of CsA, if proven

Copyright © Congress of Neurological Surgeons. Unauthorized reproduction of this article is prohibited.

effective, will be combined with surgery, hypothermia, or other neuroprotective agents to more effectively treat patients with secondary brain injury. Once CsA shows positive results in phase III trials, it is expected that further clinical studies will be conducted to explore the use of CsA in different treatment paradigms.

Although preliminary animal laboratory studies on the efficacy of CsA in TBI were very promising, they prompted a rush to clinical trials before more transitional research was conducted. Such enthusiasm was present for other agents that showed promising effects in animal models of TBI, only to fall short of expectations in later trials. Thus, we should proceed with caution and focus on transitional research to better characterize the mechanism of action and efficacy of CsA. Because animal studies have varied with respect to the TBI model, dose, and route of administration of CsA, 1 way to focus future research might be to establish certain standards. For example, in a TBI patient, CsA was administered intravenously; therefore, it seems logical to use the same administration route in animal models of TBI. Additionally, it is important to explore the effects of CsA in both female rats and on the developing brain by examining the impact of CsA on TBI in neonates. Other animals such as mice and sheep have also been used as a model of TBI. Thus, further characterization of the differences between the models should be conducted.

TBI caused by blast injuries has been on the rise since the start of the wars in Afghanistan and Iraq, and this type of TBI displays different pathology and complications. Therefore, creation of blast injury animal models of TBI can help examine the role of CsA or other neuroprotective agents in this type of TBI.

Although phase II clinical data showed that CsA was safe to use in patients with TBI, we should not await the results of phase III trials on CsA, but should focus on translational research on CsA. Additional attempts should investigate other agents such as NIM811 as potential candidates for neuroprotection in TBI.

Disclosure

C.V.B. is supported by James and Esther King Biomedical Research Program Grants 09KB-01-23123 and 1KG01-33966. The authors have no personal financial or institutional interest in any of the drugs, materials, or devices described in this article.

REFERENCES

1. Sosin DM, Sniezek JE, Waxweiler RJ. Trends in death associated with traumatic brain injury, 1979 through 1992. Success and failure. *JAMA*. 1995;273(22):1778-1780.
2. Waxweiler RJ, Thurman D, Sniezek J, Sosin D, O'Neil J. Monitoring the impact of traumatic brain injury: a review and update. *J Neurotrauma*. 1995;12(4):509-516.
3. Thurman D. Epidemiology and economics of head trauma. In: Miller LP, Hayes RL, eds. *Head Trauma: Basic, Preclinical, and Clinical Directions*. New York: Wiley-Liss; 2001:327-347.
4. Guidelines for the management of severe traumatic brain injury. *J Neurotrauma*. 2007;24(Suppl 1):S1-S106.
5. Maas AI, Stocchetti N, Bullock R. Moderate and severe traumatic brain injury in adults. *Lancet Neurol*. 2008;7(8):728-741.
6. Paci GM, Sise MJ, Sise CB, et al. Preemptive craniectomy with craniotomy: what role in the management of severe traumatic brain injury? *J Trauma*. 2009;67(3):531-536.
7. Schouten JW. Neuroprotection in traumatic brain injury: a complex struggle against the biology of nature. *Curr Opin Crit Care*. 2007;13(2):134-142.
8. Vink R, Nimmo AJ. Multifunctional drugs for head injury. *Neurotherapeutics*. 2009;6(1):28-42.
9. Wang KK, Larner SF, Robinson G, Hayes RL. Neuroprotection targets after traumatic brain injury. *Curr Opin Neurol*. 2006;19(6):514-519.
10. Faden AI, Demediuk P, Panter SS, Vink R. The role of excitatory amino acids and NMDA receptors in traumatic brain injury. *Science*. 1989;244(4906):798-800.
11. Okonkwo DO, Povlishock JT. Immunosupresants in traumatic brain injury. In: Borlongan CV, Isacson O, Sanberg PR, eds. *Immunosuppresants Analogs in Neuroprotection*. Totowa, NJ: Humana Press; 2003.
12. Sun DA, Deshpande LS, Sombati S, et al. Traumatic brain injury causes a long-lasting calcium (Ca2+)-plateau of elevated intracellular Ca levels and altered Ca2+ homeostatic mechanisms in hippocampal neurons surviving brain injury. *Eur J Neurosci*. 2008;27(7):1659-1672.
13. Buki A, Okonkwo DO, Povlishock JT. Postinjury cyclosporin A administration limits axonal damage and disconnection in traumatic brain injury. *J Neurotrauma*. 1999;16(6):511-521.
14. Povlishock JT, Marmarou A, McIntosh T, Trojanowski JQ, Moroi J. Impact acceleration injury in the rat: evidence for focal axolemmal change and related neurofilament sidearm alteration. *J Neuropathol Exp Neurol*. 1997;56(4):347-359.
15. Pettus EH, Povlishock JT. Characterization of a distinct set of intra-axonal ultrastructural changes associated with traumatically induced alteration in axolemmal permeability. *Brain Res*. 1996;722(1-2):1-11.
16. Lifshitz J, Sullivan PG, Hovda DA, Wieloch T, McIntosh TK. Mitochondrial damage and dysfunction in traumatic brain injury. *Mitochondrion*. 2004;4(5-6):705-713.
17. Castilho RF, Kowaltowski AJ, Vercesi AE. The irreversibility of inner mitochondrial membrane permeabilization by Ca2+ plus prooxidants is determined by the extent of membrane protein thiol cross-linking. *J Bioenerg Biomembr*. 1996;28(6):523-529.
18. Crompton M, Virji S, Doyle V, Johnson N, Ward JM. The mitochondrial permeability transition pore. *Biochem Soc Symp*. 1999;66:167-179.
19. Green DR, Reed JC. Mitochondria and apoptosis. *Science*. 1998;281(5381):1309-1312.
20. Halestrap AP, McStay GP, Clarke SJ. The permeability transition pore complex: another view. *Biochimie*. 2002;84(2-3):153-166.
21. Sullivan PG, Rabchevsky AG, Waldmeier PC, Springer JE. Mitochondrial permeability transition in CNS trauma: cause or effect of neuronal cell death? *J Neurosci Res*. 2005;79(1-2):231-239.
22. Hayashi T, Kaneko Y, Yu S, et al. Quantitative analyses of matrix metalloproteinase activity after traumatic brain injury in adult rats. *Brain Res*. 2009;1280:172-177.
23. Vilalta A, Sahuquillo J, Rosell A, Poca MA, Riveiro M, Montaner J. Moderate and severe traumatic brain injury induce early overexpression of systemic and brain gelatinases. *Intensive Care Med*. 2008;34(8):1384-1392.
24. Dawson VL, Kizushi VM, Huang PL, Snyder SH, Dawson TM. Resistance to neurotoxicity in cortical cultures from neuronal nitric oxide synthase-deficient mice. *J Neurosci*. 1996;16(8):2479-2487.
25. Xia Y, Dawson VL, Dawson TM, Snyder SH, Zweier JL. Nitric oxide synthase generates superoxide and nitric oxide in arginine-depleted cells leading to peroxynitrite-mediated cellular injury. *Proc Natl Acad Sci U S A*. 1996;93(13):6770-6774.
26. Fee D, Crumbaugh A, Jacques T, et al. Activated/effector CD4+ T cells exacerbate acute damage in the central nervous system following traumatic injury. *J Neuroimmunol*. 2003;136(1-2):54-66.
27. Hailer NP. Immunosuppression after traumatic or ischemic CNS damage: it is neuroprotective and illuminates the role of microglial cells. *Prog Neurobiol*. 2008;84(3):211-233.
28. Borel JF, Feurer C, Gubler HU, Stahelin H. Biological effects of cyclosporin A: a new antilymphocytic agent. *Agents Actions*. 1976;6(4):468-475.
29. Dawson VL, Brahmbhatt HP, Mong JA, Dawson TM. Expression of inducible nitric oxide synthase causes delayed neurotoxicity in primary mixed neuronal-glial cortical cultures. *Neuropharmacology*. 1994;33(11):1425-1430.

Copyright © Congress of Neurological Surgeons. Unauthorized reproduction of this article is prohibited.

30. Palladini G, Caronti B, Pozzessere G, et al. Treatment with cyclosporine A promotes axonal regeneration in rats submitted to transverse section of the spinal cord–II–Recovery of function. *J Hirnforsch*. 1996;37(1):145-153.
31. Kaminska B, Gaweda-Walerych K, Zawadzka M. Molecular mechanisms of neuroprotective action of immunosuppressants–facts and hypotheses. *J Cell Mol Med*. 2004;8(1):45-58.
32. Liu J, Farmer JD Jr, Lane WS, Friedman J, Weissman I, Schreiber SL. Calcineurin is a common target of cyclophilin-cyclosporin A and FKBP-FK506 complexes. *Cell*. 1991;66(4):807-815.
33. Cardenas ME, Muir RS, Breuder T, Heitman J. Targets of immunophilin-immunosuppressant complexes are distinct highly conserved regions of calcineurin A. *EMBO J*. 1995;14(12):2772-2783.
34. Fruman DA, Klee CB, Bierer BE, Burakoff SJ. Calcineurin phosphatase activity in T lymphocytes is inhibited by FK 506 and cyclosporin A. *Proc Natl Acad Sci U S A*. 1992;89(9):3686-3690.
35. Snyder SH, Sabatini DM, Lai MM, Steiner JP, Hamilton GS, Suzdak PD. Neural actions of immunophilin ligands. *Trends Pharmacol Sci*. 1998;19(1):21-26.
36. Goldner FM, Patrick JW. Neuronal localization of the cyclophilin A protein in the adult rat brain. *J Comp Neurol*. 1996;372(2):283-293.
37. Borlongan CV, Fujisaki T, Watanabe S. Chronic cyclosporine-A injection in rats with damaged blood-brain barrier does not impair retention of passive avoidance. *Neurosci Res*. 1998;32(3):195-200.
38. Leventhal L, Sortwell CE, Hanbury R, Collier TJ, Kordower JH, Palfi S. Cyclosporin A protects striatal neurons in vitro and in vivo from 3-nitropropionic acid toxicity. *J Comp Neurol*. 2000;425(4):471-478.
39. Inamura T, Black KL. Bradykinin selectively opens blood-tumor barrier in experimental brain tumors. *J Cereb Blood Flow Metab*. 1994;14(5):862-870.
40. Nomura T, Inamura T, Black KL. Intracarotid infusion of bradykinin selectively increases blood-tumor permeability in 9L and C6 brain tumors. *Brain Res*. 1994;659(1-2):62-66.
41. Bartus RT, Elliott PJ, Dean RL, et al. Controlled modulation of BBB permeability using the bradykinin agonist, RMP-7. *Exp Neurol*. 1996;142(1):14-28.
42. Okonkwo DO, Melon DE, Pellicane AJ, et al. Dose-response of cyclosporin A in attenuating traumatic axonal injury in rat. *Neuroreport*. 2003;14(3):463-466.
43. Diaz-Ruiz A, Rios C, Duarte I, et al. Cyclosporin-A inhibits lipid peroxidation after spinal cord injury in rats. *Neurosci Lett*. 1999;266(1):61-64.
44. Vercesi AE, Kowaltowski AJ, Grijalba MT, Meinicke AR, Castilho RF. The role of reactive oxygen species in mitochondrial permeability transition. *Biosci Rep*. 1997;17(1):43-52.
45. Baines CP, Kaiser RA, Sheiko T, Craigen WJ, Molkentin JD. Voltage-dependent anion channels are dispensable for mitochondrial-dependent cell death. *Nat Cell Biol*. 2007;9(5):550-555.
46. Woodfield K, Ruck A, Brdiczka D, Halestrap AP. Direct demonstration of a specific interaction between cyclophilin-D and the adenine nucleotide translocase confirms their role in the mitochondrial permeability transition. *Biochem J*. 1998;336(Pt 2):287-290.
47. Waldmeier PC, Feldtrauer JJ, Qian T, Lemasters JJ. Inhibition of the mitochondrial permeability transition by the nonimmunosuppressive cyclosporin derivative NIM811. *Mol Pharmacol*. 2002;62(1):22-29.
48. Schinzel AC, Takeuchi O, Huang Z, et al. Cyclophilin D is a component of mitochondrial permeability transition and mediates neuronal cell death after focal cerebral ischemia. *Proc Natl Acad Sci U S A*. 2005;102(34):12005-12010.
49. Malouitre S, Dube H, Selwood D, Crompton M. Mitochondrial targeting of cyclosporin A enables selective inhibition of cyclophilin-D and enhanced cytoprotection after glucose and oxygen deprivation. *Biochem J*. 2010;425(1):137-148.
50. Wang X, Carlsson Y, Basso E, et al. Developmental shift of cyclophilin D contribution to hypoxic-ischemic brain injury. *J Neurosci*. 2009;29(8):2588-2596.
51. Wang X, Han W, Du X, et al. Neuroprotective effect of bax-inhibiting peptide on neonatal brain injury. *Stroke*. 2010;41(9):2050-2055.
52. Nicolli A, Basso E, Petronilli V, Wenger RM, Bernardi P. Interactions of cyclophilin with the mitochondrial inner membrane and regulation of the permeability transition pore, and cyclosporin A-sensitive channel. *J Biol Chem*. 1996;271(4):2185-2192.
53. He L, Lemasters JJ. Regulated and unregulated mitochondrial permeability transition pores: a new paradigm of pore structure and function? *FEBS Lett*. 2002;512(1-3):1-7.
54. Santos JB, Schauwecker PE. Protection provided by cyclosporin A against excitotoxic neuronal death is genotype dependent. *Epilepsia*. 2003;44(8):995-1002.
55. Cousin MA, Robinson PJ. The dephosphins: dephosphorylation by calcineurin triggers synaptic vesicle endocytosis. *Trends Neurosci*. 2001;24(11):659-665.
56. Dawson TM, Steiner JP, Dawson VL, Dinerman JL, Uhl GR, Snyder SH. Immunosuppressant FK506 enhances phosphorylation of nitric oxide synthase and protects against glutamate neurotoxicity. *Proc Natl Acad Sci U S A*. 1993;90(21):9808-9812.
57. Shou Y, Li L, Prabhakaran K, Borowitz JL, Isom GE. Calcineurin-mediated Bad translocation regulates cyanide-induced neuronal apoptosis. *Biochem J*. 2004;379(Pt 3):805-813.
58. Wang HG, Pathan N, Ethell IM, et al. Ca2+-induced apoptosis through calcineurin dephosphorylation of BAD. *Science*. 1999;284(5412):339-343.
59. Costantini LC, Chaturvedi P, Armistead DM, McCaffrey PG, Deacon TW, Isacson O. A novel immunophilin ligand: distinct branching effects on dopaminergic neurons in culture and neurotrophic actions after oral administration in an animal model of Parkinson's disease. *Neurobiol Dis*. 1998;5(2):97-106.
60. Costantini LC, Isacson O. Immunophilin ligands and GDNF enhance neurite branching or elongation from developing dopamine neurons in culture. *Exp Neurol*. 2000;164(1):60-70.
61. Gabryel B, Bernacki J. Effect of FK506 and cyclosporine A on the expression of BDNF, tyrosine kinase B and p75 neurotrophin receptors in astrocytes exposed to simulated ischemia in vitro. *Cell Biol Int*. 2009;33(7):739-748.
62. Okonkwo DO, Buki A, Siman R, Povlishock JT. Cyclosporin A limits calcium-induced axonal damage following traumatic brain injury. *Neuroreport*. 1999;10(2):353-358.
63. Okonkwo DO, Povlishock JT. An intrathecal bolus of cyclosporin A before injury preserves mitochondrial integrity and attenuates axonal disruption in traumatic brain injury. *J Cereb Blood Flow Metab*. 1999;19(4):443-451.
64. Scheff SW, Sullivan PG. Cyclosporin A significantly ameliorates cortical damage following experimental traumatic brain injury in rodents. *J Neurotrauma*. 1999;16(9):783-792.
65. Gogarten W, Van Aken H, Moskopp D, et al. A case of severe cerebral trauma in a patient under chronic treatment with cyclosporine A. *J Neurosurg Anesthesiol*. 1998;10(2):101-105.
66. Suehiro E, Povlishock JT. Exacerbation of traumatically induced axonal injury by rapid posthypothermic rewarming and attenuation of axonal change by cyclosporin A. *J Neurosurg*. 2001;94(3):493-498.
67. Van Den Heuvel C, Donkin JJ, Finnie JW, et al. Downregulation of amyloid precursor protein (APP) expression following post-traumatic cyclosporin-A administration. *J Neurotrauma*. 2004;21(11):1562-1572.
68. Selkoe DJ. Translating cell biology into therapeutic advances in Alzheimer's disease. *Nature*. 1999;399(6738 Suppl):A23-A31.
69. Gabbita SP, Scheff SW, Menard RM, Roberts K, Fugaccia I, Zemlan FP. Cleaved-tau: a biomarker of neuronal damage after traumatic brain injury. *J Neurotrauma*. 2005;22(1):83-94.
70. Zemlan FP, Mulchahey JJ, Gudelsky GA. Quantification and localization of kainic acid-induced neurotoxicity employing a new biomarker of cell death: cleaved microtubule-associated protein-tau (C-tau). *Neuroscience*. 2003;121(2):399-409.
71. Sullivan PG, Thompson MB, Scheff SW. Cyclosporin A attenuates acute mitochondrial dysfunction following traumatic brain injury. *Exp Neurol*. 1999;160(1):226-234.
72. Signoretti S, Marmarou A, Tavazzi B, et al. The protective effect of cyclosporin A upon N-acetylaspartate and mitochondrial dysfunction following experimental diffuse traumatic brain injury. *J Neurotrauma*. 2004;21(9):1154-1167.
73. Albensi BC, Sullivan PG, Thompson MB, Scheff SW, Mattson MP. Cyclosporin ameliorates traumatic brain-injury-induced alterations of hippocampal synaptic plasticity. *Exp Neurol*. 2000;162(2):385-389.
74. Alessandri B, Rice AC, Levasseur J, DeFord M, Hamm RJ, Bullock MR. Cyclosporin A improves brain tissue oxygen consumption and learning/memory performance after lateral fluid percussion injury in rats. *J Neurotrauma*. 2002;19(7):829-841.
75. Riess P, Bareyre FM, Saatman KE, et al. Effects of chronic, post-injury Cyclosporin A administration on motor and sensorimotor function following severe, experimental traumatic brain injury. *Restor Neurol Neurosci*. 2001;18(1):1-8.
76. Magnasco A, Rossi A, Catarsi P, et al. Cyclosporin and organ specific toxicity: clinical aspects, pharmacogenetics and perspectives. *Curr Clin Pharmacol*. 2008;3(3):166-173.

Copyright © Congress of Neurological Surgeons. Unauthorized reproduction of this article is prohibited.

77. Sullivan PG, Rabchevsky AG, Hicks RR, Gibson TR, Fletcher-Turner A, Scheff SW. Dose-response curve and optimal dosing regimen of cyclosporin A after traumatic brain injury in rats. *Neuroscience*. 2000;101(2):289-295.
78. Sullivan PG, Thompson M, Scheff SW. Continuous infusion of cyclosporin A postinjury significantly ameliorates cortical damage following traumatic brain injury. *Exp Neurol*. 2000;161(2):631-637.
79. Gijtenbeek JM, van den Bent MJ, Vecht CJ. Cyclosporine neurotoxicity: a review. *J Neurol*. 1999;246(5):339-346.
80. Wijdicks EF. Neurotoxicity of immunosuppressive drugs. *Liver Transpl*. 2001;7(11):937-942.
81. Jayakumar AR, Rao KV, Panickar KS, Moriyama M, Reddy PV, Norenberg MD. Trauma-induced cell swelling in cultured astrocytes. *J Neuropathol Exp Neurol*. 2008;67(5):417-427.
82. Redell JB, Zhao J, Dash PK. Acutely increased cyclophilin a expression after brain injury: a role in blood-brain barrier function and tissue preservation. *J Neurosci Res*. 2007;85(9):1980-1988.
83. Fukui S, Signoretti S, Dunbar JG, Marmarou A. The effect of cyclosporin A on brain edema formation following experimental cortical contusion. *Acta Neurochir Suppl*. 2003;86:301-303.
84. Serkova NJ, Christians U, Benet LZ. Biochemical mechanisms of cyclosporine neurotoxicity. *Mol Interv*. 2004;4(2):97-107.
85. Setkowicz Z, Guzik R. Injections of vehicle, but not cyclosporin A or tacrolimus (FK506), afford neuroprotection following injury in the developing rat brain. *Acta Neurobiol Exp (Wars)*. 2007;67(4):399-409.
86. Borlongan CV. Motor activity-mediated partial recovery in ischemic rats. *Neuroreport*. 2000;11(18):4063-4067.
87. Cramer SC. Repairing the human brain after stroke: I. Mechanisms of spontaneous recovery. *Ann Neurol*. 2008;63(3):272-287.
88. Liu Z, Zhang RL, Li Y, Cui Y, Chopp M. Remodeling of the corticospinal innervation and spontaneous behavioral recovery after ischemic stroke in adult mice. *Stroke*. 2009;40(7):2546-2551.
89. Anand P, Birch R. Restoration of sensory function and lack of long-term chronic pain syndromes after brachial plexus injury in human neonates. *Brain*. 2002;125(Pt 1):113-122.
90. Ashwal S, Tone B, Tian HR, Chong S, Obenaus A. Serial magnetic resonance imaging in a rat pup filament stroke model. *Exp Neurol*. 2006;202(2):294-301.
91. Burgess JW, Villablanca JR. Recovery of function after neonatal or adult hemispherectomy in cats. II. Limb bias and development, paw usage, locomotion and rehabilitative effects of exercise. *Behav Brain Res*. 1986;20(1):1-17.
92. Derugin N, Dingman A, Wendland MF, Fox C, Bollen A, Vexler ZS. Magnetic resonance imaging as a surrogate measure for histological sub-chronic endpoint in a neonatal rat stroke model. *Brain Res*. 2005;1066(1-2):49-56.
93. Villablanca JR, Burgess JW, Olmstead CE. Recovery of function after neonatal or adult hemispherectomy in cats: I. Time course, movement, posture and sensorimotor tests. *Behav Brain Res*. 1986;19(3):205-226.
94. McEwen ML, Sullivan PG, Springer JE. Pretreatment with the cyclosporin derivative, NIM811, improves the function of synaptic mitochondria following spinal cord contusion in rats. *J Neurotrauma*. 2007;24(4):613-624.
95. Mbye LH, Singh IN, Carrico KM, Saatman KE, Hall ED. Comparative neuroprotective effects of cyclosporin A and NIM811, a nonimmunosuppressive cyclosporin A analog, following traumatic brain injury. *J Cereb Blood Flow Metab*. 2009;29(1):87-97.
96. Mbye LH, Singh IN, Sullivan PG, Springer JE, Hall ED. Attenuation of acute mitochondrial dysfunction after traumatic brain injury in mice by NIM811, a nonimmunosuppressive cyclosporin A analog. *Exp Neurol*. 2008;209(1):243-253.
97. Yu S, Kaneko Y, Bae E, et al. Severity of controlled cortical impact traumatic brain injury in rats and mice dictates degree of behavioral deficits. *Brain Res*. 2009;1287:157-163.
98. Kasturi BS, Stein DG. Progesterone decreases cortical and sub-cortical edema in young and aged ovariectomized rats with brain injury. *Restor Neurol Neurosci*. 2009;27(4):265-275.
99. Sayeed I, Stein DG. Progesterone as a neuroprotective factor in traumatic and ischemic brain injury. *Prog Brain Res*. 2009;175:219-237.
100. Empey PE, McNamara PJ, Young B, Rosbolt MB, Hatton J. Cyclosporin A disposition following acute traumatic brain injury. *J Neurotrauma*. 2006;23(1):109-116.
101. Boddie DE, Currie DG, Eremin O, Heys SD. Immune suppression and isolated severe head injury: a significant clinical problem. *Br J Neurosurg*. 2003;17(5):405-417.
102. Mazzeo AT, Kunene NK, Gilman CB, Hamm RJ, Hafez N, Bullock MR. Severe human traumatic brain injury, but not cyclosporin a treatment, depresses activated T lymphocytes early after injury. *J Neurotrauma*. 2006;23(6):962-975.
103. Mazzeo AT, Alves OL, Gilman CB, et al. Brain metabolic and hemodynamic effects of cyclosporin A after human severe traumatic brain injury: a microdialysis study. *Acta Neurochir (Wien)*. 2008;150(10):1019-1031; discussion 1031.
104. Marcoux J, McArthur DA, Miller C, et al. Persistent metabolic crisis as measured by elevated cerebral microdialysis lactate-pyruvate ratio predicts chronic frontal lobe brain atrophy after traumatic brain injury. *Crit Care Med*. 2008;36(10):2871-2877.
105. Vespa P, Bergsneider M, Hattori N, et al. Metabolic crisis without brain ischemia is common after traumatic brain injury: a combined microdialysis and positron emission tomography study. *J Cereb Blood Flow Metab*. 2005;25(6):763-774.
106. Vespa PM, McArthur D, O'Phelan K, et al. Persistently low extracellular glucose correlates with poor outcome 6 months after human traumatic brain injury despite a lack of increased lactate: a microdialysis study. *J Cereb Blood Flow Metab*. 2003;23(7):865-877.
107. Richards DA, Tolias CM, Sgouros S, Bowery NG. Extracellular glutamine to glutamate ratio may predict outcome in the injured brain: a clinical microdialysis study in children. *Pharmacol Res*. 2003;48(1):101-109.
108. Hatton J, Rosbolt B, Empey P, Kryscio R, Young B. Dosing and safety of cyclosporine in patients with severe brain injury. *J Neurosurg*. 2008;109(4):699-707.
109. Mazzeo AT, Brophy GM, Gilman CB, et al. Safety and tolerability of cyclosporin a in severe traumatic brain injury patients: results from a prospective randomized trial. *J Neurotrauma*. 2009;26(12):2195-2206.

COMMENTS

The authors are to be complimented for having done an uncommonly complete job of reviewing the neuroprotective pharmacology of cyclosporin A in rodent models of TBI as well as the phase Ib and II clinical trial results in obtained in patients with severe traumatic brain injury (TBI) obtained at the University of Kentucky[1] and the Medical College of Virginia.[2] Based on this impressive body of work, plans for a multicenter phase III clinical trial of cyclosporin A in moderate and severe TBI patients are currently being refined by the PI, Dr. Byron Young, Professor of Neurosurgery at the University of Kentucky and his colleagues. In the planning of this trial, we are trying diligently to design the trial in a manner that avoids past mistakes made in phase III trials of other neuroprotective compounds and mechanistic approaches. In particular, we are basing the dosing selection, duration of treatment, and timing of treatment initiation on the body of preclinical TBI studies across multiple laboratories that have laboriously defined the neuroprotective efficacy in multiple TBI models,[3-6] mechanism of action (mitochondrial protection),[4,7] dose-response for those effects,[8] optimal duration of treatment,[8,9] and therapeutic window.[8]

Past phase III trials typically were based on inadequate preclinical documentation of these important pharmacological parameters. Moreover, in those few instances in which the body of preclinical work was reasonably complete, the design of the subsequent clinical trials did not take the preclinical data as seriously as it should have. We hope that with cyclosporin A, we will now get it right. Having worked on the discovery of neuroprotective compounds for TBI for nearly 30 years, it is my belief from the preclinical and early phase clinical data that cyclosporin A will be our best shot on goal to date. As we carefully plan the phase III trial, which has been named Cyclosporine A in Severe Traumatic Brain Injury (CASTBI), we are doing everything we can to not miss this time.

Edward D. Hall
Lexington, Kentucky

Copyright © Congress of Neurological Surgeons. Unauthorized reproduction of this article is prohibited.

1. Hatton J, Rosbolt B, Empey P, Kryscio R, Young B. Dosing and safety of cyclosporine in patients with severe brain injury. *J Neurosurg.* 2008;109(4):699-707.
2. Mazzeo AT, Brophy GM, Gilman CB, et al. Safety and tolerability of cyclosporin a in severe traumatic brain injury patients: results from a prospective randomized trial. *J Neurotrauma.* 2009;26(12):2195-2206.
3. Buki A, Okonkwo DO, Povlishock JT. Postinjury cyclosporin A administration limits axonal damage and disconnection in traumatic brain injury. *J Neurotrauma.* 1999;16(6):511-521.
4. Okonkwo DO, Povlishock JT. An intrathecal bolus of cyclosporin A before injury preserves mitochondrial integrity and attenuates axonal disruption in traumatic brain injury. *J Cereb Blood Flow Metab.* 1999;19(4):443-451.
5. Scheff SW, Sullivan PG. Cyclosporin A significantly ameliorates cortical damage following experimental traumatic brain injury in rodents. *J Neurotrauma.* 1999;16(9):783-792.
6. Alessandri B, Rice AC, Levasseur J, DeFord M, Hamm RJ, Bullock MR. Cyclosporin A improves brain tissue oxygen consumption and learning/memory performance after lateral fluid percussion injury in rats. *J Neurotrauma.* 2002;19(7):829-841.
7. Sullivan PG, Thompson MB, Scheff SW. Cyclosporin A attenuates acute mitochondrial dysfunction following traumatic brain injury. *Exp Neurol.* 1999;160(1):226-234.
8. Sullivan PG, Rabchevsky AG, Hicks RR, Gibson TR, Fletcher-Turner A, Scheff SW. Dose-response curve and optimal dosing regimen of cyclosporin A after traumatic brain injury in rats. *Neuroscience.* 2000;101(2):289-295.
9. Sullivan PG, Thompson M, Scheff SW. Continuous infusion of cyclosporin A postinjury significantly ameliorates cortical damage following traumatic brain injury. *Exp Neurol.* 2000;161(2):631-637.

Dr. Lulic and colleagues provide an excellent, thorough review of the published data to date regarding the use of cyclosporin A in the treatment of TBI, both in the experimental and human clinical situations. Since the first report of its efficacy in experimental traumatic brain injury,[1] cyclosporin A has gone on to become one of the most, if not the most, extensively studied compounds in TBI. Cyclosporin A is almost unique in the world of pharmacologic treatment of TBI in that robust phase II human studies, including pharmacokinetics, have been performed.

No phase III clinical trial investigating a pharmacologic compound for the treatment of TBI has ever succeeded.[2] The failure of many of these clinical trials can be traced to insufficient/inadequate phase I and II studies. In fact, one would be hard pressed to explain why the dose used in several studies was ever chosen,[3,4] rendering the history of drug trials of TBI as 1 shot-in-the-dark after another. This review is a timely reminder that a phase III randomized, prospective trial of cyclosporin A in TBI is both warranted and due.

David O. Okonkwo
Pittsburgh, Pennsylvania

1. Okonkwo DO, Povlishock JT. An intrathecal bolus of cyclosporin A before injury preserves mitochondrial integrity and attenuates axonal disruption in traumatic brain injury. *J Cereb Blood Flow Metab*. 1999;19(4):443-451.
2. Narayan RK, Michel ME, Ansell B, et al. Clinical trials in head injury. *J Neurotrauma*. 2002;19(5):503-57.
3. Wright DW, Kellermann AL, Hertzberg VS, et al. ProTECT: a randomized clinical trial of progesterone for acute traumatic brain injury. *Ann Emerg Med*. 2007;49(4):391-402.
4. Temkin NR, Anderson GD, Winn HR, et al. Magnesium sulfate for neuroprotection after traumatic brain injury: a randomised controlled trial. *Lancet Neurol*. 2007;6(1):29-38.

The International Podcast Series. Article abstracts translated for our international audience at www.neurosurgery-online.com

NEUROSURGERY
THE REGISTER OF THE NEUROSURGICAL MIND

Copyright © Congress of Neurological Surgeons. Unauthorized reproduction of this article is prohibited.

Early Recognition of Lumbar Overdrainage by Lumboventricular Pressure Gradient

Dimitre Staykov, MD*
Verena Speck, MD*
Bastian Volbers, MD*
Ingrid Wagner, MD*
Marc Saake, MD‡
Arnd Doerfler, MD‡
Stefan Schwab, MD*
Juergen Bardutzky, MD*

*Department of Neurology, and ‡Department of Neuroradiology, University of Erlangen, Schwabachanlage 6, 91054 Erlangen, Germany

Correspondence:
Dimitre Staykov, MD,
Department of Neurology,
University of Erlangen,
Schwabachanlage 6,
91054 Erlangen, Germany.
E-mail: dimitre.staykov@uk-erlangen.de

Received, February 2, 2010.
Accepted, August 6, 2010.

Copyright © 2011 by the
Congress of Neurological Surgeons

BACKGROUND: Lumbar drainage (LD) represents a promising treatment strategy for prevention of vasospasm after aneurysmal subarachnoid hemorrhage (SAH).

OBJECTIVE: To report on transient herniation caused by lumbar overdrainage in 3 patients with severe SAH who were treated with early LD within an ongoing feasibility study.

METHODS: Patients with first-time aneurysmal SAH received LD within 72 hours of symptom onset, after aneurysm clipping or coiling. LD, with a target drainage amount of 5 to 10 mL, was continued for 6 to 9 days. External ventricular drainage (EVD) was begun on admission when hydrocephalus was present. With both catheters in place, intracranial pressure (ICP) and lumbar pressure (LP) were monitored simultaneously.

RESULTS: Three of 22 patients developed a progressive lumboventricular pressure gradient, likely due to cerebrospinal fluid (CSF) overdrainage. Two patients showed signs of herniation. Clamping of LD resulted in complete reversal of symptoms in those patients. The lumboventricular pressure gradient began to evolve at least 12 hours before clinical symptoms developed, and gradually disappeared in all 3 patients after LD clamping.

CONCLUSION: Lumbar overdrainage should be avoided in severe SAH, and lumboventricular pressure measurement may be a useful monitoring tool. Herniation due to lumbar overdrainage is a feared complication that can be avoided by following a strict LD management protocol.

KEY WORDS: Herniation, Intracranial pressure monitoring, Lumbar drainage, Subarachnoid hemorrhage

Neurosurgery 68:1187–1191, 2011 DOI: 10.1227/NEU.0b013e31820c0274 www.neurosurgery-online.com

Two larger studies have suggested beneficial effects of early lumbar drainage (LD) for prevention of vasospasm after subarachnoid hemorrhage (SAH),[1,2] and this new treatment approach currently is being investigated (www.clinicaltrials.gov, NCT00842049). Other evolving uses of LD in neurocritical care include therapy of refractory intracranial hypertension[3,4] or communicating hydrocephalus after intracerebral hemorrhage with severe ventricular involvement.[5-7] Results from those studies also have been encouraging, and few complications directly attributable to LD have been reported.

Transtentorial herniation is the most feared complication of LD, and it remains a major concern and matter of debate when LD is being used.[8] The pathophysiological concept of a downward pressure gradient caused by diversion of cerebrospinal fluid (CSF) from the lumbar compartment is plausible. However, actual reports of herniation clearly due to LD are rare. In such cases, overdrainage most often has been suspected as the causative mechanism.[9] To our knowledge, measurement of a lumboventricular pressure gradient in patients developing signs of herniation due to lumbar overdrainage has not been reported. Lumbar pressure (LP) monitoring is not commonly used in neurocritical care units, and only a few studies mention its use.[10,11]

In our institution, patients with severe SAH and large amounts of blood in the subarachnoid space (Fisher grade 3), who are at high risk of developing vasospasm, receive early (<72 hours) LD to facilitate blood removal from the lumbar and basal cisterns. Following this institutional protocol, which has been in place since 2007, we

ABBREVIATIONS: EVD, external ventricular drainage; **ICP,** intracranial pressure; **LD,** lumbar drainage; **LP,** lumbar pressure; **SAH,** subarachnoid hemorrhage

Copyright © Congress of Neurological Surgeons. Unauthorized reproduction of this article is prohibited.

treated a total of 13 consecutive patients with early LD. Within an ongoing prospective feasibility study on the use of early LD in patients with severe SAH, simultaneous LP and intracranial pressure (ICP) monitoring also was performed in 22 patients. In this preliminary report, we focus on complications caused by lumbar overdrainage in 3 patients with SAH treated with early LD, 2 of whom showed signs of transient herniation in the course of a developing lumboventricular pressure gradient.

METHODS

Patient Selection

This prospective study was approved by our local ethics committee. Patients older than 18 years of age with a first-time aneurysmal SAH, Fisher grade 2 to 4, Hunt and Hess grade 1 to 5, and aneurysm treatment within 48 hours from symptom onset were included in the study after informed consent was obtained from the patient or the next of kin. Exclusion criteria were casting of the third and/or fourth ventricle by intraventricular hematoma with obstructive hydrocephalus, parenchymal hemorrhage >30 mL, pregnancy, or a pre-existing disability (modified Rankin scale >1).

Treatment Protocol

General management followed the guidelines of the German Neurological Society[12] and the Stroke Council of the American Heart Association for treatment of SAH.[13] SAH was diagnosed by cranial CT. Hydrocephalus was defined by measuring the bicaudate index, considered present if it exceeded the 95th percentile for age,[14] and evaluating temporal horn diameter. Hydrocephalus present on admission was treated with external ventricular drainage (EVD) prior to aneurysm treatment. All patients underwent digital subtraction angiography. After the source of bleeding was identified, either aneurysm clipping or coiling was performed. Within 72 hours after symptom onset, a silicone lumbar catheter (Codman Lumbar Drainage Kit, Codman, Raynham, Massachusetts) was placed at the L3-L4 level under sterile conditions on the neurocritical care unit. The catheter was threaded approximately 15 cm from the skin level. After catheter placement, a sterile, closed CSF drainage system was connected to the lumbar catheter, and LD was performed against a hydrostatic pressure gradient of 5 to 10 cm above the point of catheter insertion with a target CSF drainage amount of 5 to 10 mL per hour. When traces of blood were present in the third or fourth ventricle (or both), LD was started only after complete clearance of blood from those ventricles was confirmed on CT. If additional CSF drainage was necessary, it was performed via EVD. The CSF drainage amount was documented hourly, and adjustments were made to the hydrostatic pressure gradient (position of the CSF collection chamber). LD was continued for 6 to 9 days. If a communicating hydrocephalus persisted after 9 days of LD, CSF diversion was continued via LD or EVD based on an individual decision. A permanent shunt was indicated when communicating hydrocephalus persisted for more than 2 weeks from symptom onset.

Monitoring of Intracranial and Lumbar Pressure

ICP and LP were recorded via a hydrostatic pressure transducer connected to the drainage system. If drainage was not performed via EVD, ICP was monitored continuously. The lumbar catheter was used for intermittent hourly pressure recordings after clamping for at least 5 minutes. Hydrostatic pressure was always measured using pressure transducers positioned at the same level (ie, the foramen of Monro) for both catheters. The patient was first placed in a supine position. Communication between the ventricular system and the lumbar cistern was then tested by (1) a short compression of the abdomen and (2) compression of the jugular vein for 30 seconds (ie, the Queckenstedt maneuver), which led to corresponding simultaneous changes in the pressure curves of both catheters. The ICP and LP were then recorded separately. After positioning the patient in a 30-degree elevated upper body position and adjusting the pressure transducers to the level of the foramen of Monro, ICP and LP were recorded again. Then the pressure gradient was adjusted for drainage of CSF, and LD was reopened. Using this technique, a high correlation between ICP and LP was found despite the different caliber and wall thickness of the lumbar and ventricular catheters (R^2 = 0.96; unpublished data).

RESULTS

As of January 2010, a total of 22 consecutive patients with severe SAH were prospectively included in the study. In 2 of the 22 patients (9%), LD was complicated by signs of transient herniation, likely due to lumbar CSF overdrainage. The records of 13 additional patients treated with early LD after severe SAH were retrospectively reviewed for similar complications. The patients, in whom a lumboventricular pressure gradient was measured within the current prospective study, are described in detail in the following case series. Catheter obstruction of the lumbar catheter was observed in 4 of 35 patients (11%) and EVD obstruction in 1 case (3%). Those catheters had to be exchanged.

Case Series

Three patients, a 57-year-old man (patient 1), a 50-year-old woman (patient 2), and a 48-year-old woman (patient 3) were admitted with aneurysmal SAH of Hunt and Hess grade 5 and acute hydrocephalus. The Fisher grade was 3 + 4 in patient 1 (frontal parenchymal hematoma) and patient 2 (involvement of the lateral ventricles), and 3 in patient 3. All patients primarily received EVD. Cerebral angiography revealed anterior communicating artery aneurysms, which were treated by endovascular coiling in all 3 cases. The patients received early LD (< 72 hours after bleeding onset), and CSF diversion was provided simultaneously through the EVD and LD in the first 2 days after LD insertion. After that, the EVD was clamped and used for continuous ICP monitoring, while CSF drainage via the LD was continued.

Measurements obtained initially showed no difference between the ICP and LP values. After 2 days of CSF drainage via LD alone, patient 1 showed a slowly increasing difference between ICP and LP, with a decreasing LP value and constant ICP. Recorded CSF drainage amount via the LD was continuously close to 10 mL per hour. The pressure gradient gradually increased over a period of 20 hours, reaching a maximum value of 12 mm Hg. At this time, no change in clinical status was observed. However, compression tests of the jugular vein, which earlier had led to simultaneous increases in both pressure levels, no longer provoked changes in pressure measured via the lumbar

Copyright © Congress of Neurological Surgeons. Unauthorized reproduction of this article is prohibited.

catheter. Twelve hours later, the patient developed a unilateral fixed dilated pupil, and CT revealed compressed basal cisterns, indicating impending herniation. The LD was then immediately clamped, and measurement of LP was performed continuously with EVD opened and intermittent ICP measurement for correlation. The patient was brought into a flat position. The difference of 12 mm Hg between lumbar and ventricular pressure gradually decreased, and the initially observed pressure gradient was completely reversed after approximately 2.5 hours. Clinical signs resolved completely after LD clamping. On the next day, LD was continued with a reduced maximum target amount of CSF drainage (5 mL/h) with no further pressure gradient development. The course of ICP and LP in this patient is shown in Figure 1, along with corresponding CT images.

Patient 2 developed identical symptoms 10 hours after reaching a maximum pressure gradient of 11 mm Hg within 5 days of CSF drainage via LD. Basal cistern appearance on CT imaging was similar to that shown in Figure 1. After clamping of the lumbar catheter and flat positioning, signs of herniation also were completely reversed within 2 hours.

In patient 3, a similar pattern of progressively increasing lumboventricular pressure gradient (maximum, 8 mm Hg) was observed during LD with a drainage rate of about 10 mL/h. In this patient, however, CSF drainage was then continued solely via

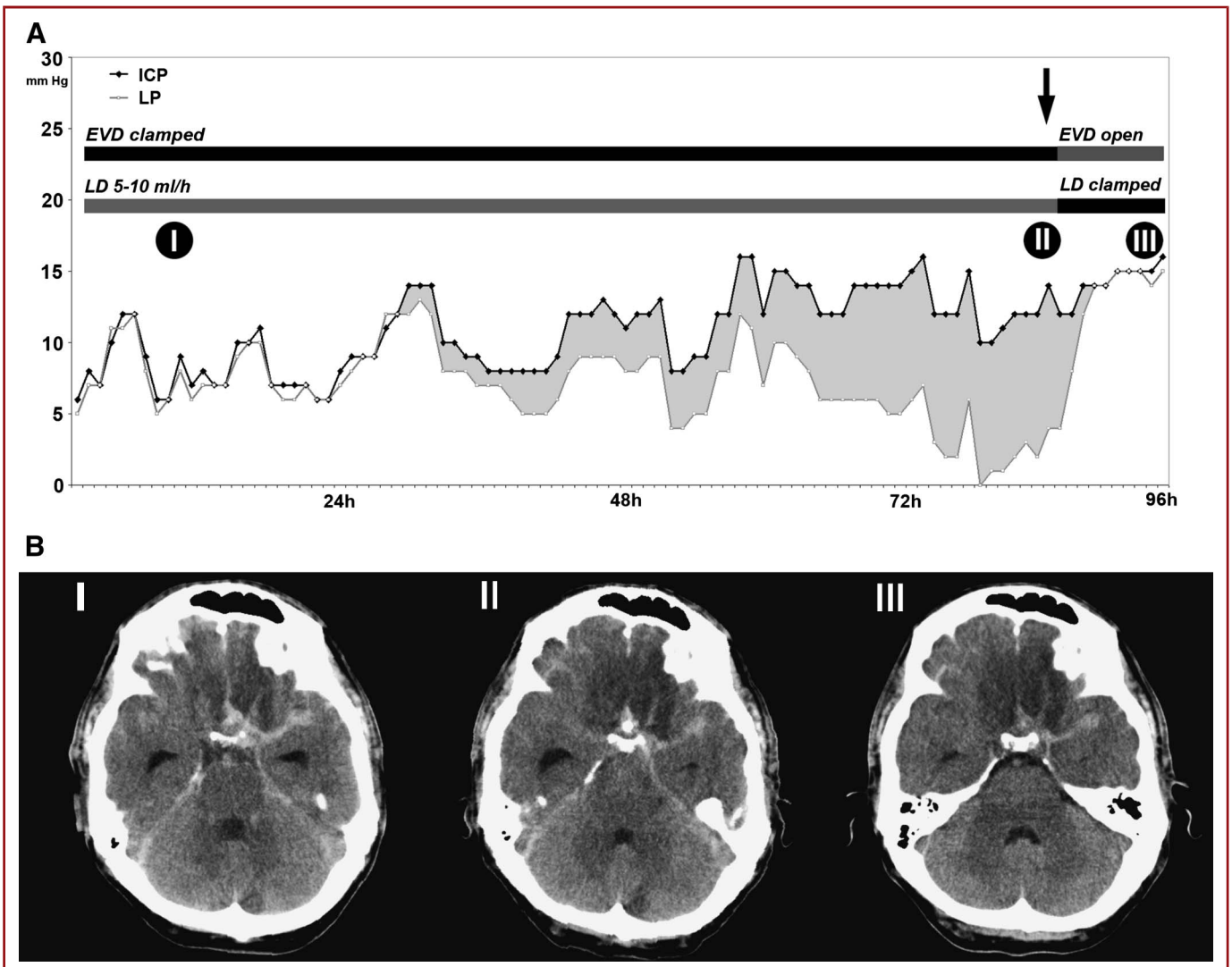

FIGURE 1. *Intracranial and lumbar pressure course in patient 1 (A) with corresponding CT imaging (B). Marks with roman numbers indicate time points of CT imaging. CT I shows a clearly distinguishable pontine cistern partially filled with blood. CT II, performed immediately after appearance of signs of herniation (indicated by arrow in A), reveals a compressed pontine cistern. After cessation of lumbar drainage and reversal of the lumboventricular pressure gradient, CT III again shows a clearly visible pontine cistern. EVD, external ventricular drainage; ICP, intracranial pressure; LD, lumbar drainage; LP, lumbar pressure.*

Copyright © Congress of Neurological Surgeons. Unauthorized reproduction of this article is prohibited.

EVD, and LD was left clamped until complete reversal of the pressure gradient was obtained. Thereafter, LD was continued with a maximum rate of 5 mL/h. Patient 3 did not show any signs of herniation during the course of LD treatment.

DISCUSSION

LD has been shown to be safe in the setting of different conditions including SAH.[1,2,4,5,7] However, communication between the compartments of CSF circulation is essential to avoid formation of pressure gradients, potentially staving off the threat of herniation. Therefore, use of LD usually is considered dangerous in obstructive hydrocephalus, where communication between the internal and the external CSF spaces is compromised.[5,7] Intraventricular hemorrhage with casting of the third and fourth ventricle is one example of such a condition.

In patients with SAH, blood usually is located mainly in the basal cisterns. Therefore, CSF outflow from the ventricles into the subarachnoid space should not be substantially impaired. This distribution of the blood clot may, however, represent a barrier to CSF downstream flow within the subarachnoid space, namely from the convexity of the cerebral hemispheres through the foramen magnum into the spinal compartment. Although this barrier does not block CSF circulation into the lumbar cistern completely, a partial obstruction may be present, and some limitation to the capacity for communication—lower than that in healthy individuals—could be assumed. CSF diversion via LD, when it exceeds the capacity of CSF communication over the blood clot in the vicinity of the foramen magnum, may, therefore, produce a pressure gradient in such patients, as illustrated in our case series.

Close monitoring of CSF drainage is essential in patients with severe SAH, and simultaneous measurements of lumbar and ventricular pressure may be helpful for early identification of lumbar overdrainage. As we demonstrated, a considerable lumboventricular pressure gradient could be measured up to 12 hours before clinical signs of herniation were noted. In addition, with increasing pressure gradient, the jugular vein compression test no longer induced a rise in pressure measured via the lumbar catheter.

In patient 3, we used these measurements to guide further therapy and did not observe any signs of herniation in the course of treatment. Although the therapeutic impact of LD clamping in this case remains speculative, it illustrates the need for further research on this promising monitoring modality. Disappearance of basal cisterns on CT may show overdrainage; however, CT is not suitable for frequent or continuous monitoring. On the other hand, clinical signs may already indicate irreversible damage; hence, their usage for purposes of drainage monitoring may be potentially dangerous. Therefore, the simultaneous measurement of ventricular pressure and LP may have potential as a useful monitoring tool in such patients.

Our case series illustrates some pitfalls of lumbar CSF drainage in the setting of severe SAH. As LD represents a novel approach, possibly capable of a substantial reduction of vasospasm after SAH,[1,2] this treatment strategy still remains promising. However, looking at the whole cohort of patients with severe SAH who were treated with early LD (including the 13 retrospective record reviews), transient signs of herniation were observed in 2 of 35 patients (6%). This complication rate occurred despite the use of closed continuous drainage systems, which allow good control over the drained CSF amount. Therefore, treatment protocols strictly avoiding lumbar overdrainage should be developed to avert potentially life-threatening complications. Fixed small intermittent CSF drainage amounts (e.g., 2 mL every 30 minutes) may be safer in patients at risk (with severe SAH) than continuous LD against a pressure gradient with hourly controls and drainage amount documentation. This regimen may be considered at least in the first days of LD until a substantial amount of the blood clot is cleared. The presence of parenchymal hemorrhage as an additional supratentorial mass represents another safety aspect for the use of LD in such patients. However, previous studies on patients with SAH and parenchymal hemorrhage do not report herniation in the course of lumbar CSF diversion.[1,2] Furthermore, LD has been shown to be safe in patients with supratentorial intracerebral hemorrhage smaller than 40 mL and severe ventricular involvement.[5] Based on those studies, we considered the presence of a parenchymal hemorrhage of less than 30 mL to be safe in the context of the present study. However, this issue and the possible impact of perihemorrhagic edema as an additional cause of mass effect in the course of treatment deserve further investigation.

CONCLUSION

The use of LD in patients with SAH may be a promising treatment strategy for prevention of vasospasm, according to the results of 2 larger studies.[1,2] However, lumbar overdrainage should be avoided in such patients, because it may cause the life-threatening complication of transtentorial herniation. The usage of a strict LD management protocol may be helpful for prevention of this complication. Herniation occurs as a consequence of an evolving pressure gradient between the supratentorial and the infratentorial compartment. This pressure gradient may be identified early by simultaneous intracranial and LP monitoring, as shown in our report. Therefore, the utilization of lumboventricular pressure monitoring in such patients deserves further investigation.

Disclosure

The authors have no personal financial or institutional interest in any of the drugs, materials, or devices described in this article.

REFERENCES

1. Klimo P Jr, Kestle JR, MacDonald JD, Schmidt RH. Marked reduction of cerebral vasospasm with lumbar drainage of cerebrospinal fluid after subarachnoid hemorrhage. *J Neurosurg.* 2004;100(2):215-224.

Copyright © Congress of Neurological Surgeons. Unauthorized reproduction of this article is prohibited.

2. Kwon OY, Kim YJ, Cho CS, Lee SK, Cho MK. The utility and benefits of external lumbar CSF drainage after endovascular coiling on aneurysmal subarachnoid hemorrhage. *J Korean Neurosurg Soc*. 2008;43(6):281-287.
3. Munch EC, Bauhuf C, Horn P, Roth HR, Schmiedek P, Vajkoczy P. Therapy of malignant intracranial hypertension by controlled lumbar cerebrospinal fluid drainage. *Crit Care Med*. 2001;29(5):976-981.
4. Tuettenberg J, Czabanka M, Horn P, et al. Clinical evaluation of the safety and efficacy of lumbar cerebrospinal fluid drainage for the treatment of refractory increased intracranial pressure. *J Neurosurg*. 2009;110(6):1200-1208.
5. Staykov D, Huttner HB, Struffert T, et al. Intraventricular fibrinolysis and lumbar drainage for ventricular hemorrhage. *Stroke*. 2009;40(10): 3275-3280.
6. Huttner HB, Nagel S, Tognoni E, et al. Intracerebral hemorrhage with severe ventricular involvement: lumbar drainage for communicating hydrocephalus. *Stroke*. 2007;38(1):183-187.
7. Huttner HB, Schwab S, Bardutzky J. Lumbar drainage for communicating hydrocephalus after ICH with ventricular hemorrhage. *Neurocrit Care*. 2006;5(3):193-196.
8. Grady MS. Editorial. Lumbar drainage for increased intracranial pressure. *J Neurosurg*. 2009;110(6):1198-1199.
9. Acikbas SC, Akyuz M, Kazan S, Tuncer R. Complications of closed continuous lumbar drainage of cerebrospinal fluid. *Acta Neurochir (Wien)*. 2002;144(5): 475-480.
10. Hanggi D, Liersch J, Turowski B, Yong M, Steiger HJ. The effect of lumboventricular lavage and simultaneous low-frequency head-motion therapy after severe subarachnoid hemorrhage: results of a single center prospective Phase II trial. *J Neurosurg*. 2008;108(6):1192-1199.
11. Scheithauer S, Burgel U, Ryang YM, et al. Prospective surveillance of drain associated meningitis/ventriculitis in a neurosurgery and neurological intensive care unit. *J Neurol Neurosurg Psychiatry*. 2009;80(12):1381-1385.
12. Diener HC, Putzki N, eds. *Leitlinien für Diagnostik und Therapie in der Neurologie*. 4th ed. Stuttgart: Thieme; 2008.
13. Bederson JB, Connolly ES Jr, Batjer HH, et al. Guidelines for the management of aneurysmal subarachnoid hemorrhage: a statement for healthcare professionals from a special writing group of the Stroke Council, American Heart Association. *Stroke*. 2009;40(3):994-1025.
14. van Gijn J, Hijdra A, Wijdicks EF, Vermeulen M, van Crevel H. Acute hydrocephalus after aneurysmal subarachnoid hemorrhage. *J Neurosurg*. 1985; 63(3):355-362.

COMMENT

Staykov et al. present a small series of patients who were treated with simultaneous ventricular and lumbar drainage and pressure monitoring during the acute phase of aneurysmal subarachnoid hemorrhage. Three of 22 patients developed a cranial / spinal pressure gradient, and 2 of these 3 patients showed clinical signs of herniation. A gradient in excess of 8 mm Hg may be worrisome. Clamping the lumbar drain resulted in reversal of the impending herniation in each case. Staykov et al. conclude that lumbar and ventricular monitoring may be a way to avoid the serious consequences of herniation while yielding the benefits of lumbar cerebrospinal fluid (CSF) drainage.

I am convinced that lumbar CSF drainage is a superior method for clearance of subarachnoid blood and that it can attenuate the severity of post-aneurysmal subarachnoid hemorrhage–induced vasospasm. There are patients however, who do not tolerate this treatment because of ventricular obstruction, brain edema, or mass effect related to intraparenchymal hemorrhage. I routinely install both an external ventricular drain and a lumbar drain in these patients during the early stages of their hospitalization, but I do not actively drain from the lumbar region until the brain CT suggests that it is safe. I prefer a patient with open cisterns and no midline shift, but I have had success with small intraparenchymal clots. I believe this paper proposes a viable technique for quantitating the craniospinal gradient and prevention of brain herniation. Although this method is more resource intensive than intracranial pressure monitoring and ventricular drainage alone, it would likely be extremely useful in a patient with focal deficits or altered mental status that could mask the early signs of herniation. In my experience, these tend to be the patients with the most to gain from minimizing the effects of vasospasm. I, too, have observed complete reversal of herniation signs when the lumbar drain is clamped and the patient is leveled. The authors are to be commended for pursuing a strategy that may avert a serious complication in a group of patients who are already critically ill.

Joel D. MacDonald
Salt Lake City, Utah

Copyright © Congress of Neurological Surgeons. Unauthorized reproduction of this article is prohibited.

Awake Craniotomy vs Surgery Under General Anesthesia for Resection of Supratentorial Lesions

Oumar Sacko, MD*‡
Valérie Lauwers-Cances, MD§
David Brauge, MD‡
Musa Sesay, MD¶
Adam Brenner, MD‖
Franck-Emmanuel Roux, MD, PhD*‡

*UMR Unité 825, Faculté Paul Sabatier, IFR 96, ‡Pole Neurosciences, §Service de Statistiques et d'Epidémiologie, Centres Hospitalo-Universitaires de Toulouse, Toulouse, France; ¶Pole d'anesthesie, CHU Pellegrin, Bordeaux, France; ‖Harrison Medical Center, Bremerton, Washington

Correspondence:
Franck-Emmanuel Roux, MD, PhD,
INSERM 825 et service de Neurochirurgie,
Hôpital Purpan,
F-31059 Toulouse, France.
E-mail: franck_emmanuel.roux@yahoo.fr

Received, March 27, 2010.
Accepted, August 23, 2010.

Copyright © 2011 by the
Congress of Neurological Surgeons

BACKGROUND: The use of an awake craniotomy in the treatment of supratentorial lesions is a challenge for both patients and staff in the operation theater.

OBJECT: To assess the safety and effectiveness of an awake craniotomy with brain mapping in comparison with a craniotomy performed under general anesthesia.

METHODS: We prospectively compared 2 groups of patients who underwent surgery for supratentorial lesions: those in whom an awake craniotomy with intraoperative brain mapping was used (AC group, n = 214) and those in whom surgery was performed under general anesthesia (GA group, n = 361, including 72 patients with lesions in eloquent areas). The AC group included lesions in close proximity to the eloquent cortex that were surgically treated on an elective basis.

RESULTS: Globally, the 2 groups were comparable in terms of sex, age, American Society of Anesthesiologists score, pathology, size of lesions, quality of resection, duration of surgery, and neurological outcome, and different in tumor location and preoperative neurological deficits (higher in the AC group). However, specific data analysis of patients with lesions in eloquent areas revealed a significantly better neurological outcome and quality of resection ($P < .001$) in the AC group than the subgroup of GA patients with lesions in eloquent areas. Surgery was uneventful in AC patients and they were discharged home sooner.

CONCLUSION: AC with brain mapping is safe and allows maximal removal of lesions close to functional areas with low neurological complication rates. It provides an excellent alternative to craniotomy under GA.

KEY WORDS: Anesthesia, Awake, Craniotomy, Neurological deficit, Tumor

Neurosurgery 68:1192–1199, 2011 DOI: 10.1227/NEU.0b013e31820c02a3 www.neurosurgery-online.com

Awake craniotomy (AC) is mainly reserved for epilepsy surgery and resection of tumors affecting the functional eloquent cortex in order to reduce the risks of deficits. It remains the standard for identifying functional areas during brain surgery.[1,2] Further development of the procedure, combined with novel anesthetic agents, has recently made AC more tolerable during brain surgery[3-5] and other types of surgery.[6,7] Hence, AC is considered as a viable alternative to general anesthesia (GA) for the resections of intracerebral lesions.[5,8]

Nevertheless, the usefulness or patients' perceptions of awake surgery with brain mapping is an ongoing debate,[4,5,8,9] with its effectiveness being questioned.[10] Because of the paucity of comparative data, the present study was designed to assess the safety and effectiveness of AC with brain mapping vs craniotomy performed under GA for resection of supratentorial brain lesions.

ABBREVIATIONS: AC, awake craniotomy; **GA**, general anesthesia

MATERIALS AND METHODS

Between January 2002 and December 2007, we prospectively collected clinical, histological, and radiological data on 575 adult patients who underwent open brain surgery of supratentorial mass lesions. All patients and their families gave informed consent to study their functional areas by direct brain mapping. National consultative committee of Institut National de la Santé et de la Recherche Médicale gave its approval for patients' data storage and preservation of anonymity in this study. The patients were divided

Copyright © Congress of Neurological Surgeons. Unauthorized reproduction of this article is prohibited.

into 2 groups: those with lesions in eloquent areas, in whom AC and intraoperative brain mapping were used (AC group, n = 214; 244 operations); and patients with lesions in various locations, in whom surgery was performed under general anesthesia without functional brain mapping (GA group, n = 361; 421 operations). The GA group included patients unable to cooperate for AC for various reasons (aphasia, mental disorders, requirement for prone position). In this group, a subset of 72 patients with lesions in eloquent areas (GA_{72}) was studied separately for a better comparison of postoperative neurological complications. Patients were not randomly assigned, but were treated electively by 6 different neurosurgeons using AC or GA in the same department. The allocation to the different groups was decided by a multidisciplinary team comprising the neurosurgeon, the neuroanesthesiologist, and the neuropsychologist based on the patient's preference when applicable. We defined "eloquent zones" as dominant temporal, supramarginal, and angular gyri; dominant and nondominant supplementary motor area, internal capsule, deep grey nuclei; primary sensory-motor cortices and posterior part of the frontal lobes (<2 cm from precentral sulcus).

Preoperative neurological evaluation was done to determine the extent of deficits. The patients and their attendants were educated to the expected course of the procedure and the potential complications. The degree of handedness of the AC patients was assessed by an independent neuropsychologist using the Edinburgh handedness inventory test.[11] The patients in both groups underwent a preoperative magnetic resonance imaging (MRI) with a neuronavigation technique, which was interpreted independently by a neuroradiologist.

Anesthetic Protocol for Awake Craniotomy

One hour before admission in the operating room, a patch (EMLA, AstraZeneca, Paris, France) containing the eutectic mixture of prilocaine (2.5 mg/g) and lidocaine (2.5 mg/g) was applied in the supraorbital and auriculotemporal regions.

In the operating room, the patients were connected to the cardiorespiratory monitor for noninvasive monitoring of blood pressure, heart rate, pulse oximetry, and end-expiratory CO_2. An 18-gauge catheter was placed for intravenous infusion of fluids and drugs. Oxygen (6 L/min) was provided via a face mask. The patient was then positioned in the lateral or supine position using a gel-filled mattress and warming blankets, with careful attention to padding pressure areas to ensure patient comfort.

Lidocaine 1% with epinephrine 1:100 000 was infiltrated to block the supraorbital, auriculotemporal, and occipital nerves. In addition, the Mayfield head holder (Ohio Medical, Cincinnati, Ohio) pin site and the surgical skin incision line were infiltrated. The patients were then draped, making sure that the anesthesiologist had an adequate corridor to the patient's face throughout the procedure. Prior to skin incision, all patients received intravenous medications including an antibiotic (cefazolin, 2 g), an anticonvulsant (levetiracetam, 500 mg), and a corticosteroid (methylprednisolone, 1 mg/kg). Sedation was provided by continuous infusion of propofol (1 to 3 $mg \cdot kg^{-1} \cdot h^{-1}$). Fentanyl (1-3 $\mu g \cdot kg^{-1} \cdot h^{-1}$) or remifentanil 0.01 to 0.25 $\mu g \cdot kg^{-1} \cdot h^{-1}$ was used for analgesia. The depth of procedural sedation was adjusted to maintain acceptable patient comfort and stable vital signs. Propofol infusion was stopped during the dural opening and restated after complete resection of the tumor until the end of the procedure.

Functional Brain Mapping

After installation of the video materials, a microphone was placed beside the patient. The boundaries of the lesion were verified with the surgical navigation system, which has been described elsewhere.[1,12] Before tumor excision, the cortex was directly stimulated to identify the eloquent sites that must be avoided during corticotomy. We used the bipolar electrode of the multifunctional stimulator, 1-mm electrodes separated by 5 mm (Nimbus cortical stimulator, Newmedic, Toulouse, France). The current amplitude was initially set at 2 mA and progressively increased by 1 mA. We used a standard procedure of stimulation with biphasic square wave pulses of 1 ms at 60 Hz and a maximum train duration of 4 seconds.

For brain mapping, patients were asked to perform at least 2 different tasks in the appropriate languages (bilinguals being tested in both languages): a naming task to detect standard anomia (ie, "This is a. . ."), and a reading task involving various basic unrelated sentences (and not previously rehearsed by the patients). During naming procedures, the patients were shown a set of 30 pictures of various objects (ie, a car, a wheelbarrow, a plane, a chair, a bird, a ball, a lion, a tomato, grapes, a bomb, a bottle, a boat, a key, a strawberry, a screwdriver, a rose, a saw, a chicken, a computer, slippers, bread, hands, a book, a rubber, a clock, a fridge, a pencil, a flute, a camera, and a door). The patients were trained to name each object as it appeared. These pictures were shown randomly, and the stimulation was applied as soon as they appeared. For the reading tasks, we used a set of 30 different sentences. The patients were asked to read rather slowly and stimulation was applied randomly on the cortex while they were reading. Naming and reading tasks are elaborate tasks known to activate similar or different areas in the brain.[1] One of the differences between the reading and picture-naming paradigms is that reading involves syntactic processing and multiple word types (verbs, grammatical words) in addition to concrete nouns. To test reading in bilingual persons, we have a data set of sentences translated from French into the major world languages or specific languages spoken in our region.

To be accepted as language location, the language sites found were tested meticulously at least 3 separate times. During direct brain mapping, single anomia sites can occasionally be found[1] and the interpretation of this phenomenon remains complex. Although this can be a matter of debate, sites showing no reproducible language interference were not included in this study. In multilingual patients, languages were tested sequentially (one language-mapping session after another). Nevertheless, at the end of language mapping, the language-specific sites found were confirmed by alternate mapping in both languages to carefully validate such sites. During tumor resection, further subcortical stimulations were performed to identify eloquent white matter. A picture of the brain was systematically taken after each brain mapping along with a written record of the findings during stimulation. Intraoperative photographs of the brain indicated the sites of positive or negative response to cortical stimulation. Standard brain mapping in a monolingual with 2 tasks (naming and reading) lasted less than 20 minutes.

Before mapping, and thus in the absence of any functional data, the surgeon evaluated which approach he would choose to remove the tumor and where he would place the cortectomy. This initial approach could be modified by functional data obtained by stimulation, ie, presence or absence of language interference sites. Our policy was to spare language areas found by electrostimulation during the tumor removal by avoiding the resection of tissue located closer than 1 cm to an "eloquent" brain area. Gross-total removal was attempted in all cases. The rule was to spare eloquent areas unless in selected rare oncological cases.

Scientific (brain-mapping data) and clinical data from these successive brain mappings were prospectively collected by the same team using the same protocol over the years. This series focused on the possible usefulness of AC with brain mapping vs GA without brain mapping, and

Copyright © Congress of Neurological Surgeons. Unauthorized reproduction of this article is prohibited.

not on the results of brain mapping itself. Brain-mapping data from such large series of patients bring a very large amount of data. These data cannot be detailed here because of the limited space allowed for each article and will be discussed further in the future.

Postoperative Management

After the procedure, all patients were admitted to the postanesthesia care unit and intensive care unit (ICU). Postoperative MRI was performed within 48 hours to determine the quality of lesion removal. The extent of tumor resection was assessed by a neuroradiologist according to a classification reported by Berger et al.[13] Resection was considered as total if there was no residual signal abnormality, subtotal (ie, <10 mL of residue), or partial indicating more than 10 mL of residual tumor. In both groups, all survivors had a follow-up MRI, clinical examination, and Karnofsky Performance scoring at 3 months and 1 year after surgery.

Statistical Analysis

Comparison between groups included the quality of tumor resection, duration of surgery, anesthetic and surgical complications, rate of postoperative neurological deficits, and hospital unit stay. Statistical analysis was performed by an independent statistician using the Sigma Stat® 3.5 software package (Systat Inc., Point Richmond, California). Qualitative variables were compared using the χ^2or Fisher exact test, and variance analysis or nonparametric tests were used for continuous variables. Cumulative survival rates were estimated by use of Kaplan-Meier methods and multiple comparison procedures (Holm-Sidak method). A P value of <.05 was considered significant.

TABLE 1. Clinical Characteristics of the Study Population[a]

	AC (n = 214)	GA (n = 361)	GA_{72} (n = 72)
Median age, y	46.5	46	46.3
Female, %	46.7	50.7	52.7
Right-handed, %	94	95.6	96
ASA I and II, %	45	43	39
ASA III, %	54	55.6	59.6
ASA IV, %	1	1.4	1.4
KPS ≥ 70, %	78	76.5	73.6
Overall preop deficit	45%	15%	47%
Motor deficit, %	12	6	20.5
Speech deficit, %	22.5	2	5.4
Other deficits, %	10.7	7.2	20.8
Brain lesion localization			
Right frontal, %	14	16.5	13.8
Left frontal, %	38.8	4.3	7
Right temporal, %	6.5	18	15.2
Left temporal, %	15	7	8.3
Right parietal, %	5.3	4.5	2.7
Left parietal, %	16.4	3.4	4.1
Right T-O or P-O, %	1.2	18.	16.6
Left T-O or P-O, %	2.8	28	32

[a]ASA, American Society of Anesthesiologists; AC, awake craniotomy; GA, general anesthesia; preop, preoperative; GA_{72}, subset of 72 patients with lesions in eloquent areas; KPS, Karnofsky Performance Score; T-O, temporo-occipital; P-O, parieto-occipital.

RESULTS

The median follow-up period was 34.7 months (range, 21-111 months). The 2 groups are comparable in their clinical and histological characteristics (Tables 1 and 2) but differ with regard to tumor location and preoperative neurological deficits. All AC patients had tumors in eloquent areas. The GA group had tumors in eloquent (72 cases, 20%) and noneloquent areas (80%). Thus, not surprisingly, patients in the GA group had fewer clinical deficits than AC patients. However, no statistical difference was found between the AC and GA_{72} groups concerning preoperative neurological deficits and tumor location (P = .65).

The awake and GA groups underwent a first-time craniotomy in 86% and 88%, respectively. Presenting symptoms include seizure in both groups (52%), sensory, motor, speech, visual, and writing deficits, Gerstmann syndrome, or cognitive disorder. Lesions were larger than 5 cm in diameter in 28.5% of AC cases and in 34% of GA cases; they were smaller than 3 cm in 32% and 31.6% of AC and GA series, respectively.

Peroperative Events

In the AC group, monitored procedural sedation was performed without significant anesthetic complications and no conversion to GA. There were no instances of severe respiratory depressions or significant increased arterial pressure and tachycardia. Intraoperative seizures occurred in 14 procedures (5.7%). The seizures resolved by irrigation of the cortex with cold saline in all but one case. In the latter, propofol administration was effective. Cortical and/or subcortical mapping identified the eloquent cortex in 179 patients (84%). We directly performed resection in these patients or alternate routes were taken to avoid neurological deficits, while the 35 patients (16%) with absence of a functionally active cortex during mapping had gross-total resection.

In the GA group, significant peroperative hemorrhages forced us to abandon the tumor resection in 4 patients; only biopsies were performed.

The durations of operations were equivalent in both the AC and GA groups with P = .83 (Table 3). Complete and subtotal resections were achieved in 82% of awake patients vs 40% of the GA_{72} group (P < .001). However, no significant difference (P = .24) was found between the AC and GA group in terms of quality of resection (Table 3). Postoperatively, 98% of the AC patients were admitted to the ICU with a mean ICU stay of 1 day (range, 1-2 days), whereas all the patients in the GA group were admitted to the ICU with a mean duration of 3.8 days (range, 1-29 days). Second-look surgery was performed in 30 patients of the AC group from 2 days to 5 years after first surgery. Of those 30 patients, tumor removal was qualified as complete on postoperative MRI in 19 of the patients. Finally, to evaluate the perception of the awake surgery procedure, a postoperative anesthetic interview was recorded in 186 patients, and 96.5% expressed satisfaction with their experience.

Copyright © Congress of Neurological Surgeons. Unauthorized reproduction of this article is prohibited.

TABLE 2. Pathology of the Brain Lesions of the Study Population[a]

	AC (n = 214) n (%)	GA (n = 361) n (%)	GA_{72} (n = 72) n (%)
Gliomas	143 (67)	213 (59)	45 (62.5)
Astrocytoma I/II	24 (11)	49 (13.5)	7 (10)
Astrocytoma III	7 (3)	15 (4)	8 (11)
Glioblastoma	45 (21)	75 (20.7)	17 (23.6)
Oligodendroglioma II	30 (14)	40 (11)	4 (5.5)
Oligodendroglioma III	18 (8.4)	19 (5)	3 (4)
Oligoastrocytoma II	16 (7.4)	12 (3.3)	3 (4)
Oligoastrocytoma III	1 (0.4)	1 (0.2)	3 (4)
Ganglioglioma	2 (0.9)	2 (0.5)	0 (0)
Tumor metastases	42 (20)	77 (21.3)	16 (22.2)
From lung cancer	19 (8.8)	45 (12.4)	10 (1.3)
Breast	10 (4.6)	16 (4.4)	4 (5.5)
Colorectal	4 (1.8)	4 (1)	0 (0)
Melanoma	3 (1.4)	6 (1.6)	1 (1.3)
Renal	2 (0.9)	3 (0.8)	0 (0)
Other metastases	4 (1.8)	3 (0.8)	1 (1.3)
Miscellaneous	29 (13)	71 (19.7)	11 (15.3)
Cavernous malformation	22 (10)	23 (6.3)	3 (4)
Meningioma	2 (0.9)	40 (11)	7 (10)
Others[b]	5 (2)	8 (2)	1 (1.3)

[a]AC, awake craniotomy; GA, general anesthesia; GA_{72}, subset of 72 patients with lesions in eloquent areas.
[b]Others: Dysembryoplastic neuroepithelial tumors, arteriovenous malformation, abscess.

TABLE 4. Complications in the Study Population[a]

Nature of Complication	AC Group (n = 214) n (%)	GA Group (n = 361) n (%)	GA_{72} Group (n =72) n (%)
Regional	8 (3.7)	12 (3.2)	5 (6.9)
Wound infection	3 (1.4)	4 (1.1)	1 (1.3)
Abscess/empyema	1 (0.4)	2 (0.5)	1 (1.3)
CSF leak	0	2 (0.5)	1 (1.3)
Hematoma	4 (1.8)	4 (1.1)	2 (2.7)
Medical	2 (0.9)	24 (6.6)	10 (14)
Deep vein thrombosis	1 (0.4)	5(1.4)	2 (2.7)
Pulmonary embolus	0	2 (0.5)	1 (1.3)
Hyponatremia	1 (0.4)	5 (1.4)	2 (2.7)
Urinary tract infection	0	7 (1.9)	3 (4.1)
Pulmonary infection	0	5 (1.4)	2 (2.7)
Neurological[b]	62 (28.9)	65 (18.0)	60 (83.3)
Speech deficit	25 (11.6)	22 (6.1)	20 (27.7)
Seizure	10 (4.6)	7 (1.9)	6 (8.3)
Motor deficit	13 (6.0)	24 (6.6)	22 (30.5)
Sensory deficit	2 (0.9)	3 (0.8)	3 (4.1)
Visual deficit	3 (1.4)	4 (1.1)	4 (5.5)
Cognitive deficit[c]	9 (4.2)	5 (1.4)	5 (6.9)
Total,[c] n (%)	72 (33.6)	111 (30.7)	72 (100)

[a]AC, awake craniotomy; GA, general anesthesia; GA_{72}, subset of 72 patients with lesions in eloquent areas.
[b]Transient and permanent neurological complications.
[c]Three patients in the GA_{72} group had mixed complications.

Morbidity and Mortality

Table 4 represents the morbidity of the study population. The median length of stay was 5.4 days in the AC group, 8.5 days in the GA group, and 12.7 days in the GA_{72} patients.

Within 90 days of the operation, the mortality in the AC and GA groups was 0% and 0.5%, respectively. At 3 months, there were 2 deaths in the GA_{72} group. The neurological outcomes of the study population are presented in Table 5.

The permanent neurological deficits were significantly lower ($P < .001$) in the AC group (4.6%), compared with the GA_{72} group (16%). These deficits were more common in patients with preoperative mild neurological deficits. Conversely, patients who were without deficit before surgery had a lower neurological complication rate than patients with preoperative deficits. Thus, in the AC group, among 118 patients without preoperative neurological deficits, 4 patients (3%) had deficits postsurgically, compared with 55% (53/96) in patients with deficits presurgically ($P < .001$).

Patients in whom mapping successfully identified functional tissue had more transient neurological deficits (27%, 48/179) than patients with negative brain mapping (11.4%, 4/35), with $P = .08$.

New neurological deficits were seen in 3.3% of patients (7/214) in the AC series, compared with 58% (42/72) in the GA_{72} cohort ($P < .001$).

In both groups, the rate of new neurological deficits was much higher in the redo surgery than in the primary operation. Three other factors were significant independent predictors of poor neurological outcome: preoperative Karnofsky Performance Score <70, histological diagnosis of a glioma or metastasis, and age at surgery >70.

Figures 1 to 4 show overall mortality between groups including patients with malignant lesions (metastasis, low- and high-grade gliomas). Survival at 80 months was better in the AC group than in the GA or GA_{72} groups.

TABLE 3. Operating Room Stay, Operation Duration in Minutes, and Quality of Tumor Removal in the Study Population[a]

	AC (n = 214)	GA (n = 361)	GA_{72} (n = 72)
Operating room stay, min	244.3	246.5	258
Operation duration, min	135	132	149
Total removal, %	37	52	14
Subtotal removal, %	45	34	26

[a]AC, awake craniotomy; GA, general anesthesia; GA_{72}, subset of 72 patients with lesions in eloquent areas.

Copyright © Congress of Neurological Surgeons. Unauthorized reproduction of this article is prohibited.

TABLE 5. Neurological Outcome in Study Population at 3 Months After Surgery[a]

Groups[b]	Preoperative Status	n	New Deficit, n (%)	Transient Deficit, n (%)	Permanent Deficit, n (%)
AC	All patients	214	7 (3.3)	52 (24)	10 (4.6)
	No deficit	118	4 (3.3)	2 (1.7)	2 (1.7)
	With deficit	96	3 (3.1)	50 (52)	8 (8.3)
GA_{72}[c]	All patients	70	40 (57)	59 (84)	11 (16)
	No deficit	38	38 (100)	35 (92)	3 (7.8)
	With deficit	32	2 (6.2)	24 (75)	8 (25)
GA	All patients	359	47 (13)	81 (22.5)	13 (3.6)
	No deficit	306	43 (14)	37 (12)	4 (1.3)
	With deficit	53	4 (7.5)	44 (83)	9 (17)

[a]No significant difference was found between the AC and GA group. The neurological outcome was better in the AC group than in the GA_{72} group.
[b]AC, awake craniotomy; GA, general anesthesia; GA_{72}, subset of 72 patients with lesions in eloquent areas.
[c]There were 2 deaths in the GA_{72} group at 3 months.

DISCUSSION

This study shows that patients with supratentorial lesions in proximity to the eloquent cortex had better neurological outcome and maximal tumor removal with AC than surgery under GA. Studies comparing these 2 anesthetic options are rare in the literature. Ethical considerations, particularly the need for randomizations, are plausible reasons for such paucity. Comparative studies can also be biased by the variability of surgical procedures among teams and small sample sizes. Even though we studied a large series with similar surgical procedures, we initially decided not to randomly select patients for ethical and clinical reasons. Consequently, patients with tumors in the eloquent areas were preferentially allocated to the AC group, while uncooperative or other patients were placed in the GA group. Preoperatively, patients in the AC group had more neurological deficits. However, their functional outcome and the quality of tumor resection were similar to the entire GA group but significantly better than the subgroup of GA_{72} patients. AC was well tolerated by our patients and was not considered as a psychologically traumatic experience. This is in line with other studies[14,15] in which some authors[4] found that

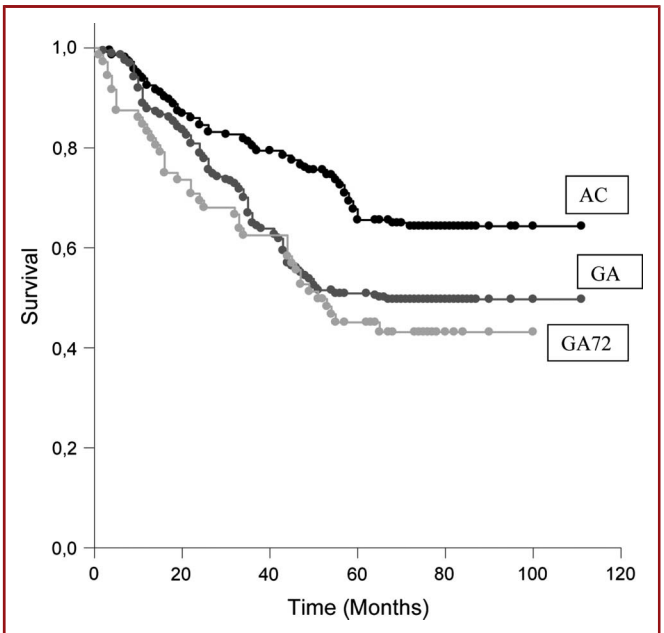

FIGURE 1. *Survival graph showing the overall mortality in AC, GA, and GA_{72} groups, P < .001 (log-rank statistic test = 19).*

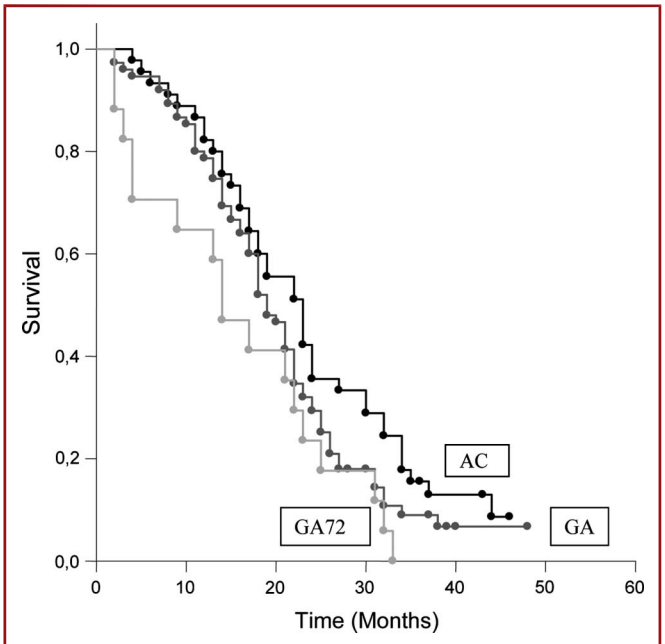

FIGURE 2. *Survival graph displaying the mortality in patients with glioblastoma in AC, GA, and GA_{72} groups, P = .06 (log-rank test statistic = 5.818).*

Copyright © Congress of Neurological Surgeons. Unauthorized reproduction of this article is prohibited.

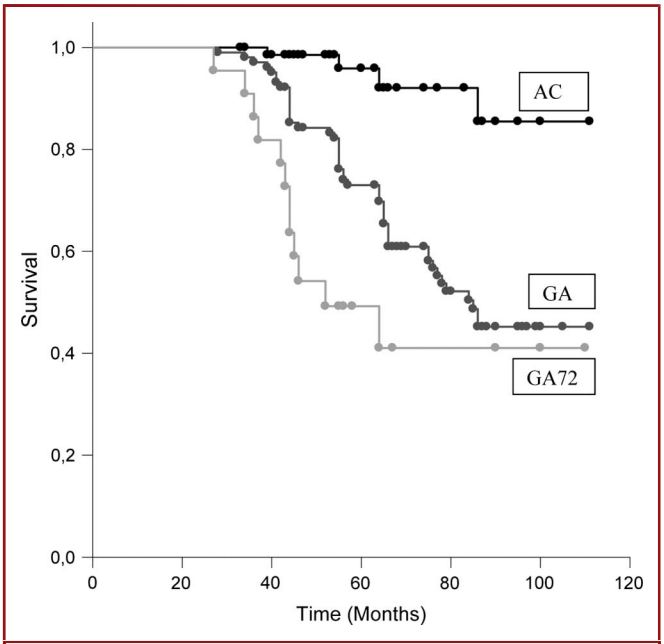

FIGURE 3. *Survival graph depicting the mortality in patients with low-grade glioma in AC, GA, and GA_{72} groups,* $P < .001$ *(log-rank test statistic = 25.646).*

most patients were amnesic to the procedure. In general, considered as an improvement of the management of brain lesions, the topic can nevertheless be controversial.[10]

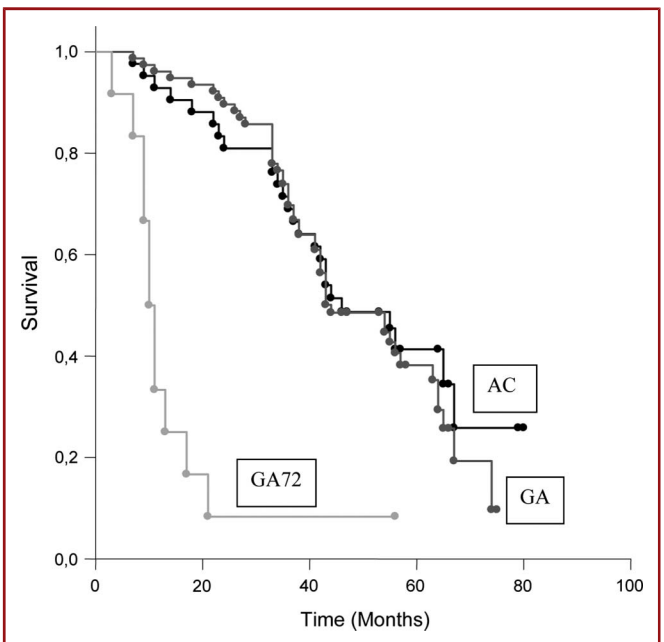

FIGURE 4. *Survival graph showing the mortality in patients with metastasis in AC, GA, and GA_{72} groups,* $P < .001$ *(log-rank test statistic = 46.186).*

In this large series, we observed no significant anesthetic complications with no conversion from awake to GA. Airway control is a serious concern in AC with particular apprehension of hypercapnia-induced brain swelling despite an incidence of less than 1%.[4,5] We observed no such complication in our study. The intraoperative seizures (5.7%) that occurred in this study were rapidly and effectively treated with cold irrigation or propofol boluses.

Our study corroborates other studies regarding short hospital stay limiting nosocomial infection or thromboembolism.[16,17] Like others, we confirm that AC was more economically advantageous from a cost and resource perspective.[5,8] The advantages of AC without brain mapping over GA in patients with significant medical comorbidities had been reiterated by other authors.[8]

Quality of Resection

Previous reports have indicated the positive correlation between prognosis and the quality of tumor resection.[18] In some patients with low-grade gliomas (or in some patients with high-grade gliomas), brain plasticity allows a reorganization of the brain functions. This gives the opportunity to operate on these patients a few months or years after the first operation and complete tumor removal. This reorganization of functional structures is especially true for cortical "nonprimary" functional structures. Although possible, primary sensorimotor cortices are less plastic than secondary cortices. We did not observe such reorganization.

Functional Outcome

Previous reports have indicated a wide range (4% to 23%) of postoperative neurological deficit after awake surgery.[4,5,10,19] Such difference among series could be explained in part by the length of follow-up. In their study on AC, Bernstein et al[8] observed new postoperative neurological deficits in 13% and permanent deficits in 4.5% of patients. Duffau et al[19] found that 6.5% of patients operated on under AC had permanent deficits vs 17% under GA. However, Gupta et al[10] observed more postoperative neurological complications with AC than with GA. They observed new neurological deficits in 19% of AC patients vs 11% of the GA group. In the present series, there were 4.6% permanent neurological deficits in the AC group and 16% in the GA_{72} group. Nevertheless, we found that the absence of response to electrical brain stimulation in eloquent areas does not always guarantee the absence of postoperative dysfunction; 11.4% of awake patients (4/35) in this series sustained transient postoperative neurological deficits despite negative stimulation vs 13.6% in the study of Bernstein et al.[8]

CONCLUSION

Patients with supratentorial lesions in proximity to the eloquent cortex had better neurological outcome and maximal tumor removal with AC than surgery under GA. AC provides a feasible alternative to craniotomy under GA.

Copyright © Congress of Neurological Surgeons. Unauthorized reproduction of this article is prohibited.

Disclosure

The authors have no personal financial or institutional interest in any of the drugs, materials, or devices described in this article.

REFERENCES

1. Berger MS, Ojemann GA. Intraoperative brain mapping techniques in neuro-oncology. *Stereotactic Funct Neurosurg*. 1992;58(1-4):153-161.
2. Berger M. Functional mapping-guided resection of low-grade gliomas. *Clin Neurosurg*. 1995;42:437-452.
3. Sanai N, Berger MS. Mapping the horizon: techniques to optimize tumor resection before and during surgery. *Clin Neurosurg*. 2008;55:14-19.
4. Danks RA, Aglio LS, Gugino LD, Black PM. Craniotomy under local anesthesia and monitored conscious sedation for the resection of tumors involving eloquent cortex. *J Neurooncol*. 2000;49(2):131-139.
5. Taylor MD, Bernstein M. Awake craniotomy with brain mapping as the routine surgical approach to treating patients with supratentorial intraaxial tumors: a prospective trial of 200 cases. *J Neurosurg*. 1999;90(1):35-41.
6. Chakravarthy M, Mitra S, Muralimanohar V, Jawali V. Congenital pleuropericardial fistula complicating awake cardiac surgery. *J Cardiothorac Vasc Anesth*. 2010. [Epub ahead of print]. PMID: 20005743.
7. Torres HM, López SC. Awake laminotomy and discectomy using Dexmedetomidine as anesthetic. *P R Health Sci J*. 2009;28(4):354-355.
8. Serletis D and Bernstein M. Prospective study of awake craniotomy used routinely and nonselectively for supratentorial tumors. *J Neurosurg*. 2007;107(1):1-6.
9. Khu KJ, Doglietto F, Radovanovic I, et al. Patients' perceptions of awake and outpatient craniotomy for brain tumor: a qualitative study. *J Neurosurg*. 2010;112(5):1056-1060.
10. Gupta DK, Chandra PS, Ojha BK, Sharma BS, Mahapatra AK, Mehta VS. Awake craniotomy versus surgery under general anesthesia for resection of intrinsic lesions of eloquent cortex—a prospective randomised study. *Clin Neurol Neurosurg*. 2007;109(4):335-343.
11. Oldfield RC. The assessment and analysis of handedness: the Edinburgh inventory. *Neuropsychologia*. 1971;9(1):97-113.
12. Roux FE, Lubrano V, Lauwers-Cances V, Tremoulet M, Mascott CR, Demonet JF. Intra-operative mapping of cortical areas involved in reading in mono- and bilingual patients. *Brain*. 2004;127(pt 8):1796-1810.
13. Berger MS, Deliganis AV, Dobbins J, Keles GE. The effect of extent of resection on recurrence in patients with low grade cerebral hemisphere gliomas. *Cancer*. 1994;74(6):1784-1791.
14. Manninen PH, Balki M, Lukitto K, Bernstein M. Patient satisfaction with awake craniotomy for tumor surgery: a comparison of remifentanil and fentanyl in conjunction with propofol. *Anesth Analg*. 2006;102(1):237-242.
15. Whittle IR, Midgley S, Georges H, Pringle AM, Taylor R. Patient perceptions of "awake" brain tumor surgery. *Acta Neurochir (Wien)*. 2005;147(3):275-277.
16. Boulton M, Bernstein M. Outpatient brain tumor surgery: innovation in surgical neurooncology. *J Neurosurg*. 2008;108(4):649-654.
17. Baker GR, Norton PG, Flintoft V, et al. The Canadian Adverse Events Study: the incidence of adverse events among hospital patients in Canada. *CMAJ*. 2004;170(11):1678-1686.
18. Duffau H. Lessons from brain mapping in surgery for low-grade glioma: insights into associations between tumor and brain plasticity. *Lancet Neurol*. 2005;4(8):476-486.
19. Duffau H, Lopes M, Arthuis F, et al. Contribution of intraoperative electrical stimulations in surgery of low grade gliomas: a comparative study between two series without (1985–96) and with(1996–2003) functional mapping in the same institution. *J Neurol Neurosurg Psychiatry*. 2005;76(6):845-851.

Acknowledgments

The authors thank Drs Trémoulet, Gigaud, Sabatier, Boetto, Fourcade, Vironneau, Sacrista, Ramonda, Ferrier, and Schmidt for their participation in the clinical management of these patients.

COMMENTS

The authors prospectively compared 214 patients who underwent awake surgery with intraoperative mapping for a brain lesion in eloquent areas, and 361 patients in whom a surgical resection was performed under general anesthesia (in functional regions in 72 cases). The results showed similar functional outcomes between the 2 groups, despite a higher rate of preoperative deficits in the patients operated on under local anesthesia. In addition, when comparing patients with lesion in eloquent areas, both neurological outcome and extent of resection were significantly better in patients who underwent awake craniotomy. The authors conclude that awake surgery with brain mapping is safe and allows maximal resection in functional regions with a low neurological complication rate.

This is a very interesting and original study. Despite an abundant literature on awake surgery and intraoperative brain mapping for lesions involving eloquent areas, few data are available on the comparison between surgical resection under local vs general anesthesia. Here, the authors report a prospective study supporting the significant impact of awake mapping on the optimization of both the functional outcome and extent of resection, at least for lesions located in eloquent structures. Interestingly, these results are in agreement with our own data. Indeed, we have previously reported by comparing 2 groups of patients who underwent surgery for a WHO grade II glioma without mapping vs with mapping, that the use of awake surgery enabled (i) to significantly increase the surgical indications in eloquent areas classically considered "inoperable," (ii) to significantly decrease the rate of permanent deficit, and even to improve the quality of life, and (iii) to significantly increase the extent of resection.[1] More recently, we showed that inpatients who underwent a first surgery under general anesthesia and who benefited thereafter from a second operation with awake conditions for a WHO grade II glioma, the resection was significantly increased in all cases – while brain function was preserved or improved.[2] The results reported by Sacko et al also plead in favor of a more systematic use of awake mapping for all lesions located near or within eloquent areas. These data are very important for the surgical community, because they show that neurosurgeons should change their mind and methodology when operating on the "functional brain."

Hugues Duffau
Montpellier, France

1. Duffau H, Lopes M, Arthuis F, et al. Contribution of intraoperative electrical stimulations in surgery of low grade gliomas: a comparative study between two series without (1985-96) and with (1996-2003) functional mapping in the same institution. *J Neurol Neurosurg Psychiatry*. 2005;76:845-851.
2. De Benedictis A, Moritz-Gasser S, Duffau H. Awake mapping optimizes the extent of resection for low-grade gliomas in eloquent areas. *Neurosurgery* 2010;66:1074-1084.

The authors provide a prospective review of patients undergoing awake craniotomies vs those undergoing surgical resection for brain lesions under general anesthesia. The sample size was large for each group at 214 for the awake craniotomy and 361 under general anesthesia, with 72 undergoing resection with general anesthesia in eloquent cortex. The findings are clear that the patients with awake craniotomies did better in survival, reversing preoperative deficits, and cost savings while those undergoing GA resections near eloquent cortex had a fourfold increase in the number of deficits. The authors have replicated multiple other studies showing the advantages of awake craniotomies for resections near

Copyright © Congress of Neurological Surgeons. Unauthorized reproduction of this article is prohibited.

eloquent cortex. The strength of this study is the large sample size and the overwhelming advantages of awake craniotomies over those done under general anesthesia when operating near eloquent cortex. However, I would disagree with the author's description that the use of awake craniotomies for mapping eloquent cortex "remains controversial" or puts patients at "high risk," rather it is the routine, not the exception at many centers. The authors have appropriately noted that the introduction of new anesthetic agents has greatly eased the ability to perform awake craniotomies, making it more readily available. The authors are to be congratulated for compiling such a large series, and their findings contribute to the already overwhelming evidence that awake craniotomies increase safety of the resections, decrease the length of stay, and lead to more favorable outcomes in both function and survival.

Michael M. Haglund
Durham, North Carolina

Copyright © Congress of Neurological Surgeons. Unauthorized reproduction of this article is prohibited.

Stereotactic Radiosurgery of Cranial Nonvestibular Schwannomas: Results of Single- and Multisession Radiosurgery

Clara Y.H. Choi, MD, PhD*
Scott G. Soltys, MD‡
Iris C. Gibbs, MD‡
Griffith R. Harsh, MD*
Gordon T. Sakamoto, MD*
Deep A. Patel, MD‡
Robert E. Lieberson, MD*
Steven D. Chang, MD*
John R. Adler, MD*

*Department of Neurosurgery, Stanford University Medical Center, Stanford, California; ‡Department of Radiation Oncology, Stanford University Medical Center, Stanford, California

Correspondence:
Clara Y.H. Choi, MD, PhD,
Department of Neurosurgery,
300 Pasteur Drive,
Stanford, CA 94305.
E-mail: cyhchoi@stanford.edu

Received, April 26, 2010.
Accepted, August 23, 2010.

Copyright © 2011 by the
Congress of Neurological Surgeons

BACKGROUND: Surgical resection of nonvestibular cranial schwannomas carries a considerable risk of postoperative complications. Stereotactic radiosurgery (SRS) offers a non-invasive treatment alternative. The efficacy and safety of multi-session SRS of nonvestibular cranial schwannomas has not been well studied.

OBJECTIVE: To analyze the results of single- and multi-session SRS of nonvestibular cranial schwannomas.

METHODS: From 2001 to 2007, 42 lesions in 40 patients were treated with SRS at Stanford University Medical Center, targeting schwannomas of cranial nerves IV (n = 1), V (n = 18), VII (n = 6), X (n = 5), XII (n = 2), jugular foramen (n = 8), and cavernous sinus (n = 2). SRS was delivered to a median marginal dose of 18 Gy (range, 15-33 Gy) in 1 to 3 sessions, targeting a median tumor volume of 3.2 cm^3 (range, 0.1-23.7 cm^3). The median doses for treatments in 1 (n = 18), 2 (n = 9), and 3 (n = 15) sessions were 17.5, 20, and 18 Gy, respectively.

RESULTS: With a median follow-up of 29 months (range, 6-84 months), tumor control was achieved in 41 of the 42 lesions. Eighteen of 42 lesions (43%) decreased in size; 23 tumors (55%) remained stable. There were 2 cases of new or worsening cranial nerve deficits in patients treated in single session; no patient treated with multi-session SRS experienced any cranial nerve toxicity ($P = 0.18$).

CONCLUSION: SRS of nonvestibular cranial schwannomas provides excellent tumor control with minimal risk of complications. There was a trend towards decreased complications with multi-session SRS.

KEY WORDS: CyberKnife, Multisession, Nonvestibular schwannoma, Radiation, Stereotactic radiosurgery

Neurosurgery 68:1200–1208, 2011 DOI: 10.1227/NEU.0b013e31820c0474 www.neurosurgery-online.com

Cranial schwannomas are, for the most part, benign, Schwann cell–derived tumors. Most of them originate from the vestibular portion of cranial nerve (CN) VIII. Nonvestibular schwannomas are rare, accounting for less than 10% of intracranial schwannomas.[1] Patients typically present with neurological deficits caused by tumor compression, dysfunction of the affected cranial nerve, or hydrocephalus. Surgery traditionally has been the standard primary treatment.[2] Despite advances in surgical techniques, the risk of morbidity continues to be significant, with postoperative cranial nerve dysfunction reported in 6% to 64% of cases.[3-7]

ABBREVIATIONS: CN, cranial nerve; **GTV,** gross tumor volume; **IPEH,** intravascular papillary endothelial hyperplasia; **LQ,** linear-quadratic; **PIV,** prescribed isodose volume; **SRS,** stereotactic radiosurgery; **TIV,** tumor volume encompassed by the prescription isodose line

Stereotactic radiosurgery (SRS) offers an alternative treatment option to surgical therapy of schwannomas. SRS precisely and accurately targets the tumor with high doses of ionizing radiation. Excellent tumor control rates have been seen after the treatment of vestibular schwannomas with SRS.[8-11] Due to their rarity, the outcome data are far less abundant for nonvestibular cranial schwannomas, however. We retrospectively reviewed the outcomes of patients with nonvestibular cranial schwannomas treated with SRS in our institution. Most of the patients in this series were treated using a multisession treatment scheme, with the goal of reducing long-term radiation toxicity. Our outcomes demonstrated excellent efficacy and safety.

Copyright © Congress of Neurological Surgeons. Unauthorized reproduction of this article is prohibited.

MATERIALS AND METHODS

Patients

Patient data were obtained from an institutional review board–approved review of a prospectively maintained database of patients treated with SRS at Stanford University Medical Center. From May 2001 to November 2007, 45 patients with nonvestibular cranial schwannomas were treated. Five patients were lost to follow-up, yielding 42 lesions in 40 patients. The diagnosis was made histologically in 18 patients and radiographically in the remaining 22 patients.

Patient characteristics are listed in Table 1. Thirteen women and 27 men received SRS at a median age of 50 years (range, 15-80 years). Six had a known diagnosis of neurofibromatosis type 1 (n = 1) or type 2 (n = 5). The cranial schwannoma nerve of origin could be named in 32 lesions (76%).

Because the exact nerve of origin could not be identified for the remaining 10 lesions, they are listed by their location: jugular foramen (n = 8) and cavernous sinus (n = 2). Tissue diagnosis was available for 6 of the 10 lesions: 5 jugular foramen and 1 cavernous sinus schwannomas. For the remaining 4 without tissue diagnosis, MRI scans were reviewed by experienced neuroradiologists at our institution; the imaging characteristics were most consistent with schwannomas.

TABLE 1. Patient Characteristics (n = 40)[a]

Age at treatment, y	
Median	50 (range, 15-80)
Sex	
Women	13 (32%)
Men	27 (68%)
Location (n = 42)	
CN IV	1 (2%)
CN V	18 (43%)
CN VII	6 (14%)
CN X	5 (12%)
CN XII	2 (5%)
Jugular foramen[b]	8 (19%)
Cavernous sinus[b]	2 (5%)
Presenting symptoms for patients receiving primary SRS[c] (n = 32)	
Headache	2 (6%)
Facial pain	2 (6%)
Facial numbness	7 (22%)
Facial palsy	4 (13%)
Hearing loss	7 (22%)
Diplopia	2 (6%)
Swallowing difficulty	2 (6%)
Tongue weakness	1 (3%)
Tinnitus	4 (13%)
Ataxia	1 (3%)
Comorbidity	
Neurofibromatosis 1	1
Neurofibromatosis 2	5
Patients with previous surgery or biopsy (n = 40)	17 (43%)

[a]CN, cranial nerve; SRS, stereotactic radiosurgery.
[b]The exact nerve of origin could not be identified. These are listed by their location.
[c]Some patients presented with more than 1 symptom.

Eighteen patients (45%) had undergone 1 to 2 (median, 1) prior surgical resections 1 to 167 months before SRS (median, 7 months). Indications for SRS were radiographically progressive, recurrent, and/or symptomatic tumors. Patients in the present series underwent SRS for primary treatment for symptomatic tumors (n = 21), residual tumor after subtotal resection (n = 9), recurrent tumor after previous surgery (n = 8), and asymptomatic tumor treated to prevent neurological symptoms (n = 4).

Treatment Characteristics

Treatment characteristics are outlined in Table 2. The prescribed dose and fractionation schedule were based on the preference of the treating physicians, size of the lesion, and the proximity of the lesion to critical structures. Patients were treated in a single session unless the tumor was located adjacent to critical structures, eg, optic apparatus (n = 3), brainstem (n = 4), CN VII/VIII complex (n = 4), or other cranial nerves (n = 2); was of large volume (median volume 22 cm^3, n = 5); or was both large and located adjacent to a critical structure (n = 6). Due to the range in prescribed dose and number of sessions, the biologically effective dose and equivalent single-session dose were derived using the linear quadratic model,[12] with an α/β ratio of 3.

A total of 42 lesions were treated in 1 to 3 sessions, using a median marginal dose of 18 Gy (range, 15-33 Gy) prescribed to the median 80% (range, 67% to 85%) isodose line, targeting a median volume of 3.2 cm^3 (range, 0.1-23.7 cm^3). The median conformity index was 1.38 (range, 1.12-2.42). Eighteen lesions (43%) were treated in a single session, and the remaining 24 lesions (57%) were treated in 2 (n = 9) or 3 (n = 15) sessions. The median doses for treatments in 1, 2, and 3 sessions were 17.5, 20, and 18 Gy, respectively. The median calculated biologically effective single-session equivalent dose was 15 Gy_3 (range, 11-20 Gy_3).

Radiosurgical Technique

The CyberKnife Robotic Radiosurgical System (Accuray, Sunnyvale, California) was used to deliver the radiosurgical treatments. A high-resolution, thin-slice (1.25 mm) CT scan was obtained using a GE Light Speed 8i or 16i Scanner (Milwaukee, Wisconsin) after administration of 125 mL of Omnipaque intravenous contrast (iohexol, 350 mg I/mL; Nycomed, Inc., Princeton, New Jersey). A stereotactic MRI scan was obtained and fused to the stereotactic CT scan to improve target identification.

The neurosurgeon, radiation oncologist, and radiation physicist performed tumor delineation, dose selection, and planning. Treatment plans were generated using the CyberKnife non-isocentric iterative inverse treatment planning software. Quality of treatment plans was assessed by evaluating target coverage, dose heterogeneity, and conformity. The conformity index (calculated as the prescribed isodose volume [PIV]/tumor volume encompassed by the prescription isodose line [TIV]) and the modified conformity index ([PIV × TIV]/tumor volume^2) were calculated.[13-16] Digitally reconstructed radiographs were computationally synthesized to allow real-time patient tracking throughout radiosurgery. Informed consent for treatment was obtained for all patients. Patients received 4 mg of dexamethasone immediately after each treatment. For multisession treatments, the typical interfraction time interval was 24 hours.

Follow-up

Patients were followed with physician clinic visits and imaging studies every 6 months for the first 1 to 2 years and then annually thereafter.

Copyright © Congress of Neurological Surgeons. Unauthorized reproduction of this article is prohibited.

TABLE 2. Treatment Characteristics (n = 42)

Number of lesions treated per patient	
Median	1 (range, 1-2)
Sessions, no. (%)	
1	18 (43)
2	9 (21)
3	15 (36)
Marginal dose, Gy, median (range)	
Median	18 (15-33)
1 session	17.5 (15-20)
2 sessions	20 (18-20)
3 sessions	18 (18-33)
Prescription isodose line, %	
Median (range)	80 (67-85)
Target volume, cm^3	
Median (range)	3.2 (0.1-23.7)
Conformity index	
Median (range)	1.38 (1.12-2.42)
Biologically effective single-session equivalent dose ($\alpha/\beta = 3$), Gy_3	
Median (range)	15 (11-20)

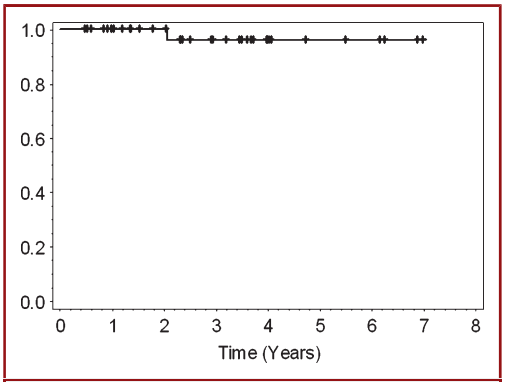

FIGURE 1. *Kaplan-Meier expansion-free tumor control rate for all 42 lesions, calculated from the date of SRS.*

Statistics

Tumor control rate is defined as having no evidence of tumor enlargement on follow-up MRI scans. Tumor volume estimates were calculated using

$$\text{volume} = \frac{4}{3}\pi(\text{abc}),$$

where a, b, and c are equatorial and polar radii. The expansion-free tumor control rate was calculated using the Kaplan- Meier product-limit method[17] using Stat View, version 5.0.1 (SAS Institute Inc, Cary, North Carolina). Fisher's exact test was used to compare crude rates of complications between single- and multisession SRS.

RESULTS

Tumor Control

With a median follow-up of 29 months (range, 6-84 months), expansion-free tumor control has been achieved in 41 of the 42 treated lesions. A Kaplan-Meier plot of expansion-free tumor control is shown in Figure 1. The 3-year actuarial tumor control rate is 96%. Eighteen of the 42 lesions (43%) decreased in size, including 3 with complete responses (ie, no residual tumor seen on follow-up imaging; Figure 2); 23 tumors (55%) have remained stable.

Analysis of patients with more than 1 year of follow-up yielded 37 treated lesions in 35 patients. With a median follow-up of 3 years (range, 1-7 years), expansion-free tumor control has been achieved in 36 of the 37 treated lesions. Twenty-five patients had more than 2 years of follow-up (median, 3.6 years; range, 2.1-7 years), with tumor control achieved in 24 of the 25 treated lesions.

There has been one case of tumor expansion. Twenty-five months following SRS to treat a trigeminal schwannoma (18 Gy in a single session prescribed to the 83% isodose line), a follow-up MRI scan revealed a slight increase in the size of the lesion, with development of a cyst—an increase from 1.1 × 1.7 × 1.5 cm to 1.5 × 2.1 × 2.1 cm. None of the patients treated with multisession SRS has had tumor expansion (P = .43). Extrapolating from the vestibular schwannoma literature, which illustrates that transient tumor expansion requiring no additional treatment can be seen in approximately 14% of the vestibular schwannomas treated with SRS,[18] we have elected to manage this patient with close observation and serial imaging studies.

Six patients had cystic schwannomas at the time of SRS. Following SRS, there was a reduction in cyst volume in 3 of the 6 and a complete disappearance of the cyst in 1 patient; 2 cystic lesions have remained unchanged. The patient with tumor expansion, described earlier, did not have a cystic tumor at the time of SRS; however, the follow-up MRI scan showed an increase in tumor volume with development of a cyst.

Neurological Outcomes

Eleven of the 18 patients with prior surgery presented for SRS with pre-existing neurological deficits attributed to their prior surgical resection: facial numbness (n = 5), facial weakness (n = 3), hearing loss (n = 3), and lower cranial nerve palsies (n = 4). None of these postsurgical cranial neuropathies worsened following SRS.

Of the 23 patients receiving primary SRS, 4 patients had incidentally discovered schwannomas on routine follow-up imaging studies with no neurological symptoms attributable to their lesions but opted for treatment with the goal of preventing neurological symptoms; all remain symptom-free following SRS. Pre-SRS neurological deficits experienced by the 19 patients undergoing primary SRS are listed in Table 1. Of these 19 patients, 5 patients reported improvement of their symptoms following SRS. Those symptoms, and the causative schwannomas, were as follows:

- Headache (vagal schwannoma);
- Headache (cavernous sinus schwannoma);
- Diplopia (cavernous sinus schwannoma);

Copyright © Congress of Neurological Surgeons. Unauthorized reproduction of this article is prohibited.

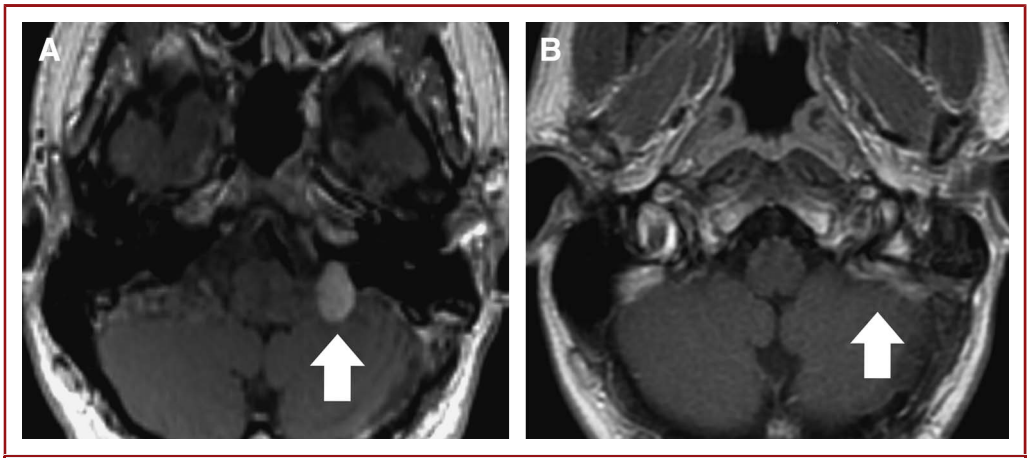

FIGURE 2. **A**, *pre-SRS MRI scan showing a left jugular bulb schwannoma.* **B**, *follow-up MRI scan obtained 12 months following SRS (18 Gy in a single session prescribed to the 80% isodose line).*

- Hoarseness and globus sensation (vagal schwannoma); and
- Ataxia, tinnitus, and decreased hearing (trigeminal schwannoma).

Complications

Two patients (5%) experienced new or worsening cranial nerve deficits: The first patient received SRS (17 Gy in a single session prescribed to the 72% isodose line) to treat a 2.0-cm^3 left trigeminal schwannoma after presenting with tongue and facial numbness. After a 3-month period of complete symptom resolution following SRS, the patient experienced recurrence of the facial numbness, along with ipsilateral jaw weakness and facial dysesthesia. An MRI scan demonstrated edema of the adjacent lateral pons. The patient was observed closely without corticosteroids, with ultimate resolution of the edema and improvement of numbness and jaw weakness by 12 months. The Common Terminology Criteria for Adverse Events (CTCAE) v3.0 Grade 2 facial dysesthesia improved after treatment with gabapentin. The second patient, 18 months following SRS (18 Gy in a single session prescribed to the 83% isodose line targeting a 17.7 cm^3 gross tumor volume [GTV]) for a large hypoglossal schwannoma involving the skull base, recurrent after prior surgery, developed left facial weakness and tinnitus. An MRI scan revealed that the treated tumor was smaller; however, there was an increased signal in the lateral left brainstem, adjacent to the tumor, likely representing radiation necrosis. He is being managed conservatively. Both of these patients were treated with single-session SRS. None of the patients treated with multisession SRS experienced any cranial nerve toxicity; however, this difference did not reach statistical significance (P = .18).

Two patients reported nausea following SRS to treat vagal schwannomas. One patient experienced acute nausea and vomiting 1 day after undergoing SRS for a vagal schwannoma with extension into the right jugular foramen (16 Gy in a single session prescribed to the 80% isodose line targeting a GTV of 6.4 cm^3). This patient was hospitalized overnight and treated with IV fluids and corticosteroids. His symptoms resolved during the hospital stay, and he was discharged home with a 2-week course of corticosteroids. He has remained well. A second patient reported intermittent nausea and multiple, vague symptoms involving the right head and neck (pain involving the right side of the head, eye, and neck, right neck spasm, and right throat pressure) following tri-session SRS (21 Gy total dose targeting a GTV of 22.1 cm^3) to treat a right-sided vagal schwannoma. The nausea has since resolved. The vague and intermittent nature of his other complaints makes it difficult to assess whether they are due to radiation.

Finally, we observed 1 unusual case of a possible radiation-associated complication. Four years following SRS for a cavernous sinus schwannoma (20 Gy in a single session prescribed to the 82% isodose line targeting a GTV of 4.4 cm^3), the patient presented with headache and short-term memory loss. An MRI scan revealed enlargement of a heterogeneously enhancing lesion within the medial temporal lobe with a large area of surrounding edema. He underwent a stereotactic biopsy and subsequent surgical resection. The pathology was not radiation necrosis but, rather, intravascular papillary endothelial hyperplasia (IPEH) or Masson's vegetative hemangioendothelioma.[19] This patient's IPEH is temporally and spatially associated with radiation. We have observed 1 additional case of a radiation-associated IPEH at our institution in an unrelated case (ie, not a schwannoma); these cases will be reported in a future publication.

Survival

Two patients in this series have died. One patient died of an unrelated esophageal cancer. The second patient presented to our institution following multiple surgeries for a cystic trigeminal schwannoma with consequent facial paralysis, hearing loss, and severe dysfunction of CN IX, X, and XI resulting in dysphasia and chronic aspiration pneumonia. The patient was referred due to a residual, progressive tumor near the foramen magnum. After discussing the treatment options, risks, and benefits, the patient

Copyright © Congress of Neurological Surgeons. Unauthorized reproduction of this article is prohibited.

elected to proceed with radiosurgery. His postsurgical neurological deficits did not improve following SRS. The MRI scan, obtained 7 months following SRS, showed a stable tumor. Eleven months following radiosurgery, the patient died as a result of seizures. The location of this patient's schwannoma makes it unlikely that either the tumor or the treatment would be the cause of this patient's seizure disorder. The etiology of this patient's seizures was not identified.

DISCUSSION

Surgery

Nonvestibular cranial schwannomas are rare. Most are benign, and symptoms often are related to the affected cranial nerve, compression of the brainstem, or hydrocephalus. Surgical resection has traditionally been the standard treatment, and advances in surgical techniques have led to tumor control rates of 81% to 100%.[4-6,20-26] Despite such improvements, the risk of serious postoperative complications and cranial nerve deficits remain significant.[5,6,21,23-29] The rate of new cranial nerve dysfunction following surgical resection of nonvestibular cranial schwannomas ranges from 0% to 71%,[5,6,21,23-29] with meningitis, cerebrospinal fluid leak, arterial vasospasm, hydrocephalus, hemiplegia, and death occurring in up to 2% of patients.[2]

Neurological deficits involving the lower cranial nerves are of particular concern because subsequent breathing difficulty, dysphagia, and aspiration pneumonia can be life-threatening. In the 3 largest jugular foramen schwannoma surgical series, the rates of new or worsening lower cranial nerve deficits were observed in 30% to 50%.[6,21,24] Additionally, schwannomas extending into multiple fossae may carry a higher risk of postoperative complications. Yoshida and Kawase[25] performed surgery on 27 patients with trigeminal schwannomas extending into multiple fossae. Five patients had recurrences, and 20 patients experienced complications, including CN VI palsy (n = 3), CN VII paresis (n = 2), total ophthalmoplegia (n = 2), CN V hypesthesia (n = 8), CN V anesthesia (n = 2), temporal lobe contusion (n = 2), and lower extremity peripheral neuropathy (n = 1).[25]

Conventionally Fractionated External Beam Radiotherapy

Published reports on the efficacy and safety of conventionally fractionated external beam radiotherapy treatment of vestibular schwannomas reveal 93% to 98% tumor control.[30-35] Due to its rarity, the data on cranial nonvestibular schwannoma treated with conventionally fractionated radiotherapy are limited (Table 3). Although the patient numbers are small, ranging from 8 to 24 patients, recent publications report excellent results, with 0% to 6% local failure rate and no new cranial nerve deficits.[36-40] A major disadvantage of conventionally fractionated radiation compared to SRS is the inconvenience of the protracted treatment course, requiring 25 to 32 daily radiation sessions. Therefore, a therapeutic approach that can deliver similar tumor control and complication outcomes is an attractive option.

Stereotactic Radiosurgery

Stereotactic radiosurgery is a noninvasive treatment option with proven efficacy and safety in treatment of vestibular schwannoma.[8-11] Kondziolka et al[11] reported a 98% resection-free tumor control rate in their series of 162 patients treated with 14 to 20 Gy single-session gamma knife radiosurgery. The same group later published their series of 252 patients with acoustic neuromas who were treated with gamma knife radiosurgery using a median marginal dose of 13 Gy (range, 10-20 Gy), resulting in a 98% tumor control rate.[9] In our own experience, 98% of patients with acoustic neuromas achieved tumor control with multisession SRS.[10]

Extrapolating from these excellent outcomes, we and other researchers have employed SRS to treat nonvestibular cranial schwannomas. Because of its rarity, series reporting SRS treatment of nonvestibular cranial schwannoma include fewer patients. As seen in the summary of published series presented in Table 4, the majority are of single-session SRS. SRS results in tumor control rates of 86% to 100%, similar to those of the best surgical series.[1] Perhaps more importantly, the rate of cranial nerve dysfunction following SRS is markedly lower than that observed in the modern surgical series (0% to 17% vs 0% to 75%, respectively). However, comparisons of surgery and SRS based on retrospective studies should be done with caution, as there is no way to adjust for selection bias.

Several studies in the literature have reported SRS complications, Martin and colleagues[42] reported their results treating jugular foramen schwannomas and trigeminal schwannomas using gamma knife radiosurgery. Only 1 patient experienced cranial nerve dysfunction, which occurred in the setting of a transient increase in tumor volume following SRS. Kano et al[41] reported that, of 33 patients with trigeminal schwannomas who underwent gamma knife SRS, new trigeminal deficits developed in 2 patients, both of them in the setting of tumor progression. Similarly, Sheehan et al[46] reported that 3 patients (12%) suffered worsening facial pain and were treated with surgical resection (n = 2) or a second course of gamma knife SRS (n = 1). Hasegawa and colleagues[8] performed gamma knife radiosurgery on 37 patients with trigeminal schwannomas; development of new or worsening symptoms could be attributed to treatment failure in 4 patients and radiation toxicity in 1 patient who developed facial numbness despite tumor regression. The results reported herein (ie, 5% rate of new or worsening cranial nerve deficit) are in line with previous studies.

Dose and Fractionation

An important question that warrants further study is whether there is any benefit to fractionating SRS over multiple sessions compared to single-session treatment. The theoretical radiobiological advantage of fractionation is clear; fractionation spares normal tissues by allowing for repair of sublethal damage between fractions.[12] Whether this radiobiological advantage translates into improved clinical outcomes when comparing single- vs three-session treatment requires further research.

Our usual practice is to treat in a single session unless the tumor is located adjacent to critical structures (eg, optic

Copyright © Congress of Neurological Surgeons. Unauthorized reproduction of this article is prohibited.

TABLE 3. Review of Conventionally Fractionated External Beam Radiotherapy of Nonvestibular Cranial Schwannomas[a]

Author and Year	No. of Patients	Location	Median Tumor Volume in cm^3 (range)	Dose, Gy	Local Failure	New or Worsening Cranial Nerve Deficit	Median Follow-up in Months (range)
Nishioka et al, 2009[37]	17	CN III (n = 1)	Mean 8.2 (0.3-31.3)	40-54	1 (6%)	0	60 (2-123)
		CN V (n = 5)					
		CN VII (n = 4)					
		Jugular foramen (n = 7)					
Showalter et al, 2008[36]	24	CN V (n = 9)	5.25	45-50	0	0	24
		CN VII (n = 5)					
		Jugular foramen (n = 4)					
Hamm et al, 2008[38]	19	CN V (n = 13)	Mean 14.1 (4.2-43.1) (n = 15) *or* mean 4.1 (2.2-6.2) (n = 4)	54-59.4 (n = 15) *or* 6-7 × 5 Gy (n = 4)	1 (5%)	0	Mean 35 (11-63)
		Jugular foramen (n = 5)					
		Orbital region (n = 1)					
Zabel et al, 2001[39]	13	CN V (n = 5)	19.8 (4.5-76.0)	54-57.6	0	0	33 (13-70)
		Lower CN (n = 3)					
		CP angle (n = 3)					
Wallner et al, 1988[40]	8	CN IV (n = 1)	NR	45-50	4 (50%)		
		CN V (n = 6)					
		CN IX (n = 1)					

[a]CN, cranial nerve; CP, cerebellopontine; NR, not reported.

apparatus, brainstem, other cranial nerves [eg, VII/VIII complex]), and/or is large. For those exceptions, based on our experiences of successfully treating perioptic lesions[49] and large tumors[50] with multisession SRS, our practice is to treat these types of tumors with multisession SRS. However, no prospective, randomized studies comparing single- vs multisession SRS have yet been published. Therefore, our practice paradigm stems from retrospective analyses, including our experience of treating vestibular schwannomas. With the goal of translating the potential radiobiological advantage into improved clinical outcomes, our practice of using tri-session SRS to treat vestibular schwannomas has resulted in no incidence of trigeminal dysfunction.[10] In comparison, 5% of patients have experienced trigeminal nerve dysfunction following single session SRS.[51] Although in no way a substitute for a prospective, randomized study, it is, at minimum, hypothesis-generating.

In our experience of nonvestibular cranial schwannoma radiosurgery, only 2 patients experienced new or worsening cranial nerve deficits, and both were treated with single-session SRS. However, due to the relatively small number of events, this difference did not reach statistical significance. We advocate further clinical studies to better understand whether there is benefit to multisession SRS.

Isoeffective Doses at Large Doses per Fraction

What is the optimal method of comparing different dose and fractionation schemes? To compare the different dose schedules in this series, we calculated the biologically equivalent dose using the linear-quadratic (LQ) model.[52] Although the LQ model is the most widely used model, whose simplicity makes it practical for clinical use, there are shortcomings. Some have raised concern about the accuracy of the LQ model to predict effects at large doses per fraction,[53] whereas others have argued that it would be reasonable to use the LQ model up to 18 Gy per fraction.[54] Although alternative models have been proposed,[55-57] these also have been assessed critically[58-60]; moreover, validation using in vitro and clinical studies is still needed. In short, which model best describes cell survival after radiation remains controversial. Given all the uncertainties, we have chosen to use the LQ model to present biologically equivalent doses, acknowledging its limitations at high dose per fraction.

Limitations of the Present Study

The duration of follow-up (median of 2.4 years) in the present series is relatively short, particularly when considering the long natural history of benign tumors such as schwannomas. Longer follow-up is necessary to assess the long-term tumor control rate

Copyright © Congress of Neurological Surgeons. Unauthorized reproduction of this article is prohibited.

TABLE 4. Review of Radiosurgical Series of Nonvestibular Cranial Schwannoma Treatments[a]

Author and Year	No. of Patients	Location	SRS System	Median Tumor Volume in cm^3 (range)	Median Rx dose in Gy (range)	Local Failure	New or Worsening Cranial Nerve Deficit	Median Follow-up in Months (range)
Kano et al, 2009[41]	33	CN V	GKS	4.2 (0.5-18)	15 (12-20)	4 (12%)	2 (6%), both with tumor progression	72 (mean) (7-148)
Showalter et al, 2008[36]	15	CN V (n = 10)	GKS	4	12 (12-15)	1 (7%)	8% (1 of 12 patients evaluable)	24
		Jugular foramen (n = 3)						
Martin et al, 2007[42]	34	Jugular foramen	GKS	4.2 (0.6-10.4)	14 (12-18)	2 (6%)	1 (3%)	83 (mean)
Sheehan et al, 2007[46]	25	CN V	GKS	4.0 (0.6-8.5)	15 (10-17)	3 (12%)	3 (12%) with worsening facial pain	49
Hasegawa et al, 2007[48]	37	CN V	GKS	Mean 10	Mean 14 Gy	5 (14%)	5 (14%)	54 (mean)
Pan et al, 2005[43]	56	CN V	GKS	Mean 8.7 (0.8-33)	Mean 13.3 (10-15)	4 (7%)	0	68 (mean)
Zhang et al, 2002[47]	25	Jugular foramen	GKS	Mean 13.5 (4.7-35.7)	Mean 14.6 (9.8-20)	1 (4%)	0	39 (mean)
Pollock et al, 2002[44]	23	CN IV (n = 1)	GKS	8.9 (0.2-17.6)	18 (12-20)	1 (4%)	4 (17%)	43
		CN V (n = 10)						
		Jugular foramen (n = 10)						
		CN XII (n = 2)						
Mabanta et al, 1999[1]	18	CN V (n = 7)	Linac	Mean 5.5 (0.7-15.4)	Mean 13 (10-15)	0 (0%)	3 (17%)	32 (mean)
		CN VII (n = 2);						
		Jugular foramen (n = 9)						
Present Series	40	CN IV (n = 1)	CKS	3.2 (0.1-23.7)	15 SFED Gy_3 (11-20)	1 (3%)	2 (5%)	29 (6-84)
		CN V (n = 18)						
		CN VII (n = 6)						
		CN X (n = 5)						
		CN XII (n = 2)						
		Jugular foramen (n = 8)						
		Cavernous sinus (n = 2)						

[a]CKS, CyberKnife radiosurgery; CN, cranial nerve; GKS, gamma knife radiosurgery; IDL, isodose line; Linac, linear accelerator; Rx, prescription; SFED, single fraction equivalent dose.

Copyright © Congress of Neurological Surgeons. Unauthorized reproduction of this article is prohibited.

accurately. The decision to include patients with shorter follow-up was made to allow for complete reporting of radiosurgery complications; 2 cases of complications occurred within 18 months following SRS.

In addition, despite extensive efforts, including contacting patients, family members listed as contacts, and referring doctors, as well as web-based searches, follow-up information on 5 patients could not be found. Given the rarity of these tumors, not having follow-up information on every patient treated is a shortcoming.

CONCLUSION

Nonvestibular cranial schwannomas are rare. The standard treatment of surgical resection carries a high risk of postoperative complications and cranial nerve deficits. SRS is an alternative treatment option for patients who are nonsurgical candidates or those wishing to avoid a craniotomy. The results presented in this article demonstrate an excellent tumor control rate with minimal short- and long-term toxicity. Although late complications were less common in patients treated in multiple sessions, this difference did not reach statistical significance. Whether there is benefit to multisession SRS compared to single-session treatment needs further examination through clinical studies.

Disclosure

The authors have no personal financial or institutional interest in any of the drugs, materials, or devices described in this article.

REFERENCES

1. Mabanta SR, Buatti JM, Friedman WA, et al. Linear accelerator radiosurgery for nonacoustic schwannomas. *Int J Radiat Oncol Biol Phys*. 1999;43(3):545-548.
2. MacNally SP, Rutherford SA, Ramsden RT, Evans DG, King AT. Trigeminal schwannomas. *Br J Neurosurg*. 2008;22(6):729-738.
3. Sharma BS, Ahmad FU, Chandra PS, Mahapatra AK. Trigeminal schwannomas: experience with 68 cases. *J Clin Neurosci*. 2008;15(7):738-743.
4. Goel A, Muzumdar D, Raman C. Trigeminal neuroma: analysis of surgical experience with 73 cases. *Neurosurgery*. 2003;52(4):783-790.
5. Sarma S, Sekhar LN, Schessel DA. Nonvestibular schwannomas of the brain: a 7-year experience. *Neurosurgery*. 2002;50(3):437-448.
6. Sanna M, Bacciu A, Falcioni M, Taibah A. Surgical management of jugular foramen schwannomas with hearing and facial nerve function preservation: a series of 23 cases and review of the literature. *Laryngoscope*. 2006;116(12):2191-2204.
7. McCormick PC, Bello JA, Post KD. Trigeminal schwannoma. Surgical series of 14 cases with review of the literature. *J Neurosurg*. 1988;69(6):850-860.
8. Hasegawa T, Kida Y, Kobayashi T, et al. Long-term outcomes in patients with vestibular schwannomas treated using gamma knife surgery: 10-year follow up. *J Neurosurg*. 2005;102(1):10-16.
9. Lunsford LD, Niranjan A, Flickinger JC, Maitz A, Kondziolka D. Radiosurgery of vestibular schwannomas: summary of experience in 829 cases. *J Neurosurg*. 2005;102(Suppl):195-199.
10. Chang SD, Gibbs IC, Sakamoto GT, et al. Staged stereotactic irradiation for acoustic neuroma. *Neurosurgery*. 2005;56(6):1254-1261.
11. Kondziolka D, Lunsford LD, McLaughlin MR, Flickinger JC. Long-term outcomes after radiosurgery for acoustic neuromas. *N Engl J Med*. 1998;339(20):1426-1433.
12. Hall E, Giaccia A. *Radiobiology for the Radiologist*. 6th ed. Philadelphia, PA: Lippincott Williams & Wilkins; 2006.
13. Gibbs IC, Kamnerdsupaphon P, Ryu MR, et al. Image-guided robotic radiosurgery for spinal metastases. *Radiother Oncol*. 2007;82(2):185-190.
14. Feuvret L, Noel G, Mazeron JJ, Bey P. Conformity index: a review. *Int J Radiat Oncol Biol Phys*. 2006;64(2):333-342.
15. Gibbs IC, Chang SD. Radiosurgery and radiotherapy for sacral tumors. *Neurosurg Focus*. 2003;15(2):E8.
16. Lomax NJ, Scheib SG. Quantifying the degree of conformity in radiosurgery treatment planning. *Int J Radiat Oncol Biol Phys*. 2003;55(5):1409-1419.
17. Kaplan E, Meier P. Nonparametric estimation for incomplete observation. *J Am Stat Assoc*. 1958;53:457-481.
18. Pollock BE. Management of vestibular schwannomas that enlarge after stereotactic radiosurgery: treatment recommendations based on a 15 year experience. *Neurosurgery*. 2006;58(2):241-248.
19. Crocker M, deSouza R, Epaliyanage P, et al. Masson's tumour in the right parietal lobe after stereotactic radiosurgery for cerebellar AVM: case report and review. *Clin Neurol Neurosurg*. 2007;109(9):811-815.
20. Al-Mefty O, Ayoubi S, Gaber E. Trigeminal schwannomas: removal of dumbbell-shaped tumors through the expanded Meckel cave and outcomes of cranial nerve function. *J Neurosurg*. 2002;96(3):453-463.
21. Bulsara KR, Sameshima T, Friedman AH, Fukushima T. Microsurgical management of 53 jugular foramen schwannomas: lessons learned incorporated into a modified grading system. *J Neurosurg*. 2008;109(5):794-803.
22. Kadri PA, Al-Mefty O. Surgical treatment of dumbbell-shaped jugular foramen schwannomas. *Neurosurg Focus*. 2004;17(2):E9.
23. Lee SK, Park K, Kong DS, et al. Surgical tactics and outcome of treatment in jugular foramen schwannomas. *J Clin Neurosci*. 2001;8(Suppl 1):32-39.
24. Samii M, Babu RP, Tatagiba M, Sepehrnia A. Surgical treatment of jugular foramen schwannomas. *J Neurosurg*. Jun 1995;82(6):924-932.
25. Yoshida K, Kawase T. Trigeminal neurinomas extending into multiple fossae: surgical methods and review of the literature. *J Neurosurg*. 1999;91(2):202-211.
26. Zhou LF, Mao Y, Zhang R. Surgical treatment of dumbbell-shaped neurinomas: report of an experience with 57 cases in a single hospital. *Surg Neurol*. 2007;68(6):594-602.
27. Day JD, Fukushima T. The surgical management of trigeminal neuromas. *Neurosurgery*. 1998;42(2):233-240.
28. Moffat D, De R, Hardy D, Moumoulidis I. Surgical management of trigeminal neuromas: a report of eight cases. *J Laryngol Otol*. 2006;120(8):631-637.
29. Ramina R, Maniglia JJ, Fernandes YB, et al. Tumors of the jugular foramen: diagnosis and management. *Neurosurgery*. 2005;57(1 suppl):59-68.
30. Chan AW, Black P, Ojemann RG, et al. Stereotactic radiotherapy for vestibular schwannomas: favorable outcome with minimal toxicity. *Neurosurgery*. 2005;57(1):60-70.
31. Combs SE, Volk S, Schulz-Ertner D, et al. Management of acoustic neuromas with fractionated stereotactic radiotherapy (FSRT): long-term results in 106 patients treated in a single institution. *Int J Radiat Oncol Biol Phys*. 2005;63(1):75-81.
32. Fuss M, Debus J, Lohr F, et al. Conventionally fractionated stereotactic radiotherapy (FSRT) for acoustic neuromas. *Int J Radiat Oncol Biol Phys*. 2000;48(5):1381-1387.
33. Kim CJ, Yoo SJ, Nam SY, Kim SY. A hearing preservation technique for the resection of extensive jugular foramen tumors. *Laryngoscope*. 2001;111(11 pt 1):2071-2076.
34. Koh ES, Millar BA, Menard C, et al. Fractionated stereotactic radiotherapy for acoustic neuroma: single-institution experience at The Princess Margaret Hospital. *Cancer*. 2007;109(6):1203-1210.
35. Szumacher E, Schwartz ML, Tsao M, et al. Fractionated stereotactic radiotherapy for the treatment of vestibular schwannomas: combined experience of the Toronto-Sunnybrook Regional Cancer Centre and the Princess Margaret Hospital. *Int J Radiat Oncol Biol Phys*. 2002;53(4):987-991.
36. Showalter TN, Werner-Wasik M, Curran WJ Jr, Friedman DP, Xu X, Andrews DW. Stereotactic radiosurgery and fractionated stereotactic radiotherapy for the treatment of nonacoustic cranial nerve schwannomas. *Neurosurgery*. 2008;63(4):734-740.
37. Nishioka K, Abo D, Aoyama H, et al. Stereotactic radiotherapy for intracranial nonacoustic schwannomas including facial nerve schwannoma. *Int J Radiat Oncol Biol Phys*. 2009;75(5):1415-1419.
38. Hamm KD, Gross MW, Fahrig A, et al. Stereotactic radiotherapy for the treatment of nonacoustic schwannomas. *Neurosurgery*. 2008;62(5 suppl):A29-A36.
39. Zabel A, Debus J, Thilmann C, Schlegel W, Wannenmacher M. Management of benign cranial nonacoustic schwannomas by fractionated stereotactic radiotherapy. *Int J Cancer*. 2001;96(6):356-362.
40. Wallner KE, Pitts LH, Davis RL, Sheline GE. Radiation therapy for the treatment of non-eight nerve intracranial neurilemmoma. *Int J Radiat Oncol Biol Phys*. 1988;14(2):287-290.
41. Kano H, Niranjan A, Kondziolka D, Flinkinger JC, Dade Lunsford L. Stereotactic radiosurgery for trigeminal schwannoma: tumor control and functional preservation. *J Neurosurg*. 2009;110(3):553-558.

Copyright © Congress of Neurological Surgeons. Unauthorized reproduction of this article is prohibited.

42. Martin JJ, Kondziolka D, Flickinger JC, Mathieu D, Niranjan A, Lunsford LD. Cranial nerve preservation and outcomes after stereotactic radiosurgery for jugular foramen schwannomas. *Neurosurgery*. 2007;61(1):76-81.
43. Pan L, Wang EM, Zhang N, et al. Long-term results of Leksell gamma knife surgery for trigeminal schwannomas. *J Neurosurg*. 2005;102(suppl):220-224.
44. Pollock BE, Foote RL, Stafford SL. Stereotactic radiosurgery: the preferred management for patients with nonvestibular schwannomas? *Int J Radiat Oncol Biol Phys*. 2002;52(4):1002-1007.
45. Sakamoto GT, Borchers DJ III, Xiao F, et al. Cyberknife radiosurgery for trigeminal schwannomas. *Neurosurgery*. 2009;64(2 suppl):A14-A18.
46. Sheehan J, Yen CP, Arkha Y, Schlesinger D, Steiner L. Gamma knife surgery for trigeminal schwannoma. *J Neurosurg*. 2007;106(5):839-845.
47. Zhang N, Pan L, Dai JZ, Wang BJ, Wang EM, Cai PW. Gamma knife radiosurgery for jugular foramen schwannomas. *J Neurosurg*. 2002;97(5 suppl):456-458.
48. Hasegawa T, Kida Y, Yoshimoto M, Koike J. Trigeminal schwannomas: results of gamma knife surgery in 37 cases. *J Neurosurg*. 2007;106(1):18-23.
49. Adler JR Jr, Gibbs IC, Puataweepong P, Chang SD. Visual field preservation after multisession cyberknife radiosurgery for perioptic lesions. *Neurosurgery*. 2008;62(suppl 2):733-743.
50. Tuniz F, Soltys SG, Choi CY, et al. Multisession cyberknife stereotactic radiosurgery of large, benign cranial base tumors: preliminary study. *Neurosurgery*. 2009;65(5):898-907.
51. Chopra R, Kondziolka D, Niranjan A, Lunsford LD, Flickinger JC. Long-term follow-up of acoustic schwannoma radiosurgery with marginal tumor doses of 12 to 13 Gy. *Int J Radiat Oncol Biol Phys*. 2007;68(3):845-851.
52. Liu L, Bassano DA, Prasad SC, Hahn SS, Chung CT. The linear-quadratic model and fractionated stereotactic radiotherapy. *Int J Radiat Oncol Biol Phys*. 2003; 57(3):827-832.
53. Kirkpatrick JP, Meyer JJ, Marks LB. The linear-quadratic model is inappropriate to model high dose per fraction effects in radiosurgery. *Semin Radiat Oncol*. Oct 2008;18(4):240-243.
54. Brenner DJ. The linear-quadratic model is an appropriate methodology for determining isoeffective doses at large doses per fraction. *Semin Radiat Oncol*. 2008;18(4):234-239.
55. Park C, Papiez L, Zhang S, Story M, Timmerman RD. Universal survival curve and single fraction equivalent dose: useful tools in understanding potency of ablative radiotherapy. *Int J Radiat Oncol Biol Phys*. 2008;70(3):847-852.
56. Astrahan M. Some implications of linear-quadratic-linear radiation dose-response with regard to hypofractionation. *Med Phys*. 2008;35(9):4161-4172.
57. Guerrero M, Li XA. Extending the linear-quadratic model for large fraction doses pertinent to stereotactic radiotherapy. *Phys Med Biol*. 2004;49(20):4825-4835.
58. Kavanagh BD, Newman F. Toward a unified survival curve: in regard to Park et al. (*Int J Radiat Oncol Biol Phys*. 2008;70:847-852) and Krueger et al. (*Int J Radiat Oncol Biol Phys*. 2007;69:1262-1271). *Int J Radiat Oncol Biol Phys*. Jul 1 2008; 71(3):958-959.
59. McKenna F, Ahmad S. Toward a unified survival curve: in regard to Kavanagh and Newman (*Int J Radiat Oncol Biol Phys*. 2008;71:958-959) and Park et al. (*Int J Radiat Oncol Biol Phys*. 2008;70:847-852). *Int J Radiat Oncol Biol Phys*. 2009;73(2):640; author reply 640-641.
60. Astrahan M. BED calculations for fractions of very high dose: in regard to Park et al. (Int J Radiat Oncol Biol Phys 2007;69:S623-S624). *Int J Radiat Oncol Biol Phys*. 2008;71(3):963; author reply 963-964.

COMMENTS

In this paper, the Stanford group reports on its experience with Cyberknife radiosurgery for treatment of nonvestibular schwannomas. With a median follow-up period of 29 months, tumor control was achieved in 41 of 42 patients. Three-year actuarial tumor control in this study is 96%. Two cases of new or worsened cranial nerve deficits were observed after radiosurgery. In addition, one case of radiation-associated intravascular papillary endothelial hyperplasia was observed 4 years after radiosurgery.

In general, the authors selected those patients with perioptic lesions and large tumors for multisession radiosurgery. Radiologic or clinical outcomes were not statistically different between single and multisession radiosurgical groups. Considering the large size of some of these tumors (up to 23.7 cm^3), comparable results in these groups are an important finding.

The authors recommend further clinical studies to evaluate the benefits of the multisession radiosurgical approach. In comparing single- vs multisession radiosurgery, patient and tumor attributes must be controlled to mitigate for study and clinician biases. Moreover, one should identify in advance the level of significance that constitutes a ''trend'' in post hoc statistical analysis. Otherwise, one can fall prey to an ''optimism bias.''[1]

From a purely radiobiological standpoint, there are advantages and disadvantages to a multisession approach as compared to single-session or conventional fractionated techniques. There is no doubt that multisession radiosurgery will play a role in the neurosurgical management of benign skull-base tumors. This research confirms its efficacy and safety. I look forward to further work by this luminary group in defining the indications and refining the techniques associated with multisession radiosurgery.

Jason Sheehan
Charlottesville, Virginia

1. Chalmers I, Matthews R. What are the implications of optimism bias in clinical research? *Lancet*. 2006;367:449-450.

While surgery remains the gold standard for the management of both vestibular and nonvestibular schwannoma, nonsurgical alternative treatments including observation, stereotactic radiosurgery (SRS), and fractionated radiotherapy have been employed and reported by various groups. The authors of this analysis present a retrospective series of Cyberknife-delivered SRS in 40 patients with 42 residual or recurrent/progressive (after prior surgery) nonvestibular schwannoma. The analysis describes the technique and early results in the form of local control and complications in a good number of these relatively uncommon tumors. Outcome data at a relatively short follow-up of 29 months is as expected for other well-published series of stereotactic and even conventional fractionated irradiation. Interestingly, authors have used both single-fraction and short multi-fraction treatments basing their decision on the size of the lesion and its location adjacent to a critical site. The authors have attempted to highlight the advantages of fractionation in larger tumors close to critical structures (eg, pons), but in view of the retrospective nature of analysis with its usual biases, one cannot arrive at a fair conclusion, which the authors freely admit. This may well have been the chief strength of the analysis. Five patients (>10%) have been lost to follow-up, and absence of data for these patients in a relatively indolent disease such as a schwannoma is a concern, because losing information (eg, a complication or a progression) for even a small number of patients may change the outcome data quite considerably. Nevertheless, the report adds important information in a growing body of evidence for nonsurgical approaches as a reasonable management strategy in complex, critically located benign tumors including nonvestibular schwannoma. Although there are several limitations to the present study, including short follow-up, it should serve as a useful platform to conduct prospective (even multi-institutional) studies to obtain robust information regarding local control, adverse events, and quality of life to ascertain the true efficacy of these techniques. Such treatments are likely to remain, however, as useful adjuncts or alternatives in our management armamentarium for improved care of our patients.

R. Jalali and A.Goel
Mumbai, India

Copyright © Congress of Neurological Surgeons. Unauthorized reproduction of this article is prohibited.

Stereotactic ^{125}Iodine Brachytherapy for the Treatment of Singular Brain Metastases: Closing a Gap?

Maximilian I. Ruge, MD, PhD*
Bogdana Suchorska, MD‡
Mohammad Maarouf, MD, PhD*
Matthias Runge, MD*
Harald Treuer, PhD*
Jurgen Voges, MD, PhD‡
Volker Sturm, MD, PhD*

*Department of Stereotactic and Functional Neurosurgery, Albertus Magnus University of Cologne, Otto v. Guericke University, Magdeburg, Germany; and ‡Department of Stereotactic Neurosurgery, Otto v. Guericke University, Magdeburg, Germany

Correspondence:
Maximilian I. Ruge, MD, PhD,
Department of Stereotactic and Functional Neurosurgery,
University Clinics of Cologne,
Kerpener Straße 62,
Main Clinic Bldg,
11th Floor,
50937 Cologne, Germany.
E-mail: maximilian.ruge@uk-koeln.de

Received, January 31, 2010.
Accepted, August 30, 2010.

Copyright © 2011 by the Congress of Neurological Surgeons

BACKGROUND: Brain metastases represent the most common intracranial tumors and are associated with very poor prognosis.

OBJECTIVE: To investigate the feasibility, survival, and cerebral disease control of patients with singular brain metastases treated with stereotactic ^{125}iodine brachytherapy (SBT), to identify prognostic factors, and to compare results with other local treatment methods.

METHODS: Complications, survival (overall and separated by recursive partitioning analysis [RPA] classes), and local and distant disease control were evaluated retrospectively in 90 patients. Prognostic factors were identified by forming subgroups of patients based on age, Karnofsky Performance Status, status of extracranial disease, interval since initial diagnosis, absence/presence of prior whole-brain radiation therapy, localization, morphology, and tumor volume.

RESULTS: There was no treatment-related mortality, and morbidity was transient and low (3.3%). Median survival was 8.5 months overall and 18.1 months for RPA class 1 patients. After 1 year, the actuarial incidence of local and distant cerebral relapse was 5.4% and 46.4%, respectively. Karnofsky Performance Status $\geq$ 70 ($P < .002$), stable systemic disease ($P < .02$), RPA class 1 ($P < .02$), and a prolonged ($>$ 12 month) interval between initial diagnosis and SBT ($P < .05$) significantly improved survival. No significant influence of previous whole-brain radiation therapy on survival or cerebral disease relapse was found.

CONCLUSION: SBT represents a safe, minimally invasive, and, compared with SRS and microsurgery, a similarly effective local treatment option in terms of survival and cerebral disease control. It allows histological (re-)evaluation and treatment within 1 stereotactic operation. Because it is less restricted by tumor localization or size, it greatly advances local treatment options, and on the basis of its favorable biological irradiation effect, SBT does not limit additional irradiation treatment in the event of disease relapse.

KEY WORDS: Singular brain metastases, Stereotactic radiosurgery (SRS), Stereotactic ^{125}iodine brachytherapy (SBT)

Neurosurgery 68:1209–1219, 2011 DOI: 10.1227/NEU.0b013e31820b526a www.neurosurgery-online.com

With increasing incidence, brain metastases represent the most common intracranial tumors and are associated with very poor prognosis in the majority of cases.

ABBREVIATIONS: KPS, Karnofsky Performance Status; **RPA,** recursive partitioning analysis; **RTOG,** Radiation Therapy Oncology Group; **SBT,** stereotactic ^{125}iodine brachytherapy; **SRS,** stereotactic radiosurgery; **WBRT,** whole-brain radiation therapy

Currently, several treatment options are available for cerebral metastases.

Although whole-brain radiation therapy (WBRT) is considered mainly for patients with multiple brain metastases, there is evidence that WBRT without concomitant local treatment (surgical resection, stereotactic radiosurgery [SRS]) is significantly less effective for patients with singular brain metastases in terms of survival.[1-3] Thus, combining surgical resection with WBRT, as well as SRS with or without WBRT, is widely accepted.[3-7] Surgical resection and intraoperative

Copyright © Congress of Neurological Surgeons. Unauthorized reproduction of this article is prohibited.

implantation of ^{125}iodine seeds for brachytherapy of the resection cavity[8-11] are also possible, which in some protocols is completed by WBRT.[12] These treatment strategies, however, have limitations.

Despite the improvement in surgical methods with the advent of advanced imaging techniques, intraoperative imaging, and navigation systems, the number of cases allowing safe resection of a singular metastatic tumor remains rather limited, ie, < 30% of all cases.[13,14]

SRS, on the other hand, is generally limited by tumor size. Treatment of metastases exceeding a diameter of 3 cm or a volume of 14 cm^3 increases the radiation burden for surrounding tissue and might elevate the risk of edema and/or tissue necrosis. Similar considerations reduce the indication for external reirradiation in cases of tumor relapse after WBRT.[15,16]

Furthermore, (re-)confirmation of the histology of a newly arising cerebral lesion with unknown or undetectable primary cancer is required before irradiation in the majority of cases, thus indicating a stereotactic biopsy. The same holds true for local recurrences after previous irradiation treatment to differentiate between tumor relapse and radiation-induced necrosis.

For these selected cases, stereotactic (interstitial) ^{125}iodine brachytherapy (SBT) has been reported to represent a feasible and minimally invasive treatment option, as initially described by Prados et al.[17] This group applied temporary high-activity ^{125}iodine seeds in 14 patients with progressive metastatic brain lesions after undergoing therapy (WBRT in 13 cases, surgical resection in 4 cases) as a salvage treatment and demonstrated a reasonable overall survival of 20 months.

In 1995, Ostertag and Kreth[13] confirmed the value of this treatment strategy for singular cerebral metastases. They observed fair overall survival of up to 17 months and low procedural risk by comparing 3 groups of patients: those receive brachytherapy only before WBRT or as a salvage treatment for recurrent disease after surgery or WBRT. The authors also emphasized the possibility of performing a stereotactic biopsy and SBT (referred to here as interstitial radiosurgery) within the same operation.

More recently, laser thermal therapy instead of brachytherapy, also using stereotactic guidance, was introduced for the focal treatment of metastatic brain tumors in a pilot study involving 6 patients and demonstrated promising results in terms of local response.[18]

The present retrospective study reports a single-institution experience using STB to treat singular brain metastases. We reviewed all patients with singular cerebral metastases who underwent STB with ^{125}iodine seeds at the Department of Stereotactic and Functional Neurosurgery, University of Cologne, Cologne, Germany, from 1994 to 2008. A total of 90 patients were chosen for further analysis. Survival, local and distant disease control, radiological treatment response, procedure-related complications, and prognostic factors related to these parameters were evaluated.

MATERIAL AND METHODS

Eligibility of Patients

Patients were selected for our SBT protocol if they fulfilled at least one of the following criteria (Figure 1): (1) unclassified histology: need for stereotactic biopsy in the case of first diagnosis of an intracerebral lesion together with unknown or undetectable but suspected primary systemic disease, or an interval between primary cancer diagnosis and appearance of cerebral disease > 3 years; (2) tumor size: metastasis exceeds a diameter of > 3 cm or a volume of > 14 cm^3; and (3) previous WBRT and/or SRS. In addition, the patient should not be a candidate for microsurgical tumor removal because of the eloquent and/or deep-seated location of the metastasis with only moderate mass effect or patient refusal to undergo surgery.

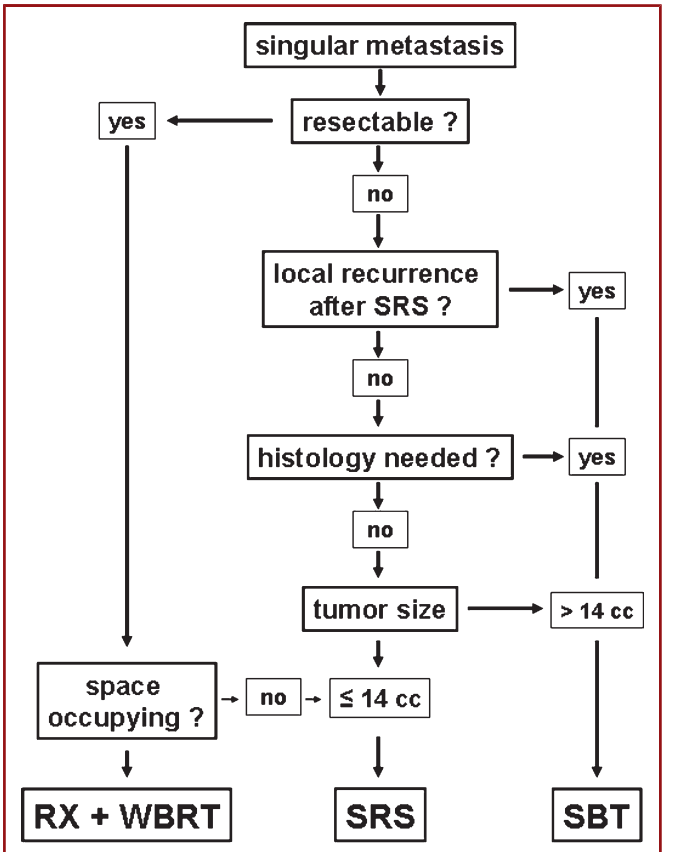

FIGURE 1. *Algorithm diagram showing the decision process for selecting treatment for singular brain metastases. SBT, stereotactic (interstitial) ^{125}iodine brachytherapy; SRS, stereotactic radiosurgery; WBRT, whole-brain radiation therapy.*

All patients signed informed consent after detailed explanation of procedure-related risks. Patients agreed that their data would be used for scientific evaluation.

Initial and Follow-up Evaluations

Before treatment, we performed computed tomography (CT) examinations of the abdomen and thorax and blood analysis focusing on tumor markers to restage the patient's disease status. Patients with a low Karnofsky Performance Status (KPS)[19] (< 60) and/or a poor estimated survival (< 3 months) caused by uncontrollable systemic disease (progression) were excluded from this treatment protocol.

We evaluated the patient's medical history, histology of the original cancer, neurological symptoms, intraoperative and postoperative complications, and need for steroid medication. KPS and neurological status

Copyright © Congress of Neurological Surgeons. Unauthorized reproduction of this article is prohibited.

were documented and rated as improved, stable, or deteriorated at the following intervals: initially, at hospital discharge, 42 days later at the time of seed catheter removal, and thereafter in 3-month intervals.

To assess local tumor response on magnetic resonance imaging (MRI) scans, we used the Macdonald et al[20] criteria. The definition of complete remission, however, had to be modified because of the frequently observed presence of residual traces of contrast enhancement around the implanted seeds, a result of treatment-induced local blood-brain barrier disruption.

Local relapse was defined as either the appearance of a new enhancing lesion in exactly the same site as the treated metastasis after complete response or histological confirmation by stereotactic biopsy after (re-) growth of a previous partial response or stable disease. Distant relapse was defined as the appearance of a new enhancing lesion at a site other than the original tumor.

The treatment response recorded by MRI was documented, along with clinical data, after 6 weeks (time of removal of ^{125}iodine seed catheter) and thereafter at the follow-up examinations in 3-month intervals until the patient's death or last contact. To collect a reasonable amount of response data, an interim evaluation was performed at the first 3-month follow-up after removal of the seeds (4.5 months after beginning the SBT), taking into account both the variable radiological response to treatment resulting from the heterogeneous characteristics of the study population in terms of size and histology of the metastases and the presumed low overall survival.

Survival and cause of death (progression of systemic vs neurological disease) were evaluated by reviewing medical records before death and/or interviewing the last treating physician. Cause of death was determined according to the prospective study protocol of Patchell et al[1]; ie, patients with stable extracerebral disease and progressive neurological dysfunction, patients with severe neurological disability who died of intercurrent illness, and patients with progressive systemic and neurological disease were considered neurological deaths; otherwise, a systemic death was assumed. Autopsy data were available in 5 cases.

MRI scans were reviewed by neuroradiologists, and all clinical ratings were performed by neurosurgeons or radiation oncologists with experience in neurooncology. All data were approved independently by an interdisciplinary tumor board.

Treatment Planning and Surgical Procedures

After induction of general anesthesia, the patient's head was fixed in a modified, CT-compatible Riechert-Mundinger stereotactic frame with an attached stereotactic localizer.[21] Although SBT could also be performed under local anesthesia, we used general anesthesia for the patient's convenience. Contrast medium (Solutrast 300R; ALTANA Pharma, Wesel, Germany) was administered, and a CT (1.5-2 mm slice thickness, 290 × 290 mm field of view, 512 × 512 matrix) with a stereotactic localizer was performed. Specialized software (STP3; until February 1996, STP2; Leibinger GmbH, Heidelberg, Germany) was used to plan the trajectory and treatment dose. In all cases, the CT images, generally not susceptible to distortions, were merged with preoperative axial T1 contrast-enhanced and T2-weighted MRIs (2 mm slice thickness, 256 × 256 mm field of view, 512 × 512 matrix) by means of anatomic landmarks. Then the surface of the metastasis was manually outlined, and the volume of the target was calculated.[22,23] This combination of imaging modalities ensured optimum precision and imaging quality for identifying tumor, tissue, and vessels. The dose prescribed at the surface of the target volume was 50 Gy, with irradiation times ranging from 35 to 42 days at an initial dose rate of 175 to 150 cGy/d. The specified doses correspond to the TG43 protocol.[24] The objective of radiation treatment planning is always to determine a seed configuration with as few seed catheters as possible (to minimize operative risk) to achieve an optimal conformation of the therapeutic isodose with the surface of the target volume. In the operating room, the stereotactic arc was adjusted according to the calculated coordinates on a phantom and then mounted on the patient's stereotactic frame. The ^{125}iodine seeds (Amersham Buchler GmbH & CoKG, Braunschweig, Germany) were introduced into Celcon nylon or silicon catheters (Best Industries Inc, Springfield, Virginia; Phoenix-Biomedical Corp, Ontario, Canada). After skin incision and placement of an 8-mm burr hole, the catheters were inserted into the tumor. If histology was requested, a stereotactic biopsy was taken and evaluated during the operation. To ensure correct placement, intraoperative x-ray images were captured in 2 planes (anterior/posterior and lateral) with a stationary stereotactic x-ray source and matched with images of the calculated trajectory. Compared with intraoperative CT or MRI scanning used by some groups to monitor laser thermal therapy or placement of deep brain stimulation electrodes, this technique does not require movement of the patient or a time-consuming imaging session. Furthermore, it is comparatively fast and repeatable and allows monitoring of the (re-) positioning of the catheters containing the ^{125}iodine seeds with high precision and a comparatively low radiation burden for the patient.[25] For stabilization, the catheters were fixated within the burr hole using bone cement. In addition, the catheter tip, protruding out of the cement by approximately 3 to 5 mm, was fixed with a vessel clip to further avoid displacement.

In the rare cases of intraoperatively detected incorrect placement of the implanted seeds, we primarily revised the catheter position. If this revision was not satisfactory, the isodose plan was recalculated and the irradiation time was adjusted accordingly.

Finally, the emitted radiation was measured at 1- and 2-m distances from the patient's head. In cases when the dose exceeded 2 μSv/h at 1-m distance, the patient had to wear a lead cap temporarily.[25,26]

The surgical procedure usually took between 40 minutes and 1.5 hours, depending on the number of catheters used. The patient's hospital stay varied between 3 and 5 days.

Seed catheters were removed 42 days (86 patients) or 35 days (4 patients) later under local anesthesia. This involved removing the vessel clip and extracting the catheter by leaving the cement within the burr hole. This procedure required a hospital stay of 1 day in most cases. At this time, every patient received a follow-up MRI using the same imaging protocol as in the SBT planning to ensure comparability.

Statistical Analysis and Outcome Measures

For statistical analysis, we used SPSS 17.0 for Windows (SPSS Inc, Chicago, Illinois). The end of the observation period was March 2009. The reference point was the date of SBT. End points of the analysis were the patient's death regardless of the cause, the date of the patient's last contact, and the date of occurrence of local or distant tumor relapse on MRI after SBT.

Length of survival and actuarial local or distant relapse were calculated with Kaplan-Meier estimates from the time of SBT to death or last contact.[27] Living patients were censored. The Log-rank test was used to compare survival estimates between subgroups, and the χ^2 test was used to identify differences in dichotomized epidemiological data. Data are given as medians and SDs. Values of $P < .05$ were considered significant.

Copyright © Congress of Neurological Surgeons. Unauthorized reproduction of this article is prohibited.

Subgroups of Patients and Correlations Between Measures

To determine possible prognostic factors regarding survival and time to progression of metastatic disease (relapse), we performed multivariate and univariate survival analyses. The following factors were considered to influence overall survival and time to progression: age ≤ 65 or > 65 years, gender, KPS < 70 or ≥ 70, stable vs progressive extracranial disease, solid vs necrotic morphology on MRI, interval between initial diagnosis ≤ 12 or > 12 months, stereotactic brachytherapy treatment before vs after the year 2000, with or without prior cerebral treatment, with or without prior WBRT, location of metastasis (lobar vs other and brainstem/basal ganglia vs other), responsiveness to irradiation (radiosensitive/radioresistant), and tumor volume ≤ 14 or > 14 cm^3. Metastases from renal cell cancer, malignant melanoma, and sarcoma were considered radioresistant. Following the Radiation Therapy Oncology Group (RTOG), we used the recursive partitioning analysis (RPA) and also compared RPA class 1 vs 2 and 3.[28]

Furthermore, the number of patients showing either radiologically complete or partial remission vs stable or progressive disease, as well as cerebral vs systemic death, was correlated with previous irradiation (yes/no), volume (≤ 14 or > 14 cm^3), morphology (solid/necrotic), and responsiveness to irradiation (radiosensitive/radioresistant) of the metastasis. The differences in these groups regarding remission status and cause of death were calculated using the χ^2 test.

RESULTS

Selection Criteria for SBT

In 55 of 90 cases (61.1%), SBT was offered primarily because a stereotactic biopsy was necessary. Of these 55 patients, 27 underwent biopsy because the interval between initial cancer diagnosis and occurrence of the brain metastasis was > 36 months. In 6 cases, biopsy revealed cancer of an unknown primary tumor, and in 21 patients with previous irradiation treatment, it served to distinguish between tumor relapse and irradiation-induced necrosis. In all these cases, biopsy and SBT were performed as a 1-stage procedure, and histology confirmed the cancer diagnosis in all cases.

Additional selection criteria in favor of SBT and against SRS included tumor size > 3 cm in diameter or a volume of 14 cm^3 in 20 patients (22.2%) and local tumor recurrence after previous SRS and/or WBRT in 26 patients (28.8%). Five patients (5.55%) considered candidates for microsurgical removal refused to undergo open resection of their tumors.

Clinical and epidemiological characteristics are listed in Table 1.

Survival

With a median follow-up time of 8.8 ± 18.8 months, the survival for the entire population was 8.5 months (range, 0.2-95.3 months; Figure 2). After adjustment by the RTOG RPA, patients with class 1 characteristics showed a median survival of 18.1 month, and those in class 2 and 3 had a median survival of 6.9 and 4.4 months, respectively (Figure 3).

Clinical Follow-up

During the first follow-up period of 4.5 months (duration of SBT plus 3 months after extraction of the seed catheters),

TABLE 1. Baseline and Treatment Characteristics[a]

Total patients, n	90
Female/male, n (%)	42/48 (46.7/53.3)
Age, mean/median, y	58.5/59.0
Range	17-80
KPS, mean/median	74/70
Range	60-90
RPA, n/%	
Class 1	34/37.8
Class 2	49/54.4
Class 3	7/7.8
Volume of tumor, mean ± SD/median, mL	10.1 ± 6.7/8.9
Range	1.2-35.7
Volume class, n/%	
0.5-14 mL	70/77.8
> 14 mL	20/22.2
Initial cancer diagnosis to STB, mean ± SD/median, mo	39.2 ± 53.6/20.0
Range	0-244
Time from initial cancer diagnosis to SBT, n (%)	
≤ 12 mo	36/40.0
> 12 mo	54/60.0
Stable systemic disease, n/%	49/54.4
Histology, n/%	
Kidney	12/13.3
Breast	17/18.9
NSCLC	27/30.0
Melanoma	8/8.9
Colorectal	7/7.8
CUP	6/6.7
Other	13/14.4
Prior cerebral treatment, n/%	29/32.2
Prior WBRT treatment, n/%	21/23.3
Localization, n/%	
Lobar (frontal/temporal/parietal/occipital)	26/28.9
Insular	6/6.7
Pre/post central sulcus	19/21.1
Pontine	12/13.3
Basal ganglia/diencephalon	13/14.4
Cerebellum	12/13.3
Other	2/2.2
Located "eloquent," n/%	71/78.9
Located cortical, n/%	20/22.2
Stereotactic biopsy performed, n/%	55/61.1
Solid	33/36.7
Necrotic	57/63.3
Radioresponsivness, n/%	
Radioresistant	20/22.2
Radiosensitive	70/77.8
Average stay as inpatient (at time of implantation of ^{125}iodine seeds), mean ± SD/median	3.8 ± 1.2/3.0
Range	3-10

[a]CUP, cancer of unknown primary; KPS, Karnofsky Performance Status; NSCLC, non–small-cell lung cancer; RPA, recursive partition analysis; SBT, stereotactic ^{125}iodine brachytherapy; WBRT, whole-brain radiation therapy.

Copyright © Congress of Neurological Surgeons. Unauthorized reproduction of this article is prohibited.

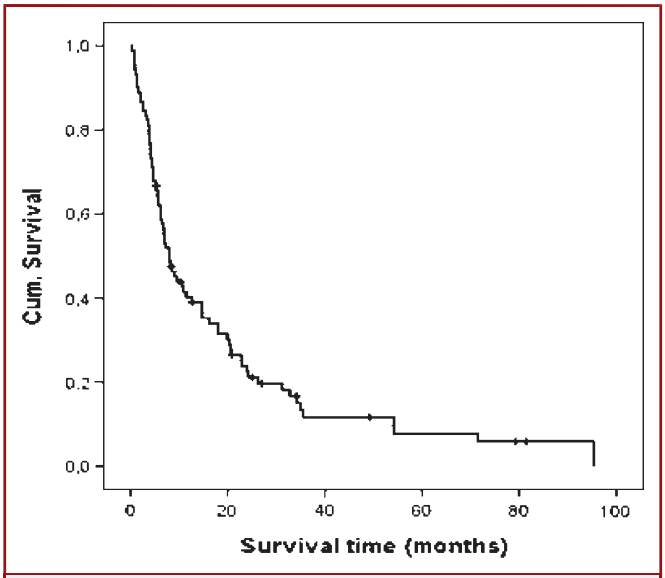

FIGURE 2. *Kaplan-Meier survival curves for patients treated with stereotactic ^{125}iodine brachytherapy for singular brain metastases. Median survival was 8.5 months.*

24 patients died: 16 as a result of progressive systemic disease and 8 as a result of newly occurring disseminated cerebral disease.

In 63 of the remaining 66 patients (95.5%), the neurological status and KPS were stable or improved after brachytherapy. The 3 remaining patients (4.5%) showing deterioration in clinical status died within the following 3 weeks after the first follow-up evaluation. None of the patients were on steroid medication for $>$ 2 weeks during the observation period, and no patient suffered from a space-occupying radiation-induced necrosis requiring microsurgical intervention.

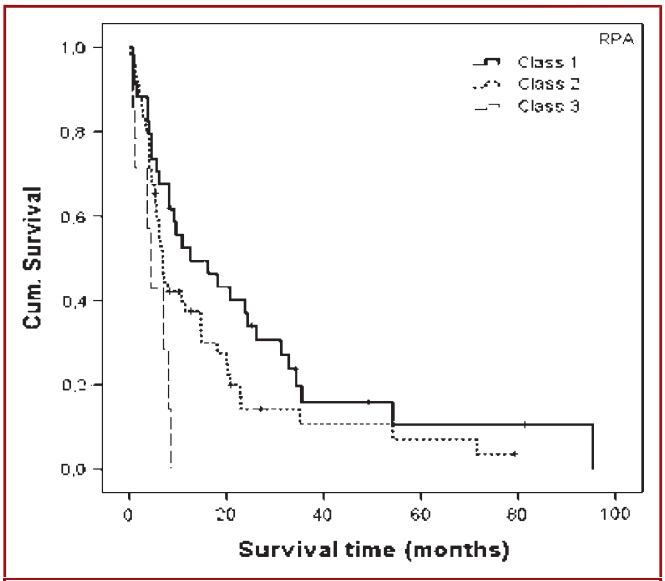

FIGURE 3. *After adjustment by Radiation Therapy Oncology Group recursive partitioning analysis (RPA), patients with class 1 characteristics showed a median survival of 18.1 months. Class 2 and 3 medians were 6.9 and 4.4 months, respectively.*

Cause of Death

Considering all patients, the cause of death was systemic progression of the disease in half of the population and cerebral progression in 31.1% (28 patients). In 5 cases, further information about the cause of death was not available. At the end of the observation period in March 2009, 12 patients (13.3%) were alive with a median follow-up time of 23.1 ± 26.6 months.

Local Response and Occurrence of Disease Relapse

MRI examinations of 65 patients were available for the interim evaluation of the treatment response at the 3-month follow-up after removal of the seed catheters. These showed complete remission of the treated metastasis in 5 patients (7.7%), partial response in 40 patients (61.5%), and stable disease in 19 patients (29.2%) according to the modified Macdonald et al[20] criteria mentioned above. In 1 patient, progressive local disease was observed.

Local tumor relapse after SBT was observed in 3 cases after 9.17 ± 3.75 months (mean ± SD). Local relapse was observed after complete remission in 1 patient and proved by histological confirmation in 2 patients. For 1 patient, brachytherapy was repeated with a reduced dose (35 Gy), resulting in a survival time of 22 months with partial response of the tumor. In another case, the recurrent metastasis was surgically removed 9.2 months after SBT (survival thereafter for 11 months), and in 1 patient, salvage SRS was performed after 5.4 months (survival thereafter for 18.5 months).

In 6 patients, the follow-up MRI showed new disease within the path of the implanted catheters, suggesting growth of tumor cells by inoculation. This phenomenon occurred as early as 6 weeks and as late as 11 months after implantation of the ^{125}iodine seeds, emphasizing the necessity for periodic imaging controls. In four of these cases, brachytherapy was repeated and complete remission was achieved, substantially prolonging survival. Two patients died within 1 month after identification of tumor progression: 1 after repeated SBT and 1 while beginning WBRT (see Table 2 for details).

Cerebral tumor progression distant from the original site of the treated metastasis (excluding the above-mentioned procedure-related tumor relapse) was found in 33 patients after a median time interval of 13.6 months (range, 1.1-34.2 months). Thirty of these patients died after a median of 6.5 ± 1.5 months (range, 0.7-26.0 months). Salvage treatment included SRS (Gamma Knife/linear accelerator) in 11 cases, WBRT in 8 patients, and microsurgical resection in 1 patient. Thirteen patients received palliative care.

Overall, after 1 year, the actuarial rate of distant relapse was 46.4%, whereas the local control rate was 94.6%. (Figure 4A and 4B).

Copyright © Congress of Neurological Surgeons. Unauthorized reproduction of this article is prohibited.

TABLE 2. Course of Patients With Occurred Inoculation Tumors[a]

ID, Sex	DX	Interval: SBT to Occurrence of Inoculated Tumor	Salvage Therapy	Local Response (on MRI Follow-up)/mo	Cause of Death	Interval: Salvage Therapy to Death, mo
B.G., male	NSCLC	4.5	SBT	CR/20.0	Alive	21.0
E.H., female	NSCLC	1.5	SBT	SD/1.0	Cerebral relapse	1.1
F.L., female	Ovarian cancer	6.0	SBT	CR/95.1	Systemic relapse	99.0
G.W., male	NSCLC	10.7	SRS	CR/3.0	Alive	3.2
S.O., male	NSCLC	6.2	WBRT	PD/6.0	Cerebral relapse	0.6
S.M., male	RCC	9.8	SBT	CR/18	Systemic/cerebral relapse	20.9

[a]CR, complete remission; DX, histological diagnosis; MRI, magnetic resonance imaging; NSCLC, non-small cell lung cancer; PD, progressive disease; RCC, renal cell cancer; SBT, stereotactic ^{125}iodine brachytherapy; SD, stable disease; SRS, stereotactic radiosurgery; WBRT, whole-brain radiation therapy.

Prognostic Factors for Survival

Improved survival was correlated with a KPS ≥ 70 ($P < .002$), stable systemic disease ($P < .02$), RPA class 1 ($P < .02$), and a prolonged (> 12 months) interval between initial diagnosis and SBT ($P < .05$). Previous treatment, tumor volume, responsiveness to irradiation, and other epidemiological factors did not correlate with better survival (Table 3).

Correlation of Treatment Response

The number of patients fulfilling the radiological criteria of stable or progressive disease was significantly higher with metastases displaying a necrotic morphology on the pretreatment MRI than those with a solid appearance ($P < .03$). A significantly better local response was associated with metastases ≤ 14 cm^3 ($P < .04$). There was no significant difference in response between radiosensitive and radioresistant metastases.

The Role of WBRT

The use of WBRT in the course of the disease did not correlate with the cause of death (cerebral vs systemic), and prior WBRT was not significantly correlated with the occurrence of new cerebral disease ($P < .09$) or with improved survival ($P = .4$) in this population. None of the factors considered for analysis proved to be significant in the multivariate analysis.

Complications

There was no procedure-related mortality. One patient died 14 days after surgery as a result of acute renal failure. The 30-day

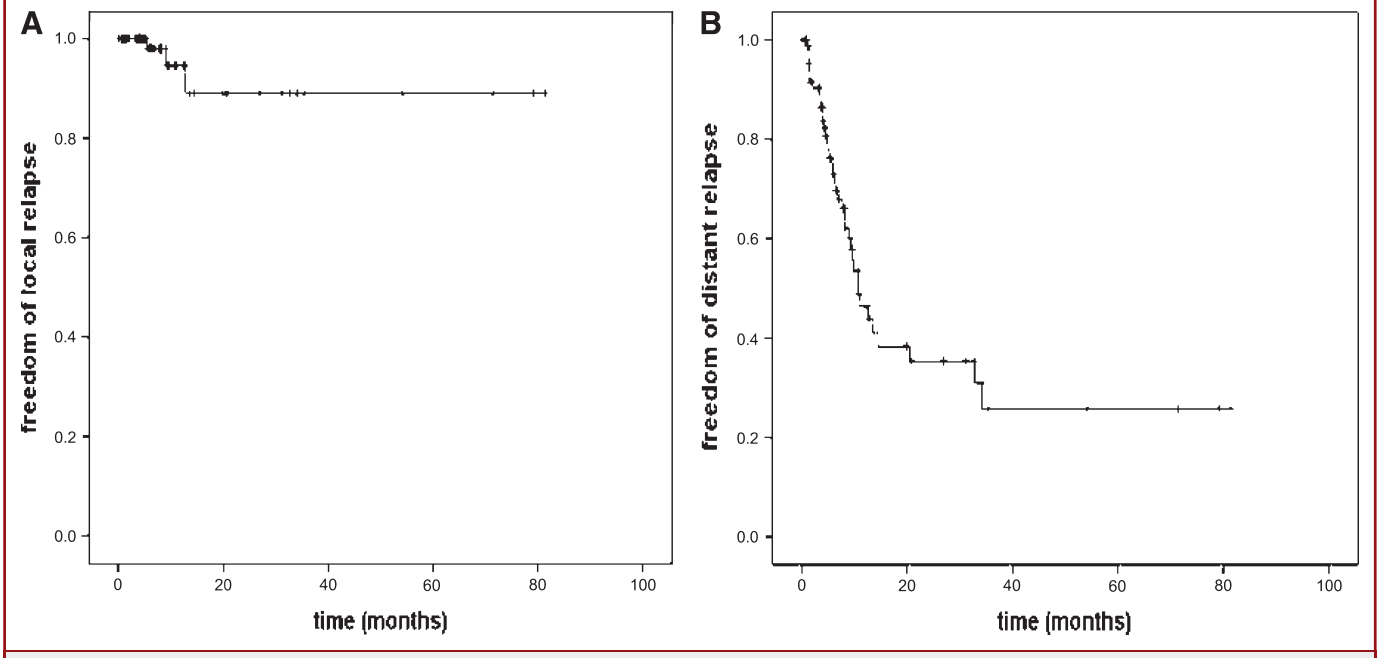

FIGURE 4. *Graphs show relapse of cerebral disease at the original site of the treated metastasis (**A**, left) and distant cerebral progression (including the procedure-related inoculated tumors; **B**, right).*

Copyright © Congress of Neurological Surgeons. Unauthorized reproduction of this article is prohibited.

TABLE 3. Prognostic Factors for Survival (n = 90)[a]

			P
Age, y	≤ 65 (n = 57)	> 65 (n = 33)	NS
Sex	Male (n = 48)	Female (n = 42)	NS
KPS	< 70[b] (n = 7)	≥ 70 (n = 83)	< .002
Stable systemic disease	Yes[b] (n = 49)	No (n = 41)	< .02
RPA class	1[b] (n = 34)	2 + 3 (n = 56)	< .02
Morphology of metastasis	Solid (n = 33)	Necrotic (n = 57)	NS
Interval: initial cancer diagnosis to SBT, mo	> 12[b] (n =54)	≤ 12 (n = 36)	< .05
Time of SBT	1990-1999 (n = 14)	2000 and after (n = 76)	NS
Previous cerebral treatment	Yes (n = 29)	No (n = 61)	NS
Previous WBRT	Yes (n = 21)	No (n = 69)	NS
Localization	Lobar (n = 49)	Other (n = 41)	NS
	Brainstem/basal ganglia (n = 29)	Other (n = 61)	NS
Volume, cm^3	≤ 14 (n = 70)	> 14 (n = 20)	NS
Radioresponsiveness	Radioresistant (n = 20)	Radiosensitive (n = 70)	NS

[a]KPS, Karnofsky performance status; RPA, recursive partition analysis, SBT, stereotactic ^{125}iodine brachytherapy; SRS, stereotactic radiosurgery; WBRT, whole brain radiation therapy.
[b]Factors for a favorable survival.

morbidity was 3.3%: 2 patients developed superficial wound infections and 1 had a cerebrospinal fluid fistula. All 3 patients underwent surgical revision, and the implanted seed catheters could be preserved in all patients.

DISCUSSION

The possibility of obtaining histological confirmation by biopsy and treating the metastasis within 1 stereotactically guided surgical procedure represents the main indication of SBT, especially when the deep-seated and/or eloquent localization of the tumor excludes microsurgical removal. SBT can be considered a safe technique, with a minimal 3.3% surgical risk of transient complications, no procedure-related mortality, and no deterioration of neurological status and KPS in 95.5% of cases.

A limited stay as an inpatient (3 days in median) and the minimally invasive nature of the stereotactic procedure do not hinder subsequent administration of any systemic treatment regiments (eg, chemotherapy).

From 1992 to 2008, we treated 90 patients with SBT, while about five-fold more patients received linear accelerator SRS in our institution for cerebral metastases displaying the strict inclusion criteria for SBT. However, according to our treatment standards, we did not offer SRS to patients with lesions > 3 cm in diameter (or a volume of 14 cm^3) or to patients who had already undergone prior radiation treatment (SRS and/or WBRT). For such cases, we indicated SBT, taking into account the favorable radiobiological characteristics of this irradiation technique in terms of its effectiveness for tumor treatment and protection of the surrounding tissue.

Radiobiological Effects of SBT

The core principle of (stereotactic) brachytherapy is the application of a lethal irradiation dose inside the tumor while optimally sparing the surrounding healthy tissue, thus allowing an almost strictly local treatment regimen. To achieve such a favorable biological effect, the desired irradiation dose is administered continuously over a prolonged time interval. This results in a substantially reduced dose rate compared with externally delivered irradiation and is therefore called "low-dose-rate irradiation."

This effect is complemented by placing the irradiation source inside the tumor. Because of the inverse-square law of radiation, this results in a very steep dose falloff toward the periphery within a 1-mm range, also considerably reducing the radiation burden on surrounding tissue. This means the option of further external irradiation (conventional fractionated or radiosurgery) or even the repetition of stereotactic brachytherapy is preserved as much as possible.

On the basis of experimental findings and clinical experience from numerous treatments of gliomas, we implanted ^{125}iodine seeds temporarily for 42 days, achieving a cumulative reference dose of 50 Gy on the surface of the tumor and resulting in a comparatively low initial dose rate of 0.1 cGy/min.[5,26]

^{125}Iodine emits photons at 28 to 35 keV and has a half-life of 59.4 days. In comparison, external (conventional fractionated/radiosurgery) irradiation uses dose rates of about 150 to 500 cGy/min with an energy of 6 MeV.

The use of computer-based planning for the stereotactic irradiation combined with stereotactically guided positioning of the ^{125}iodine seeds within the tumor allows highly conformed irradiation with maximum precision within a 1-mm range.[25] This technique provides irradiation planning even for geometrically

Copyright © Congress of Neurological Surgeons. Unauthorized reproduction of this article is prohibited.

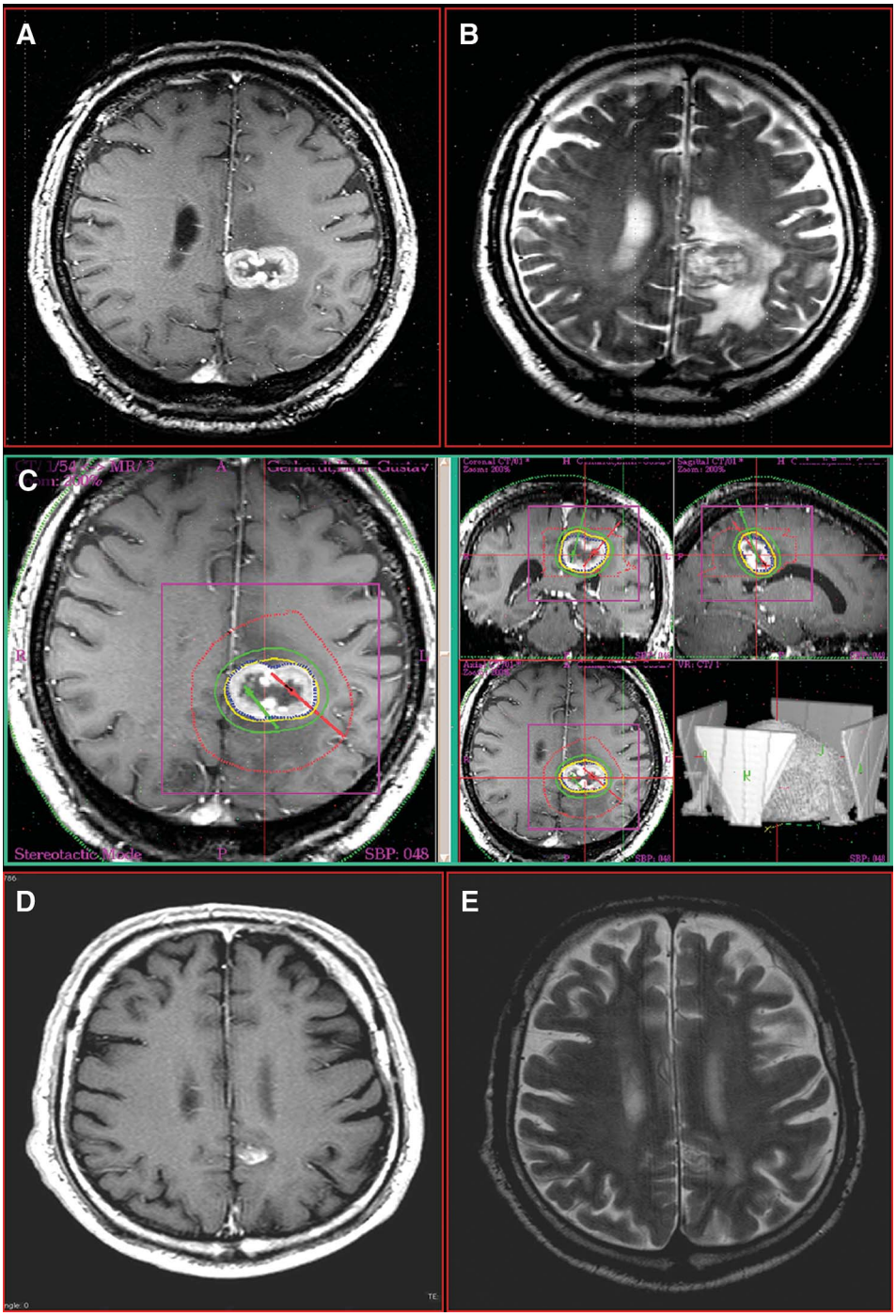

FIGURE 5. *Illustrative case.* **A** *and* **B**, *T1 contrast– and T2-weighted magnetic resonance imaging (MRI) scans of a 69-year-old male patient with adenocarcinoma of the lung presenting a left parietal, partially cystic metastases with a volume of 15.2 cm*^{3}. *On examination, progressive hemiparesis, Karnofsky Performance Status (KPS) 70.* **C**, *the stereotactic* ^{125}*iodine brachytherapy computer plan shows 2 catheters (red and green trajectory) and the marked tumor surface (dotted blue line), the 50-Gy isodose (yellow line), and the 30-Gy isodose (green line). The surface dose was 50 Gy applied for 42 days. Each catheter was loaded with three* ^{125}*iodine seeds.* **D** *and* **E**, *follow-up MRI (T1 contrast and T2 weighted) reveals partial remission after 24 months. Patient displayed no neurological deficit and had stable systemic disease (KPS 90).*

Copyright © Congress of Neurological Surgeons. Unauthorized reproduction of this article is prohibited.

complex-shaped growth patterns of the tumor, and the irradiation plan with the applied dose distribution can be reproduced at any time. An illustrative case is shown in Figure 5.

Results of Other Local Treatment Methods

Under the proposition that SBT represents a local treatment option, we put our results in perspective with other local methods.

Surgery

Patchell et al[29] conducted a multicenter randomized trial comparing survival and tumor control in patients treated for singular metastases with or without WBRT after complete surgical resection. Survival rates were 43 weeks (10.75 months) for the surgery-only group vs 48 weeks (12 months) for the group receiving additional WBRT. After 6.75 months (median), recurrence at the primary site of the metastasis occurred in 46% and elsewhere in 70% of all patients.

Radiosurgery

For SRS alone, median survival in patients treated for singular metastases ranges from 8.2 to 10.3 months.[6,7,30] When selected by RPA criteria, class 1 patients displayed a better median survival of 14.0 to 16.0 months. The actuarial rate for the development of new metastases treated after 1 year was 25.8% in patients with singular and 76.4% for patients with up to 3 metastases.[7]

Surgery Combined With Brachytherapy

A combination of microsurgical resection and intraoperative application of ^{125}iodine seeds for brachytherapy, as reported by Huang et al[10] and Petr et al[11] resulted in a median survival of 12 and 14 months, respectively. Both studies achieved local control in $>$ 90% of cases within the initial 12 to 16 months, and distant cerebral progression was evident in 32% to 37% of patients within the first year.

Comparison With SBT Results

Although patients selected for our study displayed a worse median KPS score (KPS 70) compared with those in the studies mentioned above (KPS 80), the median survival in the RPA class 1 subgroup (18.1 months) correlated well with populations receiving SRS only.[6,7,10,11,29,30]

This disparity in the KPS might also contribute to the fact that the overall survival in our population was slightly worse (8.5 months) compared with the patients treated with microsurgery only (10.75 months; Patchell et al[29]) or the population receiving microsurgery and adjacent ^{125}iodine seed placement in the resection cavity (11.3 months, Huang et al[10]; 14 months, Petr et al[11]).

With a local control failure rate of 5.4% and 46.4% for newly developed cerebral disease distant from the originally treated metastasis after 12 months, SBT compares well with other local irradiation techniques. In addition, it delivers far more favorable results compared with patients receiving surgical treatment only, as reported by Patchell and other authors (local recurrence in 34%-46%, distant recurrence 47%-75%).[7,29-33] Whether this difference in local control derives from the decline of radiation toward the periphery, providing a therapeutic safety margin and terminating possible malignant satellite cells adjacent to the visible tumor surface, has to be evaluated further.

The occurrence of new metastatic disease along the implanted seed catheters in 6.7% of our patients is difficult to explain. Possible reasons might be a dislocation of tumor cells caused by the circulation of cerebrospinal fluid along the implanted catheters or the catheter itself serving as a growth matrix for the tumor cells. However, we could demonstrate that in these cases a repetition of SBT represents a feasible salvage treatment option.

Prognostic Factors

As far as prognostic markers are concerned, those factors relating to a steady neurological status, namely a KPS score of $>$ 70, stable systemic disease, and an interval of $>$ 12 months between the initial cancer diagnosis and SBT treatment, all correlated with significantly longer survival.

As mentioned, patients with RPA class 1 disease had considerably higher median survival rates than those displaying characteristics of RPA class 2 and 3 patients, reflecting the generally favorable selection criteria of RPA class 1 patients within the RTOG classification system. However, none of the factors had an influence on the time to progression period.

Furthermore, a volume $>$ 14 cm^3 and necrotic morphology of the metastasis compromised the local response to therapy. However, the fact that 19 of 20 patients with a metastasis $>$ 14 cm^3 still displayed the criteria for partial response/stable disease on the interim follow-up evaluation and only 1 patient has shown signs of progressive disease demonstrates that even in the case of a large lesion, therapeutic efficacy could be achieved.

As reported for SRS, the responsiveness of metastatic tissue to irradiation did not influence the outcome or tumor response documented on MRI for our study population, further indicating the radiobiological effectiveness of SBT.[16,34-36]

The majority of our patients did not receive previous WBRT. In agreement with Ostertag and Kreth,[13] the survival, chance of developing new cerebral disease, or destiny to die of cerebral disease in this population was not yet significantly different compared with those receiving additional WBRT.

The divergence of this observation with the otherwise widely reported benefit of adjuvant WBRT for reducing distant cerebral disease relapse might be due to the restricted number of patients in this study. Additional studies with larger patient populations must be performed and further compared with other treatment options for patients with (singular) cerebral metastases.

CONCLUSION

We demonstrated that SBT represents a minimally invasive, safe, and feasible method for treating singular brain metastases, allowing histological confirmation and treatment within

Copyright © Congress of Neurological Surgeons. Unauthorized reproduction of this article is prohibited.

stereotactic procedures. Overall survival and survival of the RPA class 1 patients were comparable to other local treatment methods. In terms of local and distant control of cerebral disease, this method appears to be more favorable than surgical resection only and almost identically as effective as SRS alone or surgery combined with adjuvant brachytherapy of the resection cavity. The favorable biological effect of the low activity irradiation from within the tumor allows future irradiation treatment or repetition of the method without causing radiation-induced necrosis. Thus, SBT can be considered a safe and effective treatment option in cases ''left behind'' by surgery or SRS and might therefore close a gap for patients harboring singular brain metastases.

Disclosure

The authors have no personal financial or institutional interest in any of the drugs, materials, or devices described in this article.

REFERENCES

1. Patchell RA, Tibbs PA, Walsh JW, et al. A randomized trial of surgery in the treatment of single metastases to the brain. *N Engl J Med*. 1990;322(8):494-500.
2. Vecht CJ, Haaxma-Reiche H, Noordijk EM, et al. Treatment of single brain metastasis: radiotherapy alone or combined with neurosurgery? *Ann Neurol*. 1993;33(6):583-590.
3. Andrews DW, Scott CB, Sperduto PW, et al. Whole brain radiation therapy with or without stereotactic radiosurgery boost for patients with one to three brain metastases: phase III results of the RTOG 9508 randomised trial. *Lancet*. 2004;363(9422):1665-1672.
4. Sturm V, Kober B, Höver KH, et al. Stereotactic percutaneous single dose irradiation of brain metastases with a linear accelerator. *Int J Radiat Oncol Biol Phys*. 1987;13(2):279-282.
5. Voges J, Treuer H, Erdmann J, et al. Linac radiosurgery in brain metastases. *Acta Neurochir Suppl*. 1994;62:72-76.
6. Sneed PK, Suh JH, Goetsch SJ, et al. A multi-institutional review of radiosurgery alone vs. radiosurgery with whole brain radiotherapy as the initial management of brain metastases. *Int J Radiat Oncol Biol Phys*. 2002;53(3):519-526.
7. Aoyama H, Shirato H, Tago M, et al. Stereotactic radiosurgery plus whole-brain radiation therapy vs. stereotactic radiosurgery alone for treatment of brain metastases: a randomized controlled trial. *JAMA*. 2006;295(21):2483-2491.
8. Bogart JA, Ungureanu C, Shihadeh E, et al. Resection and permanent I-125 brachytherapy without whole brain irradiation for solitary brain metastasis from non-small cell lung carcinoma. *J Neurooncol*. 1999;44(1):53-57.
9. Dagnew E, Kanski J, McDermott MW, et al. Management of newly diagnosed single brain metastasis using resection and permanent iodine-125 seeds without initial whole-brain radiotherapy: a two institution experience. *Neurosurg Focus*. 2007;22(3):E3.
10. Huang K, Sneed PK, Kunwar S, et al. Surgical resection and permanent iodine-125 brachytherapy for brain metastases. *J Neurooncol*. 2009;91(1):83-93.
11. Petr MJ, McPherson CM, Breneman JC, Warnick RE. Management of newly diagnosed single brain metastasis with surgical resection and permanent I-125 seeds without upfront whole brain radiotherapy. *J Neurooncol*. 2009;92(3):393-400.
12. Schulder M, Black PM, Shrieve DC, Alexander E III, Loeffler JS. Permanent low-activity iodine-125 implants for cerebral metastases. *J Neurooncol*. 1997;33(3):213-221.
13. Ostertag CB, Kreth FW. Interstitial iodine-125 radiosurgery for cerebral metastases. *Br J Neurosurg*. 1995;9(5):593-603.
14. Bradley KA, Mehta MP. Management of brain metastases. *Semin Oncol*. 2004;31(5):693-701.
15. Voges J, Treuer H, Sturm V, et al. Risk analysis of linear accelerator radiosurgery. *Int J Radiat Oncol Biol Phys*. 1996;36(5):1055-1063.
16. Kocher M, Treuer H, Voges J, et al. Computer simulation of cytotoxic and vascular effects of radiosurgery in solid and necrotic brain metastases. *Radiother Oncol*. 2000;54(2):149-156.
17. Prados M, Leibel S, Barnett CM, et al. Interstitial brachytherapy for metastatic brain tumors. *Cancer*. 1989;63(4):657-660.
18. Carpentier A, McNichols RJ, Stafford RJ, et al. Real-time magnetic resonance-guided laser thermal therapy for focal metastatic brain tumors. *Neurosurgery*. 2008;63(1 suppl 1):ONS21-ONS28.
19. Karnofsky DA, Burchenal JH. The clinical evaluation of chemotherapeutic agents in cancer. In: MacLeod CM, ed. *Evaluation of Chemotherapeutic Agents*. New York, NY: Columbia University Press; 1949:191-205.
20. Macdonald DR, Cascino TL, Schold SC Jr, Cairncross J. Response criteria for phase II studies of supratentorial malignant glioma. *J Clin Oncol* 1990;8(7):1277-1280.
21. Sturm V, Pastyr O, Schlegel W, et al. Stereotactic computer tomography with a modified Riechert-Mundinger device as the basis for integrated stereotactic neuroradiological investigations. *Acta Neurochir*. 1983;68(1-2):11-17.
22. Sumanaweera TS, Adler JR Jr, Napel S, Glover GH. Characterization of spatial distortion in magnetic resonance imaging and its implications for stereotactic surgery. *Neurosurgery*. 1994;35(4):696-703.
23. Hunsche S, Sauner D, Maarouf M, et al. MR-guided stereotactic neurosurgery: comparison of fiducial-based and anatomical landmark transformation approaches. *Phys Med Biol*. 2004;49(12):2705-2716.
24. Nath R, Anderson LL, Luxton G, et al. Dosimetry of interstitial brachytherapy sources: recommendations of the AAPM radiation therapy committee task group no 43. *Med Phys*. 1995;22(2):209-234.
25. Treuer H, Klein D, Maarouf M, et al. Accuracy and conformity of stereotactically guided interstitial brain tumor therapy using I-125 seeds. *Radiother Oncol*. 2005;77(2):202-209.
26. Voges J, Sturm V. Interstitial irradiation with stereotactically implanted I-125 seeds for the treatment of cerebral glioma. *Crit Rev Neurosurg*. 1999;9(4):223-233.
27. Kaplan EL, Meier P. Nonparametric estimation from incomplete observations. *J Am Stat Assoc*. 1958;53:457-481
28. Gaspar L, Scott C, Rotman M, et al. Recursive partitioning analysis (RPA) of prognostic factors in three Radiation Therapy Oncology Group (RTOG) brain metastases trials. *Int J Radiat Oncol Biol Phys*. 1997;37(4):745-751.
29. Patchell RA, Tibbs PA, Regine WF, et al. Postoperative radiotherapy in the treatment of single metastases to the brain: a randomized trial. *JAMA*. 1998;280(17):1485-1489.
30. Muacevic A, Wowra B, Siefert A, et al. Microsurgery plus whole brain irradiation versus Gamma Knife surgery alone for treatment of single metastases to the brain: a randomized controlled multicentre phase III trial. *J Neurooncol*. 2008;87(3):299-307.
31. Armstrong JG, Wronski M, Galicich J, et al. Postoperative radiation for lung cancer metastasic to the brain. *J Clin Oncol*. 1994;12(11):2340-2344.
32. Hagen NA, Cirrincione C, Thaler HT, DeAngilis LM. The role pf radiation therapy following resection of single brain metastases from melanoma. *Neurology*. 1990;40(1):158-160.
33. Skibber JM, Soong SJ, Austin L, Blach CM, Sawaya RE. Cranial irradiation after surgical excision of brain metastases in melanoma patients. *Ann Surg Oncol*. 1996;3(2):118-123.
34. Brown PD, Brown CA, Pollock BE, Gorman DA, Foote RL. Stereotactic radiosurgery for patients with ''radioresistant'' brain metastases. *Neurosurgery*. 2008;62(Suppl 2):790-801.
35. Powell JW, Chung CT, Shah HR, et al. Gamma Knife surgery in the management of radioresistant brain metastases in high-risk patients with melanoma, renal cell carcinoma, and sarcoma. *J Neurosurg*. 2008;109(suppl):122-128.
36. Clarke JW, Register S, McGregor JM, et al. Stereotactic radiosurgery with or without whole brain radiotherapy for patients with a single radioresistant brain metastasis. *Am J Clin Oncol*. 2010;33(1):70-74.

COMMENT

The implantation of radioactive sources (brachytherapy or ''near'' therapy) to treat patients with brain tumors is a method nearly as old as neurosurgery. It was first used a century ago and was described by many authors, including Harvey Cushing. Brachytherapy largely fell out of favor for various reasons, including improved methods of external

Copyright © Congress of Neurological Surgeons. Unauthorized reproduction of this article is prohibited.

radiotherapy, safety concerns with radioactive sources, and the uncertain dosimetry of these sources. In the 1980s, computed tomography and then magnetic resonance imaging stereotaxis led to a revival of interest in brachytherapy, especially because afterloading techniques allowed control of the delivered dose. The now-defunct Gliasite balloon system promoted this further by providing a standardized method for implantation and dosimetry. The unavailability of Gliasite and the increasing preference for stereotactic radiosurgery (SRS) have led to another decline in neurosurgical enthusiasm for the use of brachytherapy.

Patients with metastatic tumors might seem to be the least likely candidates for brachytherapy, an invasive and highly focal treatment, because their management is palliative by definition. Plus, SRS now has a well-established track record for controlling brain metastases. Despite this, Ruge et al make a convincing case for using of brachytherapy for treating selected patients with single metastatic tumors. They present a retrospective review of 90 patients treated over 15 years. Selection criteria included the need for tissue diagnosis, tumor volume > 14 cm^3, Karnofsky Performance Status ≥ 60, previous radiotherapy and/or SRS, and/or eloquent tumor location. Low-activity I-125 seeds were loaded into catheters that were then stereotactically inserted into the tumor; they were removed 5 to 6 weeks later. Only 3 patients had a local relapse of tumor, and median patient survival was 8.5 months. Tumor control was better in patients who were younger and in better condition (Radiation Therapy Oncology Group recursive partitioning analysis class 1) and with tumor volumes < 14 cm^3. Complications were few: 2 patients sustained wound infections, and 1 had a cerebrospinal fluid leak.

Of course, no focal treatment will have a major impact on survival of patients with brain metastases. But, we should continue to strive to improve local control of their brain tumors so that they are not the cause of a patient's demise. The neurosurgical community should not give up on this powerful, safe, and century-old technique.

Michael Schulder
Manhasset, New York

Follow NEUROSURGERY® on FaceBook

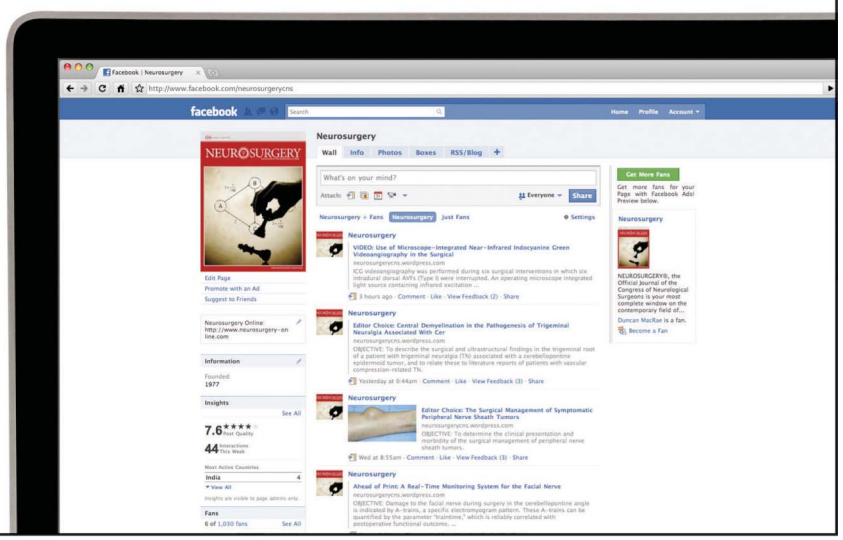

Follow NEUROSURGERY® at http://www.facebook.com/neurosurgerycns

NEUROSURGERY
THE REGISTER OF THE NEUROSURGICAL MIND

Copyright © Congress of Neurological Surgeons. Unauthorized reproduction of this article is prohibited.

Anterior Thoracolumbar Corpectomies: Approach Morbidity With and Without an Access Surgeon

Seunggu J. Han, MD*
Darryl Lau, BA*
Daniel C. Lu, MD, PhD‡
Pierre Theodore, MD§
Dean Chou, MD*

*Department of Neurological Surgery, University of California San Francisco, San Francisco, California; ‡Department of Neurological Surgery, University of California Los Angeles, Los Angeles, California; §Division of General Thoracic Surgery, Department of Surgery, University of California San Francisco, San Francisco, California

Correspondence:
Dean Chou, MD,
Department of Neurological Surgery,
University of California at San Francisco,
505 Parnassus Ave, Box 0112,
San Francisco, CA 94143.
E-mail: choud@neurosurg.ucsf.edu

Received, February 2, 2010.
Accepted, September 10, 2010.

Copyright © 2011 by the
Congress of Neurological Surgeons

BACKGROUND: Anterior approaches for thoracolumbar corpectomies can have significant morbidity. Spine surgeons have historically performed their own anterior approaches, but recently access surgeons are being used more frequently.

OBJECTIVE: To evaluate the morbidity rates of approaches performed by an access surgeon and by an approach-trained spinal neurosurgeon.

METHODS: From 2004 to 2008, 46 patients undergoing anterior thoracolumbar corpectomies (levels T2-L5) by the senior author (D.C.) were identified and subdivided into 2 groups based on whether an access surgeon was involved. Nine patients were excluded, leaving 37 patients in the final analysis. Blood loss, operative times, length of hospital stay, complications, and neurological outcomes were evaluated.

RESULTS: Eighteen patients had anterior spinal access by an approach-trained spinal neurosurgeon, and 19 patients underwent the approach by an access surgeon. Surgeries performed by the spinal neurosurgeon alone were comparable to those performed by an access surgeon with respect to operative time, days spent in the hospital, blood loss, complication rates, and improvement in neurological function.

CONCLUSION: There appears to be no increased morbidity of anterior approaches performed by an approach-trained spinal neurosurgeon compared with approaches performed by an access surgeon in terms of operative time, complication rate, and improvement in neurological function.

KEY WORDS: Access, Anterior, Approach, Morbidity, Surgeon, Thoracic, Thoracolumbar

Neurosurgery 68:1220–1226, 2011 DOI: 10.1227/NEU.0b013e31820eb287 www.neurosurgery-online.com

The anterior approach is useful to address pathologies of the anterior thoracolumbar spine. However, the transthoracic, thoracolumbar, and retroperitoneal approaches may carry associated morbidities.[1-5] Although historically spine surgeons have performed their own approaches, there has been a trend toward using access surgeons for a multitude of reasons: complication management, decreased stress for the spine surgeon, and medical-legal ramifications.

However, there are no formal criteria for the involvement of access surgeons, and there are urgent situations when access surgeons are not available. Although a posterior approach is an option, in some of these instances, an anterior approach may be ideal. In the interest of salvaging neurological function and timely surgery, it is often necessary for an approach-trained spine surgeon to perform the approach without an access surgeon. This may be particularly true in otherwise healthy patients with no significant cardiopulmonary dysfunction, no previous anterior surgery, and straightforward anatomy. Because the approaches are not always performed by access surgeons at our institution, we wished to evaluate whether anterior approaches performed by an approach-trained spinal neurosurgeon carried an increased morbidity compared with anterior approaches performed by access surgeons.

ABBREVIATION: ASIA, American Spinal Injury Association

CLINICAL MATERIALS AND METHODS

Between 2004 and 2008, 46 consecutive patients who underwent anterior thoracolumbar corpectomies by the senior author (D.C.) were identified. These corpectomies included levels T2 to L5. T1 was excluded because of the often-used transcervical approach

Copyright © Congress of Neurological Surgeons. Unauthorized reproduction of this article is prohibited.

to this level. The patients' clinical histories, perioperative outcomes, and postoperative follow-up data were collected by a detailed retrospective chart review. The data were stratified on the basis of the number of levels and analyzed on the basis of whether the approach was performed by an access surgeon or an approach-trained spinal neurosurgeon (D.C.). Access surgeons were cardiothoracic surgeons in 13 cases, vascular surgeons in 2, general surgeons in 2, and urologists in 2 cases. These operations were done with 3 cardiothoracic surgeons (with 1 performing 11 approaches), 2 individual vascular surgeons, 2 general surgeons, and 2 urologists. The spinal neurosurgeon was trained as a resident and as a fellow to perform these anterior thoracolumbar approaches.

Levels involved were divided into thoracic (T2-11), thoracolumbar (T12-L1), and lumbar (L2). All anterior corpectomies involving the L3-4-5 levels (n = 3) were performed with the assistance of an access surgeon for mobilization of the iliac veins, and these patients were excluded from final comparison analysis because of a lack of adequate equivalent controls in the group without an access surgeon. In addition, all 3-level corpectomies were performed with an access surgeon only, and these patients were also excluded from final analysis (n = 6). Thus, after exclusion of the 9 patients described above, the remaining series of patients used for comparison analyses included 18 patients who underwent corpectomies by the neurosurgeon alone and 19 patients who underwent corpectomies with an access surgeon.

Analysis of morbidity outcomes included the following factors: operative time, blood loss, length of stay, complications, and postoperative neurologic recovery. Complications were defined as any intraoperative or postoperative event that required medical or surgical intervention. Neurological function and recovery were evaluated with the American Spinal Injury Association (ASIA) Impairment Scale monitored preoperatively and postoperatively.

Statistical analysis used the 2-tailed t test or Fischer exact test when appropriate. Statistical significance was determined at a threshold of $P = .05$.

RESULTS

Clinical Data

Of the 37 patients who underwent thoracolumbar corpectomies by an anterior approach, 18 approaches were performed by the approach-trained spinal neurosurgeon (Figure 2), and 19 were performed by an access surgeon (Figure 3).

Of the patients whose corpectomies were performed by a neurosurgeon, the mean age was 48 years, 10 patients (56%) were male, and the average follow-up was 18.2 months. Among the patients whose corpectomies were performed with the assistance of an access surgeon, the mean age was 51 years, 18 patients (69%) were male, and the mean follow-up was 10.5 months. There was no statistically significant difference in the mean ages of the 2 groups ($P = .40$). In the group whose surgeries did not use an access surgeon, 7 patients carried a diagnosis of a burst fracture, 5 patients had osteomyelitis, 3 had metastatic cancer, 2 had multiple myeloma (pathological fractures), and 1 patient had lymphoma (diagnosed at surgery) (Table 1). In the group whose corpectomies had the assistance of an access surgeon, 6 patients had osteomyelitis, 4 patients had metastatic cancer, 4 had burst fractures, 3 had sarcomas, 1 had hemangioma, and 1 had chordoma (Table 2). In each group (access surgeon and no access surgeon), 1 revision case was performed; the rest of the patients did not have previous anterior surgery (Table 3).

Of the corpectomies performed by the neurosurgeon alone, 5 cases (27.8%) involved 2 vertebral levels, and 13 cases (72.2%) involved 1 level only. The mean number of levels performed was 1.28. Of the corpectomies performed with the access surgeon,

TABLE 1. Clinical Profile of Patients Who Underwent Anterior Surgery by an Access-Trained Spinal Neurosurgeon[a]

Patient	Corpectomy Level	Pathological Diagnosis	Complication	Preoperative ASIA	Postoperative ASIA
1	T6	Lymphoma	None	E	E
2	L2	Renal cell carcinoma	None	E	E
3	T9–10	Osteomyelitis	Recurrence of infection	E	E
4	T8	Melanoma	None	C	E
5	T10	Osteomyelitis	Pleural effusion	E	N/A
6	L2	Burst fracture	Wound infection	D	D
7	T7	Metastatic breast cancer	None	E	C
8	T8	Burst fracture	None	E	E
9	L1	Burst fracture	None	E	E
10	T10	Osteomyelitis	None	D	E
11	L1	Burst fracture	None	D	E
12	L2	Burst fracture	None	C	E
13	T7–8	Pott disease	None	D	E
14	L1	Burst fracture	None	E	E
15	L1	Burst fracture	Pleural effusion	B	D
16	T9–10	Multiple myeloma	Death	C	N/A
17	T7–8	Multiple myeloma	None	C	N/A
18	T12–L1	Multiple myeloma	None	C	E

[a]ASIA, American Spinal Injury Association; N/A, not available.

Copyright © Congress of Neurological Surgeons. Unauthorized reproduction of this article is prohibited.

TABLE 2. Clinical Profile of Patients Who Underwent Anterior Surgery With the Assistance of an Access Surgeon[a]

Patient	Corpectomy Level	Pathologic Diagnosis	Complication	Preoperative ASIA	Postoperative ASIA
1	T8–9	Osteomyelitis	Death	A	N/A
2	T6	Metastatic colon cancer	None	C	C
3	T9–10	Osteomyelitis	None	D	N/A
4	T5–6	Pott disease	Pleural effusion	C	E
5	T6–7	Osteomyelitis	Pleural effusion	C	D
6	T3–4	Osteomyelitis	UTI	C	D
7	T12–L1	Osteomyelitis	None	C	D
8	L1	Burst fracture	None	E	N/A
9	T7	Liposarcoma	Wound infection	E	E
10	T4	Sarcoma	None	E	C
11	L1	Cordoma	Implant failure	E	C
12	L2	Burst fracture	Adjacent-level vertebral body fracture	E	D
13	T4	Hemangioma	None	D	E
14	L1	Burst fracture	None	E	D
15	L1–2	Metastatic renal cell carcinoma	Splenic hemorrhage	E	E
16	T12	Burst fracture	None	A	B
17	L2	Metastatic renal cell carcinoma	Wound infection	D	C
18	L1	Sarcoma	None	E	E
19	T12–L1	Metastatic renal cell carcinoma	None	E	E

[a]ASIA, American Spinal Injury Association; N/A, not available; UTI, urinary tract infection.

7 cases (36.8%) involved 2 levels, and 11 cases (57.9%) involved 1 level. The mean number of levels operated on was 1.47. This difference in mean number of levels performed was not statistically significant (P = .28). In the group whose corpectomies were performed without an access surgeon, 10 cases involved the thoracic spine, 1 case involved the thoracolumbar spine, and 7 cases involved the lumbar spine. Of the corpectomies performed with an access surgeon, 9 cases were on the thoracic spine, 3 were on the thoracolumbar spine, and 7 were on the lumbar spine.

Perioperative Factors

The mean operative time for patients undergoing anterior corpectomy by the neurosurgeon was 423 minutes; for patients undergoing anterior corpectomy with the help of an access surgeon, it was 479 minutes. This difference was not statistically significant (P = .17). There was, however, a significantly lower mean blood loss in the corpectomies performed without an access surgeon than in those done with an access surgeon (1123 vs 2420 cm^3, respectively; P = .03). There was no significant difference in mean number of days the patients spent in the hospital (14.7 days without access surgeon vs 12.0 days with access surgeon; P = .38).

When stratified by number of levels involved, this difference in blood loss remained significant for 1-level corpectomies (859 cm^3 with neurosurgeon vs 2468 cm^3 with access surgeon; P = .03) but not for 2 levels (1850 cm^3 with neurosurgeon vs 2159 cm^3 with access surgeon; P = .72). Stratification by levels did not yield a significant difference in operative times between the 2 groups for 1-level (420 minutes with neurosurgeon vs 495 minutes with access surgeon; P = .19) and 2-level (428 minutes with neurosurgeon vs 464 minutes with access surgeon; P = .56) corpectomies.

TABLE 3. Comparison of Data Between Neurosurgeon-Performed Approaches and Access Surgeon–Performed Approaches[a]

	EBL, mL	Operative Time, min	Neurological Recovery, n/T	Length of Hospital Stay, d	Complication, n/N	Number of Patients With Prior Anterior Surgery, n/N
Neurosurgeon (n = 18)	1123	423	6/18	14.7	5/18	1/18
Access surgeon (n = 19)	2420	479	6/19	12.0	9/19	1/19
P	.03	.17	.27	.38	.29	.74

[a]EBL, estimated blood loss.

Copyright © Congress of Neurological Surgeons. Unauthorized reproduction of this article is prohibited.

When stratified by region of surgery, the difference in operative blood loss was no longer statistically significant for the thoracic, thoracolumbar, or lumbar level (819 vs 1575 cm^3, $P = .17$; 3600 vs 1900 cm^3, no P value because of small sample size; 1117 vs 2872 cm^3, $P = .12$, neurosurgeon vs access surgeon, respectively). Operative times were significantly shorter for the corpectomies performed by the neurosurgeon alone compared with those done by the access surgeon for thoracic corpectomies (384 vs 477 minutes; $P = .04$) but not for thoracolumbar or lumbar corpectomies (480 vs 525 minutes, no P value because of small sample size; 480 vs 486 minutes, $P = .95$, neurosurgeon vs access surgeon, respectively).

Complications

The overall complication rate for patients with corpectomies performed by the spine neurosurgeon was 22% (4 of 18). One patient suffered a postoperative death resulting from myocardial infarction, 2 patients suffered pleural effusions, and 2 patients had a wound infection (Table 1). For patients whose corpectomies were performed with an access surgeon, the overall complication rate was 47% (9 of 19). In this group of patients, there was 1 perioperative death, 2 patients with pleural effusions, 2 wound infections, 1 implant failure, 1 incidence of fracture of the adjacent vertebral body, 1 splenic injury, and 1 urinary tract infection (Table 2). There was no statistically significant difference between the overall complication rates for the 2 groups ($P = .29$).

Neurological Outcomes

The preoperative and postoperative neurological outcomes were measured with the ASIA scale (A–E). Preoperatively, in the group whose corpectomies did not use an assisting access surgeon, no patient had a score of A, 1 patient had a score of B, 5 had a score of C, 3 had a score of D, and 8 had a score of E (Figure 1A). Postoperatively, no patient had a score of A or B, 1 patient had a score of C, 2 had a score of D, and 12 had a score of E (Figure 1B). From preoperative to postoperative states, the ASIA score improved in 6 of these patients (33.3%). Among the patients whose surgeries were assisted by an access surgeon, preoperatively, there were 3 patients with a score of A, no patients with a score of B, 5 with a score of C, 3 with a score of D, and 9 with a score of E (Figure 1A). Postoperatively, no patient had a score of A, 1 patient had a score of B, 4 had a score of C, 5 had a score of D, and 6 had a score of E (Figure 1B). After the corpectomy, 6 of these patients (31.6%) improved neurologically by at least 1 ASIA score. There was no statistically significant difference in the proportion of patients who had an improved ASIA score between the group who were operated on with an access surgeon and those who were not ($P = .27$).

DISCUSSION

Anterior access to the thoracic and lumbar spine carries significant morbidities, often necessitating a thoracotomy, splitting of the diaphragm, or retroperitoneal dissection with mobilization of vessels.[1] A number of complications are associated with anterior procedures of the thoracolumbar spine. Pulmonary problems, including atelectasis, pneumonia, and respiratory failure, are the most common among reported complications for procedures of the thoracic spine.[1] Other complications described

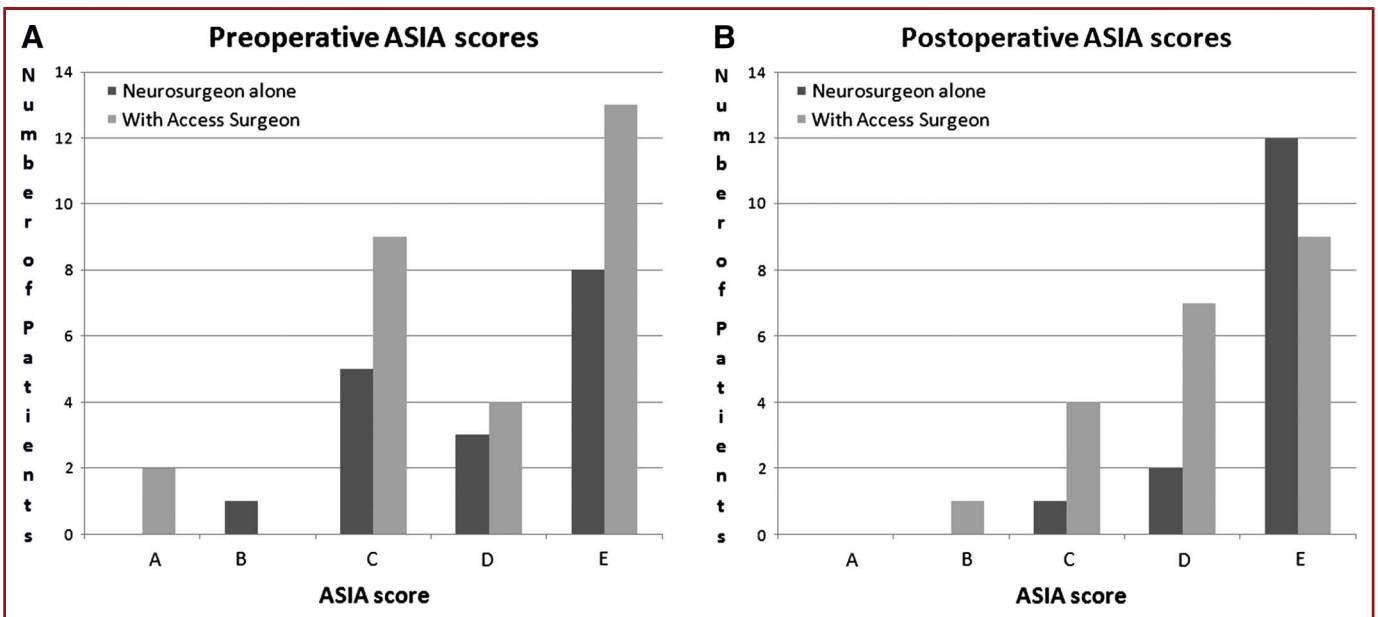

FIGURE 1. *Histogram representing neurological functions of patients preoperatively (A) and postoperatively (B). Function is scored on the American Spinal Injury Association (ASIA) Impairment Scale.*

Copyright © Congress of Neurological Surgeons. Unauthorized reproduction of this article is prohibited.

include spinal cord ischemia,[6] cardiac arrhythmias and myocardial infarctions,[7] chylothorax,[8,9] and ileus. Complications for anterior access to the lumbar spine include vascular injury to a major retroperitoneal vessel[10]; thrombotic occlusion of vessels[2,11]; injury to the ureter[5]; injury to the hypogastic sympathetic plexus leading to retrograde ejaculation[12]; injury to somatic nerves such as the iliohypogastric, ilioinguinal, and genitofemoral nerves[13]; and ileus. A higher risk of complications is frequently reported for older patients,[4,14] women, and those with multiple comorbidities.[15]

The current literature regarding the comparison of presence and absence of an access surgeon during anterior thoracolumbar spine surgery is limited and not conclusive. Holt et al[16] reported a lower rate of complications, less blood loss, and shorter operative time in anterior procedures performed by the spine surgeon compared with anterior procedures described in the literature as having been performed by a spine surgeon with the assistance of a general surgeon or a vascular surgeon. They also concluded that the anterior thoracolumbar spine can be accessed safely by a spine surgeon alone.[16] However, Jagannathan et al, when comparing anterior spine operations performed by a neurosurgeon alone and operations assisted by vascular surgeons at the same center, found significantly shorter operative times and less blood loss when a vascular access surgeon was used.[17] However, this study focused on the lumbar spine, specifically the lower lumbar spine (L3-S1). The L3-S1 levels were excluded from our study, which included only the thoracic, thoracolumbar, and upper lumbar spine.

McDonnell and colleagues[4] performed a detailed study of perioperative complications in 447 patients undergoing anterior procedures of the thoracolumbar spine and found an overall complication rate of 31%. Those authors found that pulmonary complications, including pneumonia, respiratory failure necessitating reintubation or prolonged intubation, and genitourinary complications such as cystitis, were most common.[4] Janik et al[2] reported an overall complication rate of 9.8%; respiratory complications such as pleural effusion consisted of $>$ 50% of the complications and vascular injury was found in 1.4% of cases. Stulik and colleagues[5] focused on vascular injury of anterior procedures and found injury to thoracic duct in 1 patient (0.4%), vascular injury to major blood vessels in 1% (1.26% of lumbar procedures), and damage to ureter in 1 patient (0.4%).[5] Baker and colleagues[10] noted a vascular injury rate of procedures of the anterior lumbar spine of 15.6%. Kang and colleagues[3] found a 12.1% overall complication rate in their series of 412 anterior lumbosacral procedures, and the most common complication encountered was sympathetic dysfunction (6%).

Although varied by region and institution, these procedures are performed both in conjunction with an access surgeon and by the spine surgeon alone. In our report, the age, distribution of sex, indications for operation, and preoperative neurological function (measured by ASIA) were similar between the 2 groups analyzed. Our analysis found that the operative time and number of days the patients spent in the hospital were similar whether an access surgeon assisted in the operation or not. We found that the blood loss of the operation was significantly higher when an access surgeon was present, a finding that remained significant when stratified for 1-level corpectomies. This finding may be due to a selection bias, which is an inherent difficulty of retrospective analyses. Although the numbers of revision cases performed by the spine surgeon alone and with an access surgeon were equivalent, the spine neurosurgeon may have felt comfortable doing the approaches without an access surgeon for straightforward cases without a propensity for high blood loss. Complex cases with significant comorbidities likely incorporated the use of an access surgeon. This would have induced a selection bias that could not be borne out by standard statistical measurements alone. A T7 osteomyelitis case completely within the bone could

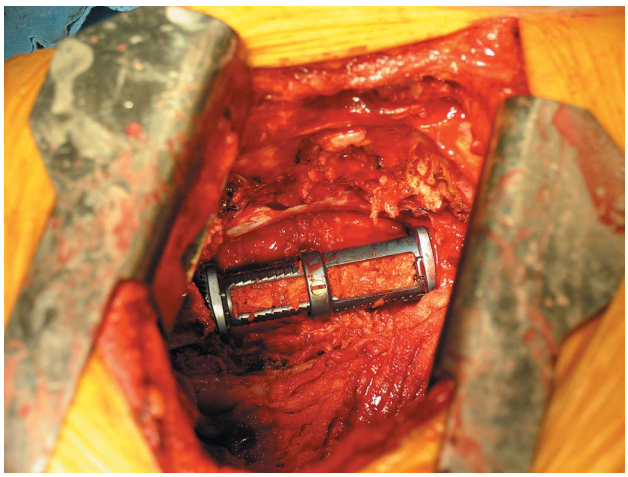

FIGURE 2. *Thoracotomy for T9-10 corpectomy performed by a neurosurgeon alone.*

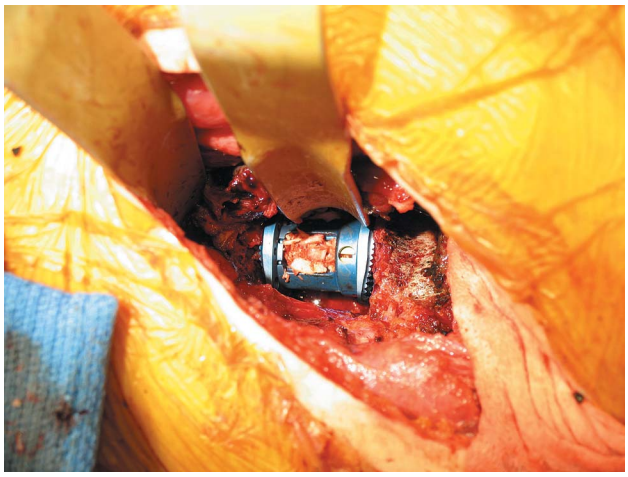

FIGURE 3. *Thoracotomy for L2 spondylectomy performed in conjunction with a cardiothoracic surgeon.*

Copyright © Congress of Neurological Surgeons. Unauthorized reproduction of this article is prohibited.

have been selected to be performed by the neurosurgeon alone, but a T7 osteomyelitis that eroded ventrally into the segmental vessels and the great vessels would probably have been selected to be performed with a thoracic surgeon. Thus, the less blood loss seen in the cases done by a neurosurgeon alone should be carefully considered when such a selection bias probably existed. Thus, there were factors related to clinical judgment that were not easily quantifiable for analysis. However, counting the numbers of revision surgeries in each group was easily performed, and we did not find a significant difference between the 2 groups in this regard.

In our series, the complication rates for patients who underwent corpectomies performed by the neurosurgeon alone and with an access surgeon's assistance were 22% and 47%, respectively. This difference was not statistically significant. In concordance with previous reports, the most complications encountered were pleural effusions from thoracotomy and wound infections for both groups in our series. Two patients died as a complication of the operation, a rate of 4.3% of all patients included. A review of complications in anterior exposure of the thoracic and lumbar spine by Ikard and colleagues[1] reported an overall mortality rate of 0.7%. Overall, there was no statistical difference in the improvement in neurological function of patients operated on by the neurosurgeon alone compared with the neurological improvement seen in cases operated on with an access surgeon. In our series, about one-third of patients showed an improvement to the next ASIA grade.

Although a single spine neurosurgeon performed the approach, the access surgeons varied. There are a few reasons for this difference. Because this study population consisted of corpectomies for nondegenerative pathologies, many of the patients were inpatients who needed fairly urgent procedures because of either cord compression or severe deformity precluding ambulation. Thus, specifying a single access surgeon was not practical in such situations because it would have resulted in delay of surgery. In other situations, the referring physician was the access surgeon. A urologist would have referred a patient with metastatic renal cell cancer for resection and wished to perform a nephrectomy during the same surgery. In such an instance, the access surgeon was the referring physician. Because of the retrospective nature of this study and the nonelective nature of these cases, various access surgeons were used.

CONCLUSION

Anterior thoracolumbar approaches from T2 to L2 performed by an access-trained spinal neurosurgeon did not demonstrate a clear difference in morbidity compared with approaches performed by an access surgeon in terms of operative time, complication rate, blood loss, and improvement in neurological function.

Disclosure

Dr Han was supported by the Howard Hughes Medical Institute. The authors have no personal financial or institutional interest in any of the drugs, materials, or devices described in this article.

REFERENCES

1. Ikard R. Methods and complications of anterior exposure of the thoracic and lumbar spine. *Arch Surg*. 2006;141(10):1025-1034.
2. Janik J, Burrington JD, Janik JE, Wayne ER, Chang JH, Rothenberg SS. Anterior exposure of spinal deformities and tumors: a 20-year experience. *J Pediatr Surg*. 1997;32(6):852-859.
3. Kang B, Choi WC, Lee SH, et al. An analysis of general surgery-related complications in a series of 412 minilaparotomic anterior lumbosacral procedures. *J Neurosurg Spine*. 2009;10(1):60-65.
4. McDonnell M, Glassman SD, Dimar JR II, Puno RM, Johnson JR. Perioperative complications of anterior procedures on the spine. *J Bone Joint Surg Am*. 1996;78(6):839-847.
5. Stulik J, Vyskocil T, Bodlak P, et al. Injury to major blood vessels in anterior thoracic and lumbar spinal surgery. *Acta Chir Orthop Traumatol Cech*. 2006;73(2):92-98.
6. Hodgson A, Stock FE. Anterior fusion: a preliminary communication on radical treatment of Pott's disease and Pott's paraplegia. *Br J Surg*. 1956;44(185):266-275.
7. Hodgson A, Stock FE. Anterior spine fusion for the treatment of tuberculosis of the spine. *J Bone Joint Surg*. 1960;42:295-310.
8. Nakai S, Zieklke K. Chylothorax: a rare complication after anterior and posterior spinal correction: report on six cases. *Spine (Phila Pa 1976)*. 1986;11(8):830-833.
9. Colletta A, Mayer PJ. Chylothorax: an unusual complication of anterior thoracic interbody fusion. *Spine (Phila Pa 1976)*. 1982;7(1):46-49.
10. Baker J, Reardon PR, Reardon MJ, Heggeness MH. Vascular injury in anterior lumbar surgery. *Spine (Phila Pa 1976)*. 1993;18(15):2227-2230.
11. Marsicano J, Mirovsky Y, Remer S, Bloom N, Neuwirth M. Thrombotic occlusion of the left common iliac artery after an anterior retroperitoneal approach to the lumbar spine. *Spine (Phila Pa 1976)*. 1994;19(3):357-359.
12. Flynn J, Price CT. Sexual complications of anterior fusion of the lumbar spine. *Spine (Phila Pa 1976)*. 1984;9(5):489-492.
13. Mirovsky Y, Neuwirth M. Injuries to the lateral femoral cutaneous nerve during spine surgery. *Spine (Phila Pa 1976)*. 2000;25(10):1266-1269.
14. Spivak J, Neurwirth MG, Giordano CP, Bloom N. The perioperative course of combined anterior and posterior spinal fusion. *Spine (Phila Pa 1976)*. 1994;19(5):520-525.
15. Faciszewski T, Winter RB, Lonstein JE, Denis F, Johnson L. The surgical and medical perioperative complications of anterior spinal fusion surgery in the thoracic and lumbar spine in adults: a review of 1223 procedures. *Spine (Phila Pa 1976)*. 1995;20(14):1592-1599.
16. Holt R, Majd ME, Vadhva M, Castro FP. The efficacy of anterior spine exposure by an orthopedic surgeon. *J Spinal Disord Tech*. 2003;16(5):477-486.
17. Jagannathan J, Chankaew E, Urban P, et al. Cosmetic and functional outcomes following paramedian and anterolateral retroperitoneal access in anterior lumbar spine surgery. *J Neurosurg Spine*. 2008;9(5):454-465.

COMMENTS

In this study, Han et al present the results of a retrospective nonrandomized study of approach morbidity in thoracolumbar corpectomies with and without an access surgeon. Patients with T1 lesions and lower lumbar lesions were excluded. Overall, 37 patients were analyzed. Examination of the data revealed no significant difference in patient demographics, distribution of lesion types or locations, operative time, complication rate, or length of hospital stay. Mean blood loss was not statistically different between the 2 groups, although a statistically lower blood loss was noted in patients who underwent a single-level corpectomy when the exposure was performed by a neurosurgeon.

These results suggest that, in specific circumstances, anterior exposure of the thoracolumbar spine can be performed by a neurosurgeon with a morbidity comparable to that experienced by access surgeon. The ability to extrapolate these data to other centers and other patient

Copyright © Congress of Neurological Surgeons. Unauthorized reproduction of this article is prohibited.

populations is unknown because the level of training and adeptness of individual surgeons are variable. In addition, as noted by the authors, selection bias is inherent in a study of this type and is, in fact, thought to be likely in the present study. Nevertheless, the data suggest that appropriately trained and experienced spinal surgeons may be able to perform this type of exposure in accordance with community standards.

Christopher A. Wolfla
Milwaukee, Wisconsin

Neurosurgeons are physicians and surgeons. Most of us did a full year of general surgery in our training and have been exposed to the full breadth of surgery. In practice, we have, by choice or external factors, become highly specialized, and most of us rely on our surgical colleagues to provide exposure in thoracic and thoracolumbar surgeries. Our specialty demands specific knowledge of general anatomy. We have a greater understanding of the exact exposure required to affect the appropriate neurosurgical component of the operation than many of our surgical colleagues who do not do this type of procedure with frequency. There are occasions when a fully trained surgical colleague is either not available or not willing to assist on certain cases. This excellent article shows that, in properly trained hands, the thoracic and thoracoabdominal approaches can be performed safely and expediently by the neurosurgeon. I would challenge our future generations to maintain their general surgical skills.

William C. Welch
Philadelphia, Pennsylvania

The authors compare the approach morbidity of anterior thoracolumbar spinal procedures performed by a neurosurgeon and an access surgeon. Overall, this is a thoughtful, well-written article. On first glance, it appears as though there is not a significant difference in the complication rate, operative time, and neurological outcome between the approach-trained spinal neurosurgeon and the access surgeon. However, the authors appropriately noted that there may have been some bias in this retrospective study because some of the more complicated cases may have been performed by the access surgeon and straightforward cases by the neurosurgeon. This, combined with the relatively small sample size, makes it difficult to state conclusively that there is no difference in approach-related morbidity between an appropriately trained neurosurgeon and an access surgeon. The challenge for neurosurgeons is not performing the exposure but how to intraoperatively deal with any significant vascular complication during the approach.

Langston T. Holly
Los Angeles, California

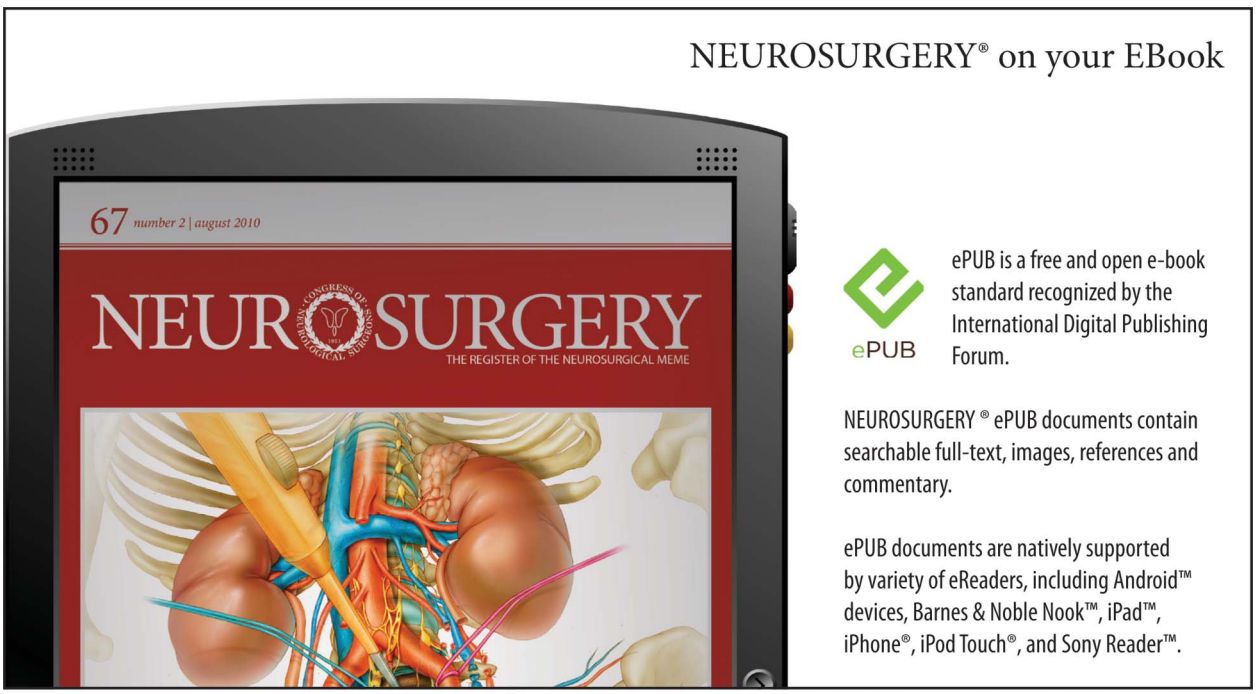

Find NEUROSURGERY® ePUB content at www.neurosurgery-online.com

NEUROSURGERY

Copyright © Congress of Neurological Surgeons. Unauthorized reproduction of this article is prohibited.

Epilepsy After Bypass Surgery in Adult Moyamoya Disease

Sung-Chul Jin, MD*
Chang Wan Oh, MD*
O-Ki Kwon, MD*
Gyojun Hwang, MD*
Jae Seung Bang, MD*
Hyun-Seung Kang, MD‡
Jeong Eun Kim, MD‡
Sang Hyung Lee, MD§
Young-Seob Chung, MD§

*Department of Neurosurgery, Seoul National University Bundang Hospital, Seongnam, Korea; ‡Department of Neurosurgery, Seoul National University Hospital, Seoul, Korea; §Department of Neurosurgery, Seoul National University Boramae Hospital, Seoul, Korea

Correspondence:
Chang Wan Oh, MD,
Seoul National University Bundang Hospital,
300 Gumi-dong,
Bungdang-gu,
Seongnam-si,
Gyeonggi-do, 463-707, Korea.
E-mail: wanoh@snu.ac.kr

Received, February 11, 2010.
Accepted, September 10, 2010.

Copyright © 2011 by the
Congress of Neurological Surgeons

BACKGROUND: Postoperative seizure, well-known in association with other pathologies, has been rarely discussed in adult moyamoya disease.

OBJECTIVE: We evaluated postoperative seizures in adult patients with moyamoya undergoing revascularization surgery.

METHODS: From 2001 to 2007, 43 adult patients with moyamoya disease underwent 53 revascularization surgeries, consisting of direct bypass with or without indirect bypass. Incidence and profile of postoperative seizures were investigated, with evaluation of influencing factors. Multivariable analysis using a generalized estimation equation was performed to determine which factors were related to postoperative seizure.

RESULTS: Seizures developed in 10 sides (18.9%) after revascularization for moyamoya disease, including immediate (<24 hours, n = 0), early (1-7 days, n = 5), late (8-30 days, n = 0), and delayed seizures (≥1 month, n = 7). Early and subsequent delayed seizures developed in the same lesions in 2 patients. Seizures developed only in the patients with combined direct and indirect revascularization. Postoperative temporary neurological deficits with imaging abnormalities were significantly related to postoperative non-delayed seizures ($P = .02$). Delayed seizures were significantly different according to the location of the recipient artery ($P = .03$), especially with the frontal branches. By multivariable analysis, revascularization using frontal branches trended toward increased incidence of delayed postoperative seizure, with adjusted odds ratio of 13.78 (95% confidence interval, 1.7-114.1).

CONCLUSION: In adult patients with moyamoya disease, the incidence of delayed postoperative seizure seems to be higher than that of other pathologies. The delayed, pronounced formation of synangiosis in moyamoya disease may be related to the development of such delayed postoperative seizures, especially when the location of the recipient artery is frontal.

KEY WORDS: Adults, Moyamoya disease, Postoperative seizure, Revascularization

Neurosurgery 68:1227–1232, 2011 DOI: 10.1227/NEU.0b013e31820c045a www.neurosurgery-online.com

Postoperative seizure after craniotomy is a well-known clinical presentation,[1-5] the incidence of which varies according to the primary disease and procedure.[5] Moyamoya disease is a rare occlusive cerebrovascular disease with unknown etiology characterized by bilateral progressive stenosis of the terminal portion of the internal carotid arteries and abnormal vascular network at the base of the brain.[6] Revascularization surgery for moyamoya disease is believed to prevent cerebral ischemic attacks by improving cerebral blood flow,[7-10] and superficial temporal artery (STA)-to-middle cerebral artery (MCA) anastomosis with or without indirect bypass is actively performed for adult patients with moyamoya disease after an ischemic insult. However, epilepsy after revascularization of adult moyamoya disease has rarely been discussed. To evaluate the incidence of seizures and influencing factors in adult

ABBREVIATIONS: AED, antiepileptic drug; **DSA,** digital subtraction angiography; **EMS,** encephalomyosynangiosis; **ICH,** intracerebral hemorrhage; **MCA,** middle cerebral artery; **SPECT,** single photon emission-computed tomography; **STA,** superficial temporal artery; **TIA,** transient ischemic attack; **TND,** temporary neurological deficit

Copyright © Congress of Neurological Surgeons. Unauthorized reproduction of this article is prohibited.

patients with moyamoya disease who underwent direct bypass with or without indirect bypass, we reviewed our data retrospectively.

MATERIALS AND METHODS

Patient Population and Perioperative Studies

From January 2001 to May 2007, 43 symptomatic patients with moyamoya disease or probable moyamoya disease (ie, unilateral involvement, n = 9) underwent 53 STA-MCA bypasses with or without indirect revascularization (ie, encephaloduroarteriosynangiosis, encephalomyosynangiosis [EMS], or encephaloduroarteriomyosynangiosis) performed in our institution by senior author CWO (Table 1). Patients included 13 men and 30 women, with a mean age of 37.3 years (range, 14-67 years). All of the patients included in this analysis presented with ischemic symptoms and signs; we usually do not perform surgery for patients with hemorrhagic type moyamoya unless the cerebral perfusion is severely decreased or a combined aneurysm (especially in the basal perforators) is present. Clinical assessment after discharge consisted mainly of outpatient visits combined with telephone interviews (mean duration of follow-up, 54.8 months; range; 18-95 months). This retrospective study was approved by the institutional review board.

TABLE 1. Baseline Characteristics of the Patients (n = 43)[a]

Characteristics	No. (%)
Sex	
Female	30 (69.8)
Male	13 (30.2)
Mean age: 37.3 y (range, 14-67)	
Lesions for revascularization (n = 53)	
Right side	26 (49.1)
Left side	27 (50.9)
Preoperative symptoms	
TIA	34 (64.2)
Ischemic stroke	19 (35.8)
Preoperative basal perfusion	52
Normal	13 (24.5)
Focal decrease	18 (34.0)
Extended decrease	21 (39.6)
Misery perfusion	31 (58.5)
Surgical methods	
Direct revascularization	11 (20.8)
Direct plus indirect revascularization	42 (79.2)
Indirect revascularization methods	
EMS	15 (35.7)
EDAS	17 (40.5)
EDAMS	10 (23.8)
Recipient artery site	
Frontal branches	22 (41.5)
Others	29 (54.7)
Double-barrel	2 (3.8)

[a]EDAMS, encephaloduroarteriomyosynangiosis; EDAS, encephaloduroarteriosynangiosis; EMS, encephalomyosynangiosis; TIA, transient ischemic attack.

Preoperative evaluation consisted mainly of clinical assessment, brain MRI, digital subtraction angiography (DSA), and single photon emission computed tomography (SPECT) with acetazolamide challenge. Surgery was performed within 3 months of the last ischemic event, and the preoperative Karnofsky performance scale was more than 80. *Misery perfusion* was defined as decrease of both basal perfusion and reserve capacity on SPECT. Basal perfusion was categorized into 3 groups: (1) normal; (2) focal, ie, perfusion decreased only in 1 or 2 of the frontal, temporal, parietal, and occipital lobes; and (3) extended, ie, 3 or 4 lobes involved.

DSA, SPECT, and/or perfusion CT were performed 6 months after surgery. *Postoperative temporary neurological deficit* was defined as full recovery from neurological deficits and no residual neurological deficits within 1 month after surgery. Postoperative imaging abnormalities included cerebral infarction, subdural fluid collection or sudural hemorrhage, subarachnoid hemorrhage, intraventricular hemorrhage, intracerebral hemorrhage (ICH), and epidural hemorrhage.

Evaluation of Postoperative Seizures and Antiepileptic Medication

Postoperative seizures were divided into non-delayed (within 1 month) and delayed (after 1 month) groups based on the time interval following surgery. The non-delayed group consisted of 3 types, again based on timing after surgery: immediate seizures (within 24 hours); early seizures (between 1 and 7 days); and late seizures (between 8 and 30 days).

This analysis included focal motor type seizures, and abnormal events consisting of sensory or visual symptoms only were excluded from the analysis, because their features were difficult to differentiate from postoperative transient ischemic attacks (TIAs) or other nonspecific discomforts. It may be difficult to differentiate focal motor seizures from limb shaking or other TIAs.[11] Clinical features such as provoking factors, rhythms of involuntary movement, associated head or eye turning, and change of consciousness were used to distinguish focal motor seizures from limb shaking or other TIAs. Simple episodes of paralysis were regarded as TIAs. For inpatients, response to intravenous antiepileptic medication also was regarded as an important criterion for postoperative seizures. Electroencephalography was done in patients with repeated seizures, but those interictal electroencephalograms were not useful for the differential diagnosis, demonstrating "nonspecific abnormal waves" only, which usually is observed in most patients after craniotomy.

Antiepileptic medication (valproic acid, 500-600 mg twice daily) was given to all patients for 2 to 3 weeks after surgery. If no seizures occurred, it was discontinued. In patients who did experience 1 or more seizures, it was continued for another 3 to 4 weeks after the last seizure. Further medication depended on whether the patient experienced additional seizures.

Surgical Strategies for Adult Patients With Moyamoya

Our perioperative management during direct revascularization with or without indirect bypass in moyamoya disease has been previously reported.[12] The detailed surgical techniques we used for STA-MCA anastomosis also were described in the previous report.[13] In patients with bilateral symptomatic hypoperfusion, we performed the first operation on the hemisphere with more recent or severe symptoms, and the other side usually was revascularized more than 1 month after the first surgery. The recipient artery was chosen on the basis of cerebral perfusion status and angiographic features. Indirect bypass of EMS was performed using a thin slice of temporalis muscle to avoid the excessive mass effect caused by swelling of the muscle flap.

Copyright © Congress of Neurological Surgeons. Unauthorized reproduction of this article is prohibited.

Statistical Analysis

Statistical analysis was performed to evaluate the influencing factors for non-delayed or delayed seizures after bypass surgery in moyamoya disease. Nominal data were analyzed with the Fisher exact or χ^2 test and numerical data with the Mann-Whitney U test. $P < .05$ was considered significant. Multivariable analysis using a generalized estimation equation was performed to determine influencing factors for postoperative delayed seizure. Based on results of univariate analysis and our anticipation of influencing factors, independent factors consisted of preoperative symptoms, sites of recipient artery, temporary neurological deficit (TND) with imaging abnormalities, and imaging abnormalities in multivariable analysis.

RESULTS

The preoperative presenting symptoms of the patients in our study (43 adult patients with 53 symptomatic lesions) included TIAs in 34 lesions and ischemic stroke in 19 lesions. No patient presented with a seizure attack. A basal SPECT study was normal in 13 lesions (24.5%), focal decrease was normal in 18 (34.0%), and extended decrease was normal in 21 lesions (39.6%). Misery perfusion was demonstrated in 31 lesions (58.5%). Treatment modalities for symptomatic moyamoya disease were as follows:

- STA-MCA anastomosis without indirect bypass: 11 lesions;
- STA-MCA anastomosis with EMS: 15 lesions;
- STA-MCA anastomosis with encephaloduroarteriosynangiosis: 17 lesions; and
- STA-MCA anastomosis with encephaloduroarteriomyosynangiosis: 10 lesions.

Recipient arteries for direct bypass included frontal branches (n = 22), parietal branches (n = 16), and temporal branches (n = 13) of the middle cerebral artery. We performed a double-barrel bypass using the frontal and parietal branch in 2 lesions. TND without imaging abnormality developed postoperatively in 6 lesions (11.3%). TND with imaging abnormality after bypass surgery developed in 8 lesions (15.1%), as follows: infarction, 4 lesions;ICH subarachnoid hemorrhage, or intraventricular hemorrhage, 2 lesions; subdural hemorrhage, 1 lesions; and subdural fluid collection, 1 lesions. None of the hemorrhagic complications in this group were severe, and the hemorrhage and symptoms resolved completely. Persistent neurological deficits after revascularization developed in 7 lesions (13.2%), as follows: a large basal ganglia ICH, which required hematoma evacuation leading to severe deficit, in 1 lesion a large bifrontal infarction leading to severe deficit in 1 patient; a small ipsilateral infarction (with or without a small amount of hemorrhage) with mild to moderate deficit in 5 lesions DSA performed 6 months after bypass surgery in adult patients with moyamoya disease showed good direct anastomosis and synangiosis in 51 hemispheres (96.2%) and poor revascularization in 2 hemispheres (3.8%). Results of SPECT or CT perfusion 6 months after bypass surgery included improved perfusion in 47 hemispheres (88.7%), no change of perfusion in 4 hemispheres (7.5%), and decreased perfusion in 2 hemispheres (3.8%).

All of the postoperative seizures developed in patients who underwent combined direct and indirect revascularization. Postoperative seizure, which developed in 10 hemispheres (18.9%), included early seizure in 5 lesions (9.4%) and delayed seizure in 7 lesions (13.2 %, Table 2). Early seizure and subsequent delayed seizure developed in 2 patients. There were no immediate or late seizures after revascularization. All early seizures were controlled well with routine perioperative antiepileptic medication (2-3 weeks). Among 7 patients with delayed seizures, 4 required medication for several weeks only without further seizure; in the other 2 cases, seizures were controlled with the maintenance of antiepileptic drugs; the remaining patient showed intermittent repeated seizures even after trying several antiepileptic medications. The last patient had undergone bilateral surgeries, and uncontrolled seizures began to develop 4 months after the second surgery. All of the patients with delayed seizure showed good direct anastomosis and synangiosis on DSA, and improvement of perfusion on SPECT or perfusion CT 6 months after bypass surgery.

In patients with moyamoya, the influence of several factors on the development of early (ie, non-delayed) or delayed seizures was analyzed statistically for the following variables:

- Sex;
- Age;
- Preoperative symptoms;
- Degree of decrease in basal perfusion;
- Presence of misery perfusion;
- Infection;
- Onset time of seizure;
- Sites of recipient artery;
- Surgical modalities (direct bypass only or direct with indirect revascularization);
- Methods of indirect revascularization;
- Use of temporalis muscle as method of indirect revascularization;
- TND with imaging abnormalities;
- TND without imaging abnormalities;
- Persistent neurological deficits;
- Imaging abnormalities, including no symptomatic presentation.

In univariate analysis, nondelayed seizures demonstrated a relationship with preoperative symptoms presenting with stroke (P = .05) and TND with imaging abnormalities (P = .02). For delayed seizures, the site of the recipient artery in the frontal branch (P = .04) showed a significant influence on the development of seizures. Revascularization using frontal branches also trended toward significantly increased postoperative delayed seizure in multivariable analysis (adjusted odds ratio [OR], 13.74, 95% confidence interval [CI], 1.66-114.07) (Table 3). No seizures occurred in the patients who underwent direct bypass only, although this was not statistically significant.

Copyright © Congress of Neurological Surgeons. Unauthorized reproduction of this article is prohibited.

TABLE 2. Clinical Characteristics of Adult Moyamoya Patients With Postoperative Seizures[a]

Case No.	Sex/Age, y	Diagnosis	Presentation	Surgical Methods	Location of Recipient Artery	TND Without Image Abnormalities	TND With Image Abnormalities	PND	Seizure Onset Time	Present Status of Seizure
1	F/25	MMD	Stroke	Dir + EMS	Frontal	No	No	No	Early	Free
2	M/49	MMD	Stroke	Dir + EDAMS	Frontal	No	Flap swelling	No	Early	Free
3	F/55	MMD	Stroke	Dir + EDAMS	Frontal	No	SDFC	No	Early	Free
4	F/15	MMD	Stroke	Dir + EDAS	Frontal	No	SAH	No	Early, delay	Free
5	F/48	MMD	TIA	Dir + EMS	Parietal	No	No	No	Delay	Free
6	F/22	MMD	TIA	Dir + EMS	Frontal	No	No	No	Delay	Uncontrolled
7	M/47	MMD	TIA	Dir + EDAS	Frontal	No	No	Infarction	Delay	Controlled
8	M/36	MMD	TIA	Dir + EDAS	Frontal	No	No	No	Delay	Free
9	M/14	MMD	TIA	Dir + EDAS	Frontal	No	No	No	Early, delay	Controlled
10	M/32	MMD	Stroke	Dir + EDAMS	Frontal	No	No	Infarction, IVH	Delay	Free

[a]Controlled, seizure free with anti-epileptic medication; Dir, direct bypass; EDAMS, encephaloduroarteriomyosynangiosis; EDAS, encephaloduroarteriosynangiosis; EMS, encephalomyosynangiosis; Free, seizure free; IVH, intraventricular hemorrhage; MMD, moyamoya disease; PND, persistent neurological deficit; SAH, subarachnoid hemorrhage; SDFC, subdural fluid collection; Stroke, ischemic stroke; TIA, transient ischemic attack; TND, temporary neurological deficit; Uncontrolled, intermittent seizure despite anti-epileptic medication.

DISCUSSIONS

Postoperative seizure is a well-recognized clinical presentation, with higher frequency in supratentorial lesions.[2,5,14-16] Its incidence varies according to the primary diseases in the supratentorial region, ranging from 3% to 92%.[2,16-21] Surgeries for arteriovenous malformation, intracerebral hematoma, ruptured middle cerebral artery aneurysm, cerebral abscess, and meningioma carry the highest risk for the development of postoperative seizure.[2] However, reports on postoperative seizure in adults with moyamoya who underwent revascularization surgery are limited. In our study, the overall incidence of seizure after revascularization in adult moyamoya disease was 18.9%, which is not lower than those of other pathologies.

Postoperative seizures usually are classified into 3 types based on the time interval after surgery: (1) immediate seizures, ie, within 24 hours; (2) early seizures, ie, within 1 week; and (3) late seizures, ie, 1 week or more after craniotomy.[22] Late seizures are considered to be true epilepsy and probably will require use of an antiepileptic drug (AED), because a fixed epileptic focus may have been formed. In this analysis, we arbitrarily defined *delayed seizures* as those developing later than 1 month after surgery, because our data showed that adults with moyamoya disease had a tendency to develop seizures beyond 1 month after revascularization, and this point seemed to deserve discussion. After revascularization surgery, adults with moyamoya disease showed a high incidence of delayed seizures compared with other pathologies reported in the literature.[23,24]

In the present series, among 7 patients with moyamoya with delayed-onset seizures, 4 patients became seizure-free after short-term (3-4 weeks) use of AED and 3 patients (5.7% of all MMD surgeries) required continuous maintenance of AED for the control of seizures. The mean onset time after surgery was shorter in the group who finally became seizure-free without AED than in those who required continuous use of AED (mean interval, 3.1 vs 11.7 months; range, 1-6 vs 4-23 months), suggesting that later onset implies formation of more intractable epileptogenic focus. Formation of such cortical vessels usually requires several months, and it may have a causal relationship with the increased incidence of delayed seizures in patients with moyamoya. Selecting frontal branches of the MCA as a recipient for STA-MCA anastomosis contributed significantly to the development of delayed seizures in moyamoya disease in univariate analysis (P = .03), and this significance also was confirmed by multivariable analysis (adjusted OR, 13.74; 95% CI, 1.66-114.07). These selected recipient arteries (prefrontal or precentral) are close to the motor

TABLE 3. Multivariable Analysis of Delayed Postoperative Seizure for Adult Moyamoya Patients[a]

Factors	Adjusted OR	Adjusted 95% CI	*P* Value
Preoperative symptoms			
TIA	1.00	1.00	
Stroke	0.82	0.18-3.87	.81
Recipient artery using frontal branches	13.74	1.66-114.07	.02
TND with image abnormalities	1.99	0.10-41.17	.66
Image abnormalities	0.80	0.12-5.16	.82

[a]CI, confidence interval; OR, odds ratio; TIA, transient ischemic attack; TND, transient neurologic deficit.

Copyright © Congress of Neurological Surgeons. Unauthorized reproduction of this article is prohibited.

cortex, and their location may be more vulnerable to the development of an epileptogenic focus of motor type than other sites of recipient arteries (eg, the anterior temporal or angular arteries). In moyamoya disease, even after direct bypass surgery only, abundant synangiosis is often observed around the surgery site,[9] and this difference in seizure incidence according to the location of the recipient artery may also suggest the relationship between synangiosis and the increased incidence of delayed seizures in such cases. In this series, all moyamoya patients with delayed postoperative seizure also showed good direct anastomosis and synangiosis on DSA 6 months after surgery. Postoperative delayed seizure in moyamoya disease developed only in those patients who underwent combined direct and indirect revascularization procedures, also suggesting that formation of more synangiosis by adding indirect bypass may have contributed to the development of delayed seizures.

In adults with moyamoya, combined direct and indirect surgery, however, usually provides more extensive revascularization compared with simple direct or indirect bypass only (unpublished data of our institute). Although the incidence of delayed seizures increased when indirect bypass was added, most of those seizures could be controlled by medication (except 1 patient in this series), and therefore we think that extensive revascularization is more important. For this reason, we still routinely perform combined direct and indirect surgery for most adult patients with moyamoya, with appropriate attention to the possible development of delayed seizures. Use of the frontal branches of the MCA as a recipient for direct anastomosis does not seem to be absolutely contraindicated, although we now try to use the anterior temporal artery for direct anastomosis whenever its size is appropriate.

Hyperperfusion syndrome, after revascularization such as carotid endarterectomy or extracranial–intracranial bypass, is characterized by unilateral headache, face and eye pain, seizures, and focal symptoms secondary to cerebral edema or hemorrhage.[25-27] Fujimura et al[28] reported that clinical features of hyperperfusion in adults with moyamoya who underwent revascularization included typical hyperperfusion syndrome and focal neurological deficit mimicking ischemic attack. In our studies, postoperative temporary focal neurological deficits with imaging abnormalities, which may be partially related to hyperperfusion syndrome, significantly influenced the development of early postoperative seizures ($P = .02$). Theoretical explanations for postoperative seizure and hyperperfusion syndrome include similar features, such as involvement of free radical species,[3,29] a theory that also supports the suggestion that early postoperative seizure after bypass in adult moyamoya disease may be related to hyperperfusion syndrome.

In patients with moyamoya who underwent direct bypass only, it is not clear why there was no seizure, especially for the nondelayed seizures. It may be due partially to the small number of patients in this group (n = 10). The increased area of contact of the cerebral cortex with the surface of a galeal or muscular flap, which may be more irritating than the inner surface of dura mater, may have contributed to the development of nondelayed seizures.

CONCLUSION

After revascularization surgery for adult patients with moyamoya, the incidence of delayed seizures (ie, onset later than 1 month after surgery) seems to be higher than that with other pathologies. Revascularization surgery using frontal branches and formation of synangiosis may have a causal relationship with the development of such delayed postoperative seizures. Most postoperative seizures were controlled with short-term or continued use of anti-epileptic medication, although the delayed seizures showed a tendency of intractability.

Disclosure

This study was supported by a grant of the Korea Health 21 R&D Project, Ministry of Health, Welfare and Family Affairs, Republic of Korea (grant no: A080588-26). The authors have no personal financial or institutional interest in any of the drugs, materials, or devices described in this article.

REFERENCES

1. Deutschman CS, Haines SJ. Anticonvulsant prophylaxis in neurological surgery. *Neurosurgery*. 1985;17(3):510-517.
2. Foy PM, Copeland GP, Shaw MD. The natural history of postoperative seizures. *Acta Neurochir (Wien)*. 1981;57(1-2):15-22.
3. Manaka S, Ishijima B, Mayanagi Y. Postoperative seizures: epidemiology, pathology, and prophylaxis. *Neurol Med Chir (Tokyo)*. 2003;43(12):589-600.
4. North JB, Penhall RK, Hanieh A, Frewin DB, Taylor WB. Phenytoin and postoperative epilepsy. A double-blind study. *J Neurosurg*. 1983;58(5):672-677.
5. Shaw MD, Foy PM. Epilepsy after craniotomy and the place of prophylactic anticonvulsant drugs: discussion paper. *J R Soc Med*. 1991;84(4):221-223.
6. Suzuki J, Takaku A. Cerebrovascular "moyamoya" disease. Disease showing abnormal net-like vessels in base of brain. *Arch Neurol*. 1969;20(3):288-299.
7. Karasawa J, Kikuchi H, Furuse S, Kawamura J, Sakaki T. Treatment of moyamoya disease with STA-MCA anastomosis. *J Neurosurg*. 1978 Nov;49(5):679-688.
8. Karasawa J, Kikuchi H, Furuse S, Sakaki T, Yoshida Y. A surgical treatment of "moyamoya" disease "encephalo-myo synangiosis." *Neurol Med Chir (Tokyo)*. 1977;17(1 pt 1):29-37.
9. Yoshida YK, Shirane R, Yoshimoto T. Non-anastomotic bypass surgery for childhood moyamoya disease using dural pedicle insertion over the brain surface combined with encephalogaleomyosynangiosis. *Surg Neurol*. 1999;51(4):404-411.
10. Mizoi K, Kayama T, Yoshimoto T, Nagamine Y. Indirect revascularization for moyamoya disease: is there a beneficial effect for adult patients? *Surg Neurol*. 1996;45(6):541-548.
11. Im SH, Oh CW, Kwon OK, et al. Involuntary movement induced by cerebral ischemia: pathogenesis and surgical outcome. *J Neurosurg*. 2004;100(5):877-882.
12. Kim JE, Oh CW, Kwon OK, et al. Transient hyperperfusion after superficial temporal artery/middle cerebral artery bypass surgery as a possible cause of postoperative transient neurological deterioration. *Cerebrovasc Dis*. 2008;25(6):580-586.
13. Newell DW, Vilela MD. Superficial temporal artery to middle cerebral artery bypass. *Neurosurgery*. 2004;54(6):1441-1448.
14. Lee ST, Lui TN, Chang CN, Cheng WC. Early postoperative seizures after posterior fossa surgery. *J Neurosurg*. 1990;73(4):541-544.
15. Suri A, Mahapatra AK, Bithal P. Seizures following posterior fossa surgery. *Br J Neurosurg*. 1998;12(1):41-44.
16. Wang EC, Geyer JR, Berger MS. Incidence of postoperative epilepsy in children following subfrontal craniotomy for tumor. *Pediatr Neurosurg*. 1994;21(3):165-172.
17. Foy PM, Chadwick DW, Rajgopalan N, Johnson AL, Shaw MD. Do prophylactic anticonvulsant drugs alter the pattern of seizures after craniotomy? *J Neurol Neurosurg Psychiatry*. 1992;55(9):753-757.
18. Legg NJ, Gupta PC, Scott DF. Epilepsy following cerebral abscess. A clinical and EEG study of 70 patients. *Brain*. 1973;96(2):259-268.
19. Mahaley MS Jr, Dudka L. The role of anticonvulsant medications in the management of patients with anaplastic gliomas. *Surg Neurol*. 1981;16(6):399-401.
20. North JB, Penhall RK, Hanieh A, et al. Postoperative epilepsy: a double-blind trial of phenytoin after craniotomy. *Lancet*. 1980;1(8165):384-386.

Copyright © Congress of Neurological Surgeons. Unauthorized reproduction of this article is prohibited.

21. Sbeih I, Tamas LB, O'Laoire SA. Epilepsy after operation for aneurysms. *Neurosurgery*. 1986;19(5):784-788.
22. Jennett WB. Early traumatic epilepsy. Definition and identity. *Lancet*. 1969;1(7604):1023-1025.
23. Keränen T, Tapaninaho A, Hernesniemi J, Vapalahti M. Late epilepsy after aneurysm operations. *Neurosurgery*. 1985;17(6):897-900.
24. Hwang SL, Lieu AS, Kuo TH, et al. Preoperative and postoperative seizures in patients with astrocytic tumours: analysis of incidence and influencing factors. *J Clin Neurosci*. 2001;8(5):426-429.
25. Piepgras DG, Morgan MK, Sundt TM Jr, Yanagihara T, Mussman LM. Intracerebral hemorrhage after carotid endarterectomy. *J Neurosurg*. 1988;68(4):532-536.
26. Solomon RA, Loftus CM, Quest DO, Correll JW. Incidence and etiology of intracerebral hemorrhage following carotid endarterectomy. *J Neurosurg*. 1986;64(1):29-34.
27. Sundt TM Jr, Sharbrough FW, Piepgras DG, et al. Correlation of cerebral blood flow and electroencephalographic changes during carotid endarterectomy: with results of surgery and hemodynamics of cerebral ischemia. *Mayo Clin Proc*. 1981;56(9):533-543.
28. Fujimura M, Kaneta T, Mugikura S, Shimizu H, Tominaga T. Temporary neurologic deterioration due to cerebral hyperperfusion after superficial temporal artery-middle cerebral artery anastomosis in patients with adult-onset moyamoya disease. *Surg Neurol*. 2007;67(3):273-282.
29. van Mook WN, Rennenberg RJ, Schurink GW, et al. Cerebral hyperperfusion syndrome. *Lancet Neurol*. 2005;4(12):877-888.

Acknowledgment

We would like to thank the Medical Research Collaborating Centre for statistical analysis on the manuscript of this paper.

COMMENTS

The authors report their experience with incidence of seizure, influencing factors of postoperative seizure after revascularization surgery in adult patients with moyamoya. The article is well written and explores an important aspect of seizure manifestation following revascularization procedures. The mean age of adults with moyamoya is 37.3 years, as opposed to 56.3 years in atherosclerotic disease. Although statistics do not suggest an influencing factor, older patients are more likely to have cerebral atrophy and infarcts that are chronic and stable. The seizure occurrence and the manifesting time would probably differ from those of younger patients with moyamoya disease. Postoperative delayed seizure in moyamoya disease developed only in those patients who underwent combined direct and indirect revascularization procedures, also suggesting that formation of more synangiosis by adding indirect bypass may have contributed to the development of delayed seizures. There were no seizures in the patients with moyamoya who underwent direct revascularization only. It is interesting to note that indirect revascularization leads to seizures, when revascularization, direct or indirect, will cause hyperperfusion in any instance.

Dattatraya Muzumdar
Mumbai, India

In this article, the authors present a useful descriptive series examining seizure risk after revascularization surgery in adults with moyamoya, and provide some insights into the potential risk factors. Early seizures were found to be associated with stroke (as opposed to transient ischemic attack) on presentation, and with postoperative transient neurological deficits in the setting of imaging abnormalities; these seizures occurred at a frequency similar to that seen in a contemporaneous cohort of patients undergoing revascularization for atherosclerotic disease, and despite the routine use of 2 to 3 weeks of prophylactic anticonvulsant therapy. Delayed seizures (>1 month postoperative), on the other hand, were seen exclusively in the patients with moyamoya, and appeared to be associated with frontal location of the bypass recipient branch. Furthermore, all seizures in the moyamoya group occurred in patients with combined direct and indirect bypass, possibly implicating additional cortical manipulation for early seizures, and greater synangiosis in the delayed ones. Despite the higher seizure incidence in the moyamoya group, these seizures were generally well controlled with additional anticonvulsant medication. Although it is difficult to draw definitive conclusions or alter therapies based upon a small series, these observations draw attention to potential risk factors and can guide modification of technique (such as use of a temporal rather than frontal recipient branch) as long as the primary objective of successful revascularization is not compromised.

Sepideh Amin-Hanjani
Chicago, Illinois

Copyright © Congress of Neurological Surgeons. Unauthorized reproduction of this article is prohibited.

Weight Changes in Subthalamic Nucleus vs Globus Pallidus Internus Deep Brain Stimulation: Results From the COMPARE Parkinson Disease Deep Brain Stimulation Cohort

Maren C. Locke, BS*
Samuel S. Wu, PhD‡
Kelly D. Foote, MD§
Marco Sassi, MD¶
Charles E. Jacobson, BS*
Ramon L. Rodriguez, MD*
Hubert H. Fernandez, MD*
Michael S. Okun, MD*§

*Department of Neurology, University of Florida Movement Disorders Center McKnight Brain Institute; Departments of ‡Biostatistics and §Neurosurgery, University of Florida Movement Disorders Center McKnight Brain Institute, Gainesville, Florida; ¶Department of Neurosurgery, Instituto Galeazzi IRCCS, Milan, Italy

Correspondence:
Michael S. Okun, MD,
Department of Neurology,
3rd Floor, McKnight Brain Institute, 101 South Newell Drive,
Room L3-101,
Gainesville, FL 32611.
E-mail: okun@neurology.ufl.edu

Received, March 2, 2010.
Accepted, September 10, 2010.

Copyright © 2011 by the
Congress of Neurological Surgeons

BACKGROUND: Parkinson's patients, on average, gain weight after deep brain stimulation (DBS).

OBJECTIVE: To determine potential differences in weight gain when comparing the subthalamic nucleus and the globus pallidus internus target.

METHODS: A retrospective analysis was performed on the prospective, randomized cohort of National Institutes of Health COMPARE trial DBS patients who received unilateral subthalamic nucleus or globus pallidus internus DBS. Baseline weights were recorded before DBS surgery and at 6, 12, and 18 months postoperatively. Relationships between weight change and changes in Beck Depression Inventory score, Unified Parkinson's Disease Rating Scale (UPDRS) motor score (part III) (also the dyskinesia duration and disability subscores from UPDRS IV), and Hoehn-Yahr stage were determined via Spearman's rank-order correlation coefficients. Regression analyses were performed to investigate the effects of potential factors on weight change over time.

RESULTS: Patients in the COMPARE DBS cohort gained a significant amount of weight, a mean of 4.86 lb (standard deviation = 8.73) (P = .001), but there was no significant difference between subthalamic nucleus and globus pallidus internus targets (weight gain of 4.29 $\pm$ 6.79 and 5.38 $\pm$ 10.32 lb, respectively; P = .68). Weight gain did not correlate with Beck Depression Inventory score change, UPDRS motor score, dyskinesia duration, dyskinesia disability change, or the Hoehn-Yahr stage (P = .62, .21, and .31, respectively). No specific variable was associated with weight gain, and there were no differences in binge eating post-surgery in either target.

CONCLUSION: There were significant changes in weight over time after DBS therapy. However, neither Beck Depression Inventory score change nor UPDRS score change or dyskinesia was correlated with weight gain. No significant factor was associated with the weight change.

KEY WORDS: Binge, Deep brain stimulation, Diet, Hypothalamus, Outcome

Neurosurgery 68:1233–1238, 2011 DOI: 10.1227/NEU.0b013e31820b52c5 www.neurosurgery-online.com

Patients with advanced Parkinson disease (PD) have been increasingly implanted with deep brain stimulation (DBS) devices to better control both motor symptoms and fluctuations.[1] US Food and Drug Administration–approved approaches to DBS include placing a lead(s) in either the globus pallidus internus (GPi) or the subthalamic nucleus (STN). Despite promising motor outcomes, a noticeable weight gain has been observed post-DBS surgery in many of the implanted patients.[2,3] There are open and debated questions about DBS-related weight change including target specificity, underlying cause, and

ABBREVIATIONS: BDI, Beck Depression Inventory; **BES**, Binge Eating Scale; **DBS**, deep brain stimulation; **GDNF**, glial cell line–derived neurotrophic factor; **GPi**, globus pallidus internus; **STN**, subthalamic nucleus; **UPDRS**, Unified Parkinson's Disease Rating Scale

Copyright © Congress of Neurological Surgeons. Unauthorized reproduction of this article is prohibited.

mechanism of action. Additionally, there has been concern that postoperative weight gain may detract from the overall benefits of surgery and/or induce metabolic disorders.[4] Most available studies on weight gain have focused on bilateral STN stimulation, and there have been few data on GPi. In the COMPARE Parkinson disease DBS cohort, patients were randomized to receive unilateral STN or alternately GPi DBS. Cognitive, motor, and quality of life outcomes for this cohort were recently reported.[5,6] Before randomization, it was hypothesized that there would be significant weight gain after DBS surgery and that STN DBS would be a greater offender. We further hypothesized that weight gain would be caused by the spread of current into the hypothalamus-associated circuits and that post-DBS changes would involve behaviors such as binge eating and carbohydrate craving.

METHODS

Fifty-two patients were randomized to receive either unilateral STN or unilateral GPi DBS in the parent study. Forty-four of these patients had a complete data set that included weight values (pre- and postoperatively at specific intervals) as well as other outcome measures. Institutional review board approval was obtained for the study, and all patients signed informed consents. Baseline weights in pounds were recorded before the first DBS surgery and at 6, 12, and 18 months postoperatively. The weight measurement for comparison between targets was conducted at 6 months post-DBS when all patients had a unilateral lead. Weight measurements were also collected at 12 and 18 months. After 6 months post-DBS, select patients received a second DBS (bilateral) lead. A mixed-effects model was used to determine the trend in weight change between targets with a correction for the discrepancy of unilateral vs bilateral leads. Other data to explore potential factors that may have affected weight change were collected including age, sex, Unified Parkinson's Disease Rating Scale (UPDRS) motor score, and dyskinesias duration and disability scores at baseline in the off dopaminergic medication state, the on medication state, and at 4 months postoperatively in the off dopaminergic medication/on DBS state; Hoehn and Yahr off staging score; and the Beck Depression Inventory (BDI) (at baseline and 6 months).

A Binge Eating Scale (BES) was administered to all available and willing patients but was notably not performed at baseline (at the study onset, the authors did not appreciate that binge eating would be an important factor to measure). A BES was administered in all patients after the 6-month follow-up visits. Based on these results, the total scores were compared for the patients with STN stimulation and those with GPi stimulation to determine whether there was a weight change and whether there was target specificity in binge-eating behavior.

Statistical analysis was performed on the complete data set using SAS version 9.1 (SAS Institute, Cary, North Carolina). Descriptive statistics were obtained for the clinical variables. Differences between the GPi group and STN group were compared using a 2-sample t test for continuous variables and χ^2 test for categorical variables. We examined relationships between weight change and changes in the BDI score, the UPDRS motor score, and dyskinesia duration and disability via Spearman's rank-order correlation coefficients. Furthermore, a linear regression analysis was performed to examine the effects of potential factors on weight change between baseline and 6 months post-DBS surgery. In addition, a mixed-effects model was applied to investigate the difference between DBS targets in trend of weight change from baseline to 18 months post-DBS surgery.

RESULTS

Descriptive statistics for the clinical variables (Table 1) showed that average values of BDI score change (−3.0 vs 1.06) and Stigma (39.95 vs 27.08) were different at a 0.1 trend level between those patients who received unilateral GPi DBS and those who received STN DBS, whereas other variables were approximately the same.

There was a significant weight gain of 4.86 lb ($P = .0006$) at 6 months post-DBS surgery when analyzing the complete COMPARE cohort. However, unlike what was hypothesized, there was no significant difference in weight change between the STN and GPi targets, with a weight gain of 4.29 ± 6.79 lb and 5.38 ± 10.32 lb, respectively ($P = .68$). The range of weight changes was broad for both targets (STN target, −7 to 19 lb; GPi target, −14 to 25 lb). For the patients with GPi stimulation, 16 (70%) gained weight (10.65 ± 6.98 lb), 6 (24%) lost weight (7.77 ± 4.55), and the weight in 1 patient (4%) remained unchanged. In comparison, 15 patients (71%) who received STN stimulation gained weight (7.20 ± 5.55 lb), 4 patients (19%) lost weight (4.50 ± 2.38 lb), and the weight in 2 patients (10%) remained unchanged. Once again, there was no significant difference between STN and GPi targets for those patients who did gain weight ($P = .14$). There was no difference in postoperative BES scores when comparing targets (28.07 at STN vs 24.8 at GPi; $P = .32$). Furthermore, in our cohort, 23 post-DBS patients answered subjective questions on eating behavior. Of these patients, 14 reported carbohydrate cravings (60.9%) and 9 reported no cravings (39.1%). There was no target specificity in carbohydrate cravings (7 were from STN DBS group and 7 were from GPi DBS group, respectively).

Weight gain did not correlate with BDI score change, UPDRS motor score/dyskinesia duration and disability changes, or the HY stage ($P = .62$, .21, .19, .79, and .31, respectively). In addition, we did not find any variables that were significantly associated with weight change between baseline and 6 months post-DBS surgery. Furthermore, time from the first DBS was found to be the only variable that was significantly associated with the weight change ($P = .002$) according to the mixed-effects model analysis, which used the recorded weights from 6, 12, and 18 months post-DBS surgery. The results showed that the longer the time was since surgery, the more weight gain occurred in patients (Figure 1).

DISCUSSION

When carefully examining the 44 patients who were studied using available data from the COMPARE cohort, 31 patients (70%) gained weight by the 6-month follow-up, 10 patients (23%) had lost weight, and 3 patients (7%) remained unchanged. Although there was an overall weight gain in both groups (4.86 lb), the change was not target specific, as we had hypothesized. Results from this study can be used in preoperative counseling for

Copyright © Congress of Neurological Surgeons. Unauthorized reproduction of this article is prohibited.

TABLE 1. Descriptive Statistics Comparing Patients Who Received Globus Pallidus Internus vs Subthalamic Nucleus Deep Brain Stimulation[a]

Variable	All	GPi, n = 23	STN, n = 21	*P* Value
Laterality				
Bilateral	25 (56.8%)	10 (43.5%)	15 (71.4%)	.06
Unilateral	19 (43.2%)	13 (56.5%)	6 (28.6%)	
Weight change at 6-mo follow-up	4.86 (8.73)	5.38 (10.32)	4.29 (6.79)	.68
BDI score change	−1.18 (6.81)	−3 (5.34)	1.06 (7.86)	.07
UPDRS III change	−11.48 (13.59)	−12.05 (16.42)	−10.84 (9.98)	.78
Height	56.99 (4.05)	57.29 (4.11)	56.6 (4.07)	.63
Binge Eating Scale	26.38 (8.74)	24.8 (6.7)	28.07 (10.5)	.32
Mobility	45.63 (24.33)	43.59 (22.84)	47.86 (26.25)	.57
Activities of daily living	38.73 (20.06)	36.23 (17.74)	41.47 (22.46)	.39
Emotional	32.67 (20.57)	30.43 (19.03)	35.12 (22.34)	.46
Stigma	33.81 (22.81)	39.95 (22.67)	27.08 (21.5)	.06
Social	19.51 (20.72)	23.19 (23.02)	15.48 (17.54)	.22
Cognitions	30.54 (21.41)	30.71 (22.68)	30.36 (20.47)	.96
Communication	33.52 (22.19)	33.33 (22.61)	33.73 (22.28)	.95
Discomfort	43.37 (25.2)	42.03 (25.19)	44.84 (25.75)	.72
Baseline UPDRS III	42.43 (11.91)	39.83 (9.48)	45.29 (13.77)	.13
Baseline BDI score	8.8 (6.54)	9.43 (7.28)	8.1 (5.72)	.50
H-Y stage	2.94 (0.65)	2.8 (0.67)	3.11 (0.61)	.13
Dyskinesias duration	−0.57 (1.14)	−0.83 (1.1)	−0.32 (1.16)	.17
Dyskinesias disability	−1.05 (1.09)	−1.16 (1.21)	−0.95 (0.97)	.56

[a]Values shown are mean (standard deviation) or number (%).
GPi, globus pallidus internus; STN, subthalamic nucleus; BDI, Beck Depression Inventory; H-Y, Hoehn-Yahr; UPDRS, Unified Parkinson's Disease Rating Scale.

patients considering STN vs GPi DBS. Approximately 70% of patients who undergo DBS can expect an average weight gain of 10.65 ± 6.98 lb with GPi target stimulation compared with 7.20 ± 5.55 lb with the STN target.

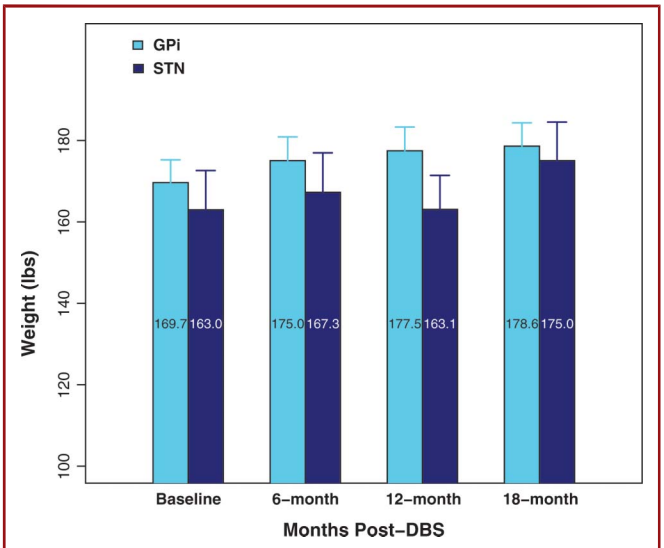

FIGURE 1. *Weight at baseline and at 6, 12, and 18 months after deep brain stimulation (DBS) surgery by stimulation targets. The I bars indicate standard error. GPi, globus pallidus internus; STN, subthalamic nucleus.*

The results also did not reveal a significant difference in the BES or eating behavior between the groups. Furthermore, time from the first DBS was found to be the only variable that was significantly associated with the weight change ($P = .002$). These data should help us to begin to evolve our understanding of the mechanisms underlying DBS-related weight change and its clinical implications.

PD as a neurodegenerative phenomenon has been strongly associated with weight loss, with some experts believing the issue to be related to Lewy body deposition in nonmotor basal ganglia circuitry as well as potential involvement of hypothalamus-related circuits.[7-9] Proposed mechanisms for weight loss in PD have included increased energy expenditure, early satiety because of decreased gastrointestinal motility, olfactory impairment, bulbar dysfunction, and decreased dopaminergic stimulation of the central reward system.[10] Although weight loss has been associated with PD, it is weight gain that has been associated with DBS in the PD population.[2] It is unknown whether this weight gain will prove beneficial or protective in this population.

Although increases in weight after DBS surgery may be undesirable, they have not been specifically linked to an increased risk of cardiovascular events, diabetes, or other health risks.[11] Weight gain after DBS surgery might, in fact, be a protective factor against adverse events such as a greater susceptibility to falls/fractures, poor nutritional status, and nursing home placement, which often accompany weight loss in the PD population.[11] Furthermore, it is plausible that weight gain might be

Copyright © Congress of Neurological Surgeons. Unauthorized reproduction of this article is prohibited.

beneficial in men, who tend to gain fat-free mass, while potentially deleterious in women who gain primarily fat mass.[4] On the other hand, the underlying mechanism for this sex difference is still to be explained.

Similar to PD, Huntington disease is a neurodegenerative disease associated with weight loss in affected patients, and this is perhaps attributable to hypermetabolism.[12] Oral nutritional supplements have been suggested for Huntington disease patients, and the gaining of weight in this population is thought to be helpful in improving longevity.[13] Whether weight gain proves to be beneficial or deleterious, a recent study showed that nutritional intervention immediately after DBS surgery may be useful in controlling weight change.[14] In comparing a group of PD patients who received nutritional intervention immediately after surgery (1 week) with a group who received delayed intervention (2.5 ± 1.6 years), the early intervention group did not gain a significant amount of weight.

A review of the available literature regarding DBS and the associated weight changes (usually gain) reveals that most studies included only the STN target, and all studies uniformly reported weight gain (Table 2). In some studies, the experimental group of patients (STN DBS) was compared with a control PD group without DBS. The STN DBS patients in these investigations experienced gain, whereas non-DBS PD patients lost weight. The time frames for each of the studies varied, but the weight gain was approximately 6.6 lb at 3 months and 19.8 lb at 1 year (in bilateral STB-DBS cases). According to these published experiences, for unilateral STN DBS, the approximate weight gain was 7.5 ± 6.6 lb at 6 months, and we observed less weight gain in the unilateral groups included in our study. The findings from these many studies have suggested that the weight gain may have been attributable to decreased energy expenditure that was in part caused by reduced dyskinesia and in part by a reduction in dopaminergic therapy.

Decreased overall energy expenditure directly resulting from DBS-related dyskinesia reduction has been posited as a leading explanation for weight gain.[1,4,15] In our study, dyskinesia improved in both STN and GPi patients, and although 1 target was not statistically better, this overall improvement may have contributed to weight gain. Montaurier et al[4] observed that energy metabolism was decreased post-DBS surgery, whereas energy intake was unchanged. The relationship of energy metabolism to dyskinesia and dyskinesia reduction remains unknown. In future studies, more careful correlation of dyskinesia score (with dyskinesia diaries, which were not done as part of COMPARE) and weight gain will need to be documented. Most authors do not believe, however, that dyskinesia reduction in itself is responsible for the weight gain. One interesting finding that was not unique to this study was that approximately 20% of patients with DBS lost weight. One wonders whether a comparison of the groups (gainers vs losers) may indicate a potential underlying mechanism.

Several potential mechanisms have been proposed as explanations for the weight gain after DBS surgery. In 1 case report involving STN DBS, 1 patient had a remarkable improvement in PD symptoms, gained 22 lb, and developed an increased craving for sweets.[16] Our own observations have revealed several cases similar to this report, and we wondered whether carbohydrate craving could be more common post-DBS than previously recognized. Additionally, a recent study showed that there was a significant difference in body mass index change between STN and GPi bilateral DBS surgery. At 6 months post-bilateral DBS surgery, the body mass index had increased by an average of 8.4% in the STN group and only 3.2% in the GPi group ($P < .05$). Perhaps the placement of the second electrode may prove to be a significant contributor to weight gain in this population of patients.[3] Much skepticism, however, remains in these studies and in their interpretation. One leading thought is

TABLE 2. Review of the Relevant Literature of Deep Brain Stimulation and Weight Change[a]

Author	DBS target site	No. of patients in study	Results	Notes
Walker et al[11]	STN	39 (27 men, 12 women)	Weight gain	Unilateral STN DBS patients gained 7.5 ± 6.6 lbs at 6 mo
Montaurier et al[4]	STN	23 (16 men, 7 women)	Weight gain	Bilateral STN patients gained an average 6.6 lbs at 3 mo post-surgery; quality of weight gain was sex specific
Macia et al[15]	STN	19 (11 men, 8 women)	Weight gain	Bilateral STN patients had a significant weight gain (+21.4 ± 15.4 lbs)
Barichella et al[1]	STN	30 (22 men, 8 women)	Weight gain	Bilateral STN patients gained an average of 20.5 ± 13.7 lbs in 1 y
Bannier et al[19]	STN	22 (15 men, 7 women)	Weight gain	Bilateral STN patients showed an average weight gain of 6.8 lbs in 3 mo

[a]STN, subthalamic nucleus; DBS, deep brain stimulation.

Copyright © Congress of Neurological Surgeons. Unauthorized reproduction of this article is prohibited.

that spread of current to the hypothalamic satiety centers may play a larger role than previously appreciated.

A regional or circuit effect of STN DBS on the hypothalamic satiety center may therefore be hypothesized as one potential contributing cause for weight gain.[4] Weight gain has been reported in multiple targets after PD surgical therapy, including unilateral pallidotomy, bilateral pallidal DBS, and bilateral STN DBS.[1] A strong piece of evidence against an exclusive current spread mechanism is that weight gain has been observed after GPi ablation.[17] Our data, which showed no difference in BES scores or carbohydrate cravings between targets, argues against an exclusive and simple regional/circuit spread of stimulation hypothesis, unless the DBS is affecting the same circuit both up and downstream (ie, connectivity in STN and GPi).

Results from recent glial cell line–derived neurotrophic factor (GDNF) studies revealed that GDNF-mediated activation of various hypothalamic areas was important in observed weight loss.[18] There are resident hypothalamic dopaminergic neurons, the nigrostriatal dopaminergic tract (known to be involved in feeding and weight loss) passing through the lateral hypothalamus and through the medial forebrain bundle. It is plausible that DBS neuromodulates and stimulates the same or similar circuitry. DBS, unlike GDNF in the medial forebrain bundle, may have affected fibers of passage in the nigrostriatal pathway, which may have induced weight gain instead of loss in the majority of cases. Alternatively, the 20% of patients who lost weight post-DBS might have invoked circuitry similar to that seen in GDNF.

There are several limitations associated with this study. The cohort consisted of a small sample size of only 44 patients. Additionally, the BES was only administered after implantation of the DBS device, and there was no baseline analysis of binging and carbohydrate craving. Further, the regression analysis, which used the 6-, 12-, and 18-month weights post-DBS surgery, included both bilateral and unilateral DBS patients. Despite these limitations, however, we believe that the prospective, randomized nature of the study has provided important insights, particularly in weight gain in more than just the STN target. Additionally, the data that revealed depressive symptoms (ie, the BDI) were not related to weight gain further eliminate another potential factor.

Future studies should include more information on activity (ie, exercise) levels before and after surgery. Further, the BES and a food diary (ie, carbohydrate intake) should be administered at baseline and at 6 months after DBS to more effectively draw conclusions.

Although DBS has great benefits for motor symptoms and fluctuations, patients should be aware there is associated weight gain with either STN or GPi DBS. Future studies will need to focus more closely on potential underlying mechanisms, and there will need to be focused preoperative education plans for patients.

Disclosure

This article was supported by a grant from the NINDS/NIH (PI: M. Okun, the COMPARE Trial, K23 NS044997) and was also supported by the UF National Parkinson Foundation Center of Excellence. No authors have any conflicts of interest since 2009. The authors have no personal financial or institutional interest in any of the drugs, materials, or devices described in this article.

REFERENCES

1. Barichella M, Marczewska AM, Mariani C, Landi A, Vairo A, Pezzoli G. Body weight gain rate in patients with Parkinson's disease and deep brain stimulation. *Mov Disord*. 2003;18(11):1337-1340.
2. Gironell A, Pascual-Sedano B, Otermin P, Kulisevsky J. [Weight gain after functional surgery for Parkinsons disease]. *Neurologia*. 2002;17(6):310-316.
3. Sauleau P, Leray E, Rouaud T, et al. Comparison of weight gain and energy intake after subthalamic vs pallidal stimulation in Parkinson's disease. *Mov Disord*. 2009;24(14):2149-2155.
4. Montaurier C, Morio B, Bannier S, et al. Mechanisms of body weight gain in patients with Parkinson's disease after subthalamic stimulation. *Brain*. 2007;130(Pt 7):1808-1818.
5. Okun MS, Fernandez HH, Wu SS, et al. Cognition and mood in Parkinson's disease in subthalamic nucleus versus globus pallidus interna deep brain stimulation: the COMPARE trial. *Ann Neurol*. 2009;65(5):586-595.
6. Zahodne LB, Okun MS, Foote KD, et al. Greater improvement in quality of life following unilateral deep brain stimulation surgery in the globus pallidus as compared to the subthalamic nucleus. *J Neurol*. 2009;256(8):1321-1329.
7. Langston JW, Forno LS. The hypothalamus in Parkinson disease. *Ann Neurol*. 1978;3(2):129-133.
8. Braak H, Ghebremedhin E, Rub U, Bratzke H, Del Tredici K. Stages in the development of Parkinson's disease-related pathology. *Cell Tissue Res*. 2004;318(1):121-134.
9. Braak H, Braak E. Pathoanatomy of Parkinson's disease. *J Neurol*. 2000;247 (Suppl 2):II3-II10.
10. Nirenberg MJ, Waters C. Compulsive eating and weight gain related to dopamine agonist use. *Mov Disord*. 2006;21(4):524-529.
11. Walker HC, Lyerly M, Cutter G, et al. Weight changes associated with unilateral STN DBS and advanced PD. *Parkinsonism Relat Disord*. 2009;15(9):709-711.
12. Aziz NA, van der Burg JM, Landwehrmeyer GB, Brundin P, Stijnen T, Roos RA. Weight loss in Huntington disease increases with higher CAG repeat number. *Neurology*. 2008;71(19):1506-1513.
13. Trejo A, Boll MC, Alonso ME, Ochoa A, Velasquez L. Use of oral nutritional supplements in patients with Huntington's disease. *Nutrition*. 2005;21(9): 889-894.
14. Guimaraes J, Matos E, Rosas MJ, et al. Modulation of nutritional state in Parkinsonian patients with bilateral subthalamic nucleus stimulation. *J Neurol*. 2009 [Epub ahead of print].
15. Macia F, Perlemoine C, Coman I, et al. Parkinson's disease patients with bilateral subthalamic deep brain stimulation gain weight. *Mov Disord*. 2004;19(2):206-212.
16. Doshi P, Bhargava P. Hypersexuality following subthalamic nucleus stimulation for Parkinson's disease. *Neurol India*. 2008;56(4):474-476.
17. Benabid AL, Koudsie A, Benazzouz A, et al. Deep brain stimulation of the corpus luysi (subthalamic nucleus) and other targets in Parkinson's disease. Extension to new indications such as dystonia and epilepsy. *J Neurol*. 2001;248(Suppl 3): III37-III47.
18. Manfredsson FP, Tumer N, Erdos B, et al. Nigrostriatal rAAV-mediated GDNF overexpression induces robust weight loss in a rat model of age-related obesity. *Mol Ther*. 2009;17(6):980-991.
19. Bannier S, Montaurier C, Derost PP, et al. Overweight after deep brain stimulation of the subthalamic nucleus in Parkinson disease: long term follow-up. *J Neurol Neurosurg Psychiatry*. 2009;80(5):484-488.

COMMENT

This article compares changes in body weight in patients with Parkinson disease (PD) after deep brain stimulation (DBS) of either the globus pallidus internus or the subthalamic nucleus. Data were drawn from a cohort in which the target choice was randomized. The body weight changes at 6 months reflect exclusively unilateral stimulation,

Copyright © Congress of Neurological Surgeons. Unauthorized reproduction of this article is prohibited.

whereas later time points include some bilaterally implanted patients. The authors show that patients in both groups had a mean weight increase, with no overall difference in weight gain between the patient groups.

All who perform surgery for PD have noted weight gain as an effect of surgery. Many patients are underweight before surgery, but even those who are not can nevertheless gain wait. This article helps to clarify the degree of expected gain and the percentage of patients who can expect to gain weight and shows that the effect occurs from DBS of either of the 2 predominant targets for PD treatment.

Philip Starr
San Francisco, California

NEUROSURGERY® on your EBook

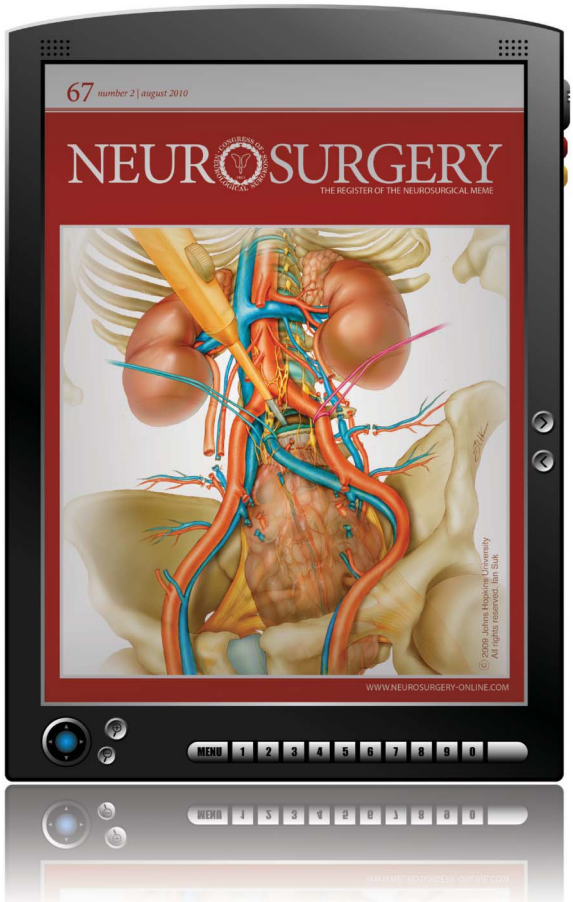

ePUB

ePUB is a free and open e-book standard recognized by the International Digital Publishing Forum.

NEUROSURGERY ® ePUB documents contain searchable full-text, images, references and commentary.

ePUB documents are natively supported by variety of eReaders, including Android™ devices, Barnes & Noble Nook™, iPad™, iPhone®, iPod Touch®, and Sony Reader™.

Find NEUROSURGERY® ePUB content at www.neurosurgery-online.com

NEUROSURGERY

Copyright © Congress of Neurological Surgeons. Unauthorized reproduction of this article is prohibited.

Optic Radiation Fiber Tracking Using Anteriorly Angulated Diffusion Tensor Imaging: A Tested Algorithm for Quick Application

Lennart H. Stieglitz, MD*
Wolf O. Lüdemann, MD‡
Mario Giordano, MD‡
Andreas Raabe, MD, PhD*
Rudolf Fahlbusch, MD, PhD‡
Madjid Samii, MD, PhD‡

*Department of Neurosurgery, Inselspital Bern, Bern, Switzerland; ‡Department of Neurosurgery, International Neuroscience Institute Hannover, Hannover, Germany

Correspondence:
Lennart Henning Stieglitz, MD,
Department of Neurosurgery,
Inselspital Bern,
3010 Bern, Switzerland.
E-mail: Lennart.Stieglitz@insel.ch

Portions of this work were published as proceedings at the Schweizer Gesellschaft für Neurochirurgie, Schweizer Gesellschaft für Intensivmedizin, Schweizer Gesellschaft für Neuroradiologie, Interessengemeinschaft Intensivplflege Schweiz, Interessengemeinschaft Neurochirirgisches Operationspersonal Schweiz Congress, St. Gallen, Switzerland, September 24–26, 2009.

Received, March 14, 2010.
Accepted, September 10, 2010.

Copyright © 2011 by the Congress of Neurological Surgeons

BACKGROUND: Fiber tracking (FT) of the optic pathways (OPs) is difficult because there is no standard for the parameters of diffusion tensor imaging (DTI), placement of seed volumes, or interpreting the results.

OBJECTIVE: To determine optimal conditions and parameters for DTI and FT of the optic radiation under intraoperative conditions, we performed a multivariate prospective study.

METHODS: A healthy man underwent magnetic resonance imaging and DTI scans using various scan parameters. The slice thicknesses were 2.7 mm, 5 mm, and 7 mm, and the gantry of the slices was 0 degrees and 44 degrees. The OPs were tracked using different settings for focal anisotropy and minimal length of the visualized fibers. The time needed for DTI, image processing, and uploading as well as the difficulty of depicting the OPs, the time needed for FT, quality, and volume of the tracked fiber object were registered and analyzed.

RESULTS: The DTI took between 2 minutes 14 seconds for the axial scan with 7-mm slice thickness and 6 minutes 14 seconds for the 44-degree angulated scan with 2.7-mm slice thickness. Splitting the data into a 3-dimensional mosaic data set took between 1 minute 42 seconds (44 degrees, 7 mm; 0 degrees, 7 mm) and 4 minutes 21 seconds (44 degrees, 2.7 mm). The best results were achieved using 44-degree, 2.7-mm DTI. The optimal setting for focal anisotropy was 0.1 and 11 mm for minimal length. Using these parameters, tracking of the OPs was possible in 1 minute 22 seconds and with high quality and correlating with anatomic studies.

CONCLUSION: The use of anteriorly angulated DTI improves the FT work flow and the results of tractography of the OP. The quality of the resulting objects can be judged by anatomic landmarks.

KEY WORDS: Diffusion tensor imaging, Fiber tracking, Functional imaging, Intraoperative magnetic resonance imaging, Optic radiation

Neurosurgery 68:1239–1251, 2011 DOI: 10.1227/NEU.0b013e31820b52e1 www.neurosurgery-online.com

Surgery in eloquent areas of the human brain is possible with good patient outcome with increased experience, knowledge of the patient's functional anatomy, improved microneurosurgical skills, and technical progress. In addition to cortical anatomy and function, the subcortical structures come more and more into focus. Knowledge of the composition and function of white matter is acquired by clinical experience with lesions and corresponding neurological deficits, electrophysiological research, and anatomic dissection of cadaver brains. The possibility of gaining information about the individual subcortical anatomy of a patient and its integration in the surgical planning and the surgical procedure represents an important advance in microneurosurgery.

ABBREVIATIONS: DTI, diffusion tensor imaging; **FA**, focal anisotropy; **FT**, fiber tracking; **LGB**, lateral geniculate body; **MFL**, minimal fiber length; **OP**, optic pathway

Diffusion tensor imaging (DTI) is a noninvasive technique for the visualization of major fiber tracts. It is based on a magnetic resonance

Copyright © Congress of Neurological Surgeons. Unauthorized reproduction of this article is prohibited.

imaging (MRI) technique that visualizes the mean movement of water molecules inside a 3-dimensional matrix.[1] In free water, the movement is even in all directions, whereas it is hindered in most directions in fibrous structures. This can be measured as focal anisotropy (FA). FA maps can be color coded to show the direction of the passing fibers. Specialized software can be used to track fibers from 1 volume of interest (VOI) to another. Although this technology is sometimes criticized because there is no proof that the tracts shown follow the true subcortical fibers, there is a striking similarity to the results of cadaver dissection studies, so it can be assumed that fiber tracking (FT) truly produces a model of white matter connectivity.

High-quality FT requires substantial experience of the performing physician. The identification of the corticospinal tracts is relatively easy and is already part of the clinical routine at many institutions, as the large and constantly growing number of publications on this topic proves. Tracking of other fiber systems is far more difficult and needs extensive knowledge of the white matter anatomy. Furthermore, the whole procedure from image acquisition and image processing to FT is very time-consuming. This may be one of the main problems of its integration in surgical planning. Especially in intraoperative MRI controls, additional time-consuming procedures increase the overall duration of surgery.

The optic radiation is one of the fiber systems that require some experience with FT. First, adequate VOIs must be chosen as seed volumes for tracking. Then other fibers that cross the seed VOIs, sometimes described as "noise," must be carefully removed. The anterior part of the optic radiation, Meyer's loop, which takes a turn deep into the temporal lobe, is especially a challenge for FT algorithms because of its sharp turn.

The aim of this study was to identify adequate technical means for image acquisition, processing, and interpretation with which a time-efficient and simple segmentation of the optic radiation is possible. We wanted to demonstrate ways that make their inclusion in routine preoperative planning procedures and even in intraoperative MRI controls possible without the increasing of the patient's narcosis.

MATERIAL AND METHODS

Patients and Surgical Technique

Between September and December 2008 at the International Neuroscience Institute, Hannover, 7 patients with temporal, parieto-occipital, and occipital lesions underwent pre- and intraoperative MRI scans with 44-degree anteriorly angulated DTI with 2.7-mm slice thickness. There were 6 male and 1 female patients of ages 11 to 70 years. There were 3 glioblastomas, 1 pilocytic astrocytoma, 1 recurrence from an oligoastrocytoma, 1 hamartoma, and 1 metastasis of renal clear cell cancer. The radicality of tumor removal and pre- and postoperative neurological status were recorded (Table 1).

The lesions were removed microsurgically with the assistance of neuronavigation (VectorVision2; BrainLab, Feldkirchen, Germany) and intraoperative imaging.

The MRI scanner for intraoperative MRI is included in the neurosurgical operating room (Siemens BrainSUITE iMRI; Siemens Healthcare, Erlangen, Germany). The patient is placed on a special operating table that can be rotated inward for MRI control and outward for placing the patient's head outside the 5-G line for surgery with normal instruments.

Tumor removal was considered radical if the T1-weighted contrast-enhancing lesion was totally removed in cases of glioblastomas and metastases. In cases of oligoastrocytoma and hamartoma, the radicality was judged from the T2-weighted fast imaging with steady procession (true fast imaging with steady procession) images.

Conventional MRI and DTI

To identify the optimal parameters for DTI and FT, we acquired 6 different DTI data sets from a 31-year-old healthy man. All imaging and image processing were performed by 1 technical assistant, and all FT procedures were done by 1 physician (first author) at 1 institution.

Before intraoperative MRI, all bleeding was carefully stopped to prevent hemorrhage during the imaging procedure. The resection cavity was filled with water to reduce inhomogeneities of the magnetic field and occurrence of additional susceptibility artifacts.

All MRI scans were performed on a Siemens 1.5-T Magnetom Espree (Siemens Healthcare). First, a T1-weighted 3-dimensional magnetization prepared rapid-acquisition gradient-echo sequence was measured. TE was 4.38 ms, TR was 2020 ms, matrix size was 256 $\times$ 256, field of view was 250 $\times$ 250, slice thickness was 1 mm, and slab size was 16 cm.

DTI was performed using 6 motion-probing gradients. In all 6 measurements, we applied a single-shot spin-echo diffusion-weighted echo planar imaging sequence (TE, 86 ms; TR, 9200 ms; matrix size, 128 $\times$ 128; field of view, 240 mm; b values of 0 and 1000 s/mm^2, no intersection gap). The slice thicknesses were 2.7 mm, 5 mm, and 7 mm; each slice thickness was measured in straight axial modality and angulated by 44 degrees anteriorly. The number of slices was chosen in that way so that in all cases, the optic chiasm, the occipital lobe, the corpus callosum, and the upper two thirds of the temporal lobe were covered. The time needed for image acquisition was recorded.

The images then had to be processed before transfer to the surgical planning station. For this we used the Espree (Syngo MR B13) Numais/4 2006 software (Siemens Healthcare) on a computer with an Intel Xeon 3, 6 GHz, 3 GB RAM running Windows XP Professional 2002, service pack 2. The time needed for image mosaic splitting was recorded. Finally, the time for data transfer via the Ethernet from the MRI console to the surgical planning station was recorded.

In a second step, we tested 44 degrees anteriorly angulated DTI on the pre- and intraoperative scans of 7 patients with temporal, parieto-occipital, and occipital lesions with possible affection of the optic radiation.

FT

For visualization of the fiber tracts, we used PatXfer 5.2 and iPlan 2.6.1 (BrainLab) on a computer with an Intel P4 3 GHz, 1 GB RAM running Windows XP Professional 202, service pack 1. The optic chiasm was selected as the first seed volume. All the fibers that crossed this VOI were tracked. The second seed volume was the occipital lobe. All tracts that did not reach this VOI were removed. Third, a seed volume was selected at the roof of the lateral ventricle at the level of the trigone. Additionally, the tracking procedure was performed with the lateral geniculate body (LGB) as the first seed volume to compare the results and decide whether the optic chiasm or the LGB was more appropriate as the first seed volume (Figure 1A and B). The adjustment for FA threshold was mutated from 0.05 to 0.1, 0.2, and 0.3, and the setting for the minimal fiber length (MFL) threshold from 5 to 10, 20, and 30 mm for all FT procedures.

Copyright © Congress of Neurological Surgeons. Unauthorized reproduction of this article is prohibited.

TABLE 1. Patients Operated on for Lesions Affecting the Optic Radiation Using Anteriorly Tilted Intraoperative Diffusion Tensor Imaging[a]

No.	Sex/ Age, y	Pathology	Radicality	Neuroimaging	Preoperative Neurology	Postoperative Neurology
1	M/70	Right temporoparietal glioblastoma	95% tumor removal in first intraoperative scan, complete tumor removal in second intraoperative scan	MPRAGE, DTI, fMRI	Left-sided dysmetria	Unchanged
2	M/11	Left temporal hamartoma	Residual tumor in first intraoperative scan, complete tumor removal in second intraoperative scan	MPRAGE, TrueFISP, DTI, fMRI	No visual deficit	No visual deficit
3	M/70	Right temporal metastasis of clear cell cancer	Complete removal in first intraoperative scan	MPRAGE, TrueFISP, DTI, fMRI	No visual deficit; fine motor skill deficit of the left hand	Unchanged
4	M/67	Left temporoparietal glioblastoma	Complete removal in first intraoperative scan	MPRAGE, TrueFISP, DTI, fMRI	Homonymous hemianopsia	Slight improvement of the hemianopsia to the right side (right eye > left eye)
5	M/43	Left frontotemporal recurrence of a oligoastrocytoma (WHO grade II)	Subtotal tumor removal	MPRAGE, TrueFISP, DTI, fMRI	No visual deficit, minor Broca aphasia	Unchanged
6	M/19	Left occipital pilocytic astrocytoma	Complete removal in first intraoperative scan	MPRAGE, TrueFISP, DTIfMRI	No visual deficit	Homonymous hemianopsia to the right side (worse on the upper right quadrant)
7	F/61	Right occipital glioblastoma	Complete removal in second intraoperative scan	MPRAGE, DTI	Homonymous hemianopsia	Unchanged

[a]No residual contrast enhancement in intraoperative MPRAGE was considered complete tumor removal. MPRAGE, magnetization prepared rapid-acquisition gradient-echo imaging; DTI, diffusion tensor imaging; TrueFISP, true fast imaging with steady procession; fMRI, functional magnetic resonance imaging; WHO, Word Health Organization.

The time needed for the whole procedure was recorded. Finally, the fibers were converted into a 3-dimensional object by virtually covering every fiber with a narrow tube and combining them. Because in some cases there were fiber artifacts rostral of the optic chiasm, the fiber objects were cut off rostral of the optic chiasm center. The volumes of these fiber objects were compared.

Grading of Optic Radiation FT Quality

Despite the fact that the feasibility of FT of the optic radiation ranged from impossible to very easy depending on the different slice thickness, image angulation, and adjustments for FA and MFL, the quality of the obtained fiber objects was different. For comparison, the results were graded from 0 to 8 points as follows: (1) 1 point if the fibers could be tracked inside the optic nerve, (2) 1 point if they passed the optic chiasm and 1 more point if they touched the LGB, (3) 1 point if they could be found inside the roof of the lateral ventricle at the level of the trigone (sagittal stratum, (4) 1 point if the fibers reached the calcarine cortex, (5) 1 point if the fibers ended somewhere outside the occipital lobe, (6) 1 point if the optic radiation could be tracked as 1 branch, (7) 1 point if the anterior temporal portion (Meyer's loop) could be identified, and (8) 1 more point if 3 different branches could be identified, as described by Yamamoto et al[2] in 2005 (Table 2).

RESULTS

Fiber Object Quality

The quality of the tracked fiber objects of the optic radiation was different depending on the imaging modalities and the chosen values for FA and MFL threshold (Table 3). The use of the LGB vs the optic chiasm resulted in a more anatomic visualization of the medial and anterior parts of the optic radiation. Meyer's loop was not tracked with the LGB as the first seed VOI at all. The anterotemporal portion of the optic radiation was better visualized with the optic chiasm as the first seed VOI, although the portion between the chiasm and anterior part of Meyer's loop was not shaped anatomically and left the LGB out (Figure 1). The posterior portion of the optic radiation was comparable using both optic chiasm and LGB as first seed VOI (Figure 1). The best results (grades 7 and 8) regarding the quality scale shown in Table 2 were achieved with a slice thickness of 2.7 mm and a FA threshold of 0.05 (Figure 2). The quality decreased as well with increasing slice thickness as with higher FA thresholds. The results with slice thicknesses of 5 and 7 mm were

Copyright © Congress of Neurological Surgeons. Unauthorized reproduction of this article is prohibited.

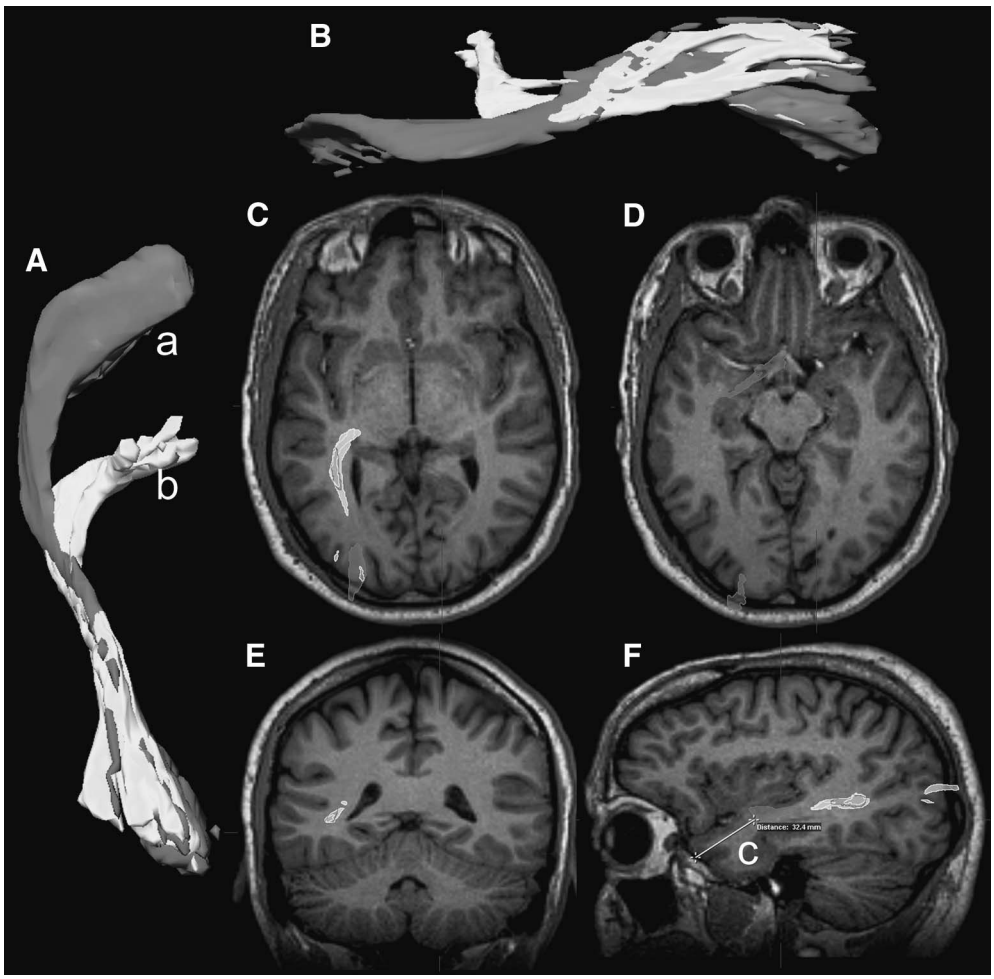

FIGURE 1. *Comparison of the lateral geniculate body (LGB) and the optic chiasm for first seed volume. Because fiber tracking of the optic radiation produces many artifacts, the fiber objects resulting from different seed volumes are different. The fiber object, which results from tracking with the LGB as first seed volume, is shown in yellow (b). Tracking from the optic chiasm is shown in magenta (a). Cranial view (**A**); lateral view (**B**). The posterior part of the optic radiation is tracked identically. Meyer's loop is better shown tracking from the optic chiasm, although the fibers shown seem to take a shortcut to the chiasma not passing the LGB as they should. Axial (**C**) and coronal (**E**) views showing the fiber objects in the roof of the trigone. **D**, the fiber object resulting from the optic chiasm as first seed volume shows a reasonable Meyer's loop. The sharp curve that the fibers make inside the temporal lobe is indicated. **F**, the distance between the most anterior part of Meyer's loop and the temporal pole can be measured (c).*

better with the use of strictly axial image sets than for 44 degrees anteriorly angulated image sets. On the other hand, the angulated image sets allowed higher FA thresholds of 0.1 with good quality results.

The second quality parameter was the distance of the most anterior fibers to the temporal pole. For FA values of 0.05 and 0.1 and a slice thickness of 2.7 mm, the mean distance was 26.9 mm as well for an angulation of 44 degrees and strictly axial images. For the angulated images, the variation was very low (range, 26.1-26.9 mm), whereas for the strictly axial images, the results ranged from 19.3 mm to 31 mm (Figure 3).

Image Acquisition Time

The time needed for image acquisition and processing depended on the slice thickness and the number of slices. It ranged from 7 minutes 34 seconds for 15 slices 7 mm thick to 18 minutes 7 seconds for 38 slices 2.7 mm thick (Table 4). The time needed for network transfer to the surgical planning station was

Copyright © Congress of Neurological Surgeons. Unauthorized reproduction of this article is prohibited.

TABLE 2. Optic Pathway Fiber Tracking Quality Scale[a]

	−1	0	1	1	1	1	1
Anatomic plausibility	Fibers end outside the occipital lobe	Fibers cannot be tracked	Fibers can be tracked inside the optic nerve	Fibers pass the optic chiasm	Fibers pass the lateral geniculate body	Fibers pass the roof of the trigonum	Fibers reach the calcarine cortex
Optic radiation branches		Fibers cannot be tracked	Posteromedial portion of the or can be tracked	Meyer's loop can be identified	3 separate branches can be identified		

[a]The quality of the tracked fiber objects is judged after 2 parameters: The anatomic plausibility and the visualization of the 3 different branches of the optic radiation, including Meyer's loop. For each condition fulfilled, 1 point is added to the score. For an ending of the tracked fibers outside the occipital lobe, 1 point is deducted.

TABLE 3. Fiber Object Quality[a]

Angulation, deg		0			44		
Slice Thickness, mm		2.7	5	7	2.7	5	7
FA 0.05	MFL 5 mm	7	4	3	8	4	3
	MFL 11 mm	8	6	4	8	4	3
	MFL 20 mm	8	6	3	8	4	0
	MFL 30 mm	8	6	3	8	4	0
FA 0.1	MFL 5 mm	6	5	2	8	3	0
	MFL 11 mm	6	5	2	8	3	0
	MFL 20 mm	6	5	2	8	3	0
	MFL 30 mm	6	5	2	7	3	0
FA 0.2	MFL 5 mm	3	3	0	4	0	0
	MFL 11 mm	3	0	0	3	0	0
	MFL 20 mm	3	0	0	3	0	0
	MFL 30 mm	3	0	0	3	0	0
FA 0.3	MFL 5 mm	0	0	0	0	0	0
	MFL 11 mm	0	0	0	0	0	0
	MFL 20 mm	0	0	0	0	0	0
	MFL 30 mm	0	0	0	0	0	0

[a]The quality of the tracked fiber objects depending on the thickness of diffusion tensor imaging slices, the angulation of diffusion tensor imaging, and the thresholds for focal anisotropy and minimal fiber length (MFL). The quality is graded following the quality scale shown in Table 1.

about half the total time needed. The image acquisition alone took about one fourth of the total time needed.

Time Needed for FT

FT of the optic radiation took between 1 minute 22 seconds and 4 minutes 44 seconds in cases in which good or acceptable results were achieved (quality grades 7-8, Table 2). The time needed decreased logarithmically with increasing FA -thresholds (Figure 4). It was also dependent on the DTI slice thickness, but the time needed for tracking the quality of the resulting fiber objects decreased as well. Good results were only achieved for the 2.7-mm slice thickness. FT went faster when the images were angulated by 44 degrees anteriorly (Figure 4B) and achieved better results for higher FA thresholds.

Application of DTI Angulation to the Pre- and Intraoperative Scan Routine

In all 7 patients shown in Table 1, the pre- and intraoperative MRI included DTI scans with angulation by 44 degrees anteriorly. The scanning procedure, image processing, transfer to the planning station, and FT took less than 25 minutes in all cases. Right after finishing the scanning procedure, the magnetization prepared rapid-acquisition gradient-echo and true fast imaging with steady procession were closely examined for tumor remnants while the DTI scan was still running.

In patients 1, 2, and 7, there were small contrast-enhancing tumor remnants found, and we decided to continue surgery. In all 3 patients, total tumor removal was achieved and proved by

Copyright © Congress of Neurological Surgeons. Unauthorized reproduction of this article is prohibited.

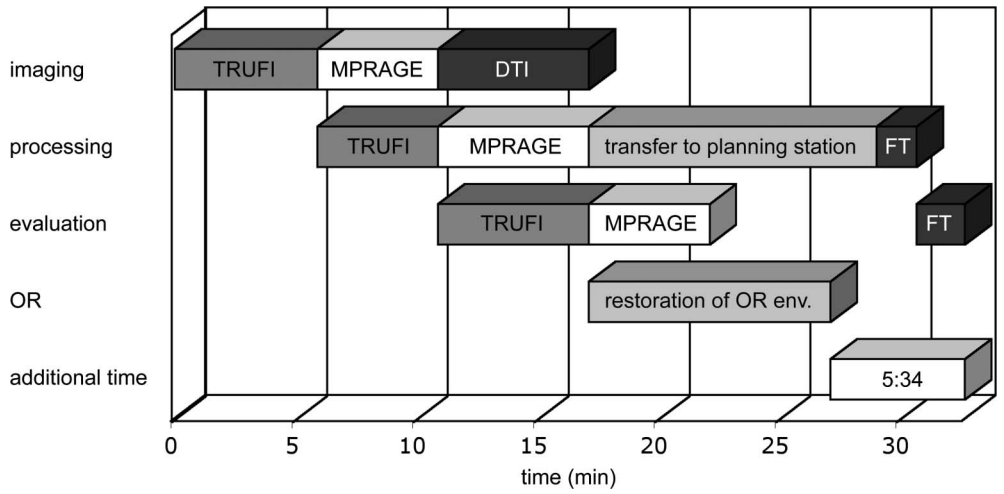

FIGURE 2. *Time schedule for intraoperative magnetic resonance imaging (MRI) including diffusion tensor imaging (DTI). The approximate time needed to perform the different procedures for intraoperative MRI with DTI is shown. The figure illustrates that the different tasks are not performed serially, but overlap so that most of the additional work necessary for intraoperative fiber tracking can be performed while the operating room (OR) is restored to the surgical setup. The additional time needed for intraoperative fiber tracking is less than 6 minutes. True fast imaging (TRUFI) with steady procession image acquisition took 5 minutes 57 seconds, magnetization prepared rapid-acquisition gradient-echo (MPRAGE) image acquisition took 5 minutes, DTI acquisition (44-degree gantry, 2.7-mm slicing) took 6 minutes 14 seconds, image transfer to the planning station took 11 minutes 53 seconds, fiber tracking ([FT] in the processing row) took 1 minute 40 seconds and evaluation of the FT results about 2 minutes (FT in the evaluation row), and restoration of a sterile surgical setup took approximately 10 minutes; the additional time needed for DTI and FT was 5 minutes 34 seconds.*

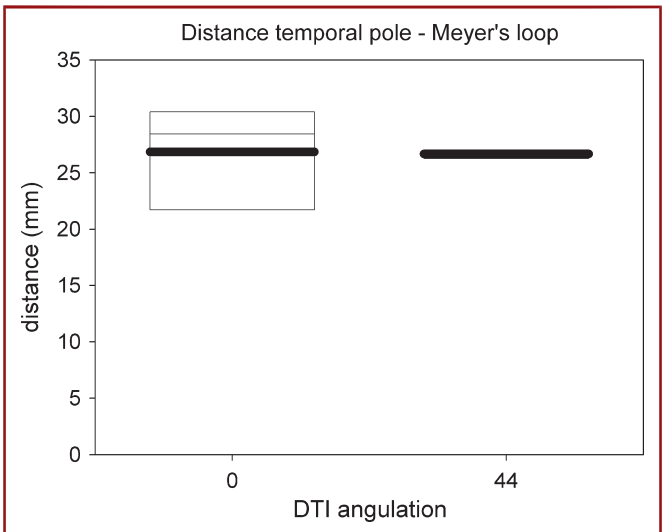

FIGURE 3. *Distance temporal pole: Meyer's loop. The distance of the most anterior part of the optic radiation (Meyer's loop) from the temporal pole is shown. All good-quality results (quality grades 7 and 8) were taken into consideration. DTI, diffusion tensor imaging.*

a second intraoperative MRI scan. Returning the operating table to the surgery position with the patient's head placed outside the 5-G line, removal of the drapes that covered the surgical site during the MRI, and restoration of a sterile environment took about 10 minutes. During this time, image transfer and FT were performed, and the additional time needed for the FT procedure was less than 6 minutes (Figure 2). In patient 4, subtotal tumor removal was planned from the start because of extension of the tumor into eloquent white matter, and we decided not to continue surgery after the first intraoperative scan. In patients 3, 4, and 6, the first intraoperative MRI proved total tumor removal, and, therefore, surgery was not continued.

Of the 5 patients with no preoperative visual field deficit, 1 patient (20%) improved and 4 remained unchanged (80%). One patient (patient 4) with preoperative homonymous hemianopsia improved postoperatively, and 1 remained unchanged (patient 7).

Patients 1, 3, 4, and 7 received adjuvant oncological treatment. The preoperative and second intraoperative MRI scans of patient 7 are shown in Figure 5. The optic radiation is visible in its spatial relationship to the tumor and the tumor resection cavity.

DISCUSSION

FT allows visualization of the individual subcortical anatomy of the patient. Inclusion of fiber objects in neuronavigation

Copyright © Congress of Neurological Surgeons. Unauthorized reproduction of this article is prohibited.

TABLE 4. Image Acquisition and Processing Details[a]

Angulation, deg	Slice Thickness, mm	No. of Slices	No. of Images	Image Acquisition Time	Mosaic Splitting Time	Time Image Transfer via Network	Σ
0	2.7	35	1855	5 min 5 s	4 min 2 s	8 min 20 s	17 min 27 s
	5	19	1007	2 min 47 s	2 min 8 s	3 min 54 s	8 min 49 s
	7	15	795	2 min 14 s	1 min 42 s	3 min 38 s	7 min 34 s
44	2.7	38	2014	6 min 14 s	4 min 21 s	7 min 32 s	18 min 7 s
	5	21	1113	5 min 46 s	2 min 23 s	5 min 17 s	13 min 26 s
	7	15	795	2 min 33 s	1 min 42 s	3 min 38 s	7 min 53 s

[a]Σ, overall time.
The table shows the number of slices and of images needed for diffusion tensor imaging with different settings for slice thickness and angulation as well as the time needed for image acquisition, processing and transfer to the computer system, where the ber tracking is performed.

systems may improve the outcome in surgeries affecting eloquent cortical and subcortical structures. Recently, Gharabaghi et al[3,4] demonstrated a positive influence of computer-assisted surgery on the operation time and complication rate in cranial base surgeries. Better knowledge of the patient's individual subcortical anatomy through FT might prove to have similar positive effects.

Information on the optic pathways is of great interest in epilepsy surgery because the fibers follow a course deep into the temporal lobe before they take a sharp turn back and follow the roof of the temporal horn of the lateral ventricle to the trigone and toward the calcarine cortex,[5,6] only separated from the ventricles by the 2- to 3-mm thick tapetum[2] and with their most anterior part frontally bordered by the uncinate fascicle.[7]

Visual field deficits are among the most common complications after anterotemporal lobectomy for temporal lobe epilepsy.[8-12] Estimating to what extent anterior temporal lobectomy was possible without visual field deficit is inconsistent in the literature and tends toward shorter distances from the temporal pole in more recent studies. The most anterior portion of the optic radiation, which is also called Meyer's loop, is expected between 20.9 mm and 51.5 mm posterior of the temporal pole.[13] Anatomic dissections of human brain (Kriegler fiber dissection technique) identified Meyer's loop at 27 mm[14] (standard deviation, 3.5) 25 mm[6] (range, 22-30 mm), and 31.4[5] mm (range, 28.0-34.0 mm) posterior the temporal pole. There is a considerable interindividual variety concerning the exact course of the

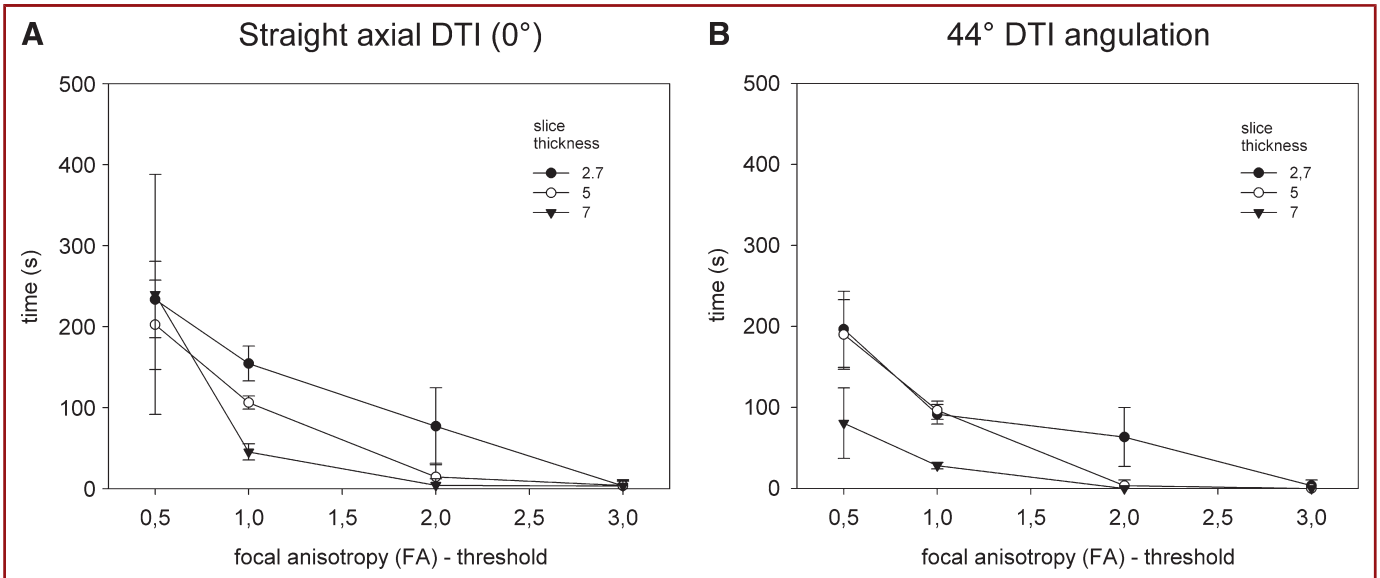

FIGURE 4. *Time needed for the fiber tracking procedure to the focal anisotropy (FA) threshold and comparison of the different diffusion tensor imaging (DTI) acquisition modalities, 2.7-, 5-, and 7-mm slice thickness. The values are the means of all 4 measurements with different minimal fiber length thresholds (5, 10, 20, and 30 mm), visualized as mean and error bars.* **A**, *DTI was acquired in straight axial manner.* **B**, *DTI was angulated anteriorly by 44 degrees. The illustrations show that fiber tracking went faster when the images were angulated by 44 degrees.*

Copyright © Congress of Neurological Surgeons. Unauthorized reproduction of this article is prohibited.

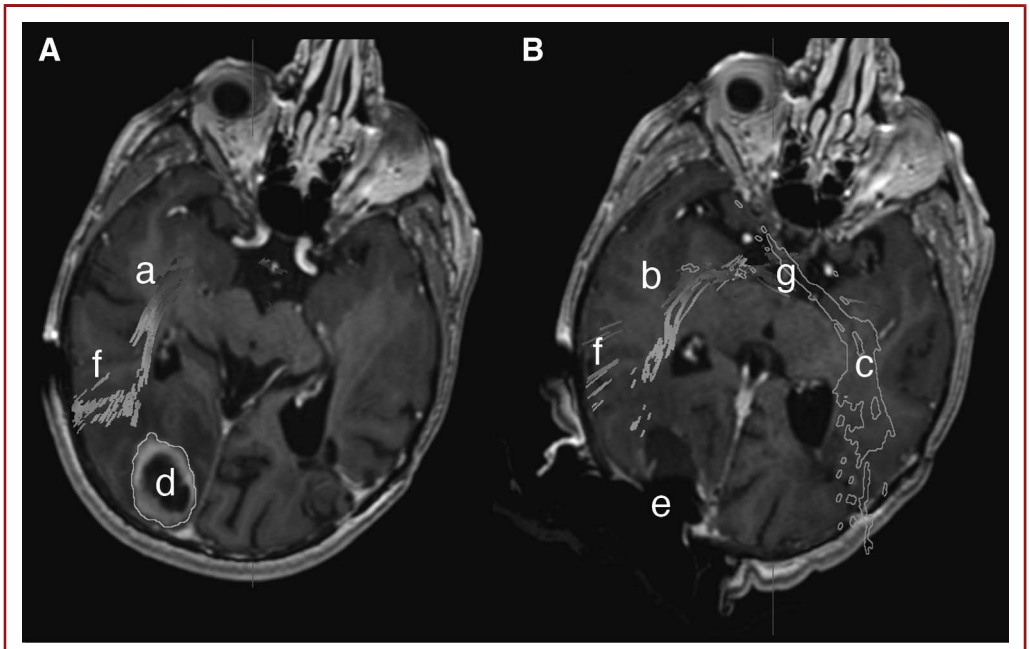

FIGURE 5. *Pre- and intraoperative magnetic resonance imaging (MRI) of patient 7.* **A**, *preoperative MRI.* **B**, *second intraoperative MRI. Right-sided optic radiation (a,b). The anterior portion (Meyer's loop) could not be tracked. A few artifacts not belonging to the optic pathways (f) remain. The spatial relationship to the tumor (d) and the resection cavity (e) is shown. Optic chiasm (g); contralateral fibers (c), in part belonging to the optic pathways.*

optic radiation.[14] Damage to Meyer's loop will lead to a homonymous superior quadrantanopia.[15] Barton et al[16] proposed that each 10-mm resection of the optic radiation anteriorly will result in an additional 20% quadrant loss.

Approaches to the trigone as described by Yaşargil[17] or surgery of occipital lesions hold the risk of damage to the optic radiation. Although the course of the optic radiation is well-known, the great interindividual variety as shown for Meyer's loop[14] underscores the need to acquire information about the patient's individual anatomy for the surgical planning.

Of course, modern MRI scanners allow fusion of pre- and intraoperatively acquired images. Thus, initial tractography is possible based on high-quality DTI. In intraoperative controls, fusion with preoperative tractography results is not possible because of mass effects. In the future, flexible image-fusion algorithms will probably be available, but at the moment, acquisition of new DTI and tractography based on actual images is the only way to judge fiber position and integrity.

FT of the optic radiation is time-consuming and requires considerable experience by the physician performing it. The selection of proper seed volumes and distinguishing relevant from irrelevant fibers adds several minutes to the time required for scanning DTI, processing the raw data, and transferring them into FT software. Even then, the results often are not satisfactory.

With the use of extremely thin DTI slices, high imaging resolution, and the use of multiple motion-probing gradients, excellent FT is possible (Figure 6). Only the imaging takes time and produces a large amount of data to be stored and processed. The aim of our study was to optimize modalities for image acquisition and processing to allow sufficient quality of FT of the optic pathways within a short time for regular preoperative and even intraoperative application and to test its applicability to routine clinical use.

DTI Modalities

In our experience, use of 6 motion-probing gradients is sufficient for basic FT. This is supported by Yamamoto et al,[18] who compared imaging with the use of 6, 12, 40, and 81-directional motion-probing gradients in 12 healthy volunteers without finding relevant differences in the quality of FT results. For regular preoperative DTI, we use 21 or even 42 gradients. To save time in intraoperative imaging, 6 gradients were considered sufficient. In addition, we compared different slice thicknesses. There is a linear relationship between the slice thickness, the number of slices needed to cover the required volume, and the time needed for imaging and processing. More than 20 minutes from image acquisition to FT seemed inappropriate for intraoperative use. Therefore, we chose the 2.7-mm slice thickness as the smallest slice thickness and even tried 5 and 7 mm to find out what thickness was really needed for tractography (Table 4).

Angulation of DTI

We thought that fibers that run orthogonally to the images can more easily be tracked than fibers that run parallel to the slice

Copyright © Congress of Neurological Surgeons. Unauthorized reproduction of this article is prohibited.

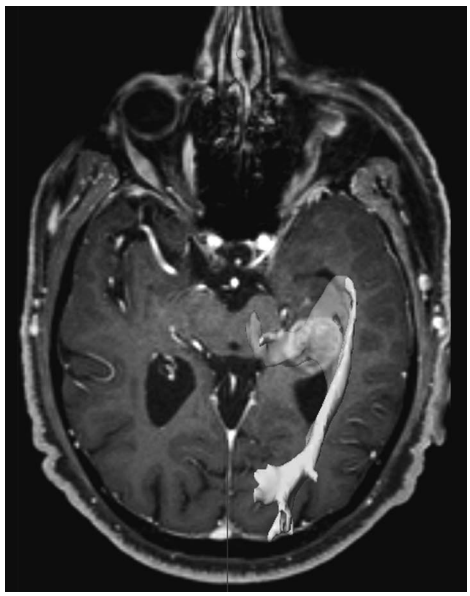

FIGURE 6. *Overlay of an optic radiation fiber tracking object with contrast-enhanced T1-weighted magnetic resonance imaging (MRI) scan at the level of the temporomesial tumor. The image is shown in feet -first supine projection to visualize the spatial relationship between the optic radiation and the lateral ventricle. The optic radiation is shown in anatomically correct shape with nearly complete visualization of Meyer's loop. To achieve a fiber tracking result of this quality, diffusion tensor imaging was performed using 42 gradients in a 3-T MRI scanner.*

layer. In straight axial planes, for example, the corticospinal tracts can be tracked with excellent quality with little effort, whereas the optic pathways are a challenge. This may be a consequence of the nonisometric voxels that are acquired in DTI, especially when the slice thickness is not minimal. The resulting tensors, which represent a fiber bundle parallel to the image layer, are located at a greater distance from each other and represent more of a challenge for the tractography algorithm to be identified as belonging together (Figure 7). This effect is even more significant if an intersection gap is used. The fibers can easily be lost "between the slices" this way. We had the idea to tilt the DTI to bring the mainly anteroposterior fibers as the optic radiation into a nearly orthogonal relation to the images. For technical reasons, the maximum angulation allowed by the FT software was 44 degrees. We compared the results for the angulated DTI with the straight axial (0 degrees) DTI to find out whether tilting allowed better FT of the optic radiation results for lower performance DTI.

Quality of FT Results

High-quality visualization of the optic radiation was possible as well as using angulated as straight axial DTI for tractography. The quality scale (Table 2) that we used for judging the quality of the results proved useful and applicable. The best of our results with a quality grades of 7 and 8 also showed the most anterior part of the optic radiation (Meyer's loop) at a distance from the temporal pole, which is comparable to anatomic dissection studies[5,6,14] (Figures 1F and 3).

As we expected, angulated DTI allowed higher settings for FA and MFL thresholds but still produced results of grades 7 to 8 quality, whereas straight axial DTI needed the very low FA threshold of 0.05 at least (Table 3). At the same time, higher FA and MFL thresholds reduced the noise and made FT easier and faster. The results for larger slice thicknesses such as 5 or 7 mm were poor overall. This was unfortunate because the image acquisition and processing took most of the total time until the completed visualization of the optic radiation. Although we were not able to show a possible decrease in the image acquisition time by reducing the slice thickness to 5 or even 7 mm, we were able to show that 2.7 mm were sufficient for FT, and thus there is no need for a 1-mm or thinner slice thickness, which is far more time-consuming and will not be suitable for routine intraoperative use.

Duration of FT

The FT procedure in scans, which produced good results, took between 1 minute 22 seconds and 4 minutes 44 seconds. The decrease in tracking time by 3 minutes 22 seconds by choosing relatively high FA and MFL thresholds is not significant given that the total time for image acquisition, processing, transfer, and FT is more than 20 minutes, but it reflects the decreased difficulty of the tracking procedure, which will be relevant for less experienced physicians.

Clinical Application

After identification of the angulated DTI with a slice thickness of 2.7 mm as suitable for routine use, we applied these parameters to all operative cases with temporal, temporoparietal, and occipital lesions, which we expected to have anatomic relationships with the optic radiation. In all cases, image acquisition, image processing, and FT did not add more than 6 minutes to the whole intraoperative MRI procedure (Figure 2).

Altogether, total tumor removal was achieved only in 3 of 7 patients at the time of the first intraoperative MRI (50%). Detailed information about the spatial relationships of remaining tumor parts with the optic radiation allowed further resection and finally total tumor removal in 3 more patients. In 1 patient with a low-grade glioma, the close proximity to eloquent white matter precluded continuing with tumor resection to prevent a disabling neurological deficit.

With the help of intraoperative DTI of the optic radiation, 5 of 7 patients (71%) had no new neurological deficit postoperatively. One patient's visual field deficit even partially recovered after decompression of the optic radiation through tumor removal, the condition of 1 patient remained unchanged, and only 1 patient experienced a new homonymous hemianopsia postoperatively (Table 1).

Copyright © Congress of Neurological Surgeons. Unauthorized reproduction of this article is prohibited.

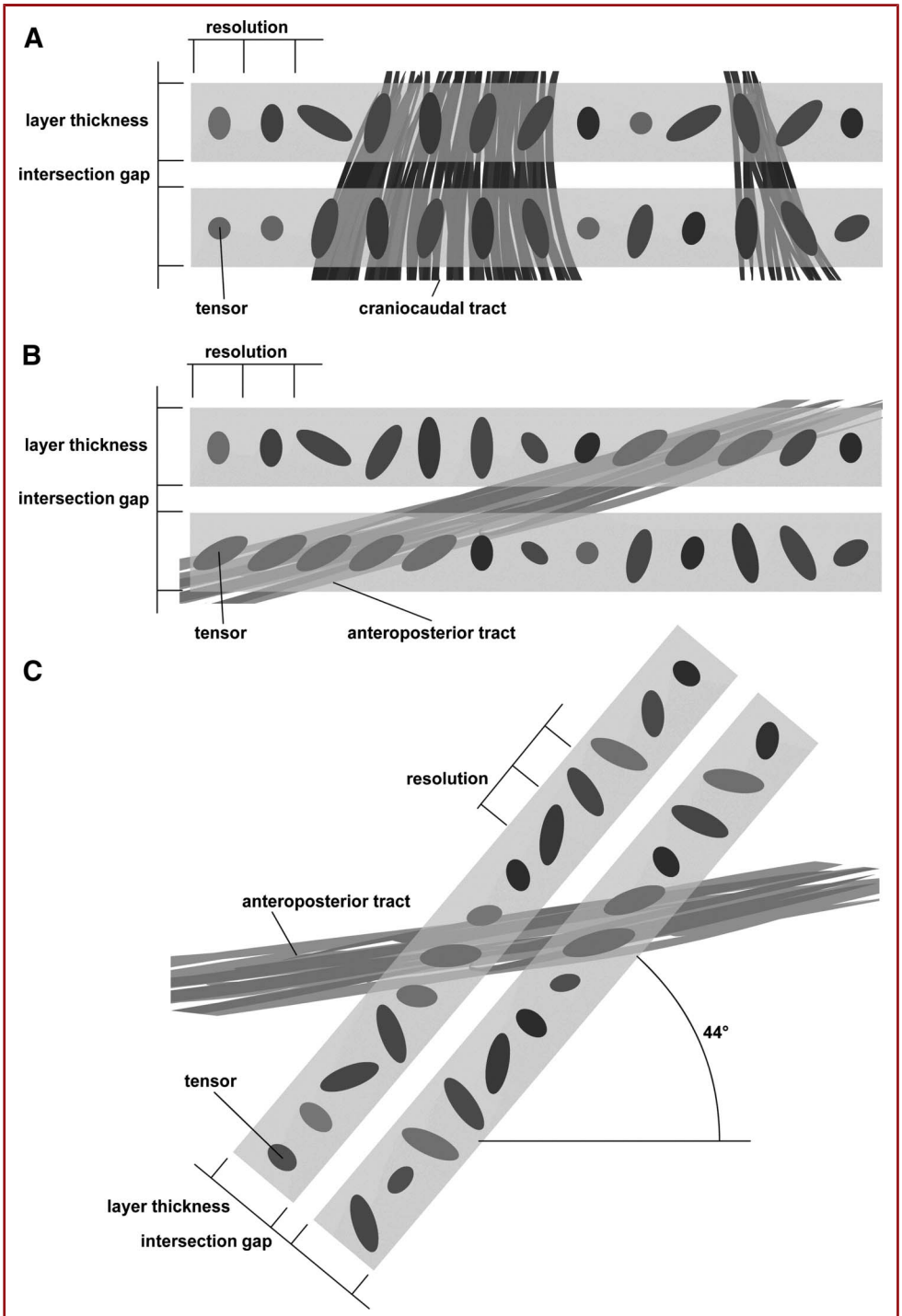

FIGURE 7. *Improvement of fiber tracking results by changing the diffusion tensor imaging (DTI) orientation.* **A**, *model of 2 straight axial DTI layers with tensors illustrating a craniocaudal tract. Even with a large DTI layer thickness and use of an intersection gap, the tensors can easily be tracked by the fiber tracking algorithm if the fibers are in nearly orthogonal relation to the DTI images.* **B**, *in the case of nearly parallel orientation of a fiber bundle toward the DTI, the tensors are at greater distance from each other, and curving fibers can easily be lost "between the slices."* **C**, *how angulation of DTI can improve the tracking quality by bringing the fiber bundle of interest into a nearly orthogonal relation with the DTI is shown.*

Copyright © Congress of Neurological Surgeons. Unauthorized reproduction of this article is prohibited.

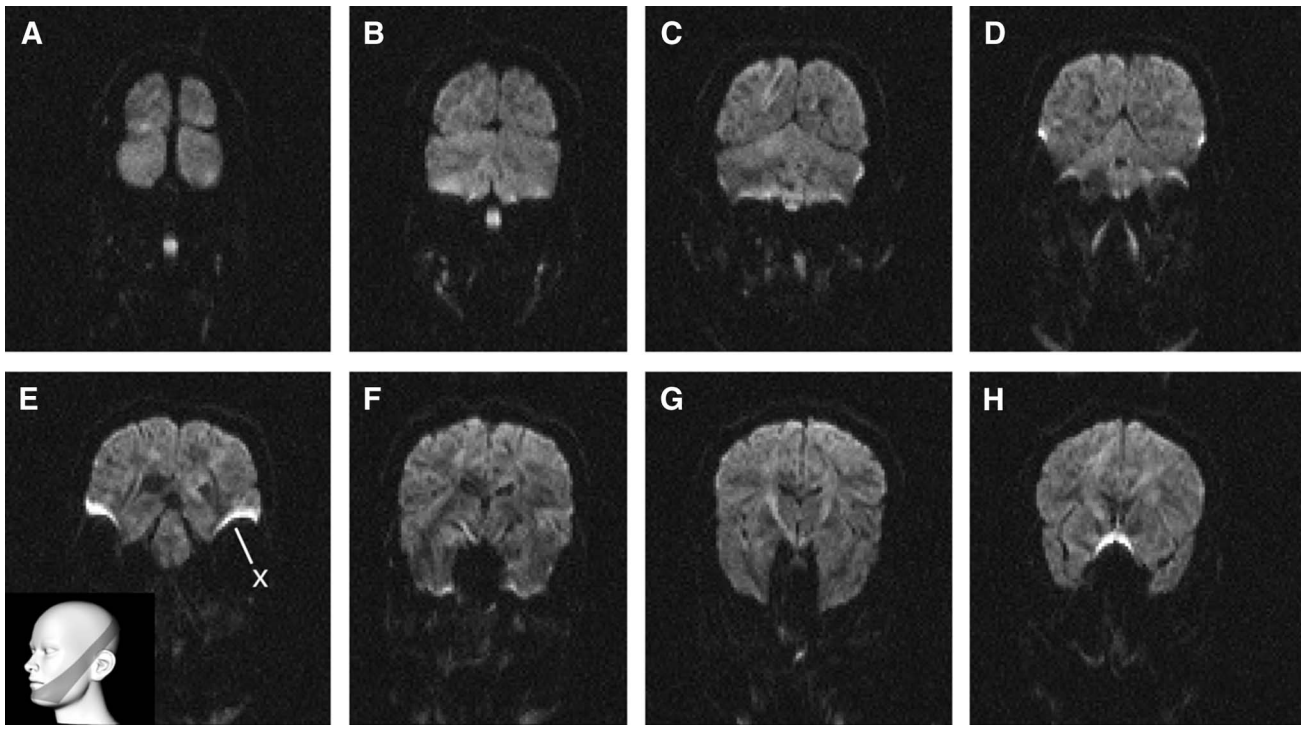

FIGURE 8. *Original diffusion tensor images acquired in a 44-degree angulated manner. Although increased artifacts by greater inhomogeneity of the magnetic field could be expected, artifacts were comparable with images acquired in the usual way.*

The quality of the FT results was good in all cases, so the additional 5 minutes 34 seconds for the DTI scan are acceptable.

Angulated DTI as Standard Protocol?

Although we had good experience with angulated DTI, there are also disadvantages to consider. First, color coding is standardized for straight axial imaging and will lead to wrong color codes if the DTI is angulated. This could easily be corrected by the software manufacturer by adding the capability to define the axis of the patient's head manually, but with the FT software that we used, the color coding was lost anyway after transforming the tracked fibers into 3-dimensional objects for transfer to the neuronavigation system. Still, this is a true disadvantage that one might consider. Furthermore, angulation seems to be beneficial for anteroposterior fiber bundles, but other fibers, for example, the corticospinal tracts, come into the unfortunate position nearly parallel to the image layers. If angulation of the DTI is considered, the tracts, which will be tracked in these data, must be determined beforehand.

Angulation of the image plane may lead to increased artifacts caused by inhomogeneities of the magnetic field at brain-bone and brain-air interface. The scans that we obtained in the manner described did not show more artifacts compared with usual scans. To illustrate, Figure 8 shows exemplary slides of the angulated DTI scan. Depending on the scanner used, the occurrence of artifacts can vary substantially.

FT Seed Volumes

The main factor in the quality of the resulting fiber objects and the time needed for the whole tracking procedure is the physician's experience in FT. In addition to our attempts to delineate suitable parameters for DTI acquisition and FT thresholds, we also suggest using seed volumes, which are easy to find even in patients with an anatomy that is compromised by tumor compression or edema. The seed volumes used in this study were easy to select and led to good and reproducible results. The optic chiasm was as good as the first seed volume as the LGB for the posterior part of the optic radiation, which is shown in Figure 1. It was even superior for tracking Meyer's loop, although the fiber objects did not show the complete sharp curve of the anterior part of the optic radiation from the LGB to the temporal lobe, but a shortcut. Edema and compression by a space-occupying lesion can still reduce the FT ability.

DTI and FT Parameters in the Literature

Table 5 shows other publications on FT of the optic radiation and other tracts with regard to the technical conditions and the imaging and FT parameters used. In most cases, DTI for clinical use and for neuronavigation purposes is acquired with 1.5-T MRI

Copyright © Congress of Neurological Surgeons. Unauthorized reproduction of this article is prohibited.

TABLE 5. Optic Radiation Diffusion Tensor Imaging and Fiber-Tracking Modalities in the Current Literature[a]

Publication		Image Acquisition						
Author/Year	Target Fiber System	Machine	MPG	b Value, s/mm^2	Slice Thickness, mm	Matrix Size	FOV, mm	IS Gap, mm
Chen et al[13] (Erlangen, Germany)/2009	OR	1.5-T Siemens Magnetom Sonata[b]	6	1000	1.9	128 × 128	240	0
Duffau et al[19] (Montpellier, France)/2008	OR, ILF, UF, IOF, SLF	1.5-T GE Signa[d]	200	3000	2			
Taoka et al[20] (Nara, Japan)/2008	OR	1.5-T Siemens Magnetom Sonata[b]	6	1000	3	128 × 128	230	3
Yamamoto et al[18] (Kyoto, Japan)/2007	OR	3 T Siemens Magnetom Trio[b]	6, 12, 40, 81	700	2.5	96 × 96	240	0
Powell et al[23] (London, UK)/2005	OR	1.5-T GE Signa Horizon[g]	6	1148	2.3	96 × 96 (128 × 128 reconstructed)	220	0
Taoka et al[22] (Nara, Japan)/2005	OR	1.5-T Siemens Magnetom Sonata[b]	6	1000	4	128 × 128	230	2
Yamamoto et al[2] (Kyoto, Japan)/2005	OR	1.5-T Gyroscan Intera[i]	32	1000	2	128 × 106	230	0
Witwer et al[21] (Madison, WI)/2002	CST, AF, CoC, ILF, OR	1.5-T GE Signa[g]	6	1000	3	128 × 128	240	

Publication	Image Processing/Fiber Tracking					
Author/Year	Software	Ang, deg	FA	Maximum Angle, deg	MFL	Seed VOI
Chen et al[13] (Erlangen, Germany)/2009	iPlan 2.5[c]	0	0.15		50	LGB, CC
Duffau et al[19] (Montpellier, France)/2008	Brainvisa 3.0.2	0	0.2	45		
Taoka et al[20] (Nara, Japan)/2008	dTV II[e]	0	0.18	––		Anterior of LGB Sagittal striatum at level of trigone
Yamamoto et al[18] (Kyoto, Japan)/2007	DtiStudio V2.3+	0	0.25	70		CC, LGB
Powell et al[23] (London, UK)/2005		0				Anterior of LGB
Taoka et al[22] (Nara, Japan)/2005	Dr. View[h]	0				
Yamamoto et al[2] (Kyoto, Japan)/2005	PRIDE[j]	0				Lateral LGB, CC
Witwer et al[21] (Madison, WI)/2002	DTI analysis software toolbox[k]	0				

[a]MPG, number of motion probing gradients; FOV, field of view; IS, intersection; Ang, DTI angulation; FA, focal anisotropy threshold; MFL, minimal fiber length threshold; VOI, volume of interest; OR, optic radiation; LGB, lateral geniculate body; CC, calcarine cortex; ILF, inferior longitudinal fasciculus; UF, uncinate fasciculus; IOF, inferior occipitofrontal fasciculus; SLF, superior longitudinal fasciculus; CST, corticospinal tract; AF, arcuate fasciculus; CoC, corpus callosum; DTI, diffusion tensor imaging.
[b]Siemens Healthcare, Erlangen, Germany.
[c]BrainLab, Feldkirchen, Germany.
[d]General Electric Healthcare, Chalfont St. Giles, UK.
[e]Masutani et al, University of Tokyo, Toky, Japan.
[f]H. Jiang, S. Mori, Johns Hopkins University, Baltimore, Maryland.
[g]General Electric Healthcare, Milwaukee, Wisconsin.
[h]Asahi-Kasei Information Systems, Tokyo, Japan.
[i]Philips Medical Systems, Best, the Netherlands.
[j]Philips Medical Systems, Amsterdam, the Netherlands.
[k]Research Systems Inc, Boulder, Colorado.

Copyright © Congress of Neurological Surgeons. Unauthorized reproduction of this article is prohibited.

scanners. The most common number of motion-probing gradients is 6; in 1 case it was 32[2] and in a other it was 200.[19] Yamamoto et al[18] compared the results after using 6, 12, 40, and 81 different motion-probing gradients and found no significant differences.

The b value, a parameter that describes the strength of diffusion weighting in DTI, is between 700[18] and 3000[19] in the listed publications; 1000 is the most common setting.[2,13,20,21]

The listed publications use values between 1.9 mm[13] and 4 mm,[22] which supports our own finding that the optimal slice thickness will be found within this range. In no case was angulation of the images attempted.

Although about half of the MRI scanners used were by Siemens and half were by GE, there were hardly 2 publications in which the same FT software was used. Many of them were locally written. One reason may be that FT still is a relatively new technology that found its way into routine use in surgical planning only a few years ago. With the improvement of commercially available software solutions, fewer software products used in the near future may allow a better comparison of the results of different centers.

The FA threshold for optic radiation FT was between 0.15 and 0.25. In 4 publications referring to optic radiation FT, the FA thresholds used were not reported.[2,21-23] Our own finding was that the FA threshold had to be much lower (0.05) to achieve high-quality results. Unfortunately, it is not possible to compare the results of different centers because in none of the publications is there a quality grading for the resulting fiber objects used.

One drawback of our study is that the data are from only 7 patients with different pathologies. Further research on optic radiation FT in larger numbers of subjects and with intracranial pathologies is needed. Second, we did not perform DTI with slice thicknesses less than 2.7 mm. Although we achieved very good results with this slice thickness, it is possible that thinner slices would allow even better visualization of the optic radiation.

The results demonstrated in this study are only to be used for optic radiation FT and can not be applied to other fiber systems such as the fornix, the superior or inferior longitudinal fasciculi, the arcuate fasciculus, the corpus callosum, or the corticospinal tract.

The most important consideration is that FT is a very time- and resource-consuming technology that still must be proved beneficial for the patient's outcome.

CONCLUSION

Good-quality results of FT of the optic radiation are possible and in a short amount of time for routine pre- and intraoperative use. For this purpose, it is possible to choose a moderate slice thickness of the DTI data set. Angulation of the images can bring the fibers of interest into a nearly orthogonal relationship with the image set and improve the ease of the tracking procedure and the quality of the results. An algorithm to track optic radiation is proposed.

Disclosure

The authors have no personal financial or institutional interest in any of the drugs, materials, or devices described in this article.

REFERENCES

1. Pierpaoli C, Jezzard P, Basser PJ, Barnett A, Di Chiro G. Diffusion tensor MR imaging of the human brain. *Radiology*. 1996;201(3):637-648.
2. Yamamoto T, Yamada K, Nishimura T, Kinoshita S. Tractography to depict three layers of visual field trajectories to the calcarine gyri. *Am J Ophthalmol*. 2005;140(5):781-785.
3. Gharabaghi A, Rosahl SK, Feigl GC, et al. Image-guided lateral suboccipital approach: part 1-individualized landmarks for surgical planning. *Neurosurgery*. 2008;62(3 Suppl 1):18-22; discussion 22-23.
4. Gharabaghi A, Rosahl SK, Feigl GC, et al. Image-guided lateral suboccipital approach: part 2-impact on complication rates and operation times. *Neurosurgery*. 2008;62(3 Suppl 1):24-29; discussion 29.
5. Choi C, Rubino PA, Fernandez-Miranda JC, Abe H, Rhoton AL Jr. Meyer's loop and the optic radiations in the transsylvian approach to the mediobasal temporal lobe. *Neurosurgery*. 2006;59(4 Suppl 2):ONS228-ONS235; discussion ONS235-ONS236.
6. Rubino PA, Rhoton AL Jr, Tong X, Oliveira E. Three-dimensional relationships of the optic radiation. *Neurosurgery*. 2005;57(4 Suppl):219-227; discussion 219-227.
7. Kier EL, Staib LH, Davis LM, Bronen RA. MR imaging of the temporal stem: anatomic dissection tractography of the uncinate fasciculus, inferior occipitofrontal fasciculus, and Meyer's loop of the optic radiation. *AJNR Am J Neuroradiol*. 2004;25(5):677-691.
8. Anderson DR, Trobe JD, Hood TW, Gebarski SS. Optic tract injury after anterior temporal lobectomy. *Ophthalmology*. 1989;96(7):1065-1070.
9. Falconer MA, Wilson JL. Visual field changes following anterior temporal lobectomy: their significance in relation to Meyer's loop of the optic radiation. *Brain*. 1958;81(1):1-14.
10. Hughes TS, Abou-Khalil B, Lavin PJ, Fakhoury T, Blumenkopf B, Donahue SP. Visual field defects after temporal lobe resection: a prospective quantitative analysis. *Neurology*. 1999;53(1):167-172.
11. Krolak-Salmon P, Guenot M, Tiliket C, et al. Anatomy of optic nerve radiations as assessed by static perimetry and MRI after tailored temporal lobectomy. *Br J Ophthalmol*. 2000;84(8):884-889.
12. Wieshmann UC, Symms MR, Clark CA, et al. Wallerian degeneration in the optic radiation after temporal lobectomy demonstrated in vivo with diffusion tensor imaging. *Epilepsia*. 1999;40(8):1155-1158.
13. Chen X, Weigel D, Ganslandt O, Buchfelder M, Nimsky C. Prediction of visual field deficits by diffusion tensor imaging in temporal lobe epilepsy surgery. *Neuroimage*. 2009;45(2):286-297.
14. Ebeling U, Reulen HJ. Neurosurgical topography of the optic radiation in the temporal lobe. *Acta Neurochir (Wien)*. 1988;92(1-4):29-36.
15. Jacobson DM. The localizing value of a quadrantanopia. *Arch Neurol*. 1997;54(4):401-404.
16. Barton JJ, Hefter R, Chang B, Schomer D, Drislane F. The field defects of anterior temporal lobectomy: a quantitative reassessment of Meyer's loop. *Brain*. 2005;128(Pt 9):2123-2133.
17. Yaşargil M. Microneurosurgery of CNS tumors. *Microneurosurgery*. Vol IVB. Stuttgart: Georg Thieme; 1996:313-318.
18. Yamamoto A, Miki Y, Urayama S, et al. Diffusion tensor fiber tractography of the optic radiation: analysis with 6-, 12-, 40-, and 81-directional motion-probing gradients, a preliminary study. *AJNR Am J Neuroradiol*. 2007;28(1):92-96.
19. Duffau H, Thiebaut de Schotten M, Mandonnet E. White matter functional connectivity as an additional landmark for dominant temporal lobectomy. *J Neurol Neurosurg Psychiatry*. 2008;79(5):492-495.
20. Taoka T, Sakamoto M, Nakagawa H, et al. Diffusion tensor tractography of the Meyer loop in cases of temporal lobe resection for temporal lobe epilepsy: correlation between postsurgical visual field defect and anterior limit of Meyer loop on tractography. *AJNR Am J Neuroradiol*. 2008;29(7):1329-1334.
21. Witwer BP, Moftakhar R, Hasan KM, et al. Diffusion-tensor imaging of white matter tracts in patients with cerebral neoplasm. *J Neurosurg*. 2002;97(3):568-575.
22. Taoka T, Sakamoto M, Iwasaki S, et al. Diffusion tensor imaging in cases with visual field defect after anterior temporal lobectomy. *AJNR Am J Neuroradiol*. 2005;26(4):797-803.
23. Powell HW, Parker GJ, Alexander DC, et al. MR tractography predicts visual field defects following temporal lobe resection. *Neurology*. 2005;65(4):596-599.

Acknowledgment

We thank Friederike Mühler for assistance with image acquisition.

Copyright © Congress of Neurological Surgeons. Unauthorized reproduction of this article is prohibited.

Differential Efficacy of Electric Motor Cortex Stimulation and Lesioning of the Dorsal Root Entry Zone for Continuous vs Paroxysmal Pain After Brachial Plexus Avulsion

Mohamed Ali, MD*
Youichi Saitoh, MD, PhD‡
Satoru Oshino, MD, PhD§
Koichi Hosomi, MD, PhD‡
Haruhiko Kishima, MD, PhD§
Shayne Morris, MD§
Masahiko Shibata, MD, PhD¶
Toshiki Yoshimine, MD, PhD§

*Neurosurgery Department, Mansoura University, Mansoura, Egypt; ‡Department of Neuromodulation and Neurosurgery, Osaka University, Japan; Departments of §Neurosurgery and ¶Pain Medicine, Osaka University Graduate School of Medicine, Osaka, Japan

Correspondence:
Youichi Saitoh, MD, PhD,
Department of Neurosurgery,
Osaka University Graduate School of Medicine,
2-2 Yamadaoka, Suita, 565-0871, Japan.
E-mail: saitoh@nsurg.med.osaka-u.ac.jp

Received, May 11, 2010.
Accepted, September 10, 2010.

Copyright © 2011 by the
Congress of Neurological Surgeons

BACKGROUND: Pain after traumatic brachial plexus avulsion (BPA) has 2 distinct patterns: continuous burning pain and paroxysmal shooting pain. Lesioning of the dorsal root entry zone (DREZotomy) is more effective for paroxysmal than continuous pain. It is unknown, however, whether electric motor cortex stimulation (EMCS) has a differential effect on continuous vs paroxysmal BPA pain.

OBJECTIVE: To analyze the differential effect of EMCS and DREZotomy on continuous vs paroxysmal BPA pain in a series of 15 patients.

METHODS: Fifteen patients with intractable BPA pain underwent DREZotomy alone (n = 7), EMCS alone (n = 4), or both procedures (n = 4). Pain intensity was evaluated with the Visual Analog Scale, and separate ratings were recorded for paroxysmal and continuous pain. Pain relief was categorized as excellent (> 75% pain relief), good (50%-75%), or poor (< 50%). Favorable outcome was defined as good or better pain relief.

RESULTS: Eight patients had EMCS; 7 were followed up for an average of 47 months. Of those 7 patients, 3 (42%) with continuous pain had favorable outcomes compared with no patients with paroxysmal pain. Eleven patients had DREZotomy; 10 were followed up for an average of 31 months. Of those 10 patients, 7 (70%) with paroxysmal pain had favorable outcomes compared with 2 (20%) with continuous pain.

CONCLUSION: EMCS was ineffective for paroxysmal pain but moderately effective for continuous pain. DREZotomy was highly effective for paroxysmal pain but moderately effective for continuous pain. It may be prudent to use EMCS for residual continuous pain after DREZotomy.

KEY WORDS: Brachial plexus avulsion pain, Continuous pain, Differential efficacy, DREZotomy, Motor cortex stimulation, Paroxysmal pain

Neurosurgery 68:1252–1258, 2011 DOI: 10.1227/NEU.0b013e31820c04a9 www.neurosurgery-online.com

Deafferentation pain is a major disabling symptom after traumatic brachial plexus avulsion (BPA).[1] Of patients with BPA, as many as 90% complain of significant early pain, but only 25% continue to experience severe pain 4 years after injury.[1] Post-BPA pain is known to be almost constantly unbearable and resistant to all classes of analgesic drugs.[2]

ABBREVIATIONS: BPA, brachial plexus avulsion; **CS,** central sulcus; **DREZotomy,** lesioning of the dorsal root entry zone; **EMCS,** electric motor cortex stimulation; **VAS,** Visual Analog Scale

Typically, post-BPA pain has 2 distinct types: continuous background pain described as burning, throbbing, and/or aching sensations and electric shooting paroxysms lasting a few seconds to minutes.[1,2] These 2 distinct types of pain appear to be the clinical expression of 2 different pain generators. Paroxysmal pain is thought to originate from hyperactive neurons in the dorsal horn, whereas continuous pain is thought to originate from supraspinal structures, particularly the thalamus.[2-4]

Since the early work of Sindou et al[5] and Nashold et al[6] in the 1970s, lesioning of the dorsal root entry zone (DREZotomy) has been

Copyright © Congress of Neurological Surgeons. Unauthorized reproduction of this article is prohibited.

the preferred procedure for treatment of intractable BPA pain. DREZotomy is designed to destroy hyperactive neurons in the substantia gelatinosa either by microsurgical incision and bipolar coagulation[5] or by thermocoagulation.[6] The reported pain relief rate immediately after DREZotomy is 75% to 98%, but sustained benefit is observed in only two-thirds of patients after 2 years.[2,7] The major complications of the DREZotomy are weakness in the ipsilateral leg and sensory disturbances, which are seen in 5% to 10% of patients.[7,8]

During the past 2 decades, electric motor cortex stimulation (EMCS) has been used to treat deafferentation pain, particularly central post-stroke pain and trigeminal neuropathic pain.[9-11] Recently, several groups, including ours, used EMCS as a "last resort" treatment for patients with BPA pain who failed or refused DREZotomy.[12-16] In these small studies, EMCS yielded a moderate success rate of 40% to 50%.[12-16] A major limitation for the use of EMCS for BPA pain remains the lack of reliable predictive factors for success, which is particularly important considering the modest success rate of EMCS for BPA and the high cost of treatment.[9-11]

Sindou et al[2] first reported that DREZotomy has a differential effect on the 2 patterns of BPA pain by showing that DREZotomy was more effective for paroxysmal than continuous pain. Conversely, none of the previous EMCS studies analyzed the differential effect of EMCS on continuous vs paroxysmal BPA pain.[12-16] Such a differential effect may be important with regard to selection of treatment for patients. We report our observations in 15 patients with BPA pain who underwent EMCS or DREZotomy and our analysis of the differential effect of EMCS and DREZotomy on continuous vs paroxysmal BPA pain.

PATIENTS AND METHODS

Patient Population

Between January 1997 and January 2010, 15 consecutive patients with intractable pain after BPA were referred to our institute and underwent a total of 19 procedures: DREZotomy alone (n = 7), EMCS alone (n = 4), or both procedures (n = 4). Two patients had EMCS after failed DREZotomy, whereas 2 patients had DREZotomy after failed EMCS. All patients were men. The mean age was 47 years (range, 31-72 years) for DREZotomy patients and 51 years (range, 30-67 years) for EMCS patients. The mean duration of pain was 12.8 years (range, 2-35 years) before DREZotomy and 10 years (range, 0.8-28 years) before EMCS. Injuries were sustained in motorcycle accident (n =13), after a fall from a height (n =1), and by a falling tree (n =1). In the majority of patients (n = 9), pain appeared within 1 month of injury; the longest interval between injury and onset of pain was 2 years. All patients had sensory and motor deficits of varying degrees (Table 1).

Patient Selection

Most patients showed pseudomeningocele on CT myelography. In all patients, pain was severe enough to interfere with normal daily activities. Pain was unresponsive to a wide variety of medications, including tricyclic antidepressants, anticonvulsants, and narcotic analgesics, for at least 12 months.

TABLE 1. Patient Clinical Characteristics[a]

Patient	Procedure	Age y, Sex	Level of Injury	Cause of Injury	Side	Pain Duration, y	Pain Onset	Pain Pattern	Pain Quality	Global VAS	Previous Treatments
1	DREZ	40/M	C6-C8	Motorcycle	R	18	Immediate[b]	Con + Paroxy	B + Elec	8	Medicine
2	DREZ	72/M	C5-C8	Motorcycle	L	12	Immediate	Con + Paroxy	B + Elec	8	Medicine
3	DREZ	35/M	C6-T1	Motorcycle	L	7	3 mo	Con + Paroxy	B + Elec	9	SCS
4	DREZ	43/M	C8-T1	Motorcycle	R	23	Immediate	Con + Paroxy	Squeezing + Elec	8	Medicine
5	DREZ	52/M	C6-T1	Motorcycle	R	35	Immediate	Con + Paroxy	B+ Elec	7	Medicine
6	DREZ	47/M	C5-T1	Motorcycle	L	2	Immediate	Con + Paroxy	B+ Elec	9	Medicine
7	DREZ	35/M	C5-C8	Motorcycle	R	18	1 y	Con + Paroxy	B + Elec	10	Medicine
8	EMCS	64/M	C7-T1	Motorcycle	L	28	NA	Con	Cramping	8	Medicine, SCS
9	EMCS	67/M	C5-T1	Falling tree	R	0.8	Immediate	Con + Paroxy	Cramping + Elec	8	Medicine
10	EMCS	55/M	C5-C7	Motorcycle	L	2.5	Immediate	Con	Paresthesia	8	Medicine, SCS
11	EMCS	30/M	C6-T1	Motorcycle	L	23	1.5 y	Con + Paroxy	B + Elec	7	Medicine
12	DREZ + EMCS	56/M	C5-T1	Fall from a height	L	4.3	Immediate	Con + Paroxy	Throb + Elec	9	Medicine, SCS, DBS
13	EMCS + DREZ	59/M	C6-T1	Motorcycle	L	10.2	2 y	Con + Paroxy	B + Elec	9	Medicine, DBS
14	DREZ + EMCS	31/M	C7-T1	Motorcycle	L	5.9	NA	Con + Paroxy	B + Elec	7	Medicine, rTMS, SCS
15	EMCS + DREZ	49/M	C7-T1	Motorcycle	L	6	Immediate	Con + Paroxy	B + stabbing	3	Medicine, rTMS

[a]B, burning; Con, continuous; DBS, deep brain stimulation; DREZ, dorsal root entry zone lesioning; Elec, electric shooting-like; EMCS, electric motor cortex stimulation; Paroxy, paroxysmal; rTMS, repetitive transcranial magnetic stimulation; SCS, spinal cord stimulation; VAS, Visual Analog Scale.
[b]Within 1 month of injury; throb, throbbing.

Copyright © Congress of Neurological Surgeons. Unauthorized reproduction of this article is prohibited.

We typically recommend DREZotomy as a primary option for intractable BPA and reserve EMCS for intractable residual pain after DREZotomy. However, in the present study, some patients declined DREZotomy and preferred EMCS as a first choice for fear of DREZotomy-related complications such as leg weakness.

Previous Treatment Trials

Six patients (40%) had previous surgical procedures for pain treatment without adequate relief. Four patients had undergone spinal cord stimulation, 1 had deep brain stimulation, and 1 had both procedures. Two patients had undergone repetitive transcranial magnetic stimulation preoperatively to predict the efficacy of permanent EMCS.[14]

Pain Characteristics

Thirteen patients (86%) suffered from both continuous and paroxysmal pain, whereas 2 patients (14%) had isolated continuous pain. Ten patients described the quality of continuous pain as burning, 2 as cramping, 1 as throbbing, 1 as squeezing, and 1 as paresthesia. Twelve patients described the quality of paroxysmal pain as electric, whereas 1 patient described it as stabbing. The frequency of paroxysmal pain was available in 10 patients. Three patients had paroxysms at a rate of 10 to 12 per day, 1 at 2 to 3 per day, 4 at 3 to 5 per hour, 1 at 1 per hour, and 1 at 3 per minute. In most patients, pain predominated in the distal portion of the upper limb, particularly the hand. Median Visual Analog Scale (VAS) for pain was 8 of 10 (range, 3-10; Table 1).

Evaluation of Pain Relief

We distinguished between continuous and paroxysmal pain by their distinct quality and duration (please see above). Using VAS, we recorded separate ratings of pain intensity for each type of pain ranging from 0 (no pain) to 10 (worst possible pain).[17] VAS was evaluated before surgery, immediately after surgery, and at follow-up visits every 6 months.[14] The degree of pain relief was categorized as excellent for VAS reduction $> 75\%$, good for VAS reduction of 50% to 75%, and poor for VAS reduction $< 50\%$. A favorable outcome was defined as good or better pain relief.[2]

Surgical Procedure

EMCS

Eight patients were treated with EMCS alone or in combination with DREZotomy (Table 1). Trial electrodes were implanted in the subdural space over the precentral gyrus in all patients and additionally within central sulcus (CS) in 4 patients. We restricted implantation within CS to patients with severe persistent motor weaknesses, who therefore had low potential for further deterioration.

The location of the CS was identified by its characteristic omega shape on magnetic resonance surface images. Under general anesthesia, a craniotomy of a 5- to 6-cm area was performed over the sensorimotor cortex corresponding to the upper extremity. A 20-grid electrode (4-5 array, 0.3-cm electrode diameter, 0.7-cm separation; Unique Medical Co, Tokyo, Japan) was placed subdurally. The location of the CS was then confirmed by phase reversal of somatosensory evoked potentials. Occasionally, somatosensory evoked potentials could not be obtained because of complete deafferentation. In that case, we relied solely on CS anatomic localization by magnetic resonance imaging.

In case of CS implantation, the arachnoid membrane of the CS was microsurgically dissected, and the vessels within that sulcus were freed to expose the hidden lateral walls of precentral and postcentral gyri. One or two 4-plate electrodes were then additionally implanted within the CS[14] (0.3-cm electrode diameter, 0.7-cm separation; Unique Medical Co, or Resume; Medtronic, Inc, Minneapolis, Minnesota).

After implantation of test electrodes, electrical stimuli were delivered to various parts of the grid electrode and the 4-plate electrode aiming to identify the best location for pain relief. One or 2 weeks later, a second surgery was performed under general anesthesia. The test electrodes were replaced by a Resume electrode, and an implantable pulse generator (ITREL III; Medtronic, Inc.) was then placed subcutaneously in the chest or abdomen.

The stimulation parameters used were an amplitude of 0.9 to 5 V, frequency of 25 to 50 Hz, and pulse width of 210-350 microseconds with bipolar configuration. Chronic stimulation was applied continuously for 15 to 30 minutes on each occasion 3 to 6 times a day.[14]

DREZotomy

DREZotomy was performed in 11 patients (Table 1) according to the Nahold et al[6] radiofrequency thermocoagulation technique. The lesioning electrode was introduced into the intermediolateral sulcus at the site of rootlet avulsion for a depth of 2 mm and angled 25° to 30° in the sagittal plane. A series of radiofrequency coagulation lesions were made along the longitudinal extent of the intermediolateral sulcus, including 1 level above and 1 level below the injured segments. The lesions are made at intervals of 1 mm at 70°C for 30 seconds (Model RFG-3C Graphics RF Lesion Generator, Radionics, Burlington, Massachusetts). Thermocoagulation was performed under monitoring of somatosensory evoked potentials and motor evoked potentials.

Statistical Analysis

We compared the percent VAS reduction of continuous and paroxysmal pain for EMCS using the 2-sample t test and for DREZotomy using the paired t test. A value of $P < .05$ was considered statistically significant.

Ethical Considerations

Written informed consent was given by each patient before the procedure. Approval was obtained from the local Ethics Review Board of Osaka University Hospital for data analysis.

RESULTS

EMCS

Eight patients had trial EMCS: 6 had both paroxysmal and continuous pain, and 2 had isolated continuous pain. Of those 8 patients, 1 patient who had both types of pain declined permanent electrode implantation. The remaining 7 patients underwent permanent EMCS and were followed up long term for an average of 47 months (range, 12-112 months).

The percentage of patients with favorable outcomes ($> 50\%$ VAS reduction) was higher for continuous than paroxysmal pain, both during the trial and with long-term stimulation (Figure 1; Table 2). During the trial, 4 of 8 patients (50%) with continuous pain had favorable outcomes compared with 2 of 6 patients (33%) with paroxysmal pain (Table 2). At the latest follow-up visit, 3 of 7 patients (42%) with continuous pain had favorable outcomes compared with 0 of the 5 patients (0%) with paroxysmal pain

Copyright © Congress of Neurological Surgeons. Unauthorized reproduction of this article is prohibited.

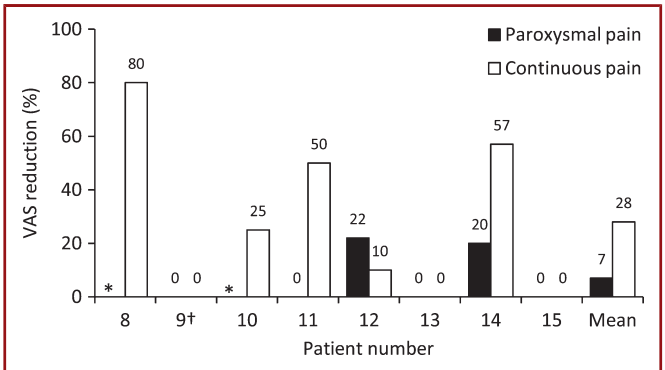

FIGURE 1. *Visual Analog Scale (VAS) reduction percent for paroxysmal and continuous pain in 8 patients who underwent electric motor cortex stimulation (EMCS) and had long-term follow-up. The mean VAS reduction percent tended to be greater for continuous pain than for paroxysmal pain (28% vs 7%;* P = *.11, 2-sample t test). EMCS was ineffective for paroxysmal pain but moderately effective for continuous pain. *These 2 patients had isolated continuous pain. †Patient 9 failed trial stimulation and had no permanent implantation.*

(Figure 1), and the mean percent VAS reduction was greater for continuous pain than for paroxysmal pain (28% vs 7%; $P = .11$, 2-sample t test). Of the 2 patients who underwent EMCS after DREZotomy, 1 patient had good pain relief for continuous pain, whereas the other had poor pain relief for both types of pain.

DREZotomy

All 11 patients who underwent DREZotomy suffered from both paroxysmal and continuous pain. One patient had < 6 months of follow-up and therefore was excluded from analysis of long-term results. The remaining 10 patients were followed up long-term for an average of 31 months (range, 12-61 months).

The percentage of patients with favorable outcomes was higher for those with paroxysmal than for those with continuous pain in both initial and long-term results (Figure 2 and Table 2). Immediately after surgery, 10 of 11 patients (91%) with paroxysmal pain had favorable outcomes compared with 8 of 11 patients (72%) with continuous pain (Table 2). At the latest follow-up, 7 of 10 patients (70%) with paroxysmal pain had favorable outcomes compared with 2 of 10 patients (20%) with continuous pain (Figure 2), and the mean percent VAS reduction was greater for paroxysmal pain than continuous pain (63% vs 26%; $P = .01$, paired t test).

Complications

There was no perioperative mortality for either procedure.

EMCS

One patient (Patient 13; 12%) had local infection 9 months after implantation. This diabetic patient presented with a deep wound infection and dehiscence but no †meningeal irritation

TABLE 2. Results of 15 Patients With Electrical Motor Cortex Stimulation or Dorsal Root Entry Zone Lesioning for Brachial Plexus Avulsion Pain[a]

Patient	Age, y/Sex Initial	Pain Pattern	Procedure	VAS Reduction, % Paroxysmal Pain Long-term	Paroxysmal Pain Initial	Continuous Pain Long-term	Continuous Pain Initial	Follow-up, mo	Complications or Comments
1	40/M	Con + Paroxy	DREZ	100	100	0	33	61	No
2	72/M	Con + Paroxy	DREZ	88	57	66	0	28	No
3	35/M	Con + Paroxy	DREZ	100	66	80	0	15	No
4	43/M	Con + Paroxy	DREZ	100	0	0	0	24	No
5	52/M	Con + Paroxy	DREZ	100	100	100	100	17	No
6	47/M	Con + Paroxy	DREZ	88	100	86	14	12	Sensory disturbances and transient leg weakness
7	35/M	Con + Paroxy	DREZ	100	100	100	100	9	Sensory disturbances
8	64/M	Con	EMCS	NA	NA	90	80	36	Death after 36 mo (ICH)
9	67/M	Con + Paroxy	EMCS	0	0	25	0	0	No permanent implantation
10	55/M	Con	EMCS	NA	NA	25	25	76	Removal after 76 mo
11	30/M	Con +Paroxy	EMCS	88	0	84	50	50	No
12	56/M	Con + Paroxy	DREZ	0	0	0	0	24	No
			EMCS	56	22	76	10	112	No
13	59/M	Con + Paroxy	EMCS	0	0	30	0	9	Removed after 9 mo owing to infection
			DREZ	100	100	75	14	53	No
14	31/M	Con + Paroxy	DREZ	100	11	57	0	60	No
			EMCS	33	20	71	57	19	No
15	49/M	Con + Paroxy	EMCS	0	0	33	0	24	No
			DREZ	100	NA	100	NA	6	Follow-up < 6 mo

[a]Con, continuous; DREZ, dorsal root entry zone lesioning; ICH, intracerebral hematoma; EMCS, electrical motor cortex stimulation; Paroxy, paroxysmal; VAS, Visual Analog Scale.

Copyright © Congress of Neurological Surgeons. Unauthorized reproduction of this article is prohibited.

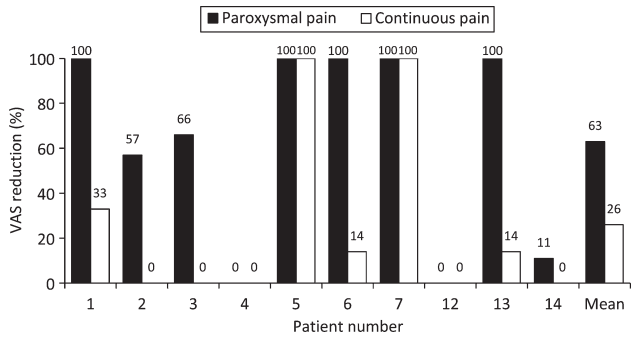

FIGURE 2. *Visual Analog Scale (VAS) reduction percent for paroxysmal and continuous pain in 10 patients who underwent lesioning of the dorsal root entry zone (DREZotomy) and had long-term follow-up. The mean percent VAS reduction was greater for paroxysmal pain than continuous pain (63% vs 26%; P = .01; paired t test). DREZotomy was highly effective for paroxysmal pain but moderately effective for continuous pain.*

signs. The infection was cured after removal of the EMCS device and bone flap and antibiotic therapy. At operation, the infection was limited to the subgaleal space and did not extend to epidural or subdural space. No electrode dislocation, cerebrospinal fluid leak, new neurological deficit, or any other complications were recorded in our patients. One patient died 3 years after implantation of a cause unrelated to the surgical procedure (intracerebral hemorrhage).

DREZotomy

Two patients had postoperative neurological complications (18%). Patient 6 had paresthesia and mild weakness of the ipsilateral leg along with diminished pain sensation in the left hemibody. Both sensory disturbances and weakness improved on further follow-up. Patient 7 showed postoperative diminished sensations in the right hemibody, which improved on later follow-up.

DISCUSSION

DREZotomy has been reported to be more effective for paroxysmal than continuous BPA pain.[2] Conversely, there is no report describing a differential effect of EMCS on these 2 types of BPA pain.[12-16] The main finding of this study is that EMCS also had a differential effect. We found that EMCS was ineffective for paroxysmal pain but moderately effective for continuous pain. We also found that DREZotomy was effective for both types of pain but was more effective for paroxysmal pain. With EMCS, 3 of 7 patients with continuous pain (42%) had a long-term favorable outcome, whereas no patients reported improvement of paroxysmal pain. With DREZotomy, 7 of 10 patients with paroxysmal pain (70%) had a long-term favorable outcome compared with 2 of 10 patients (20%) with continuous pain.

Our finding that DREZotomy was more effective for paroxysmal pain than continuous pain is consistent with a previous report.[2] To the best of our knowledge, this is the first study to show that EMCS is effective only for continuous BPA pain.[12-16] Before our investigation, only 10 patients have been reported in the literature to receive EMCS for BPA pain. The overall success rate of EMCS for BPA pain in our study was 42% (3 of 7 patients), which is comparable to the 50% (5 of 10 patients) reported in these previous studies.[12,13,15,16] However, each of these studies evaluated only a single global rating for BPA pain and did not distinguish between continuous and paroxysmal pain.[12-16] Increasingly, the distinction between different patterns of neuropathic pain is thought to be important to better understand the underlying mechanisms for each pattern of pain and to study the differential effects of treatment.[17]

From a practical point of view, the differential effect of DREZotomy and EMCS on the 2 types of BPA pain may be helpful in setting the indication for treatment. The efficacy of DREZotomy for both types of BPA pain makes it the procedure of first choice. On the other hand, EMCS was moderately effective only for continuous pain; therefore, EMCS may be most appropriate for isolated continuous pain or residual continuous pain after DREZotomy. For isolated continuous pain, we had a 50% success rate (1 of 2 patients) after EMCS in our series, which is identical to the 50% success rate (5 of 10 patients) after DREZotomy in the previous report.[2] For residual pain after DREZotomy, EMCS represents one of the few viable therapeutic options.[2,18] Spinal cord stimulation is another option but is associated, in our experience and in that of others, with inconsistent results.[18,19] In our study, some patients preferred EMCS over DREZotomy as a primary option because they wished to avoid the surgical risks associated with DREZotomy such as leg weakness and sensory dysfunction.[7,8] This reflects the most attractive aspects of EMCS, which are its reversible and less invasive nature. Overall, the evidence regarding EMCS for BPA pain is still very limited, long-term follow-up is unavailable, and the cost of treatment is high.

The mechanism by which BPA pain is generated is still not completely understood.[8] Both animal and human studies suggested that neuronal hyperactivity from deafferented dorsal horn neurons is the main generator of BPA pain.[3,20,21] However, neuronal hyperactivity has been also detected in thalamic nuclei, suggesting that supraspinal mechanisms contribute to pain generation.[4] Sindou et al[2] first reported that DREZotomy was more effective for paroxysmal than continuous pain. A possible explanation of this differential effect is that paroxysmal pain originates from hyperactive neurons in the dorsal horn, whereas continuous pain originates from supraspinal structures, particularly the thalamus.[2,3,20,21] Knowing that EMCS is able to modulate the activity of supraspinal structures, particularly the sensory thalamus and cingulate gyrus, may explain its efficacy for continuous pain.[22,23] The failure of EMCS to relieve paroxysmal pain is more difficult to explain. It was reported that EMCS exerts a descending inhibitory effect on the dorsal horn neuronal activity[24]; however, that effect may be interrupted as a result of deafferentiation.[25] It seems that each procedure acted through

Copyright © Congress of Neurological Surgeons. Unauthorized reproduction of this article is prohibited.

a distinct mechanism related to a particular type of pain: DREZotomy eliminated hyperactive neurons responsible for paroxysmal pain, whereas EMCS modulated the activity of supraspinal structures responsible for continuous pain.

Limitations

The main limitations of this study are the small sample size, particularly for subgroup analysis and retrospective design. Although the number of patients is small, it represents the largest population of patients receiving EMCS for BPA in a single center. However, our results are preliminary and should be reproduced in a larger patient population.

In 4 patients who underwent both EMCS and DREZotomy procedures, a residual effect after the first surgery, a "carryover" effect, may be argued. However, such a carryover effect is unlikely to occur after EMCS because its effects are reversible on discontinuation of treatment. Moreover, the negligible pain relief effects of the first procedure (either DREZotomy or EMCS) in those patients (Table 2) argue against such a carryover effect. However, because DREZotomy causes irreversible changes in dorsal horn, a residual effect after DREZotomy cannot be completely ruled out and remains a limitation of the present study.

Despite these limitations, our findings are of interest as the only study to describe a differential effect of EMCS on BPA pain and suggest that treatment and study of BPA pain in the future should carefully distinguish between continuous and paroxysmal pain.

CONCLUSION

We analyzed the differential effect of EMCS and DREZotomy for different types of BPA pain. EMCS was ineffective for paroxysmal pain but moderately effective for continuous pain. DREZotomy was highly effective for paroxysmal pain but moderately effective for continuous pain. It may be prudent to use EMCS for patients who continue to have intractable pain after DREZotomy.

Disclosures

The authors have no personal financial or institutional interest in any of the drugs, materials, or devices described in this article.

REFERENCES

1. Parry CB. Pain in avulsion lesions of the brachial plexus. *Pain*. 1980;9(1):41-53.
2. Sindou MP, Blondet E, Emery E, Mertens P. Microsurgical lesioning in the dorsal root entry zone for pain due to brachial plexus avulsion: a prospective series of 55 patients. *J Neurosurg*. 2005;102(6):1018-1028.
3. Guenot M, Bullier J, Sindou M. Clinical and electrophysiological expression of deafferentation pain alleviated by dorsal root entry zone lesions in rats. *J Neurosurg*. 2002;97(6):1402-1409.
4. Rinaldi PC, Young RF, Albe–Fessard D, Chodakiewitz J. Spontaneous neuronal hyperactivity in the medial and intralaminar thalamic nuclei of patients with deafferentation pain. *J Neurosurg*. 1991;74(3):415-421.
5. Sindou M, Fischer G, Goutelle A, Mansuy L. Selective surgery of posterior nerve roots: first results of surgery for pain [in French]. *Neurochirurgie*. 1974;20(5):391-408.
6. Nashold BS Jr, Ostdahl RH. Dorsal root entry zone lesions for pain relief. *J Neurosurg*. 1979;51(1):59-69.
7. Cetas JS, Saedi T, Burchiel Kim J. Destructive procedures for the treatment of nonmalignant pain: a structured literature review. *J Neurosurg*. 2008;109 (3):389-404.
8. Samii M, Bear-Henney S, Ludemann W, Tatagiba M, Blomer U. Treatment of refractory pain after brachial plexus avulsion with dorsal root entry zone lesions. *Neurosurgery*. 2001;48(6):1269-1277.
9. Saitoh Y, Yoshimine T. Stimulation of primary motor cortex for intractable deafferentation pain. *Acta Neurochir Suppl (Wien)*. 2007;9(2):751-756.
10. Fontaine D, Hamani C, Lozano A. Efficacy and safety of motor cortex stimulation for chronic neuropathic pain: critical review of the literature. *J Neurosurg*. 2009;110(2):251-256.
11. Cruccu G, Aziz TZ, Garcia-Larrea L, et al. EFNS guidelines on neurostimulation therapy for neuropathic pain. *Eur J Neurol*. 2007;14(9):952-970.
12. Delavallée M, Abu-Serieh B, de Tourchaninoff M, Raftopoulos C. Subdural motor cortex stimulation for central and peripheral neuropathic pain: a long-term follow-up study in a series of eight patients. *Neurosurgery*. 2008;63(1):101-108.
13. Lefaucheur JP, Drouot X, Cunin P, et al. Motor cortex stimulation for the treatment of refractory peripheral neuropathic pain. *Brain*. 2009;132(pt 6):1463-1471.
14. Hosomi K, Saitoh Y, Kishima H, et al. Electrical stimulation of primary motor cortex within the central sulcus for intractable neuropathic pain. *Clin Neurophysiol*. 2008;119(5):993-1001.
15. Nuti C, Peyron R, Garcia-Larrea L, et al. Motor cortex stimulation for neuropathic pain: four year outcome and predictors of efficacy. *Pain*. 2005;118(1-2):43-52.
16. Pirotte B, Voordecker P, Joffroy F, et al. The Zeiss-MKM system for frameless image-guided approach in epidural motor cortex stimulation for central neuropathic pain. *Neurosurg Focus*. 2001;11(3):E3.
17. Bouhassira D, Attal N, Fermanian J, et al. Development and validation of the neuropathic pain symptom inventory. *Pain*. 2004;108(3):248-257.
18. Lai HY, Lee CY, Lee ST. High cervical spinal cord stimulation after failed dorsal root entry zone surgery for brachial plexus avulsion pain. *Surg Neurol*. 2009;72(3)286-289.
19. Garcia-March G, Sanchez-Ledesma MJ, Diaz P, et al. Dorsal root entry lesion versus cord stimulation in the management of pain from brachial plexus avulsion. *Act Neurochir Suppl (Wien)*. 1987;39:155-158.
20. Loeser JD, Ward AA, White LE. Chronic deafferentation of human spinal cord neurons. *J Neurosurg*. 1968;29(1):48-50.
21. Guenot M, Bullier J, Rospars JP, Lansky P, Mertens P, Sindou M. Single-unit analysis of the spinal dorsal horn in patients with neuropathic pain. *Clin Neurophysiol*. 2003;20(2):143-150.
22. Kishima H, Saitoh Y, Osaki Y, et al. Motor cortex stimulation in patients with deafferentation pain: activation of the posterior insula and thalamus. *J Neurosurg*. 2007;107(1):43-48.
23. Garcia-Larrea L, Peyron R, Mertens P, et al. Electrical stimulation of motor cortex for pain control: a combined PET-scan and electrophysiological study. *Pain*. 1999;83(2):259-273.
24. Senapati AK, Huntington PJ, Peng YB. Spinal dorsal horn neuron response to mechanical stimuli is decreased by electrical stimulation of the primary motor cortex. *Brain Res*. 2005;1036(1-2):173-179.
25. Velasco F, Carrillo-Ruiz JD, Castro G, et al. Motor cortex electrical stimulation applied to patients with complex regional pain syndrome. *Pain*. 2009;147(1-3):91-98.

Acknowledgment

This work was supported by grants from the Ministry of Health, Labor and Welfare of Japan.

COMMENT

Brachial plexus injuries are classically considered a homogeneous traumatic entity, and consecutive pain is thought to be a clinical replica of experimental peripheral deafferentation. In fact, the so-called brachial plexus avulsion (BPA) syndrome has some heterogeneous aspects.

BPA is followed by chronic pain in the deafferented area in 60% of the cases on average (30% to 90% according to the published series). Incidence is quite different in relation to location of the disruptive lesion:

Copyright © Congress of Neurological Surgeons. Unauthorized reproduction of this article is prohibited.

< 33% for postganglionic location, ie, distal to the dorsal root ganglion, as opposed to 90% for predominantly preganglionic locations.[1-4]

Classically, pain after BPA appears in a standard clinical manner: a continuous background of pain described as burning, throbbing, and/or aching sensations or pain with electric shooting–like violent paroxysms. These 2 components may coexist with equal intensity; 1 type may predominate over the other; or, rarely, 1 of the 2 may exist in isolation.

In a previous article devoted to outcome after dorsal root entry zone microsurgical lesioning (DREZotomy) for pain resulting from BPA,[5] we suggested that the 2 distinct types of pain be considered the clinical expression of 2 different mechanisms. There are strong arguments that paroxysmal pain arises from deafferented hyperactive neurons in the dorsal horn.[6–10] Continuous pain might rather be in relation to supraspinal generators, particularly at the thalamus, as the consequence of destruction of the neurons at origin of the ascending spinoreticulothalamic pathways.[11]

So, as pointed out by the Japanese team, to study independently the effects of surgery on the 2 components of pain is wise and of practical importance. We have shown that microsurgical DREZotomy, although effective on both components, had better effectiveness on the paroxysmal component. Pain relief was obtained, in all the patients with paroxysms only, in 75% of the patients suffering from both pain components and in 50 % of the patients who had continuous background only (P = .04).[5]

Like us, the authors of the present article found a differential effect by the DREZ procedure: 70% of the patients with paroxysmal pain had favorable outcomes compared with 20% with continuous pain. In addition, they carried out motor cortex stimulation and compared the results; 42% with continuous pain had favorable outcomes compared with no patients with paroxysmal pain. Our experience with motor cortex stimulation for pain after BPA is quite similar.

Because the pain after BPA is almost constantly unbearable and is resistant to all classes of analgesic agents (including opioids), anticonvulsants, and antidepressants, neurosurgery is the only recourse. When patients are referred to the neurosurgeon, the majority have already undergone attempts to nerve repair. According to literature and our experience, spinal cord stimulation is not particularly effective, especially when preganglionic lesions predominate. The reason is that most of the fibers targeted by stimulation underwent degeneration up to the brainstem. Lack of corresponding valid fibers in the dorsal column can be ascertained by somatosensory evoked potentials. It has been shown that impairment in central conduction time, ie, between dorsal root ganglion cells and brain: N13 to N20 for upper limb and N22 to P39 for lower limb, is a valuable predictor of failure of SCS.[12] Thalamic deep brain stimulation, although quite logical from an anatomical/physiological point of view, has not been confirmed as effective on pain after BPA. As proposed by the Japanese authors, DREZotomy has to be considered the first option, at least when paroxysmal pain predominates; motor cortex stimulation[13] may be proposed when the continuous pain component persists after completion of DREZ-lesioning surgery.

The authors have to be acknowledged for adding useful insights to pain surgery. This article shows how surgery for neuropathic pain can be effective if the neurosurgical method precisely targets the appropriate anatomical site(s) and accurately corrects the various pathophysiological mechanisms (and therefore components) of the pain.

Marc Sindou
Lyon, France

1. Narakas A. Les syndromes douloureux dans les arrachements du plexus brachial. *Douleur et Analgésie*. 1992;3:83-101.
2. Narakas A. Surgical treatment of traction injuries of the brachial plexus. *Clin Orthop Relat Res*. 1978;133:71-90.
3. Parry CB. Pain in avulsion lesions of the brachial plexus. *Pain*. 1980;9(1):41-53.
4. Parry CB. Pain in avulsion of the brachial plexus. *Neurosurgery*. 1984;15(6):960-965.
5. Sindou M, Blondet E, Emery E, Mertens P. Microsurgical lesioning in the dorsal root entry zone for pain due to brachial plexus avulsion: a prospective series of 55 patients. J Neurosurg. 2005;102(6):1018-1028.
6. Guenot M, Bullier J, Rospars JP, Lansky P, Mertens P, Sindou M.Single-unit analysis of the spinal dorsal horn in patients with neuropathic pain. *J Clin Neurophysiol*. 2003;20:134-150.
7. Guenot M, Bullier J, Sindou M. Clinical and electrophysiological expression of deafferentation pain alleviated by dorsal root entry zone lesions in rats. J Neurosurg. 2002;97(6):1402-1409.
8. Jeanmonod D, Sindou M, Magnin M, Boudet M. Intra-operative unit recordings in the human dorsal horn with a simplified floating microelectrode. *Electroencephalogr Clin Neurophysiol*. 1989;72(5):450-454.
9. Loeser JD, Ward AA Jr, White LE Jr. Chronic deafferentation of human spinal cord neurons. *J Neurosurg*. 1968;29:48-50.
10. Ovelmen-Levitt J. Abnormal physiology of the dorsal horn as related to the deafferentation syndrome. *Appl Neurophysiol*. 1988;51(2-5):104-116.
11. Lombard MC, Larabi Y. Electrophysiological study of cervical dorsal horn cells in partially deafferented rats. In: Bonica JJ, Lindblom U, Iggo A, eds. *Advances in Pain Research and Therapy. Proceedings of the Third world Congress on Pain*. New York, NJ: Raven Press, 1983;5:147-153.
12. Sindou M, Mertens P, Bendavid U, Garcia-Larrea L, Maugiere F. Predictive value of somatosensory evoked potentials for long-lasting pain relief after spinal cord stimulation: practical use for patient selection. *Neurosurgery*. 2003;52(6):1374-1384.
13. Tsubokawa T, Katayama Y, Yamamoto T, Hirayama T, Koyama S. Chronic motor cortex simulation for the treatment of central pain. *Acta Neurochir Suppl*. 1991;52:137-139.

Copyright © Congress of Neurological Surgeons. Unauthorized reproduction of this article is prohibited.

Surgical Mortality at 30 Days and Complications Leading to Recraniotomy in 2630 Consecutive Craniotomies for Intracranial Tumors

Benjamin Lassen, MD*
Eirik Helseth, MD, PhD*‡
Pål Rønning, MD‡
David Scheie, MD§
Tom Børge Johannesen, MD, PhD¶
Jan Mæhlen, MD, PhD#
Iver A. Langmoen, MD, PhD*‡
Torstein R. Meling, MD, Dr Phil‖

*Faculty of Medicine, University of Oslo, Oslo, Norway; ‡Department of Neurosurgery, Oslo University Hospital, Ullevål, Oslo, Norway; §Department of Pathology, Oslo University Hospital, Rikshospitalet, Oslo, Norway; ¶The Norwegian Cancer Registry, Oslo, Norway; #Department of Pathology, Oslo University Hospital, Ullevål, Oslo, Norway; ‖Department of Neurosurgery, Oslo University Hospital, Rikshospitalet, Oslo, Norway

Correspondence:
Torstein R. Meling, MD, Dr Phil,
Senior Consultant,
Department of Neurosurgery,
Oslo University Hospital,
Rikshospitalet,
N-0027 Oslo, Norway.
E-mail: torstein.meling@rikshospitalet.no

Received, January 17, 2010.
Accepted, September 10, 2010.

Copyright © 2011 by the
Congress of Neurological Surgeons

BACKGROUND: In order to weigh the risks of surgery against the presumed advantages, it is important to have specific knowledge about complication rates.

OBJECTIVE: To study the surgical mortality and rate of reoperations for hematomas and infections after intracranial surgery for brain tumors in a large, contemporary, single-institution consecutive series.

METHODS: All adult patients from a well-defined population of 2.7 million inhabitants who underwent craniotomies for intracranial tumors at Oslo University Hospital from 2003 to 2008 were included (n = 2630). The patients were identified from our prospectively collected database and their charts studied retrospectively. Follow-up was 100%.

RESULTS: The overall surgical mortality, defined as death within 30 days of surgery, was 2.3% (n = 60). The mortality rates for high- and low-grade gliomas, meningiomas, and metastases were 2.9%, 1.0%, 0.9%, and 4.5%, respectively. Age >60 (odds ratio 1.84, $P < 0.05$) and biopsy compared with resection (odds ratio 4.67, $P < 0.01$) were significantly positively associated with increased surgical mortality. Hematomas accounted for 35% of the surgical mortality. Postoperative hematomas needing evacuation occurred in 2.1% (n = 54). Age >60 was significantly correlated to increased risk of postoperative hematomas (odds ratio 2.43, $P < 0.001$). A total of 39 patients (1.5%) were reoperated for postoperative infection. Meningiomas had an increased risk of infections compared with high-grade gliomas (odds ratio 4.61, $P < 0.001$).

CONCLUSION: The surgical mortality within 30 days of surgery was 2.3%, with age >60 and biopsy vs resection being the 2 factors significantly associated with increased mortality. Postoperative hematomas caused about one third of the surgical mortality.

KEY WORDS: Complications, Craniotomy, Intracranial tumor, Postoperative hematoma, Postoperative infection, Surgical mortality, Survival

Neurosurgery 68:1259–1269, 2011 DOI: 10.1227/NEU.0b013e31820c0441 www.neurosurgery-online.com

According to The Central Brain Tumor Registry of the United States, the incidence rate of all primary brain and central nervous system tumors is 16.5 cases per 100 000 person-years (9.2 per 100 000 person-years for nonmalignant tumors and 7.3 per 100 000 person-years for malignant tumors).[1] The prevalence rate for all primary brain and central nervous system tumors was estimated to be 130.8 per 100 000 inhabitants.[1] Metastatic brain tumors are thought to have a higher incidence than primary brain tumors.[2]

ABBREVIATIONS: ABP, antibiotic prophylaxis; **cSDH**, chronic subdural hematomas; **HGG**, high-grade gliomas; **LGG**, low-grade gliomas

The cornerstone of brain tumor treatment is surgery. The objective of surgery is to remove as much tumor as possible, as well as to establish an exact tissue diagnosis. The possible benefits of tumor removal include symptom relief, improved quality of life, smaller tumor burden for other treatment modalities, and improved survival.[3-9]

However, craniotomies are not without inherent risks, be it surgical mortality,[10,11] postoperative hematomas,[12,13] or infection.[14] With

Copyright © Congress of Neurological Surgeons. Unauthorized reproduction of this article is prohibited.

respect to surgical mortality, the reported series are often of limited size[15] and based on a selected patient group.[16] Furthermore, to ascertain surgical deaths, either death before discharge (in-hospital mortality) or within 30 days of surgery is used, with the former missing more than 25% of surgery-related deaths and creating potential for bias across institutions (J. D. Birkmeyer, personal communication, September 21, 1999). With respect to intracranial hematomas, the consequences are often devastating, with a mortality rate of 30% and a significant morbidity rate.[17] With respect to infections after neurosurgical procedures, these often present as meningitis, subdural empyema, or cerebral abscess. Although meningitis can often be treated with intravenous antibiotics, cases that involve a bone flap infection, subdural empyema, or cerebral abscess usually require a repeated operation.

In order to weigh the risks of surgery against the presumed advantages, it is important to have specific knowledge about the institution's complication rate. We therefore wanted to determine the 30-day surgical mortality rate as well as the rate of postcraniotomy hematomas and infections that required reoperation, reviewing our prospectively collected database of 2630 craniotomies for tumors performed between 2003 and 2008.

MATERIALS AND METHODS

Patients

The defined neurosurgical catchment area for Oslo University Hospital is the south and eastern health region of Norway. It has 2.7 million inhabitants (56% of the Norwegian population) and Oslo University Hospital treats approximately 99% of the neurosurgical tumor patients within this region (The Norwegian Cancer Registry, unpublished data). All patients ≥18 years who underwent craniotomy for an intracranial tumor at the 2 departments of Oslo University Hospital (Rikshospitalet and Ullevål) from 2003 to 2008 were included in this study. Thus, this study can also serve as a population study in terms of incidence of craniotomies for particular tumor types in Norway. Patients who underwent stereotactic biopsy were not included.

The patients were identified from our prospectively collected database and their charts were studied retrospectively. The following data were recorded: sex, age, biopsy or resection, primary or secondary (repeated) surgery, histology, reoperation for postoperative hematoma, and reoperation for deep postoperative infection (infected bone flap, epidural abscess, subdural empyema, or intracerebral abscess). Superficial wound infections that required simple wound revision were not included. Surgical mortality was defined as death within 30 days of surgery. Vital status (dead or alive) and time of death was obtained from the Norwegian Population Registry (Folkeregisteret) on February 28, 2009.

The charts of the patients who died within 30 days, or who were reoperated for hematoma or infection, were studied more thoroughly. The cause of death for those who died within 30 days was recorded as directly surgery-related, ie, hemorrhage or postoperative edema with subsequent herniation, or not surgery-related, ie, either tumor progression-related, systemic complications, or other causes. The time from initial surgery to reoperation for hematoma or infection was recorded. The long-term outcome for those reoperated for hematoma or infection was determined, based on preoperative status, postoperative recovery, both after the original craniotomy and reoperation, and status at follow-up contacts with the hospital. Patients' conditions at follow-up were compared with patients' expected disabilities had they not experienced such complications, thus giving an estimate of additional disability likely caused by the hematoma or infection. The following scale was used: no additional disability, minor additional disability, major additional disability, and death.

The major histological groups were used (Table 1), with low-frequency tumor types grouped as others. The gliomas were divided into 2 groups: high-grade gliomas (HGG), and low-grade gliomas (LGG). The HGG group included glioblastoma multiforme (World Health Organization [WHO] grade IV), primitive neuroectodermal tumor (WHO grade IV), anaplastic astrocytoma, anaplastic oligoastrocytoma, anaplastic oligodendroglioma, and anaplastic ependymoma (all WHO grade III). The LGG group included all other astrocytic, oligodendroglial, and ependymal tumors (WHO grade I and II), and also ganglioglioma (WHO grade I), dysembryoplastic neurepithelial tumor (DNET) (WHO grade I), and choroid plexus tumors (WHO grade I and II).

TABLE 1. Patient Characteristics[a]

	N	%
Patients	2630	100
Department		
Rikshospitalet	1693	64.4
Ullevål	937	35.6
Sex		
Male	1275	48.5
Female	1355	51.5
Age, y		
18-29.9	141	5.4
30-39.9	300	11.4
40-49.9	437	16.6
50-59.9	604	23.0
60-69.9	649	24.7
70-79.9	411	15.6
>80	88	3.3
Type of surgery		
Primary	2141	81.4
Second	489	18.6
Craniotomy		
Resection	2556	97.2
Open biopsy	74	2.8
Main histology		
(HGG)	890	31.6
Meningioma	693	26.3
Metastases	449	17.1
(LGG)	289	11.0
Schwannoma	73	2.8
Primary CNS lymphoma	51	1.9
CNS hemangioblastoma	39	1.5
Cavernous hemangioma	38	1.4
Pituitary adenoma	8	0.3
Others	160	6.1

[a]CNS, central nervous system; HGG, high-grade glioma; LGG, low-grade glioma.

Copyright © Congress of Neurological Surgeons. Unauthorized reproduction of this article is prohibited.

TABLE 2. Patients Who Died Within 30 Days of Tumor Surgery (Surgical Mortality Cases) (n = 60)[a]

Age, y	Sex	Histology	Operation Type[b]	Time[c]	Comments
43	M	Hemangioblastoma	R	3	Postop. hematoma
29	F	HGG	R	17	Tumor progression
41	M	HGG	R	13	Postop. brain edema/herniation
41	F	HGG	R	3	Postop. hematoma
48	M	HGG	B	10	Pneumonia
49	F	HGG	R	11	Tumor progression
54	F	HGG	R	2	Tumor progression
56	F	HGG	B	8	Postop. hematoma
60	M	HGG	R	30	Postop. hematoma
64	M	HGG	R	17	Tumor progression
64	F	HGG	R	4	Postop. brain edema/herniation
65	F	HGG	R	22	Postop. hematoma
66	F	HGG	R	24	Tumor progression
67	F	HGG	R	5	Tumor progression
67	M	HGG	R	19	Tumor progression
69	M	HGG	B	29	Tumor progression
74	F	HGG	R	30	Tumor progression
75	M	HGG	R	11	Postop. hematoma
75	M	HGG	R	22	Tumor progression
76	M	HGG	R	15	Postop. hematoma
76	F	HGG	R	4	Postop. hematoma
77	F	HGG	R	8	Postop. hematoma
81	F	HGG	B	28	Tumor progression
82	M	HGG	R	21	Pulmonary embolism
84	F	HGG	R	14	Postop. brain edema/herniation
32	F	LGG	R	17	Shunt failure
48	M	LGG	R	18	Pneumonia
68	M	LGG	R	24	Postop. hematoma
62	M	Lymphoma	B	12	Tumor progression
75	F	Lymphoma	B	13	Tumor progression
78	M	Lymphoma	B	26	Tumor progression
31	F	Melanocytoma	R	11	Tumor progression
55	F	Meningioma	R	6	Postop. brain edema/herniation
73	M	Meningioma	R	11	Postop. hematoma
77	M	Meningioma	R	4	Postop. hematoma
79	F	Meningioma	R	12	Postop. hematoma
83	M	Meningioma	R	15	Pneumonia
83	M	Meningioma	R	29	Cardiac arrest
35	M	Metastasis	R	12	Tumor progression
40	M	Metastasis	R	27	Pneumonia
45	F	Metastasis	R	4	Postop. hematoma
46	F	Metastasis	R	9	Hydrocephalus
49	F	Metastasis	R	25	Postop. hematoma
49	F	Metastasis	R	26	Postop. hematoma
52	M	Metastasis	R	6	Postop. hematoma
53	F	Metastasis	R	5	Tumor progression
56	M	Metastasis	R	3	Cardiac arrest
60	M	Metastasis	R	1	Postop. hematoma
61	M	Metastasis	R	30	Postop. hematoma
61	F	Metastasis	R	12	Pneumonia
62	M	Metastasis	R	19	Tumor progression
62	M	Metastasis	R	29	Postop. hematoma
65	F	Metastasis	R	22	Sepsis
71	F	Metastasis	R	25	Tumor progression
73	M	Metastasis	R	24	Sepsis
77	F	Metastasis	R	19	Tumor progression
78	M	Metastasis	R	29	Subdural empyema
81	F	Metastasis	R	25	Tumor progression
48	M	Pituitary adenoma	R	16	Cerebral infarction
69	M	Pituitary adenoma	R	9	Postop. hematoma

[a]M, male; F, female; HGG = high-grade glioma; LGG, low-grade glioma; postop, postoperative.
[b]Operation type is resection (R) or biopsy (B).
[c]Time is the time to death in days after primary surgery.

Perioperative Routines

A consultant anesthetist sees patients preoperatively. Elderly patients (>70 y) and patients on multiple medications are routinely also seen by a consultant internist to optimize the general medical condition and medications. Patients with a known heart condition are referred to a cardiologist for cardiac ultrasound and electrocardiogram stress test. Patients with a past hematological history are referred to a consultant hematologist. Aspirin is stopped at least 10 days before surgery and, when on anticoagulation, the international normalized ratio should be below 1.5. All patients receive compressive stockings the day before surgery and keep them until fully mobilized. At initiation of surgery, a second-generation cephalosporin is administered intravenously and continued every 90 minutes until the case is completed or the maximum daily dose of 8 g is reached. For long cases, erythromycin or a third-generation cephalosporin is started after the maximum daily dose of a second-generation cephalosporin is reached and continued until completion of the case. Postoperatively, the patients are observed in recovery for 3 to 6 hours, where after they are transferred to a level 2 bed. After a craniotomy for a supratentorial tumor, the patients are generally observed for 24 hours. For infratentorial tumors, the length of observation is a minimum of 48 hours. Low-molecular-weight heparin is given the first postoperative day. The patients are mobilized either in the afternoon on the day of surgery or on the first postoperative day.

Ethics

The hospital's Data Protection Officials approved the study.

Statistics

Uni- and multivariate logistic regression was used to determine the impact of the different independent variables on 30-day mortality, postoperative hematoma, and postoperative infection. The independent

Copyright © Congress of Neurological Surgeons. Unauthorized reproduction of this article is prohibited.

variables were binary, with the exception of histology, where high-grade glioma was used as the reference category against which all other histology classes were compared. The fit of the multivariate models was investigated and reported using Pseudo-R2 and the Hosmer-Lemeshow goodness-of-fit test. *P* values less than .05 were considered significant. Stata v10.1 (Stata Corp, Austin, TX) was used for all statistical analyses.

RESULTS

Patient Population

A total of 2630 consecutive craniotomies at the Oslo University Hospital from 2003 to 2008 were included in this study (Table 1). The mean age at surgery was 56 years (range, 18-89 years), with a male-to-female ratio of 1:1.06. Follow-up was 100%.

Incidence of Craniotomies

First-time craniotomies with primary resection were performed in 2073 cases, 483 cases were reoperations with repeated resection, and 74 cases were open biopsies. Thus, the incidence of first-time craniotomy for a brain tumor was 12.8/100 000 inhabitants per year and for a repeat resection 3.0/100 000 inhabitants per year.

Surgical Mortality

The surgical mortality, defined as death within 30 days of surgery, was 2.3% (n = 60). The cause of death was postoperative hematomas in 21 cases (35.0 %), tumor progression in 21 (35.0%), infectious diseases in 8 cases (13.3%), postoperative edema and subsequent herniation in 4 cases (6.7%), and other causes in 6 cases (10%) (Table 2). The surgical mortality rate for HGG, LGG, meningiomas, and metastases was 2.9% (n = 24), 1.0% (n = 3), 0.9% (n = 6), and 4.5% (n = 20), respectively.

Using multivariate Cox regression analyses, age $>$ 60 (odds ratio [OR] 1.84, 95%CI [1.05, 3.22], $P < .05$) and biopsy compared with resection (OR 4.67, 95% CI [1.80, 12.14], $P < .01$) were shown to be significantly associated with increased surgical mortality (Table 3). Compared with HGG, metastases were associated with a higher mortality in the univariate analysis ($P < .01$), but this did not reach significance in the multivariate analysis. Compared with HGG, meningiomas were associated with a lower surgical mortality ($P < .05$).

Postoperative Hematomas Requiring Recraniotomy

The total occurrence of surgically evacuated postoperative hematomas was 2.1% (n = 54) (Table 4). Of the 54 evacuated hematomas, 23 (42.6%) were intracerebral, 13 (24.1%) were acute epidural, 2 (3.7%) were acute subdural, 4 (7.4%) were intracerebellar, 1 (1.9%) was in the brainstem, 8 (14.8%) were chronic subdural hematomas (cSDH), and 3 (5.6%) were subcutaneous (Table 4).

Risk Factors for Reoperation for Postoperative Hematomas

Using multivariate Cox regression analyses, age $>$60 was shown to be significantly associated with increased risk of developing postoperative hematoma (OR 2.43 95% CI [1.35,4.39], $P < .001$) (Table 3). Neither sex, resection vs biopsy, primary vs secondary craniotomy, nor tumor type were significantly associated with risk of developing postoperative hematoma. The occurrence of postoperative hematoma was: HGG 2.0% (n = 17), LGG 0.7% (n = 2), meningiomas 2.3% (n = 16), and metastases 2.2% (n = 10).

Time to Reoperation for Postoperative Hematomas

The surgically evacuated hematomas were reoperated within 6 hours in 11 cases (20.4%), within 12 hours in 14 cases (25.9%), within 24 hours in 21 cases (38.9%), within 48 hours in 35 cases (64.8%), and within 72 hours in 40 cases (74.1%) (Table 4). Four patients were operated on between day 3 and day 7 after surgery, 3 patients were operated on between day 7 and day 30, and 7 patients after 30 days of surgery. All 7 patients in the latter group had cSDHs. Excluding the cSDHs, the median time from tumor surgery to reoperation for hematoma was 1 day (mean, 2.2 days; range, 0-26).

Consequences of Postoperative Hematoma

Twenty patients (37.0%) had no additional disability, 16 (29.6%) had minor additional disability, 4 (7.4%) had major additional disability, and 12 (22.2%) died of their hematoma. Long-term data are inconclusive for 2 patients (3.7%). Six of 23 (26.1%) patients with intracerebral hematomas died, whereas 2 of 13 (15.4%) patients with epidural hematomas died ($P > .05$) (Table 4).

Postoperative Infection Requiring Recraniotomy

A total of 39 patients (1.5%) were reoperated for deep postoperative infection (Table 5). Of these infections, 23 (59.0%) were extradural, 6 (15.4%) were intradural, and 10 (25.6%) were both intra- and extradural.

Risk Factors of Reoperation for Postoperative Infection

Multivariate Cox regression analysis demonstrated that meningiomas had an increased risk of infection compared with gliomas (OR 5.88, 95%CI [2.47,13.87], $P < .001$) (Table 3). Men also had an increased risk of infections ($P < .01$). Neither resection vs biopsy, nor primary vs secondary craniotomy were significantly associated with risk of developing postoperative deep infection. The postoperative infection rate was 1.0% (n = 8) for HGG, 0.0% (n = 0) for LGG, 3.2% (n = 22) for meningiomas, and 1.1% (n = 5) for metastases.

Time to Reoperation for Postoperative Infection

The median time from tumor surgery to reoperation for infection was 42 days (mean, 95.7 days; range, 16-667 days). The number of patients who were reoperated within 1, 2, 3, 6, and 12 months, were 11 (28.2%), 27 (69.2%), 29 (74.4%), 32 (82.1%), and 37 (94.9%), respectively.

Consequences of Postoperative Infection

Of the 39 patients with deep infection, 29 (74.4%) had no additional disability, 5 (12.8%) had minor additional disability, 3 (7.7%) had major additional disability, and 2 (5.1%) died because of the infection (Table 4).

Copyright © Congress of Neurological Surgeons. Unauthorized reproduction of this article is prohibited.

TABLE 3. Univariate and Multivariate Analysis of Factors Possibly Associated With Surgical Mortality, Surgery for Postoperative Infection, and Surgery for Postoperative Hematoma[a]

	30-Day Mortality		Infection		Postoperative Hematoma	
	Univariate Odds Ratio [95% CI]	Multivariate Odds Ratio [95% CI]	Univariate Odds Ratio [95% CI]	Multivariate Odds Ratio [95% CI]	Univariate Odds Ratio [95% CI]	Multivariate Odds Ratio [95% CI]
Age >60 (No/Yes)	2.27[c] [1.34,3.86]	1.84[d] [1.05,3.22]	1.11 [0.59,2.09]	0.97 [0.50,1.86]	2.42[c] [1.38,4.26]	2.43[c] [1.35,4.39]
Sex (Male/Female)	0.94 [0.56,1.57]	1.09 [0.64,1.84]	0.47[d] [0.24,0.91]	0.33[c] [0.16,0.66]	0.94 [0.55,1.61]	0.94 [0.54,1.64]
Primary Op (Primary/secondary)	0.77 [0.38,1.57]	1.01 [0.48,2.13]	1.74 [0.86,3.51]	2.01 [0.97,4.17]	0.99 [0.50,1.99]	1.14 [0.56,2.31]
Operation (Resection/Biopsy)	4.93[e] [2.16,11.26]	4.67[c] [1.80,12.14]	–[b]	–[b]	–[b]	–[b]
Histology						
HGG	1	1	1	1	1	1
LGG	0.53 [0.16,1.69]	0.44 [0.13,1.53]	–[b]	–[b]	0.38 [0.09,1.58]	0.59 [0.13,2.66]
Meningioma	0.30[c] [0.13,0.71]	0.30[d] [0.12,0.76]	3.70[e] [1.95,7.02]	4.61[e] [1.98,10.73]	1.18 [0.65,2.13]	1.08 [0.53,2.19]
Metastasis	2.50[c] [1.44,4.31]	1.51 [0.81,2.80]	0.71 [0.28,1.83]	1.34 [0.43,4.21]	1.11 [0.55,2.22]	0.95 [0.43,2.10]
Lymphoma	2.77 [0.84,9.14]	0.91 [0.23,3.64]	1.34 [0.18,9.94]	3.43 [0.41,28.80]	–[b]	–[b]
Capillary hemangioblastoma	1.13 [0.15,8.37]	1.01 [0.13,7.72]	–[b]	–[b]	2.64 [0.62,11.24]	2.67 [0.59,12.12]
Schwannoma	0.42 [0.13,1.34]	0.40 [0.12,1.34]	0.43 [0.10,1.79]	0.75 [0.16,3.56]	1.00 [0.42,2.36]	1.21 [0.47,3.15]
Others	0.42 [0.13,1.34]	0.40 [0.12,1.36]	0.92 [0.12,6.80]	1.61 [0.20,13.19]	0.66 [0.09,4.81]	0.76 [0.10,5.84]
Observations		2557		2286		2523
Pseudo-R^2		0.064		0.069		0.025
H-L test		$P = .66$		$P = .85$		$P = .78$

[a]HGG, high-grade glioma; LGG, low-grade glioma; H-L, Hosmer-Lemeshow; CI, confidence interval.
[b]Insufficient events in one of the contrasting categories to calculate odds ratio.
[c]$P = .01$.
[d]$P = .05$.
[e]$P = .001$.

Copyright © Congress of Neurological Surgeons. Unauthorized reproduction of this article is prohibited.

TABLE 4. Patients Reoperated for Postoperative Hematoma (n = 54)[a]

Age, y	Sex	Histology	Location[b]	Time to Reoperation, hh:mm[c]	Outcome[d]	Time to Death, d[e]
63	F	Carcinoma	SC	19:45	NAD	
65	M	Carcinoma	EDH	69:53	Minor	
43	M	Hemangioblastoma	Brainstem	28:35	Death	3
77	M	Hemangioblastoma	Cerebellum	47:04	NAD	
31	M	HGG	ICH	14:15	NAD	
33	M	HGG	cSDH	107 days	NAD	
34	M	HGG	Cerebellum	152:57	Minor	
46	F	HGG	EDH	26:22	NAD	
48	F	HGG	ICH	01:36	Minor	
55	F	HGG	ICH	06:20	Minor	
57	M	HGG	cSDH	43 days	NAD	
58	M	HGG	ICH	44:10	NA	
65	F	HGG	ICH	16:58	Death	22
70	F	HGG	EDH	74:25	NAD	
72	F	HGG	EDH	02:50	Minor	
75	M	HGG	ICH	01:35	Death	11
76	M	HGG	SC	03:15	NAD	
76	F	HGG	ICH	30:38	Minor	
76	F	HGG	ICH	04:12	Death	4
77	F	HGG	EDH	07:57	Death	8
81	M	HGG	EDH	30:17	Minor	
51	M	LGG	EDH	46:06	Minor	
60	F	LGG	ICH	27:35	NAD	
52	M	Melanocytoma	EDH	42:45	NAD	
51	M	Meningioma	EDH	48:50	NAD	
52	F	Meningioma	aSDH	10 days	NAD	
54	F	Meningioma	ICH	93:35	Major	
60	F	Meningioma	ICH	02:20	Minor	
67	F	Meningioma	ICH	14:20	Minor	
69	F	Meningioma	ICH	01:45	NAD	
69	F	Meningioma	cSDH	47 days	NAD	
69	F	Meningioma	ICH	22:00	Minor	
70	M	Meningioma	SC	06:20	NAD	
70	M	Meningioma	cSDH	73 days	NAD	
71	F	Meningioma	Cerebellum	22:20	Major	
75	F	Meningioma	ICH	167:45	NA	
76	M	Meningioma	ICH	03:27	Major	
78	M	Meningioma	ICH	03:40	Minor	
78	F	Meningioma	cSDH	383 days	Death	390
80	F	Meningioma	cSDH	13 days	Minor	
45	F	Metastasis	ICH	45:20	Death	4
49	F	Metastasis	ICH	26 days	Death	26
52	M	Metastasis	EDH	17:41	Death	6
54	M	Metastasis	EDH	53:07	NAD	
61	M	Metastasis	Cerebellum	38:05	Death	30
63	F	Metastasis	ICH	32:40	Minor	
68	M	Metastasis	ICH	03:40	Minor	
72	F	Metastasis	EDH	04:15	NAD	
73	F	Metastasis	cSDH	68 days	NAD	
73	M	Metastasis	ICH	47:17	Death	54
62	M	Pituitary adenoma	ICH	58:10	Major	
69	M	Pituitary adenoma	aSDH	45:15	Death	9
69	M	Pituitary adenoma	cSDH	107 days	Minor	
46	M	Schwannoma	EDH	61:08	NAD	

[a]M, male; F, female; HGG, high-grade glioma; LGG, low-grade glioma.
[b]Location of hematoma: SC, subcutaneous hematoma; EDH, epidural hematoma; aSDH, acute subdural hematoma; cSDH, chronic subdural hematoma; ICH, intracerebral hematoma.
[c]Time = time of reoperation in hours and minutes after primary surgery
[d]Outcome is a hematoma-inflicted disability; NAD, no additional disability; Minor, minor additional disability; Major, major additional disability; NA, no information available.
[e]Time to death is the time from tumor surgery to death, when death is caused by the hematoma.

Copyright © Congress of Neurological Surgeons. Unauthorized reproduction of this article is prohibited.

TABLE 5. Patients Reoperated for Postoperative Infections (n = 39)[a]

Age, y	Sex	Histology	Location[b]	Time to Reoperation, d[c]	Outcome[d]
18	M	HGG	ED	16	NAD
40	M	HGG	ED	46	NAD
57	M	HGG	ED	20	NAD
59	M	HGG	ED	307	NAD
64	M	HGG	ED	49	Death
69	M	HGG	ED	80	Major
70	M	HGG	ED	20	NAD
70	F	HGG	ID	25	NAD
34	M	Lymphoma	ED	667	NAD
26	F	Meningioma	ED	71	NAD
33	F	Meningioma	ED	119	NAD
38	M	Meningioma	ED	248	NAD
40	F	Meningioma	ED	270	NAD
42	F	Meningioma	ED/ID	25	Minor
49	M	Meningioma	ED/ID	29	NAD
51	M	Meningioma	ID	31	NAD
53	F	Meningioma	ED	42	NAD
55	M	Meningioma	ED	18	NAD
56	M	Meningioma	ID	45	NAD
56	F	Meningioma	ED/ID	38	Minor
56	M	Meningioma	ED	35	NAD
58	M	Meningioma	ED	59	NAD
64	M	Meningioma	ID	59	NAD
66	M	Meningioma	ED/ID	40	NAD
71	M	Meningioma	ED/ID	37	NAD
72	M	Meningioma	ED	37	NAD
74	F	Meningioma	ED	190	Minor
74	M	Meningioma	ID	36	NA
75	M	Meningioma	ED/ID	38	NAD
76	M	Meningioma	ED/ID	56	NAD
78	F	Meningioma	ED	17	Minor
45	M	Metastasis	ED/ID	25	NAD
59	F	Metastasis	ED/ID	116	Minor
63	M	Metastasis	ED	25	NAD
71	M	Metastasis	ED/ID	109	Major
78	M	Metastasis	ID	20	Death
66	F	Other (MFH)	ED	393	NAD
62	M	Pituitary adenoma	ED	232	Major
40	F	Schwannoma	ED	43	NAD

[a]M, male; F, female; HGG, high-grade glioma; LGG, low-grade glioma.
[b]Location is the location of infection: ED, extradural infection; ID, intradural infection; ED/ID, both intradural and extradural infection.
[c]Time is the time of reoperation in days after primary surgery.
[d]Outcome is the clinical outcome after postoperative infection: NAD, no additional disability; Minor, minor additional disability; Major, major additional disability.

DISCUSSION

Epidemiology

The neurosurgical catchment area for Oslo University Hospital is well defined, consisting of 2.7 million inhabitants (56% of the Norwegian population) and with very little loss of patients (1%) to other health regions or countries (The Norwegian Cancer Registry, unpublished data). Because all patients ≥18 years who underwent craniotomy for an intracranial tumor at Oslo University Hospital within a defined time period of 6 years were included in this study, it can serve as a population study in terms of incidence of craniotomies for particular tumor types in the Norwegian population. The incidence of first-time craniotomy for a brain tumor was 12.8/100 000 inhabitants per year and for a repeat resection 3.0/100 000 inhabitants per year.

Surgical Mortality at 30 Days

The overall surgical mortality in this series was 2.3%. The incidence of surgical mortality after craniotomy for tumors is previously reported to be between 0% and 9.6%, varying with the diagnosis.[10,15,18-26] Long et al[23] reported in 2003 a mortality rate at high-volume hospitals (>50 craniotomies/y) of 2.5% after craniotomy for various intracranial tumors, both benign and malignant. Barker et al[20] reported in their series of primary supratentorial brain tumors a mortality rate of 2.9%. However, both these studies were in-hospital mortality rates, whereas we report a 30-day mortality rate. Nevertheless, our mortality rates are comparable to, or even lower than, most published rates.

The causes of surgical mortality include complications to surgery and factors not directly related to surgery, as well as other factors, like tumor progression or other morbidity. Several risk factors are associated with increased hazard of death, eg, advanced age,[10,15,20,24] a low preoperative Karnofsky Performance score,[15] and comorbidity.[10,20] Several of the complications are avoidable, and should be paid close attention.

Postoperative hematomas carry a high mortality rate.[17] In our series, hematomas were suspected to be the cause of, or significant contributor to, 35% of the deaths within 30 days of surgery. Consequently, avoiding hematomas is the single most important factor to reduce surgical mortality.

Pulmonary embolism has an incidence rate of between 1.5% and 3%, and a mortality rate between 9% and 50%, and is a frequent cause of death among neurosurgical patients.[27] In our study, one patient died of a pulmonary embolism postoperatively. The prevention of pulmonary embolism in neurosurgical patients is controversial, because the commonly used medical prophylaxis, ie, unfractioned or low-molecular-weight heparin, may increase the rate of intracranial bleeding, with its deleterious effects.[28] Danish et al[28] showed that mechanical prophylaxis yields outcomes in patients undergoing craniotomy superior to those of heparin, but the field remains controversial. In our practice, patients with a past hematological history are referred to a consultant hematologist; all patients receive compressive stockings the day before surgery and keep them until fully mobilized. Low-molecular-weight heparin is given the first postoperative day. The patients are mobilized very early, either the same afternoon or on the first postoperative day.

Age is an independent risk factor for surgical mortality. Still, age should not be used as a selection criterion for surgery for intracranial tumors alone.[29] A careful selection among patients

Copyright © Congress of Neurological Surgeons. Unauthorized reproduction of this article is prohibited.

with a low preoperative Karnofsky Performance score and with comorbidity should be performed to lower operative mortality rates.

In our series, undergoing open biopsy was significantly associated with 30-day mortality, a finding that probably has more to do with a selection bias that favors good candidates for resection, whereas those undergoing biopsy already have a poorer prognosis. A total of 74 patients underwent open biopsy (Table 1). Seven of these patients died within 30 days postoperatively (9.5%), the majority of whom (5 of 7, or 71.4%) died of tumor progression (Table 2).

In our series, meningiomas had a significantly lower 30-day mortality rate than HGG and metastases, with a rate of 0.9% vs 2.9% and 4.5%. One factor contributing to this difference might be that all 6 deaths in the meningioma group were surgery related, whereas several deaths in the other groups were not surgery related. However, this factor alone does not explain the discrepancy, indicating that the inherent risk of undergoing a craniotomy will vary according to the diagnosis.

Postoperative Hematomas Requiring Reoperation

In our series, we found a rate of postoperative hematomas of 2.1%. This includes 3 subcutaneous hematomas and 8 cSDH. Other studies have reported a hematoma rate of 0.6% to 4.0%.[15,18-22,25,26,29,30]

Risk Factors

Advanced age was significantly associated with development of postoperative hematoma in both uni- and multivariate analyses. This finding is supported by other studies[13,17,31] and has been attributed to the tissue fragility observed in the elderly.[28] Palmer et al[17] showed in their series of 6668 intracranial procedures an increased risk of postoperative hematoma for meningiomas compared with intrinsic tumors. We did not find an association between histology and risk of postoperative hematoma.

In the aforementioned series, Palmer et al[17] identified several risk factors associated with postoperative hematoma, including thrombocytopenia, anticoagulants, a history of heavy alcohol intake, coagulopathy, malignancy outside the central nervous system, and the administration of antiplatelet agents during the 2 weeks preceding surgery. Administration of antiplatelet agents was the most frequent risk factor; it was used by 43% of those reoperated for hematoma.[17] In our practice, patients with a past hematological history are referred to a consultant hematologist, aspirin is stopped at least 10 days before surgery, and when on anticoagulation, the international normalized ratio should be below 1.5. Low-molecular-weight heparin is not given until the first postoperative day.

Mortality Rate of Postoperative Hematomas

The reported mortality rate of postoperative hematomas is 18% to 32%.[17,32,33] We found a mortality rate of 22%, with an additional 2% being severely disabled because of the hematoma. Consequently, postoperative hematomas may have deleterious consequences and it is important to reduce or eliminate as many risk factors as possible, and thereby reduce the incidence of postoperative hematomas. Vassilouthis et al[34] indicated in their series of 526 patients undergoing craniotomy that the incidence of postoperative intracranial hematoma should become negligible, provided that necessary modifications regarding anesthesia are adopted. Their strict anesthesiological protocol included a deep opioid analgesia to eliminate any acute elevations of the arterial pressure during and immediately after craniotomy. Furthermore, emergence from anesthesia was delayed for an average of 1.5 to 2 hours following the neurosurgical procedure. Even though postoperative hematomas occur rarely, more studies on how to avoid them are needed, as the consequences of them are often devastating.

Timing of Postoperative Intracranial Hematoma Development

Taylor et al[32] reported a 2.2% rate of postoperative hematomas in their series of 2305 patients undergoing intracranial surgery of miscellaneous reasons. Clinical deterioration as a result of postoperative hematoma occurred within 6 hours of surgery in 88% of the cases and $<$24 hours after surgery in the remaining 12% of hematoma cases. They concluded that a 6-hour observation period in the recovery area/intensive care unit after craniotomy before transfer to further nursing on a neurosurgical ward should be sufficient for most patients, but they recommended longer observation times after emergency craniotomies and posterior fossa surgery. In our series, only 11 patients (25%) were reoperated within 6 hours, indicating that a 6-hour observation period in recovery may be insufficient to sift out the majority of the patients in need of emergency surgery for a postoperative hematoma. However, close observation on a specialized neurosurgical ward may overcome this problem. Furthermore, our results indicate that a patient undergoing a craniotomy should be observed closely for a total of at least 48 hours postoperatively, because 80% of our patients that needed a recraniotomy for postoperative hematoma were operated on within 2 days.

Postoperative Infections Requiring Reoperation

Contemporary neurosurgical series have reported an incidence of postoperative infections after craniotomy of 0.6% to 6.6%,[18,19,30,35-37] although some of these series have included nonoperative cases as well. Our rate of postoperative infections requiring surgical treatment was 1.5%, thus being in the lower end of the scale.

Risk Factors

We observed a statistically significant association between male sex and postoperative infections. This has not been noted in other large neurosurgical series,[38-40] but Korinek et al[41] observed an increased risk of nosocomial meningitis after craniotomy in males. At present, we have no explanation for our finding.

Meningioma surgery was significantly associated with the development of postoperative infection in both uni- and multivariate analyses. This was also shown by Korinek et al[35] in 2005, although only in univariate analysis. They attributed this to hemostasis and closure difficulties in meningioma surgery.

Copyright © Congress of Neurological Surgeons. Unauthorized reproduction of this article is prohibited.

Korinek et al[35] also showed an association between infection and a surgery duration longer than 4 hours, a finding that also has been demonstrated by others.[40,42] Because meningioma operations are often time-consuming procedures, this might be a contributing factor to the higher incidence of infections after meningioma surgery.

Korinek et al[35] studied the effect of antibiotic prophylaxis (ABP) on neurosurgical site infections after craniotomy for various reasons, eg, tumor surgery, vascular surgery, and trauma surgery. Among the 4578 patients studied, 77 (1.7%) developed bone flap osteitis, and 126 (2.7%) developed brain abscess or subdural empyema, for a total of 4.4%. Because patients with both osteitis and abscess/empyema were counted once in each group, the number of patients with infections was a bit lower. ABP significantly reduced the incidence of bone flap osteitis (3.1% in patients with no ABP and 1.3% in patients with ABP, $P < .001$) and abscess/empyema (5.6% vs 2.0%, $P < .001$). In our practice, we use a second-generation cephalosporin intravenously at the initiation of surgery and continue every 90 minutes until the case is completed or the maximum daily dose of 8 g is reached, where after erythromycin or a third-generation cephalosporin is started and continued until completion of the case.

Consequences of Postoperative Infection

The consequences of postoperative infection are not at all as severe as the consequences of postoperative hematoma. In our series, 2 patients (5%) died of the infection, while 33 (85%) had a good outcome, with no or only a mild disability (Table 2). We did not include patients with meningitis.

Timing of Postoperative Infection Development

In our series, almost 75% of the patients with infection were reoperated within 3 months of tumor surgery. Korinek et al[35] showed a mean time between surgery and onset of infection of 118 ± 157 days for bone flap osteitis, and 25 ± 27 days for brain abscesses or subdural empyema. Dashti et al[36] reported a median duration between craniotomy and presentation of postoperative infection of 1.5 months (range, 4 days to 5 years). In our series, most postoperative infections requiring reoperation occur within 3 months of surgery, but some infections, in particular, bone flap osteitis, may occur later than 1 year after surgery, reportedly as late as 5 years later.[40,43]

Strengths of the Study

The strengths of this study lie in the setting, design, and follow-up. The data were restricted to one health center only (Oslo University Hospital), thereby reducing the possible confounding effect of differences in the access to health care services between health centers. Thus, we avoided the selection bias inherently present in large multicenter studies, because there are only 2 neurosurgical units performing these surgeries in a geographically well-defined area. As Dashti et al[36] pointed out, it is reasonable to assume that a number of patients with postoperative infection were not included in their study if they presented to, and were subsequently treated at, other facilities than the one where they were operated on in the first place. They also point out that this number might be high, but that there is no way to determine how high.[36] This problem may have occurred in several other studies as well. Furthermore, our data were prospectively registered in a database. Because the study includes all craniotomies performed for a histologically verifiable brain tumor, there is no selection bias. The study is contemporary, thereby reflecting current neurosurgical practice, and was performed within a relatively short time span, thereby reducing confounding factors as changes in antibiotic prophylaxis regimen or operating theaters. With respect to data, we only used end points that are easily verifiable (mortality, reoperation for hematomas, reoperations for infections). Last, we obtained 100% follow-up. To the best of our knowledge, our study is the largest study with regard to postoperative complications within 30 days of craniotomy for brain tumors. Previous studies are either smaller than our study, or they use in-hospital mortality rates.

Limitations of the Study

The first limitation of the study is the retrospective design. Second, the follow-up on some patients may be too short with regard to postoperative infections, because bone flap infections may occur later than 1 year after surgery.

CONCLUSION

The annual incidence of first-time craniotomy for a brain tumor was 12.8/100 000 inhabitants. The mortality rate, rate of postoperative hematomas, and infections were low. Although advanced age was significantly associated with a higher 30-day surgical mortality and risk of postoperative hematomas, surgery in selected elderly patients is worthwhile and not futile. The single most important way to reduce surgical mortality is avoidance of postoperative hematomas.

Disclosure

A research grant to the project was given by Schering-Plough (4000 Euro). The authors have no personal financial or institutional interest in any of the drugs, materials, or devices described in this article.

REFERENCES

1. CTBRUS. Statistical Report: Primary Brain Tumors in the United States, 2000–2004. Available at: http://www.cbtrus.org/reports//2007-2008/2007report.pdf. 2008.
2. Percy AK, Elveback LR, Okazaki H, Kurland LT. Neoplasms of the central nervous system. Epidemiologic considerations. *Neurology*. 1972;22(1):40-48.
3. Claus EB, Horlacher A, Hsu L, et al. Survival rates in patients with low-grade glioma after intraoperative magnetic resonance image guidance. *Cancer*. 2005;103(6):1227-1233.
4. McGirt MJ, Chaichana KL, Gathinji M, et al. Independent association of extent of resection with survival in patients with malignant brain astrocytoma. *J Neurosurg*. 2009;110(1):156-162.
5. Keles GE, Chang EF, Lamborn KR, et al. Volumetric extent of resection and residual contrast enhancement on initial surgery as predictors of outcome in adult patients with hemispheric anaplastic astrocytoma. *J Neurosurg*. 2006;105(1):34-40.
6. Mirimanoff RO, Dosoretz DE, Linggood RM, Ojemann RG, Martuza RL. Meningioma: analysis of recurrence and progression following neurosurgical resection. *J Neurosurg*. 1985;62(1):18-24.

Copyright © Congress of Neurological Surgeons. Unauthorized reproduction of this article is prohibited.

7. Hart MG, Grant R, Walker M, Dickinson H. Surgical resection and whole brain radiation therapy versus whole brain radiation therapy alone for single brain metastases. *Cochrane Database Syst Rev*. 2005;(1):CD003292.
8. Vecht CJ, Avezaat CJ, van Putten WL, Eijkenboom WM, Stefanko SZ. The influence of the extent of surgery on the neurological function and survival in malignant glioma. A retrospective analysis in 243 patients. *J Neurol Neurosurg Psychiatry*. 1990;53(6):466-471.
9. Nitta T, Sato K. Prognostic implications of the extent of surgical resection in patients with intracranial malignant gliomas. *Cancer*. 1995;75(11):2727-2731.
10. Barker FG II. Craniotomy for the resection of metastatic brain tumors in the U.S., 1988-2000: decreasing mortality and the effect of provider caseload. *Cancer*. 2004;100(5):999-1007.
11. Fadul C, Wood J, Thaler H, et al. Morbidity and mortality of craniotomy for excision of supratentorial gliomas. *Neurology*. 1988;38(9):1374-1379.
12. Kalfas IH, Little JR. Postoperative hemorrhage: a survey of 4992 intracranial procedures. *Neurosurgery*. 1988;23(3):343-347.
13. Gerlach R, Raabe A, Scharrer I, Meixensberger J, Seifert V. Post-operative hematoma after surgery for intracranial meningiomas: causes, avoidable risk factors and clinical outcome. *Neurol Res*. 2004;26(1):61-66.
14. Mahaley MS Jr, Mettlin C, Natarajan N, Laws ER Jr, Peace BB. National survey of patterns of care for brain-tumor patients. *J Neurosurg*. 1989;71(6):826-836.
15. Sawaya R, Hammoud M, Schoppa D, et al. Neurosurgical outcomes in a modern series of 400 craniotomies for treatment of parenchymal tumors. *Neurosurgery*. 1998;42(5):1044-1055.
16. Paek SH, Audu PB, Sperling MR, Cho J, Andrews DW. Reevaluation of surgery for the treatment of brain metastases: review of 208 patients with single or multiple brain metastases treated at one institution with modern neurosurgical techniques. *Neurosurgery*. 2005;56(5):1021-1034; discussion 1021-1034.
17. Palmer JD, Sparrow OC, Iannotti F. Postoperative hematoma: a 5-year survey and identification of avoidable risk factors. *Neurosurgery*. Dec 1994;35(6):1061-1064.
18. Morokoff AP, Zauberman J, Black PM. Surgery for convexity meningiomas. *Neurosurgery*. 2008;63(3):427-433.
19. Chang SM, Parney IF, McDermott M, et al. Perioperative complications and neurological outcomes of first and second craniotomies among patients enrolled in the Glioma Outcome Project. *J Neurosurg*. 2003;98(6):1175-1181.
20. Barker FG II, Curry WT Jr, Carter BS. Surgery for primary supratentorial brain tumors in the United States, 1988 to 2000: the effect of provider caseload and centralization of care. *Neuro Oncol*. 2005;7(1):49-63.
21. Curry WT, McDermott MW, Carter BS, Barker FG II. Craniotomy for meningioma in the United States between 1988 and 2000: decreasing rate of mortality and the effect of provider caseload. *J Neurosurg*. 2005;102(6):977-986.
22. Boviatsis EJ, Bouras TI, Kouyialis AT, Themistocleous MS, Sakas DE. Impact of age on complications and outcome in meningioma surgery. *Surg Neurol*. 2007;68(4):407-411.
23. Long DM, Gordon T, Bowman H, et al. Outcome and cost of craniotomy performed to treat tumors in regional academic referral centers. *Neurosurgery*. 2003;52(5):1056-1063.
24. Cowan JA Jr, Dimick JB, Leveque JC, et al. The impact of provider volume on mortality after intracranial tumor resection. *Neurosurgery*. 2003;52(1):48-53.
25. Stark AM, Tscheslog H, Buhl R, Held-Feindt J, Mehdorn HM. Surgical treatment for brain metastases: prognostic factors and survival in 177 patients. *Neurosurg Rev*. 2005;28(2):115-119.
26. Brell M, Ibanez J, Caral L, Ferrer E. Factors influencing surgical complications of intra-axial brain tumours. *Acta Neurochir (Wien)*. 2000;142(7):739-750.
27. Danish SF, Burnett MG, Stein SC. Prophylaxis for deep venous thrombosis in patients with craniotomies: a review. *Neurosurg Focus*. 2004;17(4):E2.
28. Danish SF, Burnett MG, Ong JG, et al. Prophylaxis for deep venous thrombosis in craniotomy patients: a decision analysis. *Neurosurgery*. 2005;56(6):1286-1292; discussion 1292-1284.
29. Rogne SG, Konglund A, Meling TR, et al. Intracranial tumor surgery in patients >70 years of age: is clinical practice worthwhile or futile? *Acta Neurol Scand*. 2009;120(5):288-284.
30. Rabadan AT, Hernandez D, Eleta M, et al. Factors related to surgical complications and their impact on the functional status in 236 open surgeries for malignant tumors in a Latino-American hospital. *Surg Neurol*. 2007;68(4):412-420; discussion 420.
31. Boviatsis EJ, Bouras TI, Kouyialis AT, Themistocleous MS, Sakas DE. Impact of age on complications and outcome in meningioma surgery. *Surg Neurol*. 2007;68(4):407-411; discussion 411.
32. Taylor WA, Thomas NW, Wellings JA, Bell BA. Timing of postoperative intracranial hematoma development and implications for the best use of neurosurgical intensive care. *J Neurosurg*. 1995;82(1):48-50.
33. Basali A, Mascha EJ, Kalfas I, Schubert A. Relation between perioperative hypertension and intracranial hemorrhage after craniotomy. *Anesthesiology*. 2000;93(1):48-54.
34. Vassilouthis J, Anagnostaras S, Papandreou A, Dourdounas E. Is postoperative haematoma an avoidable complication of intracranial surgery? *Br J Neurosurg*. 1999;13(2):154-157.
35. Korinek AM, Golmard JL, Elcheick A, et al. Risk factors for neurosurgical site infections after craniotomy: a critical reappraisal of antibiotic prophylaxis on 4,578 patients. *Br J Neurosurg*. 2005;19(2):155-162.
36. Dashti SR, Baharvahdat H, Spetzler RF, et al. Operative intracranial infection following craniotomy. *Neurosurg Focus*. 2008;24(6):E10.
37. McClelland S III, Hall WA. Postoperative central nervous system infection: incidence and associated factors in 2111 neurosurgical procedures. *Clin Infect Dis*. 2007;45(1):55-59.
38. Mollman HD, Haines SJ. Risk factors for postoperative neurosurgical wound infection. A case-control study. *J Neurosurg*. 1986;64(6):902-906.
39. Lietard C, Thebaud V, Besson G, Lejeune B. Risk factors for neurosurgical site infections: an 18-month prospective survey. *J Neurosurg*. 2008;109(4):729-734.
40. Korinek AM. Risk factors for neurosurgical site infections after craniotomy: a prospective multicenter study of 2944 patients. The French Study Group of Neurosurgical Infections, the SEHP, and the C-CLIN Paris-Nord. Service Epidemiologie Hygiene et Prevention. *Neurosurgery*. 1997;41(5):1073-1079.
41. Korinek AM, Baugnon T, Golmard JL, et al. Risk factors for adult nosocomial meningitis after craniotomy: role of antibiotic prophylaxis. *Neurosurgery*. 2006;59(1):126-133.
42. Idali B, Lahyat B, Khaleq K, et al. [Postoperative infection following craniotomy in adults]. *Med Mal Infect*. 2004;34(5):221-224.
43. Blomstedt GC. Infections in neurosurgery: a retrospective study of 1143 patients and 1517 operations. *Acta Neurochir (Wien)*. 1985;78(3-4):81-90.

Acknowledgments

We thank Elisabeth Elgesem and Hanne Vebenstad for excellent secretarial assistance.

COMMENTS

This is a uniquely useful article; it nicely points up the scientific advantages of regionalized specialty care and centralized reporting in relatively small, well-defined populations of patients. Scandinavian studies are exemplary in this regard. I well remember that one of the first reliable estimates of the incidence and prevalence of subarachnoid hemorrhage as a cause of sudden death came from a Finnish study of this type.[1] Meling and his team from Oslo University Hospital have a catchment area that encompasses more than half the population of Norway. Their institution treats 99% of all the brain tumor cases in this region of the country and they are able to achieve 100% follow-up in their patients! Moreover, their data on the risks of craniotomy in patients with brain tumors have been obtained in the very latest era of surgical and diagnostic advances. This study has the distinct methodological advantage of combining an epidemiological approach with the experience of a major institution, ie, it manages complete capture of all the data from a defined population subjected to uniform treatment in a single facility. The results validate the methodology since the various rates for tumor incidence, craniotomy mortality, frequency of postoperative bleeding and infection, all fall within previously reported ranges in our literature. One can never be reminded too frequently of the importance of achieving perfect hemostasis since postoperative bleeding, age of the patient, and histology of the tumor are chief determinants of 30-day mortality. Tumors differ in their propensity for hemorrhage and even without surgical manipulation not

Copyright © Congress of Neurological Surgeons. Unauthorized reproduction of this article is prohibited.

infrequently present as unsuspected causes of intracranial hemorrhage.[2] I envy the authors their uniform management scheme of employing a consulting hematologist for all patients with risk factors for hemorrhage. One of the few glaring omissions in the study is the failure to present data on the length of surgery, an important variable in regard to the likelihood of bleeding and the incidence of postoperative infection. I am certain that further data-mining in this retrospective study would be a useful exercise. For example, the authors report a nearly 20% incidence of reoperation for tumor resection but do not tell us whether the incidence of complications and risk factors varies between primary resections and reoperations. Other authors have noted that postoperative infection is more common in debilitated tissues previously exposed to radiation and chemotherapy.[3] Meling and colleagues speculate on the reasons for the higher mortality experience in open biopsies as opposed to attempts at radical resection, an observation that has been made since the earliest days of glioma surgery.[4] They ascribe this finding to the age and condition of the patient but do not present data on tumor location, a factor that may be just as important, even in the era of image-guided surgery.

Michael Salcman
Baltimore, Maryland

1. Pakarinen S. Incidence, aetiology, and prognosis of subarachnoid hemorrhage. A study based on 589 cases diagnosed in a defined urban population during a defined period. *Acta Neurol Scand.* 1967;43(suppl 29):1-28.
2. Salcman M. Intracranial hemorrhage caused by brain tumor. In: Kaufman, HH, ed. Intracerebral Hematomas. New York, NY: Raven Press; 1992:95-106.
3. Tenney JH, Vlahov D, Salcman M et al. Wide variation in risk of wound infection following clean neurosurgery: implications for perioperative antibiotic prophylaxis. *J Neurosurg.* 1985;62:243-247.
4. Salcman M. Historical development of surgery for glial tumors. *J Neurooncol.* 1999;42:195-204.

This study provides highly valuable information on the complication rate and mortality in the early period following craniotomy for brain tumor removal. Even though this is a retrospective study, the number of studied cases, covering all patients subjected to brain tumor craniotomy in the study period, increases the validity of the results. The strengths and weaknesses of the study design are well described by the authors. This article makes a good reference source for similar clinically based research in neurosurgery.

Tomasz Trojanowski
Lublin, Poland

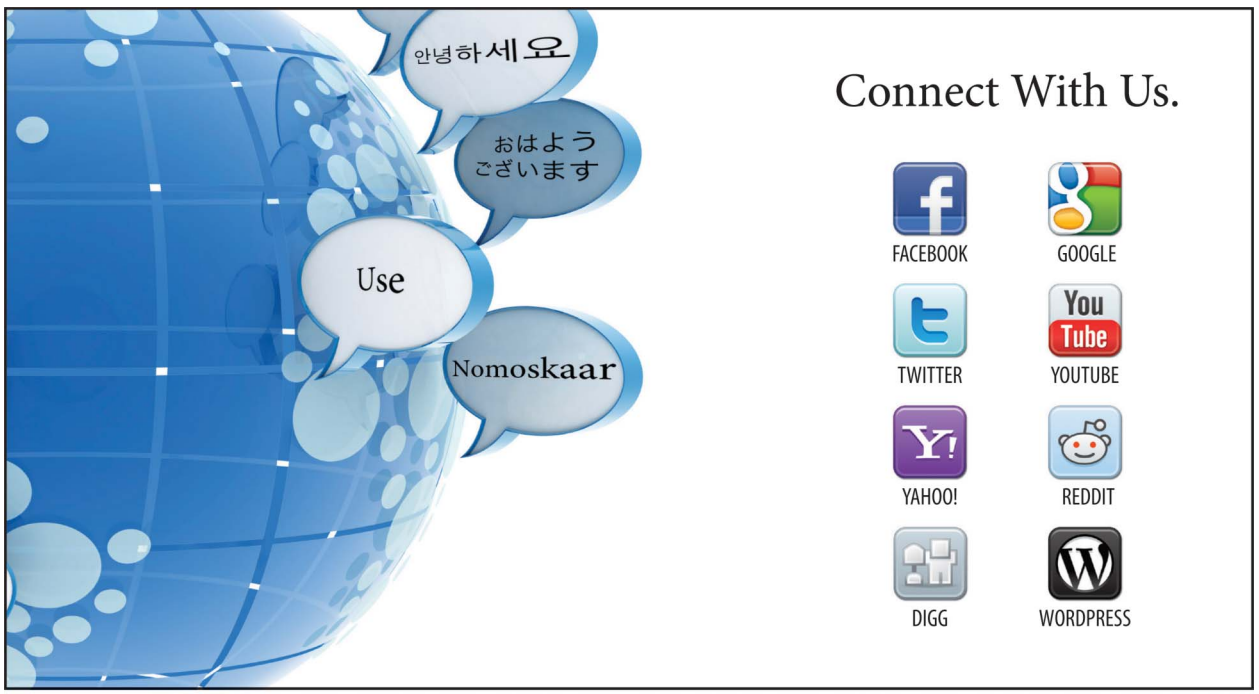

Find NEUROSURGERY® content on a growing number of social media sites.
Links at www.neurosurgery-online.com

NEUROSURGERY

Copyright © Congress of Neurological Surgeons. Unauthorized reproduction of this article is prohibited.

Geometry of the Internal Carotid Artery and Recurrent Patterns in Location, Orientation, and Rupture Status of Lateral Aneurysms: An Image-Based Computational Study

Marina Piccinelli, EngD*‡
Susanna Bacigaluppi, MD§¶
Edoardo Boccardi, MD‖
Bogdan Ene-Iordache, EngD*
Andrea Remuzzi, EngD*#
Alessandro Veneziani, PhD‡
Luca Antiga, PhD* **

*Department of Bioengineering, Mario Negri Institute, Bergamo, Italy; ‡Department of Mathematics and Computer Science, Emory University, Atlanta, Georgia; §Department of Neurosurgery, Niguarda Ca' Granda Hospital Milan, University of Milano, Milan, Italy; ¶Department Neurosciences and Biomedical Technologies, University of Milan-Bicocca, Monza, Italy; ‖Neuroradiology Division, Niguarda Hospital, Milan, Italy; #Department of Industrial Engineering, University of Bergamo, Bergamo, Italy; **Orobix Srl, Bergamo, Italy

Correspondence:
Luca Antiga, PhD,
Biomedical Engineering Department,
Mario Negri Institute for Pharmacological Research,
24020 Ranica (BG), Italy.
E-mail: antiga@marionegri.it

Received, January 23, 2010.
Accepted, September 23, 2010.

Copyright © 2011 by the
Congress of Neurological Surgeons

BACKGROUND: Intracranial aneurysm development and rupture may be associated to the morphology of the parent vessel.

OBJECTIVE: To quantitatively characterize the geometry of the internal carotid artery (ICA) in relation to the location and orientation of lateral aneurysms and to identify recurrent patterns associated with their rupture status.

METHODS: The geometry of 54 ICAs hosting lateral aneurysms was analyzed by means of computational geometry techniques. The ICA was split into individual bends, and the bend hosting the aneurysm was described in terms of curvature, torsion, length, and radius. Aneurysm position and orientation with respect to the parent vessel and specifically the hosting bend were characterized, as well as angles between the portions of the parent artery immediately upstream of and downstream from the aneurysm and the aneurysm ostium. Differences in geometric parameters with respect to rupture status and their performance as classifiers were evaluated.

RESULTS: ICA bends hosting ruptured aneurysms were shorter with a smaller radius, lower maximum curvature, and lower proximal torsion compared with those hosting unruptured lesions. Ruptured aneurysms occurred in more distal portions of the ICA, along the outer wall of the vessel, and closer to the curvature peak within the hosting bend than unruptured ones. The proximal portions of ICAs hosting ruptured aneurysms approached the ostium region at a smaller angle.

CONCLUSION: Geometric factors relative to the ICA were associated with the distribution of aneurysms and their rupture status. The present work has potential implications in the quest for hemodynamic factors contributing to the development, progression, and rupture of intracranial aneurysms.

KEY WORDS: Hemodynamics, Intracranial aneurysm, Parent vessel, Rotational angiography, Rupture risk 3D geometry

Neurosurgery 68:1270–1285, 2011 DOI: 10.1227/NEU.0b013e31820b5242 www.neurosurgery-online.com

Evidence gathered in the last decades supports the hypothesis that cerebral aneurysm formation, development, and rupture are the result of a complex interplay between systemic factors, changes in the biomechanical properties of vessel walls, and local hemodynamic factors such as wall shear stress (WSS) and pressure.[1] In particular, the involvement of hemodynamics in aneurysmal disease is supported by the circumstantial evidence that cerebral aneurysms tend to develop in areas generally associated with altered hemodynamic forces such as bends and bifurcations.[2,3]

ABBREVIATIONS: ACA, anterior cerebral artery; **AUC,** area under the curve; **BTR,** bend-torsion ratio; **HB,** hosting bend; **ICA,** internal carotid artery; **RA,** rotational angiography; **WSS,** wall shear stress

In the attempt to gain further insight into the key hemodynamic factors responsible for the pathogenesis and evolution of the disease, aneurysmal hemodynamics has been the subject of numerous studies leveraging on both

Copyright © Congress of Neurological Surgeons. Unauthorized reproduction of this article is prohibited.

experimental and computational approaches.[4,5] Still, strong relationships between specific hemodynamic-related quantities and aneurysm formation and development have yet to be identified.

Recent image-based computational studies have shown how a major determinant of hemodynamic patterns is represented by the morphology of blood vessels[6] and that geometry can constitute a simple surrogate for complex hemodynamic behaviors.[7] In this context, the study of three-dimensional (3D) geometry of cerebral aneurysms and their parent vasculature in vivo may provide strong clues to the key hemodynamic factors contributing to the initiation and progression of the disease.

To date, the majority of works dealing with cerebral aneurysm geometry have focused on the extraction of morphological features of aneurysmal sacs (eg, aneurysm volume, aspect ratio) with the purpose of identifying prognostic indexes correlated with risk of rupture or evaluating the efficacy of treatments.[8,9] Nevertheless, a few authors have recognized the importance of characterizing the geometric relations between aneurysms and their hosting vessels and exploring the effects of different geometric configurations on hemodynamic quantities.[10-14] This approach poses a few challenges, related mainly to the difficulty of performing geometric quantifications in 3D and to the interindividual variability that characterizes cerebral vasculature. To overcome these problems, robust and objective methods for the definition and measurement of geometric quantities in 3D have recently been proposed.[15-17]

In this work, the same methods are applied to a population of lateral aneurysms located along the internal carotid artery (ICA), with the aim of quantitatively characterizing the geometric relations between aneurysms and their parent vessels and identifying recurrent geometric patterns associated with their rupture status. The present approach may suggest new criteria for the stratification of lesions based of their risk of rupture and new hints for the definition of hemodynamic factors linked to aneurysm formation and rupture.

This work originated within the Aneurisk study, a wider project focused on the development of geometric, biomechanical, computational, and statistical tools for the analysis of cerebral aneurysms and their parent vasculature.[18]

MATERIALS AND METHODS

Patient Population, Image Acquisition, and Surface Reconstruction

Between September 2002 and September 2006, 153 patients underwent 3D rotational angiography (3D-RA) for cerebral aneurysm assessment at the Neuroradiology Division of the Niguarda Ca' Grande Hospital in Milan following clinical routine. All cases presenting 1 or more aneurysms along the course of the ICA were considered for inclusion; terminal aneurysms and cases without anterior cerebral artery (ACA) perfusion were excluded. In the end, 51 patients with lateral aneurysm were included in the study for a total of 54 aneurysms. Patient demographic data, aneurysm occurrence, and rupture status are summarized in Table 1.

All 3D-RA images were obtained with an Integris Allura Unit (Philips, Best, the Netherlands) with the following acquisition parameters: C-arm rotation speed, 55° per second; matrix size, 512 × 512; and frame rate, 25 frames per second. Before acquisition, 18 mL nonionic hydrosoluble contrast agent was injected at 4 mL/s with a catheter positioned in the ICA providing continuous filling of cerebral vessels. All images were reviewed by a senior neuroradiologist (E.B.), who also reported information on rupture status.

After tomographic reconstruction, 3D-RA images were collected in digital imaging and communications in medicine (DICOM) format for subsequent processing. Surface models of the ICA and associated aneurysms were reconstructed from 3D-RA DICOM images using a gradient-driven level-set approach,[19] as implemented in the Vascular Modeling Toolkit.[20] The aneurysm sac and the ICA, including its bifurcation into ACA and middle cerebral artery, were reconstructed for every subject (Figure 1A).

Geometric Characterization

The geometry of the reconstructed models was analyzed using the approach recently described by Piccinelli et al[15] and implemented in the Vascular Modeling Toolkit. Specifically, we refer to section V-B of the Piccinelli et al[15] article, which specifically addresses the geometric characterization of lateral aneurysms. In the following sections, we briefly describe the operations performed to characterize the 3D geometry of aneurysms with respect to their parent vessel, referring to the Piccinelli et al[15] article for technical details.

Centerline Extraction and Bifurcation Characterization

As depicted in Figure 1A and 1B, 2 centerlines were generated for each model from the intracranial ICA (inlet) to the ACA and the middle cerebral artery origin (outlets) and 1 centerline from the ICA inlet to the distal end of the aneurysm sac running through the aneurysm ostium; local estimates of vessel radius, namely the radius of maximal spheres locally inscribed within the vessel, were computed.[15]

Two bifurcations were automatically identified along the ICA: the distal ICA bifurcation originating in the ACA and middle cerebral artery and a bifurcation at the aneurysm, referred to as an aneurysm bifurcation, defined as the bifurcation between the ICA centerline and the centerline entering the aneurysm through the ostium. At both locations, local reference systems were computed. In Figure 1C, the ICA bifurcation plane and its reference system are illustrated for one of the models. Each reference system is composed of an origin (o) positioned at the center of the bifurcation, a normal (n) that defines the plane in which the centerlines lie while departing from each other (the bifurcation

TABLE 1. Patients' Demographics Data and Occurrence of Aneurysms[a]

	Subjects, n	Age, y	Aneurysms, n	Ruptured, n
Patients with ICA lateral aneurysms	51	56 ± 15	54	17
Female	42	57 ± 16	43	14
Male	9	52 ± 10	11	3

[a]ICA, internal carotid artery.

Copyright © Congress of Neurological Surgeons. Unauthorized reproduction of this article is prohibited.

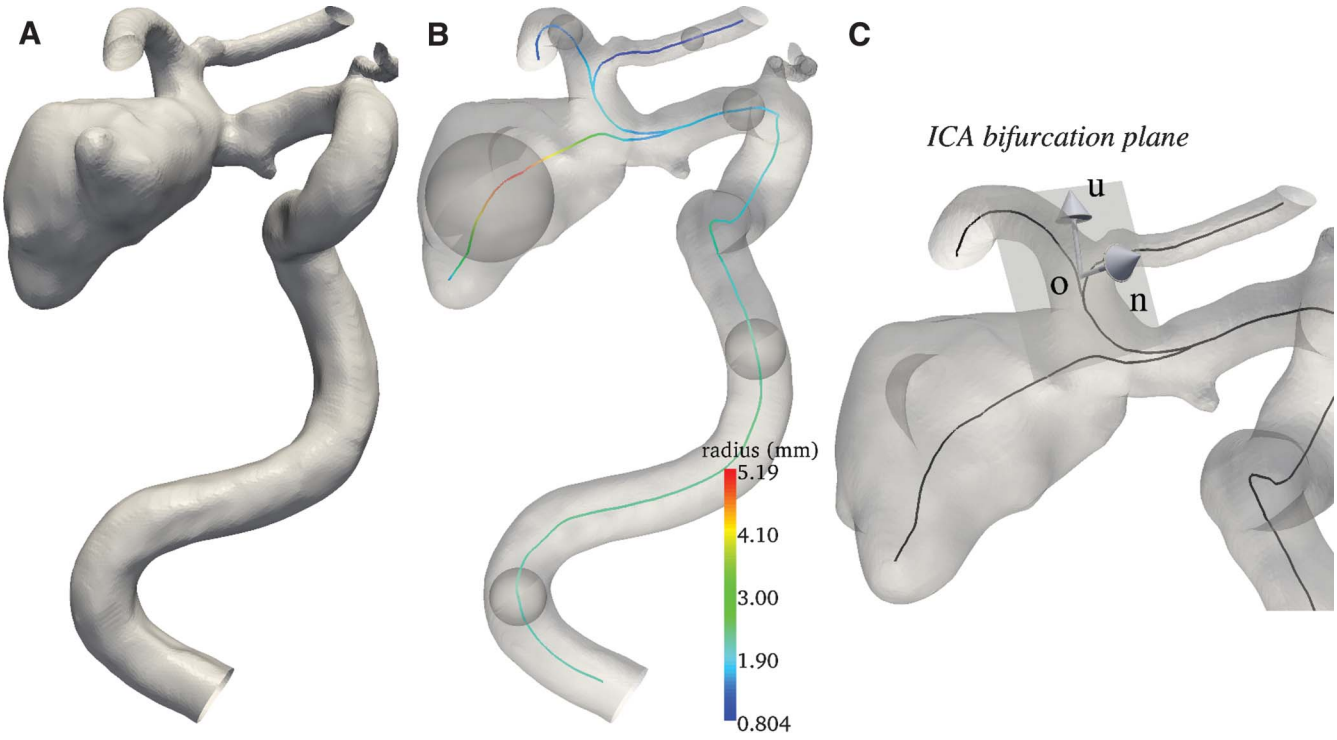

FIGURE 1. **A**, *3-dimensional model of an internal carotid artery (ICA) bearing an aneurysm.* **B**, *artery and aneurysmal sac centerlines; a few maximal inscribed spheres are included.*[15] **C**, *definition of the ICA bifurcation reference system composed of normal (n), up-normal (u), and origin (o), and the ICA bifurcation plane.*

plane), and an up-normal (u) lying on the bifurcation plane and pointing toward the flow divider.

The origin o_{ica} of the ICA bifurcation was chosen as a reference point with respect to which locations along the ICA were measured and thus compared consistently among patients, namely by measuring their distance to the ICA bifurcation. The aneurysm bifurcation reference system was instead used to characterize the location and orientation of the aneurysm ostium with respect to the parent vessel by means of the origin o_{an} and the bifurcation plane normal n_{an}, respectively.

Bifurcation vectors,[15] representing the directions of centerlines as they approach the bifurcation, characterize the directions of the upstream and downstream portions of the ICA and of the aneurysm ostium by means of vectors $v_{upstream}$, $v_{downstream}$, and v_{an}, respectively. Figure 2A graphically shows the aneurysm bifurcation for 1 aneurysm model, and Figure 2B illustrates the projections of bifurcation vectors on the aneurysm bifurcation plane, referred to as in-plane bifurcation vectors $\left(v^{ip}_{upstream}, v^{ip}_{downstream}, v^{ip}_{an}\right)$. Such in-plane vectors are important for measuring angles because any measurement of the angle between vectors in 3D strictly requires first projecting the vectors onto a plane and then measuring the angle between their in-plane components.

Geometry of the ICA and Individual Siphon Bends

The centerline relative to the ICA was defined from the most proximal ICA portion available in the source images to the ICA bifurcation origin o_{ica}; its length, curvature, and torsion were computed according to classic differential geometry formulas.[15] Intuitively, curvature measures the deviation of the curve from a straight line and is the inverse of the radius of the osculating circle, ie, the circle that locally approximates the curve; torsion measures its deviation from lying on a plane (the osculating plane) or equivalently how rapidly the osculating circle twists around the curve.[15] These concepts are graphically sketched in Figure 3, in which the osculating plane and the osculating circle are depicted at a single location (A) and at 2 different locations (B) along the ICA siphon.

Using curvature and torsion, we operated an objective subdivision of the carotid siphon into bends. Subdivision of individual siphon bends was performed by identifying locations of curvature and torsion peaks along the siphon and defining a bend for each curvature peak delimited by 3 enclosing (proximal and distal) torsion peaks. Figure 4 shows the splitting of the ICA siphon for a representative case. The subdivision in bends is shown on the curvature and torsion profiles and on the 3D model.

The position of the curvature peak within the corresponding bend was computed as a percentage of the bend length. In addition, to provide a robust description of bend geometry not influenced by the transition between 2 consecutive bends, 10% of the bend length was discarded at each end of the bend (light gray areas in Figure 4), and a geometric quantity was computed to characterize the remaining central portion. In particular, a bend-torsion ratio (BTR) was defined as the ratio between the average torsion of the central portion of the bend (the gray area in Figure 4) and the average torsion for the whole bend. Given that a bend is delimited by 2 torsion peaks, BTR quantifies the planarity of the central portion of the bend away from the peaks. A BTR close to 1 means that torsion is uniform along the length of the bend, whereas a torsion ratio close to 0 identifies bends with a low-torsion central portion

Copyright © Congress of Neurological Surgeons. Unauthorized reproduction of this article is prohibited.

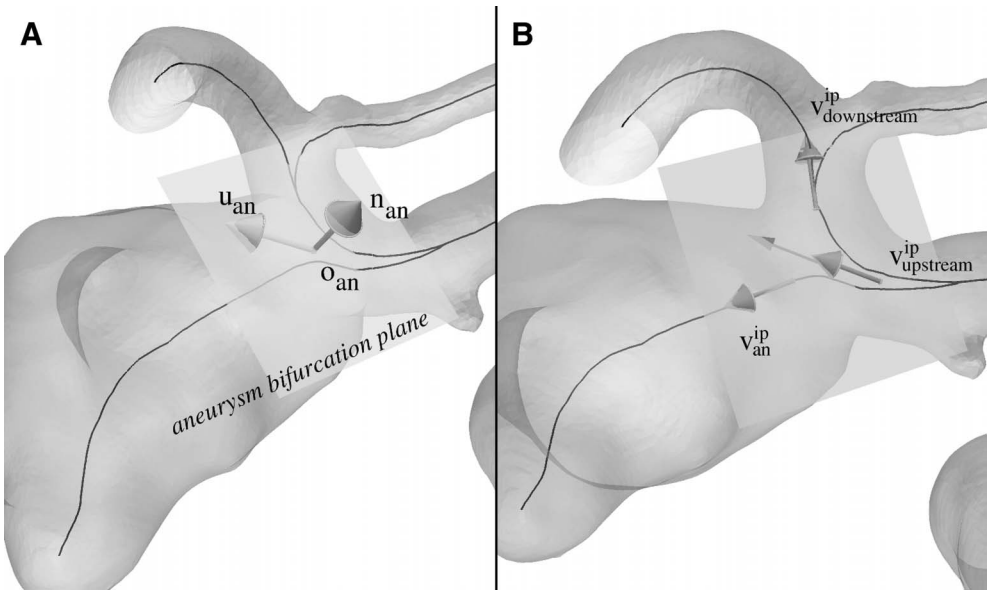

FIGURE 2. **A**, *definition of the aneurysm bifurcation reference system composed of normal (n_{an}), up-normal (u_{an}), and origin (o_{an}) and the aneurysm bifurcation plane.* **B**, *in-plane aneurysm bifurcation vectors characterizing the directions of the internal carotid artery and aneurysm branches arriving at and departing from the aneurysm bifurcation. The upstream vector lying on the bifurcation plane is also shown.*

compared with their extrema. The amount of 10% is somewhat arbitrary; it is derived only from the need to identify the "core" of a bend. However, we found that quantitative conclusions based on this index do not depend on this particular choice; we obtained similar statistical significance when adopting values of 5% through 15% for the percent length of the extrema.

To characterize the configuration of the parent vessel in relation to the presence of the aneurysm, the hosting bend (HB) was specifically investigated in terms of bend length (l_{HB}), radius (r_{HB}), mean and maximum curvature $\left(c^{mean}_{HB}, c^{max}_{HB}\right)$, mean torsion $\left(t^{mean}_{HB}\right)$, torsion peaks at the proximal and distal end points of the bend $\left(t^{prox}_{HB}, t^{dist}_{HB}\right)$, and BTR.

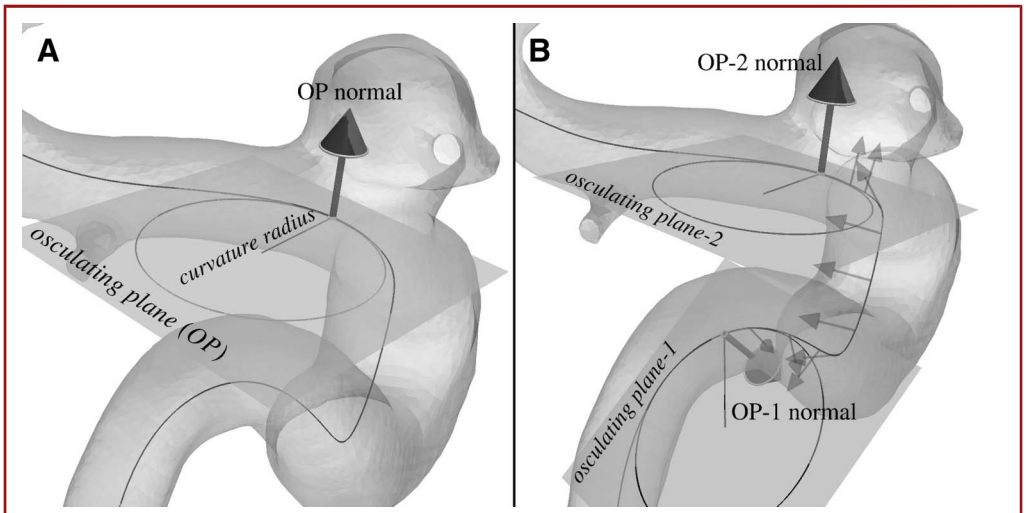

FIGURE 3. *Local geometrical characterization of the internal carotid artery (ICA).* **A**, *representation of the local osculating plane (OP) and the osculating circle tangent to the curve at one point of the ICA centerline. The curvature at each point is defined as the inverse of the radius of the osculating circle.* **B**, *rotation of the local osculating plane between 2 points of the siphon centerline.*

Copyright © Congress of Neurological Surgeons. Unauthorized reproduction of this article is prohibited.

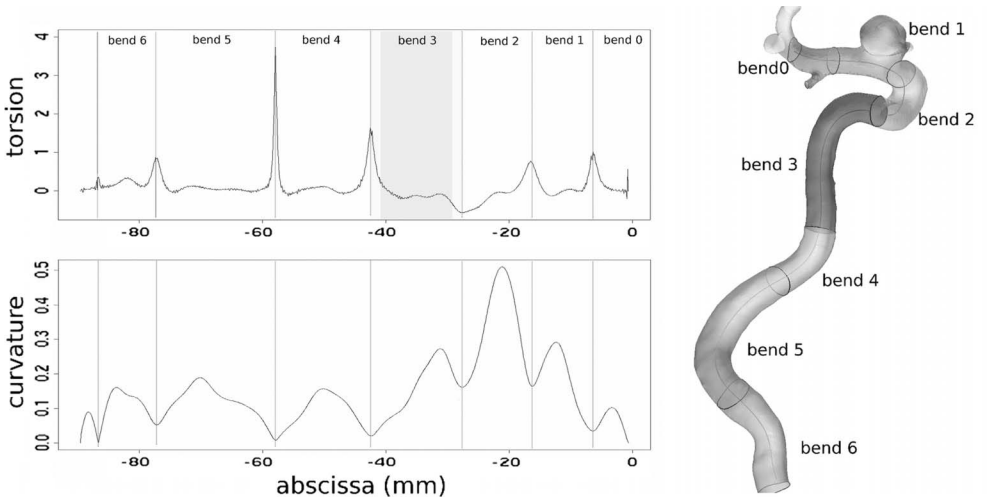

FIGURE 4. *Subdivision of the internal carotid artery siphon in bends. Each bend is identified by a curvature peak and is delimited by 2 enclosing (proximal and distal) torsion peaks. For bend 3, the regions of the definition of the bend-torsion ratio are highlighted: the inner part of the bend (gray) and the 2 boundary regions close to the torsion peaks (light gray), set to 10% of the bend length. Right, subdivision of the siphon centerline in bends applied to the corresponding 3-dimensional model.*

The described ICA geometric parameters are shown in Figure 5A through 5E for a representative case.

Aneurysm Ostium Location and Orientation

The location of the aneurysm ostium along the ICA was characterized by the curvilinear abscissa of the ostium origin o_{an}, ie, its distance from the ICA bifurcation along the ICA (abs_{ost}). In addition, the distance between the ostium origin and the curvature peak of the HB ($D_{ost\text{-}HB}$) was computed.

The local orientation of the ostium around the siphon was investigated by means of the angle α_{ost} between the local ICA osculating plane and the aneurysm bifurcation plane at the location of the ostium. The same angle was used to determine whether aneurysms were located on the inner or outer wall of the hosting ICA bend.

The aneurysm ostium parameters are depicted in Figure 5F through 5H for a representative case.

Angles Between Aneurysm Bifurcation Branches

The orientation of the portions of ICA immediately upstream of and downstream from the aneurysm and the orientation of the aneurysm ostium were characterized in terms of the angles measured between the in-plane aneurysm bifurcation vectors, as previously described. By means of the vectors $v^{ip}_{upstream}$, $v^{ip}_{downstream}$ and v^{ip}_{an}, the angles $\beta_{upstream}$, $\beta_{downstream}$, and β_{an} were computed, as shown in Figure 5i. $\beta_{upstream}$ was measured between the $v^{ip}_{upstream}$ and the up-normal unit vector u_{an}, whereas $\beta_{downstream}$ and β_{an} were calculated as the angles between the respective vectors and $v^{ip}_{upstream}$. $\beta_{upstream}$ measures the degree of alignment of the upstream portion of the ICA with the flow divider of the aneurysm bifurcation; $\beta_{downstream}$ and β_{an} quantitatively assess the deviation of the downstream portion of the ICA or the aneurysm sac.

All the geometric parameters described above are summarized in Table 2.

Statistical Analysis

For all geometric parameters listed in Table 2, mean, SD (in the following reported as mean $\pm$ SD), and range were computed.

Aneurysms were divided into 2 groups according to their rupture status at the time of acquisition, as clinically reported. Means and SDs of each parameter were calculated separately for each group. The statistical significance of the differences in the distribution of the geometric parameters between the 2 groups was assessed by means of a Student *t* test. A value of $P = .05$ was chosen for statistical significance.

To identify the performance of individual geometric parameters as classifiers of rupture status, receiver-operating characteristics analysis was performed on each of them, and the area under the curve (AUC) taken as a global figure of classifier performance. Optimal thresholds for the classifiers were obtained by maximizing the Matthews correlation coefficient, which aims at finding the levels that jointly maximize the sensitivity and specificity.

Multivariate logistic regression analysis was performed to assess the potential for a combination of geometric parameters in discriminating rupture status. Multivariate logistic regression models built from different combinations of geometric parameters taken as independent variables underwent a selection process based on the minimization of the Akaike information criterion. Because the Akaike information criterion penalizes models with large numbers of covariates, models with > 5 independent variables were systematically associated with low Akaike information criterion values. For this reason, the search was restricted to all models with up to 7 covariates generated by considering all possible combinations of up to 7 geometric parameters, for a total of 57 344 models. Estimates of coefficients, *P* values, odds ratios, and their 95% confidence intervals were reported for the obtained optimal model, as well as the model AUC.

All statistical analyses were performed with the R statistical package.[21]

Copyright © Congress of Neurological Surgeons. Unauthorized reproduction of this article is prohibited.

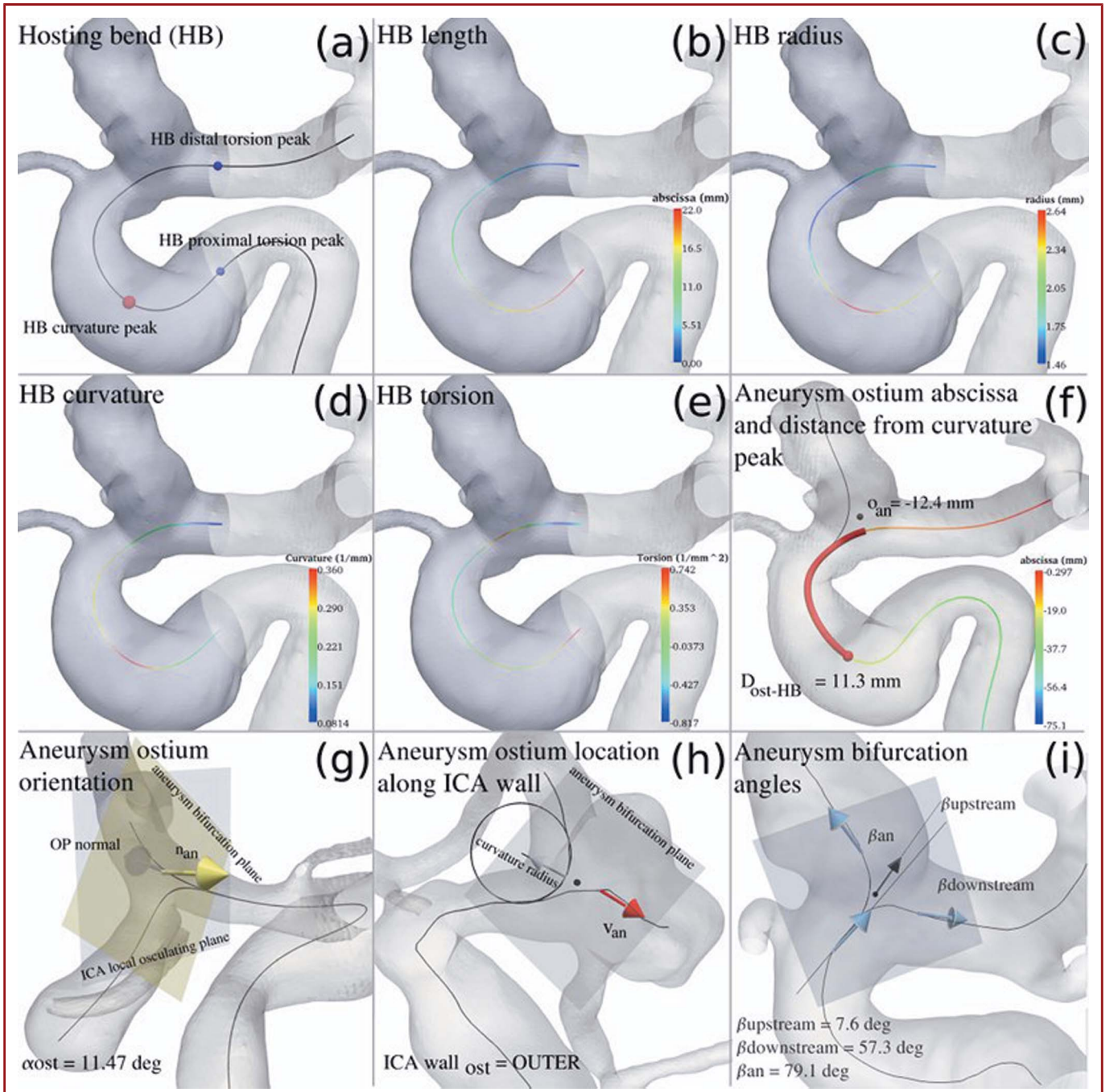

FIGURE 5. *Parameters for the geometric characterization of the internal carotid artery (ICA) and aneurysms with respect to the parent vessel.* **A**, *definition of the bend hosting the aneurysm (HB).* **B**, *length of the HB.* **C**, *radius values along the HB.* **D**, *curvature along the HB.* **E**, *torsion along the HB.* **F**, *position of the aneurysm ostium along the ICA centerline in terms of distance from the ICA bifurcation (abs_{ost}) and distance from the HB curvature peak ($D_{ost\text{-}HB}$).* **G**, *aneurysm ostium orientation (α_{ost}) calculated as the angle between the local ICA osculating plane normal (OP normal) and the aneurysm bifurcation plane normal (n_{an}).* **H**, *location of the aneurysm on the inner or outer wall of the hosting ICA.* **I**, *in-plane angles between the vascular branches arriving at and departing from the aneurysm bifurcation. Computed values are reported for a subset of the parameters.*

Copyright © Congress of Neurological Surgeons. Unauthorized reproduction of this article is prohibited.

TABLE 2. Terminology, Symbols, and Descriptions of Geometric Parameters[a]

Symbol	Description
ICA bends terminology and geometric parameters	
HB	The bend hosting the aneurysm
l_{HB}	Length of the hosting bend
$misr_{HB}$	Maximum inscribed sphere radius of the hosting bend
c_{HB}^{mean}	Mean curvature of the hosting bend
c_{HB}^{max}	Maximum curvature of the hosting bend
t_{HB}^{mean}	Mean torsion of the hosting bend
t_{HB}^{prox}	Torsion value at the proximal hosting bend end point
t_{HB}^{dist}	Torsion value at the distal hosting bend endpoint
HB BTR	Ratio between inner bend mean torsion value and t_{HB}^{mean}
Aneurysm ostium geometric parameters	
abs_{ost}	Curvilinear abscissa of the ostium origin measured along the ICA centerline
$D_{ost\text{-}HB}$	Distance measured along the ICA centerline between the ostium origin and curvature peak of the hosting bend
α_{ost}	Angle between 2 planes defined at the ostium location: the ICA local osculating plane and the aneurysm bifurcation plane
ICA $wall_{ost}$	Classification of aneurysm ostia according to their position along the inner or outer wall of the ICA wall
Angles between aneurysm bifurcation branches	
$\beta_{upstream}$	Angle between the bifurcation vector of the upstream branch of the ICA and the up-normal unit vector of the aneurysm bifurcation reference system
$\beta_{downstream}$	Angle between the bifurcation vectors of the upstream and the downstream branches of the ICA
β_{an}	Angle between the bifurcation vector of the upstream branch of the ICA and the aneurysm vector

[a]ICA, internal carotid artery.

RESULTS

Surface reconstruction was performed successfully for all 54 cases included in the study. Figure 6 shows a subset of 3D models hosting ruptured aneurysms; Figure 7A and 7B shows 3D models with unruptured aneurysms. In each model, centerlines were successfully computed for all the branches and the aneurysm sac, and the ICA and aneurysm bifurcations were identified accordingly. Means, SDs, and range of all geometric parameters listed in Table 2 computed for all cases are reported in Table 3.

ICA Geometry

The length of the acquired carotid siphon was measured up to the ICA bifurcation origin and ranged from a minimum of 26 mm to a maximum of 113 mm (mean, 66.1 ± 21.8 mm). The mean radius of the siphons was 1.9 ± 0.2 mm, in accordance with a value of about 2 mm commonly found in the literature.[22] Because of anatomic differences in the course of the ICA among subjects, the number of curvature maxima and consequently of bends identified was mildly variable. To quantify such variability, we considered the models with ICA coverage of at least 60 mm (n = 34, 63% of the subjects), and we identified bends starting from the ICA bifurcation origin back along the artery upstream direction of 60 mm. Of 34 cases, 5 bends were identified in 18 cases, 4 bends in 7 cases, 6 bends in 6 cases, and 3 and 7 bends in 1 case each.

On average, the position of the curvature peak was found to be located roughly at the center of its bend, more precisely at 0.49 ± 0.17 of its length (Figure 8). Analysis of torsion profiles revealed the consistent presence of large peaks corresponding to abrupt changes in the orientation of osculating planes, which visually also corresponded to bend boundaries (Figure 4). The analysis of BTR indicates that the mean torsion of bends excluding the extrema (light gray regions in Figure 4) is 0.64 ± 0.18 times the mean torsion of whole bends (Figure 8). From these results, we conclude that, as a first approximation, the carotid siphon can be described as a sequence of near-planar bends concatenated in a nonplanar fashion. Therefore, their spatial arrangement is well represented by a sequence of planes centered at curvature peaks and oriented as the local plane of curvature (osculating plane) at the peak, as represented in Figure 9.

When bends were subdivided into 2 groups based on whether they hosted an aneurysm, a statistically significant difference was detected (mean BTR, 0.71 ± 0.19 vs 0.62 ± 0.17 for HBs vs non-HBs; $P = .002$), indicating that the inner portion of HBs was more tortuous than that of non-HBs.

Copyright © Congress of Neurological Surgeons. Unauthorized reproduction of this article is prohibited.

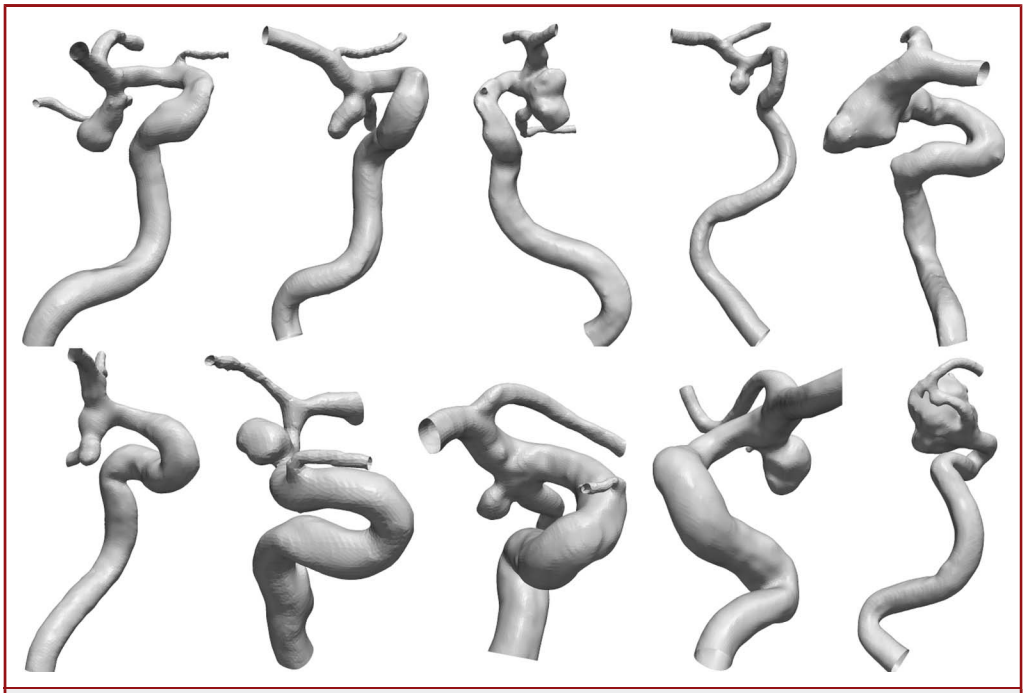

FIGURE 6. *Subset of 3-dimensional models of internal carotid arteries hosting ruptured aneurysms.*

Ruptured/Unruptured Status

Distributions of all the geometric parameters listed in Table 2 computed separately according to rupture status are given in Table 4, which also reports mean values, SDs, and *P* values of *t* tests.

To provide a clear overview of the distribution of geometric parameters within the 2 groups, box-and-whiskers plots are shown for each variable from Figure 10 through 12 according to the quantities being investigated, namely HB geometry, aneurysm position, and orientation with respect to the ICA and angles between aneurysm bifurcation branches. Here, usual graphical conventions are applied: The black continuous line within the box represents the median; the lower and upper bounds of the box represent the 25th and 75th percentiles, respectively; and the whiskers on either side of the box represent the last points that lie within 1.5 of the box height from the lower to the upper bound.

Of all the above parameters, significant differences between ruptured and unruptured groups were found in 7 parameters: 4 were related to the HB geometry $\left(I_{HB}, misr_{HB}, c_{HB}^{max}, t_{HB}^{prox}\right)$ and 3 to the location and orientation of the aneurysm ostium with respect to the parent vessel (abs_{ost}, $D_{ost\text{-}HB}$, $\beta_{upstream}$). Bends hosting ruptured aneurysms are shorter (l_{HB}, 7.32 vs 10.97 mm; $P < .05$), are characterized by a smaller radius ($misr_{HB}$, 1.70 vs 2.00 mm; $P < .05$), and exhibit a lower maximum curvature (c_{HB}^{max}, 0.22 vs 0.29 mm^{-1}; $P < .05$) and a less abrupt torsion peak at the proximal bend boundary (t_{HB}^{prox} , 0.69 vs 1.22 mm^{-2}; $P < .05$) compared with those with unruptured aneurysms.

Ruptured lesions were located in the distal portion of the ICA, significantly closer to the ICA bifurcation and significantly closer to the peak of curvature of the HB than unruptured ones. The majority of aneurysms, 46 of 54, developed along the outer wall of the ICA and 15 were ruptured; the remaining 8 aneurysms were located along the inner wall of the siphon and 2 were ruptured.

Ruptured aneurysms were also characterized by a significantly smaller value of $\beta_{upstream}$ (6.9° vs 12.0°; $P < .001$); ie, the portion of the ICA immediately proximal to the ostium approached the aneurysm with a smaller angle, with the proximal portion of the ICA more aligned to the flow divider in the ruptured group than in the unruptured one.

The remaining parameters did not show any statistically significant difference in their distribution in relation to rupture status. As far as the parent vessel geometry is concerned, c^{mean}, t^{mean}, t^{dist}, and BTR were not different in the 2 groups, and analogously, the bifurcation angles $\beta_{downstream}$ and β_{an} and the angle α_{ost}, quantifying the ostium orientation in relation to the parent vessel, did not differ significantly. The wide distributions of values of the angle α_{ost} imply no preferential orientation of the aneurysm ostium with respect to the HB, emphasizing the presence of high interindividual heterogeneity in the angular location of the ostium around the ICA.

Receiver-operating characteristics analysis for the individual geometric parameters is reported in Table 5 in terms of AUC, optimal threshold of parameters based on the Matthews

Copyright © Congress of Neurological Surgeons. Unauthorized reproduction of this article is prohibited.

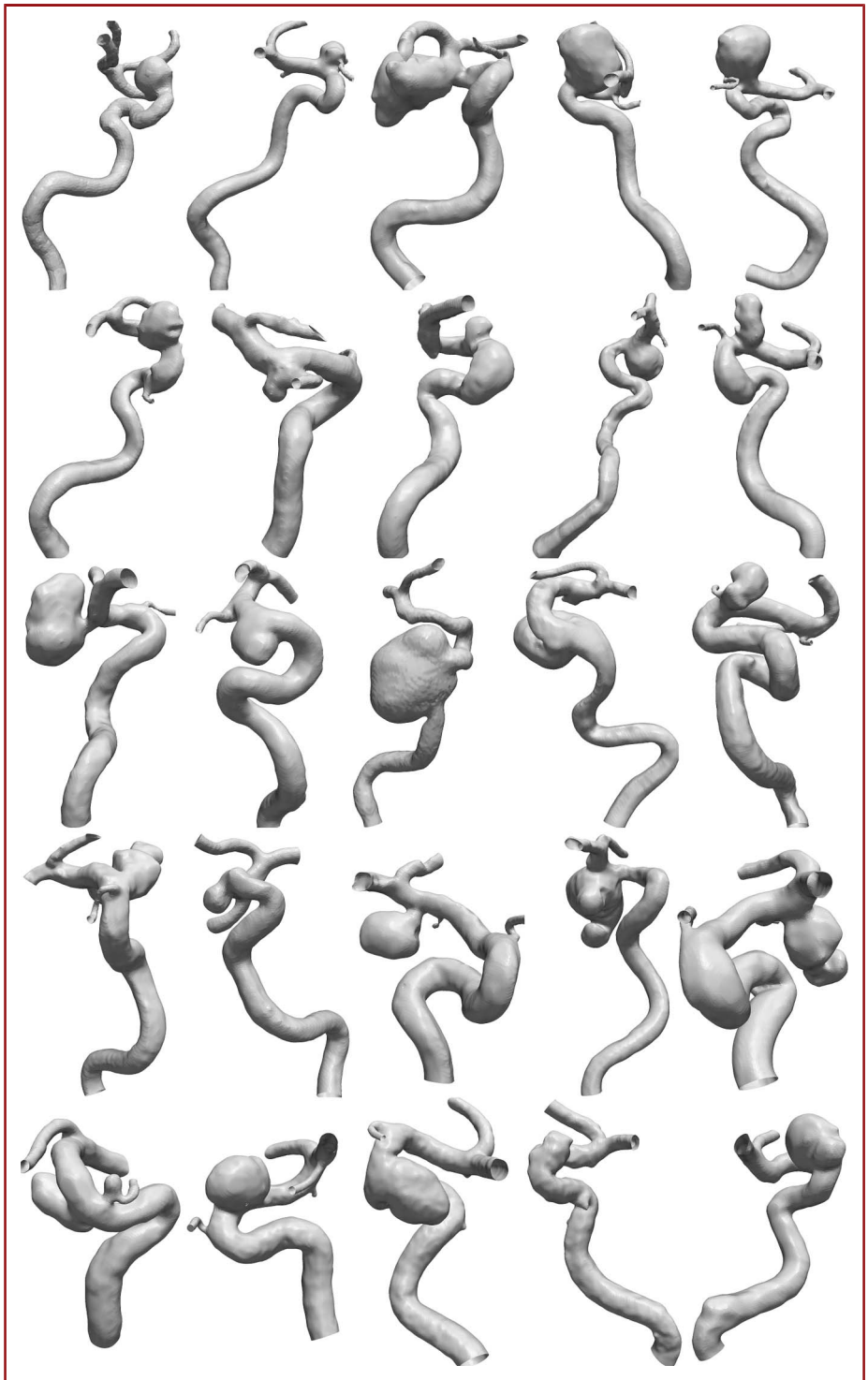

FIGURE 7. *Subset of 3-dimensional models of internal carotid arteries hosting unruptured aneurysms.*

Copyright © Congress of Neurological Surgeons. Unauthorized reproduction of this article is prohibited.

TABLE 3. Mean ± SD, Minimum, and Maximum Values for All Geometric Parameters[a]

Geometric Parameter	Mean ± SD	Minimum	Maximum
l_{HB}	9.82 ± 5.61	3.10	22.90
$misr_{HB}$	1.90 ± 0.49	0.98	3.83
c_{HB}^{mean}	0.19 ± 0.06	0.08	0.36
c_{HB}^{max}	0.27 ± 0.10	0.11	0.51
t_{HB}^{mean}	0.28 ± 0.10	0.10	0.67
t_{HB}^{dist}	0.68 ± 0.78	0.01	4.40
t_{HB}^{prox}	1.05 ± 0.91	0.23	4.04
HB BTR	0.71 ± 0.19	0.28	1.01
abs_{ost}	−12.73 ± 8.38	−1.70	−39.26
$D_{ost\text{-}HB}$	2.08 ± 2.70	0.00	11.30
α_{an}	38.53 ± 22.80	1.51	86.83
$\beta_{upstream}$	10.44 ± 7.44	0.18	31.67
$\beta_{downstream}$	46.59 ± 23.37	4.67	108.78
β_{an}	51.35 ± 22.77	4.78	95.19

[a]See Table 2 for definitions of parameters.

correlation coefficient, and odds ratios. In that table, parameters with AUC ≥ 0.7 are highlighted because they demonstrate some effectiveness in discriminating ruptured from unruptured aneurysms. Of all quantities, abs_{ost} was associated with the highest AUC (0.79), reflecting the fact that ruptured lesions had a tendency to be clustered in the intracranial tract of the ICA. t^{dist} had the second-largest AUC (0.77), followed by c^{max} (0.73). Disregarding the 2 outliers for t^{dist} in the ruptured group led to a statistically significant difference between the groups for the parameter, which explains this seemingly contradictory finding.

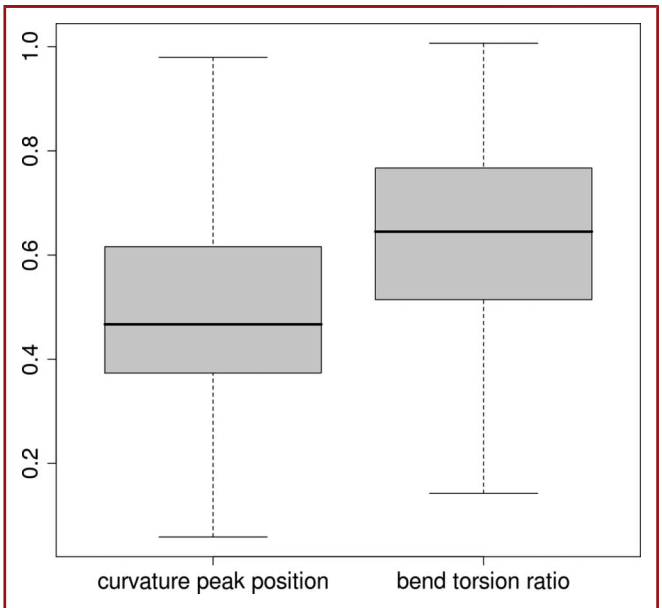

FIGURE 8. *Box plots showing the distribution of the curvature peak within the bend and bend-torsion ratio for all the bends extracted from the models under analysis.*

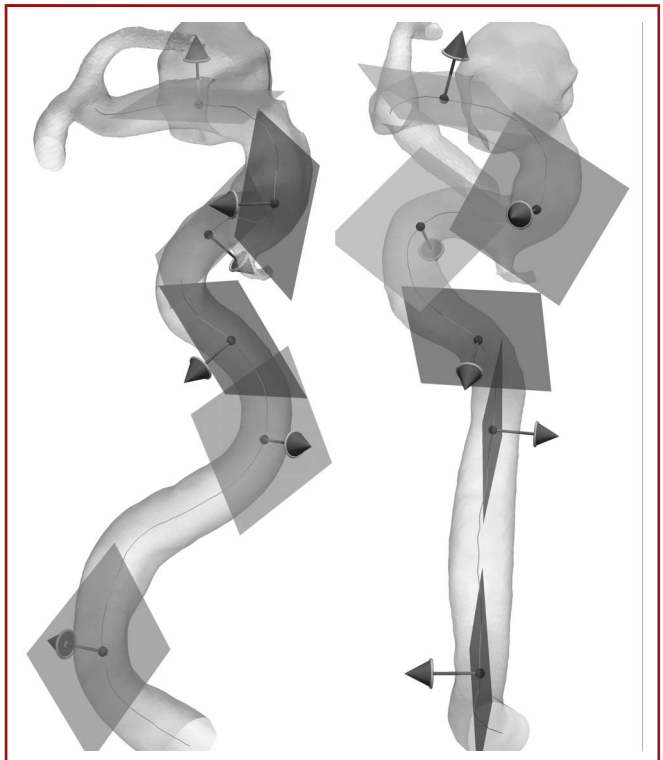

FIGURE 9. *Two views of a 3-dimensional model reporting the internal carotid artery local osculating planes centered at the bend curvature peaks, showing how the carotid siphon can be described as the sequence of near-planar bends concatenated in a nonplanar fashion.*

Multivariate logistic analysis followed by model selection led to an optimal model including only l_{HB}, $\beta_{upstream}$, and $\beta_{downstream}$ as independent variables. The multivariate logistic model takes the form

$$\text{Odds} = \exp\left(0.28 * I_{HB} + 0.239 * \beta_{upstream} + 0.046 * \beta_{downstream} - 6.076\right)$$

where odds in this case expresses the odds of finding an unruptured aneurysm. A summary of the coefficients, *P* values, odds ratios, and 95% confidence intervals is reported in Table 6. The model was characterized by an AUC of 0.84, higher than that of the best individual geometric parameter. The fact that the 3 geometric parameters having the greater AUC did not enter the optimal model has to be evaluated in light of the relations existing between the individual geometric parameters. For instance, distal ICA bends tend to be shorter as they approach the ICA bifurcation, and higher values of $\beta_{upstream}$ and $\beta_{downstream}$ in general imply that the parent vessel is bending more abruptly around the ostium. In other words, the 3 geometric parameters included in the optimal model may not be strongly associated with rupture

Copyright © Congress of Neurological Surgeons. Unauthorized reproduction of this article is prohibited.

TABLE 4. Statistical Analysis of All Geometric Parameters for Ruptured and Unruptured Aneurysm Groups[a]

Geometric Parameter	Ruptured Mean ± SD	Unruptured Mean ± SD	P
l_{HB}	**7.32 ± 3.95**	**10.97 ± 5.93**	**.011**
$misr_{HB}$	**1.70 ± 0.47**	**2.00 ± 0.48**	**.039**
c_{HB}^{mean}	0.16 ± 0.05	0.20 ± 0.07	.053
c_{HB}^{max}	**0.22 ± 0.06**	**0.29 ± 0.10**	**.003**
t_{HB}^{mean}	0.25 ± 0.12	0.29 ± 0.09	.251
t_{HB}^{dist}	0.54 ± 1.16	0.75 ± 0.54	.486
t_{HB}^{prox}	**0.69 ± 0.39**	**1.22 ± 1.04**	**.009**
HB BTR	0.77 ± 0.21	0.68 ± 0.17	.12
abs_{ost}	**−8.48 ± 8.01**	**−14.68 ± 7.89**	**.006**
$D_{ost\text{-}HB}$	**1.18 ± 1.14**	**2.50 ± 3.10**	**.012**
α_{ost}	37.92 ± 23.71	38.82 ± 22.70	.90
$\beta_{upstream}$	**6.93 ± 4.95**	**12.05 ± 7.89**	**.027**
$\beta_{downstream}$	46.01 ± 20.30	46.86 ± 24.92	.90
β_{an}	50.30 ± 20.40	51.84 ± 24.03	.81

[a]Bold indicates statistically significant *t* tests.

status individually, but when taken in combination, they tend to carry a part of the information represented in other parameters.

DISCUSSION

In the study of aneurysm hemodynamics, several authors have underlined the importance of considering the configuration of the parent artery and its geometric relation to the aneurysm itself. Castro et al[10] investigated the sensitivity of computational fluid dynamics simulations to the truncation of the parent artery included in patient-specific models, stressing the impact of the upstream parent artery curvature on the computed flow fields. Sato et al[11] performed a parametric study of idealized models that showed how differences in the aneurysm configuration relative to the parent artery affected intra-aneurysmal flow patterns and hemodynamic variables to a higher degree than sac shape and size.

To the best of our knowledge, however, few works have directly coped with a quantitative characterization of the 3D geometry of cerebral aneurysms and their parent vessels and with the search for evidence of relationships between specific morphological features and aneurysm formation, progression, or risk of rupture. Such effort has 2 possible levels of interest. On one hand, it is a step toward the identification of candidate markers to be monitored for the global evaluation of aneurysms status; in this respect, a strong correlation between morphological indexes and rupture status could have a significant prognostic role. On the other hand, because geometry affects hemodynamics, this is a step toward the identification of possible links between blood flow and related indexes (such as WSS) and aneurysm development.

In this study, the complex geometric relationships between ICA lateral aneurysms and their parent vessels were quantitatively investigated in a population of 54 aneurysms. For each case, a 3D model of the ICA including the aneurysm was reconstructed, and centerlines were automatically generated along the carotid siphon and through the aneurysm ostium. Global ICA geometry and the geometry of individual bends were characterized in relation to the presence, location, and orientation of aneurysms. All geometric parameters were tested for differences between ruptured and unruptured aneurysm groups.

ICA Geometry

In light of the present results, the ICA can be described as a sequence of near-planar bends concatenated in a nonplanar fashion. These concepts are shown in Figure 9, in which the spatial arrangement of ICA bends is well represented by the sequence of planes located at curvature peaks and oriented as the local plane of curvature.

The geometric description of the ICA siphon confirmed the heterogeneity that characterizes cerebral vasculature, reflected by the variability in the number and magnitude of curvature and torsion peaks. Nevertheless, common patterns could be identified. The curvature peak was almost invariably found very close to the middle of the bend, and torsion exhibits mild changes in the central portion of the bend, in contrast to abrupt changes at its outer boundaries.

Among the geometric parameters studied in this work, t^{prox} basically quantifies the rate of rotation between the bend preceding the HB and the HB itself. Different configurations in the concatenation of ICA bends may give rise to a wide range of possible hemodynamic solicitations along the arterial wall.[23] Lee et al[24] recently studied fluid dynamics in double bends, paying particular attention to the effect of their nonplanar concatenation. In their simulations, the terminal bend influences the outflow pattern to a different extent, depending on the orientation of its upstream bend.

To the best of our knowledge, with the exception of selected works,[23,24,25] fluid dynamics in tortuous vessels has not been thoroughly investigated. Further studies are needed to fully understand the coupled effects of torsion and curvature that seem to be dominant in determining hemodynamic patterns in the ICA siphon and how such patterns are eventually involved in the development of lateral aneurysms.

Aneurysm Location and Orientation

Aneurysmal lesions in our population developed preferably in the intracerebral space and within the HB, close to the peak of curvature and mostly along the outer wall of the parent vessel. In addition, the tract of artery hosting an aneurysm appears more tortuous than portions of parent artery without lesions.

As a first observation, aneurysms most commonly developed in the intracerebral space. Here, different structural and biological properties of the vessel wall and of the perianeurysmal environment may amplify the effects of hemodynamic forces acting on the wall.[26] The position of aneurysms inside their HBs revealed that they are, in general, located close to the point of maximal curvature within the HB, where the region of flow impingement

Copyright © Congress of Neurological Surgeons. Unauthorized reproduction of this article is prohibited.

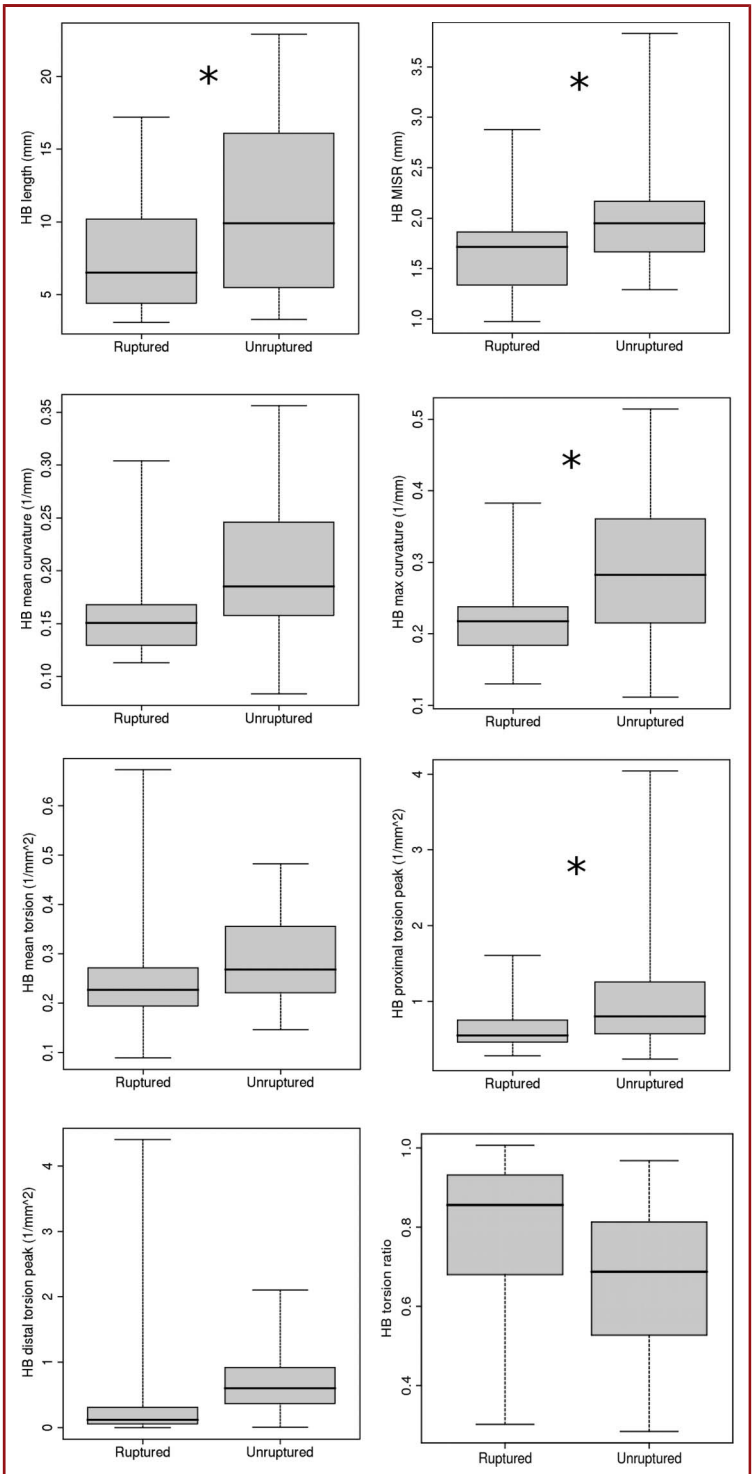

FIGURE 10. *Box plots showing the distribution of the geometric parameters relative to the hosting bend (HB) computed separately for the ruptured and unruptured groups. Top row, l_{HB} (left) and $misr_{HB}$ (right); second row, c_{HB}^{mean} (left) and c_{HB}^{max} (right) curvature; third row, t_{HB}^{mean} (left) and t_{HB}^{prox}; bottom row, t_{HB}^{dist} (left) and HB bend-torsion ratio (right). *Statistically significant difference.*

Copyright © Congress of Neurological Surgeons. Unauthorized reproduction of this article is prohibited.

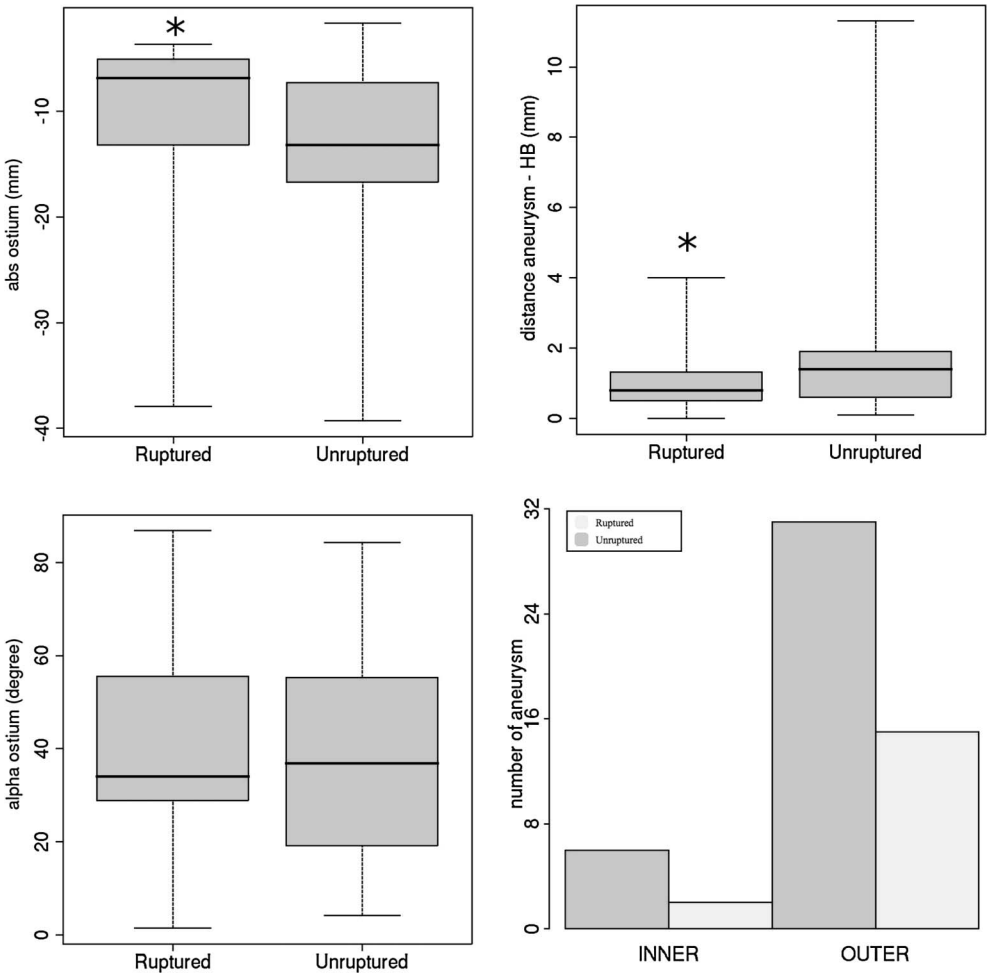

FIGURE 11. *Box plots showing the distribution of geometric parameters computed separately for the ruptured and unruptured groups. Top row, abs_{ost} (left) and $D_{ost\text{-}HB}$ (right); bottom row, α_{ost} (left) and ICA $wall_{ost}$ (right). *Statistically significant difference.*

is expected to occur. In addition, almost all aneurysm ostia were positioned on the outer wall of siphon bends, where the action of hemodynamic forces is expected to be stronger as a result of the effect that curvature exerts on flow.

The analysis of the BTR of ICA bends revealed a statistically significant difference between bends hosting a lesion and those that did not, the former being more uniformly tortuous than the latter. Whether the increased tortuosity of bends hosting aneurysms is an effect rather than a cause of aneurysm development is not possible to assess in the context of the present study.

Tortuosity and nonplanarity may explain the lack of a uniform orientation of aneurysm ostia with respect to the osculating plane of the HB as a result of their tight link with complex hemodynamics. In a recent study,[25] blood flow patterns and WSS distribution were studied in 5 transparent postmortem casts of the ICA siphon. The authors underlined the presence of low WSS in areas other than the inner bends because of the presence of a strong helicoidal flow determined by the sequence of bends along the ICA.

The connections between our findings and hemodynamic factors are provided as a possible key for interpretation and as a hint for future investigations on this subject. Because of the nature of our study, we cannot provide any evidence on a role for hemodynamics in determining aneurysmal pathogenesis.

Aneurysm Rupture Status

Given the dramatic clinical consequences of aneurysm rupture, identification of prognostic indexes for the detection of lesions that are more likely to rupture is of utmost importance. From our

Copyright © Congress of Neurological Surgeons. Unauthorized reproduction of this article is prohibited.

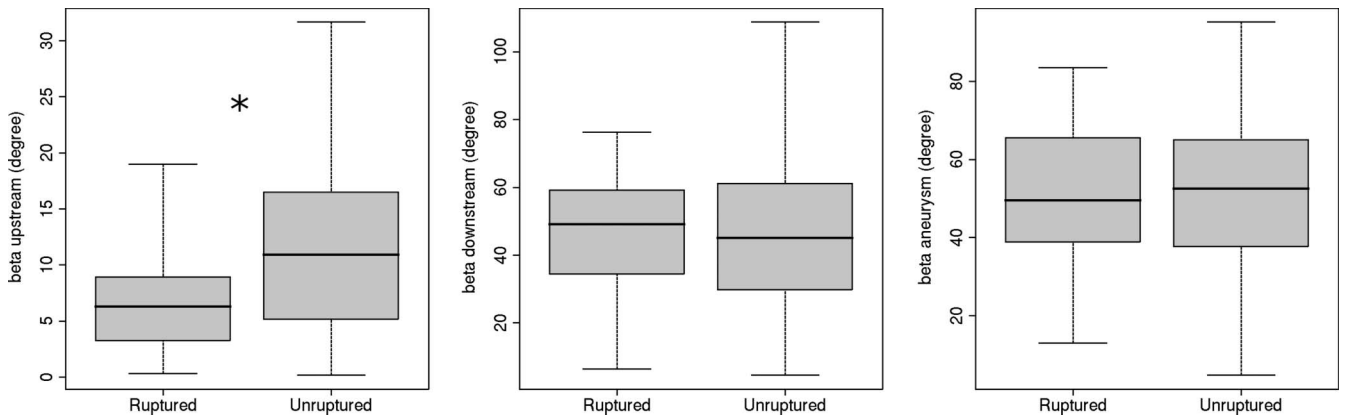

FIGURE 12. *Box plots showing the distribution of the angles between aneurysm bifurcation branches computed separately for the ruptured and unruptured group. From left to right,* $\beta_{upstream}$, $\beta_{downstream}$, *and* β_{an}. **Statistically significant difference.*

results, a geometric description of ruptured aneurysms in relation to the hosting vessel in our patient population can be outlined:

1) Ruptured lesions occurred in distal portions of the ICA, along the outer wall of the parent vessel, with various orientations with respect to the curvature plane and closer to the bend peak of curvature than unruptured ones.
2) Bends hosting ruptured aneurysms were shorter with a smaller radius, a less marked peak of curvature, and a less abrupt torsion peak at the proximal bend boundary compared with those hosting unruptured aneurysms.
3) The upstream tracts of the parent vessel in ruptured aneurysms approached the aneurysm ostium at a smaller angle, so that they tended to align more with the flow divider than their unruptured counterparts.

Ruptured aneurysms occurred in the distal tract of the ICA, significantly closer to the distal ICA bifurcation, hinting at differences in ICA aneurysm rupture status between the intracerebral and extracerebral spaces. Within the HB, ruptured lesions were also located closer to the curvature peak than unruptured ones. Ruptured aneurysms therefore seemed to be consistently closer to the expected site of flow impingement on the lateral wall of the bend.

At the same time, bends hosting ruptured aneurysms exhibited smaller curvature peaks than unruptured aneurysms, a finding also indirectly reflected by the results of the multivariate logistic regression analysis. Hoi et al[13] studied idealized models of an aneurysm developing on a curved artery for increasing curvature radius of the vessel; they observed that the flow impingement area linearly intensifies with the parent artery curvature, but the orientation of the aneurysm and the geometry of the upstream portion of the vessel were not considered in the analysis. As for proximal torsion, also significantly different in the 2 groups, Lee

TABLE 5. Receiver-Operating Characteristics Curve Analysis of the Geometrical Parameters[a]

Geometric Parameter	AUC	Optimal Threshold	Odds Ratio
l_{HB}	**0.70**	**11.00**	**6.38**
$misr_{HB}$	0.69	1.29	Infinity
c_{HB}^{mean}	0.66	0.18	6.13
c_{HB}^{max}	**0.73**	**0.25**	**9.72**
t_{HB}^{mean}	0.67	0.24	4.33
t_{HB}^{dist}	**0.77**	**0.27**	**12.40**
t_{HB}^{prox}	0.67	0.76	5.34
HB torsion ratio	0.33	0.38	7.86
abs_{ost}	**0.79**	**8.51**	**20.00**
$D_{ost\text{-}HB}$	0.63	0.90	3.82
α_{ost}	0.52	4.16	Infinity
$\beta_{upstream}$	**0.70**	**9.93**	**6.13**
$\beta_{downstream}$	0.49	83.02	Infinity
β_{an}	0.52	88.79	Infinity

[a]See Table 2 for a definition of parameters. Area under the curve (AUC), optimal threshold according to the Matthews correlation coefficient, and odds ratio are reported.
Parameters having AUC ≥ 0.70 are shown in bold.

TABLE 6. Multivariate Logistic Regression Model Selected Through Minimization of the Akaike Information Criterion Among All Models with up to 7 Covariates

Geometric Parameter	β	*P*	Odds Ratio	95% Confidence Interval
l_{HB}	0.288	0.003	1.333	1.099-1.618
$\beta_{upstream}$	0.239	0.005	1.270	1.073-1.502
$\beta_{downstream}$	0.046	0.04	1.047	1.003-1.093

Copyright © Congress of Neurological Surgeons. Unauthorized reproduction of this article is prohibited.

et al[24] demonstrated a dependence of flow patterns on the geometry and orientation of the upstream bend and showed a strong relationship between flow patterns and the magnitude of the rotation angle, here reflected by proximal torsion. On the other hand, an intuitive interpretation of the role of distal torsion as a predictor of rupture status, as evidenced by receiver-operating characteristics analysis, remains elusive and deserves further study.

Finally, the angle of approach of the ICA at the aneurysm region was found to be smaller in the ruptured compared with the unruptured group. The smaller the value of $\beta_{upstream}$ is, the more the upstream parent artery is aligned to the aneurysm bifurcation flow divider, ie, to the aneurysm wall at the distal side of the ostium. A smaller $\beta_{upstream}$ and, to a lesser extent, a concomitant smaller $\beta_{downstream}$, as highlighted by the multivariate analysis, may therefore affect the extension of the impingement area and aneurysm inflow rates.

It is important to underline that the connections to hemodynamics reported above are only given as possible keys for interpretation and are speculative. A thorough evaluation of the role of each parameter in determining aneurysmal hemodynamics and an assessment of any link of causality between geometric features and rupture status are beyond the scope of the present paper.

Study Limitations

A first limitation of the present study is related to the imaging modality used. Patients were selected from a population that underwent 3D-RA following clinical routine, but indication for 3D-RA sometimes derives from the presence of large or complex aneurysms. The increasing availability of high-resolution computed tomography and magnetic resonance scanners will make it possible to extend a 3D arterial study to a larger number of subjects and to decrease the bias in the selection of the population in future studies.

Related to the above, the skew of the population toward larger aneurysms may have led to cases in which the presence of aneurysms affects the geometry of the parent vessel. This is a problem common to all retrospective studies on this topic, and it is not easily solvable unless prospective, follow-up data are collected, which is extremely challenging because of the nature of the disease.

Also related to subject selection as a result of indications for 3D-RA, our consecutive sample unavoidably included a greater number of unruptured aneurysms (37) than ruptured aneurysms (17). This discrepancy did not translate into systematic differences in the SDs of geometric parameters between the 2 groups, which allowed us to consider the patient distribution appropriate for our analysis.

Because of a lack in the systematic visibility of ICA side branches in the imaging data such as the ophthalmic, posterior communicating, and choroidal arteries, the presence and position of such side branches in the aneurysm region, a frequent occurrence in vivo, were not taken into account in the present analysis. Improvements in the resolution of image acquisition systems may allow proper inclusion of this important aspect in future studies.

In some, if not all, of the hemodynamic implications for the geometric quantities under scrutiny, the size of the ostium may play an important role in determining the history of the disease, for instance, through its influence on the volume of blood entering the aneurysm and on washout mechanisms. Although we are aware of its importance, this parameter, as well as all parameters related to the aneurysm sac, was not investigated in the present work. A detailed geometric characterization of the aneurysmal sac is the subject of ongoing work on the present population.

We have shown how our results are, in principle, in accordance with hemodynamic findings provided by previous works available in the literature. However, we have not demonstrated these associations directly by computational fluid dynamics analysis in the present study, which was instead focused on geometric characterization. At this point, our findings are subject to verification in the context of a study on patient-specific hemodynamics, currently being performed as part of the ANEURISK project.

CONCLUSION

In the present study, the potential of 3D geometric analysis for highlighting features of the ICA associated with the position and orientation of cerebral aneurysms and their rupture status has been demonstrated. Our results may provide a first step toward the definition of new geometric quantities to be used as surrogates for rupture risk stratification, as well as hints for future studies aimed at the identification of hemodynamic factors influencing the natural history of intracranial aneurysms.

Disclosure

The Aneurisk project has been supported by Fondazione Politecnico di Milano, Italy, with the fundamental support of SIEMENS Medical Solutions, Italy. The authors have no personal financial or institutional interest in any of the drugs, materials, or devices described in this article.

REFERENCES

1. Van Gijn J, Kerr RS, Rinkel GJ. Subarachnoid haemorrhage. *Lancet*. 2007;369(9558):306-318.
2. Sforza DM, Putman CM, Cebral JR. Hemodynamics of cerebral aneurysms. *Annu Rev Fluid Mech*. 2009;41(1):91-107.
3. Foutrakis GN, Yonas H, Sclabassi RJ. Saccular aneurysm formation in curved and bifurcating arteries. *AJNR Am J Neuroradiol*. 1999;20(7):1309-1317.
4. Steinman DA, Milner JS, Norley CJ, Lownie SP, Holdsworth DW. Image-based computational simulation of flow dynamics in a giant intracranial aneurysm. *AJNR Am J Neuroradiol*. 2003;24(4):559-566.
5. Cebral JR, Castro MA, Appanaboyina S, et al. Efficient pipeline for image-based patient-specific analysis of cerebral aneurysm hemodynamics: technique and sensitivity. *IEEE Trans Med Imaging*. 2005;24(4):457-467.
6. Friedman MH. Variability of 3D arterial geometry and dynamics, and its pathologic implications. *Biorheology*. 2002;39(3–4):513-517.
7. Lee SW, Antiga L, Spence JD, Steinman DA. Geometry of the carotid bifurcation predicts its exposure to disturbed flow. *Stroke*. 2008;39(8):2341-2347.
8. Raghavan ML, Ma B, Harbaugh RE. Quantified aneurysm shape and rupture risk. *J Neurosurg*. 2005;102(2):355-362.
9. Ma B, Harbaugh RE, Raghavan ML. Three-dimensional geometrical characterization of cerebral aneurysms. *Ann Biomed Eng*. 2004;32(2):264-273.
10. Castro MA, Putman CM, Cebral JR. Computational fluid dynamics modeling of intracranial aneurysms: effects of parent artery segmentation on intra-aneurysmal hemodynamics. *AJNR Am J Neuroradiol*. 2006;27(8):1703-1709.
11. Sato K, Imai Y, Ishikawa T, Matsuki N, Yamaguchi T. The importance of parent artery geometry in intra-aneurysmal hemodynamics. *Med Eng Phys*. 2008;30(6):774-782.

Copyright © Congress of Neurological Surgeons. Unauthorized reproduction of this article is prohibited.

12. Imai Y, Sato K, Ishikawa T, Yamaguchi T. Inflow into saccular cerebral aneurysms at arterial bends. *Ann Biomed Eng*. 2008;36(9):1489-1495.
13. Hoi Y, Meng H, Woodward SH, et al. Effects of arterial geometry on aneurysm growth: three-dimensional computational fluid dynamics study. *J Neurosurg*. 2004;101(4):676-681.
14. Dhar S, Tremmel M, Mocco J, et al. Morphology parameters for intracranial aneurysm rupture risk assessment. *Neurosurgery*. 2008;63(2):185-196.
15. Piccinelli M, Veneziani A, Steinman DA, Remuzzi A, Antiga L. A framework for geometric analysis of vascular structures: application to cerebral aneurysms. *IEEE Trans Med Imaging*. 2009;28(8):1141-1155.
16. Antiga L, Steinman DA. Robust and objective decomposition and mapping of bifurcating vessels. *IEEE Trans Med Imaging*. 2004;23(6):704-713.
17. Sangalli ML, Secchi P, Vantini S, Veneziani A. Efficient estimation of three dimensional curves and their derivatives by free knot regression splines, applied to the analysis of inner carotid artery centerlines. *J Roy Stat Soc C, Appl Stat*. 2009;58(3):285-306.
18. Sangalli ML, Secchi P, Vantini S, Veneziani A. A case study in exploratory functional data analysis: geometrical features of the internal carotid artery. *J Am Stat Assoc*. 2009;104(485):37-48.
19. Antiga L, Piccinelli M, Botti L, et al. An image-based modeling framework for patient-specific computational hemodynamics. *Med Biol Eng Comput*. 2008;46(11):1097-1112.
20. Vascular Modeling Toolkit.http://www.vmtk.org. Accessed October19, 2009.
21. R Development Core Team. *R: A Language and Environment for Statistical Computing*. Vienna, Austria: R Foundation for Statistical Computing. http://www.R-project.org. Accessed October 19, 2009.
22. Müller HR, Brunhölzl C, Radü EW, Buser M. Sex and side differences of cerebral arterial caliber. *Neuroradiology*. 1991;33(3):212-216.
23. Caro CG, Doorly DJ, Tarnawski M, et al. Non-planar curvature and branching of arteries and non-planar-type flow. *Proc Roy Soc*. 1996;452(1944):185-197.
24. Lee KE, Parker KH, Caro CG, Sherwin SJ. The spectral/hp element modeling of steady flow in non planar double bends. *Int J Numer Meth Fluids*. 2006;57(5):519-529.
25. Takeuchi S, Karino T. Flow patterns and distributions of fluid velocity and wall shear stress in the human internal carotid and middle cerebral arteries [published online ahead of print October 22, 2009]. *Surg Neurol*. doi: 10.1016/j.surneu.2009.03.030.
26. Sforza DM, Putman CM, Cebral JR. Hemodynamics of cerebral aneurysms. *Annu Rev Fluid Mech*. 2009;41(1):91-107.

Acknowledgment

In memory of Dr M. Collice.

COMMENT

Dr Piccinelli and colleagues are to be congratulated for this important work. Their analysis of the geometry of the intracranial vasculature associated with unruptured or ruptured intracranial aneurysms adds to the growing body of work on the importance of geometric features other than aneurysm size as regards aneurysm rupture.

Identifying prognostic indicators of cerebral aneurysm rupture is an area of considerable importance. Aneurysm size is widely regarded as one determinant of rupture. It is easily measured from routine angiograms and would seem to be a logical choice given that larger aneurysms are more likely to rupture.[1] However, data from large population studies suggest that size alone is not a reliable index of rupture risk.[2] It is reasonable to speculate that other aspects of aneurysm morphology such as lesion shape or the configuration of the parent vessel may also play a role.

Since I first reported the use of 3-dimensional computed tomographic angiography in the diagnosis of intracranial vascular disease $>$ 18 years ago,[3] this imaging modality has proven to be of considerable value not only for clinical neurosurgery but also for giving us considerably greater insight into the geometry of the intracranial vasculature. Three-dimensional digital imaging reveals that geometric features of intracranial aneurysms and the associated vasculature vary widely among aneurysms of similar sizes. However, there has been little research to rigorously assess geometric features other than size as prognostic indicators of rupture.

Until recently, studies on lesion shape have been confined to using 2-dimensional data (eg, aspect ratio), which do not reveal the complex 3-dimensional features of the aneurysm and parent vessels. Data from computed tomography angiography, rotational digital subtraction angiography, or magnetic resonance angiography, on the other hand, allow complete characterization of 3-dimensional lesion geometry.

Our group first reported on a methodology to quantify 3-dimensional size and shape of cerebral aneurysms.[4] Using data from 3-dimensional computed tomographic angiography of aneurysm patients, we developed and reported a methodology to quantify the 3-dimensional size and shape of these lesions using techniques in differential and computational geometry.[4] Subsequently, we performed a preliminary investigation of ruptured and unruptured intracranial aneurysms and found that certain 3-dimensional shape features statistically distinguished ruptured lesions from unruptured ones, whereas all the size indexes failed to do so.[5]

We need to continue to look for ways to improve our ability to predict the risk of rupture of intracranial aneurysms. Ideally, we will find indexes that integrate geometric characteristics of the aneurysm with other factors such as the geometry of the surrounding vasculature, blood pressure, and aneurysm wall characteristics. Such an integrated biomechanical index, along with a better understanding of the genetic, epigenetic, and environmental factors that lead to aneurysm growth and rupture, will be needed to accurately assess the risk of aneurysm rupture. Preferably, such integrative indexes will not be based on phenomenological regression models alone but will include the logic and physics of biomechanics.[6,7]

From a biomechanical standpoint, the hemodynamics inside the aneurysm sac and the mechanical tension on the sac wall will be affected by lesion size and shape and the configuration of the surrounding vasculature. For instance, recent computational fluid dynamics investigations and finite-element analyses of selected aneurysms by our group suggest that aneurysm shape is a determinant of wall shear stress and pressure-induced wall tension.[6,7] Because shear stress and wall stress may be related to the phenomenon of rupture, we believe that aneurysm geometry and biomechanics will be important components of the integrative indexes needed to accurately assess the risk of aneurysm rupture. I believe the authors of this article share this vision and have made a significant contribution to this field of study.

Robert E. Harbaugh
Hershey, Pennsylvania

1. Wiebers DO, Whisnant JP, Huston J III, et al. Unruptured intracranial aneurysms: natural history, clinical outcome, and risks of surgical and endovascular treatment. *Lancet*. 2003;362(9378):103-10.
2. Weir B. Unruptured intracranial aneurysms: a review. *J Neurosurg*. 2002;96(1):3-42.
3. Harbaugh RE, Schlusselberg DS, Jeffery R, Hayden S, Cromwell LD, Pluta D. Three dimensional computerized tomography angiography in the diagnosis of cerebrovascular disease. *J Neurosurg*. 1992;76:408-414.
4. Ma B, Harbaugh RE, Raghavan ML. Three-dimensional geometrical characterization of cerebral aneurysms. *Ann Biomed Eng*. 2004;32(2):264-273.
5. Raghavan ML, Ma B, Harbaugh RE. Quantified aneurysm shape and rupture risk. *J Neurosurg*. 2005;102(2):355-362.
6. Ma B, Lu J, Harbaugh RE, Raghavan ML. Nonlinear anisotropic stress analysis of anatomically realistic cerebral aneurysms. *J Biomed Eng*. 2007;129:88-96.
7. Zhou1 X, Raghavan ML, Harbaugh RE, Lu J. Patient-specific wall stress analysis in cerebral aneurysms using inverse shell model. *Ann Biomed Eng*. 2010;38(2):478-489.

Copyright © Congress of Neurological Surgeons. Unauthorized reproduction of this article is prohibited.

Packed Red Blood Cell Transfusion and Decreased Mortality in Intracerebral Hemorrhage

Kevin N. Sheth, MD*
Aaron J. Gilson, BA‡
Yuchiao Chang, PhD§
Mona A. Kumar, MD#
Rosanna M. Rahman, PhD‡
Natalia S. Rost, MD‖
Kristin Schwab, BA‡
Lynelle Cortellini, BA‡
Joshua N. Goldstein, MD, PhD¶
Eric E. Smith, MD, MPH**
Steven M. Greenberg, MD, PhD‖
Jonathan Rosand, MD, MSc‡‖

*Department of Neurology, Division of Stroke and Neurocritical Care, University of Maryland Medical Center, Baltimore, Maryland; ‡Center for Human Genetic Research, §Department of Medicine, ‖Division of Neurocritical Care and Emergency Neurology, ¶Department of Emergency Medicine, Massachusetts General Hospital, Boston, Massachusetts; #Department of Neurology, Stroke and Neurocritical Care Division, Thomas Jefferson University Hospital, Philadelphia, Pennsylvania; **Calgary Stroke Program, Department of Clinical Neurosciences, University of Calgary, Calgary, Alberta, Canada

Correspondence:
Kevin N. Sheth, MD,
Department of Neurology,
University of Maryland Medical Center,
110 S. Paca Street, 3rd Floor,
Baltimore, MD 21201.
E-mail: ksheth@som.umaryland.edu

Received, April 8, 2010.
Accepted, September 27, 2010.

Copyright © 2011 by the
Congress of Neurological Surgeons

BACKGROUND: Accumulating data suggest that anemia worsens outcomes in critically ill patients, including those with subarachnoid and intracerebral hemorrhage (ICH). Although packed red blood cell (PRBC) transfusion appears to increase brain tissue oxygen, it is unknown whether such transfusions, which are commonly administered in patients with intracranial hemorrhage, alter outcome.

OBJECTIVE: Following up on our observation that anemia is associated with poor outcome in patients with ICH, we investigated whether PRBC transfusion was associated with any benefit.

METHODS: Five hundred forty-six consecutive subjects were identified from an ongoing single-center, prospective cohort study of nontraumatic ICH over a 6-year period. Clinical and radiographic characteristics, laboratory values including admission and daily mean hemoglobin values, and all instances of PRBC transfusion were recorded. Aggressiveness of care was assessed by whether the patient had a "do not resuscitate" order activated during hospitalization. The primary endpoint was 30-day survival.

RESULTS: Anemia was present in 144 of 546 patients (26%) on admission and developed subsequently in an additional 250, leaving just 152 of 546 patients (28%) who never developed anemia. PRBC transfusion was administered to 100 patients (18%) during their hospital stay, 98% of whom were anemic. In multivariable analysis, PRBC transfusion was associated with improved survival at 30 days (odds ratio: 2.76; 95% confidence interval: 1.45-5.26; $P = .002$).

CONCLUSION: Anemia develops in the majority of patients with ICH at some point during their hospitalization. PRBC transfusion was associated with improved outcome in these patients.

KEY WORDS: Anemia, Cerebral Hemorrhage, Intensive care unit, Stroke, Transfusion

Neurosurgery 68:1286–1292, 2011 DOI: 10.1227/NEU.0b013e31820cccb2 www.neurosurgery-online.com

Intracerebral hemorrhage (ICH) is the most devastating form of stroke. As many as 40% of those afflicted die within 30 days, and only 20% of survivors are functionally independent at 6 months.[1,2] Currently, there are no proven treatments for acute ICH. Recent studies suggest that hemoglobin concentrations inversely correlate with outcome in subarachnoid hemorrhage,[3,4] and a previous study from our group demonstrated a similar relationship in patients with ICH.[5]

ABBREVIATIONS: CMO, comfort measures only; **DNR**, do not resuscitate; **GCS**, Glasgow Coma Scale; **ICH**, intracerebral hemorrhage; **PRBC**, packed red blood cell

Despite data suggesting that lower hemoglobin concentrations may adversely affect outcome, there is controversy over whether correction of anemia will, in turn, provide benefit. Transfusion of packed red blood cells (PRBCs) appears to improve brain tissue oxygenation in patients with traumatic brain injury[6] and subarachnoid hemorrhage,[7] but whether this effect translates to a clinical benefit is unknown.

In search of an optimal hemoglobin level for critically ill patients, the landmark TRICC (transfusion requirements in critical care) trial compared a restrictive (target hemoglobin level 7-9 g/dL) and liberal (target hemoglobin level 10-12 g/dL) strategy in intensive care unit patients and found that patients with liberal targets had higher mortality rates.[8] However, less than 10% of

Copyright © Congress of Neurological Surgeons. Unauthorized reproduction of this article is prohibited.

patients in this study had a neurological diagnosis, and the majority of those patients were in the restrictive group. There are other groups of critically ill patients, such as those with ST-segment elevation myocardial infarction in whom a liberal transfusion strategy may be beneficial.[9]

Prompted by our observations that anemia on presentation was an independent predictor of 30-day mortality in patients with ICH and that this effect appeared to be mediated in part by a relationship between lower hemoglobin values and larger hematoma volumes,[5] we investigated the natural history of anemia during hospitalization for acute ICH and whether PRBC transfusion was associated with improved outcome.

METHODS

Study subjects consisted of consecutive patients with primary computed tomography scan-confirmed ICH computed, admitted through the emergency department (ED) of the Massachusetts General Hospital (MGH) between January 1, 1999, and October 31, 2005, for whom serial laboratory data were available. As described previously,[2] patients were recruited as participants in an ongoing prospective cohort study of ICH outcome and were followed after discharge for 30-day survival.[10] Patients younger than 18 years of age or with ICH secondary to antecedent head trauma, acute ischemic stroke with hemorrhagic transformation, brain tumor, vascular malformation, venous thrombosis, vasculitis of the central nervous system, or other secondary causes were excluded. Subjects with hematological malignances, blood dyscrasia, or coagulopathy were also excluded. All aspects of this study were approved by the local institutional review board, and all patients provided informed consent.

This was a retrospective review of prospectively collected data. Demographic data, including age, sex, and race, as well as clinical and laboratory data, were recorded at time of admission. Patients were identified as hypertensive on the basis of clinical history or if they required antihypertensive therapy at least 2 weeks after the onset of ICH. Diabetes mellitus was defined by a history of the diagnosis or by regular use of insulin or oral hypoglycemic agents before hemorrhage. Coronary artery disease was defined by a history of coronary artery disease, angina, or myocardial infarction. Previous ischemic stroke was defined as any clinical history of cerebral infarction as reported by the patient. A complete medical and medication history was obtained, including regular use of warfarin or an antiplatelet agent. Any history of alcohol or tobacco use was recorded as positive. Glasgow Coma Scale (GCS) scores were assessed and recorded on admission.

As in previous studies,[5] anemia was defined as a hemoglobin level less than 12.1 g/dL for women and less than 13.1 for men, according to World Health Organization criteria.[11] The first recorded hemoglobin value (g/dL) in the MGH ED was used to determine anemic status on admission. Among patients transferred from referring hospital EDs to the MGH ED, none received transfusions of PRBCs before transfer. The MGH Research Patient Data Registry was queried using an online tool to retrieve serial laboratory data from each patient's hospitalization. Patients were assessed daily for the development of anemia based on their average daily hemoglobin values. Transfusion status was assigned based on whether the patient received a PRBC transfusion during his or her hospital stay.

All baseline computed tomography scans were analyzed using computer-assisted methods for ICH location and ICH volume as previously described.[2] Image analysis was performed by study staff blinded to the patient's clinical status and other radiographic studies according to a method with high interrater reliability.[12] Patients with primary intraventricular hemorrhage were excluded from the analysis.

Physiological parameters such as admission systolic and diastolic blood pressure were obtained from ED intake forms. Recorded laboratory parameters included baseline serum glucose level (g/dL), white blood cell (WBC) count (g/dl), first platelet count, and first coagulation profile. The intensity of anticoagulation, recorded as the prothrombin time (PT), was the value determined in the ED on presentation. For those patients initially evaluated at a referring hospital, the PT recorded is the value determined in the referring ED before administration of therapy. The institution of a "do not resuscitate" (DNR) order was used as an indication of aggressiveness of care. Paper charts, electronic admission notes, and discharge summaries were reviewed for any text including the terms DNR, do not resuscitate, comfort measure only (CMO), or withdrawal of care by trained research assistants. Text that was unclear was reviewed by a physician (J.G.). In addition, the hospital's computerized order entry system was reviewed for all orders regarding limitation of care of any kind.

The primary outcome of interest was mortality at 30 days after ICH. For patients in whom 30-day outcome was not available from medical records, follow-up phone calls were made to determine mortality. Survival after 30 days was systematically confirmed using the Social Security Death Index.[13]

STATISTICAL METHODS

Continuous variables are summarized using median and interquartile range unless stated otherwise. Patient characteristics were compared using the Fisher exact test for categorical variables and Wilcoxon rank-sum test for continuous variables. The Fisher exact tests were used to identify univariate predictors of 30-day mortality. The multivariable model predicting 30-day mortality included predictors identified in the univariate analysis with $P < .2$. All analyses were performed using SAS software (SAS Institute, Cary, North Carolina).

RESULTS

There were 546 patients who met eligibility criteria. The median age was 73 years. The majority of patients were white, and 238 (44%) were female; 121 (22%) were taking warfarin at the time of their ICH and 227 (45%) patients were taking an antiplatelet agent. One hundred patients (18%) received at least 1 transfusion. There were no differences in baseline characteristics and DNR/CMO status between patients who did and did not receive a transfusion (Table 1). Patients who ultimately received a transfusion had lower admission hemoglobin levels and were more likely to be anemic on presentation. They also had higher serum glucose levels at presentation.

Anemia developed in nearly three fourths of patients (394/546; 72%) at some point during their hospital course. Median hemoglobin on admission was 13.6 g/dL, with 144 patients (26%) meeting criteria for anemia. Review of daily hemoglobin levels revealed that an additional 250 patients experienced

Copyright © Congress of Neurological Surgeons. Unauthorized reproduction of this article is prohibited.

TABLE 1. Patient Characteristics at Presentation to the Emergency Department[a]

	Transfused, n = 100	Not Transfused, n = 446	*P* Value
Demographic			
Age, y, median (IQR)	74 (66-80)	73 (63-80)	.85
Women	45 (45)	193 (43)	.82
White race	86 (88)	381 (87)	.87
Hypertension	83 (83)	353 (80)	.49
Diabetes mellitus	23 (23)	81 (18)	.32
Coronary artery disease	25 (25)	93 (21)	.42
Previous ischemic stroke	20 (20)	71 (16)	.37
Warfarin	28 (28)	93 (21)	.14
Antiplatelet agent	42 (42)	185 (45)	.91
Baseline physiological			
Mean systolic blood pressure, mm Hg (range)	181 (165-209)	181 (158-200)	.30
Mean diastolic blood pressure, mm Hg (range)	90 (78-105)	94 (80-107)	.30
Baseline radiologic (range)			
Intracerebral hemorrhage volume, mL	36 (13-58)	21 (8-54)	0.06
Supratentorial location	86 (89)	398 (93)	0.14
Presence of intraventricular hemorrhage	49 (49)	206 (46)	0.66
Baseline laboratory test results (range)			
Glucose, g/dL	156 (134-192)	135 (115-177)	.001
Prothrombin time, s	13 (13-15)	13 (13-15)	0.22
White blood cell count, 1000/cm^3	11 (8-13)	10 (7-13)	0.25
Platelets, 1000/cm^3	236 (197-292)	227 (185-280)	0.16
Hemoglobin, g/dL	13.0 (11.8-14.1)	13.7(12.7-14.8)	<.001
Anemia	40 (40)	104 (23)	.001
DNR/CMO	23 (23)	82 (18)	.32

[a]IQR, interquartile range; DNR/CMO, do not resuscitate/comfort measures only.

a postadmission decrease in hemoglobin to the threshold that qualified for anemia, and 59 of those (23.6%) were subsequently transfused. Hemoglobin trends over the 14-day period revealed an initial drop in all patients except those few with the lowest admission hemoglobin levels (Figure 1). In all groups, there was a convergence in hemoglobin levels over time; the median value on day 0 was 13.6 g/dL and 10.6 by day 14.

Despite transfusion, median hemoglobin values among transfused patients remained lower than those in patients who were not transfused (Figure 2). Although nearly all transfused patients were anemic (89 patients) before transfusion, only 40 patients were anemic on presentation; anemia developed in the remainder over the 14-day period. In addition, 20 patients underwent surgical hematoma evacuation, and 10 of these received PRBC transfusion during their critical illness.

Univariate predictors of 30-day mortality included anemia at presentation, development of anemia subsequent to admission, age, admission glucose, warfarin use, antiplatelet agent use, admission GCS score, hematoma volume, hematoma location, presence of intraventricular hemorrhage, and DNR/CMO status (Table 2). In multivariable analysis, controlling for anemia, warfarin use, admission GCS score, hematoma volume, hematoma location, and DNR/CMO status, transfusion was independently associated with decreased mortality at 30 days (odds ratio: .40; P = .02; 95% confidence interval: 0.19-0.69) (Table 3). Despite transfusion, however, there was no significant increase in hemoglobin in patients with improved outcome. Although age was associated with increased mortality at 30 days, this relationship did not persist in the multivariable analysis, likely because advanced age was strongly related to DNR status. In addition to conventional predictors of mortality such as hematoma volume, admission GCS score, hematoma location, warfarin use, and DNR/CMO status, anemia at presentation was also associated with increased mortality at 30 days. Because patients who required surgery may represent a unique subset of individuals, we also performed an analysis with surgical patients excluded. PRBC transfusion remained independently associated with decreased mortality at 30 days (odds ratio: 402; P .02).

DISCUSSION

Our data demonstrate that hospital-acquired anemia is common in ICH and generate the hypothesis that PRBC transfusion may improve outcome in ICH. Our observation of an effect of transfusion on outcome is particularly notable because we were able to control for the potential confounding effects of aggressiveness of care. This makes the explanation that transfused patients were simply those who received more aggressive care less likely.

Copyright © Congress of Neurological Surgeons. Unauthorized reproduction of this article is prohibited.

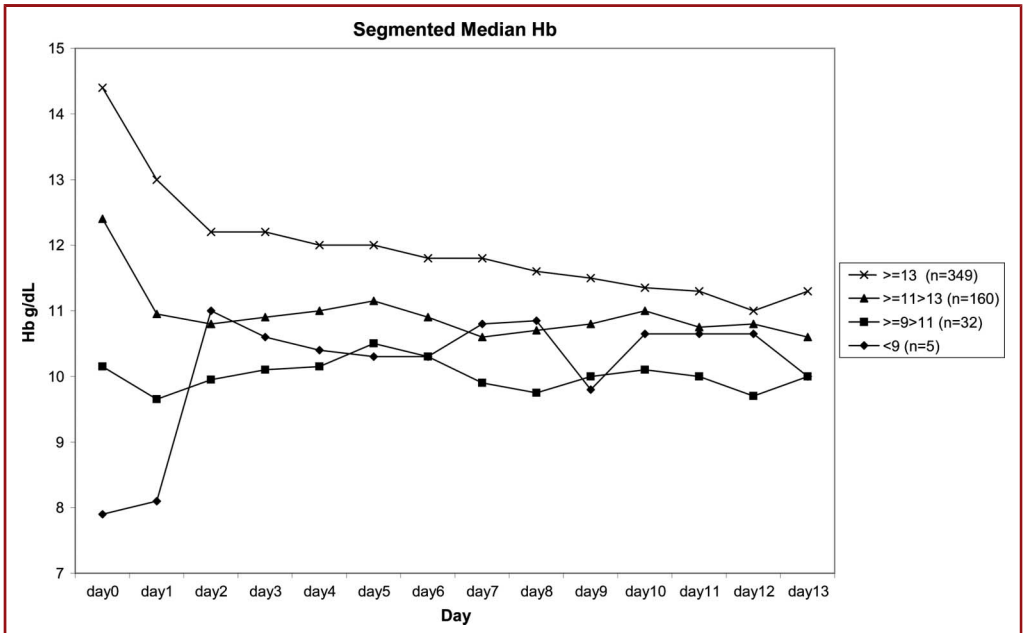

FIGURE 1. *Hemoglobin trends over time are shown for patients, stratified by admission hemoglobin level. There is a convergence of hemoglobin levels over time.*

Previous work from our cohort demonstrates that patients with anemia were older and had increased prevalence of coronary artery disease.[5] There was no difference, however, in admission prothrombin time or platelet counts. In this report, anemia was an independent predictor of hematoma volume, previously shown to be the most important determinant of mortality.[13,14] Consequently, in ICH, patients with anemia may be at inherently greater risk of death. The mechanism or causality of this

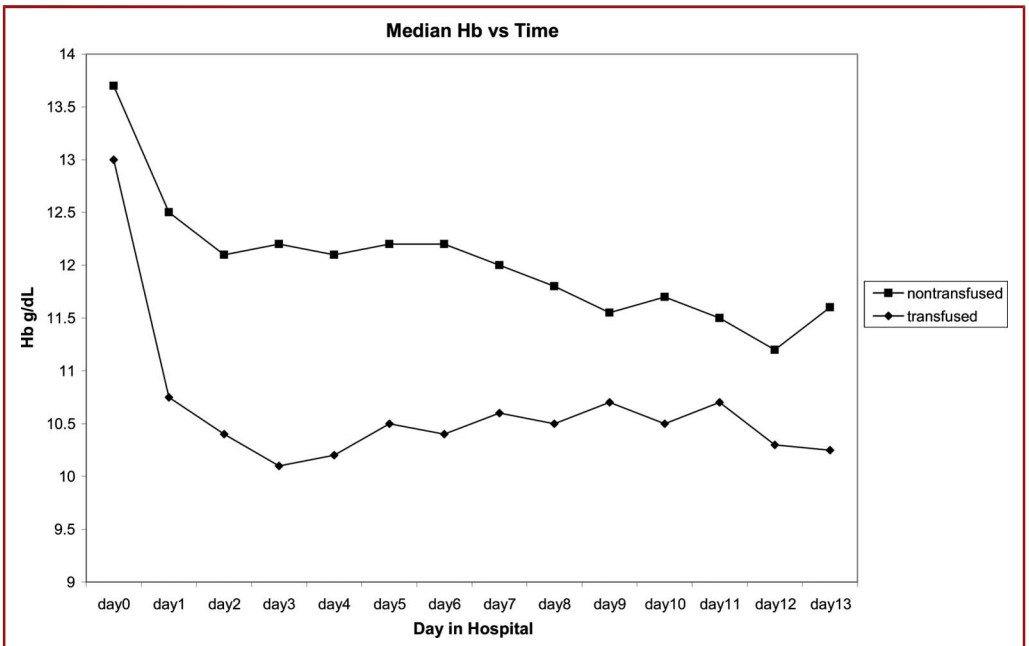

FIGURE 2. *Hemoglobin trends over time are shown for patients, stratified by their transfusion status. After an initial drop in both groups, the nontransfused group continues to see a rate of gradual decline not seen in the transfused group.*

Copyright © Congress of Neurological Surgeons. Unauthorized reproduction of this article is prohibited.

TABLE 2. Univariate Predictors of 30-Day Mortality[a]

	No.	30-Day Mortality, n (%)	*P* Value
Age, y			
≥70	341	145 (43)	.01
<70	205	64 (31)	
Warfarin			
Yes	121	60 (50)	.003
No	419	145 (35)	
Antiplatelet agent			
Yes	227	87 (38)	.005
No	276	96 (35)	
Anemia at presentation			
Yes	144	69 (48)	.007
No	402	140 (35)	
Glucose			
≥140	273	129 (47)	<.001
<140	272	79 (29)	
Glasgow Coma Scale score			
3-9	115	77 (67)	<.001
10-13	76	29 (38)	
14-15	194	25 (13)	
Intracerebral hemorrhage location			
Brainstem	18	15 (83)	.001
Cerebellar	33	15 (45)	
Deep	234	85 (36)	
Lobar	190	75 (39)	
Intracerebral hemorrhage volume, mL			
<30	308	60 (19)	<.001
30-60	120	57 (48)	
>60	118	92 (78)	
Intraventricular hemorrhage			
Presence	255	141 (55)	<.001
Absence	29	68 (23)	
DNR/CMO			
Yes	125	101 (81)	<.001
No	157	13 (8)	
Anemia over 2 wk, %			
Yes	394	138 (35)	.014
No	152	71 (47)	
Received packed red blood cells			
Yes	100	31 (31)	0.11
No	446	178 (40)	

[a]DNR/CMO, do not resuscitate/comfort measures only.

TABLE 3. Multivariable Predictors of 30-Day Mortality[a]

	Odds Ratio	95% CI	*P* Value
Age, y (<70 reference)			
≥70	1.35	0.77-2.36	.29
Intracerebral hemorrhage volume, mL (<30 reference)			
30-60	3.21	1.61-6.38	<.001
>60	15.1	7.09-32.1	
Glasgow Coma Scale score (14-15 reference)			
3-9	7.35	3.43-15.8	<.001
10-13	2.70	1.19-6.15	
Location (lobar reference)			
Brainstem	18.7	4.03-88.4	.001
Cerebellar	4.77	1.53-14.8	
Deep	1.62	0.83-3.16	
Warfarin	2.08	1.07-4.06	.029
DNR/CMO	37.8	15.7-90.9	<.001
Anemia at presentation	1.85	1.04-3.29	.04
Received transfusion	0.36	0.19-0.69	.002

[a]DNR/CMO, do not resuscitate/comfort measures only.

association is not established, and, in addition, the etiology of anemia in this patient population has not been clarified but is likely multifactorial. Anemia may be a marker of an unrecognized coagulopathy or a reduction of blood viscosity, which may impair interactions between platelets and endothelium. To ascertain the possibility of increased coagulopathy in patients on both aspirin and warfarin, when 32 such patients in our cohort were analyzed in the multivariate model, there was no significant relationship between transfusions and mortality, although this may be because of the small number of events (5 deaths in this group). In the overall cohort, because hemoglobin levels did not increase, each transfusion may have also delivered benefit by increasing intravascular volume and cerebral blood volume.

There is evidence to suggest that patients with brain injury may benefit from maintenance of higher hemoglobin levels. Previous observations in patients with subarachnoid hemorrhage have shown that higher hemoglobin is associated with improved functional outcome.[15] In reports of patients with subarachnoid hemorrhage and traumatic brain injury, PRBC transfusions raise levels of brain tissue oxygen, as measured by a direct probe in the white matter.[16-18] Alternatively, tissue hypoxia activates endothelium and increases vascular permeability and coagulopathy.[19] In our cohort, patients who were transfused had lower hemoglobin levels. Relative to nontransfused patients, however, hemoglobin levels did not continue to decrease (Figure 2). From these results, we cannot conclude whether the protective effect of PRBC transfusion was mediated by its relationship to hemoglobin level or via an alternative mechanism.

With the highest metabolic demands of any organ in the body, even the briefest interruption in adequate oxygen delivery to the brain can result in substantial irreversible injury. Furthermore, it is possible that a need for increased oxygen-carrying capacity exists during periods of increased demand or diminished supply. In the case of ICH, that period may persist for days after the initial hemorrhage, particularly during times of swelling, hydrocephalus, increased intracranial pressure, or seizures. Recent evidence also suggests that the secondary insult of ICH is one of inflammation, characterized by the toxic effects of red cell lysis, matrix metalloproteinases, and macrophage activation,[20,21] and such secondary insults may, in turn, contribute to the need for increased oxygen delivery. Although PRBC transfusion may

Copyright © Congress of Neurological Surgeons. Unauthorized reproduction of this article is prohibited.

improve oxygen delivery, blood flow, or coagulopathy, complications such as transfusion-associated lung injury must be considered as well. Recent in vitro studies have suggested that donor blood may contain proinflammatory mediators and that some of this response may be antibody mediated.[22] In addition, several studies have suggested that older blood may have reduced levels of nitric oxide, and as was suggested in a recent study of tissue oxygenation in trauma patients, older blood may lead to decreased tissue oxygenation.[23] In our study, the age of blood products used was not available, but this is an important area for future investigation.

How can one reconcile the potential need to adopt a "liberal" transfusion strategy in ICH patients with previous clinical trial results that suggest benefit for a "restrictive" strategy? A significant number of patients who die of ICH within 30 days do so as a result of the self-fulfilling prophecy of withdrawal of care.[25] ICH patients may not, as a group, have an equivalent rate and degree of medical comorbidity as part of their acute illness compared with other medical and surgical intensive care unit patients. The major medical cause of short-term death in ICH patients is because of the primary cerebral insult rather than sepsis or myocardial failure. As a result, predictors of mortality may not have a high degree of overlap with those of medical critical care patients, and the cost-benefit analysis for transfusion may lead to a different conclusion. Moreover, in a single-center study of severe sepsis and septic shock, Rivers et al[24] reported that an early goal-directed therapy targeting a central venous oxygen saturation goal reduced mortality. PRBC transfusions to reach a goal hematocrit of 30 was one of the interventions used to increase oxygen delivery. Although patients in the intervention arm did receive more pressors and fluids in addition to transfusion, this report was a striking example of the benefit from a liberal strategy during a critical period of tissue hypoxia.

Our results must be interpreted with caution. We demonstrate an association between PRBC transfusion and survival in patients with ICH but do not suggest a particular transfusion trigger. Future studies will be needed to identify optimal transfusion triggers, which may or may not be hemoglobin level. In our intensive care unit, because of the relative paucity of data regarding transfusion guidelines in neurocritical care patients, strict transfusion triggers have not been used. Instead, a combination of hemoglobin values, class of brain injury, and individual patient characteristics are all considered. Transfusion did not seem to increase hemoglobin levels in our population, perhaps because of ongoing phlebotomy of critically ill patients, fluid administration, or ongoing inflammation. The etiology of persistent anemia in this population, as well as the mechanisms of protection while patients are anemic, will require further study. Finally, in our study, we used mean hemoglobin as the measure of anemia, but it is possible that nadir hemoglobin or total anemia burden are alternative summary measures that may be informative.

Our cohort is from a single center of prospectively ascertained patients with ICH, and we cannot exclude the potential influence of unmeasured confounders. The development of anemia during the hospital course is likely multifactorial; however, we do not have information regarding the amount of loss attributed to blood sampling or age of blood. We do not have available the indications for (PRBC) transfusion and the number of transfusions received. However, more than 98% of patients who received a transfusion were anemic during their course.

We considered the possibility that those patients who continued to stay alive were more likely to receive a transfusion and that those in whom aggressive care was withdrawn would be less likely to undergo transfusion. In this case, the direction of causality would be in the opposite direction. In other words, survivors, by virtue of their being in the hospital longer, would have more of an opportunity for anemia to develop and receive a transfusion. However, 69% of the transfusions occurred in the first 4 days of the hospital stay, whereas more than 50% of deaths occurred after day 5. Furthermore, we considered DNR/CMO status in our analysis to account for the impact from aggressiveness of care. There was no difference in the proportion of patients who were made DNR/CMO when comparing those who received a transfusion with those who did not. The effect of transfusion on outcome was independent of DNR/CMO status, further suggesting that the association between transfusion and survival was not simply the result of the fact that those patients receiving aggressive care (including transfusion) were more likely to survive. The association between transfusion and decreased mortality remained even when excluding those patients who received surgery. Although combined DNR/CMO status may not be an entirely sensitive and specific measure of aggressiveness of care, its effect on ICH outcome has been well validated.[24] Withdrawal of care is the most potent predictor of mortality in ICH patients,[25] although the decision to withdraw care is driven, presumably, by the presence of additional poor prognostic indicators such as GCS score and increased hematoma volume.[26]

Because we are studying an intervention that was applied in an ad hoc basis, it is possible that some degree of confounding by indication is likely to be present. Although it is impossible to fully control for this type of confounding in a retrospective study, we noted the early transfusion of blood in the majority of cases and incorporated DNR/CMO status into our analysis. In addition, we note that a small number of patients in our cohort underwent surgical hematoma evacuation, and PRBC transfusion in this group represents only 10% of all transfusions. Therefore, it is unlikely that PRBC transfusion was simply a marker of aggressive care. Ultimately, only a prospective study with strict protocols for transfusion or a randomized clinical trial will ultimately resolve this possibility. These results are from a single center, and patient characteristics as well as transfusion practices are likely to vary in other centers, making it essential that similar studies such as ours be performed in other centers to assess the generalizability of our findings.

Well-designed prospective studies could provide information regarding the contributors to anemia, examine the effect of age and amount of blood transfused, and incorporate further physiological and functional outcome endpoints. With regard to

Copyright © Congress of Neurological Surgeons. Unauthorized reproduction of this article is prohibited.

potential administration of other blood products, it is important to note that vitamin K and fresh frozen plasma are critical components of international normalized ratio reversal in warfarin-related hemorrhage. Additional agents such as prothrombin complex concentrate, recombinant factor VII, and platelets may be considered as well in some cases.

CONCLUSION

Anemia is common in patients with ICH and associated with increased mortality. Our data generate the hypothesis that PRBC transfusions may improve survival. Future studies will be necessary to confirm these observations and determine the mechanism through which transfusions may affect the clinical course of ICH.

Disclosure

Funding provided by the National Institute of Neurological Disorders and Stroke (R01 NS059727), American Heart Association Grant-in-Aid (0755984T), Deane Institute for Integrative Research in Atrial Fibrillation and Stroke, American Academy of Neurology. Support provided by the American Heart Association Clinical Research Award 11CRP5480009. The authors have no personal financial or institutional interest in any of the drugs, materials, or devices described in this article.

REFERENCES

1. Broderick J, Connolly S, Feldmann E, et al. Guidelines for the management of spontaneous intracerebral hemorrhage in adults: 2007 update: a guideline from the American Heart Association/American Stroke Association Stroke Council, High Blood Pressure Research Council, and the Quality of Care and Outcomes in Research Interdisciplinary Working Group. *Stroke*. 2007;38(6):2001-2023.
2. Rosand J, Eckman MH, Knudsen KA, et al. The effect of warfarin and intensity of anticoagulation on outcome of intracerebral hemorrhage. *Arch Intern Med*. 2004;164(8):880-884.
3. Naidech AM, Jovanovic B, Wartenberg KE, et al. Higher hemoglobin is associated with improved outcome after subarachnoid hemorrhage. *Crit Care Med*. 2007;35(10):2383-2389.
4. Kramer AH, Zygun DA, Bleck TP, et al. Relationship between hemoglobin concentrations and outcomes across subgroups of patients with aneurysmal subarachnoid hemorrhage. *Neurocrit Care*. 2009;10(2):157-165.
5. Kumar MA, Rost NS, Snider RW, et al. Anemia and hematoma volume in acute intracerebral hemorrhage. *Crit Care Med*. 2009;37(4):1442-1447.
6. Zygun DA, Nortje J, Hutchinson PJ, et al. The effect of red blood cell transfusion on cerebral oxygenation and metabolism after severe traumatic brain injury. *Crit Care Med*. 2009;37(3):1074-1078.
7. Smith MJ, Stiefel MF, Magge S, et al. Packed red blood cell transfusion increases local cerebral oxygenation. *Crit Care Med*. 2005;33(5):1104-1108.
8. Hebert PC, Wells G, Blajchman MA, et al. A multicenter, randomized, controlled clinical trial of transfusion requirements in critical care. Transfusion Requirements in Critical Care Investigators, Canadian Critical Care Trials Group. *N Engl J Med*. 1999;340(6):409-417.
9. Sabatine MS, Morrow DA, Giugliano RP, et al. Association of hemoglobin levels with clinical outcomes in acute coronary syndromes. *Circulation*. 2005;111(16):2042-2049.
10. O'Donnell HC, Rosand J, Knudsen KA, et al. Apolipoprotein e genotype and the risk of recurrent lobar intracerebral hemorrhage. *N Engl J Med*. 2000;342(4):240-245.
11. Nutritional anaemias. Report of a who scientific group. *World Health Organ Tech Rep Ser*. 1968;405:5-37.
12. Flibotte JJ, Hagan N, O'Donnell J, et al. Warfarin, hematoma expansion, and outcome of intracerebral hemorrhage. *Neurology*. 2004;63(6):1059-1064.
13. Hemphill JC, Bonovich DC, Besmertis L, et al. The ICH score: a simple, reliable grading scale for intracerebral hemorrhage. *Stroke*. 2001;32(4):891-897.
14. Broderick JP, Brott TG, Duldner JE, et al. A powerful and easy-to-use predictor of 30 day mortality. *Stroke*. 1993;24(7):987-993.
15. Lash TL, Silliman RA. A comparison of the national death index and social security administration databases to ascertain vital status. *Epidemiology*. 2001;12(2):259-261.
16. Naidech AM, Jovanovic B, Wartenberg KE, et al. Higher hemoglobin is associated with improved outcome after subarachnoid hemorrhage. *Crit Care Med*. 2007;35(10):2383-2389.
17. Leal-Noval SR, Munoz-Gomez M, Arellano-Orden V, et al. Impact of age of transfused blood on cerebral oxygenation in male patients with severe traumatic brain injury. *Crit Care Med*. 2008;36(4):1290-1296.
18. Smith MJ, Stiefel MF, Magge S, et al. Packed red blood cell transfusion increases local cerebral oxygenation. *Crit Care Med*. 2005;33(5):1104-1108.
19. Zygun DA, Nortje J, Hutchinson PJ, et al. The effect of red blood cell transfusion on cerebral oxygenation and metabolism after severe traumatic brain injury. *Crit Care Med*. 2009;37(3):1074-1078.
20. Karimova A, Pinsky DJ. The endothelial response to oxygen deprivation: biology and clinical implications. *Intensive Care Med*. 2001;27(1):19-31.
21. Power C, Henry S, Del Bigio MR, et al. Intracerebral hemorrhage induces macrophage activation and matrix metalloproteinases. *Ann Neurol*. 2003;53(6):731-742
22. Silliman CC, Fung YL, Ball JB, et al. Transfusion-related acute lung injury (TRALI): current concepts and misconceptions. *Blood Rev*. 2009;23(6):245-255.
23. Kiraly LN, Underwood S, Differding JA, et al. Transfusion of aged packed red blood cells results in decreased tissue oxygenation in critically injured trauma patients. *J Trauma*. 2009;67(1):29-32.
24. *Deleted in proof*.
25. Hemphill JC III, Newman J, Zhao S, et al. Hospital usage of early do-notresuscitate orders and outcome after intracerebral hemorrhage. *Stroke*. 2004;35(5):1130-1134.
26. Rivers E, Nguyen B, Havstad S, et al. Early goal-directed therapy in the treatment of severe sepsis and septic shock. *N Engl J Med*. 2001;345(19):1368-1377.
27. Becker KJ, Baxter AB, Cohen WA, et al. Withdrawal of support in intracerebral hemorrhage may lead to self-fulfilling prophecies. *Neurology*. 2001;56(6):766-772.
28. Rost NS, Smith EE, Chang Y, et al. Prediction of functional outcome in patients with primary intracerebral hemorrhage: the FUNC score. *Stroke*. 2008;39(8):2304-2309.

Copyright © Congress of Neurological Surgeons. Unauthorized reproduction of this article is prohibited.

World Health Organization Grade II Gliomas and Subventricular Zone: Anatomic, Genetic, and Clinical Considerations

Francesco Vergani, MD*
Juan Martino, MD‡
Catherine Gozé, PhD§‖
Valérie Rigau, MD, PhD¶
Hugues Duffau, MD, PhD‖#

*Department of Neurosurgery, The Newcastle Upon Tyne Hospitals, Newcastle, United Kingdom; ‡Department of Neurosurgery, Hospital Universitario Marqués de Valdecilla, Cantabria, Spain; §Laboratoire de Biologie Cellulaire et Hormonale, Hôpital Arnaud de Villeneuve, Montpellier, France; ‖Team "Plasticity of Central Nervous System, Stem Cells and Glial Tumors," INSERM U1051, Institute of Neurosciences of Montpellier, Hôpital Saint Eloi, Montpellier, France; Departments of ¶Neuropathology and #Neurosurgery, Hôpital Gui de Chauliac, Montpellier, France

Correspondence:
Hugues Duffau, MD, PhD,
Department of Neurosurgery,
Hôpital Gui de Chauliac,
80 Avenue Augustin Fliche,
34295 Montpellier Cedex 5, France.
E-mail: h-duffau@chu-montpellier.fr

Received, December 12, 2009.
Accepted, September 27, 2010.

Copyright © 2011 by the
Congress of Neurological Surgeons

BACKGROUND: Recent studies suggest a possible origin of human gliomas from subventricular zone (SVZ) stem cells.

OBJECTIVE: To evaluate the relationship of World Health Organization grade II gliomas (GIIGs) with the SVZ and to investigate the presence of different genetic patterns, depending on their relationship with the SVZ.

METHODS: Forty-three consecutive patients were operated on for GIIG. Preoperative fluid-attenuated inversion recovery-weighted magnetic resonance images were reviewed to assess the presence of cortical involvement and the relationship between gliomas and the SVZ. Patients were divided into 2 groups: group 1, tumors in contact with the SVZ; and group 2, tumors not in contact with the SVZ. Preoperative and postoperative tumor volumes were calculated. Genetic analysis was performed to study 1p19q allelic loss.

RESULTS: Twenty-four patients were in group 1 and 19 in group 2. All tumors were in contact with the cortex. Preoperative volume was significantly larger in group 1 than in group 2 ($P = .003$). The proportion of total and subtotal resections was higher in group 2 ($P = .01$). Insular tumors never showed 1p19q codeletions. Noninsular tumors exhibited a significantly different incidence of complete 1p19q codeletion, with allelic loss more common in group 1 ($P = .03$).

CONCLUSION: GIIGs showed a constant relationship with the cortex and a larger volume when they came in contact with the ventricles. A distinct genetic pattern was found in noninsular SVZ GIIGs. This parameter can be considered for therapeutic management.

KEY WORDS: Subventricular zone, Surgery, 1p19q deletion, WHO grade II glioma

Neurosurgery 68:1293–1299, 2011 DOI: 10.1227/NEU.0b013e31820b522a www.neurosurgery-online.com

Previous studies have demonstrated the presence of neural stem cells in the subventricular zone (SVZ), ie, the region located under the ependyma of the brain ventricles.[1,2] Recent data show a possible relationship between the SVZ and the development of gliomas.[3-5] In particular, Lim et al[6] studied the relationship between glioblastoma multiforme and the SVZ neural stem cells region. They found that tumors in contact with the SVZ were most likely to be multifocal at diagnosis and to recur a distance from the initial lesion. Two recent works in murine models established in vivo a lineage relationship between SVZ multipotent precursors and tumoral glial cells.[7,8]

Human gliomas constitute a heterogeneous disease, with genetic and clinical differences occurring despite the same pathology. This is especially true for World Health Organization (WHO) grade II gliomas (GIIGs), in which a partial explanation for these differences might be relative to different molecular profiles, especially regarding the deletion of chromosomes 1p19q.[9,10] Moreover, recent studies show a correlation between the presence of specific genetic patterns and the location of WHO GIIGs, particularly for tumors located in frontal[11] and insular[12] areas.

ABBREVIATIONS: FLAIR, fluid-attenuated inversion recovery; **GBM,** glioblastoma multiforme; **GIIG,** grade II glioma; **OPC,** oligodendrocyte progenitor cell; **SVZ,** subventricular zone

Copyright © Congress of Neurological Surgeons. Unauthorized reproduction of this article is prohibited.

In the present study, we considered a consecutive, homogeneous series of patients operated on for WHO GIIGs with the following aims: to investigate the relationship of WHO GIIGs with the SVZ and to evaluate the possible presence of different genetic patterns in WHO GIIGs (as assessed on the basis of 1p19q deletion) depending on their relationship with the SVZ. The clinical implications of such results are also discussed.

MATERIALS AND METHODS

Patient Population

Forty-three consecutive patients (29 men, 14 women) with a first diagnosis who were operated on for GIIGs at the Department of Neurosurgery in Montpellier from January 2007 to June 2008 were included. Mean age at surgery was 37.5 years (range, 19-68 years). Presenting symptoms included seizures in 41 patients and headache in 2 patients.

Intraoperative cortical and subcortical mapping was performed in 42 of the 43 surgeries to define the margins of resection according to functional limits.[13,14] Twenty-nine patients in whom intraoperative mapping was used were operated on while awake.[15,16] The other surgeries were performed under general anesthesia. Histology was defined according to the WHO classification.[17]

Magnetic Resonance Imaging

All patients underwent a preoperative and a postoperative magnetic resonance imaging (MRI; within 24 hours from surgery) with the acquisition of fluid-attenuated inversion recovery (FLAIR) sequences. Preoperative MRIs were reviewed independently by 2 investigators (F.V. and H.D.). For any differences between the 2 observers, a final consensus was obtained by joint review. T2-weighted and FLAIR sequences were reviewed to evaluate the relationship between WHO GIIGs and the SVZ. Tumors were considered to be in contact with the SVZ when a margin of < 1 mm was assessed between the T2 and FLAIR hypersignal and the ventricle walls (Figure). Edema is rather exceptional in WHO GIIG, and all signal abnormality on FLAIR-weighted MRIs should be considered tumoral invasion. On the basis of this relationship, patient tumors were divided into 2 groups: tumors in contact with the SVZ (group 1) and tumors not in contact with the SVZ (group 2). In the same way, the presence of cortical involvement by the tumor was evaluated, with particular attention to insular cortex infiltration. Tumor location was defined as the lobe of the brain where the bulk of the tumor was found. Tumor volume was calculated by the ellipsoid approximation formula[18] on both preoperative and postoperative MRIs. In addition, the quality of resection was evaluated according to the Berger classification as partial (< 10 cm^3 on postoperative MRI), subtotal (< 10 cm^3), or total (no visible tumoral residue).[19]

Analysis of 1p19q Deletion

Tumors and blood were obtained from the 43 patients. Tumor DNA was isolated from frozen tumor samples according to the standard salting-out procedure. Reference DNA was extracted from the patient's EDTA peripheral blood with the QIAamp DNA mini-kit (Qiagen, GmbH, Hilden, Germany).

Blood DNA and tumor DNA were genotyped for a panel of highly polymorphic markers: on 1p (D1S2660, D1S450, D1S507, D1S234, D1S2892, D1S230, D1S207, D1S206) and 19q (D19S414, D19S420, D19S903, D19S571) with pairs of primers, one of which was labeled with FAM, VIC, or NED fluorochromes (ABI PRISM Linkage Mapping Set version 2.5; Applied Biosystems, Foster City, California).

Polymerase chain reaction amplification was performed in separate reactions. Analysis of pooled polymerase chain reaction products was run by capillary electrophoresis on an automatic sequencer (3130XL, Applied Biosystems) and analyzed with the GeneMapper version 4.0 software (Applied Biosystems).

The ratio of the peak heights of the 2 alleles amplified from tumor DNA was compared with that obtained for the same alleles from blood reference DNA to calculate an imbalance ratio. Diagnostic criteria for loss of heterozygosity required the calculated imbalance ratio to be < 0.7 or > 1.43.

Statistical Analysis

A Kolmogorov-Smirnov test was done to study the distribution of each variable, and P-P and Q-Q charts were used to confirm it. It was observed that the majority did not follow a normal distribution, and given that the number of patients was small (n = 43), nonparametric tests were used for the comparisons. Values are expressed as median and range. A Mann-Whitney *U* test was used to determine the relationship between the binary independent variable (tumor in contact with the SVZ vs tumor not in contact with the SVZ) and quantitative variables. The relationship between the binary independent variable (tumor in contact with the SVZ vs tumor not in contact with the SVZ) and the qualitative values were determined by the Fisher exact test, which was also used to assess the significance of association between tumor location (frontal, parietal, temporal, or insular) and 1p19q codeletion. A significance level of 5% ($P < .05$) was accepted in all cases. SPSS software version 15.0 (SPSS, UK, Feltham, Middlesex, United Kingdom) was used for the statistical analysis.

Moreover, a Mann-Whitney *U* test was used to determine the relationship between the binary independent variable (insular tumor vs non insular tumor) and the preoperative tumor volume.

RESULTS

Surgery and Neuropathology

Pathological examination was consistent with WHO GIIG in all patients. There were no enhanced tumors in our series. The mean preoperative tumor volume was 50 mL (range, 10-150 mL), and the mean postoperative tumor volume was 5 mL (range, 0-25 mL). The mean percentage of resection was 91% (range, 77%-100%). In total, there were 22 frontal (51%), 12 insular (28%), 5 parietal (12%), and 4 temporal (9%) tumors. There was neither mortality nor permanent morbidity in the series.

Tumor Location and Contact With the SVZ

In 24 patients, the tumor was in contact with the SVZ (group 1; Table). In 19 patients, the tumor did not reach the ventricle walls (group 2; Table). The 2 groups were homogeneous regarding age, sex, and tumor location. The reviewers never disagreed about whether there was SVZ involvement.

Preoperative tumor volume was statistically significantly larger in group 1 (mean tumor volume, 64 mL; range, 18.5-150 mL) compared with group 2 (mean tumor volume, 34 mL; range,

Copyright © Congress of Neurological Surgeons. Unauthorized reproduction of this article is prohibited.

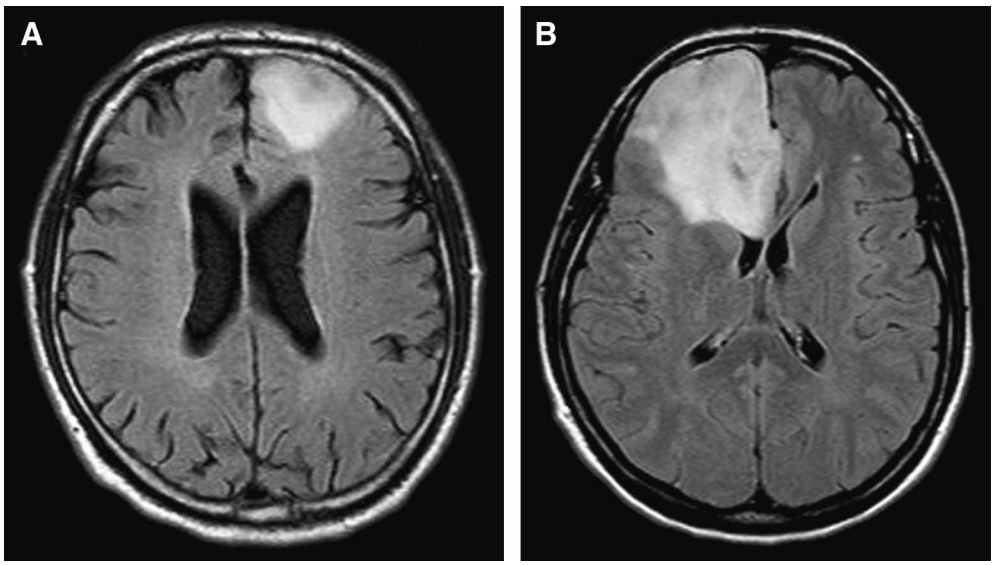

FIGURE. A, *axial fluid-attenuated inversion recovery–weighted magnetic resonance image showing a left frontal World Health Organization grade II glioma not in contact with the subventricular zone.* **B**, *axial fluid-attenuated inversion recovery–weighted magnetic resonance image showing a right frontal World Health Organization grade II glioma in contact with the subventricular zone.*

14.5-70 mL; $P = .003$). A difference between the 2 groups was also found in the postoperative residual tumor (group 1: 7 mL; range, 0-30 mL; group 2: 2.5 mL; range, 0-6 mL), but it was not statistically significant.

Nevertheless, taking into account the extent of resection, a total or subtotal resection was achieved in all tumors in group 2 compared with 17 of 24 tumors in group 1 (70.8%). The difference between these proportions was statistically significant ($P = .01$; Table). All tumors in both groups showed cortical infiltration.

A total of 12 tumors showed insular involvement: 9 in group 1 and 3 in group 2. The incidence of insular tumors was not significantly different in the 2 groups. Details of glioma location in the 2 groups are provided in the Table.

Analysis of 1p19q Deletions

Overall, 12 complete deletions of both 1p and 19q were observed in 43 patients (35%). In group 1, 9 complete deletions of both 1p and 19q were found. In the remaining 15 patients, no deletions were observed in both 1p and 19q. In group 2, 3 complete deletions of both 1p and 19q were found. In the remaining 16 patients, no deletions were observed. Taking into account the complete codeletions, no significant differences were observed between the 2 groups (Table).

Concerning brain tumor location, 7 complete codeletions were found in 21 frontal lobe tumors (33%), 1 codeletion in 5 parietal tumors (20%), 3 codeletions in 4 temporal tumors (75%), and 0 codeletions in 12 insular tumors (0%). When the proportion of 1p19q codeletion vs no deletion was compared in the frontal, parietal, and temporal tumors, no statistically significant differences were found ($P > .05$). Nevertheless, the proportion of 1p19q codeletions was statistically significantly lower in the group of insular tumors (0%) compared with the other locations (38%) ($P = .05$).

Our team previously analyzed the genetic pattern of insular GIIGs. We reported that these gliomas, arising from the insula anatomic entity, displayed a different genetic profile compared with gliomas originating from other brain subregions.[12] Therefore, we decided to analyze the presence of 1p19q codeletion in the subgroup of noninsular tumors, according to contact with the SVZ. Taking into account only the noninsular tumors, 9 of the 15 tumors in group 1 presented a 1p19q codeletion compared with 3 of the 16 tumors in group 2. The difference between the 2 proportions was statistically significant ($P = .03$; Table).

We also measured the volume of gliomas with codeleted status (mean, 45 mL; range, 15-130 mL) and in gliomas with no codeletion (mean, 48 mL; range, 10-110 mL). We compared these means with a statistical test (Mann-Whitney U test), and the difference was statistically not significant ($P = .92$). The volume of insular gliomas (mean, 66 mL; range, 19-150 mL) was larger than in the noninsular tumors (mean, 46 mL; range, 10-130 mL). When a Mann-Whitney U test was used, the difference between the preoperative tumor volume of insular and noninsular gliomas was statistically nonsignificant ($P > .05$).

Copyright © Congress of Neurological Surgeons. Unauthorized reproduction of this article is prohibited.

TABLE. Clinical, Anatomic, Surgical, and Molecular Characteristics of the 43 Patients With World Health Organization Grade II Glioma[a]

	Group 1, n = 24	Group 2, n = 19	*P*
Contact with SVZ	Yes	No	. . .
Male:female	15:9	14:5	> .05
Age at surgery, y	36.8	37.9	> .05
Preoperative volume (range), mL	64 (18.5-150)	34 (14.5-70)	< .05 (.003)
Postoperative volume (range), mL	7 (0-30)	2.5 (0-6)	> .05
Extent of resection, n/N			
Partial	7/24	0/19	< .05 (.01)
Subtotal	11/24	15/19	
Total	6/24	4/19	
Subtotal/total	17/24	19/19	
Cortex infiltration, n/N	24/24	19/19	> .05
Tumor location, n/N			
Insular	9/24	3/19	> .05
Frontal	10/24	12/19	> .05
Parietal	1/24	4/19	> .05
Temporal	4/24	0/19	> .05
Complete 1p19q deletion, n/N			
Overall	9/24	3/19	> .05
Insular tumors	0/9	0/3	> .05
Noninsular tumors	9/15	3/16	< .05 (.03)

[a]SVZ, subventricular zone.

DISCUSSION

In recent years, different studies have suggested a relationship between the human stem cells regions, with particular emphasis on the SVZ, and the development of high-grade gliomas.[3,4,6] Glioblastoma multiforme (GBM) contains a subset of cancer cells that resemble human neural stem cells.[20] Lim et al[6] studied the relationship between GBM (WHO grade IV gliomas) and the SVZ. They found that GBMs in contact with both the SVZ and the cerebral cortex were most likely to be multifocal at diagnosis and to recur a distance from the initial lesion. Conversely, tumors that were in contact with neither the SVZ nor the cortex were always single at diagnosis and usually recurred within 2 cm from the resection margin. The authors concluded that GBMs in contact with the SVZ and infiltrating the cortex could be most closely related to neural stem cells.

Corroborating biological data have been provided. Recent experiments realized in transgenic mice showed a lineage link between neural stem/progenitor and tumoral glial cells isolated from tumors induced in these mice. The tumors exhibited the characteristics of human GBMs. First, Wang et al[7] demonstrated in tumoral cells the persistent expression of a mutated p53 protein encoded by a transgene specifically expressed in the radial glial cells in the developing brain. Second, the somatic inactivation of some tumor suppressor genes, targeted to neural stem/progenitor cells, in mice embryos or adult mice led to high-grade astrocytomas.[8]

The present study specifically addresses the issue of the relationship between the SVZ and WHO GIIGs. The main difference compared with the data reported by Lim et al[6] was that in WHO GIIGs at diagnosis, we always found an involvement of the cerebral cortex, either neocortex or insular cortex. We never observed a WHO GIIG in contact with the SVZ and not reaching the cortex.

In a recent study performed on a heterogeneous series of mixed-grade gliomas, Barami et al[21] reported that the majority of tumors (93%) came in contact with the ventricular walls. A different proportion of WHO GIIGs not in contact with the SVZ was reported in that work (2 of 28, 7%) compared with our study (19 of 43, 44%). This difference could be explained by the smaller sample of WHO grade II tumors (28) in the study of Barami et al. Furthermore, Barami et al reported that oligodendrogliomas tended to be in contact with the SVZ more often than astrocytomas and oligoastrocytomas. These findings were not replicated in our series, which consisted of a larger number of WHO GIIGs; no statistical differences were found between oligodendrogliomas and astrocytomas or mixed gliomas (Table). Similar to our study, Barami et al reported that the average diameter of gliomas adjacent to the ventricular walls was higher than that of gliomas without ventricular contact. Nonetheless, analyzing the proportion of gliomas contacting the ventricles as a function of lesion size, these authors found that contact with the ventricular walls was independent of size (smaller gliomas were equally prone to contact the ventricular walls as larger ones). This finding could be explained by the larger proportions of WHO grade IV gliomas in the series of Barami et al.

To the best of our knowledge, there are no articles in the literature reporting the occurrence of WHO GIIGs not in contact with the cortex, even if we cannot exclude some isolated cases. Moreover, in the present series, tumors in contact with the ventricle were also significantly larger in volume than tumors with cortical involvement only. Indeed, because all the gliomas were in contact with the cortex, those also in contact with the SVZ were by definition the tumors with the larger size. Two hypotheses could explain these findings. First, a "centripetal" pattern of growth for WHO GIIGs can be proposed. In this scenario, tumors develop at the cortical/subcortical level and involve the SVZ only secondarily through white matter extension[22] when a considerable volume is reached. The absence of a direct origin from the SVZ could suggest that WHO GIIGs do not arise from SVZ progenitor cells. Their possible origin could rather be at the cortical level. Preliminary studies performed both in animal[23] and in human[24] highlighted the presence of pluripotent neural progenitors at the cortical or subcortical level. Lindberg et al[25] recently provided more accurate data relative to the possible origin of WHO GIIGs. In vivo, in transgenic mice, they specifically targeted platelet-derived growth factor-B overexpression to the oligodendrocyte progenitor cells (OPCs). Gliomas arose in 33 % of these transgenic mice; all the tumors exhibited

Copyright © Congress of Neurological Surgeons. Unauthorized reproduction of this article is prohibited.

histopathological features of human WHO GIIGs and expressed markers of OPCs. These first results support the OPC as a potential candidate to be the cell of origin of WHO GIIGs. Interestingly, OPCs are widely scattered throughout the gray and white matter in the brain.[26]

According to the second hypothesis, gliomas originate from SVZ progenitor cells, but because of their high proliferative rate and the rapid migration of tumor cells, the original anatomic links with the SVZ are not visible at diagnosis on conventional MRI.[27] For high-grade gliomas, the aforementioned clinical data about human GBMs by Lim et al[6] are in accordance with this hypothesis. Biological studies reinforce the SVZ origin hypothesis for GBMs.[7,8]

The hypothesis of a centripetal growth pattern cannot be unequivocally derived from our data. As stated, we cannot exclude that the origin of GIIG is at the level of the SVZ, and then tumoral cells migrate toward the subcortical/cortical level. An experimental way to corroborate the present study would be to follow the evolution of GIIGs over the time. Because we always found a cortical involvement, it would be of great interest to follow up the earlier stages of GIIGs to verify whether, from the cortical involvement, they later come in contact with the SVZ. Such a study can be performed with the experimental animal model developed by Lindberg et al.[25]

Concerning WHO GIIGs, their slow growth rate[18] and the extreme rarity of multifocal localizations[28] contribute to the idea that the cells of origin of WHO GIIGs are less broadly migratory than cells found in SVZ-derived gliomas. Our clinical data could therefore suggest a different cellular origin of WHO GIIGs compared with de novo high-grade gliomas, in accordance with preliminary biological results obtained in animal models.[25] These findings could account for the radically different natural history of these glial tumors and for the differences retrieved in molecular patterns of de novo GBMs and secondary GBMs.

In the present article, noninsular WHO GIIGs showed a significant difference in the incidence of 1p19q complete codeletion, with tumors reaching the SVZ displaying a higher incidence of codeletion. In a previous article, our team reported the absence of 1p19q deletion in a consecutive series of insular GIIGs.[12] The insular lobe shows peculiar developmental, anatomic, and cytoachitectonic characteristics, being an interface between the allocortex and the neocortex.[29,30] This could account for a different genetic behavior in insular GIIGs. In noninsular gliomas, the different incidence of 1p19q deletions between groups 1 and 2 raises the question whether WHO GIIGs that come in contact with the SVZ can be considered distinct on genetic grounds. Other studies from the literature found a ''genetic signature'' (ie, different patterns of 1p19q allelic loss) in gliomas, depending on their location.[11,31,32] None of these previous studies, however, focused on the relationship between genetic signature of WHO GIIGs and contact with the SVZ. In the present series, the distinct genetic patterns observed in the 2 groups could help to explain the different tumor extensions observed. Noninsular ''SVZ tumors,'' which show more frequent 1p19q deletions and therefore a more favorable genetic pattern,[33] could have a less aggressive behavior. Brain plasticity mechanisms would then have a greater possibility to compensate for slower tumor growth.[34,35] In a centripetal hypothesis, this could explain the extension to the SVZ and the larger volumes seen in this group of patients.

Regardless of the possible differences in genetic patterns, these findings yield potential clinical relevance. In group 1, larger tumors in contact with the SVZ appeared to be more difficult to treat surgically. The percentage of partial resections for patients in group 1 was significantly more elevated than for patients in group 2 because of invasion of functional subcortical pathways. This was the case with the superior longitudinal fasciculus, the arcuate fasciculus, and the inferior fronto-occipital fasciculus in the dominant hemisphere and the corticospinal tract, the thalamocortical tract, and the optic radiations in both hemispheres.[36] The presence of a higher proportion of 1p19q codeletion for WHO GIIGs in group 1 might represent a more favorable spontaneous prognostic factor and a more favorable chemosensitive molecular pattern, as previously suggested in oligodendrogliomas[37,38] and more recently in WHO GIIGs in general.[39] We therefore suggest that in patients with SVZ tumors that are less amenable to complete resection, which is currently the first treatment in WHO GIIGs,[40,41] chemotherapy or radiotherapy could be discussed earlier.

CONCLUSION

In our series, all WHO GIIGs showed a constant relationship with the cortex. WHO GIIGs that came in contact with the SVZ showed a larger volume. These findings differentiate WHO GIIGs from high-grade tumors. Taking into account noninsular tumors, SVZ GIIGs exhibited a distinct genetic signature, with a significantly higher proportion of 1p19q deletions. This parameter can be considered for therapeutic management.

Disclosure

The authors have no personal financial or institutional interest in any of the drugs, materials, or devices described in this article.

REFERENCES

1. Alvarez-Buylla A, Garcia-Verdugo JM. Neurogenesis in adult subventricular zone. *J Neurosci*. 2002;22(3):629-634.
2. Sanai N, Tramontin AD, Quinones-Hinojosa A, et al. Unique astrocyte ribbon in adult human brain contains neural stem cells but lacks chain migration. *Nature*. 2004;427(6976):740-744.
3. Sanai N, Alvarez-Buylla A, Berger MS. Neural stem cells and the origin of gliomas. *N Engl J Med*. 2005;353(8):811-822.
4. Uchida K, Mukai M, Okano H, Kawase T. Possible oncogenicity of subventricular zone neural stem cells: case report. *Neurosurgery*. 2004;55(4):977-978.
5. Vescovi AL, Galli R, Reynolds BA. Brain tumour stem cells. *Nat Rev Cancer*. 2006;6(6):425-436.
6. Lim DA, Cha S, Mayo MC, et al. Relationship of glioblastoma multiforme to neural stem cell regions predicts invasive and multifocal tumor phenotype. *Neuro Oncol*. 2007;9(4):424-429.
7. Wang Y, Yang J, Zheng H, et al. Expression of mutant p53 proteins implicates a lineage relationship between neural stem cells and malignant astrocytic glioma in a murine model. *Cancer Cell*. 2009;15(6):514-526.

Copyright © Congress of Neurological Surgeons. Unauthorized reproduction of this article is prohibited.

8. Alcantara Llaguno S, Chen J, Kwon CH, et al. Malignant astrocytomas originate from neural stem/progenitor cells in a somatic tumor suppressor mouse model. *Cancer Cell*. 2009;15(1):45-56.
9. Kujas M, Lejeune J, Benouaich-Amiel A, et al. Chromosome 1p loss: a favorable prognostic factor in low-grade gliomas. *Ann Neurol*. 2005;58(2):322-326.
10. Ricard D, Kaloshi G, Amiel-Benouaich A, et al. Dynamic history of low-grade gliomas before and after temozolomide treatment. *Ann Neurol*. 2007;61(5):484-490.
11. Laigle-Donadey F, Martin-Duverneuil N, Lejeune J, et al. Correlations between molecular profile and radiologic pattern in oligodendroglial tumors. *Neurology*. 2004;63(12):2360-2362.
12. Gozé C, Rigau V, Gibert L, Maudelonde T, Duffau H. Lack of complete 1p19q deletion in a consecutive series of 12 WHO grade II gliomas involving the insula: a marker of worse prognosis? *J Neurooncol*. 2009;91(1):1-5.
13. Duffau H, Capelle L, Denvil D, et al. Usefulness of intraoperative electrical subcortical mapping during surgery for low-grade gliomas located within eloquent brain regions: functional results in a consecutive series of 103 patients. *J Neurosurg*. 2003;98(4):764-778.
14. Duffau H, Lopes M, Arthuis F, et al. Contribution of intraoperative electrical stimulations in surgery of low grade gliomas: a comparative study between two series without (1985–96) and with (1996–2003) functional mapping in the same institution. *J Neurol Neurosurg Psychiatry*. 2005;76(6):845-851.
15. Duffau H, Gatignol P, Mandonnet E, et al. New insights into the anatomo-functional connectivity of the semantic system: a study using cortico-subcortical electrostimulations. *Brain*. 2005;128(pt 4):797-810.
16. Duffau H, Gatignol P, Mandonnet E, Capelle L, Taillandier L. Intraoperative subcortical stimulation mapping of language pathways in a consecutive series of 115 patients with hrade II glioma in the left dominant hemisphere. *J Neurosurg*. 2008;109(3):461-471.
17. Louis DN, Ohgaki H, Wiestler OD. *WHO Classification of Tumours of the Central Nervous System*. Lyon, France: IARC; 2007.
18. Mandonnet E, Delattre JY, Tanguy ML, et al. Continuous growth of mean tumor diameter in a subset of grade II gliomas. *Ann Neurol*. 2003;53(4):524-528.
19. Berger MS, Deliganis AV, Dobbins J, Keles GE. The effect of extent of resection on recurrence in patients with low grade cerebral hemisphere gliomas. *Cancer*. 1994;74(6):1784-1791.
20. Galli R, Binda E, Orfanelli U, et al. Isolation and characterization of tumorigenic, stem-like neural precursors from human glioblastoma. *Cancer Res*. 2004;64(19):7011-7021.
21. Barami K, Sloan AE, Rojiani A, et al. Relationship of gliomas to the ventricular walls. *J Clin Neurosci*. 2009;16(2):195-201.
22. Mandonnet E, Capelle L, Duffau H. Extension of paralimbic low grade gliomas: toward an anatomical classification based on white matter invasion patterns. *J Neurooncol*. 2006;78(2):179-185.
23. Costa MR, Kessaris N, Richardson WD, Götz M, Hedin-Pereira C. The marginal zone/layer I as a novel niche for neurogenesis and gliogenesis in developing cerebral cortex. *J Neurosci*. 2007;27(42):11376-11388.
24. Nunes MC, Roy NS, Keyoung HM, et al. Identification and isolation of multipotential neural progenitor cells from the subcortical white matter of the adult human brain. *Nat Med*. 2003;9(4):439-447.
25. Lindberg N, Kastemar M, Olofsson T, Smits A, Uhrbom L. Oligodendrocyte progenitor cells can act as cell of origin for experimental glioma. *Oncogene*. 2009;28(23):2266-2275.
26. McTigue DM, Tripathi RB. The life, death, and replacement of oligodendrocytes in the adult CNS. *J Neurochem*. 2008;107(1):1-19.
27. Stiles CD, Rowitch DH. Glioma stem cells: a midterm exam. *Neuron*. 2008;58(6):832-846.
28. Vergani F, Sanson M, Duffau H. Combined multiple surgical intervention and chemotherapy for multicentric WHO grade II glioma: a long-term follow-up study. *Acta Neurochir (Wien)*. 2009;151(12):1699-1704.
29. Augustine JR. Circuitry and functional aspects of the insular lobe in primates including humans. *Brain Res Brain Res Rev*. 1996;22(3):229-244.
30. Duffau H, Capelle L, Lopes M, et al. The insular lobe: physiopathological and surgical considerations. *Neurosurgery*. 2000;47(4):801-810.
31. Zlatescu MC, TehraniYazdi A, Sasaki H, et al. Tumor location and growth pattern correlate with genetic signature in oligodendroglial neoplasms. *Cancer Res*. 2001;61(18):6713-6715.
32. Mueller W, Hartmann C, Hoffmann A, et al. Genetic signature of oligoastrocytomas correlates with tumor location and denotes distinct molecular subsets. *Am J Pathol*. 2002;161(1):313-319.
33. Mariani L, Deiana G, Vassella E, et al. Loss of heterozygosity 1p36 and 19q13 is a prognostic factor for overall survival in patients with diffuse WHO grade 2 gliomas treated without chemotherapy. *J Clin Oncol*. 2006;24(29):4758-4763.
34. Duffau H. Lessons from brain mapping in surgery for low-grade glioma: insights into associations between tumour and brain plasticity. *Lancet Neurol*. 2005;4(8):476-486.
35. Desmurget M, Bonnetblanc F, Duffau H. Contrasting acute and slow-growing lesions: a new door to brain plasticity. *Brain* 2007;130(Pt 4):898-914.
36. Duffau H. New concepts in surgery of WHO grade II gliomas: functional brain mapping, connectionism and plasticity: a review. *J Neurooncol*. 2006;79(1):77-115.
37. Smith JS, Perry A, Borell TJ, et al. Alterations of chromosome arms 1p and 19q as predictors of survival in oligodendrogliomas, astrocytomas, and mixed oligoastrocytomas. *J Clin Oncol*. 2000;18(3):636-645.
38. Hoang-Xuan K, Capelle L, Kujas M, et al. Temozolomide as initial treatment for adults with low-grade oligodendrogliomas or oligoastrocytomas and correlation with chromosome 1p deletions. *J Clin Oncol*. 2004;22(15):3133-3138.
39. Kaloshi G, Benouaich-Amiel A, Diakite F, et al. Temozolomide for low-grade gliomas: predictive impact of 1p/19q loss on response and outcome. *Neurology*. 2007;68(21):1831-1836.
40. Smith JS, Chang EF, Lamborn KR, et al. Role of extent of resection in the long-term outcome of low-grade hemispheric gliomas. *J Clin Oncol*. 2008;26(8):1338-1345.
41. Duffau H. Surgery of low-grade gliomas: towards a ''functional neurooncology''. *Curr Opin Oncol*. 2009;21(6):543-549.

Acknowledgments

We wish to thank Dr Xavier Vasques for his advice on statistical analysis and Dr Claire Nicholson for reviewing the English in the manuscript.

COMMENTS

The authors have conducted an original study of low-grade gliomas in terms of their relationship to neural stem cells (based on location) and 1p19q codeletion. Their results indicate that these lesions are quite heterogeneous in terms of location and genetically. Their pattern of growth also seems to be different compared with higher-grade gliomas. The authors' findings are the groundwork for future studies that will allow improved patient stratification and development of new therapeutic strategies.

Kaveh Barami
Jacksonville, Florida

From the results of 43 patients with World Health Organization grade II gliomas, the authors hypothesize that there is a different cellular origin (subventricular zone stem cells) for low-grade tumors opposed to high-grade tumors. Furthermore, they allude to a distinct genetic pattern of noninsular low-grade gliomas with regard to the incidence of 1p19q codeletion.

This article is interesting, has certainly novel aspects, and comes from a respected group with great experience. The ''evidence,'' however, is weak or circumstantial for several reasons, although I tend to believe it. It remains on the level of assumptions and hypothesis. The results provide a trend that has to be substantiated by further studies.

Bernhard Meyer
Munich, Germany

In this article, a distinguished group of authors observe that grade II gliomas (n = 43) can be divided into 2 distinct types by magnetic

Copyright © Congress of Neurological Surgeons. Unauthorized reproduction of this article is prohibited.

resonance imaging. Although all tumors in both groups involve the cortex, tumors in group I are also in contact with the subventricular zone and are significantly larger than those in group 2 with decreased incidence of total/subtotal resection and increased rate of codeletion of 1p/19q among noninsular tumors. The authors suggest that involvement of the subventricular zone may implicate neural or glioma stem cell in group 1 tumors, which appear to have a "centripetal" pattern of growth. Furthermore, they propose that group 1 tumors, which tend to be more difficult to resect completely, should be considered for early chemotherapy or radiotherapy.

The authors' observations are novel and intriguing and suggest that the patterns of growth in grade II gliomas are different from those in grade IV gliomas. However, as they themselves acknowledge, the evidence for a centripetal growth pattern is somewhat lacking. Furthermore, the role of chemotherapy and radiotherapy for grade II gliomas remains controversial. It would be interesting to know more about the subtype of gliomas in each group. Does group 1 have more oligodendrogliomas or oligoastrocytomas than group 2? Is there a difference in the incidence of astrocytomas in the 2 groups? Do the 2 groups differ in prognosis? Given the current interest in the putative role of stem cells in gliomagenesis, it would also be interesting to know if there is a difference in stem cell markers in the 2 groups of neoplasms. The answers to such questions may lead to further understanding of the etiology and behavior of these neoplasms.

Andrew Sloan
Cleveland, Ohio

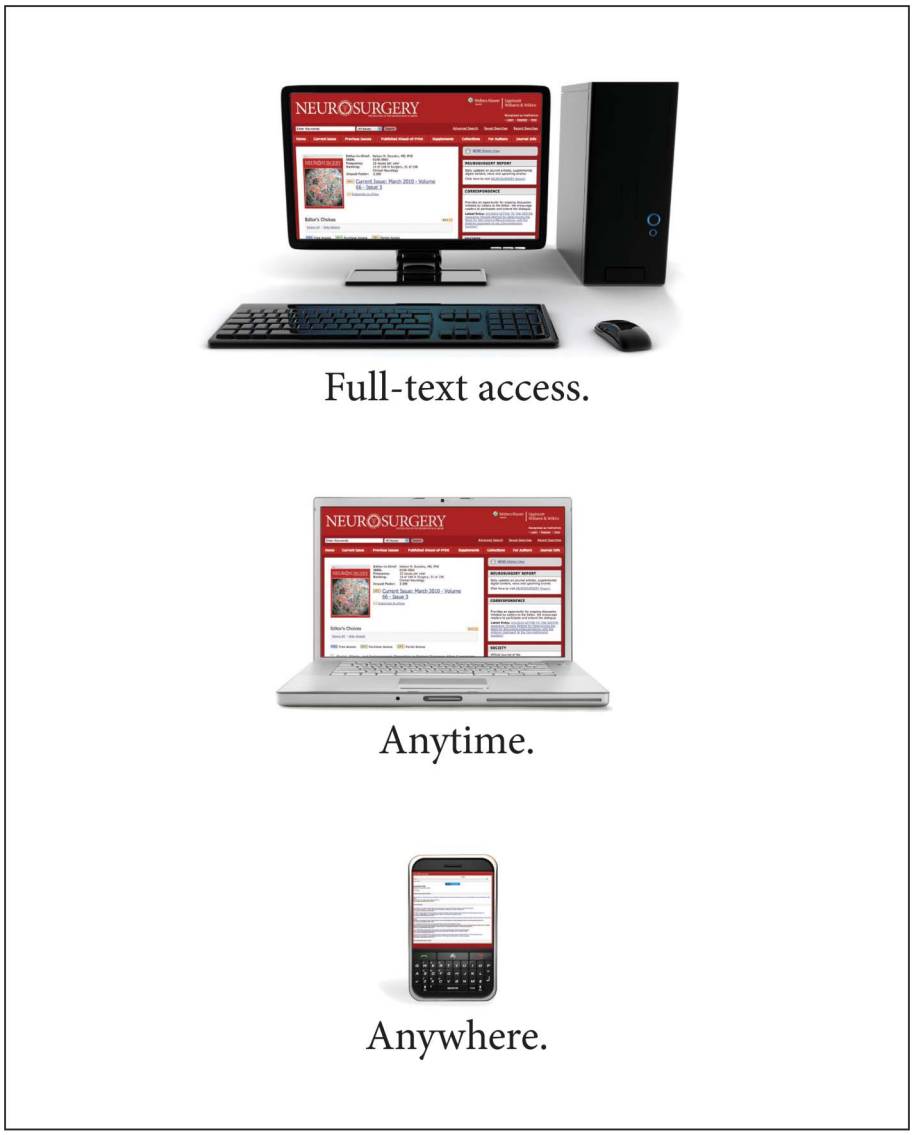

Copyright © Congress of Neurological Surgeons. Unauthorized reproduction of this article is prohibited.

Treatment of Severe Trigeminal Headache in Patients With Pituitary Adenomas

Tiago da Silva Freitas, MD*
Ivan Coelho Ferreira, MD*
Aldo Pereira Neto, MD, PhD*
Oswaldo R.M. Neto, MD*
Gustavo do Vale Gomes, MD§
Luis Augusto Casulari Roxo da Mota, MD, PhD‡
Luciana Ansaneli Naves, MD, PhD‡
Monalisa F. Azevedo, MD, PhD‡

Departments of *Neurosurgery and ‡Endocrinology, University Hospital of Brasília, Brasília, Brazil; §Radiology Department, Hospital Santa Lúcia, Brasília, Brazil

Correspondence:
Tiago da Silva Freitas, MD,
Departamento de Neurocirurgia,
Faculdade de Medicina,
Universidade de Brasília,
SGAN Quadra 605,
Asa Norte,
Prédio Novo de Ambulatórios,
70840-901 Brasília DF, Brazil.
E-mail: tmosca@gmail.com

Received, November 22, 2009.
Accepted, October 2, 2010.

Copyright © 2011 by the
Congress of Neurological Surgeons

BACKGROUND: The incidence of headache in patients with pituitary adenomas is high, and the underlying pathological mechanisms are not completely understood.

OBJECTIVE: We tested the efficacy of percutaneous ganglion block and trigeminal rhizotomy in the treatment of severe trigeminal/autonomic headache associated with pituitary tumors.

METHODS: Eleven patients treated surgically for pituitary adenomas in whom intractable trigeminal headaches developed were enrolled in the study and underwent ictal cerebral single-photon emission computed tomography before starting treatment. Initially, all patients underwent a 6-month medical treatment trial. Patients who did not experience improvement in headache severity, addressed by the Headache Impact Test-6 scale, underwent trigeminal percutaneous ganglion blockade. Two patients subsequently underwent trigeminal balloon rhizotomy.

RESULTS: Among the 11 patients, 6 did not have improved Headache Impact Test-6 scale scores after 6 months of treatment with medications and underwent trigeminal ganglion blockade. Significant improvement in headache severity was noted in 3 of them. Long-term response was obtained in 1 patient, and the other 2, in whom the response was transient, were then successfully treated with trigeminal rhizotomy. Cerebral single-photon emission computed tomography showed increased uptake in the thalamus/hypothalamus region in patients who responded well to manipulation of the trigeminal-hypothalamic system.

CONCLUSION: Percutaneous ganglion blockade and trigeminal rhizotomy may be promising alternative options for the treatment of severe headache in selected patients with pituitary adenomas.

KEY WORDS: Autonomic headache, Ganglion block, Pituitary tumor, Trigeminal rhizotomy

Neurosurgery 68:1300–1308, 2011 DOI: 10.1227/NEU.0b013e31820c6c9e www.neurosurgery-online.com

Headache is a common presenting feature of pituitary tumors, and the incidence of this symptom in pituitary adenomas ranges from 33% to 72%.[1-3] A variety of headache phenotypes is reported to be associated with pituitary tumors, including migraine[4] and also the trigeminal autonomic cephalalgias, which comprise cluster headache (severe unilateral pain accompanied by restlessness or agitation and cranial autonomic symptoms); short-lasting, unilateral, neuralgiform headache attacks with conjunctival injection and tearing; and paroxysmal hemicranias.[4-10] Migraine, the most common form of headache associated with pituitary adenomas, is a common disabling trigeminal headache disorder, defined as moderate or severe recurring headache, usually unilateral, accompanied by phono/photophobia, nausea, or vomiting.[11]

ABBREVIATIONS: HIT-6, Headache Impact Test-6; **SPECT**, single-photon emission computed tomography

The underlying mechanism for the headache in the context of pituitary tumors has long been thought to be mechanical, eg, stretching of the dura mater in the presence of suprasellar extension of the tumor, and/or invasion of the cavernous sinus with trigeminal nerve irritation.[1,12] However, some patients with huge pituitary tumors with suprasellar extension and

Copyright © Congress of Neurological Surgeons. Unauthorized reproduction of this article is prohibited.

cavernous sinus invasion do not report pain, whereas others present with severe headache associated with relatively small lesions.[13,14] The fact that headache can be either dramatically improved or worsened by endocrine treatments with somatostatin analogs or dopamine agonists, even in the absence of any measurable change in pituitary size,[5,15] suggests that pituitary tumor–associated headache may also have a biochemical-neuroendocrine origin. Although some candidate peptides have been demonstrated in pituitary adenomas,[16,17] no association with headache was found, and the etiology of cephalalgias associated with pituitary lesions remains to be determined.

The treatment of pituitary tumor–associated headache remains entirely empirical because of the lack of trials in this area, which is not unexpected given the rarity of the disease and heterogeneity of the presentation.[18] Generally, the first approach for these patients is the treatment of the tumor, if the lesion warrants treatment on its own merit. Although the indication for treating the pituitary tumor is not headache per se, a number of patients experience improvement in this symptom after surgical or medical treatment of the pituitary lesion.[19,20]

Nevertheless, a subgroup of patients with trigeminal/autonomic headache present with refractory pain after surgery and/or medical treatment, even with the use of various prophylactic and abortive analgesic medications. In a previous study[4] and also in our experience at the Endocrinology Unit of the University Hospital of Brasilia (unpublished data), the analgesic effect of somatostatin analogs was observed in some patients with growth hormone–secreting adenomas. However, it was noted that some of them experienced rebound phenomenon and dependency, discouraging the routine use of these agents in the treatment of acromegaly-associated headache.

We describe an alternative approach to patients presenting with pituitary tumors that evolve with severe and intractable trigeminal headache after pituitary surgery.

PATIENTS AND METHODS

Patients and Classification of the Headache

Among the 345 consecutive patients who underwent pituitary surgery at the University Hospital of Brasilia from 1998 to 2007, 20 presented with persistent headache and were referred to the Clinic of Functional Neurosurgery for evaluation. These patients underwent a semiological analysis of their headache (Table 1), and classification of their symptoms was based on the International Headache Society Classification.[11] Patients with a diagnosis of persistent headache with a trigeminal/autonomic pattern (n = 11) were selected to undergo further analysis. All but 1 patient were hormonally controlled, and the study was conducted from 2007 to 2008.

The severity of headache in these patients was addressed using the Headache Impact Test-6 (HIT-6)[21] (Table 1). This scale consists of 6 items that evaluate social functioning, pain intensity, and emotional impact of headache as well as well-being, cognitive function, and vitality of the individuals. According to the score in each subclass, the headache is graded as small (≤49 points), moderate (50-55 points), substantial (56-59 points), or severe (≥60 points). The HIT-6 score was translated to more than 27 languages, including Brazilian Portuguese, and this instrument of evaluation has been shown to correlate across different diagnostic groups of headache with both headache severity and quality of life.[22-24]

The study protocol was approved by the Research Ethics Committee of the University of Brasília, Brazil, and written informed consent as obtained. HIT-6 scale classification of the patients was performed 2 months before starting the protocol treatment twice monthly and 3 and 6 months after clinical and surgical treatment at a frequency of twice monthly. For the analysis, we considered the medium-range results on the HIT-6 scale during the pretreatment period and the medium-range results on the HIT-6 scale during the follow-up.

Cerebral Single-Photon Emission Computed Tomography (SPECT)

The 11 patients involved in the study were submitted to functional analysis with cerebral SPECT in the pretreatment period using the GE Millennium MG–Multi-geometry digital CSE dual-detector gamma camera (General Electric, Milwaukee, Wisconsin). The radionuclide used was technetium 99m-ethylene cysteinate dimer at a dose of 30 mCi intravenously, and we used a high-resolution collimator with a 15% window at 140 KeV. Acquisition started 60 minutes after radionuclide administration, with a resolution of 64 × 64 pixels and 1.5 zoom.

In the supine position, the patient's head was fixed with a strap so that the brain was fully visible in the inferior portion of the field. We used a circular orbit, 360-degree projections, and 64 frames of 30-second acquisition. The reconstruction type used at the image processing was the iterative method and the attenuation correction was the Chang Order method.

In the SPECT images, which are tomographic images reconstructed in 3 planes (coronal, sagittal, and transaxial) representing the encephalic parenchyma blood flow, the radionuclide was administered intravenously, passed through the blood-brain barrier, and concentrated in the brain according to the perfusion of each site. In the color scale used (GE cool), darker tones meant decreased perfusion and whiter tones meant increased perfusion. In all patients, the examination was performed during an episode of intense headache (ictal SPECT).

Study Protocol

The study protocol included the following. Medical treatment with different medications routinely was used to treat trigeminal/autonomic headaches for a period of 6 months. The impact of the treatment on the relief of headache was determined by the HIT-6 scale score. Improvement of at least 1 level in this scale was considered relevant, and patients who experienced benefit with this approach (n = 5) were kept only on medical treatment and were not considered eligible for surgical treatment. The 6 patients who did not experience headache control with medical treatment underwent additional interventional procedures.

Interventional Procedures

The intervention treatment consisted of 2 stages. In the first stage, we performed percutaneous trigeminal ganglion blockade, with the aim of modulating the trigeminal-hypothalamus system possibly involved in the genesis and symptoms of headache in these patients. A series of 3 consecutive blocks using a 2-mL solution containing 120 μg clonidine and 1 mL of 1% bupivacaine was administered using the

Copyright © Congress of Neurological Surgeons. Unauthorized reproduction of this article is prohibited.

TABLE 1. Protocol Used for the Semiological Analysis of the Headache in the Patients (A) and the Headache Impact Test-6 Scale Parameters (B)[a]

A. Semiological Analysis
1. Identification:
Name: Age: Sex:
2. Headache semiology:
2.1 Headache character: pulsatile ( ) heavy weight ( ) shocklike ( ) burning ( ) other_____
2.2. Localization: unilateral ( ) bilateral ( )
2.2.2. Frontoparietal ( ) temporal ( ) occipital ( )
2.3. Intensity: VAS:_____HIT-6:_____
2.4. Frequency:_____
2.5. Autonomic phenomenon: conjunctival ( ) nasal block ( ) tear drop ( )
2.6. Other symptoms: visual aura ( ) sensitive aura ( ) nausea ( ) photophobia ( ) phonophobia ( )
2.7. Time of the symptom:_____
3. Lesion characteristics: Histology:_____ microadenoma ( ) macroadenoma ( )
4. Treatment:
4.1. Medications: beta-blocker ( ) tricyclic antidepressants ( ) anticonvulsants ( ) calcium channel blocker ( ) corticosteroid ( ) lithium ( )
Other_____
4.2. Medications in pain crisis: _____
4.3. Surgical procedures: Gasser ganglion block ( ) Balloon compression ( )
5. Response

	1 month	3 months	6 months
HIT-6			
VAS			

6. Radiological examinations: Ictal SPECT:

B. Headache Impact Test-6
1. Pain intensity: When you have headaches, how often is the pain severe?
Never ( ) Rarely ( ) Sometimes ( ) Very often ( ) Always ( )
2. Social functioning: How often do headaches limit your ability to do usual daily activities including household work, work, school, or social activities?
Never ( ) Rarely ( ) Sometimes ( ) Very often ( ) Always ( )
3. Well-being: When you have a headache, how often do you wish you could lie down?
Never ( ) Rarely ( ) Sometimes ( ) Very often ( ) Always ( )
4. Vitality: In the past 4 weeks, how often have you felt too tired to do work or daily activities because of your headaches?
Never ( ) Rarely ( ) Sometimes ( ) Very often ( ) Always ( )
5. Emotional impact: In the past 4 weeks, how often have you felt fed up or irritated because of your headaches? Never ( ) Rarely ( ) Sometimes ( ) Very often ( ) Always ( )
6. Cognitive function: In the past 4 weeks, how often did headaches limit your ability to concentrate on work or daily activities? Never ( ) Rarely ( ) Sometimes ( ) Very often ( ) Always ( )

(6 points) + (8 points) + (10 points) + (11 points) + (13 points)
Classification:

a) Small (≤49 points)
b) Moderate (50-55 points)
c) Substantial (56-59 points)
d) Severe (≥60 points)

[a]VAS, Visual Analog Scale; HIT-6, Headache Impact Test-6; SPECT, single-photon emission computed tomography.

Copyright © Congress of Neurological Surgeons. Unauthorized reproduction of this article is prohibited.

TABLE 2. Characteristics of the 11 Patients Enrolled in the Study[a]

Patient	Sex, y/Age	Pattern of Autonomic Headache	Headache Main Symptom at Diagnosis of Pituitary Tumor	Tumor Size Before Pituitary Surgery	Histology	Treatment
1	M/28	Migraine-like	Yes	Macroadenoma	Nonfunctioning	Surgery
2	F/38	Cluster	Yes	Microadenoma	GH	Surgery/somatostatin analog[d]
3	F/41	Cluster	No	Macroadenoma	GH	Surgery/somatostatin analog[e]
4	F/29	Migraine-like	Yes	Microadenoma	Prolactin	Dopamine agonist[f]
5	F/26	Migraine-like	Yes	Macroadenoma	Prolactin	Dopamine agonist/surgery[g]
6	F/28	No class	No	Macroadenoma	GH	Surgery/radiotherapy/ somatostatin analog[h]
7	M/39	Trigeminal neuralgia	Yes	Macroadenoma	Prolactin	Dopamine agonist/surgery[i]
8	F/52	Migraine-like	Yes	Macroadenoma	Prolactin	Dopamine agonist/surgery[j]
9	F/45	Cluster	No	Macroadenoma	Nonfunctioning	Surgery
10	M/45	Cluster	No	Microadenoma	GH	Surgery/somatostatin analog[k]
11	F/34	No class	Yes	Macroadenoma	Prolactin	Dopamine agonist/surgery[l]

Patient	Cerebral Ictal SPECT Showing an Increased Uptake in Thalamic-Hypothalamic Region	HIT-6 Scale Score		Percutaneous Ganglion Block	HIT-6 Scale Score[b]		Trigeminal Rhizotomy	HIT-6 Scale Score[c]
		Before Medical Treatment	After Medical Treatment		After 3 mo	After 6 mo		
1	No	58	58	Yes	50	50	No	—
2	Yes	62	62	Yes	62	62	No	—
3	Yes	58	58	Yes	50	58	Yes	48
4	No	50	44	No	—	—	No	—
5	No	52	46	No	—	—	No	—
6	No	70	70	Yes	70	70	No	—
7	No	48	42	No	—	—	No	—
8	No	51	46	No	—	—	No	—
9	Yes	58	58	Yes	50	58	Yes	46
10	Yes	54	46	No	—	—	No	—
11	No	73	73	Yes	73	73	No	—

[a]Patients who did not respond to medical treatment subsequently underwent interventional procedures. HIT-6 score: 40 to 49, small; 50 to 55, moderate; 56 to 59, substantial; more than 59, severe. SPECT, single-photon emission computed tomography; HIT-6, Headache Impact Test-6; GH, growth hormone; IGF-I, insulinlike growth factor I.
[b]HIT-6 score determined after the interventional treatment: 3 and 6 months after percutaneous ganglion block intervention.
[c]HIT-6 score determined after the interventional treatment: 3 months after trigeminal rhizotomy.
[d-l]Hormonal levels when the patient was enrolled in the study.
[d]IGF-I 595 ng/mL (normal range, 106-277).
[e]IGF-I 92 ng/mL (normal range, 98-261).
[f]Prolactin 19.3 ng/mL (normal range, 0.33-27.33).[g]Prolactin 10.4 ng/mL (normal range, 0.33-27.33).
[h]IGF-I 174 ng/mL (normal range, 117-321).
[i]Prolactin 22 (normal range, 0.33-27.33).
[j]Prolactin 12 ng/mL (normal range, 0.33-27.33).
[k]IGF-I 110 ng/mL (normal range, 98- 261).
[l]Prolactin 17 (normal range, 0.33-27.33).

percutaneous Härtel technique, traditionally used to treat trigeminal neuralgias[25] (Figure 1).

Two patients who showed transitory pain relief with the percutaneous trigeminal ganglion blockade underwent the second stage of the surgical treatment: trigeminal percutaneous rhizotomy with a balloon, which was performed in the operating room with the aid of fluoroscopic imaging. Light general anesthesia was induced, and then an external pacemaker was placed on the patient's chest to set the depressor response. Preoperative atropine was not given so that the depressor response could be used as a parameter of trigeminal compression.

Patients were positioned supine, with a roll under their shoulders, allowing approximately 20 degrees of extension. A 14-gauge introducing cannula was percutaneously passed to the foramen using Härtel guidelines and aided by lateral fluoroscopic imaging. Often a brief trigeminal depressor response occurs from mechanical compression of the mandibular nerve at the foramen. Once the cannula had engaged the foramen ovale, the blunt obturator was removed and a straight guiding stylet inserted. Using the anteroposterior image (with the petrous ridge positioned in the radiographic center of the orbit), the stylet was directed at the medial dip in the petrous bone, which is the proximal entrance to

Copyright © Congress of Neurological Surgeons. Unauthorized reproduction of this article is prohibited.

TABLE 3. Medium-Range Results on Headache Impact Test-6 Scale Determined Throughout the Study[a]

HIT-6 Scale Topics	Pretreatment Period											After Conservative Treatment										
Patient	1	2	3	4	5	6	7	8	9	10	11	1	2	3	4	5	6	7	8	9	10	11
Pain intensity	13	11	11	10	10	13	8	11	13	11	11	13	11	11	6	8	13	6	11	13	8	11
Social functioning	11	13	13	8	10	11	8	8	11	11	13	11	13	13	6	6	11	6	8	11	6	13
Well-being	8	10	8	8	10	11	8	8	8	8	13	8	10	8	8	10	11	6	8	8	8	13
Vitality	10	10	10	10	8	11	8	8	8	8	10	10	10	10	10	8	11	8	8	8	8	10
Emotional impact	8	10	8	6	8	13	8	8	10	8	13	8	10	8	6	8	13	8	8	10	8	13
Cognitive functioning	8	8	8	8	6	11	8	8	8	8	13	8	8	8	8	6	11	8	8	8	8	13
Final HIT-6 scale score	58	62	58	50	52	70	48	51	58	54	73	58	62	58	44	46	70	42	46	58	46	73

HIT-6 Scale Topics	After Percutaneous Gasser Ganglion Block													After Balloon
Patient	1		2		3		6		9		11		3	9
Follow-up, mo	3	6	3	6	3	6	3	6	3	6	3	6	3	3
Pain intensity	8	8	11	11	8	11	13	13	10	13	11	11	8	10
Social functioning	10	10	13	13	10	13	11	11	8	11	13	13	10	8
Well-being	8	8	10	10	8	8	11	11	8	8	13	13	8	8
Vitality	10	10	10	10	10	10	11	11	8	8	10	10	8	6
Emotional impact	6	6	10	10	6	8	13	13	8	10	13	13	6	6
Cognitive functioning	8	8	8	8	8	8	11	11	8	8	13	13	8	8
Final HIT-6 scale score	50	50	62	62	50	58	70	70	50	58	73	73	48	46

[a]HIT-6, Headache Impact Test-6. HIT-6 scale score: 40 to 49, small; 50 to 55, moderate; 56 to 59, substantial; more than 59, severe.

the Meckel cave, the porus trigeminus, found approximately 17 mm beyond the foramen ovale. The tip of the stylet was set approximately 2 mm beyond the edge of the petrous ridge as seen through the orbit. Once properly positioned, the stylet was withdrawn and the balloon catheter inserted into the same site.

The lateral view of the cranium was used during the balloon compression. Air was evacuated from the balloon with a tuberculin syringe connected to a 3-way stopcock. The balloon was inflated with 0.7 to 0.75 mL of 180 mg% iohexol, and once a corresponding pear shape was observed, the balloon was left inflated for 1 to 1.5 minutes. The pear shape indicates that the tip of the balloon lies within the porus trigeminus, which is where it must lie to compress the trigeminal nerve adequately.

The depressor response was observed in both patients at this point, briefly triggering the external pacemaker. Intermittent lateral imaging was obtained to monitor the balloon's position and shape. The needle and catheter were then removed, and sterile bandage applied to the cheek. Both patients were discharged the following morning.

RESULTS

The characteristics of the 11 patients with trigeminal/autonomic headache are shown in Table 2. Four patients had growth hormone–secreting adenomas; all but 1 (patient 2) were under endocrine control after surgery and with the use of somatostatin analog. Another 4 patients with prolactinomas were initially treated with dopamine agonists and were cured after pituitary surgery. One patient with microprolactinoma was treated only with dopamine agonist. The other 2 patients had nonfunctioning pituitary adenomas. In 8 of the 11 patients, headache was the main symptom at the time of diagnosis of pituitary adenoma.

All individuals enrolled had their headache severity quantified by the HIT-6 scale, as detailed in Table 3, and functionally studied through cerebral SPECT performed during an ictal period. All but 1 patient (number 7) had their headache classified as, at least, moderate, and 3 of them had severe headache, by the HIT-6 scale. As shown in Figure 2, cerebral SPECT showed increased uptake in the peri-insular/insular and thalamic/hypothalamic regions in the 4 patients who presented with trigeminal/autonomic headache of a cluster-like pattern (patients 2, 3, 9, and 10). The other 7 patients had their trigeminal/autonomic headache subclassified as migraine-like (patients 1, 4, 5, and 8), trigeminal neuralgia (patient 7), and "no class" (patients 6 and 11), and none of them showed the same alterations in the cerebral SPECT (Figure 3).

All patients were initially submitted to medical treatment, and the intensity of the headaches was readdressed after 6 months. Three patients with migraine-like pain and one with cluster-like symptoms presented a significant decrease in scoring in the HIT-6 scale classification, changing their headache status from moderate to small (Table 2). These 4 patients together with the patient with trigeminal neuralgia, who experienced a 6-point decrease in the HIT-6 scale score, were kept on medical treatment with no further procedures because the benefit of the conservative approach was considered evident and relevant. Medications used, side effects, and final doses for each patient are shown in Table 4.

Copyright © Congress of Neurological Surgeons. Unauthorized reproduction of this article is prohibited.

TABLE 4. Clinical Treatment: Medications, Side Effects, and Doses Used During the Study Protocol[a]

Patient	Medications Prescribed	Side Effects	Final Medications and Final Doses
1	AMT, PRO, TOP, VAL	VAL: nausea, drowsiness	AMT: 75 mg/d
			PRO: 120 mg/d
			TOP: 75 mg/d
2	LIT, VAL, VER	None	LIT: 1200 mg/d
			VAL: 1000 mg/d
			VER: 240 mg/d
3	LIT, VAL, VER	VER: water retention, drowsiness	LIT: 1200 mg/d
			VAL: 1000 mg/d
4	NTP, TOP	None	NTP: 50 mg/d
			TOP: 75 mg/d
5	AMT, PRO	None	AMT: 75 mg/d
			PRO: 160 mg/d
6	AMT, TOP, VAL, VEN, VER	VAL: nausea, drowsiness VEN: nausea	AMT: 75 mg/d
			TOP: 100 mg/d
			VER: 240 mg/d
7	CBZ, TOP	None	CBZ: 1000 mg/d
			TOP: 50 mg/d
8	AMT, PRO, VAL	None	AMT: 50 mg/d
			PRO: 120 mg/d
			VAL: 1000 mg/d
9	LIT, VAL, VER	None	LIT: 1800 mg/d
			VAL: 1000 mg/d
			VER: 360 mg/d
10	VAL, VER	None	VAL: 1000 mg/d
			VER: 480 mg/d
11	AMT, VAL, PRO, TOP	None	AMT: 75 mg/d
			VAL: 1000 mg/d
			PRO: 120 mg/d
			TOP: 75 mg/d

[a]AMT, amitriptyline; PRO, propranolol; TOP, topiramate; VAL, valproic acid; LIT, lithium carbonate; VER, verapamil; NTP, nortriptyline; VEN, venlafaxine; CBZ, carbamazepine.

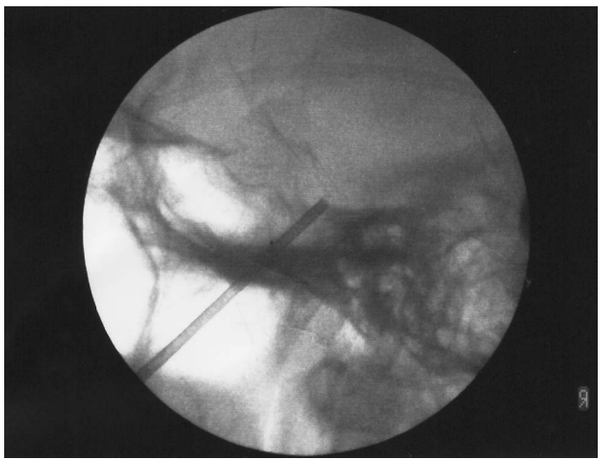

FIGURE 1. *Puncture of the ganglion of Gasser guided by radioscopy, performed using the Härtel technique.*

The other 6 patients who did not experience improvement in headache after 6 months of medical treatment underwent percutaneous trigeminal ganglion blockade. One patient with migraine-like pain (patient 1) had his headache classification changed from substantial to moderate after 3 and 6 months of follow-up (Table 2). One patient with cluster headache (patient 2, the only patient who was not hormonally controlled when enrolled in the study) and 2 patients with an unclassified pattern (patients 6 and 11) did not experience any benefit as shown by the HIT-6 scale score after the percutaneous ganglion blockade and did not undergo any additional procedures. Patients 3 and 9, presenting with cluster headache, showed an initial response to treatment, with the HIT-6 scale classification changing from substantial to moderate after 4 months. However, this effect was transitory, and the score returned to moderate after 6 months (Table 2).

Based on the initial response to the ganglion blockade, these 2 patients (patients 3 and 9) were assigned for the trigeminal rhizotomy with balloon compression. Three months after the procedure, significant changes in the HIT-6 scale score were noted. In both patients, the headache was reclassified from substantial to small, according to the HIT-6 scale score (Table 2). The benefit was also maintained after more than 1 year of follow-up (data not shown).

No complications related to the interventional procedures (percutaneous trigeminal ganglion blockade and trigeminal rhizotomy with balloon compression) were observed in any patient involved in the study.

DISCUSSION

Although headache has long been recognized as a common symptom associated with pituitary lesions,[1-3] the pathophysiology of pituitary tumor–related cephalalgias is still unknown. Dural stretch and invasion of the cavernous sinus explain many, but not all, cases of headache in this setting. The hypothesis of a biochemical cause has been postulated to justify the pain in a subgroup of patients with pituitary tumors that respond to somatostatin analogs, perhaps via the inhibition of some local nociceptive peptide,[20] but a definite mechanism is still to be established.

Pituitary adenomas require an intervention, eg, surgical removal or treatment with somatostatin analogs (for growth hormone–secreting adenomas) or dopamine agonists (for prolactinomas)

Copyright © Congress of Neurological Surgeons. Unauthorized reproduction of this article is prohibited.

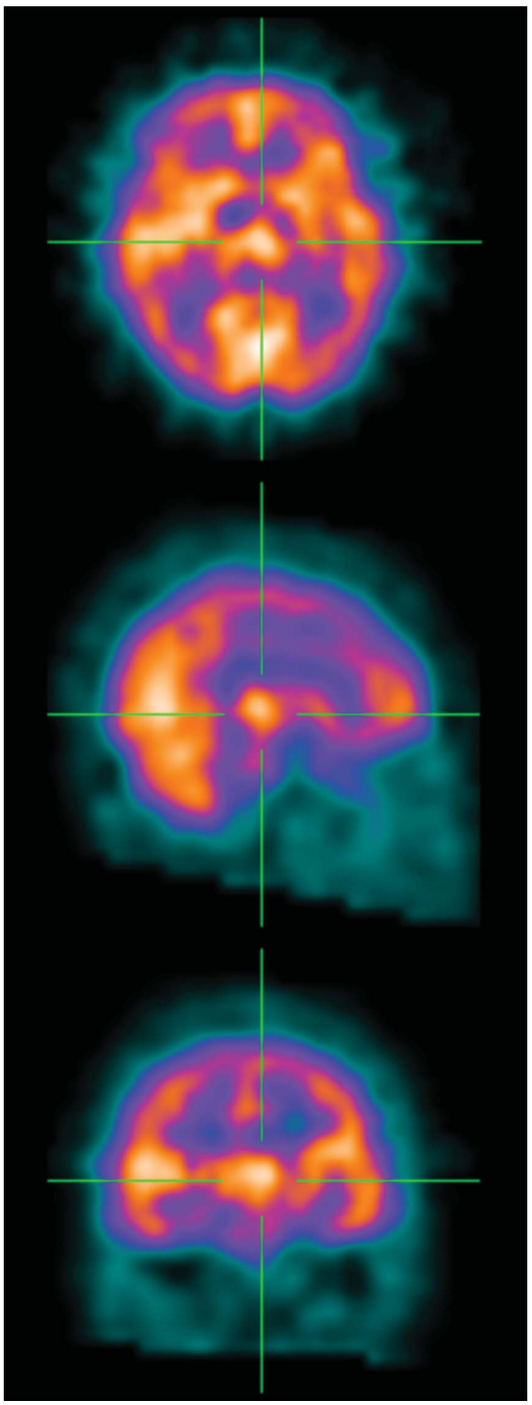

FIGURE 2. *Cerebral ictal single-photon emission computed tomography (SPECT) performed in patient 2, showing increased uptake in the thalamic/hypothalamic region, bilaterally. Patients 3, 9, and 10 also presented a similar pattern on the SPECT scan.*

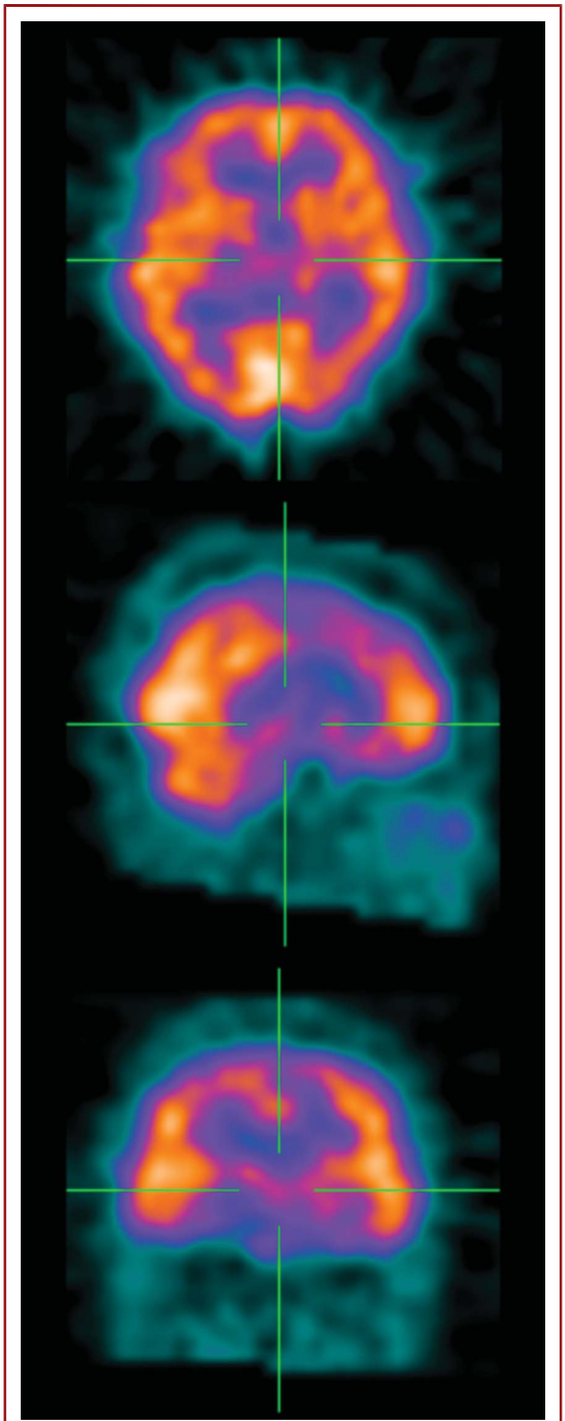

FIGURE 3. *Cerebral ictal single-photon emission computed tomography performed in patient 1. Note the absence of increased uptake in the thalamic/hypothalamic region. The same pattern was observed in patients 4, 5, 6, 7, 8, and 11.*

Copyright © Congress of Neurological Surgeons. Unauthorized reproduction of this article is prohibited.

when any threat to the optic chiasm or endocrine hypersecretion is observed.[26-29] Headache may be aborted with the pituitary tumor approach, although this is not a rule nor is the presence of headache an indication for treatment.

After surgical removal of the pituitary tumor, a minority of patients evolve with persistent and severe headache, most of the time with an autonomic pattern, which is resistant to conservative treatments such as tricyclic antidepressants, anticonvulsants, beta-blockers, calcium channel blockers, dopamine agonists, and corticosteroids.[6,14,30] Some of these patients obtain relief with subcutaneous injections of somatostatin analogs, but our experience shows that these patients become addicted to the drug: they require progressively higher doses of the medication, with loss of the analgesic effect, thus discouraging this approach as a routine. In this study, 8 of the 11 patients with persistent headache after surgery had this symptom as the main manifestation at the time of diagnosis of pituitary adenoma. All patients were kept on medical treatment throughout the study, regardless of the interventional procedures to which they were assigned, and our main goal was to investigate alternative approaches that could provide pain relief in this setting.

To our knowledge, this is the first time that percutaneous Gasser ganglion block and trigeminal percutaneous rhizotomy were used for the treatment of trigeminal/autonomic headache associated with pituitary tumors. Although the placebo effect cannot be ruled out in this study, according to our results, the interventional procedures may be promising options for the treatment of such patients, in addition to conventional medical treatment. The effectiveness of percutaneous Gasser ganglion block was observed in 1 patient with migraine-like headache, whereas a transitory benefit was seen in 2 patients with cluster autonomic headache.

Moreover, based on previous reports in the literature of the successful use of trigeminal rhizotomy in patients with primary cluster headache,[31-33] we performed this surgical technique in the 2 patients with cluster headache who presented a previous transitory response to percutaneous ganglion block. A significant and sustained improvement in the pain intensity was observed in both after rhizotomy, suggesting that this procedure may be an alternative for the treatment of cluster headache in the context of pituitary adenomas.

In an effort to better define the trigeminal pattern of headache in our patients, we performed functional studies with cerebral SPECT during the ictal period. In 4 of the 11 patients, an increased uptake of the contrast was observed in the peri-insular/insular and thalamic/hypothalamic regions, suggesting a possible role for reduced blood flow in this area in the underlying mechanism for the headache. Previous studies of cerebral blood flow in trigeminal headaches, using SPECT, are few in number, and the results have been heterogeneous.[34-38] In the most recent study, a reduced cerebral blood flow was observed in the thalamus region in patients with cluster headache compared with healthy volunteers.[39] In this study, the alterations were seen outside the active period of headache.[39]

In our study, the 4 patients who presented altered cerebral blood flow in SPECT had cluster headache, and 1 of them was successfully treated with trigeminal ganglion blockade, whereas 2 others who presented a transitory response to this procedure were successfully treated with percutaneous rhizotomy. These findings may suggest a relationship between the thalamic/hypothalamic pattern on SPECT and the response to surgical procedures. Unfortunately, it was not possible to perform the SPECT during a headache-free period, which limits our conclusions about the utility of this modality of functional study in the approach of the headache associated with pituitary adenomas.

Our study, performed in a small number of patients, represents the first insight for a potential benefit of percutaneous Gasser ganglion block and percutaneous balloon compression (trigeminal rhizotomy) in the treatment of severe trigeminal/autonomic headache associated with pituitary tumors.

Disclosure

The authors have no personal financial or institutional interest in any of the drugs, materials, or drugs described in this article.

REFERENCES

1. Suwanwela N, Phanthumchinda K, Kaoropthum S. Headache in brain tumor: a cross-sectional study. *Headache*. 1994;34(7):435-438.
2. Yamagiwa S, Niwa K, Yokoyama Y, et al. Primary adenoid cystic carcinoma of Bartholin's gland. A case report. *Acta Cytol*. 1994;38(1):79-82.
3. Ferrante E, Ferraroni M, Castrignano T, et al. Non-functioning pituitary adenoma database: a useful resource to improve the clinical management of pituitary tumors. *Eur J Endocrinol*. 2006;155(6):823-829.
4. Levy MJ, Matharu MS, Meeran K, Powell M, Goadsby PJ. The clinical characteristics of headache in patients with pituitary tumours. *Brain*. 2005;128 (Pt 8):1921-1930.
5. Levy MJ, Matharu MS, Goadsby PJ. Prolactinomas, dopamine agonists and headache: two case reports. *Eur J Neurol*. 2003;10(2):169-173.
6. Porta-Etessam J, Ramos-Carrasco A, Berbel-Garcia A, Martinez-Salio A, Benito-Leon J. Clusterlike headache as first manifestation of a prolactinoma. *Headache*. 2001;41(7):723-725.
7. Sarov M, Valade D, Jublanc C, Ducros A. Chronic paroxysmal hemicrania in a patient with a macroprolactinoma. *Cephalalgia*. 2006;26(6):738-741.
8. Tfelt-Hansen P, Paulson OB, Krabbe AA. Invasive adenoma of the pituitary gland and chronic migrainous neuralgia. A rare coincidence or a causal relationship? *Cephalalgia*. 1982;2(1):25-28.
9. Friedman AH, Wilkins RH, Kenan PD, Olanow CW, Dubois PJ. Pituitary adenoma presenting as facial pain: report of two cases and review of the literature. *Neurosurgery*. 1982;10(6 Pt 1):742-745.
10. Gazioglu N, Tanriover N, Tuzgen S. Pituitary tumour presenting with trigeminal neuralgia as an isolated symptom. *Br J Neurosurg*. 2000;14(6):579.
11. Classification and diagnostic criteria for headache disorders, cranial neuralgias and facial pain. Headache Classification Committee of the International Headache Society. *Cephalalgia*. 1988;8(suppl 7):1-96.
12. Forsyth PA, Posner JB. Headaches in patients with brain tumors: a study of 111 patients. *Neurology*. 1993;43(9):1678-1683.
13. Abe T, Matsumoto K, Kuwazawa J, Toyoda I, Sasaki K. Headache associated with pituitary adenomas. *Headache*. 1998;38(10):782-786.
14. Levy MJ, Jager HR, Powell M, Matharu MS, Meeran K, Goadsby PJ. Pituitary volume and headache: size is not everything. *Arch Neurol*. 2004;61(5):721-725.
15. Williams G, Ball JA, Lawson RA, Joplin GF, Bloom SR, Maskill MR. Analgesic effect of somatostatin analogue (octreotide) in headache associated with pituitary tumours. *Br Med J (Clin Res Ed)*. 1987;295(6592):247-248.
16. Levy MJ, Classey JD, Maneesri S, Meeran K, Powell M, Goadsby PJ. The association between calcitonin gene-related peptide (CGRP), substance P and headache in pituitary tumours. *Pituitary*. 2004;7(2):67-71.

Copyright © Congress of Neurological Surgeons. Unauthorized reproduction of this article is prohibited.

17. Nathoo S, Classey JD, Levy MJ, Meeran K, Powell M, Goadsby PJ. No relationship between vasoactive intestinal polypeptide expression and headache in pituitary tumours. *Acta Neurol Scand*. 2005;111(5):317-322.
18. Levy MJ, Matharu M, Goadsby PJ. Chronic headache and pituitary tumors. *Curr Pain Headache Rep*. 2008;12(1):74-78.
19. Fleseriu M, Yedinak C, Campbell C, Delashaw JB. Significant headache improvement after transsphenoidal surgery in patients with small sellar lesions. *J Neurosurg*. 2009;110(2):354-358.
20. Levy MJ, Bejon P, Barakat M, Goadsby PJ, Meeran K. Acromegaly: a unique human headache model. *Headache*. 2003;43(7):794-797.
21. Gandek B, Alacoque J, Uzun V, Andrew-Hobbs M, Davis K. Translating the Short-Form Headache Impact Test (HIT-6) in 27 countries: methodological and conceptual issues. *Qual Life Res*. 2003;12(8):975-979.
22. Nachit-Ouinekh F, Dartigues JF, Henry P, et al. Use of the headache impact test (HIT-6) in general practice: relationship with quality of life and severity. *Eur J Neurol*. 2005;12(3):189-193.
23. Shin HE, Park JW, Kim YI, Lee KS. Headache Impact Test-6 (HIT-6) scores for migraine patients: their relation to disability as measured from a headache diary. *J Clin Neurol*. 2008;4(4):158-163.
24. Dahlof CG. Measuring disability and quality of life in migraine. *Drugs Today (Barc)*. 2003;39(suppl D):17-23.
25. Hartel F. Die Leitungsanästhesie und Injektionsbehanlung des Ganglion Gasseri und der Trigemenisstäne. *Arch Klin Chir*. 1912;100:193-292.
26. Buchfelder M, Schlaffer S. Surgical treatment of pituitary tumours. *Best Pract Res Clin Endocrinol Metab*. 2009;23(5):677-692.
27. Greenman Y, Stern N. Non-functioning pituitary adenomas. *Best Pract Res Clin Endocrinol Metab*. 2009;23(5):625-638.
28. Melmed S. Medical progress: acromegaly. *N Engl J Med*. 2006;355(24):2558-2573.
29. Schlechte JA. Clinical practice. Prolactinoma. *N Engl J Med*. 2003;349(21):2035-2041.
30. Evans RW. Migrainelike headache in a patient with a hemorrhagic pituitary macroadenoma. *Headache*. 1997;37(7):455-456.
31. Mathew NT. Cluster headache. *Neurology*. 1992;42(3 suppl 2):22-31.
32. Mathew NT, Hurt W. Percutaneous radiofrequency trigeminal gangliorhizolysis in intractable cluster headache. *Headache*. 1988;28(5):328-331.
33. Pieper DR, Dickerson J, Hassenbusch SJ. Percutaneous retrogasserian glycerol rhizolysis for treatment of chronic intractable cluster headaches: long-term results. *Neurosurgery*. 2000;46(2):363-368; discussion 368-370.
34. Henry PY, Vernhiet J, Orgogozo JM, Caille JM. Cerebral blood flow in migraine and cluster headache. Compartmental analysis and reactivity to anaesthetic depression. *Res Clin Stud Headache*. 1978;6:81-88.
35. Krabbe AA, Henriksen L, Olesen J. Tomographic determination of cerebral blood flow during attacks of cluster headache. *Cephalalgia*. 1984;4(1):17-23.
36. Nelson RF, du Boulay GH, Marshall J, Russell RW, Symon L, Zilkha E. Cerebral blood flow studies in patients with cluster headache. *Headache*. 1980;20(4):184-189.
37. Norris JW, Hachinski VC, Cooper PW. Cerebral blood flow changes in cluster headache. *Acta Neurol Scand*. 1976;54(4):371-374.
38. Sakai F, Meyer JS, Ishihara N, Naritomi H, Deshmukh VD. Noninvasive 133XE inhalation measurements of regional cerebral blood flow in migraine and related headaches. *Acta Neurol Scand Suppl*. 1977;64:196-197.
39. Di Piero V, Fiacco F, Tombari D, Pantano P. Tonic pain: a SPET study in normal subjects and cluster headache patients. *Pain*. 1997;70(2-3):185-191.

COMMENTS

The pathomechanisms of pituitary adenoma associated facial pain is still unsolved. The authors present a series of 11 patients (3.2%) out of a total of 345 patients who still had untractable trigeminal headaches persisting after pituitary adenoma surgery. Unfortunately there are no data on the remaining 96.8% of patients according to their pre- and postoperative status regarding headaches. Among the 11 investigated patients, medical treatment had no significant effect in 6 patients, so that these were treated by percutaneous ganglion block and/or additional trigeminal rhizotomy, reducing the pain in 3 of them. This study illustrates that pituitary adenoma associated pain is a definite challenge that necessitates a sophisticated therapeutic strategy in selected cases. Hopefully, further insight in the pathophysiological mechanism will offer additional treatment options in the future.

Christopher Nimsky
Marburg, Germany

The authors evaluated their experience in managing medically intractable headaches in a small subset of patients after removal of pituitary tumors. Several of these patients had growth hormone–secreting tumors, which can notoriously cause headaches even after surgical cure or hormonal control of insulinlike growth factor I with somatostatin analogs. The authors classified 11 of these patients as having trigeminal headaches of a presumed autonomic origin. They provide single-photon emission computed tomography data to suggest involvement of the hypothalamic region in mediating the control of these headaches and document improvement in headache symptoms after trigeminal blockade or rhizotomy in 3 patients.

Although this is a very nice effort to classify an unusual headache syndrome and provide a treatment rationale, I am left with many questions and uncertainties. Headache is extremely common in patients with pituitary tumors, and almost 75% will report improvement in symptoms after surgery. However, not all patients with headaches and pituitary tumors have their symptoms relieved by surgery. Headache is one of the most common medical disorders known, and it is quite reasonable that the subset of patients described here had headaches that had nothing to do with their pituitary tumor. Also, of note, these patients did not have trigeminal neuralgia, but rather trigeminal headache. Unilateral rhizotomy or trigeminal blockade was effective in reducing headache in 3 of 6 patients treated, but even these patients were not completely cured of symptoms. A similar efficacy may be seen in headache sufferers without pituitary tumors. Further, placebo effect may play a large role because it often does in headache sufferers. Placebo effects can account for up to 40% of response to any treatment for headache. Unfortunately, this article does not really provide the practitioner any new guidelines for treatment or a clear way to determine who might benefit from this invasive and potentially risky treatment. It may suggest further lines of headache research, but I do not believe that the current data are compelling enough to recommend trigeminal blockade in patients with intractable headaches, and I would not suggest such treatment for my patients based on this report. Nonetheless, I laud the efforts of the authors in collecting and reporting these data and provoking further inquiry into the nature of these debilitating headaches.

Adam N. Mamelak
Los Angeles, California

The authors present their experience gleaned from 345 patients with pituitary adenoma. However, details of only a few patients were presented. Criteria for selecting those patients are not clear nor are the details of symptoms of the majority of the patients presented. In how many of the entire group was pituitary adenoma discovered during evaluation for headache? Consequently, this cannot be considered a study of the entire population of patients seen by the authors, but rather case histories of the patients, presumably randomly selected, that are presented in detail. Because there was no consistent response to management, no firm conclusions or recommendations for treatment have emerged. However, the experience demonstrates how difficult it can be to manage headache that persists after treatment of pituitary adenoma.

Philip L. Gildenberg
Houston, Texas

Copyright © Congress of Neurological Surgeons. Unauthorized reproduction of this article is prohibited.

Prospective, Randomized, Double-Blind Clinical Study Evaluating the Correlation of Clinical Outcomes and Cervical Sagittal Alignment

Alan T. Villavicencio, MD*‡
Jason M. Babuska, BA‡
Alex Ashton, PA-C*
Eric Busch, PA-C*
Cassandra Roeca, BA*
E. Lee Nelson, MD*‡
Alexander Mason, MD*‡
Sigita Burneikiene, MD*‡

*Boulder Neurosurgical Associates, Boulder, Colorado; ‡Justin Parker Neurological Institute, Boulder, Colorado

Correspondence:
Sigita Burneikiene, MD,
Boulder Neurosurgical Associates,
1155 Alpine Ave, Ste 320,
Boulder, CO 80304.
E-mail: sigitab@bnasurg.com

Received, December 10, 2009.
Accepted, October 1, 2010.

Copyright © 2011 by the
Congress of Neurological Surgeons

BACKGROUND: Sagittal alignment of the cervical spine has received increased attention in the literature as an important determinant of clinical outcomes after anterior cervical diskectomy and fusion. Surgeons use parallel or lordotically fashioned grafts depending on preference or simple availability.

OBJECTIVE: To quantitatively assess and compare cervical sagittal alignment and clinical outcome when lordotic or parallel allografts were used for fusion.

METHODS: A prospective, randomized, double-blind clinical study that enrolled 122 patients was performed. The mean follow-up was 37.5 months (range, 12-54 months).

RESULTS: The mean postoperative cervical sagittal alignment was 19° (range, −7°-36°) and 18° (range, −7°-37°) in the lordotic and parallel graft patient groups, respectively. The mean segmental sagittal alignment was 6° (range, −4°-19°) and 7° (range, −3°-19°) in the lordotic and parallel graft patient groups, respectively. There were no statistically significant differences in clinical outcome scores between the lordotic and parallel graft patient groups. However, patients who had maintained or improved segmental sagittal alignment, regardless of graft type, achieved a higher degree of improvement in Short Form-36 Physical Component Summary and Neck Disability Index scores. This was statistically significant ($P < .038$).

CONCLUSION: The use of lordotically shaped allografts does not increase cervical/segmental sagittal alignment or improve clinical outcomes. Maintaining a consistent segmental sagittal alignment or increasing segmental lordosis was related to a higher degree of improvement in clinical outcomes.

KEY WORDS: Anterior cervical diskectomy and fusion, Cervical sagittal alignment, Clinical outcomes, Prospective clinical study

Neurosurgery 68:1309–1316, 2011 DOI: DOI:10.1227/NEU.0b013e31820b51f3 www.neurosurgery-online.com

Compared with lumbar sagittal alignment, which has received a large amount of attention in the literature, much less is known regarding the alteration of cervical sagittal alignment (CSA) and clinical outcomes. Although it is generally accepted that the physiological sagittal balance is important for normal function of the spine, whether maintenance and improvement of cervical and/or segmental lordosis have an effect on clinical outcomes after cervical spine surgeries remains to be proven. This could be partially related to the facts that the greatest normal physiological variations in spinal curvature occur between C2 and C7 in the cervical spine[1] and that most of the published studies examined sagittal alignment as the postoperative result without studying its relationships to the preoperative status. In addition, it is not easy to clearly demonstrate that the correction of kyphotic cervical deformity promotes improvement in clinical outcome scores when such improvement could be attributed to the spinal cord decompression itself.[2]

Device manufacturers and tissue banks offer cervical allografts and other interbody spacers

ABBREVIATIONS: ACDF, anterior cervical diskectomy and fusion; **CSA,** cervical sagittal alignment; **MCS,** Mental Component Summary + Score; **NDI,** Neck Disability Index; **PCS,** Physical Component Summary; **SSA,** segmental sagittal alignment; **VAS,** Visual Analog Scale

Copyright © Congress of Neurological Surgeons. Unauthorized reproduction of this article is prohibited.

that come in various sagittal profiles, including lordotic, parallel, or even convex designs that, according to indications, should restore lordosis, maximize surface area contact,or allow for patient-specific needs. However, these statements or improved long-term clinical outcomes have never been proven in any prospective, randomized clinical studies. The purpose of this study was to determine whether lordotic sagittal alignment and clinical outcomes could be improved in patients undergoing anterior cervical diskectomy and fusion (ACDF) with lordotically shaped vs parallel allografts.

METHODS

A prospective, randomized, double-blind clinical study was performed. Institutional Review Board approval was granted, and the study was initiated in January 2003. The study objectives and surgical procedure were explained, and informed consent was obtained from all patients who agreed to participate in the study. Patients were randomly assigned to 1 of the 2 groups and received either lordotic or parallel allograft(s) during the ACDF procedure. The allograft selection was performed after enrollment but before the surgery with the use of the JavaScript random-number generator (Research Randomizer version 3.0). Both the patient and the independent radiographic reviewer were blinded to whether lordotic or parallel allografts were used during surgery.

Clinical Outcome Assessment and Analysis

Standardized questionnaires were used to evaluate clinical outcomes. Health-related quality of life or functional outcomes were assessed with the Health-Related Quality of Life Questionnaire (Short Form-36 [SF-36] version 2). Two scores within the scoring algorithm were analyzed: the Physical Component Summary (PCS) and Mental Component Summary + Score (MCS). The Neck Disability Index (NDI) was used to evaluate chronic disability and activities of daily living. The severity of neck and arm pain was evaluated using VAS (Visual Analog Scale). In addition, patients were asked to complete a self-reported Patient Satisfaction With Results survey. A sample of the patient satisfaction survey and scoring methods are presented in Figure 1. A total score was calculated for each patient by averaging the scores from all 6 responses, and the means were compared between the lordotic and parallel allograft patient groups.

Surgical Procedure

The surgical procedure has been previously described.[3] All ACDF procedures were performed with either lordotic or parallel allograft cortical spacers manufactured by Synthes Spine (West Chester, Pennsylvania) or Lanx (Broomfield, Colorado). The lordotic allografts had a 5° profile. Both parallel and lordotic allografts were available in variable heights ranging from 5 to 12 mm and were selected depending on the height of the intervertebral disk space. Two anterior cervical arthrodesis plating systems were used for patients in the study: the Zephir and Atlantis systems (Medtronic Sofamor Danek, Memphis, Tennessee).

Radiographic Assessment and Analysis

Two parameters were measured preoperatively and postoperatively on lateral neutral views of cervical radiographs: CSA and segmental sagittal alignment (SSA) (Figure 2A and 2B). Sagittal alignment was measured using the posterior tangent method described by Gore et al.[4] This method uses a technique in which the tangent to the C2 and C7 posterior vertebral body margins is calculated to determine the overall CSA. The SSA was determined by measuring sagittal alignment of the fused segment(s). The posterior tangent method has been regarded in the literature as more reliable than the Cobb method for lateral cervical radiographic analysis[5] and was therefore chosen for this study. We chose positive angulation as indicative of lordosis and negative angulation to represent kyphosis. The mean postoperative CSA and SSA values were compared between the 2 groups of patients who received lordotically shaped or parallel allografts during the surgery.

Correlation of Change in Sagittal Alignment and Clinical Outcomes

We also performed a posthoc analysis to examine whether the maintenance or enhancement of CSA and/or SSA regardless of allograft shape was predictive of a higher degree of improvement in clinical outcome scores. This was accomplished by calculating the difference between the preoperative and postoperative CSA and SSA for each patient. Changes in clinical outcome scores were calculated for each patient by the difference

The following are statements that people make about what they expect following a spinal surgery. For each statement indicate how true or false you think it is.

	Definitely true	Mostly true	Don't know	Mostly false	Definitely false
01. I can do the things I thought I would be able to after surgery.	○	○	○	○	○
02. I was helped as much as I though I would be by my surgery.	○	○	○	○	○
03. My pain was reduced as much as I expected it to be after surgery.	○	○	○	○	○
04. The benefits of my care outweight the setbacks it caused me.	○	○	○	○	○
05. Overall I am happy with the care I am receiving for my neck and/or arms.	○	○	○	○	○
06. All things considered, I would have the surgery again for the same condition.	○	○	○	○	○

FIGURE 1. *Patient Satisfaction With Results survey. Answers were scored on a scale from 0 to 100: 100 = definitely true; 75 = mostly true; 50 = don't know; 25 = mostly false; 0 = definitely false. Total (overall satisfaction) was calculated by averaging the scores from all 6 responses.*

Copyright © Congress of Neurological Surgeons. Unauthorized reproduction of this article is prohibited.

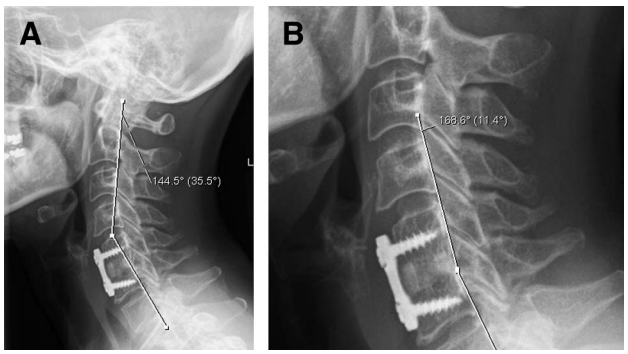

FIGURE 2. *Lateral neutral radiographs demonstrating cervical sagittal alignment (A) and segmental sagittal alignment (B) measurements.*

between preoperative and postoperative scores. The difference in clinical outcome scores was then compared for the subgroups (maintenance/change toward lordosis vs change toward kyphosis) for both SSA and CSA.

Statistical Analyses

Data are expressed descriptively as means (range) and percentages when applicable. Groups were compared by the use of Student *t* tests for all independent continuous quantitative variables. All categorical values were compared between groups with χ^2 analysis (with or without Yates continuity correction). Regression analyses were conducted to evaluate the relationship of the change in SSA with the change in CSA, as well as relationships between the SSA and CSA with each of the clinical outcome measures. Statistical significance was considered at values of $P \leq .05$.

RESULTS

Patients

The study analyzed 122 patients who underwent 1- to 3-level ACDF surgeries between March 2003 and March 2006. All patients enrolled in the study failed at least 6 weeks of conservative therapy before surgery unless immediate surgical intervention was required (eg, severe progressive myelopathy). There were 63 male (51.6%) and 59 female (48.4%) patients. The average patient age was 49.9 years (range, 17-80 years). Patients were selected for surgery on the basis of clinical symptoms and included 84 patients (68.8%) who had intractable neck pain and radiculopathy caused by spondylosis and/or disk herniation, foraminal and/or central stenosis, or spondylolisthesis and 38 patients (31.2%) with myelopathy.

Clinical and radiographic patient evaluation was performed preoperatively and then at 3, 6, 12, 24, 36, and 48 months after surgery. The mean follow-up time was 37.5 months (range, 12-54 months).

Lordotic vs Parallel Allograft Patient Groups: Clinical Outcome and Sagittal Alignment Analysis

There were 57 and 65 patients in the lordotic and parallel allograft patient groups, respectively. Selected demographic and clinical patient data are presented in Table 1. There were no statistically significant differences in clinical diagnoses, duration of symptoms, previous surgeries, or preoperative clinical symptoms between the 2 patient groups. Selected operative data, including surgical levels, estimated blood loss, duration of procedure (operating room time), and length of hospital stay, for the lordotic and parallel allograft patient groups are presented in Table 2. There were no statistically significant differences identified between any of these parameters.

TABLE 1. Selected Demographic and Clinical Data for Lordotic and Parallel Allograft [a]Patient Groups

	Lordotic	Parallel	*P*
Demographic data			
Patients, n (%)	57	65	
Age, y	49.2 (34-78)	50.6 (17-80)	.52
Male/female	25:32	38:27	.11[b]
Clinical data			
Diagnosis			
Cervical radiculopathy, n (%)	39 (68.4)	45 (69.2)	.38[b]
Myelopathy, n (%)	18 (31.6)	20 (30.8)	
Pre-Op VAS neck	5.4 (0-10)	5.8 (0-10)	.53
Pre-Op VAS arm	5.1 (0-10)	4.5 (0-10)	.34
Pre-Op SF-36 PCS	38.5 (16.4-54.9)	37.3 (20.8-57.4)	.45
Pre-Op SF-36 MCS	41.9 (10.2-69.4)	43.4 (17.8-74.2)	.54
Pre-Op NDI	20.1 (1-45)	20.4 (0-41)	.88
Previous surgeries, n (%)	1 (1.7)	8 (12.3)	.06[c]
Duration of symptoms, mo	25.3 (0.5-240)	31.2 (0.1-288)	.53

[a]MCS, Mental Component Summary + Score; NDI, Neck Disability Index; PCS, Physical Component Summary; Pre-Op, preoperative; SF-36, Short-Form version 2 Health Survey; VAS, Visual Analog Scale. Student *t* tests were used for all calculations comparing the 2 groups except when noted, in which case χ^2 tests [b]without or [c]without the Yates correction were performed. Values are presented as means (ranges) when appropriate.

The mean clinical outcomes scores were almost identical in both patient groups that received either lordotic or parallel allografts (Table 3). Although improvement was noted in all postoperative clinical outcome measures, we found no statistically significant differences between the lordotic and parallel allograft patient groups. A power analysis was conducted using *t*-test sample sizes of 57 and 65 to evaluate the detectable effect size of our data. With the recommended power of 0.8, the present sample size would have been able to detect an effect size as small as 0.5.

The lordotic and parallel allograft patient groups did not significantly differ in their CSA or SSA ($P = .67$) preoperatively. The mean CSA was measured at 16° degrees (range, −8°-34°) and 17° (range, −10°-34°) in the patient groups that received lordotically shaped or parallel allografts, respectively. The mean SSA was measured at 1° (range, −10°-12°) and 2° (range, −13°-25°) in the lordotic and parallel allograft patient groups, respectively (Figure 3). Although both the lordotic and parallel allograft patient groups had increased mean CSA and SSA scores postoperatively, no statistically significant differences were found in mean

Copyright © Congress of Neurological Surgeons. Unauthorized reproduction of this article is prohibited.

TABLE 2. Selected Surgical Parameters[a]

	Lordotic	Parallel	P
1-Level fusions, n (%)	29 (50.9)	37 (56.9)	.65[b]
C2-C3	0	1	
C3-C4	2	3	
C4-C5	5	5	
C5-C6	13	14	
C6-C7	9	11	
C7-T1	0	3	
2-Level fusions, n (%)	23 (40.3)	21 (32.3)	
C3-C5	2	1	
C4-C6	9	8	
C5-C7	12	12	
3-Level fusions, n (%)	5 (8.8)	7 (10.8)	
C3-C6	2	3	
C4-C7	2	2	
C5-T1	0	1	
C3-C5, C6-C7	1	0	
C3-C5, C7-T1	0	1	
Operative and hospitalization data			
EBL, mL	98.3 (25-500)	107.7 (25-500)	.59
Operation time, min	89.8 (50-190)	98.1 (40-240)	.26
LOS, d	1.3 (0.2-8.4)	1.0 (0.1-4.0)	.24

[a]EBL, estimated blood loss; LOS, length of hospital stay. Values are presented as means (ranges) when appropriate. Student *t* tests were used for all calculations comparing the 2 groups except when noted, in which a [b]χ^2 test was performed.

postoperative CSA and SSA scores. The mean postoperative CSA was 19° (range, −7°-36°) and 18° (range, −7°-37°) in the lordotic and parallel graft patient groups, respectively. The mean postoperative SSA was 6° (range, −4°-19°) and 7° (range, −3°-19°) in the lordotic and parallel graft patient groups, respectively.

Change in Sagittal Alignment and Clinical Outcomes

Thirteen patients were lost to follow-up, and 22 patients had either adjacent-level or posterior cervical fusion surgeries preventing the change in sagittal alignments to be calculated, leaving 85 of 122 patients for these analyses. Results were analyzed in the following subgroups. One subgroup consisted of 68 patients who had improved (change toward lordosis) or preserved sagittal alignment at the surgical level (SSA). Another 17 patients had a loss of sagittal alignment (change toward kyphosis) at the surgical level (SSA). Both groups were quite different before the surgery in terms of the SSA and were comparable postoperatively; thus, a considerably higher degree of angle correction was achieved in the patient group with maintained or improved SSA (Figure 4). The average loss of 3° (range, −9°-−1°) at the surgical level was detected in patients who lost SSA.

Postoperatively, both groups had decreased mean VAS (arm and neck) and NDI scores, as well as increased mean SF-36 (PCS and MCS) scores, indicating an improvement in all clinical outcome measures. However, analysis of the change in clinical scores between the 2 groups showed that patients who had maintained or improved SSA also achieved a statistically significant and higher degree of improvement in SF-36 PCS and NDI

TABLE 3. Postoperative Clinical Outcome Data for Lordotic and Parallel Allograft Patient Groups[a]

Clinical Outcome Data	Lordotic	Parallel	P
Post-Op VAS (neck)	2.8 (0-7.5)	2.8 (0-8)	.93
Post-Op VAS (arm)	2.1 (0-8)	2.2 (0-9)	.87
Post-Op SF-36 PCS	44.9 (16.5-60.3)	45.3 (19.7-58.2)	.85
Post-Op SF-36 MCS	47.0 (25.2-64.7)	47.7 (11.7-63.2)	.71
Post-Op NDI	11.1 (0-32.5)	11.5 (0-36)	.83
Patient Satisfaction Survey	77.2 (9.4-100)	73.1 (15-100)	.36

[a]MCS, Mental Component Summary + Score; NDI, Neck Disability Index; PCS, Physical Component Summary; Post-Op, postoperative; SF-36, Short-Form version 2 Health Survey; VAS, Visual Analog Scale.
Values are presented as means (ranges).
Student t-tests were used for all calculations comparing the 2 groups.

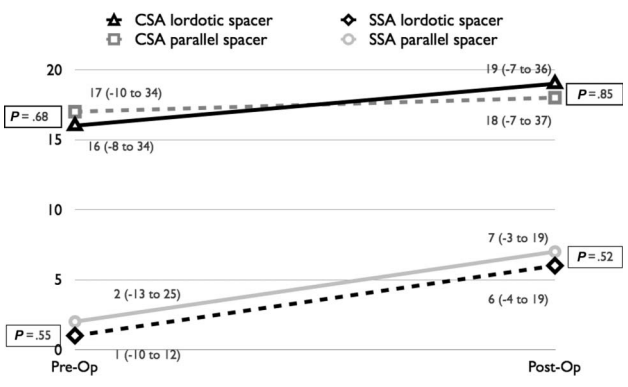

FIGURE 3. *Mean sagittal alignment in lordotic vs parallel allograft patient groups. Student t tests were used for all calculations comparing the 2 groups. CSA, cervical sagittal alignment; Post-Op, postoperative; Pre-Op, preoperative; SSA, segmental sagittal alignment.*

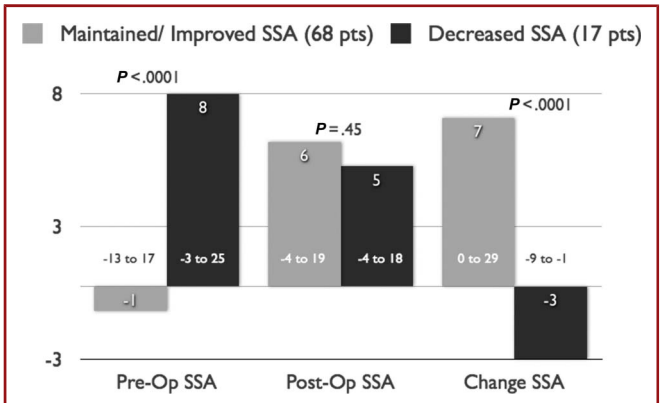

FIGURE 4. *Change in segmental sagittal alignment (SSA) radiographic analysis. Student t tests were used for all calculations comparing the 2 groups. Post-Op, postoperative; Pre-Op, preoperative.*

Copyright © Congress of Neurological Surgeons. Unauthorized reproduction of this article is prohibited.

scores. Although there was a higher degree improvement in VAS neck and SF-36 MCS scores in the maintained or improved SSA patient group, it did not reach statistical significance (Figure 5).

In addition to demonstrating that a higher degree of improvement in clinical outcomes was related to qualitative change in the alignment (change toward lordosis in SSA), regression analyses were conducted to determine a possible quantitative relationship between improvement in clinical outcomes and degree change in SSA. In other words, the analyses tested whether a higher degree change in SSA was associated with a greater change in each of the clinical outcome measures. The results illustrate that a higher degree of SSA change was not directly proportional to the changes in either of the quantitatively significant clinical outcome scores: NDI (R^2 = 0.004, B = −0.08, $F_{(1,72)}$ = 0.25, P = .62) and SF-36 PCS (R^2 = 0.010, B = 0.16, $F_{(1,73)}$ = 0.76, P = .39).

We also analyzed 52 patients who had maintained or improved (change toward lordosis) CSA and 33 patients who had lost (change toward kyphosis) CSA. These 2 subgroups of patients were compared to establish how changes in CSA correlated with clinical outcomes. The CSA preoperative and postoperative measurements are presented in Figure 6. The 2 subgroups of patients did not significantly differ in the changes of their clinical outcome scores (Figure 7).

To compare the effect of the change in SSA on the change in CSA, a regression analysis was conducted (Figure 8). As can be predicted, the regression analysis found that a change in SSA was a significant predictor of a change in CSA (R^2 = 0.25, B = 0.37, $F_{(1,83)}$ = 28.08, P < .0001).

Fusion Rates and Additional Surgeries

The nonunion rate was 7.4% (9 of 122) for the entire patient population. A total of 22 patients required additional surgery, 13 of which were performed for symptomatic adjacent-level degenerative disease. There were no statistically significant differences in the number of patients who underwent surgery for adjacent-level degenerative disk disease between the lordotic and parallel allograft patient groups or improved/maintained and decreased SSA patient groups.

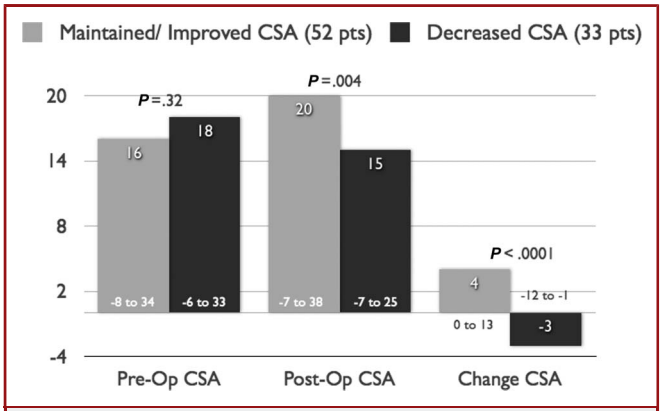

FIGURE 6. *Change in cervical sagittal alignment (CSA) radiographic analysis. Student t tests were used for all calculations comparing the two groups. Post-Op, postoperative; Pre-Op, preoperative.*

DISCUSSION

Despite the continuous progress in surgical instrumentation and techniques, little is known regarding the relationship of cervical alignment and clinical outcomes. Several authors concluded that the degree of cervical lordosis is important in achieving good outcomes for cervical surgical interventions in patients with neurological deficits, and postoperative kyphosis would deteriorate neurological function. Jenkins et al[6] indicated that there was a significant increase in complaints of cervical pain

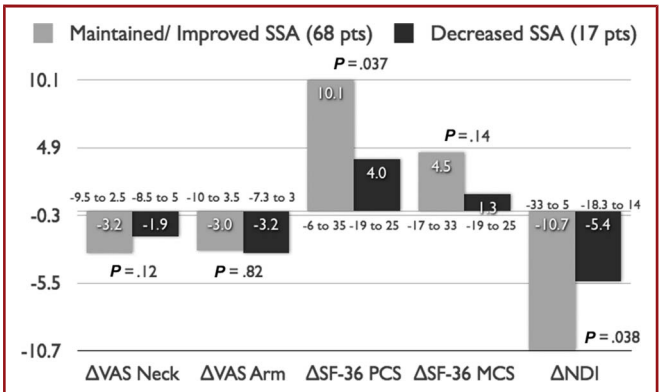

FIGURE 5. *Correlation between segmental sagittal alignment (SSA) and clinical outcomes. Values are presented as changes between preoperative and postoperative clinical outcomes scores. MCS, Mental Component Summary + Score; NDI, Neck Disability Index; PCS, Physical Component Summary; SF, Short Form; VAS, Visual Analog Scale.*

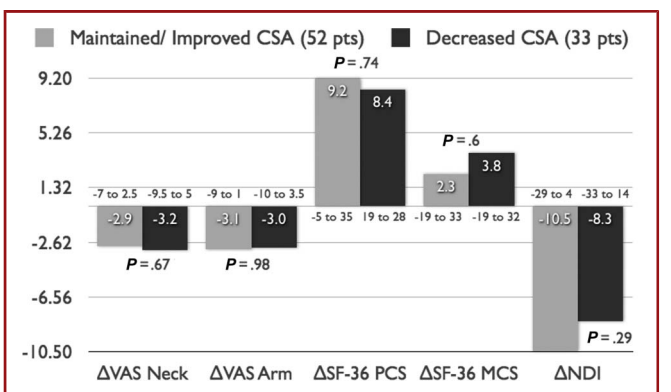

FIGURE 7. *Correlation between cervical sagittal alignment (CSA) and clinical outcomes. Values are presented as changes between preoperative and postoperative clinical outcomes scores. MCS, Mental Component Summary + Score; NDI, Neck Disability Index; PCS, Physical Component Summary; SF, Short Form; VAS, Visual Analog Scale.*

Copyright © Congress of Neurological Surgeons. Unauthorized reproduction of this article is prohibited.

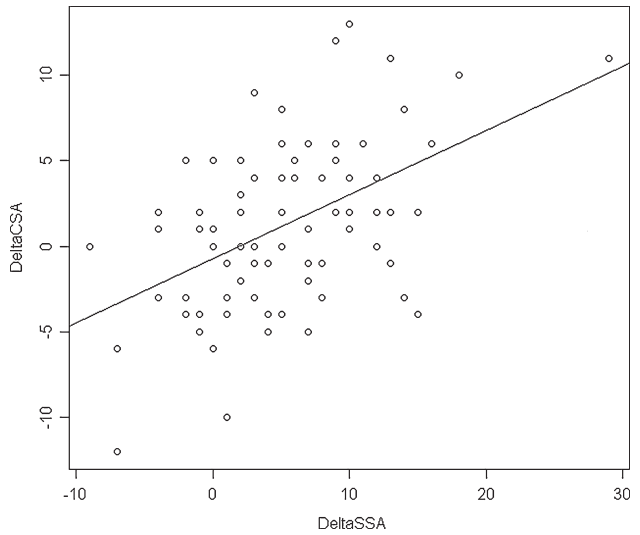

FIGURE 8. *Correlation between the changes (delta) in segmental sagittal alignment (SSA) and cervical sagittal alignment (CSA).*

in patients with kyphosis of > 20° after cervical spine trauma surgery. Naderi et al[7] studied correlations between sagittal and coronal geometry of the spine and neurological deficit and concluded that the presence of abnormal cervical curvature correlated with less neurological improvement. After examining patients undergoing an open-door laminoplasty, Baba et al[8] suggested that posterior cord migration plays an important role in recovery of spinal cord function. The authors showed that reduced lordosis postoperatively is associated with a negative impact for neurological recovery. Kawakami et al[9] reported that axial symptoms such as neck pain and stiffness, shoulder pain, neck dullness, and interscapular pain are directly related to the loss in cervical lordosis.

There have also been reports that argued the importance of cervical alignment and any significant relationships with clinical outcomes.[10-14] Jagannathan et al[15] investigated sagittal alignment and clinical outcome in 170 patients who underwent single-level ACDF with allograft and no plating. They reported a mean change of 7.4° toward kyphosis postoperatively in all 36 patients (21%) who had preoperative kyphotic segmental angles. No significant relationship was determined between change in the segmental angle and postoperative functional status. In addition, no significant changes in the mean C2-C7 Cobb angles were detected. Kwon et al[16] investigated 30 patients who underwent single-level ACDF with anterior cervical plating and 4 patients who underwent ACDF with threaded cervical cage and no plate. They found no significant relationship between disk space angulation and clinical outcomes but noted a trend that more kyphosis correlates with greater VAS scores for neck pain. Xie et al[17] compared anterior cervical diskectomy vs diskectomy with fusion and diskectomy with fusion and instrumentation. They found a significant loss of segmental lordosis in the patient group that had anterior cervical diskectomy but did not detect any differences in clinical outcome scores.

The occurrence of segmental kyphosis after Bryan cervical disk implantation has recently received attention in the literature, but no significant relationship with clinical outcomes was reported.[18-22]

Lordotic vs Parallel Allografts

One of the hypotheses tested in this study was that the use of lordotically shaped allografts during ACDF would improve sagittal alignment and subsequently clinical outcomes. Considering that normal lordosis of the cervical spine is determined mainly by lordotically shaped intervertebral disks, it may seem intuitive to think that such an allograft shape would increase lordotic curvature of the cervical spine and therefore hold potential for promoting better clinical outcomes than parallel allografts. In our study, both lordotic and parallel allograft patient groups demonstrated a slight average increase toward lordosis in overall CSA of 3° and 1°, respectively. A larger mean increase toward lordosis was observed at the surgical level (SSA) with a mean change of 5° for both the lordotic and parallel allograft patient groups. However, there were no statistically significant differences in restoration of CSA or SSA, and we did not find any significant differences in clinical outcomes between the lordotic and parallel allograft patient groups. There are likely other factors in this equation that need to be considered like the height of the allograft, angle and depth of the insertion, or anatomic characteristics of the endplates. Some degree of the allograft or bone collapse probably took place, but then it would most likely have the same effect on the parallel and lordotic allograft patient groups.

Change in Sagittal Alignment and Clinical Outcomes

Although all patients improved postoperatively, we analyzed whether the alterations in sagittal alignment influenced clinical outcomes. It was determined that the maintenance of or change in SSA toward lordosis was an important factor responsible for a higher degree of improvement in clinical outcomes after single and multilevel ACDF. In our investigation, patients who had the SSA change toward lordosis demonstrated a significantly higher degree of improvement in NDI and SF-36 scores. This conclusion potentially supports all previously published findings that postoperative kyphosis may or may not be responsible for inferior clinical outcomes compared with lordotic postoperative sagittal alignment. This could be attributed to the fact that regardless of sagittal alignment, a majority of the patients still improve as a result of decompression and restoration of the intervertebral disk height even if the segmental/sagittal alignment becomes kyphotic. From our results, it seems that a change in segmental alignment toward lordosis may have a positive impact in this process. The mechanism of this effect is not clear but most likely acts through complex muscle and ligament interactions related to posture rather than affecting a radicular component of the cervical pain. Although not significant, the

Copyright © Congress of Neurological Surgeons. Unauthorized reproduction of this article is prohibited.

patients in our study had a higher degree of improvement in neck VAS scores but not arm VAS scores in the maintained/improved SSA patient group.

Further examination of the clinical outcome regression analysis results suggests that the actual angle measure that the SSA changes is not what predicts or relates to the bettering of the patient clinical outcomes. This supports the decision to test clinical outcome improvement by comparing the difference in means of the clinical outcomes between those whose sagittal alignment stayed constant or improved and those whose alignment decreased. The very close mean values for these 2 groups' postoperative SSA (Figure 4), along with the results of the clinical outcome regression analyzes, highlight the notion that it does not appear to be the mean postoperative SSA itself or the actual degree measure of change but whether or not the patients maintained/ improved or decreased their SSA.

Preservation or improvement in SSA has directly affected some of the clinical outcome measures, whereas the alterations in CSA did not. Overall, after a mean 37.5-month average follow-up of our entire patient population, we found a significant mean SSA increase toward lordosis of 5° ($P < .0001$), from a mean preoperative SSA of 1° to the mean postoperative 6°. We found a nonsignificant mean CSA increase toward lordosis of 2°, from a mean preoperative CSA of 16° to a mean 18°, postoperatively for the entire patient population. It is likely that adjacent-level intervertebral disks "absorb" a significant proportion of such segmental alterations before any substantial and significant effect on cervical alignment or clinical outcomes can be noted.

The regression coefficient of the regression analysis evaluating the effect of SSA change on CSA change shows that 25% of the variance in CSA measures can be attributed to the change in SSA measures (see Change in SSA vs Change in CSA). Although a significant result, this model suggests that 75% of the change in CSA measures is left unexplained. As outlined by the model, for every 1° change in SSA, the CSA changes about 0.37°.

When considering the comparison between degree changes in one's CSA and SSA, we can dilute a degree measure change in SSA in 1- to 3-level procedures when including all cervical levels. Ferch et al[2] suggested that "correction of local kyphotic deformity had a variable effect on the regional sagittal alignment." These findings have also been repeatedly reported in the literature related to ACDF[13] or cervical artificial disk replacement surgeries.[18,22] Jagannathan et al[15] investigated sagittal alignment and clinical outcome in 170 patients who underwent single-level nonplated ACDF with allograft and noted: "The fact that the overall alignment between C2 and C7 did not change significantly in spite of kyphosis indicates that the untreated segments of the cervical spine compensated for focal kyphosis." Our study further contributes to this idea.

Limitations

We investigated only whether lordotic allografts can improve sagittal alignment and subsequently affect clinical outcomes. Although we have accounted for demographic, surgical, and clinical variables that may contribute to the final outcome, multiple variables such as height of the disk, angle and depth of the allograft insertion, allograft subsidence, or patient positioning remained unaccounted and require further investigation.

The study did not specifically analyze the postoperative loss of sagittal alignment, but we did not observe any excessive variations in that regard. This study also most likely was affected by sagittal alignment measurement errors, which are unavoidable with the measurement techniques available to us.

The kyphotic alignment could be among multiple factors that contribute to acceleration of the degenerative changes in the cervical spine. A correlation between the progress of degeneration and loss of lordosis has been demonstrated,[23,24] and kyphotic alignment of the cervical fusion segment was shown to increase the load sharing of the anterior plate under flexion.[25] We have not been able to demonstrate this correlation but will investigate it further in subsequent studies.

CONCLUSION

This is the first study that compared lordotic and parallel allografts in clinical settings and in a prospective, randomized, long-term clinical study. The use of lordotically shaped allografts does not increase CSA or SSA and does not correlate with improved clinical outcomes. However, maintaining a consistent or improving SSA was related to a higher degree of improvement in clinical outcome scores.

Disclosure

No funds or benefits in any form have been received in support of this study from commercial parties related directly or indirectly to the subject of this manuscript. Alan T. Villavicencio, MD, and E. Lee Nelson, MD, are stock holders (Lanx, Bromfeld, Colorado). The other authors have no personal financial or institutional interest in any of the drugs, materials, or devices described in this article.

REFERENCES

1. Kuntz CT, Levin LS, Ondra SL, Shaffrey CI, Morgan CJ. Neutral upright sagittal spinal alignment from the occiput to the pelvis in asymptomatic adults: a review and resynthesis of the literature. *J Neurosurg Spine*. 2007;6(2):104-112.
2. Ferch RD, Shad A, Cadoux-Hudson TA, Teddy PJ. Anterior correction of cervical kyphotic deformity: effects on myelopathy, neck pain, and sagittal alignment. *J Neurosurg*. 2004;100(1)(suppl spine):13-19.
3. Villavicencio AT, Pushchak E, Burneikiene S, Thramann JJ. The safety of instrumented outpatient anterior cervical discectomy and fusion. *Spine J*. 2007;7(2):148-153.
4. Gore DR, Sepic SB, Gardner GM. Roentgenographic findings of the cervical spine in asymptomatic people. *Spine (Phila Pa 1976)*. 1986;11(6):521-524.
5. Harrison DE, Harrison DD, Cailliet R, et al. Cobb method or Harrison posterior tangent method: which to choose for lateral cervical radiographic analysis. *Spine (Phila Pa 1976)*. 2000;25(16):2072-2078.
6. Jenkins LA, Capen DA, Zigler JE, Nelson RW, Nagelberg S. Cervical spine fusions for trauma: a long-term radiographic and clinical evaluation. *Orthop Rev*. 1994;suppl:13-19.
7. Naderi S, Ozgen S, Pamir MN, Ozek MM, Erzen C. Cervical spondylotic myelopathy: surgical results and factors affecting prognosis. *Neurosurgery*. 1998;43(1):43-49.
8. Baba H, Uchida K, Maezawa Y, et al. Lordotic alignment and posterior migration of the spinal cord following en bloc open-door laminoplasty for cervical myelopathy: a magnetic resonance imaging study. *J Neurol*. 1996;243(9):626-632.

Copyright © Congress of Neurological Surgeons. Unauthorized reproduction of this article is prohibited.

9. Kawakami M, Tamaki T, Yoshida M, et al. Axial symptoms and cervical alignments after cervical anterior spinal fusion for patients with cervical myelopathy. *J Spinal Disord*. 1999;12(1):50-56.
10. Kaptain GJ, Simmons NE, Replogle RE, Pobereskin L. Incidence and outcome of kyphotic deformity following laminectomy for cervical spondylotic myelopathy. *J Neurosurg*. 2000;93(2)(suppl):199-204.
11. Rajshekhar V, Arunkumar MJ, Kumar SS. Changes in cervical spine curvature after uninstrumented one- and two-level corpectomy in patients with spondylotic myelopathy. *Neurosurgery*. 2003;52(4):799-804.
12. Sasai K, Saito T, Akagi S, Kato I, Ogawa R. Cervical curvature after laminoplasty for spondylotic myelopathy: involvement of yellow ligament, semispinalis cervicis muscle, and nuchal ligament. *J Spinal Disord*. 2000;13(1):26-30.
13. Troyanovich SJ, Stroink AR, Kattner KA, Dornan WA, Gubina I. Does anterior plating maintain cervical lordosis versus conventional fusion techniques? A retrospective analysis of patients receiving single-level fusions. *J Spinal Disord Tech*. 2002;15(1):69-74.
14. Haden N, Latimer M, Seeley HM, Laing RJ. Loss of inter-vertebral disc height after anterior cervical discectomy. *Br J Neurosurg*. 2005;19(6):69-74.
15. Jagannathan J, Shaffrey CI, Oskouian RJ, et al. Radiographic and clinical outcomes following single-level anterior cervical discectomy and allograft fusion without plate placement or cervical collar. *J Neurosurg Spine*. 2008;8(5):420-428.
16. Kwon B, Kim DH, Marvin A, Jenis LG. Outcomes following anterior cervical discectomy and fusion: the role of interbody disc height, angulation, and spinous process distance. *J Spinal Disord Tech*. 2005;18(4):304-308.
17. Xie JC, Hurlbert RJ. Discectomy versus discectomy with fusion versus discectomy with fusion and instrumentation: a prospective randomized study. *Neurosurgery*. 2007;61(1):116-127.
18. Pickett GE, Mitsis DK, Sekhon LH, Sears WR, Duggal N. Effects of a cervical disc prosthesis on segmental and cervical spine alignment. *Neurosurg Focus*. 2004;17(3):E5.
19. Johnson JP, Lauryssen C, Cambron HO, et al. Sagittal alignment and the Bryan cervical artificial disc. *Neurosurg Focus*. 2004;17(6):E14.
20. Sears WR, Duggal N, Sekhon LH, Williamson OD. Segmental malalignment with the Bryan cervical disc prosthesis: contributing factors. *J Spinal Disord Tech*. 2007;20(2):111-117.
21. Sears WR, Sekhon LH, Duggal N, Williamson OD. Segmental malalignment with the Bryan Cervical Disc prosthesis: does it occur? *J Spinal Disord Tech*. 2007;20(1):1-6.
22. Kim SW, Shin JH, Arbatin JJ, et al. Effects of a cervical disc prosthesis on maintaining sagittal alignment of the functional spinal unit and overall sagittal balance of the cervical spine. *Eur Spine J*. 2008;17(1):20-29.
23. Katsuura A, Hukuda S, Saruhashi Y, Mori K. Kyphotic malalignment after anterior cervical fusion is one of the factors promoting the degenerative process in adjacent intervertebral levels. *Eur Spine J*. 2001;10(4):320-324.
24. Miyazaki M, Hymanson HJ, Morishita Y, et al. Kinematic analysis of the relationship between sagittal alignment and disc degeneration in the cervical spine. *Spine (Phila Pa 1976)*. 2008;33(23):E870-E876.
25. Wang M, Gourab K, McGrady LM, Rao RD. Alteration of load sharing of anterior cervical implants with change in cervical sagittal alignment. *Med Eng Phys*. 2008;30(6):768-773.

Acknowledgment

We would like to thank Frances Carr, BA, for help with the data analysis.

COMMENT

In this article, the authors present the results of a prospective, randomized study of 122 patients who underwent anterior cervical diskectomy and fusion with instrumentation for a variety of indications. The patients were randomized to receive either parallel or lordotic allograft bone grafts.

The results showed no differences between the 2 groups in terms of segmental or regional lordosis, functional outcome, or pain scores. Further analysis demonstrated that patients with preserved or improved segmental lordosis experienced significantly greater improvements in Short Form-36 Physical Component Summary and Neck Disability Index scores.

As stated by the authors, the significance of sagittal alignment as an important parameter in cervical spine surgery is complex and a subject of great interest. It is interesting to note that, in the present study, preservation or improvement in segmental lordosis appeared to have a direct bearing on certain outcome measures, whereas regional lordosis did not. It is not clear whether this is an effect of sample size or the result of some other yet-to-be-defined parameter. It is also interesting to note that in this study there does not appear to be a threshold for negative cervical sagittal balance below which outcomes begin to fall. Finally, although studies regarding thoracolumbar global sagittal balance have noted an increase in the nonunion rate for patients with postoperative positive sagittal balance, it is intriguing that this study showed no such effect in the cervical region.

Although there is clearly much more to this story, the present article provides useful and applicable information for the practicing spinal surgeon.

Christopher Wolfla
Milwaukee, Wisconsin

Copyright © Congress of Neurological Surgeons. Unauthorized reproduction of this article is prohibited.

Navigated Transcranial Magnetic Stimulation and Functional Magnetic Resonance Imaging: Advanced Adjuncts in Preoperative Planning for Central Region Tumors

Marie-Thérèse Forster, MD*
Elke Hattingen, MD, PhD‡
Christian Senft, MD, PhD*
Thomas Gasser, MD, PhD*
Volker Seifert, MD, PhD*
Andrea Szelényi, MD, PhD*

Departments of *Neurosurgery and ‡Neuroradiology, Johann Wolfgang Goethe University Hospital, Frankfurt am Main, Germany

Correspondence:
Marie-Thérèse Forster, MD,
Department of Neurosurgery,
Johann Wolfgang Goethe University Hospital, Schleusenweg 2-16,
D-60528 Frankfurt/Main, Germany.
E-mail: marie-therese.forster@med.uni-frankfurt.de

Received, February 4, 2010.
Accepted, October 1, 2010.

Copyright © 2011 by the Congress of Neurological Surgeons

BACKGROUND: Tumor resection in the vicinity of the motor cortex poses a challenge to all neurosurgeons. For preoperative assessment of eloquent cortical areas, functional magnetic resonance imaging (fMRI) is used, whereas intraoperatively, direct cortical stimulation (DCS) is performed. Navigated transcranial magnetic stimulation (nTMS) is comparable to DCS in activating cortical pyramidal neurons.

OBJECTIVE: To evaluate the reliability of nTMS compared with fMRI and DCS for preoperative resection planning of centrally located tumors.

METHODS: In a prospective series, 11 patients (ages, 20-63 years; mean, 41.9 ± 14.9 years, 2 women) with tumors located in or adjacent to the motor cortex were evaluated for surgery. fMRI and nTMS were applied for preoperative assessment of the extent of tumor resection. A 3-dimensional anatomic data set with superimposed fMRI data was integrated in the eXimia Navigated Brain Stimulation station for ensuing motor cortex mapping by nTMS. Responses from nTMS were evaluated by electromyographic response. During surgery, the coordinates of each DCS site were unambiguously defined and integrated into neuronavigation. A post hoc comparison of the coordinates of nTMS, fMRI, and DCS was performed.

RESULTS: Distances from nTMS to DCS (10.5 ± 5.67 mm) were significantly smaller than those from fMRI to DCS (15.0 ± 7.6 mm).

CONCLUSION: nTMS anticipates information usually only enabled by DCS and therefore allows surgical planning in eloquent cortex surgery.

KEY WORDS: Direct cortical stimulation, Functional magnetic resonance imaging, Motor cortex, Navigated transcranial magnetic stimulation, Tumor resection

Neurosurgery 68:1317–1325, 2011 DOI: 10.1227/NEU.0b013e31820b528c www.neurosurgery-online.com

Brain tumors located within the motor cortex or adjacent to it are often regarded as not resectable. With the introduction of functional magnetic resonance imaging (fMRI) in the early 1990s, the "visualization" of cortical function became possible. To visualize preoperatively eloquent cortex regions, the risk of postoperative deficit is supposed to be minimized.[1,2] Nevertheless, fMRI provides indirect information about neuronal function by visualizing the function-dependent changes in paramagnetic deoxyhemoglobin.[1,3] Although many imaging parameters have been tested to improve the quality of imaging results, fMRI still does not allow precise functional cartography, as shown by several authors.[4-6] Furthermore, the intraoperative use of a preoperative fMRI data set in navigation systems is limited by brain shift, and intraoperative fMRI has only anecdotally been described.[7] Therefore, neurophysiological procedures still represent the gold standard for evaluating eloquent cerebral structures. Direct cortical stimulation (DCS) provides the neurosurgeon with a real-time assessment of functional

ABBREVIATIONS: DCS, direct cortical stimulation; **ICC**, intraclass correlation coefficient; **MEP**, motor evoked potential; **NBS**, Navigated Brain Stimulation; **nTMS**, navigated transcranial magnetic stimulation; **TMS**, transcranial magnetic stimulation

Copyright © Congress of Neurological Surgeons. Unauthorized reproduction of this article is prohibited.

cortex, thus reducing the rate of postoperative permanent deficit as well as enabling a larger amount of resection.[8-10] Recently, Picht et al[6] revealed the imprecision of fMRI compared with DCS of 13.8 mm on average.

In 1985, Barker et al[11] introduced a noninvasive alternative to DCS by proving the reliability of transcranial magnetic stimulation (TMS) in transcranially activating pyramidal neurons of the hand motor area. Since then, TMS has become a widespread diagnostic and research tool in clinical neurology and neuroscience with an increasing number of publications.[12,13] So far, only a small number of publications have described this new technique for neurosurgical planning in which a combination of TMS with a neuronavigation system is necessary for its practical use.[14-16] Despite an early report by Krings et al[17] on the correlation of real-time neuronavigated TMS (nTMS) and fMRI for presurgical planning, it was not applied for preoperative planning until more user-friendly systems were developed. At this time, they stated that nTMS may not only be used in addition to fMRI but may even replace it, especially because there might be some applications for which TMS is superior to fMRI. However, they correlated the distances between the peak TMS response and the peak parenchymal fMRI activation, but did not compare the results of these activations with the gold standard of DCS.

Another study recently published by Picht et al[18] compared nTMS with DCS, proving the high congruence between these 2 methods, but did not address fMRI.

We report our experience with nTMS to evaluate its feasibility and its value in the preoperative assessment of eloquent cortex in patients with central region tumors. Therefore, its correlation with fMRI and DCS hot spots was evaluated.

PATIENTS AND METHODS

In a prospective series, we studied 10 patients (8 men and 2 women, ages 20-63 years; mean, 41.9 $\pm$ 14.9 years) with lesions in or adjacent to the motor cortex in 11 sessions. In 1 patient, the tumor was situated in the medial frontal gyrus (F2) in close proximity to the motor tongue area. In all but 1 patient, fMRI could be performed. This patient had a very large tumor, making it impossible for her to perform the motor tasks for fMRI. The patient who was included twice had a subtotally resected ganglioglioma World Health Organization grade II that had recurred after 4 months, now contrast enhancing in the magnetic resonance imaging (MRI), histologically transformed into an anaplastic astrocytoma WHO grade III.

All patients were clinically evaluated before and after surgery (within 1 week before and immediately after surgery as well as at the end of the hospital stay).

Preoperative fMRI

The MRI study was performed with a 3-T Magnetom Allegra Scanner (Siemens Medical Solutions, Erlangen, Germany). Structural 3-dimensional (3D) isovolumetric T1-weighted data were acquired using a magnetization-prepared rapid-acquisition gradient echo sequence (TR, 2250 ms; TE, 26 ms; inversion time, 900 ms; 192 sagittal slices, flip angle, 9 degrees, field of view, 256×256 mm^2; and voxel size, $1 \times 1 \times 1$ mm^3).

fMRI was performed in a block design experiment using a blood oxygen level–dependent sensitive echo planar imaging sequence (TR, 2640 ms; TE, 30 ms; flip angle, 90 degrees; 36 transverse slices; 0.75-mm gap, voxel size, $3 \times 3 \times 3$ mm; base resolution, 64×64). For online echo-planar imaging, distortion correction point spread function mapping was used as described by others.[19]

Subjects performed a simple visually guided motor task. Instructions were projected on a screen mounted on the rear end of the head coil. A total of 192 scans were acquired while subjects performed 3 blocks of alternating movements of the tongue and flexion movements of the fingers and feet, each contralateral to the affected brain hemisphere (21 seconds per condition). Subjects were instructed to perform the movements at a self-paced rate of approximately 2 Hz.

Data processing involved interslice scan time correction with sinc interpolation, 3D motion correction, and high-pass temporal filtering of 3 data points and signal linear drift removal. No severe motion artifacts were observed, and, therefore, all data were used for further statistical analysis. To guarantee good alignment of functional and 3D anatomic data sets, the coregistration process was split into 2 main stages with an initial automatic header-based alignment, followed by fine-tuning alignment with manual adjustment of rotational and translational parameters.

For statistical analysis, a linear correlation analysis was performed. A reference time course function predicting the expected BOLD signal was correlated with the time course of the measured data, resulting in a correlation coefficient r, which indicates the strength of covariation. The resting condition for 1 motor task was defined by the other 2 conditions; for example, the time periods of finger and foot movements were used as a resting period to analyze the tongue activation map. Voxels with significant ($P < .05$) signal increase that correlated with the motor tasks at a correlation coefficient r greater than 0.4 were color coded. The threshold values for the single motor areas were adjusted by visual inspection. The functional areas were superimposed on the anatomic T1-weighted images and exported as DICOM files.

nTMS

We used an eXimia Navigated Brain Stimulation (NBS) System–controlled eXimia TMS Stimulator (Nexstim Ltd., Helsinki, Finland) with a focal biphasic figure-of-8 coil of a mean winding diameter of 50 mm for delivering TMS. The eXimia NBS System locates the TMS coil with an optical tracking system that can recognize the TMS tracking tolls with a precision of less than 1 mm.

Preoperatively acquired 3D MRI, an anatomic data set with coregistrated fMRI activations was loaded in the eXimia NBS System. In the 1 patient for which fMRI was not available because of the patient's inability to perform the motor tasks for fMRI, a 3D magnetization-prepared rapid-acquisition gradient echo image was used instead. The head of the patient was coregistered with MRI data by using anatomic landmarks and 9 scalp points, allowing alignment to the patient's actual head with an accuracy of 2 mm. Once the registration was completed, a 3D head model was created by the system and displayed on the screen. The depth of the displayed calculated 3D head model was adjusted so that the rendered cortical 3D surface and the tumor were both visualized. Navigation-integrated 6-channel electromyography with a frequency band of 10 to 500 Hz was used for motor evoked potential (MEP) registration. Therefore, surface electromyography electrodes were attached in a belly-tendon fashion over the contralateral muscles. These were the first interosseus dorsal muscle and the tibialis anterior muscle as well as additional muscles according to the region of interest. MEPs were registered continuously.

Copyright © Congress of Neurological Surgeons. Unauthorized reproduction of this article is prohibited.

First, the hot spot of the first interosseous dorsal muscle was determined by stimulating the precentral gyrus above the resting motor threshold. For this, a coil position was chosen; the induced and displayed electric field was anterior to the central sulcus. Second, the resting motor threshold of the first interosseous dorsal muscle was determined at the hot spot according to the method described by Awiszus, meaning that 5 of 10 responses were obtained with a peak-to-peak amplitude exceeding 50 μV.[20] Motor cortex mapping was then undertaken at a stimulator output corresponding to 110% of the resting motor threshold, as shown in Figure 1. Each spot was stimulated twice. The same procedure was undertaken to determine the resting motor threshold of the tibialis anterior muscle. So as not to exceed the mapping session, we decided to map the hand area with 110% of the resting motor threshold of the first interosseous dorsal muscle and the leg area with 110% of the resting motor threshold of tibialis anterior muscle.

DCS

All patients underwent general anesthesia (propofol 200 μg/kg, fentanyl 250 μg, and midazolam 2 mg for intubation and propofol 4-8 mg/kg/h and remifentanyl 0.2-0.5 mg/kg/min for maintaining anesthesia) and received a short-acting muscle relaxant (cisatracurium 20 mg) only for intubation. Pairs of subdermal needle electrodes were used for recording MEPs of contralateral thenar, extensor digitorum, and biceps and tibialis anterior muscles. Moreover, responses of hypothenar, first interosseous dorsal, biceps, quadriceps, long abductor hallucis, orbicularis oris, and genioglossus muscles were registered according to the localization of the tumor.

For cortical mapping, a monopolar anodal probe with a 2-mm diameter was used, which was referenced to a cathodal frontopolar electrode positioned at Fpz. A strip electrode containing 4 or 8 electrodes was placed over the precentral gyrus, thus allowing cortical stimulation for continuous MEP recording during the resection. To elicit MEPs, short trains of 5 stimuli with a pulse width of 0.5 ms and an interstimulus interval of 4 ms at a repetition rate of 0.5 Hz were applied. Stimulation intensity was increased in steps of 1 mA until an MEP response could be recorded with an upper intensity limit of 25 mA. In this way, the motor cortex was mapped according to the craniotomy and the tumor location. Intraoperative neurophysiological investigations were performed using the ISIS IOM Neuromonitoring system (Inomed Medizintechnik GmbH, Emmendingen, Germany).

All cortical points where DCS elicited MEPs accordingly were manually and unambiguously coregistered in the navigation system (StealthStation; Medtronic, Minneapolis, Minnesota) and could be displayed any time.

Data Analysis: Comparison of nTMS, fMRI, and DCS

Intraoperatively, the results of nTMS as well as fMRI were not displayed on the navigation system to exclude a bias of the stimulation side toward the preoperative nTMS and fMRI results.

A post hoc comparison of the preoperative nTMS and fMRI with intraoperatively registered data sets was performed.

First, the largest MEPs (ie, responses with the maximal EMG peak-to-peak amplitude) of all muscle responses elicited by nTMS were defined for each muscle. In a next step, the intraoperatively acquired cortical points where DCS triggered MEPs were selected. For each muscle, the spot of lowest stimulation intensity eliciting MEPs was defined and registered as coordinates in the fMRI-nTMS data set. For this purpose, the coordinates of the intraoperative system (StealthStation; Medtronic) needed to be converted to the NBS coordinate system. Thus, all 3 methods could simultaneously be visualized on the individually calculated 3D head model, as shown in Figure 2. A pairwise euclidean distance between DCS coordinates and corresponding nTMS coordinates was calculated by the eXimia NBS System for each specific muscle MEP. The same was true for the distance between DCS coordinates and the centroid of fMRI activation. Because the eXimia NBS System can display all coordinates at a selected peeling depth of the 3D head model, which can

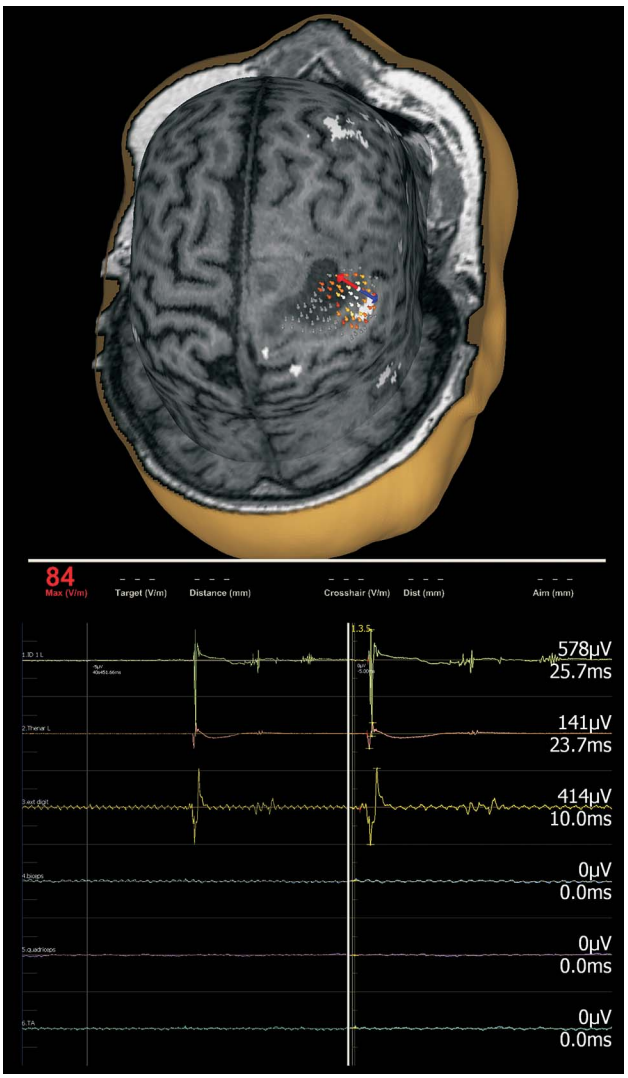

FIGURE 1. *Preoperative navigated transcranial magnetic stimulation of cortical hand representation area. The cortical sites are colored according to the strength of motor responses of the left first interosseous dorsal muscle. In this example, the greatest response at 110% of the first interosseous dorsal muscle resting motor threshold is shown and marked by an arrow indicating the direction of the electric field. Corresponding electromyography of the first interosseous dorsal, thenar, extensor digitorum, biceps, quadriceps, and tibialis anterior muscles are displayed on the lower half.*

Copyright © Congress of Neurological Surgeons. Unauthorized reproduction of this article is prohibited.

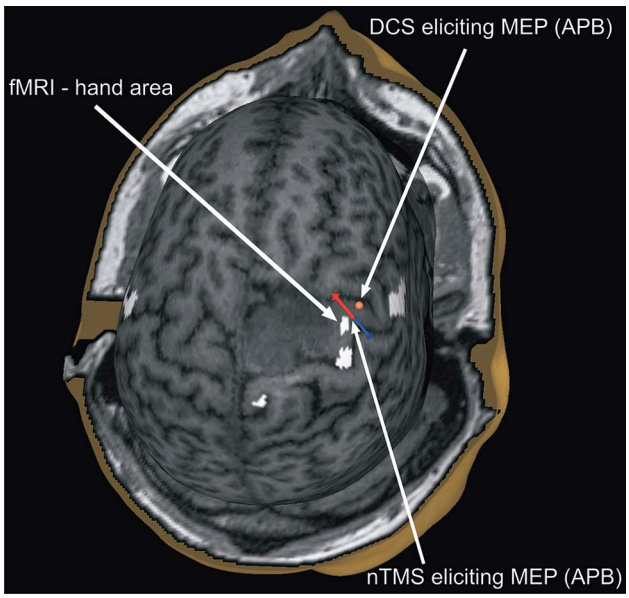

FIGURE 2. *Postoperative calculation of distances between eloquent motor cortex areas determined by navigated transcranial magnetic stimulation (nTMS), functional magnetic resonance imaging (fMRI), and direct cortical stimulation (DCS). Here the spots where motor evoked potentials (MEPs) of the abductor pollicis brevis muscle (APB) could be elicited by nTMS and DCS are displayed. The bicolored arrow standing for activation by nTMS appears immediately on the screen of the eXimia Navigated Brain Stimulation System after single-pulse TMS. After mapping of the motor cortex, we chose the stimulus eliciting the greatest MEPs for each specific muscle. During the operation, cortical points where DCS triggered MEPs are coregistered in the neuronavigation system. Postoperatively, these data are all displayed on the same screen based on preoperative fMRI. The eXimia Navigated Brain Stimulation System calculates the distances between corresponding nTMS and DCS coordinates for each specific muscle. With regard to fMRI, coordinates of the center of the visualized fMRI area are also calculated by the system, thus enabling the distances of fMRI to DCS and to nTMS, respectively, to be determined.*

be adjusted manually, comparison of all responses was performed in a depth equivalent to cortical surface, hence the depth of DCS.

For all calculations, a paired *t* test was used.

RESULTS

Ten patients with tumors in the vicinity of the motor cortex were studied. All patients completed the study, and there were no adverse events. For all patient characteristics, histopathological examination, and pre- and postoperative deficit, see Table 1.

Regarding postoperative outcome, 7 patients demonstrated an unchanged clinical status. Three patients had a transient slight paresis that improved during the hospital stay. One patient with a recurrent tumor had a slight permanent paresis. In 1 patient, delayed postoperative intracerebral hemorrhage developed, causing permanent left hemiparesis.

The motor threshold for eliciting MEPs of the first interosseous dorsal muscle and the tibialis anterior muscle by nTMS was defined at 41.5 ± 10.9% (range, 30%-65%) and 71.7 ± 12.6% (range, 54%-95%) of the stimulator output, respectively.

DCS was performed without any side effects, particularly no intraoperative seizures. The mean stimulation intensity eliciting MEPs was 15.3 ± 5.0 mA (range, 5-25 mA).

Comparison of nTMS and DCS was possible in all patients; correlation of fMRI and DCS could be calculated in all but 1 patient; this patient was not able to perform the tasks for preoperative fMRI. Correlation of stimulated muscles both by nTMS and DCS was possible for 9 different muscles, according to tumor location and craniotomy. In 5 patients, the thenar and extensor digitorum muscles were elicited by both methods. The same was true for recording of MEPs of the tibialis anterior muscle in 4 patients, MEPs of the first interosseous dorsal muscle and the abductor hallucis muscle in 3, MEPs of the biceps and the quadriceps in 2, and MEPs of the hypothenar and the orbicularis oris muscle in 1 patient. Cortical hot spots where nTMS and DCS were elicited in the corresponding muscle differed by 10.49 ± 5.67 mm (range, 2.6-27.6 mm). The center of fMRI activation areas obtained from the first interosseous dorsal muscle or toe movement was situated at a distance of 15.03 ± 7.59 mm (range, 3.4-22.2 mm) from the corresponding DCS site (see illustration, Figure 2). Size, location, or histology of the tumor had no influence on the distances.

A detailed analysis of the lowest stimulation intensity eliciting MEPs by DCS and of distances from the stimulated DCS sites to both the corresponding nTMS sites and the center of fMRI activation areas is shown in Table 2. Moreover, an example of intraoperatively recorded MEPs in correlation with preoperatively elicited MEPs by nTMS is presented in Figure 3.

DISCUSSION

Test-Retest-Reliability

An important fact often neglected when discussing the reliability of fMRI is intrasubject variability over time. Havel et al[21] described the reproducibility of activation in motor paradigms for fMRI, observing a high test-retest-reliability for movements of the foot and the hand, with a reliability coefficient of 0.78 and 0.62, respectively. Movements of the tongue and mouth, however, could practically not be reproduced. Similar results were reported by Zandbelt et al,[22] who found a variability of fMRI signal changes of about 20% in the primary motor cortex. On the other hand, the test-retest reliability of TMS may even be higher according to investigated parameters. According to the literature and using the intraclass correlation coefficient (ICC), the motor threshold has the highest reliability (ICC = 0.90-0.98), followed by the location of motor representation (ICC = 0.69-0.86) and the mapping area (ICC = 0.63-0.86).[23-25] Whether nTMS may even increase this reliability has not been investigated, but may be anticipated.

Copyright © Congress of Neurological Surgeons. Unauthorized reproduction of this article is prohibited.

TABLE 1. Characteristics of Patients, Tumors, and Pre- and Postoperative Motor Deficit[a]

Patient	Sex/ Age, y	Tumor Location	Histology/WHO Grade	Preoperative Motor Deficit	Postoperative Motor Deficit
1[b]	M/20	Pre R	Ganglioglioma II	None	Transient distal leg paresis (MRC 4)
2	M/23	Central R	Papillary glioneural tumor I	None	Transient hand paresis (MRC 4)
3	F/64	Post R	GBM IV	Apraxia of left hand	None
4	M/48	Central R	Anaplastic astrocytoma III	None	None
5[b]	M/21	Pre R	Anaplastic astrocytoma III	None	Leg paresis (MRC 3), arm paresis (MRC 4)
6	M/42	Central L	GBM IV	None	None
7	M/47	Post L	Diffuse reactive astrogliosis	None	Permanent distal leg paresis (MRC 4)
8	F/45	F2 R	Oligoastrocytoma II	None	None
9	M/44	Central R	Astrocytoma II	Distal leg plegia, proximal leg paresis (MRC 4)	None
10	M/42	Central L	GBM IV	None	Transient hand paresis (MRC 4)
11	M/44	Post L	Metastasis of melanoma	None	None

[a]WHO, World Health Organization; Pre, precentral; R, right; MRC, Medical Research Council Scale for Muscle strength, grades 1 to 5; Post, postcentral; GBM, glioblastoma; L, left; F2, medial frontal gyrus.
[b]This patient was included twice in the study because of tumor recurrence.

Comparison of nTMS and DCS

For the comparison of nTMS and DCS, the presumable site of neuronal excitation is important.

Using epidural recordings from the high cervical cord during transcranial electrical stimulation and TMS of the motor cortex, Di Lazzaro et al[23] confirmed that the first volley with a latency of 2.0 to 2.6 ms, known as a D wave (direct wave), was produced by transcranial electrical stimulation, whereas the wave appearing 1.4 ms later, known as I-wave (indirect wave), was produced by TMS. These latencies are compatible with the direct activation of the pyramidal tract axons just below the gray matter and with the synaptic activation of the same pyramidal tract neurons, respectively.[24]

Most effective TMS can be achieved by an optimal coil orientation to induce a current that runs perpendicular to the central sulcus.[23,26] This can be explained by the theory that axons are best stimulated when there is a large change in voltage along its length. However, prediction of the maximal current density evoked by the magnetic field can be perturbed by tissue anisotropies as, for example, between sulci and gyri. Concerning the identification of the latter navigated TMS, a combination of a neuronavigation system based on the individual MRI with TMS may help. Also, the orientation of individual neurons within the magnetic and induced electric field in relation to the coil placement has an impact on the efficacy of stimulation.[27] According to Balslev et al,[28] a posterolateral orientation of the induced current in the brain creates a most effective stimulation, thus implicating the need for an anteromedial orientation of the stimulating magnetic field. Nevertheless, stimulation focality only can be estimated. In a study performing ^{14}C-labeled deoxyglucose mapping during repetitive TMS in cats, a stimulation field of about 176 mm^2 could be registered.[29] Affecting larger cortical regions also means that competing effects such as inhibition and facilitation in surrounding neurons may potentially influence the targeted stimulated cortex.

Keeping the inaccuracies of the methods in mind, this nevertheless allows direct comparison and explains the closer relationship between nTMS and DCS compared with fMRI.

Limitations of nTMS

Functional areas determined by TMS also depend on the actual excitability of the stimulated cortex. This state dependency on the effect of TMS has recently been the subject of several studies.[30]

It is probably because of this state dependency that in 4 excluded patients with preoperative paresis we did not elicit MEPs by nTMS despite a maximal stimulator output. In 2 of these patients, we observed good excitability by DCS, even if mainly subcortically. Their tumors were located partly cortically and partly in the white matter. Concerning the other 2 patients, no MEPs could be elicited at all when stimulating cortically with an upper stimulation intensity limit of 25 mA. In these cases, no functional area could be determined in the peritumoral cortex.

Particularly in patients with preexisting paresis, nTMS may be time-consuming. In our experience, 30 to 60 minutes are needed to examine 1 patient by nTMS. Moreover, the postprocessing of results including the visualization of MEPs of separate muscles and the integration of the data into the intraoperative navigation system may

Copyright © Congress of Neurological Surgeons. Unauthorized reproduction of this article is prohibited.

TABLE 2. Listing of the 3 Most Mapped Muscles[a]

	APB Hot Spot: Distances				Ext Dig Hot Spot: Distances				TA Hot Spot: Distances				MT of nTMS	
	SI, mA	nTMS-DCS, mm	fMRI-DCS, mm	nTMS-fMRI, mm	SI, mA	nTMS-DCS, mm	fMRI-DCS, mm	nTMS-fMRI, mm	SI, mA	nTMS-DCS, mm	fMRI-DCS, mm	nTMS-fMRI, mm	ID1, % Output	TA, % Output
Range	5-25	2.6-27.6	7.7-37.2	12.5-16.2	6-20	7.8-16.4	7.7-20.9	6.4-19	5-22	5.9-15.9	5.7-19.1	4.1-8.4	30-65	54-95
Median	12	12.8	20.7	13.0	11.5	10.6	12.2	13	15.5	11.1	9.4	6.4	37.5	69
Mean	14	14.4	18.2	13.9	12.2	12.1	13.1	12.1	14.5	11.0	10.9	6.3	40.4	71.2
SD	6.7	8.7	11.1	1.6	7.2	3.6	4.3	4.3	7.1	5.6	6.4	1.8	10.4	12.6

[a]Stimulation intensity during direct cortical stimulation, postoperatively calculated distances of navigated transcranial magnetic stimulation hotspot to direct cortical stimulation hotspot and of functional magnetic resonance imaging hotspot to direct cortical stimulation hotspot as well as the distances of navigated transcranial magnetic stimulation to functional magnetic resonance imaging hotspot are shown. Moreover, the motor thresholds of transcranial magnetic mapping of the hand and leg area are demonstrated. APB, abductor pollicis brevis muscle; Ext dig, extensor digitorum muscle; TA, tibial anterior muscle; MT, motor threshold; nTMS, navigated transcranial magnetic stimulation; SI, stimulation intensity; DCS, direct cortical stimulation; fMRI, functional magnetic resonance imaging; ID1, first interosseous dorsal muscle; SD, standard deviation.

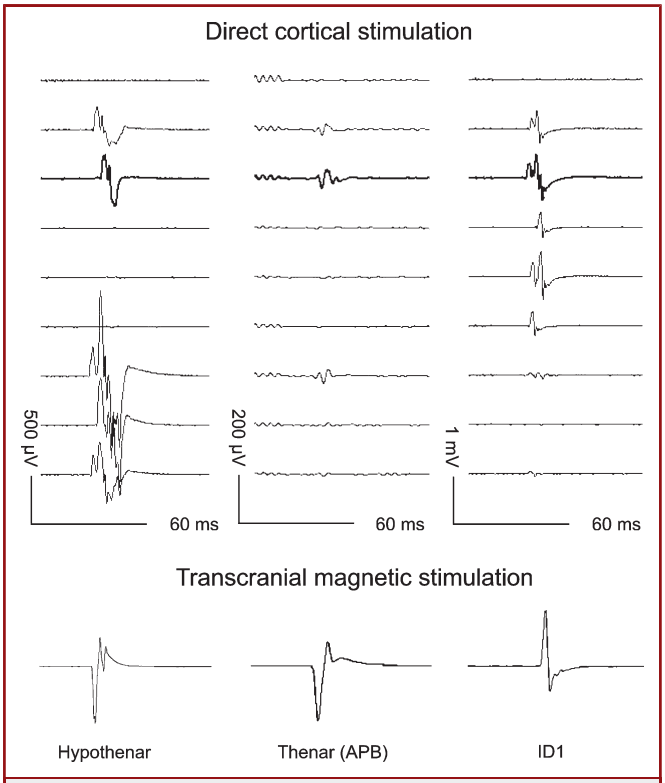

FIGURE 3. *Motor evoked potentials recorded during resection of a grade III glioma in the motor cortex by direct cortical stimulation. At the bottom, the corresponding MEPs recorded during preoperative navigated transcranial magnetic stimulation are shown. APB, abductor pollicis brevis muscle.*

take another 30 minutes. This may pose a time challenge to neurosurgeons and therefore affect the practicality for daily routine.

Comparison of All 3 Methods

There are some drawbacks in comparing these 3 methods. Functional imaging provides maps of cortex activation during performing tasks, including all cortical areas involved in planning and execution. Because isolated movement of 1 muscle is barely possible, fMRI will mostly reflect the cortical representation of all muscles involved in the movement. This fact and the examiner-dependent analysis threshold lead to variability in fMRI maps. In TMS, stimulation by a focal coil at the motor threshold allows activation of pyramidal axons for individual muscles. This results in smaller representational maps. For the sake of a faster stimulation session and to minimize the potential risk of stimulation-related seizures, mapping was undertaken after defining the motor threshold only for 1 muscle of the upper and lower extremity. Thus, when comparing the 3 methods, only the hot spots of those muscles for which the resting motor threshold was determined were included. This is a bias toward nTMS.

Another source of error lies in the brain shift once craniotomy, opening of the dura, and tumor debulking have begun. In a series of 6 patients undergoing resection of brain tumors,

Copyright © Congress of Neurological Surgeons. Unauthorized reproduction of this article is prohibited.

Trantakis et al[31] investigated the extent of brain shift using a 0.5-T MRI unit at different time points intraoperatively, demonstrating a maximal brain shift up to 25 mm. Nevertheless, as in this study, DCS was performed shortly after the dura opening; the extent of brain shift was apparently not this critical.

Accuracy of Spatial Calculation

The comparison of localization results yielded mean distances of 10.49 ± 5.67 mm and 15.03 ± 7.59 mm for nTMS and fMRI, respectively, from the corresponding DCS electrode location. These distances are a combination of the intrinsic uncertainties associated with all 3 methods. To better understand the comparative accuracies, it is possible to judge the reported average distances against the theoretical capability of DCS to replicate its own localization results. This follows the logic behind the statistical methods proposed for the estimation of accuracies among different methods.[32] The accuracy of DCS depends on the stimulation probe type and the stimulation intensity and is mostly less than 10 mm.[33] Conservatively estimated DCS errors are less than 10 mm with 95% confidence. The use of neuro navigation for electrode localization adds uncertainty; a conservative estimate of the neuronavigation errors is 4 mm with 95% confidence.[34,35] Because the 95% limits add up quadratically, the combined error of DCS and neuronavigation is $\sqrt{(10^2 + 4^2)} = 10.77$ mm. This is supported by a study by Schiffbauer et al,[36] who found that in 1 DCS mapping, similar motor responses were obtained from cortical electrode locations more than 10 mm apart. Applying statistical formulations, the DCS and neuronavigation errors can be represented as 2-variate uncorrelated gaussian random variables, which leads to a distribution of the distances as Rayleigh variable[37] representing the square root of the χ^2 variable with 2 *df*. From Rayleigh formulations, it is possible to derive the expected mean distance between 2 replicate trials, which can be shown to be equal to $\sqrt{2}\sigma E(\omega)$, where $\sigma = 4.40$ mm is the combined standard deviation of error for DCS and neuronavigation corresponding to the 95% confidence limit of 10.77 mm, and where $E(\omega) = \sqrt{\pi}$ is the expectancy value of the Rayleigh distribution. From the previous calculations, the resulting expected mean distance between 2 DCS replicate localizations is hence 7.80 mm. The observed 10.5 mm for nTMS is therefore comparable to the expected capability of 7.80 mm for DCS to replicate its own findings.

Therefore, postoperative calculations of distances must be imprecise. Nevertheless, because in the current study both fMRI and nTMS were undertaken before surgery, they could be compared when correlated with the intraoperatively registered data.

CONCLUSION

Our results suggest that nTMS enables the visualization of eloquent cortex, not only in normal but also in distorted anatomy, as is often encountered with cerebral tumors. As a noninvasive neurophysiological tool, it may complement the preoperative estimation of possible tumor removal. In contrast to fMRI, in which only a slight movement of the patient as well as tumor tissue can lead to motion artifacts with potential misregistration of the data, nTMS can be easily recalibrated. Moreover, patients with claustrophobia mostly need sedation during MRI, so that motor tasks for fMRI are not possible. This is also true for patients with paresis who are not able to adequately perform the motor tasks. In these patients, nTMS represents a perfect alternative to evaluate eloquent areas of the motor cortex preoperatively.

Comparing the accuracy of these visualized eloquent areas, we could show that nTMS is more precise than fMRI when correlated with intraoperative DCS. Therefore, our results indicate that, at the moment, nTMS is an excellent tool. Nevertheless, intraoperative verification by direct cortical and subcortical electrical stimulation must be performed.

Disclosure

Drs Forster and Szelényi have received consulting fees from Nexstim for serving as speakers. Dr Senft has received honoraria as consultant for Medtronic. Dr Gasser is member of the scientific advisory board of Medtronic. Technical support was provided by Nexstim Ltd, Helsinki, Finland. The authors have no personal financial or institutional interest in any of the drugs, materials, or devices described in this article.

REFERENCES

1. Kwong KK, Belliveau JW, Chesler DA, et al. Dynamic magnetic resonance imaging of human brain activity during primary sensory stimulation. *Proc Natl Acad Sci U S A*. 1992;89(12):5675-5679.
2. Lehericy S, Duffau H, Cornu P, et al. Correspondence between functional magnetic resonance imaging somatotopy and individual brain anatomy of the central region: comparison with intraoperative stimulation in patients with brain tumors. *J Neurosurg*. 2000;92(4):589-598.
3. Bandettini PA, Wong EC, Hinks RS, Tikofsky RS, Hyde JS. Time course EPI of human brain function during task activation. *Magn Reson Med*. 1992;25(2):390-397.
4. Kober H, Nimsky C, Moller M, Hastreiter P, Fahlbusch R, Ganslandt O. Correlation of sensorimotor activation with functional magnetic resonance imaging and magnetoencephalography in presurgical functional imaging: a spatial analysis. *Neuroimage*. 2001;14(5):1214-1228.
5. Korvenoja A, Kirveskari E, Aronen HJ, et al. Sensorimotor cortex localization: comparison of magnetoencephalography, functional MR imaging, and intraoperative cortical mapping. *Radiology*. 2006;241(1):213-222.
6. Picht T, Wachter D, Mularski S, et al. Functional magnetic resonance imaging and cortical mapping in motor cortex tumor surgery: complementary methods. *Zentralbl Neurochir*. 2008;69(1):1-6.
7. Gasser T, Ganslandt O, Sandalcioglu E, Stolke D, Fahlbusch R, Nimsky C. Intraoperative functional MRI: implementation and preliminary experience. *Neuroimage*. 2005;26(3):685-693.
8. Duffau H, Lopes M, Arthuis F, et al. Contribution of intraoperative electrical stimulations in surgery of low grade gliomas: a comparative study between two series without (1985-96) and with (1996-2003) functional mapping in the same institution. *J Neurol Neurosurg Psychiatry*. 2005;76(6):845-851.
9. Ebeling U, Schmid UD, Ying H, Reulen HJ. Safe surgery of lesions near the motor cortex using intra-operative mapping techniques: a report on 50 patients. *Acta Neurochir (Wien)*. 1992;119(1-4):23-28.
10. Kombos T, Suess O, Funk T, Kern BC, Brock M. Intra-operative mapping of the motor cortex during surgery in and around the motor cortex. *Acta Neurochir (Wien)*. 2000;142(3):263-268.
11. Barker AT, Jalinous R, Freeston IL. Non-invasive magnetic stimulation of human motor cortex. *Lancet*. 1985;1(8437):1106-1107.
12. Chen R, Cros D, Curra A, et al. The clinical diagnostic utility of transcranial magnetic stimulation: report of an IFCN committee. *Clin Neurophysiol*. 2008;119(3):504-532.
13. Rossini PM, Rossi S. Transcranial magnetic stimulation: diagnostic, therapeutic, and research potential. *Neurology*. 2007;68(7):484-488.

Copyright © Congress of Neurological Surgeons. Unauthorized reproduction of this article is prohibited.

14. Boroojerdi B, Foltys H, Krings T, Spetzger U, Thron A, Topper R. Localization of the motor hand area using transcranial magnetic stimulation and functional magnetic resonance imaging. *Clin Neurophysiol*. 1999;110(4):699-704.
15. Hannula H, Neuvonen T, Savolainen P, et al. Navigated transcranial magnetic stimulation of the primary somatosensory cortex impairs perceptual processing of tactile temporal discrimination. *Neurosci Lett*. 30 2008;437(2):144-147.
16. Sparing R, Hesse MD, Fink GR. Neuronavigation for transcranial magnetic stimulation (TMS): where we are and where we are going. *Cortex*. 2010;46(1): 118-120.
17. Krings T, Foltys H, Reinges MH, et al. Navigated transcranial magnetic stimulation for presurgical planning–correlation with functional MRI. *Minim Invasive Neurosurg*. 2001;44(4):234-239.
18. Picht T, Mularski S, Kuehn B, Vajkoczy P, Kombos T, Suess O. Navigated transcranial magnetic stimulation for preoperative functional diagnostics in brain tumor surgery. *Neurosurgery*. 2009;65(6 suppl):93-98; discussion 98-99.
19. Zaitsev M, Hennig J, Speck O. Point spread function mapping with parallel imaging techniques and high acceleration factors: fast, robust, and flexible method for echo-planar imaging distortion correction. *Magn Reson Med*. 2004;52(5): 1156-1166.
20. Saisanen L, Julkunen P, Niskanen E, et al. Motor potentials evoked by navigated transcranial magnetic stimulation in healthy subjects. *J Clin Neurophysiol*. 2008; 25(6):367-372.
21. Havel P, Braun B, Rau S, et al. Reproducibility of activation in four motor paradigms. An fMRI study. *J Neurol*. 2006;253(4):471-476.
22. Zandbelt BB, Gladwin TE, Raemaekers M, et al. Within-subject variation in BOLD-fMRI signal changes across repeated measurements: quantification and implications for sample size. *Neuroimage*. 2008;42(1):196-206.
23. Di Lazzaro V, Oliviero A, Pilato F, et al. The physiological basis of transcranial motor cortex stimulation in conscious humans. *Clin Neurophysiol*. 2004;115(2):255-266.
24. Di Lazzaro V, Oliviero A, Profice P, et al. Comparison of descending volleys evoked by transcranial magnetic and electric stimulation in conscious humans. *Electroencephalogr Clin Neurophysiol*. 1998;109(5):397-401.
25. Siebner HR, Hartwigsen G, Kassuba T, Rothwell JC. How does transcranial magnetic stimulation modify neuronal activity in the brain? Implications for studies of cognition. *Cortex*. 2009;45(9):1035-1042.
26. Mills KR, Boniface SJ, Schubert M. Magnetic brain stimulation with a double coil: the importance of coil orientation. *Electroencephalogr Clin Neurophysiol*. 1992; 85(1):17-21.
27. Wagner T, Rushmore J, Eden U, Valero-Cabre A. Biophysical foundations underlying TMS: setting the stage for an effective use of neurostimulation in the cognitive neurosciences. *Cortex*. 2009;45(9):1025-1034.
28. Balslev D, Braet W, McAllister C, Miall RC. Inter-individual variability in optimal current direction for transcranial magnetic stimulation of the motor cortex. *J Neurosci Methods*. 2007;162(1-2):309-313.
29. Valero-Cabre A, Payne BR, Rushmore J, Lomber SG, Pascual-Leone A. Impact of repetitive transcranial magnetic stimulation of the parietal cortex on metabolic brain activity: a 14C-2DG tracing study in the cat. *Exp Brain Res*. 2005;163(1): 1-12.
30. Silvanto J, Pascual-Leone A. State-dependency of transcranial magnetic stimulation. *Brain Topogr*. 2008;21(1):1-10.
31. Trantakis C, Tittgemeyer M, Schneider JP, et al. Investigation of time-dependency of intracranial brain shift and its relation to the extent of tumor removal using intra-operative MRI. *Neurol Res*. 2003;25(1):9-12.
32. Bland JM, Altman DG. Measuring agreement in method comparison studies. *Stat Methods Med Res*. 1999;8(2):135-160.
33. Tharin S, Golby A. Functional brain mapping and its applications to neurosurgery. *Neurosurgery*. Apr 2007;60(4 Suppl 2):185-201; discussion 201-182.
34. Shamir RR, Freiman M, Joskowicz L, Spektor S, Shoshan Y. Surface-based facial scan registration in neuronavigation procedures: a clinical study. *J Neurosurg*. 2009;111(6):1201-1206.
35. Woerdeman PA, Willems PW, Noordmans HJ, Tulleken CA, van der Sprenkel JW. Application accuracy in frameless image-guided neurosurgery: a comparison study-of three patient-to-image registration methods. *J Neurosurg*. 2007;106(6): 1012-1016.
36. Schiffbauer H, Berger MS, Ferrari P, Freudenstein D, Rowley HA, Roberts TP. Preoperative magnetic source imaging for brain tumor surgery: a quantitative comparison with intraoperative sensory and motor mapping. *Neurosurg Focus*. 2003;15(1):E7.
37. Weisstein EW. Rayleigh distribution. *From MathWorld - A Wolfram Web Resource*. http://mathworld.wolfram.com/RayleighDistribution.html. Accessed February 23, 2011.

Acknowledgment

We thank Katja Ziehmayer for help in editing the manuscript.

COMMENTS

In this study, the authors compare the data provided by preoperative navigated transcranial magnetic stimulation (nTMS), presurgical functional MRI (fMRI), and intraoperative direct cortical stimulation (DCS) in a prospective study of 11 patients who underwent surgery for a tumor located near or within the motor cortex. They show that distance from nTMS to DCS (10.5 $\pm$ 5.67 mm) is significantly less than that from fMRI to DCS (15.0 $\pm$ 7.6 mm). On the basis of these data, they conclude that nTMS enables the visualization of eloquent cortex, even in distorted anatomy caused by brain tumor and even in patients with paresis (thus who are not able to adequately perform motor tasks during fMRI). They advocate that nTMS is more accurate than fMRI when correlated with intrasurgical DCS and thus that nTMS is currently the best method to estimate preoperatively the respectability of lesions of the motor cortex.

This is the first study to compare the 3 methods of nTMS, fMRI, and DCS. The authors have to be congratulated for these original data. However, beyond the correlations between these different techniques of mapping, it is important to emphasize that the underlying mechanisms are different. fMRI uses the blood oxygen level dependent–effect, which is an indirect reflection of neuronosynaptic activity, whereas noninvasive nTMS and invasive DCS elicit a transient inhibition of brain functions. As a consequence, even if intraoperative direct cortical and subcortical electrostimulation is currently the gold standard, the future aim is to combine the 3 complementary methods to benefit from a better understanding of the individual organization of the anatomofunctional networks, ie, to detect the crucial vs the compensable functional epicenters and their connectivity, to optimize the surgical indications and planning in eloquent structures. To this end, the association of these 3 techniques should also be applied to language areas.

Hugues Duffau
Montpellier, France

The authors are to be congratulated for making the effort to carefully evaluate and report on their use of a relatively new functional mapping technology. Presurgical localization of functional anatomy has become a standard methodology for evaluating the resectability of tumors in or adjacent to eloquent cortex. The most widely available technique for noninvasive functional localization is fMRI, and its spatial correlation with the gold-standard technique for cortical functional localization, intraoperative DCS, has been well studied. The authors present the results of a study comparing nTMS with fMRI and DCS and report that nTMS shows a greater spatial correlation with DCS. Aside from the obvious concern regarding the ability to generalize these observations, given the small sample size of this study, it remains unclear whether the small differences in spatial accuracy between fMRI and nTMS are of clinical relevance when neither precludes the use of DCS (and I would suggest subcortical mapping as well) to guide intraoperative decision making.

Nevertheless, it appears that nTMS, where available, is a useful tool for planning surgery. Ultimately, our desire to both maximize the extent

Copyright © Congress of Neurological Surgeons. Unauthorized reproduction of this article is prohibited.

of resection and avoid loss of function means that we need to understand both cortical and subcortical functional anatomy. Hence, incorporation of preoperative fiber maps (eg, diffusion tensor imaging–based tractography) into our image guidance models also is necessary to guide decision making regarding how aggressive we should plan to be and what expectations we should give our patients.

Michael A. Vogelbaum
Cleveland, Ohio

As Forster et al note, the concept of maximal safe resection is tested maximally in tumors surrounding the motor area. In a relatively small series of 10 patients undergoing 11 operations (1 procedure was a second stage for recurrence), 3 mapping modalities are compared for their accuracy in surgical guidance to prevent postoperative deficits. In particular, nTMS is compared with DCS and fMRI. The authors found that nTMS provided information that closely predicts the location of the motor neurons as validated by intraoperative DCS.

At many centers, including our own, where functional mapping (fMRI, diffusion tractography, electrophysiological recording) is routinely performed for tumors in eloquent areas, the combination of mapping techniques informs the neurosurgeon of the best surgical approach to these challenging tumors and the limits of resection that complement standard 3-dimensional frameless neuronavigation. We find fMRI to be useful and diffusion tractography especially valuable.[1] Other techniques, including nTMS, electrophysiological recording with subdural electrodes, and magnetoencephalography[2] focus mainly on the cortical surface, and not the subcortical, pyramidal tract fibers that are at risk during surgery for tumors in this region.

Predictors of outcome after motor area surgery include the distance to the central sulcus and the extent of resection.[3] A key determinant of outcome is whether the tumor is infiltrative or whether it is relatively well circumscribed. In the former situation, the tumor replaces motor fibers (eg, invasive gliomas) vs displacement of these fibers (eg, metastatic nodules). In the current series, the 1 patient with a cerebral metastasis remained intact neurologically. Of the other 10 patients undergoing intrinsic glioma surgeries, 5 of 10 (50%) had postoperative deficits, although the majority were transient, reflecting the risks of surgery in this area. Fortunately, there is long-term neuroplasticity that enables functional recovery if fiber tracts are preserved.[4]

Both fMRI and nTMS are limited in patients who have preoperative deficits because of the tumor location and size caused by loss of signal. In the current report, 4 patients could not be included because of preoperative paresis. Another practical limitation is the time required for preoperative evaluation and postprocessing with integration into the intraoperative navigation. The additional time (1 hour) is an obstacle to overcome. The elegant discussion, using mathematical formulae, details the inherent limitations of any single modality, including the gold standard of DCS. We agree that nTMS complements other established tools of mapping, and if it can be efficient and cost-effective, it could be widely adapted.

Steven Brem
Surbhi Jain
Tampa, Florida

1. Jain S, Murtagh R, Murtagh R, Vrionis F, Brem S. Combined fiber-tracking, f-MRI, integrated neuronavigation and intraoperative motor mapping in the protection of brain functions. *Neuro-oncology*. 2008;10:915.
2. Mäkelä JP, Forss N, Jääskeläinen J, Kirveskari E, Korvenoja A, Paetau R. Magnetoencephalography in neurosurgery. *Neurosurgery*. 2006;59:493-511.
3. Krishnan R, Raabe A, Hattingen E. Functional magnetic resonance imaging-integrated neuronavigation: correlation between lesion-to-motor cortex distance and outcome. *Neurosurgery*. 2004;55:904-914.
4. Robles SG, Gatignol P, Lehéricy S, Duffau H. Long-term brain plasticity allowing a multistage surgical approach to World Health Organization Grade II gliomas in eloquent areas. *J Neurosurg*. 2008;109:615-624.

eTOCS ALERTS

Receive Neurosurgery Tables of Contents automatically via email.

1. At the Neurosurgery Online home page (*http://www.neurosurgery-online.com*), click Login. If you have not yet registered, you will be prompted to do so.

2. Click on the eTOCs link in the top-right navigation menu.

3. You can manage your subscription to Neurosurgery eTOCs and add other LWW titles in the eTOCs and Alerts tab of your account information.

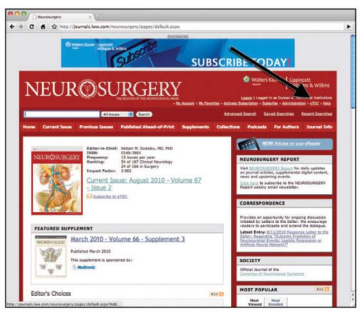

Scan the QR Code to access video tutorial

NEUROSURGERY

Copyright © Congress of Neurological Surgeons. Unauthorized reproduction of this article is prohibited.

Seizures and the Natural History of World Health Organization Grade II Gliomas: A Review

Anja Smits, MD, PhD*
Hugues Duffau, MD, PhD‡

*Department of Neuroscience and Neurology, Uppsala University, University Hospital, Uppsala, Sweden; ‡Department of Neurosurgery and INSERM U583, Institute of Neurosciences of Montpellier, Hôpital Gui de Chauliac, CHU de Montpellier, Montpellier, France

Correspondence:
Anja Smits, MD, PhD,
Department of Neuroscience,
Neurology,
Uppsala University,
University Hospital,
S-751 85 Uppsala, Sweden.
E-mail: Anja.Smits@neuro.uu.se

Received, February 2, 2010.
Accepted, October 27, 2010.

Copyright © 2011 by the
Congress of Neurological Surgeons

OBJECTIVE: The majority of adults with low-grade gliomas have seizures. Despite the frequency of seizures as initial symptoms and symptoms of later disease, seizures in relation to the natural course of low-grade gliomas have received little attention.

METHODS: In this review, we provide an update of the literature on the prognostic impact of preoperative seizures and discuss the tumor- and treatment-related factors affecting seizure control at later stages of the disease.

RESULTS: Seizures occur most frequently at disease presentation and predict a more favorable outcome. Initial seizures are correlated with tumor location and possibly indirectly to the molecular profile of the tumor. About 50% of all patients with seizures at presentation continue to have seizures before surgery. Maximal tumor resection, including resection of epileptic foci, is a valuable strategy for improving seizure control. In addition, radiotherapy and chemotherapy, as single therapies or in combination with surgery, have shown beneficial effects in terms of seizure reduction. Recurrent seizures after macroscopically complete tumor resection may be a marker for accelerated tumor growth. Recurrent seizures after an initial transient stabilization after radiotherapy and/or chemotherapy may be a marker for anaplastic tumor transformation.

CONCLUSION: Preoperative seizures likely reflect, apart from tumor location, intrinsic tumor properties as well. Change in seizure control in individual patients is frequently associated with altered tumor behavior. Including seizures and seizure control as clinical parameters is recommended in future trials of low-grade gliomas to further establish the prognostic value of these symptoms and to identify the factors affecting seizure control.

KEY WORDS: Epilepsy, Low-grade glioma, Survival, Tumor progression

Neurosurgery 68:1326–1333, 2011 DOI: 10.1227/NEU.0b013e31820c3419 www.neurosurgery-online.com

Low-grade gliomas (LGGs) in adults are brain tumors affecting otherwise healthy people with a mean age of approximately 40 years at the time of diagnosis. The annual incidence of the disease is estimated to be 1.5 to 1.8 per 100.000 inhabitants.[1] There is a slight male predominance, making up about 60% of all patients. According to the World Health Organization (WHO) classification of brain tumors, adult LGGs are of malignancy grade II and consist mainly of astrocytomas, oligodendrogliomas, and oligoastrocytomas.[2] The etiology of gliomas is basically unknown, with high-dose ionizing radiation exposure as one of the few accepted risk factors.[3] Evidence of the role of other risk factors such as occupational exposure, the use of mobile phones, exposure to tobacco, diet, and trauma is insufficient.

ABBREVIATIONS: EORTC, European Organization for Research and Treatment of Cancer; **LGG**, low-grade glioma

Seizures are the most common presenting symptoms in patients with LGGs.[4,5] Epilepsy may be the only symptom for months or years in the initial phase of disease. Poor seizure control can have sustained negative effects on daily functioning and quality of life.[6] Seizures may also occur during later disease and be affected by surgery and postoperative treatment.[5] Recent developments in imaging techniques have shown that LGGs in adults grow slowly but continuously, with a growth rate that is mainly dependent on the intrinsic properties of the tumor.[7-9] Furthermore, there is evidence that the

Copyright © Congress of Neurological Surgeons. Unauthorized reproduction of this article is prohibited.

molecular profiles of tumor subtypes with similar histopathology may vary among different brain locations, indicating a correlation between tumor behavior and specific locations in the brain.[10] Thus, it is of interest to study the specific symptoms of disease in this patient group in correlation with the natural course of the tumor.

Despite seizures being the most frequent symptom at disease presentation as well as a common symptom during later disease, the correlation between seizures and the natural history of LGGs has not been systematically studied. Important clinical questions, such as whether seizure control during early disease is of prognostic value or the likelihood of growth acceleration with anaplastic tumor transformation in patients with recurrent seizures after a long seizure-free interval, remain unanswered.

In this review, we provide an update on the association of preoperative seizures with the prognosis of adult LGGs and discuss the tumor- and treatment-related factors that may affect seizure control during later disease. We also offer suggestions for including seizures and seizure control as clinical parameters in future trials to increase our understanding of this issue. Literature references were identified through searches of PubMed with the search terms "low-grade glioma," "epilepsy," "prognosis," "survival," "surgery," "radiotherapy," "chemotherapy," and "progression" from January 1989 to December 2009. Articles were identified also through searches of the authors' own files including information from international congress proceedings focused on clinical neuro-oncology. Only papers published in English were reviewed. Because almost all published studies on this subject consist of retrospective studies and case reports, patients are simply divided into seizure free or not seizure free. Patients who are not seizure free have either ongoing or recurrent seizures, ie, seizures after an initial seizure-free period. Grading of the severity of epilepsy and of seizure control by various antiepileptic treatments as well as classification of the seizure types has not been possible. Additional important parameters for seizure control, such as the dose and plasma levels of antiepileptic drugs, could not be evaluated and are assumed to be optimally adjusted in all patient groups.

PREOPERATIVE SEIZURES IN RELATION TO PROGNOSIS

Seizures as the Presenting Symptom

Seizures as the presenting symptom occur in 70% to 90% of all patients with LGGs.[11,12] Seizures frequently predate other symptoms or diagnosis by many years and may occur when the magnetic resonance imaging (MRI) shows only subtle changes.[13] The seizure risk in patients with LGGs is strongly related to the proximity of the tumor to the cortical gray matter.[12-14,17-19] Patients with deeply located tumors are less likely to present with seizures.

The tumor growth rate is another important determinant for seizure risk faced by patients with gliomas. There is evidence that epileptogenic pathways vary for different tumor types. In slowly growing gliomas, seizure development is related to deafferentation and disconnection of functionally isolated cortical areas rather than disturbed microcirculation and direct effects of tissue damage.[12-14] There is an inverse correlation between seizure risk and the growth rate of the tumor.[13-15] Seizures are more common in the slowly growing oligodendrogliomas than in WHO grade II astrocytomas.[16]

The majority of studies on survival of patients with LGGs provide support for a correlation between seizures as initial symptom and a more favorable outcome, as shown in Table 1.[4,9,11,20,21] Another factor associated with seizure risk, but with a less clear correlation with prognosis, is the specific lobe affected by the tumor. Patients with tumors in the frontal, temporal, and parietal lobes more often manifest with seizures than patients with occipital tumors. LGGs are frequently located in the supplementary motor area and the insular cortex, which are all areas with a presumed role in epileptogenesis.[17,18] Patients with inoperable insular LGGs have traditionally been considered to have a poor prognosis, but recent data indicate that total or subtotal resection can be achieved safely in as many as 80% of these cases.[22] A substantial improvement in seizure control (78% relief of seizures) as well as good survival (82% alive at follow-up of 4 years) by means of extensive surgery was observed for these tumor locations.[22]

It is important to realize that the presence of seizures is a predictor of favorable outcome only if present as a single initial symptom.[23] Other symptoms and signs at presentation, such as cognitive deficits and poor clinical performance status of patients, were found to be associated with unfavorable prognosis.[24-26] The presence of seizures, the absence of neurological and/or cognitive deficits, and a good performance status are 3 interrelated parameters. A strong negative correlation between the presence of seizures and the presence of other symptoms was shown in the final analysis of the European Organization for Research and Treatment of Cancer (EORTC) phase III trials on LGGs.[21] (Table 1). Likewise, once neurological or cognitive deficits are present, a decrease in performance status is to be expected.[21]

Duration of Seizure History and Overall Survival

The earlier concept that patients with chronic epilepsy as the single symptom of disease represent a subtype of LGGs with a particularly favorable prognosis needs some modification.[27,28] Many of the earlier studies on survival and chronic epilepsy in LGGs consisted of histopathological diagnoses of a benign nature, such as gangliogliomas, grade I astrocytomas, and dysembryoblastic neuroepithelial tumors.[29] When analyzing survival of patients with astrocytomas WHO grade II exclusively, a long preoperative seizure history is associated with a higher risk of progression and death.[30] This is in line with the current view that malignant transformation eventually occurs in most, if not in all, grade II gliomas.[31]

The question remains whether the association between long seizure history and higher risk of transformation is true for all WHO grade II gliomas. Rare histological tumor subtypes may exist in patients with chronic epilepsy with an unexpectedly indolent disease course without risk of tumor transformation.[32,33]

Copyright © Congress of Neurological Surgeons. Unauthorized reproduction of this article is prohibited.

TABLE 1. Examples of Studies on Epileptic Seizures in Relation to Prognosis in Adult Low-Grade Gliomas[a]

Study	Study Design	Tumor Subtype/No. of Patients	Conclusions
Leighton et al,[4] 1997	Retrospective review, single institution	A, OA, O/167	Seizures at presentation favorable prognostic factor
El-Hateer et al,[9] 2009	Retrospective review, single institution	O 69	Seizures at presentation favorable prognostic factor
Bauman et al,[20] 2009	Retrospective review, single institution	A, OA, O/145	Seizures at presentation favorable prognostic factor
van Veelen et al,[23] 1998	Retrospective review, single institution	A/90	Epilepsy as only symptom favorable prognostic factor
Lote et al,[24] 1997	Retrospective review, single institution	A, OA, O/379	Seizures at presentation not significant; cognitive changes unfavorable prognostic factor
Chang et al,[11] 2008	Retrospective review, single institution	A, OA, O/332	Seizures at presentation more common in histological subtypes with favorable prognosis
Danfors et al,[19] 2009	Retrospective review, single institution	A, OA, O/101	Seizures at presentation favorable prognostic factor; preoperative seizure-control prognostic factor
Pignatti et al,[21] 2002	Multivariate analysis of EORTC 22844 (construction set) and EORTC 22845 (validation set) phase III trials	A, OA, O/322 + 288	Seizures at presentation significant in univariate but not in multivariate analysis; neurological deficits at presentation unfavorable prognostic facto

[a]A, astrocytoma World Health Organization grade II; OA, oligoastrocytoma World Health Organization grade II; O, oligodendroglioma World Health Organization grade II; EORTC, European Organization for Research and Treatment of Cancer.

Preoperative Seizure Control

In general, as many as 50% of all patients presenting with seizures continue to have seizures despite antiepileptic drug treatment[11,19] (Figure 1). Tumor location affects the risk of the development of medically intractable seizures (ie, seizures so frequent or severe that they limit daily life) despite the use of antiepileptic drugs at adequate serum concentrations.[34] In particular, LGGs in the insular region and in the mesiotemporal lobe are frequently associated with medically refractory seizures.[12] In a retrospective chart review involving adults with LGGs who underwent initial surgery at the University of California, San Francisco, temporal lobe location together with the presence of simple partial seizures and a longer duration of preoperative seizures were associated with pharmacoresistant seizures.[11]

Whether large preoperative tumor size is a predisposing factor for poor seizure control is not clear. Patients with persisting preoperative seizures had a larger mean tumor diameter compared with patients who became seizure free, but the study sample size was too small for multivariate analysis.[19]

POSTOPERATIVE SEIZURE CONTROL

Frequency of Postoperative Seizures

Several studies have supported the beneficial role of surgery in seizure control of tumor-related epilepsy.[35-37] A retrospective analysis of the spatial and causal relationship between brain tumors and epilepsy reported a postoperative seizure-free rate of 62.5% for all patients with chronic tumor-related seizures during the preoperative phase, consisting of mainly, but not exclusively, LGGs[38] (Figure 1). Only patients with frontal and temporal tumor locations were included in this study. In another report, 57% of all patients with preoperative tumor-related seizures continued to have seizures postoperatively compared with 11% of the preoperatively seizure-free population.[18] This series consisted of a mixture of high- and low-grade gliomas. Comparable results have been found in studies of WHO grade II gliomas exclusively, showing a 50% postoperative seizure-free rate for all patients with uncontrolled preoperative seizures at 12 months after surgery and a 67% seizure-free rate for the total population presenting with seizures[11] (Figure 1).

Factors Affecting Postoperative Seizure Control

As expected, the presence of preoperative seizures was strongly associated with the persistence of seizures after surgery.[18] The parameters of radical tumor resection including seizure foci mapping and short preoperative seizure history (<1 year) were identified as predictors of good postoperative seizure control.[38] The authors demonstrated that, whereas lesionectomy was sufficient for obtaining seizure control in patients with seizures less than a year before surgery, optimal relief of chronic seizures

Copyright © Congress of Neurological Surgeons. Unauthorized reproduction of this article is prohibited.

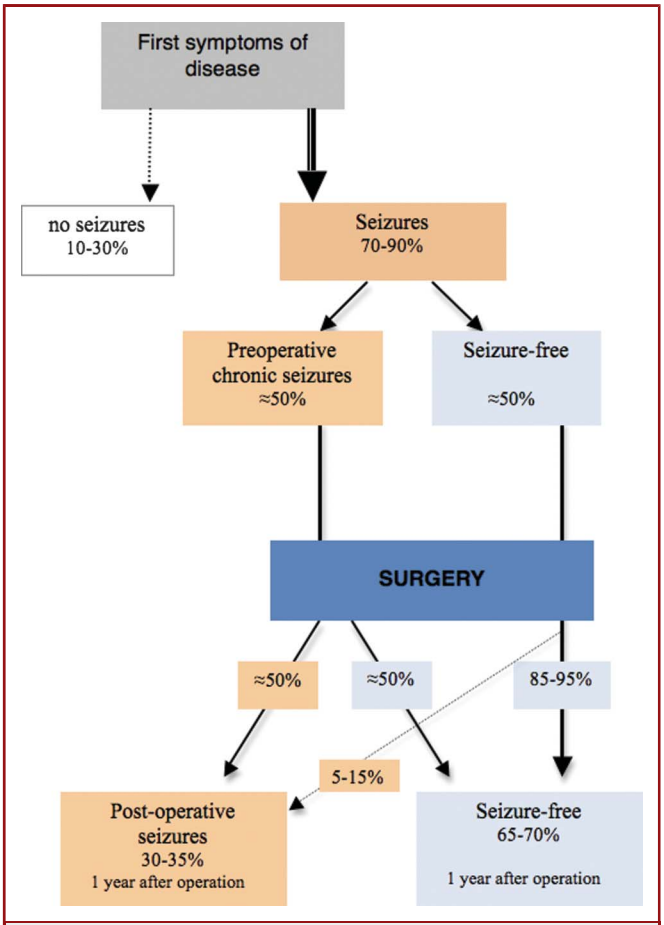

FIGURE 1. *Illustration of the frequency of preoperative and postoperative seizures in adults with low-grade gliomas.*

required additional resection of the epileptogenic zone. The importance of short seizure duration and early surgical intervention for good postoperative seizure control has been confirmed by several studies.[36] The parameter of extent of surgery with the use of cortical and subcortical mapping has been more controversial but is now generally accepted as an additional predictor for seizure control.[39,40] This is probably true for all tumor locations, including the highly epileptogenic insula and the mesiotemporal region.[41] Intraoperative electrostimulation mapping has made it possible to increase the extent of resection while preserving the eloquent areas (glioma removal according to functional boundaries), but also to extend the indications for surgery within brain regions classically considered as inoperable such as the insular lobe or the rolandic area, both very epileptogenic.[40,41] Moreover, the use of intraoperative electrocorticography monitoring may further improve postoperative seizure control by identifying surrounding seizure foci separated from the tumor.[12] Further support for the role of radical surgery for postoperative seizure control, rather than preoperative tumor size and tumor location, comes from the study of Chang et al.[11]

SEIZURE CONTROL BY POSTOPERATIVE THERAPY

Radiotherapy

Seizure outcome after radiotherapy was included as a secondary endpoint in the randomized EORTC 22845 phase III trial, designed to compare survival of patients with LGGs treated with early vs delayed radiotherapy.[42] Neurological symptoms were analyzed in patients still progression free 2 years after randomization, and better seizure control was found in patients who underwent radiotherapy compared with patients who did not[42] (Table 2). Because there was no difference in seizure control at baseline between the 2 groups, it was concluded from this trial that seizures were better controlled in the group receiving radiotherapy. Consistent findings have been found in retrospective reviews and case reports, reporting a significant seizure reduction with radiotherapy in patients with LGGs[43,44] (Table 2).

In the EORTC 22845 trial, external radiotherapy with 1.8-Gy fractions to a total dose of 54 Gy was used.[42] The earlier EORTC 22844 trial compared high-dose (59.4 Gy in 6.6 weeks) and low-dose (45 Gy in 5 weeks) radiotherapy in patients with LGGs, with survival as the primary endpoint.[45] Reduced quality of life was found for patients who received high-dose radiation, but seizure control did not differ between the 2 treatment arms.[46] Although no definite conclusions can be drawn from this trial in which the assessment of the quality of life including seizures was an optional part, it seems likely that high-dose radiation does not improve seizure control for this patient group.

Any other treatment- or tumor-related parameters that affect seizure control after radiotherapy have not yet been identified. It is also not clear to what extent seizure control and tumor control by radiotherapy are related. No correlation was found between seizure reduction and tumor response on computed tomography and MRI in a preliminary report of 25 irradiated patients.[43]

Chemotherapy

The alkylating chemotherapeutic agent temozolomide was shown to induce seizure reduction in a phase II study of LGGs[47] (Table 2). Patients recruited for this study had not previously undergone radiotherapy, but were included at varying postoperative time points and not selected on the basis of progressive tumor disease. Interestingly, significantly better seizure control with temozolomide was found in nonenhancing than in enhancing tumors in a study on progressive LGGs.[48] In the subset of patients with seizure reduction, progression occurred mainly by volumetric tumor expansion on MRI without clear-cut signs of tumor transformation such as contrast enhancement. The authors concluded that the heterogeneity in biological behavior and response to treatment in this patient group should be considered in selection criteria for clinical trials.[48] Likewise,

Copyright © Congress of Neurological Surgeons. Unauthorized reproduction of this article is prohibited.

TABLE 2. Studies That Include Reports on the Effect on Seizure Control in Adult Low-Grade Gliomas by Different Postoperative Tumor Treatments[a]

Study	Study Design	Tumor Subtype/No. of Patients	Results
Seizure control by radiotherapy			
van den Bent et al,[42] *2005*	EORTC 22845 phase III trial Seizure outcome by radiotherapy included as secondary endpoint	A, OA, O/102 irradiated, 71 not irradiated	Better seizure control in irradiated patients (25%) than in patients not irradiated (41%) at 2 y from randomization
Soffietti et al,[43] *2005*	Retrospective review of adjuvant radiotherapy or at tumor progression	A/25	Significant reduction in seizures in 19 (of 25) patients (2 seizure free); no response in 5 patients; deteriorated seizure control in 1 patient
Rogers et al,[44] *1993*	Case reports of unresected biopsy-proven low-grade gliomas with medically intractable seizures	A/5	>90% seizure reduction in 3 patients (1 seizure free); >75% seizure reduction in 1 patient; no response in 1 patient
Seizure control by chemotherapy			
Brada et al,[47] *2003*	Phase II study of efficacy of primary temozolomide in low-grade gliomas	A, OA, O/30	Seizure reduction in 15 (of 28) patients (6 seizure free)
Pace et al,[48] *2003*	Retrospective review of temozolomide in progressive low-grade gliomas	A, OA, O/43	Seizure reduction in 15 (of 31) patients (4 seizure free)
Sherman et al,[49] *2008*	Retrospective review of primary temozolomide in low-grade gliomas	A, OA, O/40	>50% seizure reduction in 24 (of 40) patients (13 seizure free)
Taillandier and Duffau,[50] *2009*	Retrospective review of insular low-grade gliomas treated with surgery, chemotherapy or combined chemotherapy/surgery	A, OA, O/46	Improved seizure control in 80% of patients with first- or second-line chemotherapy; in 90% of patients with surgery as first-line and in 80% as second-line therapy
Seizure control by reoperation			
Martino et al,[51] *2009*	Review of consecutive series of patients re-operated for low-grade gliomas in eloquent areas	A, OA, O/19	Improved seizure control in 14 (of 17) patients (9 seizure free)

[a]A, astrocytoma World Health Organization grade II; OA, oligoastrocytoma World Health Organization grade II; O, oligodendroglioma World Health Organization grade II.

a retrospective analysis of the impact of temozolomide chemotherapy on seizure frequency in LGGs reported a subset of patients who became seizure free during treatment irrespective of radiographic tumor response.[49]

In a retrospective chart review of patients with exclusively paralimbic LGG treated by surgery, chemotherapy, or a combination of the 2, chemotherapy was shown to produce excellent seizure control results[50] (Table 2). These patients had not previously undergone surgery and received chemotherapy as first- or second-line treatment for progressive tumors: temozolomide in 19 patients, PCV (procarbazine, lomustine [CCNU], and vincristine) in 6 patients, and fotemustine in 1 patient.[50] Favorable seizure control results were also obtained in the group treated by surgical resection. It was concluded that, despite the technical difficulties, surgery combined with chemotherapy is indicated in pharmacoresistant epilepsy because of insular gliomas independently of the oncological indications.[50]

Seizure Control After Reoperation

Reoperation of recurrent LGGs is a therapeutic option that may have beneficial effects on seizure control. Traditionally, surgery for patients with recurrent LGGs in eloquent areas has been controversial, but safe and efficacious results can be obtained by using intraoperative functional mapping. In a recent study of patients with recurrent LGGs in eloquent areas who underwent reoperation, with a minimum of 1 year and a median of 4.1 years between the 2 resections, all but 1 patient improved or retained normal neurological function after reoperation[51] (Table 2). The authors hypothesize that brain plasticity is not exhausted after the first operation and that reorganization of functional areas continues to take place between initial and recurrent operations.[51] After the second operation, seizures disappeared in 9 of 17 patients with refractory seizures and were reduced in another 5 patients. Histopathology of the recurrent tumors showed transformation

Copyright © Congress of Neurological Surgeons. Unauthorized reproduction of this article is prohibited.

to high-grade gliomas in 11 cases, but no correlation was found between the presence of seizures as the initial symptom and malignant transformation of the tumor in this series.[51]

SEIZURE CONTROL DURING TUMOR PROGRESSION

It is a common experience for clinical neuro-oncologists that recurrent seizures after an initial seizure-free period may be the first signs of tumor progression. However, the exact predictive value of this symptom has not been studied in any longitudinal trials.[46,52] One can speculate that altered seizure control reflects a change in tumor growth rate or, in the case of transformation, in tumor behavior. This way, recurrent seizures will occur when a switch to an accelerated growth rate or to anaplastic tumor transformation takes place, whereas seizure reduction (temporarily obtained by radiotherapy or chemotherapy) could represent a transient conversion to slower growth.

Data on seizure control at progression have come mainly from cross-sectional series, consisting of mixed samples of patients with high- and low-grade tumors who received varying previous treatment modalities.[18] Hildebrand et al[53] examined 234 consecutive ambulatory patients treated for chemotherapy of a supratentorial brain tumor during a 3-month period. Less than 50% of the study population received radiotherapy earlier in the course of disease. Of the 93 patients with grade II gliomas included in this series, 84 patients (92%) had seizures at study presentation.[53] In a series of patients with grade II gliomas presenting with clinical and radiological progressive disease, 31 of 43 patients had pharmacoresistant seizures.[48] Thirty of these 43 patients were previously treated by radiotherapy.[48]

Further support for a causal relationship between changes in tumor growth rate and changes in seizure control comes from a recent study on LGGs in pregnant women.[54] The tumors in these patients, monitored by successive MRI during pregnancy, showed a significant increase in growth rate compared with corresponding prepregnancy measures, and 40% of the patients reported a simultaneous increase in seizure frequency.[54]

DISCUSSION

The understanding and management of LGGs is evolving as randomized clinical trials have begun to address issues related to the effect and timing of treatment on progression-free and overall survival.[55] These trials offer new opportunities for studying the time course of symptoms during the evolution of this disease. Epilepsy is the most frequent symptom of LGGs. From a clinical point of view, a better understanding of how seizures and seizure control are related to tumor behavior will optimize individual treatment strategies.

The etiology of tumor-related seizures is multifactorial, involving tumor as well as host factors. Furthermore, some of the molecular pathways leading to tumor growth may contribute to the development of seizures as well.[56] The original concept for tumor-associated seizures proposed that seizures arise as a result of tissue damage and edema, leading to impaired vascularization and peritumoral ischemia, and suggested that the occurrence of seizures was related to the degree of mass effect by the tumor.[13] It did not explain why seizures were less common in high-grade gliomas and why seizures could return or sometimes appear for the first time after tumor resection. Deafferentation of the adjacent cortex during the slow growth of LGGs may cause epileptogenic changes of the microenvironment surrounding the tumor. Various morphological changes associated with seizure activity have been found in the peritumoral tissue, including aberrant neuronal migration, persistent neurons in the white matter, and altered number, size, and distribution of synaptic vessels.[13,14] In addition, neurochemical alterations take place that can modulate neuronal excitability, such as changes in pH and amino acids and an imbalance in inhibitory and excitatory neurotransmittors.[5,12]

For tumor-related epilepsy, the question has been raised whether the tumor may have intrinsic epileptogenic properties. This has never been shown for common types of WHO grade II gliomas but may be true for certain benign histological entities consisting of neuronal and glial components such as gangliogliomas and dysembryoblastic neuroepithelial tumors. These tumors are associated with a seizure incidence of almost 100% and a high degree of refractory epilepsy. They typically occur in childhood or young adults and are predominantly located in the temporal lobe. The neurochemical profiles of these tumor cells including enzyme and receptor expression showed similarities to neocortical neurons, pointing out the tumor itself as the generator of seizure activity.[57] A microarray analysis study, comparing human ganglioglioma with normal temporal cortex, revealed differential expression levels for various genes with a presumed role in the pathogenesis and the epileptogenesis of these tumors.[58] Interestingly, the most prominent differences were found for genes involved in the immune and inflammatory response.

Sometimes the epileptic focus does not correspond to the tumor or peritumoral region, leading to paroxysmal discharges distant to the tumor.[59] Such secondary epileptogenesis may occur in patients with temporal tumors for whom young age and long seizure history are strong predisposing factors, but is rare in adult WHO grade II gliomas.

Cognitive impairment is a frequent symptom in patients with brain tumors and may be caused by tumor growth, surgery, radiotherapy, chemotherapy, refractory seizures, antiepileptic drugs, or a combination of these factors.[60] In general, patients with LGGs have more diffuse disturbances of cognition, such as executive or attentional difficulties, in contrast to the focal deficits characteristically found in patients with high-grade gliomas. Such a diffuse pattern of cognitive dysfunction in patients with LGGs may be attributed to the growth and invasion of the tumor into the white matter, causing a functional imbalance of the different cortical neuronal networks connected by white matter fibers.[12] It

Copyright © Congress of Neurological Surgeons. Unauthorized reproduction of this article is prohibited.

has been suggested that the extremely complex structural networks can be modified by slow tumor growth in a way that either enhances brain plasticity, thereby preserving major cortical functions such as language or induces conversion into pathological networks of random structure leading to seizures.[12] Thus, disarrangement of the same functional cerebral networks may underlie the diverse symptoms of disease in LGGs, ie, cognitive disturbances as a result of diffuse destruction and seizures as a result of pathological excess of functional network structures.

Different aspects of antiepileptic drug treatment have to be taken into account in the clinical management of seizures in patients with LGGs. These include the optimal use of antiepileptic drugs, interactions between antiepileptic and chemotherapeutic drugs or dexamethasone, and the possibility of multidrug-resistance proteins causing refractory epilepsy.[5] These issues are beyond the scope of this review and not discussed further here, but illustrate the complexity of tumor-related seizures in LGGs.

CONCLUSION

LGG in adults is a disease with a fatal outcome, but long-term survival with good function is possible. Survival is determined primarily by disease factors with treatments having less influence on outcome. Seizures occur most commonly at disease presentation but are frequent symptoms during later disease as well. Seizures as initial symptom predict more favorable outcome and are correlated with tumor growth rate and tumor location and possibly indirectly with the molecular profile of the tumor. Despite optimal treatment with antiepileptic drugs, good preoperative seizure control is achieved in only 50% of patients presenting with seizures. Preoperative seizures are related to the location and likely also to the intrinsic properties of the tumor. Maximal surgical resection including resection of epileptic foci is a valuable strategy for improving seizure control in patients with refractory seizures. Radiotherapy and chemotherapy as single therapies or in combination with surgery have also shown beneficial effects on seizure control. Changes in seizure control after a seizure-free interval or a period with controlled seizures may reflect changes in tumor growth rate or tumor behavior. Ongoing and future randomized trials on LGGs will offer new opportunities to unravel the relationship between preoperative seizures and disease outcome and between seizure control and tumor control.

Disclosure

Financial support for this study was provided by the Uppsala University, the Selanders Foundation and the Lions Cancer Foundation at the Uppsala University Hospital. The authors have no personal financial or institutional interest in any of the drugs, materials, or devices described in this article.

REFERENCES

1. Davies FG, Preston-Martin S. *Russell & Rubenstein's Pathology of Tumors in the Nervous System*. In: Bigner DD, McLendon RE, Bruner JM, eds. Arnold. London: 1998.
2. Louis DN, Ohgaki H, Wiestler OD, et al. The 2007 WHO classification of tumors of the central nervous system. *Acta Neuropathol*. 2007;114(2):97-109.
3. Ohgaki H, Kleihues P. Epidemiology and etiology of gliomas. *Acta Neuropathol*. 2005;109(1):93-108.
4. Leighton C, Fisher B, Bauman G, et al. Supratentorial low-grade gliomas in adults: an analysis of prognostic factors and timing of radiation. *J Clin Oncol*. 1997;15(4):1294-1301.
5. van Breemen MS, Wilms EB, Vecht CJ. Epilepsy in patients with brain tumours: epidemiology, mechanisms, and management. *Lancet Neurol*. 2007;6(5):421-430.
6. Klein M, Engelberts NH, van der Ploeg HM, et al. Epilepsy in low-grade gliomas: the impact on cognitive function and quality of life. *Ann Neurol*. 2003;54(4):514-520.
7. Mandonnet E, Delattre JY, Tanguy ML, et al. Continuous growth of mean tumor diameter in a subset of grade II gliomas. *Ann Neurol*. 2003;53(4):524–528.
8. Rees J, Watt H, Jäger HR, et al. Volumes and growth rates of untreated adult low-grade gliomas indicate risk of early malignant transformation. *Eur J Radiol*. 2009;72(1):54-64.
9. El-Hateer H, Souhami L, Roberge D, et al. Low-grade oligodendroglioma: an indolent but incurable disease? *J Neurosurg*. 2009;111(2):265-271.
10. Zlatescu MC, TehraniYazdi A, Sasaki H, et al. Tumor location and growth pattern correlate with genetic signature in oligodendroglial neoplasms. *Cancer Res*. 2001;61(18):6713-6715.
11. Chang EF, Potts MB, Keles GE, et al. Seizure characteristics and control following resection in 332 patients with low-grade gliomas. *J Neurosurg*. 2008;108(2):227-235.
12. Brogna C, Gil Robles S, Duffau H. Brain tumors and epilepsy. *Expert Rev Neurother*. 2008;8(6):941-955.
13. Beaumont A, Whittle IR. The pathogenesis of tumour associated epilepsy. *Acta Neurochir (Wien)*. 2000;142(1):1-15.
14. Schaller B, Ruegg SJ. Brain tumor and seizures: pathophysiology and its implications for treatment revisited. *Epilepsia*. 2003;44(9):1223-1232.
15. Rosati A, Tomassini A, Pollo B, et al. Epilepsy in cerebral glioma: timing of appearance and histological correlations. *J Neurooncol*. 2009;93(3):395-400.
16. Van den Bent MJ, Reni M, Gatta G, Vecht C. Oligodendroglioma. *Crit Rev Oncol Hematol*. 2008;66(3):262-272.
17. Duffau H, Capelle L. Preferential brain locations of low-grade gliomas. *Cancer*. 2004;100(12):2622-2626.
18. Hwang SL, Lin CL, Lee KS, et al. Factors influencing seizures in adult patients with supratentorial astrocytic tumors. *Acta Neurochir (Wien)*. 2004;146(6):589-594.
19. Danfors T, Ribom D, Berntsson SG, Smits A. Epileptic seizures and survival during early disease in grade 2 gliomas. *Eur J Neurol*. 2009;16(7):823-831.
20. Bauman G, Fisher B, Watling C, Cairncross JG, Macdonald D. Adult supratentorial low-grade glioma: long-term experience at a single institution. *Int J Radiat Oncol Biol Phys*. 2009;75(5):1401-1407.
21. Pignatti F, van den Bent M, Curran D, et al. Prognostic factors for survival in adult patients with cerebral low-grade glioma. *J Clin Oncol*. 2002;20(8):2076-2084.
22. Duffau H. A personal consecutive series of surgically treated 51 cases of insular WHO Grade II glioma: advances and limitations. *J Neurosurg*. 2009;110(4):696-708.
23. van Veelen ML, Avezaat CJ, Kros JM, van Putten W, Vecht C. Supratentorial low grade astrocytoma: prognostic factors, dedifferentiation, and the issue of early versus late surgery. *J Neurol Neurosurg Psych*. 1998;64(5):581-587.
24. Lote K, Egeland T, Hager B, et al. Survival, prognostic factors, and therapeutic efficacy in low-grade glioma: a retrospective study in 379 patients. *J Clin Oncol*. 1997;15(9):3129-3140.
25. Soffietti R, Chiò A, Giordana MT, Vasario E, Schiffer D. Prognostic factors in well-differentiated cerebral astrocytomas in the adult. *Neurosurgery*. 1989;24(5):686-692.
26. Kreth FW, Faist M, Rossner R, Volk B, Ostertag CB. Supratentorial World Health Organization Grade 2 astrocytomas and oligoastrocytomas. A new pattern of prognostic factors. *Cancer*. 1997;79(2):370-379.
27. Piepmeier J, Christopher S, Spencer D, et al. Variations in the natural history and survival of patients with supratentorial low-grade astrocytomas. *Neurosurgery*. 1996;38(5):872-878.
28. Bartolomei JC, Christopher S, Vives K, Spencer DD, Piepmeier JM. Low-grade gliomas of chronic epilepsy: a distinct clinical and pathological entity. *J Neurooncol*. 1997;34(1):79-84.

Copyright © Congress of Neurological Surgeons. Unauthorized reproduction of this article is prohibited.

29. Plate KH, Wieser H-G, Yasargil MG, Wiestler OD. Neuropathological findings in 224 patients with temporal lobe epilepsy. *Acta Neuropathol*. 1994;86(5):433-438.
30. Afra D, Osztie E, Sipos L, Vitanovics D. Preoperative history and postoperative survival of supratentorial low-grade astrocytomas. *Br J Neurosurg*. 1999;13(3):299-305.
31. Piepmeier JM. Current concepts in the evaluation and management of WHO grade II gliomas. *J Neurooncol*. 2009;92(3):253-259.
32. Schramm J, Luyken C, Urbach H, Fimmers R, Blümcke I. Evidence for a clinically distinct new subtype of grade II astrocytomas in patients with long-term epilepsy. *Neurosurgery*. 2004;55(2):340-347.
33. Blumcke I, Luyken C, Urbach H, Schramm J, Wiestler OD. An isomorphic subtype of long-term epilepsy-associated astrocytomas associated with benign prognosis. *Acta Neuropathol*. 2004;107(5):381-388.
34. Devinsky O. Patients with refractory seizures. *N Engl J Med*. 1999;340(20):1565-1570.
35. Bauer R, Dobesberger J, Unterhofer C, et al. Outcome of adult patients with temporal lobe tumors and medically refractory epilepsy. *Acta Neurochir (Wien)*. 2007;149(2):1211-1216.
36. Zaatreh MM, Firlik KS, Spencer DD, et al. Temporal lobe tumoral epilepsy: characteristics and predictors of surgical outcome. *Neurology*. 2003;61(5):636-641.
37. Peraud A, Meschede M, Eisner W, Ilmberger J, Reulen HJ. Surgical resection of grade II astrocytomas in the superior frontal gyrus. *Neurosurgery*. 2002;50(5):966-975.
38. Kim OJ, Yong AJ, Chung YS, et al. Significance of chronic epilepsy in glial tumors and correlation with surgical strategies. *J Clin Neurosci*. 2004;11(7):702-705.
39. Lombardi D, Marsh R, de Tribolet N. Low grade glioma in intractable epilepsy: lesionectomy versus epilepsy surgery. *Acta Neurochir*. 1997;68(suppl):70-74.
40. Duffau H. Surgery of low-grade gliomas: towards a 'functional neurooncology'. *Curr Opin Oncol*. 2009;21(6):543-549.
41. Duffau H, Capelle L, Lopes M, Bitar A, Sichez JP, van Effenterre R. Medically intractable epilepsy from insular low-grade gliomas: improvement after an extended lesionectomy. *Acta Neurochir (Wien)*. 2002;144(6):563-572.
42. van den Bent MJ, Afra D, de Witte, et al. Long-term efficacy of early versus delayed radiotherapy for low-grade astrocytoma and oligodendroglioma in adults: the EORTC 22845 randomised trial. *Lancet*. 2005;366(9490):985-990.
43. Soffietti R, Borgognone M, Ducati A, et al. Efficacy of radiation therapy on seizures in low-grade astrocytomas. *Neuro-Oncol*. 2005(suppl):389.
44. Rogers LR, Morris HH, Lupica K. Effect of cranial irradiation on seizure frequency in adults with low-grade astrocytoma and medically intractable epilepsy. *Neurology*. 1993;43(8):1599-1601.
45. Karim AB, Maat B, Hatlevoll R, et al. A randomized trial on dose-response in radiation therapy of low-grade cerebral glioma: European Organization for Research and Treatment of Cancer (EORTC) Study 22844. *Int J Radiat Oncol Biol Phys*. 1996;36(3):549-556.
46. Kiebert GM, Curran D, Aaronson NK, et al. Quality of life after radiation therapy of cerebral low-grade gliomas of the adult: results of a randomised phase III trial on dose response (EORTC trial 22844). EORTC Radiotherapy Co-operative Group. *Eur J Cancer*. 1998;34(12):1902-1909.
47. Brada M, Viviers L, Abson C, et al. Phase II study of primary temozolomide chemotherapy in patients with WHO grade II gliomas. *Ann Oncol*. 2003;14(12):1715-1721.
48. Pace A, Vidiri A, Galiè E, et al. Temozolomide chemotherapy for progressive low-grade glioma: clinical benefits and radiological response. *Ann Oncol*. 2003;14(12):1722-1726.
49. Sherman J, Yeoh H, Pouratian N, et al. Impact of temozolomide chemotherapy on seizure frequency in patients with low-grade glioma. *Neuro-Oncol*. 2008;832. (abstr)
50. Taillandier L, Duffau H. Epilepsy and insular Grade II gliomas: an interdisciplinary point of view from a retrospective monocentric series of 46 cases. *Neurosurg Focus*. 2009;27(2):E8.
51. Martino J, Taillandier L, Moritz-Gasser S, Gatignol P, Duffau H. Re-operation is a safe and effective therapeutic strategy in recurrent WHO grade II gliomas within eloquent areas. *Acta Neurochir (Wien)*. 2009;151(5):427-436.
52. Wick W, Menn O, Meisner C, et al. Pharmacotherapy of epileptic seizures in glioma patients: who, when, why and how long? *Onkologie*. 2005;28(8-9):391-406.
53. Hildebrand J, Lecaille C, Perennes J, Delattre JY. Epileptic seizures during follow-up of patients treated for primary brain tumors. *Neurology*. 2005;65(2):212-215.
54. Pallud J, Mandonnet E, Deroulers C, et al. Pregnancy increases the growth rates of WHO grade II gliomas. *Ann Neurol*. 2010;67(3):398-404.
55. Ruiz J, Lesser GJ. Low-grade gliomas. *Curr Treat Options Oncol*. 2009;10(3-4):231-242.
56. Berntsson SG, Malmer B, Bondy ML, Qu M, Smits A. Tumor-associated epilepsy and glioma: are there common genetic pathways? *Acta Oncol*. 2009;48(7):955-963.
57. Wolf HK, Wiestler OD. Surgical pathology of chronic epileptic seizure disorders. *Brain Pathol*. 1993;3(4):371-380.
58. Aronica E, Boer K, Becker A, et al. Gene expression profile analysis of epilepsy-associated gangliogliomas. *Neuroscience*. 2008;151(1):272-292.
59. Gilmore R, Morris H III, Van Ness PC, Gilmore-Pollak W, Estes M. Mirror focus: function of seizure frequency and influence on outcome after surgery. *Epilepsia*. 1994;35(2):258-263.
60. Taphoorn MJ, Klein M. Cognitive deficits in adult patients with brain tumours. *Lancet Neurol*. 2004;3(3):159-168.

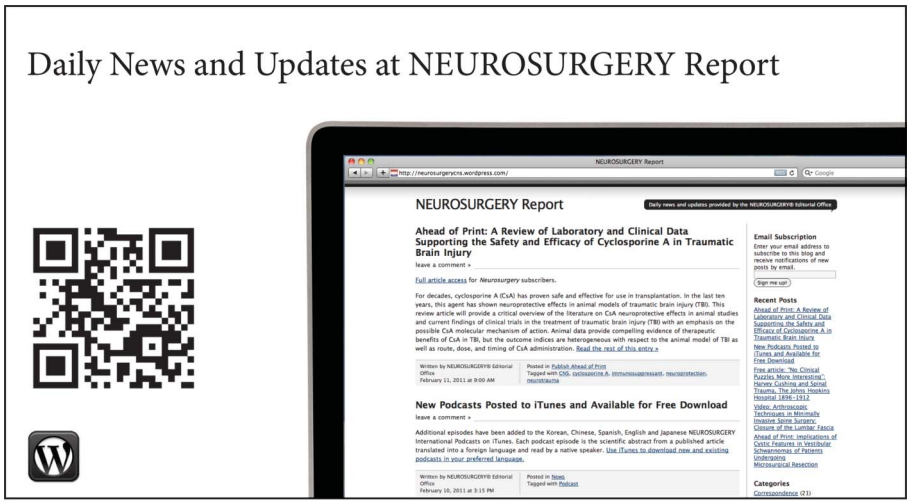

Copyright © Congress of Neurological Surgeons. Unauthorized reproduction of this article is prohibited.

Neuroprotection With Intraventricular Brain-Derived Neurotrophic Factor in Rat Venous Occlusion Model

Yasuhiro Takeshima, MD
Mitsutoshi Nakamura, MD
Hitoshi Miyake, MD
Ryo Tamaki, MD
Toshitaka Inui, MD
Kaoru Horiuchi, MD
Daisuke Wajima, MD
Hiroyuki Nakase, MD

Department of Neurosurgery, Nara Medical University School of Medicine, Nara, Japan

Correspondence:
Yasuhiro Takeshima, MD,
Department of Neurosurgery,
Nara Medical University School of Medicine,
840 Shijo-cho, Kashihara,
Nara, 634-8521, Japan.
E-mail: yasu-77@qj8.so-net.ne.jp

Received, May 11, 2010.
Accepted, October 1, 2010.

Copyright © 2011 by the Congress of Neurological Surgeons

BACKGROUND: The increasing number of neurosurgical procedures for elderly patients and the development of skull base neurosurgery have increased interest in cerebral venous injury that might occur in a neurosurgical setting. Brain-derived neurotrophic factor (BDNF) may have neuroprotective effects against cerebral venous ischemia.

OBJECTIVE: To investigate the intraventricular effects of BDNF infusion on infarct size, suppression of apoptosis, and regional cerebral blood flow (rCBF) in cerebral venous ischemic lesions in a rat 2-vein occlusion model.

METHODS: Thirty-three male Wistar rats were randomly divided into BDNF-treated and vehicle control groups; each group was further randomly divided into 2-day and 7-day postocclusion groups. BDNF (2.1 μg/day) or vehicle was delivered continuously via intraventricular infusion pumps. Two adjacent contralateral cortical veins were then photochemically occluded. Two and 7 days after occlusion, we histologically measured ratios of infarct volume to contralateral hemisphere volume and counted (2-day group) terminal deoxynucleotidyl transferase–mediated deoxyuridine triphosphate nick-end labeling (TUNEL)-positive apoptotic cells in the penumbra. rCBF was measured via full-field laser perfusion imaging.

RESULTS: The mean infarct volume after venous occlusion was significantly smaller in BDNF-treated rats than in controls at 2 days (1.49 ± 1.44% vs 3.66 ± 1.51%; $P < .05$) and 7 days (0.93 ± 0.47% vs 1.69 ± 0.58%; $P < .05$). Two days after occlusion, there were significantly fewer TUNEL-positive apoptotic cells in the BDNF-treated rats (17.0 ± 15.1) than in the controls (39.0 ± 19.6; $P < .05$). There were no differences in rCBF.

CONCLUSION: After 2-vein occlusion, continuous intraventricular administration of BDNF protected the cerebral cortex against apoptosis and reduced infarct size without affecting rCBF.

KEY WORDS: Apoptosis, BDNF, Cerebral venous ischemia, Regional CBF, 2-Vein occlusion model

Neurosurgery 68:1334–1341, 2011 DOI: 10.1227/NEU.0b013e31820c048e www.neurosurgery-online.com

Cerebral venous ischemia (CVI), which may be experienced in a neurosurgical setting, is one of the general components of cerebral stroke. Recently, there has been considerable interest in CVI because of the increasing number of neurosurgical procedures for elderly patients and the development of skull base neurosurgery.[1-3] However, because of its intricate nature, the treatment for CVI remains clinically and experimentally uncertain compared with the treatment for cerebral arterial ischemia, and a new treatment for CVI has been sought for several decades.

ABBREVIATIONS: BDNF, brain-derived neurotrophic factor; **CVI,** cerebral venous ischemia; **MCA,** middle cerebral artery; **rCBF,** regional cerebral blood flow; **TUNEL,** terminal deoxynucleotidyl transferase–mediated deoxyuridine triphosphate nick-end labeling

There are 2 important factors to consider in the search for a treatment for cerebral ischemia. First, it is necessary to look for a treatment that interrupts the process of neuronal death. Recently, we revealed the mechanisms of neuronal death in the terminal stage of CVI as necrosis and apoptosis.[4,5] Finding a candidate that

Copyright © Congress of Neurological Surgeons. Unauthorized reproduction of this article is prohibited.

interrupts the process of commitment to apoptosis and contributes to the survival of cells in CVI may require a novel treatment. A second concern for a cerebral ischemia treatment is its effect on cerebral blood flow (CBF). The cerebral ischemic region comprises tissues that have a sufficiently reduced CBF to put the cells at risk. Thus, to salvage this region from ischemia, one treatment would be to increase regional CBF (rCBF).

In this study, we focused on brain-derived neurotrophic factor (BDNF) as a candidate to treat CVI. BDNF, a member of the neurotrophin family of growth factors, has a neuroprotective effect in various cerebral ischemias. BDNF suppresses apoptosis after middle cerebral occlusion,[6] has well-known stimulatory effects on neuroplasticity and a neurologically functional recovery effect,[7,8] and improves long-term outcome after focal ischemia in rats.[9] In addition, recent animal studies showed that BDNF affects neurogenesis in cerebral ischemia.[8,10] However, no studies have been conducted to evaluate the neuroprotective effects of BDNF in CVI, and it is not known whether BDNF affects rCBF.

The aim of this study is to determine whether BDNF has neuroprotective effects in CVI. We used a rat 2-vein occlusion model, which is based on photochemically induced cortical vein occlusion that was developed as a good approximation of the intraoperative venous injury that might be experienced in a neurosurgical setting,[11] to examine whether intraventricular administration of BDNF reduced infarct volume through suppression of apoptosis and its effect on rCBF.

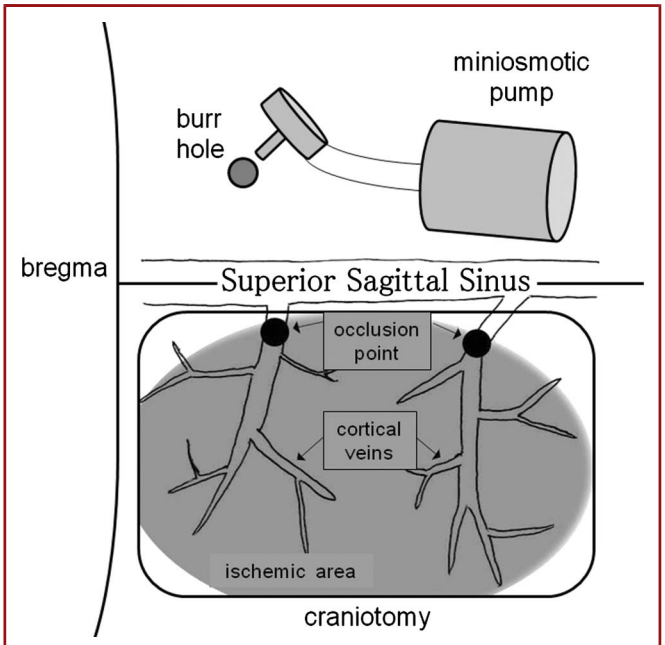

FIGURE 1. *Schematic of a rat brain from a 2-vein occlusion model. A burr hole was drilled over the right lateral ventricle, and a cannula connected to a miniosmotic pump filled with brain-derived neurotrophic factor or vehicle was inserted stereotactically into the contralateral ventricle. A left parietal cranial window was made, and 2 adjacent cortical veins were photochemically occluded. After venous occlusion, regional cerebral blood flow decreased, and a mild ischemic area spread widely.*

MATERIALS AND METHODS

Animals

All experimental protocols were approved by the Animal Welfare Committee of Nara Medical University (Kashihara, Nara, Japan). Thirty-three male Wistar rats (CLEA Japan, Inc, Osaka, Japan) weighing 240 to 280 g were used in the study. The rats were housed and maintained on a 12-hour light-dark cycle with free access to food and water.

Surgical Procedures and BDNF Preparation

The 2-vein occlusion model is different from the well-known 2-vessel occlusion model, which occludes arterial supply to the circle of Willis.[12] The 2-vein occlusion method followed the precedents described by Kimura et al[13] and the intraventricular infusion method followed that of Schäbitz et al[14] (Figure 1). The rats were anesthetized with chloral hydrate (36 mg/100 g body weight IP) after premedication with 0.5 mg atropine sulfate. The anesthesia was maintained with chloral hydrate (12 mg/100 g body weight) administered hourly through a peritoneal catheter. All rats were intubated with silicon tubing (outer diameter, 2.5 mm) and mechanically ventilated (model 683; Harvard Apparatus, Holliston, Massachusetts). Rectal temperature was maintained at 37°C with a feedback heating pad (CMA 150; Carnegie Medicine AB, Stockholm, Sweden). Polyethylene catheters were inserted into the tail artery and right femoral vein. The arterial line was used for continuous monitoring of mean arterial blood pressure and arterial blood gas sampling, and the venous line was used to administer drugs. The Pa_{O_2}, Pa_{CO_2}, and arterial pH were measured with a blood gas analyzer (ABL 330; Radiometer Ltd, Copenhagen, Denmark), and blood pressure was continuously monitored through an intra-arterial catheter connected to a pressure transducer (Polygraph System RM-600; Nihon Koden, Tokyo, Japan). Each rat was mounted on a stereotactic frame (SR-6; Narishige Inc, Tokyo, Japan).

BDNF (450-02; Peprotech EC LTD, London, United Kingdom) was stored at 8°C before use. In accordance with the Schäbitz et al[14] protocol, 15 μg BDNF was dissolved in 175 μL phosphate-buffered saline. BDNF was delivered intraventricularly at a rate of 2.1 μg/d (0.086 μg/h) until sacrifice. Controls received similar infusions of the vehicle alone. Intraventricular infusions were carried out with miniosmotic pumps (Alzet Brain Infusion Kits 2; Alzet, Palo Alto, California; Alzet2001, 200-μL fill volume, 1.0-μL/h pump rate) implanted subcutaneously in the back with the cannula positioned over the right lateral ventricle contralateral to the venous occlusion (1.6 mm lateral, 0.8 mm posterior to the bregma, and 4 mm beneath the surface of the skull; Figure 1). The reliabilities of the pumps were assessed by weighing them before and after the experiment; there was no residual drug in any of the pumps at the time of transcardial perfusion.

Experimental Design and Groups

Thirty-three male Wistar rats were randomly divided into 2 groups: a BDNF-treated group (n = 18) and a control (n = 15) group. The rats in each group were further divided (blindly) into 2 subgroups according to the time of death: a 2-day and a 7-day postocclusion group. Thus, there were 8 and 10 rats in the 2-day and 7-day subgroups, respectively, in the BDNF group and 6 and 9 rats in the 2-day and 7-day subgroups,

Copyright © Congress of Neurological Surgeons. Unauthorized reproduction of this article is prohibited.

respectively, in the control group. To assess the neuroprotective effect of BDNF, the infarct volume was evaluated in both groups 2 days and 7 days after venous occlusion. In addition, DNA fragmentation was analyzed in cells 2 days after venous occlusion for the assessment of apoptosis.

Measurement of rCBF and Cortical Vein Occlusion by Photochemical Thrombotic Technique

A left parietal cranial window (4.5 × 6 mm) on the side contralateral to the agent infusion was made with a high-speed drill. The entire procedure was performed under an operating microscope (Carl Zeiss, Oberkochen, Germany). During the craniectomy, the drill tip was cooled continuously with physiological saline to avoid thermal injury to the cerebral cortex. The left parietal cortex was visible through the dura mater, and the rCBF was measured from above the dura mater following the method described by Dusch et al.[15] A full-field laser perfusion imager (FLPI; Moor Instruments Ltd, Axminster, United Kingdom) was mounted perpendicular to and at a distance of 25 cm from the dural surface after craniectomy, and the image focus of the FLPI was adjusted to cover the field. After FLP images were taken of each cranial window just before and at 15-minute intervals for 90 minutes after intraventricular insertion of the miniosmotic pump, the images were analyzed with offline software (FLPI software package, version 1, Moor Ltd) to measure the rCBF of the area between the adjacent cortical veins. To measure average rCBFs, we set up regions of interest in each image, taking care to avoid large dural or pial vessels (Figure 2). After FLPI, 2 adjacent cortical veins were photochemically occluded with Rose Bengal dye and fiberoptic illumination as described previously (Figure 1).[4,13]

Histopathological Evaluation

Histopathological evaluation followed the method described by Nishioka et al.[4] Two and 7 days after venous occlusion, rats were transcardially perfused with 100 mL heparinized saline, followed by 100 mL of 10% formaldehyde. The brains were excised, and coronal blocks from the middle frontal cortex containing the 2 dorsal cerebral veins were embedded in paraffin. Sections 5 μm thick were cut and stained with hematoxylin and eosin. To control for individual differences, the ratio of infarct volume to the volume of the contralateral hemisphere was calculated with the use of an image processing software package (NIH Image; Macintosh, Apple, Cupertino, California).

The DNA fragmentation of cells undergoing apoptosis was analyzed in sections from the 2-day group through the use of the terminal deoxynucleotidyl transferase–mediated deoxyuridine triphosphate nick-end labeling (TUNEL) assay; sections were processed in accordance with the instructions of the ApopTag Peroxidase In Situ Apoptosis Detection Kit (Chemicon International, Eastleigh, United Kingdom) with minor modifications. Digoxigenin-deoxyuridine 5-phosphate was used to label 3′-OH ends by terminal deoxynucleotidyl transferase, and digoxigenin was detected by antidigoxigenin peroxidase labeling and then by the 3,3′ diaminobenzidine-HCl reaction. We used the thymus of the rat as a positive control. When evaluating the apoptotic cell number, we confirmed the presence of standard morphological characteristics of apoptosis; only those cells showing nuclear pyknosis, chromatin condensation or fragmentation, and cytoplasmic shrinkage were recognized as TUNEL-positive apoptotic cells. Three microscopic fields (magnification × 200) in each section containing the most abundant distribution of TUNEL-positive cells in the penumbral areas were selected for counts. These evaluations were performed by an experimenter blinded to rat allocation.

Statistical Analysis

All statistical comparisons were performed with SigmaStat software version 9.0 (Jandel Scientific, Erkrath, Germany). Physiological variables, infarct volumes, and the number of TUNEL-positive apoptotic cells in the various groups were compared by use of unpaired *t* tests. Changes in rCBF after BDNF administration were compared by use of 2-factor, repeated-measures ANOVA. The values presented in this study are mean ± SD. Differences were considered significant at $P < .05$.

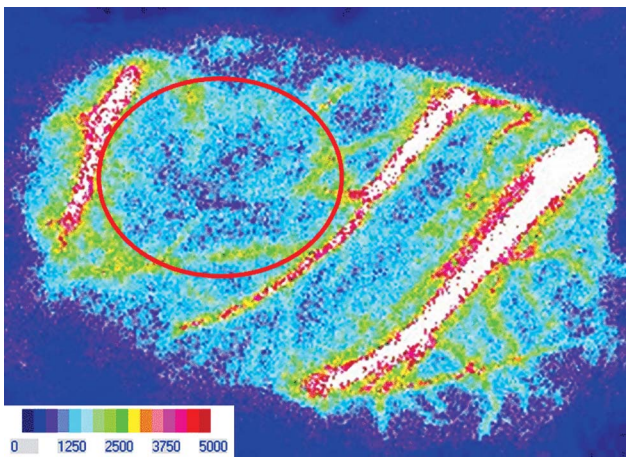

FIGURE 2. *A typical pseudo–color-coded, full-field laser perfusion image of the left parietal cranial window. The circle indicates the region of interest set up to measure average regional cerebral blood flow (rCBF) between 2 cortical veins and not to include these vessels. Numbers on the pseudocolor bar represent relative rCBF values.*

RESULTS

Measurement of rCBF

During the intraventricular administration of BDNF, we observed the time course of rCBF. Physiological variables for the rats in both the BDNF and control groups were within normal limits as shown in Table 1. The mean arterial blood pressure did not change significantly during surgical procedures and remained between 80 and 110 mm Hg. The other parameters, including weight, body temperature, pH, Pao_2, and $Paco_2$, were stable before and after rCBF measurements. Time courses of rCBF are shown in Figure 3. Although rCBF values in the BDNF group were lower than those in the control group at all time points, there were no significant differences in rCBF between the 2 groups ($P = .74$).

Histopathological Evaluation

Physiological variables of the BDNF-treated and control rats 2 and 7 days after venous occlusion are shown in Table 2. There were no significant intergroup differences in any of the physiological variables,

Copyright © Congress of Neurological Surgeons. Unauthorized reproduction of this article is prohibited.

TABLE 1. Physiological Variables at the Time of Regional Cerebral Blood Flow Measurements[a]

Treatment	Weight, g	Body Temperature, °C	Mean Arterial Blood Pressure, mm Hg	Arterial Blood Gas		
				pH	$Paco_2$, mm Hg	Pao_2, mm Hg
Control	257.2 ± 8.1	37.1 ± 0.4	98.8 ± 9.2	7.41 ± 0.05	35.7 ± 4.6	176.6 ± 70.0
BDNF	262.2 ± 15.0	37.0 ± 0.3	99.3 ± 11.8	7.42 ± 0.06	35.0 ± 4.4	182.8 ± 77.3

[a]BDNF, brain-derived neurotrophic factor.
Data are mean ± SD.
Differences in physiological variables between groups were not statistically signicant.

including weight, body temperature, mean arterial blood pressure, pH, PaO_2, and $PaCO_2$. All rats in the experimental groups developed typical venous infarcts in the cortex near the superior sagittal sinus. Areas showing morphological changes in the neurons were considered to be infarction cores, and the border zones around ischemic cores were identified as the penumbra areas.

Representative histological findings at 2 and 7 days after occlusion are shown in Figure 4. Light microscopic examination showed parenchymal damage, neuronal loss, vacuole formation, infiltration of inflammatory ells, and edematous changes with enlarged extracellular spaces in the infarcted areas. There was a visible reduction in infarct volume in the rats treated with BDNF. The mean infarct volumes were significantly smaller in BDNF-treated rats than in controls at 2 days (1.49 ± 1.44% vs 3.66 ± 1.51%, respectively; $P = .03$; Figure 5). At 7 days, the infarct volumes were smaller in each group than in the respective groups at 2 days and were significantly smaller in BDNF-treated rats than in controls (0.93 ± 0.47% vs 1.69 ± 0.58%; $P = .006$; Figure 5). The average decreases in infarct volumes were 54% in controls and 38% in the BDNF-treated group.

Because TUNEL staining may detect cells undergoing necrotic and apoptotic cell death, we considered the presence of various types of chromatin condensation (perinuclear ring formation, patches, or apoptotic bodies) as TUNEL-apoptotic neurons, and we considered cells showing weak, diffuse, cytoplasmic staining or light nuclear labeling without nuclear condensation or apoptotic bodies as TUNEL-positive necrotic neurons. In all rats examined at 2 days after occlusion, TUNEL-positive apoptotic cells were detected in infarction cores and penumbra areas; in the penumbra area, there were significantly fewer such cells in BDNF-treated rats (17.0 ± 15.1) than in controls (39.0 ± 19.6; $P = .003$; Figure 6).

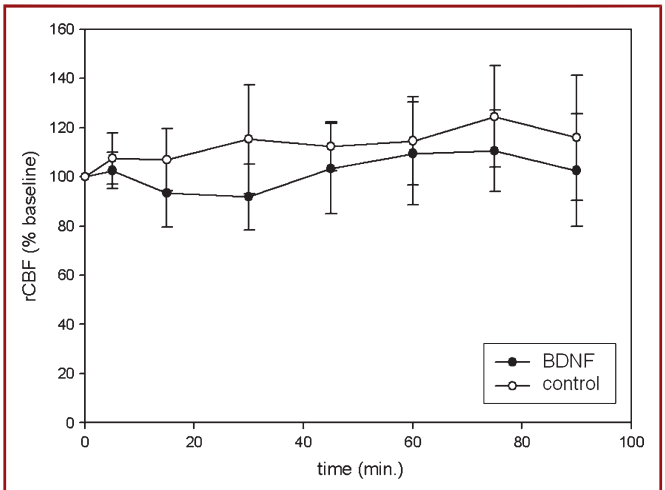

FIGURE 3. *Line graph shows changes in regional cerebral blood flow (rCBF) in the left parietal cranial window as measured by the full-field laser perfusion imager. Time lines indicate the times after administration of brain-derived neurotrophic factor (BDNF) or vehicle alone. Although rCBFs in the BDNF group were lower than those in controls at all time points, there were no significant differences in rCBF between the 2 groups (P = .740, 2-factor, repeated-measures analysis of variance). Data points represent mean ± SD.*

DISCUSSION

Cerebral Venous Ischemia

Data in the present study demonstrated that intraventricular BDNF reduces venous infarct volumes, suggesting that it may be a new candidate for the treatment of CVI. In an attempt to determine the mechanism of CVI, several experimental studies examined factors related to CVI and the subsequent brain damage that occurs.[11,16,17] CVI may cause local ischemia adjacent to occluded veins lacking sufficient collateral flow; the ischemia appears even in the very early period after venous occlusion and results in an expanding venous thrombus, local critical ischemia, and severe brain damage.[11,16] Venous occlusion leads to an increase in cerebral blood volume and cerebral fluid content, resulting in intracranial hypertension, decreased regional CBF, and long-term changes in brain function.[16] Cerebral venous occlusion also leads to neurological deterioration with a subsequent increase in intracranial pressure and development of brain tissue edema, brain tissue infarction, and intracerebral hemorrhage.[17] These various complex factors may eventually cause neuronal cell death in CVI. Because of the intricate nature of CVI, its treatment remains clinically and experimentally uncertain compared with that of other brain insults. Thus, we examined treatment with BDNF in a rat 2-vein occlusion model, the results of which might provide a new therapeutic regimen for the treatment of CVI.

Copyright © Congress of Neurological Surgeons. Unauthorized reproduction of this article is prohibited.

TABLE 2. Physiological Variables in Brain-Derived Neurotrophic Factor–Treated and Control Rats[a]

Treatment	n	Weight, g	Body Temperature, °C	Mean Arterial Blood Pressure, mm Hg	Arterial Blood Gas		
					pH	$Paco_2$, mm Hg	Pao_2, mm Hg
At 2 d							
Control	6	260.9 ± 12.8	37.0 ± 0.3	98.2 ± 6.7	7.41 ± 0.04	35.9 ± 3.5	170.0 ± 60.8
BDNF	8	264.8 ± 9.2	37.1 ± 0.5	96.2 ± 6.5	7.41 ± 0.06	35.7 ± 4.1	181.2 ± 64.2
At 7 d							
Control	9	259.2 ± 8.1	37.1 ± 0.3	99.0 ± 3.5	7.39 ± 0.06	33.6 ± 4.2	157.4 ± 40.7
BDNF	10	260.8 ± 15.0	37.0 ± 0.3	97.8 ± 5.5	7.41 ± 0.05	36.8 ± 3.2	158.9 ± 39.4

[a]BDNF, brain-derived neurotrophic factor.
Data are mean ± SD.
Differences in physiological variables between groups were not statistically signicant.

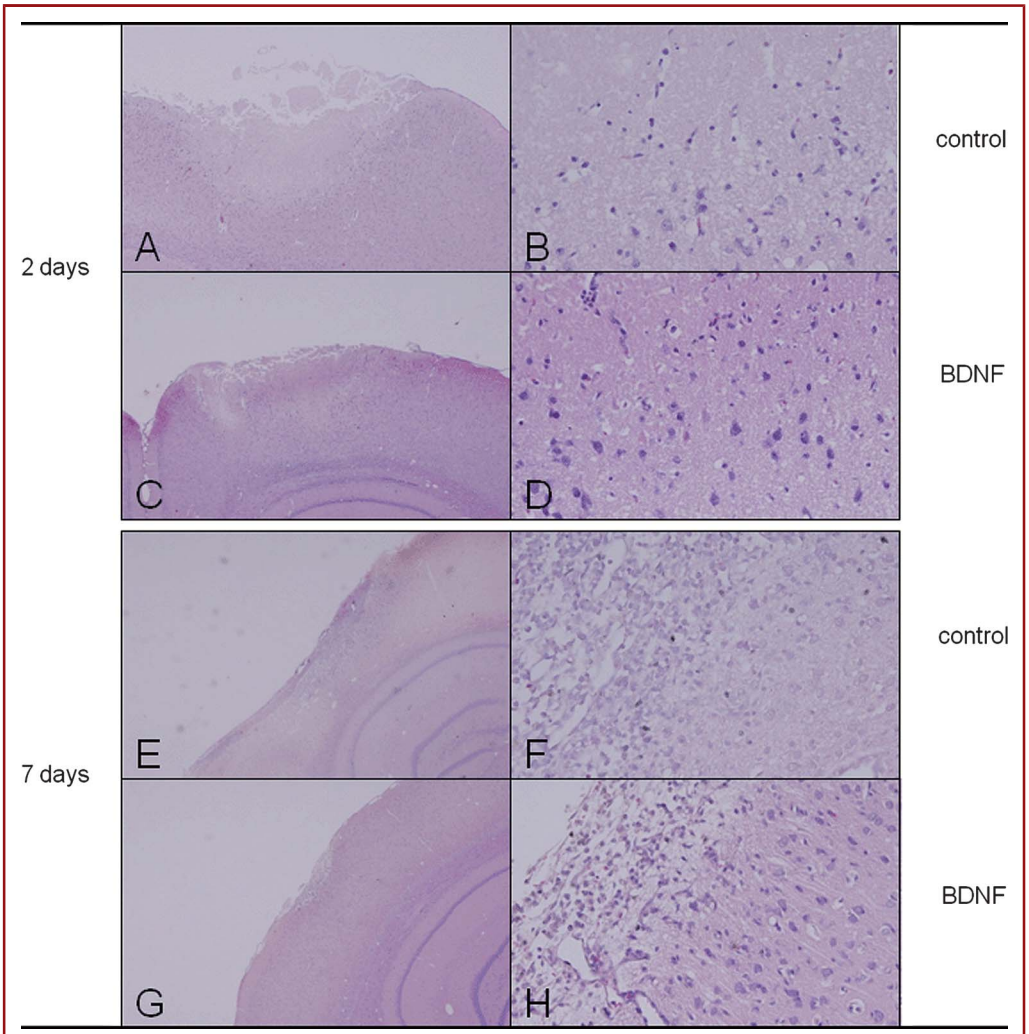

FIGURE 4. *Coronal sections from brain-derived neurotrophic factor (BDNF)–treated and control rats stained with hematoxylin and eosin. Representative histological findings at 2 days after 2-vein occlusion in controls (**A** and **B**) and BDNF-treated (**C** and **D**) rats. Typical infarct features at 7 days in controls (**E** and **F**) and BDNF-treated (**G** and **H**) rats. Note the large infarct size and the ischemic lesion composed of brain edema in the 2-day BDNF group vs the 7-day group. Original magnification × 20 (**A**, **C**, **E**, and **G**) and × 200 (**B**, **D**, **F**, and **H**).*

Copyright © Congress of Neurological Surgeons. Unauthorized reproduction of this article is prohibited.

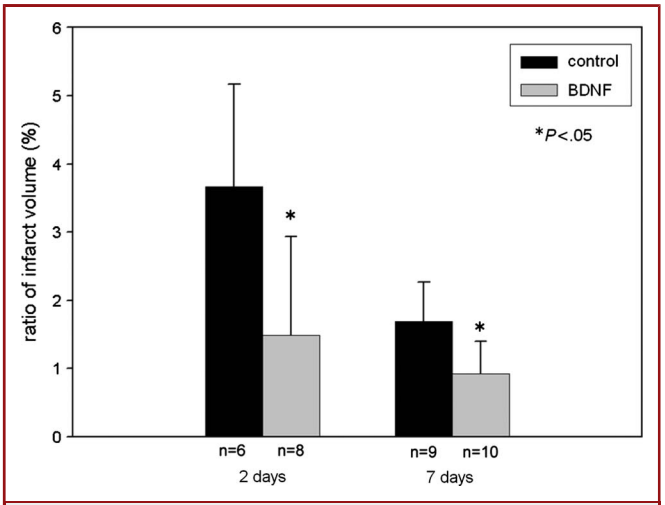

FIGURE 5. *Bar graphs comparing infarct sizes after 2 days and 7 days of 2-vein occlusion. The brain-derived neurotrophic factor (BDNF)–treated group had significantly smaller venous infarctions than the control group at both time points (P < .05, unpaired t test).*

Neuroprotective Effects of BDNF

We examined whether BDNF has neuroprotective effects in CVI similar to those demonstrated in various other brain insults. BDNF is more widely distributed throughout the central nervous system than nerve growth factor and promotes survival, differentiation, and nerve extension in many types of mammalian central nervous system neurons.[18-20] Neuroprotective effects of BDNF were observed both in vitro and in vivo after various brain insults. In cell culture, BDNF ameliorates degeneration of hippocampal neurons caused by glutamate.[21] BDNF also protects cultured dentate granule cells and hippocampal, striatal, septal, and cortical neurons against hypoglycemic insult evoked by glucose deprivation.[21-26] A reduction in the endogenous biological activity of BDNF by replacement of the coding sequence in a single allele of the BDNF gene resulted in markedly enlarged infarctions after middle cerebral artery (MCA) occlusion.[27] In addition, it is well known that BDNF is strongly associated with the pathophysiology of acute stroke and has particularly potent antiapoptotic functions. BDNF was shown to be neuroprotective after MCA occlusion, inducing suppression of apoptosis.[6,14] After hypoxia and/or ischemia, BDNF induced the extracellular signal–regulated kinase signaling pathway, counteracted the proapoptotic caspase 3 and Bax, and upregulated the antiapoptotic Bcl-2.[28,29] Although research on BDNF is making steady progress, it was still unclear whether BDNF would have similar neuroprotective efficacy in CVI. To the best of our knowledge, the present study shows for the first time that intraventricular BDNF administration was neuroprotective against CVI.

There are at least 2 possible explanations for the neuroprotective effects of BDNF in cases of cerebral arterial ischemia.

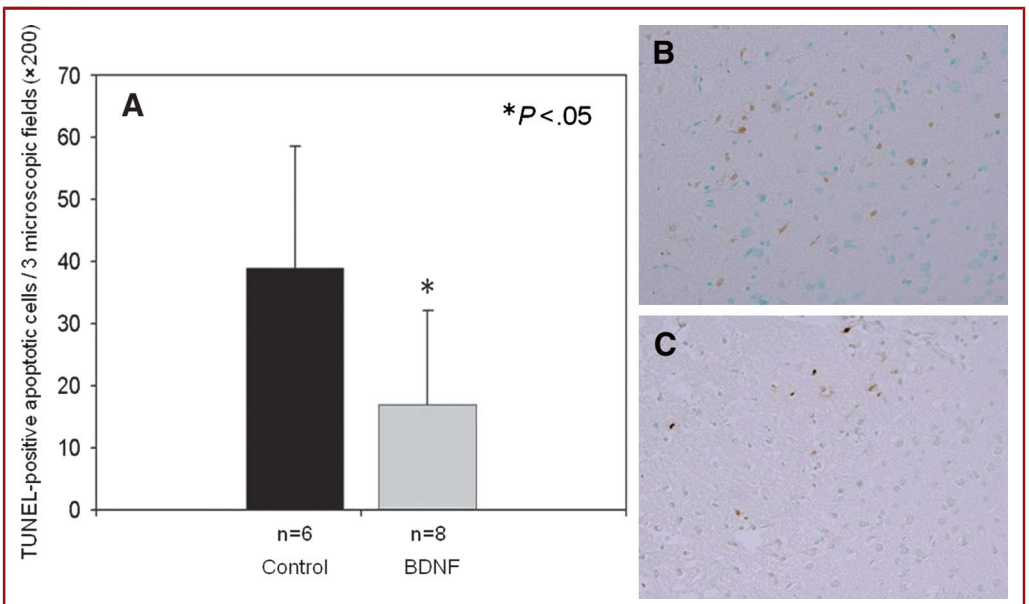

FIGURE 6. *Intraventricular brain-derived neurotrophic factor (BDNF) administration suppresses the number of terminal deoxynucleotidyl transferase–mediated deoxyuridine triphosphate nick-end labeling (TUNEL)–positive apoptotic cells after 48 hours of 2-vein occlusion.* **A**, *bar graph comparing the number of TUNEL-positive apoptotic cells. The BDNF-treated group had significantly fewer TUNEL-positive apoptotic cells than the control group (P < .05, unpaired t test).* **B** *and* **C**, *TUNEL staining assay (brown staining) in the penumbra area of control (***B***) and BDNF-treated (***C***) rats demonstrating more TUNEL-positive apoptotic cells in the control group than in the BDNF-treated group. Original magnification × 200.*

Copyright © Congress of Neurological Surgeons. Unauthorized reproduction of this article is prohibited.

One might be the prevention of apoptotic cell death confined to the penumbral border of the infarction, as evidenced by the fact that in a rat arterial stroke model, BDNF reduced expression of the proapoptotic protein Bax and counterregulated the anti-apoptotic protein Bcl-2 in the penumbra zone.[6] Another possible mechanism is the prevention of excitotoxicity.[30] BDNF protects in vitro neuronal cells against glutamate-induced neurotoxicity and the subsequent high levels of intracellular calcium.[21,24] BDNF attenuates striatal glutamate release and reduces early infarct size in the acute stage of ischemia.[31] In the present study, we demonstrated the ability of BDNF to suppress apoptotic neuronal death in the penumbral zone after CVI, but further studies are required to determine whether other mechanisms are involved in the neuroprotective effects of BDNF in CVI.

In the present experiment, we administrated BDNF intraventricularly at a rate of 2.1 μg/day. This dose of BDNF was based on its previous use for cerebral arterial ischemia[2] and was higher than that used in other studies so as to increase the potential effect of the drug. Even with this relatively high dose, no significant side effects were observed.

In another experimental study involving cerebral arterial ischemia,[14] administration of BDNF was started 1 day before cerebral arterial occlusion, but we started the intraventricular infusion just before the venous occlusion because of differences in the 2 models. It is well known that CVI usually develops much more slowly than arterial stroke. In CVI, partial interruption of regional CBF maintained for a long time causes mild ischemia. In addition, the penumbral areas with moderate reduction of CBF surrounding a core infarct in CVI are wider than those in arterial stroke.[4,32] Therefore, the therapeutic window in time and space is much wider in CVI than in arterial strokes. Therefore, starting the intraventricular administration of BDNF just before the venous occlusion in the present study was appropriate. However, the potential clinical utility of BDNF for treating CVI requires demonstration of its effectiveness after cerebral venous infarction; further studies are needed to examine the effectiveness of BDNF delivered at various times after venous occlusion.

Effect of Intraventricular BDNF on rCBF

In focal cerebral ischemia, critical rates of local blood flow determine the penumbra. This region comprises all tissues that have a reduced sufficiently CBF that its cells are at risk. One way to salvage this region from ischemia is to increase rCBF. Research on neurotrophic factors shows that their effects on CBF are still controversial. Regli et al[33] observed no changes in CBF in normal rabbits receiving intracarotid administration of basic fibroblast growth factor. Tanaka et al[34] demonstrated that intracarotid administration of basic fibroblast growth factor (100 ng) reduced infarct size after MCA occlusion as a result of increased CBF in the penumbra areas of the MCA. However, there are no reports indicating the effects of BDNF on CBF, and previous studies on cerebral arterial ischemia did not examine whether BDNF affects rCBF.[6,14] We report here that intraventricular administration of BDNF had no significant effect on rCBF, suggesting that BDNF reduces cerebral infarct not by increasing rCBF.

In this study, we assessed the effect of BDNF on rCBF using the FLPI system, recently introduced as a novel method of spatial blood flow evaluation at a uniquely high temporal resolution of image capture.[15] It provides video frame rate images of blood flow in the microvasculature up to 25 images per second. Compared with standard laser Doppler imaging, the effective sampling depth with FLPI is less and the resulting image is mainly blood flow in the microvessels of the surface layers of the tissue.[15] Because the ischemic area in the 2-vein occlusion model spreads mainly on the surface of the brain tissue, FLPI was a good choice for evaluating the effect of BDNF on rCBF.

Relationship of Infarct Volume and Brain Edema

Contrary to the findings from the MCA occlusion model that infarct volume is greatest 24 hours after the ischemic insult and smallest at 1 week,[35] in our study, the infarct volumes in both groups 7 days after venous occlusion were smaller than those observed at 2 days. These results directly demonstrate 2 features of CVI. The first is that it is greatly influenced by focal edema. Recent studies demonstrated a relationship between CVI and brain edema. Cerebral venous occlusion leads to an increase in venous and capillary pressure, and this significant dilatation of venules and capillaries without dilatation of arteries suggests that venous congestion in sinus vein occlusion occurs at the post-arterial level[36] and leads to brain tissue edema.[17] Vasogenic edema develops as a result of an increase in vascular permeability and breakdown of the blood-brain barrier,[37] and it is especially important with CVI.[13] Kimura et al[13] revealed that CVI leads to expression of vascular endothelial growth factor, which is associated with the formation of vasogenic edema in the acute stage of CVI and the inhibition of vascular endothelial growth factor–attenuated vascular permeability and reduces CVI in the acute stage.[38]

The second feature of CVI is that it progresses more slowly than cerebral arterial ischemia. In previous studies using the same model, we showed that cells in the ischemic region died of necrosis and apoptosis.[4,5] These cells died gradually, and the peak of TUNEL-positive apoptotic cells occurred 48 hours after venous occlusion.[4] Similarly, in the present study, we observed apoptotic death 2 days after venous occlusion in both the BDNF and control groups. It is also well known that mild transient focal ischemia in the rat arterial reperfusion model progresses more slowly than the normal cerebral arterial ischemia seen in the permanent occlusion model.[39] However, the mechanism by which mild transient focal ischemia occurs is intricately related to the fact that the neuronal degeneration appears in a delayed fashion after reperfusion despite recovery of blood flow.[39] Therefore, it is speculated that these 2 factors, vasogenic edema and the slow progression of CVI, led to the overestimation of infarct volume 2 days after venous occlusion in the present study.

Copyright © Congress of Neurological Surgeons. Unauthorized reproduction of this article is prohibited.

CONCLUSION

We observed for the first time that continuous intraventricular administration of BDNF protected the rat brain cortex from apoptotic changes and reduced infarct volume in a rat venous infarction model but had no effect on rCBF. We believe this finding will provide consequent benefits in the clinical treatment of CVI.

Disclosure

This work was supported by a Grant-in-Aid for Scientific Research from the Ministry of Education, Culture, Sports, Science and Technology of Japan (No. 18390402). The authors have no personal financial or institutional interest in any of the drugs, materials, or devices described in this article.

REFERENCES

1. Nakase H, Shin Y, Nakagawa I, Kimura R, Sakaki T. Clinical features of postoperative cerebral venous infarction. *Acta Neurochir (Wien)*. 2005;147(6):621-626.
2. Roberson JB Jr, Brackmann DE, Fayad JN. Complications of venous insufficiency after neurotologic-skull base surgery. *Am J Otol*. 2000;21(5):701-705.
3. Sindou M, Auque J. The intracranial venous system as a neurosurgeon's perspective. *Adv Tech Stand Neurosurg*. 2000;26:131-216.
4. Nishioka T, Nakase H, Nakamura M, Konishi N, Sakaki T. Sequential and spatial profiles of apoptosis in ischemic penumbra after two-vein occlusion in rats. *J Neurosurg*. 2006;104(6):938-944.
5. Wajima D, Nakamura M, Horiuchi K, et al. Enhanced cerebral ischemic lesions after two-vein occlusion in diabetic rats. *Brain Res*. 2009;1309:126-135.
6. Schabitz WR, Sommer C, Zoder W, Kiessling M, Schwaninger M, Schwab S. Intravenous brain-derived neurotrophic factor reduces infarct size and counterregulates Bax and Bcl-2 expression after temporary focal cerebral ischemia. *Stroke*. 2000;31(9):2212-2217.
7. Ploughman M, Windle V, MacLellan CL, White N, Dore JJ, Corbett D. Brain-derived neurotrophic factor contributes to recovery of skilled reaching after focal ischemia in rats. *Stroke*. 2009;40(4):1490-1495.
8. Schabitz WR, Steigleder T, Cooper-Kuhn CM, et al. Intravenous brain-derived neurotrophic factor enhances poststroke sensorimotor recovery and stimulates neurogenesis. *Stroke*. 2007;38(7):2165-2172.
9. Muller HD, Hanumanthiah KM, Diederich K, Schwab S, Schabitz WR, Sommer C. Brain-derived neurotrophic factor but not forced arm use improves long-term outcome after photothrombotic stroke and transiently upregulates binding densities of excitatory glutamate receptors in the rat brain. *Stroke*. 2008;39(3):1012-1021.
10. Keiner S, Witte OW, Redecker C. Immunocytochemical detection of newly generated neurons in the perilesional area of cortical infarcts after intraventricular application of brain-derived neurotrophic factor. *J Neuropathol Exp Neurol*. 2009;68(1):83-93.
11. Nakase H, Kakizaki T, Miyamoto K, Hiramatsu K, Sakaki T. Use of local cerebral blood flow monitoring to predict brain damage after disturbance to the venous circulation: cortical vein occlusion model by photochemical dye. *Neurosurgery*. 1995;37(2):280-285.
12. Clark DL, DeButte-Smith M, Colbourne F. Spontaneous temperature changes in the 2-vessel occlusion model of cerebral ischemia in rats. *Can J Physiol Pharmacol*. 2007;85(12):1263-1268.
13. Kimura R, Nakase H, Sakaki T, Taoka T, Tsuji T. Vasogenic edema and VEGF expression in a rat two-vein occlusion model. *Acta Neurochir Suppl*. 2003;86:213-217.
14. Schäbitz WR, Schwab S, Spranger M, Hacke W. Intraventricular brain-derived neurotrophic factor reduces infarct size after focal cerebral ischemia in rats. *J Cereb Blood Flow Metab*. 1997;17(5):500-506.
15. Dusch M, Schley M, Rukwied R, Schmelz M. Rapid flare development evoked by current frequency-dependent stimulation analyzed by full-field laser perfusion imaging. *Neuroreport*. 2007;18(11):1101-1105.
16. Nakase H, Heimann A, Kempski O. Local cerebral blood flow in a rat cortical vein occlusion model. *J Cereb Blood Flow Metab*. 1996;16(4):720-728.
17. Schaller B, Graf R. Cerebral ischemia and reperfusion: the pathophysiologic concept as a basis for clinical therapy. *J Cereb Blood Flow Metab*. 2004;24(4):351-371.
18. Kaplan DR, Hempstead BL, Martin-Zanca D, Chao MV, Parada LF. The trk proto-oncogene product: a signal transducing receptor for nerve growth factor. *Science*. 1991;252(5005):554-558.
19. Kaplan DR, Martin-Zanca D, Parada LF. Tyrosine phosphorylation and tyrosine kinase activity of the trk proto-oncogene product induced by NGF. *Nature*. 1991;350(6314):158-160.
20. Lamballe F, Klein R, Barbacid M. trkC, a new member of the trk family of tyrosine protein kinases, is a receptor for neurotrophin-3. *Cell*. 1991;66(5):967-979.
21. Cheng B, Mattson MP. NT-3 and BDNF protect CNS neurons against metabolic/excitotoxic insults. *Brain Res*. 1994;640(1-2):56-67.
22. Cheng B, Mattson MP. NGF and bFGF protect rat hippocampal and human cortical neurons against hypoglycemic damage by stabilizing calcium homeostasis. *Neuron*. 1991;7(6):1031-1041.
23. Kokaia Z, Zhao Q, Kokaia M, et al. Regulation of brain-derived neurotrophic factor gene expression after transient middle cerebral artery occlusion with and without brain damage. *Exp Neurol*. 1995;136(1):73-88.
24. Lindholm D, Dechant G, Heisenberg CP, Thoenen H. Brain-derived neurotrophic factor is a survival factor for cultured rat cerebellar granule neurons and protects them against glutamate-induced neurotoxicity. *Eur J Neurosci*. 1993;5(11):1455-1464.
25. Nakao N, Kokaia Z, Odin P, Lindvall O. Protective effects of BDNF and NT-3 but not PDGF against hypoglycemic injury to cultured striatal neurons. *Exp Neurol*. 1995;131(1):1-10.
26. Shimohama S, Tamura Y, Akaike A, et al. Brain-derived neurotrophic factor pretreatment exerts a partially protective effect against glutamate-induced neurotoxicity in cultured rat cortical neurons. *Neurosci Lett*. 1993;164(1-2):55-58.
27. Endres M, Fan G, Hirt L, Jaenisch R. Stroke damage in mice after knocking the neutrophin-4 gene into the brain-derived neurotrophic factor locus. *J Cereb Blood Flow Metab*. 2003;23(2):150-153.
28. Schabitz WR, Berger C, Kollmar R, et al. Effect of brain-derived neurotrophic factor treatment and forced arm use on functional motor recovery after small cortical ischemia. *Stroke*. 2004;35(4):992-997.
29. Han BH, Holtzman DM. BDNF protects the neonatal brain from hypoxic-ischemic injury in vivo via the ERK pathway. *J Neurosci*. 2000;20(15):5775-5781.
30. Mattson MP, Murrain M, Guthrie PB, Kater SB. Fibroblast growth factor and glutamate: opposing roles in the generation and degeneration of hippocampal neuroarchitecture. *J Neurosci*. 1989;9(11):3728-3740.
31. Berger C, Schabitz WR, Wolf M, Mueller H, Sommer C, Schwab S. Hypothermia and brain-derived neurotrophic factor reduce glutamate synergistically in acute stroke. *Exp Neurol*. 2004;185(2):305-312.
32. Otsuka H, Ueda K, Heimann A, Kempski O. Effects of cortical spreading depression on cortical blood flow, impedance, DC potential, and infarct size in a rat venous infarct model. *Exp Neurol*. 2000;162(1):201-214.
33. Regli L, Anderson RE, Meyer FB. Basic fibroblast growth factor increases cortical blood flow in vivo. *Brain Res*. 1994;665(1):155-157.
34. Tanaka R, Miyasaka Y, Yada K, Ohwada T, Kameya T. Basic fibroblast growth factor increases regional cerebral blood flow and reduces infarct size after experimental ischemia in a rat model. *Stroke*. 1995;26(11):2154-2158.
35. Lin TN, He YY, Wu G, Khan M, Hsu CY. Effect of brain edema on infarct volume in a focal cerebral ischemia model in rats. *Stroke*. 1993;24(1):117-121.
36. Ueda K, Nakase H, Miyamoto K, Otsuka H, Sakaki T. Impact of anatomical difference of the cerebral venous system on microcirculation in a gerbil superior sagittal sinus occlusion model. *Acta Neurochir (Wien)*. 2000;142(1):75-82.
37. Go KG. The normal and pathological physiology of brain water. *Adv Tech Stand Neurosurg*. 1997;23:47-142.
38. Kimura R, Nakase H, Tamaki R, Sakaki T. Vascular endothelial growth factor antagonist reduces brain edema formation and venous infarction. *Stroke*. 2005;36(6):1259-1263.
39. Du C, Hu R, Csernansky CA, Hsu CY, Choi DW. Very delayed infarction after mild focal cerebral ischemia: a role for apoptosis? *J Cereb Blood Flow Metab*. 1996;16(2):195-201.

Copyright © Congress of Neurological Surgeons. Unauthorized reproduction of this article is prohibited.

Thrombospondin-1 Modulates the Angiogenic Phenotype of Human Cerebral Arteriovenous Malformation Endothelial Cells

Christopher J. Stapleton, BS*§
Don L. Armstrong, PhD*
Raphael Zidovetzki, PhD¶
Charles Y. Liu, MD, PhD*‖
Steven L. Giannotta, MD*
Florence M. Hofman, PhD*‡

Departments of *Neurological Surgery and ‡Pathology, Keck School of Medicine, University of Southern California, Los Angeles, California; §Harvard-MIT Division of Health Sciences and Technology, Harvard Medical School, Boston, Massachusetts; ¶Department of Cell Biology and Neuroscience, University of California, Riverside, California; ‖Division of Chemistry and Chemical Engineering, California Institute of Technology, Pasadena, California

Correspondence:
Florence M. Hofman, PhD,
Departments of Pathology and Neurological Surgery,
Keck School of Medicine,
University of Southern California,
2011 Zonal Avenue,
Hoffman Medical Research Building 315,
Los Angeles, CA 90033.
E-mail: hofman@usc.edu

Received, May 18, 2010.
Accepted, October 4, 2010.

Copyright © 2011 by the
Congress of Neurological Surgeons

BACKGROUND: The management of cerebral arteriovenous malformation (AVM) is challenging, and invasive therapies place vital intracranial structures at risk of injury. The development of noninvasive, pharmacologic approaches relies on identifying factors that mediate key angiogenic processes. Previous studies indicate that endothelial cells (ECs) derived from cerebral AVM (AVM-ECs) are distinct from control brain ECs with regard to important angiogenic characteristics.

OBJECTIVE: To determine whether thrombospondin-1 (TSP-1), a potent angiostatic factor, regulates critical angiogenic features of AVM-ECs and to identify factors that modulate TSP-1 production in AVM-ECs.

METHODS: EC proliferation, migration, and tubule formation were evaluated with bromodeoxyuridine incorporation, Boyden chamber, and Matrigel studies, respectively. TSP-1 and inhibitor of DNA binding/differentiation 1 (Id1) mRNA levels were quantified with microarray and quantitative real-time polymerase chain reaction analyses. TSP-1 protein expression was measured using Western blotting, immunohistochemical, and enzyme-linked immunosorbent assay techniques. The mechanistic link between Id1 and TSP-1 was established through small interfering RNA–mediated knockdown of Id1 in AVM-ECs followed by Western blot and enzyme-linked immunosorbent assay experiments assessing TSP-1 production.

RESULTS: AVM-ECs proliferate faster, migrate more quickly, and form disorganized tubules compared with brain ECs. TSP-1 is significantly down-regulated in AVM-ECs. The addition of TSP-1 to AVM-EC cultures normalizes the rate of proliferation and migration and the efficiency of tubule formation, whereas brain ECs are unaffected. Id1 negatively regulates TSP-1 expression in AVM-ECs.

CONCLUSION: These data highlight a novel role for TSP-1 in the pathobiology of AVM angiogenesis and provide a context for its use in the clinical management of brain AVMs.

KEY WORDS: Angiogenesis, Cerebral arteriovenous malformations, Endothelium, Inhibitor of DNA binding/differentiation 1, Thrombospondin-1

Neurosurgery 68:1342–1353, 2011 DOI: 10.1227/NEU.0b013e31820c0a68 www.neurosurgery-online.com

ABBREVIATIONS: AVM, arteriovenous malformation; **AVM-ECs**, endothelial cells derived from cerebral arteriovenous malformation; **BEC**, brain endothelial cell; **EC**, endothelial cell; **ELISA**, enzyme-linked immunosorbent assay; **ET-1**, endothelin-1; **FDR**, false discovery rate; **GAPDH**, glyceraldehyde-3-phosphate dehydrogenase; **Id1**, inhibitor of DNA binding/differentiation 1; **IL-8**, interleukin-8; **PBS**, phosphate-buffered saline; **TGF-β**, transforming growth factor-β; **TSP-1**, thrombospondin-1; **VEGF**, vascular endothelial growth factor

Cerebral arteriovenous malformations (AVMs) consist of a conglomerate of tortuous, dysplastic blood vessels (nidus) that lack traditional capillary beds and vascular organization at the subarteriolar level. Often surrounded by gliotic brain parenchyma, AVMs are characterized by pathologic shunting between their system of associated feeding arteries and draining veins. Considered a congenital lesion, approximately 0.001% to 0.52% of the general population have a brain AVM.[1] Patients most commonly present with symptoms secondary to

Copyright © Congress of Neurological Surgeons. Unauthorized reproduction of this article is prohibited.

hemorrhage (42%-72%), although seizures and complications of mass effect and steal phenomenon are not infrequently seen.[1,2] Current therapies are open microsurgery, embolization, and stereotactic radiosurgery, and the modality used depends on the location, size, and venous drainage of the lesion. The neurosurgical management is complex and challenging, and despite the advent of minimally invasive techniques, the treatment of brain AVMs still poses a significant risk to nearby eloquent cortical, subcortical, and neurovascular structures.[3,4]

With the increasing availability of advanced noninvasive imaging techniques, the population of patients with an unruptured AVM is steadily increasing, and several studies estimate that unruptured lesions outnumber their ruptured counterparts by at least twofold.[5,6] Recent data pertaining to the natural history of cerebral AVMs suggest that patients who undergo prophylactic invasive treatment of unruptured lesions fare worse in the long term than those who receive medical management alone.[6,7] In addition, AVM hemorrhage facilitates surgical resection because hematoma formation often creates a workable space between normal brain tissue and the dysplastic vascular structures.[8] In fact, a new brain AVM grading system designed to supplement the traditional Spetzler-Martin scale includes an unruptured presentation as an independent predictor of poor postoperative neurologic outcome.[9,10] The treatment of unruptured AVMs, therefore, is especially onerous, and ARUBA (A Randomized Trial of Unruptured Brain Arteriovenous Malformations) is currently investigating the optimal management for such lesions.[11] Undoubtedly, future therapies for both ruptured and unruptured cerebral AVMs will favor advanced minimally invasive techniques and pharmacologic approaches.

Previous research into the pathobiology of brain AVMs focused on the abnormal expression patterns of numerous factors involved in regulating angiogenesis.[12-17] Although these reports offer invaluable insight into the molecular underpinnings of cerebral AVMs, the studies were often performed on whole AVM tissue, which contains numerous cell types. As a result, it is difficult to ascertain specifically which cell type(s) is dysfunctional. Previous work from this laboratory described several abnormal angiogenic properties of endothelial cells (ECs) derived from cerebral AVM (AVM-ECs) when compared with control brain ECs (BECs).[18] To further delineate the molecular aberrations present in AVM-ECs, we performed gene microarray analyses and found that the expression of thrombospondin-1 (TSP-1), an endogenous angiostatic factor, was significantly dysregulated in AVM-ECs. TSP-1 is a large matricellular glycoprotein involved in a variety of biological processes, including angiogenesis, inflammation, hemostasis and thrombosis, and neuronal synaptogenesis and synaptic plasticity.[19-23] Furthermore, the role of TSP-1 in tumor biology has been described extensively,[21,24,25] and clinical reports indicate that low intratumoral TSP-1 levels predict poor clinical outcomes.[26,27] Synthesized predominantly by ECs, fibroblasts, and smooth muscle cells, TSP-1 directly inhibits the angiogenic activity of vascular endothelial growth factor (VEGF), basic fibroblast growth factor, and interleukin-8 (IL-8) and alters cell adhesion, proliferation, and migration.[21-23]

Despite a robust literature on the importance of TSP-1 in tumor angiogenesis, its role in the pathobiology of cerebral AVMs remains unknown. In the current study, we demonstrate that TSP-1 is significantly down-regulated at the mRNA and protein levels in AVM-ECs compared with control BECs. In addition, reconstitution of TSP-1 to AVM-EC cultures normalizes important abnormal angiogenic functions. Finally, we identify a critical role for the inhibitor of DNA binding/differentiation 1 (Id1), a transcriptional repressor of TSP-1 production,[28] in the regulation of TSP-1 expression in AVM-ECs. Taken together, these data offer a unique insight into the molecular pathobiology of AVM-ECs and provide a context for the potential role of TSP-1 in the clinical management of brain AVMs.

MATERIALS AND METHODS

EC Isolation and Culture

Surgical specimens were obtained and handled in accordance with guidelines set forth by the Institutional Review Board at the Keck School of Medicine, University of Southern California. AVM-ECs were isolated from surgical specimens from 7 patients who underwent microsurgical AVM resection (Table) and control BECs were derived from structurally normal cortex from 9 patients who underwent temporal lobectomy for intractable epilepsy. Tissue specimens were gently homogenized and microvessels were isolated on a 30% dextran gradient followed by enzymatic dissociation with collagenase/dispase. For AVM-ECs, distinctions between vein, artery, and nidus were not made. ECs were cultured in RPMI 1640 growth media (Mediatech Inc., Manassas, Virginia) supplemented with 100 ng/mL EC growth supplement (Millipore, Temecula, California), 2 mmol/L L-glutamine (Invitrogen Corp., Carlsbad, California), 10 mmol/L *N*-2-hydroxyethylpiperazine-*N*-2-ethanesulfonic acid (Invitrogen), 24 mmol/L sodium pyruvate (Invitrogen), 300 U heparin (Sigma-Aldrich, St. Louis, Missouri), 1× MEM (minimal essential medium) vitamin solution (Invitrogen), 1× MEM nonessential amino acids (Mediatech Inc.), 1% penicillin/streptomycin (Invitrogen), and 10% fetal calf serum (Omega Scientific Inc., Tarzana, California). Once grown to 80% confluency, the cells were labeled with 10 μg/mL Dil-Ac-LDL (Biomedical Technologies Inc., Stoughton, Massachusetts) and purified by fluorescence-activated cell sorting. The purity of control BECs and AVM-ECs was confirmed by positive immunohistochemical staining for the endothelial cell markers CD31/platelet-EC adhesion molecule-1 (Santa Cruz Biotechnology Inc., Santa Cruz, California) and von Willebrand factor (Dako North America Inc., Carpinteria, California) and negative staining for glial fibrillary acidic protein (Chemicon International Inc., Temecula, California) and smooth muscle actin (Vector Laboratories, Burlingame, California) (data not shown). For all experiments, cells were cultured in complete RPMI 1640 growth media without EC growth supplement in a 37°C incubator with 5% CO_2. Only ECs between passages 3 through 5 were used. Unless otherwise noted, all ECs were grown on 1% gelatin-coated surfaces. All images were captured using Canon EOS Rebel XSi (Lake Success, New York) or Nikon Coolpix P1 (Tokyo, Japan) digital cameras mounted to Olympus BH-2 and Nikon TMS microscopes.

Gene Microarray

Cells were seeded at a density of 5×10^5 per 10-cm dish and grown for 48 hours. Total RNA was isolated using the RNeasy Plus Mini Kit (Qiagen Inc., Valencia, California) according to the manufacturer's instructions. Total RNA quantity and quality were assessed using an Agilent 2100 Bioanalyzer (Agilent Technologies Inc., Santa Clara, California). The RNA

Copyright © Congress of Neurological Surgeons. Unauthorized reproduction of this article is prohibited.

TABLE. Summary of Patient Clinical Characteristics[a]

Patient	Age, y/Sex	Presenting Symptom(s)	Location of Pathology	History of Hemorrhage	No. of Embolizations	Spetzler-Martin Score
AVM 1	42/F	HA	L occipital lobe	Yes	5	2
AVM 2	22/M	Seizures	L frontal lobe	No	4	3
AVM 3	26/F	HA	R parietal lobe	No	3	1
AVM 4	35/F	HA, seizures	L frontal lobe	No	3	2
AVM 5	22/M	HA	R temporal lobe	Yes	0	3
AVM 6	28/M	HA, seizures	R frontal lobe	Yes	0	1
AVM 7	22/F	HA	R occipital lobe	Yes	1	1

[a]AVM, arteriovenous malformation; HA, headache; L, left; R, right.

duplicate with the highest quality was reverse-transcribed and hybridized with an Affymetrix HU133 Plus 2.0 (Affymetrix Inc., Santa Clara, California) microarray system. Probe pair intensities were extracted using the statistical software package R (R Foundation for Statistical Computing, Vienna, Austria), and normalized using the MvA kernel density method. *P* values were calculated using the Student *t* test modified with a Bayesian prior.[29] The Storey q-value procedure,[30] an estimate of the false discovery rate (FDR), was used to correct for multiple testing. An FDR <0.05 was considered statistically significant.

Western Blot

Cells were seeded at a density of 5×10^5 per 10-cm dish and grown for 48 hours. Total protein was extracted with radioimmunoprecipitation assay buffer supplemented with 1 mM phenylmethylsulfonyl fluoride (Sigma-Aldrich), 1× Halt Protease Inhibitor Cocktail (Thermo Fisher Scientific Inc., Rockford, Illinois), and 1× Phosphatase Inhibitor Cocktail 1 (Sigma-Aldrich). Total protein was quantified using the bicinchoninic acid Protein Assay Kit (Thermo Fisher Scientific). Equal amounts of protein were separated by sodium dodecylsulfate polyacrylamide gel electrophoresis and electrotransferred to 0.45-μm nitrocellulose membranes. The membranes were blocked with SEA BLOCK (Thermo Fisher Scientific), probed with anti-TSP-1 (R&D Systems Inc., Minneapolis, Minnesota) or anti–glyceraldehyde-3-phosphate dehydrogenase (GAPDH) (Santa Cruz Biotechnology) polyclonal antibodies, and incubated with the appropriate fluorescent secondary antibodies (Thermo Fisher Scientific). Protein bands were detected by Odyssey infrared imaging (LI-COR Biosciences, Lincoln, Nebraska) and densitometric studies were performed using ImageJ (National Institutes of Health, Bethesda, Maryland). GAPDH levels were measured for internal standardization.

Enzyme-Linked Immunosorbent Assay (ELISA)

Cells were seeded at a density of 6×10^4 per well in 6-well plates and grown for 48 hours. Recombinant human TSP-1 (1000 ng/mL; R&D Systems) or vehicle control (phosphate-buffered saline [PBS]) was added as appropriate. Supernatants were collected and filtered through a 0.2-μm cellulose acetate membrane (VWR International, West Chester, Pennsylvania) and analyzed for TSP-1 (R&D Systems), VEGF (Invitrogen), IL-8 (Invitrogen), and endothelin-1 (ET-1) (R&D Systems) content using commercially available ELISA kits per the manufacturers' instructions.

Immunohistochemistry

Cytocentrifuge cell preparations (1×10^5 cells/mL) and cryostat-sectioned tissues (8 μm) were fixed in acetone, blocked with SEA BLOCK (Thermo Fisher Scientific), and probed with anti-TSP-1 or anti–von Willebrand factor polyclonal antibodies. The samples were incubated with biotinylated secondary antibodies (Vector Laboratories) and coupled to avidin using the VECTASTAIN Elite ABC System (Vector Laboratories). Cell and tissue preparations were then stained with 3-amino-9-ethylcarbazole substrate (Sigma-Aldrich), which resulted in a red precipitate at the site of antigen-antibody complex formation. Specimens were counterstained with hematoxylin (Sigma-Aldrich).

Cell Proliferation Assay

Cells were seeded at a density of 3×10^3 per well in 96-well plates and grown for 12, 24, or 48 hours. TSP-1 (100, 500, or 1000 ng/mL) or vehicle control (PBS) was added as appropriate. The bromodeoxyuridine cell proliferation assay (Roche Diagnostics Corp., Indianapolis, Indiana) was conducted according to the manufacturer's instructions. For cell death analyses, cells were seeded at a density of 6×10^4 per well in 6-well plates and grown for 12, 24, or 48 hours. TSP-1 (1000 ng/mL) or vehicle control (PBS) was added as appropriate. At the designated time points, cells were treated with trypan blue (Sigma-Aldrich) and the numbers of dead (blue) and viable cells were counted using a standard hemacytometer.

Migration Assay

Cells were seeded at a density of 4×10^4 per modified transwell Boyden chamber (BD BioCoat, Bedford, Massachusetts). Each chamber housed a 6.5-mm diameter polyethylene terephthalate filter with 8-μm pores coated with 0.5% gelatin. Migration was stimulated by adding complete growth media to the lower compartment of the experimental apparatus; TSP-1 (1000 ng/mL) or vehicle control (PBS) was added as appropriate. After 6 hours, the filters were fixed and stained with Harleco Hemacolor staining solution (EMD Chemicals, Gibbstown, New Jersey). Cells that migrated to the underside of the filter were quantified under high-power magnification (×400). A 6-hour migration period was used to eliminate the effect of disparate rates of cell proliferation.

Tubule Formation Assay

Cells were seeded at a density of 1.5×10^4 per well onto 96-well plates coated with growth factor-reduced Matrigel (BD Biosciences). TSP-1 (1000 ng/mL) or vehicle control (PBS) was added as appropriate. After 12 hours, 3 to 5 images (magnification, ×100) per sample were captured of regions randomly selected throughout the area of tube formation. Relative tubule length was quantified using ImageJ. To determine tubule

Copyright © Congress of Neurological Surgeons. Unauthorized reproduction of this article is prohibited.

formation efficiency, the total number of completed tubelike structures was compared with the total number of tubule branches or sprouts.[31]

Small Interfering RNA Transfection and Quantitative Real-Time Polymerase Chain Reaction

Cells were seeded at a density of 6×10^4 per well in 6-well plates and transfected with small interfering Id1 (Ambion Inc., Austin, Texas) or small interfering control (Santa Cruz Biotechnology) constructs using the Lipofectamine 2000 Transfection Reagent (Invitrogen) per the manufacturer's instructions. After 48 hours, whole-cell lysates and cell culture supernatants were collected as described earlier for Western blot and ELISA analyses, respectively. Knockdown of Id1 was confirmed by quantitative real-time polymerase chain reaction using the SYBR GreenER Reagent System (Invitrogen) on a Stratagene Mx3000P Bioanalyzer (Agilent Technologies). GAPDH was measured for sample normalization. The forward and reverse primers for Id1 were 5′-GCCGAGGCGGCATGCGTTC-3′ and 5′-TCCCTCAGATCCGGCGAGGC-3′, respectively.

Statistical Analyses

Data analysis was performed with the statistical software package PRISM (GraphPad, San Diego, California). Data are presented as mean ± standard error of the mean. Multigroup comparisons were made using 1-way analysis of variance with post hoc Bonferroni or Dunnett test. Comparisons between 2 groups were performed with the unpaired Student *t* test. A value of $P < .05$ was considered significant.

RESULTS

TSP-1 Is Differentially Expressed Between AVM-ECs and BECs

Previous reports from our laboratory indicate that AVM-ECs display abnormal angiogenic properties compared with control BECs.[18] To determine the molecular basis for these observed differences, we performed gene microarray analyses to identify potential targets of interest. The expression of TSP-1, a critical regulator of physiologic and pathologic angiogenesis, was 13.2-fold (FDR <0.05) lower in AVM-ECs compared with control BECs (Figure 1A). To validate that this decrease in mRNA expression correlated with functional protein levels, we conducted Western blot, immunohistochemical, and ELISA studies. Western blotting demonstrated that AVM-ECs produce 10-fold ($P < .01$) less intracellular TSP-1 protein than BECs (Figure 1B), and immunohistochemistry showed qualitatively similar findings (Figure 1C). In addition, analysis of cell culture supernatants by ELISA indicated that AVM-ECs secrete 3.8-fold less TSP-1 into the extracellular environment than control BECs (314 ± 130 vs 1204 ± 223 ng/mL/10^5 cells, $P < .05$) (Figure 1D). To determine whether this decrease in TSP-1 expression was observed in situ and not secondary to cell culture conditions, we performed immunohistochemical studies on fresh-frozen whole AVM and normal human brain tissues. The endothelial layer of both cerebral AVM and normal brain tissues exhibited similar levels of von Willebrand factor staining. By contrast, ECs in the normal human brain sections expressed greater amounts of TSP-1 protein than ECs of the cerebral AVM specimens (Figure 2). These data indicate that a reduced level of TSP-1 expression is an inherent property of AVM-ECs.

TSP-1 Does Not Alter the Expression of VEGF, IL-8, or ET-1 in AVM-ECs

VEGF, IL-8, and ET-1 are important proangiogenic growth factors. Previous research suggests that the expression of these factors is differentially regulated between cerebral AVM and normal human brain.[12,13,18,32,33] Given the observed lack of TSP-1 production by AVM-ECs compared with control BECs, we asked whether treatment of AVM-ECs with exogenous TSP-1 could alter the expression profiles of VEGF, IL-8, and ET-1. We performed ELISAs on AVM-EC culture supernatants treated with vehicle control or recombinant TSP-1 (1000 ng/mL). At 48 hours, there was no significant difference in the secretion patterns of VEGF (124.6 ± 4.2 vs 151.9 ± 27.5 pg/mL/10^5 cells, $P = .43$), IL-8 (215.9 ± 34.4 vs 220.0 ± 67.5 pg/mL/10^5 cells, $P = .96$), or ET-1 (54.3 ± 17.8 vs 59.0 ± 20.4 pg/mL/10^5 cells, $P = .88$) for vehicle- and TSP-1-treated AVM-ECs (Figure 3).

TSP-1 Normalizes the Aberrant Angiogenic Functions of AVM-ECs

The formation of new blood vessels and stable vascular networks requires coordinated EC proliferation, migration, and 3-dimensional tube formation. These processes occur under the guidance of EC-derived growth factors and regulatory proteins present in the surrounding extracellular matrix. To clarify the relevant functional differences distinguishing AVM-ECs from control BECs, we conducted in vitro cell proliferation, migration, and tubule formation assays to determine whether reconstitution of TSP-1 to AVM-EC cultures could normalize their activated angiogenic phenotype.

To assess the baseline rate of AVM-EC and BEC proliferation, we performed bromodeoxyuridine incorporation studies. AVM-ECs proliferated 7 ± 7.2%, 46 ± 5.2% ($P < .05$), and 28 ± 8.4% ($P < .05$) faster than control BECs at 12, 24, and 48 hours, respectively (Figure 4A). The addition of TSP-1 (1000 ng/mL) reduced AVM-EC proliferation by 16 ± 1.7% ($P < .01$) at 48 hours, whereas BEC proliferation was unaffected (Figure 4B). To ensure that this differential response to exogenous TSP-1 treatment was not solely attributable to preferential AVM-EC death, we conducted cell death assays using the trypan blue exclusion method. After treatment with TSP-1 (1000 ng/mL) for 12, 24, and 48 hours, the percentage of cell death in AVM-EC and BEC cultures was equal in vehicle- and TSP-1-treated groups (Figure 4C).

EC migration is a critical component of new blood vessel formation. As the ECs proliferate, they must migrate into the surrounding matrix to form vascular networks. AVM-EC and BEC migration was analyzed via the modified transwell Boyden chamber method (Figure 5A). At baseline, AVM-ECs migrated 50% more quickly than BECs over a 6-hour period (35.6 ± 1.6 vs 23.7 ± 2.9 cells per high-power field; $P < .05$). Treatment

Copyright © Congress of Neurological Surgeons. Unauthorized reproduction of this article is prohibited.

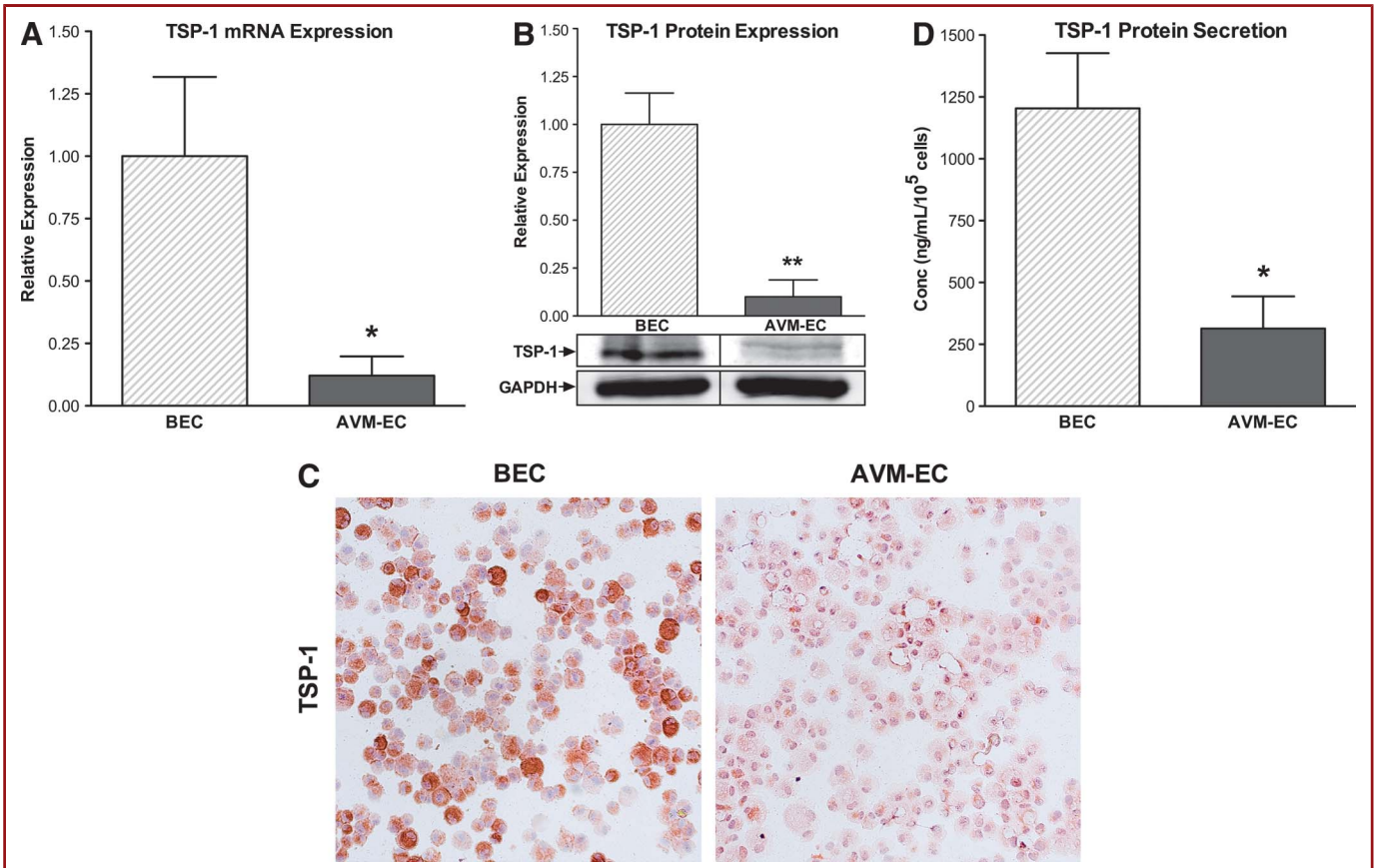

FIGURE 1. *Thrombospondin-1 (TSP-1) is differentially expressed between arteriovenous malformation endothelial cells (AVM-ECs) and brain endothelial cells (BECs). Gene microarray (A) and Western blot (B) analyses show that AVM-ECs express 13.2-fold less mRNA and 10-fold less intracellular protein, respectively, than control BECs. C, immunohistochemical staining of AVM-ECs and BECs for TSP-1 qualitatively demonstrates a similar degree of differential expression. D, quantitative enzyme-linked immunosorbent assay indicates that AVM-ECs secrete 3.8-fold less TSP-1 into the extracellular environment than BECs. Magnification, ×100. *P < .05, **P < .01. GAPDH, glyceraldehyde-3-phosphate dehydrogenase.*

with TSP-1 (1000 ng/mL) reduced AVM-EC migration by 38.2% (35.6 ± 1.6 vs 22.0 ± 0.3 cells per high-power field; $P < .01$), whereas BEC migration did not change over the 6-hour period (23.7 ± 2.9 vs 22.4 ± 1.3 cells per high-power field; $P = .71$) (Figure 5B).

In addition to coordinated cell proliferation and migration, the ability of ECs to form functional tubes is a hallmark of neovascularization. To assess the ability of AVM-ECs and BECs to form efficient tubelike structures, we performed tubule formation assays in growth factor–reduced Matrigel. Tubule length and tubule formation efficiency were evaluated at 12 hours (Figure 6A). At baseline, AVM-ECs formed tubules that were 37.7 ± 4.9% shorter ($P < .05$) than those formed by BECs. The addition of TSP-1 (1000 ng/mL) increased AVM-EC tubule length by 23.5 ± 5.2% ($P < .05$), whereas BEC tubule length remained relatively constant (Figure 6B). To quantify tubule formation efficiency, we calculated the ratio of complete, uninterrupted tubelike structures to the total number of tubule branches or sprouts. AVM-ECs formed tubules with an efficiency of 68 ± 3.5%, whereas 88 ± 1.2% of BEC tubule sprouts resulted in unabridged tubule structures ($P < .01$). With exogenous TSP-1 (1000 ng/mL), the tubule formation efficiency of AVM-ECs increased to 84 ± 3% ($P < .01$), whereas the efficiency of BEC tubule formation remained constant (Figure 6C).

Taken together, these data suggest that AVM-ECs are functionally distinct from control BECs with respect to essential angiogenic functions. Although exogenous TSP-1 did not alter AVM-EC secretion of VEGF, IL-8, or ET-1, TSP-1 did correct the observed functional aberrations of our brain AVM-ECs. Therefore, TSP-1 mediates critical cellular processes irrespective of proangiogenic growth factor levels.

Copyright © Congress of Neurological Surgeons. Unauthorized reproduction of this article is prohibited.

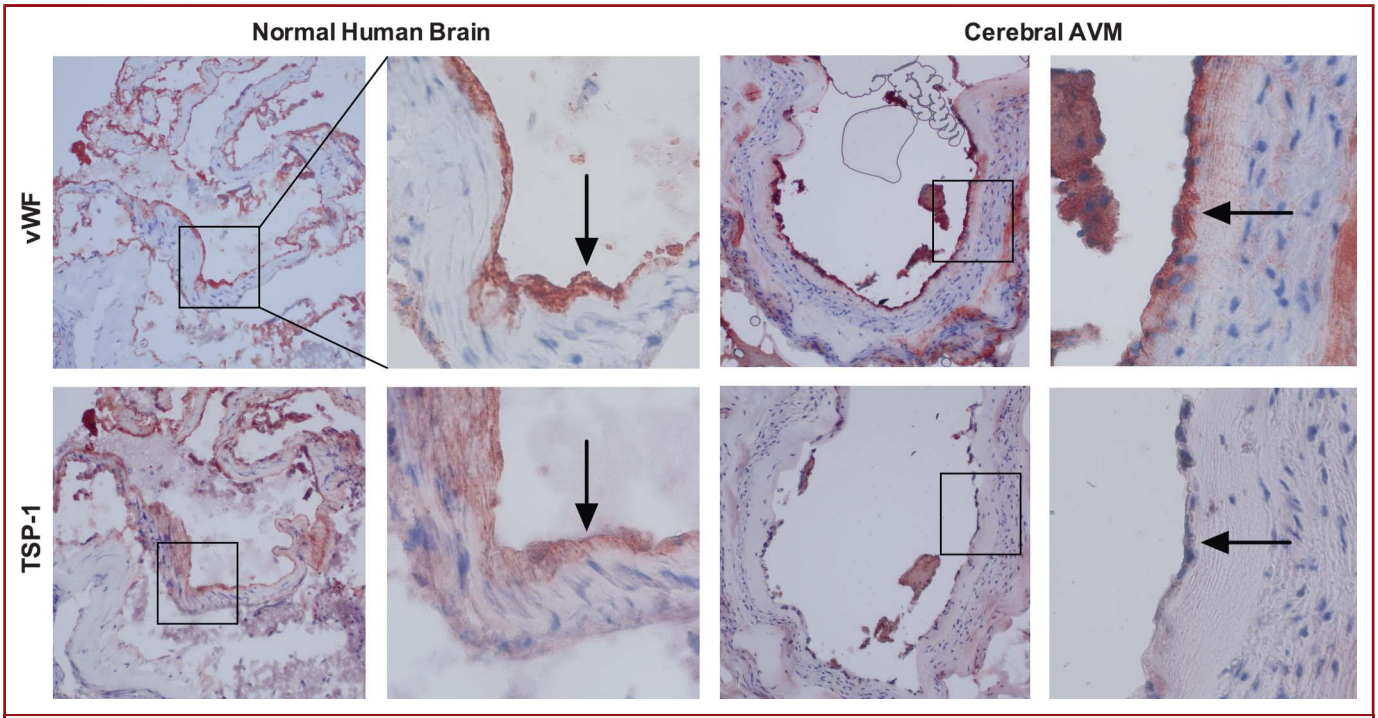

FIGURE 2. *Thrombospondin-1 (TSP-1) is differentially expressed between endothelial cells of cerebral arteriovenous malformation (AVM) and normal human brain tissue in situ. The endothelial layer (arrows) of cerebral AVMs and normal brain tissue is denoted by positive von Willebrand factor (vWF) immunostaining. Endothelial cells of cerebral AVM tissue express qualitatively less TSP-1 protein than endothelial cells of normal human brain specimens. Original magnification, ×100; zoom magnification, ×400.*

Id1 Regulates TSP-1 Expression in AVM-ECs

Because our ultimate aim is to develop targeted therapeutics for cerebral AVMs, we next investigated the molecular factors that regulate TSP-1 expression. Data from our gene microarray indicated that Id1, a transcriptional repressor of TSP-1, was up-regulated 25.2-fold (FDR <0.05) in AVM-ECs compared with control BECs (Figure 7A), and quantitative real-time polymerase chain reaction analysis confirmed this finding (data not shown). To establish the mechanistic importance of Id1 in regulating TSP-1 expression in AVM-ECs, we performed small interfering RNA–mediated knockdown of Id1 and subsequently analyzed TSP-1 production with Western blot and ELISA experiments. Western blotting demonstrated that Id1 knockdown (120 nM) increases TSP-1 expression 11.2-fold ($P < .05$) (Figure 7B). To determine whether this increase in production augmented secretion of TSP-1 protein, we performed ELISAs on cell culture supernatants. Treatment of AVM-ECs with 60, 120, and 240 nM of small interfering Id1 increased TSP-1 secretion by 1.3-, 1.5- ($P < .05$), and 2.5-fold ($P < .01$), respectively, compared with small interfering control-treated samples (Figure 7C). These results confirm that Id1 is a potent inhibitor of TSP-1 production and identify a unique role for Id1 in brain AVM pathogenesis.

DISCUSSION

In this study, we define a role for TSP-1 in modulating the angiogenic phenotype of ECs derived from human brain AVMs. Through detailed mRNA and protein studies, we provide evidence that TSP-1 is significantly underexpressed by AVM-ECs compared with control BECs. Moreover, our immunohistochemical analyses on whole cerebral AVM and normal human brain tissue show that underexpression of TSP-1 is an inherent property of AVM-ECs. Although the origin of TSP-1 dysregulation in AVM-ECs is multifold in nature, our gene microarray demonstrated that Id1, a transcriptional repressor of TSP-1 expression, was significantly overexpressed in AVM-ECs. Through small interfering RNA–mediated knockdown of Id1 production, we demonstrate that Id1 is an important inhibitor of TSP-1 expression in AVM-ECs. Furthermore, AVM-ECs are functionally distinct from control BECs and possess the phenotype of ECs in dysregulated angiogenesis. Reconstitution of TSP-1 to AVM-ECs cultures normalizes the rate of cell proliferation and migration and the length and efficiency of AVM-EC tubule formation to levels similar to those of control BECs. Despite the important role that proangiogenic factors play in regulating neovascularization, the TSP-1–induced changes in AVM-EC

Copyright © Congress of Neurological Surgeons. Unauthorized reproduction of this article is prohibited.

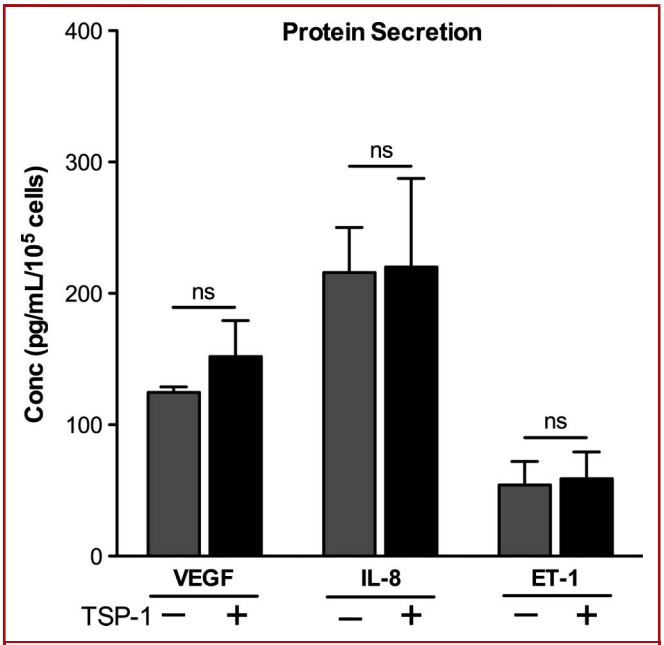

FIGURE 3. *Thrombospondin-1 (TSP-1) does not alter the expression patterns of vascular endothelial growth factor (VEGF), interleukin-8 (IL-8), or endothelin-1(ET-1). Quantitative enzyme-linked immunosorbent assays indicate that treatment of arteriovenous malformation endothelial cells with TSP-1 for 48 hours does not significantly affect levels of secreted VEGF, IL-8, or ET-1. Conc, concentration; ns, not significant.*

function are not explained by altered expression patterns of VEGF, IL-8, or ET-1, suggesting that TSP-1 operates through direct cellular pathways. Although many reports have described the importance of TSP-1 in tumor growth and angiogenesis, this is the first study to systematically define a role for TSP-1 in modulating the dysregulated angiogenic phenotype of AVM-ECs and to implicate Id1 as being an important regulator of TSP-1 expression in brain AVMs.

Previous research indicates that TSP-1 modifies various phases of new blood vessel formation, including EC proliferation and apoptosis, adhesion, migration, and 3-dimensional tubule formation.[21-23,34] Our data demonstrate that treatment of AVM-EC and BEC cultures with TSP-1 selectively decreases the rate of AVM-EC proliferation without comparatively increasing the rate of cell death. Cellular analyses suggest that TSP-1 can alter EC proliferation and survival through both apoptotic and non-apoptotic mechanisms. Acting through the cell-surface receptor CD36,[35,36] TSP-1 activates a signaling cascade that culminates in caspase activation and eventual apoptosis. Although the direct activation of programmed cell death is 1 method by which TSP-1 regulates cell proliferation, recent studies performed on human umbilical vein ECs, which naturally lack CD36, provide evidence that TSP-1 also operates through nonapoptotic means.[37,38] Preliminary data from our laboratory indicate that AVM-ECs underexpress CD36 compared with control BECs (data not shown). Taken together, reduced CD36 cell-surface expression and equal rates of AVM-EC death after vehicle and TSP-1 treatment suggests that TSP-1 may function in a largely non-apoptotic manner in AVM-ECs.

In addition to EC proliferation, cell migration is a necessary component of new blood vessel formation. Our data show that AVM-ECs exhibit significantly greater rates of chemotactic migration than control BECs. Charalambous et al[39] similarly demonstrate that tumor-associated brain ECs migrate more rapidly than BECs, underscoring the notion that AVM-ECs are highly activated ECs. The mechanisms underlying EC migration are complex and rely on the concerted activity of extracellular growth factors, matricellular and cytoskeletal proteins, and cell-surface integrins. Integrins are key mediators of cell adhesion and migration, and numerous reports indicate that cerebral AVMs have altered expression patterns of various integrin proteins.[34,40,41] Several studies indicate that β_1 integrins are

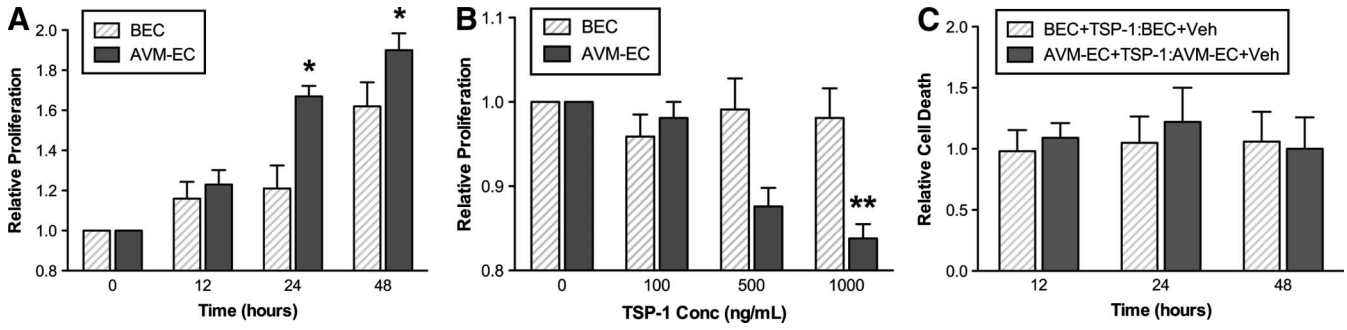

FIGURE 4. *Thrombospondin-1 (TSP-1) reduces the proliferation rate of arteriovenous malformation endothelial cells (AVM-ECs).* **A**, *the proliferation rate of AVM-ECs is 46% and 28% greater than the proliferation rate of brain endothelial cells (BECs) at 24 and 48 hours, respectively.* **B**, *the addition of TSP-1 (1000 ng/mL) reduces the proliferation rate of AVM-ECs by 16% at 48 hours, whereas the proliferation rate of BECs is not altered.* **C**, *relative rates of cell death at 12, 24, and 48 hours are equivalent for vehicle (Veh)- and TSP-1-treated groups of AVM-ECs and BECs. *P < .05, **P < .01. Conc, concentration.*

Copyright © Congress of Neurological Surgeons. Unauthorized reproduction of this article is prohibited.

significantly overexpressed in whole-brain AVM tissue.[15] Because TSP-1 reportedly inhibits EC migration through β_1-integrin activation,[34,40] overexpression of this integrin in brain AVMs would support our observation that TSP-1 selectively decreases AVM-EC migration. Although the precise molecular aberrations governing AVM-EC and tumor-associated EC migration rates remain elusive, our results validate TSP-1's role as an angiostatic factor and are consistent with previous reports of TSP-1's ability to inhibit EC migration.

The creation of a functional vascular network requires the efficient formation of 3-dimensional tubule structures. In our analysis, AVM-ECs form tubules in a highly disorganized manner compared with control BECs. As a matricellular protein, TSP-1 binds cell-surface receptors and growth factors and coordinates essential interactions between cells and extracellular matrix scaffolds, such as laminins, proteoglycans, collagens, and fibronectin.[22,23] Although BEC cultures are naturally replete with TSP-1, reconstitution of TSP-1 to AVM-EC cultures may allow for the cell-matrix interactions necessary for proper tubule formation. Given our observations, it is conceivable that reduced TSP-1 expression in cerebral AVM contributes to their lack of functional capillary beds and normal vascular organization.

The abnormal angiogenic features of AVM-ECs are strikingly similar to the activated phenotype of ECs derived from human gliomas.[39] However, although the proangiogenic character of tumor-associated brain ECs is driven by factors produced by the tumor, the functional abnormalities of AVM-ECs observed in this study are likely primary defects of the AVM vasculature. Research into the molecular genetics of both syndrome-associated and sporadic cerebral AVMs has implicated variants of the *Endoglin* (*ENG*), *Activin-like kinase receptor 1* (*ALK-1*), and *SMAD4* genes, all members of the transforming growth factor β (TGF-β) signaling family, as root causes of these vascular dysplasias of the brain.[17,32,42-45] The importance of TGF-β proteins in brain AVM pathogenesis has been described,[40] and numerous studies have implicated TSP-1 as a critical regulator of latent TGF-β.[23] Because bioactive TGF-β mediates important functions in vasculogenesis and vessel stability,[22] primary defects in TSP-1 expression would adversely alter tissue levels of active TGF-β and significantly impair blood vessel integrity. Moreover, apart from being a transcriptional repressor of TSP-1 expression, Id1 is a transcription factor involved in an array of biological processes, including cell fate and lineage determination, development, and angiogenesis.[46] Unlike TSP-1, Id1 acts to augment cell proliferation and migration and to promote new blood vessel formation. Recent studies show that Id1 expression is upregulated on VEGF stimulation in ECs, supporting a proangiogenic role for this transcription factor.[47] In addition, Id1 is critical for the differentiation of human embryonic stem cells into ECs[48] and is a key mediator of endothelial progenitor cell proliferation and migration.[49] The idea that aberrant Id1 expression in an endothelial progenitor cell could facilitate development of a complex cerebrovascular lesion is interesting and warrants future consideration.

Despite identifying novel roles for TSP-1 and Id1 in AVM-EC biology, certain study limitations preclude more definitive conclusions. The use of primary ECs isolated from human cerebral AVMs is unique and allows for detailed molecular and functional studies of a single cell type not capable with whole-tissue specimens. However, this type of experimentation removes the cell of interest from its native environment and exposes the cell to artificial culture conditions. As a result, we cannot exclude the possibility that the observed molecular and functional abnormalities of AVM-EC are secondary to blood flow–related alterations in shear stress or to factors present solely within the AVM microenvironment.[50,51] In addition, the majority of patients from whom AVM-ECs were isolated had undergone previous embolization of their AVMs. The presence of either platinum coils or Onyx within the AVM may induce an artificial proangiogenic state as a result of thrombosis, hypoxia, and ischemia.[44,52] Future studies, therefore, will attempt to include a greater proportion of patients who have not undergone preoperative embolization. Finally, because of the relative infrequency of open microsurgery for the treatment of unruptured cerebral AVMs, the majority of our AVM specimens were from patients with a hemorrhagic presentation. Although we generalize our results to brain AVMs regardless of rupture status, this fact must be taken into consideration when evaluating the translational potential of our findings.

The management of both unruptured and ruptured cerebral AVMs is challenging and even minimally invasive treatments place vital intracranial structures at risk of injury. The development of pharmacotherapies that specifically attack the AVM vasculature relies on the elucidation of critical molecular differences between the ECs of brain AVMs and normal BECs. Pioneering work has demonstrated that oral tetracyclines may reduce matrix metalloproteinase levels in patients with brain AVMs, thus stabilizing the fragile, malformed vasculature and reducing the risk of hemorrhage.[53,54] In addition, in vivo experiments demonstrate that ABT-510, a peptide mimetic derived from the antiangiogenic domain of TSP-1, suppresses malignant glioma growth specifically by reducing tumor angiogenesis.[55,56] Our results clearly demonstrate that TSP-1 is differentially expressed between AVM-ECs and control BECs, that AVM-EC overexpression of Id1 is responsible for the down-regulation of TSP-1, and that reconstitution of TSP-1 to AVM-EC cultures normalizes their dysfunctional angiogenic phenotype. These discoveries highlight a novel role for TSP-1 in the biology of brain AVMs and may aid in the rational design of therapies that target the dysplastic AVM vasculature to complement current treatment modalities.

CONCLUSION

The results of this study offer a unique insight into the molecular pathobiology of ECs derived from human brain AVMs. Although the role of TSP-1 in tumor angiogenesis is well defined, we demonstrate the novel finding that TSP-1 is a critical regulator

Copyright © Congress of Neurological Surgeons. Unauthorized reproduction of this article is prohibited.

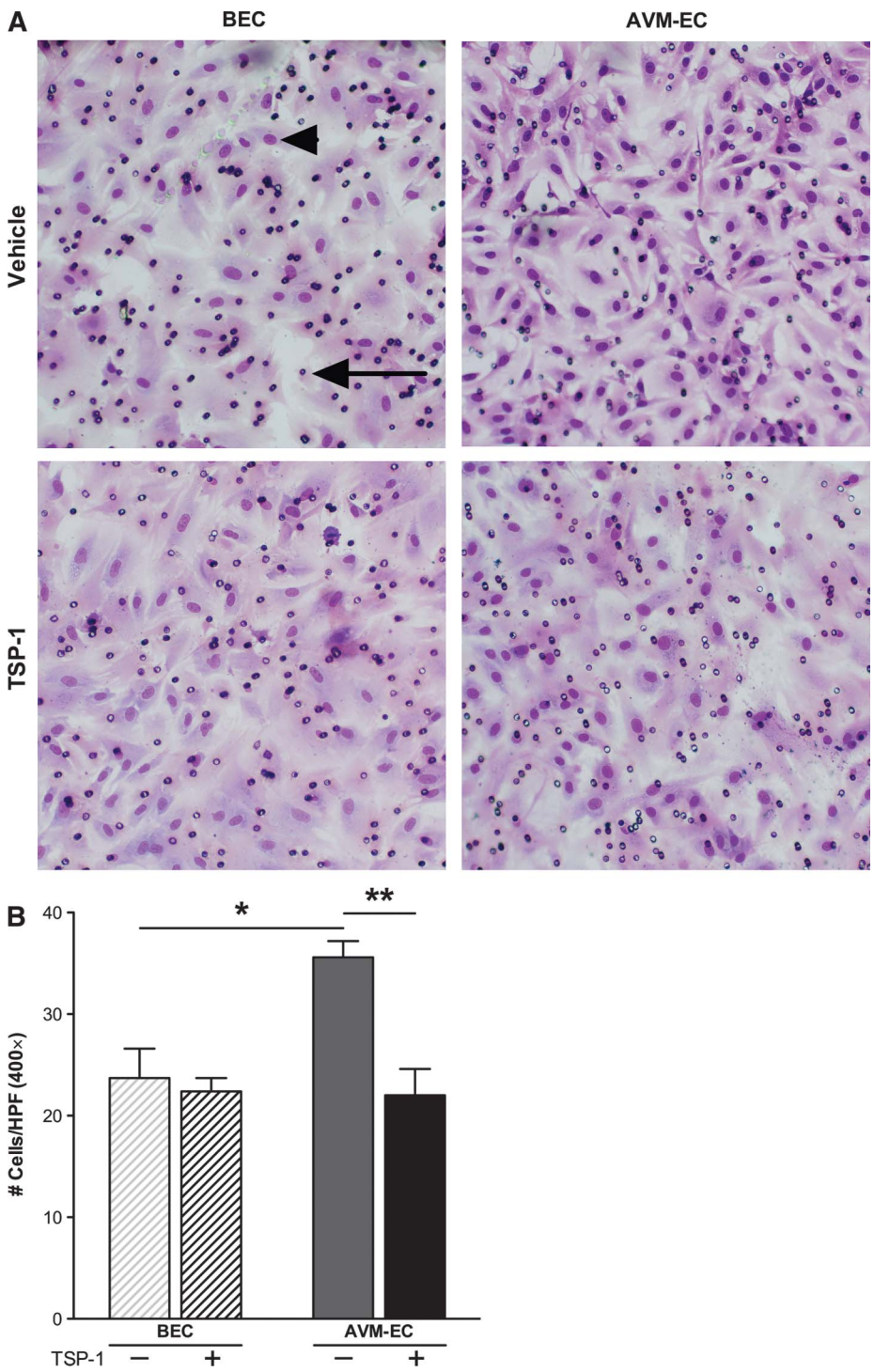

FIGURE 5. *Thrombospondin-1 (TSP-1) normalizes the migration rate of arteriovenous malformation endothelial cells (AVM-ECs).* **A**, *representative images of the underside of modified transwell Boyden chamber filters, demonstrating the migration of endothelial cells (arrowhead) through the 8-μm pores (arrow).* **B**, *at baseline, AVM-ECs migrate 50% more quickly than brain endothelial cells (BECs). TSP-1 decreases the migration rate of AVM-ECs by 38%, whereas the migration rate of BECs is not changed. Magnification, ×100. *P < .05, **P < .01. HPF, high-power field.*

Copyright © Congress of Neurological Surgeons. Unauthorized reproduction of this article is prohibited.

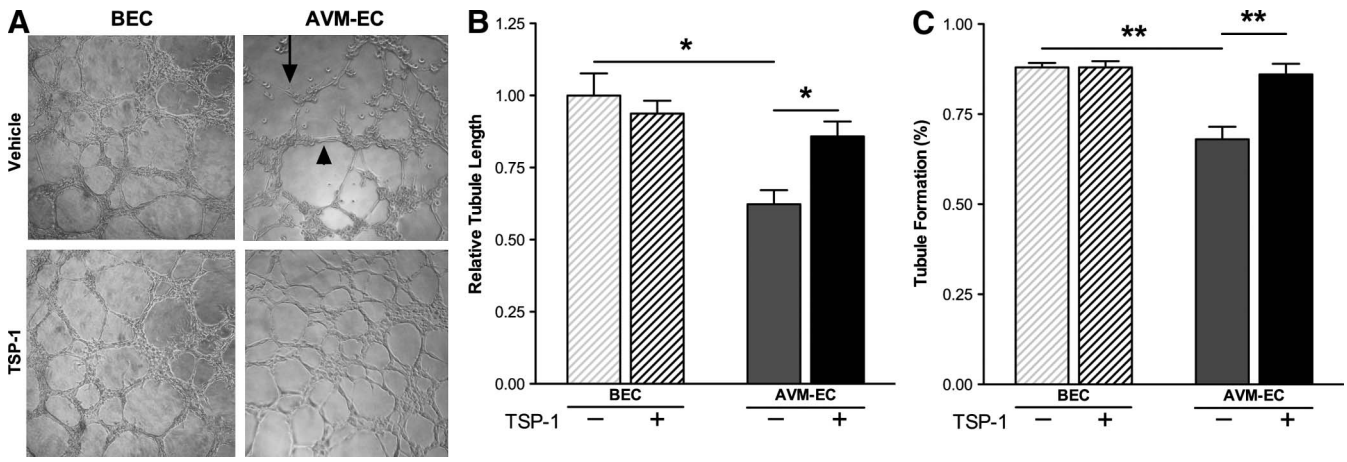

FIGURE 6. *Thrombospondin-1 (TSP-1) increases the length and efficiency of tubule formation of arteriovenous malformation endothelial cells (AVM-ECs).* **A**, *representative images of tubule formation in AVM-ECs and brain endothelial cells (BECs) in growth factor–reduced Matrigel, illustrating complete tubule structures (arrowhead) and tubule sprouts or branches (arrow).* **B**, *AVM-ECs form tubule structures that are 38% shorter and more irregular than those formed by control BECs. The addition of TSP-1 increases the tubule length of AVM-ECs by 24%, whereas the length of BEC tubules remains constant.* **C**, *AVM-ECs form complete tubule structures with an efficiency of 66%, whereas BECs form unabridged tubules with an efficiency of 88%. AVM-EC tubule formation efficiency increases to 84% after TSP-1 treatment. Magnification, ×100. *P < .05, **P < .01.*

of the aberrant angiogenic functions of AVM-ECs. Furthermore, we identify Id1 as a potent repressor of TSP-1 expression in AVM-ECs. As current invasive therapies for cerebral AVMs are fraught with risk, future treatment modalities will favor advanced minimally invasive strategies and pharmacologic approaches. Additional in vitro and in vivo studies are necessary to identify the molecular factors mediating TSP-1 dysregulation in AVM-ECs as well as to delineate the signaling pathways through which TSP-1

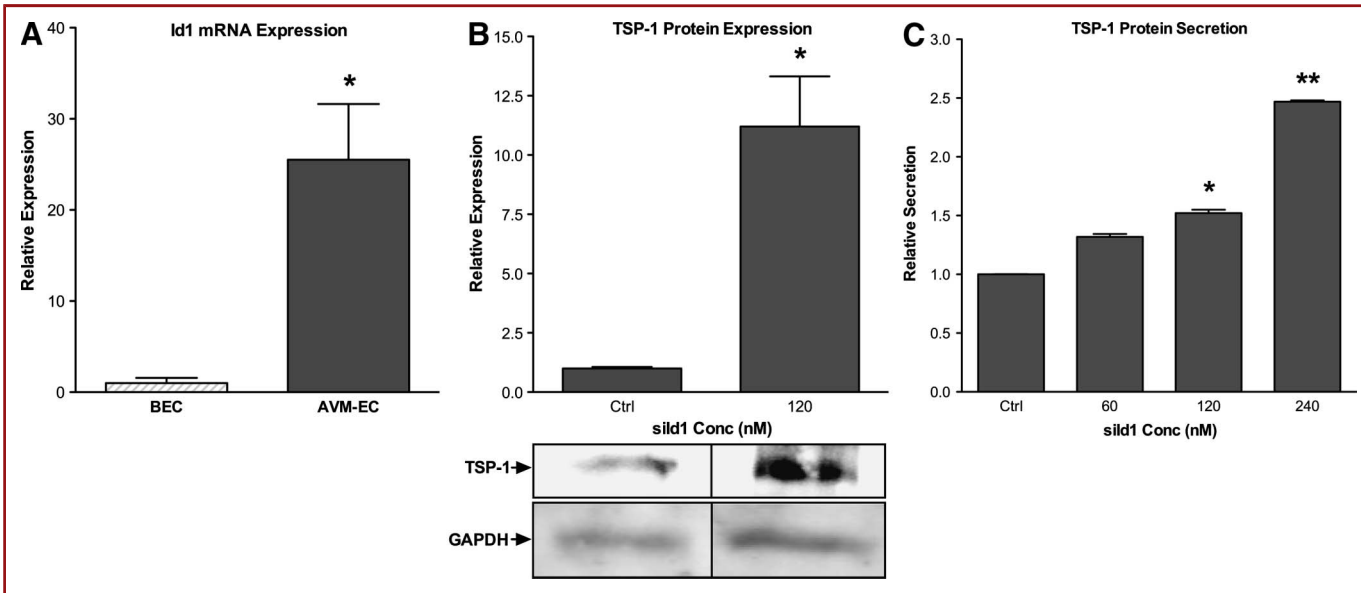

FIGURE 7. *Inhibitor of DNA binding/differentiation 1 (Id1) regulates thrombospondin-1 (TSP-1) expression in of arteriovenous malformation endothelial cells (AVM-ECs).* **A**, *gene microarray analysis indicates that AVM-ECs express 25.2-fold more Id1 mRNA than control brain endothelial cells (BECs).* **B**, *knockdown of Id1 expression with small interfering RNA constructs increases intracellular TSP-1 production 11.2-fold compared with small interfering control (Ctrl)-treated samples.* **C**, *transient transfection of AVM-EC with 120 and 240 nM of small interfering (si) Id1 increases TSP-1 secretion by 1.5- and 2.5-fold, respectively, as demonstrated by enzyme-linked immunosorbent assays. *P < .05, **P < .01. Conc, concentration.*

Copyright © Congress of Neurological Surgeons. Unauthorized reproduction of this article is prohibited.

normalizes AVM-EC function. Nevertheless, the data in this study provide a springboard for future investigations and a context for the potential role of TSP-1 in the clinical management of brain AVMs.

Disclosure

These studies were supported by the Neithart Foundation (S.L.G.) and the Sarnoff Cardiovascular Research Foundation (C.J.S.). The authors have no personal financial or institutional interest in any of the drugs, materials, or devices described in this article.

REFERENCES

1. Friedlander RM. Arteriovenous malformations of the brain. *N Engl J Med*. 2007;356(26):2704-2712.
2. Stapf C, Mast H, Sciacca RR, et al. Predictors of hemorrhage in patients with untreated brain arteriovenous malformation. *Neurology*. 2006;66(9):1350-1355.
3. Hartmann A, Pile-Spellman J, Stapf C, et al. Risk of endovascular treatment of brain arteriovenous malformations. *Stroke*. 2002;33(7):1816-1820.
4. Haw CS, terBrugge K, Willinsky R, Tomlinson G. Complications of embolization of arteriovenous malformations of the brain. *J Neurosurg*. 2006;104(2):226-232.
5. Berman MF, Sciacca RR, Pile-Spellman J, et al. The epidemiology of brain arteriovenous malformations. *Neurosurgery*. 2000;47(2):389-397.
6. Stapf C, Mast H, Sciacca RR, et al. The New York Islands AVM Study: design, study progress, and initial results. *Stroke*. 2003;34(5):e29-e33.
7. Stapf C, Mohr JP. Unruptured brain arteriovenous malformations should be treated conservatively: yes. *Stroke*. 2007;38(12):3308-3309.
8. Lawton MT, Du R, Tran MN, et al. Effect of presenting hemorrhage on outcome after microsurgical resection of brain arteriovenous malformations. *Neurosurgery*. 2005;56(3):485-493.
9. Spetzler RF, Martin NA. A proposed grading system for arteriovenous malformations. *J Neurosurg*. 1986;65(4):476-483.
10. Lawton MT, Kim H, McCulloch CE, Mikhak B, Young WL. A supplementary grading scale for selecting patients with brain arteriovenous malformations for surgery. *Neurosurgery*. 2010;66(4):702-713.
11. Stapf C. The rationale behind "A Randomized Trial of Unruptured Brain AVMs" (ARUBA). *Acta Neurochir Suppl*. 2010;107(3):83-85.
12. Sonstein WJ, Kader A, Michelsen WJ, Llena JF, Hirano A, Casper D. Expression of vascular endothelial growth factor in pediatric and adult cerebral arteriovenous malformations: an immunohistochemical study. *J Neurosurg*. 1996;85(5):838-845.
13. Hashimoto T, Emala CW, Joshi S, et al. Abnormal pattern of Tie-2 and vascular endothelial growth factor receptor expression in human cerebral arteriovenous malformations. *Neurosurgery*. 2000;47(4):910-918.
14. Uranishi R, Baev NI, Ng PY, Kim JH, Awad IA. Expression of endothelial angiogenesis receptors in human cerebrovascular malformations. *Neurosurgery*. 2001;48(2):359-367.
15. Hashimoto T, Lawton MT, Wen G, et al. Gene microarray analysis of human brain arteriovenous malformations. *Neurosurgery*. 2004;54(2):410-425.
16. Chen Y, Pawlikowska L, Yao JS, et al. Interleukin-6 involvement in brain arteriovenous malformations. *Ann Neurol*. 2006;59(1):72-80.
17. Chen Y, Hao Q, Kim H, et al. Soluble endoglin modulates aberrant cerebral vascular remodeling. *Ann Neurol*. 2009;66(1):19-27.
18. Jabbour MN, Elder JB, Samuelson CG, et al. Aberrant angiogenic characteristics of human brain arteriovenous malformation endothelial cells. *Neurosurgery*. 2009;64(1):139-148.
19. Christopherson KS, Ullian EM, Stokes CCA, et al. Thrombospondins are astrocyte-secreted proteins that promote CNS synaptogenesis. *Cell*. 2005;120(3):421-433.
20. Liauw J, Hoang S, Choi M, et al. Thrombospondins 1 and 2 are necessary for synaptic plasticity and functional recovery after stroke. *J Cereb Blood Flow Metab*. 2008;28(10):1722-1732.
21. Lawler J. Thrombospondin-1 as an endogenous inhibitor of angiogenesis and tumor growth. *J Cell Mol Med*. 2002;6(1):1-12.
22. Bornstein P. Thrombospondins as matricellular modulators of cell function. *J Clin Invest*. 2001;107(8):929-934.
23. Adams JC, Lawler J. The thrombospondins. *Int J Biochem Cell Biol*. 2004;36(6):961-968.
24. Kazerounian S, Yee KO, Lawler J. Thrombospondins in cancer. *Cell Mol Life Sci*. 2008;65(5):700-712.
25. Ren B, Yee KO, Lawler J, Khosravi-Far R. Regulation of tumor angiogenesis by thrombospondin-1. *Biochim Biophys Acta*. 2006;1765(2):178-188.
26. Zubac DP, Bostad L, Kihl B, Seidal T, Wentzel-Larsen T, Haukaas SA. The expression of thrombospondin-1 and p53 in clear cell renal cell carcinoma: its relationship to angiogenesis, cell proliferation and cancer specific survival. *J Urol*. 2009;182(5):2144-2149.
27. Pour L, Svachova H, Adam Z, et al. Levels of angiogenic factors in patients with multiple myeloma correlate with treatment response. *Ann Hematol*. 2010;89(4):385-389.
28. Volpert OV, Pili R, Sikder HA, et al. Id1 regulates angiogenesis through transcriptional repression of thrombospondin-1. *Cancer Cell*. 2002;2(6):473-483.
29. Long AD, Mangalam HJ, Chan BY, Tolleri L, Hatfield GW, Baldi P. Improved statistical inference from DNA microarray data using analysis of variance and a Bayesian statistical framework. Analysis of global gene expression in Escherichia coli K12. *J Biol Chem*. 2001;276(23):19937-19944.
30. Storey JD, Tibshirani R. Statistical significance for genomewide studies. *Proc Natl Acad Sci U S A*. 2003;100(16):9440-9445.
31. Arnaoutova I, Kleinman HK. In vitro angiogenesis: endothelial cell tube formation on gelled basement membrane extract. *Nat Protoc*. 2010;5(4):628-635.
32. Xu B, Wu YQ, Huey M, et al. Vascular endothelial growth factor induces abnormal microvasculature in the endoglin heterozygous mouse brain. *J Cereb Blood Flow Metab*. 2004;24(2):237-244.
33. Rhoten RL, Comair YG, Shedid D, Chyatte D, Simonson MS. Specific repression of the preproendothelin-1 gene in intracranial arteriovenous malformations. *J Neurosurg*. 1997;86(1):101-108.
34. Short SM, Derrien A, Narsimhan RP, Lawler J, Ingber DE, Zetter BR. Inhibition of endothelial cell migration by thrombospondin-1 type-1 repeats is mediated by β_1 integrins. *J Cell Biol*. 2005;168(4):643-653.
35. Jiménez B, Volpert OV, Crawford SE, Febbraio M, Silverstein RL, Bouck NP. Signals leading to apoptosis-dependent inhibition of neovascularization by thrombospondin-1. *Nat Med*. 2000;6(1):41-48.
36. Dawson DW, Pearce SFA, Zhong R, Silverstein RL, Frazier WA, Bouck NP. CD36 mediates the in vitro inhibitory effects of thrombospondin-1 on endothelial cells. *J Cell Biol*. 1997;138(3):707-717.
37. Oganesian A, Armstrong LC, Migliorini MM, Strickland DK, Bornstein P. Thrombospondins use the VLDL receptor and a nonapoptotic pathway to inhibit cell division in microvascular endothelial cells. *Mol Biol Cell*. 2008;19(2):563-571.
38. Yamauchi M, Imajoh-Ohmi S, Shibuya M. Novel antiangiogenic pathway of thrombospondin-1 mediated by suppression of the cell cycle. *Cancer Sci*. 2007;98(9):1491-1497.
39. Charalambous C, Chen TC, Hofman FH. Characteristics of tumor-associated endothelial cells derived from glioblastoma multiforme. *Neurosurg Focus*. 2006;20(4):E22-E26.
40. Calzada MJ, Zhou L, Sipes JM, et al. $\alpha_4\beta_1$ integrin mediates selective endothelial cell responses to thrombospondins 1 and 2 in vitro and modulates angiogenesis in vivo *Circ Res*. 2004;94(4):462-470.
41. Su H, Kim H, Pawlikowska L, et al. Reduced expression of integrin $\alpha_v\beta_8$ is associated with brain arteriovenous malformation pathogenesis. *Am J Pathol*. 2010;176(2):1018-1027.
42. Kim H, Pawlikowksa L, Chen Y, Su H, Yang G-Y, Young WL. Brain arteriovenous malformation biology relevant to hemorrhage and implication for therapeutic development. *Stroke*. 2008;40(3 Suppl):S95-S97.
43. Leblanc GG, Golanov E, Awad IA, Young WL, Biology of Vascular Malformations of the Brain NINDS Workshop Collaborators. Biology of vascular malformations of the brain. *Stroke*. 2009;40(12):e694-e702.
44. Zhang H, Akman HO, Smith ELP, Zhao J, Siddiqui JEM-UMAQ, Batuman OA. Cellular response to hypoxia involves signaling via Smad proteins. *Blood*. 2003;101(6):2253-2260.
45. Schwarte-Waldhoff I, Volpert OV, Bouck NP, et al. Smad4/DPC4-mediated tumor suppression through suppression of angiogenesis. *Proc Natl Acad Sci U S A*. 2000;97(17):9624-9629.
46. Sikder HA, Devlin MK, Dunlap S, Ryu B, Alani RM. Id1 proteins in cell growth and tumorigenesis. *Cancer Cell*. 2003;3(6):525-530.

Copyright © Congress of Neurological Surgeons. Unauthorized reproduction of this article is prohibited.

47. Sakurai D, Tsuchiya N, Yamaguchi A, et al. Crucial role of inhibitor of DNA binding/differentiation in the vascular endothelial growth factor-induced activation and angiogenic processes of human endothelial cells. *J Immunol*. 2004;173(9):5801-5809.
48. James D, Nam H-S, Seandel M, et al. Expansion and maintenance of human embryonic stem cell-derived endothelial cell by TGFβ inhibition is Id1 dependent. *Nat Biotechnol*. 2010;28(2):161-166.
49. Gao D, Nolan D, McDonnell K, et al. Bone marrow-derived endothelial progenitor cells contribute to the angiogenic switch in tumor growth and metastatic progression. *Biochim Biophys Acta*. 2009;1796(1):33-40.
50. Desai SY, Marroni M, Cucullo L, et al. Mechanisms of endothelial survival under shear stress. *Endothelium*. 2002;9(2):89-102.
51. Krizanac-Bengez L, Kapural M, Parkinson F, et al. Effects of transient loss of shear stress on blood-brain barrier endothelium: role of nitric oxide and IL-6. *Brain Res*. 2003;977(2):239-246.
52. Akakin A, Ozkan A, Akgun E, et al. Endovascular treatment increases but gamma knife radiosurgery decreases angiogenic activity of arteriovenous malformations: an in vivo experimental study using a rat cornea model. *Neurosurgery*. 2010;66(1):121-129.
53. Lee CZ, Yao JS, Huang Y, et al. Dose-response effect of tetracyclines on cerebral matrix metalloproteinase-9 after vascular endothelial growth factor stimulation. *J Cereb Blood Flow Metab*. 2006;26(9):1157-1164.
54. Lee CZ, Xue Z, Zhu Y, Yang GY, Young WL. Matrix metalloproteinase-9 inhibition attenuates vascular endothelial growth-factor-induced intracerebral hemorrhage. *Stroke*. 2007;38(9):2563-2568.
55. Anderson JC, Grammer JR, Wang W, et al. ABT-510, a modified type 1 repeat peptide of thrombospondin, inhibits malignant glioma growth in vivo by inhibiting angiogenesis. *Cancer Biol Ther*. 2007;6(3):454-462.
56. Nabors LB, Fiveash JB, Markert JM, et al. A Phase 1 trial of ABT-510 concurrent with standard chemoradiation for patients with newly diagnosed glioblastoma. *Arch Neurol*. 2010;67(3):313-319.

COMMENTS

Stapleton et al demonstrated that thrombospondin-1 (TSP-1) modulates the angiogenic phenotype of endothelial cells from brain arteriovenous malformations (AVMs). Using endothelial cell proliferation, migration, and tubule formation assays, this angiostatic factor was differentially underexpressed in AVMs compared with control brain. Reconstitution of TSP-1 to AVM endothelial cell cultures normalized their angiogenic phenotype. Id1, a transcriptional repressor of TSP-1 production, was overexpressed in AVMs to down-regulate TSP-1. This study provides important evidence that dysregulated angiogenesis is part of AVM pathophysiology. The UCSF AVM Study Project has also demonstrated increased angiogenesis activity in AVMs, which we think is part of the vasculature's reparative response to erosive blood flow through the nidus and subsequent inflammatory degradation. It is difficult to determine whether abnormalities in angiogenesis relate to AVM pathogenesis or its pathophysiology. Nonetheless, these data implicate TSP-1 and suggest intriguing pharmacological interventions for further investigation.

Michael T. Lawton
San Francisco, California

1. Chen Y, Zhu W, Bollen AW, et al. Evidence of inflammatory cell involvement in brain arteriovenous malformations. *Neurosurgery*. 2008;62(6):1340-1350.
2. Zhu Y, Lawton MT, Du R, et al. Expression of hypoxia-inducible factor-1 and vascular endothelial growth factor in response to venous hypertension. *Neurosurgery*. 2006;59(3):687-696.
3. Pawlikowska L, Tran MN, Achrol AS, et al, for the UCSF BAVM Study Project. Polymorphisms in transforming growth factor-<beta>-related genes ALK1 and ENG are associated with sporadic brain arteriovenous malformations. *Stroke*. 2005;36:2278-2280.

Stapleton et al performed a series of elegant experiments that examined endothelial cells derived from AVMs and found that AVM endothelial cells have higher proliferation and migration and less ability to form tubes compared with normal brain endothelial cells. They have demonstrated that this difference is caused by the down-regulation of TSP-1 in AVM endothelial cells, which in turn are regulated by Id1. Although this study is an in vitro study and the results must therefore be interpreted with caution, the findings provide a mechanism by which angiogenesis occurs in AVMs and point to TSP-1 as a promising candidate in the pathogenesis of AVMs that can be further investigated in future in vivo studies.

Rose Du
Boston, Massachusetts

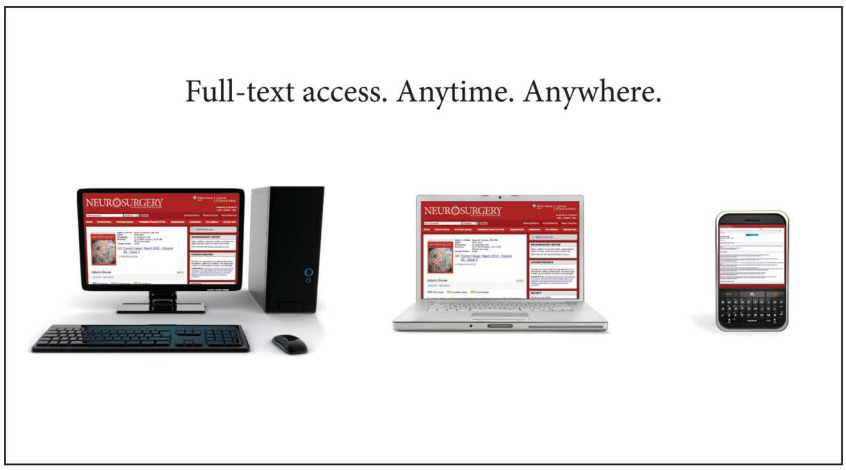

Access for your favorite mobile devices now available at www.neurosurgery-online.com
NEUROSURGERY

Copyright © Congress of Neurological Surgeons. Unauthorized reproduction of this article is prohibited.

A Long Peripheral Nerve Autograft Model in the Sheep Forelimb

Joanne Forden
Qing-Gui Xu, PhD
Kathleen Joy Khu, MD
Rajiv Midha, MD, MSc, FRCS(C)

Division of Neurosurgery, Department of Clinical Neurosciences and Hotchkiss Brain Institute, University of Calgary, Calgary, Alberta, Canada

Correspondence:
Rajiv Midha, MD, MSc, FRCS(C),
Division of Neurosurgery,
Department of Clinical Neurosciences,
University of Calgary,
Room 1195,
1403–29 St NW,
Calgary, Alberta, Canada T2N 2T9.
E-mail: rajmidha@ucalgary.ca

Received, March 31, 2010.
Accepted, July 19, 2010.

Copyright © 2011 by the
Congress of Neurological Surgeons

BACKGROUND: Autologous nerve grafts remain the only proven means of bridging lengthy gaps in peripheral nerve. However, there is very little literature on a reliable long (> 5 cm) nerve autograft animal model.

OBJECTIVE: To establish a reproducible long nerve gap and autograft animal model that is clinically relevant but not cost prohibitive.

METHODS: The extent of nerve regeneration and electrophysiological recovery after segmental repair of a long nerve defect was evaluated with a sheep model. Thirteen Suffolk sheep were used. An 18-cm segment of radial sensory nerve was harvested from the forelimb, trimmed, divided into 2 equal segments of 7 cm each, and microsurgically repaired to a surgically created defect of 5 cm in the median nerve within the same forelimb. Electrophysiological studies were performed on 6 sheep at 6 months and 6 sheep at 9 months. Samples of the grafted segments were obtained for histology, immunohistochemistry, and morphometric analyses. Electric studies were also performed on an uninjured median nerve of a control animal in tissue that was similarly harvested and processed.

RESULTS: At 6 and 9 months, all sheep had recordable robust nerve action potentials. Nerve conduction velocity and amplitude were slightly decreased compared with control, but the difference was statistically insignificant. Histomorphometric assessment demonstrated that the autografts contained a large number of regenerating axons through graft fascicles in all animals.

CONCLUSION: The median nerve in the sheep forelimb is a reproducible and reliable model for assessing regeneration through long peripheral nerve grafts.

KEY WORDS: Autograft, Large animal, Nerve regeneration, Nerve repair

Neurosurgery 68:1354–1362, 2011 DOI: 10.1227/NEU.0b013e31820c08de www.neurosurgery-online.com

Injuries to peripheral nerves are a major source of disability because of impairment of motor and/or sensory function. Unfortunately, such injuries are undertreated primarily because the options for repair are limited and the functional outcomes are less than ideal. Injuries resulting in short gaps (2-3 cm) have more treatment options such as end-to-end suture repair after extensive mobilization of the nerve or graft repair using autografts, allografts, or nerve conduits.[1] In addition, they are technically easier to repair and produce better outcomes because of the shorter distance necessary for the regenerating axons to traverse.[2] On the other hand, injuries resulting in longer defects (≥ 5 cm) are more difficult to manage and necessitate implantation of a graft to bridge the proximal and distal nerve stumps and to promote regeneration. Among the different sources of nerve grafts, an autologous nerve graft or autograft (nerve graft harvested from the same patient) is considered the gold standard for graft repair.[3,4] Historically, autografts have shown the greatest efficacy for inducing axonal regeneration because they provide appropriate alignment and cellular constituents of the normal nerve.[2] The use of nerve autografts in bridging lengthy defects in the peripheral nerve has resulted in good outcomes for both nerve injuries and lesions requiring nerve resection such as tumors.

Short-segment graft repair and nerve regeneration have been studied in various small-animal

ABBREVIATION: NAP, nerve action potential

Copyright © Congress of Neurological Surgeons. Unauthorized reproduction of this article is prohibited.

models such as mice, rats, and rabbits, but the length of the graft ranged from only 1 to 4 cm.[5] Large-animal models would allow larger gaps to be created and have longer regeneration distances that would more closely mimic the clinical condition in human nerve injuries.[6] Moreover, a longer segment of autologous nerve graft used for repair can be harvested from large animals with no significant morbidity. To date, very few large animal models have been used in the study of peripheral nerve regeneration.[1,3,6-13]

This study aimed to establish a reproducible long nerve gap and nerve autograft animal model that would be clinically relevant but not cost prohibitive. Using a sheep forelimb model, we evaluated the extent of nerve regeneration and electrophysiological recovery after repair of a segmental nerve defect in the median nerve with 7-cm autograft cables. We also evaluated graft revascularization and cellular infiltration after graft repair.

METHODOLOGY

Surgical Procedure

Thirteen juvenile Suffolk ewes (Nagel Veterinary Service, Crossfield, Alberta, Canada) weighing 27 to 30 kg each were used for the study. The sheep were divided into 2 experimental groups of 6 animals each; 1 group was sacrificed after 6 months and the other at 9 months. One unoperated animal served as the control for electric studies and normal nerve histomorphometry. All animal care, housing, and surgical procedures were approved by the University of Calgary animal care committee and were in accordance with the guidelines set by the Canadian Council on Animal Care. The surgical procedures were conducted under general anesthesia and followed aseptic technique.

The animals were fasted for 12 hours before surgery. General anesthesia was administered with 4% to 5% isoflurane via an induction mask and atropine injected intramuscularly at 0.5 mg/kg. Each animal was then intubated with a cuffed endotracheal tube and ventilated with oxygen at 2 L/min. Anesthesia was maintained with 3% isoflurane. Buprenorphine 0.01 to 0.02 mg/kg IM was given as an analgesic perioperatively. With the sheep supine, the right forelimb and axilla were shaved and prepared with an iodine solution. A skin incision was made, starting medially from the axilla and curving anterolaterally as it progressed down the distal forelimb to expose the radial nerve. The nerve was then dissected free of its surrounding tissues, and an 18-cm segment was excised (Figure 1). The nerve segment was placed in a sterile saline (0.9%)-soaked gauze to prevent desiccation while awaiting autologous transplantation.

Using the proximal portion of the same skin incision, we dissected the median nerve and exposed it in a deeper intermuscular plane where it ran with the segmental vessels. At this point, the previously harvested radial nerve segment was brought back into the surgical field and cut into 2 equal segments, each measuring 7 cm in length, after excess tissue was trimmed off each end. These 2 segments were placed adjacent to each other and sutured together at each end with a single stitch of 9-0 nylon suture under microscopic guidance. The "paired" cables of radial nerve graft were then sutured onto the median nerve, from which 5 cm of nerve segment had been removed, using 3 stitches of 9-0 nylon suture at each end (Figure 1). Because the median nerve gap was approximately 6 cm after retraction of the nerve ends, the resulting graft lengths of 7 cm allowed tension-free repair.

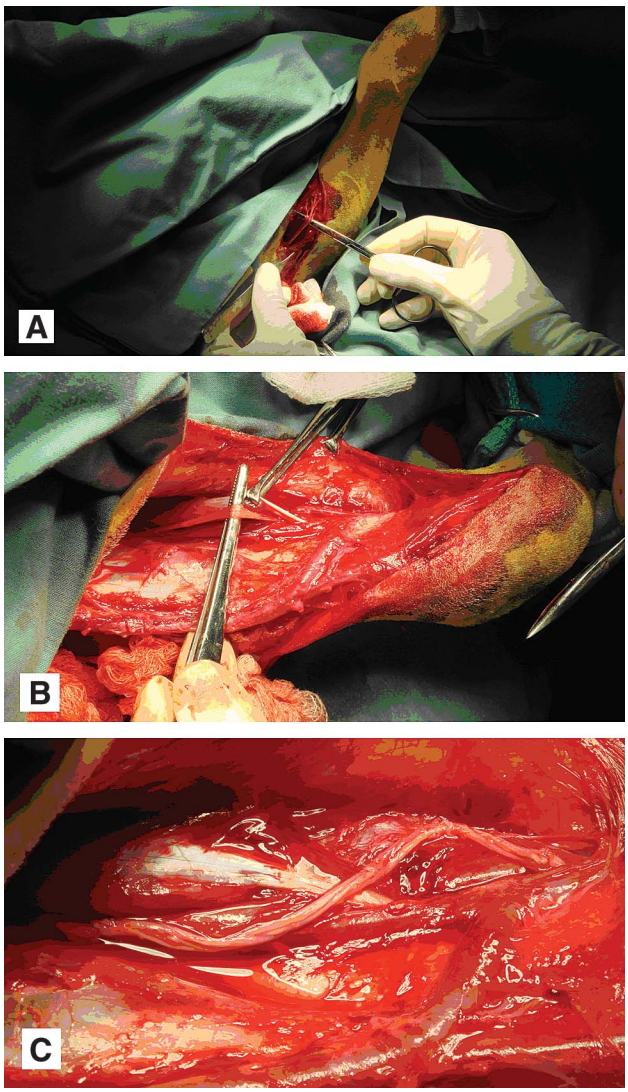

FIGURE 1. *Under general anesthesia, an 18-cm segment of radial sensory nerve was harvested from the anterolateral aspect of the forelimb of each sheep (A). The radial nerve was trimmed and divided into two 7-cm segments and then microsurgically repaired to a surgically created median nerve injury gap of 5 cm. The median nerve in the medial aspect of the sheep's proximal forelimb was shown before sectioning (B). The radial nerve autograft cables were apposed to the median nerve defect, so the 2 grafts ensured cross-sectional coverage of the parent nerve stumps. Because the nerve graft was slightly longer than the defect, the repair was tension free (C).*

Copyright © Congress of Neurological Surgeons. Unauthorized reproduction of this article is prohibited.

The grafts were placed in the gap in a reverse manner; ie, the distal end of the graft was sutured to the proximal end of the median nerve stump to prevent regenerating axons to be lost within branches and thus not attain the distal nerve repair. The donor nerve and the graft were well matched in terms of size and number of fascicles. The diameter of each radial nerve segment ranged from 1 to 2 mm; that of the median nerve ranged from 2 to 3 mm. The median nerve contained an average of 13 fascicles, whereas each radial nerve had an average of 9 somewhat smaller-diameter fascicles, ensuring a good match once the 2 graft segments were apposed to the median nerve. After irrigation with sterile saline and penicillin solution, the wound was closed. Postoperatively, the sheep were allowed to ambulate and were given food and water ad libitum. Analgesia in the form of intramuscular injections of buprenorphine 0.1 to 0.2 mg/kg was provided as needed.

Nerve Exploration and Harvesting

Electrophysiological Studies

All animals underwent electrophysiological assessment before sacrifice. Under general anesthesia, the forelimb wound was reopened and the nerve graft site was carefully exposed with external neurolysis so as not to disrupt the graft segments. Electric studies and nerve action potential (NAP) recordings were obtained with a Cadwell Sierra 6200A electrodiagnostic machine (Cadwell Laboratories, Kennewick, Washington). Bipolar stimulating and recording electrodes were placed 2 cm proximal and distal to the graft suture site to ensure that NAPs were measured across the entire graft. Primary measures include the presence or absence of NAP, as well as the determination of latency, conduction velocity, and amplitude and area of the waveform. The secondary measure was to observe for the presence or absence of a hoof twitch in response to electric stimulation, which was elicited with a stimulating current of 1 to 2 mA delivered to the median nerve proximal to the nerve graft. Care was taken not to stretch the nerve grafts, and all tissues were kept moist with normal saline at 37° centigrade. After the electric testing was completed, the animals were euthanized with an overdose of intracardiac Euthanyl Forte (Bimeda-MTC, Cambridge, Ontario, Canada). The entire regenerated nerve segment in place of the graft, along with nerve tissue 2 cm proximal and distal to it, was harvested for histological evaluation, immunohistochemistry studies, and morphometric analysis. Electric studies were also performed on an uninjured median nerve of the single age- and sex-matched control animal in tissue that was similarly harvested and processed.

Histological Evaluation

After harvesting, each segment was divided into five 3- to 5-mm sections and two 10-mm sections and processed accordingly (Figure 2). Sections for morphometry were obtained from the midpoint of the graft and from each end, whereas sections for histology and immunohistochemistry (transverse and longitudinal sections) were taken from the segments in between. The remaining segments were preserved for future use.

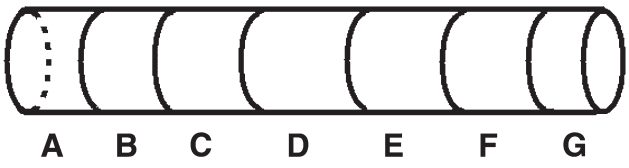

FIGURE 2. *Schematic diagram of the grafted nerve segment after explantation. A denotes the proximal end; G, the distal end. Segments A, D, and G were processed for EPON embedding and histomorphometry studies, but data from segment D, the center of the graft segment, is reported in this article for the actual morphometric analysis. Segments B and F were used for hematoxylin and eosin and immunohistochemistry studies; segment B, for longitudinal studies; and segment F, for transverse studies. Segments C and E were preserved and set aside for future use.*

The tissue was fixed by immersion in 10% formalin, embedded in paraffin, and stained with hematoxylin and eosin for routine histology. Immunostaining with anti-sera to neurofilaments (Sigma mouse monoclonal anti-neurofilament 200 Clone N52; Sigma, St Louis, Missouri), laminin (Sigma rabbit anti-laminin), and Schwann cells (DakoCytomation polyclonal rabbit anti-Cow S-100a; DakoCytomation, Carpinteria, California) was also done. For the morphometric analysis, nerve graft segments and control median nerve segments were fixed overnight in 2.5% glutaraldehyde buffered in cacodylate (0.025 mol/L), postfixed in osmium tetroxide (2%) for 2 hours, and then embedded in EPON. Semithin transverse sections 1 μm thick were cut and stained with toluidine blue. Five fields of view per section were photographed at high-power light microscopy (× 400; Olympus BX51) for analysis, in which all myelinated axons were evaluated in 3 to 4 representative fascicles. Images were digitized with a WacomIntuos3 digitizing tablet (Vancouver, Washington) and analyzed with Image Pro Plus 5.0 imaging software (Media Cybernetics, Bethesda, Maryland). The following parameters were measured: total number of axons, total number of myelinated axons (total estimated count equal to the number of myelinated axons counted in sampling area times the cross-sectional area divided by the sampling area), mean fiber diameter, G ratio (axon diameter/nerve fiber diameter), and percent neural tissue (sum of the total fiber area divided by the total area sampled times 100).

Statistical Analysis

Statistical analysis was performed with the Tukey and Student *t* tests to compare differences between groups. The level of significance was set at $P < .05$, and all results are presented as the mean ± SEM.

RESULTS

General Observations

All animals tolerated the surgical procedure well, and their surgical incisions exhibited good wound healing. There were no obvious clinical deficits from either the median or radial sensory

Copyright © Congress of Neurological Surgeons. Unauthorized reproduction of this article is prohibited.

nerve injury. Ambulation was normal, and there were no pressure sores or ulcerations around the hoof or forelimb.

On re-exploration of the wound at 6 and 9 months postoperatively, the graft sites showed very little scarring or fibrosis, thus allowing relatively easy external neurolysis. The autografts resembled normal nerves in size, color, and appearance, and no neuromas were seen at the suture site of the grafts.

Electrophysiological Findings

All the sheep demonstrated readily recordable NAPs and hoof twitch responses with 1 to 2 mA of stimulation. The average conduction velocity at 6 months was 17.7 ± 2.0 m/s, whereas that at 9 months was 20.6 ± 2.3 m/s. Meanwhile, the amplitude at 6 months was 23.09 ± 5.8 mV; at 9 months, it was 32.12 ± 6.4 mV. There were no statistical differences between groups. Both conduction velocity and amplitude increased with the passage of time from surgery but did not attain normal values within the observation period (Table 1).

Histological Findings

Microscopic Appearance

Hematoxylin and eosin sections showed that there was a greater amount of extrafascicular connective tissue in the grafted nerve than seen in the control nerve (Figure 3). There were approximately twice as many fascicles in the grafted nerves compared with the control nerve, and each fascicle was slightly smaller in the regenerated nerve. Very few extrafascicular axons were visible in the grafted nerve sections.

Immunohistochemistry

Almost all regenerating axons were confined to within the fascicle in the graft as demonstrated by S100 and laminin staining, which showed Schwann cells and endoneurial tubes nicely constrained within the intrafascicular environment (Figures 4 and 5). S100 immunoreactivity represents Schwann cells that ensheath and encapsulate the regenerating axon. Sustained axonal growth was manifested by the appearance of neurofilament-immunopositive axons in transverse sections across the graft (Figure 6).

Morphometric Analysis

The paucity of extrafascicular axons was confirmed in the EPON sections from midgraft segments (Figure 7). Morphometric assessment showed that the mean myelinated axon density was not significantly different from the control, whereas the mean fiber diameters at both 6 and 9 months were significantly lower than the control (Figure 8A and 8B). The myelination indexes (G ratio) showed that the axons were already well myelinated at 6 months and remained so at 9 months (Figure 8C). The differences in G ratio were not statistically significant from each other at any time point.

TABLE 1. Results of Electrophysiological Studies

	Conduction Velocity, m/s	Amplitude, mV
Control	23.7	49.42
At 6 mo	17.7 ± 2.0[a]	23.09 ± 5.8
At 9 mo	20.6 ± 2.3	32.12 ± 6.4

[a]Data are presented as mean ± SEM. There is no statistical difference between groups.

DISCUSSION

Animal models of repair and regeneration play an important role in the trial of various therapeutic modalities aimed at regaining function and improving neurological outcome from nerve injury. In contrast to small-animal models, large-animal models permit the creation of longer and more clinically relevant nerve defects and the harvest of long segments of donor nerves. This reflects the actual situation in most human nerve injuries in which damage to the nerve often extends over several centimeters.[14]

Sheep may prove to be an excellent model in which to investigate nerve regeneration because their nerves are polyfascicular and more akin to human nerve in histomorphology than the rat nerve.[1] Specifically, the median nerve in the sheep's foreleg was chosen as a model because it is a large mixed nerve with a size similar to that of the ulnar nerve at the wrist in humans. High division of the median nerve in the sheep weakens flexion of the forefoot and wrist but does not affect limb extension required for weight bearing and locomotion.[10] This would enable the sheep to function normally and prevent morbidity associated with paralysis and disuse. In addition, the hoof of the sheep receives overlapping sensory innervation from the ulnar and radial nerves, so hoof anesthesia and subsequent trauma and sepsis rarely occur.[10] In terms of costs, the amount of money needed to purchase, house, and feed sheep is reasonable compared with other large animals (Table 2).

Previous studies of nerve regeneration in large animal models are few, and even when performed on large animals, models often only investigate short (≤ 3 cm) nerve gaps (Table 3). Bratton et al[8] created small 1-cm defects in the tibial nerve of a primate and evaluated nerve regeneration after direct fascicular repair, epineurial repair, and repair with autografts. Mackinnon et al[11] investigated nerve regeneration across a 3-cm defect in the ulnar nerve of a primate model repaired with a pseudosynovial sheath. Glasby et al[9] used freeze-thawed muscle grafts to bridge 3-cm defects in the radial and ulnar nerves of marmoset monkeys and measured regeneration across the graft using histomorphometric, electrophysiological, and gross behavioral parameters. In another primate model used by Archibald et al,[7] a collagen-based nerve guide was used to bridge a 0.5-cm nerve defect. The degree of nerve regeneration was comparable to that using autografts and direct repair. Brenner et al[13] also used a primate model to study the effects of immunosuppression on allografts used to repair ulnar nerve defects 5 cm long. Lawson and Glasby[10] performed a series of experiments on Scottish blackface sheep to determine the success of nerve regeneration through a muscle graft

Copyright © Congress of Neurological Surgeons. Unauthorized reproduction of this article is prohibited.

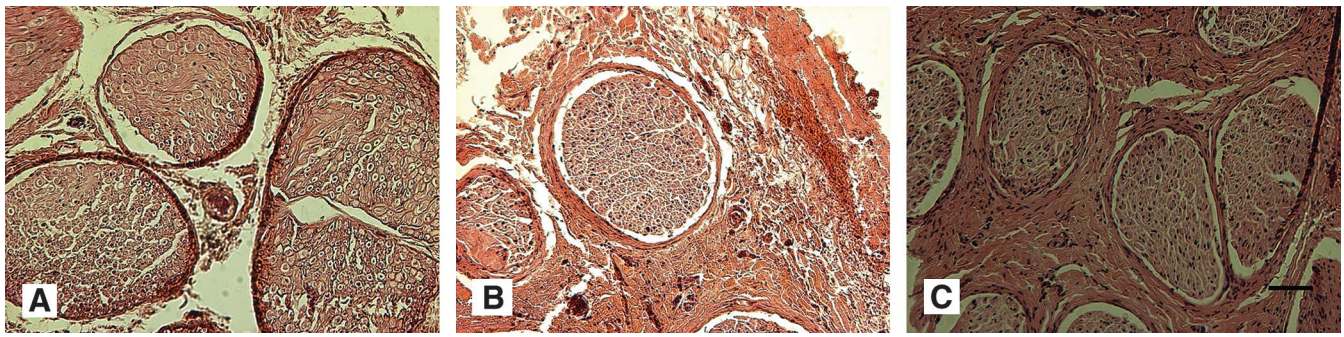

FIGURE 3. *Representative light micrographs of a cross section of the control nerve (A), distal autograft at 6 months (B), and distal autograft at 9 months (C). This section was obtained from the distal graft segment (F in Figure 2). Note that fascicles are smaller and more numerous in the autografts compared with the control median nerve and that the extrafascicular connective tissue is more abundant. Hematoxylin and eosin, × 10. Scale bar = 100 μm.*

compared with a nerve autograft. However, the defect made in the median nerve was only 3 cm and thus cannot be considered a long-segment graft model. Strasberg et al[12] implanted 8-cm-long radial sensory nerve allografts compared with autografts in sheep and found that although excellent regeneration occurred across the autografts, long nerve allografts could not support axonal elongation. Matsuyama et al[1] similarly used 8-cm-long sensory radial nerve grafts in the sheep model to study the effect of immunosuppression on the regeneration properties of long-segment autografts and allografts. These prior sheep studies were deficient because they evaluated regeneration only across pure sensory, cutaneous nerves. Atchabahian et al[6] used a swine model to investigate nerve regeneration in 8-cm ulnar nerve autografts or allografts without immunosuppression. Regeneration was excellent in the autografts at 6 and 10 months but very poor across the allografts. Matsumoto et al[3] created 8-cm gaps across the peroneal nerves of beagle dogs and implanted a polyglycolic acid–collagen nerve conduit across the defect. However, they did not include an autograft group for comparison. For researchers who wish to study longer nerve defects, the median nerve gap in this model can be further increased to a 7-cm gap by dissecting slightly more proximally into the plexus and by additionally exposing the distal segment of nerve that can be incised just before it reaches the joint. With the use of a 7-cm gap and 9- to 10-cm graft lengths, a longer regeneration distance can be evaluated if desired.

In our study, nerve regeneration was assessed using several parameters: electrophysiology, histology, immunohistochemistry, and morphometry. The minimum time point for evaluation was set at 6 months to allow the majority of the regenerating axons to have extended beyond the distal end of the graft and to be able to measure electrophysiological recovery. Behavioral studies are not applicable for this model because injury to the median or the sensory radial nerves of sheep does not produce any discernible functional deficit.

Morphological and electrophysiological features seldom regain preinjury values after injury and repair of a nerve.[10] On microscopic analysis, the grafted nerves showed structural preservation with recognizable fascicles within the nerve, although there was a greater amount of extrafascicular connective tissue. This finding was consistent with other histological studies in which a fascicular

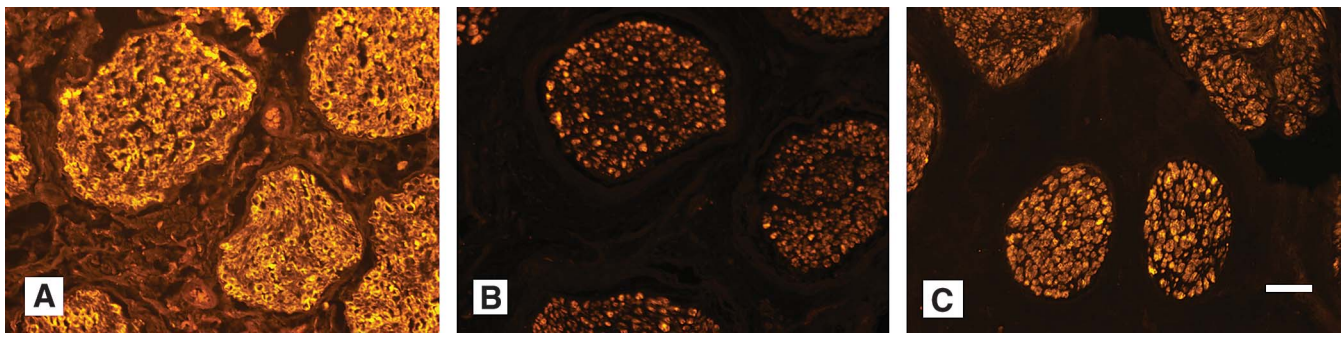

FIGURE 4. *Anti-S100 immunohistochemistry performed on a cross section of the control nerve (A), distal autograft at 6 months (B), and distal autograft at 9 months (C). This section also was obtained from segment F in Figure 2. Note the brightly fluorescent S100-stained Schwann cells confined within the fascicles. Scale bar = 100 μm.*

Copyright © Congress of Neurological Surgeons. Unauthorized reproduction of this article is prohibited.

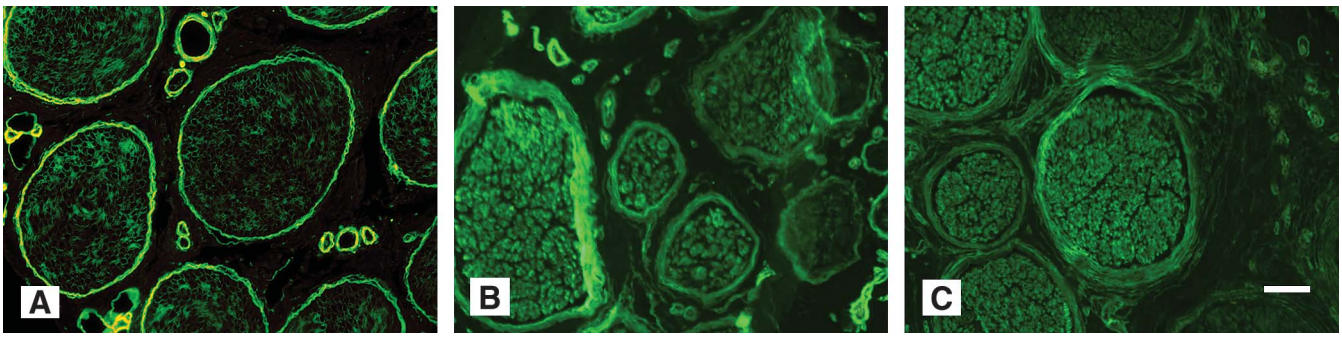

FIGURE 5. *Anti-laminin immunohistochemistry performed on a cross section of the control nerve (A), distal autograft at 6 months (B), and distal autograft at 9 months (C). This section was obtained from segment F in Figure 2. Note that laminin stains the basal lamina of the blood vessels, perineurium, and endoneurium. Specifically, the laminin stains demonstrate the presence of endoneurial tubes within the intrafascicular environment. Scale bar = 100 μm.*

pattern was usually discerned within the grafted segment, with the majority of regenerating axons in an intrafascicular location and only rare clusters of regenerating axons seen interspersed within connective tissue.[15] However, some of the regenerating axons were in an extrafascicular location, and it was only in the distal stump sections that the fascicles were consistently well defined, with very few extrafascicular axons visible.[15]

Immunohistochemistry revealed considerable infiltration of Schwann cells into the graft as shown by S100 immunostaining. The extent of axonal regeneration in the grafts was indicated by neurofilament immunolabeling,[16] whereas the integrity of the basal lamina encasing the axons was demonstrated by anti-laminin stains. Normally, a neurofilament-immunolabeled axon is accompanied by an S100-immunolabeled Schwann cell and surrounded by a laminin-immunopositive endoneurial sheath,[16] so a regenerating nerve should have sufficient quantities of all 3 components.

In addition to histological studies, morphometric assays were analyzed to confirm successful regeneration of axons through nerve grafts and into the targeted reinnervation site. Indexes of regeneration include axon counts, fiber size, and degree of myelination. Generally, the greater the number of myelinated axons is, and the thicker the layer of myelin is and the more successful the degree of nerve regeneration and maturation is.

When nerves are injured, there is a shift to the left in the fiber diameter spectrum of the nerve, so that repaired nerves contain a population of much smaller nerve fibers.[10] This is presumed to be due to a failure of either regeneration or maturation of the larger-diameter, faster-conducting fibers.[10] However, the diameter of regenerated myelinated nerve fibers has been shown to increase gradually with time, approaching but not exactly attaining the normal level over a long period of regeneration.[11] Despite having a population of smaller nerve fibers, repaired nerves may have a G ratio that approaches normal, suggesting that

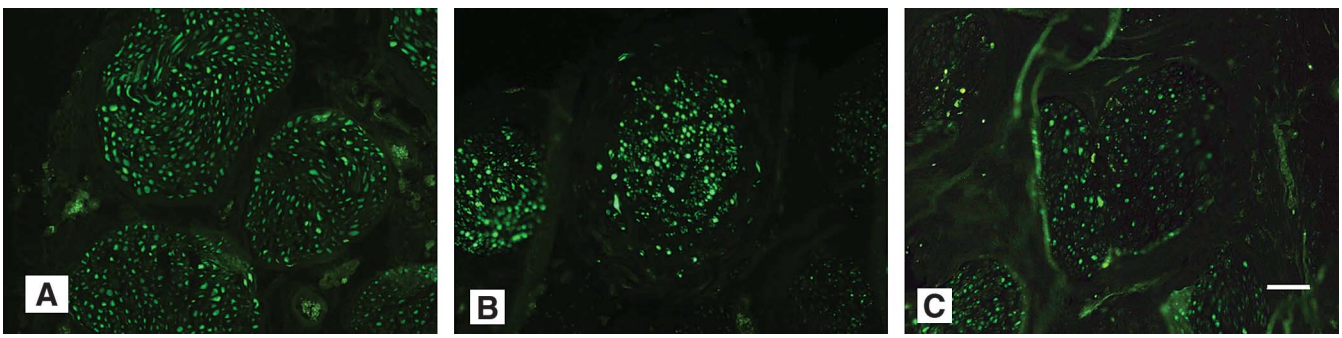

FIGURE 6. *Anti-neurofilament immunohistochemistry performed on a cross section of the control nerve (A), distal autograft at 6 months (B), and distal autograft at 9 months (C). This section was obtained from segment F in Figure 2. Note the brightly fluorescent immunolabeled neurofilaments within the endoneurium, indicating the presence of axons. Scale bar = 100 μm.*

Copyright © Congress of Neurological Surgeons. Unauthorized reproduction of this article is prohibited.

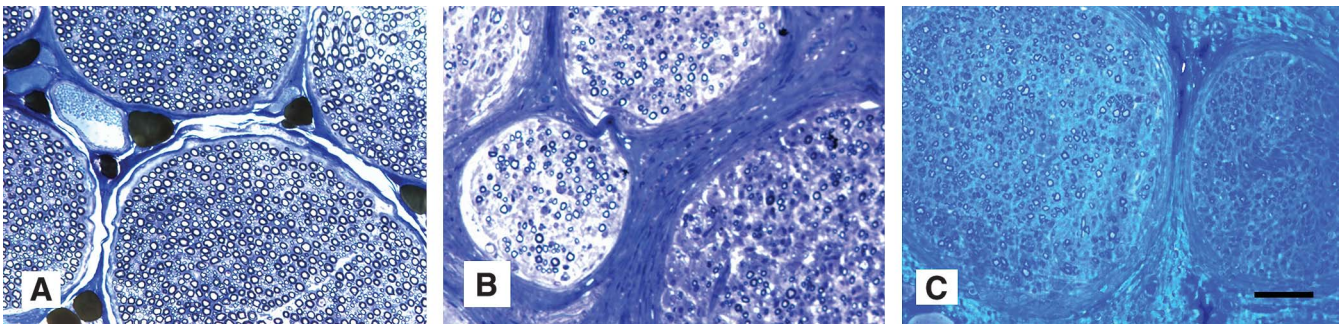

FIGURE 7. *Representative light micrographs of semithin transverse sections from the control nerve (A), autograft at 6 months (B), and autograft at 9 months (C). The control nerve demonstrates normal morphology, with numerous large, well-myelinated axons. Both autografts exhibit the appearance of regenerating nerve tissue, with greater numbers of small-diameter axons and a greater amount of extrafascicular and endoneurial connective tissue throughout the nerve. Scale bar = 100 μm.*

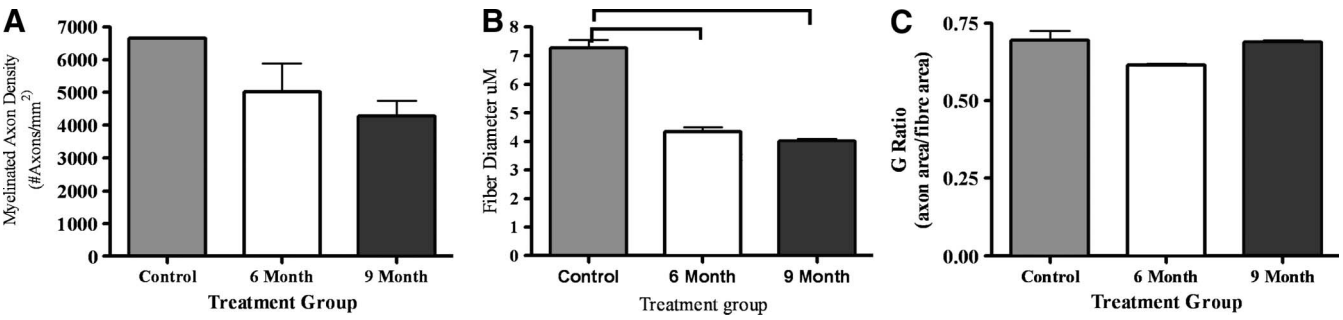

FIGURE 8. *Histograms of the morphometric measurements for control nerve and autografts at 6 and 9 months. A, mean myelinated axon density shows no statistically significant difference between the three, which is indicative of excellent nerve regeneration. B, mean fiber diameters at 6 and 9 months are significantly smaller than the control ($P < .001$, the Tukey test), as is evidenced by the smaller fascicles on histology. C, the mean G ratio or myelination index among the 3 are similar with no statistically significant differences between the groups. All bars represent mean ± SEM.*

axons that do regenerate are in fact well myelinated and have reached full maturity.[10] In this study, mean fiber diameter was significantly smaller in the 2 experimental groups compared with the control; however, the axon densities and G ratio had no significant difference even if they were nominally decreased in value.

As mentioned previously, electrophysiological features rarely return to normal levels after nerve repair.[10] Although all the grafted nerves exhibited a NAP across its length, the nerve conduction velocities at 6 and 9 months were only 74.7% and 86.9%, respectively, of the normal nerve. Likewise, the amplitude of the NAP's was less than the control. The difference between the grafted and control nerves, however, was not significant. The values also exhibited an upward trend with the passage of time, approaching but not reaching the control values. This implies that either full regeneration has not yet been achieved or the electrophysiological properties of a repaired nerve never truly become normal, consistent with prior literature.[10]

The decreased conduction velocity of grafted nerves can be inversely correlated with the G ratio because the thickness of the myelin sheath can affect the conduction velocity of myelinated nerve fibers.[4,10] Other factors that may contribute to the slower conduction velocity include the smaller diameter of the regenerating axons, shorter internodes, and immaturity of the regenerated nerve fibers as a whole.[4]

The median nerve in the sheep forelimb is a reproducible and reliable model for assessing regeneration through long peripheral

TABLE 2. Comparative Costs for Purchasing, Feeding, and Housing Select Laboratory Animals at the University of Calgary

	Purchase Cost, Can$	Housing and Feeding Costs, Can$/d
Rat	49.80	2.06
Rabbit	128.80	2.32
Dog	486.00	9.65
Pig	290.00	8.09
Sheep	375.00	8.04

Copyright © Congress of Neurological Surgeons. Unauthorized reproduction of this article is prohibited.

TABLE 3. Review of the Literature on Large Animals and/or Animals With Long Nerve Graft (> 5 cm)

Author/Year	Animal Model	Size of Defect/Graft, Location, Intervention	Assessment of Regeneration	Outcome
Bratton et al[8] (1979)	Primate (rhesus monkeys)	Group 1: tibial nerves transected, trimmed, and repaired with autografts vs direct fascicular repair; group 2: 1-cm defect in tibial nerve repaired with autografts vs direct epineurial repair under some tension	Histology, morphometry, electrophysiology	Assessment at 4, 6, 9, and 12 mo shows that results of direct end-to-end suture repair is superior to graft repair, but if this cannot be achieved, use of short nerve grafts for repair is a good alternative because of evidence of regeneration across it
MacKinnon et al[11] (1985)	Primate	A 3-cm defect in the ulnar nerve repaired with a pseudosynovial sheath	Histology, morphometry	Histological evaluation at 3, 5, 7, and 9 mo showed evidence of nerve regeneration across the defect
Glasby et al[9] (1986)	Primate (marmosets)	A 3-cm defect in the radial and ulnar nerves repaired with freeze-thawed muscle grafts; no autograft group	Histology, morphometry, electrophysiology, behavior	At 6 mo, there was return of normal hand function and normal compound action potentials; morphometry showed normal axon numbers and axon maturity across the graft, but myelination is significantly poorer than the control
Archibald et al[7] (1995)	Primate (macaques)	A 0.5-cm defect in 15 median nerves and 1 ulnar nerve bridged by collagen-based nerve guides vs autografts vs direct suture repair	Histology, morphometry, electrophysiology	Assessment was done over 3.5 y; nerve regeneration after repair with a collagen nerve guide was similar to that after graft repair; final level of electrophysiological recovery was comparable in all 3 groups
Strasberg et al[12] (1996)	Sheep	An 8-cm radial nerve allograft vs autograft, comparing fresh and cold-preserved samples of each	Histology, morphometry, electrophysiology	Assessment was done at 6 and 10 mo; regeneration was excellent across the autografts but poor across the allografts; cold nerve preservation did not enhance regeneration
Lawson and Glasby[10] (1998)	Sheep	A 3-cm defect in median nerve repaired with freeze-thawed muscle grafts vs autografts	Histology, morphometry, electrophysiology, nerve blood flow	At 6 mo, nerve blood flow and nerve conduction velocity were comparable between the regenerating nerves repaired with muscle grafts and autografts, although both were reduced compared with the control
Atchabahian et al[6] (1998)	Pig	An 8-cm ulnar nerve allograft vs autograft; no immunosuppression given	Histology, morphometry	Assessment was done at 6 and 10 mo; nerve regeneration was excellent across the autografts and very poor across the allografts
Matsuyama et al[1] (2000)	Sheep	An 8-cm radial nerve allografts vs autografts; effect of immunosuppression with cyclosporine was assessed	Histology, immunologic assays	Assessment was done between 35 and 47 d postoperatively because of severe opportunistic infections necessitating early sacrifice; evidence of nerve regeneration seen in the autografts and allografts that were treated with cyclosporine; nonimmunosuppressed allografts were rejected
Matsumoto et al[3] (2000)	Dog (beagles)	An 8-cm defect in the peroneal nerve bridged by a polyglycolic acid–collagen nerve conduit; no autograft group	Histology, immunohistochemistry, morphometry, electrophysiology, behavior	After 12 mo, there was good evidence of axonal regeneration across the conduit; there was also favorable functional recovery
Brenner et al[13] (2004)	Primate (macaques)	A 5-cm ulnar allograft vs autograft; effect of CD40 antibody assessed	Histology, morphometry, immunologic assays	Assessment was done between 4 and 6 mo postoperatively; allografts were rejected without CD40 or after withdrawal of CD40

Copyright © Congress of Neurological Surgeons. Unauthorized reproduction of this article is prohibited.

nerve grafts. It mimics the human nerve graft model in that it is a multifascicular mixed motor and sensory nerve with electrophysiological and morphometric indexes that are much more akin to humans than the more commonly used rodent graft models. The main limitation is that sheep exhibit no easily demonstrable clinical deficit with median nerve injury, so it is not possible to measure functional outcome. However, compound muscle action potentials can also be recorded from the flexor carpi radialis muscle, which is innervated by the median nerve. The compound muscle action potential amplitude from this muscle would serve as an additional means of assessing nerve regeneration to augment the other measures described here.

Disclosure

The authors have no personal financial or institutional interest in any of the drugs, materials, or devices described in this article.

REFERENCES

1. Matsuyama T, Midha R, Mackinnon SE, Munro CA, Wong PY, Ang LC. Long nerve allografts in sheep with cyclosporin A immunosuppression. *J Reconstr Microsurg*. 2000;16(3):219-225.
2. Cai J, Peng X, Nelson KD, Eberhart R, Smith GM. Synergistic improvements in cell and axonal migration across sciatic nerve lesion gaps using bioresorbable filaments and heregulin-B1. *J Biomed Mater Res*. 2004;69A(2):247-258.
3. Matsumoto K, Ohnishi K, Kiyotani T, et al. Peripheral nerve regeneration across an 80-mm gap bridged by a polyglycolic acid (PGA)-collagen tube filled with laminin-coated collagen fibers: a histological and electrophysiological evaluation of regenerated nerves. *Brain Res*. 2000;868(2):315-328.
4. Wang X, Hu W, Cao Y, Yao J, Wu J, Gu X. Dog sciatic nerve regeneration across a 30-mm defect bridged by a chitosan/PGA artificial nerve graft. *Brain*. 2005;128(8),1897-1910.
5. Evans PJ, Midha R, Mackinnon SE. The peripheral nerve allograft: a comprehensive review of regeneration and neuroimmunology. *Prog Neurobiol*. 1994;43(3):187-233.
6. Atchabahian A, Genden EM, Mackinnon SE, Doolabh VB, Hunter DA. Regeneration through long nerve grafts in the swine model. *Microsurgery*. 1998;18(6):379-382.
7. Archibald SJ, Shefner J, Krarup C, Madison RD. Monkey median nerve repaired by nerve graft or collagen nerve guide tube. *J Neurosci*. 1995;15(5):4109-4123.
8. Bratton BR, Kline DG, Coleman W, Hudson AR. Experimental interfascicular nerve grafting. *J Neurosurg*. 1979;51(3):323-332.
9. Glasby MA, Gschmeissner SE, Huang CL, De Souza BA. Degenerated muscle grafts used for peripheral nerve repair in primates. *J Hand Surg Br*. 1986;11(3):347-351.
10. Lawson GM, Glasby MA. Peripheral nerve reconstruction using freeze-thawed muscle grafts: a comparison with group fascicular nerve grafts in a large animal model. *J R Coll Surg Edinb*. 1998;43(5):295-302.
11. Mackinnon SE, Dellon AL, Hudson AR, Hunter DA. Nerve regeneration through a pseudosynovial sheath in a primate model. *Plast Reconstr Surg*. 1985;75(6):833-841.
12. Strasberg SR, Mackinnon SE, Genden EM, et al. Long-segment nerve allograft regeneration in the sheep model: experimental study and review of the literature. *J Reconstr Microsurg*. 1996;12(8):529-537.
13. Brenner MJ, Jensen JN, Lowe JB, et al. Anti-CD40 ligand antibody permits regeneration through peripheral nerve allografts in a nonhuman primate model. *Plast Reconstr Surg*. 2004;114(7):1802-1814.
14. Midha R. Mechanisms and pathology of injury. In: Kim DH, Midha R, Murovic JA, et al, eds. *Kline and Hudson's Nerve Injuries: Operative Results for Major Nerve Injuries, Entrapments, and Tumors*. 2nd ed. Beijing, China: Elsevier Saunders; 2008:23-42.
15. Hudson AR, Hunter D, Kline DG, Bratton BR. Histological studies of experimental interfascicular graft repairs. *J Neurosurg*. 1979;51(3):333-340.
16. Neubauer D, Graham JB, Muir D. Chondroitinase treatment increases the effective length of acellular nerve grafts. *Exp Neurol*. 2007;207(1):163-170.

Acknowledgments

We would like to thank AxoGen Inc, Alachua, Florida, for financial support that aided this work and Dr Jacob Alant for his assistance in preparing this manuscript.

COMMENT

This article describes a large-animal model of long-segment median nerve repair with radial nerve autograft. This study is important for several reasons.

First, the sheep model provides a large animal platform to study long segment graft repairs, a procedure that is technically impossible in small-animal (eg, rodent) models. Thus, promising therapies that could potentially be used to enhance the recovery across long segment graft repairs can be tested in a translational model before their introduction in human clinical trials.

Second, the sheep model is technically straightforward, including the relative paucity of scar tissue in the previously operated field. I personally find the amount of scar tissue in the cat model I use in my laboratory completely aggravating during reoperative peripheral nerve surgery. In addition, a sheep model is far less expensive and less problematic than a primate model. Thus, larger studies can be used to evaluate novel graft therapies with relative cost-effectiveness. Plus, the use of primate animal models tends to attract the attention of ecoterrorists, who can really complicate the effective completion of good animal research studies. Sheep models typically do not.

That median nerve injury has minimal impact on the sheep neurological examination is a mixed blessing. Large animals with severe neurological deficits can require a lot of labor-intensive postoperative care, and seeing these animals day after day can be discouraging. Investigators using this sheep model do not have to address these issues. On the other hand, the lack of obvious neurological deficits limits the ability to use functional outcome measures, as the authors acknowledge.

One limitation of this study is the excellent recovery seen in the grafted animals. That there were only insignificant electrodiagnostic differences between experimental and control animals could be problematic in powering future studies with this model. For example, using this model to asses a new therapy designed to enhance nerve graft recovery might require a very large number of subjects to discern a significant difference between control animals, grafted animals, and grafted and treated animals. Perhaps using an even longer graft construct could help with this.

Christopher J. Winfree
New York, New York

Copyright © Congress of Neurological Surgeons. Unauthorized reproduction of this article is prohibited.

Induction of Angiogenesis and Modulation of Vascular Endothelial Growth Factor Receptor-2 by Simvastatin After Traumatic Brain Injury

Hongtao Wu, MD*§
Hao Jiang, PhD‡
Dunyue Lu, MD, PhD¶
Changsheng Qu, MD*
Ye Xiong, MD, PhD*
Dong Zhou, MD§
Michael Chopp, PhD‡‖
Asim Mahmood, MD*

Departments of *Neurosurgery and ‡Neurology, Henry Ford Hospital, Detroit, Michigan; §Department of Neurology, West China Hospital, Sichuan University, Chengdu, People's Republic of China; ¶Department of Psychiatry, State University of New York at Downstate Medical Center, Brooklyn, New York; ‖Department of Physics, Oakland University, Rochester, Michigan

Correspondence:
Asim Mahmood, MD,
Henry Ford Hospital,
Neurosurgery Department,
2799 W Grand Blvd,
Detroit, MI 48202.
E-mail: nsaam@neuro.hfh.edu

Received, March 24, 2010.
Accepted, July 23, 2010.

Copyright © 2011 by the
Congress of Neurological Surgeons

BACKGROUND: Our previous studies demonstrated that simvastatin reduced neuronal death, increased neurogenesis, and promoted functional recovery after traumatic brain injury (TBI).

OBJECTIVE: To investigate the effect of simvastatin on angiogenesis after TBI and the related signaling pathways.

METHODS: Saline or simvastatin (1 mg/kg) was administered orally to rats starting at day 1 after TBI or sham surgery and then daily for 14 days. Rats were sacrificed at 3 and 14 days after treatment. Brain sections and tissues were prepared for immunohistochemical staining, enzyme-linked immunosorbent assay, and Western blot analysis. Cultured rat brain microvascular endothelial cells were subjected to oxygen-glucose deprivation followed by immunocytochemical staining with phallotoxins and vascular endothelial growth factor receptor-2 (VEGFR-2). Western blot analysis was carried out to examine the simvastatin-induced activation of the v-akt murine thymoma viral oncogene homolog (Akt) signaling pathway. The expression of VEGFR-2 was detected by enzyme-linked immunosorbent assay.

RESULTS: Simvastatin significantly increased the length of vascular perimeter, promoted the proliferation of endothelial cells, and improved the sensorimotor function after TBI. Simvastatin stimulated endothelial cell tube formation after oxygen-glucose deprivation in vitro. VEGFR-2 expression in both brain tissues and cultured rat brain microvascular endothelial cells was enhanced after simvastatin treatment, which may be modulated by activation of Akt. Akt-dependent endothelial nitric oxide synthase phosphorylation was also induced by simvastatin in vivo and in vitro.

CONCLUSION: Simvastatin augments TBI-induced angiogenesis in the lesion boundary zone and hippocampus and improves functional recovery. Simvastatin also promotes angiogenesis in vitro. These beneficial effects on angiogenesis may be related to simvastatin-induced activation of the VEGFR-2/Akt/endothelial nitric oxide synthase signaling pathway.

KEY WORDS: Angiogenesis, Simvastatin, Traumatic brain injury, VEGFR-2

Neurosurgery 68:1363–1371, 2011 DOI: 10.1227/NEU.0b013e31820c06b9 www.neurosurgery-online.com

ABBREVIATIONS: BrdU, bromodeoxyuridine; **BSA,** bovine serum albumin; **DAPI,** 4′-6-diamidino-2-pheylindole; **ELISA,** enzyme-linked immunosorbent assay; **eNOS,** endothelial nitric oxide synthase; **GSK-3,** glycogen synthase kinase-3; **OGD,** oxygen-glucose deprivation; **PBS,** phosphate-buffered saline; **PI3K,** phosphatidylinositol 3-kinase; **RBMVEC,** rat brain microvascular endothelial cell; **TBI,** traumatic brain injury; **VEGF,** vascular endothelial growth factor; **VEGFR,** vascular endothelial growth factor receptor; **vWF,** von Willebrand factor

Traumatic brain injury (TBI) remains a major cause of serious, long-term disability worldwide. Despite the extensive research being conducted in this field, there still is no effective clinical treatment for TBI. Regional ischemia early after TBI and a relationship between the volume of ischemic tissue and neurological outcomes have been reported.[1]

After TBI, there is a substantial increase in angiogenesis, and focal angiogenesis may provide oxygen and nutrition for cerebral

Copyright © Congress of Neurological Surgeons. Unauthorized reproduction of this article is prohibited.

reconstruction.[2] Solely targeting neuroprotection after TBI has not proven sufficient for promoting functional recovery.[3] To reduce brain tissue damage and restore neural function, one may have to rescue all the complex signals and interactions between a network of multiple cell types, including neurons, astrocytes, and microvascular endothelial cells.[4] Therefore, cerebral vasculature–based therapy combined with neuroprotection may be a reasonable approach for TBI therapy.

The 3-hydroxy-3-methylglutaryl co-enzyme A reductase inhibitors (statins) have pleiotropic effects that are independent of cholesterol metabolism. A low dose of statins activates angiogenesis in a number of animal models, including ischemic stroke[5-7] and TBI.[8] Simvastatin at the same dose is superior to atorvastatin in treating TBI because of its ability to cross the blood-brain barrier.[9] In previous studies, we demonstrated that simvastatin modulates neuronal death, increases neurogenesis, and promotes neurological functional recovery after TBI.[10] Angiogenesis and neurogenesis are coupled in the brain,[11] and simvastatin treatment promotes angiogenesis.[9] However, the present study is the first endeavor to seek the molecular basis of induction of angiogenesis by simvastatin after TBI.

Simvastatin upregulates vascular endothelial growth factor (VEGF) expression after TBI,[12] and VEGF is an important mitogen in the process of angiogenesis. The binding of VEGF to its receptor VEGFR-2 (flk-1) on the surface of endothelial cells activates intracellular tyrosine kinases, triggering multiple downstream signals that promote angiogenesis. Among these signals, Akt-dependent endothelial nitric oxide synthase (eNOS) phosphorylation is crucial for angiogenesis.[13]

In this study, we investigate the effect of simvastatin on angiogenesis after TBI. To examine a possible mechanism for the angiogenic effects of simvastatin that subsequently enhanced the functional recovery, we focused on the VEGFR-2/Akt/eNOS pathway, which has been implicated as a key signaling pathway for angiogenesis.

MATERIALS AND METHODS

Materials

Simvastatin for in vivo study was purchased from Merck (Whitehouse Station, New Jersey). Simvastatin 5 mg for in vitro study was obtained from Sigma Aldrich (St Louis, Missouri), dissolved in 0.2 mL of 100% ethanol, and then diluted to a volume of 1 mL with dimethyl sulfoxide. The stock solution of simvastatin (12 mmol/L) was further diluted to appropriate concentrations with cell culture medium immediately before use. The control experiments used dimethyl sulfoxide only. Rat brain microvascular endothelial cells (RBMVECs) were purchased from American Type Culture Collection (ATCC catalog No. R840-05; Manassas, Virginia). Von Willebrand factor (vWF) antibody was obtained from DakoCytomation (Carpinteria, California). Glycogen synthase kinase-3 (GSK-3) inhibitor (lithium chloride [LiCl]) and bromodeoxyuridine (BrdU) were purchased from Sigma Aldrich. A specific phosphatidylinositol 3-kinase (PI3K) inhibitor, LY294002 [2-(4-morpholinyl)-8-phenyl-4H-1-benzopyran-4-one], was obtained from Calbiochem (La Jolla, California). A selective VEGFR-2 antagonist, SU1498, was obtained from LC Laboratories (Woburn, Massachusetts). DC101, a neutralizing antibody against VEGFR-2, was obtained from ImClone Systems, Inc (New York, New York). Antibodies against VEGFR-2, phospho-Akt (ser473), Akt, phosphor–GSK-3β (Ser9), and phospho-eNOS (Ser1177) were purchased from Cell Signaling Technology (Beverly, Massachusetts). Antibodies against actin (I-19) were obtained from Santa Cruz Biotechnology (Santa Cruz, California).

TBI Model

A modified controlled cortical injury model of TBI in rats was used in the present study.[14] Adult male Wistar rats weighing 300 to 400 g were anesthetized intraperitoneally with chloral hydrate (350 mg/kg body weight). Rectal temperature was maintained at 37°C by use of a feedback-regulated water heating pad. A controlled cortical injury device was used to induce injury. Rats were placed in a stereotactic frame. Two 10-mm-diameter craniotomies were performed adjacent to the central suture, midway between the lambda and the bregma. The second craniotomy allowed lateral movement of cortical tissue. The dura mater was kept intact over the cortex. Injury was induced by striking the left (ipsilateral) cortex with a pneumatic piston with a 6-mm-diameter tip at a rate of 4 m/s and 2.5-mm compression. Velocity was measured with a linear velocity displacement transducer. Sham-injured animals were similarly anesthetized, and craniectomy was performed without cortical injury.

Experimental Groups

Male Wistar rats were randomly divided into 3 groups (n = 12 per group). Rats in the first group were subjected to TBI and given saline orally 1 day later and then consecutively for 14 days. Rats in the second group were subjected to TBI, and simvastatin was administered orally 1 day later at a dose of 1 $mg \cdot kg^{-1} \cdot d^{-1}$ for 14 consecutive days. Rats in the third group were subjected to sham surgery. Four rats in each group were sacrificed at 3 days after administration of simvastatin, and cortical tissues in lesion boundary zone were harvested for enzyme-linked immunosorbent assay (ELISA) of VEGFR-2. The other 8 rats were sacrificed at 14 days after administration of simvastatin.

Foot-Fault Functional Test

The foot-fault test[15] was performed before TBI and at 1, 3, 7, and 14 days after treatment by an investigator blinded to the experimental groups. A total of 50 steps were measured for each right hind limb. The percentage of foot faults of the right hind limb to total steps was determined.

vWF Staining

To identify vascular structure, coronal sections were immunohistochemically stained with vWF antibody.[16] Brain sections were deparaffinized and then incubated with 0.4% pepsin solution at 37°C for 1 hour. After washing, the sections were blocked with 1% bovine serum albumin (BSA) at room temperature for 1 hour and then incubated with rabbit anti-human vWF (1:200; DakoCytomation) at 4°C overnight. After washing, sections were incubated with biotinylated anti-rabbit antibody (1:200; Vector Laboratories, Inc, Burlingame, California) and then with an avidin-biotin-peroxidase system, visualized with diaminobenzidine, and counterstained with hematoxylin.

Immunofluorescent Staining

Newly generated endothelial cells were identified by double labeling for BrdU and vWF. After dehydration, tissue sections were boiled in

Copyright © Congress of Neurological Surgeons. Unauthorized reproduction of this article is prohibited.

10-mmol/L citric acid buffer (pH 6) for 10 minutes. Sections were incubated with 1% BSA containing 0.3% Triton-X-100 in phosphate-buffered saline (PBS). Sections were then incubated with rabbit anti-vWF antibody (1:200; Chemicon, Temecula, California) at 4°C overnight. FITC-conjugated anti-rabbit antibody (1:400; Jackson ImmunoResearch, West Grove, Pennsylvania) was added to sections at room temperature for 2 hours. The sections were then treated with 50% formamide in 2 × SSC (300 mM NaCl, 30 mM sodium citrate, pH 7.0) at 65°C for 30 minutes, followed by 10 minutes at 37°C in 2N HCl and 3 minutes at room temperature in 0.1 mol/L boric acid. After PBS wash, sections were then incubated with mouse anti-BrdU antibody (1:200; Dako, Glostrup, Denmark) at 4°C overnight. Sections were then incubated with Cy3-conjugated anti-mouse antibody (1:400; Jackson ImmunoResearch) at room temperature for 2 hours. Each of the steps was followed by three 5-minute rinses in PBS. Tissue sections were mounted with Vectashield mounting medium (Vector Laboratories). Sections were observed with the aid of a fluorescent microscope.

Stereology

The unbiased stereology method was used in cell counting using MCID stereology software (version 7.0; Linton, Cambridge, United Kingdom). A series of coronal sections were cut from the bregma −2.12 to −6.04 mm of each rat.[17] A pilot study was performed to determine Gunderson coefficients and counting space.[18] From the pilot study, we determined the appropriate grid size (distance between sampling sites on each section), counting frame size, dissector height, top and bottom guard zone sizes, and target coefficient of error for the sampling parameters to achieve an acceptable level of sampling error. Using these parameters, we then implemented the 3-dimensional fractionator (MCID). Using the automated optical fractionator method, we drew the lesion boundary zone and hippocampus areas on coronal sections at low magnification. A higher power was selected, and the system used random systematic sampling to sample a 5% to 10% defined region of interest, depending on cellular density within the region.

Enzyme-Linked Immunosorbent Assay

Using ELISA kits (R&D Systems, Minneapolis, Minnesota; catalog No. MVR200B), we measured VEGFR-2 expression using equal amounts of lysate from brain tissue samples in lesion boundary zone or from cultured RBMVECs.

Cell Culture

RBMVECs were cultured in RBMVECs groin ain 0-05r Biostatistician sed in this proprosal wth medium (ATCC, catalog No. R819-500) at 37°C in a humidified incubator containing 5% CO_2. To explore the signaling pathways and proteins mediating the proangiogenetic effects of simvastatin on endothelial cells, the PI3K inhibitor LY294002 (10 μmol/L; which subsequently inhibits phosphorylation of Akt), the GSK-3 activation inhibitor LiCl (3 mmol/L), and the VEGFR-2 antagonist SU1498 (5 μmol/L) were added in the culture medium along with simvastatin treatment to block the corresponding signaling targets.

In Vitro Oxygen Glucose Deprivation/ Reoxygenation Model

RBMVECs were seeded in tissue culture plates containing normal medium until they attached to the plates. Normal growth medium was then replaced with Dulbecco modified Eagle medium without glucose, and the cells were incubated in an anaerobic chamber (model 1025; Forma Scientific, Marietta, Ohio) for 3 hours. The oxygen level within the anaerobic chamber was routinely measured with a BD Disposable Anaerobic Indicator (Becton Dickinson Co, Sparks, Maryland), which confirmed that the oxygen level remained below 0.2%. After oxygen-glucose deprivation (OGD), glucose-free Dulbecco modified Eagle medium was replaced with normal growth medium, and the cells were incubated under normal culture conditions. Simvastatin was added at the start of OGD and maintained during the reoxygenation process. After 24 hours, cells were detached and collected for further study.

Immunocytochemistry

Cells were fixed with a fixing solution (ie, 4% paraformaldehyde in 0.01 mol/L PBS, pH 7.5) at 25°C for 15 minutes. Cells were then washed 3 times for 5 minutes with PBS and permeabilized with a solution containing 1% BSA and 0.3% Triton X-100 in PBS for 30 minutes. Cells were incubated with fluorescent phallotoxins (200 U/mL; Invitrogen, Carlsbad, California) for 20 minutes in the dark. After PBS washing, cells were incubated with a monoclonal rabbit anti–VEGFR-2 antibody (diluted 1:100, Cell Signaling Technology) in 1% BSA overnight at 4°C. Cells were then washed 3 times for 5 minutes with PBS. VEGFR-2 immunoreactivity was visualized with a goat anti-rabbit secondary antibody conjugated to CY-3 (Jackson ImmunoResearch). Cell nucleus was counterstained with 4′-6-diamidino-2-pheylindole (DAPI). Slides were mounted with Fluoromount-G mounting media on glass and analyzed under a fluorescence microscope (Nikon, Tokyo, Japan).

Western Blot Analysis

After various treatments, cells were collected and washed once with 1 × PBS, lysed in lysis buffer on ice for 30 minutes, and briefly sonicated. Protein concentrations were determined. Equal amounts of cell lysate were subjected to sodium dodecyl sulfate–polyacrylamide electrophoresis on Novex Tris-glycine gels (Invitrogen); then, separated proteins were electrotransferred to polyvinylidene fluoride membranes (Millipore, Bedford, Massachusetts). After exposure to various antibodies, specific proteins were detected with the SuperSignal West Pico chemiluminescence substrate system (Pierce, Rockford, Illinois). The band intensity was analyzed with Scion image software (Scion, Frederick, Maryland).

Matrigel-Based Capillary Tube Formation Assay

Matrigel was thawed on ice overnight and diluted 1:3 in serum free cell culture medium. Diluted Matrigel (100 μL) was put on a prechilled well of a 96-well plate and then placed in an incubator at 37°C for 30 minutes until solidified. The cells to be tested (2×10^4 cells per well) were resuspended in growth medium, carefully placed onto the solidified Matrigel, and incubated at 37°C with 5% CO_2. Development of capillarylike networks was evaluated between 2 and 4 hours after plating. The plates were photographed with an inverted microscope (Leica, Bensheim, Germany). The length of completed tubelike structures in 5 random fields (10-fold magnification) was quantified in a blinded fashion with the MCID image analysis software (Linton).http://www.mcid.co.uk/

Statistical Analyses

All data are presented as means with SDs. For cell counting and vWF-stained vascular density, a 1-way analysis of variance test followed by

Copyright © Congress of Neurological Surgeons. Unauthorized reproduction of this article is prohibited.

a posthoc Student-Newman-Keuls test was used to compare the difference between different groups. Data were analyzed by repeated-measures analysis of variance for sensorimotor function. Statistical significance was taken at values of $P < .05$.

RESULTS

Simvastatin Improves Sensorimotor Function After TBI

The incidence of right forelimb (contralateral to TBI) foot faults before TBI was approximately 3%. Animals in the sham group showed only a slight increase in the incidence of foot-fault 1 day after surgery.

TBI significantly increased the incidence of right hind limb foot faults at 1 to 14 days after injury compared with the sham rats ($P = .001$ vs sham; Figure 1). Simvastatin treatment significantly reduced the incidence of foot faults from 4 days after injury ($P = .003$ vs saline), and this effect persisted to the last observation time point ($P = .012$ vs saline; Figure 1). There is no significant difference in the incidence of foot faults between the simvastatin-treated group and the sham group on day 14 after injury ($P = .061$ vs sham), which suggests that simvastatin promotes the sensorimotor functional recovery after TBI.

Simvastatin Treatment of TBI Increases Angiogenesis in the Injured Brain

To evaluate the angiogenesis after TBI, vascular perimeter was measured with vWF staining. Figure 2A through 2G shows that the vascular perimeter ($P = .008$ vs saline in cortex, $P = .006$ vs saline in hippocampus; Figure 2G) increased significantly in the simvastatin treatment group compared with the saline control group after TBI. Figure 2H through 2K show that BrdU-positive endothelial cells were significantly increased in the TBI rats ($P = .003$ vs sham; Figure 2K) compared with sham rats. Furthermore, simvastatin increased the BrdU-positive endothelial cells ($P = .001$ vs saline; Figure 2K) compared with saline treatment after TBI, suggesting that simvastatin enhanced the proliferation of endothelial cells after TBI.

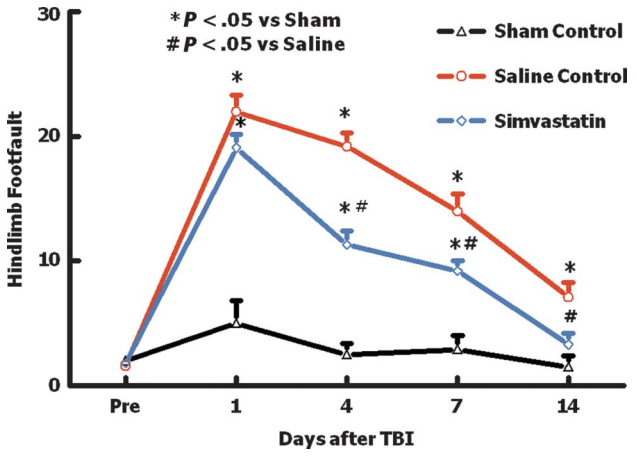

FIGURE 1. *Plot showing the temporal profile of sensorimotor function (foot-fault) before and after traumatic brain injury (TBI) or sham. TBI impaired sensorimotor performance in the contralateral hind limb. Simvastatin enhanced the recovery of sensorimotor function. Data are presented as mean ± SD. n = 8 per group. Pre, preinjury level.*

Simvastatin Stimulates Endothelial Cell Tube Formation After OGD

Capillarylike tube formation was performed to examine the effects of simvastatin on endothelial cells after OGD. Simvastatin significantly ($P = .001$) increased RBMVEC tube formation (5.6 ± 0.6 mm/mm^2; Figure 3C) compared with OGD (2.4 ± 0.3 mm/mm^2; Figure 3B). However, treatment with simvastatin did not increase the tube formation in the presence of the PI3K/Akt inhibitor LY29402 (2.8 ± 0.2 mm/mm^2; Figure 3D). Inhibition of GSK-3 with LiCl (6.1 ± 0.6 mm/mm^2; Figure 3E) enhanced the effect of simvastatin after OGD. Blockage of VEGFR-2 with SU1498, a specific antagonist of VEGFR-2, suppressed capillarylike tube formation induced by the simvastatin ($P = .001$; Figure 3F). These data suggest that simvastatin induces in vitro angiogenesis of RBMVECs after ischemic injury.

Simvastatin Enhances VEGFR-2 Expression in Brain Tissues and in Cultured RBMVECs

To elucidate the mechanism of simvastatin on angiogenesis, we examined VEGFR-2 expression in the injured brain tissues by ELISA (Figure 4C). The lesion boundary zone is a special area where active angiogenesis takes place after TBI and ischemic stroke.[19,20] Therefore, tissues from the lesion boundary zone were sampled to study the expression of proteins related to angiogenesis. TBI alone increased the expression of VEGFR-2 in the lesion boundary zone in cortex (1298.3 ± 64 pg/mg) compared with the sham rats (856.2 ± 89 pg/mg; $P = .003$). Simvastatin further enhanced the expression of VEGFR-2 (1634.1 ± 151 pg/mg) in the injured cortex compared with the saline-treated rats ($P = .020$ vs saline). In addition, the expression of VEGFR-2 in cultured RBMVECs was tested by immunocytochemistry and ELISA (Figure 4A and 4B). VEGFR-2 expression in hypoxic cells was significantly upregulated compared with normoxic cells. Simvastatin increased the expression of VEGFR-2 in both the cytoplasm and nucleus of the RBMVECs compared with the OGD-alone cells. The effects of simvastatin on VEGFR-2 were enhanced by the GSK-3 inhibitor LiCl and were reversed by the PI3K/Akt inhibitor LY29402 and the VEGFR-2 neutralizing protein DC101. A similar pattern of VEGFR-2 expression in cultured RBMVECs was detected by ELISA (Figure 4B). OGD alone induced VEGFR-2 expression ($P = .033$ vs control) compared with the control cells. Simvastatin further increased the VEGFR-2 level compared with OGD ($P = .011$ vs OGD). LY29402 ($P = .006$ vs simvastatin) and DC101 ($P = .008$ vs simvastatin) suppressed the effects of simvastatin on VEGFR-2 expression, whereas LiCl ($P = .022$ vs simvastatin) did not alter the effect of simvastatin.

Copyright © Congress of Neurological Surgeons. Unauthorized reproduction of this article is prohibited.

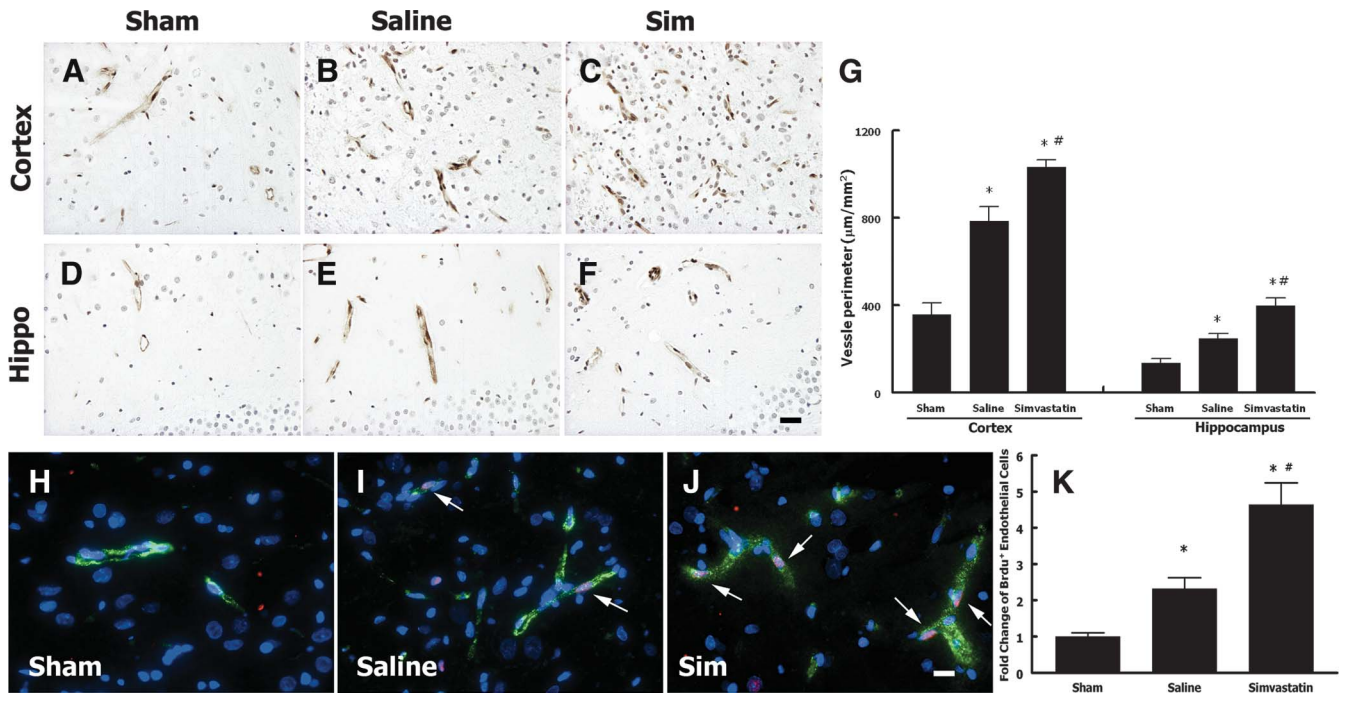

FIGURE 2. *Simvastatin treatment of traumatic brain injury (TBI) increases angiogenesis in the cortex and hippocampus.* **A**, *through* **F**, *von Willebrand factor (vWF) immunostaining in the ipsilateral cortex and hippocampus after TBI.* **G**, *quantitative data of cerebral vascular perimeters (vWF).* **H** *through* **J**, *immunofluorescent staining of vWF (green) and bromodeoxyuridine (BrdU; red). Nuclei were counterstained with 4' -6-diamidino-2-pheylindole (DAPI; blue). Arrows show BrdU-reactive cells colocalized with vWF in the vessel. n = 4 per group. Scale bar = 50 μm in* **F** *and* **J**. *Sim, simvastatin.*

Simvastatin Induces Phosphorylation of eNOS via the Akt Pathway In Vivo and In Vitro

eNOS plays a key role in the process of angiogenesis after brain insult.[21] To explore the signal transduction pathway related to the simvastatin-induced angiogenesis, phosphorylation of eNOS and Akt was examined by Western blot analyses. The cortical tissues from the lesion boundary zone were harvested and homogenized for immunoblotting (Figure 5A and 5C). Simvastatin induced the phosphorylation of eNOS in the injured cortex compared with the saline-treated animals (P = .002 vs saline; Figure 5C). The phosphorylation of Akt and GSK-3 was also increased in the simvastatin-treated rats compared with the saline-treated rats (Figure 5A). The effect of simvastatin on phosphorylation of eNOS was also tested in the cultured RBMVECs (Figure 5B and 5D). Simvastatin promoted the phosphorylation of eNOS in the RBMVECs after OGD, whereas LY29402 and SU1498 suppressed this simvastatin-induced phosphorylation. These results suggest that simvastatin-induced phosphorylation of eNOS may be related to activation of the VEGFR-2/PI3K/Akt pathway.

DISCUSSION

The primary findings in the present study are that treatment with simvastatin promotes angiogenesis and evokes the functional recovery after TBI; that simvastatin stimulates in vitro angiogenesis after OGD, which could be suppressed by inhibition of Akt or blockage of VEGFR-2; and that simvastatin-induced proangiogenetic effects may be related to the activation of the VEGFR-2/PI3K/Akt/eNOS pathway in endothelial cells.

One of the most prominent pathophysiological changes after TBI is ischemia and hypoxia in the lesion boundary area.[22] Early after the injury, the direct trauma causes necrotic neuronal cell death, followed by increased neuronal apoptosis hours and days later as a result of secondary injury.[23] Posttraumatic ischemia plays an important role in secondary injury after TBI. Regional ischemia early after TBI has been shown to correlate with neurological outcome,[1] which suggests that TBI and ischemic stroke share fundamental mechanisms of cell damage.[22] To date, drugs that target solely neuroprotection have not been proven efficacious for TBI amelioration.[3] The failure of therapies directed only at neuronal protection is attributable in part to the lack of concomitant effects on cerebral blood vessels after injury. The "neurovascular unit" has emerged as a new paradigm for understanding the pathology of central nervous system disease[24] and injury.[25] To improve neurological function after TBI, one may need not only to promote neuroprotection but also to enhance angiogenesis.

Recent studies show significant benefit of statins in models of TBI[26] and related disease processes, including cerebral ischemia,[7]

Copyright © Congress of Neurological Surgeons. Unauthorized reproduction of this article is prohibited.

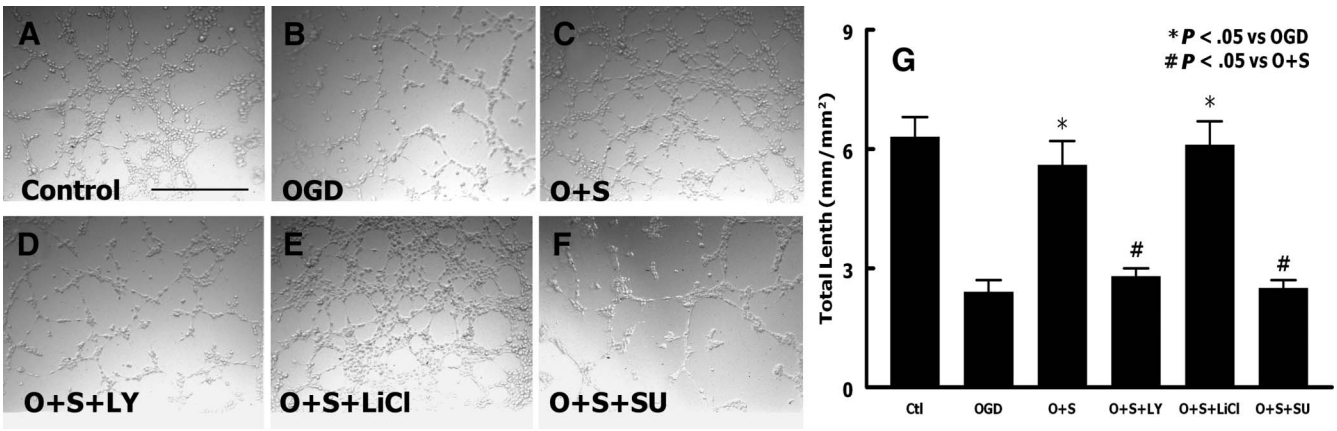

FIGURE 3. *Simvastatin regulates capillarylike tube formation.* **A** *through* **F**, *tube formation of rat endothelial cells under various conditions.* **G**, *quantitative data of capillarylike tube formation. O + S, simvastatin treatment after oxygen-glucose deprivation (OGD); O + S + LiCl, simvastatin plus lithium chloride after OGD; O + S + LY, simvastatin plus LY294002 after OGD; O + S + SU: simvastatin plus SU1498 after OGD. n = 3 per group, Scale bar = 0.5 mm in* **A**.

intracerebral hemorrhage,[27] and subarachnoid hemorrhage.[28] We reported earlier that simvastatin increases neurogenesis and reduces neuronal apoptosis in TBI rats. Simvastatin also increases angiogenesis in limb ischemic rabbits[13] and stroke rats.[7] Therefore, simvastatin possesses the potential to promote angiogenesis after TBI. In the present study, fluorescent double-staining with BrdU and vWF was performed to identify the newly generated endothelial cells. Our data show that TBI alone induces angiogenesis in the lesion boundary zone and ipsilateral hippocampus, which is consistent with a previous study.[2] However, simvastatin enhanced the TBI-induced angiogenesis identified by increasing endothelial cell proliferation and vascular length (Figure 2). These data are consistent with the previous findings using atorvastatin.[8] In this study, simvastatin induces angiogenesis and promotes functional recovery (Figure 1), although recovery of neurological function after TBI is mediated by many

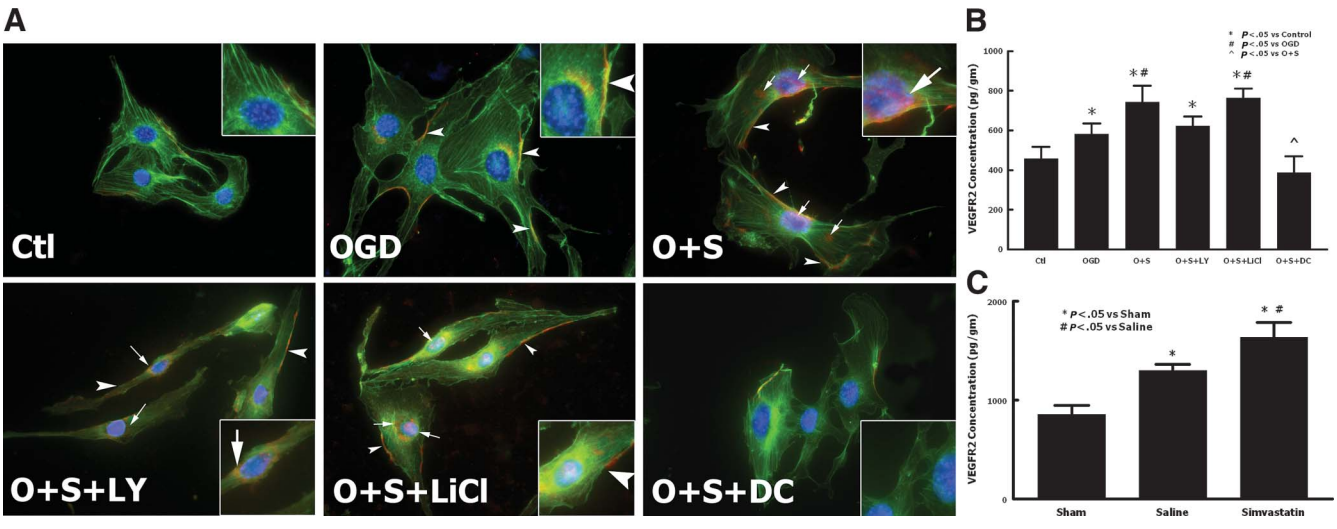

FIGURE 4. *Effect of simvastatin on vascular endothelial growth factor receptor-2 (VEGFR-2) expression in brain tissue after traumatic brain injury (TBI) and in cultured rat endothelial cells.* **A**, *double-fluorescent immunostaining of F-actin (green) and VEGFR-2 (red) in rat endothelial cells. Nuclei were counterstained with 4′-6-diamidino-2-pheylindole (DAPI; blue). Arrows show VEGFR-2 expression in nucleus and cytoplasm; arrowheads, VEGFR-2 expression in cell membrane.* **B**, *enzyme-linked immunosorbent assay (ELISA) on expression of VEGFR-2 in rat endothelial cells.* **C**, *ELISA on expression of VEGFR-2 in rat brain tissue after TBI. n = 3 (***B***) and 4 (***C***). Scale bar = 25 μm.*

Copyright © Congress of Neurological Surgeons. Unauthorized reproduction of this article is prohibited.

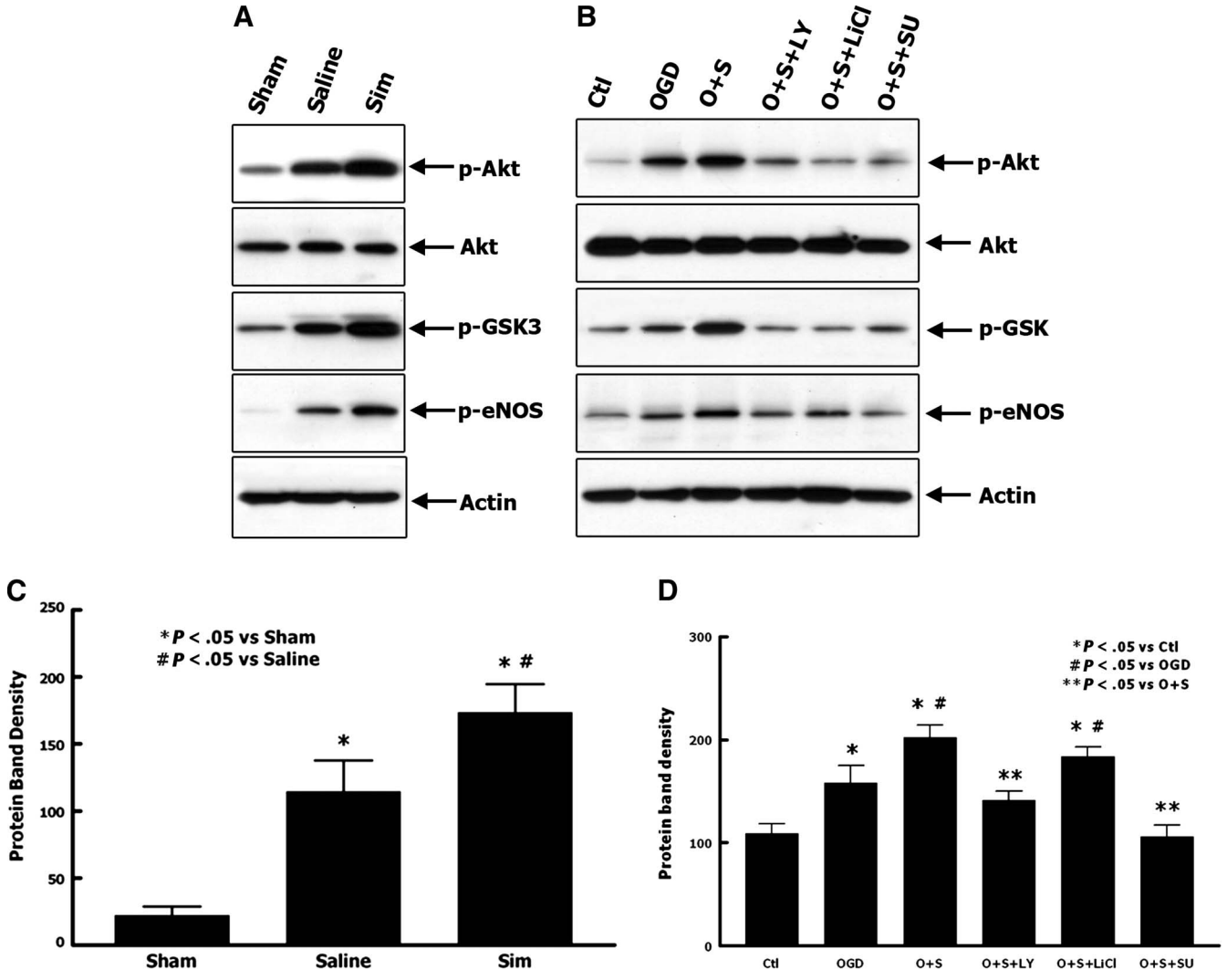

FIGURE 5. *Simvastatin enhanced Akt-dependent phosphorylation of endothelial nitric oxide synthase (eNOS) in brain after traumatic brain injury (TBI) and in cultured rat endothelial cells. Western blot analyses show the effects of simvastatin on phosphorylation of Akt and eNOS in brain tissue after TBI (A) and the quantitative data of protein band density (C); n = 4. Western blot analysis shows the effects of simvastatin on phosphorylation of eNOS in cultured rat endothelial cells (B) and the quantitative data of protein band density (D); n = 3.*

coupled events, including vascular remodeling, neurogenesis, and synaptogenesis. In treatment with simvastatin, it is possible that other restorative events, in addition to angiogenesis, contribute to recovery of function.

To investigate the mechanism of the proangiogenic effects of simvastatin on TBI, endothelial cell tube formation was used as an in vitro angiogenesis model.[29] Because ischemia is a fundamental pathophysiological process after TBI,[22] OGD was used to induce the injury. Simvastatin significantly increases the RBMVEC capillarylike tube formation compared with OGD. Simvastatin-induced tube formation is inhibited by LY29402, a PI3K/Akt inhibitor; enhanced with LiCl, a GSK-3 inhibitor; and blocked by SU1498, a VEGFR-2 antagonist (Figure 3). These data suggest that simvastatin-induced angiogenesis is related to activation of the VEGFR-2/Akt/GSK-3 signaling pathway. Endothelial cell capillary tube formation is enhanced by activating VEGFR-2, and Akt is involved in these activities.[13,30] Akt plays an important role in ischemic and VEGF-mediated angiogenesis.[31] It regulates many aspects of endothelial cellular functions, including apoptosis, cell motility, and tube formation.[32] Our previous studies also demonstrate that simvastatin activates Akt in the rat brain after TBI.[10]

VEGFR-2 mediates the majority of the downstream angiogenic effects of VEGF, including microvascular permeability and

Copyright © Congress of Neurological Surgeons. Unauthorized reproduction of this article is prohibited.

endothelial cell proliferation, migration, and survival.[33] VEGFR-2 transduces VEGF signals through several intracellular signaling pathways, including the Raf-Mek-Erk and PI3K/Akt pathways.[34] In light of the critical role of VEGFR-2 on angiogenesis, VEGFR-2 expression was examined both in the brain tissues after TBI and in the cultured RBMVECs subjected to OGD. Our results show that there is an upregulation of VEGFR-2 after TBI, which is consistent with the previous report about VEGFR-2 expression in brain injury,[35] and simvastatin further enhances the level of VEGFR-2 in the injured cortex. A similar pattern is seen in the cultured RBMVECs. Hypoxia induces expression of VEGFR-2 in RBMVECs, and simvastatin promotes this induction both in the cytoplasm and in the nucleus of RBMVECs (Figure 4A). Recent reports show that VEGFR-2 can internalize and extend its proliferative signaling activity for longer periods within intracellular compartments.[36] Simvastatin-induced intracellular distribution of VEGFR-2 may also contribute to the enhanced angiogenesis because the intracellular receptor has longer signal transduction capacity. Simvastatin-induced upregulation of VEGFR-2 expression may be partially related to Akt activity because LY29402 attenuates this effect (Figure 4B). These data indicate that simvastatin modulates VEGFR-2 expression in RBMECs both in vitro and in vivo, which results in an increased endothelial cell proliferation and OGD resistance that may enhance angiogenesis in the injured brain.

eNOS is a downstream mediator of VEGFR-2 and is critical for angiogenesis.[21] Enhanced phosphorylated eNOS induces a broad range of effects, including the promotion of angiogenesis and mural cell recruitment to immature angiogenic sprouts.[37] Our data show that treatment with simvastatin activates Akt/GSK-3 and promotes phosphorylation of eNOS in the TBI brain. Simvastatin treatment of RBMVECs significantly increases phosphorylated eNOS activity after OGD compared with controls, which could be suppressed by inhibition of PI3K/Akt and blockade of VEGFR-2 (Figure 5). These results suggest that simvastatin evokes phosphorylation of eNOS in a VEGFR-2/PI3K/Akt–dependent manner and that eNOS plays an important role in simvastatin-induced angiogenesis after TBI.

The studies reported here show an association between increased overall expressions of VEGFR-2, elevated Akt/eNOS phosphorylation levels, and higher angiogenesis rates in simvastatin treatment compared with control.

CONCLUSION

Treatment with simvastatin significantly promotes angiogenesis and improves functional outcome after TBI. The proangiogenic effect of simvastatin is mediated by activation of VEGFR-2/Akt/eNOS pathway.

Disclosure

This work was supported by National Institutes of Health grants R01NS052280-01A1 (Dr Mahmood) and PO1NS23345 (Dr Chopp). The authors have no personal financial or institutional interest in any of the drugs, materials, or devices described in this article.

REFERENCES

1. Coles JP, Fryer TD, Smielewski P, et al. Incidence and mechanisms of cerebral ischemia in early clinical head injury. *J Cereb Blood Flow Metab*. 2004;24(2):202-211.
2. Morgan R, Kreipke CW, Roberts G, Bagchi M, Rafols JA. Neovascularization following traumatic brain injury: possible evidence for both angiogenesis and vasculogenesis. *Neurol Res*. 2007;29(4):375-381.
3. Jain KK. Neuroprotection in traumatic brain injury. *Drug Discovery Today*. 2008;13(23-24):1082-1089.
4. del Zoppo GJ. Stroke and neurovascular protection. *N Engl J Med*. 2006;354(6):553-555.
5. Shimamura M, Sato N, Sata M, et al. Delayed postischemic treatment with fluvastatin improved cognitive impairment after stroke in rats. *Stroke: J Cereb Circ*. 2007;38(12):3251-3258.
6. Weis M, Heeschen C, Glassford AJ, Cooke JP. Statins have biphasic effects on angiogenesis. *Circulation*. 2002;105(6):739-745.
7. Chen J, Zhang ZG, Li Y, et al. Statins induce angiogenesis, neurogenesis, and synaptogenesis after stroke. *Ann Neurol*. 2003;53(6):743-751.
8. Lu D, Goussev A, Chen J, et al. Atorvastatin reduces neurological deficit and increases synaptogenesis, angiogenesis, and neuronal survival in rats subjected to traumatic brain injury. *J Neurotrauma*. 2004;21(1):21-32.
9. Lu D, Qu C, Goussev A, et al. Statins increase neurogenesis in the dentate gyrus, reduce delayed neuronal death in the hippocampal CA3 region, and improve spatial learning in rat after traumatic brain injury. *J Neurotrauma*. 2007;24(7):1132-1146.
10. Wu H, Lu D, Jiang H, et al. Increase in phosphorylation of Akt and its downstream signaling targets and suppression of apoptosis by simvastatin after traumatic brain injury. *J Neurosurg*. 2008;109(4):691-698.
11. Palmer TD, Willhoite AR, Gage FH. Vascular niche for adult hippocampal neurogenesis. *J Comp Neurol*. 2000;425(4):479-494.
12. Wu H, Lu D, Jiang H, et al. Simvastatin-mediated upregulation of VEGF and BDNF, activation of the PI3K/Akt pathway, and increase of neurogenesis are associated with therapeutic improvement after traumatic brain injury. *J Neurotrauma*. 2008;25(2):130-139.
13. Kureishi Y, Luo Z, Shiojima I, et al. The HMG-CoA reductase inhibitor simvastatin activates the protein kinase Akt and promotes angiogenesis in normocholesterolemic animals. *Nat Med*. 2000;6(9):1004-1010.
14. Mahmood A, Lu D, Wang L, Chopp M. Intracerebral transplantation of marrow stromal cells cultured with neurotrophic factors promotes functional recovery in adult rats subjected to traumatic brain injury. *J Neurotrauma*. 2002;19(12):1609-1617.
15. Hernandez TD, Schallert T. Seizures and recovery from experimental brain damage. *Exp Neurol*. 1988;102(3):318-324.
16. Xiong Y, Mahmood A, Lu D, et al. Histological and functional outcomes after traumatic brain injury in mice null for the erythropoietin receptor in the central nervous system. *Brain Res*. 2008;1230:247-257.
17. Paxinos G WC. *The Rat Brain in Stereotaxic Coordinates*. Burlington, MA: Academic Press; 2007.
18. Schmitz C, Hof PR. Design-based stereology in neuroscience. *Neuroscience*. 2005;130(4):813-831.
19. Beck H, Plate KH. Angiogenesis after cerebral ischemia. *Acta Neuropathol*. 2009;117(5):481-496.
20. Guo X, Liu L, Zhang M, Bergeron A, Cui Z, Dong JF, Zhang J. Correlation of CD34+ cells with tissue angiogenesis after traumatic brain injury in a rat model. *J Neurotrauma*. 2009;26(8):1337-1344.
21. Murohara T, Asahara T, Silver M, et al. Nitric oxide synthase modulates angiogenesis in response to tissue ischemia. *J Clin Invest*. 1998;101(11):2567-2578.
22. Werner C, Engelhard K. Pathophysiology of traumatic brain injury. *Br J Anaesth*. 2007;99(1):4-9.
23. Greve MW, Zink BJ. Pathophysiology of traumatic brain injury. *Mt Sinai J Med*. 2009;76(2):97-104.
24. Iadecola C. Neurovascular regulation in the normal brain and in Alzheimer's disease. *Nat Rev*. 2004;5(5):347-360.
25. Khan M, Im YB, Shunmugavel A, et al. Administration of S-nitrosoglutathione after traumatic brain injury protects the neurovascular unit and reduces secondary

Copyright © Congress of Neurological Surgeons. Unauthorized reproduction of this article is prohibited.

injury in a rat model of controlled cortical impact. *J Neuroinflammation*. 2009;6:32.
26. Wang H, Lynch JR, Song P, et al. Simvastatin and atorvastatin improve behavioral outcome, reduce hippocampal degeneration, and improve cerebral blood flow after experimental traumatic brain injury. *Exp Neurol*. 2007;206(1):59-69.
27. Karki K, Knight RA, Han Y, et al. Simvastatin and atorvastatin improve neurological outcome after experimental intracerebral hemorrhage. *Stroke*. 2009; 40(10):3384-3389.
28. Sugawara T, Ayer R, Jadhav V, Chen W, Tsubokawa T, Zhang JH. Simvastatin attenuation of cerebral vasospasm after subarachnoid hemorrhage in rats via increased phosphorylation of Akt and endothelial nitric oxide synthase. *J Neurosci Res*. 2008;86(16):3635-3643.
29. Chen J, Cui X, Zacharek A, Roberts C, Chopp M. eNOS mediates TO90317 treatment-induced angiogenesis and functional outcome after stroke in mice. *Stroke*. 2009;40(7):2532-2538.
30. Morales-Ruiz M, Fulton D, Sowa G, et al. Vascular endothelial growth factor-stimulated actin reorganization and migration of endothelial cells is regulated via the serine/threonine kinase Akt. *Circ Res*. 2000;86(8):892-896.
31. Ackah E, Yu J, Zoellner S, et al. Akt1/protein kinase Balpha is critical for ischemic and VEGF-mediated angiogenesis. *J Clin Invest*. 2005;115(8):2119-2127.
32. Shiojima I, Walsh K. Role of Akt signaling in vascular homeostasis and angiogenesis. *Circ Res*. 2002;90(12):1243-1250.
33. Hicklin DJ, Ellis LM. Role of the vascular endothelial growth factor pathway in tumor growth and angiogenesis. *J Clin Oncol*. 2005;23(5):1011-1027.
34. Freitas-Andrade M, Carmeliet P, Stanimirovic DB, Moreno M. VEGFR-2-mediated increased proliferation and survival in response to oxygen and glucose deprivation in PlGF knockout astrocytes. *J Neurochem*. 2008;107(3):756-767.
35. Lafuente JV, Argandona EG, Mitre B. VEGFR-2 expression in brain injury: its distribution related to brain-blood barrier markers. *J Neural Transm*. 2006;113(4):487-496.
36. Lampugnani MG, Orsenigo F, Gagliani MC, Tacchetti C, Dejana E. Vascular endothelial cadherin controls VEGFR-2 internalization and signaling from intracellular compartments. *J Cell Biol*. 2006;174(4):593-604.
37. Kashiwagi S, Izumi Y, Gohongi T, et al. NO mediates mural cell recruitment and vessel morphogenesis in murine melanomas and tissue-engineered blood vessels. *J Clin Invest*. 2005;115(7):1816-1827.

COMMENT

This excellent experimental study demonstrates the role of simvastatin in inducing angiogenesis as a contribution to functional recovery from traumatic brain injury (TBI). Simvastatin has already been shown to have a neuroprotective effect in experimental studies on models of TBI, acute ischemic stroke, and neurodegenerative disorders. The neuroprotective effect of simvastatin is attributed to counteraction of apoptosis and enhancement of neurogenesis, and the authors have proposed that angiogenesis, related to activation of the vascular endothelial growth factor receptor-2 (VEGFR-2)/Akt/endothelial nitric oxide synthase signaling pathway, counteracts ischemia/hypoxia in the penumbra zone surrounding the damaged brain. Simvastatin was shown to enhance proliferation of endothelial cells. Endothelial injury in cerebral ischemia is also associated with production of reactive oxygen species and inflammatory mediators. Statins are among the substances that have a protective effect against vascular endothelial injury.[1] A recent study surprisingly shows that simvastatin has antiangiogenic effects in retinal endothelial cells, which is due at least in part to the reduction of VEGFR2 phosphorylation in these cells.[2] Perhaps there is an explanation for this disparity in actions of simvastatin.

Delivery of statins across the blood-brain barrier (BBB) also requires some comments. The authors participated in one of the earlier studies showing that simvastatin at the same dose provides a therapeutic effect superior to treatment with atorvastatin and attributed this to improved delivery across the BBB. It is difficult to compare the penetration of different drugs across the BBB without measuring its permeability because the lipophilic or hydrophilic nature is only one of the factors affecting drug transport across membranes. Damage to the BBB or attempts to forcibly open it for drug delivery aggravate the pathology of TBI, and passage of drugs across it is unreliable. Therefore, it is desirable to reduce the increased permeability of BBB after TBI. Although a neuroprotective agent should have access to the brain parenchyma, enhancement of angiogenesis by simvastatin does not need passage across the BBB.

The potential neuroprotective effect of simvastatin in human TBI may be described as follows. The primary aim in acute TBI is neuroprotection by counteracting the cascades that aggravate the initial damage, whereas the aim in subacute/chronic stages is neuroregeneration, which contributes to prevention of delayed damage and improves the functional outcome. Simvastatin, in addition to neuroprotection in the acute phase, contributes to regeneration in the subacute phase by promoting angiogenesis, which may counteract any long-term neurodegenerative sequelae of severe TBI. Simvastatin may contribute to central nervous system regeneration in other ways. Studies have been done to explore the effect of statins in enhancing the number of circulating stem cells in vivo. It is worthwhile to investigate the combination of simvastatin with stem cell transplants to enhance regeneration after severe TBI. Combination methods such as the use of biological therapies and pharmaceuticals that induce angiogenesis are promising strategies for research in regeneration of central nervous system after trauma.[3] Because of its multiple actions, simvastatin plays an important role in both neuroprotection and neuroregeneration after TBI.

Angiogenesis does not occur fast enough to play a significant role in revascularization in the acute stage of TBI. The authors pointed out a parallel between ischemia in TBI and stroke, but counteraction of ischemia requires different strategies, and the cascades of pathomechanism in the 2 conditions do not overlap. Whereas restoration of blood flow in acute stroke caused by vascular occlusion may be beneficial, an increase in regional cerebral blood flow in acute head injury resulting from vasodilatation may be harmful, particularly in the presence of BBB damage, and may aggravate cerebral edema. Hypoxia in TBI patients can be corrected without increasing blood flow by hyperbaric oxygen, which has been shown to have a neuroprotective effect and reduces cerebral edema.[4] Hyperbaric oxygen may reduce cerebral blood flow by vasoconstriction but increases tissue oxygenation.

In conclusion, this study and previous information on this topic support further investigation of simvastatin in the management of TBI. Although simvastatin has been shown to be neuroprotective against the toxic effects of some chemicals on the brain, myotoxicity is a known adverse effect of this drug. Further studies are also needed to rule out any potential for neurotoxicity of simvastatin.

K. K. Jain
Basel, Switzerland

1. Fisher M. Injuries to the vascular endothelium: vascular wall and endothelial dysfunction. *Rev Neurol Dis*. 2008;5(suppl 1):S4-S11.
2. Hata Y, Miura M, Asato R, et al. Antiangiogenic mechanisms of simvastatin in retinal endothelial cells. *Graefes Arch Clin Exp Ophthalmol*. 2010;248:667-673.
3. Jain KK. Regenerative therapy for central nervous system trauma. In: Steinhoff G, ed. *Regenerative Medicine? From Protocol to Patient*. London, UK: Springer; 2010.
4. Sukoff MH, Jain KK. Hyperbaric oxygen therapy in neurosurgery. In: Jain KK, ed. *Textbook of Hyperbaric Medicine*. 5th ed. Seattle, WA: Hogrefe; 2009: 263-277.

Copyright © Congress of Neurological Surgeons. Unauthorized reproduction of this article is prohibited.

Granulocyte Colony-Stimulating Factor Enhances the Angiogenetic Effect of Indirect Bypass Surgery for Chronic Cerebral Hypoperfusion in a Rat Model

Yuki Ohmori, MD
Motohiro Morioka, MD, PhD
Yasuyuki Kaku, MD
Takayuki Kawano, MD, PhD
Jun-ichi Kuratsu, MD, PhD

Department of Neurosurgery, Kumamoto University School of Medicine, Kumamoto, Japan

Correspondence:
Motohiro Morioka, MD, PhD, Department of Neurosurgery, Kumamoto University School of Medicine, Kumamoto, Japan 1-1-1, Honjo Kumamoto 860-8556, Japan.
E-mail: mmorioka@kumamoto-u.ac.jp

Received, February 4, 2010.
Accepted, October 1, 2010.

Copyright © 2011 by the Congress of Neurological Surgeons

BACKGROUND: Granulocyte colony-stimulating factor (G-CSF) mobilizes hematopoietic bone marrow cells into systemic circulation and has been used clinically to treat chemotherapy-induced neutropenia. Recently, G-CSF was shown to have neuroprotective and angiogenetic effects in acute cerebral infarction.

OBJECTIVE: To evaluate the effects of G-CSF for angiogenesis after indirect bypass surgery.

METHODS: Chronic cerebral hypoperfusions were induced in male Wistar rats by permanent bilateral internal carotid artery occlusion (BICAO). After BICAO, unilateral indirect bypass and encephalogaleosynangiosis (EGS) were performed, and human recombinant G-CSF (10 μg/kg) or saline was injected intramuscularly for 5 consecutive days. We measured regional cerebral blood flow (rCBF) by laser Doppler flowmetry and performed immunohistochemical analysis 21 days after BICAO.

RESULTS: BICAO decreased rCBF to 62.52% ± 5.8% of control ($P < .01$). The rCBF increased significantly 21 days after BICAO in all treatment groups (n = 10; $P < .05$) except the G-E- group. The rCBF increase observed in the G+E+ group was significantly higher than that observed in other groups. Both G-CSF and EGS treatments significantly increased the number of small vessels ($P < .01$), and G-CSF and EGS showed additive effect in increasing the number of small vessels.

CONCLUSION: Combined use of G-CSF and indirect bypass surgery induces an increase in rCBF and angiogenesis under conditions of cerebral chronic hypoperfusion. This is the first report to demonstrate that G-CSF can enhance angiogenesis induced by indirect bypass surgery, and that this combined therapy is a safe and easy method of treatment.

KEY WORDS: Angiogenesis, Cerebral blood flow, Granulocyte colony-stimulating factor, Hypoperfusion Indirect bypass

Neurosurgery 68:1372–1379, 2011 DOI: 10.1227/NEU.0b013e31820c0289 www.neurosurgery-online.com

Chronic cerebral hypoperfusion is found in diseases with progressive, severe stenosis of the major cerebral arteries, such as the internal carotid artery (ICA) and its distal arteries. Clinically, this condition is found in diseases such as ICA stenosis (or occlusion), middle cerebral artery (MCA) stenosis (or occlusion), and moyamoya disease, among others. Progressive stenosis of the ICA and MCA is induced mainly by atherosclerosis, but the cause of moyamoya disease is still unclear. Moyamoya disease is characterized by progressive stenosis of the terminal portion of the bilateral ICA and is associated with an abnormal vascular network, the so-called "moyamoya vessels."[1] Chronic hypoperfusion conditions often cause cerebral

ABBREVIATIONS: BICAO, bilateral internal carotid artery occlusion; **EGS,** encephalogaleosynangiosis; **EPC,** endothelial progenitor cell; **G-CSF,** granulocyte colony-stimulating factor; **ICA,** internal carotid artery; **MCA,** middle cerebral artery; **PBS**, phosphate buffered saline; **STA,** superficial temporal artery; **VEGF,** vascular endothelial growth factor; **vWF,** von Willebrand factor

Copyright © Congress of Neurological Surgeons. Unauthorized reproduction of this article is prohibited.

infarction and require direct bypass surgery (eg, superficial temporal artery [STA]-to-MCA anastomosis). Evidence regarding the benefit of direct bypass surgery for patients with mildly decreased cerebral blood flow (CBF) is controversial or lacking.[2,3] For patients with a mild decrease in CBF, the only available treatments are anti-platelet or anticoagulant therapy. Patients with moyamoya disease have the option of "indirect bypass surgery," even in cases of mild CBF decrease. Indirect bypass surgery, which is relatively easy and safe, can create transgaleal and/or transdural anastomoses from external arteries to a hypoperfused brain via angiogenesis. This surgery is widely acknowledged to be effective in the treatment of moyamoya disease in humans[4-7] and in miniature pigs[8]; however, in some patients with moyamoya disease this treatment fails to provide optimal revascularization from the perspective of collateral vessel formation. Furthermore, for hypoperfused patients with atherosclerotic ICA or MCA stenosis (or occlusion), indirect bypass surgery has little effect on angiogenesis. A drug that could enhance angiogenesis after indirect bypass surgery and improve the CBF to a hypoperfused brain clearly is needed.

G-CSF can mobilize hematopoietic bone marrow cells to enter systemic circulation[9] and has been used clinically to counter the side effects of chemotherapy-induced neutropenia and prepare donors for peripheral cell harvesting.[10-12] Recently, G-CSF was shown to act as a neuroprotective agent in acute cerebral infarction.[10,13-18] Furthermore, several studies have suggested that G-CSF increases collateral angiogenesis after cerebral ischemia.[19-22]

We hypothesized that the combined use of G-CSF and indirect surgery could enhance the angiogenesis compared to indirect bypass surgery alone. In this study, we investigated the effects of G-CSF on rCBF and angiogenesis after indirect bypass surgery in a rat chronic cerebral hypoperfusion model.

MATERIAL AND METHODS

Animal Care and Use

All experimental procedures used in this investigation were performed in accordance with the institutional guidelines of the Kumamoto University Graduate School of Medical Sciences. Male Wistar rats weighing 300 to 350 g were used. All surgical procedures were performed under anesthesia with 4% halothane and maintained with 1.5% halothane in 70%/30% nitrous oxide/oxygen. Normothermia (37°C) was maintained in each animal using a rectal thermistor probe connected to a feedback-regulated heating blanket.

Experimental Groups

Animals were divided into 4 experimental treatment groups: (1) G-CSF injection with encephalogaleosynangiosis (EGS) (G+E+); (2) G-CSF injection without EGS (G+E-); (3) saline injection with EGS (G-E+); and (4) saline injection without EGS (G-E-).

Bilateral ICA Occlusion/Chronic Cerebral Hypoperfusion Model

Bilateral ICAs were exposed via a ventral midline cervical incision. An incision was made between the sternocleidomastoid and the sternohyoid muscles, carefully dissecting them from the sympathetic and vagal nerves. Bilateral ICAs were doubly ligated with 4-0 silk sutures.

Encephalogaleosynangiosis

After the BICAO, rats were placed in a stereotactic head holder with the top of the skull positioned horizontally. The scalp was then incised on the parieto-occipital midline, the galea was peeled off the skull, and the galeal flap was prepared. A 7-mm^2 craniectomy was performed by drilling just behind the coronal suture, 1 mm lateral from the midline, and dural incision was performed with the use of microsurgical forceps and microscope to avoid brain injury. The galeal flap was seated on the region of removed dura. A right-side EGS procedure of about 7 mm^2 was performed just behind the coronal suture. (In the sham-operated animals [the E- group], dural incision was not performed.)

Measurement of Regional Cerebral Blood Flow

The rCBF was measured 3 times—before, immediately after, and 21 days after BICAO—for the 10 rats in each experimental group using transcranial laser Doppler flowmeter (ALF21, Advance, Tokyo, Japan). Details of this procedure have been described previously.[23] Rats were anesthetized with halothane and fixed in a stereotactic headholder. A midline scalp skin incision was made, and the flowmeter probe was fixed. rCBF was measured 5 times each at the bilateral frontal lobes and cerebellums. Mean rCBF values from 10 animals per group were calculated. We calculated percent values of each frontal rCBF and compared them with the ipsilateral rCBF of the cerebellum.

G-CSF Injection

Recombinant human G-CSF was donated by Kyowa Hakko Kirin Co. Ltd. (Tokyo, Japan). Rats were randomly assigned to either the G-CSF (10 μg/kg) or saline injection groups. Injections were administered at the right temporal region intramuscularly. G-CSF (G+ group) or saline (G- group) was injected following carotid artery occlusion once a day for 5 consecutive days.

Histology and Immunohistochemistry

Rats were deeply anesthetized 21 days after BICAO, and their aortas were perfused with 300 to 400 mL of phosphate-buffered saline (PBS, pH 7.4), followed by perfusion of 400 mL of 4% paraformaldehyde in PBS. Brain tissue (with EGS tissue) was carefully removed, fixed with 4% paraformaldehyde overnight, and embedded in paraffin. Coronal sections measuring 5 μm and including EGS tissue were taken from each brain, and nonspecific binding sites were blocked using blocking solution (3% bovine serum albumin in PBS). The sections were sequentially incubated overnight at 4°C with an antibody against von Willebrand factor (vWF; 1:200). Immunostaining procedures were carried out using the Vectastain ABC kit (Vector Laboratories, Burlingame, California) according to manufacturer instructions, using 3,3′-diaminobenzidine as a chromogen. Adjust sections were stained with hematoxylin and eosin (H&E) for histological evaluation. Sections were photographed at 40× magnification. Five photographs from different sites in the cerebral cortex were obtained from each brain section (n = 10), and the number and diameter of vWF-positive vessels in each section were recorded. Sections were analyzed blindly by 2 independent co-authors (Y.K. and T.K.), and the mean value was used for final analysis.

Copyright © Congress of Neurological Surgeons. Unauthorized reproduction of this article is prohibited.

Data Analysis

Data are expressed as mean ± standard error (SE). Changes in laser Doppler flowmetry were calculated in percent of mean baseline value. *P* values indicate results of a Student's *t*-test, and values of $P < .05$ were considered statistically significant.

RESULTS

rCBF Change After BICAO in the Absence of G-CSF Treatment

The relative bilateral frontal lobe rCBFs before and after BICAO were decreased to 55.20 ± 9.27% and 58.24 ± 8.50 % in the right and left sides, respectively ($P < .001$ compared to cerebellum rCBF values). There was no statistically significant difference between the rCBF rates of the right and left sides. Without G-CSF treatment, the rCBFs of the right and left sides increased to 75.21 ± 3.01% and 64.89 ± 3.36%, respectively, 21 days after BICAO. The rCBF rate of the right side (EGS treatment side) was significantly higher than that of the left side (Table). Thus, in this hypoperfusion model, a decreased rCBF rate was maintained for 21 days post-BICAO. EGS treatment was associated with a statistically significant increase in rCBF.

The Effect of G-CSF on rCBF

Twenty-one days after operation, the increased rCBF rates of the G+E+, G+E- and G-E+ groups were 91.53%, 59.8%, and 37.0%, respectively, and a statistical difference was observed when these groups were compared with the increase rate of 11.4% of the G-E- group (rate increase of 11.4%, $P < .01$).The increase rate of rCBF of the G+E+ group was significantly higher than that of the G-E+ group ($P < .01$) or the G+E- group ($P < .05$). Furthermore, there was a significant difference between the increase rates of rCBF the G+E- and G-E+ groups (Figure 1). Thus, G-CSF treatment significantly increases rCBF, and an additive effect is observed when G-CSF is combined with indirect bypass surgery/EGS treatment.

TABLE. Changes in rCBF Measured by Transcranial Laser Doppler Flowmeter Pre- Post-BICAO and 21 Days After BICAO[a]

	% rCBF Compared to Cerebellum[b]		
	Right Side (EGS+)	Left Side (EGS-)	*P* Value Right vs Left
0 day/pre-BICAO	95.34 ± 7.42	99.68 ± 7.82	NS
0 day/post-BICAO	55.20 ± 9.27	58.24 ± 8.50	NS
21 day post-BICAO	75.21 ± 3.01	64.89 ± 3.36	<.05
%[c]	136.25 ± 5.45	111.41 ± 5.77	<.05

[a]BICAO, bilateral internal carotid artery occlusion; EGS, encephalogaleasynangiosis; NS, not significant; rCBF, regional cerebral blood flow.
[b]Mean ± SE.
[c]% of rCBF 21days after BICAO, compared with rCBF value 0 days after BICAO.

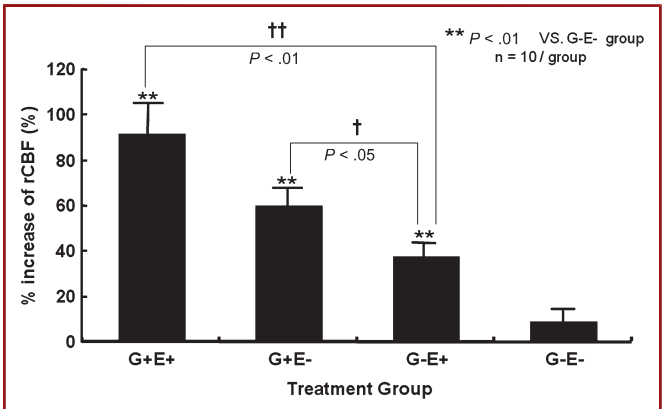

FIGURE 1. *Percent increase in rCBF at 21 days after BICAO in each treatment group. G, G-CSF treatment; E, EGS treatment; **, P < .01, compared with G-E- group; †, P < .05, compared with G-E+ group; ††, P < .01, compared with G+E+ group.*

Immunohistochemical Findings of Angiogenesis

We performed immunohistochemical analysis of vWF staining at the boundary zone between brain and EGS tissue (galea), using tissues collected 21 days post-BICAO in animals that had been treated with G-CSF (Figure 2A, B). There was a blurred boundary between the cerebral cortex, arachnoid, fibrous coat, and galeal tissue in patients in both the G+ and G- groups who received indirect bypass. Numerous vessels smaller than 50 μm were found at the boundary zone, giving the appearance of a thin fibrous coat[8] and extending to the cortex and white matter. There was no brain injury at the EGS site (Figure 2 B, C, E, F).We counted the vessels in a 100 × 400 μm square field at the boundary zone and found that the number of vessels in the G+ group was higher than that in the G- group (13.5 ± 4.43 vs 7.7 ± 2.64, respectively; mean ± SD, Figure 2G, H), a statistically significant difference.

Figure 3 shows staining for vWF of cerebral cortex at the sites near the EGS in each experimental group. Three different representative pictures from three different animals are shown for each group. The G+E+ group had the greatest number of vWF-positive vessels. The size of these vessels was generally small, with a considerable number under 30 μm.

Analysis of Angiogenesis

G-CSF injection (in the G+E+ and G+E- group) significantly increased the number of vessels per field, compared with the control G-E- group (G+E+, 65.3 ± 1.8; G+E-, 54.6 ± 2.9; and G-E-, 38.9 ± 2.8; $P < .01$). In the EGS treatment groups (G+E+ and G-E+), G-CSF injection significantly increased the number of vessels per field (G+E+, 65.3 ± 1.8 vs. G-E+.43.9 ± 2.6; $P < .01$). Thus, G-CSF injection has a significant angiogenetic effect regardless of EGS. In the saline injection groups (G-E+ and G-E-), however, EGS treatment did not significantly increase the

Copyright © Congress of Neurological Surgeons. Unauthorized reproduction of this article is prohibited.

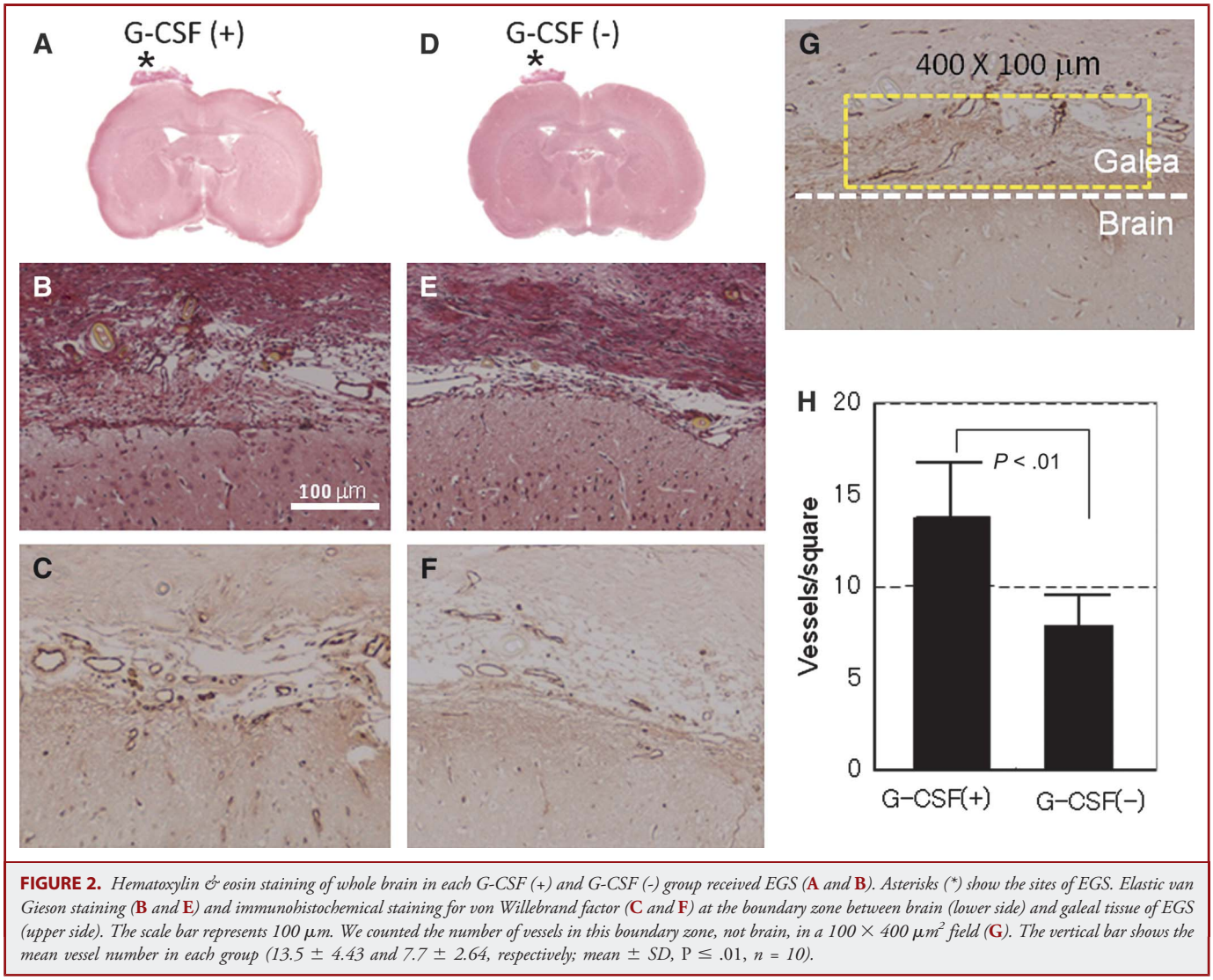

FIGURE 2. *Hematoxylin & eosin staining of whole brain in each G-CSF (+) and G-CSF (-) group received EGS (**A** and **B**). Asterisks (*) show the sites of EGS. Elastic van Gieson staining (**B** and **E**) and immunohistochemical staining for von Willebrand factor (**C** and **F**) at the boundary zone between brain (lower side) and galeal tissue of EGS (upper side). The scale bar represents 100 μm. We counted the number of vessels in this boundary zone, not brain, in a 100 × 400 μm² field (**G**). The vertical bar shows the mean vessel number in each group (13.5 ± 4.43 and 7.7 ± 2.64, respectively; mean ± SD,* P ≤ .01, *n = 10).*

number of vessels. Thus, although EGS treatment is effective in addition to G-CSF treatment, EGS treatment alone does not significantly impact angiogenesis in this hypoperfusion model (Figure 4).

G-CSF Increases the Number of Vessels Smaller Than 40 μm and Modifies the Effects of EGS Treatment

In addition to number of vessels, we also analyzed the size of the proliferated vessels. Figure 5 shows vessel diameter and vessel number at 21 days after operation for each experimental group. The number of vessels smaller than 40 μm was significantly increased in the G+E+ group, compared with the G-E- group (G+E+, 53.8 ± 2.8; G-E-, 28.1 ± 1.9; $P < .01$). In particular, vessels between 20 μm and 40 μm significantly increased in the G+E+ group compared with the G-E+ group (G+E+, 22.7 ± 2.2; G-E+, 13.1 ± 1.4; $P < .01$). The G+E- group also demonstrated a significantly increased number of vessels between 20 and 40 μm, compared with the G+E- group (G+E-, 16.6 ± 0.9; G-E-, 9.7 ± 1.1; $P < .01$). There was no significant increase in the size of vessels over 40 μm in any of the groups, however. The G-CSF treatment groups (G+E+ and G+E-) had significantly higher numbers of vessels in both the 0- to 20-μm and 20- to 40-μm diameter vessel groups compared with the G- groups.

DISCUSSION

In animal studies examining chronic cerebral hypoperfusion, the bilateral common carotid artery occlusion model is generally used. In this study, we used the bilateral internal carotid artery occlusion (BICAO) model, because (1) the BICAO model is

Copyright © Congress of Neurological Surgeons. Unauthorized reproduction of this article is prohibited.

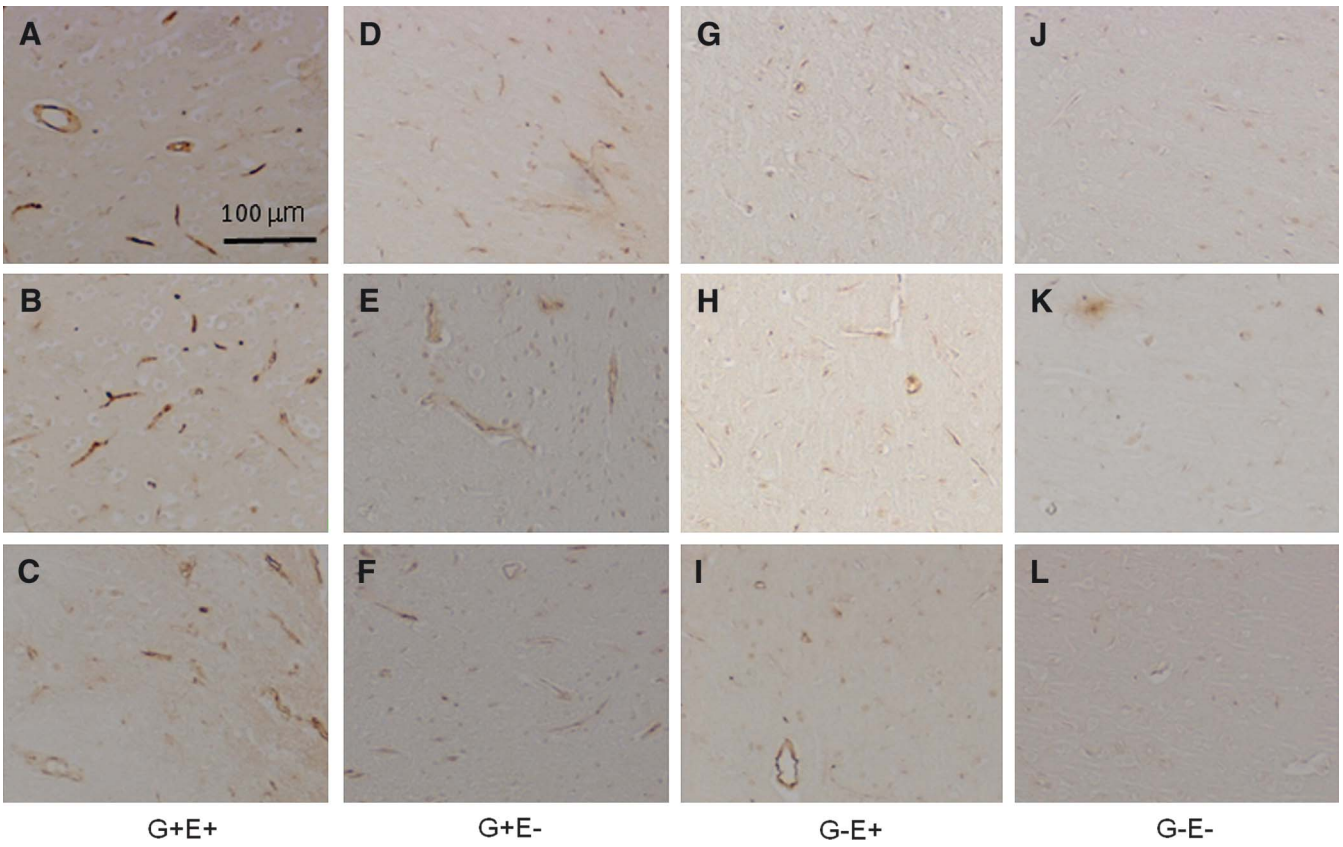

FIGURE 3. *Representative immunohistochemical staining for von Willebrand factor in brain sections from 3 different animals for each treatment group.* **A-C**, *G+E+ group;* **D-F**, *G+E- group;* **G-I**, *G-E+ group;* **J-L**, *G-E- control group. Scale bar shows 100 µm.*

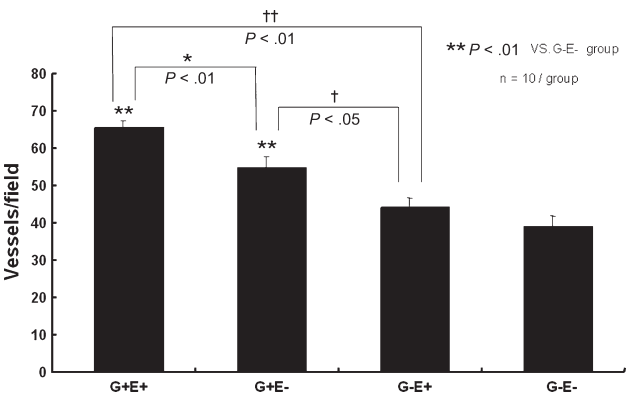

FIGURE 4. *Vessel number for each treatment group 21 days after BICAO. *,* P < .01 *compared with G+E- group; **,* P < .01, *compared with G-E- group; †,* P < .05, *compared with G-E+ group; ††,* P < .01, *compared with G-E+ group.*

more similar to human chronic hypoperfused cerebrovascular diseases, such as moyamoya disease and major cerebral vessel stenosis (or occlusion) than the bilateral common carotid artery occlusion model, and (2) preservation of the blood flow of the external carotid artery was important because we sought to examine angiogenesis after indirect bypass, which creates transcranial anastomosis via the external carotid artery. In contrast to the bilateral common carotid artery occlusion method, which induces severe hypoperfusion,[1,24] there was the possibility with the BICAO method that the decrease in rCBF would not be adequate to induce experimental hypoperfusion conditions. This could have been due to the development of collateral circulation from the ophthalmic artery and other factors. In our study model, bilateral frontal lobe rCBF decreased mildly, to 50% to 60% of that observed in the cerebellum after BICAO (Table). Therefore, our BICAO model mimics human cerebral hypoperfusion disease well.

The main findings of this study were as follows: (1) G-CSF injection and EGS treatment significantly increased rCBF; (2) G-CSF treatment significantly increased rCBF compared to EGS treatment; (3) the effects of rCBF increase induced by G-CSF and

Copyright © Congress of Neurological Surgeons. Unauthorized reproduction of this article is prohibited.

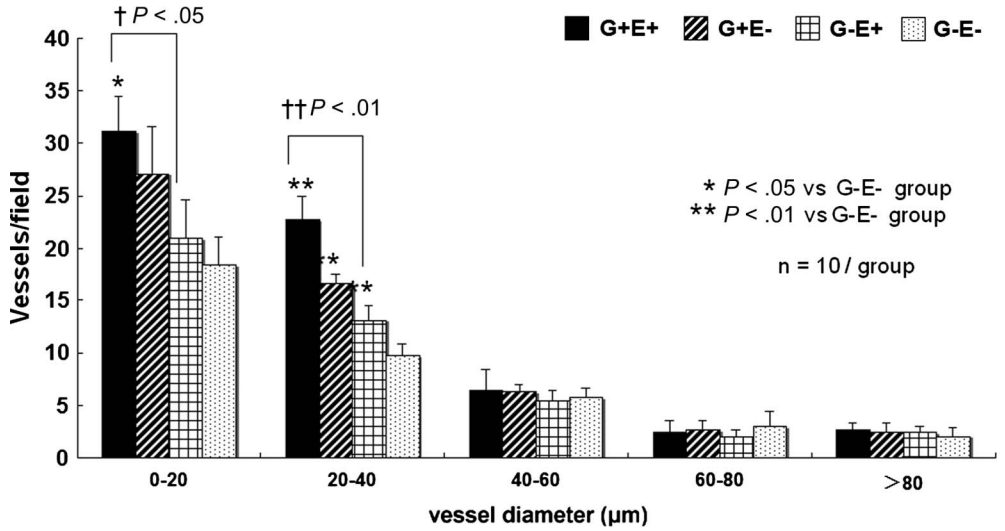

FIGURE 5. *Vessel number distribution for each vessel diameter size group.* **, P < .01, *compared with G-E- group;* †, P < .05, *compared with G-E+ group;* ††, P < .01, *compared with G+E+ group.*

EGS were additive; and (4) both G-CSF and EGS significantly increased the number of blood vessels 40 μm or less in diameter. Thus, G-CSF and EGS treatment increased rCBF by inducing angiogenesis, and G-CSF can be considered a powerful angiogenetic enhancer when coupled with indirect bypass (EGS treatment).

Although these results suggest the efficiency of G-CSF for indirect bypass surgery, we did not show the functional revascularization from the external carotid artery to the intracranial artery via indirect bypass surgery. The best way to prove such revascularization is to perform cerebral angiography. However, it is hard to perform cerebral angiography in rats. Nakamura et al[8] reported on the histopathological evaluation of indirect bypass surgery in miniature pigs in a study in which cerebral angiography was performed. If we use such a large animal, we must show the functional revascularization.

The concept of angiogenesis was first described by Folkman et al,[25] who observed the growth of new capillaries during tumor progression. Vascular endothelial growth factor (VEGF) was the first angiogenetic factor isolated, and since that time, several other angiogenetic factors have been found and tested for therapeutic use in the improvement of microcirculation.[26] Most studies have used single angiogenetic agents for the treatment of cerebral acute and chronic hypoperfusion conditions; there is a lack of studies focusing on combination therapy using angiogenetic agents and indirect bypass surgery. Kusaka et al[27] injected plasmids bearing the human *VEGF* gene into rats following indirect bypass for chronic cerebral hypoperfusion and reported a remarkable increase in capillary number following the *VEGF* injection. Our study, the second report of a combination therapy that includes angiogenetic factor treatment and indirect bypass surgery, demonstrates significant increases in rCBF and vessel number. While most therapeutic trials using angiogenetic factors involve gene therapy, our study used G-CSF, a protein that is safe and widely used in humans.

G-CSF is known to have neuroprotective and neurogenesis activities in acute cerebral ischemia in experimental animals[13-15,17,18,28] and humans.[16] Recently, it was reported that G-CSF has angiogenetic activity when administrated after cerebral infarction.[19-22] The mechanism of angiogenesis by G-CSF is not well known. G-CSF mobilizes CD34+ hematopoietic stem cells from the bone marrow into peripheral blood.[29] It has been suggested that bone marrow–derived endothelial progenitor cells (EPCs) participate in cerebral neovascularization after cerebral ischemia.[30,31] Because bone marrow-derived CD34+ cells contain EPCs,[32] EPCs mediating the angiogenesis induced by G-CSF are very likely to originate in the bone marrow.[33] Furthermore, G-CSF activates endothelial cell proliferation in vitro and demonstrates angiogenetic activity in the corneal angiogenesis assay.[34] Ohki et al[35] reported that VEGF was released by neutrophils that had been prestimulated with G-CSF in vitro and in vivo, which suggests that G-CSF may stimulate the VEGF-mediated angiogenesis system. Thus, G-CSF may contribute to several pathways of angiogenesis in ischemic or hypoperfusion conditions.

In moyamoya disease, direct bypass (STA-to-MCA anastomosis) is considered more effective than indirect bypass. However, in some patients (especially pediatric patients), direct STA-MCA bypass can be difficult, due to both the size and progressive occlusion of the MCAs. In contrast, indirect bypass and cerebral revascularization has been shown to be beneficial in both younger patients[36-39] and adult patients.[36,40,41] Although indirect bypass is considered a beneficial surgery for most moyamoya disease

Copyright © Congress of Neurological Surgeons. Unauthorized reproduction of this article is prohibited.

patients, indirect bypass surgery fails to provide satisfactory revascularization in some patients. Therefore, the addition of G-CSF treatment would be a powerful enhancer for angiogenesis in cases in which surgery alone proved unsatisfactory.

In contrast to its use in the treatment of moyamoya disease, indirect bypass does not appear to be beneficial in patients with medically refractory symptomatic intracranial athero-occlusive disease and secondary hemodynamic failure.[42] It has been suggested that the reason is that patients with atherosclerotic disease may have impaired angiogenesis secondary to reduced endothelial repair capacity. For example, EPCs (which have been characterized as KDR+/CD133+ cells) are reduced in patients with atherosclerotic risk factors and cardiovascular disease.[32,43] Rafat et al[44] reported that circulating EPCs increase in moyamoya disease patients and may play a role in angiogenesis. They also found that the level of circulating EPCs in patients with atherosclerotic cerebrovascular disease was higher than that of healthy controls, but lower than that of patients with moyamoya disease. Furthermore, G-CSF treatment has been demonstrated to increase the number of EPCs in patients with myocardial infarction.[45] The combination of these data and our data suggests that combination therapy consisting of G-CSF treatment and indirect bypass surgery could increase circulating EPCs, which could induce angiogenesis in patients with atherosclerotic hypoperfusion conditions.

The present study is the first to report that G-CSF treatment stimulates angiogenesis of intraparenchymal microvessels and enhances angiogenesis at EGS sites in a model of cerebral hypoperfusion. G-CSF and EGS treatment increases cerebral blood flow and induces angiogenesis in a rat chronic cerebral hypoperfusion model. Moreover, G-CSF enhances angiogenesis associated with indirect bypass surgery. Although G-CSF clinically has some side effects such as bone pain, fever, and allergic reaction, most of them are rare and transient.[10] Thus, G-CSF is considered a highly safe drug and is used for many patients. Our results imply that G-CSF treatment combined with indirect bypass surgery could become a new and novel method for treating chronic cerebral hypoperfusion.

Disclosure

This work was supported by Grants-in-Aid for Scientific Research from the Ministry of Education, Sports, Science and Culture of Japan. The authors have no personal financial or institutional interest in any of the drugs, materials, or devices described in this article.

REFERENCES

1. Coyle P, Panzenbeck MJ. Collateral development after carotid artery occlusion in Fischer 344 rats. *Stroke*. 1990;21(2):316-321.
2. Jet Study Group. Japanese EC-IC Bypass Trial (JET Study): the second interim analysis. *Surg Cereb Stroke (Jpn)*. 2002;30:434-437.
3. The EC-IC bypass study. *N Engl J Med*. 1987;317(16):1030-1032.
4. Karasawa J, Kikuchi H, Furuse S, et al. A surgical treatment of "moyamoya" disease: "encephalo-myo-synangiosis." *Neurol Med Chir (Tokyo)*. 1977;17(1 Pt 1): 29-37.
5. Matsushima Y, Fukai N, Tanaka K, et al. A new surgical treatment of moyamoya disease in children: a preliminary report. *Surg Neurol*. 1981;15(4):313-320.
6. Ozgur BM, Aryan HE, Levy ML. Indirect revascularization for paediatric moyamoya disease: the EDAMS technique. *J Clinic Neurosc*. 2006;13(1):105-108.
7. Shirane R, Yoshida Y, Takahashi T, Yoshimoto T. Assessment of encephalo-galeomyo-synangiosis with dural pedicle insertion in childhood Moyamoya disease: characteristics of cerebral blood flow and oxygen metabolism. *Clin Neurol Neurosurg*. 1997;99(suppl 2):79-85.
8. Nakamura M, Imai H, Konno K, et al. Experimental investigation of encephalomyosynangiosis using gyrencephalic brain of the miniature pig: histopathological evaluation of dynamic reconstruction of vessels for functional anastomosis. *J Neurosurg Pediatr*. 2009;3(6):488-495.
9. Nagata S, Tsuchiya M, Asano S, et al. Molecular cloning and expression of cDNA for human granulocyte colony-stimulating factor. *Nature*. 1986;319(6052):415-418.
10. Morstyn G, Lieschke GJ, Sheridan W, Layton J, Cebon J, Fox RM. Clinical experience with recombinant human granulocyte colony-stimulating factor and granulocyte macrophage colony-stimulating factor. *Semin Hematol*. 1989;26(2 suppl 2):9-13.
11. Neidhart J, Mangalik A, Kohler W, et al. Granulocyte colony-stimulating factor stimulates recovery of granulocytes in patients receiving dose-intensive chemotherapy without bone marrow transplantation. *J Clin Oncol*. 1989;7(11):1685-1692.
12. Sheridan WP, Morstyn G, Wolf M, et al. Granulocyte colony-stimulating factor and neutrophil recovery after high-dose chemotherapy and autologous bone marrow transplantation. *Lancet*. 1989;2(8668):891-895.
13. Gibson CL, Bath PM, Murphy SP. G-CSF reduces infarct volume and improves functional outcome after transient focal cerebral ischemia in mice. *J Cereb Blood Flow Metab*. 2005;25(4):431-439.
14. Matchett GA, Calinisan JB, Matchett GC, Martin RD, Zhang JH. The effect of granulocyte-colony stimulating factor in global cerebral ischemia in rats. *Brain Res*. 2007;1136(1):200-207.
15. Schabitz W, Kollmar M, Schwaninger E, Juettler J, Bardutzky M, Scholzke N. Neuroprotective effect of granulocyte colony stimulating factor after focal cerebral ischemia. *Stroke*. 2003;34(3):745-751.
16. Shyu WC, Lin SZ, Lee CC, Liu DD, Li H. Granulocyte colony-stimulating factor for acute ischemic stroke: a randomized controlled trial. *Can Med Assoc J*. 2006;174(7):927-933.
17. Six I, Gasan G, Mura E, Bordet R. Beneficial effect of pharmacological mobilization of bone marrow in experimental cerebral ischemia. *Eur Pharmacol*. 2003;458(3):327-328.
18. Solaroglu IS, Cahill J, Jadhav V, Zhang JH. A novel neuroprotectant granulocyte-colony stimulating factor. *Stroke*. 2006;37(4):1123-1128.
19. Lee ST, Chu K, Jung KH, et al. Granulocyte colony-stimulating factor enhances angiogenesis after focal cerebral ischemia. *Brain Res*. 2005;1058(1-2):120-128.
20. Piao CS, Gonzalez-Toledo ME, Xue YQ, et al. The role of stem cell factor and granulocyte-colony stimulating factor in brain repair during chronic stroke. *J Cereb Blood Flow Metab*. 2009;29(4):759-770.
21. Sehara Y, Hayashi T, Deguchi K, et al. Potentiation of neurogenesis and angiogenesis by G-CSF after focal cerebral ischemia in rats. *Brain Res*. 2007;1151:142-149.
22. Toth ZE, Leker RR, Shahar T, et al. The combination of granulocyte colony-stimulating factor and stem cell factor significantly increases the number of bone marrow-derived endothelial cells in brains of mice following cerebral ischemia. *Blood*. 2008;111(12):5422-5423.
23. Hasegawa Y, Hamada J, Morioka M, et al. Neuroprotective effect of postischemic administration of sodium orthovanadate in rats with transient middle cerebral artery occlusion. *J Cereb Blood Flow Metab*. 2003;23(9):1040-1051.
24. Ulrich PT, Kroppenstedt S, Heimann A, et al. Laser-doppler scanning of local cerebral blood flow and reserve capacity and testing of motor and memory functions in a chronic 2-vessel occlusion model in rats. *Stroke*. 1998;29(11):2412-2420.
25. Folkman J, Merler E, Abernathy C, et al. Isolation of a tumor factor responsible for angiogenesis. *J Exp Med*. 1971;133(2):275-288.
26. Gupta R, Tongers J, Losordo DW. Human studies of angiogenetic gene therapy. *Circ Res*. 2009;105(8):724-736.
27. Kusaka N, Sugiu K, Tokunaga K, et al. Enhanced brain angiogenesis in chronic cerebral hypoperfusion after administration of plasmid human vascular endothelial growth factor in combination with indirect vasoreconstructive surgery. *J Neurosurg*. 2005;103(5):882-890.
28. Sevimli S, Diederich K, Strecker JK, et al. Endogenous brain protection by granulocyte-colony stimulating factor after ischemic stroke. *Exp Neurol*. 2009;217(2):328-335.
29. Grigg AP, Roberts AW, Raunow H, et al. Optimizing dose and scheduling of filgrastism (granulocyte colony-stimulating factor) for mobilization and collection of peripheral blood progenitor cells in normal volunteers. *Blood*. 1995;86(12):4437-4445.

Copyright © Congress of Neurological Surgeons. Unauthorized reproduction of this article is prohibited.

30. Taguchi A, Soma T, Tanaka H, et al. Administration of CD34(+) cells after stroke enhances neurogenesis via angiogenesis in a mouse model. *J Clin Invest*. 2004;114(3):330-338.
31. Zhang ZG, Zhang L, Jiang Q, Chopp M. Bone marrow-derived endothelial progenitor cells participate in cerebral neovascularization after focal cerebral ischemia in the adult mouse. *Circ Res*. 2002;90(3):284-288.
32. Asahara T, Murohara T, Sullivan A, Silver M, van der Zee R, Li T. Isolation of putative progenitor endothelial cells for angiogenesis. *Science*. 1997;275(5302):964-967.
33. Natori T, Sata M, Washida M, Hirata Y, Nagai R, Makuuchi M. GCSF stimulates angiogenesis and promotes tumor growth: potential contribution of bone marrow-derived endothelial progenitor cells. *Biochem Biophys Res Commun*. 2002;297:1058-1061.
34. Bussolino F, Ziche M, Wang JM, et al. In vitro and in vivo activation of endothelial cells by colony-stimulating factors. *J Clin Invest*. 1991;87(3):986-995.
35. Ohki Y, Heissig B, Sato Y, et al. Granulocyte colony-stimulating factor promotes neovascularization by releasing vascular endothelial growth factor from neutrophils. *FASEB J*. 2005;19(14):2005-2007.
36. Houkin K, Ishikawa T, Yoshimoto T, Abe H. Direct and indirect revascularization for moyamoya disease surgical techniques and peri-operative complications. *Clin Neurol Neurosurg*. 1997;99(Suppl 2):S142-S145.
37. Ishikawa T, Houkin K, Kamiyama H, Abe H. Effects of surgical revascularization on outcome of patients with pediatric moyamoya disease. *Stroke*. 1997;28(6):1170-1173.
38. Lee SK, Kim DI, Jeong EK, et al. Postoperative evaluation of moyamoya disease with perfusion-weighted MR imaging: initial experience. *AJNR Am J Neuroradiol*. 2003;24(4):741-747.
39. Matsushima Y, Aoyagi M, Koumo Y, Takasato Y, Yamaguchi T, Masaoka H. Effects of encephalo-duro-arterio-synangiosis on childhood moyamoya patients—swift disappearance of ischemic attacks and maintenance of mental capacity. *Neurol Med Chir (Tokyo)*. 1991;31(11):708-714.
40. Han DH, Nam DH, Oh CW. Moyamoya disease in adults: characteristics of clinical presentation and outcome after encephalo-duro-arterio-synangiosis. *Clin Neurol Neurosurg*. 1997;99(suppl 2):S151-S155.
41. Starke RM, Komotar RJ, Hickman ZL, et al. Clinical features, surgical treatment and long-term outcome in adult patients with moyamoya disease. *J Neurosurg*. 2009;111(5):936-942.
42. Komotar RJ, Starke RM, Otten ML, et al. The role of indirect extracranial-intracranial bypass in the treatment of symptomatic intracranial atheroocclusive disease. *J Neurosurg*. 2009;110(5):896-904.
43. Hill JM, Zalos G, Halcox JP, et al. Circulating endothelial progenitor cells, vascular function, and cardiovascular risk. *N Engl J Med*. 2003;348(7):593-600.
44. Rafat N, Beck GH, Pena-Tapia PG, Schmiedek P, Vajkoczy P. Increased levels of circulating endothelial progenitor cells in patients with moyamoya disease. *Stroke*. 2009;40(2):432-438.
45. Bruno S, Bussolati B, Scacciatella P, et al. Combined administration of G-CSF and GM-CSF stimulates monocyte-derived pro-angiogenic cells in patients with acute myocardial infarction. *Cytokine*. 2006;34(1-2):56-65.

COMMENT

This study uses a well-thought-out experimental approach with the aim of revealing the possible function of granulocyte colony-stimulating factor (G-CSF)and unilateral indirect bypass surgery in stimulation of angiogenesis in the course of reperfusion after induced ischemia.

Reperfusion therapy is crucial after chronic or acute ischemic conditions; therefore, the study provides crucial clinical support for the use of G-CSF, given that it is already in use treating other clinical issues such as chemotherapy-induced neutropenia and also introduces indirect bypass surgery as a therapeutic method combined with G-CSF. The study also provides support for the utilization of a valid ischemia model and the use of laser Doppler flowmetry for analysis of regional cerebral blood flow and immunohistochemistry methods to assess the angiogenesis in the ischemic cerebral tissues.

Ischemia/reperfusion field is extensively critical, and each step taken forward to discover new therapeutic options should be treated accordingly. This study will further the therapeutic options supporting more effective reperfusion modalities. Additionally, understanding the role of angiogenesis in ischemia is vital and eventually will make it possible to direct the angiogenic cascade of events toward more efficient treatments.

Turker Kılic
Istanbul, Turkey

The International Podcast Series. Article abstracts translated for our international audience at www.neurosurgery-online.com

NEUROSURGERY

Copyright © Congress of Neurological Surgeons. Unauthorized reproduction of this article is prohibited.

Computed Tomography Imaging of Transferrin Targeting Liposomes Encapsulating Both Boron and Iodine Contrast Agents by Convection-Enhanced Delivery to F98 Rat Glioma for Boron Neutron Capture Therapy

Shiro Miyata, MD*
Shinji Kawabata, MD, PhD*
Ryo Hiramatsu, MD*
Atsushi Doi, MD, PhD*
Naokado Ikeda, MD, PhD*
Taro Yamashita, MD*
Toshihiko Kuroiwa, MD, PhD*
Satoshi Kasaoka, PhD‡
Kazuo Maruyama, PhD§
Shin-Ichi Miyatake, MD, PhD*

*Department of Neurosurgery, Osaka Medical College, Osaka, Japan; ‡Faculty of Pharmaceutical Sciences, Hiroshima International University, Hiroshima, Japan; §Faculty of Pharmaceutical Sciences, Teikyo University, Tokyo, Japan.

Correspondence:
Shinji Kawabata, MD, PhD,
Department of Neurosurgery,
Osaka Medical College,
2-7 Daigaku-machi,
Takatsuki City,
Osaka 569-8686, Japan.
E-mail: neu046@poh.osaka-med.ac.jp.

Received, February 4, 2010.
Accepted, October 2, 2010.

Copyright © 2011 by the
Congress of Neurological Surgeons

WHAT IS THIS BOX?
A QR Code is a matrix barcode readable by QR scanners, mobile phones with cameras, and smartphones. **The QR Code above links to Supplemental Digital Content from this article.**

BACKGROUND: To achieve potent tumor-selective antitumor efficacy by boron neutron capture therapy (BNCT), it is important to have a significant differential uptake of 10B between tumor cells and normal cells. This should enable BNCT to reduce damage to normal tissues compared with other radiation therapies.

OBJECTIVE: To augment the therapeutic efficacy of BNCT, we used transferrin-conjugated polyethylene glycol (PEG) (TF-PEG) liposome encapsulating sodium borocaptate and lomeprol, an iodine contrast agent, with intratumoral convection-enhanced delivery (CED) in a rat glioma tumor model.

METHODS: The in vitro ^{10}B concentration of F98 rat glioma cells was determined by inductively coupled plasma atomic emission spectrometry after incubation with either TF-PEG or PEG liposomes. For in vivo biodistribution studies, ^{10}B concentrations within blood, normal brain tissue, and intracerebrally transplanted F98 cells were measured with inductively coupled plasma-atomic emission spectrometry after CED of the compounds, and computed tomography was performed at selected time intervals.

RESULTS: ^{10}B concentrations of F98 cultured glioma cells in vitro 6 hours after exposure to PEG and TF-PEG liposome were 16.1 and 51.9 ng^{10}B/10^6 cells, respectively. ^{10}B concentrations in F98 glioma tissue 24 hours after CED were 22.5 and 82.2 μg/g, by PEG and TF-PEG liposome, respectively, with lower ^{10}B concentrations in blood and normal brain. Iomeprol provided vivid and stable enhanced computed tomography imaging of the transplanted tumor even 72 hours after CED by TF-PEG liposome. Conversely, tissue enhancement had already washed out at 24 hours after CED of the PEG liposomes.

CONCLUSION: The combination of TF-PEG liposome encapsulating sodium borocaptate and lomeprol and intratumoral CED enables not only a precise and potent targeting of boron delivery to the tumor tissue, but also the ability to follow the trace of boron delivery administered intratumorally by real-time computed tomography.

KEY WORDS: Boron neutron capture therapy, Computed tomography, Convection-enhanced delivery, Liposome, Transferrin

Neurosurgery 68:1380–1387, 2011 DOI: 10.1227/NEU.0b013e31820b52aa www.neurosurgery-online.com

ABBREVIATIONS: **^{10}B**, boron-10; **BBB**, blood-brain barrier; **BDS**, boron delivery system; **BNCT**, boron neutron capture therapy; **BSH**, sodium borocaptate; **CED**, convection-enhanced delivery; **PEG**, polyethylene glycol; **TF-PEG**, transferrin-conjugated polyethylene glycol

Supplemental digital content is available for this article. Direct URL citations appear in the printed text and are provided in the HTML and PDF versions of this article on the journal's Web site (www.neurosurgery-online.com).

Therapeutic modalities such as stereotactic radiosurgery, intensity-modulated radiation therapy, particle radiation therapy, and novel therapeutic agents with molecular targeting have been developed to improve the prognosis of some types of brain tumors. However, over the past few decades, there has been little improvement in the prognosis of

Copyright © Congress of Neurological Surgeons. Unauthorized reproduction of this article is prohibited.

patients with malignant gliomas because of the tumor's tendency to microscopically infiltrate the surrounding normal tissue. To overcome this infiltrative nature, it is necessary to selectively deliver a higher concentration of anticancer or radiation sensitizing agents into tumor tissue compared with the surrounding normal brain tissue. We are focusing on developing boron neutron capture therapy (BNCT) to achieve greater tumor-selective killing and therefore therapeutic efficacy.

At our institution, we have clinically applied BNCT since 2002 as an essential adjuvant therapy for patients with recurrent or newly diagnosed malignant gliomas[1-4] and have achieved superior outcomes compared with those by standard therapies using fractionated radiographic treatments.[5] BNCT is based on the nuclear capture and fission reactions that occur when boron-10 (^{10}B), a nonradioactive constituent of natural elemental boron, is irradiated with low-energy thermal neutrons to produce high-energy α particles and recoiling lithium-7 nuclei. These have high linear energy transfer and path lengths of approximately 9 and 5 μm, respectively, which theoretically allow them to discharge their energy within ^{10}B-containing cells.[6] Thus, to achieve potent tumor-selective antitumor efficacy, it is important to have a significant differential uptake of ^{10}B between tumor cells and normal cells. This should enable BNCT to reduce damage to normal tissues compared with other radiation therapies.

Today, clinically used sodium borocaptate (BSH) is transferred to brain tumors only through the disrupted blood-brain barrier (BBB), so it is difficult for BSH to reach regions that tumor cells invade microscopically where the BBB seems to be intact. On the other hand, boronophenylalanine, which transfers boron via L-type amino acid transporter, can deliver ^{10}B even in the infiltrating tumor cell population where the BBB is intact. However, some amounts of ^{10}B are inevitably taken into the normal cells by boronophenylalanine systemic administration. Moreover, the native heterogeneity of malignant gliomas interferes with the ability to accurately target the tumor. Recent reports have delineated boron delivery systems (BDSs) to improve molecular targeting of malignant gliomas.[7,8] Previously we reported on the effectiveness of transferrin-conjugated polyethylene glycol (PEG) (TF-PEG) liposome encapsulating BSH administered intravenously, with regard to its ability to target tumor cells and to increase the accumulation of ^{10}B in tumor tissue.[9]

To improve the efficacy of tumor targeting under systemic administration, the circulation time of a BDS in the blood needs to be lengthened. Unfortunately, systemic administration of a BDS increases the capture of ^{10}B-labeled molecules in the reticuloendothelial system of the liver and spleen, which may cause adverse effects. To solve these problems, we adopted convection-enhanced delivery (CED) for drug administration. This technique enables the delivery of boron compounds to the tumor cells in the brain without going through the disrupted BBB. CED, a method for local drug infusion directly into the brain,[10] enables the distribution of any drugs homogeneously in the brain, keeping high concentration at the target site without mechanical damage to the surrounding normal tissue. CED depends on the bulk flow in the interstitial space produced by continuous slow infusion into the brain under low positive pressure. Using this method, it is theoretically possible to deliver drugs to regions where tumor cells invade microscopically with little accumulation in the blood and other organs. Moreover, because it does not depend on the molecular weight of the infused agent, this method allows us to widely select many kinds of therapeutic agents or carriers for them, such as liposomes, dendrimers, and nanotubes.[7,11-15] Today, some clinical trials of targeted toxins with epidermal growth factor receptor, transferrin receptor, interleukin-13 receptor, and interleukin-4 receptor are reported.[8,11,16-18]

In BNCT, there is some interval before neutron irradiation, unlike with chemotherapies or therapies by toxins. This interval derives from the nontoxicity of BDS, and it enables us to estimate the distribution of infusion agents before neutron irradiation. We developed a novel liposomal BDS mechanism that encapsulates BSH and an iodine contrast agent, making it possible to trace the intracerebral distribution of the drug by computed tomography (CT).[19] We evaluated 2 BDSs: PEG liposome encapsulating both BSH and Iomeprol (PEG liposome [BSH, Iomeprol]) and TF-PEG liposome (BSH, Iomeprol) administered by CED in rat brain tumor models.

MATERIALS AND METHODS

Preparation of the Boron Compounds

BSH was purchased from Katchem (Prague, Czech Republic). Iomeprol was used as an iodine contrast agent for CT scanning. Iomeprol (MW777.09, concentration 612.4 mg/mL; Iomeron 300; Eisai, Tokyo, Japan), which is very soluble in water and contains 300 mg/mL organically bound iodine, was used as the imaging tracer. PEG liposome (BSH, Iomeprol) and TF-PEG liposome (BSH, Iomeprol) were prepared by one of the authors (S.K.) as reported previously.[20] Transferrin (1:60 transferrin:phospholipid molar ratio; phospholipid concentration, 0.2 mM) (Wako Pure Chemical Industries, Osaka, Japan) was conjugated to the distal ends of 1,2-dioleoyl-sn-glycero-3-phosphoethanolamine-n-[poly(ethyleneglycol)]-hydroxy succinamide (Nippon Oil and Fats, Tokyo, Japan) in micelles at room temperature for 1 hour with gentle stirring. TF-PEG distearoylphosphatidylethanolamine (DSPE) was transferred to preformed PEG liposomes (64:33:3 dipalmitoylphosphatidylcholine (DPPC):cholesterol:DSPE-PEG molar ratio; size $<$150 nm) loaded with 300 mM BSH:Iomeprol at a 1:1 volume ratio using the micelle transfer method at a 1:33 TF-PEG-DSPE:liposome molar ratio, at 45°C for 3 hours. Both PEG liposome (BSH, Iomeprol) and TF-PEG liposome (BSH, Iomeprol) were prepared using the protocol described by Wei et al[7] with slight modifications.

To evaluate possible adverse effects of PEG liposome (BSH, Iomeprol) and TF-PEG liposome (BSH, Iomeprol) on normal brain parenchyma, 12 Fischer 344 male rats (200-230 g, F344 NSlc; Japan SLC, Shizuoka, Japan) were given a 20-μg ^{10}B infusion of either BDS (n = 6 per BDS) into the right hemisphere by CED. Body weight was measured just before the CED procedure and on days 7 and 14 after the procedure. Some of the rats that were administered either BDS were euthanized on day 7 after the CED procedure for histological evaluation and were perfused with 4% paraformaldehyde; their brains were then processed for histological examination with hematoxylin and eosin staining.

Copyright © Congress of Neurological Surgeons. Unauthorized reproduction of this article is prohibited.

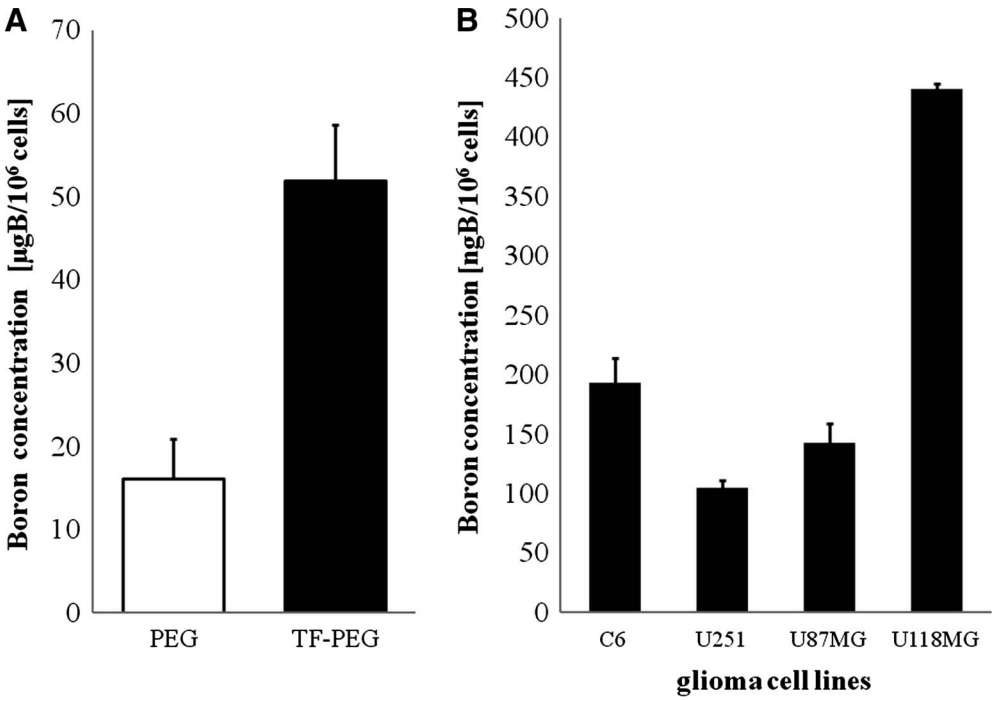

FIGURE 1. **A**, *boron concentration of F98 glioma cells 6 hours after incubation in media including 10 μg^{10}B/mL of each boron delivery system. Transferrin-conjugated polyethylene glycol (TF-PEG) group (■) and the polyethylene glycol (PEG) group (□). The boron concentrations of tumor cells were significantly higher in the TF-PEG group than in the PEG group: 51.9 ± 6.8 ng^{10}B/10^6 cells and 16.1 ± 4.8 ng^{10}B/10^6 cells, respectively (P < .05).* **B**, *boron concentration of glioma cells (C6, U251, U87MG, and U118MG) 6 hours after incubation for 10 μg^{10}B/mL of TF-PEG liposome. F98 glioma cells showed the minimum accumulation of sodium borocaptate by this liposome among these glioma cell lines.*

In Vitro Cellular Uptake Study

For the in vitro boron uptake study, F98 rat glioma cells (provided by Rolf F. Barth MD, The Ohio State University, Columbus, Ohio) were used. One million F98 glioma cells were seeded onto a tissue culture dish (100 × 20 mm; Becton Dickinson, Franklin Lakes, New Jersey) with Dulbecco modified Eagle medium with 10% fetal bovine serum with penicillin and streptomycin at 37°C in an atmosphere of 5% CO_2. All the materials for the culture medium were purchased from Invitrogen (Carlsbad, California). After incubation for 24 hours at 37°C, the medium was replaced with Dulbecco modified Eagle medium containing 10 μg^{10}B/mL PEG liposome (BSH, Iomeprol) or TF-PEG liposome (BSH, Iomeprol), and the cells were incubated for an additional 6 hours at 37°C. The medium was then removed, and the cells were washed twice with phosphate-buffered saline and detached with trypsin–ethylenediamine tetraacetic acid solution. Medium was then added, and the cells were counted and sedimented. Cells were digested overnight with 1 N nitric acid solution (Wako Pure Chemical Industries), and boron uptake was determined by inductively coupled plasma-atomic emission spectrometry (Hitachi, Tokyo, Japan). Cellular uptake of boron by TF-PEG liposome (BSH, Iomeprol) for other glioma cell lines (C6, U251, U87MG, and U118MG) was also evaluated.

Tumor Model

The male Fischer 344 rats were generally anesthetized with an intraperitoneal injection of pentobarbital sodium (50 mg/kg) and placed in a stereotactic frame (Model 900; David Kopf Instruments, Tujunga, California). A midline incision was made in the scalp, and the skull target (3.5 mm right to the bregma) was identified. A hand-held drill was used to create a small burr hole at this location. A 25 μL Hamilton infusion syringe (model 1700 RN, Hamilton Bonaduz AG, Bonaduz, Switzerland) was fixed on the clamping device of the stereotactic frame. A 26-gauge needle attached to a microsyringe was first inserted to a depth of 6.0 mm from the skull and then withdrawn to its target depth in the brain (5.5 mm from the skull surface). Ten thousand F98 cells diluted in 10 μL of Dulbecco modified Eagle medium were then injected over approximately 10 minutes. The needle was kept in place for 1 minute after infusion and withdrawn slowly. The skull hole was sealed with bone wax, and the scalp was sutured. Under these conditions, the procedure results in tumor growth in all rats, with a median survival time of 23 days.

In Vivo Biodistribution Study

For biodistribution study, 10 days after tumor implantation, rats bearing F98 brain tumors were generally anesthetized and placed in a stereotactic frame as described above. They were administered either PEG liposome (BSH, Iomeprol) or TF-PEG liposome (BSH, Iomeprol) by CED with an infusion syringe pump over 30 minutes at a rate of 0.33 μL/min. The total amount of ^{10}B administered to each rat was 20 μg. We then assayed the ^{10}B concentration of tumor, blood, and normal brain by inductively coupled plasma-atomic emission spectrometry. In this study, we sampled normal tissues from both

Copyright © Congress of Neurological Surgeons. Unauthorized reproduction of this article is prohibited.

TABLE 1. Boron Concentrations in Brain Tumors in Rats Bearing F98 Gliomas to Which Polyethylene Glycol Liposome (Sodium Borocaptate, Iomeprol) or Transferrin-Conjugated Polyethylene Glycol Liposome (Sodium Borocaptate), Iomeprol) Was Administered by Convection-Enhanced Delivery[a]

		Boron Concentration, μg/g				Tumor Brain Ratio	
BDS	Time, h[b]	Tumor	Brain Ipsilateral	Brain Contralateral	Blood	Ipsilateral Normal Brain	Contralateral Normal Brain
PEG liposome (BSH, Iomeprol)	0[c]	33.5 ± 10.5	0.6 ± 0.6	0.3 ± 0.1	0.4 ± 0.2	55.8	111.7
	24	22.5 ± 6.1	1.7 ± 1.5	1.0 ± 0.6	0.4 ± 0.1	13.2	22.5
	48	8.5 ± 7.9	1.5 ± 0.7	0.4 ± 0.3	0.4 ± 0.1	5.7	21.3
	72	4.9 ± 4.6	0.2 ± 0.1	0.2 ± 0.1	0.5 ± 0.2	24.5	24.5
TF-PEG liposome (BSH, Iomeprol)	0[c]	55.2 ± 26.6	2.1 ± 2.5	0.4 ± 0.2	0.6 ± 0.3	26.3	138.0
	24	82.2 ± 18.6	0.7 ± 0.4	0.3 ± 0.2	0.6 ± 0.1	117.0	274.0
	48	41.2 ± 14.4	1.2 ± 1.0	0.9 ± 0.6	0.9 ± 0.1	34.3	45.8
	72	25.8 ± 13.5	0.4 ± 0.2	0.4 ± 0.2	0.6 ± 0.2	64.5	64.5

[a]Each point represents the mean ± standard deviation. BDS, boron delivery system; PEG, polyethylene glycol; BSH, sodium borocaptate; TF-PEG, transferrin-conjugated polyethylene glycol.
[b]Hours after convection-enhanced delivery of each BDS.
[c]The time point of 0 means the point just after rats were killed.

hemispheres and defined the normal tissue from the tumor-bearing hemisphere as ipsilateral normal brain and the normal tissue from the other hemisphere as contralateral normal brain. The normal brain of the ipsilateral side, at least a couple of millimeters away from the tumor border, was sampled with approximately 1 g for ^{10}B content measurement. The normal brain of the contralateral side, symmetrical for the ipsilateral sampling, was sampled for the measurement.

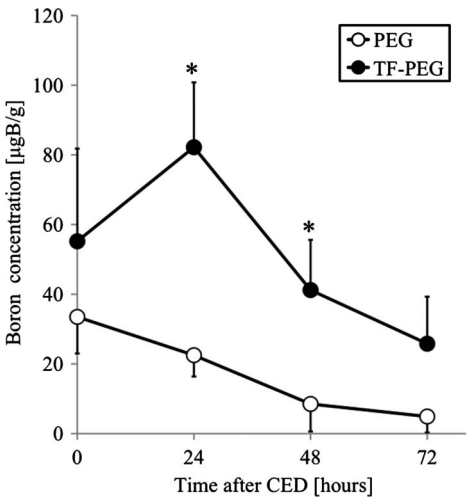

FIGURE 2. *Boron concentration of the tumor at selected times after convection-enhanced delivery (CED) administration of each boron delivery system, polyethylene glycol (PEG) liposome (sodium borocaptate [BSH], Iomeprol) or transferrin-conjugated polyethylene glycol (TF-PEG) liposome (BSH, Iomeprol). The TF-PEG group (●) and the PEG group (○). At all the time points, the tumor boron concentration in the TF-PEG group was higher than that in the PEG group. Especially at 24 and 48 hours after CED, the boron concentrations in the TF-PEG group were significantly higher than those in the PEG group (P < .05).*

Imaging Study

For the imaging study, at selected times (0, 24, 48, and 72 hours) after termination of CED, rats were analyzed by CT to evaluate the distribution of BDS and were then euthanized. In this study, we used a high-speed helical CT imaging system (Aquilion 64; Toshiba Medical Systems, Tochigi, Japan). Real-time coronal CT scans (1-mm slice thickness, 1-mm spacing) were performed. We also did a covisualization study using iodine contrast agent (Iomeprol) and fluorescence dye, co-encapsulated into the TF-PEG liposome infused by CED with the CT scan the same as for BDS.

All procedures were performed according to the Osaka Medical College Regulations on Animal Experimentation.

Statistical Analysis

Pairwise comparisons were conducted using Student's *t* test. Group differences resulting in *P* values of $<.05$ were considered statistically significant.

RESULTS

Evaluation of the Normal Rat Brain Infused BDS by CED

Fischer 344 rats receiving a 20-μg ^{10}B infusion of PEG liposome (BSH, Iomeprol) or TF-PEG liposome (BSH, Iomeprol) by CED into their right hemisphere showed no substantial evidence of adverse effects over a 14-day period. Daily observations revealed no clinical deficits during the study. The rats appeared healthy and gained or maintained body weight at the same rate as did normal rats. Histological evaluation from a representative rat euthanized on day 7 after infusion revealed some evidence of

Copyright © Congress of Neurological Surgeons. Unauthorized reproduction of this article is prohibited.

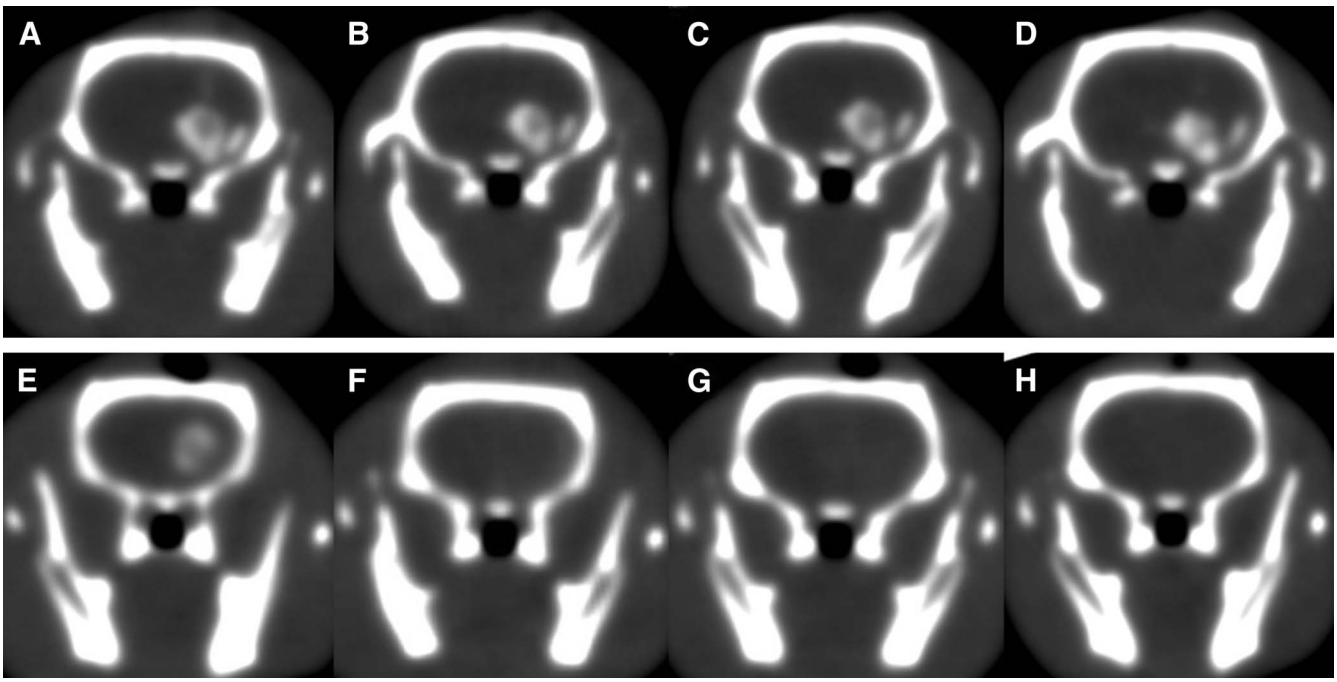

FIGURE 3. *Computed tomography (CT) imaging of iodine contrast agent distributions from each boron delivery system (BDS). These are images from CT scans at selected times (0, 24, 48, 72 hours) after the termination of convection-enhanced delivery (CED) with each BDS. The upper column (**A-D**) shows one of the polyethylene glycol (PEG) group, and the lower (**E-H**) shows one of the transferrin-conjugated polyethylene glycol (TF-PEG) group (**E-H**) The images are from the TF-PEG group, and the contrast enhancement was retained in the tumor until 72 hours after CED. (**A-D**) The images are from the PEG group. The contrast enhancement had already disappeared 24 hours after CED.*

tissue inflammation in the striatal regions proximal to the needle track on the site. This tissue reaction was observed only adjacent to the needle tract (data not shown).

In Vitro Uptake Study

The boron concentrations of F98 glioma cells 6 hours after exposure to TF-PEG liposome (BSH, Iomeprol) were significantly higher than those after exposure to PEG liposome (BSH, Iomeprol): 51.9 ± 6.8 and 16.1 ± 4.8 ng^{10}B/10^6 cells, respectively. (Figure 1) ($P < .05$).

F98 glioma line showed the minimum accumulation of BSH by TF-PEG liposomes among other glioma lines (C6, U251, U87MG, and U118MG).

In Vivo Biodistribution Study

Table 1 summarizes the biodistribution data for PEG liposome (BSH, Iomeprol) and TF-PEG liposome (BSH, Iomeprol) after CED administration to rats bearing F98 brain tumors. The boron concentrations in tumors were significantly higher in the TF-PEG group than in the PEG group at 24 and 48 hours after CED (Figure 2) ($P < .05$). Especially at 24 hours after CED, the TF-PEG group showed a higher mean tumor boron concentration (82.2 ± 18.6 μg^{10}B/g) and a higher tumor-to-normal brain ratio (274). On the other hand, at that time point, the boron concentrations of blood and contralateral normal brain were less than 1.0 μg^{10}B/g. In addition, the boron concentrations in the other organs such as liver, spleen, kidney, heart, lung, muscle, and skin were also less than 1.0 μg^{10}B/g (data not shown).

Imaging Study

Figures 3 and 4 show the results of the imaging study by CT and histological study of the brain from same rats, respectively, at 4 time points (0, 24, 48, and 72 hours). The CT images showed that the contrast enhancement of the tumor in the TF-PEG group was retained for at least until 72 hours after CED, whereas in the PEG group, the enhancement had already disappeared by 24 hours after CED. The mean Hounsfield unit values in the PEG group and the TF-PEG group were 269 ± 33.3 and 281 ± 88.4, respectively, at 0 hours, and 142 ± 40.6 and 256 ± 39.2, respectively, at 24 hours ($P < .05$) (Figure 5).

In the covisualization study using iodine contrast agent (Iomeprol) and fluorescence dye, co-encapsulated into the TF-PEG liposome administered by CED shows compatible distribution of both agents (left, fluorescencephotography; right, CT scan) (see Figure, Supplemental Digital Content 1, http://links.lww.com/NEU/A371).

Copyright © Congress of Neurological Surgeons. Unauthorized reproduction of this article is prohibited.

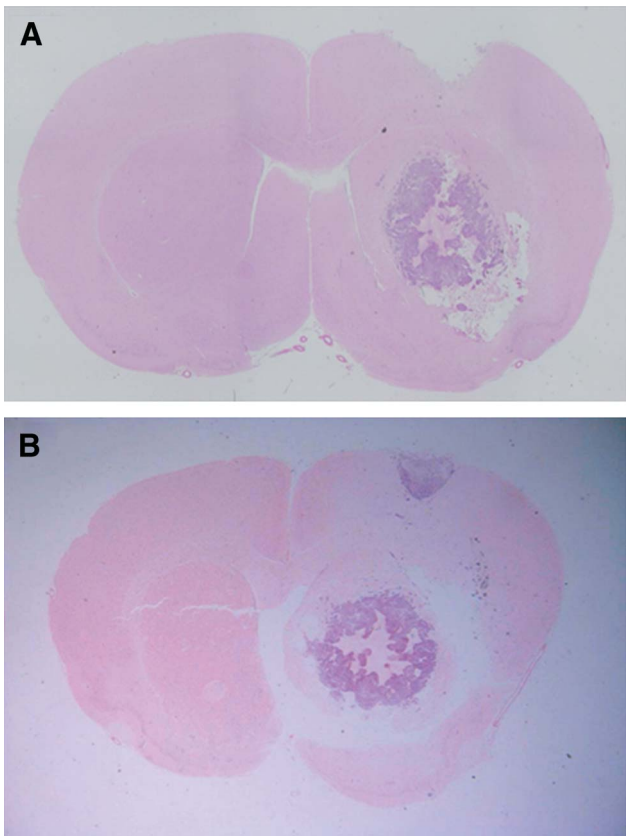

FIGURE 4. *Histological study of the brain shown in Figure 3.* **A** *is from the TF-PEG group and* **B** *is from the polyethylene glycol (PEG) group. Each case shows that the tumor location on hematoxylin and eosin staining corresponds to the tumor contrast on computed tomography imaging in Figure 3.*

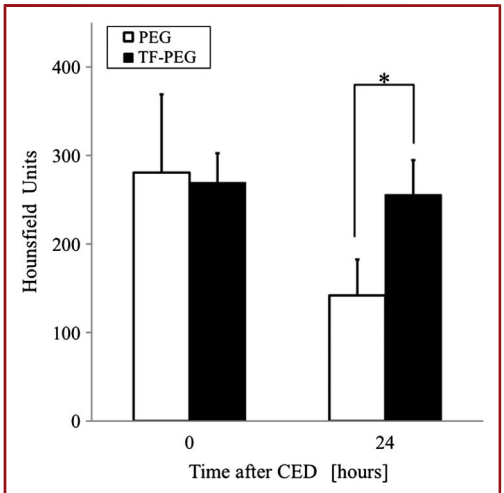

FIGURE 5. *The Hounsfield unit graph measured on each computed tomography image shown in Figure 3. Transferrin-conjugated polyethylene glycol (TF-PEG) group (□) and the polyethylene glycol (PEG) group (■). In both cases, the Hounsfield units at 0 hours after convection-enhanced delivery (CED) are almost the same. In the TF-PEG group, the Hounsfield units remained high until 24 hours after CED, but in the PEG group, the Hounsfield units decreased until 24 hours after CED.*

DISCUSSION

We previously reported that significantly higher concentrations of ^{10}B in tumor tissues in U87Δ brain tumor-bearing nude mice were achieved with systemic TF-PEG liposome (BSH) administration compared with mice administered PEG liposome (BSH) or bare BSH.[9] However, the results of that study led us to speculate on 2 problems: the limitation on ^{10}B accumulation because of the BBB, especially in the microscopic tumor cell invasion area, and the unexpected accumulation into other organs. In this study, to overcome these problems, we devised a combination of tumor targeting by transferrin and CED as a method for local drug injection directly into the brain independent of the BBB. Moreover, we devised a novel liposomal BDS that contained Iomeprol as an iodine contrast agent simultaneously with BSH to visualize the distribution of these BDSs in the brain by using CT.

The results of this in vitro boron uptake study confirmed that TF-PEG liposome can deliver BSH into F98 cells efficiently. As for the in vivo biodistribution study, we found that TF-PEG liposome can also accumulate ^{10}B at significantly high concentrations in the tumor tissue by CED, whereas low ^{10}B concentrations are maintained in normal brain, blood, and other organs. Neutron irradiation is expected to provide immeasurable tumor control efficacy by virtue of this enormously higher contrast in ^{10}B concentration to the normal brain, allowing decreased irradiation doses to the surrounding normal tissues. F98 glioma cell line showed the minimum accumulation of BSH by TF-PEG liposomes among 5 glioma cell lines tested in this study. Therefore, if we use other cell lines in vivo study, more promising results may be expected.

CED itself is a less invasive procedure, and Lonser et al[21] reported that histological inflammation was typical only within a 50-μm radius of the catheter if the agent infused was nontoxic. They also reported that CED had been proved safe in a number of species, ranging from mice to humans, and did not produce cerebral edema or measurably increased intracranial pressure. On the other hand, Saito et al[13] reported that a heterogeneous tissue arrangement of the tumor gives rise to an irregular distribution of the infused agent and to leakage into undesirable areas. They also mentioned that ideal and expected tissue distribution after CED can be significantly decreased when the catheter tip is placed near a large blood vessel, white matter tracts, or the resection cavity because of fluid escaping along the path of least resistance.

Thus, the idea of using imaging to visualize locally injected agents would logically arise. We devised a novel liposomal BDS containing Iomeprol, an iodine contrast agent, simultaneously

Copyright © Congress of Neurological Surgeons. Unauthorized reproduction of this article is prohibited.

with BSH. Using imaging technology, such as CT, this liposomal BDS was successfully visualized and its distribution was well recognized on CT imaging even when injected into the small brain of the rat by CED.

In BNCT, unlike other therapies with cytotoxic agents such as targeted toxins[22] or anticancer drugs, the infused agent itself has no cytotoxicity until neutron irradiation is applied. So if some technical errors, such as those that Saito et al mentioned, in CED were revealed on a CT image (eg, an undesirable distribution of BDS that leaked into the cerebral ventricle or subarachnoid space), neutron irradiation could be postponed so that the safety of the therapy would be ensured. Rousseau et al[19] reported the efficacy of an iodine tracer not only as a tumor contrast agent on CT imaging but also as a dose-enhancement agent for synchrotron stereotactic radiotherapy. Their method also required precise tumor targeting, so they should have encountered the same problems as those in our study with regard to BNCT. They also adopted CED to improve iodine distribution for synchrotron stereotactic radiotherapy treatment and mentioned that its efficacy and safety in that CED can achieve high iodine concentrations in the target area and low iodine concentrations in the surrounding healthy brain tissues and blood vessels. With or without cytotoxicity of the infused agent, visualization through clinical imaging is essential for the treatment of malignant brain tumors.

In the current study, some problems arose. First, it has not been solved how the infused BDSs, liposomes, and encapsulated BSH and Iomeprol were metabolized. In Figures 2 and 4, ^{10}B concentration in tumor tissue is not proportional to Hounsfield unit value at the concerned time. This shows that there is a difference in behavior after injection between BSH and Iomeprol. If the metabolic kinetics of the BDS were disclosed, it would enable us to evaluate the ^{10}B concentration in tumor tissue by CT and Hounsfield unit value. We overcame one of the important problems of CED that caused undesirable distribution of the BDS, such as leaking into the cerebral ventricle or subarachnoid space, by co-encapsulation with drug and contrast agent for CT imaging. However, distribution of the BDS was accurately tracked by the CT imaging. Second, we could not apply neutron irradiation to evaluate the true toxicity and the therapeutic efficacy of this BDS in the current study because both reactors (KUR and JRR4) in Japan had been unavailable because of repairs and the change to uranium as fuel.

In the next step of our work, we expect to confirm that our novel strategy can obtain higher efficacy in BNCT.

Disclosure

This work was supported by Grants-in-Aid for Scientific Research for Young Scientists (B) (18791030 to S.K. and 20791022 to N.I.), by Grants-in-Aid for Scientific Research (C) (20591728 to S.K.) and (B) (19390385 to S-I.M.) from the Japanese Ministry of Education, Culture, Sports, Science and Technology, and by the Eisai Science Foundation to S.K. This work was also supported in part by the Takeda Science Foundation for Osaka Medical College. The authors have no personal financial or institutional interest in any of the drugs, materials, or devices described in this article.

REFERENCES

1. Miyatake S, Kawabata S, Nonoguchi N, et al. Pseudoprogression in boron neutron capture therapy for malignant gliomas and meningiomas. *Neuro Oncol*. 2009;11(4):430-436.
2. Miyatake S, Kawabata S, Yokoyama K, et al. Survival benefit of Boron neutron capture therapy for recurrent malignant gliomas. *J Neurooncol*. 2009;91(2):199-206.
3. Miyatake S, Kawabata S, Kajimoto Y, et al. Modified boron neutron capture therapy for malignant gliomas performed using epithermal neutron and two boron compounds with different accumulation mechanisms: an efficacy study based on findings on neuroimages. *J Neurosurg*. 2005;103(6):1000-1009.
4. Kawabata S, Miyatake S, Kajimoto Y, et al. The early successful treatment of glioblastoma patients with modified boron neutron capture therapy. Report of two cases. *J Neurooncol*. 2003;65(2):159-165.
5. Kawabata S, Miyatake S, Kuroiwa T, et al. Boron neutron capture therapy for newly diagnosed glioblastoma. *J Radiat Res (Tokyo)*. 2009;50(1):51-60.
6. Barth RF, Coderre JA, Vicente MG, Blue TE. Boron neutron capture therapy of cancer: current status and future prospects. *Clin Cancer Res*. 2005;11(11):3987-4002.
7. Wei Q, Kullberg EB, Gedda L. Trastuzumab-conjugated boron-containing liposomes for tumor-cell targeting; development and cellular studies. *Int J Oncol*. 2003;23(4):1159-1165.
8. Yang W, Barth RF, Adams DM, et al. Convection-enhanced delivery of boronated epidermal growth factor for molecular targeting of EGF receptor-positive gliomas. *Cancer Res*. 2002;62(22):6552-6558.
9. Doi A, Kawabata S, Iida K, et al. Tumor-specific targeting of sodium borocaptate (BSH) to malignant glioma by transferrin-PEG liposomes: a modality for boron neutron capture therapy. *J Neurooncol*. 2008;87(3):287-294.
10. Bobo RH, Laske DW, Akbasak A, Morrison PF, Dedrick RL, Oldfield EH. Convection-enhanced delivery of macromolecules in the brain. *Proc Natl Acad Sci U S A*. 1994;91(6):2076-2080.
11. Wu G, Barth RF, Yang W, Kawabata S, Zhang L, Green-Church K. Targeted delivery of methotrexate to epidermal growth factor receptor-positive brain tumors by means of cetuximab (IMC-C225) dendrimer bioconjugates. *Mol Cancer Ther*. 2006;5(1):52-59.
12. Mukundan S Jr, Ghaghada KB, Badea CT, et al. A liposomal nanoscale contrast agent for preclinical CT in mice. *AJR Am J Roentgenol*. 2006;186(2):300-307.
13. Saito R, Bringas JR, McKnight TR, et al. Distribution of liposomes into brain and rat brain tumor models by convection-enhanced delivery monitored with magnetic resonance imaging. *Cancer Res*. 2004;64(7):2572-2579.
14. Dickinson PJ, LeCouteur RA, Higgins RJ, et al. Canine model of convection-enhanced delivery of liposomes containing CPT-11 monitored with real-time magnetic resonance imaging: laboratory investigation. *J Neurosurg*. 2008;108(5):989-998.
15. Aoki I, Bakalova R. MR molecular imaging using drug delivery system. *Drug Delivery System*. 2008;23(1):61-68.
16. Weaver M, Laske DW. Transferrin receptor ligand-targeted toxin conjugate (Tf-CRM107) for therapy of malignant gliomas. *J Neurooncol*. 2003;65(1):3-13.
17. Murad GJ, Walbridge S, Morrison PF, et al. Real-time, image-guided, convection-enhanced delivery of interleukin 13 bound to pseudomonas exotoxin. *Clin Cancer Res*. 2006;12(10):3145-3151.
18. Vogelbaum MA. Convection enhanced delivery for the treatment of malignant gliomas: symposium review. *J Neurooncol*. 2005;73(1):57-69.
19. Rousseau J, Boudou C, Esteve F, Elleaume H. Convection-enhanced delivery of an iodine tracer into rat brain for synchrotron stereotactic radiotherapy. *Int J Radiat Oncol Biol Phys*. 2007;68(3):943-951.
20. Maruyama K, Ishida O, Kasaoka S, et al. Intracellular targeting of sodium mercaptoundecahydrododecaborate (BSH) to solid tumors by transferrin-PEG liposomes, for boron neutron-capture therapy (BNCT). *J Control Release*. 2004;98(2):195-207.
21. Lonser RR, Walbridge S, Garmestani K, et al. Successful and safe perfusion of the primate brainstem: in vivo magnetic resonance imaging of macromolecular distribution during infusion. *J Neurosurg*. 2002;97(4):905-913.
22. Rainov NG, Soling A. Clinical studies with targeted toxins in malignant glioma. *Rev Recent Clin Trials*. 2006;1(2):119-131.

Supplemental digital content *is available for this article. Direct URL citations appear in the printed text and are provided in the HTML and PDF versions of this article on the journal's Web site (www.neurosurgery-online.com).*

Copyright © Congress of Neurological Surgeons. Unauthorized reproduction of this article is prohibited.

Acknowledgments

We thank Dr Rolf F. Barth, Department of Pathology, The Ohio State University, for preparing the F98 cell line and Hitomi Kuroda for technical assistance.

COMMENTS

The authors report a novel means to introduce potential sensitizing agents into an experimental brain tumor in an animal model using convection-enhanced delivery. The goal is to introduce these potential agents into the brain surrounding a tumor mass and eventually administer neutron radiation with the hope of providing greater cell kill, especially in the infiltrated zone. In essence, this is a study showing that specially tailored pharmaceuticals can be created to increase delivery of a selected agent in the target zone and that addition of other agents may make recognition of the target by imaging possible as well. It would be even better to demonstrate in a part 2 study that this targeting of sensitizing compounds actually resulted in a therapeutic response using boron neutron capture therapy (BCNT). This technology has been advocated in a relatively few centers for more than 40 years; perhaps because of the large overhead cost and lack of major therapeutic safety window, it has never reached mainstream use. Further efforts may allow safer BNCT, especially because the authors show that tissue concentrations are significantly reduced in other tissues, an important feature that may improve the safety of BNCT during the actual radiation administration. The risk-benefit ratio in BNCT has been difficult to ascertain. In the past, neutron radiation was effective at killing the target tumor but usually resulted in unacceptable radiation toxicity in the brain. Perhaps further efforts in this field will yet allow a beneficial therapeutic window to emerge.

L. D. Lunsford
Pittsburgh, Pennsylvania

The authors describe their early preclinical findings (in vitro and in vivo) in a potentially interesting application and modification of BCNT. Their strategy directly targets glioma cells (and the surrounding region) with transferrin bound to a polyethylene glycol liposome that encapsulates sodium borocaptate and an iodine contrast agent (used for tracking the liposome distribution during computed tomography imaging). To provide high concentrations of this compound to regions in and around glioma, it was delivered to tumor and surrounding region via convection-enhanced delivery.

The data from this study indicate that the polyethylene glycol liposome encapsulated sodium borocaptate can be safely and successfully delivered by convection-enhanced delivery in rodent brain tumor models while tracking its distribution using computed tomography imaging. Although these early findings are encouraging from a distribution perspective, the next potential step in determining whether this modification of BCNT for glioma may hold promise will be in determining therapeutic dosing (irradiation) and assessing efficacy in vivo. I look forward to the authors' subsequent work in this area.

Russell R. Lonser
Bethesda, Maryland

Copyright © Congress of Neurological Surgeons. Unauthorized reproduction of this article is prohibited.

Magnetic Microparticles for Endovascular Aneurysm Treatment: In Vitro and In Vivo Experimental Results

Johanna Oechtering, MD*‡
Peter J. Kirkpatrick, FRCS (SN), FMedSci§
Alexander G.K. Ludolph, MD*¶
Franz J. Hans, MD‖
Bernd Sellhaus, MD#
Andreas Spiegelberg, PhD**
Timo Krings, MD, PhD*‡‡

*Department of Neuroradiology, University Hospital Aachen, Aachen, Germany; ‡Department of Neurology and Clinical Neurophysiology, Campus Benjamin Franklin, Charité–University Medicine Berlin, Berlin, Germany; §Neurosurgical Unit, Department of Clinical Neurosciences, Addenbrooke's Hospital, University of Cambridge, Cambridge, United Kingdom; ¶Department of Radiology and Interventional Radiology, Municipal Hospital of Fulda, Fulda, Germany; ‖Clinic for Neurosurgery, University Hospital Aachen, Aachen, Germany; #Department of Neuropathology, University Hospital Aachen, Aachen, Germany; **Spiegelberg Gmbh & Co. KG, Hamburg, Germany; ‡‡Division of Neuroradiology, Department of Medical Imaging, University of Toronto, Toronto Western Hospital, Toronto, Ontario, Canada

Correspondence:
Peter J. Kirkpatrick, FRCS (SN), FMedSci,
Consultant Neurosurgeon,
Box 167,
Block A, Level 4,
Department of Neurosurgery,
Addenbrooke's Hospital,
Cambridge, CB2 2QQ, UK.
E-mail: pjk21@medschl.cam.ac.uk

Received, March 3, 2010.
Accepted, October 1, 2010.

Copyright © 2011 by the
Congress of Neurological Surgeons

OBJECTIVE: Endovascular treatment of intracranial aneurysms employing endosaccular coiling can be associated with aneurysm perforation, coil herniation or incomplete obliteration fueling the interest to investigate novel endovascular techniques. We aimed to test a novel embolization material in experimental aneurysms in vitro and in vivo whereby intra-arterially administered magnetic microparticles (MMPs) are navigated into the lumen of vascular aneurysms with assistance from an external magnetic field.

METHODS: MMPs are core-shell particles suspended in saline that have a shell made of a polymeric material and a core made of magnetite (Fe3O4). They have a diameter of 1.4 μm. During MMP administration via a microcatheter, a magnetic field was applied externally to direct the particles with the use of a solid-state neodymium magnet. Experiments were performed in a perfused silicone vessel and aneurysm model to evaluate application techniques and fluid dynamics and in the elastase aneurysm model in rabbits to evaluate in vivo compatibility, including multiorgan histological examinations and long-term stability of aneurysm embolization.

RESULTS: It was possible to steer and hold the MMPs within the aneurismal cavity where they occluded the lumen progressively. After removal of the external magnetic field, the results remained stable in vivo for the remainder of the observational period (30 minutes); after a 12-week observational period, recanalization of the aneurysm occurred.

CONCLUSION: MMPs can be magnetically directed into aneurysms, allowing short-term obliteration. Although the method has yet to show reliable long-term stability, these experiments provide proof of concept, encouraging further investigation of intravascular magnetic compounds.

KEY WORDS: Cerebral aneurysm, Experimental interventional neuroradiology, Magnetic microparticles

Neurosurgery 68:1388–1398, 2011 DOI: 10.1227/NEU.0b013e3182125eb0 www.neurosurgery-online.com

Subarachnoid hemorrhage is a disease associated with high morbidity and mortality. In up to 85% of cases, it is caused by rupture of a cerebral aneurysm that usually arises from an artery of the basal circle of Willis.[1] The 2 principal forms of treatment for cerebral aneurysms are microsurgical clipping and endovascular therapies. Over the last few years, especially since the International Subarachnoid Aneurysm Trial,[2] endovascular therapy of cerebral aneurysms has become increasingly important. The International Subarachnoid Aneurysm Trial has shown the superiority of endovascular approaches in terms of mortality, dependency, and disability for those aneurysms considered treatable from both the neurosurgical and neuroradiological point of view. However, most of the encountered aneurysms could not be included in the study because they did not fulfill these criteria.

Embolizing cerebral aneurysms with platinum spirals, so-called coiling, is the classic approach for endovascular treatment, but this technique poses several problems resulting from the anatomic configuration of the aneurysm in relation

ABBREVIATIONS: BA, basilar artery; **MCA,** middle cerebral artery; **MMP,** magnetic microparticle; **RHS,** reticulohistiocytic system

Copyright © Congress of Neurological Surgeons. Unauthorized reproduction of this article is prohibited.

to the parent artery,[3] branches arising near the neck of the aneurysm,[1] or the wide neck of the aneurysm with potential coil herniation during the therapy.[4] Neck remnants combined with coil compaction create a risk of aneurysm recurrence and rerupture.[5] Other possible shortcomings might be the absence of permanent aneurysm obliteration and recanalization of the coil package. Moreover, peri-interventional rupture, thromboembolic events, or technical problems in steering the microcatheter into the aneurysm may cause problems with this technique.[6] Several of the above-mentioned problems can be solved by introducing new endovascular devices such as flow diverters, stents, the balloon remodeling technique, or new coiling materials and techniques.[3,6] However, not all of the above-mentioned problems have been solved yet, thereby fuelling the need to investigate new embolization devices and techniques.

Magnetic microparticles (MMPs) typically consist of a core made from magnetic material like iron oxides and a shell made from synthetic or natural polymers. Iron oxides like magnetite (Fe3O4) and maghemite (Fe2O3) are highly magnetizable and are biocompatible as required for biomedical applications.[7,8] Iron oxide nanoparticle suspensions have been used intravascularly as a contrast agent for the reticulohistiocytic system (RHS) because they accumulate shortly after intravascular injection into the RHS, especially in the liver and spleen. They do not damage the hepatocellular function, become degraded, and are even metabolized in iron metabolism.[9-12] In previous studies, neither acute nor subacute toxic or mutagen effects could be detected. The coating of the magnetic core is of great importance because it provides protection from corrosion in a hydrous medium like blood.[13] An appropriate design of the particle surface, its charges, and its functional chemical groups can enable a particle suspension to be colloidally stable. This is one of the measures to prevent particle agglomeration and thereby thromboembolic events.[7,14] Another argument for a well-considered design of the shell is related to the immunological system. Shortly after intravascular injection of the particles, opsonization begins and the macrophages of the RHS start to phagocytose. The period of time until uptake can be influenced by the characteristics of the coating.[15] Furthermore, the particles can be not only protected but also functionalized by coupling them with drugs, proteins, or antibodies. Through functionalization, they can be used for a diversity of biomedical applications, including magnetic drug targeting[8,16,17] and magnetic thermotherapy.[18-20] Recently, there have been promising reports on the potential of "quantum dot paramagnetism" to enhance imaging and therapy in various fields of neurosurgery, including neurooncology. Potential applications include imaging of angiogenesis, tumor targeting, and cellular uptake with an external magnet.[21-23] These quantum dots have also been suggested to be potential embolization materials for neoplastic processes.[23,24]

The size of the magnetic particles determines their magnetic properties. Single-domain nanoparticles made from magnetite that are typically significantly smaller than 100 nm are superparamagnetic. This implies that these particles do not remain magnetized after exposure to a magnetic field. In contrast, larger multidomain particles show ferrimagnetic behavior (ie, these particles stay magnetized after exposure). This is called "magnetic memory" and implies a considerable risk of magnetic agglomeration.[7,15,25] On the other hand, magnetic steerability improves with particle size.[26] To combine superparamagnetic behavior and good magnetic steerability, so-called microspheres have been introduced. These microparticles have cores that consist of a multiplicity of nanoparticles to prevent them from becoming permanently magnetized.[25] Particles that are < 100 nm have a larger effective surface area, improved tissue diffusion, lower sedimentation rates, and higher stability in the fluid. Particle size is also reciprocally proportional to the circulation time before uptake of the RHS and the metabolization of the particles.[15,25]

Given their magnetic properties, they can be steered by a magnetic field. Here, the use of MMPs to treat aneurysms is presented and is based on the assumption that MMPs can be injected into an aneurysm-carrying artery via a microcatheter and can be navigated into an aneurysm with the aid of an extracorporeal- or an intravascular-positioned magnetic field.

The principles of the technique are similar to an approach first described in 1967 by Alksne et al[27-29] and in 1976 by Khilko.[30] Alksne et al[27-29] injected a probe of carbonyl iron powder suspended in human serum albumin for aneurysm embolization through a burr hole with a needle puncturing the fundus of the aneurysm. The probe was held in the aneurysm with an extravascular magnet for 3 to 5 days. Because of this extravascular approach, however, not all aneurysms were anatomically suitable for this technique. Khilko[30] used 8 to 40 polystyrene balls, 2 to 3 mm in diameter, for the embolization of arteriovenous malformations. In some cases, the needed direction of the emboli movement was attained by applying a magnetic field.

Since then, biomedical engineering, nanotechnologies, and material developments have seen tremendous progress, enabling the creation of particles of a specific size, coating, and functionalization. In addition, endovascular techniques have been established with specific catheters that allow easier application of the magnetic particles. Finally, tailor-made nanoparticles and microparticles can now be used, opening a window into what has been called nanoneurosurgery, of which vascular applications are but a facet. A good overview of the different potentials of magnetic nanoparticles is given in a recent review by Khalessi et al.[23]

In the present study, we used experimental aneurysms to investigate the potential of MMPs to obliterate aneurysms, their technique of application and the current problems of this novel device.

METHODS

In Vitro Studies

The MMPs used (Magseal; APG Medical Ltd, Newbury, United Kingdom) are magnet-steerable core-shell particles with a diameter of 1.4 μm. They are suspended in saline solution. The core is made up of a multiplicity of magnetite nanoparticles and is coated with a polymeric shell. This shell is made of different synthetic polymers layer by

Copyright © Congress of Neurological Surgeons. Unauthorized reproduction of this article is prohibited.

layer; a negatively charged layer is followed by a positively charged one. The following polymers have been used: polystyrolsulfonate, polyallylamine, polystyrolsulfonate–rhodamine, polydiallyldimethyl–ammonium chloride–rhodamine, and polymethacrylate. Some layers were labeled with rhodamine for research purposes. Before the experiments, cell toxicity tests were performed in an accredited laboratory, demonstrating no cytotoxic effects in cell suspensions of mouse connective tissue fibroblasts for 72 hours.

To guide the MMPs during the subsequent experiments, a solid neodymium permanent magnet measuring 2.5 × 2.5 × 1.25 cm was used. Magnetic field strength was 400 mT at 0 cm, 300 mT at 0.4 cm, 200 mT at 0.8 cm, and 100 mT at 1.6 cm. For the application of the MMP suspensions, a microcatheter with an inner diameter of 0.685 mm was used (Renegade Hi-Flo-Microcatheter 18-302, Boston Scientific, Cork, Ireland) because during pretests we observed occlusion of smaller-diameter microcatheters.

For the in vitro experiments, a 3-dimensional silicone vessel model (Elastrat-Sarl, Geneva, Switzerland) that presents a true-to-scale imitation of the human circle of Willis was used. Two aneurysms were investigated in this model: a basilar artery (BA) tip aneurysm measuring 7.2 × 6.9 mm with a neck diameter of 7.5 mm and a middle cerebral artery (MCA) aneurysm measuring 5.2 × 2.8 mm with a neck diameter of 2.2 mm. The vessel model was perfused with saline at a rate of 34 to 53 L/h.

Fifty- and 150-mg portions of MMPs were suspended in 10 mL physiological saline and filled into a syringe. Over a period of 5 minutes, the suspended MMPs were applied constantly via a microcatheter in the vessel model as detailed above. MMPs that were not retained by the magnetic field were collected and measured. After applying the MMPs, the magnet stayed in position for 10 minutes and then was removed. In a second container, the MMPs that had been retained by the magnet were retrieved and measured. For each of the different experimental setups, 5 runs were performed. Student *t* test was used to statistically determine the differences between the means obtained in the different experimental setups.

In the first in vitro experiment, the influence of the distance between the position of the catheter tip and the aneurysm during application was investigated on the BA tip aneurysm. In 5 runs each, 3 different catheter tip positions were examined during the application of 150 mg MMPs under constant magnetic forces of 400 mT and 25 T/m. The catheter tip was positioned (a) deep in the aneurysm, (b) at the neck of the aneurysm, or (c) 10 cm distant from the aneurysm in the right vertebral artery.

In the second experiment, the influence of the magnetic field strength on the aneurysm filling was investigated on both the MCA and the BA aneurysm with the catheter tip constant at the neck of the aneurysm. The magnetic flow density and the magnetic field gradient were varied by systematic increase of the distance between the aneurysm dome and the magnet. Flow densities and magnetic field gradients of 400 mT with 25 T/m, 200 mT with 13 T/m, and 100 mT with 9 T/m were investigated. These values correspond approximately to distances of 0, 0.8, and 1.6 cm between aneurysm dome and magnet, respectively.

Animal Studies

The animal protocol for our study was approved by the Institutional Animal Care and Use Committee of our university and was conducted according to current regulations and guidelines for animal welfare (AZ: 50.203.2-AC 24, 24/01) and the international principles of laboratory animal care. Procedures were performed under general anesthesia on the intubated, spontaneously breathing rabbit. Anesthesia was induced by subcutaneous injection of 0.3 mL/kg medetomidine, 0.2 mL/kg ketamine (10%), and 0.2 mL/kg diazepam (0.5%). Maintenance of anesthesia was achieved by 6 to 10 $mg \cdot kg^{-1} \cdot h^{-1}$ propofol (1%). Aneurysms were created on the brachiocephalic trunk of 3 New Zealand White rabbits by ligation of the right common carotid artery and intraluminal incubation with elastase.[3,31] Three weeks after aneurysm induction, endovascular treatment was performed via a transfemoral approach. After documentation of the configuration of the vessels and aneurysms, a microcatheter was inserted, the solid neodymium magnet was positioned extracorporeally on the body surface of the animal, and the MMPs were applied. The distance between magnet and aneurysm was 1 cm; therefore, a magnetic influence of approximately 175 mT and 13 T/m was present on the aneurysm. The microcatheter was positioned close to the neck of the aneurysm, and MMPs were injected by hand at a rate of approximately 1 mL/min under fluoroscopic control. Immediately after the treatment and 30 minutes postinterventionally, digital subtraction angiographies were performed to evaluate and document treatment results. Twelve weeks after the endovascular treatment, a final catheter angiography was performed via a left-sided femoral approach. After final angiography, the rabbits were euthanized with intravenously injected barbiturates, and a histopathological investigation was performed. Tissues of rabbit liver and spleen and the aneurysm on the brachiocephalic trunk were embedded in paraffin. Staining with hematoxylin and eosin, elastica van Gieson, and Turnbull Blue was performed.

RESULTS

In Vitro Studies

General Comments and Influence of the Aneurysm Geometry

After removal of the magnet, it took only 20 to 90 seconds for all MMPs to be flushed out of the BA tip aneurysm. During all trials, the BA tip aneurysm was not completely filled, and there was a neck remaining. During the trials on the MCA aneurysm, not only were MMPs retained inside the lumen of the aneurysm, but also a very small proportion was assembled in the small vessels around the aneurysm within the sphere of influence of the magnet. Stenosis was caused and could be observed in these vessels, but no occlusion occurred. The minimal inner diameter of these vessels amounted to 2 mm (Figure 1). After removal of the magnet, the designated period of 5 minutes was not long enough for complete depletion of MMPs from the MCA aneurysm.

Influence of the Position of the Catheter Tip

When the catheter tip was positioned at the neck of the aneurysm, a mean of 30.6 ± 14.4 mg MMPs was retained by the magnet inside the BA tip aneurysm. A smaller amount of 24.4 ± 5.4 mg was achieved when MMPs were applied with the catheter tip in the right vertebral artery 10 cm distant from the BA tip aneurysm. Between both positions, however, there was no statistically significant difference in filling of the aneurysm ($P = .42$). When the catheter tip was positioned deep inside the aneurysm, the filling amounted to 5 ± 1.5 mg. This was statistically significantly less than the achieved amounts in the 2 other trials ($P = .02$ and $P = .00$; Figure 2A).

Copyright © Congress of Neurological Surgeons. Unauthorized reproduction of this article is prohibited.

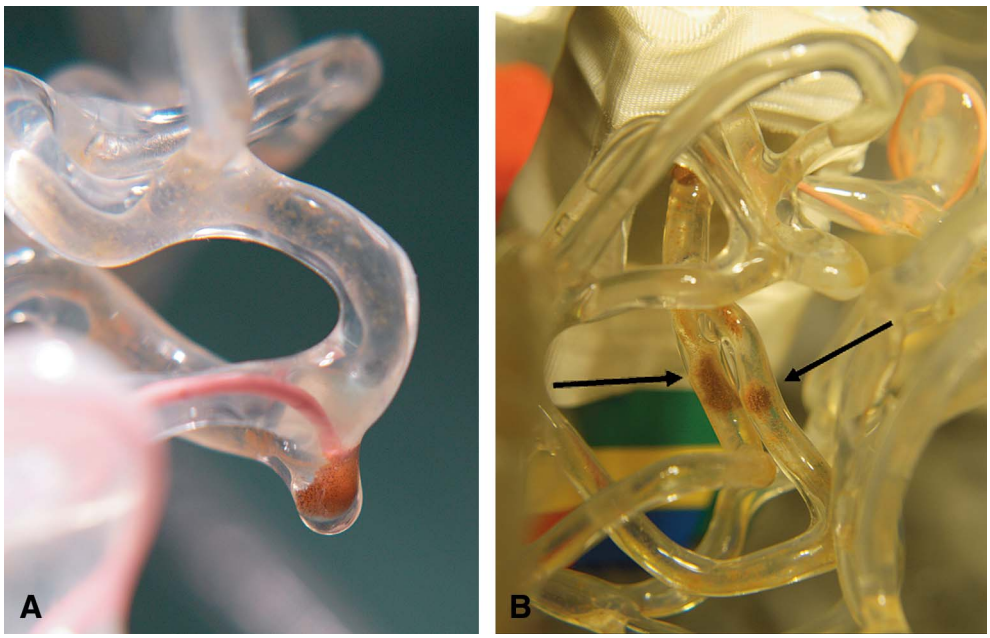

FIGURE 1. A, *right middle cerebral artery aneurysm of the vessel model filled with magnetic microparticles (MMPs) after removal of the magnetic field.* **B,** *MMPs also accumulate in small vessels with reduced flow inside the vessel model under the influence of a magnetic field.*

Influence of Magnetic Field Strength

When the MMPs were applied with a negligible distance between the aneurysm dome and the magnet, corresponding to 400 mT and 25 T/m, a mean of 30.6 ± 14.4 mg MMPs were retained in the BA aneurysm. After the distance was increased to 0.8 cm (200 mT and 13 T/m), 29.4 ± 9.5 mg MMPs were retained (P = .89). After a further increase in distance to 1.6 cm, corresponding to 100 mT and 9 T/m, 7.2 ± 1.9 mg MMPs were retained inside the aneurysm. This last result differs statistically significantly from the results of the 2 previous trials (P = .01 and P = .00; Figure 2B). Trials on the MCA aneurysm were performed with 50 mg MMPs. Under the influence of 400 mT and 25 T/m, the MCA aneurysm was fully filled and 13.6 ± 22 mg MMPs were retained. At a magnetic field of 200 mT and 13 T/m, the retained amount averaged 11.4 ± 2.4 mg (not significant, P = .22). If the aneurysm was under the influence of 100 mT and 9 T/m, 4.8 ± 2.4 mg MMPs were retained in the aneurysm (highly significant difference to both other trials; P = .00 and P = .00; Figure 2C).

Embolizate Scatter and Negative Controls

The amount of MMPs passing through the aneurysm model without being retained after injection (embolizate scatter) was collected and quantified. For the BA aneurysm, 150 mg MMPs were applied; for the MCA aneurysm, 50 mg MMPs. The embolizate scatter was the difference between the amount of particles injected and the amount of particles retained in the aneurysm (less a constant small loss of 5% to 15% resulting from the extraction method). The extraction method (drying and extracting the precipitate from a collecting container) was established during pretests before having performed the main experiments (Table).

The vessel model used had 5 other aneurysms at various sites of the circle of Willis. No accumulation of MMPs in any other aneurysm was observed during our in vitro experiments.

In addition, we observed that depletion of MMPs out of the aneurysm started immediately after removal of the magnet, whereas no such depletion was seen during the 5 minutes during which the magnet was in place.

To show that filling of the aneurysm was related to the magnetic force on the MMPs, 2 negative control experiments were also performed. In the first set of 9 experiments, MMPs were injected into the vessel model with the catheter positioned at the neck of the BA aneurysm without involvement of a magnet. In a second control experiment, nonmagnetic polyvinyl alcohol particles (Contour, Boston Scientific; size, 45 to 150 μm; 1 vial suspended in 10 mL saline) were injected via the microcatheter with the catheter tip positioned at the neck of the BA aneurysm and the magnet positioned in direct contact with the aneurysm dome. In neither control experiment was BA aneurysm filling observed, and there was no accumulation of embolizate material in the aneurysm.

Copyright © Congress of Neurological Surgeons. Unauthorized reproduction of this article is prohibited.

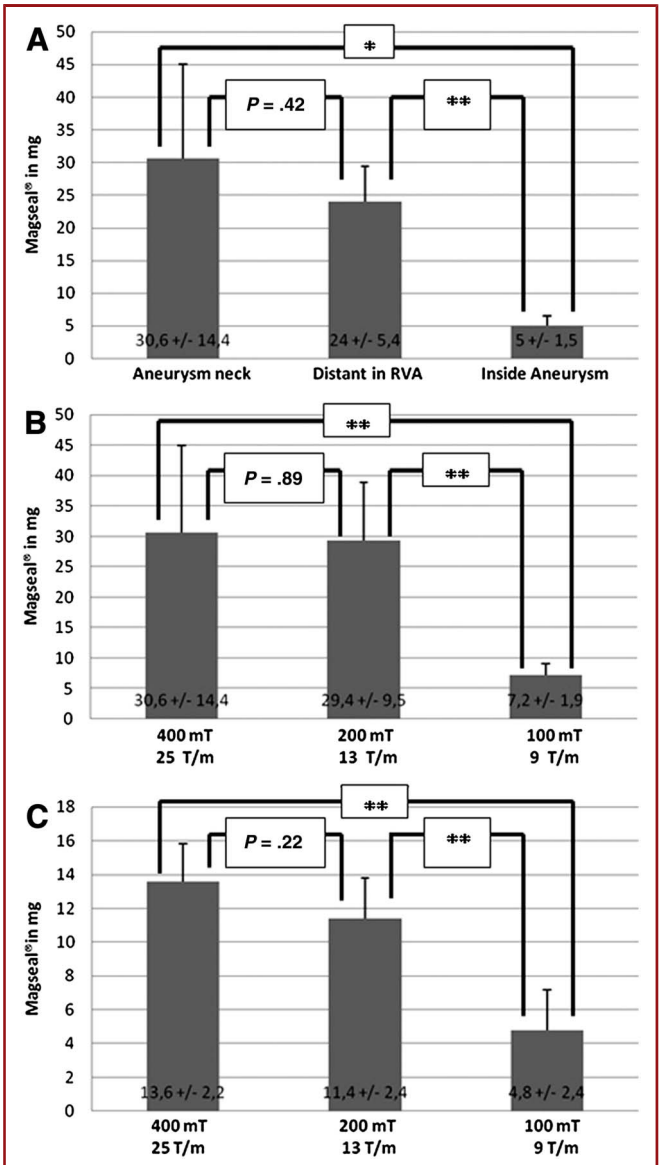

FIGURE 2. *A, filling of the basilar head aneurysm with magnetic microparticles (MMPs) in milligrams depending on the position of the catheter tip. B, filling of the basilar artery aneurysm with MMPs in milligrams depending on the magnetic field strength. C, filling of the middle cerebral artery aneurysm with MMPs in milligrams depending on the magnetic field strength. RVA, right vertebral artery. *Significant; **highly significant.*

Animal Studies

The induction of aneurysms was successful in all 3 rabbits. One animal died of anesthesia-related complications before endovascular treatment. In the other animals, it was possible to steer and hold MMPs in the aneurysmal lumens with the assistance of an extracorporeal magnet corresponding to 175 mT and 13 T/m on the aneurysm dome. Progressive and complete occlusion of both aneurysms could be achieved. These results remained stable on angiography for at least 30 minutes after removal of the magnetic field. Both animals tolerated the procedures well. During endovascular treatment and the following 12 weeks, no toxic or allergic reactions or any other signs of disease were observed. After the observational period, control angiography revealed reopening of both aneurysms. However, the larger of the 2 aneurysms had a smaller lumen compared with the initial presentation (Figures 3 and 4).

Histopathology

In the wall of the larger aneurysm, wall thickening caused by foreign-body granulomas with and without involvement of MMPs and inflammatory infiltrates dominated by lymphocytes were detected within the adventitial layer. In the lumen, unorganized thrombotic material without neovascularization was found adjacent to the intimal layer (Figure 5A). In iron stain (Turnbull blue) of both rabbit livers and spleens, an impressive iron enrichment was shown. The particles were localized mainly in the RHS. In the animal treated first, a homogenous distribution pattern of predominantly solitary particles could be seen in the liver tissue (Figure 5B), and an accumulation in the red pulp of the spleen was observed. In the other animal, liver and spleen showed agglomerates of MMPs in a range up to at least 90 × 160 μm (Figure 5C). There was no evidence for large- or small-vessel occlusions or infarctions.

DISCUSSION

In Vitro Results

Vessel Model and Methodology

The filling and application of MMPs could be investigated on the perfused vessel model regarding different types of aneurysms in unequal fluid dynamic conditions. It is advantageous that the vessel model presents a true-to-scale imitation of the circle of Willis and that all aneurysms are positioned in classic localizations. Furthermore, both the hose system and the vessel model are made of transparent material. Thus, no harmful radiation was needed for experiments, and even small amounts of residual MMPs could be detected. Its major drawback is the missing physiological reaction to blood and tissue, including thrombotic processes. For successful filling of an aneurysm, magnetic forces have to exceed local fluid forces. It has to be considered that fluid forces in this experimental circulation are only roughly comparable with limitations to those in the human circulation. The characteristics of a tube flow (laminar vs turbulent flow) depend on several factors such as flow velocity, geometric measurements, surface characteristics of the tube, and the mass density and viscosity of the fluid. Although most determining factors in the present model were similar to human physiology (similar flow rates and geometric measurements), differences in pulsatility, surface characteristics, elasticity of the model silicone vessels, and fluid features are major drawbacks of this model. In addition, in

Copyright © Congress of Neurological Surgeons. Unauthorized reproduction of this article is prohibited.

TABLE. Amount of Magnetic Microparticles Retained in the Aneurysm, Embolizate Scatter, and Overall Amount Re-extracted[a]

Experiment	Aneurysmal Filling, mg	Embolizate Scatter, mg	Amount Re-extracted, mg	Amount Re-extracted, %
BA aneurysm: catheter at aneurysm neck, 0.4 T, 25 T/m	30.6 ± 14.4	104.4 ± 13.2	135 ± 3.5	90.0 ± 2.3
BA aneurysm: catheter distant in RVA, 0.4 T, 25 T/m	24 ± 5.4	121 ± 3.3	145 ± 2.5	96.7 ± 1.7
BA aneurysm: catheter inside the aneurysm, 0.4 T, 25 T/m	5 ± 1.2	131.3 ± 7.6	136.3 ± 6.8	90.9 ± 4.5
BA aneurysm: catheter at aneurysm neck, 0.2 T, 13 T/m	29.4 ± 9.5	110.2 ± 11.3	139.6 ± 2.3	93.1 ± 1.5
BA aneurysm: catheter at aneurysm neck, 0.1 T, 9 T/m	7.2 ± 1.9	130.2 ± 3.7	137.4 ± 2.9	91.6 ± 1.9
MCA aneurysm: catheter at aneurysm neck, 0.4 T, 25 T/m	13.6 ± 2.2	29.2 ± 3.3	42.8 ± 1.7	85.6 ± 3.4
MCA aneurysm: catheter at aneurysm neck, 0.2 T, 13 T/m	11.4 ± 2.4	32.6 ± 2.2	44 ± 2.3	88.0 ± 4.6
BA aneurysm: catheter at aneurysm neck, 0.1 T, 9 T/m	4.8 ± 2.4	41.4 ± 2.2	46.2 ± 1.2	92.4 ± 2.4

[a]BA, basilar artery; MCA, middle cerebral artery; RVA, right vertebral artery.

the present model, the magnet could be placed in direct contact with the aneurysm, which is impossible in humans. Still, for a basic evaluation of proof of principle and for data concerning the best-suited application technique, the present model was deemed sufficient.

Influence of the Position of the Catheter Tip on the Success of Aneurysm Filling

We were able to show that application of the MMPs resulted in the best aneurysm filling with the catheter at the neck of the aneurysm and in the worst filling with the application catheter

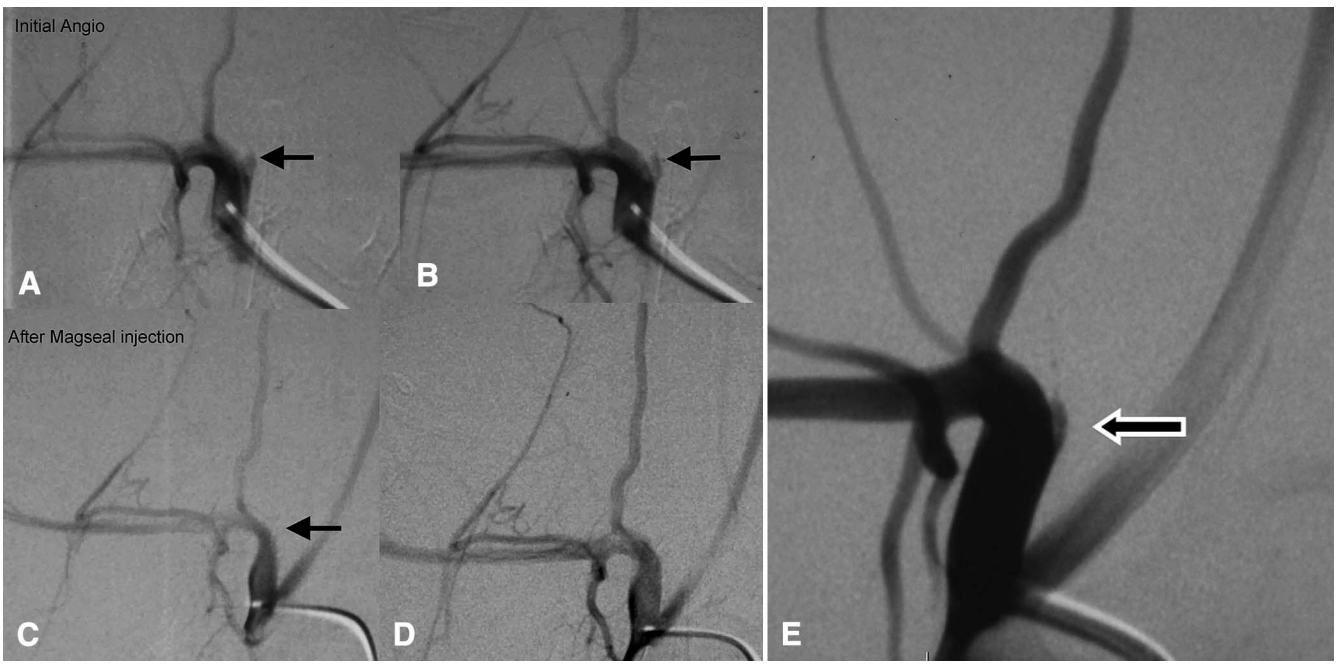

FIGURE 3. *Endovascular treatment with magnetic microparticles (MMPs).* **A** *and* **B**, *initial angiography showing the aneurysm.* **C**, *the aneurysm directly after MMP injection presents without intraluminal blood flow.* **D**, *results are stable for at least 30 minutes after removal of the magnetic field.* **E**, *the 12-week follow-up with recanalization of the aneurysm.*

Copyright © Congress of Neurological Surgeons. Unauthorized reproduction of this article is prohibited.

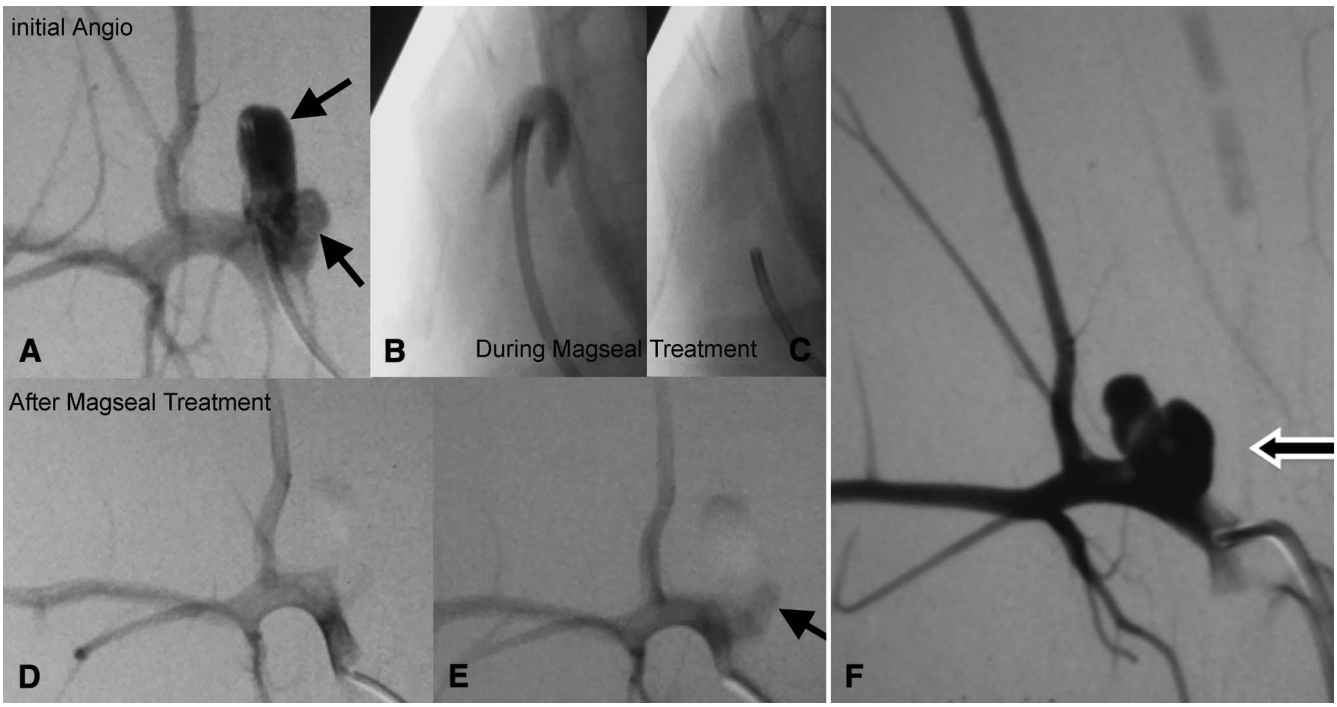

FIGURE 4. *Endovascular treatment with magnetic microparticles (MMPs).* **A**, *initial angiography showing the successfully experimentally induced aneurysm.* **B** *and* **C**, *fluoroscopy during MMP treatment.* **D**, *aneurysm after MMP injection presents without intraluminal blood flow.* **E**, *results are stable for 30 minutes after removal of the magnetic field.* **F**, *however, on follow-up after 12 weeks, the aneurysm is partly recanalized.*

in the aneurysm proper. A significant amount of filling was even possible when the catheter was distant from the aneurysm in the parent feeding artery. For filling of the aneurysm, magnetic forces have to exceed local fluid forces in and around the aneurysm. A potential explanation for the low filling rates of the aneurysm when the microcatheter was placed within the aneurysm may be related to turbulent flow and immediate washout of particles that were not fully magnetized. During the application of the MMPs, already accumulated MMPs may be washed out as a result of the jet effect of the suspended MMPs from the microcatheter tip. When MMPs were applied 10 cm distant from the aneurysm, a smaller amount was retained in the aneurysm compared with the application at the aneurysm neck. Although not statistically significant, it might be caused by a different distribution of the applied particles within the fluid and by slightly different local fluid dynamics around the aneurysm. According to this part of the experiments, we therefore concluded that MMPs are best applied slowly with the catheter tip at the neck of the aneurysm to avoid an increase in local flow velocities and forces inside the aneurysm but still providing a close application in a high concentration.

Influence of the Position of the Catheter Tip on the Success of Aneurysm Filling

When investigating the influence of the magnetic field strength and magnetic field gradient on aneurysm filling, we showed that the grade of aneurysm filling can be influenced by the strength of magnetic forces. Both aneurysms showed highest filling results under the influence of 400 mT and 25 T/m. However, there was no statistically significant reduction of aneurysm filling under the influence of 200 mT and 13 T/m. Only under the magnetic influence of 100 mT and 9 T/m was a significant reduction of filling observed. During 9 pretests functioning as negative controls, no MMPs could be accumulated in the BA aneurysm without the involvement of a magnet. The same result was seen on the BA aneurysm if non–MMP/embolizate material was given with the use of a magnet.

As stated above, the magnetic forces have to exceed the fluid forces for successful filling. In accordance with previous results, we found that a field strength of at least 200 mT is necessary for the steerability of most carriers based on magnetite.[32] The distance between magnetic field and aneurysm should be as small as possible because it was shown that particles accumulate not only in an aneurysm but also in smaller surrounding vessels with a reduced field strength. When the distance is increased, a stronger magnetic field will be necessary, which will also act on surrounding vessels, thereby increasing the likelihood of small-vessel occlusions in the vicinity of the aneurysm given the lack of focus of the magnetic field.

The present experiments were performed in a model of a broad-based large BA tip aneurysm and a small-necked small MCA

Copyright © Congress of Neurological Surgeons. Unauthorized reproduction of this article is prohibited.

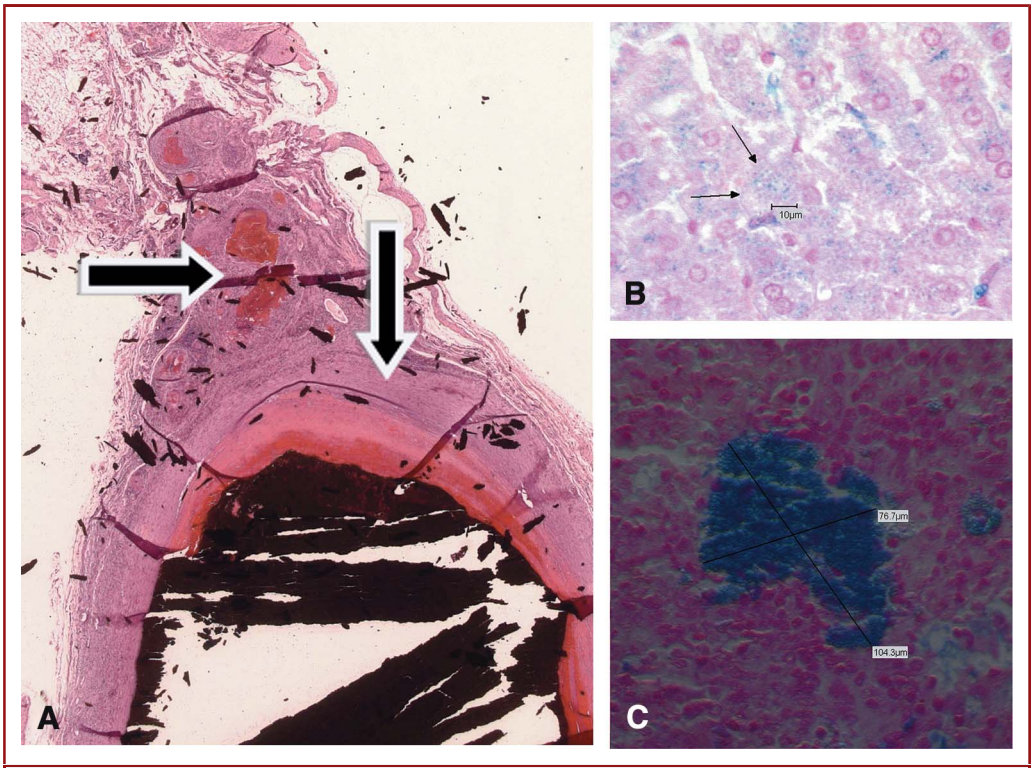

FIGURE 5. *Histological examinations.* **A**, *aneurysm with massive wall thickening, foreign-body granulomas (vertical arrow) in the vessel wall, inflammatory infiltrates in the adventitia, and focally unorganized thrombotic material circularly attached to the intimal layer (hortizontal arrow) (hematoxylin and eosin; × 5 magnification).* **B**, *homogenous distribution of predominantly solitary magnetic microparticles (MMPs) (diameter = 1.4 µm) in the liver of the rabbit treated first (Turnbull Blue, × 40 magnification).* **C**, *large MMP agglomerate (76.7 × 104.3 µm) in the spleen of the rabbit treated second (Turnbull Blue, × 40 magnification).*

aneurysm to evaluate 2 extremes of fluid dynamic situations encountered in aneurysms. In the larger and wide-necked BA tip aneurysm, flow velocity and volume flow have a stronger effect, leading to an increase in shear stress and perhaps turbulence. Therefore, complete filling was not achieved in the BA aneurysm, whereas it was possible in the MCA aneurysm, and MMP washout from the MCA aneurysm took considerably longer compared with the BA aneurysm (> 5 minutes vs 20-90 seconds). Hemodynamics are an important determining factor of the success rates of occlusion in experimental aneurysms.

Animal Results

Animal Model

This rabbit model is very suitable for investigations of endovascular therapy for cerebral aneurysms and has already been used in several experimental studies.[3,31-34] The elastase aneurysm model shows anatomic and histological configurations similar to human saccular aneurysms.[31] The aneurysms on a rabbit brachiocephalic trunk are made of an arterial vessel wall and are localized in similar hemodynamic conditions in terms of pressure and shear stress like human bifurcation aneurysms.[35] The aneurysm-carrying vessel has a diameter of 2 to 4 mm, which is comparable to human basal cerebral arteries.[36] Rabbits also have similar systolic (90 to 130 mm Hg) and diastolic (80 to 90 mm Hg) blood pressures.[37] They feature a number of similarities to the human coagulation and fibrinolysis systems.[38] However, there are also differences that must be considered. First, the histological structures of intracranial and extracranial vessels deviate from each other. The aneurysm in the rabbit model is surrounded by connective tissue, whereas a human cerebral aneurysm is embedded in the subarachnoid space. It is also important that the main arterial flow behind the brachiocephalic trunk of the rabbit is directed into the foreleg rather than the brain; therefore, potential thromboembolic events cannot be evaluated in this model. Because of the small body size of the rabbit, an aneurysm on the brachiocephalic trunk is easily reachable with an extracorporeal magnetic field, which is not the case in human aneurysms. Therefore, the current experimental results have to be regarded with caution in terms of their transfer to humans.[26]

Filling and Occlusion of the Aneurysms

In this proof-of-principle study, we were able to demonstrate that the experimentally induced aneurysms could be filled and

Copyright © Congress of Neurological Surgeons. Unauthorized reproduction of this article is prohibited.

occluded with MMPs, indicating that the forces of the external magnetic field (175 mT and 13 T/mm) countervailed against the local hemodynamic forces. Occlusion remained stable for at least 30 minutes after removal of the magnet, but after 12 weeks, final angiography showed reperfusion of the aneurysms with slight size reduction in 1 animal. Given the results from the in vitro studies, it is unlikely that the stable occlusion after magnet removal was due only to the particles because washout would likely have occurred by that time. It seems more likely, therefore, that a primary (instable) thrombus was present after the application of MMPs, which held the particles loosely within the aneurysm. The missing long-term stability might be related to an incomplete or missing transformation of the primary thrombus into a secondary, organized thrombus, which is supposed to happen, for example, after coil embolization.[39] We cannot rule out, however, that the observed short-term stability was due simply to a low-flow and low-shear-stress situation within the aneurysm.

Toxicity and Biocompatibility of MMPs

In accordance with previously performed toxicity tests, no signs of toxicity could be observed in the 12 weeks between application of the MMPs and final angiography. In analogy to former animal and human studies,[9,12,40-42] the application of iron oxide particles caused no complications in terms of allergic reactions, signs of disease, or bioincompatibility. However, the present study does not cover the period of time after 12 weeks in terms of long-term toxicity or biocompatibility. Because perivascular inflammatory infiltrates and foreign-body granulomas with and without involvement of MMPs were found in the aneurysm wall, adverse long-term effects cannot be ruled out. According to the formerly known distribution pattern of iron oxides, histopathology showed a substantial iron enrichment in the RHS of liver and spleen. In the liver and spleen of 1 rabbit, predominantly solitary particles were observed, whereas in the organs of the other rabbit, mainly large agglomerates could be found. This agglomeration implies a considerable risk of thromboembolic events because the agglomerate diameter was as large as 160 $\times$ 90 μm and therefore could have led to microembolic events. It has already been pointed out that in the rabbit model small thromboembolic events in the right foreleg would not be clinically detected as easily as in a human brain. Thus, it cannot be excluded with certainty that thromboembolic events did not occur during the experiments. In contrast to previously performed animal studies with other iron oxide nanoparticles, there was still a considerable amount of nondegraded MMPs in the spleen and liver after 12 weeks,[11,12] which raises the question of long-term biocompatibility.

PROBLEMS AND PERSPECTIVES

The present in vitro and in vivo results can be regarded as proof of principle that MMPs can be used to occlude experimental aneurysms. However, the study also demonstrates that for this new approach to be further developed for clinical use, several requirements have to be fulfilled and certain problems have to be resolved. The magnetic field has to be strong enough to overcome forces exerted by the blood flow and focused enough to prevent particle accumulation in smaller surrounding vessels while being noninvasive (ie, with the magnet placed outside the patient's skull or intravascularly). A potential solution to this problem may be the use of a catheter with an integrated magnet at its tip or the positioning of magnetically charged coils within the aneurysm before the application of MMPs. A second major problem is that of ferrimagnetic behavior with subsequent permanent magnetization leading to particle agglomeration and thromboembolic complications. Although magnetic steerability improves with increasing particle size, their ferrimagnetic behavior (resulting in permanent magnetization after exposure to a magnetic field) also increases.[7] The particle size also influences the immunological reactions and tissue diffusion.[15] Time to particle uptake by the RHS is reciprocally proportional to their size, but smaller particles diffuse more easily into the surrounding tissue, leading to potential inflammatory reactions in the vessel wall. A third problem is related to the long-term stability of the conglomerate of MMPs within the aneurysm. Even if a safe and sufficient aneurysm filling can be achieved with this method, the filling has to resist local shear stress to prevent recanalization. Therefore, for permanent embolization, advances and improvements in thrombogenicity seem necessary, keeping in mind that this may at the same time increase the risk of thromboembolic complications. Future studies should investigate different coatings that may delay immunological reactions and improve long-term stability. At the same time, one may contemplate the use of the investigated MMPS as a vehicle for transporting drugs into the aneurysm lumen and tissue diffusion into the aneurysm wall. Recently published articles have focused on the molecular pathology and inflammatory component of the pathogenesis of cerebral aneurysms and their rupture.[43-45] As a future option, therefore, specially designed MMPs could be coupled with anti-inflammatory drugs for the local treatment of the aneurysm wall.

Disclosure

Dr Andreas Spiegelberg and Mr Peter Kirkpatrick are co-owners of APG Medical Ltd., the supplier of the magnetic microparticles (Magseal) for this study. They are also the inventors of the patent application for said technology. The other authors have no personal financial or institutional interest in any of the drugs, materials, or devices described in this article.

REFERENCES

1. Van Gijn J, Kerr RS, Rinkel G. Subarachnoid haemorrhage. *Lancet*. 2007;369(9558):306-318.
2. Molyneux A, Kerr R, Stratton I, of neurosurgical clipping versus an endovascular coiling in 2143 patients with ruptured intracranial aneurysms: a randomized trial. *Lancet*. 2002;360et al; International Subarachnoid Aneurysm Trial (ISAT) Collaborative Group. International Subarachnoid Aneurysm Trial (ISAT) (9342):1267-1274.
3. Krings T, Hans FJ, Möller-Hartmann W, et al. Treatment of experimentally induced aneurysms with stents. *Neurosurgery*. 2005;56(6):1347-1359.
4. Zubillaga AF, Guglielmi G, Vinuela F, Duckwiler G. Endovascular occlusion of intracranial aneurysms with electrically detachable coils: correlation of aneurysm neck size and treatment results. *AJNR Am J Neuroradiol*. 1994;15(5):815-820.

Copyright © Congress of Neurological Surgeons. Unauthorized reproduction of this article is prohibited.

5. Malisch TW, Guglielmi G, Vinuela F, et al. Intracranial aneurysms treated with the Guglielmi detachable coil: midterm clinical results in a consecutive series of 100 patients. *J Neurosurg*. 1997;87(2):176-183.
6. Pierot L, Spelle L, Vitry F; ATENA Investigators. Immediate clinical outcome of patients harboring unruptured intracranial aneurysms treated by endovascular approach: results of the ATENA study. *Stroke*. 2008;39(9):2497-2504.
7. Dutz S. *Magnetic Nanoparticles for Biomedical Heating Applications*. Hamburg, Germany: Verlag Dr Kovac; 2008.
8. Holzapfel V. *Fluorescinating and Magnetic Polymer Nanoparticles: Functionalization and Biomedical Application*. Saarbrücken, Germany: VDM Verlag Dr Müller; 2008.
9. Bacon BR, Stark DD, Park CH, et al. Ferrite particles: a new magnetic resonance imaging contrast agent: lack of acute or chronic hepatotoxicity after intravenous administration. *J Lab Clin Med*. 1987;110(2):164-171.
10. Lübbe AS, Bergemann C, Riess H, et al. Clinical experiences with magnetic drug targeting: a phase I study with 4′-epidoxorubicin in 14 patients with advanced solid tumors. *Cancer Res*. 1996;56(20):4686-4693.
11. Lübbe AS, Bergemann C, Huhnt W, et al. Preclinical experiences with magnetic drug targeting: tolerance and efficacy. *Cancer Res*. 1996;56(20):4694-4701.
12. Weissleder R, Stark DD, Engelstad BL, et al. Superparamagnetic iron oxides: pharmacokinetics and toxicity. *AJR Am J Roentgenol*. 1989;152 (1):167-173.
13. McBain SC, Yiu HH, Dobson J. Magnetic nanoparticles for gene and drug delivery. *Int J Nanomedicine*. 2008;3(2):169-180.
14. Alexiou C, Arnold W, Klein RJ, et al. Locoregional cancer treatment with magnetic drug targeting. *Cancer Res*. 2000;60(23):6641-6648.
15. Berry CC, Curtis ASG. Functionalisation of magnetic nanoparticles for applications in biomedicine. *J Phys D Appl Phys*. 2003;36:198-206.
16. Koda J, Venook A, Walser E, et al. A multicenter phase I/II trial of hepatic intraarterial delivery of doxorubicin hydrochloride adsorbed to magnetic targeted carriers in patients with hepatocellular carcinoma. *Eur J Cancer*. 2002;38(suppl 7):18.
17. Wilson MW, Kerlan RK Jr, Fidelman NA, et al. Hepatocellular carcinoma: regional therapy with a magnetic targeted carrier bound to doxorubicin in a dual MR imaging/conventional angiography suite: initial experience with four patients. *Radiology*. 2004;230(1):287-293.
18. Johannsen M, Gneveckow U, Thiesen B, et al. Thermotherapy of prostate cancer using magnetic nanoparticles: feasibility, imaging, and three-dimensional temperature distribution. *Eur Urol*. 2007;52(6):1653-1661.
19. Jordan A, Maier-Hauff K. Magnetic nanoparticles for intracranial thermotherapy. *J Nanosci Nanotechnol*. 2007;7(12):4604-4606.
20. Maier-Hauff K, Rothe R, Scholz R, et al. Intracranial thermotherapy using magnetic nanoparticles combined with external beam radiotherapy: results of a feasibility study on patients with glioblastoma multiforme. *J Neurooncol*. 2007;81(1):53-60.
21. Udrea LE, Strachan NJ, Bădescu V, Rotariu O. An in vitro study of magnetic particle targeting in small blood vessels. *Phys Med Biol*. 2006;51(19):4869-4881.
22. Furlani EP, Ng KC.Analytical model of magnetic nanoparticle transport and capture in the microvasculature. *Phys Rev E Stat Nonlin Soft Matter Phys*. 2006;73(6)(pt 1):06 1919.
23. Khalessi A, Liu C, Apuzzo M. Neurosurgery and quantum dots, part I: state of the art. *Neurosurgery*. 2009;64(4):1015-1028.
24. Radomski A, Jurasz P, Alonso-Escolano D, et al. Nanoparticle-induced platelet aggregation and vascular thrombosis. *Br J Pharmacol*. 2005;146(6):882-893.
25. Tartaj P, Del Puerto Morales M, Veintemillas-Verdaguer S, Gonzalez-Carreno T, Serna CJ. The preparation of magnetic nanoparticles for applications in biomedicine. *J Phys D Appl Phys*. 2003;36:182-197.
26. Lübbe AS, Bergemann C, Brook J, McClure DG. Physiological aspects in magnetic drug targeting. *J Magn Magn Mater*. 1999;194(1):149.
27. Alksne JF, Fingerhut A, Rand R. Magnetic probe for the stereotactic thrombosis of intracranial aneurysms. *J Neurol Neurosurg Psychiat*. 1967;30(2): 159-162.
28. Alksne JF, Smith R. Iron-acrylic compound for stereotaxic aneurysm thrombosis. *J Neurosurg*. 1977;47(2):137-141.
29. Smith RW, Alksne JF. Stereotaxic thrombosis of inaccessible intracranial aneurysms. *J Neurosurg*. 1977;47(6):833-839.
30. Khilko VA. Artificial embolization of cerebral arteriovenous aneurysms via the vertebro-basilar system [in Russian]. *Vopr Neirokhir*. 1976;May-June(3): 15-20.
31. Krings T, Möller-Hartmann W, Hans FJ, et al. A refined method for creating saccular aneurysms in the rabbit. *Neuroradiology*. 2003;45(7):423-429.
32. Voltairas PA, Fotiadis DI, Michalis LK. Hydrodynamics of magnetic drug targeting. *J Biomech*. 2002;35(6):813-821.
33. Hans FJ, Krings T, Möller-Hartmann W, et al. Endovascular treatment of experimentally induced aneurysms in rabbits using stents: a feasibility study. *Neuroradiology*. 2003;45(7):430-434.
34. Hans FJ, Möller-Hartmann W, Brunn A, Schmitz-Rode T, Thron A, Krings T. Treatment of wide-necked aneurysms with balloon-expandable polyurethane-covered stent grafts: experience in an animal model. *Acta Neurochir (Wien)*. 2005;147(8):871-876.
35. Abruzzo T, Shengelaia GG, Dawson RC III, Owens DS, Cawley CM, Gravanis MB. Histologic and morphologic comparison of experimental aneurysms with human intracranial aneurysms. *AJNR Am J Neuroradiol*. 1998;19(7):1309-1314.
36. Kallmes DF, Helm GA, Hudson SB, et al. Histologic evaluation of platinum coil embolization in an aneurysm model in rabbits. *Radiology*. 1999;213(1):217-222.
37. Manning PJ, Ringler DH, Newcomer CE. *The Biology of the Laboratory Rabbit*. 2nd ed. San Diego, CA: Academic Press; 1994.
38. Heilman CB, Kwan ES, Wu JK. Aneurysm recurrence following endovascular balloon occlusion. *J Neurosurg*. 1992;77(2):260-264.
39. Spetzger U, Reul J, Weis J, Bertalanffy H, Gilsbach JM. Endovascular coil embolization of microsurgically produced experimental bifurcation aneurysms in rabbits. *Surg Neurol*. 1998;49(5):491-494.
40. Alexiou C, Jurgons R, Schmid RJ, et al. Magnetic drug targeting: biodistribution of the magnetic carrier and the chemotherapeutic agent mitoxantrone after locoregional cancer treatment. *J Drug Target*. 2003;11(3):139-149.
41. Alexiou C, Jurgons R, Schmid R, et al. Magnetic drug targeting: a new approach in locoregional tumor therapy with chemotherapeutic agents: experimental animal studies. *HNO*. 2005;53(7):618-622.
42. Stark DD, Weissleder R, Elizondo G, et al. Superparamagnetic iron oxide: clinical application as a contrast agent for MR imaging of the liver. *Radiology*. 1988;168(2):297-302.
43. Frösen J, Piippo A, Paetau A, et al. Growth factor receptor expression and remodeling of saccular cerebral artery aneurysm walls: implications for biological therapy preventing rupture. *Neurosurgery*. 2006;58(3):534-541.
44. Krings T, Lasjaunias PL, Geibprasert S, Pereira V, Hans FJ. The aneurysmal wall: the key to a subclassification of intracranial arterial aneurysm vasculopathies? *Interv Neuroradiol*. 2008;14(Suppl 1):39-47.
45. Niemelä M, Frösen J, Hernesniemi J, Dashti R, Palotie A. Molecular pathology of aneurysms. *Surg Neurol*. 2008;70(1):36-38.

COMMENTS

The authors merit congratulations for their strong introductory in vitro and in vivo inquiries into magnetic microparticle (MMP)–based coil embolization of intracranial aneurysms. Although far from clinical application, the research methodology essential to the adoption of emerging nanotechnologies is exemplified in this article.

Endovascular therapy for intracranial aneurysms necessitates exclusion of the weakened aneurysmal fundus from the circulation while avoiding parent artery encroachment at the aneurysm neck and sparing the distal native circulation of embolizate scatter. The authors elegantly quantify these clinical end points in their in vitro model.

Moreover, the authors aptly mention the subclinical embolic potential for individual MMP particles; aneurysm occlusion demands an amalgam of particles. The authors therefore assert that individual MMP particles scattered beyond the aneurysm are unlikely to accumulate in an individual vascular territory sufficiently to precipitate an ischemic event. Even though this claim obviously requires closer scrutiny and further study, the in vivo histopathological correlation buttresses the authors' claims regarding the ultimate fate of these wayward particles and further lays the foundation for toxicity studies of MMPs.

Finally, endovascular neurosurgery currently enjoys an era of rapid technological advancement. Increasingly sophisticated flow-directed

Copyright © Congress of Neurological Surgeons. Unauthorized reproduction of this article is prohibited.

microcatheters and microwire engineering, coupled with the introduction of Onyx HD 500, have enabled the liquid embolic treatment of intracranial aneurysms. By introducing the application of an external magnetic force beyond conventional flow and catheter manipulation, the article challenges the boundaries of even these ambitious endovascular techniques.

Although engineering advancements in nanoparticles remain speculative, studies such as this one hasten the day when interventionists may apply several different modalities to arrive at the point of pathology. We look forward to these advancements and applaud the authors for their role in this effort.

Alexander A. Khalessi
Los Angeles, California
L. Nelson Hopkins
Buffalo, New York

Magnetically controlled iron particle embolization is an old concept described for the first time in the 1960s. It was, however, long forgotten. Oechtering et al have now upgraded and refined the concept by combining it with modern endovascular catheterization techniques, modern paramagnetic microparticles, and better magnets. The result is a minimally invasive new therapeutic tool that might prove to be a valuable adjunct therapy to coiling or other embolization, although the present results suggest that it might not be sufficient alone to completely occlude an aneurysm. Even more interesting, however, is the authors' suggestion to use this method as a tool to enable local drug delivery. We have described how ongoing remodeling of the aneurysm wall structure is associated with its rupture[1] and how the remodeling and rupture are associated with the expression of receptor for vascular growth factors in the aneurysm wall.[2] It remains to be seen whether local delivery of a vascular growth factor with paramagnetic nanoparticles could reverse or reduce the degenerative processes ongoing in a still unruptured aneurysm wall.

Juhana Frösen
Mika Niemelä
Juha Hernesniemi
Helsinki, Finland

1. Frösen J, Piippo A, Paetau A, et al. Remodeling of saccular cerebral artery aneurysm wall is associated with rupture: histological analysis of 24 unruptured and 42 ruptured cases. *Stroke*. 2004;35(10):2287-2293.
2. Frösen J, Piippo A, Paetau A, et al. Growth factor receptor expression and remodeling of saccular cerebral artery aneurysm walls: implications for biological therapy preventing rupture. *Neurosurgery*. 2006;58(3):534-541.

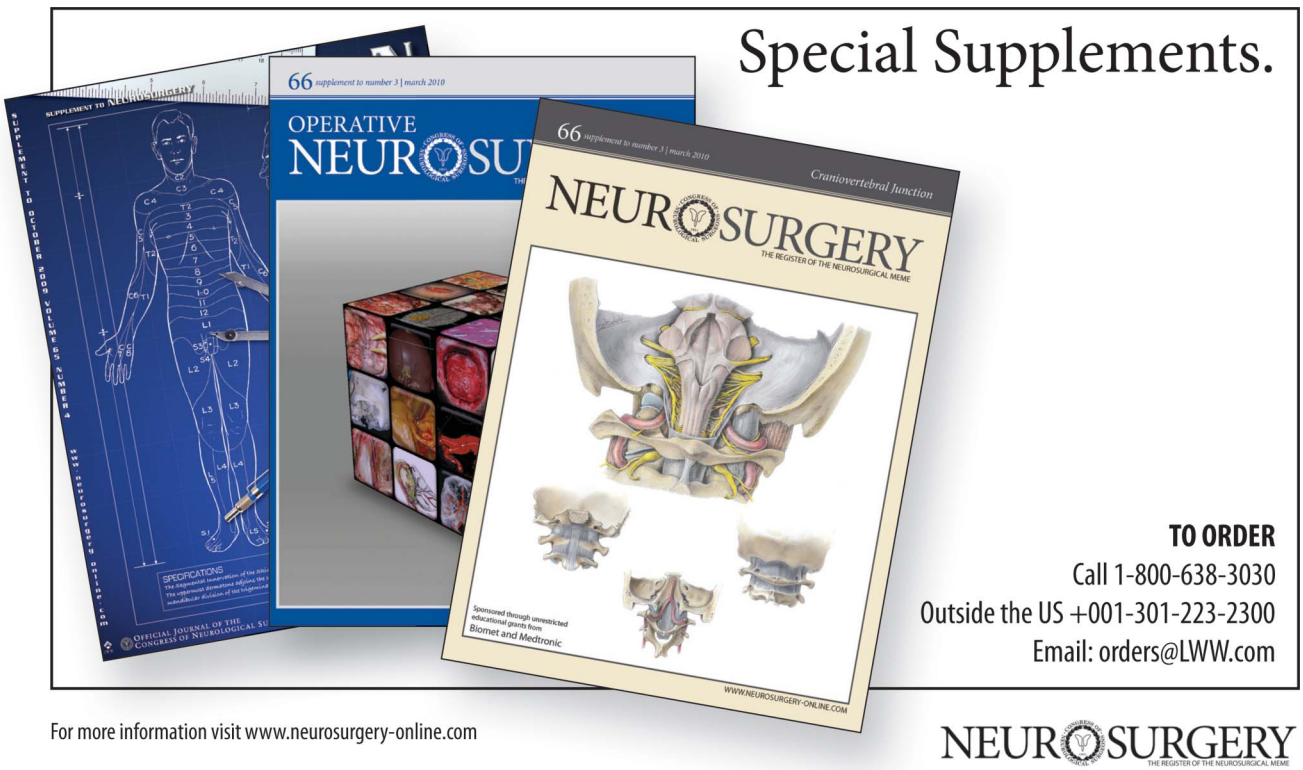

Copyright © Congress of Neurological Surgeons. Unauthorized reproduction of this article is prohibited.

Application of 2 Different Hemostatic Procedures During Microsurgical Median Nerve Reconstruction in the Rat Does Not Hinder Axonal Regeneration

Nektarios Sinis, MD*‡
Theodora Manoli, MD*§
Jennifer Lynn Schiefer, MD§
Frank Werdin, MD§
Patrick Jaminet, MD§
Armin Kraus, MD§
Michele Fornaro, PhD¶
Stefania Raimondo, PhD¶
Stefano Geuna, MD¶
Hans-Eberhard Schaller, MD§

‡Department of Plastic Surgery, Martin-Luther Hospital, Berlin, Germany; §Department of Hand, Plastic, and Reconstructive Surgery with Burn Unit, BG Trauma Centre, University of Tuebingen, Tuebingen, Germany; ¶Department of Clinical and Biological Sciences, University of Turin, San Luigi Hospital, Turin, Italy

*These authors have contributed equally contributed to this article.

Correspondence:
Nektarios Sinis, MD,
Department of Plastic Surgery,
Martin-Luther Hospital,
Caspar-Theyß-Straße 27,
14193 Berlin, Germany.
E-mail: Nektarios.sinis@gmail.com

Received, April 26, 2010.
Accepted, October 5, 2010.

Copyright © 2011 by the
Congress of Neurological Surgeons

BACKGROUND: Hemostatic procedures by means of electrical coagulation or application of topical agents are widely used to avoid postoperative bleeding during microsurgical reconstruction of peripheral nerves. It is speculated, however, that extensive hemostasis could provoke significant nerve damage.

OBJECTIVE: To examine the effects of 2 intraoperative hemostatic procedures on peripheral nerve regeneration.

METHODS: In 36 adult rats divided into 3 groups, the median nerve was transected and repaired by end-to-end neurorrhaphy. During surgery, bleeding was treated in groups 2 and 3 by application of either the topical hemostatic agent Floseal or routine bipolar coagulation. The degree of nerve regeneration was assessed in terms of motor function recovery using weekly grasping test evaluation for 3 months, muscle mass recovery of flexor digitorum sublimis, and stereological assessment of myelinated axon regeneration.

RESULTS: Neither of the 2 applied hemostatic methods induced any negative effects on nerve regeneration as defined by grip strength, muscle mass recovery, and morphology of myelinated nerve fibers. In contrast, Floseal-treated animals showed a faster progression of motor function recovery, and animals subjected to bipolar coagulation revealed a higher muscle mass recovery compared with the control group.

CONCLUSION: Controlled application of bipolar coagulation or Floseal does not exert a negative effect on the nerve regeneration outcome in rats. We propose that these methods can be applied safely to patients.

KEY WORDS: Blood coagulation, Hemostatic agent, Median nerve, Nerve reconstruction, Nerve regeneration, Rat

Neurosurgery 68:1399–1404, 2011 DOI: 10.1227/NEU.0b013e3182127bc4 www.neurosurgery-online.com

Peripheral nerve reconstruction is attracting more and more experimental and clinical research, and the progressive spread of microsurgical skills among surgeons worldwide is expected to maintain this trend over the near future.[1,2] In this evolving scenario, basic science should provide the surgeon with as much information as possible about the various factors that might influence the clinical outcome of nerve surgery. This should include information not only on the possible tools to improve the regeneration process during and after surgery but also on the potential unintentional effects or factors, which might depend on the surgical technique applied.

Among these factors, the use of bipolar coagulation to avoid bleeding might represent a possible source of damage to the nerve stumps because they can be unintentionally burned during the surgical act. Contrary to nerves treated by monopolar coagulation, application of bipolar coagulation was shown to preserve Schwann cell architecture and to cause less demyelination in previous studies.[3,4]

An alternative to electric coagulation is the application of topical hemostatic agents. There

Copyright © Congress of Neurological Surgeons. Unauthorized reproduction of this article is prohibited.

are several hemostatic agents to choose from, and their number is increasing. The most common hemostatic agents are collagen, fibrin, and thrombin sealants.[5] Floseal, a combination of a bovine-derived gelatin-based matrix and a human-derived thrombin component, is an efficient topical hemostaticum that is being widely used during microsurgical procedures.[6] Because the impact of hemostatic agents on nerve regeneration has not been specifically examined yet, one can speculate that they could negatively influence postoperative functional outcome.

The aim of the present study was to test whether unintentional nerve stump damage by bipolar coagulation or Floseal application exerts a negative effect on the outcome after end-to-end median nerve neurorrhaphy in the rat.

METHODS

Surgery, Experimental Design, and Animal Surveillance

Thirty-six Wistar adult female rats weighing 220 to 240 g each were used in this study. Good laboratory animal practice was observed according to the international standards for animal experimentation (EC Council Directive of November 1986, 86/609/EEC) and following approval by local government. Rats were fed standard laboratory food (Ssniff, Soest, Germany) and provided tap water ad libitum and an artificial light/dark cycle (12 hour light/12 hour dark). For the assessment of animal well-being, a careful daily animal surveillance was used to monitor passive and active movement, automutilation, skin ulcers, and joint contracture, especially during early postoperative times. In addition, animal body weight was measured weekly.

Rats were operated on under deep intraperitoneal anesthesia with 100 mg/kg ketamine and 5 mg/kg xylazine under clean conditions and with the aid of an operating microscope. The right median nerve was approached from the axillary region and then transected at a level where the brachial artery crosses the median nerve.

Animals were then divided into 3 experimental groups, each consisting of 12 rats. In group 1, the 2 median nerve stumps were immediately approached and repaired with a primary nerve suture in an end-to-end fashion by means of 2 epineural stitches of 10-0 monofilament nylon (Figure 1). In group 2, 20 μL Floseal was applied to each nerve stump before microsurgical repair by end-to-end neurorrhaphy. The volume was estimated according to the size of the rat median nerve. It was the amount of Floseal needed to flush the complete coaptation site with fluid because it is recommended that the entire bleeding site be kept in contact with the agent. Floseal is a combination of a bovine-derived gelatin-based matrix and a human-derived thrombin component. The gelatin component swells in the first 10 minutes up to 20% and hinders bleeding mechanically. Moreover, gelatin particles form a thrombin-rich surface on which secondary hemostasis occurs more effectively.[7] Floseal is biocompatible and is completely resorbed in 6 to 8 weeks.

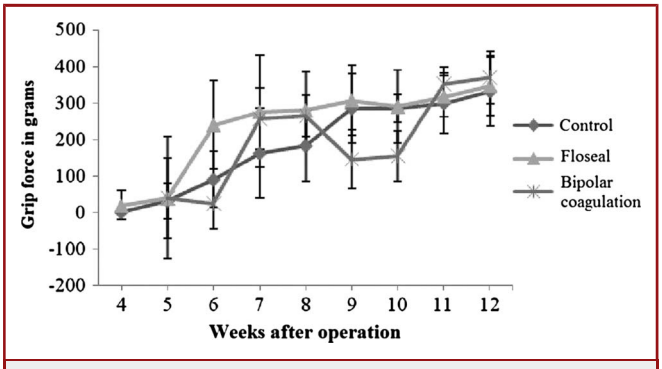

FIGURE 1. *Comparison of motor function recovery assessed by the grasping test in the 3 experimental groups.*

In group 3, the 2 nerve stumps were electrocoagulated briefly (for 1 second) by means of a microsurgical bipolar forceps. A programmed coagulation pattern with an autostop mechanism after 1 second of application time was used to standardize the electrical coagulation procedure at level 2 on the option board (Aesculap electrostimulator; output frequency, 450 kHz; modulation frequency, 1 kHz; power, 10 W). The electrostimulation was chosen in accordance with human application with the same intensity. Because of the small size of the nerve, we chose to apply the stimulus with microforceps. The 2 median nerve stumps were then approached and repaired by end-to-end neurorrhaphy as described above. All operations were performed by a single experienced microsurgeon.

To ensure an unbiased evaluation of the results, all postoperative assessments were carried out by a blinded approach. Each rat was therefore given an identification code, so that at the time of evaluation, the investigators were unaware of the group to which the rat belonged.

Assessment of Nerve Function Recovery

Functional recovery during the first 12 postoperative weeks was measured by the grasping test.[8–10] The grasping test was performed weekly beginning the first postoperative week. To obtain preoperative and postoperative comparisons within the data, all animals underwent the grasping test before surgery. Data were recorded and compared with the final results. The grasping test provides a quantitative assessment of finger flexion, which is controlled solely by the median nerve in the rat. The rat is gently lifted by the tail and allowed to grasp a grid connected to an ordinary electronic balance. While grasping, the animal continues to be lifted by the tail with increasing firmness until it loses its grip. At this precise moment, the value shown by the balance is recorded. After 3 grasping attempts, the highest value in grams displayed on the electronic balance is recorded and considered to reflect the maximum grip force for that specific animal at the respective experimental time point. To avoid grasping via the left (intact) paw, claws are covered by a piece of adhesive tape before testing.[11]

Assessment of Muscle Weight

Three months after surgery, all animals were anesthetized again with 100 mg/kg ketamine and 5 mg/kg xylazine. The flexor digitorum sublimis muscle is one of the forearm muscles in rats that are exclusively innervated by the median nerve. The right flexor digitorum sublimis muscle was carefully exposed, withdrawn, and immediately weighed.

Histological and Stereological Analyses of Nerve Fiber Regeneration

For histological and stereological quantitative analyses of regenerated nerve fibers, 1-cm-long median nerve segments were harvested immediately distally to the suture site and fixed by immediate immersion in 2.5% purified glutaraldehyde and 0.5% saccarose in 0.1 mol/L Sorensen phosphate buffer for 6 to 8 hours. Specimens were then washed in a solution containing 1.5% saccarose in 0.1 mol/L Sorensen phosphate

Copyright © Congress of Neurological Surgeons. Unauthorized reproduction of this article is prohibited.

buffer, postfixed in 1% osmium tetroxide, dehydrated, and embedded in resin. From each nerve, 2-μm-thick series of semithin transverse sections were cut starting from the distal stump of each median nerve specimen with an Ultracut UCT ultramicrotome (Leica Microsystems, Wetzlar, Germany) and stained with toluidine blue for high-resolution light microscopy examination. On 1 randomly selected section from each nerve specimen, design-based stereological analysis was carried out by a DM4000B microscope equipped with a DFC320 digital camera and an IM50 image manager system (Leica Microsystems). The final magnification was × 6.6, enabling accurate identification and analysis of myelinated nerve fibers. On the randomly selected section, the total cross-sectional area of the nerve was measured, and then 12 to 16 sampling fields were selected through the use of a systematic random sampling protocol.[12] In each sampling field, a 2-dimensional disector procedure, which is based on sampling the "tops" of fibers, was adopted to avoid the edge effect.[13] Mean fiber density was then calculated by dividing the total number of nerve fibers (n) within the sampling field by its area (n/mm^2). Total fiber number was finally estimated by multiplying the mean fiber density by the total cross-sectional area of the whole-nerve cross section.

Two-dimensional dissection probes were also used to select an unbiased representative sample of myelinated nerve fibers for measuring the following parameters: circle-fitting diameter of fiber (D) and axon (d), myelin thickness [(D − d) / 2], and axon/fiber diameter ratio, the g ratio (d/D). The precision of the estimates was evaluated by calculating the coefficient of error as previously described.[13,14] The sampling scheme was designed to keep the coefficient of error below 0.10, which ensures enough accuracy for neuromorphological studies.[15]

Statistical Analysis

Statistical analysis of quantitative data obtained by the grasping test was carried out with 1-way repeated-measures analysis of variance over time. When significant differences were detected by repeated-measures analysis of variance, posthoc multiple pairwise comparisons were carried out with the Student-Newman-Keuls test. Statistical analysis of quantitative data on muscle weight and axon number and density was carried out with 1-way ANOVA. Statistical significance was established as $P < .05$.

RESULTS

Animal surveillance showed that animal well-being was maintained during all postoperative times. All animals survived until the end of the experiment, 3 months after operation.

Figure 1 shows the results of the weekly grasping test assessment. In all experimental groups, functional recovery started between postoperative weeks 4 and 6 and increased progressively until the end of experiments at postoperative week 12, when it reached 80 % of preoperative baseline values. In general, Floseal-treated animals (group 2) showed a significantly faster progression of motor function recovery ($P < .05$) than animals treated by no hemostatic method (group 1) or by bipolar coagulation (group 3). The final function recovery at month 3 postoperatively showed no statistically significant difference between the 3 experimental groups ($P > .05$).

The mean masses of reinnervated flexor digitorum sublimis muscles in the 3 experimental groups are given with their SDs in Table 1. When *t* tests between the 3 experimental groups were performed, a significantly higher muscle mass in animals treated by bipolar coagulation (group 3) was found compared with the control group 1 ($P < .05$). There was no statistically significant difference between the Floseal-treated group 2 and bipolar coagulation–treated group 3 ($P > .05$).

TABLE 1. Comparison of Muscle Mass (Mean Weight) of Reinnervated Flexor Digitorum Muscles in the 3 Experimental Groups

Group	Wet Muscle Weight, mg[a]
1	118 ± 21.0
2	127 ± 20.0
3	140 ± 15.5

[a]Values are mean ± SD.

The morphological appearance of regenerated nerve fibers in the 3 experimental groups is shown in Figure 2. No qualitative morphological differences could be seen among the different groups. Design-based quantitative assessment of regenerated axons (Table 2) confirmed the qualitative analysis because statistical comparison revealed no significant intergroup differences for any of the morphometric parameters investigated ($P > .05$).

DISCUSSION

Hemostatic applications in the form of topical agents or electrocoagulation are a common practice during surgery of peripheral nerves. Especially at the level of brachial plexus nerves, intraoperative bleeding caused by injury of accompanying, relatively large-caliber nutritive vasa nervorum is not a rare phenomenon. In that situation, hemostatic procedures have to be applied to avoid obscuration of the operative field. However, the effects of such methods have not, to the best of our knowledge, been investigated in a controlled experimental setting. It can be postulated that the reduction of intraoperative and postoperative bleeding could have a positive impact on the quality of peripheral nerve regeneration. On the other hand, electrocoagulation or application of hemostatic agents could provoke damage to the nerve stumps, which might interfere with axonal regeneration and lead to a delayed or insufficient outcome after peripheral nerve neurorraphy. It has already been shown that monopolar coagulation provoked significant Schwann cell destruction compared with bipolar coagulation and should therefore be avoided when working around nerves.[3,4]

The present study aimed at comparatively investigating the effects of intraoperative bipolar electrocoagulation and application of the topical hemostaticum Floseal on nerve fiber regeneration after end-to-end neurorrhaphy in rats. Results revealed that neither of the 2 applied hemostatic methods induced any negative effects on nerve regeneration as defined by grip strength, muscle mass recovery, and morphology of myelinated nerve fibers

Copyright © Congress of Neurological Surgeons. Unauthorized reproduction of this article is prohibited.

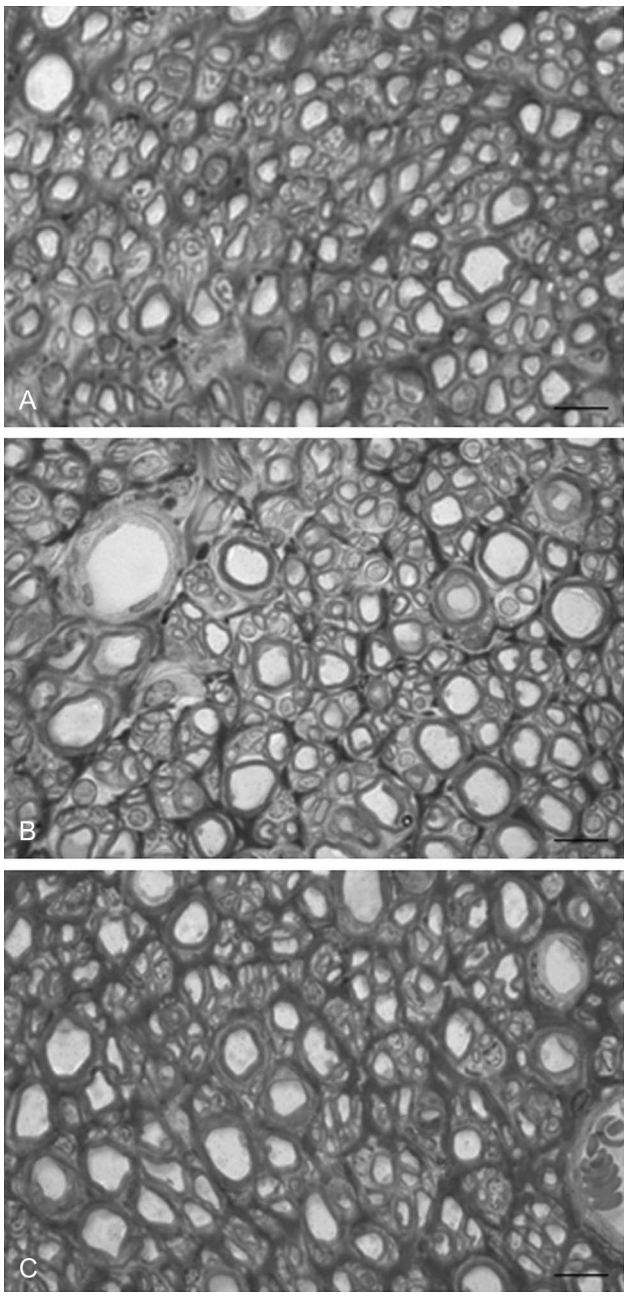

FIGURE 2. *Light microscope toluidine blue–stained micrographs of the regenerated median nerve in the 3 experimental groups:* **A**, *group 1;* **B**, *group 2;* **C**, *group 3. Magnification, × 2000.*

TABLE 2. Comparison of Stereological Predictors of Nerve Fiber Regeneration in the Regenerated Median Nerve: Total Number of Fibers, Mean Fiber Diameter, Myelin Thickness, and g Ratio

Group	Fibers, n	Fiber Diameter, μm[a]	Myelin Thickness, μm[a]	g Ratio
1	6829 ± 1430	3.65 ± 0.28	0.46 ± 0.07	0.73 ± 0.06
2	7798 ± 1698	3.86 ± 0.28	0.44 ± 0.03	0.76 ± 0.01
3	7679 ± 507	3.56 ± 0.18	0.45 ± 0.04	0.74 ± 0.02

[a]Values are mean ± SD.

as predictors of recovery. In contrast, Floseal-treated animals showed a faster progression of motor function recovery, whereas animals subjected to bipolar coagulation revealed a higher muscle mass recovery compared with the control group. One possible reason for the positive effects of the 2 tested hemostatic methods on nerve regeneration parameters could be the reduction of postoperative loss of nutrients by bleeding. An adequate nutrient supply to regenerating axons and Schwann cells through intrafascicular and epineural vessels is important for effective nerve regeneration.[16] The faster progression of motor function recovery in Floseal-treated animals is not surprising because no negative effects of the local hemostatic agent on nerve regeneration are expected. Moreover, faster axon growth in a high-viscosity gel matrix applied between the 2 nerve stumps could be postulated.[17]

On the other hand, bipolar coagulation can cause thermal damage to Schwann cells, which can compensate for or even overwhelm the positive hemostatic effect. This could explain the delayed progression of motor recovery at week 6 after operation. It is important to illustrate that in this study bipolar coagulation was applied by microsurgical forceps and a programmed coagulation pattern with an autostop mechanism after 1 second of application time. When bigger macroscopic forceps are used, the area of thermocoagulation could be unpredictably big in small nerves, provoking significant nerve damage. Moreover, it cannot be excluded that longer coagulation times or different coagulation intensities than those used in this study may have a negative impact on functional and morphological results of nerve regeneration. However, because the potential for axonal regeneration after injury is different in rodents than in humans, it is difficult to transfer the settings of bipolar intensity that generated satisfactory results to human surgery. Nevertheless, these results demonstrate, in accordance with clinical observations, that bipolar coagulation does not cause harm to nerves if applied carefully.

In addition, the results raise the question of whether axons can preserve their regenerative potential after extensive thermal damage during microsurgical reconstruction. Further research should focus on the hypothesis that a postconditioning effect like bipolar coagulation of the nerve stumps after neurotmesis and before neurorraphy can stimulate the regenerative potential of transected axons in the proximal nerve stump as well as wallerian degeneration in the distal stump. It was recently shown, for instance, that electrostimulation induces cell differentiation of fibroblasts.[18] These effects could also be visualized by observation of early changes and effects of regeneration during the first hours after application of electrocautery. Because our results showed

Copyright © Congress of Neurological Surgeons. Unauthorized reproduction of this article is prohibited.

a higher muscle mass recovery in animals treated by bipolar coagulation than in the control group, it is speculated that neuromuscular repair might have been improved by a post-conditioning mechanism. However, this question could also be addressed in an electrophysiological study in which the denervation and reinnervation of the muscle could be demonstrated according to time and place (ie, different parts of the muscle).

Our study suggests that bipolar coagulation or application of local hemostatic agents during microsurgical nerve reconstruction does not harm axon regeneration. Although implications of clinical applications obtained through experimental observations in laboratory animal models should be critically considered, the results of the present study support the view that the examined hemostatic methods can be used safely in patients.

CONCLUSION

Controlled application of the local hemostatic agent Floseal or bipolar coagulation of the nerve stumps did not hinder nerve regeneration after end-to-end neurorraphy of the median nerve in the rat. Floseal-treated animals showed a faster motor recovery than the control group.

Disclosure

This work was supported by a Fortune (01H2S) grant from the University of Tuebingen and by grants from the Regione Piemonte (Ricerca Sanitaria Finalizzata) and the Italian Ministry of University and Research. The authors have no personal financial or institutional interest in any of the drugs, materials, or devices described in this article.

REFERENCES

1. Evans GR. Peripheral nerve injury: a review and approach to tissue engineered constructs. *Anat Rec*. 2001;263(4):396-404.
2. Lundborg G. A 25-year perspective of peripheral nerve surgery: evolving neuroscientific concepts and clinical significance. *J Hand Surg Am*. 2000;25(3):391-414.
3. Zohar Y, Sadov R, Strauss M, Djialdetti M. Ultrastructural study of peripheral nerve injury induced by monopolar and bipolar diathermy. *Ann Otol Rhinol Laryngol*. 1996;105(9):673-677.
4. Schietroma JJ, Tenzel RR. The effects of cautery on the optic nerve. *Ophthal Plast Reconstr Surg*. 1990;6(2):102-107.
5. Barnard J, Millner R. A review of topical hemostatic agents for use in cardiac surgery. *Ann Thorac Surg*. 2009;88(4):1377-1383.
6. Oz MC, Cosgrove DM III, Badduke BR, et al. Controlled clinical trial of a novel hemostatic agent in cardiac surgery: the Fusion Matrix Study Group. *Ann Thorac Surg*. 2000;69(5):1376-1382.
7. Stassen JM, Arnout J, Deckmyn H. The hemostatic system. *Curr Med Chem*. 2004;11(17):2245-2260.
8. Bertelli JA, Mira JC. The grasping test: a simple behavioral method for objective quantitative assessment of peripheral nerve regeneration in the rat. *J Neurosci Methods*. 1995;58(1-2):151-155.
9. Papalia I, Tos P, Stagno d'Alcontres F, Battiston B, Geuna S. On the use of the grasping test in the rat median nerve model: a re-appraisal of its efficacy for quantitative assessment of motor function recovery. *J Neurosci Methods*. 2003;127(1):43-47.
10. Sinis N, Schaller HE, Schulte-Eversum C, et al. Nerve regeneration across a 2-cm gap in the rat median nerve using a resorbable nerve conduit filled with Schwann cells. *J Neurosurg*. 2005;103(6):1067-1076.
11. Ronchi G, Nicolino S, Raimondo S, et al. Functional and morphological assessment of a standardized crush injury of the rat median nerve. *J Neurosci Methods*. 2009;179(1):51-57.
12. Piskin A, Kaplan S, Aktas A, et al. Platelet gel does not improve peripheral nerve regeneration: an electrophysiological, stereological, and electron microscopic study. *Microsurgery*. 2009;29(2):144-153.
13. Raimondo S, Fornaro M, Di Scipio F, Ronchi G, Giacobini-Robecchi MG, Geuna S. Chapter 5: methods and protocols in peripheral nerve regeneration experimental research, part II: morphological techniques. *Int Rev Neurobiol*. 2009;87:81-103.
14. Schmitz C. Variation of fractionator estimates and its prediction. *Anat Embryol (Berl)*. 1998;198(5):371-397.
15. Pakkenberg B, Gundersen HJ. Neocortical neuron number in humans: effect of sex and age. *J Comp Neurol*. 1997;384(2):312-320.
16. Bell MA, Weddell AG. A descriptive study of the blood vessels of the sciatic nerve in the rat, man and other mammals. *Brain*. 1984;107 (pt 3):871-898.
17. Nakayama K, Takakuda K, Koyama Y, et al. Enhancement of peripheral nerve regeneration using bioabsorbable polymer tubes packed with fibrin gel. *Artif Organs*. 2007;31(7):500-508.
18. Genovese JA, Spadaccio C, Langer J, Habe J, Jackson J, Patel AN. Electrostimulation induces cardiomyocyte predifferentiation of fibroblasts. *Biochem Biophys Res Commun*. 2008;370(3):450-455.

Acknowledgment

We thank W.A. Grandy for carefully reading the manuscript.

COMMENTS

In this experimental study, the authors evaluated the degree of peripheral nerve regeneration in rats after the use of intraoperative hemostatic procedures during transection and subsequent end-to-end neurorrhaphy of the median nerve. Their goal was to determine whether the application of a topical hemostatic agent (Floseal) or the use of bipolar coagulation would have a deleterious effect on nerve regeneration. Using appropriate objective measures of motor function and muscle mass recovery, including the grasping test and gross weight of the median innervated flexor digitorum sublimis, as well as histological and stereological quantitative analyses of nerve fiber remyelination, the authors showed that these techniques did not exert any (measured) negative effects on nerve regeneration. Additionally, they demonstrated that Floseal-treated animals had a faster progression of motor function recovery and that the animals subjected to bipolar coagulation accumulated greater amounts of muscle after the surgery compared with the control group. They conclude from the results that these methods may be safely applied to human patients.

Although this experiment provides support for the previously unstudied hypothesis that these hemostatic agents do not exert deleterious effects on peripheral nerve regeneration, extrapolation of these results to clinical relevance requires the investigation of additional doses and levels of both techniques. These data are encouraging and should provide peripheral nerve surgeons with a greater degree of confidence to used such hemostatic devices without measurable risk to nerve recovery and function. As stated by the authors, however, further work should delineate specific tolerances and toxicities so that the parameters guiding their use in the operating room are more carefully defined.

Nathan J. Ranalli
Eric L. Zager
Philadelphia, Pennsylvania

This article compares the effects of chemical and thermal hemostasis in a rodent model of direct peripheral nerve end-to-end anastomosis. The first group of rats underwent median nerve transection with immediate suture repair without the application of any method of hemostasis along the nerve stumps. The second group underwent median

Copyright © Congress of Neurological Surgeons. Unauthorized reproduction of this article is prohibited.

nerve transection, and the stumps were treated with Floseal before suture repair. The third group underwent median nerve transection, and the nerve ends were treated with a standardized amount of bipolar electrocautery before suture repair. Functional, histological, and anatomic outcomes were analyzed for 3 months after repair.

Functional recovery, as measured by grip strength, was essentially the same in all 3 groups at the end of the study period, but the Floseal-treated animals recovered a bit faster than animals in the other 2 groups. The histological recovery, including the number of recovering axons and morphological appearance, was the same for all 3 groups. Lastly, the bipolar group had the least residual atrophy, and the control and Floseal groups had the same amounts of residual atrophy.

Overall, functional outcomes were the same regardless of whether hemostasis was performed or which type was used. The differences in the rates of recovery and amount of atrophy reversal by the different methods are difficult to explain. Without histological data in the immediate time period (days) after repair, all explanations are purely speculative. Perhaps not using hemostasis allows a small intraneural hematoma to form, delaying the onset of recovery as the axons are forced to first grow across the hematoma. Perhaps bipolar electrocautery burns back the axons, requiring them to grow a bit further to achieve recovery, resulting in a similar delay. A follow-up study could report short-term histological data to answer some of these questions.

In any case, these data are not likely to dramatically alter how peripheral nerve surgeons perform their repairs. I suspect that most surgeons currently perform nerve repair without the use of excessive amounts of chemical agents or bipolar electrocautery across the stumps themselves. If the application of gentle pressure to a persistent bleeder does not do the trick, then progression to chemical hemostasis followed by thermal hemostasis will likely take care of the oozing. I further suspect that these techniques will apply equally well during attempts at obtain hemostasis in the tumor beds of nerves after tumor excision.

Christopher J. Winfree
New York, New York

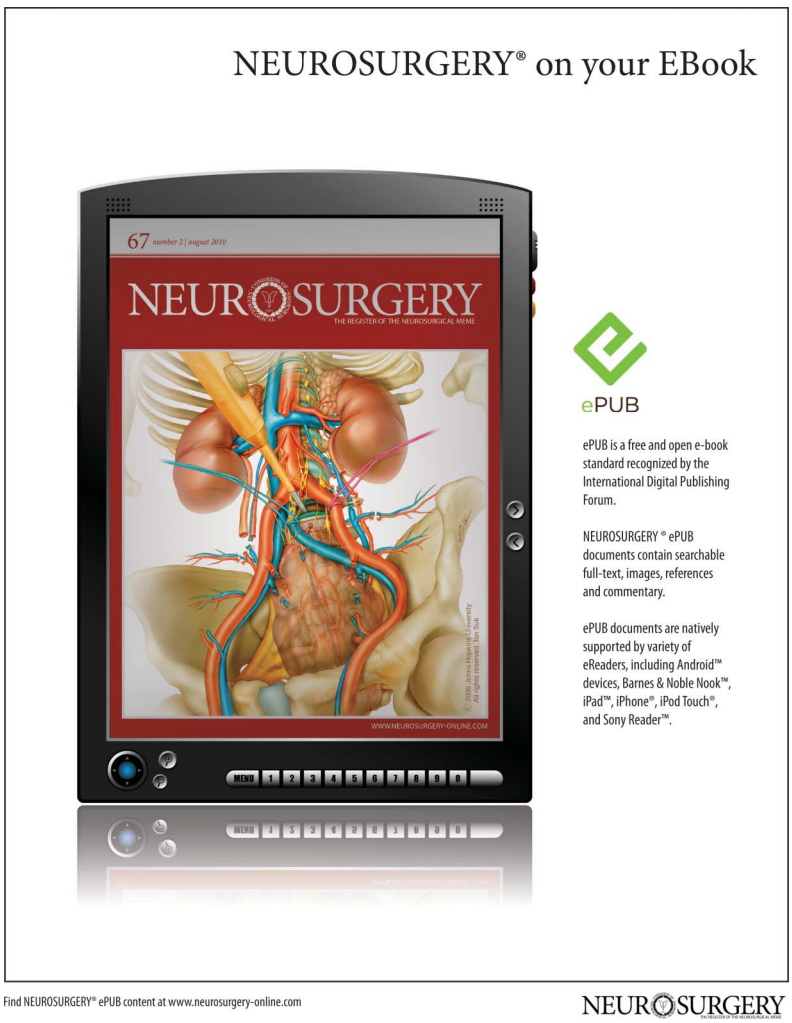

Copyright © Congress of Neurological Surgeons. Unauthorized reproduction of this article is prohibited.

Autologous Adult Cortical Cell Transplantation Enhances Functional Recovery Following Unilateral Lesion of Motor Cortex in Primates: A Pilot Study

Mélanie Kaeser, PhD*‡§
Jean-François Brunet, PhD*§
Alexander Wyss, PhD‡
Abderraouf Belhaj-Saif, PhD‡
Yu Liu, PhD‡
Adjia Hamadjida, MSc‡
Eric M Rouiller, PhD‡¶
Jocelyne Bloch, MD§¶

‡Unit of Physiology, Department of Medicine, University of Fribourg, Fribourg, Switzerland; §Department of Neurosurgery, Lausanne University Hospital (CHUV), Lausanne, Switzerland

*¶The authors contributed to this article equally.

Correspondence:
Eric M. Rouiller, PhD,
Unit of Physiology,
Department of Medicine,
University of Fribourg,
Ch. du Musée 5, CH-1700 Fribourg,
Switzerland.
E-mail: Eric Rouiller@unifr.ch

Received, May 20, 2010.
Accepted, October 4, 2010.

Copyright © 2011 by the
Congress of Neurological Surgeons

BACKGROUND: Although cell therapy is a promising approach after cerebral cortex lesion, few studies assess quantitatively its behavioral gain in nonhuman primates. Furthermore, implantations of fetal grafts of exogenous stem cells are limited by safety and ethical issues.

OBJECTIVE: To test in nonhuman primates the transplantation of autologous adult neural progenitor cortical cells with assessment of functional outcome.

METHODS: Seven adult macaque monkeys were trained to perform a manual dexterity task, before the hand representation in motor cortex was chemically lesioned unilaterally. Five monkeys were used as control, compared with 2 monkeys subjected to different autologous cells transplantation protocols performed at different time intervals.

RESULTS: After lesion, there was a complete loss of manual dexterity in the contralesional hand. The 5 "control" monkeys recovered progressively and spontaneously part of their manual dexterity, reaching a unique and definitive plateau of recovery, ranging from 38% to 98% of prelesion score after 10 to 120 days. The 2 "treated" monkeys reached a first spontaneous recovery plateau at about 25 and 40 days postlesion, representing 35% and 61% of the prelesion performance, respectively. In contrast to the controls, a second recovery plateau took place 2 to 3 months after cell transplantation, corresponding to an additional enhancement of functional recovery, representing 24% and 37% improvement, respectively.

CONCLUSIONS: These pilot data, derived from 2 monkeys treated differently, suggest that, in the present experimental conditions, autologous adult brain progenitor cell transplantation in a nonhuman primate is safe and promotes enhancement of functional recovery.

KEY WORDS: Adult, Autologous, Lesion, Monkey, Motor cortex, Neurotransplantation, Recovery

Neurosurgery 68:1405–1417, 2011 DOI: 10.1227/NEU.0b013e31820c02c0 www.neurosurgery-online.com

Brain lesions in the adult have dramatic consequences, because the spontaneous capacity of the brain to functionally recover is limited. Besides existing rehabilitative therapeutic approaches (eg, physiotherapy), several lines of research aim at developing treatments to promote and refine brain plasticity to enhance functional recovery following brain injury. Stem cell research, which represents a promising strategy to treat several nervous diseases, segregates into 2 main potential lines of treatment: implantation of exogenous cells or use of endogenous cells. The implantation of exogenous neural stem cells, either of embryonic or fetal origin, represents an encouraging approach, although there are serious limitations on the ethical, scientific, and clinical viewpoint.[1-12] Another strategy aims at stimulating and/or recruiting endogenous stem cells or precursor cells available in the adult central nervous system. These cells are located principally in the forebrain subventricular zone (SVZ) and in the subgranular zone (SGZ) of the dentate gyrus of

ABBREVIATIONS: M1, primary motor cortex; **PM**, premotor cortex; **SGZ**, subgranular zone; **SVZ**, subventricular zone

Copyright © Congress of Neurological Surgeons. Unauthorized reproduction of this article is prohibited.

the hippocampus.[12] These cells, however, migrate either only to a specific target (olfactory bulb from the SVZ) or only locally in the dentate gyrus (from the SGZ). The possibility to repair postlesion parts of the central nervous system (cerebral cortex, basal ganglia, spinal cord) remote from these 2 neurogenic niches is therefore limited. Attempts to experimentally enhance the migration of stem/precursors from the neurogenic niches to distant zones of the brain or to use resident progenitors led to a modest compensatory replacement of lost cells, without clinically relevant functional recovery.[12] Stem/precursors taken from the SVZ or SGZ and transplanted into another brain area may not develop their full potential of cell replacement in a different environment.[12] Stem/precursors residing in the cerebral cortex or basal ganglia may be too few to successfully replace lost cells after a lesion. To bypass these 2 limitations, the aim of the present pilot study was to extend preliminary experiments to fully test the feasibility and functional relevance of an original endogenous strategy in a nonhuman primate model of cerebral (motor) cortex lesion: first, to collect adult neural progenitor cells resident in the cerebral cortex of the lesioned subject itself[13]; second, to put the progenitor cells in culture to increase their number[14,15]; and third, to transplant them into the cerebral cortex, in and/or nearby an experimental lesion and assess the functional outcome.

A crucial step toward feasible, safe, and efficient clinical application requires the most appropriate animal model for the corresponding neural pathology, closely mimicking the characteristics of human diseases. The nonhuman primate model is often mandatory to address safety issues and scientific concerns, especially to include exquisite neural functions present only in primates.[16,17] In a previous study, we established in 3 monkeys the basis for feasible autologous cell reimplantation, from the point of view of safety and the fate of the implanted cells.[15] As a next step, the present pilot study aimed at providing, as proof of principle, first quantitative behavioral evidence in macaque monkeys for a beneficial outcome of cell therapy following injury of the cerebral cortex. To this aim, we used a previously established model of cerebral cortex lesion in nonhuman primates,[18] introduced originally to assess the extent and time course of "spontaneous" functional recovery.[19,20]

MATERIALS AND METHODS

Subjects

Data were collected from 7 adult macaque monkeys (*Macaca fascicularis*; 6 males and 1 female) weighing between 3 and 6 kg, ranging from 2.5 to 5 years old at onset of motor training sessions. The monkeys originated from the breeding colony in our own animal facility or were purchased from a certified supplier (Bioprim; 31450 Baziège; France), with the authorization to import delivered by the Federal Veterinary Office (BVET, Bern, Switzerland). All procedures were conducted in accordance to the Guide for Care and Use of Laboratory Animals (ISBN 0-309-05377-3; 1996) and approved by local veterinary authorities. Separate data from monkeys included in the present study were reported in previous articles or abstracts on other parameters.[18,21,22]

Seven adult macaque monkeys were subjected to unilateral lesion of the hand representation in motor cortex, producing a selective paresis of the contralesional hand.[18] Postlesion, 2 of these monkeys were "treated" (autologous adult brain progenitor cells were reimplanted) for comparison of their functional recovery of manual dexterity with 5 lesioned, untreated ("control") monkeys.

Monkeys were housed in our animal facilities in rooms of 12 m^3, in which usually 2 to 4 monkeys were free to move and interact with each other (a new swiss regulation has been introduced in September 2010 requesting a new volume of 45 m^3 at least to be given to a group of 2-5 macaque monkeys). Before behavioral testing in the morning, the animal caretaker placed the monkeys in temporary cages for subsequent transfer to a primate chair. The monkeys had free access to water and were not food deprived. The rewards (pellets) obtained during the behavioral tests represented the first daily access to food. After the tests, the monkeys received additional food (fruits, cereals). The body weight of the animals was monitored before every behavioral session. In case the body weight dropped by 10% or more, the experiment was interrupted until the monkey regained the lost weight (this criterion for interruption was not met in the course of the present experiments).

Behavioral Task

The seven monkeys were trained to perform the modified (static) Brinkman board task, aimed at assessing manual dexterity.[18-25] The subjects had to grasp food pellets from small slots oriented either vertically (n = 25) or horizontally (n = 25) by using precision grip (opposition of thumb and index finger), as described earlier in detail.[23] Each monkey was its own control, as the dexterity scores were compared prevs postlesion. The slot dimension was 15 mm long, 8 mm wide, and 6 mm deep. The monkeys performed the task daily with each hand until they reached a plateau reflecting a stable prelesion performance. The duration of the daily behavioral session was about 1 hour. After the motor cortex lesion, the behavioral sessions were pursued for a period ranging from 80 to 310 days. The main analysis was focused on the number of pellets retrieved in 30 seconds (retrieval score) from the vertical and the horizontal slots, respectively. The total retrieval score was also documented (the sum of the pellets retrieved in 30 seconds from both slot orientations). Besides the retrieval score, reflecting the entire motor sequence (reaching, grasping, and withdrawal of the hand), a second parameter was measured, namely the contact time, as recently reported.[22,23,26] The contact time is defined as the time of contact (in seconds) between the fingers and the pellet, representing the time interval between the first contact with the pellet in the slot (usually with the index finger) and the precise time of successful grasping when the pellet is removed from the slot. For each session, the contact time was determined separately for each of the first 5 vertical slots and each of the first 5 horizontal slots visited by the monkey. In general, the contact time was longer for the horizontal than the vertical slots, in line with the notion that grasping is somewhat more difficult for the horizontal slots, thus requiring a longer manipulation of the pellet before successive grasping.[23]

In addition to the modified (static) Brinkman board task, another task was introduced to test the ability to grasp moving objects (pellets), presented on a circular Brinkman board rotating at a speed of 10 rotations per minute. The monkey had to anticipate the rotation of the Brinkman board, turning either clockwise or counterclockwise. In a given behavioral session, the monkeys performed, one hand after the other, the rotating Brinkman board task once for each direction of rotation, corresponding each to the prehension of 32 pellets in slots distributed in 4 concentric circles. The contact time was measured as

Copyright © Congress of Neurological Surgeons. Unauthorized reproduction of this article is prohibited.

described above in the modified Brinkman board, for the first 10 slots aimed by the monkey. The 2 grasping tasks (modified Brinkman board and rotating Brinkman board) can be seen on the following web page: http://www.unifr.ch/neuro/rouiller/research/motorcontcadre.htm.

Animal Care for Surgery

After completion of prelesion training, the animals were subjected to the following surgical procedures. The monkeys were first tranquilized with ketamine (Ketalar; Parke-Davis, 5 mg/kg, intramuscularly); atropine was injected (0.05 mg/kg, intramuscularly) to reduce bronchial secretions. Before surgery, the animals were treated with the analgesic carprofen (Rymadil, 4 mg/kg, subcutaneously) and the antibiotic Albipen (ampicillin 10%, 30 mg/kg, subcutaneously). Subsequently, they were anesthetized with intravenous perfusion of 1% propofol (Fresenius) mixed with a 5% glucose solution (1 volume of propofol and 2 volumes of glucose solution); ketamine was added to the perfusion solution (65 mg/100 mL). To prevent edema, methylprednisolone (Solu-medrol, Pfizer) was added to the propofol/glucose solution (1 mg/mL). The level of anesthesia was kept at an optimal level with a perfusion rate of the propofol/glucose mixture of 0.1 $mL \cdot min^{-1} \cdot kg^{-1}$. All surgeries were performed under sterile conditions. Heart rate, respiration rate, expired CO_2, arterial O_2 saturation, and rectal temperature were monitored throughout the surgery. Each monkey was chronically implanted over the left forelimb area in the primary motor cortex (M1) with a stainless steel recording chamber (22 × 17 × 15 mm) allowing intracortical microstimulation sessions to map the primary motor cortex and locate the hand representation, as previously described.[18,27] After surgery, the monkeys received carprofen (pills of Rymadil mixed with food) daily and Albipen (subcutaneously) every 2 days for 1 to 2 weeks.

Biopsy of Prefrontal Cortical Tissue and Cell Preparation

In the 2 treated monkeys (Mk-JO and Mk-JA; during prelesion phase), following the same surgery protocol as described above, a squared bony sector of 8 × 8 mm was opened above the right dorsolateral prefrontal cortex. The dura mater was incised and an approximate volume of 8 to 20 mm^3 of cortical tissue was extracted using a surgical blade (no. 11, Paragon) and placed into sterile cold culture medium.[15] As previously described,[15,28] a few hours after the biopsy was performed, the cortical tissue collected was dissected to obtain gray matter cells, placed first in RPMI 1640 medium with fetal bovine serum and an antibiotic/antimycotic cocktail under horizontal agitation, and then kept in culture medium without serum, in suspension and under slow agitation. There was no specific cell sorting other than a selection imposed by the medium. Before reimplantation, a batch of cells were stained for subsequent tracking with fluorescent viable membrane dyes, PKH26 (red) for the cells reimplanted into the lesion site (Mk-JO and Mk-JA) and with PKH67 (green) for another batch of cells, reimplanted near the lesion site in the intact cortex (only Mk-JA). For the reimplantation (see below), the cells were cryopreserved, as previously reported.[14]

After the biopsy specimen was extracted, the bony sector was put back in place on the dura mater and sewed to the skull. The muscle and skin were then sutured. The extraction of brain tissue biopsy from the prefrontal cortex did not affect the motor capacity to grasp the pellets from the Brinkman board tasks.

Primary Motor Cortex Lesion

Several weeks after the biopsy, the hand area in the left M1 was permanently lesioned in the 7 monkeys by multiple injections of ibotenic acid (either Fluka 99% or Sigma 95%), as previously reported.[18,22] A volume of 1 to 1.5 μL of ibotenic acid solution (10 μg/μL in phosphate-buffered saline) was injected at each site by using a Hamilton microsyringe positioned at relevant sites previously defined by intracortical microstimulation. The total volume of ibotenic acid injected in each monkey ranged from 15 to 40 μL. More relevant than the volume of ibotenic acid injected is the volume of the actual lesion (volume of gray matter in motor cortex affected by the lesion), as determined for each monkey based on reconstruction of the lesion from consecutive histological sections stained for SMI-32. A typical lesion produced by infusion of ibotenic acid in M1 is illustrated in a recent report.[22]

Cell Reimplantation

Following the same surgical protocol as described above, cells contained in culture medium were reimplanted stereotaxically with a Hamilton microsyringe. For one monkey (Mk-JO), the reimplantation was performed into the lesion site 15 days after the motor cortex lesion. A total volume of 20 μL with PKH26 labeled cells containing 12 500 cells/μL was injected. For the other monkey (Mk-JA), the first reimplantation was performed into the lesion site (PKH26-labeled cells) and near the lesion site in the intact cortex (PKH67-labeled cells), once the monkey had reached a spontaneous functional recovery plateau. A second reimplantation was performed in the intact cortex, near the lesion site 49 days later (PKH67-labeled cells). The total volume (concentration of 3000 cells/μL) injected was 100 μL with PKH26 cells and 100 μL with PKH67-labeled cells (first implantation) and 49 μL with PKH67-labeled cells (second implantation), respectively. The 2 distinct viable membrane markers aimed at distinguishing, in the histological analysis, cells implanted in the lesion site from cells implanted in the intact cortex adjacent to the lesion (in Mk-JA).

Necropsy and Histology

At the end of the experiment, the monkeys were sacrificed as previously described,[27,29] for histological analysis of the lesion and of the implanted cells' fate. Frozen sections of the brain were cut in the frontal plane at a thickness of 50 μm, collected in 8 series for further processing to visualize different markers, such as SMI-32, glial fibrillary acidic protein, nestin, MAP2, and doublecortin, as previously reported.[15,29] Standard light, fluorescent, and confocal microscope analyses were conducted. Sectors of the brain sections where PKH26- and PKH67-labeled cells had been detected were selected and anatomically analyzed further.

RESULTS

Modified Brinkman Board

The description of the results is focused on the total score (sum of vertical and horizontal slots). Before lesion, the monkeys exhibited stable scores of manual performance (Figure 1; see http://www.unifr.ch/neuro/rouiller/ACCI/videos.htm video sequences 1, 5, and 9 for Mk-JO, Mk-JA, and Mk-GE, respectively). As a result of unilateral lesion of motor cortex, a total loss of the contralesional hand performance was observed, as reflected by a grasping score dropping to zero in the modified Brinkman board task, both in control and treated monkeys (Figure 1A and B; see http://www.unifr.ch/neuro/rouiller/ACCI/videos.htm video sequences 2, 6, and 10 for Mk-JO, Mk-JA, and Mk-GE,

Copyright © Congress of Neurological Surgeons. Unauthorized reproduction of this article is prohibited.

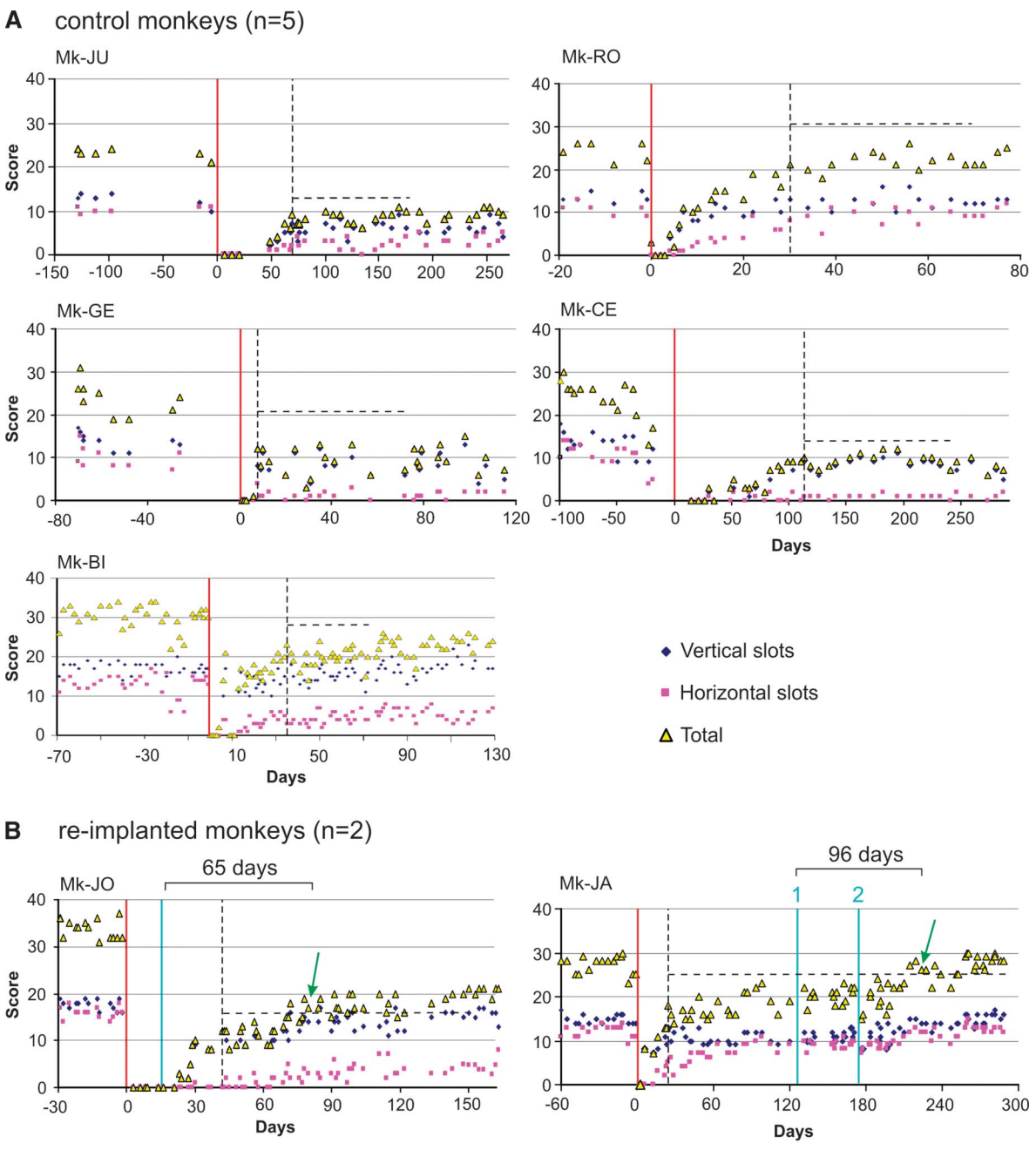

FIGURE 1. *Behavioral data (retrieval score).* **A** *and* **B**, *time course in days of manual dexterity performance (score), pre- and postlesion, as derived from the modified Brinkman board task in 5 control monkeys (***A***) and in 2 treated monkeys subjected to cell transplantation (***B***). The score is given by the number of pellets successively retrieved by the monkeys during 30 seconds. Yellow triangles represent the total score, blue diamonds the score for vertical slots, and pink squares the score for horizontal slots. The vertical red line indicates the time of the lesion (day zero). In* **A**, *the vertical dashed line shows the time point at which a spontaneous plateau of recovery was reached (see text for criterion to define the plateau). In* **B**, *the vertical dashed line represents the first (spontaneous) plateau of recovery. In the 2 treated monkeys (***B***), the vertical blue lines show the time of autologous cell implantations. The green arrows point out to the onset of a second behavioral plateau, reached following a rebound in the recovery curve (see text), occurring after a delay after cell implantation given in days above the graph. The horizontal dashed line represents a level of score defined by the median score calculated at the plateau of spontaneous recovery plus twice the difference between the highest value and the median score. In the control monkeys, the length of the horizontal dashed line represents the time window in which the spontaneous recovery was assessed quantitatively at plateau. The score level represented by the horizontal dashed line was taken as the criterion to be met to define a second plateau, representing an enhancement of functional recovery, observed in the 2 treated monkeys but not in the 5 control monkeys.*

Copyright © Congress of Neurological Surgeons. Unauthorized reproduction of this article is prohibited.

respectively). The 5 control monkeys (Figure 1A) then exhibited a progressive, spontaneous functional recovery starting after 5 to 50 days, reaching a postlesion plateau 10 to 120 days postlesion, depending on the monkey. In the recovery curve approaching saturation, the onset of the plateau was defined as the first individual data point (total score) for which, among the next 3 individual data points, none exhibits a higher score (vertical dashed line in Figure 1A). This spontaneous recovery plateau ranged across the 5 control monkeys from 38 to 98% of the prelesion score of manual performance (Figure 2, top), thus

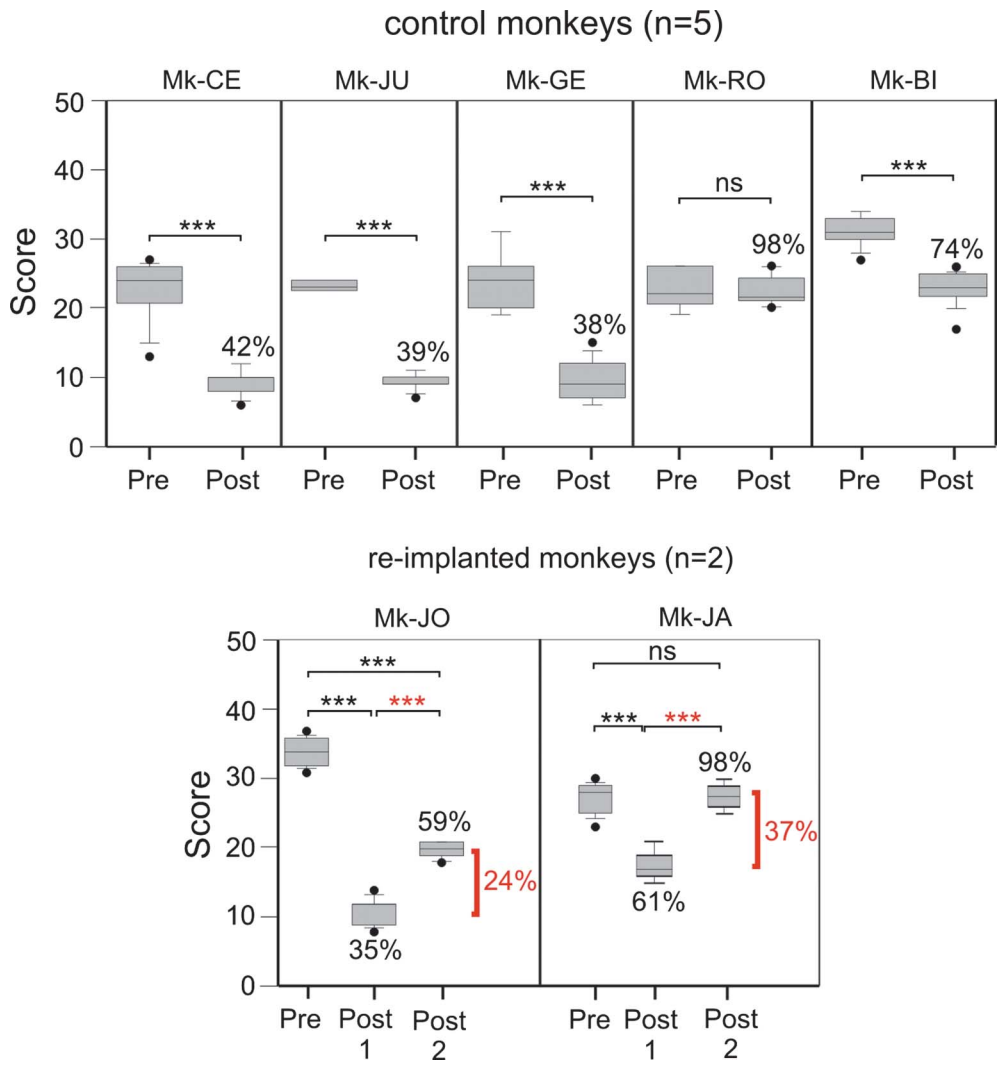

FIGURE 2. *Extent of functional recovery (retrieval score). The behavioral data are represented by box-and-whisker plots, comparing the prelesion and postlesion retrieval scores at plateau. In the 5 control monkeys (top), there was only one postlesion plateau, whereas, in the 2 treated (reimplanted) monkeys (bottom), in addition to the first plateau of spontaneous recovery (Post 1) there was a rebound in the recovery curve leading to a second plateau (Post 2) of manual dexterity scores. The different plateau scores were statistically compared (Mann-Whitney test, as previously reported[23]) with* $P < .001$ *(***) whereas "ns" is for* $P > .05$*. The percentage values in black next to each postlesion plateau represent the percentage of spontaneous functional recovery compared with the prelesion median score. The percentage values in red are for the magnitude of the behavioral rebounds in the 2 treated monkeys, compared with the first plateau of spontaneous recovery. In box-and-whisker plots, the horizontal line in the box corresponds to the median value and the top and bottom of the box are for the 75th and 25th percentile values, respectively. The top extremity of the whisker above the box is the largest data point included in the range going from the 75th percentile up to a level defined as the sum of the 75th percentile plus 1.5 times the interquartile distance. The bottom extremity of the whisker below the box is the smallest data point included in the range going from the 25th percentile down to a level defined as the 25th percentile minus 1.5 times the interquartile distance.*

Copyright © Congress of Neurological Surgeons. Unauthorized reproduction of this article is prohibited.

corresponding to an incomplete functional recovery. In the control monkey exhibiting the fastest recovery (Mk-GE), it turned out to be mainly limited to the vertical slots with a poor long-lasting recovery for horizontal slots (Figure 1A). A poor recovery for the horizontal slots was also observed in Mk-CE. The control monkey with the best recovery (Mk-RO, 98%) had the smallest lesion. In Mk-RO, because the spontaneous recovery was nearly complete already after a couple of months, the experiment was interrupted after 80 days, in contrast to much longer periods of observation in the other monkeys. A statistical comparison of pre- and postlesion plateaux is presented in Figure 2 (top) for the 5 control monkeys, showing that the spontaneous recovery remained dramatically incomplete (38% to 42%) in 3 of 5 monkeys. In the other 2 control monkeys, the spontaneous recovery was more prominent (74% to 98%), as expected for a smaller lesion of the motor cortex. The postlesion plateau then remained largely stable for several months in the control monkeys (Figure 1A).

For the 2 treated monkeys (Figure 1B), after complete loss of manual performance lasting 25 days in Mk-JO and 5 days in Mk-JA, the same progressive spontaneous recovery as seen in control monkeys took place, reaching a first plateau 40 days after lesion in Mk-JO and 25 days after lesion in Mk-JA (vertical dashed lines in Figure 1B). In Mk-JO, this first plateau represented 35% of prelesion score and lasted about 30 days (see http://www.unifr.ch/neuro/rouiller/ACCI/videos.htm video sequence 3). Meanwhile, 15 days after lesion, the autologous adult brain cell transplantation was performed. Starting around 70 days postlesion, there was a rebound of recovery, as reflected by a "second plateau" 80 days after the lesion (green arrow in Figure 1B), respectively, 65 days after the autologous transplantation. The second plateau was defined by data points in the recovery curve standing out above a level (horizontal dashed line in Figure 1B) calculated as the median score at first plateau to which twice the difference between the highest value and the median value at plateau 1 was added. The median score and the difference between the highest value and median were calculated from 15 data points taken from the beginning of the first plateau. The time onset of the second plateau was arbitrarily defined as the third data point (green arrow) greater than the limit (horizontal dashed line) defined above. This second behavioral plateau represented 59% of the prelesion score in Mk-JO. The difference between the first and second postlesion plateau (24%) was statistically significant ($P < .001$; see red stars in Figure 2; see http://www.unifr.ch/neuro/rouiller/ACCI/videos.htm video sequence 4 and compare with video sequence 3 at first plateau).

In the treated Mk-JO described above, the autologous cell transplantation was performed into the lesioned territory in the motor cortex, 15 days after the lesion during the first recovery phase. In this monkey, as shown by the histological analysis, the reimplanted cells remained mainly at a precursor stage (positive for the markers nestin, vimentin, and doublecortin), surrounded by endogenous astrocytes (glial fibrillary acidic protein reactive gliosis), although some cells were found to be either engaged in a neuronal differentiation process (positive for the marker β-tubulin III) or differentiated (positive for the marker SMI-32). Because the transplanted cells were found to be agglomerated, they did not migrate at all to occupy the whole lesioned territory. In an earlier feasibility study without behavioral assessment,[15] transplantation of autologous neural cells was performed in 3 monkeys not only in the lesion itself, but also in the adjacent intact tissue, near the lesioned territory, at a later time point after the lesion (40 days). The reimplanted cells showed in these 3 monkeys an ability to massively migrate from the reimplantation site toward the damaged area, as well as to differentiate massively (positive for the neuronal marker MAP-2). Based on these data (feasibility study and Mk-JO of the present pilot study), in the second monkey subjected here to the transplantation of autologous adult brain cells (Mk-JA), the reimplantation was performed both in and near the lesioned territory in M1, as well as at a later time point postlesion than in Mk-JO, to investigate the impact of these 2 parameters on the cell migration and differentiation ability.

In Mk-JA, the reimplantation of the autologous cells was performed in 2 steps, 125 days and 175 days postlesion. The first, spontaneous behavioral plateau represented 61% of the prelesion score and lasted more than 150 days (Figure 1; see http://www.unifr.ch/neuro/rouiller/ACCI/videos.htm video sequence 7). Then, as in the other treated monkey, a rebound of recovery took place as reflected by a second plateau (data points above the horizontal dashed line in the right panel of Figure 1B) at about 96 days after the first implantation. Moreover, this second plateau exhibited further improvement at postlesion day 260, possibly in relation to the second implantation of autologous cells (corresponding to a delay of about 85 days). The second plateau corresponded to a nearly complete recovery (98%): the enhancement of recovery presumably related to the cell transplantation was 37% (see red stars in Figure 2 for statistical comparison of plateaux 1 and 2; see http://www.unifr.ch/neuro/rouiller/ACCI/videos.htm video sequence 8 and compare with video sequence 7 at first plateau).

In the 2 treated monkeys, a rebound of manual performance score was present, as reflected by the second plateau of functional recovery. In contrast, in the 5 control monkeys, when the first plateau of recovery was reached, variations of the score across daily sessions never reached the criterion defined by the median score plus twice the difference between the highest value and the median score (horizontal dashed lines in Figure 1A). Among the 5 control monkeys, one animal (Mk-BI) exhibited some improvement after the plateau of recovery was reached, but it did not fulfill the criterion of surpassing the median score plus twice the difference between the highest value and the median score; the final level of recovery reached by Mk-BI was separated from the criterion level (horizontal dashed line in Figure 1A) by a score gap of half the difference between the median score and the highest value at plateau. The enhancement of manual performance observed in the 2 treated monkeys, corresponding to the second plateau, is illustrated qualitatively by video sequences (see http://www.unifr.ch/neuro/rouiller/ACCI/videos.htmcompare sequences 3 and 4 for Mk-JO as well as sequences 7 and 8 for Mk-JA), showing that the 2 monkeys achieved a better manual performance at the level of the second plateau than

Copyright © Congress of Neurological Surgeons. Unauthorized reproduction of this article is prohibited.

at the level of the first plateau. For comparison, video sequences taken at 2 remote time points along the unique plateau of spontaneous recovery in Mk-GE show that there was no enhancement of manual dexterity (http://www.unifr.ch/neuro/rouiller/ACCI/videos.htm, compare video sequences 11 and 12).

To further support the notion that the second plateau observed exclusively in the 2 treated monkeys corresponds to an enhancement of manual dexterity per se (better manipulation of pellets between the thumb and index finger), a further analysis was based on the contact time (see Materials and Methods). The contact time was determined in the sessions included in time windows corresponding to the first and second plateaux in Mk-JO (40-68 postlesion days and 9-164 postlesion days for plateau 1 and plateau 2, respectively) and in Mk-JA (80-180 postlesion days and 252-300 postlesion days for plateau 1 and plateau 2, respectively). The distribution of the contact times observed at plateau 1 and 2 is shown in the form of box-and-whisker plots in Figure 3A, separately for the vertical and horizontal slots, for each of the 2 treated monkeys. In Mk-JO, irrespective of the slot orientation, the contact times were significantly shorter at plateau 2 than at plateau 1, reflecting an improvement of manual dexterity when the second plateau was reached (Figure 3A). This was also the case in Mk-JA for the vertical slots, whereas there was no statistically significant difference for the horizontal slots, although the contact times were less variable at plateau 2 than at plateau 1 (Figure 3A). In agreement with the retrieval score data, the extent of decrease of median contact times going from plateau 1 to plateau 2 in Mk-JO (both slot orientations) and Mk-JA (vertical slots) ranged from 24 to 30%, representing an enhancement of manual dexterity comparable to the improvement of performance reflected by the retrieval score (24-37%; Figure 2).

Rotating Brinkman Board Task

A separate assessment was made of whether the 2 monkeys (Mk-JO; Mk-JA) subjected to transplantation of autologous adult cortical cells achieved a second level of recovery that reflected a significant improvement of manual dexterity over the first plateau. In this assessment, the contact times were measured in the rotating Brinkman board, comparing the sessions taken within the time windows corresponding to the 2 distinct plateaux (see above). As shown in Figure 3B, irrespective of the direction of rotation of the board, there was a statistically significant decrease of contact time going from postlesion plateau 1 to postlesion plateau 2, indicative of an enhanced manual dexterity. Comparing the median values, there was a decrease of contact time from plateau 1 to plateau 2 ranging from 42% to 57%, thus even more pronounced than for the modified (static) Brinkman board task.

Relationship Between Lesion Size and Recovery

There was a substantial variation of postlesion recovery across monkeys (Figures 1 and 2). To assess the dependence on lesion size (see Figure 4B), the degree of functional recovery in the modified Brinkman board (total score) in percent was plotted as a function of lesion volume, corresponding to the extent of gray matter in motor cortex affected by the lesion (Figure 4A). As expected, a small lesion in a control monkey (Mk-RO) was followed by a nearly complete spontaneous functional recovery (98%). A somewhat larger lesion in a second control monkey (Mk-BI) was followed by a reduced, though still prominent (74%), spontaneous recovery. In contrast, still in control monkeys, above a lesion volume of about 40 mm^3 and up to a volume of about 100 mm^3, the extent of spontaneous recovery remained fairly constant near 40% (Figure 4A). The extent of spontaneous recovery across the control monkeys is quite variable and the functional recovery observed in the 2 treated monkeys is in the same range. Nevertheless, a difference between the 2 subgroups of monkeys is the presence of a rebound in the postlesion recovery curve in the 2 treated monkeys (second plateau of an extent represented by the vertical dashed line in Figure 4A), a phenomenon absent in the 5 control monkeys (see also Figures 1 and 2).

The 2 treated monkeys of the present pilot behavioral study, as well as the 3 monkeys of our previous report also subjected to autologous cell transplantation,[15] did not exhibit any sign of pain or discomfort related to the autologous cell transplantation, indicating that this procedure does not produce undesired, secondary effect.

Cell Analysis

When looking at SMI-32-stained brain sections in motor cortex in an intact territory, there were darkly stained SMI-32 positive neurons in layer III and layer V, both in control and treated monkeys (Figure 4C, panel c1). In contrast, in the lesion territory, there was no SMI-32 staining in the control monkeys as expected (Figure 4C, panel c2), whereas lightly stained SMI-32 positive neurons were present in the lesion territory of the treated monkeys (Figure 4C, panel c3). When considering more closely these SMI-32-positive cells located in the lesion site of the treated monkey (Figure 4C, panel c4), it appeared that they sometimes corresponded to PKH26 (red, designed by yellow arrows) and PKH67 (green, designed by white arrows) positive cells that were transplanted in the monkey's brain (Figure 4C, panels c5–c7). In a treated monkey, a 3D reconstruction of the motor cortical area shows the distribution of PKH26 (red)- and PKH67 (green)-labeled cells (Figure 4C, panels c8–c10), implanted respectively in the lesion and at the vicinity of the lesion. Finally, PKH67-positive cells were present in the lesion site, indicating that they migrated from the intact cortex toward the lesion territory. The proportion of surviving transplanted cells amounted to about one third on average, a proportion most likely consistent with a clinical effect. The histological observations did not reveal the presence of teratoma or tumor formation.

DISCUSSION

Survey of the Data

To the best of our knowledge, the present behavioral pilot study is the first report in nonhuman primates suggesting that transplantation of autologous adult brain progenitor cells leads to

Copyright © Congress of Neurological Surgeons. Unauthorized reproduction of this article is prohibited.

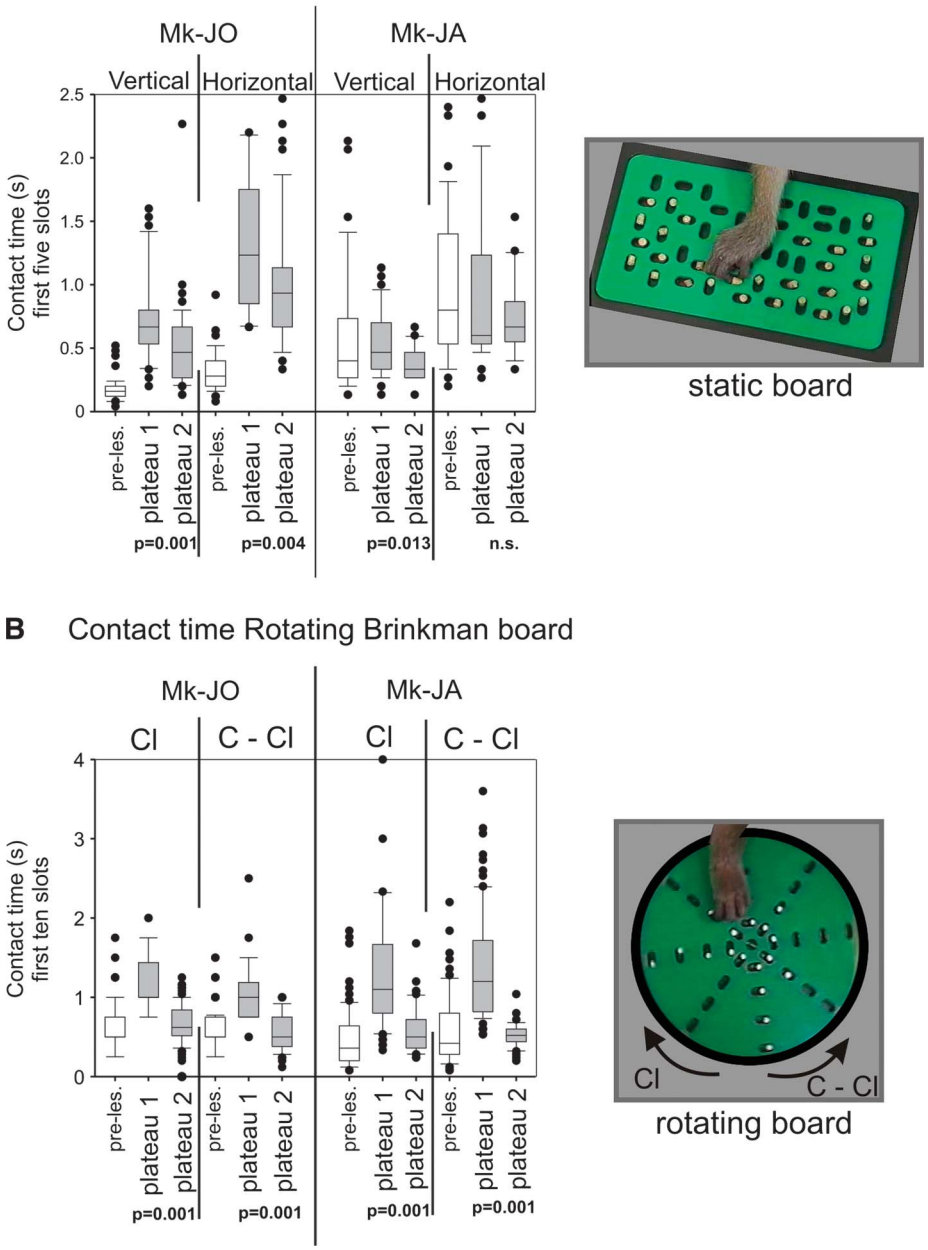

FIGURE 3. *Behavioral data (contact time). The contact times, measured separately during the postlesion plateaux 1 and 2 (gray boxes), are plotted in the form of box-and-whisker plots, for the modified (static) Brinkman board task (**A**) and the rotating Brinkman board task (**B**). The shorter contact time the better is the manual dexterity because less time of contact between the pellets and the fingers was needed to successfully grasp the pellet. In Mk-JA, data were collected from 9 behavioral sessions during the first plateau and from 4 sessions during the second plateau. In Mk-JO, data were collected from 6 behavioral sessions during the first plateau and from 12 sessions during the second plateau. n.s., nonsignificant difference between plateau 1 and plateau 2 ($P > .05$). The statistics refer to the comparison of contact times between the plateau 1 and the plateau 2 (Mann-Whitney test). For completeness of the information, the corresponding prelesion data are given by the white boxes, derived from 10 behavioral sessions. The conventions for the box-and-whisker plots are the same as in Figure 2. The insets on the right display the boards used for the 2 tests while a monkey is grasping a pellet. In the rotating Brinkman board, Cl is for clockwise rotation and C-Cl is for counterclockwise rotation.*

Copyright © Congress of Neurological Surgeons. Unauthorized reproduction of this article is prohibited.

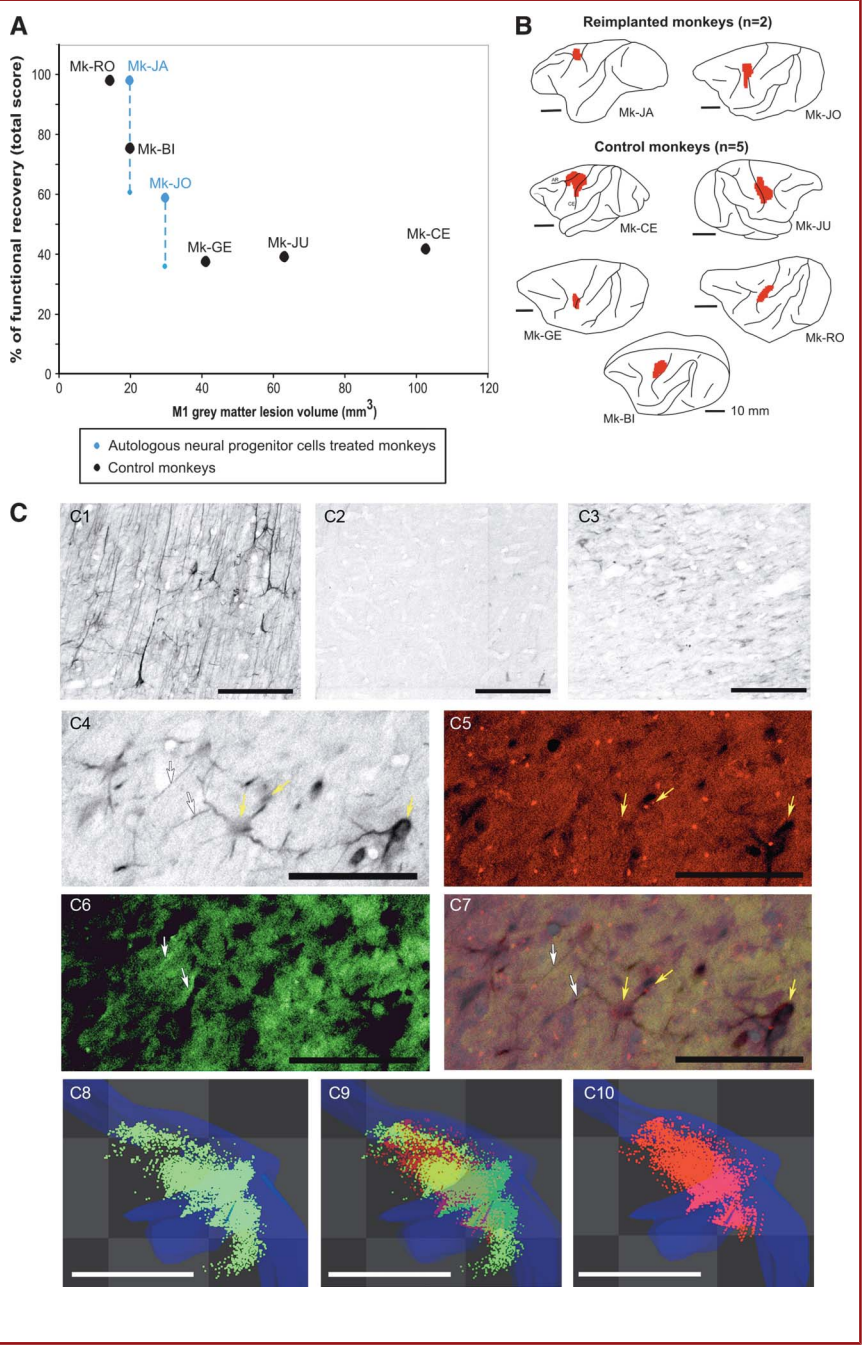

FIGURE 4. *Relationship with morphological data.* **A**, *plot of the percentage of postlesion functional recovery of the contralesional hand (total score in the modified Brinkman board) as a function of the volume of the primary motor cortical lesion. Black-filled circles represent the control monkeys and blue-filled circles represent the monkeys treated with autologous brain cells. For the 2 treated monkeys, the vertical dashed line represents the additional recovery observed (rebound), presumably in relation to the cell reimplantation (see text).* **B**, *lateral views of the projection on the cerebral cortex surface of the approximate location and extent of the left M1 gray matter lesion (red) as observed on frontal histological sections of the monkeys' brain. Theses reconstructions do not take the depth of the lesion into account. The precise extent of the lesion is given by its volume in* **A**. *At the bottom, the brain of the 4 control monkeys are shown, whereas the brain of the 2 monkeys reimplanted with autologous brain cells are represented at the top. AR, arcuate sulci; CE, central sulci. Scale bar = 10 mm.* **C**, *histological data in transplanted and control lesioned motor cortex area. (C1 to C3) Brain diaminobenzidine-immunohistology for SMI-32 neurons. In C1, SMI-32-positive neurons are as seen in the intact part of the motor cortex (at some distance from the lesion); SMI-32-positive neurons are present in layer III and layer V. The lesion territory is shown in C2 and C3 for a control monkey and a treated monkey, respectively; in the control monkey, no SMI-32 staining is visible (C2); in contrast, there are some positively stained cells in the lesion of the treated monkey (C3). Scale bar = 200 μm. (C4 to C7) High magnification of SMI-32-positive cells in the lesion site of the treated monkey (C4 and C7). These SMI-32-positive cells (yellow and white arrows in C4 and C7) correspond to PKH26-labeled cells (yellow arrows in C5) or to PKH67-labeled cells (white arrows in C6). Scale bar = 200 μm. (C8-C10) 3D reconstruction of the motor cortex lesion territory showing the distribution of PKH67-labeled cells (green dots in C8 and C9) and PKH26-labeled cells (red dots in C9 and C10). Note that the 2 sets of cells migrated in the same lesion territory in the overlay reconstruction (C9). Scale bar = 1 cm.*

an enhancement of functional recovery after brain injury. The enhancement of recovery is not directly reflected by a difference of postlesion behavioral plateau between groups of "treated" and "control" monkeys: the recovery was quite variable across monkeys because of interindividual variability of lesion volume and precise position of the lesion. Because of this high variability, an intergroup comparison would require larger numbers of monkeys in each group. The preliminary evidence for enhancement of functional recovery in relation to the treatment is rather based on the presence of a rebound (second plateau) in the postlesion recovery curve, present in the 2 treated monkeys and not in the 5 control monkeys (Figures 1, 2, and 4). The manual performance obtained at the second plateau was higher than the performance reflected by the first plateau of recovery (Figures 1,

Copyright © Congress of Neurological Surgeons. Unauthorized reproduction of this article is prohibited.

2, and 3; see also http://www.unifr.ch/neuro/rouiller/ACCI/videos.htm video sequences). Furthermore, the rebounds observed in the treated monkeys turned out to occur within a fairly comparable time window in the 2 treated monkeys (about 2-3 months; Figure 1B). The enhanced functional recovery in the 2 treated monkeys (reflected by the second plateau), compared with the control monkeys, cannot be explained by a more frequent practice of the motor tasks postlesion in the monkeys subjected to the transplantation of autologous cells, because the frequency of behavioral sessions were overall comparable across the 2 groups of monkeys.

Limitations of Interpretation

The interpretation of the present pilot results is limited by the low number of monkeys, especially in the group of treated monkeys, limited to 2 cases. Nevertheless, the consistent data obtained in the 5 control monkeys in the sense of an absence of significant rebound of functional recovery (even after a long time postlesion; see Figure 1A) represents a reliable observation, considering that 5 monkeys constitute a decent group size for nonhuman primates, although a group of 6 to 7 animals would be optimal.[23] More preliminary is the observation of a rebound of functional recovery most likely related to the autologous cell therapy, because it is based on only 2 monkeys, who underwent somewhat different injection protocols. However, the enhancement of recovery occurred with a time course consistent with plausible scenarios (see below). As far as the safety of the present therapeutic procedure is concerned, the 2 treated monkeys confirm the data previously obtained on 3 monkeys in a feasibility study.[15]

Possible Mechanisms of Enhancement of Functional Recovery

The delay of 2 to 3 months between cell reimplantation and rebound of functional recovery may reflect 2 possible mechanisms: cell replacement and/or endogenous neurogenesis induced by factor delivery. First, the reimplanted cells may integrate the neuronal network after differentiation into mature neurons that express MAP2[15] and SMI-32 (Figure 4C). As shown previously,[15] 1 month after transplantation, the cells still expressed progenitor markers such as nestin and were differentiated into neurons at 3 months postreimplantation. Furthermore, Koch et al[30] demonstrated that human embryonic neural stem cells can functionally integrate with and receive synaptic input from host brain tissue after 18 to 24 weeks. Such integration may occur in our study, where the autologous strategy is expected to facilitate the migration and integration of the transplanted cells. In line with this ability to colonize the entire lesion, the re-implanted cells express doublecortin, a migrant neuroblast marker that participates in the regulation of microtubule dynamics and stability during neuronal morphogenesis and migration.[31] Second, the cells may have a bystander effect through factor delivery and influence the endogenous brain modeling.[32] Preliminary results (data not shown) indicate that, in vitro, these adult primate brain cells secrete neurotrophic factors, such as brain derived neurotrophic factor, leukemia inhibitory factor, and ciliary neurotrophic factor. Based on the posttreatment delay of 2 to 3 months, the cell replacement mechanism appears likely but the factor delivery effect cannot be excluded at that time, although it should occur more rapidly. It is known that, after lesion of the M1 in monkey, the ipsilesional premotor cortex (PM) plays a significant role in the "spontaneous" functional recovery,[18,33-35] although other cortical areas may contribute.[36] Among possible mechanisms, it was shown that the normal projection from PM to M1 is redirected to the postcentral gyrus (somatosensory cortex[37]). It may be that the transplanted autologous adult cortical cells secrete factors favorable for such redirection of relevant projections originating from intact adjacent motor cortical areas.

Both the absence of rebound in the recovery curve of the 5 control monkeys and the consistent delay of about 2 to 3 months between autologous cells implantation and the rebound leading to a second plateau argue in favor of a positive effect of the cell transplantation on the functional recovery of manual dexterity following lesion of the hand area in M1 in macaque monkeys. In line with such interpretation, the autologous cell implantation took place at different time points with respect to the lesion in the 2 treated monkeys. If the rebounds would be due to factors independent from the autologous cells' implantation, then a consistent delay of 2 to 3 months would most likely not have been observed in the 2 treated monkeys. Another important observation derived from Mk-JA is that the rebound in the postlesion recovery curve occurred even though the autologous cell implantation took place a long time after the lesion (more than 3 months). The delay between the lesion and the cell reimplantation may play an important role, and the optimal timing remains to be determined in future experiments. For instance, it may be favorable to wait for the completion of the whole perilesional inflammatory phenomenon to obtain an optimal cell migration and differentiation.

The magnitude of the rebound of the postlesion recovery curve in the 2 treated monkeys ranged from 24 to 37%, as assessed in the modified Brinkman board task, adding to the "spontaneous" postlesion recovery score (Figure 2). In the second behavioral test (rotating Brinkman board), the effect even reached about 50% improvement of manual performance (Figure 3). In the control monkeys, there was no sham treatment (for instance, infusion of vehicle only). However, it is unlikely that the absence of rebound is due to the lack of cortical penetration in the perilesional territory with a syringe. In the entire cohort of monkeys with M1 lesion (not Mk-JO and Mk-JA, but comprising monkeys not included in the present study, eg, treated with anti-Nogo-A antibody), postlesion intracortical microstimulation sessions conducted at the level of the plateau of recovery did not exhibit a second plateau within the next 2 to 3 months, indicating that a surgical insult in itself does not enhance functional recovery.

A similar rebound effect as in the 2 monkeys with cell transplantation was found in another group of monkeys subjected to a comparable lesion of M1, but treated with anti-Nogo-A

Copyright © Congress of Neurological Surgeons. Unauthorized reproduction of this article is prohibited.

antibody,[21] a therapeutic strategy known to also enhance functional recovery after cervical cord lesion in monkeys.[23,38] The time course of rebound observed in the anti-Nogo-A antibody-treated monkeys subjected to lesion of M1 was comparable to the rebound delay of about 2 to 3 months observed here in the monkeys subjected to autologous transplantation. This observation suggests that both treatments, although based on different mechanisms, exert their effect following a comparable time course, which may represent a favorable situation to tentatively combine the 2 treatments in future experiments in monkeys, with the aim to obtain an additive, if not synergistic effect.

Comparison With Previous Studies

Following stroke, a majority of patients experience serious loss of hand function. The present monkey model focused on the recovery of hand function after cortical lesion thus represents a pertinent model to test therapeutic strategies. A direct comparison of the present data with previous animal studies is limited, because nearly all preclinical studies of cell therapy on animal models of cerebral infarct were conducted on rodents as the host animal.[10] One exception is a recent study,[39] in which human neural stem cells were transplanted in a monkey model of ischemic stroke. Evidence for cell replacement was found but the functional outcome was not tested. Considering another neurological disease (Parkinson disease), the transplantation of dopaminergic neurons generated from embryonic stem cells in monkeys into 1-methyl-4phenyl-1,2,3,6-tetrahydropyridine monkeys was followed by an attenuation of neurological symptoms,[40] based on a neurological score testing a wide repertoire of functions, but less quantitative than the present assessment of manual dexterity. In a monkey model of Parkinson disease, using the same transplantation strategy of autologous adult progenitor cells, there is also evidence for a neuroprotective effect[28] and enhancement of functional recovery compared with control monkeys.[41] Taken together, the latter study on Parkinson disease and the present one on cortical lesion, both based on reimplantation of autologous adult progenitor cells, provide new and encouraging results, as suggested by an enhanced functional recovery possibly related to the treatment. However, these 2 studies are at a pilot step and therefore the conclusion of enhanced functional recovery prompted by autologous cell transplantation needs to be confirmed on a larger sample of monkeys and, preferably, in combination with other strategies, such as neutralization of Nogo-A, for instance.[23,38] Even at the present pilot stage, these studies provide evidence that the reimplanted autologous brain cells did not form teratoma or tumor over time.

Future Perspectives

Considering that the autologous strategy does not involve as complex ethical and/or immunosuppression concerns as in heterologous strategies, there is hope to successfully translate this approach into the clinics in the reasonably close future, for instance, in case of irreversible cerebral pathology, like brain trauma or stroke. The present animal model was aimed at reflecting mechanisms taking place after cerebral insult, such as acute lesions (vascular or trauma) leading to excitotoxicity provoking cell death (mimicked here by infusion of ibotenic acid). On a more general perspective, the present study provides additional evidence in favor of a strategy aimed at recruiting endogenous stem cells or progenitor cells, associated in synergy with exogenous stems cell actions, as recently advocated.[12]

Disclosure

This work was supported by the Swiss National Science Foundation, grants 31-61857.00, 310000-110005, and 31003A-132465 (to E.M.R.), 3100A0-103924 (to J.B.), the Novartis Foundation; the National Centre of Competence in Research on ''Neural plasticity and repair'' and the Christopher Reeves Foundation (Springfield, NJ). The authors have no personal financial or institutional interest in any of the drugs, materials, or devices described in this article.

REFERENCES

1. Lindvall O, Kokaia Z, Martinez-Serrano A. Stem cell therapy for human neurodegenerative disorders-how to make it work. *Nat Med*. 2004;10(Suppl):S42–S50.
2. Rosser AE, Zietlow R, Dunnett SB. Stem cell transplantation for neurodegenerative diseases. *Curr Opin Neurol*. 2007;20(6):688-692.
3. Imitola J. Prospects for neural stem cell-based therapies for neurological diseases. *Neurotherapeutics*. 2007;4(4):701-714.
4. Ormerod BK, Palmer TD, Caldwell. MA. Neurodegeneration and cell replacement. *Philos Trans R Soc Lond B Biol Sci*. 2008;363(1489):153-170.
5. McKay R, Kittappa R. Will stem cell biology generate new therapies for Parkinson's disease? *Neuron*. 2008;58(5):659-661.
6. Kondziolka D, Wechsler L. Stroke repair with cell transplantation: neuronal cells, neuroprogenitor cells, and stem cells. *Neurosurg Focus*. 2008;24(3-4):E13.
7. Williams BA, Keating A. Cell therapy for age-related disorders: myocardial infarction and stroke–a mini-review. *Gerontology*. 2008;54(5):300-311.
8. Hess DC, Borlongan CV. Stem cells and neurological diseases. *Cell Prolif*. 2008;41(Suppl 1):94-114.
9. Bacigaluppi M, Pluchino S, Martino G, Kilic E, Hermann DM. Neural stem/precursor cells for the treatment of ischemic stroke. *J Neurol Sci*. 2008;265(1-2):73-77.
10. Locatelli F, Bersano A, Ballabio E, et al. Stem cell therapy in stroke. *Cell Mol Life Sci*. 2009;66(5):757-772.
11. Preynat-Sauve O, Burkhard PR, Villard J, et al. Pluripotent stem cells as new drugs? The example of Parkinson's disease. *Int J Pharm*. 2009;381(2):113-121.
12. Madhavan L, Collier TJ. A synergistic approach for neural repair: cell transplantation and induction of endogenous precursor cell activity. *Neuropharmacology*. 2009;58(6):835-844.
13. Brunet JF, Pellerin L, Arsenijevic Y, Magistretti P, Villemure JG. A novel method for in vitro production of human glial-like cells from neurosurgical resection tissue. *Lab Invest*. 2002;82(6):809-812.
14. Brunet JF, Pellerin L, Magistretti P, Villemure JG. Cryopreservation of human brain tissue allowing timely production of viable adult human brain cells for autologous transplantation. *Cryobiology*. 2003;47(2):179-183.
15. Brunet JF, Rouiller E, Wannier T, Villemure JG, Bloch J. Primate adult brain cell autotransplantation, a new tool for brain repair? *Ex Neurology*. 2005;196(1):195-198.
16. Courtine G, Bunge MB, Fawcett JW, et al. Can experiments in nonhuman primates expedite the translation of treatments for spinal cord injury in humans? *Nat Med*. 2007;13(5):561-566.
17. Capitanio JP, Emborg ME Contributions of non-human primates to neuroscience research. *Lancet*. 2008;371(9618):1126-1135.
18. Liu Y, Rouiller EM. Mechanisms of recovery of dexterity following unilateral lesion of the sensorimotor cortex in adult monkeys. *Exp Brain Res*. 1999;128(1-2):149-159.
19. Murata Y, Higo N, Oishi T, et al. Effects of motor training on the recovery of manual dexterity after primary motor cortex lesion in macaque monkeys. *J Neurophysiol*. 2008;99(2):773-786.
20. Darling WG, Pizzimenti MA, Rotella DL, et al. Volumetric effects of motor cortex injury on recovery of dexterous movements. *Exp Neurol*. 2009;220(1):90-108.

Copyright © Congress of Neurological Surgeons. Unauthorized reproduction of this article is prohibited.

21. Wyss A, Bloch J, Mir A, Schwab ME, Rouiller EM, Belhaj-Saif A. Enhancement of hand dexterity recovery following a lesion of the primary motor cortex (M1) with anti-Nogo-A antibody treatment: electrophysiological data in monkeys. Abstract FENS Meeting, July 12 to 16, 2008, Geneva, Switzerland.
22. Kaeser M, Wyss AF, Bashir S, et al. Effects of unilateral motor cortex lesion on ipsilesional hand's reach and grasp performance in monkeys: relationship with recovery in the contralesional hand. *J. Neurophysiol*. 2010;103(3):1630-1645.
23. Freund P, Schmidlin E, Wannier T, et al. Anti-Nogo-A antibody treatment promotes recovery of manual dexterity after unilateral cervical lesion in adult primates–re-examination and extension of behavioral data. *Eur J Neurosci*. 2009;29(5):983-996.
24. Brinkman J, Kuypers HGJM. Cerebral control of contralateral and ipsilateral arm, hand and finger movements in the split-brain rhesus monkey. *Brain*. 1973;96(4):653-674.
25. Brinkman C. Supplementary motor area of the monkey's cerebral cortex: short- and long-term deficits after unilateral ablation and the effects of subsequent callosal section. *J Neurosci*. 1984;4(4):918-929.
26. Nishimura Y, Onoe H, Morichika Y, Perfiliev S, Tsukada H, Isa, T. Time-dependent central compensatory mechanisms of finger dexterity after spinal cord injury. *Science*. 2007;318(5853):1150-1155.
27. Schmidlin E, Wannier T, Bloch J, Rouiller EM. Progressive plastic changes in the hand representation of the primary motor cortex parallel incomplete recovery from a unilateral section of the corticospinal tract at cervical level in monkeys. *Brain Res*. 2004;1017(1-2):172-183.
28. Brunet JF, Redmond DE Jr, Bloch J. Primate adult brain cell autotransplantation, a pilot study in asymptomatic MPTP-trained monkeys. *Cell Transpl*. 2009b;18(7): 787-799.
29. Wannier T, Schmidlin E, Bloch J, Rouiller EM. A unilateral section of the corticospinal tract at cervical level in primates does not lead to measurable cell loss in motor cortex. *J Neurotrauma*. 2005;22(6):703-717.
30. Koch P, Opitz T, Steinbeck JA, Ladewig J, Brustle O. A rosette-type, self-renewing human ES cell-derived neural stem cell with potential for in vitro instruction and synaptic integration. *Proc Natl Acad Sci U S A*. 2009;106(9):3225-3230.
31. Horesh D, Sapir T, Francis F, et al. Doublecortin, a stabilizer of microtubules. *Hum Mol Genet*. 1999;8(9):1599-1610.
32. Zhang ZG, Chopp M. Neurorestorative therapies for stroke: underlying mechanisms and translation to the clinic. *Lancet Neurol*. 2009;8(5):491-500.
33. Frost SB, Barbay S, Friel KM, Plautz EJ, Nudo RJ. Reorganization of remote cortical regions after ischemic brain injury: a potential substrate for stroke recovery. *J Neurophysiol*. 2003;89(6):3205-3214.
34. Plautz EJ, Barbay S, Frost SB, et al. Post-infarct cortical plasticity and behavioral recovery using concurrent cortical stimulation and rehabilitative training: a feasibility study in primates. *Neurol Res*. 2003;25(8):801-810.
35. Dancause N, Barbay S, Frost SB, et al. Effects of small ischemic lesions in the primary motor cortex on neurophysiological organization in ventral premotor cortex. *J Neurophysiol*. 2006;96(6):3506-3511.
36. McNeal DW, Darling WG, Ge J, et al. Selective long-term reorganization of the corticospinal projection from the supplementary motor cortex following recovery from lateral motor cortex injury. *J Comp Neurol*. 2010;518(5):586-621.
37. Dancause N, Barbay S, Frost SB, et al. Extensive cortical rewiring after brain injury. *J Neurosci*. 2005;25(44):10167-10179.
38. Freund P, Schmidlin E, Wannier T, et al. Nogo-A-specific antibody treatment enhances sprouting and functional recovery after cervical lesion in adult primates. *Nat Med*. 2006;12(7):790-792.
39. Roitberg BZ, Mangubat E, Chen EY, et al. Survival and early differentiation of human neural stem cells transplanted in a nonhuman primate model of stroke. *J Neurosurg*. 2006;105(1):96-102.
40. Takagi Y, Takahashi J, Saiki H, et al. Dopaminergic neurons generated from monkey embryonic stem cells function in a Parkinson primate model. *J Clin Invest*. 2005;115(1):102-109.
41. Brunet JF, Redmond DE Jr, Bloch J Primate adult brain cell autotransplantation improves the Parkinson score in a MPTP parkinsonian monkey model. Abstract. Society for Neuroscience October 17 to 21, 2009, Chicago, IL.

Acknowledgments

The authors wish to thank the technical assistance of Laurence Grollimund, Catherine Pythoud, Véronique Moret, Christine Roulin, Françoise Tinguely and Christiane Marti (histology and behavioral evaluations), Josef Corpataux, Laurent Bossy, Bernard Bapst and Bernard Morandi (animal house keeping), André Gaillard (mechanics), Bernard Aebischer (electronics), Laurent Monney (informatics). Thanks are due to Dr T. Wannier, Dr S. Bashir, and Dr E. Schmidlin for their support and advice in the course of the experiments. Julie Savidan contributed to the assessment of the volume of cortical lesion.

COMMENT

Stroke is the third leading cause of death in the United States and it is a leading cause of disability in adults. The armamentarium available for improvement of neurological function after stroke is currently limited to acute treatment in specialized stroke units, optimal therapy for medical complications, and intense physical, occupational, and speech rehabilitation. Despite many clinical trials, there is no effective intervention to improve neurological outcome following ischemic stroke. A growing number of studies have demonstrated stem cell-based therapy provides a potential approach to the restoration of lost brain function after stroke. Replacement of damaged cells and restoration of function may be accomplished by transplantation of many different cell types, such as embryonic, fetal, or adult stem cells, human fetal tissue, and genetically engineered cell lines.[1,2] Adult neural stem cells offer the advantage of avoiding the ethical problems associated with embryonic or fetal stem cells and can be harvested as autologous grafts from the individual patients. Current enthusiasm concerning the clinical applications of autologous adult stem cells in stroke is based on promising results obtained during experimental animal studies and initial clinical trials.

The authors describe a pilot study evaluating 7 monkeys that underwent a chemical lesion in their cortex. Five were followed as controls for spontaneous recovery and 2 were injected with autologous cortex progenitor cells. All 5 control monkeys achieved varying degrees of spontaneous recovery in a single phase. The 2 monkeys injected with progenitor cells achieved a spontaneous recovery in an initial phase, but also had a delayed recovery 2 to 3 months subsequent to the initial recovery. The small number of subjects studied makes it difficult to interpret the results, and with the 2 test subjects being injected differently with progenitor cells, there is no statistical power to the study. Furthermore, there is a lack of experimental consistency because each monkey tested did not undergo equal lesions, equal volume of injection, or equal locations of the injections. That being said the study does have some points that make it viable pilot research in which the authors learned enough to standardize the variables for a valid study. The authors put together an extensive control period, and most importantly, in a primate model with behavioral endpoints. It was demonstrated that there was a second boost of recovery that occurred in only the 2 monkeys injected with progenitor cells and not observed in the controls. When viewed as a pilot study it shows good initial insight into this potential treatment paradigm despite its apparent weaknesses. It will hopefully lead to a confirmation of the findings in a larger group with a more adequately designed fixed protocol.

At this point we are left to wonder: what is the plausible mechanism for this second phase of recovery? Spontaneous recovery of manual dexterity takes place to a highly variable extent across subjects and may depend on the recruitment of other motor areas.[3] Transplanted stem cells from multiple sources can generate neural cells that survive and form synaptic connections in the stroke-injured brain. More importantly, stem cells from multiple sources also exhibit neuroprotective properties that may ameliorate stroke deficits. In many cases, functional benefits observed are most likely independent of neural differentiation, although the mechanisms remain inadequately understood. A study of human umbilical cord cells showed improvement in neurobehavioral function

Copyright © Congress of Neurological Surgeons. Unauthorized reproduction of this article is prohibited.

and the reduction of infarct volume related more to the neuroprotective effects rather than the formation of a new network between host neurons and the implanted cells.[4] Endogenous neurogenesis has been observed in response to ischemic injury, and can be enhanced via transplants or infusion of appropriate cytokines. Enriched housing and voluntary running exercise enhanced migration of transplanted stem cells toward the region of injury after stroke and trends to the increase of survival of stem cells.[5] Thus the ability of transplanted stem cells in promoting recovery can be augmented by environmental factors such as rehabilitation. For maximal functional recovery, regenerative therapy will need to incorporate multidisciplinary approaches, which may include cell replacement, trophic support, protection from oxidative stress, and enhanced endogenous neuronal stem cells response. The loss of appropriate guidance cues and supporting architecture in the infarct cavity will likely impede the restoration of lost circuitry. Biologically compatible nanofiber scaffolds may provide the structure needed,[6] but getting grafted neurons to survive and make functional synapses as replacements to lost neurons is still a dream.

Before embracing clinical applications, several essential precautions must be suitably addressed. For example, the regenerative potentials of adult stem cells decline with age, and stem cells isolated from aged patients may retain dysfunctional characteristics. Functional recovery from stroke reaches a maximum level by 3 to 6 months after onset, and no further recovery occurs beyond this time. The time course for therapeutic intervention still needs to be worked out. Are the available autologous cells appropriate for therapeutic application in stroke? What are the optimal injection routes and cell doses? Success in future clinical trials will depend on careful investigation at the experimental level, to allow us to understand not only the clinical practicalities of stem cell use, but also the underlying biological principles involved. Furthermore, stimulation of endogenous adult stem cell-mediated repair mechanisms in the brain might offer new avenues for stroke therapy without the necessity of transplantation. Thus, important scientific issues need to be addressed to advance our understanding of the molecular mechanisms underlying the critical steps in cell-based repair to allow the introduction of these experimental techniques into clinical practice.

Roy Bakay
Chicago, Illinois

1. Urbaniak Hunter K, Yarbrough C, Ciacci J. Stem cells in the treatment of stroke. *Adv Exp Med Biol*. 2010;671:105-116.
2. Burns TC, Verfaillie CM, Low WC. Stem cells for ischemic brain injury: a critical review. *J Comp Neurol*. 2009;515(1):125-144.
3. Kaeser M, Wyss AF, Bashir S, et al. Effects of unilateral motor cortex lesion on ipsilesional hand's reach and grasp performance in monkeys: relationship with recovery in the contralesional hand. *J Neurophysiol*. 2010;103(3):1630-1645.
4. Koh SH, Kim KS, Choi MR, et al. Implantation of human umbilical cord-derived mesenchymal stem cells as a neuroprotective therapy for ischemic stroke in rats. *Brain Res*. 2008;1229:233-248.
5. Hicks AU, Hewlett K, Windle V, et al. Enriched environment enhances transplanted subventricular zone stem cell migration and functional recovery after stroke. *Neuroscience*. 2007;146(1):31-40.
6. Kubinova S, Sykova E. Nanotechnology for treatment of stroke and spinal cord injury. *Nanomedicine (Lond)*, 2010;5(1):99-108.

Copyright © Congress of Neurological Surgeons. Unauthorized reproduction of this article is prohibited.

Newly Synthesized Radical-Containing Nanoparticles Enhance Neuroprotection After Cerebral Ischemia-Reperfusion Injury

Aiki Marushima, MD*
Kensuke Suzuki, MD, PhD*‖
Yukio Nagasaki, PhD‖‡
Toru Yoshitomi, PhD‡
Kazuko Toh, PhD‡
Hideo Tsurushima, MD, PhD*¶
Aki Hirayama, MD, PhD§
Akira Matsumura, MD, PhD*

*Department of Neurosurgery, Graduate School of Comprehensive Human Sciences; ‡Graduate School of Pure and Applied Sciences University of Tsukuba; and §Center for Integrative Medicine, Tsukuba University of Technology, Tsukuba, Ibaraki, Japan; Department of Neurosurgery, Dokkyo Medical University Koshigaya Hospital, Koshigaya, Saitama, Japan; ¶Nanotechnology Research Institute, National Institute of Advanced Industrial Science and Technology, Tsukuba, Ibaraki, Japan

Correspondence:
Hideo Tsurushima, MD, PhD,
Department of Neurosurgery,
Graduate School of Comprehensive Human Sciences,
University of Tsukuba,
Tennoudai, Tsukuba,
Ibaraki, 305-8575, Japan.
E-mail: hideo-tsurushima@md.tsukuba.ac.jp.

Received, June 21, 2010.
Accepted, October 8, 2010.

Copyright © 2011 by the Congress of Neurological Surgeons

BACKGROUND: Antioxidant nitroxyl radicals such as 2,2,6,6-tetramethylpiperidine-1-oxyl (TEMPO) have been investigated for their ability to scavenge free radicals produced by ischemia-reperfusion injury. However, the short in vivo half-life and toxicity of TEMPO have limited their clinical application.

OBJECTIVE: We developed a core-shell-type nanoparticle, termed a radical-containing nanoparticle (RNP), to deliver nitroxyl radicals with prolonged in vivo half-life and pH-sensitivity. We evaluated the ability of RNP to deliver TEMPO radicals to the ischemic brain and scavenge free radicals in cerebral ischemia-reperfusion injury using rats.

METHODS: When RNPs were administrated to middle cerebral artery occlusion rats, the delivery and clearance of RNPs were detected using electron paramagnetic resonance (EPR) assay. The production of superoxide anion in neuronal cells was observed with dihydroethidium staining. The treatment effects were evaluated by measuring the cerebral infarction volumes, lipid peroxidation and protein oxidation, and neurological symptom scoring.

RESULTS: The TEMPO radicals contained in RNPs were detected for 6 hours after intravenous administration as a triplet EPR signal in the ischemic brain, and RNPs significantly reduced the production of superoxide anion in neuronal cells compared with saline and 4-hydroxy-2,2,6,6-tetramethylpiperidine-1-oxyls (TEMPOL). The infarction volumes of rats treated by RNPs were significantly lower than those of rats treated by saline, micelles, and TEMPOL. In addition, RNP treatment suppressed lipid peroxidation and protein oxidation, and limited the adverse effects of TEMPO radicals such as hypotension.

CONCLUSION: RNPs could be a promising neuroprotective agent with their enhanced ability to scavenge free radicals and reduced toxicity.

KEY WORDS: Free-radical scavenger, Ischemia-reperfusion injury, Ischemic brain disease, Neuroprotection, Radical-containing nanoparticle

Neurosurgery 68:1418–1426, 2011 DOI: 10.1227/NEU.0b013e31820c02d9 www.neurosurgery-online.com

Arterial recanalization by thrombolysis and intravascular intervention are the primary treatment strategies for ischemic stroke and heart attack.[1,2] However, this restoration of blood flow can result in ischemia-reperfusion injury. Ischemia-reperfusion injury is caused by reactive oxygen species (ROS) and can enhance the damage sustained in the ischemic organ.[3,4] Therefore, to minimize the damage associated with ischemia-reperfusion, protection of the organs from ROS must be considered. Previous reports revealed that nitroxyl radicals and spin-trapping compounds, such as 2,2,6,6-tetramethylpiperidine-1-oxyl (TEMPO) and α-phenyl-*N*-*tert*-butylnitrone (PBN), improved functional outcomes in ischemia-reperfusion injuries with the ability to scavenge free radicals at the same degree.[5-8]

ABBREVIATIONS: BBB, blood-brain barrier; **EPR**, electron paramagnetic resonance; **MCAO**, middle cerebral artery occlusion; **PBN**, α-phenyl-N-tert-butylnitrone; **RNP**, radical-containing nanoparticle; **RNP-H**, RNP-hydroxylamine; **ROS**, reactive oxygen species; **TBARS**, thiobarbituric acid reactive substances; **TEMPO**, 2,2,6,6-tetramethylpiperidine-1-oxyl; **TEMPOL**, 4-hydroxy-2,2,6,6-tetramethylpiperidine-1-oxyl

Copyright © Congress of Neurological Surgeons. Unauthorized reproduction of this article is prohibited.

TEMPO is a free-radical scavenger composed of a 6-membered piperidine ring structure, and it is known to have unique antioxidant properties. It acts as a self-replenishing antioxidant via catalytic reactions.[9] However, a short in vivo half-life due to acute reduction by antioxidant systems in vivo (such as catalase and glutathione peroxidase) and its toxicity have limited clinical applications.[6,8,10] 4-Hydroxy-TEMPO (TEMPOL) could induce hypotension that is a seriously adverse event in the ischemia. TEMPOL is also used as an antihypertensive agent.[9,11] If the in vivo half-life of TEMPO radicals could be prolonged and its toxicity would be erased, the modified TEMPO radicals would have a higher potential for neuroprotection than conventional free-radical scavengers containing PBN.

We developed a novel core-shell-type nanoparticle, termed a radical-containing nanoparticle (RNP), which consists of micelles containing 4-amino-2,2,6,6-tetramethylpiperidine-1-oxyl (4-amino-TEMPO).[12] RNPs demonstrated prolonged in vivo half-life due to the encapsulation of TEMPO radicals in the core of the micelle, as well as pH sensitivity to help TEMPO radicals act as antioxidants upon collapse of the nanoparticles in low pH conditions in vivo (Figure 1).[13] The purpose of this study was to evaluate the ability of RNPs to deliver nitroxyl radicals to the ischemic brain, as well as to determine the neuroprotective effects of RNPs in a rat model of transient middle cerebral artery occlusion (MCAO).

MATERIALS AND METHODS

Properties of RNPs

Amphophilic block copolymers possessing a poly(ethylene glycol) chain as a hydrophilic segment, a polystyrene hydrophobic segment, and 4-amino-TEMPO repeating unit as a side chain was prepared as described previously.[12] They formed core-shell-type RNPs in aqueous media when subjected to the dialysis method. RNPs were prepared in various concentrations for application in in vivo experiments. The average RNP diameter was measured using a light-scattering spectrometer (Nano ZS, ZEN3600, Malvern Instruments, Ltd., Malvern, Worcestershire, United Kingdom), and estimated to be about 40 nm in the low concentration and 60 nm in the high concentration. RNPs were designed to possess characteristics that enhance the effects of TEMPO radicals in low pH conditions caused by ischemia. The properties of RNPs were summarized.[12,13] The amino groups on amino-TEMPO have a pH sensitivity. The protonation of the amino group initiated below pH 7.0, and subsequently RNP, was collapsed in lower pH condition. The electron paramagnetic resonance (EPR) spectra of RNPs showed a broad signal at high pH values because of the encapsulation of TEMPO radicals in the core of RNPs. In low pH conditions, the EPR spectra changed to a triplet signal because of the collapse of RNPs, which is a typical signal of TEMPO derivatives, resulting in interaction between the 14N nuclei and the unpaired electron in the dilute solution. The in vivo half-life of TEMPOL measured by EPR signal was about 15 seconds and its pharmacological effect would disappear within 15 to 30 minutes.[6-9,14,15] On the other hand, the EPR signal of RNPs could be detected even 2 hours after intravenous injection, and the in vivo half-life was 60 times longer (15 min) than that of TEMPOL because of the encapsulation of TEMPO and the inhibition of phagocytosis by the reticuloendothelial system.

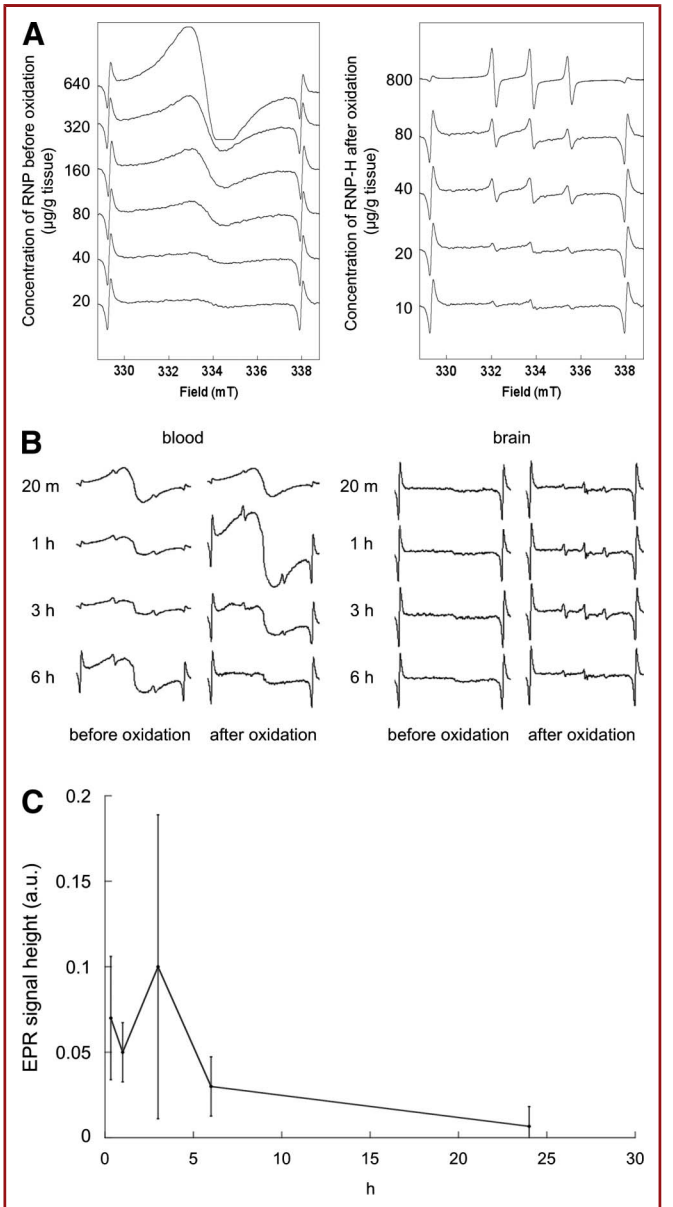

FIGURE 1. **A**, *TEMPO radicals showing broad EPR signals of RNP and triplet. The EPR signals after oxidation of RNP-H using potassium ferricyanide in proportion to the concentration of RNPs and RNP-Hs, respectively.* **B**, *in blood, the broad EPR signals were detected before and after oxidation. On the other hand, in brain, few EPR signals were detected before oxidation, but the triplet EPR signals were detected after oxidation.* **C**, *measurement of the triplet EPR signal height indicating the accumulation of TEMPO radicals for at least 6 hours with the highest peak at 3 hours after the administration of RNPs in the ischemic brain. The spectroscopy settings were: microwave frequency, 9.4133 GHz; microwave power, 7.99 mW; center field, 33.800 mT; field modulation width, 0.1 mT at 100 kHz; sweep time, 0.5 minutes; sweep width, 5.00 mT; time constant, 0.10 second. (a.u., arbitrary unit). TEMPO, 2,2,6,6-tetramethylpiperidine-1-oxyl; RNP, radical-containing nanoparticle; RNP-H, RNP-hydroxylamine; EPR, electron paramagnetic resonance.*

Copyright © Congress of Neurological Surgeons. Unauthorized reproduction of this article is prohibited.

Experimental Protocol

The dose of RNPs used for treatment of the MCAO rats was decided by measuring the 50% lethal dose (LD_{50}). The LD_{50} of RNPs was 600 to 1200 mg/kg, and the dose of RNPs was defined as about one-tenth (90 mg/kg) of the LD_{50}, containing 27.5 mg/kg TEMPO. The dose of TEMPOL contained the same amount of TEMPO included in RNPs (27.5 mg/kg), which is a tolerable dose of TEMPOL in rats according to previous reports.[6,8,16]

The first study was designed to evaluate the delivery of TEMPO radicals contained in RNPs to the ischemic brain tissue and the antioxidant effects on neuronal cells. The accumulated volume of TEMPO radicals in the ischemic brain was estimated from the EPR signal height. The production of superoxide anions in the neuronal cells was evaluated by measuring the fluorescence obtained after incubation of thin coronal brain sections with dihydroethidium.

Our second study was designed to evaluate the neuroprotective effects of RNPs in rats subjected to transient MCAO. All rats were sacrificed 24 hours after administration of saline, micelles (not containing TEMPO), TEMPOL, or RNPs. The cerebral infarction volume and neurological deficits were evaluated.

Our final study was designed to assess lipid peroxidation and protein oxidation in the ischemic brain tissue, which were measured in terms of thiobarbituric acid reactive substances (TBARS) and protein carbonyls, respectively.

Transient MCAO Model

Animal experiments were performed after approval from the Institutional Animal Experiment Committee of the University of Tsukuba. Our procedure to induce MCAO has been described previously.[6] Male Sprague-Dawley rats (Charles River, Japan; weight, 280-350 g) were anesthetized with isoflurane (4% induction, 2% maintenance) using an anesthesia machine 400 (Medicare Co., Ltd., Kanagawa, Japan). A 24-gauge cannula was introduced into the right femoral artery to monitor the factors (Table; see Figure 4). After the external and common carotid arteries were ligated, a small incision was made in the common carotid artery. A 4-0 nylon suture with a silicone-coated tip was inserted into the internal carotid artery through the common carotid artery until resistance could be felt. The cerebral blood flow (CBF) was measured at a point 2 mm rostral and 1 mm lateral from the bregma using laser Doppler (Advance Co, Ltd, Tokyo, Japan) for 30 seconds, after the laser Doppler probe was attached on the surface of cranium for 30 seconds to stabilize CBF data. We confirmed a 60 to 80% reduction of CBF after MCAO. There is no significant difference in CBF reduction rate among the saline group (68.8% reduction), TEMPOL group (69.2% reduction), and RNP group (72.0% reduction). After occlusion for 1 hour, reperfusion was accomplished by withdrawal of the suture to allow reperfusion through the circle of Willis, and drugs were administered into the right femoral vein 30 minutes after reperfusion. The arterial blood pressure was monitored using UB-103U (Unique Medical Co Ltd, Tokyo, Japan), and arterial blood gas was analyzed by iSTAT (Fuso Pharmaceutical Industries, Ltd, Japan). Body temperature was maintained at 37°C with the use of a heating pad.

EPR Signal Detection of TEMPO Radicals in the Ischemic Brain Tissue

First, the detectable threshold for TEMPO radicals contained in RNPs when using EPR spectrometry was examined in vitro. The EPR signal of TEMPO radicals was measured before oxidation of RNP and after oxidation of RNP-hydroxylamine (RNP-H) using potassium ferricyanide.[13] RNP-Hs were prepared because most TEMPO radicals contained in RNPs were reduced to EPR-silent TEMPO-H in the process of scavenging free radicals in the ischemic brain. EPR of TEMPO radicals contained in RNPs was measured after 10 μL of RNPs was added to 200 mg of homogenized rat liver in various concentrations (20, 40, 80, 160, 320, 640 μg/g tissue). The reaction mixture was then put into a flat quartz cell and placed at the center of the cavity of the X-band EPR spectrometer.[17] EPR of TEMPO radicals contained in RNP-Hs was measured after 10 μL of RNP-Hs was added to 200 mg of homogenized rat livers, followed by 10 μL of 200 mM potassium ferricyanide at different concentrations (10, 20, 40, 80, 800 μg/g tissue). It was confirmed that EPR of TEMPO radicals contained in RNPs and RNP-Hs were equally reproduced by homogenized rat brain at some concentrations of RNPs and RNP-Hs. The amount of TEMPO radicals accumulated in the tissue was estimated by measuring the EPR signal height.

Second, rats with MCAO were sacrificed 20 minutes, 1 hour, 3 hours, 6 hours, and 24 hours after intravenous administration of RNPs (each, n = 3), following collection of blood and perfusion through the left ventricle with phosphate-buffered saline to drain RNPs from blood. Blood was centrifuged at 2000 rpm for 5 minutes and the brain was homogenized. The EPR signal of 200 mg of blood plasma and homogenized brain was measured before oxidation and after oxidation using 200 μL of 200 mM potassium ferricyanide and an X-band EPR spectrometer. The time course of TEMPO radical accumulation in the ischemic brain was estimated by measuring the EPR signal height.

TABLE. Physiological Parameters During the Operations[a]

	Saline, n = 8	Micelle, n = 8	TEMPOL, n = 20	RNP, n = 20	
Body weight, g	315.6 ± 16.5	309.7 ± 26.9	320.0 ± 19.9	322.7 ± 20	NS
MABP, mm Hg	101.6 ± 13.4	104.8 ± 6.2	104.0 ± 5.6	105.4 ± 5.1	NS
pH	7.43 ± 0.02	7.40 ± 0.04	7.41 ± 0.04	7.41 ± 0.04	NS
P_{CO_2}, mm Hg	45.9 ± 5.4	43.2 ± 2.2	42.2 ± 4.4	44.0 ± 5.8	NS
P_{O_2}, mm Hg	78.8 ± 8.8	75.8 ± 4.8	78.1 ± 7.8	79.2 ± 12.6	NS
Body temperature	36.9 ± 0.7	36.6 ± 0.3	36.7 ± 0.3	36.7 ± 0.4	NS

[a]MABP, mean arterial blood pressure, NS, not significant; RNP, radical-containing nanoparticle; TEMPOL, 4-hydroxy-2,2,6,6-tetramethylpiperidine-1-oxyl.

Copyright © Congress of Neurological Surgeons. Unauthorized reproduction of this article is prohibited.

Detection of Superoxide Anion Produced in Neuronal Cells

Rats with MCAO were sacrificed 3 hours after the administration of drugs (saline n = 4, TEMPOL n = 4, and RNP n = 4). The brains were removed after perfusion through the left ventricle with phosphate-buffered saline. Two-millimeter coronal brain sections were embedded into Tissue-Tek O.C.T compound (Sakura Finetek Japan, Co, Ltd, Japan), and 8-μm sections were prepared. The slides were incubated with 10 μmol/L dihydroethidium (Invitrogen) for 30 minutes at 37°C in a humidified chamber protected from light. Upon reaction with the superoxide anion, dihydroethidium is oxidized to ethidium bromide, which binds to DNA in the nucleus and emits red fluorescence.[18] After incubation with dihydroethidium, slides were treated with anti-NeuN (mouse monoclonal, dilution 1:500, Chemicon) applied as the primary antibody. Alexa Fluor 488 mouse IgG (Molecular Probes) was used as the secondary antibody. Using a fluorescence microscope (Biozero BZ-8000, Keyence, Japan), red fluorescence emitted from ethidium bromide was detected with excitation at 540 nm and emission at 605 nm, and green fluorescence emitted from Alexa Fluor 488 was detected with excitation at 470 nm and emission at 535 nm.

Regions of interest were placed on the ischemic core in the cerebral cortex and striatum. The intensity of red fluorescence was measured using a VH analyzer VH-H1A5 (Keyence), and the data showed the ratio of the intensity in the ipsilateral cortex and striatum to that in the contralateral cortex and striatum, respectively.

Treatment of Cerebral Infarction Using RNPs

Rats with MCAO were treated with saline (n = 8), micelles (not containing TEMPO, n = 8), TEMPOL (n = 20), or RNPs (n = 20) 30 minutes after reperfusion through the femoral vein. All rats were euthanized 24 hours after administration of the drugs. Two-millimeter coronal brain sections were immersed in 2% 2,3,5-triphenyltetrazolium chloride (Sigma Aldrich, Japan) at 37°C for 30 minutes, and the infarct volume was quantified using NIH image analysis software. The neurological symptoms were scored before and 24 hours after the administration of the drugs according to the following criteria: 0, rats extend both forelimbs straight, no observable deficit; 1, rats attach the left forelimb to the breast and extend the right forelimb straight; 2, rats decrease resistance to lateral push in addition to the behavior described in score 1; 3, rats twist the upper half of their body in addition to the behavior described in score 2.

Measurement of TBARS

Rats with MCAO were sacrificed 3 hours after the administration of drugs (saline n = 7, TEMPOL n = 7, and RNP n = 7). The third coronal brain sections were frozen and stored at −80°C until assayed. Lipid peroxidation was determined by measuring TBARS, which were generated by the reaction between thiobarbituric acid and lipid peroxides.[6] In brief, 10% homogenated brain tissues mixed with cold 1.15% potassium chloride were centrifuged. Ten microliters of 0.01% butylated hydroxytoluene (Wako Pure Chemical Industries, Osaka, Japan) was added to the supernatant (0.2 mL) to prevent auto-oxidation. Then, 0.2 mL of 8.1% sodium lauryl sulfate, 1.5 mL of 20% acetic acid buffer (pH 3.5), and 1.5 mL of 0.8% thiobarbituric acid (Sigma Aldrich, St Louis, Missouri) were added into the samples. The mixture was boiled for 1 hour at 95°C and rapidly cooled to 25°C. The absorbance was measured using a spectrophotometer (Mithral LB 940, Berthold Japan) at 530 nm and compared with the standard using 0.2 mL of 1,3,3-tetramethoxypropane (Wako Pure Chemical Industries, Osaka, Japan).

Measurement of Protein Carbonyls

Rats with transient MCAO were sacrificed 24 hours after the administration of drugs (saline n = 5, TEMPOL n = 6, and RNP n = 6). The fourth coronal brain sections were preserved at −80°C for analysis of carbonyl protein. Carbonyl protein was measured as an indicator of oxidative protein damage using a Protein Carbonyl Enzyme Immuno-Assay Kit (BioCell Co, Ltd, New Zealand).

Statistical Analysis

All values are expressed as the mean ± standard deviation (SD). Continuous data between groups were compared using 1-factor ANOVA, and the nonparametric data were compared using a Mann-Whitney U test. Differences with a value of $P < .05$ were considered statistically significant.

RESULTS

Delivery of RNP-Encapsulated TEMPO Radicals to the Ischemic Brain

The EPR signals of TEMPO radicals contained in RNPs were detected as broad signals because interaction among radicals was limited due to the encapsulation into nanoparticles. The EPR signals of TEMPO radicals contained within RNP-Hs were detected as triplet signals after oxidation using potassium ferricyanide, because interaction among radicals is unlimited due to the collapse of RNP-Hs.[13] The height of broad or triplet signals increased in proportion to the concentration of RNPs and RNP-Hs. The detectable threshold of TEMPO radicals contained in RNPs and RNP-Hs was estimated at 20 μg/g tissue and 10 μg/g tissue, respectively (Figure 1A).

In the in vivo study, EPR measurements of blood showed broad signals before and after oxidation, because RNPs were not near collapse in blood. On the other hand, in EPR measurements of brain, EPR signals before oxidation were barely detected. However, after oxidation, the EPR signals were detected as triplets, indicating that the RNPs had collapsed and had been reduced via scavenging free radicals produced in the ischemic brain (Figure 1B). The time course of the EPR signal height showed that TEMPO radicals were detected for 6 hours, with the highest peak at 3 hours, in the ischemic brain tissue after intravenous administration of RNPs (Figure 1C). The delivered and accumulated RNP concentration in the brain was estimated to be about 25 μg/g and 10 μg/g tissue at 3 hours and 6 hours after 90 mg/kg of RNPs including 27.5 mg/kg of TEMPO was administered. They contained about 8 μg/g and 3 μg/g of TEMPO radicals, respectively.

Antioxidant Effect on Superoxide Anions Produced in the Neuronal Cells

Immunofluorescent analysis showed that most cells with red fluorescence, emitted by ethidium bromide, showed good

Copyright © Congress of Neurological Surgeons. Unauthorized reproduction of this article is prohibited.

colocalization with neuronal cells, which were identified by green fluorescence emitted from Alexa Fluor 488, in the ischemic core of the cerebral cortex and striatum (Figure 2A to 2C). In addition, the fluorescence intensity of dihydroethidium in sections from the brains treated with RNPs was significantly lower than that of sections from the brains treated with saline ($P < .05$) or TEMPOL ($P < .05$) (Figure 2D and 2E). These results indicate that RNPs can scavenge superoxide anions produced in the neuronal cells.

Evaluation of the Treatment With RNPs

RNPs, TEMPOL, micelles, or saline were administered to the rats with 1-hour MCAO 30 minutes after reperfusion through the femoral vein and were euthanized 24 hours after administration of the drugs. The 4 rats were excluded from the experiments. Two rats died before euthanasia because of strong brain edema by the infarction; these rats belonged to the groups treated with saline (n = 1) and TEMPOL (n = 1). Another had respiratory acidosis and another had contralateral cerebral infarct lesion.

The infarction volume in the RNP group was significantly smaller than that in the saline ($P < .01$), micelle ($P < .05$), or TEMPOL ($P < .05$) groups (Figure 3A and 3B). These values were 79.4 ± 69.9 mm^3 in the RNP group, 166.9 ± 82.5 mm^3 in the saline group, 148.9 ± 100.8 mm^3 in the micelle group, and 126.6 ± 74.2 mm^3 in the TEMPOL group. The reduction ratios of the infarction volume were $52.4 \pm 41.9\%$ in the RNP group ($P < .01$), $10.7 \pm 60.4\%$ in the micelle group (not significant), and $24.1 \pm 44.5\%$ in the TEMPOL group (not significant) compared with the infarction volume in the saline group as the control. The RNP group showed significantly lower neurological symptom scores than the saline, micelle, or TEMPOL groups ($P < .05$, $P < .01$, and $P < .05$, respectively) (Figure 3C). The level of TBARS in the RNP group was significantly lower than that in the saline group ($P < .05$) (Figure 3D). The production of protein carbonyls was significantly reduced in the RNP group compared with the saline group ($P < .05$) (Figure 3E).

Physiological Parameters

There were no significant differences in physiological parameters such as body weight, mean arterial pressure, pH, Po_2, Pco_2, or rectal temperature when comparing the saline, micelle, TEMPOL, and RNP groups during the operations (Table). However, the mean arterial blood pressure, monitored for 5 minutes after the administration of the drugs, was significantly reduced in the TEMPOL group (n = 20, -6.6 mm Hg) compared with the saline (n = 8, +0.35 mm Hg, $P < .01$), micelle (n = 8, +0.24 mm Hg, $P < .01$), or RNP (n = 20, -1.3 mm Hg, $P < .001$) groups, presented as the change of blood pressure (Figure 4). The mean arterial blood pressure of RNP did not show significant difference compared with that of saline and micelle.

DISCUSSION

RNPs decreased the cerebral infarction volume and improved neurological deficits in a rat transient MCAO model. The nanoparticles delivered TEMPO radicals to the ischemic brain, allowing the radicals to act as neuroprotective agents in ischemia-reperfusion injury.

Nitroxyl radicals are a notable free-radical scavenger. It was known that the antioxidant effects of nitroxyl radicals act catalytically by redox transformation to oxoammonium cation and hydroxylamine, and recently the neuroprotective effects were reported.[9] However, the short in vivo half-life and marked toxicity make it difficult to apply TEMPOL to neuroprotective therapy. TEMPOL could induce hypotension due to the increase in bioavailable nitric oxide (NO) and the vasodilatation,[11] which was a seriously adverse event in the cerebral ischemia. RNP could prevent the hypotension after administration by the encapsulation of TEMPO radicals. The other toxicity, eg, body weight loss, was examined preliminary before the protocol of this experiment. The body weight of mice were lost 4.0% and 1.6% from the baseline 24 hours after administration of TEMPOL and RNP, respectively, but were recovered in both mice 2 days after administration. The toxicity of RNP was less than TEMPOL, and not recognized for the longer duration after administration.

Drug delivery systems using nanoparticles have been advanced as molecular targeting therapies. RNPs are unique free-radical scavengers consisting of a pH-sensitive core-shell-type micelle containing amino-TEMPO with 60-fold prolongation of the in vivo half-life of TEMPO radicals due to the encapsulation of TEMPO and the inhibition of phagocytosis by the reticuloendothelial system.[12,13] RNPs might have some advantages in the distribution to the ischemic brain because of pH sensitivity and the releasing profile of agents to scavenge ROS, compared with other treatment systems using nanoparticles.[19] The delivered and accumulated RNP concentration in the brain was estimated to be about 25 μg/g and 10 μg/g tissue at 3 hours and 6 hours, containing about 8 μg/g and 3 μg/g TEMPO radicals, respectively. This concentration of TEMPO radicals may be reasonable for scavenging free radicals and ameliorating oxidative brain injury, because a plasma concentration of 8.5 to 17.2 μg/g TEMPOL was sufficient for the treatment of myocardial infarction.[20] Furthermore, RNPs limited hypotension via the encapsulation of amino-TEMPO.

The molecular mechanism of neuroprotection was investigated. We speculated that RNPs would gain access to the cerebral parenchyma by crossing the blood-brain barrier (BBB) and prevent the oxidative damage. BBB is an interface between the blood and the brain. However, BBB can be disrupted by ischemic injury, resulting in increasing permeability.[21,22] Nanoparticles 40 to 60 nm in diameter would pass through BBB and leak into the extravascular space of the cerebral parenchyma. Yoshitomi et al[13] reported that RNPs started to disintegrate at the acid conditions of pH 6 to 7 and formed polymers. The differences in the EPR signals between blood

Copyright © Congress of Neurological Surgeons. Unauthorized reproduction of this article is prohibited.

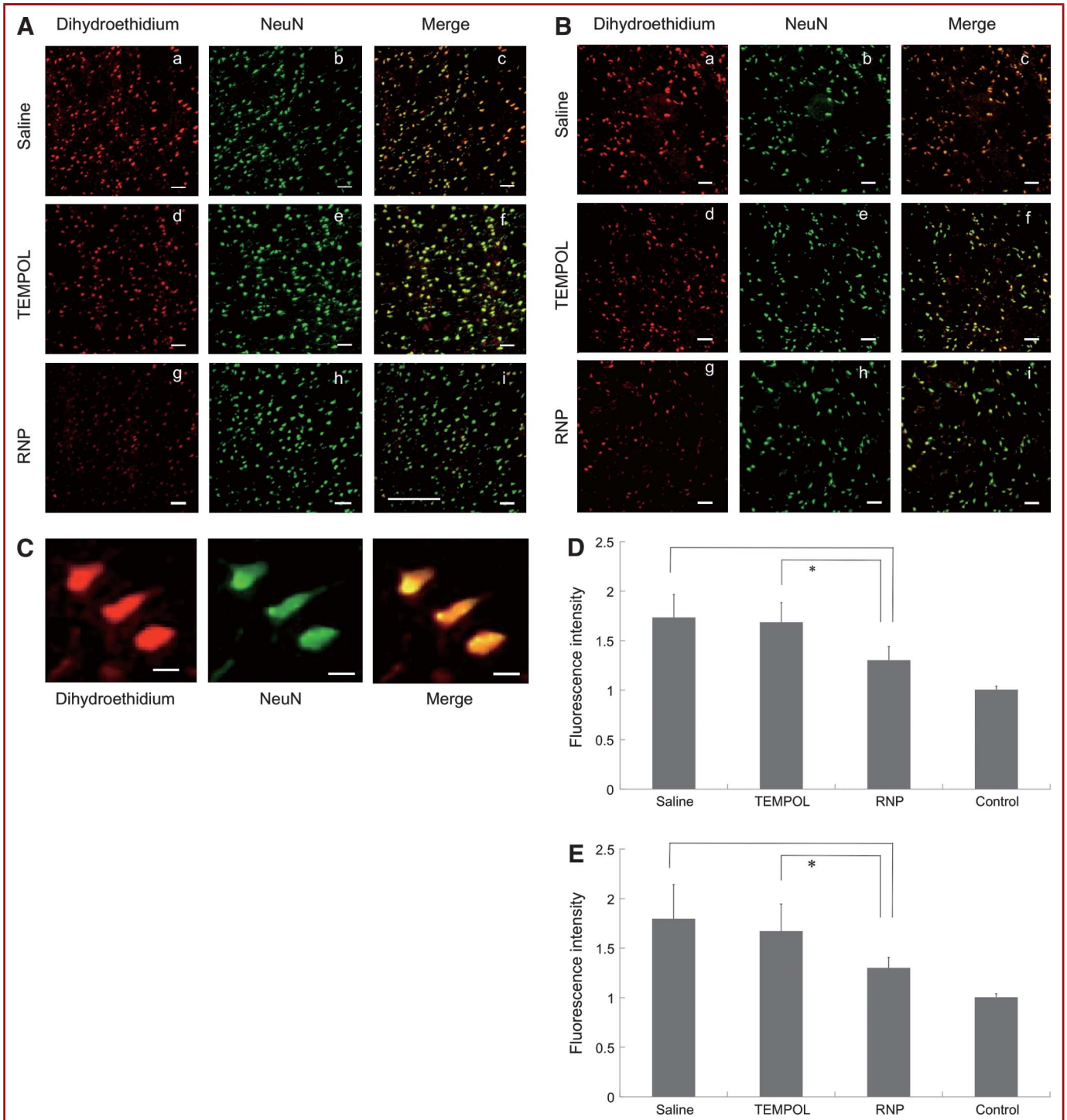

FIGURE 2. *Immunofluorescent analysis showing that dihydroethidium-positive cells with red fluorescence were detected more in the saline (n = 4) and TEMPOL (n = 4) groups than in the RNP (n = 4) group (a, d, g) in the ischemic core of the cerebral cortex (A) and the striatum (B). Merged image (c, f, i) showing that most cells with red fluorescence colocalized with anti-NeuN-positive cells with green fluorescence (b, e, h, C). Scale bar =50 μm (for A, B, and C). Bar graph showing the intensity of red fluorescence in the ischemic core of the cerebral cortex (D) and the striatum (E). The control group was prepared using anesthetized rats, but there were no MCAO nor infused drugs. *P < .05. TEMPOL, 4-hydroxy-2,2,6,6-tetramethylpiperidine-1-oxyls; RNP, radical-containing nanoparticle; MCAO, middle cerebral artery occlusion.*

Copyright © Congress of Neurological Surgeons. Unauthorized reproduction of this article is prohibited.

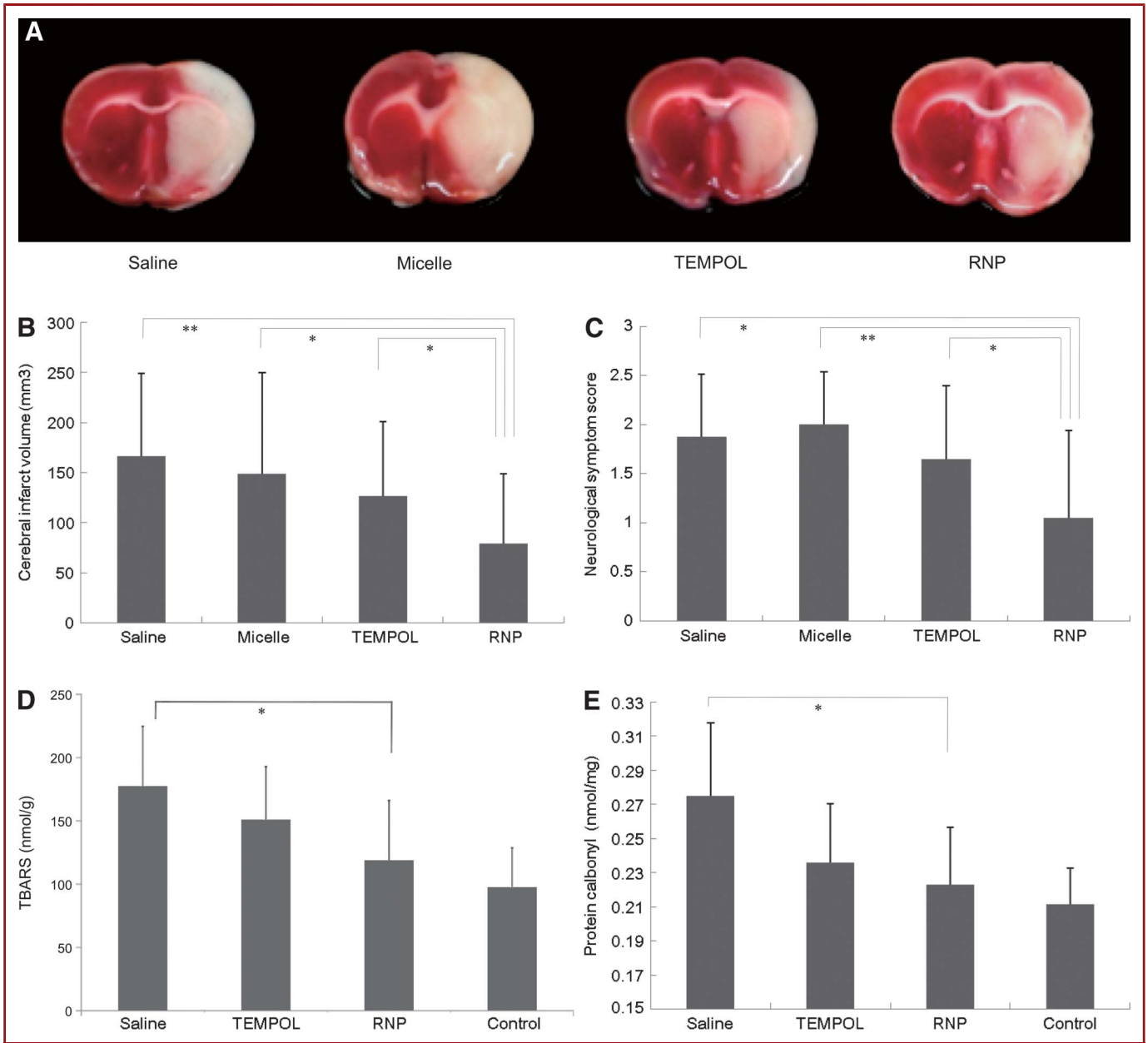

FIGURE 3. **A**, *photographs of coronal brain sections showing infarct area (white area) stained by 2,3,5-triphenyltetrazolium chloride in each group. Bar graph showing the cerebral infarct volumes (saline n = 8, micelle n = 8, TEMPOL n = 20, RNP n = 20) (***B***), the neurological symptom score (saline n = 8, micelle n = 8, TEMPOL n = 20, RNP n = 20) (***C***), the level of TBARS (saline n = 7, TEMPOL n = 7, RNP n = 7, control n = 7) (***D***), and protein carbonyls (saline n = 5, TEMPOL n = 6, RNP n = 6, control n = 3) (***E***). The control group consisted of brains of rats without transient MCAO or infused drugs. *P < .05, **P < .01. TEMPOL, 4-hydroxy-2,2,6,6-tetramethylpiperidine-1-oxyls; RNP, radical-containing nanoparticle; TBARS, thiobarbituric acid reactive substances; MCAO, middle cerebral artery occlusion.*

and brain tissue would indicate the collapse of RNPs responsive to low pH conditions in the ischemic tissue. This collapse of RNPs may enhance the leakage of TEMPO radicals to the extravascular space via BBB.

RNPs are promising, offering more effective neuroprotection than conventional free-radical scavengers such as TEMPOL or PBN. Therefore, RNPs may be a useful treatment for the ischemic heart and vascular diseases as well as ischemic stroke.

Disclosure

This work was partly supported by Grant-in-Aid for Scientific Research (A), No.21240050, and Scientific Research (C), No. 20591700, The Ministry of

Copyright © Congress of Neurological Surgeons. Unauthorized reproduction of this article is prohibited.

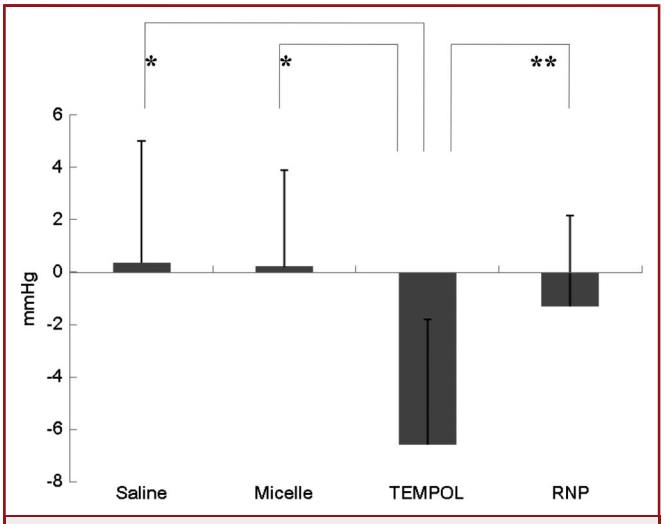

FIGURE 4. *Bar graph showing the change in blood pressure for 5 minutes after the administration of drugs. The acute blood pressure reduction seen in the TEMPOL group was significantly prevented in the RNP group (saline n = 8, micelle n = 8, TEMPOL n = 20, RNP n = 20). *P < .01, **P < .001. TEMPOL, 4-hydroxy-2,2,6,6-tetramethylpiperidine-1-oxyls; RNP, radical-containing nanoparticle.*

Education, Culture, Sports, Science, and Technology-Japan (MEXT). The authors have no personal financial or institutional interest in any of the drugs, materials, or devices described in this article.

REFERENCES

1. Hacke W, Donnan G, Fieschi C, et al. ATLANTIS Trials Investigators; ECASS Trials Investigators; NINDS rt-PA Study Group Investigators. Association of outcome with early stroke treatment: pooled analysis of ATLANTIS, ECASS, and NINDS rt-PA stroke trials. *Lancet*. 2004;363(9411):768-774.
2. The National Institute of Neurological Disorders and Stroke rt-PA Stroke Study Group. Tissue plasminogen activator for acute ischemic stroke. *N Engl J Med*. 1995;333(24):1581-1587.
3. Hermann DM, Matter CM. Tissue plasminogen activator-induced reperfusion injury after stroke revisited. *Circulation*. 2007;116(4):363-365.
4. Toledo-Pereyra LH, Lopez-Neblina F, Toledo AH. Reactive oxygen species and molecular biology of ischemia/reperfusion. *Ann Transplant*. 2004;9(1):81-83.
5. Folbergrová J, Zhao Q, Katsura K, Siesjö BK. N-tert-butyl-alpha-phenylnitrone improves recovery of brain energy state in rats following transient focal ischemia. *Proc Natl Acad Sci USA*. 1995;92(11):5057-5061.
6. Kato N, Yanaka K, Hyodo K, Homma K, Nagase S, Nose T. Stable nitroxide Tempol ameliorates brain injury by inhibiting lipid peroxidation in a rat model of transient focal cerebral ischemia. *Brain Res*. 2003;979(1-2):188-193.
7. Leker RR, Teichner A, Lavie G, Shohami E, Lamensdorf I, Ovadia H. The nitroxide antioxidant tempol is cerebroprotective against focal cerebral ischemia in spontaneously hypertensive rats. *Exp Neurol*. 2002;176(2):355-363.
8. Rak R, Chao DL, Pluta RM, Mitchell JB, Oldfield EH, Watson JC. Neuroprotection by the stable nitroxide Tempol during reperfusion in a rat model of transient focal ischemia. *J Neurosurg*. 2000;92(4):646-651.
9. Soule BP, Hyodo F, Matsumoto K, et al. The chemistry and biology of nitroxide compounds. *Free Radic Biol Med*. 2007;42(11):1632-1650.
10. Ankel EG, Lai CS, Hopwood LE, Zivkovic Z. Cytotoxicity of commonly used nitroxide radical spin probes. *Life Sci*. 1987;40:495-498.
11. Hahn SM, Sullivan FJ, DeLuca AM, et al. Hemodynamic effect of the nitroxide superoxide dismutase mimics. *Free Radic Biol Med*. 1999;27(5-6):529-535.
12. Yoshitomi T, Miyamoto D, Nagasaki Y. Design of core-shell-type nanoparticles carrying stable radicals in the core. *Biomacromolecules*. 2009;20:1792–1798.
13. Yoshitomi T, Suzuki R, Mamiya T, Matsui H, Hirayama A, Nagasaki Y. pH-sensitive radical-containing-nanoparticle (RNP) for the L-band-EPR imaging of low pH circumstances. *Bioconjugete Chemistry*. 2009;10:596-601.
14. Hahn SM, DeLuca AM, Coffin D, Krishna CM, Mitchell JB. In vivo radioprotection and effects on blood pressure of the stable free radical nitroxides. *Int J Radiat Oncol Biol Phys*. 1998;42(4):839-842.
15. Kuppusamy P, Wang P, Zweier JL, et al. Electron paramagnetic resonance imaging of rat heart with nitroxide and polynitroxyl-albumin. *Biochemistry*. 1996;35(22):7051-7057.
16. Cuzzocrea S, McDonald MC, Mazzon E, et al. Effects of tempol, a membrane-permeable radical scavenger, in a gerbil model of brain injury. *Brain Res*. 2000;875(1-2):96-106.
17. Ueda A, Nagase S, Yokoyama H, et al. Importance of renal mitochondria in the reduction of TEMPOL, a nitroxide radical. *Mol Cell Biochem*. 2003;244(1-2):119-124.
18. Shichinohe H, Kuroda S, Yasuda H, et al. Neuroprotective effects of the free radical scavenger Edaravone (MCI-186) in mice permanent focal brain ischemia. *Brain Res*. 2004;1029(2):200-206.
19. Reddy MK, Labhasetwar V. Nanoparticle-mediated delivery of superoxide dismutase to the brain: an effective strategy to reduce ischemia-reperfusion injury. *FASEB J*. 2009;23(5):1384-1395.
20. Li H, Ma L, Hsia CJ, Zweier JL, Kuppusamy P. Polynitroxyl-albumin (PNA) enhances myocardial infarction therapeutic effect of tempol in rat hearts subjected to regional ischemia-reperfusion. *Free Radic Biol Med*. 2002;32(8):712-719.
21. Belayev L, Busto R, Zhao W, Ginsberg MD. Quantitative evaluation of blood-brain barrier permeability following middle cerebral artery occlusion in rats. *Brain Res*. 1996;739(1-2):88-96.
22. Grillon E, Provent P, Montigon O, Segebarth C, Rémy C, Barbier EL. Blood-brain barrier permeability to manganese and to Gd-DOTA in a rat model of transient cerebral ischaemia. *NMR Biomed*. 2008;21(5):427-436.

Acknowledgments

We would like to thank Yoshiko Tsukada and Makiko Miyakawa (Graduate School of Comprehensive Human Sciences, University of Tsukuba) for their technical assistance.

COMMENTS

Marushima and colleagues performed a rigorous and well executed investigation into a novel nanoparticle-based approach for enhancing the neuroprotection afforded by the antioxidant TEMPO. They convincingly show that TEMPO packaged within a nanoparticle provides several advantages compared with standard Tempol therapy, including prolonged half-life of the active agent, reduced treatment-induced hypotension, improved free-radical scavenging, and greater degrees of neuroprotection. Though this is an exciting result and certainly deserves further investigation (eg, dose-finding studies, therapeutic window of opportunity studies, and validation studies in larger animal models of ischemic stroke), this result must be placed into the broader context of the multitude of failed neuroprotective drug trials that have been completed to date – a sobering history that raises the question whether any neuroprotective strategy will ultimately show efficacy in human ischemic stroke.

Gregory Joseph Zipfel
St. Louis, Missouri

The authors propose that a novel core-shell-type nanoparticle construct composed of a micelle shell containing a free-radical scavenger 2,2,6,6-tetramethylpiperidine-1-oxyl (TEMPO) can be utilized to deliver this or in vivo other antioxidant agents across the blood-brain barrier to reduce the lesion volume of cerebral infarction after middle

Copyright © Congress of Neurological Surgeons. Unauthorized reproduction of this article is prohibited.

cerebral artery occlusion in a rat model. They state that the difficulty with the delivery of the antioxidant agent alone has unacceptable toxicity at systemic dosages as well as potentially complicating hypotensive effects. Furthermore, the nanoparticle design allows delivery of the core at lower pH which can also be useful in cerebral tissue undergoing ischemic response.

It is certainly an important article in that adding a delivery system that is specific for crossing the BBB would be ideal in cerebral tissue at risk for ischemia and reperfusion injury. The idea of a delivery agent, or the radical-containing nanoparticle (RNP), while not entirely novel is certainly an original application of this technology for the delivery of a potentially toxic agent. It has the potential for widespread application not only in cerebral infarction, but also myocardial or other tissue at risk for reperfusion injury.

The MCAO model utilized in this study, despite having many limitations, has been well established for ischemic injury to the brain. Its role in reperfusion injury is less studied. The data showing neuroprotection in terms of reduced lesion size and behavioral outcome are certainly remarkable. The evidence would be more compelling if the authors would give additional data on neuronal or glial survival in terms of cell density or total cell number, but presumably this will be a future area of research for the investigators.

Arash Farahvar
G. Edward Vates
Rochester, New York

The authors investigate the feasibility and efficacy of delivering a nitroxyl radical containing nanoparticle (RNP) to an area of ischemia following reperfused stroke in rodents. The TEMPO radicals contained in the RNPs were detected for 6 hours after intravenous administration and were noted to significantly reduce neuronal superoxide anion production. Infarct volumes were significantly less and neurological scores more favorable in the treated animals compared with the control cohort. The investigators utilize a novel and intriguing delivery mechanism in conjunction with a treatment concept that has previously demonstrated significant promise in preclinical testing. They perform well-conducted experiments to demonstrate the physiologic properties, delivery mechanism, antioxidant effects, and treatment efficacy of the RNPs. Post-reperfusion dosing suggests the possibility of administration at a clinically relevant time point. I look forward to future studies from this group addressing the optimal dose and time window for treatment. It would also be helpful to determine whether treatment effect persists at a prolonged follow-up. Most encouraging is that this vehicle may lend to a host of treatment strategies that would be otherwise difficult to administer because of varying structural and biochemical restrictions.

William J. Mack
Los Angeles, California

eTOCS ALERTS

Receive Neurosurgery Tables of Contents automatically via email.

1. At the Neurosurgery Online home page (*http://www.neurosurgery-online.com*), click Login. If you have not yet registered, you will be prompted to do so.

2. Click on the eTOCs link in the top-right navigation menu.

3. You can manage your subscription to Neurosurgery eTOCs and add other LWW titles in the eTOCs and Alerts tab of your account information.

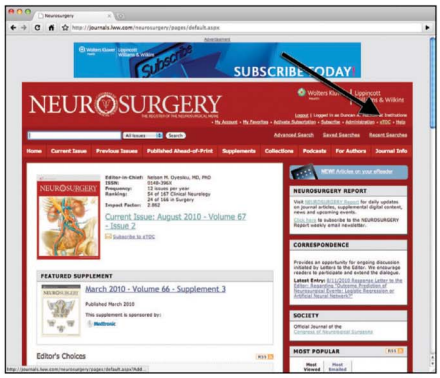

Scan the QR Code to access video tutorial

NEUROSURGERY
THE REGISTER OF THE NEUROSURGICAL MEME

Copyright © Congress of Neurological Surgeons. Unauthorized reproduction of this article is prohibited.

Robotic Digital Subtraction Angiography Systems Within the Hybrid Operating Room

Yuichi Murayama, MD
Koreaki Irie, MD
Takayuki Saguchi, MD
Toshihiro Ishibashi, MD
Masaki Ebara, MD
Hiroyasu Nagashima, MD
Akira Isoshima, MD
Hideki Arakawa, MD
Hiroyuki Takao, MD
Hiroki Ohashi, MD
Tatsuhiro Joki, MD
Masataka Kato, MD
Satoshi Tani, MD
Satoshi Ikeuchi, MD
Toshiaki Abe, MD

Division of Endovascular Neurosurgery, Department of Neurosurgery, Jikei University School of Medicine, Tokyo, Japan

Correspondence:
Yuichi Murayama, MD,
Division of Endovascular Neurosurgery,
Department of Neurosurgery,
Jikei University School of Medicine,
3-25-8 Nishi-Shinbashi, Minato-ku,
Tokyo, Japan.
E-mail: ymurayama@jikei.ac.jp

Received, February 3, 2010.
Accepted, October 1, 2010.

Copyright © 2011 by the
Congress of Neurological Surgeons

BACKGROUND: Fully equipped high-end digital subtraction angiography (DSA) within the operating room (OR) environment has emerged as a new trend in the fields of neurosurgery and vascular surgery.

OBJECTIVE: To describe initial clinical experience with a robotic DSA system in the hybrid OR.

METHODS: A newly designed robotic DSA system (Artis zeego; Siemens AG, Forchheim, Germany) was installed in the hybrid OR. The system consists of a multiaxis robotic C arm and surgical OR table. In addition to conventional neuroendovascular procedures, the system was used as an intraoperative imaging tool for various neurosurgical procedures such as aneurysm clipping and spine instrumentation.

RESULTS: Five hundred one neurosurgical procedures were successfully conducted in the hybrid OR with the robotic DSA. During surgical procedures such as aneurysm clipping and arteriovenous fistula treatment, intraoperative 2-/3-dimensional angiography and C-arm-based computed tomographic images (DynaCT) were easily performed without moving the OR table. Newly developed virtual navigation software (syngo iGuide; Siemens AG) can be used in frameless navigation and in access to deep-seated intracranial lesions or needle placement.

CONCLUSION: This newly developed robotic DSA system provides safe and precise treatment in the fields of endovascular treatment and neurosurgery.

KEY WORDS: Endovascular therapy, Cerebrovascular surgery, Digital subtraction angiography, Operating room, Spine surgery

Neurosurgery 68:1427–1433, 2011 DOI: 10.1227/NEU.0b013e31820b4f1c www.neurosurgery-online.com

Over the last few years, fully equipped high-end digital subtraction angiography (DSA) within the operating room (OR) environment has emerged as a new trend in the fields of neurosurgery and vascular surgery.[1-5] Recent improvements seen with OR-capable DSA systems provide the ability to conduct complex combined endovascular and surgical procedures in a single session.[6,7] Traditionally, these DSA systems were not developed for the OR environment. Therefore, a new technical breakthrough was necessary to overcome current limitations and to expand operative technical capabilities.

The new concept, the implementation of industrial robot technology in angiography systems, provides surgeons with a totally new image-guided surgery in the OR environment. We report our initial experience with the robotic DSA system in the hybrid OR.

ABBREVIATION: **DSA,** digital subtraction angiography

PATIENTS AND METHODS

A newly designed robotic DSA system (Artis zeego; Siemens AG, Forchheim, Germany) was installed in one of our endovascular ORs. The system consists of a multiaxis robotic C arm and surgical OR table (Figure 1). The system allows flexibility in the working position because of its 8-axis design.

The intelligent controller unit of the system allows accurate movement and positioning around the patient, and the rotational data acquisition of up to 220° around the patient at 60°/s provides high-quality imaging data. The multiple parking positions allow neurosurgeons to have more working space during surgery. If the imaging system is not being used, it can be retracted to minimize the parking space required or

Copyright © Congress of Neurological Surgeons. Unauthorized reproduction of this article is prohibited.

FIGURE 1. *Hybrid endovascular operating room comprising the robotic digital subtraction angiography system with multipurpose surgical capabilities.*

even moved to a ceiling park position. This is a highly significant feature, particularly in multipurpose operating rooms. Intraoperative or postoperative angiography and soft-tissue C-arm–based computed tomography (CT) imaging (syngo DynaCT; Siemens AG) can be directly performed with the patient in the surgical position.

In addition to the unique multiaxis robotic C arm, new technologies have been developed for the Robotic DSA system.

Large-Volume DynaCT

DynaCT has the benefit of creating soft-tissue cross-sectional images using the C arm immediately without the need to move the patient.[8] This imaging method enables real-time information to be obtained during and after neurosurgical procedures. The new unique large-volume DynaCT enables the physician to visualize large volumes (47-cm diameter × 18-cm height and 35 × 25 cm), providing cross-sectional imaging of the entire abdomen and lumbar spine. An example of its clinical use is surgery for spinal instrumentation or vertebroplasty.

iGuide-Live and Integrated Needle Guidance

iGuide is a newly developed virtual navigation software that can be used in frameless navigation and in access to deep-seated intracranial lesions or needle placement. After the DynaCT acquisition, the target area such as an intracerebral hematoma or dilated ventricle can be identified. Subsequently, a second targeted area such as a burr hole area can be selected.

The smooth on-screen and laser beam-guided workflow allows the surgeon to plan the needle path and to review the path trajectory and provides guidance during needle advancement. The method provides increased accuracy of needle placement and reliable control in procedures such as tumor biopsy, screw placement for spine instrumentation, and ventriculostomy (Figure 2).

iPilot (3-Dimensional Roadmap)

This software enables the identification of the best working angle of imaging during coil embolization of cerebral aneurysms. The difference from conventional 2-dimensional roadmap is that 3-dimensional (3D) rotational angiography acquisition can be superimposed on the 2-dimensional fluoroscopic image as an overlay. When that is done on the live 2-dimensional image, it can even update dynamically during movements of the C arm, table, zoom, and source to image distance changes. The system also allows automatic compensation of patient movements at the touch of a button. This real-time 3D visualization provides additional spatial information when microcatheter navigation is difficult because of complex vascular anatomy. With this advanced technology, placement of the microcatheter tip into a specified target spot can be performed easily.

RESULTS

Between May 2008 and December 2009, 501 neurosurgical procedures were conducted in the hybrid OR with robotic DSA. Conventional endovascular treatment, open surgery, and presurgical cerebral/spinal angiography with or without subsequent surgical procedures were performed successfully with robotic DSA.

Case Example 1

Endovascular Coil Embolization of Ruptured Aneurysm and Subsequent Ventriculostomy With iPilot and iGuide

A 74-year-old woman suffered Hunt and Hess grade 3 subarachnoid hemorrhage; acute hydrocephalus was also detected. Three-dimensional DSA confirmed a multilobular left middle cerebral artery aneurysm.

A 5F femoral sheath was placed before surgery. The sheath was continuously flushed with heparinized saline (1000 U/500 cm^3; 200 cm^3/h). Systemic heparin was administered after first coil placement. After successful coil embolization, ventriculostomy was conducted. With the use of a DynaCT with iGuide guidance, a ventricular drainage tube was placed in the lateral ventricle without difficulty (Figure 3). Postoperative DynaCT confirmed successful placement of the drainage tube.

Case Example 2

Intraoperative Angiography

A 32-year-old woman presented with homonymous hemianopsia, and 3D CT angiography revealed an unruptured complex pial arteriovenous fistula (Figure 4A). The fistula was supplied by the left middle and posterior cerebral artery feeders (Figure 4B). The draining vein was connected to the superior sagittal sinus. Surgical clipping and arteriovenous fistula removal were performed. After placement of a 5F Arrow kink-resistant sheath on the left femoral artery, the sheath was continuously flushed with heparinized saline (1000 U/500 cm^3; 200 cm^3/h). For prone procedures, a specially designed surgical cushion was used to achieve best surgical positioning.

The patient's head was secured in a carbon head clamp system (Figure 4C). The robotic C arm was placed on the ceiling parking position during microsurgery (Figure 4D). A left suboccipital craniotomy was made, and the microsurgical procedure was conducted. After clipping of the feeding arteries, intraoperative angiography was performed. The flexible C arm enabled the best working position to be obtained without moving the patient.

Copyright © Congress of Neurological Surgeons. Unauthorized reproduction of this article is prohibited.

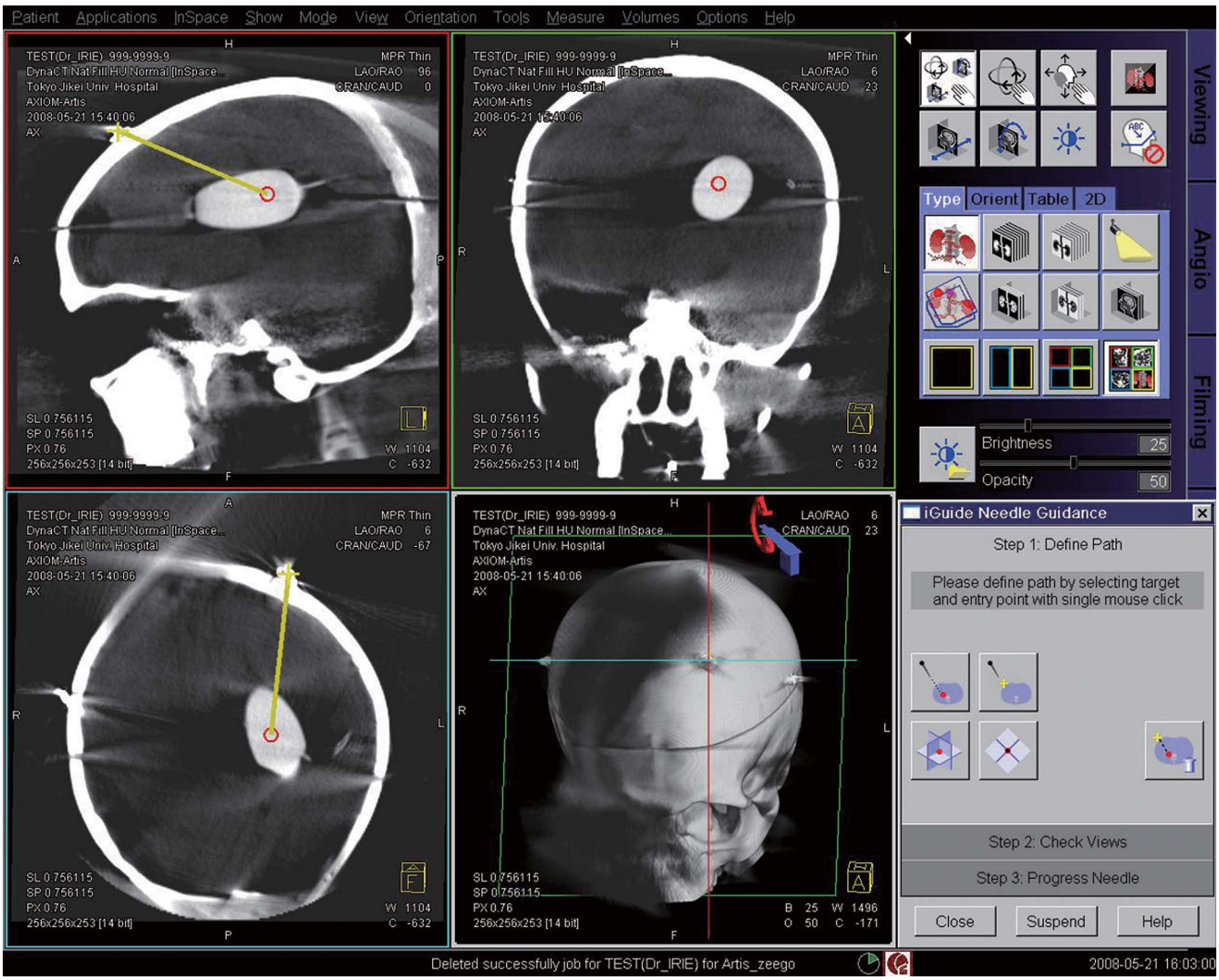

FIGURE 2. *Demonstration of iGuide on a phantom skull model with hematoma. Target area (red dot) and burr hole area (yellow X) are marked on the 3-dimensional workstation (top and bottom left). Vertical needle direction (bull's-eye position) is shown on the lower right. The workstation tells the distance and direction of the needle placement.*

Although left middle cerebral artery feeders were successfully clipped, selective left vertebral artery injection demonstrated residual fistula supplied by a small posterior cerebral artery branch (Figure 4E). Additional microsurgical clipping was conducted, and the final angiogram demonstrated complete obliteration of the fistula (Figure 4F).

Case Example 3

Spine Instrumentation

A 74-year-old woman experienced sudden onset of tetraparesis. Magnetic resonance imaging and CT demonstrated atlano-axial dislocation and instability. The patient was prepped and draped with the prone position. The robotic C arm was placed on the lateral position during microsurgery. C1 lateral mass fixation surgery was successfully conducted under guidance of real-time fluoroscopy and laser beam (iGuide; Figure 5).

DISCUSSION

Since 2003, we have used a modified biplane system in the surgical OR for both endovascular and surgical purposes.[3,8] The system was useful for most surgical clippings or combined treatments. However, this system required rotation of the surgical table from the endovascular position to the surgical position

Copyright © Congress of Neurological Surgeons. Unauthorized reproduction of this article is prohibited.

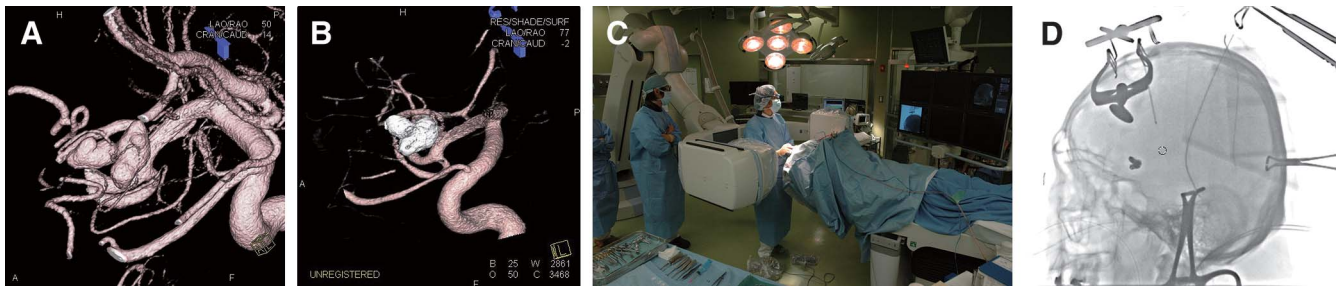

FIGURE 3. *A, pre-embolization 3-dimensional digital subtraction angiography of a multilobular ruptured right middle cerebral artery aneurysm.* **B**, *postembolization angiography of a middle cerebral artery aneurysm.* **C**, *subsequent ventricular drainage using iGuide assistance.* **D**, *live image of ventricular drainage tube placement under iGuide assistance. Target area of tube placement is indicated on the live monitor.*

because of limited OR space and C-arm positioning difficulties. With the installation of the multiaxis robotic DSA system in a surgical setting, procedures can be converted from endovascular treatment to an open surgical procedure without moving the surgical table. This improvement was extremely useful, especially for anesthesiology tubing and draping. The robotic DSA system may be of most interest to vascular and spine neurosurgeons who can perform some interventional neurovascular and spine studies at the time of conventional surgery.

The C arm of the robotic DSA system rotates around the patient at a high velocity and with great precision; in combination with the flat detector, this allows the creation of CT-like images

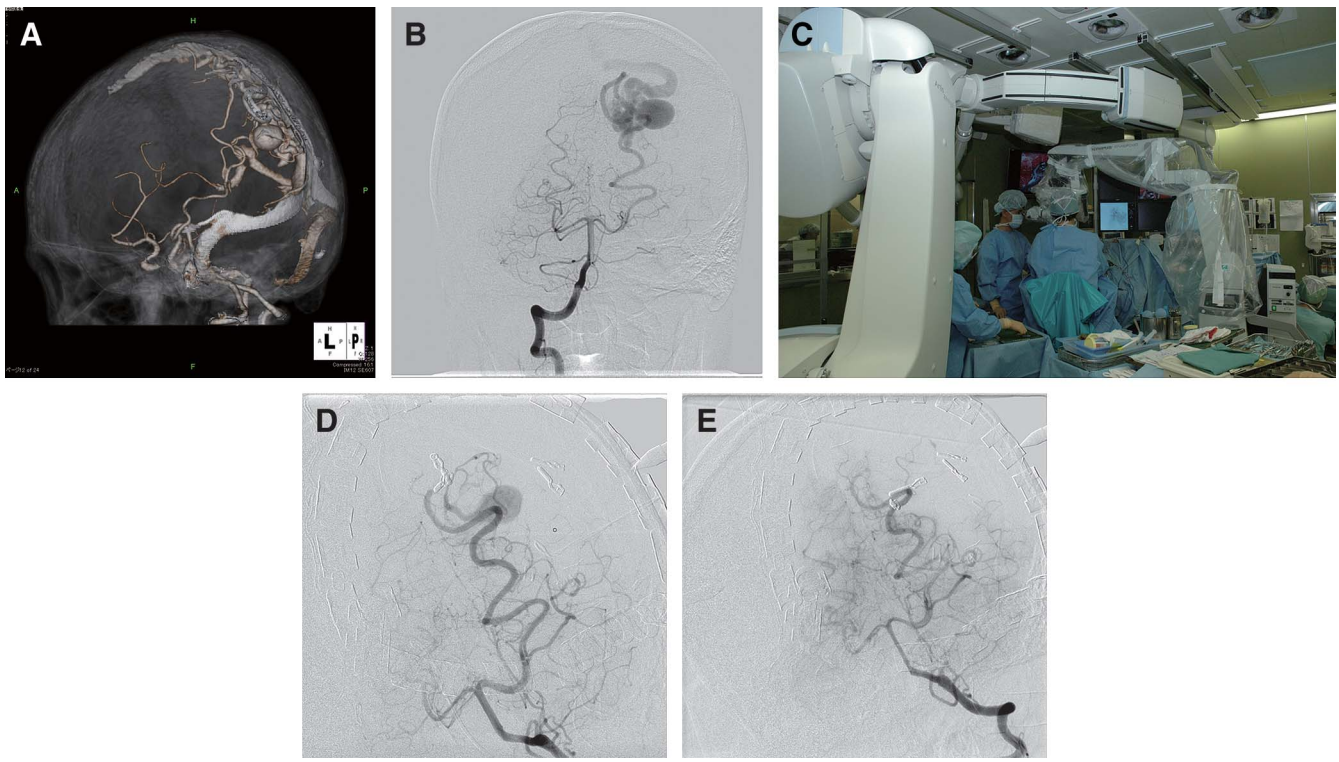

FIGURE 4. *Illustrative case of left occipital arteriovenous fistula (AVF).* **A**, *3-dimensional computed tomography angiography demonstrating left occipital AVF supplied via left middle and posterior cerebral artery feeders.* **B**, *presurgical left vertebral artery angiogram (anterior-posterior view).* **C**, *microsurgical setup in the endovascular operating room. Note the ceiling parking position for microsurgery.* **D**, *intraoperative angiogram demonstrating residual filling of the AVF.* **E**, *final intraoperative angiogram demonstrating complete obliteration of the fistula.*

Copyright © Congress of Neurological Surgeons. Unauthorized reproduction of this article is prohibited.

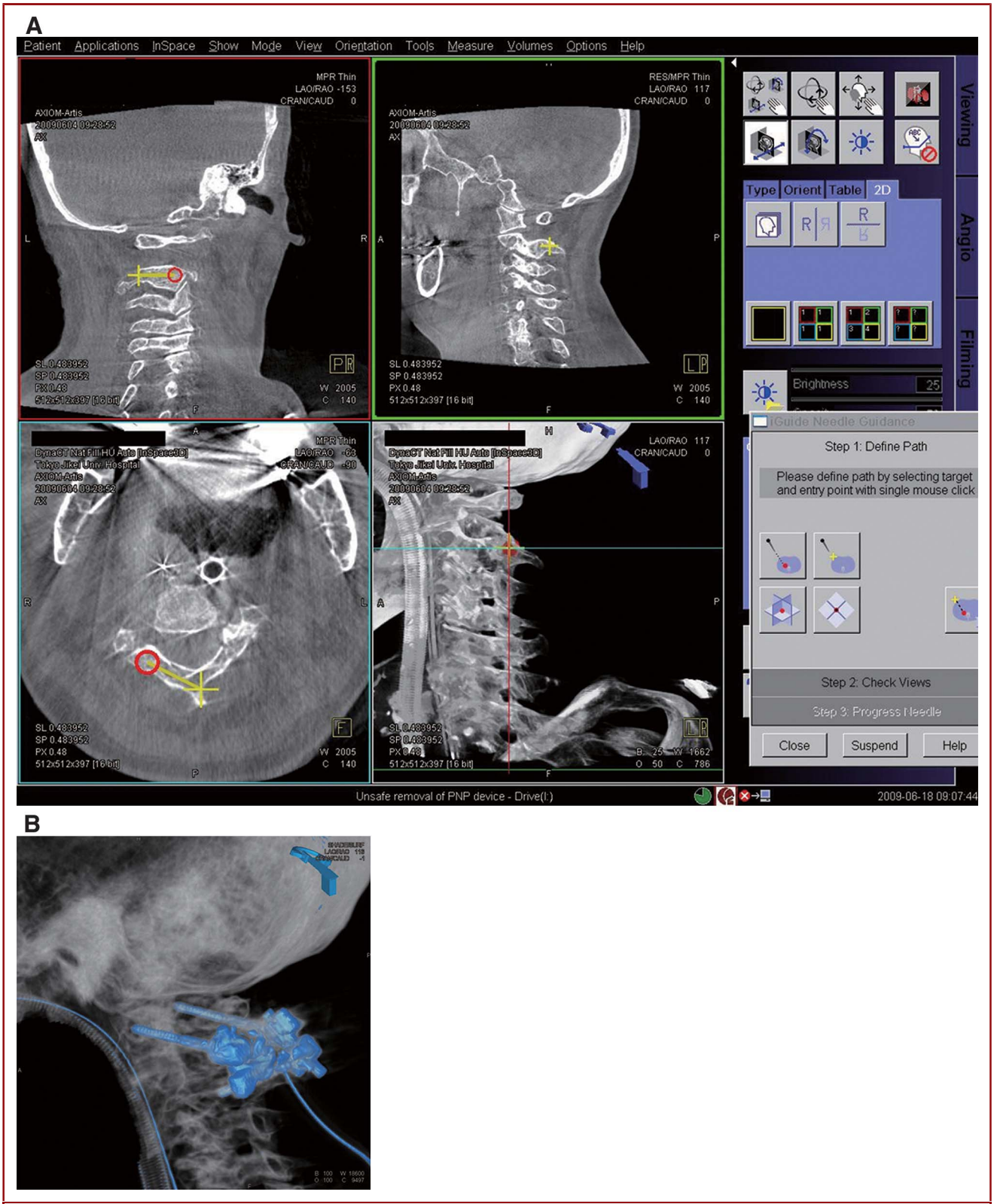

FIGURE 5. *Illustrative case of spinal instrumentation surgery.* **A**, *the screw placement using iGuide (yellow X, insertion point; red circle, end point of the screw). iGuide was also useful for identifying the direction and end point of the screw with live fluoroscopic imaging.* **B**, *3-dimensional reconstruction of DynaCT after screw placement.*

Copyright © Congress of Neurological Surgeons. Unauthorized reproduction of this article is prohibited.

(syngo DynaCT) that provide greater anatomic detail than previously possible with an angiographic system. Thus, diagnostic confidence is increased, particularly during complex neurointerventions and surgical procedures such as clipping of intracranial aneurysms or bypass surgery. During surgical clipping, the surgeon could perform intraoperative angiography with the patient table in a tilted position, the angle that created difficulties with conventional C-arm systems.

Limitations

Although the robotic DSA system has many advantages over the conventional DSA system in the OR, there are still some drawbacks that must be overcome. As with other C-arm angiographic systems, the intraoperative radiation dose for surgeons, nurses, and anesthesiologists must be monitored. In general, the average doses of 3D DSA and 3D DynaCT acquisitions were 10 and 60 mGy, respectively. These values are similar to dose values for other C-arm angiographic systems and are comparable to conventional head CT doses (20-60 mGy). To minimize intraoperative radiation dose, specially designed lead shields have been provided for the surgeons, nurses, and anesthesiologists. In addition, they wear lead aprons, lead goggles, and thyroid protectors during regular fluoroscopic procedures. During 3D DSA or DynaCT, all staff must be out of the OR. Software for tracking radiation dose is included as part of the robotic DSA system. The new 3D roadmap technology was effective when the aneurysm was located on the proximal portion of the parent artery such as the posterior communicating artery. However, a discrepancy between the 3D overlay image and the real image occurred when the microcatheter stretched out the parent artery. This discrepancy was frequently seen in distally located aneurysms such as anterior communicating artery aneurysms. Once advanced fusion technology that takes into account tissue deformation is developed, this type of limitation could be overcome.

For neuroendovascular use, the conventional biplane system is still the gold standard. Simultaneous monitoring of anteriorposterior and lateral projections may still be required during sensitive microcatheter treatment such as arteriovenous malformation embolization. Even though the robotic DSA system can potentially rotate at very high speeds, the current system does not allow rotation at such high speeds because of safety considerations. Therefore, most scheduled aneurysm coiling and AVM embolization procedures have been performed in the biplane endovascular OR unit. The industry is intensively working on a ''virtual biplane'' system that will allow high-speed rotation from the anteroposterior view to the lateral view like the biplane system with a dual-plane roadmap. The cost of the system is another limitation of the robotic DSA system. The price is close to that of a biplane system. However, this innovative system has great advantages in neurosurgical procedures. Intraoperative fluoroscopic imaging clearly improved the safety of surgical procedures. Real-time imaging with the assistance of the iGuide navigation system allows young neurosurgery residents to conduct such procedures as needle biopsy and ventriculostomy safely. Anatomic knowledge is a basic requirement, but this type of surgical assistance clearly has an advantage for less experienced physicians. Routine intraoperative angiography during surgical clipping was not always simple when portable DSA was used.[9] Precise positioning of the C arm was sometimes difficult, and high-quality 3D imaging was not possible. The current ceiling position provides quick and precise intraoperative 3D angiography just after clip placement.

Finally, to develop such an integrated operating room, there must be close cooperation between anesthesiologists, neurosurgeons, and medical engineers, as well as managers of the surgical rooms and nurses. As has been demonstrated, interdisciplinary approaches and collaboration between surgeon performing open neurosurgery and the endovascular therapist provide better patient care.

CONCLUSIONS

The multiaxis robotic DSA system was installed in a surgical setting, and the procedures could be converted from endovascular to ''open'' without moving the patient. This system requires the integration of a specially designed surgical and imaging table; otherwise, the imaging system itself has no additional requirements over conventional DSA systems. Further technical improvements of this OR imaging system include a more OR-friendly user interface and fast C-arm rotations to emulate a second imaging plane.

Disclosure

The authors have no personal financial or institutional interest in any of the drugs, materials, or devices described in this article.

REFERENCES

1. Calligaro KD, Dougherty MJ, Patterson DE, Raviola CA, DeLaurentis DA. Value of an endovascular suite in the operating room. *Ann Vasc Surg*. 1998;12(3):296-298.
2. Matsumae M, Koizumi J, Fukuyama H, et al. World's first magnetic resonance imaging/x-ray/operating room suite: a significant milestone in the improvement of neurosurgical diagnosis and treatment. *J Neurosurg*. 2007;107(2):266-273.
3. Murayama, Y, Saguchi T, Ishibashi T, et al. Endovascular operative suite: future directions for treating neurovascular disease. *J Neurosurg*. 2006;104(6):925-930.
4. Sikkink CJ, Reijnen MM, Zeebregts CJ. The creation of the optimal dedicated endovascular suite. *Eur J Vasc Endovasc Surg*. 2008;35(2):198-204.
5. ten Cate G, Fosse E, Hol PK, et al. Integrating surgery and radiology in one suite: a multicenter study. *J Vasc Surg*. 2004;40(3):494-499.
6. Ng PY, Huddle D, Gunel M, Awad IA. Intraoperative endovascular treatment as an adjunct to microsurgical clipping of paraclinoid aneurysms. *J Neurosurg*. 2000;93(4):554-560.
7. Ricci G, Ricci A, Gallucci M, et al. Combined endovascular and microsurgical approach in the treatment of giant paraclinoid and vertebrobasilar aneurysms. *J Neurosurg Sci*. 2005;49(1):1-6.
8. Irie K, Murayama, Y, Saguchi T, et al. Dyna CT soft tissue visualization using a C-arm unit: initial clinical experience in the operating room. *Neurosurgery*. 2008;62(3)(Suppl 1):266-272.
9. Foley KT, Cahan LD, Hieshima GB. Intraoperative angiography using a portable digital subtraction unit: technical note. *J Neurosurg*. 1986,64(5):816-818.

Copyright © Congress of Neurological Surgeons. Unauthorized reproduction of this article is prohibited.

COMMENTS

Increasingly, the integration of advanced dynamic imaging technologies into the operating room is viewed as an important step in improving the safety and efficacy of surgical procedures. The first generations of these integrations are often cumbersome, as was seen with early intraoperative magnetic resonance imaging suites. Similarly, initial angiography "operating rooms" were often simply an angiography table in the operating room, without accommodation of the plethora of complex patient positionings required to adequately treat a surgical lesion. Here, the authors describe a second-generation integrated operating room suite that uses robotic technology to both maximize the efficacy of the dynamic imaging during vascular neurosurgery and minimize the negative impact of limitations in positioning.

I anticipate that we will see further such integrations in the future, pushed by surgeons who are expert in multiple treatment modalities and who seek to combine those modalities simultaneously in the treatment of patients.

Bob Carter
San Diego, California

The authors report their experience with a robotic C arm capable of 3-dimensional (3D) angiography and cone-beam computed tomography (CT). Three-dimensional angiography is a particularly attractive technique for the intraoperative evaluation of surgical aneurysm clipping, among other neurovascular and spinal interventions. The neurosurgeon using a C arm capable of rotational 3D imaging can acquire a data set, allowing him/her to sit at a nearby workstation and manually rotate the angiogram image into any desired radiographic projection. This can translate into fewer angiographic runs, less radiation and contrast dose for the patient, and better visualization of angiographic anatomy, with presumably more accurate detection of aneurysm neck remnants and arterial branch issues.

Intraoperative cone-beam CT, ie, CT obtained with a rotating C arm, holds much promise for novel forms of image guidance. This exciting development will bring neurosurgeons closer to what one might call "live image guidance"—live in that it is based on intraoperative rather than preoperative axial and 3D imaging and can thus account for changes such as brain shift, change in ventricular size, and unexpected bleeding. These events will become easier to diagnose, quantify, and manage within the operating room than before.

As the authors note, this technology is expensive. Indocyanine green may serve the same purpose for vascular conditions at less cost and with fewer requirements in terms of radiology technology support and expertise. However, as more neurosurgeons become trained and capable of performing neuroangiography, this type of technology may become more frequent in operating room environments. As the authors note, most neurointerventionalists rely on biplane systems. It is unclear whether robotic single C arms would be a preferable alternative for procedures such as aneurysm coiling.

The authors are to be congratulated for contributing an important advance in this new and exciting field.

Stephen P. Lownie
London, Ontario, Canada

ALERT ME WHEN CITED

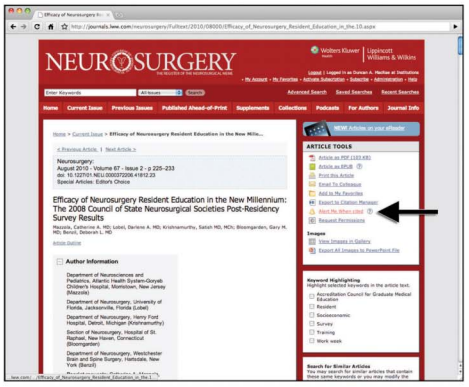

Identify an article and receive an email alert whenever that article appears in another article's reference list.

1. At the Neurosurgery Online home page (*http://www.neurosurgery-online.com*), click Login. If you have not yet registered, you will be prompted to do so.

2. Find the article you wish to add to your Alert Me When Cited notifications. Click on the Alert Me When Cited link in the Article Tools sidebar box.

3. You can manage your Citation Alerts from within the My eTOCS and Alerts tab of your account settings.

Scan the QR Code to access video tutorial

NEUROSURGERY

Copyright © Congress of Neurological Surgeons. Unauthorized reproduction of this article is prohibited.

Open and Endovascular Treatment of Unruptured Carotid-Ophthalmic Aneurysms: Clinical and Radiographic Outcomes

Sanjay Yadla, MD*
Peter G. Campbell, MD*
Bartosz Grobelny, BA‡
Jack Jallo, MD, PhD*
L. Fernando Gonzalez, MD*
Robert H. Rosenwasser, MD*
Pascal M. Jabbour, MD*

*Department of Neurological Surgery and ‡Jefferson Medical College, Thomas Jefferson University, Philadelphia, Pennsylvania

Correspondence:
Pascal M. Jabbour, MD,
Department of Neurological Surgery,
Thomas Jefferson University,
909 Walnut, 2nd Floor,
Philadelphia, PA 19107.
E-mail: sanjay.yadla@jeffersonhospital.org

Received, April 13, 2010.
Accepted, October 1, 2010.

Copyright © 2011 by the
Congress of Neurological Surgeons

BACKGROUND: Aneurysms of the carotid-ophthalmic artery present unique challenges to cerebrovascular neurosurgeons given their proximity to vital anatomic structures.

OBJECTIVE: To report our experience with a combined-modality treatment of unruptured carotid-ophthalmic aneurysms over a 12-year period.

METHODS: A retrospective review of 161 patients who underwent open, endovascular, or combined treatment of 170 aneurysms from January 1997 to July 2009 was conducted. Medical records, operative reports, office notes, and follow-up angiograms were reviewed to obtain data on patient demographics, angiographic results, and clinical outcomes.

RESULTS: One hundred forty-seven aneurysms were treated via endovascular techniques; 17 aneurysms (10%) were treated with microsurgical clip ligation; and 6 aneurysms (3.5%) were treated with a combined approach. Of the aneurysms treated via an endovascular approach alone, 81.6% of aneurysms had evidence of $\geq$ 95% occlusion on initial angiogram. There was a 1.4% rate of major complications associated with the initial procedure. Twenty-six of these aneurysms (18.9%) required further intervention on the basis of early angiographic results. Major complications occurred after 6 of 23 open microsurgical procedures (26.1%), including 2 instances of permanent visual loss. Nine clipped patients had long-term angiographic follow-up; none required further intervention.

CONCLUSION: Endovascular treatment of carotid-ophthalmic aneurysms with modern endovascular techniques can be performed safely and efficaciously in the elective setting.

KEY WORDS: Aneurysm recurrence, Carotid-ophthalmic aneurysm, Coil embolization, Endovascular therapy, Stent, Subarachnoid hemorrhage

Neurosurgery 68:1434–1443, 2011 DOI: 10.1227/NEU.0b013e31820b4f85 www.neurosurgery-online.com

Carotid-ophthalmic aneurysms represent approximately 5% of all intracranial aneurysms.[1,2] They have been associated with an increased prevalence in women and occur in multiples more often than aneurysms at other locations.[3] Microsurgical treatment of these lesions can be challenging secondary to their proximal location.[4-6] Close relationships with the cavernous sinus, carotid siphon, and optic nerve, which often covers the base of the aneurysm, can make clipping particularly hazardous.[1,3] To obtain proximal control, cervical carotid exposure and anterior clinoidectomy are often required, and these maneuvers may be additional sources of morbidity. By avoiding these difficulties, endovascular treatment of carotid-ophthalmic aneurysms has provided an attractive alternative to open surgery since its approval by the Food and Drug Administration in 1995.[5]

Outcomes for endovascular therapy of carotid-ophthalmic aneurysms have typically been reported in the setting of a multimodality approach or as a subset of paraclinoid series.[7-10] However, embolization of carotid-ophthalmic aneurysms may be associated with unique risks such as retinal artery occlusion or delayed optic

ABBREVIATIONS: GOS, Glasgow Outcome Scale

Copyright © Congress of Neurological Surgeons. Unauthorized reproduction of this article is prohibited.

ischemia that require special consideration.[11-13] To this end, this study reviews 170 carotid-ophthalmic aneurysms treated by neurosurgeons trained in both open and endovascular techniques over a 12-year period. To the best of our knowledge, the present study represents the largest reported single-institution series of electively treated aneurysms of the ophthalmic artery.

PATIENTS AND METHODS

All patients who underwent treatment of unruptured carotid-ophthalmic aneurysms at the Jefferson Hospital for Neuroscience between January 1997 and July 2009 were eligible for review. Records for 170 aneurysms treated in 161 patients over this 12-year period were available and included in the study. All patients underwent digital subtraction angiography before treatment. Carotid-ophthalmic aneurysms were distinguished from other paraclinoid or ophthalmic segment aneurysms by the principal neurosurgeon at the time of the initial angiogram.

Electronic medical records, operative reports, and outpatient charts were systematically reviewed. Data on demographics, presenting symptoms, length of stay, Hunt and Hess grade on presentation, Glasgow Outcome Scale (GOS) on discharge from initial hospitalization, and GOS score at latest follow-up were collected. Angiographic data on the size of aneurysm, use of a stent-assisted technique, initial angiographic occlusion, degree of occlusion at the 1-year follow-up, degree of occlusion at the latest follow-up if $>$ 1 year, and need for further treatment (ie, further coiling, stent-assisted coiling, or clip ligation for recurrence) were tabulated. Complications associated with angiography or surgery, including stroke, death, hemorrhage, intraoperative rupture, coil prolapse, retroperitoneal hematoma, and new visual deficits, were also recorded. The size of the aneurysm dome was categorized by International Study of Unruptured Intracranial Aneurysms criteria into $<$10 mm (average), 10 to 24 mm (large), and $\geq$ 25 mm (giant).[14] Initial and follow-up degree of occlusion was classified as total (100% occlusion), near-total (95% occlusion or neck remnant), and subtotal ($<$ 95% or aneurysm remnant) as dictated by the surgeon. This study was approved by the Institutional Review Board of Thomas Jefferson University.

Statistical Analysis

Statistical analysis was performed with JMP 7 software (SAS Institute Inc, Cary, North Carolina). Multivariate analysis was performed to identify associations between the following variables: age, sex, treatment modality (open vs endovascular), size, degree of initial occlusion, use of stent, complications, and length of stay. Recurrence was defined as a change in degree of occlusion from total to near-total, total to subtotal, or near-total to subtotal. Recurrence was evaluated by time-to-event analysis and Kaplan-Meier curves. Values of $P \leq .05$ were considered statistically significant.

Endovascular Management

Standard procedures for coil embolization at our institution evolved over the course of the series; our current practices have been reported previously.[15-17] In 2002, the introduction of intracranial microstents expanded the indications for endovascular treatment of carotid-ophthalmic aneurysms, particularly aneurysms that are wide necked or fusiform. Patients with significant medical comorbidities or age $>$ 75 years are referred for endovascular treatment. If aneurysms are amenable to both an open or endovascular approach, the endovascular approach is preferred.

The standard procedures for stent-assisted coiling at our institution have also been reported previously.[17-19] All patients are maintained on a minimum of 6 weeks of clopidogrel 75 mg daily after stent placement. If stent-assisted coiling is required, attempts to perform both stent placement and coil embolization are made at the time of initial intervention. If evidence of motion or instability is noted at the time of stent placement, the procedure may be aborted at the discretion of the surgeon. The patient subsequently returns for definitive coiling 6 to 8 weeks later to allow for stent endothelialization.

Angiographic follow-up is routinely scheduled at 6 to12 months after endovascular treatment, along with magnetic resonance angiography. If the aneurysm is completely obliterated on the follow-up angiogram, the patient next returns for 5-year follow-up angiography. During the interim period, serial magnetic resonance angiographies are obtained every 6 months for the first 18 months and annually thereafter. If magnetic resonance angiography shows evidence of recurrence at any point, the patient is scheduled for an angiogram (Figure 1). Angiographic recurrences of $<$ 10% are followed up. Angiographic recurrences of $>$ 10% are referred for further treatment.

Clinic visits are routinely scheduled 6 weeks after definitive coiling. Patients are then asked to return for an annual appointment. Both preoperative and postoperative ophthalmologic evaluations are performed if the patient presents with visual symptoms or is noted to have a deficit on preoperative exam.

Microsurgical Management

Aneurysms are considered for microsurgical clip ligation if angiography demonstrates that the ophthalmic artery emanates from the neck of the aneurysm or if an endovascular approach is otherwise technically not feasible. Intraoperative angiograms are performed to assess clip placement and aneurysm obliteration. Clinic visits are routinely scheduled 6 weeks and 1 year after surgery. The patient then returns for a 5-year follow-up angiogram.

RESULTS

One hundred seventy ophthalmic aneurysms in 161 patients were included in this review. One hundred forty-seven aneurysms were treated via endovascular techniques; 17 aneurysms (10%) were treated with microsurgical clip ligation; and 6 aneurysms (3.5%) were treated with a combined approach. The number of aneurysms treated by an endovascular approach per year increased steadily during the course of this series, whereas the number treated by an open approach remained relatively stable (Figure 2). The mean age of patients undergoing treatment was 50.8 years (Table 1). The majority (142; 88.2%) of patients were female; there were 19 male patients in this cohort (11.8%). Seventy-two aneurysms originated from the right ophthalmic artery and 98 from the left; 9 patients had bilateral aneurysms treated. The majority of aneurysms in this series were $\leq$ 10 mm (n = 139). Twenty-three aneurysms were large (10-24 mm) and 8 aneurysms were giant ($>$ 25 mm).

Thirteen patients presented with visual symptoms, including decrease in visual acuity (n = 10), scotomas (n = 1), visual field deficit (n = 1), and diplopia (n = 1). Ophthalmic aneurysms were found incidentally in the remaining 148 patients, and of those, 43 aneurysms were found on workup of headaches. The average GOS score at the time of discharge was 4.93 for all patients.

Copyright © Congress of Neurological Surgeons. Unauthorized reproduction of this article is prohibited.

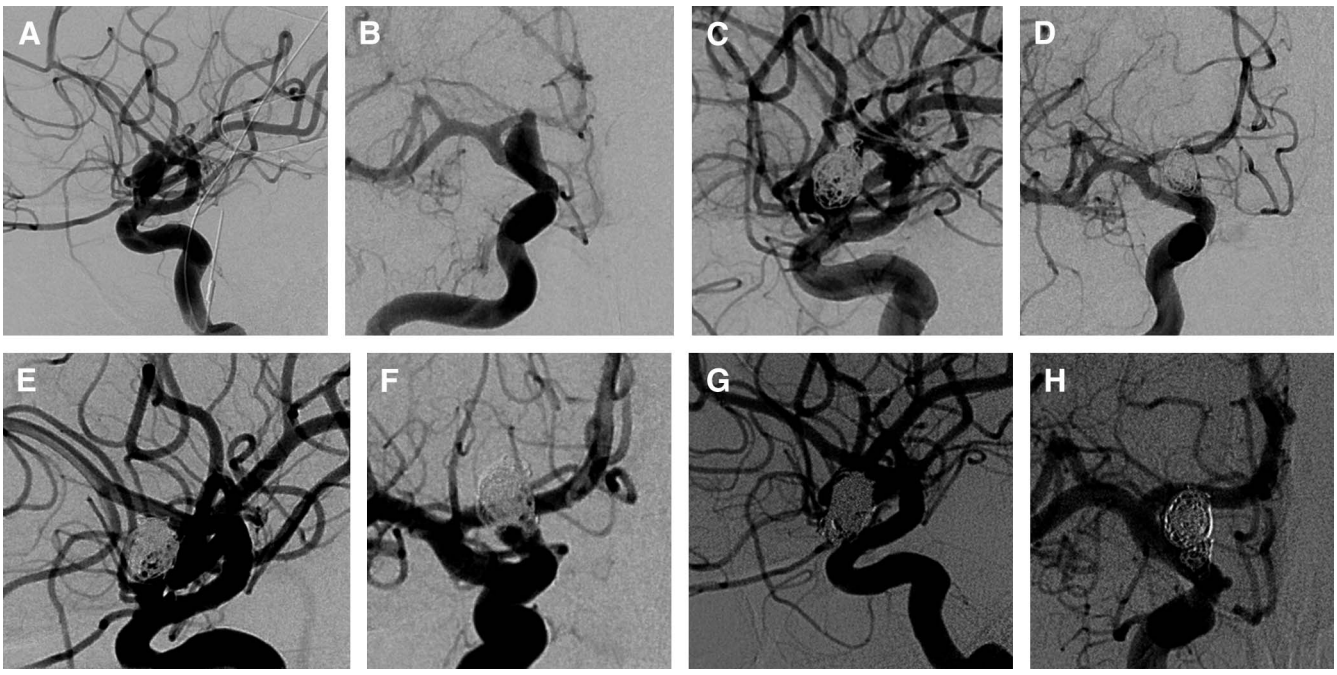

FIGURE 1. *Lateral (A) and anteroposterior (B) views of initial diagnostic angiogram of a 39-year-old man who presented with subarachnoid hemorrhage from a 12-mm right carotid-ophthalmic aneurysm. Lateral (C) and anteroposterior (D) views after initial coil embolization showing 90% occlusion. At the 9-month follow-up angiography, a 20% recurrence was noted on lateral (E) and anteroposterior (F) views. The patient returned 1 month later for recoiling with complete occlusion of the aneurysm on lateral (G) and anteroposterior (H) views.*

Guglielmi detachable coils (Boston Scientific, Natick, Massachusetts) were used exclusively during the first 8 years of this series, 1997 to 2005, and the majority of aneurysms overall were treated with them (n = 105). Both Guglielmi detachable coils (n = 57) and Cerecyte coils (Micrus Endovascular, San Jose, California; n = 36) were used regularly after 2005, depending on the primary surgeon's preference. Three other coiling systems were used in a limited number of cases throughout the series (n = 6). Balloon remodeling techniques were used in 3 cases.

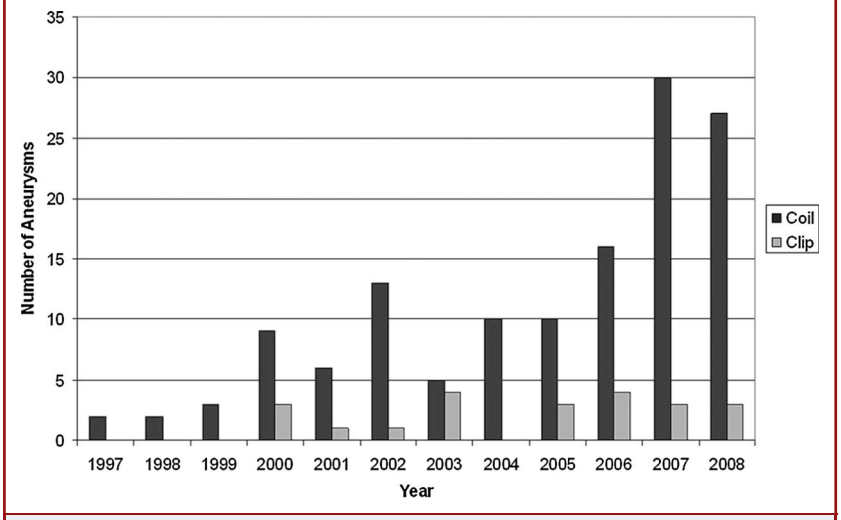

FIGURE 2. *Bar graph illustrating the number of aneurysms treated via an endovascular approach by year from 1997 to 2008 and via an open microsurgical approach from 2000 to 2008.*

Copyright © Congress of Neurological Surgeons. Unauthorized reproduction of this article is prohibited.

TABLE 1. General Characteristics of 170 Carotid-Ophthalmic Aneurysms Treated in 161 Patients From 1997 to 2009 at the Jefferson Hospital for Neuroscience

Sex, n (%)	
Male	142 (88.2)
Female	19 (11.8)
Mean age, y	50.8
Side of aneurysm, n	
Right	72
Left	98
Size of aneurysm, n (%)	
≤ 10 mm (average)	139 (81.8)
10-24 mm (large)	23 (13.5)
≥ 25 mm (giant)	8 (4.7)
Presenting symptom/signs, n	
Loss of acuity	10
Scotomas	1
Visual field deficit	1
Diplopia	1
Incidental	148

Seventy-two patients (47.1%) underwent stent-assisted coiling, and the use of stents steadily increased over the series (Figure 3). Two patients were treated definitively by a flow-reducing stent-in-stent technique without coiling. Aneurysms < 10 mm were less likely to require stent-assisted coiling than those > 10 mm (35.2% vs 61.8%; $P = .002$).

Endovascular Results

Of the 147 aneurysms treated via an endovascular approach alone, 71 aneurysms (48.3%) had 100% occlusion at the time of initial coil embolization, and 49 aneurysms (33.3%) had ≥ 95% occlusion at the time of initial coil embolization. Twenty-seven aneurysms (18.4%) had < 95% initial occlusion. In multivariate analysis, aneurysms > 10 mm were associated with lower rates of complete initial occlusion (35.7% vs 50.8%; $P = .05$). Aneurysms treated via stent-assisted technique were less likely to have 100% occlusion at the time of initial coil embolization (34.7% vs 61.3%; $P = .002$).

Early angiographic follow-up was available for 118 aneurysms (80.3%) with a mean time to follow-up of 10.9 months. Of those, 81 aneurysms (68.6%) had angiographic evidence of 100% occlusion at early follow-up, 16 aneurysms (13.6%) had evidence of ≥ 95% occlusion, and 21 aneurysms (17.8%) had evidence of < 95% occlusion. Greater degree of occlusion at follow-up was associated with smaller size (< 10 mm; $P < .001$).

Eighteen aneurysms (12.2%) required further intervention on the basis of early angiographic results. Eleven aneurysms required placement of a stent and further coiling; 5 aneurysms required further coiling alone; and 2 aneurysms were treated via a stent-in-stent flow-reducing technique.

Late angiographic follow-up was available for 39 aneurysms (26.5%) with a mean time to follow-up of 35.3 months and a range of 14 to 95 months. Of these, 25 aneurysms (64.1%) had angiographic evidence of 100% occlusion at late follow-up, 9 aneurysms (23.1%) had evidence of ≥ 95% occlusion, and 5 aneurysms (12.8%) had evidence of < 95% occlusion.

The overall recurrence rate in the 118 cases for which angiographic follow-up was available was 17.8% with a mean time to recurrence of 28.3 months. Aneurysms with 100% initial occlusion had a mean time to recurrence of 36 months, and aneurysms with 95% initial occlusion had a mean time to recurrence of 13 months, although these differences were not statistically significant ($P = .11$; Figure 4). Recurrence rates were

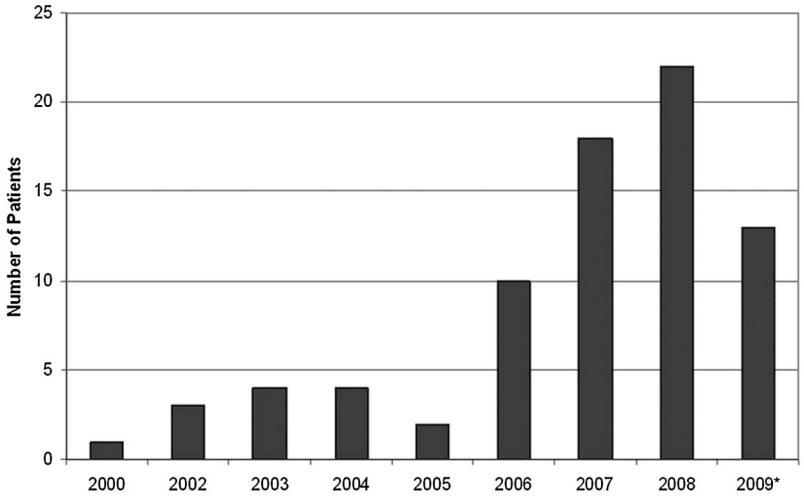

FIGURE 3. *Bar graph illustrating the number of stent-assisted coil embolizations by year from 2000 to 2009. *Only procedures from January to July 2009 were included in this analysis.*

Copyright © Congress of Neurological Surgeons. Unauthorized reproduction of this article is prohibited.

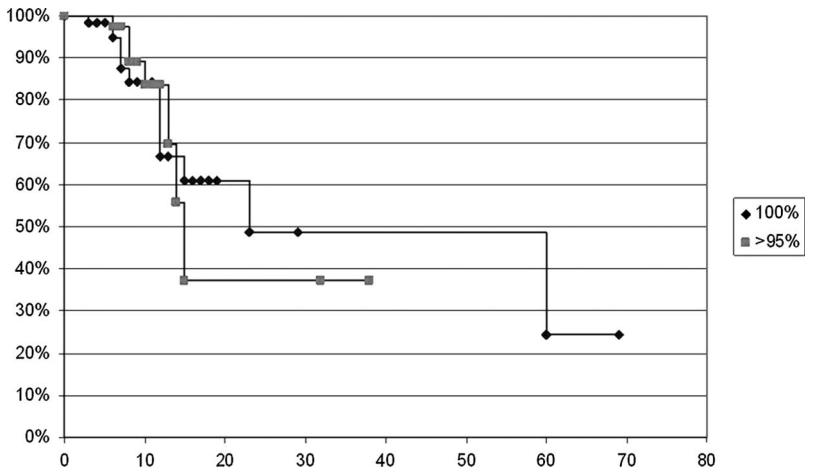

FIGURE 4. *Kaplan-Meier survival analysis for recurrence based on degree of initial angiographic occlusion.*

lower in aneurysms treated initially with a stent-assisted technique (9.4% vs 24.6%; $P = .03$). There was no statistically significant difference in recurrence rates between aneurysms treated before 2005 and those treated after (22.2% vs 14.1%; $P = .25$).

Microsurgical Results

Records for 23 patients who underwent microsurgical clip ligation from January 2000 to 2009 were available for review. The average age of patients undergoing clip ligation was 46 years. Six aneurysms were referred for clip ligation after failed attempts at endovascular treatment. Twenty aneurysms were ≤ 10 mm, and 3 were giant aneurysms. Initial occlusion based on intraoperative angiogram was 100% in all 23 cases. Long-term follow-up angiograms were available for 9 patients at an average of 43.1 months after the initial clipping. One patient had evidence of recurrence at the neck of the aneurysm; no patients required further treatment for their aneurysms.

Complications

Major complications, those with permanent or significant detrimental effects directly related to the procedure, occurred in 2 of 147 endovascular procedures (1.4%; Table 2). Minor complications, those with minimal or no detrimental effect, occurred in 13 procedures (8.8%). Minor complications included 7 instances of clinically insignificant coil prolapse and 6 cases of retroperitoneal hematoma that did not require surgical intervention. Giant aneurysms had a significantly higher rate of any complication, major or minor (40% vs 8.6%; $P = .02$). One hundred thirty-two procedures (89.8%) were not associated with complications. Stent-assisted coiling was not associated with

TABLE 2. Major Complications and Outcomes of 170 Aneurysms Treated via Open and Endovascular Means

Age, y	Sex	Method of Treatment	Side of Aneurysm	Size of Aneurysm, mm	Length of Stay, d	Complication	Follow-up, mo	Outcome
58	F	Coil	Right	5	25	Intraoperative rupture	Lost to follow-up	N/A
32	F	Coil	Left	7	48	Retroperitoneal hematoma	N/A	Underwent exploratory laparotomy for evacuation of hematoma
49	F	Clip	Right	8	18	Stroke, death	N/A	
60	M	Coil, clip	Left	7	30	Stroke	N/A	
61	F	Clip	Left	6	9	Stroke	N/A	
63	F	Clip	Left	26	9	Visual loss	12	Improved
54	F	Clip	Left	28	10	Visual loss	N/A	

Copyright © Congress of Neurological Surgeons. Unauthorized reproduction of this article is prohibited.

a higher incidence of complications (P = .67). There was no difference in complication rates between aneurysms treated with Guglielmi detachable coils or Cerecyte coils (7.8% vs 13.9%; P = .29). The rate of any complication, major or minor, did not vary significantly between aneurysms treated before 2005 and those treated after 2005 (10.5% vs 9.1%; P = .08).

Hemorrhage occurred in 1 patient after endovascular treatment. A 54-year-old woman presented with a giant right carotid-ophthalmic aneurysm found on workup of headaches. The patient's initial procedure was uneventful, resulting in a 90% occlusion. The patient was discharged but returned 5 days later after being found unresponsive by a family member. Computed tomography revealed diffuse subarachnoid hemorrhage, and the patient met brain death criteria on arrival. No patients treated by endovascular techniques experienced delayed ophthalmologic ischemic events.

Major complications occurred after 6 of 23 open microsurgical procedures (26.1%). Major complications included 3 strokes, 1 death, and permanent visual loss in the ipsilateral eye in 2 patients. Minor complications occurred after 4 of 23 open procedures (17.4%); they included 2 clinically insignificant hemorrhages and 2 episodes of transient weakness that resolved before discharge. The rates of major (30.4% vs 1.4%; P = .001) and overall (43.5% vs 10.2%; P = .002) complications with open surgery were significantly higher than with endovascular treatment.

Clinical Results

Clinical follow-up was available for 128 patients (79.5%) with a mean last follow-up of 19.1 months. The overall mean GOS score at last follow-up was 4.93. Follow-up ophthalmologic data were available for 10 of 13 patients who presented with ophthalmologic deficits. Five of these patients had no change, and 5 had improvement of their preoperative deficit at follow-up. Ophthalmologic outcomes are presented in Table 3.

The overall mean length of stay (LOS) for patients undergoing endovascular procedures was 2.96 days. The median LOS decreased over the course of the series from 3 days in 1998 to 1 day in 2008 (95% confidence interval, 1.02-1.15; Figure 5). The median LOS for uncomplicated microsurgical clipping was 4 days, but for patients who experienced complications, it was 13.5 days.

DISCUSSION

Open microsurgical approaches to carotid-ophthalmic aneurysms can be challenging because of close relationships with surrounding anatomic structures.[4,20,21] Even with advances in microsurgical techniques, the morbidity reported in modern clipping series has led some authors to advocate the endovascular approach over open surgery for paraclinoid aneurysms.[20] The present review was conducted to evaluate the management of a large series of carotid-ophthalmic aneurysms by cerebrovascular neurosurgeons trained in both open and endovascular techniques at a tertiary referral center.

This series comprises patients who underwent treatment on a nonemergent basis. The median LOS for elective endovascular treatment decreased over the course of the series from roughly 3 days to 1 day. During the first several years of the series, patients routinely presented for test balloon occlusion followed by coil embolization the next day. Currently, patients undergo intervention (coil and/or stent) on the day of admission and are discharged the next day if there are no complications.

Angiographic Results

We found that 81.6% of aneurysms had ≥ 95% occlusion at the time of initial coil embolization, with 48.3% having 100% occlusion at the time of initial coiling. The proportion of procedures in which initial embolization results in 100% occlusion of ophthalmic segment aneurysms in the reported literature ranges from

TABLE 3. Clinical Outcomes of the 13 Patients in the Present Series Who Presented With Ophthalmologic Deficits

Age, y	Sex	Treatment	Aneurysm Group[a]	Presentation	Stent Assisted	Length of Follow-up, mo	Ophthalmologic Outcome
58	F	Coil	3	Diplopia	No	6	Unchanged
56	F	Coil	1	Monocular nasal quadrantanopia	Yes	9	Unchanged
42	F	Coil	1	Scotomas	No	12	Improved
40	F	Coil	1	Loss of acuity	No	65	Improved
53	F	Coil	2	Loss of acuity	No	42	Improved
54	F	Clip	3	Loss of acuity	N/A	12	Improved
58	F	Clip	3	Loss of acuity	N/A	N/A	N/A
63	F	Clip	3	Loss of acuity	N/A	N/A	N/A
68	F	Coil	2	Loss of acuity	No	4	Improved
72	F	Coil	2	Loss of acuity	No	15	Unchanged
44	F	Coil	2	Loss of acuity	Yes	27	Unchanged
53	F	Coil	1	Loss of acuity	Yes	4	Unchanged
72	F	Coil	2	Loss of acuity	No	N/A	N/A

[a]Group 1, aneurysms < 10 mm; Group 2, aneurysms 10-24 mm; Group 3, aneurysms > 25 mm.

Copyright © Congress of Neurological Surgeons. Unauthorized reproduction of this article is prohibited.

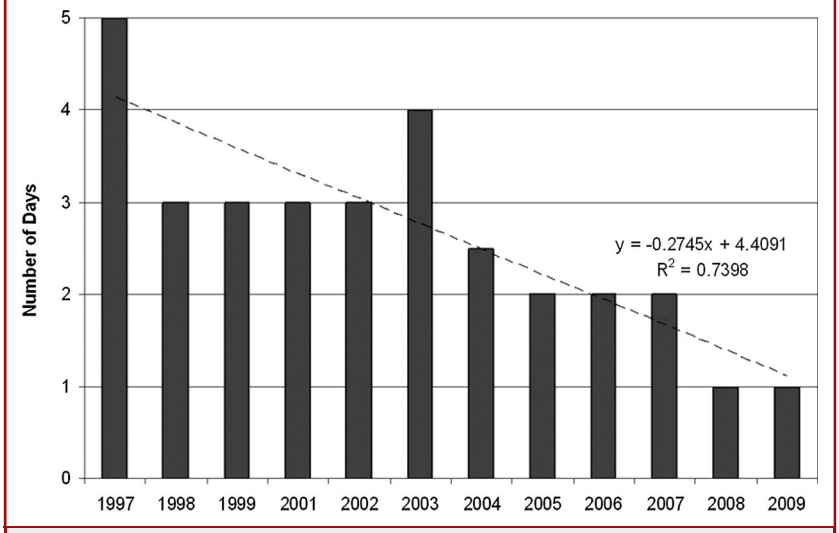

FIGURE 5. *Median length of stay in days for endovascular treatment of unruptured carotid-ophthalmic aneurysms from 1997 to July 2009.*

21% to 83% with an average of 42% (Table 4).[5,9,10,20,22-30] Statistical analysis demonstrated that 100% occlusion was less likely in aneurysms with a diameter of > 10 mm in the present series.

Choi et al[31] recently reported on long-term angiographic follow-up of 91 aneurysms, including 8 ophthalmic segment aneurysms, all of which were 100% occluded on initial embolization. These authors found a recanalization rate of 26.4% at a mean angiographic follow-up of 26.4 months (range, 3 months to 9.1 years). There were no episodes of postembolization hemorrhage, and aneurysms with wider necks were associated with higher rates of recanalization.[31] Follow-up angiography 6 months after the initial procedure and annually thereafter was recommended.

Angiographic follow-up for aneurysms treated via an entirely endovascular approach was available for 118 aneurysms at an average of 13.2 months, and there was evidence of aneurysm recurrence in 17.8%. In the previously reported literature for carotid-ophthalmic aneurysms, the rate of recurrence ranges from 7.1% to 53% with an average rate of 24.2%.[5,9,10,20,24,26-29,32]

TABLE 4. Summary of Angiographic Results in Existing Series on Endovascular Management of Carotid-Ophthalmic and Ophthalmic Segment Aneurysms With ≥ 10 Patients

Author, Year	Carotid-Ophthalmic Aneurysms (Overall Series), n	Degree of Initial Occlusion, %			Average Follow-up, mo	Rate of Recurrence, %	Retreated, %	Complications, %
		Complete (100%)	Near-Complete (> 95%)	Incomplete (< 95%)				
Sherif et al, 2009[22]	18 (64)	82.9	14.3[a]	2.8[a]	29.2	. . .	31.6[a]	10.5
Sung-Chul et al, 2009[23]	10 (67)	40[a]	40[a]	20[a]	29.7	. . .	0	7.6[a]
Fulkerson et al, 2009[24]	28 (157)	28.6	25	27.9	16.8	11	4	7.1
Heran et al, 2007[25]	10 (17)	30	40	30	34.8	. . .	70.5[a]	35
Campi et al, 2007[33]	30 (1096)	. . .	. . .	. . .	13.7	. . .	17.4[a]	. . .
Biondi et al, 2007[26]	15 (42)	35[a]	45[a]	20[a]	9	16.5[a]	11.9[a]	7.2
Boet et al, 2005[5]	15 (21)	80	20	0.0	30.5	53	46.70	0
Raymond et al, 2003[32]	73 (501)	. . .	. . .	. . .	31.3	26	. . .	0.3
Park et al, 2003[10]	18 (73)	73[a]	8[a]	19[a]	14.4	11	27.8	27.8
Iihara et al, 2003[27]	10 (111)	50	20	30	. . .	20	20	40
Hoh et al, 2001[28]	27 (238)	44[a]	26[a]	30[a]	. . .	26[a]	9[a]	21
Thornton et al, 2000[20]	35 (71)	54[a]	31[a]	15[a]	16	16.4[a]	11.5	5.5[a]
Byrne et al, 1999[29]	13 (317)	64[a]	34[a]	2[a]	. . .	14.7[a]	5	N/A
Roy et al, 1997[9]	14 (28)	21.4	50	28.6	23.5	7.1[a]	0	21.4[a]
Vinuela et al, 1997[30]	47 (403)	70.8[a]	21.4[a]	4.2[a]	. . .	. . .	. . .	9.2[a]

[a]Values were reported for the overall series and not for carotid-ophthalmic aneurysms specifically.

Copyright © Congress of Neurological Surgeons. Unauthorized reproduction of this article is prohibited.

The length of angiographic follow-up in those studies ranged from 9 to 34.8 months with an average of 22.6 months.

Raymond et al[32] reported on long-term angiographic recurrences in a cohort of 501 endovascularly treated aneurysms. Of the 73 aneurysms located on the ophthalmic segment of the carotid artery, 19 aneurysms (26%) recurred at a mean of 12.3 months. The overall recurrence rate in their series was 33.6% with significant recurrence in 20.7%. They concluded that 6-month follow-up angiography was insufficient for detecting most recurrences.[32]

Boet et al[5] reported on recurrence after multimodality treatment of 21 ophthalmic segment aneurysms over 7 years.[5] Fifteen aneurysms in that series were treated by coil embolization, and 8 patients experienced recurrence, giving a rate of 53%. They found no evidence of recurrence in 5 of 6 patients who underwent clip ligation and had follow-up angiography. The authors suggested that greater shear hemodynamic stresses at the region of the carotid siphon may slow intimal overgrowth, resulting in higher rates of recurrence in the endovascular cohort, particularly if initial occlusion was incomplete.[5]

Aneurysms in the present series with 100% initial occlusion had a median time to recurrence of 36 months, whereas aneurysms with 95% initial occlusion had a median time to recurrence of 13 months. Raymond et al,[32] Thornton et al,[33] and Campi et al[20] reported similar trends with higher rates of recurrence associated with incomplete initial occlusion. These data suggest that earlier or more frequent angiographic follow-up may be warranted in these patients.

Ophthalmologic Results

A small proportion (8.1%) of patients presented with ophthalmologic symptoms or signs. Ophthalmologic findings are more commonly associated with larger aneurysms; however, only 7 aneurysms in our series were considered giant. Thus, the low incidence of visual findings may be due to the modest number of giant aneurysms treated in the present series. Some previous reports suggested that 25% to 50% of carotid-ophthalmic aneurysms are $\geq$ 25 mm.[21,34]

Several authors have recently described progressive visual loss after coil embolization of carotid-ophthalmic or paraclinoid aneurysms.[11-13] Turner et al[11] described 6 cases of delayed ($>$ 24 hours) visual deficits in patients undergoing coil embolization of giant ophthalmic aneurysms. Five of 6 cases occurred in aneurysms treated with hydrogel-coated coiling systems, although 1 case occurred in a patient treated with bare platinum coils alone.[11] This phenomenon was not observed in the present cohort; hydrogel-coated coils were not used in this series, although bare platinum coils were used in 105 patients.

Five of 13 patients who presented with visual deficits were noted to have improvement at a mean follow-up of 27 months in the present series. Five of 13 patients had no change in their visual deficit at follow-up. The single patient who presented with a field defect underwent coil embolization and did not have improvement at 9 months. These results are comparable to those of previous endovascular series.[9,20,25] Two patients in the clipping cohort had permanent visual loss postoperatively.

A search of the microsurgical literature for carotid-ophthalmic and other paraclinoid aneurysms yielded postoperative ophthalmologic deficit rates of 0% to 28.5% with an average of 11.5%.[4,21,27,34-39] In the present series, the rate of ophthalmologic deficit after clipping was 8.6%; this rate is well within the range of previous reports. For endovascular series, published postprocedural ophthalmologic deficit rates range from 0% to 25% with an average of 4.2%.[9,10,20,22,24-28,40] The results of the present series and previous publications suggest that endovascular treatment can be performed with lower rates of ophthalmologic morbidity than open surgery. Open surgery may still be preferred in specific instances, however, such as for ligation and decompression of an aneurysm causing a visual field deficit by direct compression of the optic nerve.[34]

Complications

The rate of major complications in the present series was significantly higher in the open cohort (26.1%) than the endovascular cohort (1.4%; P = .001). A search of published endovascular series yielded overall complication rates that ranged from 0% to 40% with an average of 16.5%.[5,9,10,20,22,24-28,30,32,40] Overall complication rates of open microsurgical series range from 4.2% to 22.8% with an average of 13.5%.[3,4,21,27,34-39,41-44] The rate of major complications in the present microsurgical cohort is higher than previous reports. This cohort was relatively small, with only 17 patients treated with clipping alone and 6 patients undergoing combined treatment. The practices at our institution may have selected more technically challenging aneurysms to undergo open surgery given that aneurysms that were not amenable to endovascular treatment were referred for clip ligation. In addition, definitions of complications are variable in the literature, and there are few series restricted to carotid-ophthalmic aneurysms alone. This makes direct comparisons with other reports difficult. Interestingly, the incidence of complications with endovascular treatment was not associated with the use of stent-assisted technique or the type of coil.

Limitations

Several aspects of this study may affect interpretation of the results. First, angiographic follow-up was not available for 29 endovascularly treated aneurysms (19.7%). The angiographic outcomes of patients lost to follow-up may have varied from the outcomes of patients included in the study. Second, recurrence was defined in a specific manner to facilitate statistical analysis. The method used in this study inherently excluded aneurysms that had subtotal ($<$ 95%) initial angiographic occlusion. This could have led to an underestimate of recurrence rates in the overall cohort. Finally, there are no standard classifications for complications in the literature, and those used in this study may not be agreed on by the neurosurgical community.

Copyright © Congress of Neurological Surgeons. Unauthorized reproduction of this article is prohibited.

CONCLUSIONS

The clinical and radiographic results of a 12-year experience with combined open and endovascular management of carotid-ophthalmic aneurysms are presented. Near-total or total initial angiographic occlusion was achieved in 81.6% of aneurysms with an overall recurrence rate of 17.8% (n = 118) and a mean time to recurrence of 28.3 months. The major complication rate of endovascular treatment (1.4%) was significantly lower than that of microsurgical treatment (26.1%). Endovascular treatment of carotid-ophthalmic aneurysms is safe and efficacious in the elective setting. Further long-term angiographic follow-up is necessary to determine the durability of this technique.

Disclosure

Dr Rosenwasser and Gonzalez are consultants for Boston Scientific, Inc. Dr Jabbour is a consultant for Codman Neurovascular, Inc. The authors have no personal financial or institutional interest in any of the drugs, materials, or devices described in this article.

REFERENCES

1. Drake CG, Vanderlinden RG, Amacher AL. Carotid-ophthalmic aneurysms. *J Neurosurg*. 1968;29(1):24-31.
2. Locksley HB. Natural history of subarachnoid hemorrhage, intracranial aneurysms and arteriovenous malformations: based on 6368 cases in the cooperative study. *J Neurosurg*. 1966;25(2):219-239.
3. Sengupta RP, Gryspeerdt GL, Hankinson J. Carotid-ophthalmic aneurysms. *J Neurol Neurosurg Psychiatry*. 1976;39(9):837-853.
4. De Jesus O, Sekhar LN, Riedel CJ. Clinoid and paraclinoid aneurysms: surgical anatomy, operative techniques, and outcome. *Surg Neurol*. 1999;51(5):477-487.
5. Boet R, Wong GK, Poon WS, Lam JM, Yu SC. Aneurysm recurrence after treatment of paraclinoid/ophthalmic segment aneurysms: a treatment-modality assessment. *Acta Neurochir (Wien)*. 2005;147(6):611-616.
6. Almeida GM, Shibata MK, Bianco E. Carotid-ophthalmic aneurysms. *Surg Neurol*. 1976;5(1):41-45.
7. Solander S, Ulhoa A, Vinuela F, et al. Endovascular treatment of multiple intracranial aneurysms by using Guglielmi detachable coils. *J Neurosurg*. 1999;90(5):857-864.
8. Arnautovic KI, Al-Mefty O, Angtuaco E. A combined microsurgical skull-base and endovascular approach to giant and large paraclinoid aneurysms. *Surg Neurol*. 1998;50(6):504-518.
9. Roy D, Raymond J, Bouthillier A, et al. Endovascular treatment of ophthalmic segment aneurysms with Guglielmi detachable coils. *AJNR Am J Neuroradiol*. 1997;18(7):1207-1215.
10. Park HK, Horowitz M, Jungreis C, et al. Endovascular treatment of paraclinoid aneurysms: experience with 73 patients. *Neurosurgery*. 2003;53(1):14-23.
11. Turner RD, Byrne JV, Kelly ME, et al. Delayed visual deficits and monocular blindness after endovascular treatment of large and giant paraophthalmic aneurysms. *Neurosurgery*. 2008;63(3):469-474.
12. Castillo B Jr., De Alba F, Thornton J, DeBrun G, Pulido J. Retinal artery occlusion following coil embolization of carotid-ophthalmic aneurysms. *Arch Ophthalmol*. 2000;118(6):851-852.
13. Schmidt GW, Oster SF, Golnik KC, et al. Isolated progressive visual loss after coiling of paraclinoid aneurysms. *AJNR Am J Neuroradiol*. 2007;28(10):1882-1889.
14. Unruptured intracranial aneurysms: risk of rupture and risks of surgical intervention: International Study of Unruptured Intracranial Aneurysms Investigators. *N Engl J Med*. 1998;339(24):1725- 1733.
15. Pandey AS, Koebbe C, Rosenwasser RH, Veznedaroglu E. Endovascular coil embolization of ruptured and unruptured posterior circulation aneurysms: review of a 10-year experience. *Neurosurgery*. 2007;60(4):626-636.
16. Koebbe CJ, Veznedaroglu E, Jabbour P, Rosenwasser RH. Endovascular management of intracranial aneurysms: current experience and future advances. *Neurosurgery*. 2006;59(5)(Suppl 3):S93-S102.
17. Jabbour PM, Tjoumakaris SI, Rosenwasser RH. Endovascular management of intracranial aneurysms. *Neurosurg Clin N Am*. 2009;20(4):383-398.
18. Jabbour P, Koebbe C, Veznedaroglu E, Benitez RP, Rosenwasser R. Stent-assisted coil placement for unruptured cerebral aneurysms. *Neurosurg Focus*. 2004; 17(5):E10.
19. Benitez RP, Silva MT, Klem J, Veznedaroglu E, Rosenwasser RH. Endovascular occlusion of wide-necked aneurysms with a new intracranial microstent (Neuroform) and detachable coils. *Neurosurgery*. 2004;54(6):1359-1367.
20. Thornton J, Aletich VA, Debrun GM, et al. Endovascular treatment of paraclinoid aneurysms. *Surg Neurol*. 2000;54(4):288-299.
21. Day AL. Aneurysms of the ophthalmic segment: a clinical and anatomical analysis. *J Neurosurg*. 1990;72(5):677-691.
22. Sherif C, Gruber A, Dorfer C, et al. Ruptured carotid artery aneurysms of the ophthalmic (C6) segment: clinical and angiographic long term follow-up of a multidisciplinary management strategy. *J Neurol Neurosurg Psychiatry*. 2009;80(11):1261-1267.
23. Sung-Chul Jin, Do Hoon Kwon, Jae-Sung Ahn, et al. Clinical and radiological outcomes of endovascular detachable coil embolization in paraclinoid aneurysms: a 10-year experience. *J Korean Neurosurg Soc*. 2009;45(1):5-10.
24. Fulkerson DH, Horner TG, Payner TD, et al. Results, outcomes, and follow-up of remnants in the treatment of ophthalmic aneurysms: a 16-year experience of a combined neurosurgical and endovascular team. *Neurosurgery*. 2009; 64(2):218-229.
25. Heran NS, Song JK, Kupersmith MJ, et al. Large ophthalmic segment aneurysms with anterior optic pathway compression: assessment of anatomical and visual outcomes after endosaccular coil therapy. *J Neurosurg*. 2007; 106(6):968-975.
26. Biondi A, Janardhan V, Katz JM, et al. Neuroform stent-assisted coil embolization of wide-neck intracranial aneurysms: strategies in stent deployment and midterm follow-up. *Neurosurgery*. 2007;61(3):460-468.
27. Iihara K, Murao K, Sakai N, et al. Unruptured paraclinoid aneurysms: a management strategy. *J Neurosurg*. 2003;99(2):241-247.
28. Hoh BL, Carter BS, Budzik RF, Putman CM, Ogilvy CS. Results after surgical and endovascular treatment of paraclinoid aneurysms by a combined neurovascular team. *Neurosurgery*. 2001;48(1):78-89.
29. Byrne JV, Sohn MJ, Molyneux AJ, Chir B. Five-year experience in using coil embolization for ruptured intracranial aneurysms: outcomes and incidence of late rebleeding. *J Neurosurg*. 1999;90(4):656-663.
30. Vinuela F, Duckwiler G, Mawad M. Guglielmi detachable coil embolization of acute intracranial aneurysm: perioperative anatomical and clinical outcome in 403 patients. *J Neurosurg*. 1997;86(3):475-482.
31. Choi DS, Kim MC, Lee SK, Willinsky RA, Terbrugge KG. Clinical and angiographic long-term follow-up of completely coiled intracranial aneurysms using endovascular technique. *J Neurosurg*. 2010;112(3):575-581.
32. Raymond J, Guilbert F, Weill A, et al. Long-term angiographic recurrences after selective endovascular treatment of aneurysms with detachable coils. *Stroke*. 2003;34(6):1398-1403.
33. Campi A, Ramzi N, Molyneux AJ, et al. Retreatment of ruptured cerebral aneurysms in patients randomized by coiling or clipping in the International Subarachnoid Aneurysm Trial (ISAT). *Stroke*. 2007;38(5):1538-1544.
34. Zhao J, Wang S, Zhao Y, et al. Microneurosurgical management of carotid-ophthalmic aneurysms. *J Clin Neurosci*. 2006;13(3):330-333.
35. Barami K, Hernandez VS, Diaz FG, Guthikonda M. Paraclinoid carotid aneurysms: surgical management, complications, and outcome based on a new classification scheme. *Skull Base*. 2003;13(1):31-41.
36. Peiris JB, Ross Russell RW. Giant aneurysms of the carotid system presenting as visual field defect. *J Neurol Neurosurg Psychiatry*. 1980;43(12):1053-1064.
37. Fries G, Perneczky A, van Lindert E, Bahadori-Mortasawi F. Contralateral and ipsilateral microsurgical approaches to carotid-ophthalmic aneurysms. *Neurosurgery*. 1997;41(2):333-342.
38. Kyoi K, Gega A, Tada T, et al. Carotid-ophthalmic aneurysms and visual abnormalities [in Japanese]. *No Shinkei Geka*. 1986;14(10):1197-1204.
39. de Oliveira JG, Borba LA, Rassi-Neto A, et al. Intracranial aneurysms presenting with mass effect over the anterior optic pathways: neurosurgical management and outcomes. *Neurosurg Focus*. 2009;26(5):E3.
40. Sung-Chul J, Do Hoon K, Jae-Sung A, et al. Clinical and radiological outcomes of endovascular detachable coil embolization in paraclinoid aneurysms: a 10-year experience. *J Korean Neurosurg Soc*. 2009;45(1):5-10.

Copyright © Congress of Neurological Surgeons. Unauthorized reproduction of this article is prohibited.

41. Batjer HH, Samson DS. Retrograde suction decompression of giant paraclinoidal aneurysms: technical note. *J Neurosurg*. 1990;73(2):305-306.
42. Beretta F, Andaluz N, Zuccarello M. Aneurysms of the ophthalmic (C6) segment of the internal carotid artery: treatment options and strategies based on a clinical series. *J Neurosurg Sci*. 2004;48(4):149-156.
43. Ng PY, Huddle D, Gunel M, Awad IA. Intraoperative endovascular treatment as an adjunct to microsurgical clipping of paraclinoid aneurysms. *J Neurosurg*. 2000;93(4):554-560.
44. Kothandaram P, Dawson BH, Kruyt RC. Carotid-ophthalmic aneurysms: a study of 19 patients. *J Neurosurg*. 1971;34(4):544-548.

Acknowledgments

We would like to thank Florian Dibra, BS, for his assistance with data collection and Mitchell G. Maltenfort, PhD, for assistance with statistical analysis.

COMMENTS

The authors present a large series of unruptured carotid-ophthalmic aneurysms. They impressively show that in the elective setting endovascular therapy leads to excellent clinical results. The authors' proposed treatment strategy is based on a first-line endovascular approach with surgery reserved for those patients unsuitable for embolization. The theoretical drawbacks of embolization in this particular location are the relatively high recanalization rates and the probability of embolism of the ophthalmic artery. To minimize these risks, several authors have presented precise treatment selection criteria. For example, proposed indications for embolization could be narrow aneurysm necks, neck calcification, or close aneurysm relation to the clinoid process. Indications for surgery could be giant/large or wide-necked aneurysms and aneurysms directly at branching sites. If direct treatment seems hazardous, indirect treatment with vessel occlusion with or without bypass protection is a safe option. The challenge is to select the best treatment modality with the lowest risk for the patient on a case-by-case analysis.

Camillo Sherif
Vienna, Austria

The authors present a large body of work detailing their experience with endovascular treatment of unruptured carotid-ophthalmic aneurysms. They have shown in a high-volume cerebrovascular center that endovascular outcomes can be remarkable, and compared with their equally respectable microsurgical experience, there is a clear improvement in clinical outcomes with their approach. I applaud the authors for their diligence and hard work in not only presenting their data but also looking in the mirror and making sure that their approach is the best approach for them.

The unruptured aneurysm population represents a burden to treating physicians. These are often patients who are asymptomatic, and in most cases, their aneurysms are unlikely to rupture. Yet because of the potential bad outcome if they do rupture, many are treated. This "preventive" approach is certainly worthy of discussion, and the TEAM trial attempted to answer whether we should even be treating unruptured aneurysms endovascularly. Unfortunately, without clear evidence, we must do what we feel is best for the patient using our current (incomplete) data. One thing is certain: In the majority of the unruptured aneurysm population, in which there is a very low risk of rupture, there can be zero tolerance for poor outcomes or adverse events; thus, those who desire to treat unruptured aneurysms should do so in the safest manner possible (clip or coil) at their particular center and meticulously track their results, or they should refer the patients to a high-volume cerebrovascular center that has outstanding outcomes.

Raymond Turner
Charleston, South Carolina

ALERT ME WHEN CITED

Identify an article and receive an email alert whenever that article appears in another article's reference list.

1. At the Neurosurgery Online home page (*http://www.neurosurgery-online.com*), click Login. If you have not yet registered, you will be prompted to do so.

2. Find the article you wish to add to your Alert Me When Cited notifications. Click on the Alert Me When Cited link in the Article Tools sidebar box.

3. You can manage your Citation Alerts from within the My eTOCS and Alerts tab of your account settings.

Scan the QR Code to access video tutorial

NEUROSURGERY

Copyright © Congress of Neurological Surgeons. Unauthorized reproduction of this article is prohibited.

Endoscopic Port Surgery for Resection of Lesions of the Cerebellar Peduncles: Technical Note

Pawel G. Ochalski, MD*

Juan C. Fernandez-Miranda, MD*

Daniel M. Prevedello, MD*

Ian F. Pollack, MD‡

Johnathan A. Engh, MD*

*Department of Neurological Surgery, University of Pittsburgh Medical Center, Pittsburgh, Pennsylvania; ‡Department of Pediatric Neurosurgery, The Children's Hospital of Pittsburgh, Pittsburgh, Pennsylvania

Correspondence:
Johnathan A. Engh, MD,
Department of Neurological Surgery,
University of Pittsburgh Medical Center,
200 Lothrop St, Ste B-400, Pittsburgh,
PA 15213.
E-mail: enghja@upmc.edu

Received, April 8, 2010.
Accepted, October 8, 2010.

Copyright © 2011 by the
Congress of Neurological Surgeons

BACKGROUND: Mass lesions of the inferior, middle, and superior cerebellar peduncles (cerebellar peduncle complex [CPC]) present numerous surgical pitfalls when resection or debulking is warranted. Success has been achieved through multiple approaches, but complications can be severe.

OBJECTIVE: To report the surgical technique for and clinical results of the treatment of lesions in the CPC with an endoscopic port via a lateral transcerebellar corridor.

METHODS: Three patients underwent resection of intrinsic lesions of the CPC via a lateral transcerebellar approach with an endoscopic port. Deployment of the port was performed with frameless image-guided placement into the area of interest. Resection was performed using bimanual microsurgical technique under parallel endoscopic visualization.

RESULTS: Three patients 43, 27, and 13 years of age underwent successful resection of lesion in the CPC. Histopathological diagnosis consisted of cavernous malformation, glioblastoma multiforme, and a juvenile pilocytic astrocytoma. All had complete gross total resection except for the patient with a high-grade glioma. Clinically, all had excellent outcomes, with 1 patient suffering postoperative facial palsy after resection of her high-grade glioma.

CONCLUSION: The lateral transcerebellar approach to the CPC with an endoscopic port may be a feasible alternative to standard microsurgical resection in such difficult cases. Careful patient selection is critical to identify those who may be suitable for endoscopic port surgery on the basis of clinical, radiographic, and anatomical considerations.

KEY WORDS: Endoscopic port surgery, Neuroendoport, Transcerebellar approach

Neurosurgery 68:1444–1451, 2011 DOI: 10.1227/NEU.0b013e31820b4f6a www.neurosurgery-online.com

Open surgical resection of intrinsic mass lesions of the inferior, middle, and superior cerebellar peduncles (cerebellar peduncle complex [CPC]) can be technically challenging because of both the deep location and the proximity to critical surrounding neural structures, especially the pons. As a result, many such lesions are treated with stereotactic biopsy for histopathological diagnosis and adjuvant therapy. Some authors recommend that surgical intervention in this region be limited to aspiration of cysts or abscesses with stereotactic techniques.[1,2] However, recent advances in magnetic resonance imaging (MRI) technology, image guidance, and microneurosurgical techniques have enabled surgeons to safely pursue open surgical resections within this region with favorable outcomes.[3-6]

ABBREVIATIONS: CPC, cerebellar peduncle complex; **EPS,** endoscopic port surgery

We have developed an approach to the CPC through the lateral cerebellar hemisphere using an endoscopic port. Use of this approach is based on the technique of stereotactic surgery, which has historically enabled a safe access to the CPC via a transcerebellar approach[1,7] or a transfrontal approach.[8,9] The concept was initially developed by modifying the work of Dr Patrick Kelly, who pioneered a 20-mm-diameter stereotactic tubular retraction system for the microscopic resection of deep brain tumors.[8-11] Although the use of the endoscopic port requires partial disruption of the cerebellar hemisphere, advantages include avoidance of critical neural structures

Copyright © Congress of Neurological Surgeons. Unauthorized reproduction of this article is prohibited.

abutting the fourth ventricular floor and obviation of brain retraction. Three illustrative cases are presented (Table).

SURGICAL TECHNIQUE

Deployment of the endoscopic port is performed according to a previously described technique.[12,13] The anesthetized patient is placed in the lateral position with slight flexion and contralateral rotation of the neck. A 3-cm paramedian linear incision is performed behind the ear, and a 2-cm craniectomy is performed directly above the lateral cerebellar hemisphere, approximately 1 cm below the transverse sinus at its most superior extension. Cruciate dural opening is performed, and a 3-mm cortisectomy is made on the cerebellar surface. Subsequently, with the use of frameless image guidance, a 2-mm brain needle (Elekta, Inc, Stockholm, Sweden) is advanced through the cortical-pial surface, and the bullet-shaped dilator is passed over the needle using gentle rotation under image guidance.[12,13] Directly overlying the dilator is a clear plastic tube, 11.5 mm in outer diameter and 5.5 to 6.0 cm in length, based on measurements performed with the preoperative MRI scan. The brain needle and dilator are then removed, and the port is secured to the scalp with sutures. A 4-mm, 0° rod-lens endoscope (Karl Storz, Inc., Tuttlingen, Germany) is brought into the port for visualization. Resection is performed using bimanual microsurgical technique facilitated by teardrop suction, pituitary forceps, scissors, and bipolar electrocautery (Figure 1). The scope and port angles are adjusted multiple times throughout the resection to facilitate dynamic lesion visualization. This technique facilitates removal of lesions much larger than the 11.5-mm port itself. After resection, meticulous hemostasis is achieved, and then the cavity is irrigated with plain saline and lined with Surgicel (Ethicon, Inc, Somerville, New Jersey). The port is removed; the cerebellar cortex is also lined with Surgicel; and the dura is then closed in a watertight fashion, with or without a dural graft. In selected cases, a titanium mesh cranioplasty may be performed. Superficial wound closure is performed in the standard fashion.

CASE REPORTS

Case 1

A 43-year-old woman presented with sudden onset of headache, diplopia, gait ataxia, and right-sided discoordination. Both computed tomography scans and MRI demonstrated a hemorrhagic lesion in the middle cerebellar peduncle on the right side, extending slightly posteriorly into the cerebellum (Figure 2). She underwent digital subtraction angiography, which showed no evidence of a vascular malformation (not pictured). The suspected diagnosis was a cavernous malformation vs a hemorrhagic brain tumor. The patient was taken to the operating room for surgical evacuation of the hematoma, both for tissue diagnosis and for alleviation of regional mass effect. With the use of an endoscopic port, image-guided hematoma evacuation and total resection were successfully performed. The histopathological diagnosis was a cavernous malformation. The patient was discharged on postoperative day 2 with improvement of her gait ataxia. By the 6-month follow-up, she was both driving and ambulating independently, with no neurological deficits.

Case 2

A 27-year-old woman was initially diagnosed with a nonenhancing lesion in her right middle cerebellar peduncle after she presented with isolated vertigo. At the time of initial presentation, she was noted to have horizontal nystagmus without any other neurological findings. The patient refused a stereotactic brain biopsy and instead underwent Gamma Knife radiosurgery for initial treatment without tissue diagnosis. Nearly 2 years after radiosurgery, the patient developed increasing gait ataxia, with right-sided facial numbness, House-Brackmann grade 2 facial palsy, and nearly total hearing loss. MRI revealed a progressive increase in the size of the lesion in the right middle cerebellar peduncle with marked peripheral contrast enhancement and local mass effect (Figure 3). It appeared that the lesion now involved both the dorsal brainstem and the superior cerebellar peduncle and had its origin in the middle cerebellar peduncle. Because of clinical and radiographic progression, the patient underwent surgical exploration for the purpose of cytoreduction and tissue diagnosis.

An image-guided transcerebellar approach to the lesion was taken with an endoscopic port. Nearly total resection was accomplished. The patient awakened with improved gait and facial numbness. The facial paresis worsened to a House-Brackmann grade 5, and a gold weight was implanted into the affected eyelid. This facial paresis improved to grade 3 within 6 weeks. Pathological diagnosis was glioblastoma multiforme, and the patient subsequently was referred for chemotherapy with temozolomide combined with fractionated radiation therapy followed by dose-intensive temozolomide. At the 7-month follow-up, the patient remained neurologically stable but with radiographic evidence of remote tumor progression within the right frontal horn of the lateral ventricle. The patient was sent for palliative chemotherapy with an alternative agent.

TABLE. Summary of Surgical Management and Histopathological Diagnosis

Case	Age, y/Sex	Cerebellar Peduncle Complex Division	Surgical Approach	Pathologic Diagnosis	Complications/Outcomes
1	43/F	Ventricular division	R transcerebellar; 6-cm endoscopic port	Cavernous malformation	None; gross total resection
2	27/F	Ventricular and brainstem division	R transcerebellar; 6-cm endoscopic port	Glioblastoma World Health Organization grade IV; Ki-67: 20%	R facial palsy; nearly total resection
3	14/M	Ventricular division	R transcerebellar; 5.5-cm endoscopic port	Pilocytic astrocytoma	None; gross total resection

Copyright © Congress of Neurological Surgeons. Unauthorized reproduction of this article is prohibited.

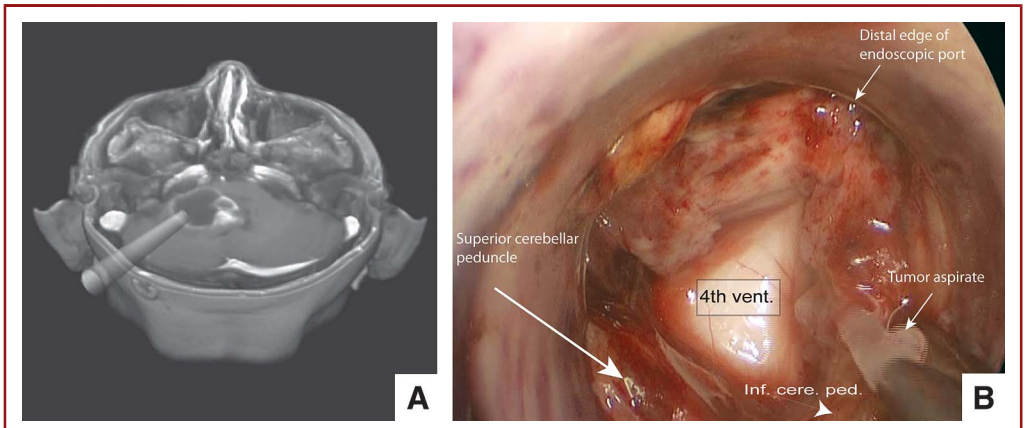

FIGURE 1. *Technique for the lateral transcerebellar approach with an endoscopic port (**A** and **B**). **A**, 3-dimensional T1-weighted postcontrast magnetic resonance axial reconstruction at the level of the pons demonstrating the simulated cannulation of the endoscopic port into the lesion. **B**, intraoperative view through the endoscopic port showing tumor resection superficial to the fourth ventricular floor with visualization of the superior and inferior cerebellar peduncles (inf. cere. ped.).*

Case 3

A 13-year-old boy presented with intermittent gait ataxia and isolated falls, with no evidence of motor weakness. A contrast-enhanced MRI scan of the head showed a small area of high signal in the left superior cerebellar peduncle with some inferior extension, most consistent with a low-grade glioma (Figure 4). Initially, his symptoms stabilized and he was managed with observation. Over a period of 2 years, serial MRI scans displayed evidence of radiographic progression, so the patient was offered surgical exploration for tissue diagnosis and attempted resection.

A transcerebellar approach with the endoscopic port was taken to the lesion with frameless image guidance. The lesion was resected without complication, and the postoperative MRI scan demonstrated no residual tumor. Pathological diagnosis was pilocytic astrocytoma. The patient developed temporary worsening of his gait ataxia, which resolved completely over the ensuing 2 weeks.

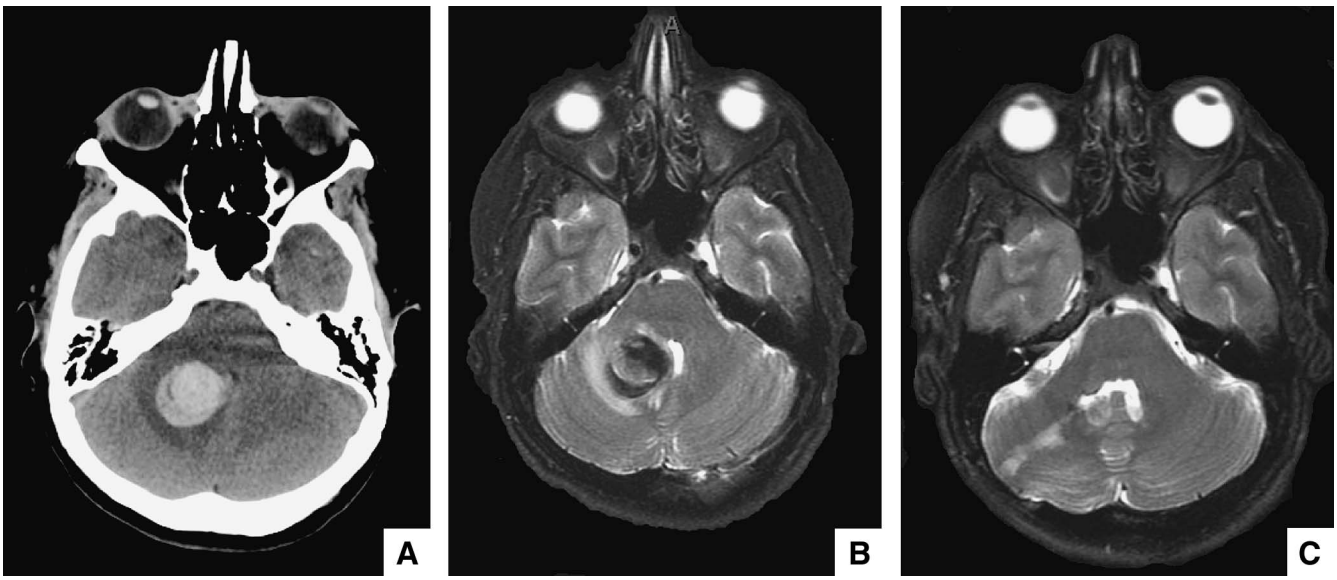

FIGURE 2. *Case 1: Axial unenhanced computed tomography (CT) scan (**A**) and magnetic resonance images (MRI; **B** and **C**) obtained on initial presentation and postoperatively. **A**, the CT scan shows a large hyperdensity within the right cerebellar peduncle complex (CPC) with extension into the cerebellum consistent with an acute hemorrhage. **B**, a T2-weighted axial image showing a mixed-intensity lesion suggestive of hemosiderin and blood product breakdown with some associated edema extending into the cerebellum. The lesion is located at the level of ventricular and cerebellar divisions of the CPC. **C**, a T2-weighted axial MRI 3.7 months postoperatively after a lateral transcerebellar endoscopic port surgery approach showing complete evacuation of the hematoma and resection of the associated cavernous malformation.*

Copyright © Congress of Neurological Surgeons. Unauthorized reproduction of this article is prohibited.

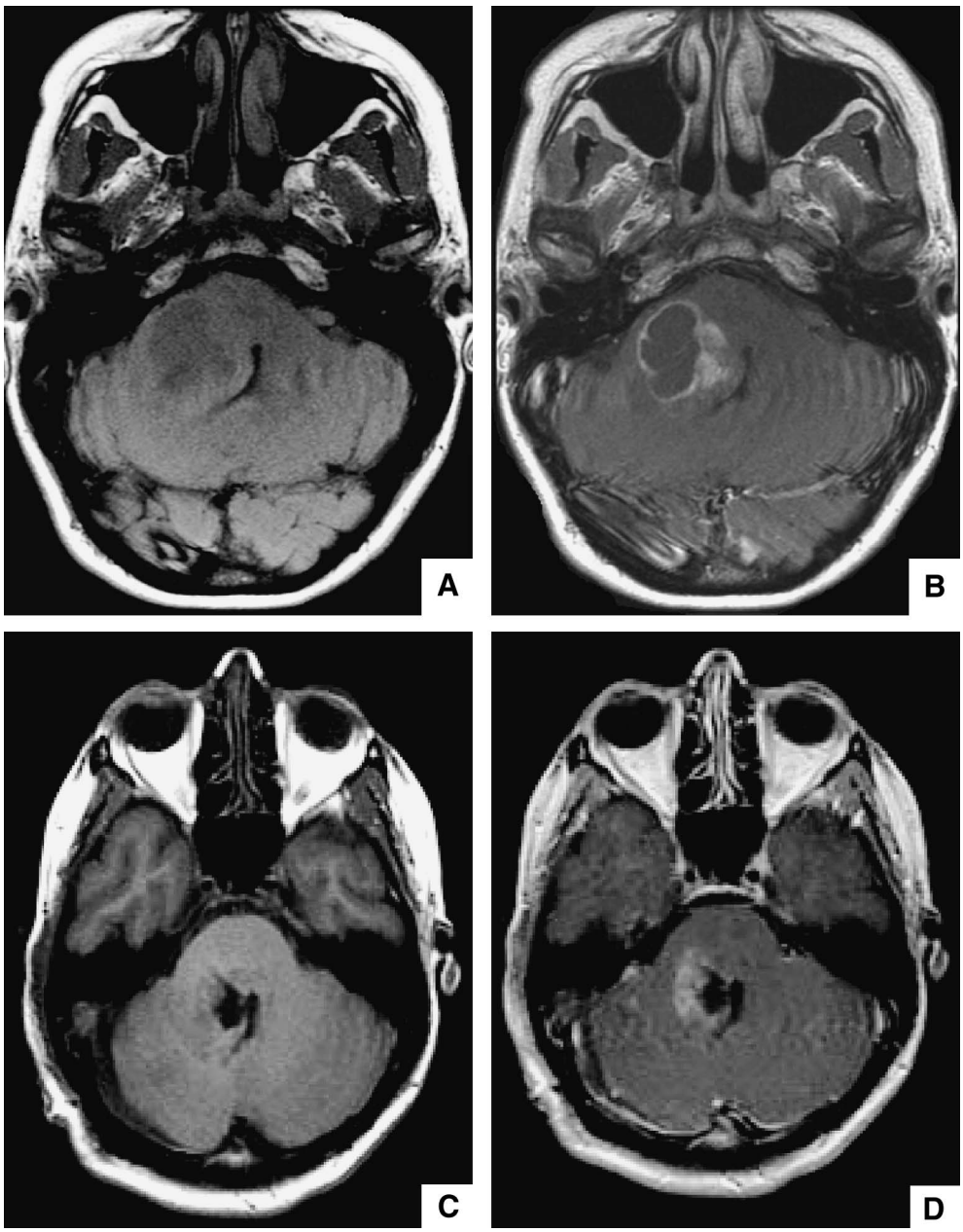

FIGURE 3. *Case 2: magnetic resonance imaging performed on initial presentation (**A** and **B**) and postoperatively (**B** and **C**) after tumor debulking. **A** and **B**, precontrast and postcontrast T1-weighted imaging showing a peripherally enhancing lesion in the cerebellar peduncle complex involving both the ventricular and brainstem divisions. **C** and **D**, T1-weighted precontrast and postcontrast imaging after resection. Some residual tumor is seen, but there has been a significant cytoreduction with resultant decompression of the fourth ventricle.*

DISCUSSION

We demonstrate the successful resection of intrinsic lesions of the CPC via a lateral transcerebellar approach using an endoscopic port. Because of the depth of these lesions below the cerebellar cortical surface, conventional microsurgical approaches to this area through the cerebellar hemisphere are not ideal. Instead, several surgical corridors for accessing lesions within the CPC, including the transventricular,[4,14-18] supracerebellar infratentorial,[6,19] retrosigmoid, and supratentorial approaches,[3,20]

Copyright © Congress of Neurological Surgeons. Unauthorized reproduction of this article is prohibited.

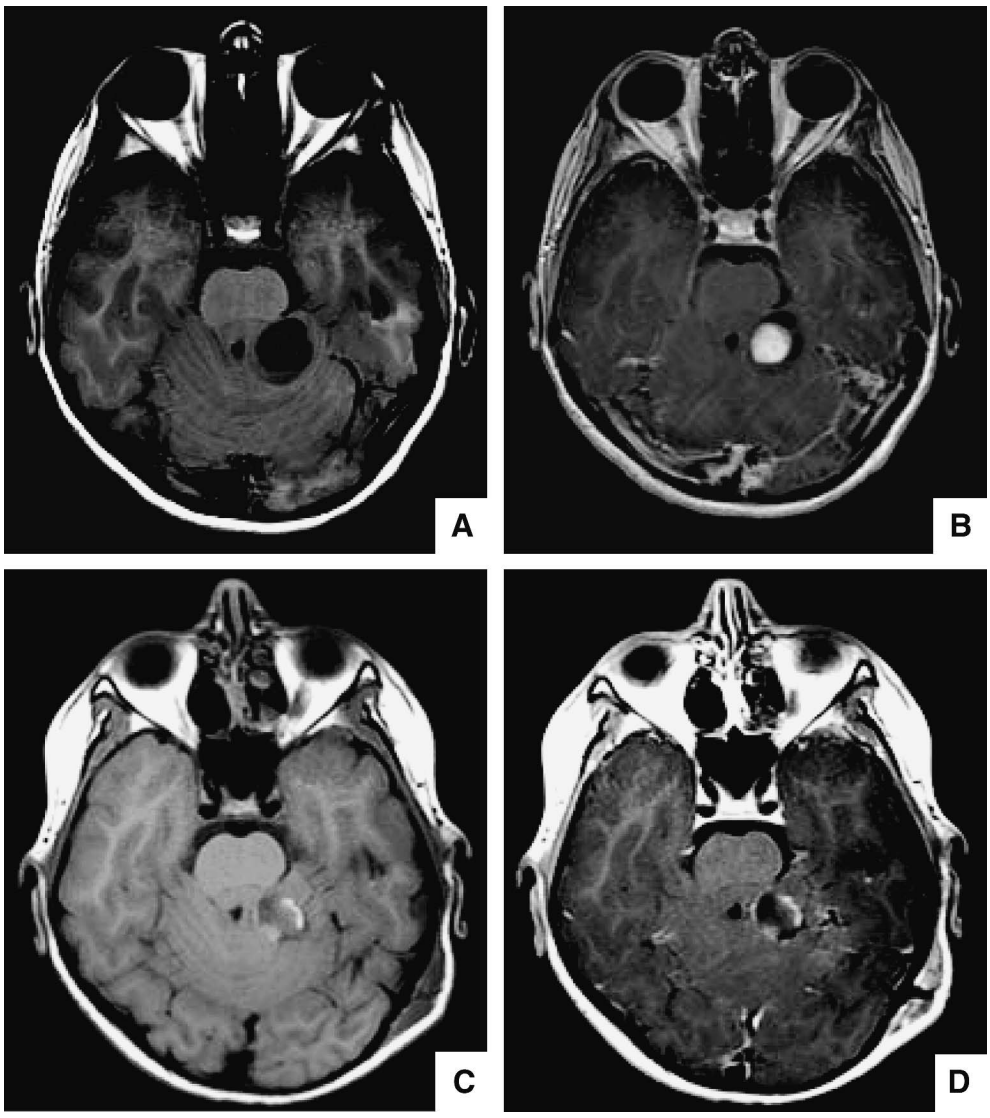

FIGURE 4. *Case 3: magnetic resonance imaging performed on initial presentation (**A** and **B**) and postoperatively (**B** and **C**) after tumor debulking. **A** and **B**, precontrast and postcontrast T1-weighted imaging showing an enhancing lesion in the cerebellar peduncle complex involving the ventricular divisions. **C** and **D**, T1-weighted precontrast and postcontrast imaging after resection. No evidence of enhancing tumor remains.*

have been advocated. Selection of the most appropriate corridor requires a thorough understanding of the neuroanatomical relationships of the CPC (Figure 5).

When viewed in the sagittal plane, the cerebellar peduncle is a complex of 3 structures consisting of (from rostral to caudal) the superior, middle, and inferior peduncles.[16] The superior cerebellar peduncle, or brachium conjunctivum, consists of efferent fibers arising from the dentate, emboliform, and globose nuclei of the cerebellum, which target the tegmentum of the midbrain. The middle cerebellar peduncle, or brachium pontis, consists of mostly afferent fibers from the pontine nuclei, which target and synapse in the cerebellum. The inferior cerebellar peduncle, also known as the restiform and juxtarestiform body, consists mainly of the spinocerebellar and olivocerebellar tracts. Another classification of the CPC, first proposed by Tomita,[4] is based on the axial plane of the CPC at the level of the pons, in which the CPC is divided into 3 separate divisions. From anteromedial to posterolateral, these divisions include the brainstem, ventricular, and cerebellar divisions (Figure 4). With this system, the location and extension of CPC lesions can be

Copyright © Congress of Neurological Surgeons. Unauthorized reproduction of this article is prohibited.

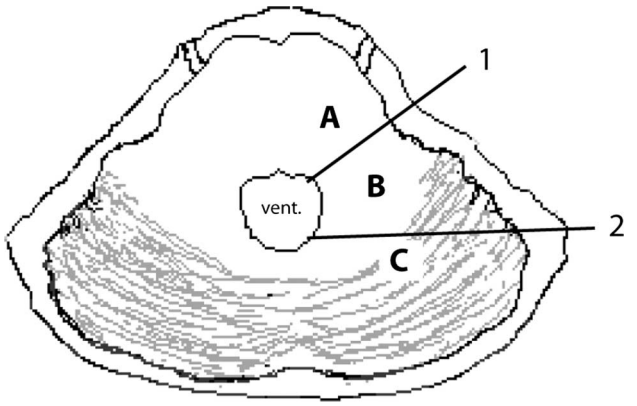

FIGURE 5. *Cerebellar peduncle complex (CPC) divisions. The CPC consists of 3 divisions based on 2 superimposed reference lines dividing the complex. Line 1 connects the anterolateral corner of the fourth ventricle and the cerebellopontine fissure. Line 2 is drawn perpendicularly to the sagittal plane of the skull through the most posterolateral corner of the fourth ventricle. This divides the CPC into brainstem (A), ventricular (B), and cerebellar (C) divisions (adapted from Tomita[4]).*

more easily evaluated and categorized radiographically among multiple patients.

For dorsal CPC lesions involving primarily the ventricular and cerebellar divisions, Tomita[4] described entry via the lateral recess of the fourth ventricle, which frequently required dissections of the posterior medullary velum as well as the vermis. In his series, he treated 4 pediatric patients with this approach, and although all patients had a favorable outcome, each had several weeks of transient postoperative ataxia. Pendl et al[17] described a transvermian approach to lesions of the CPC. Many patients in this series also had postoperative cerebellar signs and symptoms likely related to damage to the dentate nucleus, the largest of the deep cerebellar nuclei. The dentate nucleus receives afferent fibers from the premotor cortex and the supplementary motor cortex through the pontocerebellar system or middle cerebellar peduncle, and its efferents project via the superior cerebellar peduncle through the red nucleus to the ventrolateral thalamus and prefrontal and premotor cortex. More recently, Lawton et al[21] reported using a supratonsillar approach that traverses the tonsillobiventral fissure in a trajectory over the cerebellar tonsil to the inferior cerebellar peduncle. This approach differs from the transvermian and telovelar approaches to the fourth ventricle, with a more superolateral trajectory that leads instead to the inferior cerebellar peduncle. However, this approach may carry more risk of injury to the dentate nucleus.

For ventral CPC lesions, especially with abutment or involvement of the midbrain or pons, the most advocated approaches have been the subtemporal, retrosigmoid, and supracerebellar infratentorial approaches.[3,6,17,20,22] Heffez and colleagues[3] favored a retrosigmoid approach to this region, especially for lesions in the ventral brainstem. However, they also reported the use of a midline infratentorial fourth ventricular/transcerebellar technique for selected tumors. In their series, postoperative deficits were related mainly to cranial nerve palsies and gait ataxia. Both Tomita[4] and Pendl et al[17] advocated the subtemporal approach, which provided effective rostral and caudal access. Ogata and Yonekawa[6] used a paramedian supracerebellar approach first developed by Yasargil[19] to resect lesions of the superior and middle cerebellar peduncles.

The major drawback of the telovelar and transvermian approaches to lesions of the CPC is the need to expose and dissect through the lateral extent of the fourth ventricular wall, with inherent risk to associated cranial nerve nuclei, deep cerebellar nuclei, and white matter projection fibers. In addition, for lesions located more laterally within the CPC, the telovelar approach may not provide suitable lesional exposure.[21] In contrast, the retrosigmoid approach obviates the need for vermian dissection and exposure of brainstem and cerebellar nuclei, along with crossing spinocerebellar and spinocortical tracts. However, because the length and depth of the corridor are large, the disadvantage of this approach is the amount of retraction required to enable visualization with the operating microscope. This degree of retraction can be precarious in the setting of a tumor with significant regional mass effect, especially when the tumor has significant medial extension. Because of the concern of retraction injury with a subtemporal or retrosigmoid approach and the possibility of injury of the dentate nucleus with a transventricular approach, we applied endoscopic port surgery (EPS) to the lesions described in this report. Each approach has its advantages, but the most critical factors contributing to morbidity are the location of the tumor and the histopathology. In general, lesions located in the ventricular and cerebellar divisions of the peduncle are less challenging to resect than lesions of the brainstem division because of the critical nuclei in this region of the peduncle and brainstem. In addition, well-circumscribed lesions of low vascularity are generally less surgically challenging than poorly delineated, highly vascular lesions. These principles were corroborated by the cases presented here, in which the only neurological complication (worsening of facial palsy) was encountered in the patient with the most ventral, aggressive, and highly infiltrative tumor.

Careful patient selection is critical to identify those who may be suitable for EPS based on clinical, radiographic and anatomical considerations. Surgical resection should generally be considered in those patients who develop evidence of progressive neurological deficit combined with regional mass effect. All patients undergo informed consent before EPS or any other procedure. We specifically discuss the options of observation, surgical resection, and nonsurgical treatment. Once a patient opts for surgical treatment, we discuss the use of EPS as a means of resecting tumors in deep regions in an attempt to avoid damage to surrounding neurovascular structures.

The goals of EPS are similar to the goals of conventional microsurgical tumor resection: maximal tumor resection with functional neurological preservation. Our technique, as demonstrated in Figure 2, requires the creation of a corridor through the

Copyright © Congress of Neurological Surgeons. Unauthorized reproduction of this article is prohibited.

lateral cerebellar hemisphere. This approach clearly disrupts a greater volume of tissue than creating an opening through the lateral edge of the cerebellar peduncle. Thus, the transcerebellar approach described may appear counterintuitive to conventional microsurgical teaching, which generally advocates approaching intra-axial lesions via an entry point with the shortest distance to the lesion that avoids eloquent cortex. However, this channel through the lateral cerebellum may have less adverse consequences than retraction of an edematous cerebellum combined with dissection into the cerebellum and the peduncular complex to improve visualization and removal of this lesion. Therefore, we favor the transcerebellar trajectory as an alternative approach in this particular case. If the lesion presents to the lateral pial surface of the CPC, then a retrosigmoid microsurgical approach is generally recommended. However, if the lesion is subpial, then the image-guided lateral transcerebellar approach with the endoscopic port facilitates direct visualization of CPC lesions while limiting brain retraction, with potentially less trauma to the CPC than microscopic approaches using retractors to separate the white matter. However, appropriate experience with EPS is paramount to achieving acceptable outcomes in such complex cases.

CONCLUSION

Mass lesions of the cerebellar peduncles can be challenging to resect. An image-guided approach to the middle and superior cerebellar peduncles through the lateral cerebellar hemisphere with an endoscopic port may be a feasible alternative to conventional microsurgical resection in selected cases. Both careful patient selection and an understanding of the relevant neuroanatomy are necessary to achieve reasonable outcomes with this procedure.

Disclosure

The authors have no personal financial or institutional interest in any of the drugs, materials, or devices described in this article.

REFERENCES

1. Coffey RJ, Lunsford LD. Stereotactic surgery for mass lesions of the midbrain and pons. *Neurosurgery*. 1985;17(1):12-18.
2. Hood TW, Gebarski SS, McKeever PE, Venes JL. Stereotaxic biopsy of intrinsic lesions of the brain stem. *J Neurosurg*. 1986;65(2):172-176.
3. Heffez DS, Zinreich SJ, Long DM. Surgical resection of intrinsic brain stem lesions: an overview. *Neurosurgery*. 1990;27(5):789-797.
4. Tomita T. Surgical management of cerebellar peduncle lesions in children. *Neurosurgery*. 1986;18(5):568-575.
5. Epstein F, McCleary EL. Intrinsic brain-stem tumors of childhood: surgical indications. *J Neurosurg*. 1986;64(1):11-15.
6. Ogata N, Yonekawa Y. Paramedian supracerebellar approach to the upper brain stem and peduncular lesions. *Neurosurgery*. 1997;40(1):101-104.
7. Abernathey CD, Camacho A, Kelly PJ. Stereotaxic suboccipital transcerebellar biopsy of pontine mass lesions. *J Neurosurg*. 1989;70(2):195-200.
8. Kelly PJ, Goerss SJ, Kall BA. The stereotaxic retractor in computer-assisted stereotaxic microsurgery: technical note. *J Neurosurg*. 1988;69(2):301-306.
9. Kelly PJ, Kall BA, Goerss S, Earnest F IV. Computer-assisted stereotaxic laser resection of intra-axial brain neoplasms. *J Neurosurg*. 1986;64(3):427-439.
10. Morita A, Kelly PJ. Resection of intraventricular tumors via a computer-assisted volumetric stereotactic approach. *Neurosurgery*. 1993;32(6):920-926.
11. Russell SM, Kelly PJ. Volumetric stereotaxy and the supratentorial occipito-subtemporal approach in the resection of posterior hippocampus and parahippocampal gyrus lesions. *Neurosurgery*. 2002;50(5):978-988.
12. Harris AE, Hadjipanayis CG, Lunsford LD, Lunsford AK, Kassam AB. Microsurgical removal of intraventricular lesions using endoscopic visualization and stereotactic guidance. *Neurosurgery*. 2005;56(1)(suppl):125-132.
13. Kassam AB, Engh JA, Mintz AH, Prevedello DM. Completely endoscopic resection of intraparenchymal brain tumors. *J Neurosurg*. 2009;110(1):116-123.
14. Deshmukh VR, Figueiredo EG, Deshmukh P, et al. Quantification and comparison of telovelar and transvermian approaches to the fourth ventricle. *Neurosurgery*. 2006;58(4)(suppl 2):ONS202-ONS206.
15. Mussi AC, Rhoton AL Jr. Telovelar approach to the fourth ventricle: microsurgical anatomy. *J Neurosurg*. 2000;92(5):812-823.
16. Rhoton AL Jr. Cerebellum and fourth ventricle. *Neurosurgery*. 2000;47(3)(Suppl):S7–S27.
17. Pendl G, Vorkapic P, Koniyama M. Microsurgery of midbrain lesions. *Neurosurgery*. 1990;26(4):641-648.
18. Matsushima T, Fukui M, Inoue T, et al. Microsurgical and magnetic resonance imaging anatomy of the cerebello-medullary fissure and its application during fourth ventricle surgery. *Neurosurgery*. 1992;30(3):325-330.
19. Yasargil MG. Paramedian supra cerebellar approach. In: Yasargil MG, ed. *Microneurosurgery*. New York, NY: G. Thieme; 1984;1:242.
20. Jittapiromsak P, Little AS, Deshmukh P, et al. Comparative analysis of the retrosigmoid and lateral supracerebellar infratentorial approaches along the lateral surface of the pontomesencephalic junction: a different perspective. *Neurosurgery*. 2008;62(5)(suppl 2):ONS279-ONS287.
21. Lawton MT, Quinones-Hinojosa A, Jun P. The supratonsillar approach to the inferior cerebellar peduncle: anatomy, surgical technique, and clinical application to cavernous malformations. *Neurosurgery*. 2006;59(4)(Suppl 2):ONS244-ONS251.
22. Tomita T, Cortes RF. Astrocytomas of the cerebral peduncle in children: surgical experience in seven patients. *Childs Nerv Syst*. 2002;18(5):225-230.

COMMENTS

The authors have given us excellent examples of the usefulness of image-guided, endoscopically assisted port-based microsurgery. This work is essentially a modernization of the work done by Patrick Kelly in the 1980s. His was a computer-assisted, image-guided, port-based microsurgical technique for accessing and removing deep-seated tumors, mainly in the thalamus. The use of the endoscope rather than the microscope as the visual-assist device allows a much smaller port size and thus less disruption of the normal brain between the surgeon and the lesion. The approach described by the authors takes full advantage of the time-tested reliability of the transcerebellar route for stereotactic biopsy of lateral pontine or peduncular lesions and adds the ability to directly visualize and remove the lesion. This technique expands our options for managing these deep-seated lesions, and the authors are to be commended.

Franco DeMonte
Houston, Texas

Tubular retractors within the brain are not novel, but they have had a somewhat checkered history that has kept them from achieving general acceptance. This is due in part to the ongoing debate as to whether an approach that has low morbidity is minimally invasive and whether this definition should be applied more properly to one that traverses less brain. The authors describe an approach that transits the cerebellum with a tubular retractor with an apparently low morbidity and good efficacy. Nonetheless, it raises understandable concern that a large amount of healthy brain must be disrupted in the technique. The cerebellum is, however, fairly tolerant of anatomical transgressions, and more traditional routes that required cerebellar manipulation from

Copyright © Congress of Neurological Surgeons. Unauthorized reproduction of this article is prohibited.

without also can ultimately result in damage to the cerebellum. The presence or absence of a deficit seems to matter the most to patients. The amount of brain tissue disrupted in an endoscopic removal of colloid cyst of the third ventricle is more by volume than the amount disrupted in a transcallosal craniotomy; however, the patient after the former procedure typically looks better and recovers faster than the patient who undergoes the latter.

This cerebellar peduncle technique is too novel to be recommended as a routine approach. A high degree of skill with this kind of surgery is required to make it work. The report presents an intriguing initial picture of an alternative way of accessing difficult lesions in this region that deserves further investigation.

Peter Nakaji
Phoenix, Arizona

Ochalski et al present their experience with 3 patients who underwent endoscopic port surgery for resection of 3 lesions located within the cerebellar peduncles. Frameless image guidance was used to insert a tube via a lateral transcerebellar approach into the lesion. The port had a diameter of 11.5 mm. Gross total resection was achieved in the 2 benign lesions. The glioblastoma was partially resected. The glioblastoma patient was the only one who developed a permanent neurological deficit (postoperative facial palsy) after the surgery. The authors concluded that the lateral transcerebellar approach to the cerebellar peduncle with an endoscopic port may be a feasible alternative to standard microsurgical resection for lesions of this area.

This is a well-written report of a modified Kelly technique. The rationale of this approach is to avoid brain retraction, the floor of the fourth ventricle, and the cranial nerves. However, the authors used a very long surgical corridor (and the corridor size is significant, ie, $>$ 11 mm in diameter) through normal cerebellar tissue to reach the lesion. This is against the opinion of most surgeons, who would prefer to approach lesions through the thinnest mantle of normal brain. When going through the subarachnoid spaces, many lesions can be approached with minimal trauma to the surrounding healthy brain. Furthermore, tumor parts located in blind corners can be resected without excessive cerebellar retraction using endoscope-assisted microsurgical techniques. The trajectory nicely depicted in Figure 2C shows the length of the approach to reach the lesion. The lateral part of the dentate nucleus also may be at risk with this approach. Nevertheless, the results obtained by the authors are promising. More cases or, even better, randomized studies are needed to prove that this approach is really superior to our microsurgical approaches used so far.

Henry W.S. Schroeder
Greifswald, Germany

Copyright © Congress of Neurological Surgeons. Unauthorized reproduction of this article is prohibited.

The Effect of Pulse Width and Contact Configuration on Paresthesia Coverage in Spinal Cord Stimulation

Jan Holsheimer, PhD*
Jan R. Buitenweg, PhD*
John Das‡
Paul de Sutter‡
Ljubomir Manola, PhD*
Bart Nuttin, MD, PhD‡

*Institute for Biomedical Technology, University of Twente, Enschede, the Netherlands; ‡Department of Neurosurgery, University Hospital Gasthuisberg, Leuven, Belgium

Correspondence:
Jan Holsheimer, PhD,
Institute for Biomedical Technology, BSS,
Building Zuidhorst,
Room 222,
University of Twente,
PO Box 217,
NL-7500 AE Enschede, Netherlands.
E-mail: jan@holsheimer.nl

Received, February 17, 2010.
Accepted, November 1, 2010.

Copyright © 2011 by the Congress of Neurological Surgeons

BACKGROUND: In spinal cord stimulation for the management of chronic, intractable pain, a satisfactory analgesic effect can be obtained only when the stimulation-induced paresthesias cover all painful body areas completely or partially.

OBJECTIVE: To investigate the effect of stimulus pulse width (PW) and contact configuration (CC) on the area of paresthesia (PA), perception threshold (V_{PT}), discomfort threshold (V_{DT}), and usage range (UR) in spinal cord stimulation.

METHODS: Chronic pain patients were tested during a follow-up visit. They were stimulated monopolarly and with the CC giving each patient the best analgesia. V_{PT}, V_{DT}, and UR were determined for PWs of 90, 210, and 450 microseconds. The paresthesia contours at V_{DT} were drawn on a body map and digitized; PA was calculated; and its anatomic composition was described. The effects of PW and CC on PA, V_{PT}, V_{DT}, and UR were tested statistically.

RESULTS: Twenty-four of 31 tests with low thoracic stimulation and 8 of 9 tests with cervical stimulation gave a significant extension of PA at increasing PW. In 14 of 18 tests (low thoracic), a caudal extension was obtained (primarily in L5-S2). In cervical stimulation the extension was predominantly caudal as well. In contrast to V_{PT} and V_{DT}, UR is not significantly different when stimulating with any CC.

CONCLUSION: PA extends caudally with increasing PW. The mechanism includes that the larger and smaller dorsal column fibers have a different mediolateral distribution and that smaller dorsal column fibers have a smaller UR and can be activated only when PW is sufficiently large. A similar effect of CC on PA is unlikely as long as electrodes with a large intercontact distance are applied.

KEY WORDS: Contact configuration, Discomfort threshold, Paresthesia, Pulse width, Spinal cord stimulation, Usage range

Neurosurgery 68:1452–1461, 2011 DOI: 10.1227/NEU.0b013e31820b4f47 www.neurosurgery-online.com

In spinal cord stimulation (SCS) for the management of chronic, intractable pain, a satisfactory analgesic effect can be obtained only when the stimulation-induced paresthesias cover all painful body areas completely or partially.[1-7] The extent of the paresthesias is influenced by both anatomic and technical variables, eg, the nerve fiber diameter, the distance between the epidural electrode and the spinal cord, the cathode-anode configuration, the pulse amplitude, and the pulse width (PW). The cathode-anode configuration and the anatomic conditions determine the shape of the stimulus-induced potential field and thus the sites where nerve fibers can be activated. These effects have been simulated by calculating the electrical potential field in a 3-dimensional model of the spinal cord and the subsequent activation of nerve fiber models.[8-10] With an unchanged shape of the electric potential field, it depends on the combination of pulse amplitude and PW, known as the strength-duration relationship, [11,12] which nerve fibers are actually activated. In addition to the threshold stimulus, an

ABBREVIATIONS: CC, contact configuration; **DC,** dorsal column; **IPG,** implantable pulse generator; **PA,** pixel count of paresthesia area at discomfort threshold; **PW,** pulse width; **RMANOVA,** repeated-measures analysis of variance; **SCS,** spinal cord stimulation; **V_{rh},** rheobase voltage; **V_{DT},** discomfort threshold; **V_{PT},** perception threshold

Copyright © Congress of Neurological Surgeons. Unauthorized reproduction of this article is prohibited.

upper limit is set to the stimulus intensity that a patient can bear: the discomfort threshold (V_{DT}). It is rather common that at V_{DT} the painful regions are not all covered with paresthesias.

Incidentally, it has been reported that increasing PW in monopolar stimulation has an effect similar to changing monopolar into bipolar stimulation, namely a caudal extension of the initially segmental, rostral paresthesia. According to Krainick et al, [13] this increase in PW resulted in a more complete paresthesia coverage in patients with lower limb pain. These authors also reported that radicular pain is evoked in monopolar rather than bipolar stimulation. This painful segmental band around the trunk at the contacts level could be diminished by increasing PW to 600 to 1500 microseconds.[13,14] Apart from the effect of PW, these observations suggest that the change of paresthesia area at V_{DT} (PA) is also associated with the contact configuration (CC) of cathode(s) and anode(s).

However, results published so far are anecdotal, and a systematic study of the effects of PW and CC on PA in a group of subjects has not yet been presented. In this study, we analyzed the influence of the stimulation parameters PW and CC on PA. Chronic pain patients using SCS were stimulated monopolarly and bipolarly or tripolarly with pulses of 90-, 210-, and 450-microsecond PWs. At the stimulus magnitude corresponding to V_{DT}, body maps of paresthesia were drawn and their areas calculated. To gain insight into the underlying mechanisms, we also documented the perception threshold (V_{PT}) and V_{DT}. These parameters were used for posthoc calculation of the usage range (UR) and fitting strength-duration curves. Hypotheses to explain the results of this study are formulated.

PATIENTS AND METHODS

Patients

Chronic pain patients with an SCS implant came to the hospital for a periodic check of the performance of their SCS system. All patients agreed to have their stimulation parameters changed during the time of the test (ie, $<$ 1 day) according to the protocol of this study. Authorization for this study was given by the Medical Ethics Committee of the University Hospitals of Leuven.

Data Acquisition

Each patient was implanted with a pulse generator (IPG), either an Itrel 3 (model 7425; Medtronic Inc, Minneapolis, Minnesota) or a Synergy (model 7427; Medtronic Inc), and a percutaneous-type epidural electrode with 4 or, in a few cases, 8 contacts. The tests for this study were performed during a standard follow-up visit of each patient, which were scheduled at regular intervals after implantation. Each patient was sitting in a similar position on a chair or a hospital bed and was asked to stay in the same position throughout the test session.

For each test, a data acquisition form, consisting of 2 parts, was entered. The first part included the patient's initials, date of the test, electrode type, IPG, and vertebral level of the contacts. The second part included the results of each single test. In this article, an electrode is defined as the implantable device that generally embodies 4 contacts where the current flow into the spinal structures takes place.

On each patient, 2 CCs were tested at 3 different PWs each. One was the CC selected for chronic stimulation (giving the best analgesia), which was generally a bipole ($^{+\ -}$) or a guarded cathode ($^{+\ -\ +}$). The second one was a monopole (cathode) with the IPG as a distant anode. The contact selected as the cathode was the same as in the first configuration. This was done to avoid a bias in V_{PT} and V_{DT} caused by different distances between the cathode and the spinal cord.

A PW of 90, 210, and 450 microseconds was used in each patient, the last one being the maximum available PW of the IPGs. The IPG output was set to 0 V, and the cathode-anode configuration used in chronic stimulation was programmed, whereas the shortest PW (90 microseconds) was selected. The pulse rate was kept constant at the value selected for chronic stimulation. Next, the output voltage was increased stepwise until the initial perception of paresthesia, and V_{PT} was noted. The voltage was then increased stepwise up to V_{DT} and was noted. The paresthesia contours at V_{DT} were drawn on the 15.5-cm-high frontal and rear-side body map, either by the patient or by the practitioner guided by the patient. Subsequently, PWs of 210 and 450 microseconds were selected, and the procedure was repeated. Finally, the whole procedure was repeated for a second test using monopolar stimulation (if available).

Calculation of the Area of Paresthesia

The contours that patients indicated as paresthesia areas on the body maps were first enhanced and filled with a red marker. The body maps were then scanned (red-green-blue color coding system) with a resolution of 150 dpi in each direction, and the red level was equalized. The result of these procedures is shown in Figure 1.

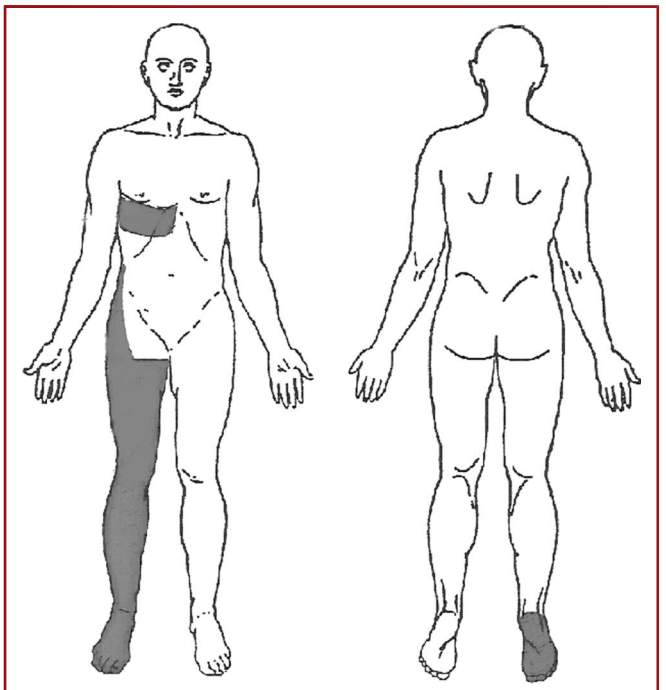

FIGURE 1. *Drawing of paresthesia contours on a body map.*

Copyright © Congress of Neurological Surgeons. Unauthorized reproduction of this article is prohibited.

Next, the body contours were removed, the contrast was enhanced, and spurious pixels and pinholes were removed with a program routine written in Matlab (Mathworks Inc, Natick, Massachusetts). This process appeared to be sufficient to identify only those pixels that represent PAs. Finally, the red pixels in the processed image were counted by the same Matlab routine. Their number represents the total PA on the frontal and rear-side of a body map.

The areas of the paresthesia drawings at V_{DT} were calculated and given as PA_{90}, PA_{210}, and PA_{450} in Kpix. The dermatomal topography of the paresthesia of each body map was determined by visual comparison with a dermatomal body map.

Calculation of UR and Strength-Duration Constants

UR was calculated from each pair of measured V_{PT} and V_{DT} according to Equation 1:

$$UR = \frac{V_{DT} - V_{PT}}{V_{PT}} = \frac{V_{DT}}{V_{PT}} - 1 \text{(modified from Law}^{4}\text{)} \quad (1)$$

To develop a hypothesis describing the relationship between PW and PA, we calculated the strength-duration time constant (τ_{sd}), or chronaxie, and the rheobase voltage (V_{rh}; minimum threshold voltage at large PW) at V_{PT} and V_{DT} of each test. A modified Lapicque equation (currents replaced by voltages) was applied to describe the strength-duration relationship[11]:

$$V_{th} = V_{rh} \cdot \left(1 + \frac{\tau_{sd}}{PW}\right) = V_{rh} \cdot \left(\frac{PW + \tau_{sd}}{PW}\right) \quad (2)$$

with V_{th} being the threshold voltage at each PW. The constants V_{rh} and τ_{sd} were obtained by fitting this relationship on the measured V_{PT} and V_{DT} using linear regression according to Weiss.[12] Only τ_{sd} and V_{rh} values obtained from linear regression lines with an explained variance of $R^2 > 0.90$ were used for further analysis.

Statistical Analysis

The outcome parameters PA, V_{PT}, V_{DT}, and UR were repeatedly measured from each single subject using different values of the independent variables PW and CC. Therefore, the effects of PW and CC on the outcome variables could be analyzed with a 2-way repeated-measures analysis of variance (RMANOVA) test. This method does not take into account differences between subjects (eg, differences in individual thresholds) but is sensitive only to variations within a subject, eg, threshold changes that might be associated with changes in PW or CC. PW was defined with 3 levels: 90, 210, and 450 microseconds; CC was defined with 2 levels: monopolar stimulation and stimulation with guarded cathodes and bipoles on adjacent contacts. Measurement data from wider bipoles were not included in this analysis because modeling studies suggest that their fields and monopolar fields are essentially the same.[15] Incomplete data sets were excluded from RMANOVA testing.

RMANOVA testing is based on the assumption that data are normally distributed. Application of the Lilliefors test of normality revealed that none of the outcome variables except UR was normally distributed. Therefore, normal distributions of PA, V_{PT}, and V_{DT} were obtained by log-transformation before 2-way RMANOVA testing was applied. This design has sufficient power ($1 - \beta = 0.80$ at $\alpha = 0.05$) to identify clinically relevant effect size indexes of 0.6 at a group size of at least 12 subjects. When a significant main effect was obtained ($P < .05$), posthoc multiple comparison testing was performed with 2-way RMANOVA on all permutations of 2 of 3 levels (in case of PW).

RESULTS

General Aspects

Twenty patients, 7 men and 13 women, were included in this study. Their mean age was 49 years. Eleven patients had Failed Back Surgery Syndrome (radicular pain), whereas 6 other patients had Complex Regional Pain Syndrome, type 2. The other 3 patients had radicular pain (tumor), spinal cord injury pain, and neuropathic pain after peripheral nerve injury, respectively.

Sixteen patients had a Pisces Quad electrode (model 3487A, 9-mm contact center distance; Medtronic, Inc) and 4 had a Pisces Compact (model 3887, 7-mm center distance; Medtronic, Inc) implanted. An electrode was implanted cervically in 5 patients and low thoracically (T7-T10) in another 15 patients.

In 15 of 20 patients (11 with an electrode placed low thoracically and 4 cervically), 2 tests have been performed in accordance to the protocol. In the first test, the configuration giving the most analgesic effect in chronic stimulation was used. This "best" configuration was never a monopole. In the second test, the cathode of this "best" configuration was used in monopolar stimulation. In 5 patients, only the "best" configuration has been tested because monopolar stimulation was not possible with the Synergy IPG. As a result of a hardware failure in 2 patients, their electrodes were replaced by a Specify (model 3998; Medtronic Inc), and their tests (13, 20a, and 20b) were repeated, as well as tests 5a, 5b, and 14.

Table 1 gives an overview of the tests and pixel counts representing PA_{90}, PA_{210}, and PA_{450} at V_{DT} of all tests and the corresponding CCs. A total of 40 tests, 9 with electrodes placed cervically and 31 with low thoracic electrodes, were performed. In 17 tests, stimulation was applied monopolarly (cathode and distant anode), 9 with a bipole on adjacent contacts, 8 with a wide bipole (on nonadjacent contacts), 5 with a guarded cathode, and 1 with a double bipole. The 8 tests with a wide bipole were excluded from the analysis of the influence of CC on PA because their bipolar field characteristic is weak and approximates the field of a monopole. In Table 1, the test numbers of the 9 pairs analyzed statistically are printed in bold.

The pulse rate was 100 pps in 34 of 41 tests. In the remaining 7 tests, the rate varied between 50 and 85 pps (mean, 74 pps).

Paresthesia Coverage

The effects of PW and CC on PA were analyzed first. In Figure 2, the PA values at V_{DT} and corresponding to levels of PW of 90, 210, and 450 microseconds are presented, and the PA values of each test are connected, thus displaying the within-subject changes. An increase in PW from 90 to 210 or 450 microseconds raised PA in 32 of 40 tests. The other 8 tests gave either a reduction of PA or no change. The median PA values are 12.15, 14.55, and 17.60 Kpix at PWs of 90, 210, and 450 microseconds, respectively. Two-way RMANOVA testing revealed that the effect of PW on PA is significant ($F = 10.75$, $P = .001$). Posthoc testing revealed that the PA values were significantly different at all PW levels: $PA_{450} > PA_{210} > PA_{90}$ (all $P < .033$). However, because of the exclusion of 5 subjects in

Copyright © Congress of Neurological Surgeons. Unauthorized reproduction of this article is prohibited.

TABLE 1. Test Results[a]

Test	PA_{90}, Kpixel	PA_{210}, Kpixel	PA_{450}, Kpixel	Contact Configurations
Thoracic				
1	66.65	67.22	67.08	Narrow bipole
2a	13.04	14.12	14.41	Wide bipole
2b	19.75	19.37	29.24	Monopole
3[b]	4.81	8.37	6.66	Wide bipole
4a	25.66	25.83	62.74	Monopole
4b	55.53	59.95	62.55	Narrow bipole
5a	33.17	33.08	41.50	Monopole
5b	36.35	53.25	52.98	Narrow bipole
6a	2.58	5.43	4.75	Monopole
6b	14.06	14.04	13.32	Narrow bipole
7	25.47	31.04	30.39	Monopole
8a[c]	10.41	38.29	73.73	Monopole
8b[c]	16.65	29.80	38.39	Narrow bipole
9a	9.85	9.90	15.18	Guarded cathode
9b	8.10	10.38	11.59	Monopole
10a	9.31	9.18	9.19	Guarded cathode
10b	1.45	3.84	24.41	Monopole
11a	5.27	11.93	13.10	Guarded cathode
11b	11.54	10.92	11.51	Monopole
12a	10.22	9.86	6.64	Wide bipole
12b	25.78	5.67	29.12	Monopole
13[b]	25.50	18.70	14.51	Wide bipole
14[c]	15.85	25.84	40.55	Guarded cathode
15	8.22	53.96	63.50	Narrow bipole
16	14.44	30.58	46.11	Double bipole
17[d]	19.37	21.42	19.39	Monopole
18a	16.55	16.49	24.39	Wide bipole
18b	34.98	25.85	28.85	Monopole
19	0.13	33.29	28.43	Narrow bipole
20a[d]	12.80	23.03	17.21	Monopole
20b[d]	13.51	32.11	17.63	Wide bipole
Cervical				
21a	2.36	4.00	3.74	Monopole
21b	6.39	7.63	1.29	Wide bipole
22a	6.37	6.22	7.66	Narrow bipole
22b	7.12	7.55	8.63	Monopole
23a	9.64	5.56	31.93	Wide bipole
23b	19.60	5.96	10.70	Monopole
24	8.35	14.26	8.58	Narrow bipole
25a	9.48	14.84	7.96	Monopole
25b	9.41	8.70	17.22	Guarded cathode

[a] PA_{90}, PA_{210}, and PA_{450}, paresthesia area in Kpixels at discomfort threshold in each single test at pulse width of 90, 210, and 450 microseconds. Test numbers followed by a and b refer to tests on same patient. Top 31 tests, low thoracic stimulation; bottom 9 tests, cervical stimulation. Bold indicates pairs of tests (a and b) used in 2-way repeated-measures analysis of variance test.
[b] Tests 3 and 13: same patient.
[c] Tests 8a, 8b, and 14: same patient but different leads.
[d] Tests 17, 20a, and 20b: same patient but different leads.

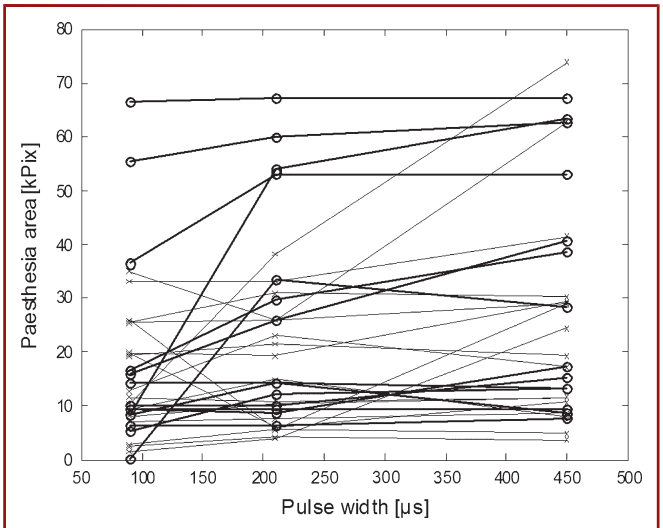

FIGURE 2. *Paresthesia areas at discomfort threshold and pulse widths of 90, 210, and 450 microseconds; 26 tests at monopolar (○, fat line) and bipolar/guarded cathode (x, thin line) stimulation.*

whom monopolar stimulation could not be applied, only 9 subjects were included in this test. As a consequence, the a priori power of this test dropped to 0.68. Furthermore, the observed effect size index for CC was still 0.61, suggesting that the nonsignificance is due to the reduced group size. Therefore, these data must be regarded as inconclusive with respect to an effect of CC on PA.

To investigate whether PA was influenced by CC, 2 CC groups were distinguished: (1) monopoles and (2) narrow bipoles and guarded cathodes. In Figure 2, these groups are designated with ○ and ×, respectively. Statistical testing did not reveal a significant effect of CC on PA ($F = 2.93$, $P = .13$).

The topography of the paresthesias at V_{DT} in low thoracic stimulation was estimated from the paresthesia body maps and is presented in Table 2. Only those tests with PA_{210} and/or PA_{450} exceeding PA_{90} by at least 25% (n = 18) were used to identify differences in the topography of paresthesia associated with different PWs. From these tests, the approximate position of the paresthesia(s) evoked by stimulation at PW = 90 microseconds is given (column 4, line 1). On line 2 of each test and an additional third line with tests 8a, 14, and 15 (continued), the main additional areas evoked at either a PW of 210 or 450 microseconds are indicated. The dermatomes corresponding to the paresthesia at PW of 90 microseconds and the additional dermatomes at PW of 210 or 450 microseconds are given in column 5.

In increasing PW from 90 to 210 or 450 microseconds in low thoracic stimulation, a caudal extension of at least 25% generally covered part of the dermatomes L5-S2 and was observed in 14 of 18 tests (types a and a + b in column 6 of Table 2). In 6 of these 14 tests, some cephalad extension was present around the L2 dermatome as well (type a + b), whereas in 4 tests, only a cephalad extension was present (type b). In cervical stimulation, the extension of paresthesia was predominantly caudal in 5 tests as well.

Thresholds and UR

To study the origins of the specific effect of PW on PA, we analyzed V_{PT}, V_{DT}, and UR. In Figure 3A and 3B, V_{PT} and

Copyright © Congress of Neurological Surgeons. Unauthorized reproduction of this article is prohibited.

TABLE 2. Topography of Paresthesia[a]

Test	PW, μs	PA, Kpixel	Paresthesia Topography	Dermatomes	a/b
2b	90	19.75	Both posterior legs, right posterior thigh, perineum	L5-S1	a
	450	29.24	Left posterior thigh	L5-S1	
3	90	4.81	Right posterior thigh	L5	a
	210	8.37	Right posterior knee	S2	
4a	90	25.66	**Left:** anterior leg + posterior leg + dorsal foot	L4-S1	a + b
	450	62.74	**Left:** anterior thigh + posterior thigh	L2-L4, L5-S2	
5a	90	33.17	**Left:** buttock + posterior thigh/leg + foot sole	L5-S2	b
	450	41.50	**Right:** inner thigh + inner leg + inner foot	L3	
5b	90	36.35	**Left:** buttock + posterior thigh/leg + foot sole	L5-S2	a
	210	53.25	**Right:** posterior thigh + posterior leg	L5-S2	
6a	90	2.58	Abdominal wall	T12	a
	210	5.43	Right anterior thigh	L3	
8a	90	10.41	Right anterior leg	L3-S1	a + b
	450	73.73	**Right:** buttock + posterior thigh + posterior leg +	L5-S2	
	450	(continued)	foot + anterior thigh; left abdomen	L2-L4	
8b	90	16.65	**Right:** posterior leg + foot sole	L4, S1	a
	450	38,39	**Right:** buttock + posterior thigh	L5-S2	
9a	90	9.85	**Right:** inner anterior thigh + inner anterior leg	L2-L4	b
	450	15.18	**Right:** buttock + posterior thigh	L5-S1	
9b	90	8.10	**Right:** inner anterior thigh + waist	T9-T10, L3	a
	450	11.59	Right inner anterior leg	L3-L4	
10b	90	1.45	Outer feet	S1	b
	450	24.41	Outer thighs + outer legs	L4-L5	
11	90	5.27	Abdomen (both sides)	L2	b
	450	13.10	Upper buttocks (both sides)	L2 (axial)	
14	90	15.85	**Left:** anterior thigh + anterior leg	L2-L3	a + b
	450	40.55	**Left:** posterior thigh, leg; complete foot	L4-S2	
	450	(continued)	**Right:** posterior thigh, anterior thighs	L2	
15	90	8.22	Right anterior thigh	L3-L4	a + b
	450	63.50	**Right:** anterior leg + foot + posterior leg + thigh	L4-S2	
	450	(continued)	**Right:** buttock + low back + abdomen	T12-L2	
16	90	14.44	Inner anterior thighs + legs	L2-L4	a + b
	450	46.11	**Left:** posterior thigh + posterior leg	L5-S2	
18a	90	16.55	**Right:** outer thigh + leg + buttock	L4-S1	a + b
	450	24.39	**Right:** low back + abdomen + waist	L3-L4	
20a	90	12.80	Ankles, right posterior leg, perineum	S1, S4	a
	210	23.03	Right posterior thigh	L5-S2	
20b	90	13.51	**Right** posterior thigh + posterior leg, ankles	L4, S1	a
	210	32.11	Right foot sole + buttock	L5, S1	

[a]All thoracic stimulation tests giving at least 25% increase of paresthesia area (PA) when pulse width (PW) is increased from 90 to 210 or 450 microseconds (columns 2 and 3). Topography of paresthesia (column 4) and corresponding dermatomes (column 5) at a PW of 90 microseconds and additional paresthesia/dermatomes at PW of 210 or 450 microseconds. Column 6 shows the extension of paresthesia caudally (a), cephalad (b), and caudally and cephalad (a + b). **Left** or **right** shows all paresthesias on the same body side.

V_{DT} are depicted vs PW for all 26 tests, with different markers for the 2 CC levels. Two-way RMANOVA testing revealed that both V_{PT} and V_{DT} were significantly influenced by PW (V_{PT}: $F = 170.99$, $P < .0001$; V_{DT}: $F = 77.49$, $P < .001$) and CC (V_{PT}: $F = 16.84$, $P = .003$, V_{DT}: $F = 26.82$, $P = .002$). In all cases, posthoc testing revealed significant differences in V_{PT} and V_{DT} between all PW levels ($P < .008$), as predicted by the strength-duration relationship.

In Figure 3C, the calculated UR values are plotted in a similar way. UR ranged from 0.1 to 2.1 and had a mean value of 0.41 (SD = 0.23). Contrary to V_{PT} and V_{DT}, no significant effects of the independent variables PW ($F = 0.089$, $P = .92$) and CC ($F = 0.379$, $P = .56$) on UR were found. The observed effect size indexes are conventionally small (0.19 and 0.12, respectively), suggesting that this nonsignificance is not likely due to a reduced test power but rather reflects a poor effect from PW and CC on UR.

Chronaxie and Rheobase

The values of τ_{sd} and V_{rh} were calculated as described earlier and are depicted by their histograms in Figure 4A and 4C. $\tau_{sd,\ PT}$ and $\tau_{sd,\ DT}$ are similarly distributed around 100 microseconds with mean values of 109 ± 12 and 99 ± 9 microseconds (mean ± SEM; n = 26), respectively. The distribution of $V_{rh,\ DT}$ is shifted

Copyright © Congress of Neurological Surgeons. Unauthorized reproduction of this article is prohibited.

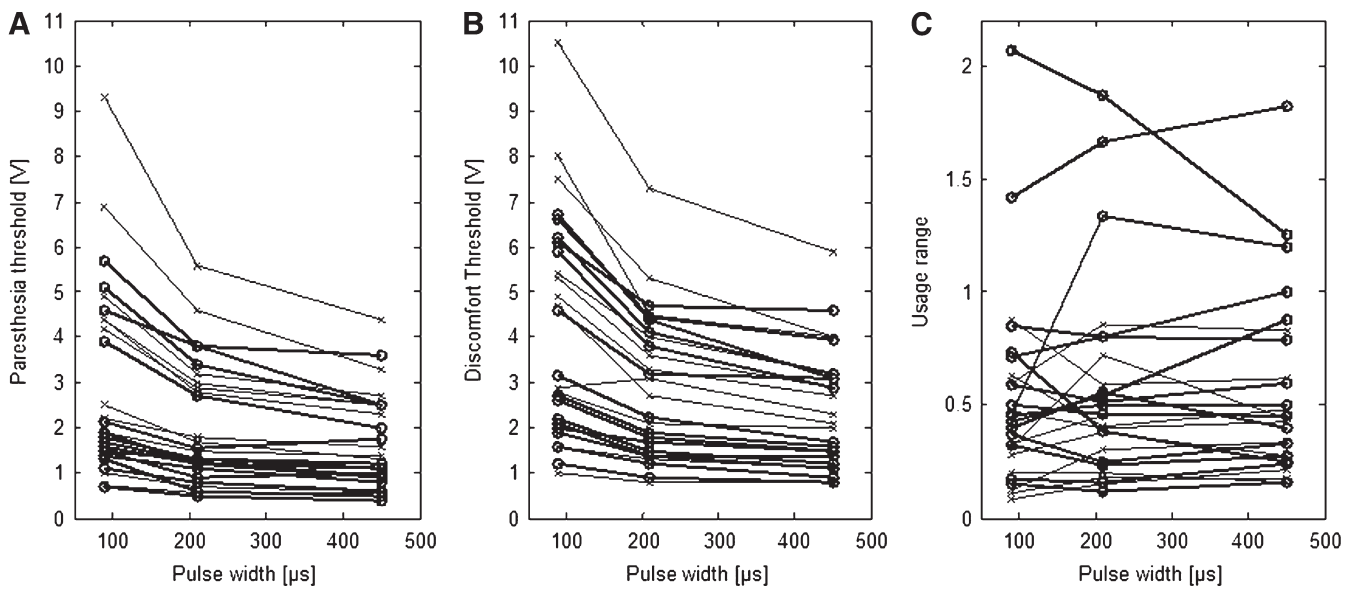

FIGURE 3. *Paresthesia thresholds (A), discomfort thresholds (B), and corresponding usage ranges (C) at pulse widths of 90, 210, and 450 microseconds; 26 tests at monopolar (○, fat line) and bipole/guarded cathode (x, thin line) stimulation.*

to slightly larger values compared with the distribution of $V_{rh,\,PT}$. This also appears from the mean values: $V_{rh,\,DT}$ = 2.0 ± 0.2 V and $V_{rh,\,PT}$ = 1.4 ± 0.2 V (mean ± SEM; n = 26). From Figure 4B and 4D, it appears that the variation of both τ_{sd} and V_{rh} originates from differences between subjects because τ_{sd} and V_{rh} derived from V_{PT} and V_{DT} data are highly correlated for individual tests (0.71 and 0.93, respectively; $P < .001$).

DISCUSSION

The primary aim of this clinical study was to reveal whether PA is influenced by PW of the stimulus pulses, as suggested by Krainick et al[13] and Burton, [14] and whether PA relates to CC. In our experiments, an increase in PW from 90 to 210 or 450 microseconds was sufficient to increase PA significantly. In contrast, Burton[14] reported that generally an increase to 600 to 1500 microseconds was required. Similarly, Krainick et al[13] reported that pulses of 1000 microseconds had to be applied to obtain an extended PA. In these studies, the reference value of PW has not been mentioned but has most likely been the usual value of 210 microseconds. The significant effect we obtained at rather small changes in PW is most likely due to our quantitative approach that used body maps and a repeated-measures test design with high statistical power.

To explore the mechanisms underlying the observed effects, V_{PT}, V_{DT}, and the corresponding UR were included as additional outcome variables. UR is considered to be associated with the maximum amount of dorsal column (DC) fibers recruited at V_{DT} and might therefore mediate changes in PA.[8] In this study, a significant effect of PW on PA, V_{PT}, and V_{DT} was found, but not on UR. The effect of PW on V_{PT} and V_{DT} immediately follows from the strength-duration relationship. Furthermore, an effect of CC on V_{PT} and V_{DT} is demonstrated, in contrast to an effect on UR, whereas an effect on PA was inconclusive. The statistical relations are summarized in Table 3.

Why Does PW Not Affect the UR?

The empirical results from this study demonstrate that PW has a significant influence on V_{PT} and V_{DT}. These threshold voltages correspond to the initial perception of paresthesia, probably evoked by the largest cutaneous Aβ fibers, and to the activation of the largest proprioceptive fibers inducing uncomfortable sensations and/or spinal reflexes.[8] The influence of PW on both V_{PT} and V_{DT} is given by the strength-duration relationship (see Equation 2). Hence, by substitution of Equation 1 in Equation 2, UR can be expressed in the strength-duration constants τ_{sd} and V_{rh} of the corresponding fibers:

$$UR = \frac{V_{\mathrm{rh,DT}} \cdot \left(\mathrm{PW} + \tau_{\mathrm{sd,DT}}\right)}{V_{rh,PT} \cdot \left(\mathrm{PW} + \tau_{\mathrm{sd,PT}}\right)} - 1 \qquad (3)$$

Because $\tau_{sd,PT}$ and $\tau_{sd,DT}$ have similar distributions and a minor difference between their mean values (109 and 99 microseconds, respectively), Equation 3 can be reduced to Equation 4, in which UR is influenced only by $V_{rh,\,PT}$ and $V_{rh,\,DT}$, not by PW:

$$UR \approx \frac{V_{\mathrm{rh,DT}}}{V_{\mathrm{rh,PT}}} - 1 \qquad (4)$$

As a result, the statistical analysis yielded a nonsignificant effect of PW on UR.

Copyright © Congress of Neurological Surgeons. Unauthorized reproduction of this article is prohibited.

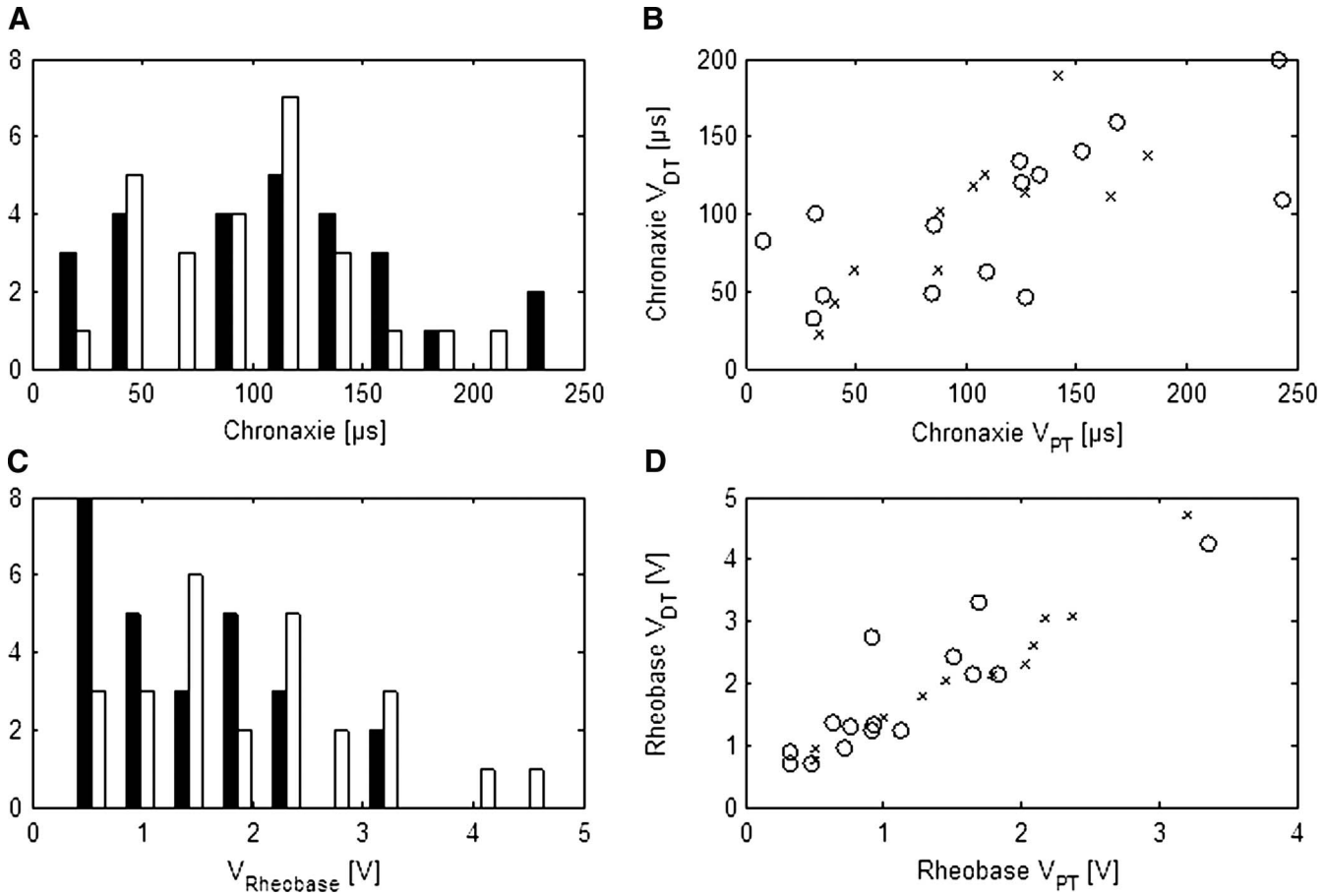

FIGURE 4. *Distributions of chronaxie (**A**) and rheobase (**C**) obtained by fitting Equation 2 on the measured perception threshold (V_{PT}; black bars) and discomfort threshold (V_{DT}; white bars) at all 3 pulse widths; 26 tests. **B**, correlation of chronaxie at V_{PT} (x axis) and V_{DT} (y axis). **D**, correlation of rheobase at V_{PT} (x axis) and V_{DT} (y axis); 26 tests at monopolar (o) and bipolar/guarded (x) cathode stimulation.*

To obtain a correct estimate of τ_{sd} and V_{rh}, these parameters should be calculated from PWs and threshold currents. However, until a few years ago, IPGs were voltage-controlled sources, as are the pulse generators used in this study. As shown in an in vitro study on deep brain stimulation electrodes, τ_{sd} calculated from voltage instead of current-controlled pulses are underestimated by 30% to 40%.[16] When compensating our empirical τ_{sd} data for this bias, the mean value of eg $\tau_{sd,\ PT}$ would rise from 109 to about 144 microseconds.

TABLE 3. Relations Between Independent Variables and Output Parameters[a]

	V_{PT}	V_{DT}	UR	PA
PW	0.0001	0.0001	**0.915**	0.0011
CC	0.0034	0.0021	**0.561**	[b]

[a]CC, contact configuration; PA, paresthesia area; PW, pulse width; UR, usage range; V_{DT}, discomfort threshold; V_{PT}, perception threshold. Tested by 2-way repeated-measures analysis of variance. Bold indicates nonsignificant.
[b]Inconclusive.

Does PW Influence the Recruitment of Smaller Nerve Fibers?

Because large DC fibers have a lower V_{rh} and τ_{sd} than smaller fibers, they are more easily activated (see elsewhere[17–20] for experimental and modeling studies on the inverse relationship between fiber diameter and τ_{sd}). Therefore, V_{PT} is most likely related to the activation of the largest DC fibers. Because we have shown that $\tau_{sd,PT}$ and $\tau_{sd,DT}$ have similar values, V_{DT} is probably related to the activation of large fibers as well. However, at stimulation amplitudes exceeding V_{PT}, DC fibers with a smaller diameter and a threshold $V_{small} > V_{PT}$ might be activated and might contribute to the paresthesia as well. Similar to large fibers, the

Copyright © Congress of Neurological Surgeons. Unauthorized reproduction of this article is prohibited.

activation of smaller fibers is limited by V_{DT}. In analogy to Equation 3, a UR for smaller fibers (UR_{small}) can be defined:

$$UR_{small} = \frac{V_{DT}}{V_{small}} - 1 = \frac{V_{rh,DT} \cdot (PW + \tau_{sd,DT})}{V_{rh,small} \cdot (PW + \tau_{sd,small})} - 1 \quad (5)$$

Note that UR_{small} has not been determined empirically. Because $\tau_{sd,\ small}$ is assumed to be larger than $\tau_{sd,\ DT}$, a simplification as made in Equation 4 is not allowed. Contrary to UR of large fibers, UR_{small} will be reduced when PW is small compared with $\tau_{sd,\ small}$. In Figure 5A, the strength-duration curves related to V_{PT} (solid line) and V_{DT} (dotted line), based on the estimated mean of V_{rh} and τ_{sd}, are depicted. Additionally, the strength-duration curve of a hypothetical, smaller fiber with a larger $V_{rh,\ small}$ (1.50 V) and $\tau_{sd,\ small}$ (200 microseconds) is presented (dashed line). From these curves, the corresponding UR and UR_{small} are calculated and depicted in Figure 5B. As expected and confirmed by empirical data, [21] UR remains at an almost constant level of about 0.4 (solid line), whereas UR_{small} has a value below 0 when PW $<$ 150 microseconds and increases with PW to a maximum value of 0.1 (dashed line). This implies that at PW $\leq$ 150 microseconds, fibers of the corresponding smaller diameter will not be recruited.

Why Does an Increase in PW Extend Paresthesia in a Caudal Direction?

We hypothesize that the intensity of the perceived paresthesia rises with the number of activated DC fibers in the corresponding somatotopic DC region and that an extension of the paresthesia toward more caudal dermatomes originates from an inhomogeneity of the mediolateral nerve fiber distribution in the DCs. Therefore, relevant aspects of this fiber distribution are presented first.

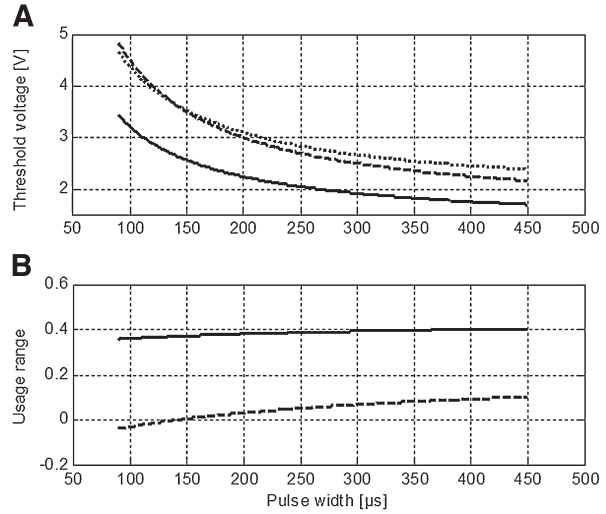

FIGURE 5. A, *strength-duration (s-d) curves from largest dorsal column fibers (L-fibers) determining perception threshold (V_{PT}; solid line) and discomfort threshold (V_{DT}; dotted line), based on averaged s-d constants (see Figure 4A and 4C); the dashed line represents a hypothetical curve for smaller fibers (S-fibers) with larger rheobase and chronaxie.* **B**, *usage range vs pulse width calculated from the s-d curves of L-fibers (solid line) and S-fibers (dashed line).*

The diameter of the largest human DC fibers is about 16 µm, and fiber density is inversely related to fiber diameter. On the basis of the morphometric study of the superficial 300-µm layer of the low thoracic DCs by Feirabend et al, [22] we distinguished 2 fiber size ranges: largest (L) fibers, with a transverse area $\geq$ 70 µm² (diameter $\geq$ 9.4 µm) and smaller (S) fibers, with an area of 40 to 70 µm² (diameter, 7.1–9.4 µm). The latter have a rather homogeneous mean fiber size and density (mean of 2.64 fibers/1000 µm²), as indicated by the gray area in the middle of Figure 6A through 6D, covering the full mediolateral extent of the DCs. In contrast, the L-fibers have an inhomogeneous density distribution, being highest (0.60 fibers/1000 µm²) at approximately 75% of the lateral extent of a DC, as shown bilaterally by the gray ovals in the top of Figure 6A through 6D and being lowest (0.24 fibers/1000 µm²) medially and 100% laterally.[22]

Modeling studies suggest that SCS electrodes, when placed on the midline of the spinal cord and programmed as a guarded cathode or a narrow bipole, result in the largest recruitment areas in the DCs, ie, at V_{DT}. These areas cover a large span from left to right, as shown by the dashed line in Figure 6A.[15] An off-midline position of the electrode reduces the recruitment area on the contralateral side. The resulting asymmetrical recruitment area extends from the ipsilateral side to the medial DC area, as shown by the dashed line in Figure 6B.

Two aspects of the recruitment areas should be noted. First, recruitment areas define the area in which DC fibers can be activated if present in this area. In turn, the presence of these fibers depends on the diameter-specific spatial distribution as described above. Therefore, most activated L-fibers in the recruitment area will be located laterally (Figure 6A and 6C, top). Second, because both PW and fiber size influence the fiber activation threshold, recruitment areas at V_{DT} depend on the fiber size and on PW. For example, at a PW of 90 microseconds, no S-fibers will be activated (see previous discussion); hence, a recruitment area exists only for L-fibers (Figure 6A and 6B, top and middle). At PW of 450 microseconds, the recruitment area for L-fibers is increased and a recruitment area for S-fibers is present (Figure 6C and 6D, top and middle).

In combination, these 2 aspects may explain the observed extension of paresthesia in a caudal direction when PW is increased. When PW is small (in this example, PW is 90 microseconds), only L-fibers are activated. Based on the first hypothesis from this section, the perceived intensity of paresthesia is expected to be highest in the dermatomes corresponding to the somatotopic representation of these lateral DC fibers. Hence, patients can be expected to report these dermatomes when drawing paresthesia maps as obtained in this study. When PW is increased (in this example to 450 microseconds), a dorsomedial superficial recruitment area of smaller fibers arises. Contrary to

Copyright © Congress of Neurological Surgeons. Unauthorized reproduction of this article is prohibited.

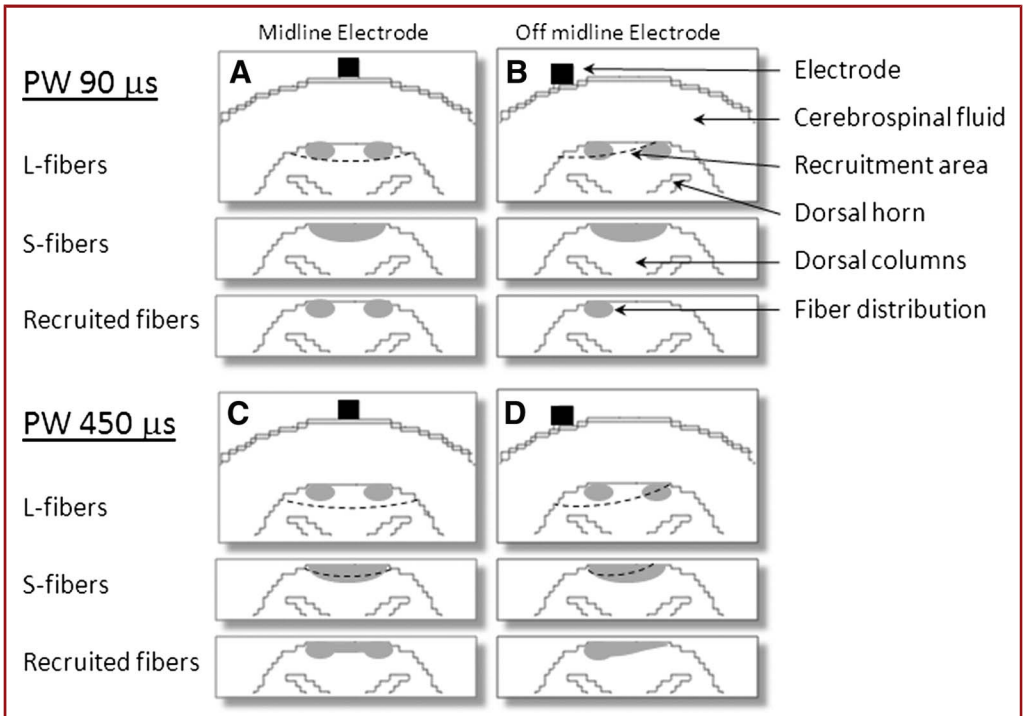

FIGURE 6. *Illustration of the hypothesis on the caudal extension of the paresthesia area shown in a transverse section of the spine at short pulse width (**A** and **B**) and long pulse width (**C** and **D**); midline (**A** and **C**) and off-midline electrode position (**B** and **D**). Gray ovals and dashed lines (top) indicate areas of highest density and ventral boundary of the recruitment area of the largest (L-) dorsal column fibers (ie, at discomfort threshold [V_{DT}]), respectively. Middle, the more abundant and homogeneously distributed small (S-) fibers (gray areas) and their recruitment area (dashed lines) for small (**A** and **B**) and large (**C** and **D**) values of pulse width (note that no S-fibers are activated at small pulse width; no dashed lines). Bottom, the resulting activated populations of both L- and S-fibers, ie, all fibers located within their specific recruitment areas.*

the L-fibers, these S-fibers are much more homogeneously distributed. As a consequence, the total number of activated fibers will increase by the superposition of activated L- and S-fiber populations. Furthermore, the total spatial distribution of activated fibers will be dominated by the more abundantly present (10-fold higher density) and more medially activated S-fibers (Figures 6C and 6D, bottom). Taking into account the somatotopic organization of the DCs, this can explain the observed caudal extension of the paresthesia. Furthermore, even the observed transitions from unilateral to bilateral paresthesia (eg, Table 2, tests 5a, 5b, and 14) are covered by this explanation. A similar study with similar outcome has been presented by Yearwood, Hershey, Bradley, and Lee.[23]

CONCLUSION

It has been shown empirically that an insufficient paresthesia coverage on the caudal side of the pain area can be compensated by increasing PW. It is likely that the largest coverage of the pain area will be obtained when a large PW is used while the stimulation is directed to the part of the DCs corresponding to the painful dermatomes. It is hypothesized that in addition to the largest DC fibers, smaller fibers may contribute substantially to the paresthesia when PW is sufficiently large. To validate this hypothesis additional, clinical data and computer modeling studies are needed. A preliminary modeling study of the effect of PW and fiber size on fiber recruitment has been presented (Lee DC, Hershey B, Bradley K, Moffitt M, Peterson D, Yearwood T. Dorsal column selectivity in pulse width programming of spinal cord stimulation: computational model for the sacral shift. Poster presented at: 11th Annual Meeting of the North American Neuromodulation Society; 2007; Acapulco, Mexico).

Disclosure

Dr Manola is currently an employee of Boston Scientific, Neuromodulation Division. The authors have no personal financial or institutional interest in any of the drugs, materials, or devices described in this article.

Copyright © Congress of Neurological Surgeons. Unauthorized reproduction of this article is prohibited.

REFERENCES

1. Nashold BS Jr, Friedman H. Dorsal column stimulation for control of pain. Preliminary report on 30 patients. *J Neurosurg*. 1972;36(5):590-597.
2. Burton CV. Session on spinal cord stimulation: safety and clinical efficacy. *Neurosurgery*. 1977;1(2):164-165.
3. Urban BJ, Nashold B. Percutaneous epidural stimulation of the spinal cord for relief of pain. Long-term results. *J Neurosurg*. 1978;48(3):323-328.
4. Law JD. Spinal stimulation: statistical superiority of monophasic stimulation of narrowly separated, longitudinal bipoles having rostral cathodes. *Appl Neurophysiol*. 1983;46(1-4):129-137.
5. North RB, Fowler K, Nigrin DJ, Szymanski R. Patient-interactive, computer-controlled neurological stimulation system: clinical efficacy in spinal cord stimulator adjustment. *J Neurosurg*. 1992:76(6):967-972.
6. North RB, Ewend MG, Lawton MT, Piantadosi S. Spinal cord stimulation for chronic, intractable pain: superiority of "multi-channel" devices. *Pain*. 1991;44(2):119-130.
7. Barolat G, Massaro F, He J, Zeme S, Ketcik B. Mapping of sensory responses to epidural stimulation of the intraspinal neural structures in man. *J Neurosurg*. 1993;78(2):233-239.
8. Holsheimer J. Effectiveness of spinal cord stimulation in the management of chronic pain: analysis of technical drawbacks and solutions. *Neurosurgery*. 1997;40(5):990-996; discussion 996-999.
9. Holsheimer J, Wesselink WA. Effect of anode-cathode configuration on paresthesia coverage in spinal cord stimulation. *Neurosurgery*. 1997;41(3):654-659.
10. Holsheimer J. Computer modelling of spinal cord stimulation and its contribution to therapeutic efficacy. *Spinal Cord*. 1998;36(8):531-540.
11. Lapicque L. Recherches quantitatifs sur l'excitation électrique des nerfs traité comme un polarisation. *J Physiol (Paris)*. 1907;9:622-635.
12. Weiss G. Sur la possibilité de rendre comparables entre eux les appareils servant à l'excitation electrique. *Arch Ital Biol*. 1901;35:413-446.
13. Krainick JU, Thoden U, Riechert T. Spinal cord stimulation in post-amputation pain. *Surg Neurol*. 1975;4(1):167-170.
14. Burton C. Dorsal column stimulation: optimization of application. *Surg Neurol*. 1975;4(1):171-176.
15. Manola LJ, Holsheimer J, Veltink PH. Technical performance of percutaneous leads for spinal cord stimulation: a modeling study. *Neuromodulation*. 2005;8(2):88-99.
16. Holsheimer J, Dijkstra EA, Demeulemeester H, Nuttin B. Chronaxie calculated from current-duration and voltage-duration data. *J Neurosci Methods*. 2000; 97(1):45-50.
17. Jankowska E, Roberts WJ. An electrophysiological demonstration of the axonal projections of single spinal interneurones in the cat. *J Physiol*. 1972;222(3):597-622.
18. Nowak LG, Bullier J. Axons, but not cell bodies, are activated by electrical stimulation in cortical gray matter: I. Evidence from chronaxie measurements. *Exp Brain Res*. 1998;118(4):477-488.
19. Wesselink WA, Holsheimer J, Boom HB. A model of the electrical behaviour of myelinated sensory nerve fibres based on human data. *Med Biol Eng Comput*. 1999;37(2):228-235. Erratum in: *Med Biol Eng Comput*. 1999;37(4):543.
20. West DC, Wolstencroft JH. Strength-duration characteristics of myelinated and non-myelinated bulbospinal axons in the cat spinal cord. *J Physiol*. April 1983;337:37-50.
21. He J, Barolat G, Ketcik B. Stimulation usage range for chronic pain management. *Analgesia*. 1994;1(1):75-80.
22. Feirabend HKP, Choufoer H, Ploeger S, Holsheimer J, van Gool JD. Morphometry of human superficial dorsal and dorsolateral column fibres: significance to spinal cord stimulation. *Brain*. 2002;125(pt 5):1137-1149. Erratum in: *Brain*. 2002;125(pt 7):1668.
23. Yearwood TL, Hershey B, Bradley K, Lee D. Pulse width programming in spinal cord stimulation: a clinical study. *Pain Physician*. 2010;13:321-335.

COMMENT

This study, which comes from the collaboration of two respected groups, advances our scientific understanding of a clinically-observed phenomenon. While it is obviously possible to stimulate an entire pathway or the entire spinal cord, the therapeutic requirement is to be as specific as possible. It seems that the more extensively the evoked paraesthesiae cover the area where the neuropathic pain is felt, the more probable is the pain relief from spinal cord stimulation. It is reasonable to aim for, and patients increasingly demand, minimal or no extraneous stimulation. As implanted neurostimulators become increasingly sophisticated the opportunities for selectivity and accuracy become greater but at the same time the programming becomes more difficult and time-consuming. This study provides some guidance and insight which will help optimize the effect of this initially expensive therapy and increase its usefulness against the misery of chronic neuropathic pain.

Brian A. Simpson
Cardiff, United Kingdom

Daily News and Updates at NEUROSURGERY Report

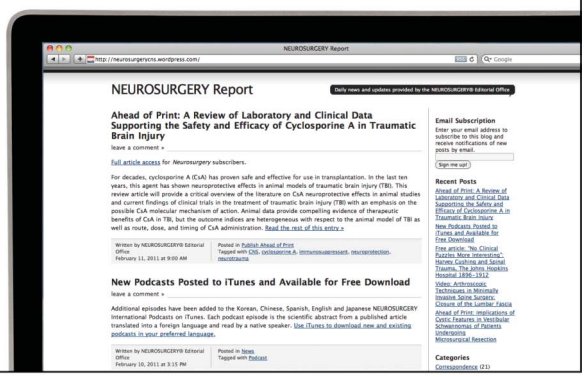

Follow NEUROSURGERY® at http://neurosurgerycns.wordpress.com

NEUROSURGERY

Copyright © Congress of Neurological Surgeons. Unauthorized reproduction of this article is prohibited.

Review of: Focal Peripheral Neuropathies (Fourth Edition)

John D. Stewart
JBJ Publishing, West Vancouver, British Columbia, Canada (2010)

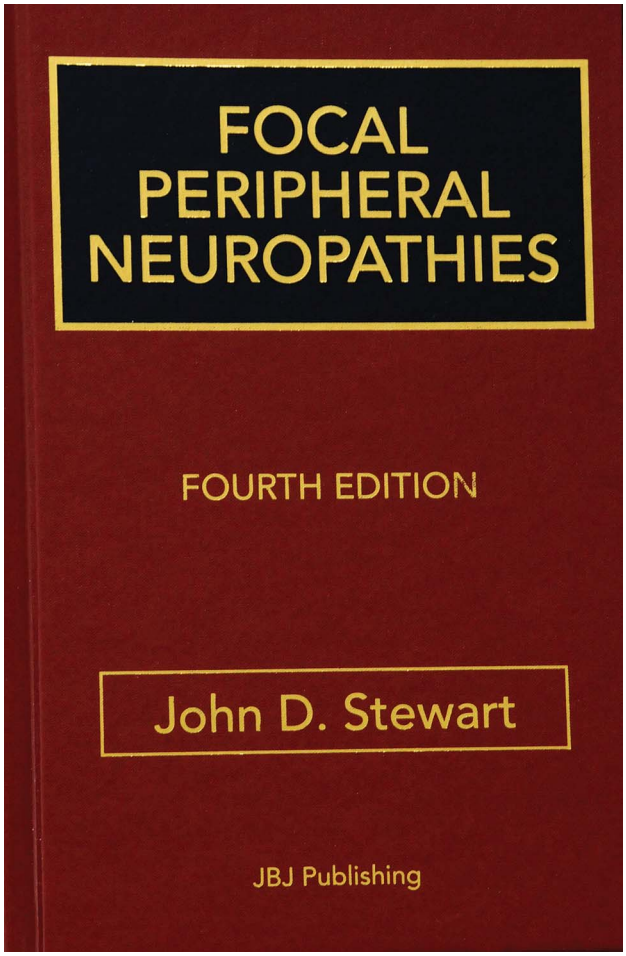

It might have been a long time coming (10 years after the third edition), but the fourth edition of *Focal Peripheral Neuropathy* will certainly benefit the peripheral nerve community by embracing an evidence-supported approach to its presentation. In the book's preface, the author stresses the great need for practitioners in this field to analyze and critique good and robust medical evidence in support of their daily practice. This overarching theme is present throughout the book, providing a consistent approach even though the content covered is diverse. This compendium of clinical presentations, diagnostic tools, and treatment options also carries with it an exhaustive list of contemporary references. Despite the rich clinical content, each chapter is divided into bite-sized sections and subsections. Each subsection attempts to address relevant clinical issues through intelligent critique of clinical dogma and evidence. More importantly, when conflicting or less vigorous research results are included, Dr Stewart has the foresight to include excellent practical summaries of what the evidence means for the practicing doctor by the patient's bedside. The author attempts, in short, to present the spectrum of conditions causing focal neuropathies but couples it with an ambitious effort to provide best-evidence information to impart practical guidance for patient management.

The signs, symptoms, anatomy, and electrophysiology nuances of peripheral nerves are covered in the first 4 chapters to provide important background. The meat of the textbook is within the subsequent 17 chapters. Using an anatomical layout and a proximal-to-distal approach, Dr Stewart covers all major peripheral nerves of the upper and lower limbs in each chapter. A separate chapter is devoted to nerves of the trunk. Of note is the concluding chapter, which discusses diagnostic approach for mononeuropathy multiplex. It is sufficiently detailed for neurologists and trainees while being succinct enough for surgeons, rehabilitative physicians, and physiotherapists. Brachial plexus and lumbosacral plexus are covered extensively in 2 excellent chapters. This discussion maintains the systematic approach seen elsewhere in the book. Surgical management and medical management are emphasized equally. This balanced critique is often missing in most publication. It offers physicians a surgical perspective and vice versa. A huge selection of illustrations in the appendix provides a pictorial summary of dermatome, cutaneous distribution of nerves, tendon reflex innervations, and myotome of the human body.

In each chapter, apart from discussions of nerve anatomy and clinical care, discriminating features between clinical syndromes are highlighted. Emphasis on signs and symptoms that help differentiate the site of pathology are succinctly summarized, often presented in table form. This provides a quick reference for residents and physicians to help localize the site of pathology to within root, plexus, peripheral nerve, or its terminal branch. The pages are filled with illustrations, clinical pictures, and diagnostic images, often covering variations of clinical deficits seen in practice. Sensory deficit is clearly marked in photographs of real patients. Also included are photographs of postures that might put individual peripheral nerves at risk, certainly making comprehension much easier than reading the textual description. Such a plethora of clinical photos imparts an easy read while stressing important points at the same time. This theme continues into the diagnostic section with many computed tomography and magnetic resonance images of peripheral nerve lesions. Diagnostic test sensitivity and specificity are included when available, thus providing a more evidence-based approach for test utilization.

Copyright © Congress of Neurological Surgeons. Unauthorized reproduction of this article is prohibited.

Professor Stewart outlines an approach for addressing less-defined clinical syndromes such as piriformis syndrome. He draws inspiration from Koch's postulate when attempting to suggest definition, management, and treatment in contentious peripheral nerve syndromes. Vague terms are avoided. The conclusion on vagueness of a commonly accepted term is intelligently argued by drawing on clinical literature. Review articles that explore contentious clinical syndromes such as quadrilateral space, disputed thoracic outlet, and piriformis syndromes are analyzed to provide up-to-date conclusions.

Discussion of disease management involves the natural history and medical and surgical options. The literature is combed for supporting evidence. A brief description of the evidence is given and its quality is taken into account for deriving the evidence-based conclusion. When robust evidence is lacking or ambiguous, a practical clinical workflow is often suggested. This is exceedingly helpful and improves on many other publications, which often end in an ambiguous conclusion because of such a lack of evidence. The thoughtful analysis, which reflects much of the work in this edition, is most clearly evident in discussions of controversial topics. Such topics include thoracic outlet syndrome, radial tunnel syndromes, piriformis syndrome, fibular tunnel syndrome, and tarsal tunnel syndrome. The author combed the literature extensively to provide an evidence-based approach to definition, diagnosis, and potential treatment. Conscious efforts are again made to identify diagnostic test accuracy and outcomes from robust studies whenever possible. A brief but clinically relevant and practical summary is provided to allow quick and easy transfer of numerous, often ambiguous studies to the bedside.

This book is unique in providing an authoritative work that focuses on focal peripheral neuropathies, unlike many textbooks that cover the general field of peripheral neuropathy in an encyclopedic fashion. Moreover, the practical considerations and evidence-based presentation make the book highly approachable and readable. This textbook will be a great reference for physicians, surgeons, rehabilitative medicine practitioners, pathologists, physical therapists, and anyone interested in the art and science of peripheral nerve disorders. It is a must read for any surgeon seriously interested in peripheral nerve disorders because focal conditions are often of surgical interest or at least consideration. Spinal surgeons in particular will find the sections on radiculopathy and the evidence-based approach to managing spinal conditions of considerable value.

Boon Pang, MBBF, FRACS
Rajiv Midha, MD, MSc, FRCSC
Calgary, Alberta, Canada

Disclosure

The authors report no disclosures relevant to the content or subject of this book review.

10.1227/NEU.0b013e31821129cb

Copyright © Congress of Neurological Surgeons. Unauthorized reproduction of this article is prohibited.

Ventral Intermediate Thalamic Stimulation for Monoclonal Gammopathy-Associated Tremor: Case Report

Donald C. Shields, MD, PhD*
Alice W. Flaherty, MD, PhD‡
Emad N. Eskandar, MD*
Ziv M. Williams, MD*

*Department of Neurosurgery, Massachusetts General Hospital and Harvard Medical School, Boston, Massachusetts; ‡Department of Neurology, Massachusetts General Hospital and Harvard Medical School, Boston, Massachusetts

Correspondence:
Ziv M. Williams, MD,
15 Parkman Street,
Wang Ambulatory Care Center,
745K, Boston, MA 02114.
E-mail address: zwilliams@partners.org

Received, July 10, 2009.
Accepted, September 10, 2010.

Copyright © 2011 by the
Congress of Neurological Surgeons

BACKGROUND AND IMPORTANCE: Peripheral and central sensory loss are often associated with significant tremor or sensory ataxia, which can be highly refractory to medical therapy.

CLINICAL PRESENTATION: We present the case of a 67-year-old man with progressive and debilitating intention tremor from monoclonal gammopathy-associated peripheral neuropathy. The patient was implanted with bilateral thalamic deep brain stimulator electrodes under microelectrode guidance. Following optimization of stimulation parameters, the patient's appendicular tremor and gait improved, as did his general activities of daily living.

CONCLUSION: These initial findings suggest that deep brain stimulation may benefit not only tremor presumed to originate from central nervous system dysfunction, but also tremor originating peripherally from neuropathy-related sensory loss.

KEY WORDS: Action tremor, Deep brain stimulation, Microelectrode recording, Monoclonal gammopathy, Polyneuropathy, Thalamus

Neurosurgery 68:E1464–E1467, 2011 DOI: 10.1227/NEU.0b013e3182124633 www.neurosurgery-online.com

Polyneuropathies affect approximately 8% of patients over 55 years of age.[1] Ten percent of polyneuropathies are associated with autoimmune inflammatory disorders including Guillain-Barre syndrome, chronic inflammatory demyelinating polyneuropathy, and neuropathies related to monoclonal gammopathies. Clinically, these patients are often found to have a slowly progressive sensory impairment, tremor, and gait ataxia.

Based on these behavioral observations, it has been speculated that delayed input to the cerebellum prompts a poorly coordinated agonist burst in distal musculature that ultimately leads to the action tremor as the cerebellum attempts to modulate distal extremity movement.[2] Here, we provide initial evidence that disrupting this circuitry at the thalamic level may improve tremor associated with such diseases.

ABBREVIATION: VIM, ventral intermediate

Supplemental digital content is available for this article. Direct URL citations appear in the printed text and are provided in the HTML and PDF versions of this article on the journal's Web site (www.neurosurgery-online.com).

CLINICAL PRESENTATION

This 67-year-old man first noted leg paresthesias at the age of 40. Approximately 10 years later he developed progressive sensory dysmetria characterized as coarse and erratic tremor combined with distal-to-proximal numbness and weakness. He was given a diagnosis of monoclonal antibody-associated polyneuropathy, and was treated with plasmapheresis, propranolol, intravenous immunoglobulin, and rituximab. Despite multiple trials of these therapies, he continued to lose useful limb function. He required a cane for balance, and both grasp and reach were greatly impaired by his severe bilateral limb tremors. On physical examination, he presented with extensor deformities of both hands, significant muscle wasting (especially interossei and gastrocnemius), hyporeflexia, and loss of distal sensation/proprioception. Magnetic resonance imaging (MRI) did not reveal abnormalities of the cerebellum or supratentorial structures. His other medical history included well-controlled hypertension and hyperlipidemia.

WHAT IS THIS BOX?
A QR Code is a matrix barcode readable by QR scanners, mobile phones with cameras, and smartphones. **The QR Code above links to Supplemental Digital Content from this article.**

Copyright © Congress of Neurological Surgeons. Unauthorized reproduction of this article is prohibited.

INTERVENTION

Consideration for surgery was discussed with the patient, including the potential risks and the option for continued medical management. On the morning of surgery, the patient underwent a head computer tomography (CT) scan with a CRW stereotactic frame (Integra Radionics, Burlington, Massachusetts) in place. Fine-cut CT images were overlaid with previously obtained MR images using a Stealth Station navigational device (Medtronic, Inc., Minneapolis, Minnesota). Bilateral ventral intermediate (VIM) thalamic nuclei were targeted at the level of the anterior commissure/posterior commissure plane (*z* axis), 5 mm posterior to the mid anterior commissure/posterior commissure point (*y* axis), and 14 mm lateral (*x* axis) to the midline. After injecting local anesthetic, we incised the scalp along the coronal plane at the level of the coronal suture and placed burr holes 3.5 cm lateral to the midline. To obtain electrophysiology data, the patient remained awake throughout the procedure. We recorded neuronal activity using 3 tungsten microelectrodes (arranged in a parasagittal orientation and spaced 2 mm apart) that were advanced to target using a motorized microdrive (Alpha Omega, Nazareth, Israel).

Recording began approximately 20 mm above the calculated target. After an initially quiescent descent, we found activity consistent with that of the thalamus in all 3 electrodes beginning at an approximate depth of 15 mm above the VIM nucleus target (Figure 1). During recording, the patient performed motor and sensory tasks. Movements of the contralateral arm evoked changes in the neuronal firing rate that also corresponded to the patient's tremor. Light touch to the patient's arms and face caused alterations in neuronal activity from 0.5 to 5 mm above the target point along the posterior-most electrode.

We then removed the recording microelectrodes, and placed the permanent stimulator electrode (model 3387; Medtronic, Inc., Minneapolis, Minnesota) in the middle tract, which demonstrated the most consistent motor-driving and tremor-correlated activity. The permanent electrodes were secured and temporarily connected to an externalized stimulator to test for speech-related changes and sensory-motor side effects; none were noted.

A week after the initial surgery, both leads were connected to an infraclavicular pulse generator (Kinetra; Medtronic, Inc.) under general anesthesia.

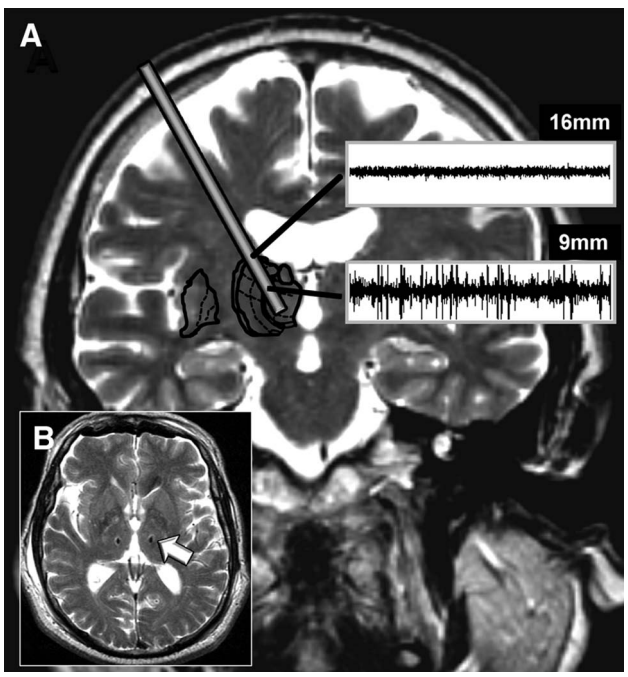

FIGURE 1. *Microelectrode-guided VIM thalamic nucleus deep brain stimulator placement.* **A**, *coronal T2-weighted MR image depicts the right-sided stimulator electrode position with corresponding 10-second microelectrode recordings at locations approximately 16 mm and 9 mm from the projected target.* **B,** *postoperative axial T2-weighted MR image demonstrates bilateral stimulator electrode (arrow) locations. VIM, ventral intermediate.*

Clinical Follow-up

Postoperative MRI demonstrated that both leads were in proper position. Benefits in both hand control and gait were apparent immediately after the first stimulator adjustment visit. At his 2-week follow up, the patient's truncal ataxia was significantly improved. His gait was more stable, and he no longer needed to use a cane for balance. He also enjoyed mild-to-moderate improvement in his limb tremor on finger-to-finger and finger-to-nose tasks, but was still functionally limited by his severe neuropathy-related hand weakness and atrophy. Significantly higher voltages resulted in slurred speech initially, but this effect was short-lived when returning to lower settings. The patient did not demonstrate any new postoperative stimulation-induced sensory or motor deficits.

At a 7-month follow-up, the patient demonstrated some improvement in his limb tremor and significant subjective gait improvement compared with his preoperative baseline. He could ambulate 20 feet within 15 seconds (similar to baseline), but

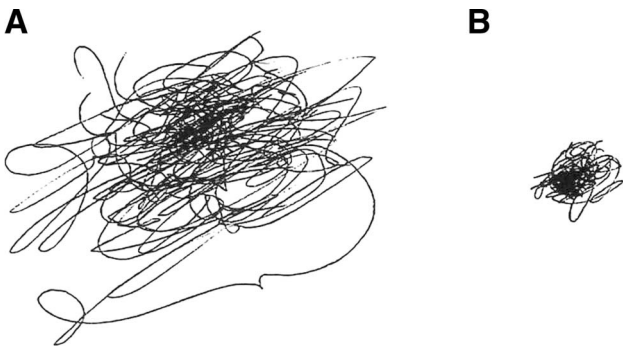

FIGURE 2. *Pen movements produced without stimulation (***A***) and with stimulation (***B***) during the Tremor Research Group dot approximation task. The average widest pen excursion was significantly greater when the stimulator was turned off vs periods when the stimulator was on (*P = .003*).*

Copyright © Congress of Neurological Surgeons. Unauthorized reproduction of this article is prohibited.

TABLE 1. Postoperative Stimulator Settings[a]

Date, mm/dd/yy	Side	Voltage	Pulse Width, μs	Frequency, Hz	Positive Contacts	Negative Contacts
10/17/08	L	1.5	90	185	Case	2
	R	0.7	90	185	Case	5
10/30/08	L	2.0	90	185	Case	2
	R	2.0	90	185	Case	5
10/31/08	L	1.5	90	185	Case	2
	R	1.2	90	185	Case	5
05/12/09	L	1.5	90	185	Case	2
	R	0.7	90	185	Case	5
05/17/10	L	1.5	90	185	Case	2
	R	0.6	90	185	Case	5

[a]L, left; R, right.

without the use of a cane. At 19 months, the patient could ambulate 20 feet in 18 seconds with stimulation; 24 seconds was required for the same distance when the stimulator was turned off (see Video, Supplemental Digital Content 1, http://links.lww.com/NEU/A372, which demonstrates ambulation with and without stimulation, 1 minute, 65 MB). His limb tremor was evaluated with the Tremor Research Group dot approximation task in which the pen was held vertically over a point on a sheet of paper for 30 seconds.[3] This task created a wider pen excursion of 11.2 cm ± 4.0 SD when the stimulator was turned off vs 4.5 cm ± 2.3 SD when the stimulator was on (P = .003, 2-tailed t test) (Figure 2). Thus, using a tremor grading scale from 0 (no tremor) to 4 (>20 cm in amplitude), he scored an average grade of 3.2 ± 0.27 SD without stimulation vs 2.5 ± 0.50 SD with stimulation (P = .009, 2-tailed t test). Stimulator settings that resulted in the most significant improvement in his arm tremor and truncal ataxia were at 2.0 V, 90 μs, and 185 Hz in a monopolar configuration (Table 1). Optimal lead position corresponded to the dorsolateral motor subterritory of the VIM nucleus.

DISCUSSION

This patient presented with a neuropathy-associated variable-frequency distal arm tremor and sensory ataxia.[2] Similar symptoms have been reported with monoclonal gammopathy, sensory neuropathy, dorsal column damage, and parietal lobe lesions.[2,4] Neuropathic tremor (or sensory dysmetria) differs from essential tremor by its more variable frequency, worsening with targeted compared with untargeted movements, and its association with sensory findings such as the Romberg sign and steppage gait. In making the diagnosis of neuropathy-related tremor, it is essential to exclude other neurological conditions (eg, cerebellar lesions) that may occasionally produce similar symptoms.[5]

Although incompletely understood, the physiological mechanisms associated with peripheral neuropathy-related tremor are believed to result from a distortion of reflex propagation within demyelinated peripheral nerves.[6] Axonal conduction from muscle spindles to central nervous nuclei is slowed, and therefore leads to prolonged agonist-antagonist-agonist activation with delay of the second agonist burst. Based on these observations, some investigators have suggested that this delayed input to the cerebellum may lead to action tremor as the cerebellum attempts to compensate for discrepancies between intended and executed distal extremity movement.[2] This is also supported by positron emission tomography and functional MRI studies demonstrating cerebellar hyperactivity during neuropathic tremor production.[7–9]

Interruption of this circuitry at the thalamic level may thus be an option for treating medically refractory ataxia and tremor.[9] In particular, high-frequency stimulation of the thalamus may override abnormal cerebellar hyperactivity within the spinocerebellar-thalamic-cortical circuit, which is affected by aberrant reflex loops generated peripherally. Although the exact pathophysiological mechanism of neuropathy-related tremor is unknown, these findings suggest the use of deep brain stimulation may benefit not only symptomatic tremor presumed to originate from the central nervous system, such as in Parkinson disease and essential tremor, but also tremor associated with disorders of the peripheral nervous system. Because the effectiveness of high-frequency stimulation may decline over time with such progressive diseases, additional studies will be needed to better define the role of deep brain stimulation in long-term treatment strategies.

Disclosure

The authors have no personal financial or institutional interest in any of the drugs, materials, or devices described in this article.

REFERENCES

1. Renaud S. Dysimmune polyneuropathies: new diagnostic and therapeutic insights. *Schweiz Arch Neurol Psychiatr*. 2006;157:307-316.
2. Bain PG, Britton TC, Jenkins IH, et al. Tremor associated with benign IgM paraproteinaemic neuropathy. *Brain* 1996;119(Pt 3):789-799.

Copyright © Congress of Neurological Surgeons. Unauthorized reproduction of this article is prohibited.

3. Tintner R for the Tremor Research Group. Eighteenth annual symposia on etiology, pathogenesis, and treatment of Parkinson's disease and other movement disorders. *Mov Disord*. 2004;19:1131-1132.
4. Smith IS. The natural history of chronic demyelinating neuropathy associated with benign IgM paraproteinaemia. A clinical and neurophysiological study. *Brain*. 1994;117(pt 5):949-957.
5. Deuschl G, Bergman H. Pathophysiology of nonparkinsonian tremors. *Mov Disord*. 2002;17(suppl 3):S41–S48.
6. Shahani BT, Young RR. Physiological and pharmacological aids in the differential diagnosis of tremor. *J Neurol Neurosurg Psychiatry*. 1976;39(8):772-783.
7. Boecker H, Brooks DJ. Functional imaging of tremor. *Mov Disord*. 1998;13:S64–S72.
8. Perlmutter JS, Mink JW, Bastian AJ, et al. Blood flow responses to deep brain stimulation of thalamus. *Neurology* 2002;58(9):1388-1394.
9. Ruzicka E, Jech R, Zarubova K, Roth J, Urgosik D. VIM thalamic stimulation for tremor in a patient with IgM paraproteinaemic demyelinating neuropathy. *Mov Disord*. 2003;18(10):1192-1195.

Supplemental digital content *is available for this article. Direct URL citations appear in the printed text and are provided in the HTML and PDF versions of this article on the journal's Web site (www.neurosurgery-online.com).*

Copyright © Congress of Neurological Surgeons. Unauthorized reproduction of this article is prohibited.

Reactive Expansive Intracerebral Process as a Complication of Endovascular Coil Treatment of an Unruptured Intracranial Aneurysm: Case Report

Marton König, MD*
Søren Jacob Bakke, MD, PhD‡
David Scheie, MD, PhD§
Wilhelm Sorteberg, MD, PhD*
Torstein Ragnar Meling, MD, PhD*

Departments of *Neurosurgery, ‡Neuroradiology, and §Pathology, Oslo University Hospital, Rikshospitalet, Oslo, Norway

Correspondence:
Torstein R. Meling, MD, PhD,
Head of Section,
Department of Neurosurgery,
Oslo University Hospital,
Rikshospitalet,
0027 Oslo, Norway.
E-mail: torstein.meling@rikshospitalet.no

Received, October 9, 2009.
Accepted, April 27, 2010.

Copyright © 2011 by the
Congress of Neurological Surgeons

BACKGROUND AND IMPORTANCE: As a consequence of the increased use of endovascular coiling of intracranial aneurysms, a growing number of case reports on complications are being reported. This article presents a case with a previously undescribed complication of coil treatment: a reactive, noninfectious process after coiling of an unruptured intracranial aneurysm

CLINICAL PRESENTATION: A 60-year-old hypertensive woman with hypoxic encephalopathy after respiratory arrest following a total thyroidectomy had extensive intentional myoclonus and reduced quality of life as sequelae. An asymptomatic 15-mm internal carotid artery bifurcation aneurysm was discovered on magnetic resonance imaging (MRI) 6 months after the thyroidectomy. After documented growth, the aneurysm was treated endovascularly with bare platinum Guglielmi detachable coils. Three months later, an expansion in the right frontal lobe cranially to the coiled aneurysm was observed. The lesion had grown at the 12-month postcoil MRI and, because of its increasing mass effect, was resected through a craniotomy 2 years after the coiling. As a result of lesion regrowth and cyst formation, she underwent a new craniotomy 5 years later with excision of the now 21-mm large coiled aneurysm, internal carotid artery clip reconstruction, and lesionectomy. Five months postoperatively, the process had not recurred. No signs of malignancy or infection were observed during the histological evaluation of the resected tissue. The tissue is described as a reactive, noninfectious process, most likely resulting from the coils acting as a foreign body.

CONCLUSION: This article presents a case with a reactive expansive intracerebral process as a complication to endovascular coil treatment of an unruptured intracranial aneurysm.

KEY WORDS: Complications, Endovascular treatment, Intracranial aneurysm, Neuropathology, Neurovascular surgery

Neurosurgery 68:E1468–E1474, 2011 DOI: 10.1227/NEU.0b013e318210c7c0 www.neurosurgery-online.com

Previously, intracranial aneurysm repair was exclusively surgical with most aneurysms being clipped.[1] However, since its introduction in 1991,[2] endovascular aneurysm repair has grown in popularity.[3,4] Consequently, a growing number of case reports on complications of this treatment such as incomplete aneurysm coiling,[5,6] aneurysm regrowth,[7] aneurysm rupture,[8] and failure to alleviate symptoms related to mass effect[9] have been published.

ABBREVIATIONS: CRP, C-reactive protein; **ICA,** internal carotid artery; **SR,** sedimentation rate; **WCC,** white cell count

Bare platinum coils within an aneurysm exert a hemodynamic effect, resulting in an immediate major reduction in aneurysm blood flow.[10] This may trigger the initial thrombus formation within the coil-filled sac that is gradually followed by inflammatory cellular responses around the coil material.[11] Approximately 2 weeks after treatment, the inflammatory changes are followed by the formation of granulation tissue, occasionally including foreign-body–type giant cells. Myofibroblasts and fibrocellular components such as collagen then progressively replace the initial thrombus, and fibrous scar tissue formation can be seen 1 month after treatment.[11]

Copyright © Congress of Neurological Surgeons. Unauthorized reproduction of this article is prohibited.

The inflammatory responses, formation of granulation tissue, and fibrous tissue formation after aneurysm coil placement may be looked on as wanted effects. Indeed, second-generation coils containing bioactive materials to facilitate or enhance the aneurysm healing process have been developed. Bioabsorbable polymeric material–coated coils are now part of the standard armamentarium in endovascular aneurysm repair. However, because bioabsorbable polymeric material coils elicit a greater inflammatory response, complications seen after the use of these coils include symptomatic chemical meningitis,[12] perimural edema,[13] and hydrocephalus.[13-15]

In this report, we present a case of exaggerated immunological response to endovascular aneurysm repair with only bare platinum coils. After treatment of a 17-mm unruptured internal carotid artery (ICA) bifurcation aneurysm, a 60-year-old female patient developed over time a 50-mm large noninfectious reactive process in the perianeurysmal region. This reactive tissue response did stop until the coiled aneurysm was excised from the brain.

CASE REPORT

Clinical Presentation

Our patient, a 60-year-old hypertensive woman, underwent total thyroidectomy in February 2000 because of nodular goiter. The surgery was complicated by a postoperative respiratory arrest and a generalized tonic-clonic seizure lasting approximately 6 to 8 minutes. She underwent emergency tracheostomy and needed respiratory support for the following 14 days. She sustained hypoxic brain damage and developed an extensive intentional myoclonus, which still reduces her quality of life and general condition. Her myoclonus is being treated with clonazepam, and she receives thyroxin substitution therapy.

On cerebral magnetic resonance imaging (MRI) 6 months after the thyroid surgery, a 15-mm asymptomatic intracranial ICA bifurcation aneurysm was discovered (Figure 1). After the aneurysm grew from 15 to 17 mm, she was admitted to our department in December 2001 for aneurysm treatment. Cerebral digital subtraction angiography showed that the aneurysm had a small neck and contained no thrombus.

Intervention and Technique

Because the standard treatment of ICA bifurcation aneurysms $<$ 20 mm at our department is endovascular, our patient underwent aneurysm coiling with multiple bare platinum Guglielmi detachable coils (Figure 2A and 2B). A neck remnant remained. The coiling procedure was carried out under total intravenous anesthesia and lasted 2 hours 20 minutes. No perioperative antimicrobial therapy was administered. Before treatment, the patient had a normal body temperature and a normal blood C-reactive protein (CRP) concentration ($<$ 5 mg/L). After treatment, she had a temporary increase in CRP (peak value, 146 mg/L), a slightly increased (18 mm) sedimentation rate (SR), but a normal (8.8 $\times$ 10.9/L) white cell count (WCC). She had no postoperative fever, headache, nuchal rigidity, or photophobia. Postoperative urine analysis and chest x-ray showed no sign of infection. She was discharged from our hospital 3 days after the coiling.

At the 3-month follow-up, she reported a decrease in her gait function and worsening of her myoclonus from approximately 2 weeks after the treatment. MRI scans demonstrated a perianeurysmal edema measuring approximately 25 mm in diameter (Figure 3). Both MR angiography and digital subtraction angiography showed moderate coil compaction in the aneurysm. A blood count showed no sign of infection (CRP $<$ 5 mg/L; WCC: 4.9 $\times$ 10^9/L). No cerebrospinal fluid (CSF) analysis was performed. We decided on no medical treatment of the perianeurysmal edema and no recoiling of the aneurysm. She was discharged to her home and scheduled for a follow-up 12 months later.

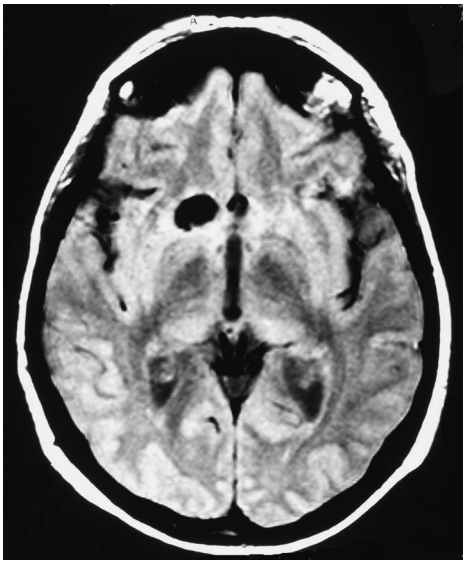

FIGURE 1. *Magnetic resonance image showing a right-sided unruptured internal carotid artery bifurcation aneurysm measuring 15 mm.*

Shortly before the scheduled follow-up, the patient was readmitted to our department because of complete loss of gait function, urine incontinence, visual hallucinations, and worsening of her cognitive functions. The MRI now showed a 22-mm perianeurysmal expansive

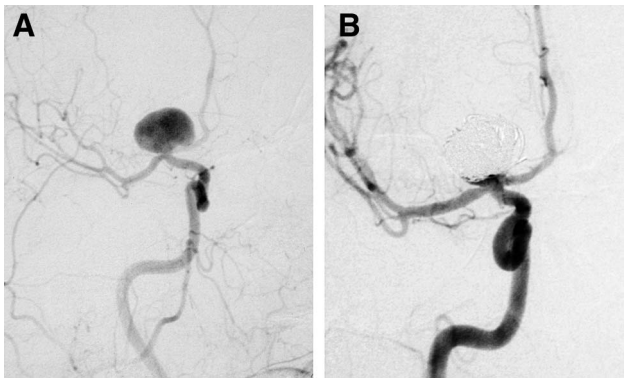

FIGURE 2. A, *digital subtraction angiography (DSA) before endovascular treatment of the aneurysm with Guglielmi detachable coils (GDCs).* **B**, *DSA after endovascular treatment of the aneurysm with GDCs.*

Copyright © Congress of Neurological Surgeons. Unauthorized reproduction of this article is prohibited.

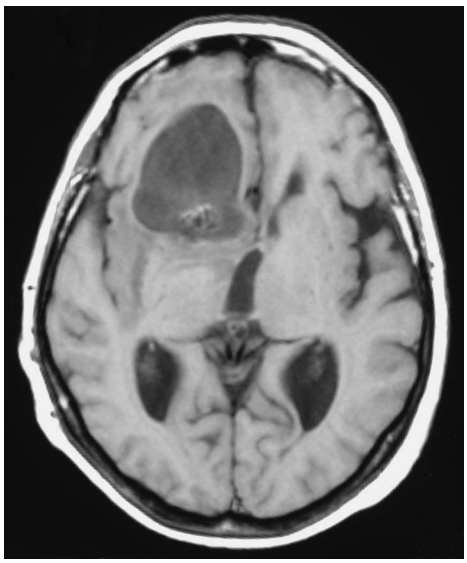

FIGURE 3. *A 3-month postoperative magnetic resonance image showing an expansive process around the coiled aneurysm (axial section).*

process (Figure 4). MR angiography documented considerable coil compaction with recirculation in a major part of the aneurysm. After routine urine investigation showed a lower urinary tract infection, she was treated with trimethoprim 320 mg/24 h PO 5 days preoperatively. The aneurysm was successfully recoiled, requiring 1.25 m of GDC. The procedure lasted 1 hour 40 minutes and was carried out under total intravenous anesthesia. Postoperative full blood count showed a temporary increase in CRP with a peak value of 30 mg/L 2 days after the intervention. Her WCC and SR remained within reference values throughout the stay.

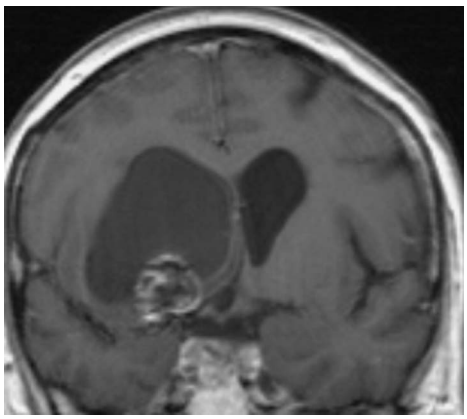

FIGURE 4. *Magnetic resonance image taken before the first craniotomy showing the expansive process lifting the floor of the lateral ventricle on the right side (coronal section).*

One month later, a new MRI showed further growth of the perianeurysmal process, now measuring 50 mm in diameter and with a perilesional cyst growing toward the foramen of Monroe. There was no contrast enhancement in the mass. A low-grade tumor was suspected. MR angiography showed no circulation within the expansion. A urinary tract infection was diagnosed and treated with trimethoprim 600 mg/24 h PO and ciprofloxacin 1 g/24 h PO through 3 and 4 days, respectively. Full blood count showed CRP, WCC, and SR within reference values. Because of her progressive neurological symptoms, she underwent a craniotomy with fenestration of the cystic lesion and a lesionectomy. The resected tissue had mucous characteristics. Numerous biopsies were taken from the periphery of the lesion. The biopsy material consisted of small fragments of subependymal brain tissue from grey and white matter with reactive gliosis, scattered eosinophilic granular bodies, and small perivascular aggregates of lymphocytes. Granulomas or foreign-body–type giant cells were not observed. Glial fibrillary acidic protein staining confirmed the presence of reactive astrocytes. Perls Prussian blue staining demonstrated no sign of iron deposition. Tumor tissue was not observed (Figure 5). The patient received perioperative steroid treatment with an intravenous methylprednisolone bolus of 40 mg followed by 80 mg/24 h, which was decreased to 10 mg/24 h IV over a period of 8 days and then stopped. A standard dose of cefalotin 2 g IV was administered at the start of the operation. Treatment with peroral ciprofloxacin 1 g/24 h was continued until the third postoperative day. After surgery, there were temporary increases in CRP (peak, 16 mg/dL), WCC (11.4×10^9/L), and SR (18 mm). The patient was discharged after an uneventful recovery. At a check-up 3 months after surgery, improvement was seen in her clinical performance, and an MRI showed no regrowth of the expansion (Figure 6).

In subsequent years, she had follow-ups at her local neurological department. Repeat MRI investigations showed a continuous growth of the expansion surrounding the previously coiled aneurysm (Figure 7A and 7B). She was readmitted to our department as an emergency case 5 years after the surgical treatment (November 2008) as a result of increasing confusion, seizures, aphasia, and decreasing level of consciousness. Cerebral computed tomography (CT) showed enlarged lateral ventricles and a multicystic lesion on the right side occluding the foramen of Monroe. She was treated with endoscopic third ventriculostomy and attempted fenestration of the cysts, together with placement of an external ventricular drain and intracerebral pressure sensor. During surgery, 2 g cefalotin was administered intravenously as prophylactic antimicrobial treatment. On the day of the surgery, CSF analysis showed glucose concentration of 5 mmol/L, total protein concentration of 1.58 g/L, and a WCC of 0 and 1×10^6/L.

The clinical condition of the patient, however, did not improve, and serial computed tomography imaging demonstrated cyst regrowth and secondary midline shift (Figure 8). The senior author (T.R.M.) therefore opted for a craniotomy to excise the coiled ICA aneurysm (now measuring 21 mm), thus removing the anticipated cause of the immunological reaction (Figure 9). Intraoperatively, part of the coil material was located outside the aneurysm wall and in contact with the gliotic, scarred brain tissue. The coiled aneurysm was excised under temporary clip ligation of the ICA, and the ICA bifurcation was subsequently reconstructed with a Sugita 15 and a Yasargil 710 clip. The remaining cysts were fenestrated, the lamina terminalis was opened, and numerous biopsies were taken from the perilesional area. Histological examination also demonstrated this time brain tissue with reactive gliosis and small collections of CD68-positive macrophages. Granulomas or foreign-body–type giant cells were not observed. Again, there were no signs of

Copyright © Congress of Neurological Surgeons. Unauthorized reproduction of this article is prohibited.

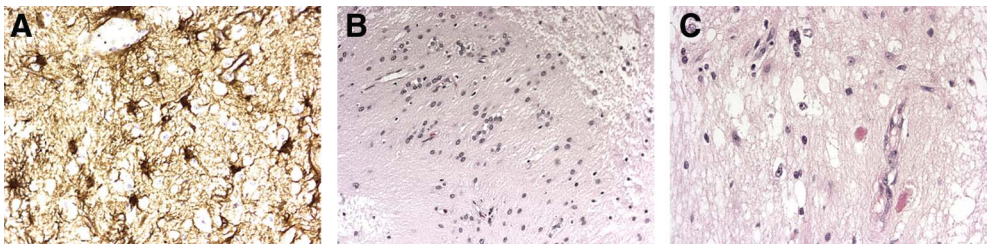

FIGURE 5. *Biopsy material consisting of subependymal brain tissue from grey and white matter with reactive gliosis. The material taken during the first craniotomy shows reactive astrocytes (A, glial fibrillary acidic protein staining; B, hematoxylin and eosin, × 40; C, hematoxylin and eosin, × 60).*

tumor tissue or infection (Figure 10). During the aneurysm surgery, a total of 6 g cefalotin was administered intravenously as prophylactic antimicrobial treatment.

The patient had later undergone intracerebral pressure monitoring to evaluate her cerebral hydrodynamics and had a ventriculoperitoneal shunt implanted. Routine CSF and blood investigations carried out perioperatively showed no evidence of infection. At a later follow-up, she was awake, alert, and able to communicate. She is using a wheelchair because of her hypoxic encephalopathy and receives daily nursing care. Postoperative MRI taken 5 months after the last aneurysm craniotomy has shown no evidence of regrowth of the expansion (Figure 11).

DISCUSSION

This case report describes a woman who developed an expansive intracerebral process secondary to endovascular coil treatment of an unruptured intracranial aneurysm with bare platinum coils. The response triggered in the brain tissue seemed to be acting slowly, lasted a period of years, and did not end until the coiled aneurysm was excised from the brain. She also developed secondary hydrocephalus that required shunt placement.

The perianeurysmal edema seen on MRI scans at the 3-month follow-up in our case resembles that seen in 1 of the 2 cases reported by Meyers et al[12] on chemical meningitis after aneurysm treatment with 2 second-generation aneurysm coils. In their cases, the MRI findings were seen 3 weeks after the coil treatment. Their patients had symptoms and signs of meningitis, a clinical picture not seen in our patient.

The blood-brain barrier, critical to the maintenance of homeostasis within nervous system tissue, is carried out by highly specialized brain microvascular endothelial cells, which lack pinocytotic vesicles and fenestrae but possess intercellular tight junctions.[16] These features limit transcellular and paracellular movement of molecules and cells. During immune-mediated events, however, blood-brain barrier function is lost, and cellular components of the immune system gain access to the nervous system.[17,18] Edema frequently accompanies these events. Our finding during aneurysm surgery that part of the coil material was located outside the aneurysm wall and in direct contact with the surrounding brain tissue could possibly have allowed exposure of the coil material to the brain cells.

Colonization of coils, which act as a foreign-body nidus, may rarely lead to localized infection.[19-24] The infective microorganism that colonizes the coils may be introduced at the time of endovascular coil placement or may be released in the circulation in the course of a concomitant infection that leads to hematogenous dissemination. Bacteremia has been documented to occur at a rate of 32% in therapeutic angiography procedures lasting $>$ 2 hours.[22,25,26] However, infectious complications are rare because the endovascular approach does not affect the brain-blood barrier significantly,[19] and thus only a few cases of infection, usually brain abscesses, of the central nervous system attributable to coils and cyanoacrylate have been reported.[19-24]

The histological evaluation of multiple biopsies, taken from the periphery and from the perianeurysmal area, in our patient demonstrated no signs of a neoplastic process or infection, only reactive gliosis and a slight, unspecific inflammation. The time interval between coil placement and the onset of the reactive event was longer than in the previously described cases[19-24] and persisted after administration of several antimicrobial agents. The

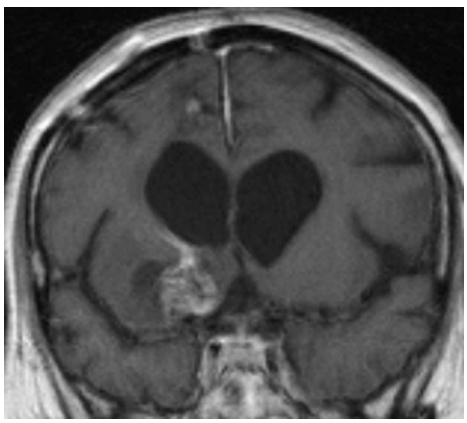

FIGURE 6. *Magnetic resonance image taken 3 months after the first craniotomy showing no evidence of regrowth of the expansion (coronal section).*

Copyright © Congress of Neurological Surgeons. Unauthorized reproduction of this article is prohibited.

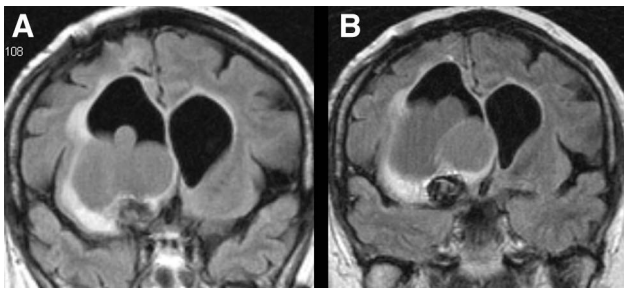

FIGURE 7. *Magnetic resonance image follow-up at 20 (A) and 27 (B) months postoperatively showing growth of the expansive process around the previously coiled aneurysm with surrounding edema of the brain tissue, causing midline shift (coronal sections).*

patient received antimicrobial therapy several times connected to her multiple treatments, and septic follow-ups did not show evidence of infection (CRP, WCC, SR). Consequently, an infectious etiology is unlikely. Moreover, the histological evaluation of the resected tissue samples demonstrated an exaggerated immunological tissue process. Although granulomas or foreign-body–type giant cells were not observed, we interpret the reactive changes as secondary to the coil material.

Despite having been treated with opening of the lamina terminalis during aneurysm surgery, thus creating an additional CSF route, our patient needed shunt placement to resolve her hydrodynamic problems. Except for mechanical blocking of CSF flow from the mass effect of giant aneurysms, development of

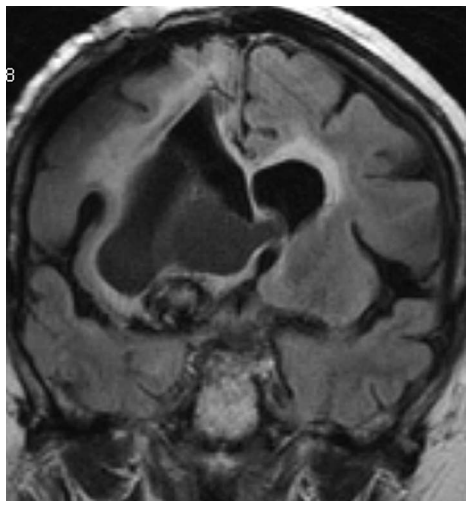

FIGURE 8. *Magnetic resonance image showing the expansive process above the previously coiled aneurysm 5 years after the first craniotomy, a few days before the second craniotomy (coronal section).*

FIGURE 9. *Photograph of the excised internal carotid artery bifurcation aneurysm with endovascular coils outside the aneurysm wall.*

delayed hydrocephalus secondary to coiling of unruptured aneurysms is rare. Recently, communicating hydrocephalus has been described secondary to the use of second-generation bioactive coils in the treatment of unruptured intracranial aneurysms.[13-15] In the series of Marchan et al[14] in which 29 patients were treated with HydroCoils, the "clean" results of the CSF analysis suggest that neither inflammation nor infection was the cause of hydrocephalus in the 4 patients who developed secondary hydrocephalus. In addition, they considered aseptic meningitis not to be the cause of the secondary hydrocephalus in their cases. In the 2 cases of secondary hydrocephalus after use of HydroCoils reported by Mitha et al,[15] the inserted shunt later had to be revised owing to shunt failure. In both cases, they found the ventricular catheter to be partially obstructed by a clear gelatinous material, with histopathological analysis of the shunt

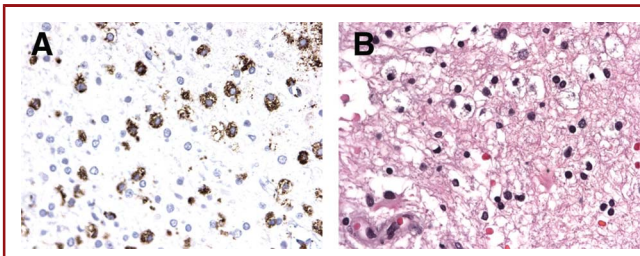

FIGURE 10. *Biopsy material taken during the second craniotomy showing reactive gliosis similar to the material taken after the first craniotomy and small collections of CD68-positive macrophages. No sign of tumor tissue (A, CD68; B, hematoxylin and eosin, × 60).*

Copyright © Congress of Neurological Surgeons. Unauthorized reproduction of this article is prohibited.

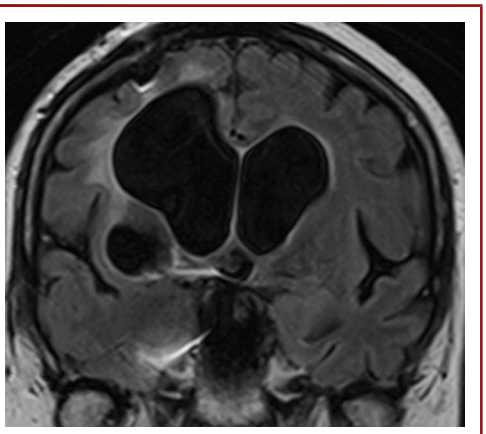

FIGURE 11. *Magnetic resonance image taken 5 months after the second craniotomy.*

revealing a basophilic, nonreactive, acellular, and amorphous foreign material with associated granulomatous inflammation. A possible explanation for the hydrocephalus secondary to the use of HydroCoils was that, by reaching the CSF, the Hydrogel polymer or an associated breakdown product altered cerebral hydrodynamics to a degree causing secondary hydrocephalus. In contrast, there was no exposure to such products in our patient.

CONCLUSION

We report on a female patient who over time developed an expansive intracerebral process secondary to endovascular coil treatment with only bare platinum coils. The response in the brain did not stop until the aneurysm with its platinum coils was excised. Except for her prior episode of major cerebral hypoxia, no previous serious damage to the brain before the aneurysm coiling could be documented or linked to her exaggerated immunological response.

Disclosure

The authors have no personal financial or institutional interest in any of the drugs, materials, or devices described in this article.

REFERENCES

1. Raftopoulos C, Goffette P, Vaz G, et al. Surgical clipping may lead to better results than coil embolization: results from a series of 101 consecutive unruptured intracranial aneurysms. *Neurosurgery*. 2003;52(6):1280-1287.
2. Guglielmi G. History of the genesis of detachable coils: a review. *J Neurosurg*. 2009;111(1):1-8.
3. Levy EI, Siddiqui AH, Hopkins LN, Langer DJ, Ogilvy CS. Cerebrovascular surgery: evolution or obsolescence. *J Neurosurg*. 2009;111(1):195-197.
4. Higashida RT, Lahue BJ, Torbey MT, Hopkins LN, Leip E, Hanley DF. Treatment of unruptured intracranial aneurysms: a nationwide assessment of effectiveness. *AJNR Am J Neuroradiol*. 2007;28(1):146-151.
5. Ferns SP, Sprengers ME, van Rooij WJ, et al. Coiling of intracranial aneurysms: a systematic review on initial occlusion and reopening and retreatment rates. *Stroke*. 2009;40(8):e523–e529.
6. Henkes H, Fischer S, Liebig T, et al. Repeated endovascular coil occlusion in 350 of 2759 intracranial aneurysms: safety and effectiveness aspects. *Neurosurgery*. 2006;58(2):224-232.
7. van Rooij WJ, Sprengers ME, Sluzewski M, Beute GN. Intracranial aneurysms that repeatedly reopen over time after coiling: imaging characteristics and treatment outcome. *Neuroradiology*. 2007;49(4):343-349.
8. Molyneux AJ, Kerr RS, Birks J, et al. Risk of recurrent subarachnoid haemorrhage, death, or dependence and standardised mortality ratios after clipping or coiling of an intracranial aneurysm in the International Subarachnoid Aneurysm Trial (ISAT): long-term follow-up. *Lancet Neurol*. 2009;8(5):427-433.
9. Tawk RG, Villalobos HJ, Levy EI, Hopkins LN. Surgical decompression and coil removal for the recovery of vision after coiling and proximal occlusion of a clinoidal segment aneurysm: technical case report. *Neurosurgery*. 2006;58(6):E1217.
10. Sorteberg A, Sorteberg W, Rappe A, Strother CM. Effect of Guglielmi detachable coils on intraaneurysmal flow: experimental study in canines. *AJNR Am J Neuroradiol*. 2002;23(2):288-294.
11. Yuki I, Lee D, Murayama Y, et al. Thrombus organization and healing in an experimental aneurysm model, part II: the effect of various types of bioactive bioabsorbable polymeric coils. *J Neurosurg*. 2007;107(1):109-120.
12. Meyers PM, Lavine SD, Fitzsimmons BF, et al. Chemical meningitis after cerebral aneurysm treatment using two second-generation aneurysm coils: report of two cases. *Neurosurgery*. 2004;55(5):1222.
13. Fanning NF, Willinsky RA, ter Brugge KG. Wall enhancement, edema, and hydrocephalus after endovascular coil occlusion of intradural cerebral aneurysms. *J Neurosurg*. 2008;108(6):1074-1086.
14. Marchan EM, Sekula RF Jr, Ku A, et al. Hydrogel coil-related delayed hydrocephalus in patients with unruptured aneurysms. *J Neurosurg*. 2008;109(2):186-190.
15. Mitha AP, Wong JH, Lu JQ, Morrish WF, Hudon ME, Hu WY. Communicating hydrocephalus after endovascular coiling of unruptured aneurysms: report of 2 cases. *J Neurosurg*. 2008;108(6):1241-1244.
16. Gloor SM, Wachtel M, Bolliger MF, Ishihara H, Landmann R, Frei K. Molecular and cellular permeability control at the blood-brain barrier. *Brain Res Brain Res Rev*. 2001;36(2-3):258-264.
17. Engelhardt B, Ransohoff RM. The ins and outs of T-lymphocyte trafficking to the CNS: anatomical sites and molecular mechanisms. *Trends Immunol*. 2005; 26(9):485-495.
18. Ransohoff RM, Kivisakk P, Kidd G. Three or more routes for leukocyte migration into the central nervous system. *Nat Rev Immunol*. 2003;3(7):569-581.
19. Jenkinson MD, Javadpour M, Nixon T, Warnke P. Intracerebral abscess formation following embolisation of an internal carotid artery aneurysm using Guglielmi detachable coils. *Acta Neurochir (Wien)*. 2003;145(8):703-705.
20. Mourier KL, Bellec C, Lot G, et al. Pyogenic parenchymatous and nidus infection after embolization of an arteriovenous malformation: an unusual complication: case report. *Acta Neurochir (Wien)*. 1993;122(1-2):130-133.
21. Zurin AA, Ushikoshi S, Houkin K, Kikuchi Y, Abe H, Saitoh H. Cerebral abscess as an unusual complication of coil embolization in a dural arteriovenous fistula: case report. *J Neurosurg*. 1997;87(1):109-112.
22. Al-Okaili R, Patel SJ. Brain abscess after endovascular coiling of a saccular aneurysm: case report. *AJNR Am J Neuroradiol*. 2002;23(4):697-699.
23. Kirollos RW, Bosma JJ, Radhakrishnan J, Pigott TD. Endovascularly treated cerebral aneurysm using Guglielmi detachable coils acting as a nidus for brain abscess formation secondary to Salmonella bacteremia: case report. *Neurosurgery*. 2002;51(1):234-237.
24. Diaz-Romero R, Zenteno M, Santos-Franco JA, Soto-Hernandez JL, Lee A. Perianeurysmal abscess and meningitis after endovascular coil placement for an intracranial aneurysm. *Surg Infect (Larchmt)*. 2009;10(4):359-362.
25. Meyer P, Reizine D, Merland JJ, Guerin JM. Nosocomial septicemia and therapeutic angiography: apropos of 4 cases [in French]. *Ann Radiol (Paris)*. 1988;31(1):34-36.
26. Shawker TH, Kluge RM, Ayella RJ. Bacteremia associated with angiography. *JAMA*. 1974;229(8):1090-1092.

COMMENT

König et al report an interesting case of a patient with an intracranial aneurysm treated with bare platinum coils who developed a significant and prolonged inflammatory response. This subsequently led to further endovascular treatment, endoscopic cyst fenestration, and then

Copyright © Congress of Neurological Surgeons. Unauthorized reproduction of this article is prohibited.

ultimately excision of the aneurysm and clip reconstruction of the parent vessel. Postcoiling inflammatory reactions have been previously reported with virtually every type of aneurysm coil. Nevertheless, there are a few interesting findings in this case report. Notably, despite the exuberant reaction to the coil mass, the aneurysm still recurred in a manner that required retreatment, which is paradoxical to bioactive coil data that a biological response to the coil mass may enhance aneurysm obliteration. In addition, the progression of the patient's inflammatory process occurred over a long follow-up period, which demonstrated that even with delayed steroid treatment, it was not a self-limiting process, ultimately requiring microsurgical intervention. Finally, given some of the eosinophilic bodies identified on initial histology, it would be interesting to test the patient for metallurgic allergies, given that even bare platinum coils can contain some trace impurities. Fortunately, severe inflammatory reactions after aneurysm coil embolization are exceedingly uncommon and are typically self-limiting with medical treatment. However, as illustrated in this report, in suspected cases, close clinical and radiographic follow-up is mandatory.

Louis J. Kim
Seattle, Washington

Copyright © Congress of Neurological Surgeons. Unauthorized reproduction of this article is prohibited.

Navigated Brain Stimulation for Preoperative Cortical Mapping in Paretic Patients: Case Report of a Hemiplegic Patient

Thomas Picht, MD*
Sein Schmidt, MD‡
Johannes Woitzik, MD*
Olaf Suess, MD*

Departments of *Neurosurgery and ‡Neurology, Charité–Universitaetsmedizin, Berlin, Germany

Correspondence:
Dr Med Thomas Picht,
Department of Neurosurgery,
Charité–Universitaetsmedizin Berlin,
Campus Virchow Klinikum,
Augustenburger Platz 1, 13353
Berlin, Germany.
E-mail: thomas.picht@charite.de

Received, October 30, 2009.
Accepted, March 25, 2010.

Copyright © 2011 by the
Congress of Neurological Surgeons

BACKGROUND AND IMPORTANCE: Navigated brain stimulation (NBS) is an emerging technology that can be used for preoperative mapping of the motor cortex. It combines conventional transcranial magnetic stimulation with neuronavigation and achieves high precision by taking into account all relevant physical factors. In contrast to functional imaging technologies, NBS does not rely on voluntary patient movements for cortical mapping. Thus, NBS can be used even on patients with severe motor impairment.

CLINICAL PRESENTATION: This article presents the case of a hemiplegic elderly woman with a brain tumor in the motor cortex. Preoperative NBS surprisingly demonstrated intact corticospinal tracts in the hemiplegic patient. The results modified the surgical strategy. Direct cortical stimulation was performed intraoperatively. The direct cortical stimulation results were in agreement with the preoperative NBS findings, and the clinical success of the surgery exceeded expectations.

CONCLUSION: NBS can be used for preoperative mapping in plegic patients. Even more important, this case report discusses why tumor resection surgery based on NBS may sometimes lead to substantially better clinical outcomes than surgery planned according to functional imaging technologies.

KEY WORDS: Brain tumor, Direct cortical stimulation, Motor cortex, Navigated brain stimulation, Preoperative mapping, Transcranial magnetic stimulation

Neurosurgery 68:E1475–E1480, 2011 DOI: 10.1227/NEU.0b013e318210c7df www.neurosurgery-online.com

Patients with tumors near the motor cortex are at risk of losing motor function from the surgical resection of the tumor. Preoperative cortical mapping is useful because it allows better planning of the surgical access route and extent of resection. It also enables better preoperative advising of the patient in regard to risk assessment and the value of surgery relative to nonsurgical treatments. Brain tumors can distort the normal anatomy by displacement resulting from tumor mass or by induction of plastic changes. When this occurs in the area of the motor cortex, preoperative functional mapping is imperative to minimize the risk of damaging motor function by the surgical intervention.

ABBREVIATIONS: DCS, direct cortical stimulation; **EMG,** electromyogram; **fMRI,** functional magnetic resonance imaging; **NBS,** navigated brain stimulation

Several technologies are currently available for preoperative functional mapping.[1] The most commonly used mapping technology is functional magnetic resonance imaging (fMRI), which maps neural activity indirectly by measuring metabolic changes during patient movements.[2,3] Similarly, magnetoencephalography detects magnetic fields generated by cortical activity during patient movement.[4] Positron emission tomography likewise measures cerebral blood flow, oxygen use, or glucose consumption of brain areas during patient performance of tasks.[5] Electroencephalography has also been used for preoperative mapping.[6] All these technologies depend on the patient making voluntary movements.

Thus, 2 problems arise if the patient cannot make voluntary movements of 1 or more limbs (or is cognitively incapable of task compliance). First, it will remain unknown whether functional recovery is possible at all after tumor removal.

Copyright © Congress of Neurological Surgeons. Unauthorized reproduction of this article is prohibited.

Second, even if recovery is possible, where the restorable functional areas are located will remain guesswork. Preoperative cortical mapping is still essential to spare functional motor cortex, but none of the available imaging technologies mentioned above can provide information on cortical areas if the patient cannot move the corresponding body part. Currently, the surgical planning and patient advising are based only on the anatomic MRIs.

Navigated brain stimulation (NBS)[7,8] is an enhanced version of navigated transcranial magnetic stimulation,[9-11] combined with 3-dimensional MRI and computer analysis, to provide feedback on the exact position of maximal stimulation. NBS differs from conventional technologies for preoperative mapping in that it does not passively record brain activity during voluntary patient movements. Instead, NBS actively stimulates the patient's motor cortex, thus producing involuntary muscle responses, which are then recorded by electromyogram (EMG) and direct observation.[10] Previous studies have shown that preoperative NBS mapping of the motor cortex in brain tumor patients is consistent with preoperative fMRI mapping[12] and intraoperative direct cortical stimulation (DCS).[7]

The aim of this article is to demonstrate with a case example that NBS can be used for preoperative cortical mapping in brain tumor patients with high-grade paresis or plegia. The patient presented here was part of a larger data analysis presented in a previous article, which contains further general discussion of NBS preoperative mapping.[7]

CASE PRESENTATION

A 63-year-old woman presented with a 5-month history of progressive left-sided weakness without other complaints. On admission, left hemiplegia was observed. Focal seizures at the initial onset of motor weakness had not recurred since she started taking antiepileptic medication. The patient was otherwise neurologically intact but quite pessimistic. She was very reluctant to undergo surgery or to receive any treatment at all because she could not move her limbs and felt she had no quality of life anyway.

Preoperative diagnostics consisted of MRI and NBS. The MRI (whole-head 256 × 256-mm scan on a Siemens 1.5-T MRI) revealed a 3 × 3 × 4-cm mass in the central region of the right hemisphere with a cyst (Figure 1). Thus, a metastasis within the precentral gyrus was suspected. Given the plegia and the MRI, we assumed that the corresponding parts of the motor system were irreversibly damaged.

Cortical mapping was performed noninvasively with the eXimia NBS system (Nexstim; Helsinki, Finland), which comprises a stereotactic navigation system, transcranial magnetic stimulation stimulator coil, 6-channel EMG recorder, central processing unit, and dual-display screens (Figure 2). Using anatomic landmarks, we coregistered the patient's head with the MR data set. Surface EMG electrodes were attached to the abductor pollicis brevis, abductor digiti minimi, first dorsal interosseous, and tibialis anterior muscles. After the patient's motor threshold was determined on the lesioned side, NBS mapping was systematically performed at 110% of the resting motor threshold, as previously described in more detail.[7,8] The coordinates of the motor representation area "hotspots" were stored in the system's database.

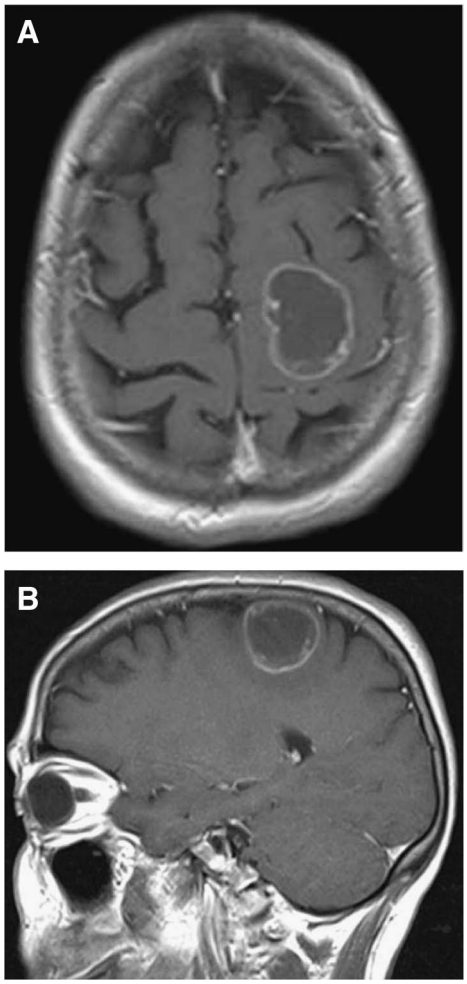

FIGURE 1. *Preoperative magnetic resonance image showing a 3 × 3 × 4-cm mass in the central region of the right hemisphere with an accompanying cyst.* **A**, *transverse view.* **B**, *sagittal view.*

Much to our surprise, preoperative mapping with NBS at stimulation intensities within the usual range elicited EMG responses from all 4 muscles. This strongly suggested that at least parts of the motor system were still intact and "only" not responding to voluntary control because of the tumor mass and/or edema. The patient saw her arm and leg move by the power of her own muscles again for the first time in weeks, so her attitude toward surgery improved substantially. These observations also led the surgical team to aim primarily for restoring motor function rather than maximizing resection and to examine motor

Copyright © Congress of Neurological Surgeons. Unauthorized reproduction of this article is prohibited.

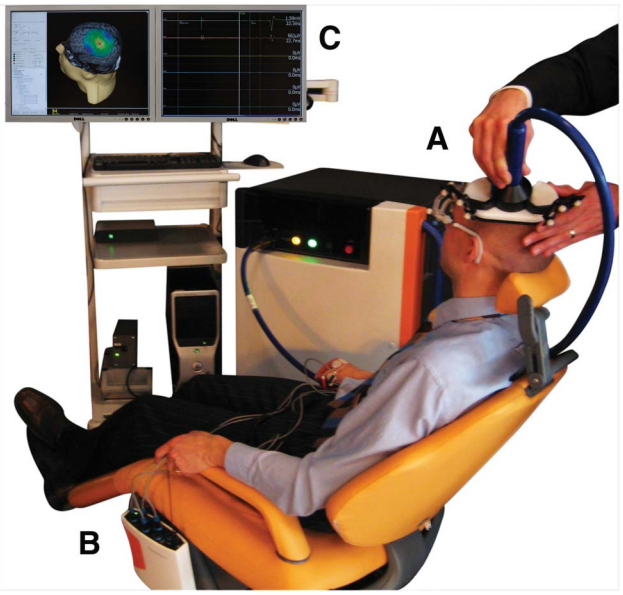

FIGURE 2. *The eXimia navigated brain stimulation system.* **A**, *handheld stimulation coil connected to the stimulator.* **B**, *electromyogram (EMG) device connected to surface electrodes on the subject's right hand.* **C**, *dual-display screens showing location of brain stimulation and EMG recording traces.*

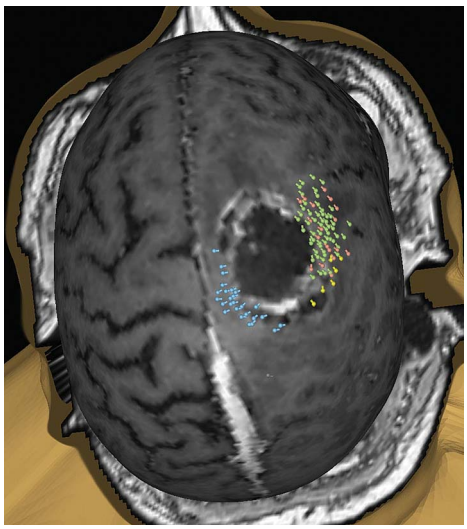

FIGURE 3. *Preoperative navigated brain stimulation showing that the tumor was immediately within the motor cortex and had split the patient's primary motor representation area. The color coding is as follows: green, abductor pollicis brevis; yellow, abductor digiti minimi; red, first dorsal interosseous; and blue, tibialis anterior (TA). The abductor pollicis brevis, abductor digiti minimi, and first dorsal interosseous were located lateral to the tumor, and the tibialis anterior was located mostly medial to the tumor with some slight response mediodorsally.*

function during resection by means of subcortical stimulation mapping in addition to DCS mapping and monitoring.

The preoperative NBS results revealed that the tumor was immediately within the motor cortex and had split the patient's primary motor representation area. The abductor pollicis brevis, abductor digiti minimi, and first dorsal interosseous were lateral to the tumor, and the tibialis anterior was medial to the tumor with some slight response mediodorsally (Figure 3). Because of these findings, our operative strategy was to start by draining the cyst in the tumor center. We would then begin the dissection in the frontal part of the tumor and continue back toward the area of direct contact (or possible infiltration) of the motor cortex only if a clear plane between the tumor and cortex could be identified.

The patient underwent surgical resection of the tumor mass, guided by intraoperative DCS[13,14] and direct subcortical stimulation.[15,16] Total intravenous anesthesia was administered. Neuromuscular blocking agents were used only during intubation. Neuronavigation was registered by anatomic landmarks. The central sulcus and primary motor cortex were identified by somatosensory phase reversal with median nerve stimulation. Neurophysiological monitoring was performed with motor evoked potentials as previously described.[17] DCS was performed for the abductor pollicis brevis and tibialis anterior with a 5-mm-diameter monopolar electrode as previously described.[13,14] Motor representation area hotspots were identified by moving the electrodes in 5-mm steps. The coordinates of the hotspot locations derived from the DCS mapping were entered into the surgical neuronavigator database. Motor areas were identified medial and frontolateral of the tumor (Figure 4). The cortex immediately above the tumor showed no motor activity. The resection was performed in a standard fashion, starting with aspiration of the cystic part. After identification of a plane between the tumor and healthy tissue, the tumor was removed by microdissection. Monitoring of motor function by repetitive DCS demonstrated stable motor evoked potentials throughout the operation. Subcortical stimulation was performed sporadically during dissection at the basal part of the tumor to avoid damaging intact motor tracts. At the lateral and medial border of the resection cavity, motor evoked potentials were observed at a stimulation of 3 mA, proving that motor tracts were in the immediate vicinity.[16]

Postoperatively, the patient had already recovered to British Medical Research Council grade 4 by the first day. An MRI taken at 24 hours postoperatively documented that the resection was complete (Figure 5). The resection also appeared complete microscopically. Histopathology confirmed that the tumor was a metastasis from lung cancer. NBS mapping on the fourth postoperative day (Figure 6) demonstrated larger amplitudes of motor evoked potentials in response to lower stimulation intensities compared with the preoperative NBS. The electric field strength at the cortical surface needed to trigger motor evoked potentials had dropped from 107 V/m preoperatively to 56 V/m

Copyright © Congress of Neurological Surgeons. Unauthorized reproduction of this article is prohibited.

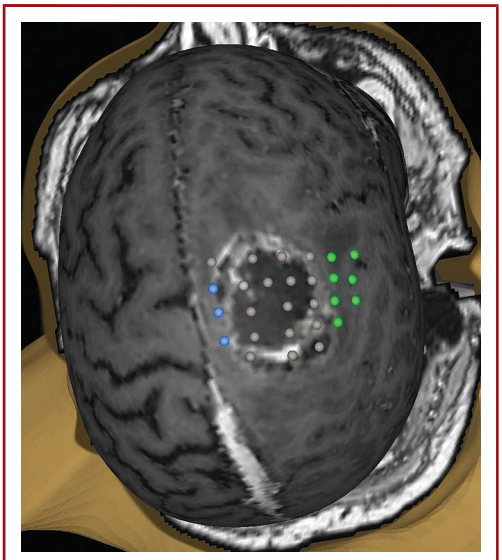

FIGURE 4. *Neuronavigation image showing where direct cortical stimulation was performed for intraoperative mapping. The color coding is as follows: green, response from the abductor pollicis brevis; blue, response from the tibialis anterior; and gray, stimulation target that yielded no response.*

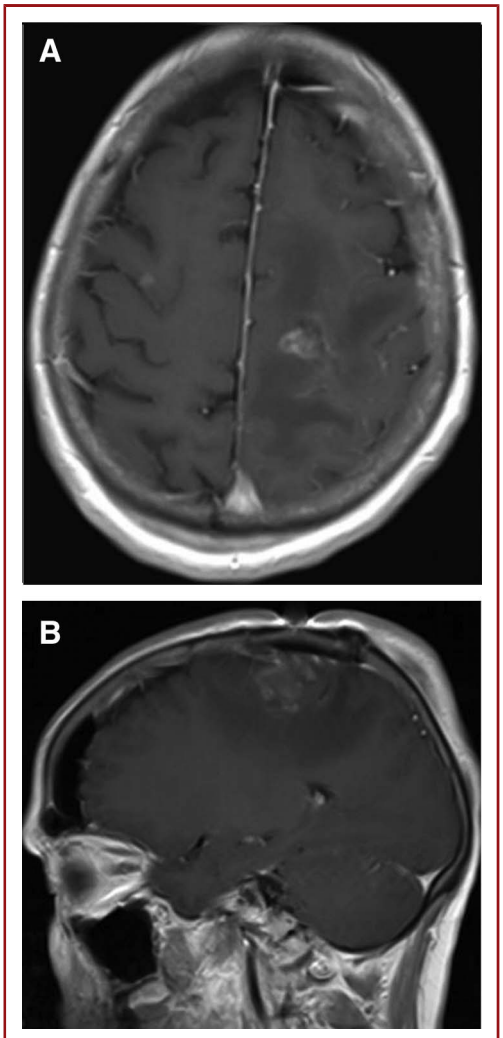

FIGURE 5. *Postoperative magnetic resonance image of a seemingly complete tumor removal.* **A**, *transverse view.* **B**, *sagittal view.*

postoperatively. At discharge on the seventh postoperative day, the patient had completely recovered with only residual impairment of fine motor skills in her left hand.

For further analysis, the DCS hotspot coordinates were transferred from the surgical neuronavigator into the NBS system. The eXimia screen simultaneously displayed the DCS and NBS results in a 3-dimensional navigational image of the patient's brain. The preoperative NBS results were consistent with the intraoperative DCS results as previously reported.[7] The distance between the NBS and DCS hotspots was 0.83 mm for the abductor pollicis brevis. For technical reasons, the DCS measurements of the tibialis anterior were off but confirmed leg representations medial of the tumor.

At the 3-month follow-up, the patient had no functionally relevant paresis and only slight impairment of fine motor skills.

DISCUSSION

During surgical removal of brain tumors, care must be taken to not damage surrounding functional brain tissue. The mass of the tumor can distort and obscure the cortical anatomy, making it difficult to know the role of brain tissue in a given spot. When this occurs in the area of the motor cortex, preoperative cortical mapping is useful to avoid causing motor deficits. If a patient has already lost most motor function preoperatively, then the existing preoperative mapping technologies (fMRI, positron emission tomography, magnetoencephalography, electroencephalography) cannot be used because the patient cannot make the voluntary movements needed for these technologies to provide data. In contrast, NBS can be used in such cases because it does not rely on voluntary patient movements but instead stimulates the brain by magnetically induced electrical currents, thus producing involuntary movements.

This case demonstrates that NBS can be used for such preoperative mapping. The clinical presentation and preoperative MRI suggested that the tumor had destroyed parts of the primary motor cortex and thus permanently eliminated motor function for the patient's left arm and leg. NBS revealed that this was not the case. It showed that viable motor cortex remained lateral to the tumor for the left arm and medial to the tumor for the left leg. NBS showed that the tumor had only "blocked" or

Copyright © Congress of Neurological Surgeons. Unauthorized reproduction of this article is prohibited.

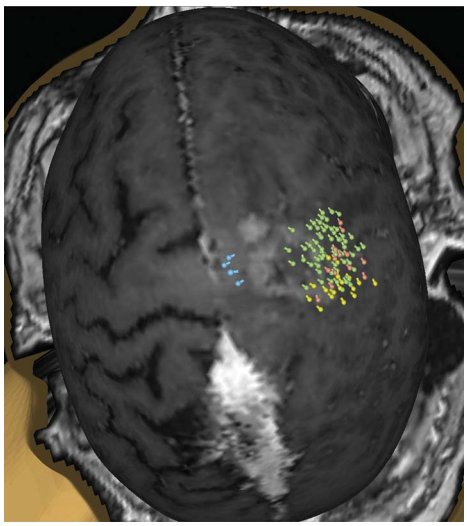

FIGURE 6. *Postoperative navigated brain stimulation showing the preservation of motor function after surgery. The color coding is as follows: green, abductor pollicis brevis; yellow, abductor digiti minimi; red, first dorsal interosseous; and blue, tibialis anterior.*

"incapacitated" voluntary motor function but had not destroyed the patient's potential capacity for motor function. It therefore became clear that motor function might be restorable if the tumor was surgically removed. These results were confirmed by the independent intraoperative mapping with the gold standard of DCS. The surgery successfully removed the tumor without causing any iatrogenic deficits. The greater postoperative responsiveness to NBS was reflective of the patient's complete clinical recovery.

Sometimes, attempts have been made to use fMRI for preoperative mapping in partially or even completely paretic patients. First, in cases in which the patient had diminished but not absent motor function, comparisons have been made of ipsilateral and contralateral activation on fMRI to provide indirect evidence that some part of the functional motor cortex has not been mapped.[18] At the same time, that study showed that lack of cortical activation in the peritumorous tissue on fMRI does not definitively prove that there is no functional motor tissue in those areas.[18] It only shows that they are not currently metabolically active during voluntary movement. In contrast, lack of motor response after NBS can be taken as more definitive evidence that a cortical area is not involved in motor output. Second, in patients with no motor activity, it appears possible to map cortical motor function by analyzing the intrinsic cortical activity on task-free fMRI,[19] thus allowing preoperative mapping of paretic patients. However, in our opinion, that method requires complicated analysis of fMRI data, is even more prone to the known inaccuracies of fMRI, and yields results that only roughly correspond to the results from standard fMRI recording of movement. So, although these 2 approaches using fMRI were better than performing no mapping at all, we believe that NBS offers a clearly superior solution for preoperative mapping in paretic patients. Two other fMRI-based approaches have been proposed in studies on healthy volunteers,[20,21] but the findings do not seem sufficiently reliable for surgical planning.

A further lesson should be drawn from this case regarding the preoperative mapping of brain tumor patients. If a patient is paretic but able to move, it is still possible to map the motor cortex with fMRI. However, voluntary movements in these patients may not activate all the areas of the motor cortex that could be functional after tumor resection. As seen in this case, areas of the motor cortex could not be activated by the patient preoperatively but were restored to function postoperatively. Similarly, even in paretic patients who can still move enough for preoperative fMRI mapping, NBS may often be better able than fMRI to detect functional motor cortex that should be spared during surgery. In other words, fMRI might map only motor cortex that is still functional at the preoperative level of paresis, whereas NBS is also able to detect motor cortex that is not active at the preoperative level of paresis but that could be restored to function after resection of the tumor.

NBS allows accurate preoperative mapping of the motor cortex. Because it does not rely on voluntary patient movements, NBS is suitable for use on paretic patients with brain tumors in the area of the motor cortex. In contrast to imaging technologies, NBS even appears able to identify areas of the motor cortex that will be restored to function after tumor resection.

Disclosure

The research reported in this article was supported by a research promotion grant from the Charité–Universitaetsmedizin Berlin (project No. 2007/29516) and by a grant from the Berliner Krebsgesellschaft. The authors have no personal financial or institutional interest in any of the drugs, materials, or devices described in this article.

REFERENCES

1. Mazziotta JC. Imaging: window on the brain. *Arch Neurol*. 2000;57(10):1413-1421.
2. Tieleman A, Deblaere K, Van Roost D, Van Damme O, Achten E. Preoperative fMRI in tumour surgery. *Eur Radiol*. 2009;19(10):2523-2534.
3. Picht T, Kombos T, Suess O, et al. Functional magnetic resonance imaging and cortical mapping in motor cortex tumor surgery: complementary methods. *Zentralbl Neurochir*. 2008;69(1):1-6.
4. Mäkelä JP, Forss N, Jääskeläinen J, Kirveskari E, Korvenoja A, Paetau R. Magnetoencephalography in neurosurgery. *Neurosurgery*. 2006;59(3):493-511.
5. Fox PT. Functional brain mapping with positron emission tomography. *Semin Neurol*. 1989;9(4):323-329.
6. Darcey TM, Hughes HC, Barkan HI, Saykin AJ. Preoperative functional mapping using intracranial EEG activation methods. *Adv Neurol*. 2000;84:331-341.
7. Picht T, Schmidt S, Brandt S, et al. Preoperative functional mapping for rolandic brain tumor surgery: a case series comparison of navigated transcranial magnetic stimulation to direct cortical stimulation. *Hum Brain Mapp*. In press.
8. Säisänen L, Julkunen P, Niskanen E, et al. Motor potentials evoked by navigated transcranial magnetic stimulation in healthy subjects. *J Clin Neurophysiol*. 2008;25(6):367-372.
9. Picht T, Mularski S, Kuehn B, Vajkoczy P, Kombos T, Suess O. Navigated transcranial magnetic stimulation for preoperative functional diagnostics in brain tumor surgery. *Neurosurgery*. 2009;65(6)(suppl):93-98.

Copyright © Congress of Neurological Surgeons. Unauthorized reproduction of this article is prohibited.

10. Krings T, Chiappa KH, Foltys H, Reinges MHT, Cosgrove GR, Thron A. Introducing navigated transcranial magnetic stimulation as a refined brain mapping methodology. *Neurosurg Rev*. 2001;24(4):171-179.
11. Julkunen P, Säisänen L, Danner N, et al. Comparison of navigated and non-navigated transcranial magnetic stimulation for motor cortex mapping, motor threshold and motor evoked potentials. *Neuroimage*. 2009;44(3):790-795.
12. Krings T, Foltys H, Reinges MHT, et al. Navigated transcranial magnetic stimulation for presurgical planning. *Minim Invas Neurosurg*. 2001;44(4): 234-239.
13. Suess O, Suess S, Brock M, Kombos T. Intraoperative electrocortical stimulation of Brodman area 4: a 10-year analysis of 255 cases. *Head Face Med*. 2006;2:20.
14. Kombos T, Suess O, Funk T, Kern BC, Brock M. Intra-operative mapping of the motor cortex during surgery in and around the motor cortex. *Acta Neurochir (Wien)*. 2000;142(3):263-268.
15. Bernstein M. Subcortical stimulation mapping. *J Neurosurg*. 2004;100(3): 365-366.
16. Keles GE, Lundin DA, Lamborn KR, Chang EF, Ojemann G, Berger MS. Intraoperative subcortical stimulation mapping for hemispheric perirolandic gliomas located within or adjacent to the descending motor pathways: evaluation of morbidity and assessment of functional outcome in 294 patient. *J Neurosurg*. 2004;100(3):369-375.
17. Kombos T, Suess O, Ciklatekerlio Ö, Brock M. Monitoring of intraoperative motor evoked potentials to increase the safety of surgery in and around the motor cortex. *J Neurosurg*. 2001;95(4):608-614.
18. Roux FE, Boulanouar K, Ibarrola D, Tremoulet M, Chollet F, Berry I. Functional MRI and intraoperative brain mapping to evaluate brain plasticity in patients with brain tumours and hemiparesis. *J Neurol Neurosurg Psychiatry*. 2000;69(4):453-463.
19. Liu H, Buckner RL, Talukdar T, Tanaka N, Madsen JR, Stufflebeam SM. Task-free presurgical mapping using functional magnetic resonance imaging intrinsic activity. *J Neurosurg*. 2009;111(4): 746-754.
20. Gasser TG, Sandalcioglu EI, Wiedemayer H, et al. A novel passive functional MRI paradigm for preoperative identification of the somatosensory cortex. *Neurosurg Rev*. 2004;27(2):106-112.
21. Stippich C, Ochmann H, Sartor K. Somatotopic mapping of the human primary sensorimotor cortex during motor imagery and motor execution by functional magnetic resonance imaging. *Neurosci Lett*. 2002;331(1):50-54.

Acknowledgments

We would like to thank Michael Hanna, PhD (Mercury Medical Research and Writing), for providing medical writing services and feedback on the figures.

COMMENT

This is a nice case presentation regarding the value of transcranial magnetic stimulation in the not-so-rare event of a preoperative severe motor impairment in a patient in whom functional magnetic resonance imaging is precluded because of the lack of voluntary limb movement. Navigated transcranial magnetic stimulation seems to be, at least when used by an experienced group, a valuable tool. This case report further serves as an example that preoperative transcranial magnetic stimulation could indicate the potential of postoperative functional recovery in patients with severe motor deficits.

J.C. Tonn
Berlin, Germany

Copyright © Congress of Neurological Surgeons. Unauthorized reproduction of this article is prohibited.

Community-Associated Methicillin-Resistant *Staphylococcus Aureus*–Infected Chronic Scalp Wound With Exposed Dura in a 10-Year-Old Boy: Vacuum-Assisted Closure Is a Feasible Option: Case Report

Ulrike Subotic, MD*
Wolfram Kluwe, MD‡
Valérie Oesch, MD§

*Pediatric Surgery, Children's Hospital, University Zurich, Zurich, Switzerland; ‡Wolfram Kluwe, Pediatric Surgery, Asklepios Hospital, Sankt Augustin, Germany; §Pediatric Surgery, Children's Hospital, University Berne, Berne, Switzerland

Correspondence:
Dr Ulrike Subotic,
Pediatric Surgery,
Kinderspital Steinwiesstrasse 75,
8032 Zurich, Switzerland.
E-mail: subotic18@gmx.net

Received, November 12, 2009.
Accepted, July 23, 2010.

Copyright © 2011 by the
Congress of Neurological Surgeons

BACKGROUND AND IMPORTANCE: Since the introduction of vacuum-assisted closure (VAC) in 1997, it has been used successfully in treating difficult wounds, including spinal wounds and wounds in pediatric patients. There are no reports on VAC therapy in pediatric patients on the scalp, especially with exposed dura. This report describes a 10-year-old boy with a chronic wound of the scalp with exposed dura after multiple neurosurgical interventions who was treated successfully with VAC.

CLINICAL PRESENTATION: A 10-year-old mentally disabled boy with Apert syndrome suffered from a chronic wound with community-associated methicillin-resistant *Staphylococcus aureus* (MRSA) infection after multiple neurosurgeon operations. For wound closure, VAC therapy was initiated on the bony defect with exposed dura. The wound healed successfully, and the MRSA disappeared.

CONCLUSION: The aims of VAC therapy are formation of new granulation tissue, wound cleansing, and bacterial clearance. In this case, the VAC device was excellent for temporary coverage of the defect and for wound cleaning, and it allowed a thick bed of granulation tissue to form over the dura, even with minimal constant negative pressure. The application and management were feasible even in a mentally disabled child. With this experience, we are encouraged to use the VAC device in difficult wounds, even in the head and neck area in children, and to bring this treatment into the outpatient clinic.

KEY WORDS: Dura, GranuFoam Silver, MRSA, Pediatric, VAC, Vacuum-assisted closure

Neurosurgery 68:E1481–E1484, 2011 DOI: 10.1227/NEU.0b013e318210c7fb www.neurosurgery-online.com

Vacuum-assisted closure (VAC) therapy was introduced by Argenta and Morykwas[1] in 1997 and has been in routine clinical use for the treatment of difficult wounds. The mechanism of treatment is exposure of the wound bed to negative pressure, resulting in removal of edema fluid, improvement in the blood supply, and stimulation of cellular proliferation of reparative granulation tissue. It has been used successfully to treat open wounds of the extremities, thoracic and abdominal walls, and pressure or diabetic ulcerative wounds.[1] It has also proved effective for the treatment of spinal wound infections, and the application is stated as being simple.[2] Since 2000, there are upcoming reports about vacuum-assisted wound closure in pediatric patients.

There are only case reports in VAC therapy on exposed dura in adults.[3,4] Reports about VAC therapy in pediatric patients on the scalp and especially on dura have not yet been published.

ABBREVIATIONS: MRSA, methicillin-resistant Staphylococcus aureus; **VAC,** vacuum-assisted closure

CLINICAL PRESENTATION

We report the treatment of a 10-year-old boy with Apert syndrome. Because of craniosynostosis vertex, craniectomy and fronto-orbital advancement were performed in 1998. After surgery, the patient developed severe wound and

Copyright © Congress of Neurological Surgeons. Unauthorized reproduction of this article is prohibited.

bone infection with resulting frontotemporal bony defect and hairless scar. Several plastic surgical interventions, including tissue expansion and pedicled flaps with recurrent wound infections, were performed, and multiple broad scars remained. In 2006, a titanium mesh was inserted to cover the bony defect. After this intervention, a wound dehiscence remained. Because of the complicated medical history, no further surgery was planned, and the titanium mesh was left exposed (Figure 1). In July 2008, the patient presented at an emergency department with an abscess in the persisting wound, and surgical intervention was mandatory. The abscess was drained. The microbiological result showed an infection with community-associated methicillin-resistant *Staphylococcus aureus* (MRSA), and a VAC (Kinetic Concepts Inc, San Antonio, Texas) was started. The patient tolerated the system change without any anesthesia in the outpatient clinic; after 2 weeks, the titanium mesh was covered with granulation tissue, and a full-thickness skin transplantation was performed. At first, the treatment seemed to be successful, and there was a take of 100%. Three weeks after transplantation, the wound recurred, MRSA was again detectable, only 20% of the graft was still vital, and the titanium mesh was again exposed (Figure 2).

INTERVENTION

An interdisciplinary team (pediatric surgeon, pediatric infectiologist, maxillofacial surgeon) decided to start a MRSA-eradication therapy that included the removal of the titanium mesh, a systemic perioperative antibiotic therapy with vancomycin, and an eradication therapy of the family.

The mesh was removed (Figure 3). During this procedure, the dura was injured. The defect was oversewn and covered with TachoSil (Nycomed, Roskilde, Denmark). TachoSil is a sterile, ready-to-use, absorbable patch for intraoperative topical application. It consists of an equine collagen patch coated with the fibrin glue components, human fibrinogen and human thrombin. It thus combines the aspects of a pliable patch material with the hemostatic and adhesive properties of the coagulation factors. The product is currently approved in Europe for supportive hemostatic treatment in surgery.[5] VAC was again applied, this time with GranuFoam Silver. The aim of this dressing was better eradication of MRSA. As a result of the concerns of negative pressure on exposed dura, sinus thrombosis, and lack of clinical experience, a constant setting of only −25 mm Hg was installed. A porous silicone sheet (Mepitel; Mölnlycke Health Care, Norcross, Georgia) was placed between foam and dura to avoid adhesions.

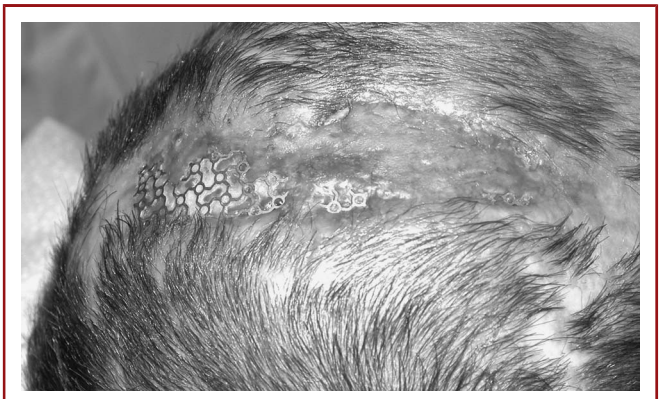

FIGURE 2. *Recurrent defect with exposed titanium mesh after full-thickness skin transplantation.*

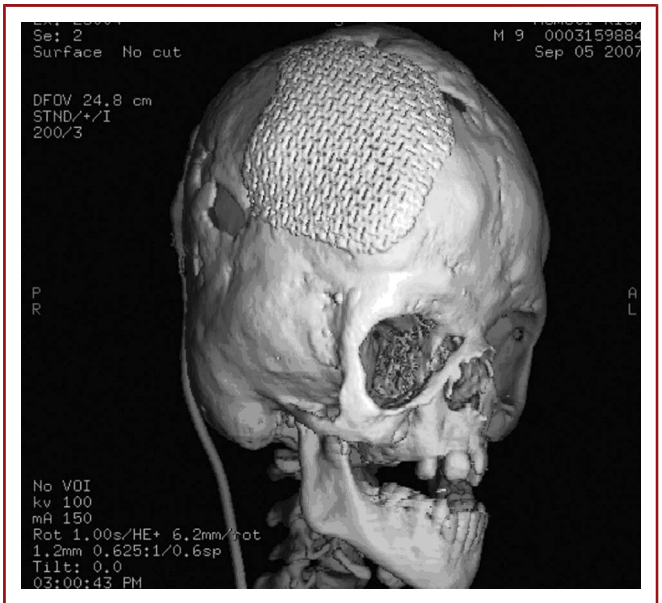

FIGURE 1. *Computed tomography scan of the bone and titanium mesh.*

FIGURE 3. *Intraoperative defect after removal of the titanium mesh.*

Copyright © Congress of Neurological Surgeons. Unauthorized reproduction of this article is prohibited.

The VAC device was changed twice a week. The patient tolerated the therapy without any difficulty, and subsequent system changes were performed in the outpatient clinic without anesthesia. There was no leakage of cerebrospinal fluid. After 3 weeks, the bony defect was covered with granulation tissue, and the VAC treatment was stopped. Because of previous failure of full-thickness transplantation, the parents refused another skin graft, and the wound was left covered with only a dressing for contraction. After 2 weeks, the wound was closed (Figure 4). Reported complications of the VAC device such as pain, excessive in-growth of granulation tissue, and late infection were not observed. Six months after this treatment, the patient is still free of MRSA.

DISCUSSION

Reconstruction of scalp and calvarial defects can be challenging because of the poor vascularity of the cortical bone. In our particular case, free flaps and tissue expansion failed, and a bony defect was covered with titanium mesh. The implant was exposed for several years and colonized with MRSA. In the literature, the failure rate of wound debridement without implant removal is between 32% and 86%.[6] In our case, this attempt failed, and removal of the implant was necessary. The question then became, How do we close the exposed dura?

The aims of vacuum therapy are the formation of new granulation tissue, wound cleansing, and bacterial clearance.[7] Andrews et al[8] described the successful use of VAC in complicated head and neck wounds, and VAC has also been proved effective in infected spinal wounds with exposed dura.[2] We have had excellent results using VAC therapy and GranuFoam Silver in the management of infected wounds in children. This device is an "open-celled, reticulated polyurethane foam" that has been microbonded with metallic silver via a proprietary metallization process. The silver-impregnated foam creates a large surface area from which Ag^+ is released on exposure to wound fluid.[9] The effectiveness of silver as an antimicrobial agent has been well established.[10] Combining the advantages of silver and VAC therapy in a silver-impregnated foam has particular appeal in treating colonized chronic wounds such as that in our patient. For this reason, we decided to apply this device. Because of concerns about creating a cerebrospinal fistula and because of a paucity of clinical experience, minimal negative pressure was installed. In neonates with abdominal wound and exposure of bowel, the lowest applicable negative pressure is recommended in VAC therapy.[11] This seems to be the most vulnerable group; therefore, we geared our therapy to this recommendation. The application was excellent for temporary coverage of the defect and for wound cleaning, and it allowed a thick bed of granulation tissue to form over the dura. In addition, management was feasible even in a mentally disabled child.

There are only 2 reports about the use of the VAC device in the treatment of scalp wounds with exposed dura in adults.[3,4] This is the first report on this treatment in a child with an injured dura. With low constant subatmospheric pressure application, there was no leakage, and the wound was closed without any complications. The VAC device is feasible for use in the treatment of scalp wounds with exposed dura and chronic infection to create a setting for wound closure, eg, secondary healing and skin transplantation. Because of this experience, we are encouraged to use the VAC device in difficult wounds, even in the head and neck area in children, and to bring this treatment in the outpatient clinic.

FIGURE 4. *Three weeks after vacuum-assisted closure therapy.*

Disclosure

The authors have no personal financial or institutional interest in any of the drugs, materials, or devices described in this article.

REFERENCES

1. Argenta LC, Morykwas MJ. Vacuum-assisted closure: a new method for wound control and treatment: clinical experience. *Ann Plast Surg*. 1997;38(6):563–577.
2. Ploumis A, Mehbod AA, Dressel TD, Dykes DC, Transfeldt EE, Lonstein JE. Therapy of spinal wound infections using vacuum-assisted wound closure: risk factors leading to resistance to treatment. *J Spinal Disord Tech*. 2008;21(5):320-323.
3. Adil Abas Khan M, Chipp E, Hardwicke J, Srinivsasn K, Shaw S, Rayatt S. The use of dermal regeneration template (Integra®) for reconstruction of a large full-thickness scalp calvarial defect with exposed dura. *J Plast Reconstr Aesthet Surg*. 2010;63(12)2168–2171.
4. Donovan D, Person D. Giant eccrine adenocarcinoma of the scalp with intracranial invasion: resection and reconstruction using a vacuum-assisted closure device: technical case report. *Neurosurgery*. 2006;58(4)(Suppl 2):ONS-E371.
5. Siemer S, Lahme S, Altziebler S, et al. Efficacy and safety of TachoSil as haemostatic treatment versus standard suturing in kidney tumour resection: a randomised prospective study. *Eur Urol*. 2007;52(4):1156-1163.
6. Zimmerli W, Ochsner PE. Management of infection associated with prosthetic joints. *Infection*. 2003;31(2):99-108.
7. Willy C. Side effects and risks of vacuum therapy. In: Willy C, ed. *The Theory and Practice of Vacuum Therapy*. Ulm, Germany: Linquist Book Publishing; 2005:87-101.
8. Andrews B, Smith R, Goldstein D, Funk F. Management of complicated head and neck wounds with vacuum-assisted closure system. *Head Neck*. 2006;28(11):974-981.
9. Ambrosio A, Barton K, Ginther D.VAC GranuoFoam Silver dressing: a new antimicrobial silver foam dressing specifically engineered for use with VAC therapy [brochure]. San Antonio, TX: Kinetic Concepts Inc; 2005.
10. Gerry R, Kwei S, Bayer L, Breuing K. Silver-impregnated vacuum-assisted closure in the treatment of recalcitrant venous stasis ulcers. *Ann Plast Surg*. 2007;59(1):58-62.
11. Lopez G, Clifton-Koeppel R, Emil S. Vacuum-assisted closure for complicated neonatal abdominal wounds. *J Pediatr Surg*. 2008;43(12):2202-2207.

Copyright © Congress of Neurological Surgeons. Unauthorized reproduction of this article is prohibited.

COMMENTS

This is an interesting approach to a fortunately unusual complication. It increases our armamentarium for handling these difficult problems and is a creative solution to a complication that eludes other solutions. Vacuum-assisted closure therapy has been used quite successfully in difficult wound complications. It has been used for spine wounds by neurosurgeons and orthopedic surgeons. Plastic surgeons have used it on the scalps and even on the dura. Although this is the first case report on a child, the child is 10 years old and thus not that different from an adult. Although a polyurethane sponge is usually used with this device, the authors used a silver sponge for its antimicrobial properties. This is another worthwhile useable technique. The setting of −25 mm Hg, determined empirically, worked and appeared to be well tolerated. I congratulate the authors on their creativity and thank them for sharing it with us.

Arthur E. Marlin
Tampa, Florida

The authors present the first successful use of a vacuum-assisted closure (VAC) device to treat an infected cranial wound with exposed dura in a child. This child with Apert syndrome had undergone several prior failed procedures to correct his cranial and scalp defects and had developed a methicillin-resistant *Staphylococcus aureus* (MRSA) abscess around his titanium mesh cranioplasty. A first attempt at VAC repair without removal of the titanium mesh healed initially but then failed after 3 weeks. The titanium mesh was removed, and the VAC device treatment was repeated with a silver-impregnated sponge to enhance eradication of the MRSA. Because of the exposed dura, the VAC device was used at a low setting. Importantly, surgical therapy was accompanied by intravenous vancomycin and MRSA-eradication therapy for the family. The child tolerated the VAC device changes in the outpatient clinic without sedation. The report suggests that VAC therapy may be used safely over exposed dura as part of a multidisciplinary treatment plan in selected rare patients who have failed the other more standard options.

Shenandoah Robinson
Cleveland, Ohio

Copyright © Congress of Neurological Surgeons. Unauthorized reproduction of this article is prohibited.

Pott Disease in a 13-Month-Old: Case Report

Giac Consigilieri, MD
Udaya K. Kakarla, MD
Nicholas Theodore, MD

Division of Neurological Surgery, Barrow Neurological Institute, St Joseph's Hospital and Medical Center, Phoenix, Arizona

Correspondence:
Nicholas Theodore, MD, FACS,
c/o Neuroscience Publications,
Barrow Neurological Institute,
350 W Thomas Rd,
Phoenix, AZ 85013.
E-mail: neuropub@chw.edu

Received, November 13, 2009.
Accepted, May 7, 2010.

Copyright © 2011 by the
Congress of Neurological Surgeons

BACKGROUND AND IMPORTANCE: Tuberculosis (TB) is a common disease worldwide that is caused by *Mycobacterium tuberculosis*. TB of the spine is the most common site of bony infection and is often referred to as Pott disease. To the best of our knowledge, our case represents the youngest patient with naturally acquired Pott disease in the United States.

CLINICAL PRESENTATION: A 13-month-old boy presented with paraplegia and a known diagnosis of TB. His evaluation revealed a kyphotic gibbus deformity in the midthoracic region associated with severe spinal cord compression. The patient underwent urgent decompressive laminectomies, T2-T4 transpedicular corpectomies, placement of an anterior tibial strut graft, and posterior instrumentation with sublaminar wires and a Steinmann pin. At his 18-month follow-up, the patient was ambulating 5 steps at a time independently, and his kyphotic deformity showed no sign of progression.

CONCLUSION: Pott disease can occur in very young children and presents a unique challenge when a patient presents with a neurological deficit and unstable deformity requiring surgical intervention.

KEY WORDS: Pediatric Pott disease, spine, tuberculosis

Neurosurgery 68:E1485–E1490, 2011 DOI: 10.1227/NEU.0b013e318210c81b www.neurosurgery-online.com

Tuberculosis (TB) is a common disease caused by mycobacteria, especially *Mycobacterium tuberculosis*. According to the World Health Organization, almost one-third of the world population has been exposed to the pathogen.[1] The incidence of the disease is highest in Africa (358 per 100 000 population). In contrast, in the United States, the incidence is estimated to be 4.6 in 100 000 and is mostly restricted to certain subsets of society.[2] Groups at high risk are the homeless, intravenous drug abusers, immigrants, refugees from high-prevalence countries, those coinfected with human immunodeficiency virus or immunocompromised, residents of prisons and nursing homes, and children exposed to infected individuals.[3]

TB of the spine is the most common site of bony infection and is often referred to as Pott disease. Spinal involvement of TB assumes many forms, including arachnoiditis, intramedullary tuberculoma, epidural abscess, diskitis, and spondylitis.[4] We report TB spondylitis in a 13-month-old boy, the youngest such case reported in the literature.

ABBREVIATION: TB, tuberculosis

PATIENTS AND METHODS

The primary complaint for this 13-month-old Hispanic boy was loss of ambulation. The patient was fully ambulatory by 9 months of age. Two months later, he and his family were diagnosed with pulmonary TB and started on multidrug therapy consisting of rifampin, isoniazid, pyrazinamide, and ethambutol. Despite a full course of broad-spectrum anti-TB medications, the child developed a progressive neurological deficit. At the time of his initial presentation, he was able to stand only with support. One month later, the child was taken to an outside facility because he was refusing to stand. Magnetic resonance (MR) imaging of the neuraxis was performed, and the patient was transferred to our facility.

On admission, the boy was paraplegic with some preserved spinal reflexes. His strength was normal in both upper extremities. His legs were spastic with no purposeful movement. He was hyperreflexic with persistent ankle clonus. Babinski sign was present. Given his age and lack of cooperation, the level of paraplegia was difficult to assess.

Sagittal MR images of the thoracic spine showed a kyphotic gibbus deformity. With contrast enhancement, a large paraspinal and epidural abscess was seen extending from T2 to T6 (Figure 1A and 1B). Axial MR images showed the paraspinal abscess located ventrally and extending into the spinal canal.

Copyright © Congress of Neurological Surgeons. Unauthorized reproduction of this article is prohibited.

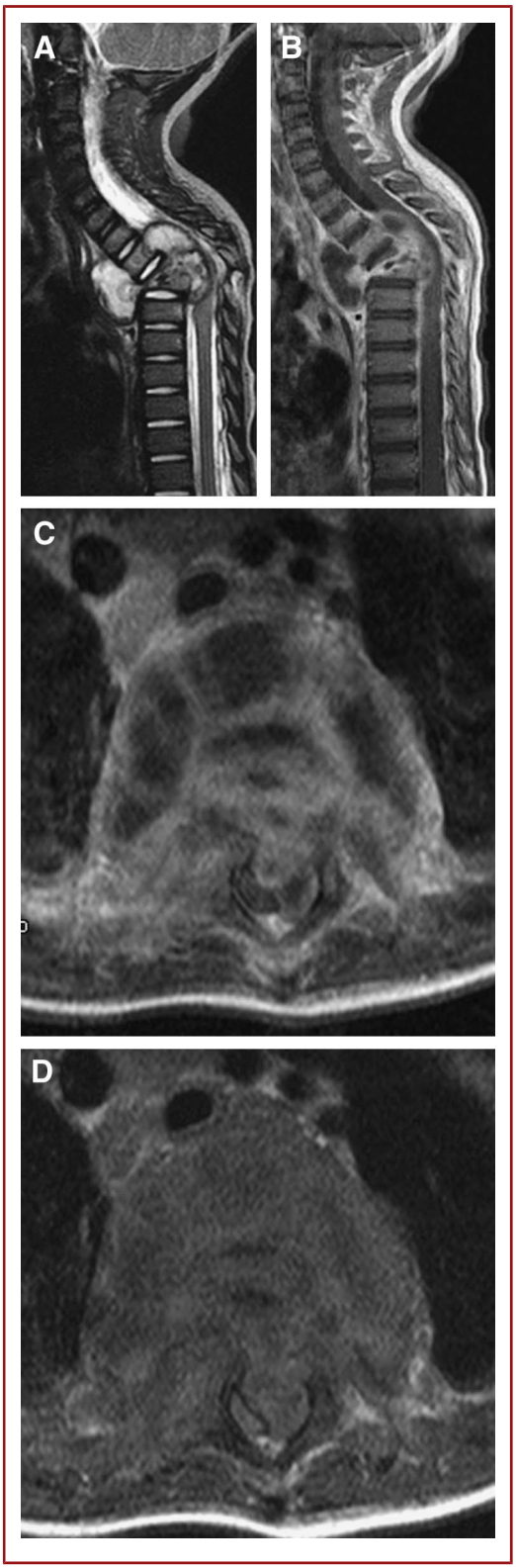

The abscess severely compressed the spinal cord and displaced it to the right (Figure 1C and 1D). Computed tomography of the thoracic spine showed complete destruction of the T4 vertebral body and collapse of T3 onto the vertebral body of T5 (Figure 2A and 2B).

The patient was continued on a solumedrol protocol that was initiated at the outside facility. He underwent an urgent laminectomy and transpedicular corpectomies from T2 to T4 via a posterior approach. The ventral abscess was drained, and the spinal sac was decompressed circumferentially until spontaneous pulsations of spinal fluid were seen. Sublaminar wires were placed from C7 to T7 and fastened to a Steinmann pin unilaterally in an attempt to partially correct the deformity. An anterior fibular strut graft was placed from T3 to T6 to reconstruct the anterior column (Figure 3). After the strut graft was placed, the contralateral Steinmann pin was fastened, providing good correction of the deformity. Structural allografts were placed posteriorly from T1 to T5 to provide additional support (Figure 4A and 4B).

RESULTS

The patient tolerated the surgery well. Postoperative dynamic imaging in a thoracolumbosacral orthosis was stable. His neurological examination remained unchanged. He was discharged home on day 10 with outpatient therapies and continued on the antibiotics for 4 months. At his most recent follow-up 26 months after surgery, the patient had made significant neurological recovery. The patient was able to walk 5 steps at a time, and he continues to improve, working with physical therapy on a regular basis. Anteroposterior and lateral films showed a stable construct with no progression of a kyphotic deformity (Figure 5A and 5B).

DISCUSSION

In the United States, pediatric Pott disease has been rare with the steady decline in the prevalence of TB since 1990.[5] The youngest reported case of Pott disease was in a 3-week-old infant who acquired the infection congenitally.[6] To the best of our knowledge, our case represents the youngest patient with naturally acquired Pott disease in the United States.

Spinal spondylitis is the most common manifestation of skeletal TB, and 1% to 3% of patients suffering from TB have skeletal involvement.[7] Most common during the first 3 decades of life,[7] it is a leading cause of paraplegia in developing countries. Patients typically present with pain after the bacterial infection has spread from the lungs to bony structures through the bloodstream. In particular, the vertebral bodies may be infected via the extensive venous plexus of Batson,[5,8] spreading the

FIGURE 1. *Sagittal T2-weighted magnetic resonance (MR) image (A), sagittal (B) and axial (C) T1-weighted MR images with gadolinium, and axial T1-weighted MR image (D) of the thoracic spine showing a kyphotic gibbus deformity in the midthoracic region. Used with permission from Barrow Neurological Institute.*

Copyright © Congress of Neurological Surgeons. Unauthorized reproduction of this article is prohibited.

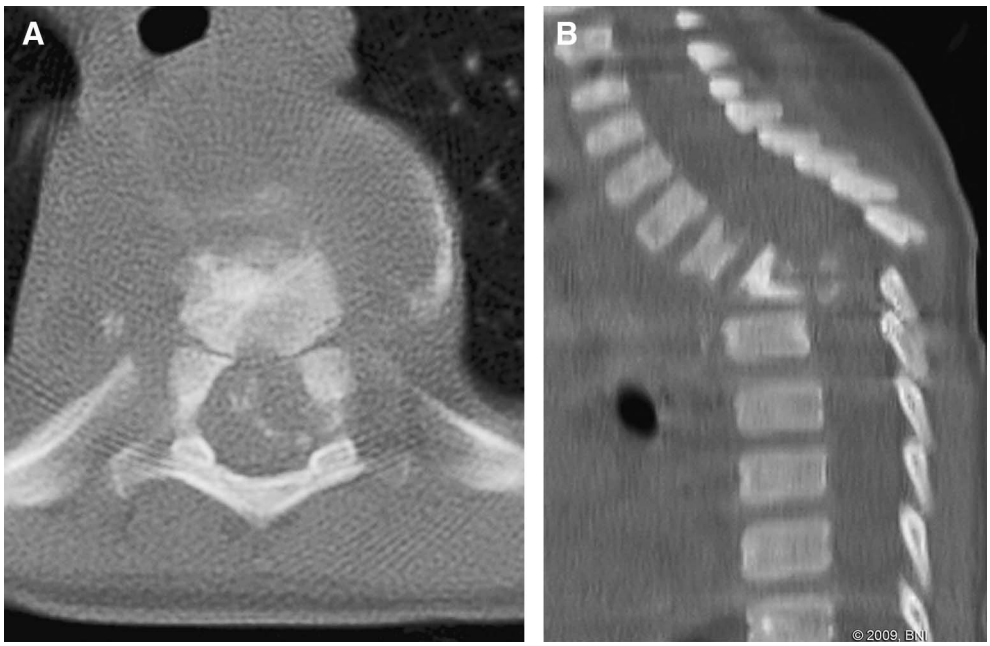

FIGURE 2. *Preoperative axial (A) and sagittal (B) computed tomographic images of the thoracic spine showing a kyphotic gibbus deformity in the midthoracic region. Used with permission from Barrow Neurological Institute.*

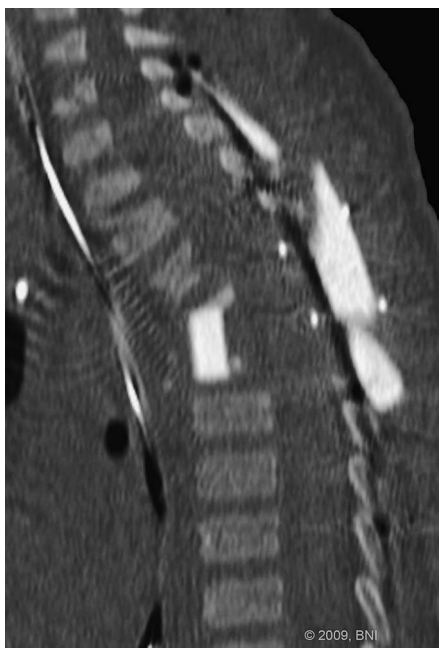

FIGURE 3. *Postoperative sagittal computed tomographic image of the thoracic spine showing the fibular strut graft. Used with permission from Barrow Neurological Institute.*

infection to multiple spinal levels while typically sparing the disk space. Early TB spondylitis without neural compression can be treated conservatively with a drug regimen. Nevertheless, surgery is recommended for patients with spinal cord compression or neurological dysfunction, significant spinal deformity, persistent severe pain, or disease progression during chemotherapy.[9,10]

Several surgical approaches have been reported in the treatment of tuberculous spondylitis. In a large prospective pediatric series, Upadhyay et al[11] showed that short- and long-term clinical outcomes were similar when radical surgery was compared with debridement alone for the treatment of TB spondylitis. However, the correction of kyphosis and deformity was better in patients undergoing radical surgery with structural grafts than in patients undergoing surgical debridement alone. The latter showed progressive deterioration at a mean of 17 years. Postoperatively, all patients were treated with a chemotherapeutic regimen. In a subsequent study by the same authors,[12] clinical and radiographic outcomes were similar for chemotherapeutic regimens prescribed for 6, 9, or 18 months when combined with radical surgery.

Although Pott disease disproportionately affects children,[5] cases involving infants are relatively rare, and their management is challenging. Several pediatric TB studies totaling 243 patients reported no patient $<$ 1 year of age.[13-16] Although chemotherapy remains the first choice for treatment,[17] surgery may be needed to correct or prevent kyphotic deformity in children. Any surgical intervention must allow for the continued growth of the patient's

Copyright © Congress of Neurological Surgeons. Unauthorized reproduction of this article is prohibited.

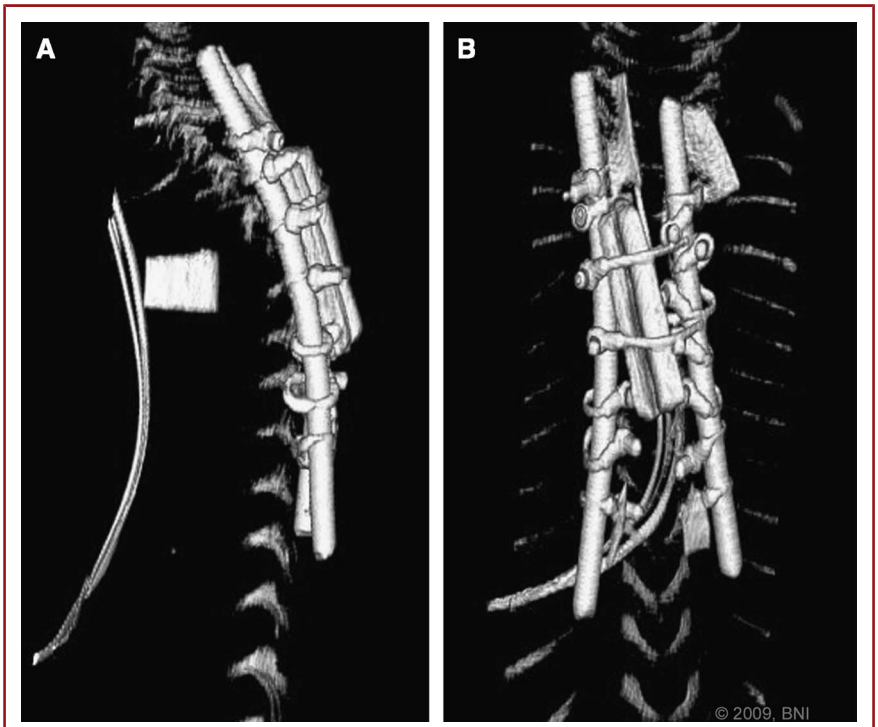

FIGURE 4. *Postoperative sagittal (A) and coronal (B) 3-dimensional computed tomographic reconstructions of the thoracic spine showing the structural allografts in place. Used with permission from Barrow Neurological Institute.*

spine and preservation of normal motion. This situation is further complicated by the fact that younger patients exhibit a more progressive form of TB, with an increased risk of extrapulmonary disease and progressive vertebral body collapse.[15,18] In the pediatric population, the dorsolumbar region is the most common site of spinal involvement in the form of an exudative abscess.[5] In the presence of spinal epidural abscesses, immediate diagnosis and urgent decompression of the spinal cord are essential.[19] Significant involvement of the vertebral column in children with Pott disease can cause progressive spinal instability, further contributing to the risk of spinal cord compression and neurological decline.[20] For these reasons, spinal TB places children at a higher risk for disabling complications than adults.

A review of the literature yielded a similar case of Pott disease in an 8-month-old Turkish infant.[21] A thorough history showed that the child had refused to bear weight after the age of 6 months and would cry if made to sit up with support. Empiric antibiotic therapy was started for 1 month, followed by anterior surgical debridement and placement of a strut allograft to reduce the spinal deformity. A cast and custom-made orthosis were used instead of internal fixation. Two-year follow-up MR imaging of the patient showed that the infection was still active, causing the graft to penetrate several adjacent vertebrae and possibly requiring additional corrective surgery.

Given the extent of the disease spread and the severity of our patient's symptoms, a combination of chemotherapy and surgical intervention was necessary. The child was evaluated thoroughly by the pediatric infectious disease team and was found to be immunocompetent. Despite his severe disease progression on an appropriate drug regimen, the final cultures showed no evidence of an atypical drug-resistant TB strain. Multilevel laminectomies and corpectomies were performed to decompress the spinal cord. Fibular allografts were placed dorsally and ventrally to facilitate fusion across the involved levels.[22] The choice to proceed with posterior surgery followed consultation with our cardiothoracic surgery consultant, who did not think that it would be safe to perform a thoracotomy on this child given the extent of the disease. The goals of the surgery were to decompress the spinal cord in an attempt to restore neurological function, to reconstruct the spine to prevent a late deformity, and to decrease the overall disease burden by wide debridement of infected tissue. The spinal instrumentation options in a child this size are limited. Given the child's age, we thought that a well-placed fibular allograft would ultimately be incorporated. Given the child's size and nonambulatory status, we entertained the use of a custom thoracic spinal orthosis but did not consider it to be crucial. Unlike the treatment reported by Tufan et al,[21] posterior fixation via sublaminar atlas cables and a Steinmann pin was used to provide

Copyright © Congress of Neurological Surgeons. Unauthorized reproduction of this article is prohibited.

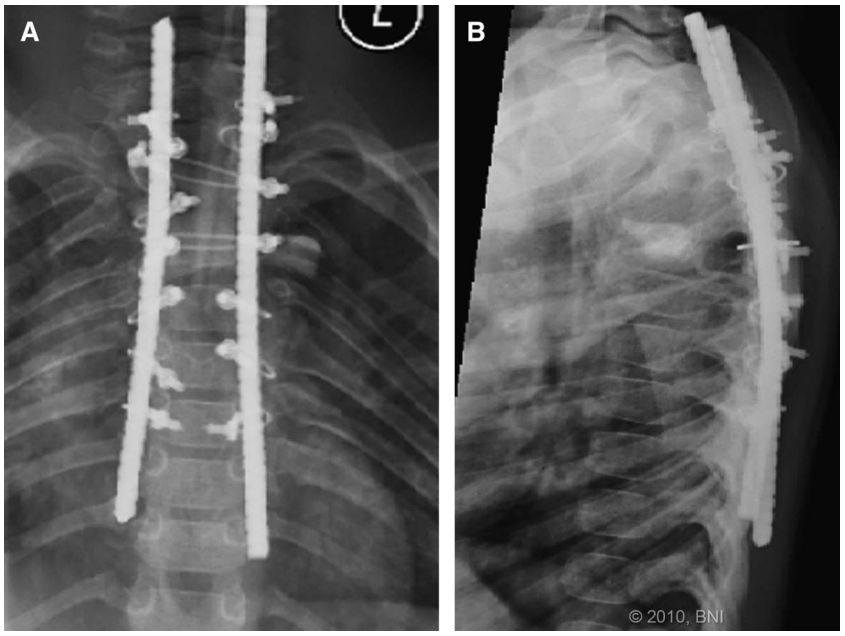

FIGURE 5. *Anteroposterior (A) and lateral (B) plain radiographs of the thoracic spine showing a stable construct and no progression of a kyphotic deformity. Used with permission from Barrow Neurological Institute.*

additional support to the fibular construct. The combination of anterior debridement and posterior instrumentation increases stability and is associated with favorable outcomes in the treatment of TB spondylitis.[23,24] Although our patient's initial neurological symptoms remained unchanged immediately after surgery, he has made significant neurological improvement since surgery. He is now ambulating 5 steps at a time and continues physical therapy. This improvement is consistent with the motor and urologic improvements of most pediatric patients that commonly occur over the course of several months.[5] At this time, our patient's kyphotic deformity has shown no signs of progression. However, he will need to be followed up into adulthood to monitor for the development of a progressive deformity.

CONCLUSION

Although still uncommon, Pott disease should be considered in infants presenting with lower-extremity paralysis, postural pain, and a history of contact with groups at high risk for TB infection.

Disclosure

The authors have no personal financial or institutional interest in any of the drugs, materials, or devices described in this article.

REFERENCES

1. According to the World Health Organization (WHO), nearly 2 billion people, one third of the world's population, have TB. 10-26- 2005. National Institute of Allergy and Infectious Diseases (NIAID). http://www.niaid.nih.gov/topics/tuberculosis/Pages/Default.aspx. Last updated, January 31, 2011. Accessed, March 2, 2011.
2. *Fact sheet: Tuberculosis in the United States*. March 17, 2005. Centers for Disease Control. *Reported Tuberculosis in the United States, 2006*. Atlanta, GA US Department of Health and Human Services, CDC, September 2007. http://www.cdc.gov/tb/statistics/reports/surv2006/pdf/FullReport.pdf. Accessed, March 2, 2011.
3. Buckner CB, Leithiser RE, Walker CW, Allison JW. The changing epidemiology of tuberculosis and other mycobacterial infections in the United States: implications for the radiologist. *AJR Am J Roentgenol*. 1991;156(2):255-264.
4. du Plessis J, Andronikou S, Theron S, Wieselthaler N, Hayes M. Unusual forms of spinal tuberculosis. *Childs Nerv Syst*. 2008;24(4):453-457.
5. Kumar R. Spinal tuberculosis: with reference to the children of northern India. *Childs Nerv Syst*. 2005;21(1):19-26.
6. Grover SB, Pati NK, Mehta R, Mahajan H. Congenital spine tuberculosis: early diagnosis by imaging studies. *Am J Perinatol*. 2003;20(3):147-152.
7. Tuli SM. Results of treatment of spinal tuberculosis by "middle-path" regime. *J Bone Joint Surg Br*. 1975;57(1):13-23.
8. Lolge S, Maheshwari M, Shah J, Patkar D, Chawla A. Isolated solitary vertebral body tuberculosis: study of seven cases. *Clin Radiol*. 2003;58(7):545-550.
9. Mehta JS, Bhojraj SY. Tuberculosis of the thoracic spine: a classification based on the selection of surgical strategies. *J Bone Joint Surg Br*. 2001;83(6):859-863.
10. Cavusoglu H, Kaya RA, Turkmenoglu ON, Tuncer C, Colak I, Aydin Y. A long-term follow-up study of anterior tibial allografting and instrumentation in the management of thoracolumbar tuberculous spondylitis. *J Neurosurg Spine*. 2008;8(1):30-38.

Copyright © Congress of Neurological Surgeons. Unauthorized reproduction of this article is prohibited.

11. Upadhyay SS, Sell P, Saji MJ, Sell B, Yau AC, Leong JC.17-year prospective study of surgical management of spinal tuberculosis in children: Hong Kong operation compared with debridement surgery for short- and long-term outcome of deformity. *Spine (Phila Pa 1976)*. 1993;18(12):1704-1711.
12. Upadhyay SS, Saji MJ, Yau AC. Duration of antituberculosis chemotherapy in conjunction with radical surgery in the management of spinal tuberculosis. *Spine (Phila Pa 1976)*. 1996;21(16):1898-1903.
13. Govender S, Ramnarain A, Danaviah S. Cervical spine tuberculosis in children. *Clin Orthop Relat Res*. 2007;460:78-85.
14. Bailey HL, Gabriel M, Hodgson AR, Shin JS. Tuberculosis of the spine in children: operative findings and results in one hundred consecutive patients treated by removal of the lesion and anterior grafting. *J Bone Joint Surg Am*. 1972;54(8):1633-1657.
15. Andronikou S, Jadwat S, Douis H. Patterns of disease on MRI in 53 children with tuberculous spondylitis and the role of gadolinium. *Pediatr Radiol*. 2002; 32(11):798-805.
16. Mushkin AI, Kovalenko KN, Bakin MN. Correction of kyphosis in tuberculous spondylitis in children [in Russian]. *Probl Tuberk*. 1999;(3):25-27.
17. Moon MS, Moon YW, Moon JL, Kim SS, Sun DH. Conservative treatment of tuberculosis of the lumbar and lumbosacral spine. *Clin Orthop Relat Res*. 2002;(398):40-49.
18. Powell DA, Hunt WG. Tuberculosis in children: an update. *Adv Pediatr*. 2006;53:279-322.
19. Reihsaus E, Waldbaur H, Seeling W. Spinal epidural abscess: a meta-analysis of 915 patients. *Neurosurg Rev*. 2000;23(4):175-204.
20. Moon MS. Tuberculosis of the spine: controversies and a new challenge. *Spine (Phila Pa 1976)*. 1997;22(15):1791-1797.
21. Tufan K, Dogulu F, Kardes O, Oztanir N, Baykaner MK. Dorsolumbar junction spinal tuberculosis in an infant: case report. *J Neurosurg*. 2005;102(4)(Suppl): 431-435.
22. Nussbaum ES, Rockswold GL, Bergman TA, Erickson DL, Seljeskog EL. Spinal tuberculosis: a diagnostic and management challenge. *J Neurosurg*. 1995;83(2): 243-247.
23. Talu U, Gogus A, Ozturk C, Hamzaoglu A, Domanic U. The role of posterior instrumentation and fusion after anterior radical debridement and fusion in the surgical treatment of spinal tuberculosis: experience of 127 cases. *J Spinal Disord Tech*. 2006;19(8):554-559.
24. Zhang HQ, Guo CF, Xiao XG, Long WR, Deng ZS, Chen J. One-stage surgical management for multilevel tuberculous spondylitis of the upper thoracic region by anterior decompression, strut autografting, posterior instrumentation, and fusion. *J Spinal Disord Tech*. 2007;20(4):263-267.

Acknowledgment

We thank Zafar Sayed, MS, for his assistance in performing background research for this case report.

COMMENT

The authors describe an interesting case of a frequent pathology in developing countries that has special characteristics because of the patient's age. This issue is the most original aspect of this report. The failed pharmacological treatment, which was supposedly adequate and sufficient in a child who was not immunocompromised, is an interesting, unresolved point. The surgical management was adapted with creativity for such a small person. Transpedicular corpectomies usually lead to an incomplete resection of the soft tissues of the vertebras, maintaining the fibular graft without contact with the upper and lower vertebras, which ultimately means a poor stabilization. In this case, the decision of going with posterior surgery (in agreement with the cardiothoracic surgeon) is not the usual management of this pathology but was made in accordance with the very special situation produced by the patient's age. The last follow-up (26 months) demonstrated good stabilization and no deformities at that time.

Ignacio Madrazo
Mexico City, Mexico

Copyright © Congress of Neurological Surgeons. Unauthorized reproduction of this article is prohibited.

"Double-Barrel" Stent Reconstruction of a Symptomatic Fusiform Basilar Artery Aneurysm: Case Report

Mark Bain, MD*
Muhammad Shazam Hussain, MD*
Alejandro Spiotta, MD*
Vivekananda Gonugunta, MD*‡
Shaye Moskowitz, MD, PhD*
Rishi Gupta, MD§

*Cerebrovascular Center, The Cleveland Clinic Foundation, Cleveland, Ohio; ‡Department of Neurosurgery, Marshfield Clinic, Marshfield, Wisconsin; §Departments of Neurology, Neurosurgery and Radiology, Emory University School of Medicine, Marcus Stroke and Neuroscience Center, Grady Memorial Hospital, Atlanta, Georgia

Correspondence:
Rishi Gupta, MD,
Department of Neurology,
Vanderbilt Stroke Center,
A-0118 Medical Center North,
Nashville, TN 37232-2551.
E-mail: rishi.gupta@emory.edu

Received, December 22, 2009.
Accepted, June 7, 2010.

Copyright © 2011 by the Congress of Neurological Surgeons

BACKGROUND AND IMPORTANCE: Giant fusiform aneurysms of the basilar artery are associated with a high rate of morbidity and mortality. Treatment of these lesions can be difficult, especially when there are poor anatomic collaterals such as posterior communicating arteries. These lesions often have no acceptable treatment. The authors present a case of a patient with a symptomatic, fusiform basilar artery aneurysm successfully treated with a side-by-side (double-barrel), telescoping stent construct.

CLINICAL PRESENTATION: A 56-year-old man presented with chief concerns of dysarthria and left-sided hemiparesis. MRI and conventional catheter-based angiography revealed a dolichoectatic basilar artery with 3 large fusiform aneurysms throughout its length. Flow through the patient's aneurysm was successfully reduced with a side-by-side stent construct and coiling of the proximal aneurysm dilation. The patient experienced stabilization of his ischemic events and neurologic recovery. A total of 6 Neurform-2 4.5 × 30-mm stents were navigated and positioned from the proximal posterior cerebral arteries to the distal vertebral arteries in a side-by-side (double-barrel), telescoping manner. These were deployed simultaneously by 2 operators to oppose the stent struts as well as the arterial wall. Next, the proximal aneurysmal dilation was coiled to near occlusion. Successful flow redirection and aneurysm thrombosis was observed.

CONCLUSION: A novel, endovascular stenting technique for successfully treating symptomatic, giant basilar artery aneurysms is presented. This patient at 4 months was living independently with no further neurologic events or decline.

KEY WORDS: Basilar artery aneurysm, Endovascular treatment, Fusiform, Giant aneurysm, Stenting

Neurosurgery 68:E1491–E1496, 2011 DOI: 10.1227/NEU.0b013e318211f982 www.neurosurgery-online.com

Fusiform basilar trunk aneurysms are associated with a high rate of morbidity and mortality, particularly if they manifest with ischemic stroke or rapid expansion.[1,2] Treatment options are limited and include surgical sacrifice of the vertebral arteries with concomitant bypass[3,4] and utilization of endovascular stent reconstruction.[5-7] More recently, the Pipeline stent (Chestnut Medical, Menlo Park, California) has been used to treat patients with this condition,[8] but currently the technology has been limited to a few centers. We report a patient who presented with clinically progressive deterioration in the setting of 3 fusiform aneurysms incorporating the entire basilar trunk treated with a "double-barrel" stent reconstruction endovascular approach.

CASE REPORT

A 56-year-old man with a history of tobacco use, hypertension, and hyperlipidemia presented to an outside medical facility with concerns about dysarthria and left-sided hemiparesis 3 months earlier. The patient underwent a magnetic resonance imaging (MRI) of the brain that revealed an acute infarct in the right basis pontis and 3 fusiform aneurysms of the basilar artery. He subsequently underwent a catheter angiogram that confirmed the presence of a dolichoectatic basilar artery with 3 fusiform aneurysms. He was placed on aspirin and clopidogrel along with a high-dose statin and discharged to home. He presented 6 weeks later with profound dysphagia and worsening of his left hemiparesis. He was found to have a new infarct in the right pons and left medulla on MRI and was

Copyright © Congress of Neurological Surgeons. Unauthorized reproduction of this article is prohibited.

discharged to rehabilitation on Coumadin therapy. Six weeks later he presented with profound dysarthria (mute), emotional lability, and right arm paresis. A repeat MRI of the brain confirmed a new ischemic stroke in the pons bilaterally, and a repeat cerebral angiogram confirmed significant expansion of the fusiform dilatation of the distal and proximal aneurysm. It was not clear if the aneurysm had truly enlarged or was related to recanalization of thrombus while the patient was on Coumadin therapy. Given the progression of ischemic injury, the patient was transferred to our institution for further evaluation.

Figure 1 reveals the cerebral angiogram performed before transfer to our institution. We were unable to obtain the Pipeline device because of an ongoing clinical trial for which the patient did not qualify. The diameter of the basilar artery was 9.5 mm precluding placement of telescoping Enterprise (Cordis Corp., Miami Lakes, Florida) or Neuroform stents (Boston Scientific, Natick, Massachusetts). Thus, we opted for side-by-side telescoping stents (double-barrel technique) that has been previously reported to preserve side branches during aortic arch Endograft reconstruction.[10]

TECHNIQUE

The patient was placed under general anesthesia with continuous hemodynamic monitoring through a radial arterial line. Before treatment the patient was given aspirin 325 mg for 3 days and clopidogrel 450 mg load followed by 75 mg daily for 3 days. We confirmed adequate inhibition of platelet function via aggregometry before proceeding with the procedure. The patient was given intermittent boluses of heparin to achieve an activated clotting time of 300 seconds or greater for the entire procedure.

A 6F sheath was placed in the right common femoral artery and left common femoral artery using the Seldinger technique. A Neuron guide catheter (Penumbra Corp., Alameda, California) was placed in the left vertebral artery because of the extensive proximal tortuosity of the extracranial vertebral artery. A 6F 80-cm Cook Shuttle sheath was placed in the right subclavian artery and a 6F 100-cm Envoy guide catheter was positioned in the extracranial right vertebral artery.

Under roadmapping guidance, a microcatheter and microwire were navigated into each posterior cerebral artery. The microcatheters were exchanged for 0.014-inch exchange length microwires (Figure 2). Two Neurform-2 4.5 × 30 mm stents were navigated and positioned in the proximal posterior cerebral artery side by side. These were deployed simultaneously by 2 operators to oppose the stent struts as well as the arterial wall. The stent catheters were removed and 4 more stents of the same size were placed in a telescoping manner overlapping the distal tines of the previously placed stents. A total of 6 stents were overlapped to the vertebrobasilar junction on each side. A Dyna CT was performed to confirm the positioning of the stents next to each other. We administered a total of 15 mg of eptifibatide at the end of the procedure for concerns of interval development of thromboembolic complications. Although the use of further antiplatelet therapy is unconventional, we felt that given the large amount of exposed metal surface area from the stents and turbulent blood flow through the stent construct of the aneurysm, administration of a glycoprotein IIb/IIIa antagonist might help in prevention of thromboembolic complications.

At this point, a microcatheter was placed in the proximal aneurysm through the stent struts and coil embolization was performed with GDC platinum coils. Sequential coil embolization was performed to partial occlusion of the aneurysm (Figure 3). The patient was then awoken from anesthesia and transferred to the intensive care unit on a heparin drip to achieve a partial thromboplastin time of 70 to 90 seconds. Aspirin 325 mg daily and clopidogrel 75 mg daily were maintained indefinitely.

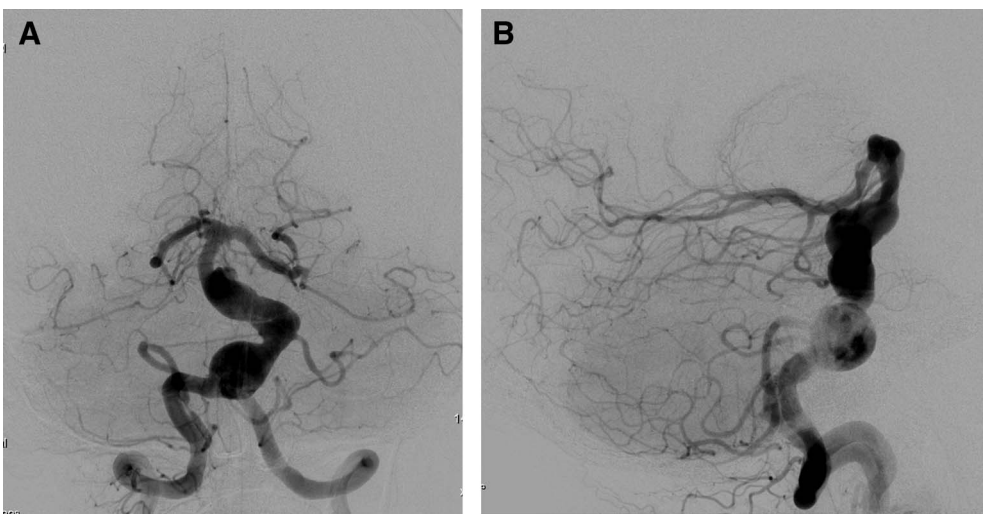

FIGURE 1. *An anteroposterior (A) and lateral (B) projection from a right vertebral artery injection showing 3 large fusiform aneurysmal dilatations of the basilar artery with reflux down the left vertebral artery.*

Copyright © Congress of Neurological Surgeons. Unauthorized reproduction of this article is prohibited.

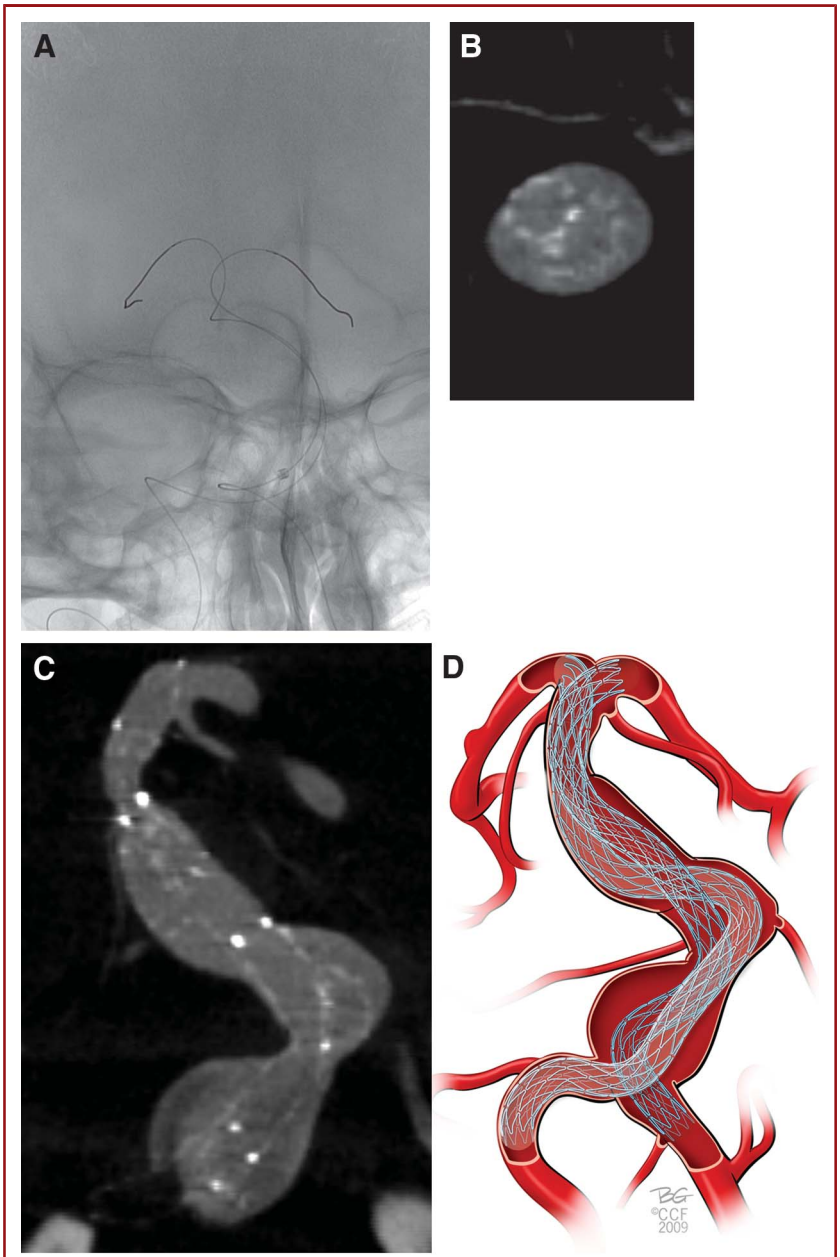

FIGURE 2. **A**, *an anteroposterior projection showing 2 exchange length microwires positioned in each posterior cerebral artery.* **B**, *DYNA CT with contrast axial view though the mid basilar artery showing the configuration of the side-by-side stents.* **C**, *DYNA CT with contrast coronal reconstruction showing the configuration of the side-by-side stents throughout the length of the basilar artery aneurysm.* **D**, *an artist's rendition of the stent construct postdeployment of the 8 stents traversing the course of the basilar artery.*

The patient required mechanical ventilation for 48 hours and then was extubated with an initial worsening of his left hemiparesis, but this returned to baseline 4 days postprocedure. He returned for follow-up at 4 months and was living independently and did not have any further clinical deterioration. He underwent a cerebral angiogram and MRI of the brain (Figure 4) that showed progressive thrombosis of the proximal and distal aneurysms.

Copyright © Congress of Neurological Surgeons. Unauthorized reproduction of this article is prohibited.

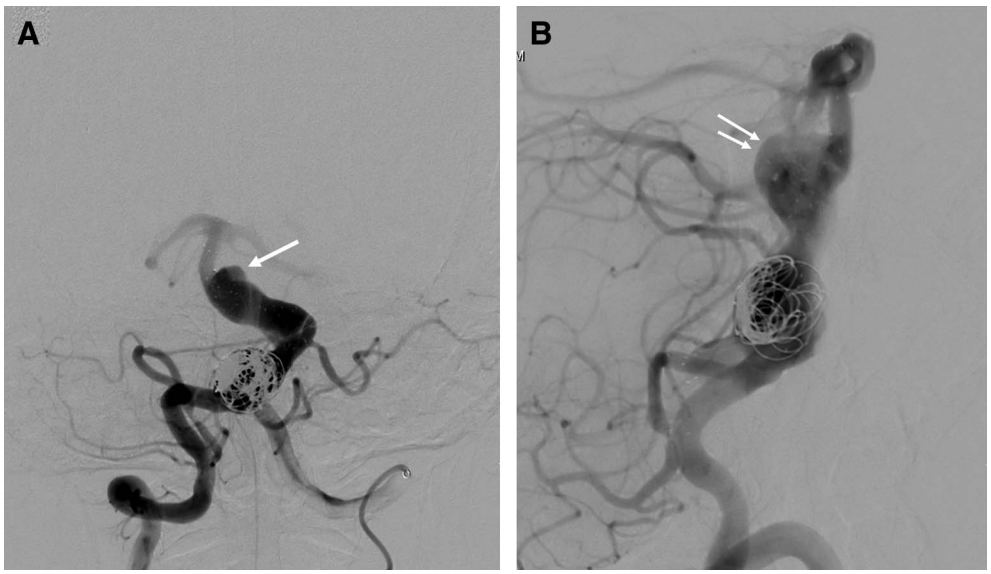

FIGURE 3. *Anteroposterior (A) and lateral (B) projection with a left vertebral angiogram showing the result post–stent reconstruction and coil embolization of the proximal aneurysm. The distal aneurysm (white arrows) will undergo progressive thrombosis in follow-up imaging.*

DISCUSSION

Fusiform basilar artery aneurysms are associated with a high rate of mortality and disability.[1,2] The mortality rate appears to be proportional to the size of the dilatation with rates of mortality as high as 30% per year when the diameter of the vessel is larger than 7 mm.[1] These lesions cause mass effect on the brainstem leading to cranial nerve dysfunction along with ischemic strokes due to formation of thrombus that may impede flow to the perforator branches.[2] The treatment of these lesions is often challenging and associated with a high degree of morbidity.

Surgical treatment with occlusion of the vertebral arteries or the basilar artery has been previously reported.[3,4] This technique was not believed to be suitable for our patient because the aneurysmal dilatation involved the length of the basilar artery and the patient had little anatomic collaterals such as posterior communicating arteries on angiography. Other studies have shown that aneurysms that extend along the length of basilar artery or are distal in nature have higher rates of ischemic complications with this occlusion technique.[11,12] From an endovascular perspective, the Pipeline embolization device was considered given the reports of recent success, but unfortunately this was not available because the device was being tested in a clinical trial for which our patient did not qualify. Prior studies have shown that utilization of stent monotherapy may occlude basilar trunk aneurysms.[5,8] The mechanism for this is likely due to the condition being a dissecting pseudoaneurysm with stents inducing healing along the dissection, thereby inducing thrombosis of the aneurysm. Alternatively, minor redirection of flow through the stent, as opposed to the dome of the aneurysm, may induce thrombosis of the aneurysm. The etiology of these lesions is often unknown, although atherosclerosis has been postulated as a potential mechanism because there is disruption of the internal elastic lamina on histopathololgy.[13]

In our patient, the vessel diameter of the nonaneurysmal portions of the artery measured 9.5 mm in diameter and, thus, it was felt that a single stent would not be opposed to the vessel wall and thereby risk becoming dislodged from the original position during placement of subsequent telescoping stents. We thus utilized the side-by-side stent delivery technique to allow sections of the stent to heal along the arterial wall. The concern with this technique was leaving a septum of 2 stents in the middle of the basilar artery, thereby potentially increasing thromboembolic complications. Prior operators have described the "kissing stent" technique intracranially without reported incidence of thromboembolic complications.[6] In addition, the kink at the level of the anterior inferior cerebellar artery was felt to be contributory to the aneurysmal dilatation distally, and, by placing stents, the hope was to change the configuration of the kink. Although we did not see a significant change in the curvature of the basilar artery, progressive thrombosis occurred within the distal aneurysm.

Giant aneurysms throughout the intracranial vasculature usually contain some evidence of thrombosis and slow or turbulent blood flow. It has been postulated that thrombus formation in these aneurysms is dynamic, and, consequently, the amount and direction of blood flow in the aneurysm changes. We also postulate that large aneurysms, because of stagnant and turbulent blood flow, are prone to thrombosis; therefore, slight

Copyright © Congress of Neurological Surgeons. Unauthorized reproduction of this article is prohibited.

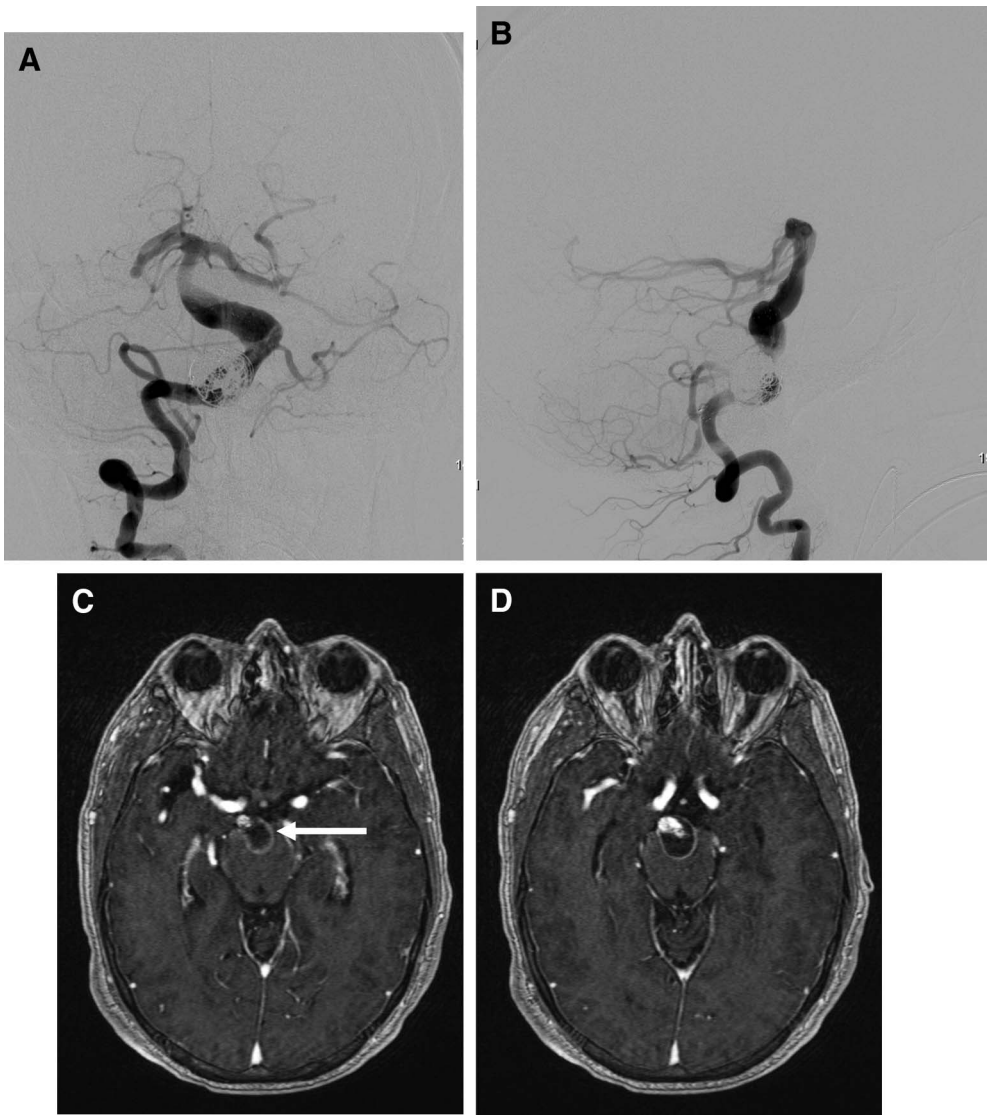

FIGURE 4. *Follow-up angiography at 4 months shows progressive thrombosis of the proximal (**A**) and distal (**B**) aneurysms. There is no significant reflux down the left vertebral artery confirming improvement of antegrade filling of the posterior circulation. (**C** and **D**) MRI with gadolinium confirming thrombus formation within the distal aneurysm (white arrows).*

manipulation or redirection of flow may induce dramatic changes in the aneurysm's overall characteristics. The placement of stents inside of these large aneurysms, regardless of metal surface area, may provide flow redirection to induce varying levels of thrombosis. In our case, we also elected to place coils in the proximal aneurysmal dilation. It was felt that this might also promote laminar flow through the stent construct by reducing turbulence through the proximal aneurysm. Follow-up angiography and MRI studies showed progressive thrombosis of the distal aneurysm.

This case describes an endovascular technique for treating giant fusiform vertebrobasilar aneurysms. This technique is off-label and may be considered in select cases when no other therapeutic option is available. A more in-depth knowledge of large fusiform posterior circulation aneurysms elucidating etiology and the effects/outcomes of endovascular treatment of these lesions is required. It also illustrates the morbid natural history of these lesions, and the etiology of stent-induced thrombus formation within aneurysms. The double-barrel technique can be considered an option for patients with progressive neurologic decline. This technique, or variations of this technique, can be considered in patients who may not be candidates for current flow-diversion technologies.

Copyright © Congress of Neurological Surgeons. Unauthorized reproduction of this article is prohibited.

REFERENCES

1. Pico F, Labreuche J, Gourfinkel-An I, Amarenco P, on behalf of the GENIC Investigators. Basilar artery diameter and 5-year mortality in patients with stroke. *Stroke*. 2006;37(9):2342-2347.
2. Milandre L, Bonnefoi B, Pestre P, Pellissier JF, Grisoli F, Khalil R. Vertebrobasilar arterial dolichoectasia: complications and prognosis. *Rev Neurol (Paris)*. 1991; 147(11):714-722.
3. Hopkins LN, Budny JL, Castellani D. Extracranial-intracranial arterial bypass and basilar artery ligation in the treatment of giant basilar artery aneurysms. *Neurosurgery*. 1983;13(2):189-194.
4. Omahen DA, Findlay JM. A giant fusiform basilar aneurysm treated by bilateral vertebral artery occlusion. *J Clin Neurosci*. 2004;11(3):324-328.
5. Crowley RW, Evans AJ, Kassell NF, Jensen ME, Dumont AS. Endovascular treatment of a fusiform basilar artery aneurysm using multiple "in-stent stents". Technical note. *J Neurosurg Pediatr*. 2009;3(6):496-500.
6. Henkes H, Kirsch M, Mariushi W, Miloslavski E, Brew S, Kuhne D. Coil treatment of a fusiform upper basilar trunk aneurysm with a combination of "kissing" neuroform stents, TriSpan-, 3D- and fibered coils, and permanent implantation of the microguidewires. *Neuroradiology*. 2004;46(6):464-468.
7. Higashida RT, Smith W, Gress D, et al. Intravascular stent and endovascular coil placement for a ruptured fusiform aneurysm of the basilar artery. Case report and review of the literature. *J Neurosurg*. 1997;87(6):944-949.
8. Ansari SA, Lassig JP, Nicol E, Thompson BG, Gemmete JJ, Gandhi D. Thrombosis of a fusiform intracranial aneurysm induced by overlapping neuroform stents: case report. *Neurosurgery*. 2007;60(5):E950–E951.
9. Fiorella D, Kelly ME, Albuquerque FC, Nelson PK. Curative reconstruction of a giant midbasilar trunk aneurysm with the pipeline embolization device. *Neurosurgery*. 2009;64(2):212-217.
10. Hiramoto JS, Schneider DB, Reilly LM, Chuter TA. A double-barrel stent-graft for endovascular repair of the aortic arch. *J Endovasc Ther*. 2006;13(1):72-76.
11. Steinberg GK, Drake CG, Peerless SJ. Deliberate basilar or vertebral occlusion in the treatment of intracranial aneurysms. Immediate results and long-term outcome in 201 patients. *J Neurosurg*. 1993;79(2):161-173.
12. Drake CG, Peerless SJ. Giant fusiform intracranial aneurysms: review of 120 patients treated surgically from 1965 to 1992. *J Neurosurg*. 1997;87(2):141-162.
13. Shokunbi MT, Vinters HV, Kaufmann JC. Fusiform intracranial aneurysms. Clinicopathologic features. *Surg Neurol*. 1988;29(4):263-270.

Acknowledgment

The authors would like to thank Bill Garriott for the medical illustration representing the technique described.

COMMENT

The authors present an interesting approach to treating a fusiform aneurysm of the basilar artery by incorporating a technique published in the treatment of abdominal aortic aneurysms. By employing the double-barrel technique, the authors provide the necessary support for each portion of the stent system across regions of aneurysm that are much broader than the maximum diameter of the aneurysm. At 4-month follow-up the authors report no further symptomatology and a significant improvement in the patient's neurological condition. They thus conclude that this technique should be considered in situations where the traditional techniques are not applicable.

There are several important observations that can be made as a result of this and other similar techniques, the most important of which is the tremendous amount of remodeling that can occur when flow through vessels is modified. The concept of flow diversion and how to successfully "tame" it to predictably alter the biology of vessels, though discussed for many years, still eludes us. However, clinical vignettes such as this may certainly serve to help investigators from many disciplines better understand the key combination of biology and flow that contribute to healing in this setting.

The technical aspects of this procedure can certainly be challenging, and should be carefully considered as one adds this technique to the endovascular armamentarium in the treatment of previously untreatable lesions.

Charles J. Prestigiacomo
Newark, New Jersey

Copyright © Congress of Neurological Surgeons. Unauthorized reproduction of this article is prohibited.

Onyx Pulmonary Artery Embolization After Treatment of a Low-Flow Dural Arteriovenous Fistula: Case Report

Bryan A. Pukenas, MD*
Sudhakar R. Satti, MD*
Robert Bailey, MD‡
John B. Weigele, MD, PhD*
Robert W. Hurst, MD*‡
Michael F. Stiefel, MD, PhD§

*Department of Radiology, Division of Interventional Neuroradiology, and ‡Department of Neurosurgery; University of Pennsylvania Medical Center, Philadelphia, Pennsylvania; §Department of Neurosurgery, Division of Cerebrovascular & Endovascular Neurosurgery, Westchester Medical Center, New York Medical Center, Valhalla, New York

Correspondence:
Bryan Pukenas, MD,
Department of Neuroradiology,
Hospital of the University of Pennsylvania,
3400 Spruce St,
Philadelphia, PA 19104.
E-mail: bryan.pukenas@uphs.upenn.edu

Received, January 4, 2010.
Accepted, June 4, 2010.

Copyright © 2011 by the Congress of Neurological Surgeons

BACKGROUND AND IMPORTANCE: Endovascular management of dural arteriovenous fistulas (DAVFs) has become an accepted primary and often definitive therapy. We present the first documented case of Onyx pulmonary embolism after embolization of a low-flow DAVF.

CLINICAL PRESENTATION: A 63-year-old man presented with subarachnoid hemorrhage secondary to a DAVF. Computed tomographic angiography, magnetic resonance imaging, and initial conventional angiogram were negative. A repeat angiogram demonstrated a DAVF, which was cured with Onyx embolization. A routine chest computed tomography after intervention revealed an asymptomatic Onyx embolization cast in a subsegmental pulmonary artery.

CONCLUSION: Endovascular treatment options include transarterial embolization with microcoils, polyvinyl alcohol particles, n-butyl-2cyanoacrylate, and Onyx (ev3 Neurovascular, Irvine, California). Complications associated with the use of Onyx are low but include embolizate pulmonary embolism. Patients often remain asymptomatic, but for symptomatic patients, conservative treatment options usually result in resolution of symptoms.

KEY WORDS: Dural arteriovenous fistula, Onyx, Pulmonary embolism

Neurosurgery 68:E1497–E1500, 2011 DOI: 10.1227/NEU.0b013e318210c83b www.neurosurgery-online.com

CLINICAL PRESENTATION

A 63-year-old man with a medical history of pulmonary fibrosis presented with headache. Unenhanced head computed tomography (CT) documented subarachnoid hemorrhage. CT angiogram demonstrated no aneurysm or dissection. Initial conventional cerebral angiogram was interpreted as no evidence of aneurysm or arteriovenous shunting. Brain magnetic resonance imaging and magnetic resonance angiography were then performed; both were also negative for aneurysm, dissection, or arteriovenous malformation (AVM). A repeat conventional angiogram performed 4 days after presentation demonstrated faint early antegrade opacification of the right sigmoid sinus with arterial feeders arising from posterior branches of the right middle meningeal artery (Figure 1A), consistent with a type 1 Borden[1] slow-flow dural arteriovenous fistula (DAVF).

ABBREVIATIONS: AVM, arteriovenous malformation; **DAVF,** dural arteriovenous fistula; **DMSO,** dimethyl sulfoxide

INTERVENTION

Through a right common femoral artery sheath, a 6F Penumbra Neuron 053 guide catheter was positioned in the left external carotid artery. A Marathon microcatheter (ev3 NeuroVascular, Irvine, California) was navigated into the squamous branch of the middle meningeal artery. The fistula was embolized with Onyx 18 (ev3 NeuroVascular), (Figure 2). The patient was discharged home on day 17. A high-resolution chest CT was performed on an outpatient basis 5 days after discharge for routine evaluation of pulmonary fibrosis. This CT revealed stable findings of pulmonary fibrosis, although a new linear radiopaque right lower lobe pulmonary artery foreign body raised concern (Figure 3). This finding was not suspected

Copyright © Congress of Neurological Surgeons. Unauthorized reproduction of this article is prohibited.

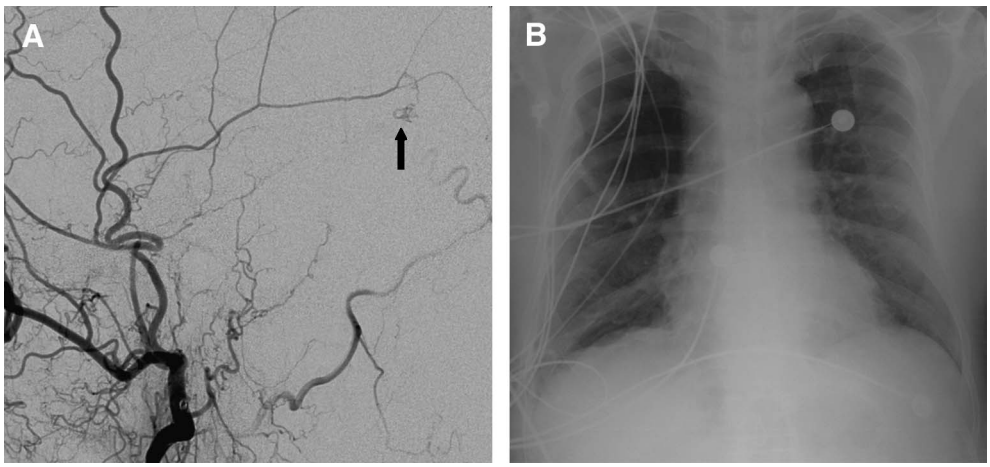

FIGURE 1. **A**, *right external carotid artery injection demonstrating faint early opacification of the sigmoid sinus from the squamous branch of the middle meningeal artery (arrow).* **B**, *routine chest radiograph performed while the patient was in the intensive care unit. The Onyx cast in a right lower lobe pulmonary artery is not seen.*

clinically and was not visible on a routine chest radiograph performed while the patient was in the intensive care unit for treatment of subarachnoid hemorrhage (Figure 1B). After careful examination and review of previous chest CT, it was apparent that Onyx material had embolized to the pulmonary artery during treatment.

DISCUSSION

As an acquired lesion, DAVFs are 10 times less frequent than brain AVMs.[2] Despite their relative infrequent occurrence, the rate of rebleeding in the first 2 weeks after hemorrhage from DAVFs has been reported as high as 35%,[3] and prompt endovascular treatment is warranted. Endovascular treatment options include transarterial embolization with microcoils,[4] polyvinyl alcohol particles, and liquid embolic agents.[5] Pulmonary embolism complicating brain AVM embolization with n-butyl-2cyanoacrylate and microcoils has been described.[6-8]

Onyx is a liquid embolic agent composed of ethylene vinyl alcohol copolymer suspended in dimethyl sulfoxide (DMSO) and tantalum that is used in the treatment of cerebral and peripheral AVMs and cerebral aneurysms.[9-11] It solidifies by precipitation when the organic solvent, DMSO, diffuses out of the polymer mass.[12] A recent report suggests that Onyx should be the primary

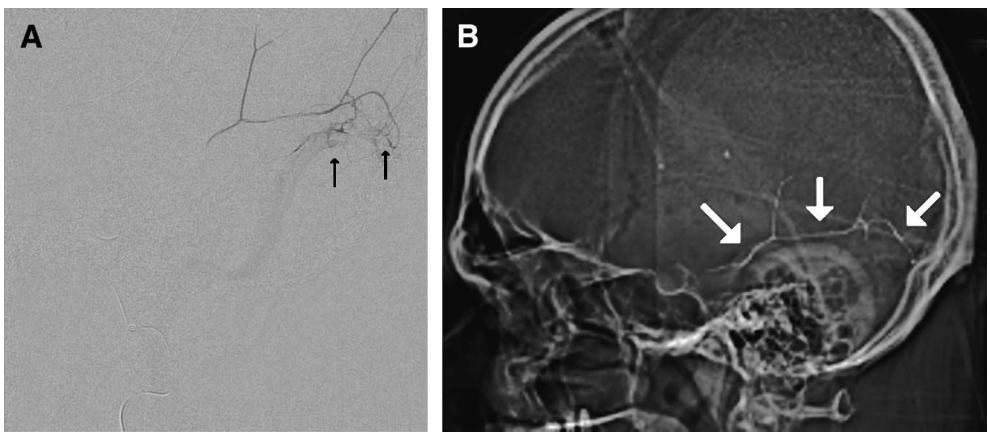

FIGURE 2. **A**, *superselective right middle meningeal artery injection demonstrating arteriovenous shunting to the right sigmoid sinus (arrows).* **B**, *sagittal scout image from a head computed tomography performed after embolization demonstrates an Onyx cast in the expected location of the squamous branch of the middle meningeal artery and the sigmoid sinus (arrows).*

Copyright © Congress of Neurological Surgeons. Unauthorized reproduction of this article is prohibited.

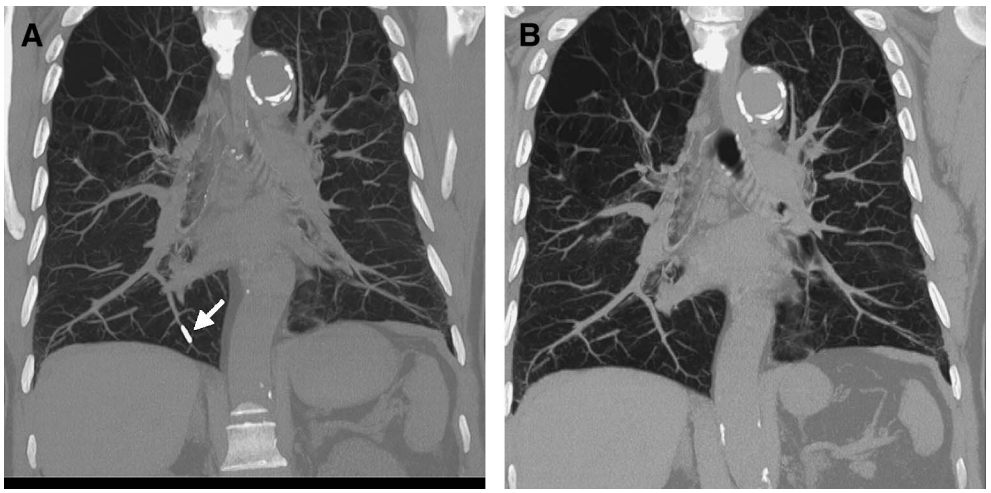

FIGURE 3. **A**, *coronal chest computed tomography (CT) reconstructed maximum-intensity projection images obtained 5 days after discharge demonstrate a new linear radiopaque foreign body in a right lower lobe pulmonary artery, consistent with Onyx liquid embolizate (arrow).* **B**, *coronal chest CT reconstructed maximum-intensity projection images obtained 4 months before Onyx embolization demonstrate the absence of the radiopaque foreign body.*

therapeutic agent for treatment of certain DAVFs,[13] and others have reported high cure rates with Onyx monotherapy,[5] perhaps as a result of its unique diffusion properties. The less adherent nature of Onyx allows greater tolerance for reflux around the infusion catheter, which can result in deeper penetration[14] without the risk of arterial avulsion when removing the microcatheter. In fact, reflux around the catheter tip is often desirable because it facilitates further antegrade injection.[15] The use of Onyx for DAVF embolization is an off-label use of an approved product.

Complications associated with the use of Onyx are low but include skin discoloration, nontarget vessel embolization, alopecia secondary to embolization of arteries supplying the scalp, and radiation-induced alopecia secondary to prolonged use of a focused x-ray beam.[5] Although Onyx pulmonary embolization has been reported in a high-flow cerebral AVM in a neonate,[16] to the best of our knowledge, we report the first case of Onyx pulmonary embolism after embolization of a low-flow dural AVM with antegrade venous sinus drainage. Nontarget embolization to the pulmonary vasculature in our patient was unsuspected because an Onyx cast was not present in the cerebral venous system and the patient's pulmonary status remained at baseline. The finding was recognized only on a routine follow-up high-resolution chest CT performed for evaluation of pulmonary fibrosis. We postulate a possible cause for the Onyx pulmonary artery embolism: When the Onyx syringe was attached to the microcatheter, an ideal DMSO/Onyx interface was not achieved, thus making the leading edge of the Onyx less visible, allowing unrecognized transit through the venous system into the pulmonary artery. As in our experience, patients are often asymptomatic, but symptoms of pulmonary artery embolization with embolic material may include cough, dyspnea, pleuritic chest pain, bloody sputum, or a drop in Pao_2.[17] Conservative treatment for symptomatic pulmonary embolism related to liquid embolic material including analgesia and oxygen therapy has been described, and patients often recover spontaneously.[18]

Disclosure

The authors have no personal financial or institutional interest in any of the drugs, materials, or devices described in this article.

REFERENCES

1. Borden JA, Wu JK, Shucart WA. A proposed classification for spinal and cranial dural arteriovenous fistulous malformations and implications for treatment. *J Neurosurg*. 1995;82(2):166-179.
2. Newton TH, Cronqvist S. Involvement of the dural arteries in intracranial arteriovenous malformations. *Radiology*. 1969;93(5):1071-1078.
3. Daffau H, Lopes M, Janosevic V, et al. Early rebleeding from intracranial dural arteriovenous fistulas. *J Neurosurg*. 1999;90(1):78-84.
4. Roy D, Raymond J. The role of transvenous embolization in the treatment of intracranial dural arteriovenous fistulas. *Neurosurgery*. 1997;40(6)1133–1141.
5. Barnwell SL, Halbach VV, Dowd CF, Higashida RT, Hieshima GB, Wilson CB. A variant of arteriovenous fistulas within the wall of dural sinuses: results of combined surgical and endovascular therapy. *J Neurosurg*. 1991;74(2):199–204.
6. Carapiet DA, Stevens JE. Pulmonary embolism following embolization of an arteriovenous malformation. *Paediatr Anaesth*. 1996;6(6):491-494.
7. Pelz DM, Lownie SP, Fox AJ, Hutton LC. Symptomatic pulmonary complications from liquid acrylate embolization of brain arteriovenous malformations. *AJNR Am J Neuroradiol*. 1995;16(1):19-26.
8. Kjellin IB, Boechat MI, Vinuela F, Westra SJ, Duckwiler GR. Pulmonary emboli following therapeutic embolization of cerebral arteriovenous malformations in children. *Pediatr Radiol*. 2000;30(4):279-283.
9. Stiefel M, Albuquerque F, Park M, Dashti S, McDougall C. Endovascular treatment of intracranial dural arteriovenous fistulae using Onyx: a case series. *Neurosurgery*. 2009;65(6)(Suppl):132-139.

Copyright © Congress of Neurological Surgeons. Unauthorized reproduction of this article is prohibited.

10. Molyneus AJ, Cekirge S, Saatci I, Gál G. Cerebral Aneurysm Multicenter European ONYX (CAMEO) trial: results of a prospective observational study in 20 European centers. *AJNR Am J Neuroradiol*. 2004;25(1):39-51.
11. Numan F, Omerloglu A, Dara B, Cantaşdemir M, Adaletli I, Kantarci F. Embolization of peripheral vascular malformations with ethylene vinyl alcohol copolymer (ONYX). *J Vasc Interv Radiol*. 2004;15(9):939-946.
12. Gailloud P. Endovascular treatment of cerebral arteriovenous malformations techniques in vascular and interventional radiology. *Tech Vasc Interv Radiol*. 2005;8(3):118-128.
13. Cognard C, Januel AC, Silva NA Jr, Tall P. Endovascular treatment of intracranial dural arteriovenous fistulas with cortical venous drainage: new management using Onyx. *AJNR Am J Neuroradiol*. 2008;29(2):235-241.
14. Elhammady MS, Wolfe SQ, Ashour R, et al. Safety and efficacy of vascular tumor embolization using Onyx: is angiographic devascularization sufficient? *J Neurosurg*. 2009;112(5):1039-1045.
15. Gore P, Theodore N, Brasiliense L, et al. The utility of Onyx for preoperative embolization of cranial and spinal tumors. *Neurosurgery*. 2008;62(6):1204-1211.
16. Herman TE, Siegel MJ, Vachharajani A, Masand P, Cross D. Cerebral arteriovenous fistula to pulmonary artery onyx embolization. *J Perinatol*. 2007;27(4):238-240.
17. Kaplan V, Hauser M, Speich R. A patient with cerebral arteriovenous malformation and multiple metallic pulmonary particles. *Chest*. 1996;110(6):1611-1612.
18. Pelz DM, Lownie SP, Fox AJ, Hutton LC. Symptomatic pulmonary complications from liquid acrylate embolization of brain arteriovenous malformations. *AJNR Am J Neuroradiol*. 1995;16(1):19-26.

COMMENT

This is the first reported case of pulmonary embolism caused by Onyx after embolization of a dural arteriovenous fistula. The risk for pulmonary embolism from embolic materials is higher with high-flow arteriovenous shunts, and the authors raise the awareness for such a complication when treating low-flow arteriovenous shunts.

Athos Patsalides
New York, New York

Copyright © Congress of Neurological Surgeons. Unauthorized reproduction of this article is prohibited.

High-Frequency Pallidal Stimulation for Camptocormia in Parkinson Disease: Case Report

Nova B. Thani, MBBS*
Arul Bala, MBBS*
Thomas E. Kimber, FRACP‡
Christopher R. P. Lind, FRACS*§

*West Australian Neurosurgical Service, Sir Charles Gairdner Hospital, Perth, Australia; ‡Royal Adelaide Hospital, Adelaide, Australia; §School of Surgery, University of Western Australia, Perth, Australia

Correspondence:
Professor Christopher Lind, FRACS,
Consultant Neurosurgeon,
Sir Charles Gairdner Hospital,
Hospital Avenue,
Nedlands, WA 6009, Australia.
E-mail:
Christopher.Lind@health.wa.gov.au

Received, January 6, 2010.
Accepted, June 11, 2010.

Copyright © 2011 by the
Congress of Neurological Surgeons

BACKGROUND AND IMPORTANCE: Camptocormia is characterized by abnormal flexion of the thoracolumbar spine that increases during upright posture and abates in the recumbent position and has been reported to occur in patients with Parkinson disease. Camptocormia causes significant spinal and abdominal pain, impairment of balance, and social stigma.

CLINICAL PRESENTATION: A 57-year-old woman with Parkinson disease developed severe camptocormia, which did not improve with trials of antiparkinsonian and muscle relaxant medications. The patient was successfully treated with bilateral globus pallidus interna deep brain stimulation surgery under general anesthesia. High-frequency neuromodulation afforded relief of camptocormia and improvement in Parkinson disease symptoms.

CONCLUSION: Camptocormia in Parkinson disease may represent a form of dystonia and can be treated effectively with chronic pallidal neuromodulation.

KEY WORDS: Camptocormia, Deep brain stimulation, Dystonia, Globus pallidus interna, Parkinson disease

Neurosurgery 68:E1501–E1505, 2011 DOI: 10.1227/NEU.0b013e318210c859 www.neurosurgery-online.com

Camptocormia is a disorder characterized by abnormal posture with excessive flexion of the thoracolumbar spine that increases during upright posture or ambulation and abates in the recumbent position.[1,2] Historically, camptocormia was considered a psychogenic conversion disorder.[3,4] Recently, however, several reports propose various etiologic factors. It has been associated with movement disorders (Parkinson disease [PD],[1,2,5-8] juvenile parkinsonism,[9] dystonia[8,10,11]), neuromuscular disorders (myopathy,[5,12,13] amyotrophic lateral sclerosis,[14-17] inclusion body myositis[18]), focal brain lesions,[19] and certain drugs.[20]

Idiopathic PD is the commonest movement disorder associated with camptocormia.[1,2,5-8] Pathophysiological mechanisms of camptocormia in PD remain elusive. Some reports have proposed camptocormia to be a form of trunk or action dystonia associated with PD[1,6,11]; others consider it to be part of the spectrum of postural abnormalities encountered in late stages of PD.[8,21]

Camptocormia appears to be refractory to medical treatments. Agents such as anticholinergics, amantadine, dopamine agonists, muscle relaxants, and tetrabenazine have been tried with no improvement in posture.[8] Botulinum toxin type A injections into the rectus abdominis muscle have been reported to alleviate muscular spasms for short periods.[8] Use of levodopa makes little difference in the symptoms of camptocormia.[2,19] Furthermore, there is no temporal relationship between camptocormia and dopaminergic doses.[11]

Encouraging results are emerging in the use of deep brain stimulation (DBS) to alleviate symptoms of camptocormia. We present a case of camptocormia in a patient with PD successfully treated with bilateral pallidal DBS and discuss the possible pathophysiological mechanisms.

ABBREVIATIONS: DBS, deep brain stimulation; **GPi,** globus pallidus interna; **PD,** Parkinson disease; **STN,** subthalamic nucleus; **UPDRS,** United Parkinson's Disease Rating Scale

CASE REPORT

A 57-year-old woman initially presented 13 years ago with right upper limb rest tremor with micrographia and no other associated neurological

Copyright © Congress of Neurological Surgeons. Unauthorized reproduction of this article is prohibited.

symptoms. She was given biperiden hydrochloride 3 mg daily, which afforded good relief of tremor. Six years later, she developed difficulty walking because of tremor and rigidity of the right upper and lower limbs. She demonstrated masked facial expression, reduced arm swing during gait, resting tremor, and cogwheel rigidity. The working diagnosis was idiopathic PD. As a result of her complaint of difficulty with memory, biperiden hydrochloride was changed to cabergoline 0.5 mg weekly. A trial of levodopa 100 mg/benserazide 25 mg TID for 12 months did not improve her symptoms. However, she suffered from medication-induced nausea, so it was discontinued.

Over the ensuing 2 years, she developed uncontrollable abdominal contractions and discomfort. She had stooped posture, which was worse while standing and was completely relieved in the recumbent position. Investigations demonstrated no tetanic activity on abdominal electromyography and normal levels of glutamate decarboxylase antibodies. Diazepam afforded some relief of the spasms. As her camptocormia progressed, she was again given levodopa 200 mg/benserazide 50 mg TID, selegiline 5 mg BID, clonidine 0.2 mg, and cabergoline 4 mg daily in various combinations. The camptocormia did not improve at all with these medications. Each combination of drug trials lasted 1 to 2 months. She went on to have continuous intrathecal morphine and baclofen infusions, again without significant improvement in camptocormia.

Despite worsening of posture and discomfort over the last 2 years, her symptoms consistently resolved in the supine position. On recent examination, she presented with right-sided rest tremor, reduced facial expression, bradykinesia, and gait with short stride length and reduced arm swing. There was no hesitancy, freezing, or festination. On ambulation, she experienced progressive dystonia of the abdominal muscles, causing flexion of the torso. This resulted in a closing of the shoulder-hip-knee angle from 147° to 133° with no change in the head-shoulder-hip angle in the sagittal plane (Figure 1A and 1B). She underwent an apomorphine challenge (maximum dose, 3 mg), resulting in improvement of tremor and bradykinesia without any significant alteration in camptocormia. Her diagnosis was levodopa-responsive idiopathic PD with camptocormia not responsive to dopa.

Magnetic resonance imaging (MRI) of the brain did not reveal any focal lesions, and x-rays of the spine showed no structural abnormalities. Previous investigations excluded myopathic or metabolic causes. All findings were consistent with idiopathic PD and camptocormia.

Given that camptocormia was the most significant symptom of the patient, she was offered bilateral globus pallidus interna (GPi) high-frequency DBS surgery. The choice of GPi as the target is discussed later.

Surgical Technique

The posteroventral GPi target was mapped out on a 1.5-T-field-strength MRI gained under general anesthesia. The borders of GPi and the optimal target were plotted in the axial and coronal planes. A Cosman-Robert-Wells (Integra Radionics, Burlington, Massachusetts) frame-mounted computed tomography (CT) was digitally fused with the preoperative MRI to calculate the stereotactic coordinates. Surgery was performed under general anesthesia. Bilateral 3389-model quadripolar brain leads were connected to an implantable pulse generator (Medtronic, Minneapolis, Minnesota).

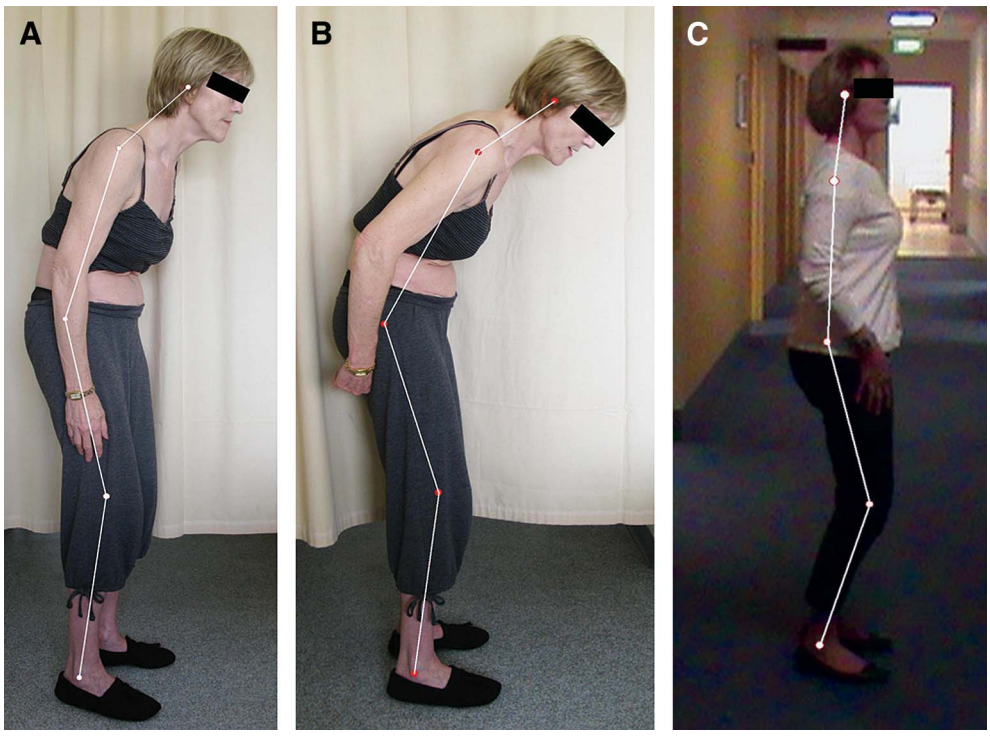

FIGURE 1. *Preoperative appearance (A) when patient stands up from recumbent position and (B) after patient has walked 25 m showing worsening of camptocormia with ambulation. C, postoperative appearance after walking 25 m showing improvement.*

Copyright © Congress of Neurological Surgeons. Unauthorized reproduction of this article is prohibited.

Postoperative stereotactic CT scan with the Cosman-Robert-Wells frame was digitally fused to the preoperative MRI/CT plan without geometric transformations (BrainLab AG, Feldkirchen, Germany). The active contacts were plotted, and anatomic positions were confirmed to be within the ventrodorsal GPi (Figure 2).

Clinical Outcome

The baseline United Parkinson's Disease Rating Scale (UPDRS) part III score was 25. This was improved to 11 with 3 mg apomorphine. Clinically, the camptocormia did not change with the apomorphine.

After surgery, the patient noted significant improvement of posture at 2 months, improving consistently over the following year. She continued to take levodopa 50 mg/benserazide 12.5 mg and benzhexol hydrochloride 2 mg TID. At the 3-month follow-up, her dose of levodopa/benserazide was doubled in an attempt to better control her resting tremor.

At 6 months, she had significant improvement of camptocormia with no resting tremor. She continued on the same medications with mild dyskinesia immediately after levodopa intake. At 12 months, she had complete resolution of camptocormia. She discontinued benzhexol hydrochloride and diazepam. She experienced mild dystonia of the abdomen only on prolonged activity. Figure 1 demonstrates the preoperative and 1-year photographs of the patient on standing after walking 25 m. The postambulation sagittal shoulder-hip-knee angle improved from 133° to 160°. Moreover, neutral gaze has been achieved with reduced neck flexion in part as a result of improvement in the sagittal head-shoulder-hip angle from 148° to 170°. Residual mild hip flexion is likely to be secondary to chronic hamstring muscle shortening because this was also present in the recumbent position.

At 14 months, our patient's on-stimulation UPDRS part III score was 14 in both the on- and off-medication states. The off-stimulation state was not assessed because of the long-term effect of neuromodulation in dystonia. This result shows a relative improvement in UPDRS part III score from 25 to 14 (56%) with stimulation that was independent of dopaminergic medication. Her current medications are levodopa 100 mg/benserazide 25 mg TID and amitriptyline 50 mg nocturnally. Her pallidal electrodes are set on bipolar mode: left (3-2+) at 3.3 V and right

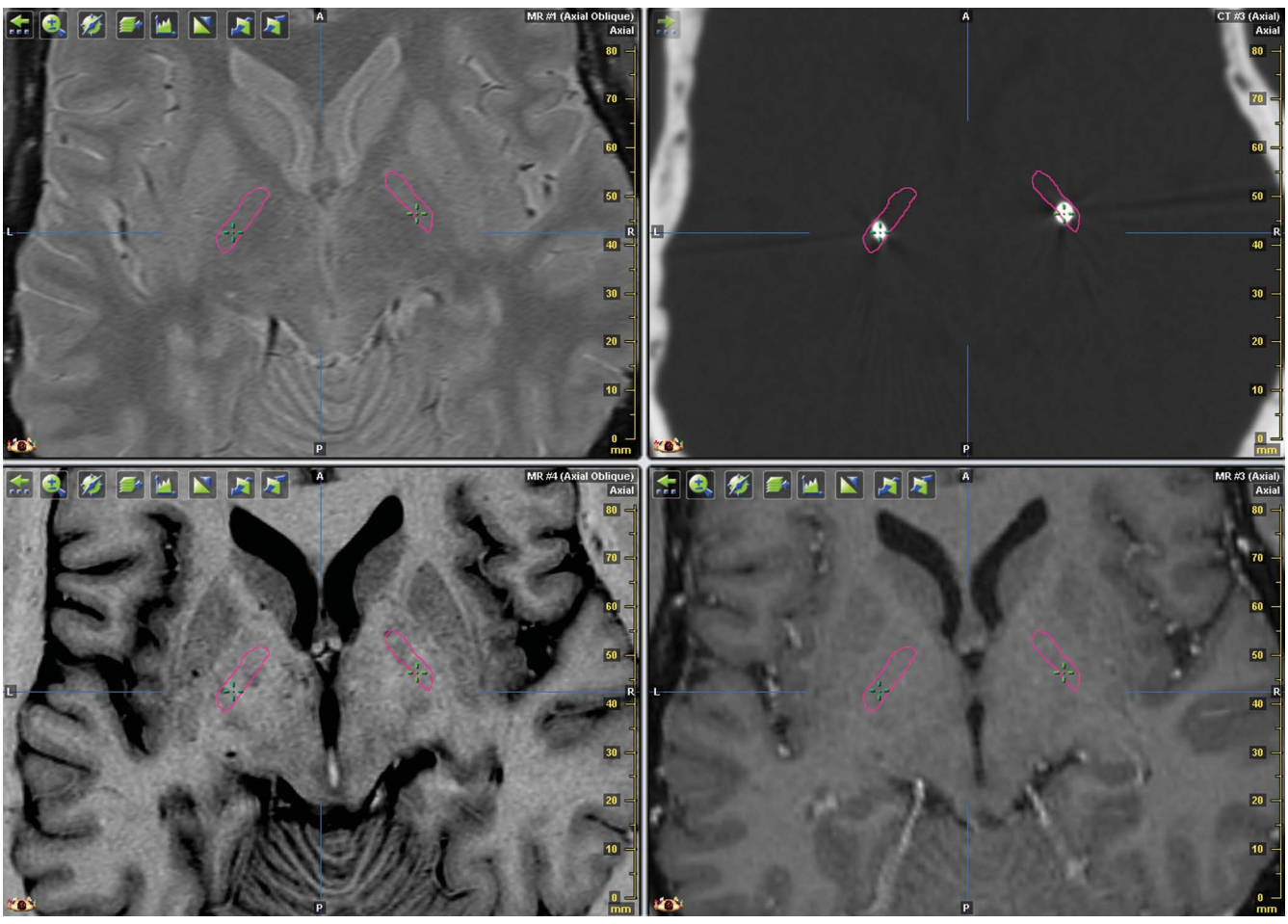

FIGURE 2. *Globus pallidus interna plotted on axial (pink) and the location of the active deep brain stimulation lead contacts plotted by digitally fusing the preoperative plan with postoperative computed tomography scan.*

Copyright © Congress of Neurological Surgeons. Unauthorized reproduction of this article is prohibited.

(7-6+) at 3.2 V, both with frequency of 130 Hz and pulse width of 120 microseconds.

DISCUSSION

Since the first report of camptocormia associated with PD in 1999,[1] it is being increasingly reported within this cohort. Camptocormia can be the most disabling symptom, as in our case, or even the presenting symptom of PD. Our patient's camptocormia was not responsive to dopamine agonists, consistent with other reports in the literature.[1,6,11,22]

Etiology of Camptocormia in PD

Camptocormia appears to have a number of similarities with dystonia. By definition, camptocormia is characterized by the dystonic flexion of the torso in erect posture that is relieved in recumbent position, features consistent with action dystonia. Electromyography of the abdominal muscle in camptocormia shows evidence of myocloniclike jerks[23] that are similar to the observations in patients with primary segmental dystonia.[24] Dystonia is a well-recognized entity among patients with PD[21] as part of the spectrum of dopa-related motor fluctuations.[25] Camptocormia in PD, however, usually has no association with or response to levodopa.[2,9,11]

Camptocormia can result from instability of the vertebral column or imbalance between core musculature. Such instability can result from vertebral spondylosis, spinal tumors, epidural hematoma, infections, various myopathies,[5,12,13] amyotrophic lateral sclerosis,[14-17] motor neurone disease,[17] or drug reactions.[20] In the primary form of camptocormia, segmental abdominal dystonia appears to be the only apparent clinical finding[17,23] likely representing central nervous system dysfunction. Two patients have been reported to have developed camptocormia as a result of lesions in the putaminal/pallidal region.[19] Camptocormia in PD may represent basal ganglia dysfunction that is not significantly altered by dopamine agonists.

DBS Surgery for Camptocormia in PD

When considering DBS therapy for a patient with camptocormia and PD, as in our case, one has to select a suitable brain structure for neuromodulation. Two randomized, controlled trials have provided Class I evidence for the use of DBS of GPi in primary generalized and segmental dystonia.[26,27] More specifically, Fukaya et al[28] recently published a report on 3 patients with camptocormia treated by high-frequency DBS of GPi, reporting 92.2 $\pm$ 5.3% improvement in the Burke, Fahn, and Marsden dystonia rating scale. Similarly, Nandi et al[23] described a patient with camptocormia with bilateral GPi stimulation leading to excellent improvement. All 4 patients suffered from camptocormia without associated PD.

One of the widely used targets for treatment of the cardinal symptoms of PD is the subthalamic nucleus (STN).[29,30] There are 2 reported cases of camptocormia associated with severe PD demonstrating improvement with STN high-frequency DBS.[7,31] One patient had UPDRS part III scores of 91 and 47 in the "off" and "on" states, which improved to 58 and 29, respectively.[31] Similarly, the second patient improved from a UPDRS part III score of 52 to 37 in the "off" state.[7] Conversely, Azher and Jankovic[2] reported on a patient with camptocormia and PD who failed to show any improvement of camptocormia with STN DBS. It appears that STN neuromodulation has the potential to improve camptocormia in patients with severe PD. High-frequency DBS of STN is known to improve dopa-responsive dystonia,[29] although it is unclear whether the camptocormia in these patients was responsive to levodopa.

The GPi is an alternative target considered for treatment of camptocormia. If camptocormia is considered a form of dystonia, then it is not surprising that high-frequency DBS of the GPi leads to improvement. Even when camptocormia is associated with PD, the GPi may be a superior target, especially for those with prominent dyskinetic or levodopa-unresponsive dystonic symptoms. Micheli et al[22] described 1 patient with PD-associated camptocormia treated with bilateral GPi high-frequency DBS. The patient's baseline UPDRS part III score was 52 in the "off" and 24 in the "on" state. The camptocormia was not responsive to levodopa. Surgery resulted in excellent improvement of camptocormia with moderate improvement of PD symptoms (UPDRS part III score of 37 in the "off" state). Interestingly, unilateral pallidotomy in a patient with severe camptocormia and PD has been reported to improve both symptoms.[11]

Although both GPi and STN DBS have been reported to be suitable for patients with camptocormia associated with PD, we chose the GPi as the target of modulation. GPi is attractive because of its direct effects on dyskinesia and dystonia. Our patient had camptocormia as the disabling symptom with mild to moderate symptoms of PD. Moreover, her camptocormia was unresponsive to levodopa and showed features consistent with segmental action dystonia. Our patient had slow but steady improvement of her dystonia with excellent resolution of camptocormia by 6 months, which was sustained at 14 months after surgery. Indeed, this progressive resolution of symptom is reminiscent of the response expected in other forms of dystonia, with optimal improvement often taking months to develop.[32,33] As expected, our patient also showed improvement in PD symptoms with GPi neuromodulation with her off-state UPDRS part III motor scores decreasing from 25 to 14, an improvement of 56%.

CONCLUSION

Camptocormia in PD differs from the common form of Parkinson dystonia in that it is not levodopa responsive and involves the abdomen rather than limbs. It fits the broad definition of dystonia and can be classified as a form of action dystonia in PD. In the absence of secondary causes such as structural, myopathic, or metabolic causes for camptocormia that are poorly treated by medication, DBS may prove a fruitful option. The GPi has efficacy in both PD and action dystonia and

Copyright © Congress of Neurological Surgeons. Unauthorized reproduction of this article is prohibited.

is therefore a suitable target for the treatment of patients with camptocormia and PD.

Disclosure

The authors have no personal financial or institutional interest in any of the drugs, materials, or devices described in this article.

REFERENCES

1. Djaldetti R, Mosberg-Galili R, Sroka H, Merims D, Melamed E. Camptocormia (bent spine) in patients with Parkinson's disease: characterization and possible pathogenesis of an unusual phenomenon. *Mov Disord*. 1999;14(3):443-447.
2. Azher SN, Jankovic J. Camptocormia: pathogenesis, classification, and response to therapy. *Neurology*. 2005;65(3):355-359.
3. Pfeiffer E, von Moers A. Camptocormia in an adolescent. *J Am Acad Child Adolesc Psychiatry*. 2000;39(8):944-945.
4. Lazare A, Klerman GL. Camptocormia in a female: a five-year study. *Br J Med Psychol*. 1970;43(3):265-270.
5. Schäbitz W-R, Glatz K, Schuhan C, et al. Severe forward flexion of the trunk in Parkinson's disease: focal myopathy of the paraspinal muscles mimicking camptocormia. *Mov Disord*. 2003;18(4):408-414.
6. Holler I, Dirnberger G, Pirker W, Auff E, Gerschlager W. Camptocormia in idiopathic Parkinson's disease: [(123)I]beta-CIT SPECT and clinical characteristics. *Eur Neurol*. 2003;50(2):118-120.
7. Yamada K, Goto S, Matsuzaki K, et al. Alleviation of camptocormia by bilateral subthalamic nucleus stimulation in a patient with Parkinson's disease. *Parkinsonism Relat Disord*. 2006;12(6):372-375.
8. Jankovic J, Tintner R. Dystonia and parkinsonism. *Parkinsonism Relat Disord*. 2001;8(2):109-121.
9. Inzelberg R, Hattori N, Nisipeanu P, et al. Camptocormia, axial dystonia, and parkinsonism: phenotypic heterogeneity of a parkin mutation. *Neurology*. 2003;60(8):1393-1394.
10. Reichel G, Kirchhöfer U, Stenner A. Camptocormia: segmental dystonia: proposal of a new definition for an old disease [in German]. *Nervenarzt*. 2001;72(4):281-285.
11. Sławek J, Derejko M, Lass P. Camptocormia as a form of dystonia in Parkinson's disease. *Eur Neurol*. 2003;10(1):107-108.
12. Wunderlich S, Csoti I, Reiners K, et al. Camptocormia in Parkinson's disease mimicked by focal myositis of the paraspinal muscles. *Mov Disord*. 2002;17(3):598-600.
13. Serratrice J, Weiller PJ, Pouget J, Serratrice G. An unrecognized cause of camptocormia: proximal myotonic myopathy [in French]. *Presse Med*. 2000;29(20):1121-1123.
14. Umapathi T, Chaudhry V, Cornblath D, Drachman D, Griffin J, Kuncl R. Head drop and camptocormia. *J Neurol Neurosurg Psychiatry*. 2002;73(1):1-7.
15. Van Gerpen JA. Camptocormia secondary to early amyotrophic lateral sclerosis. *Mov Disord*. 2001;16(2):358-360.
16. Kuncl RW, Cornblath DR, Griffin JW. Assessment of thoracic paraspinal muscles in the diagnosis of ALS. *Muscle Nerve*. 1988;11(5):484-492.
17. Feriha O, Aytul M, Hasan M. A case of camptocormia (bent spine) secondary to early motor neuron disease. *Behav Neurol*. 2004;15(1-2):51-54.
18. Hund E, Heckl R, Goebel HH, Meinck HM. Inclusion body myositis presenting with isolated erector spinae paresis. *Neurology*. 1995;45(5):993-994.
19. Nieves AV, Miyasaki JM, Lang AE. Acute onset dystonic camptocormia caused by lenticular lesions. *Mov Disord*. 2001;16(1):177-180.
20. Kiuru S, Iivanainen M. Camptocormia, a new side effect of sodium valproate. *Epilepsy Res*. 1987;1(4):254-257.
21. Djaldetti R, Hellmann M, Melamed E. Bent knees and tiptoeing: late manifestations of end-stage Parkinson's disease. *Mov Disord*. 2004;19(11):1325-1328.
22. Micheli F, Cersósimo MG, Piedimonte F. Camptocormia in a patient with Parkinson disease: beneficial effects of pallidal deep brain stimulation: case report. *J Neurosurg*. 2005;103(6):1081-1083.
23. Nandi D, Parkin S, Scott R, et al. Camptocormia treated with bilateral pallidal stimulation. *J Neurosurg*. 2002;97(2):461-466.
24. Berardelli A, Rothwell J, Hallett M, Thompson P, Manfredi M, Marsden C. The pathophysiology of primary dystonia. *Brain*. 1998;121(7):1195-1212.
25. Melamed E, Djaldetti R. Camptocormia in Parkinson's disease. *J Neurol*. 2006;253(Suppl VII):14-16.
26. Pollak P, Deste A, Agid Y, et al. Bilateral deep-brain stimulation of the globus pallidus in primary generalized dystonia. *N Engl J Med*. 2005;352(5):459-467.
27. Kupsch A, Benecke R, Muller J, et al. Pallidal deep-brain stimulation in primary generalized or segmental dystonia. *N Engl J Med*. 2006;355(19):1978-1990.
28. Fukaya C, Otaka T, Obuchi T, et al. Pallidal high-frequency deep brain stimulation for camptocormia: an experience of three cases. *Acta Neurochir Suppl*. 2006;99:25-28.
29. Krack P, Batir A, Van Blercom N, et al. Five-year follow-up of bilateral stimulation of the subthalamic nucleus in advanced Parkinson's disease. *N Engl J Med*. 2003;349(20):1925-1934.
30. Benabid AL, Chabardes S, Mitrofanis J, Pollak P. Deep brain stimulation of the subthalamic nucleus for the treatment of Parkinson's disease. *Lancet Neurol*. 2009;8(1):67-81.
31. Hellmann M, Djaldetti R, Israel Z, Melamed E. Effect of deep brain subthalamic stimulation on camptocormia and postural abnormalities in idiopathic Parkinson's disease. *Mov Disord*. 2006;21(11):2008-2010.
32. Coubes P, Cif L, El Fertit H, et al. Electrical stimulation of the globus pallidus internus in patients with primary generalized dystonia: long-term results. *J Neurosurg*. 2004;101(2):189-194.
33. Bittar RG, Yianni J, Wang S, et al. Deep brain stimulation for generalised dystonia and spasmodic torticollis. *J Clin Neurosci*. 2005;12(1):12-16.

Acknowledgments

We thank Dr Julian Rodrigues, Dr Rick Stell, Professor Frank Mastaglia, and Sue Walters from the Australian Neuromuscular Research Institute for their role in the clinical management of this patient, including the preoperative apomorphine challenge and DBS programming.

Copyright © Congress of Neurological Surgeons. Unauthorized reproduction of this article is prohibited.

Surgical Approaches to Tumors of the Gyrus Cinguli

To the Editor:

We read the article by Talacchi et al[1] entitled "Surgical Approaches to Tumors of the Anterior Gyrus Cinguli" with great interest. To their credit, the authors have successfully focused attention on a surgical site that rarely receives the attention it deserves, and we applaud them for this. In fact, we believe that it is safe to say that, apart from any functional considerations, tumors involving the cingulate gyrus are significant both because of their deep location and because they are supplied with a specific anatomic pathway like the interhemispheric fissure. In our opinion, however, based on more than 100 interhemispheric approaches performed over the course of 5 years (for a variety of lesions that lie deep in the interhemispheric fissure), there is another approach to reach this region that Talacchi et al might have considered. We are referring to the contralateral transfalcine interhemispheric approach. In 1984, Machado de Almeida et al[2] were the first to take an exclusively contralateral approach to removing a parasagittal arteriovenous malformation. In 1995, Goel[3] systematically elaborated on this specific approach as a means of reaching contralateral tumors involving the cingulate gyrus. He underscored the value of this approach in the treatment of deep-seated brain tumors, emphatically stressing that this approach, if correctly performed, is direct, safe, and helpful in the successful resection of such tumors. He further suggested that this approach also provides an exposure that obviates the need for traversing or retracting the homolateral edematous brain. In 1996, Lawton et al[4] further elaborated on this approach by introducing the concept of a gravity-aided contralateral approach. With the patient lying in a supine position and with the midline orientated horizontally, they were able to make their lesion on the upper aspect (see their Figure 1). They suggested that this position has the following 2 main advantages: Gravity alone will retract the lower hemisphere and, in so doing, open the interhemispheric fissure; and the lesion will naturally come into greater view as removal of the tumor progresses. Recently, Chi and Lawton[5] also stressed the benefits of a gravity retraction that allows a wider operative exposure, which has the additional benefit of reducing morbidity.

We have developed expertise in this approach as a result of time spent with Dr Spetzler in Phoenix in 2003. To date, we have had numerous opportunities to successfully use this approach to treat a variety of neoplastic and/or vascular lesions that were found in or around the cingulate gyrus. It is on the basis of these surgical opportunities that we fully appreciate the advantages that, we believe, are incomparable when it comes to cases of small lesions deep within a motor area that is swollen as a result of the underlying lesion.[6] Because the interhemispheric corridor is tempting but, it should also be noted, rich in dangerous snares, we offer the following strategies that we have found extremely helpful for avoiding these hazards during surgery: (1) use the Lawton-Spetzler position; (2) make a linear incision parallel to the midline; (3) perform magnetic resonance angiography– or image–guided craniotomy perfectly centered between the entry point of bridging veins in the superior sagittal sinus; (4) expose the superior sagittal sinus by ad hoc placed burr holes and craniotome only after full control and detachment of dura mater from the bone; (5) gently retract and release the brain with working instruments rather than with a fixed spatula; and (6) consider the use of indocyanine green videoangiography to evaluate the presence of collateral drainage pathways before sacrifice or putting a bridging vein at risk (Ferroli et al[7]).

Ferroli Paolo
Giovanni Tringali
Morgan Broggi
Francesco Acerbi
Edvin Zekaj
Angelo Franzini
Giovanni Broggi
Milan, Italy

1. Talacchi A, Corsini F, Gerosa M. Surgical approaches to tumors of the anterior gyrus cinguli. *Neurosurgery*. 2010;66(6)(suppl operative):245-251.
2. Machado de Almeida G, Shibata MK, Nakagawa EJ. Contralateral parafalcine approach for parasagittal and callosal arteriovenous malformations. *Neurosurgery*. 1984;14(6):744-746.
3. Goel A. Transfalcine approach to a contralateral hemispheric tumour. *Acta Neurosurg*. 1995;135(3-4):210-212.
4. Lawton MT, Golfinos JG, Spetzler RF. The contralateral transcallosal approach experience with 32 patients. *Neurosurgery*. 1996;39(4):729-734.
5. Chi JH, Lawton MT. Posterior interhemispheric approach: surgical technique, application to vascular lesion, and benefits of gravity retraction. *Neurosurgery (ONS suppl)*. 2006;59:41-49.
6. Ferroli P, Russo A, Albanese E, Tringali G, Broggi G. Gravity-aided trans-falcine removal of a contralateral subcortical ependymoma. *Acta Neurochir (Wien)*. 2007;149(11):1147-1150.
7. Ferroli P, Nakaji P, Acerbi F, Albanese E, Broggi G. ICG temporary clipping test to asses collateral circulation before venous sacrifice: technical note. *World Neurosurgery*. In press.

10.1227/NEU.0b013e31821243f1

In Reply:

Ferroli and colleagues note that anterior gyrus cinguli tumors may be approached contralaterally. In our series of anterior gyrus cinguli tumors, we used—among others—the interhemispheric bilateral approach in perigenual tumors extending contralaterally and the unilateral approach in perirolandic tumors, based on the finding that tumors never extend contralaterally at this level. From this observation and evidence for the absence of drawbacks to the ipsilateral interhemispheric approach in small lesions, we believe that the contralateral approach may not necessarily offer

Copyright © Congress of Neurological Surgeons. Unauthorized reproduction of this article is prohibited.

an additional advantage over the ipsilateral approach. Furthermore, maneuvers like falx transection with division of the inferior sagittal sinus and the falcine venous plexus, which can carry unpredictable consequences for venous drainage, are not justified in our opinion.[1] However, we were aware of this approach and mentioned it in the discussion, but, because of its limited indications and the scarce success reported in the literature, we decided not to discuss it further.

Andrea Talacchi
Massimo Gerosa
Verona, Italy

1. Tubbs RS, Loukas M, Louis RG Jr, et al. Anatomy of the falcine venous plexus. *J Neurosurg*. 2007;107(1):155-157.

10.1227/NEU.0b013e3182127bee

Spinal Cord Stimulation for Thalamic or Central Pain

To the Editor:

I have read with great interest the paper of Ali et al[1] regarding the usefulness of spinal cord stimulation (SCS) in the treatment of central pain after stroke (CPSP), also well known as thalamic pain.

Patients with focal CPSP instead of generalized pain were considered for treatment by Ali et al.[1] Two cases with complete hemibody pain had circumscribed areas of more severe pain.

Percutaneous tetrapolar epidural electrodes were implanted and held for a 2- to 7-day trial period in 30 patients. Then, the electrode was removed. The analgesic results of the trial period were discussed with the patient. Ten patients received a new tetrapolar electrode. After a second trial period (whose duration is not specified), the internal pulse generator was implanted.

In their discussion the authors claim to be the first to describe good results with the SCS for the treatment of CPSP. The work published by our group[2] shows that this statement is not true. Our series is shorter than the one by Ali et al.[1] Follow-up is longer. They have a 28-month follow-up (range, 6-62), while that ours is longer: 81.6 months (range, 36-149).

I assume with Ali et al[1] that SCS is a much less aggressive surgical method than deep brain stimulation or motor prefrontal cortex. I also agree that better results can be attained in cases of focal pain rather than generalized pain.

I disagree with Ali et al[1] on the appropriateness of a short trial period of 2 to 7 days. I disagree very much with the removal of the electrode test and the return to implant it in the case of the definite implant. It is possible that the second electrode failed to obtain the same paresthesia as did the first. In addition, the rate of local complications could be increased.

Congratulations to Ali et al[1] for his excellent work, which confirms the good results that were previously shown by our work.[2]

Jose Antonio Lopez Lopez
Cadiz, Spain

1. Ali M, Saitoh Y, Hosomi K, Oshino S, Kishima H, Yoshimiro T. Spinal cord stimulation for central poststroke pain. *Neurosurgery*. 2010;67(3): ONS206–ONS212.
2. Lopez JA, Torres LM, Gala F, Iglesias I. Spinal cord stimulation and thalamic pain: long-term results of eight cases. *Neuromodulation*. 2009;12(3):240-243.

10.1227/NEU.0b013e318210f024

In Reply:

We would like to thank Lopez and colleagues for their interest in our article.[1] Lope et al[2] reported on a small series of spinal cord stimulation (SCS) for thalamic pain; 6 of 8 patients (75%) achieved satisfactory pain relief in the long term. Lopez et al restricted their indication to patients with localized pain distribution that could be entirely covered by stimulation paraesthesia; and this may explain their relatively high success rate.[2] Unfortunately this work had not yet been published when we submitted our report for publication.

Lopez et al reported that our trial period (2–7 days) was short. Actually, within this time frame we were able to unequivocally evaluate the analgesic effect of SCS in all patients. In general, there is no consensus on the length of SCS trial period, and periods of one day to several weeks have been reported.[2,3] There is no doubt that long trial periods give a better opportunity to evaluate the exact response to SCS, but unfortunately this comes with the price of increasing the risk of infection.

In our series, we used to remove the trial electrodes, and discharge patients after the trial period. At the time of counseling the patients in the outpatient clinic, those who decided to proceed were scheduled for the second trial and permanent SCS implantation.[1] Lopez et al disagree with this approach because they think it may increase the rate of local complications and the second electrode may fail to provoke the same paresthesia. The rationale for our approach was that, during trial stimulation, patients tend to respond in an affirmative manner, and therefore overestimate the analgesic efficacy.[4] We believe that repeating trials before permanent implant of SCS electrodes will minimize this phenomenon. However, there is no evidence that our method can improve outcome. We did not have any added complications from the second trial, but it obviously increases the cost of treatment. Finally, it is interesting to find that our results of SCS for central poststroke pain (CPSP) could be reproduced at other institutes. Hopefully these reports will encourage other centers to use SCS for CPSP, particularly in the face of safety of SCS trials and limited therapeutic options for CPSP.

Mohamed M. Aly
Youichi Saitoh
Satoru Oshino
Koichi Hosomi
Haruhiko Kishima
Toshiki Yoshimine
Suita, Japan

Copyright © Congress of Neurological Surgeons. Unauthorized reproduction of this article is prohibited.

1. Aly MM, Saitoh Y, Hosomi K, Oshino S, Kishima H, Yoshimine T. Spinal cord stimulation for central poststroke pain. *Neurosurgery*. 2010;67(3): ONS206-ONS212.
2. Lopez JA, Torres LM, Gala F, Iglesias I. Spinal cord stimulation and thalamic pain: long term results of eight cases. *Neuromodulation*. 2009;12(3): 240-243.
3. Stojanovic M, Abdi S. Spinal cord stimulation. *Pain Phys*. 2002;5(2):156-166.
4. Coffey RJ, Lozano AM. Neurostimulation for chronic noncancer pain: an evaluation of the clinical evidence and recommendations for future trial designs. *J Neurosurg*. 2006;105(2):175-198.

10.1227/NEU.0b013e318210f04b

Neurosurgery Simulation

In their neurosurgery simulation technology review, Malone et al[1] address an important yet largely unaddressed surgical area that can significantly benefit from the availability of an effective simulation-based surgical training system. Further, they touch on a number of relevant aspects of developments that will underpin their work on a pedicle screw placement simulator. We would like to add some additional thoughts here, which are based our work over the past several years in developing both a hard-tissue (burr hole) drilling simulator prototype for the US Army as well as a generalized soft-tissue simulation and bleeding system for general surgical resident training.

The authors have correctly identified that the foundational step in developing a system that provides clinically useful surgical skills training is to isolate the subtasks that will benefit most from simulation. Minimizing effort devoted to already mastered or commonly acquired skills and, instead, focusing on critical skill areas that are not well addressed with currently available approaches is critical to producing a simulator that meets unmet needs. To build simulations for those subtasks, the movements and loads experienced by the surgeon during both expected and unexpected actions in the procedure need to form the basis for the mathematical modeling and haptic device interfaces that will be developed. We have also found that, as the authors note, these movements and loads are often not known/available, and we have had to obtain this information ourselves as well. Measuring how actions are done wrong is just as important, if not more so, as measuring when they are done correctly, because an effective simulator must provide learners with the complete range of possible interactions. Learning what happens when something is done right often occurs in the context of learning what happens when things are done wrong.

Also important at the earliest stage of planning a simulator is defining objective, quantitative metrics of performance that can be used to measure attainment of proficiency of the skills being learned. This enables the simulator to be designed to provide reliable, appropriate metrics of performance that can stand up to rigorous evaluation and professional scrutiny.

The authors mention the limitations of current haptic devices and illustrate with the results in their work on measuring the loads encountered in pedicle screw placement. Current, commercially available haptic devices typically provide about 1 lb of force, whereas approximately 15 lb of force are experienced during screw placement in the authors' work. Our research in drilling fresh frozen cadaver skulls showed that forces as high as 30 lb can be experienced. To approach the forces and torques we measured, however, we needed to develop a custom haptic device using augmented off-the-shelf haptic devices. We expect that the availability of haptic devices having sufficient force/torque capacity and adequate range of movement and orientation will remain a major challenge for simulators that focus on high-load situations such as bone drilling.

A final consideration is the mixture of soft-tissue-centric lower-force actions with bone-centric high-load actions in the same simulation. Typically, soft-tissue simulations are modeled with finite-element methods centered on deformation and transection, whereas bone-centric simulations are done with voxel-based techniques in which the goal is often to remove bone through an energy-based methodology that represents the action of drill or saw blades. These techniques are quite different from one another, as are the haptic interface requirements. To our knowledge, no simulator has been produced to date that supports interaction with both soft tissue and bone in the same user experience. This limitation calls for attention to how procedural subtasks are deconstructed if combined soft-tissue–bone actions are encountered, which is not uncommon in spinal procedures.

Malone and colleagues are to be congratulated for taking on an important and largely unaddressed area. Much work lies ahead in the years to come, however, before the potential of such simulators is realized.

Dwight Meglan
Howard R. Champion
Silver Spring, Maryland

1. Malone HR, Syed ON, Downes MS, D'Ambrosio AL, Quest DO, Kaiser MG. Simulation in neurosurgery: a review of computer-based simulation environments and their surgical applications. *Neurosurgery*. 2010;67(4):1105-1116.

10.1227/NEU.0b013e318210f038

In Reply:

We appreciate the remarks of Drs Meglan and Champion of SimQuest, LLC. They are right to emphasize the limitations of many available haptic interfaces in reproducing the torques and loads encountered in the operative theater. The difficulty of simultaneously modeling finite-element–based soft-tissue deformation and voxel-based bone (hard-tissue) drilling, a challenge inherent to spine surgery simulation, is also addressed. Collaboration with simulation firms like SimQuest that possess the technical expertise to customize standard haptic interfaces and merge tissue deformation modalities is

Copyright © Congress of Neurological Surgeons. Unauthorized reproduction of this article is prohibited.

essential to the continued evolution of computer-based neurosurgery simulation.

Hani Malone
Omar Syed
Michael Kaiser
New York, New York

10.1227/NEU.0b013e3182127c00

Relationship Between Decompressive Craniectomy and Hydrocephalus

To the Editor:

We read with great interest the article by Rahme et al[1] in which the authors reviewed the records of 17 patients with stroke-related increased intracranial pressure who underwent decompressive craniectomy (DC). The authors described a 0% rate of shunting after DC and concluded that hydrocephalus does not frequently occur after DC. On the other hand, in the series of Waziri et al,[2] hydrocephalus developed in 15 of 17 patients after DC, and 5 required shunting after cranioplasty. Rahme et al[1] speculated that the explanation for this discrepancy might lie in the definition of hydrocephalus and the indications for shunting.

We completely agree with the viewpoint of Rahme et al[1]; however, we wish to provide further comment on this issue. Bogousslavsky and Regli[3] reported that, in 60 cases of internal carotid artery occlusion, the occurrence of ventricular dilation was related to the volume of infarction. Additionally, Barber et al[4] reported that hydrocephalus was present in 22% of patients who had a large middle cerebral artery infarction, and they received conventional medical therapy (without surgery).

Therefore, we believe that the possibility of hydrocephalus developing in the course of a large infarction should be considered. From this viewpoint, we consider that an additional explanation for the discrepancy between the results of Rahme et al[1] and Waziri et al[2] might be differences in the area and volume of the infarction. Indeed, in the Waziri et al series, all 4 patients with internal carotid artery infarction developed hydrocephalus after DC (half required shunting), and none of the 7 patients with middle cerebral artery infarction received shunting, whereas the Rahme et al series included no patients with internal carotid artery infarction.[1]

Satoru Takeuchi
Naoki Otani
Hiroshi Nawashiro
Tokorozawa, Saitama, Japan

1. Rahme R, Weil AG, Sabbagh M, Moumdjian R, Bouthillier A, Bojanowski MW. Decompressive craniectomy is not an independent risk factor for communicating hydrocephalus in patients with increased intracranial pressure. *Neurosurgery*. 2010;67(3):675-678.
2. Waziri A, Fusco D, Mayer SA, McKhann GM II, Connolly ES Jr. Postoperative hydrocephalus in patients undergoing decompressive hemicraniectomy for ischemic or hemorrhagic stroke. *Neurosurgery*. 2007;61(3):489-493.
3. Bogousslavsky J, Regli F. Obstruction of the internal carotid artery and cerebral malacias: tomodensitometric factors of the prognosis in 150 cases [in French]. *Schweiz Arch Neurol Neurochir Psychiatr*. 1984;134(1):13-28.
4. Barber PA, Demchuk AM, Zhang J, et al. Computed tomographic parameters predicting fatal outcome in large middle cerebral artery infarction. *Cerebrovasc Dis*. 2003;16(3):230-235.

10.1227/NEU.0b013e3182124403

In Reply:

We would like to thank Drs Takeuchi, Otani, and Nawashiro for their interest in our article.[1] However, we find that the 2 studies they are referring to do not really lend support to their hypothesis that the divergence between our results and those of Waziri et al[2] lies in the difference in patient characteristics, specifically the extent of infarction.

In the article of Bogousslavsky and Regli,[3] the authors analyzed the development of unilateral ipsilateral ventricular dilation and cortical atrophy in patients with large strokes secondary to internal carotid artery occlusion or stenosis. There was no mention of hydrocephalus in their report. It is important to distinguish between true hydrocephalus, that is, mismatch between CSF production and resorption, and ventricular dilation or hydrocephalus ex vacuo, which is merely a radiological finding caused by large areas of neuronal loss and encephalomalacia after a massive infarction.

In their publication, Barber et al[4] sought to determine early CT signs predictive of death after large middle cerebral artery (MCA) infarction in a large cohort of conservatively managed patients, none of which had undergone decompressive craniectomy. The authors found that moderate or severe hydrocephalus was predictive of death on univariate, but not multivariate analysis. It must be noted, however, that these authors were referring to acute obstructive hydrocephalus, a complication of cerebral edema-related mass effect in large ischemic strokes. Conversely, in our study[1] and that of Waziri et al,[2] patients were typically protected against obstructive hydrocephalus by the wide surgical decompression. Rather, the incidence of chronic communicating hydrocephalus in survivors of malignant MCA territory infarction and other types of stroke was assessed.

To the best of our knowledge, there is no direct relationship between communicating hydrocephalus and ischemic stroke. Additionally, in our experience, hydrocephalus is not a frequent complication of decompressive craniectomy.[1] Therefore, unless new scientific evidence comes to disprove these findings, we have no reason to believe that hydrocephalus should be a major concern in the management of patients with large MCA or internal carotid artery infarctions.

Ralph Rahme
Alexander G. Weil
Michel W. Bojanowski
Montreal, Quebec, Canada

Copyright © Congress of Neurological Surgeons. Unauthorized reproduction of this article is prohibited.

1. Rahme R, Weil AG, Sabbagh M, Moumdjian R, Bouthillier A, Bojanowski MW. Decompressive craniectomy is not an independent risk factor for communicating hydrocephalus in patients with increased intracranial pressure. *Neurosurgery*. 2010;67(3):675-678.
2. Waziri A, Fusco D, Mayer SA, McKhann GM II, Connolly ES Jr. Postoperative hydrocephalus in patients undergoing decompressive hemicraniectomy for ischemic or hemorrhagic stroke. *Neurosurgery*. 2007;61(3):489-494.
3. Bogousslavsky J, Regli F. Obstruction of the internal carotid artery and cerebral malacias. Tomodensitometric factors of the prognosis in 150 cases [French]. *Schweiz Arch Neurol Neurochir Psychiatr*. 1984;134(1):13-28.
4. Barber PA, Demchuk AM, Zhang J, et al. Computed tomographic parameters predicting fatal outcome in large middle cerebral artery infarction. *Cerebrovasc Dis*. 2003;16(3):230-235.

10.1227/NEU.0b013e3182127bdc

Copyright © Congress of Neurological Surgeons. Unauthorized reproduction of this article is prohibited.

Surgical Approaches to Tumors of the Gyrus Cinguli

To the Editor:

We read the article by Talacchi et al[1] entitled "Surgical Approaches to Tumors of the Anterior Gyrus Cinguli" with great interest. To their credit, the authors have successfully focused attention on a surgical site that rarely receives the attention it deserves, and we applaud them for this. In fact, we believe that it is safe to say that, apart from any functional considerations, tumors involving the cingulate gyrus are significant both because of their deep location and because they are supplied with a specific anatomic pathway like the interhemispheric fissure. In our opinion, however, based on more than 100 interhemispheric approaches performed over the course of 5 years (for a variety of lesions that lie deep in the interhemispheric fissure), there is another approach to reach this region that Talacchi et al might have considered. We are referring to the contralateral transfalcine interhemispheric approach. In 1984, Machado de Almeida et al[2] were the first to take an exclusively contralateral approach to removing a parasagittal arteriovenous malformation. In 1995, Goel[3] systematically elaborated on this specific approach as a means of reaching contralateral tumors involving the cingulate gyrus. He underscored the value of this approach in the treatment of deep-seated brain tumors, emphatically stressing that this approach, if correctly performed, is direct, safe, and helpful in the successful resection of such tumors. He further suggested that this approach also provides an exposure that obviates the need for traversing or retracting the homolateral edematous brain. In 1996, Lawton et al[4] further elaborated on this approach by introducing the concept of a gravity-aided contralateral approach. With the patient lying in a supine position and with the midline orientated horizontally, they were able to make their lesion on the upper aspect (see their Figure 1). They suggested that this position has the following 2 main advantages: Gravity alone will retract the lower hemisphere and, in so doing, open the interhemispheric fissure; and the lesion will naturally come into greater view as removal of the tumor progresses. Recently, Chi and Lawton[5] also stressed the benefits of a gravity retraction that allows a wider operative exposure, which has the additional benefit of reducing morbidity.

We have developed expertise in this approach as a result of time spent with Dr Spetzler in Phoenix in 2003. To date, we have had numerous opportunities to successfully use this approach to treat a variety of neoplastic and/or vascular lesions that were found in or around the cingulate gyrus. It is on the basis of these surgical opportunities that we fully appreciate the advantages that, we believe, are incomparable when it comes to cases of small lesions deep within a motor area that is swollen as a result of the underlying lesion.[6] Because the interhemispheric corridor is tempting but, it should also be noted, rich in dangerous snares, we offer the following strategies that we have found extremely helpful for avoiding these hazards during surgery: (1) use the Lawton-Spetzler position; (2) make a linear incision parallel to the midline; (3) perform magnetic resonance angiography– or image–guided craniotomy perfectly centered between the entry point of bridging veins in the superior sagittal sinus; (4) expose the superior sagittal sinus by ad hoc placed burr holes and craniotome only after full control and detachment of dura mater from the bone; (5) gently retract and release the brain with working instruments rather than with a fixed spatula; and (6) consider the use of indocyanine green videoangiography to evaluate the presence of collateral drainage pathways before sacrifice or putting a bridging vein at risk (Ferroli et al[7]).

Ferroli Paolo
Giovanni Tringali
Morgan Broggi
Francesco Acerbi
Edvin Zekaj
Angelo Franzini
Giovanni Broggi
Milan, Italy

1. Talacchi A, Corsini F, Gerosa M. Surgical approaches to tumors of the anterior gyrus cinguli. *Neurosurgery*. 2010;66(6)(suppl operative):245-251.
2. Machado de Almeida G, Shibata MK, Nakagawa EJ. Contralateral parafalcine approach for parasagittal and callosal arteriovenous malformations. *Neurosurgery*. 1984;14(6):744-746.
3. Goel A. Transfalcine approach to a contralateral hemispheric tumour. *Acta Neurosurg*. 1995;135(3-4):210-212.
4. Lawton MT, Golfinos JG, Spetzler RF. The contralateral transcallosal approach experience with 32 patients. *Neurosurgery*. 1996;39(4):729-734.
5. Chi JH, Lawton MT. Posterior interhemispheric approach: surgical technique, application to vascular lesion, and benefits of gravity retraction. *Neurosurgery (ONS suppl)*. 2006;59:41-49.
6. Ferroli P, Russo A, Albanese E, Tringali G, Broggi G. Gravity-aided trans-falcine removal of a contralateral subcortical ependymoma. *Acta Neurochir (Wien)*. 2007;149(11):1147-1150.
7. Ferroli P, Nakaji P, Acerbi F, Albanese E, Broggi G. ICG temporary clipping test to asses collateral circulation before venous sacrifice: technical note. *World Neurosurgery*. In press.

10.1227/NEU.0b013e31821243f1

In Reply:

Ferroli and colleagues note that anterior gyrus cinguli tumors may be approached contralaterally. In our series of anterior gyrus cinguli tumors, we used—among others—the interhemispheric bilateral approach in perigenual tumors extending contralaterally and the unilateral approach in perirolandic tumors, based on the finding that tumors never extend contralaterally at this level. From this observation and evidence for the absence of drawbacks to the ipsilateral interhemispheric approach in small lesions, we believe that the contralateral approach may not necessarily offer

Copyright © Congress of Neurological Surgeons. Unauthorized reproduction of this article is prohibited.

an additional advantage over the ipsilateral approach. Furthermore, maneuvers like falx transection with division of the inferior sagittal sinus and the falcine venous plexus, which can carry unpredictable consequences for venous drainage, are not justified in our opinion.[1] However, we were aware of this approach and mentioned it in the discussion, but, because of its limited indications and the scarce success reported in the literature, we decided not to discuss it further.

Andrea Talacchi
Massimo Gerosa
Verona, Italy

1. Tubbs RS, Loukas M, Louis RG Jr, et al. Anatomy of the falcine venous plexus. *J Neurosurg*. 2007;107(1):155-157.

10.1227/NEU.0b013e3182127bee

Spinal Cord Stimulation for Thalamic or Central Pain

To the Editor:

I have read with great interest the paper of Ali et al[1] regarding the usefulness of spinal cord stimulation (SCS) in the treatment of central pain after stroke (CPSP), also well known as thalamic pain.

Patients with focal CPSP instead of generalized pain were considered for treatment by Ali et al.[1] Two cases with complete hemibody pain had circumscribed areas of more severe pain.

Percutaneous tetrapolar epidural electrodes were implanted and held for a 2- to 7-day trial period in 30 patients. Then, the electrode was removed. The analgesic results of the trial period were discussed with the patient. Ten patients received a new tetrapolar electrode. After a second trial period (whose duration is not specified), the internal pulse generator was implanted.

In their discussion the authors claim to be the first to describe good results with the SCS for the treatment of CPSP. The work published by our group[2] shows that this statement is not true. Our series is shorter than the one by Ali et al.[1] Follow-up is longer. They have a 28-month follow-up (range, 6-62), while that ours is longer: 81.6 months (range, 36-149).

I assume with Ali et al[1] that SCS is a much less aggressive surgical method than deep brain stimulation or motor prefrontal cortex. I also agree that better results can be attained in cases of focal pain rather than generalized pain.

I disagree with Ali et al[1] on the appropriateness of a short trial period of 2 to 7 days. I disagree very much with the removal of the electrode test and the return to implant it in the case of the definite implant. It is possible that the second electrode failed to obtain the same paresthesia as did the first. In addition, the rate of local complications could be increased.

Congratulations to Ali et al[1] for his excellent work, which confirms the good results that were previously shown by our work.[2]

Jose Antonio Lopez Lopez
Cadiz, Spain

1. Ali M, Saitoh Y, Hosomi K, Oshino S, Kishima H, Yoshimiro T. Spinal cord stimulation for central poststroke pain. *Neurosurgery*. 2010;67(3): ONS206–ONS212.
2. Lopez JA, Torres LM, Gala F, Iglesias I. Spinal cord stimulation and thalamic pain: long-term results of eight cases. *Neuromodulation*. 2009;12(3):240-243.

10.1227/NEU.0b013e318210f024

In Reply:

We would like to thank Lopez and colleagues for their interest in our article.[1] Lope et al[2] reported on a small series of spinal cord stimulation (SCS) for thalamic pain; 6 of 8 patients (75%) achieved satisfactory pain relief in the long term. Lopez et al restricted their indication to patients with localized pain distribution that could be entirely covered by stimulation paraesthesia; and this may explain their relatively high success rate.[2] Unfortunately this work had not yet been published when we submitted our report for publication.

Lopez et al reported that our trial period (2–7 days) was short. Actually, within this time frame we were able to unequivocally evaluate the analgesic effect of SCS in all patients. In general, there is no consensus on the length of SCS trial period, and periods of one day to several weeks have been reported.[2,3] There is no doubt that long trial periods give a better opportunity to evaluate the exact response to SCS, but unfortunately this comes with the price of increasing the risk of infection.

In our series, we used to remove the trial electrodes, and discharge patients after the trial period. At the time of counseling the patients in the outpatient clinic, those who decided to proceed were scheduled for the second trial and permanent SCS implantation.[1] Lopez et al disagree with this approach because they think it may increase the rate of local complications and the second electrode may fail to provoke the same paresthesia. The rationale for our approach was that, during trial stimulation, patients tend to respond in an affirmative manner, and therefore overestimate the analgesic efficacy.[4] We believe that repeating trials before permanent implant of SCS electrodes will minimize this phenomenon. However, there is no evidence that our method can improve outcome. We did not have any added complications from the second trial, but it obviously increases the cost of treatment. Finally, it is interesting to find that our results of SCS for central poststroke pain (CPSP) could be reproduced at other institutes. Hopefully these reports will encourage other centers to use SCS for CPSP, particularly in the face of safety of SCS trials and limited therapeutic options for CPSP.

Mohamed M. Aly
Youichi Saitoh
Satoru Oshino
Koichi Hosomi
Haruhiko Kishima
Toshiki Yoshimine
Suita, Japan

Copyright © Congress of Neurological Surgeons. Unauthorized reproduction of this article is prohibited.

1. Aly MM, Saitoh Y, Hosomi K, Oshino S, Kishima H, Yoshimine T. Spinal cord stimulation for central poststroke pain. *Neurosurgery*. 2010;67(3): ONS206-ONS212.
2. Lopez JA, Torres LM, Gala F, Iglesias I. Spinal cord stimulation and thalamic pain: long term results of eight cases. *Neuromodulation*. 2009;12(3): 240-243.
3. Stojanovic M, Abdi S. Spinal cord stimulation. *Pain Phys*. 2002;5(2):156-166.
4. Coffey RJ, Lozano AM. Neurostimulation for chronic noncancer pain: an evaluation of the clinical evidence and recommendations for future trial designs. *J Neurosurg*. 2006;105(2):175-198.

10.1227/NEU.0b013e318210f04b

Neurosurgery Simulation

In their neurosurgery simulation technology review, Malone et al[1] address an important yet largely unaddressed surgical area that can significantly benefit from the availability of an effective simulation-based surgical training system. Further, they touch on a number of relevant aspects of developments that will underpin their work on a pedicle screw placement simulator. We would like to add some additional thoughts here, which are based our work over the past several years in developing both a hard-tissue (burr hole) drilling simulator prototype for the US Army as well as a generalized soft-tissue simulation and bleeding system for general surgical resident training.

The authors have correctly identified that the foundational step in developing a system that provides clinically useful surgical skills training is to isolate the subtasks that will benefit most from simulation. Minimizing effort devoted to already mastered or commonly acquired skills and, instead, focusing on critical skill areas that are not well addressed with currently available approaches is critical to producing a simulator that meets unmet needs. To build simulations for those subtasks, the movements and loads experienced by the surgeon during both expected and unexpected actions in the procedure need to form the basis for the mathematical modeling and haptic device interfaces that will be developed. We have also found that, as the authors note, these movements and loads are often not known/available, and we have had to obtain this information ourselves as well. Measuring how actions are done wrong is just as important, if not more so, as measuring when they are done correctly, because an effective simulator must provide learners with the complete range of possible interactions. Learning what happens when something is done right often occurs in the context of learning what happens when things are done wrong.

Also important at the earliest stage of planning a simulator is defining objective, quantitative metrics of performance that can be used to measure attainment of proficiency of the skills being learned. This enables the simulator to be designed to provide reliable, appropriate metrics of performance that can stand up to rigorous evaluation and professional scrutiny.

The authors mention the limitations of current haptic devices and illustrate with the results in their work on measuring the loads encountered in pedicle screw placement. Current, commercially available haptic devices typically provide about 1 lb of force, whereas approximately 15 lb of force are experienced during screw placement in the authors' work. Our research in drilling fresh frozen cadaver skulls showed that forces as high as 30 lb can be experienced. To approach the forces and torques we measured, however, we needed to develop a custom haptic device using augmented off-the-shelf haptic devices. We expect that the availability of haptic devices having sufficient force/torque capacity and adequate range of movement and orientation will remain a major challenge for simulators that focus on high-load situations such as bone drilling.

A final consideration is the mixture of soft-tissue-centric lower-force actions with bone-centric high-load actions in the same simulation. Typically, soft-tissue simulations are modeled with finite-element methods centered on deformation and transection, whereas bone-centric simulations are done with voxel-based techniques in which the goal is often to remove bone through an energy-based methodology that represents the action of drill or saw blades. These techniques are quite different from one another, as are the haptic interface requirements. To our knowledge, no simulator has been produced to date that supports interaction with both soft tissue and bone in the same user experience. This limitation calls for attention to how procedural subtasks are deconstructed if combined soft-tissue–bone actions are encountered, which is not uncommon in spinal procedures.

Malone and colleagues are to be congratulated for taking on an important and largely unaddressed area. Much work lies ahead in the years to come, however, before the potential of such simulators is realized.

Dwight Meglan
Howard R. Champion
Silver Spring, Maryland

1. Malone HR, Syed ON, Downes MS, D'Ambrosio AL, Quest DO, Kaiser MG. Simulation in neurosurgery: a review of computer-based simulation environments and their surgical applications. *Neurosurgery*. 2010;67(4):1105-1116.

10.1227/NEU.0b013e318210f038

In Reply:

We appreciate the remarks of Drs Meglan and Champion of SimQuest, LLC. They are right to emphasize the limitations of many available haptic interfaces in reproducing the torques and loads encountered in the operative theater. The difficulty of simultaneously modeling finite-element–based soft-tissue deformation and voxel-based bone (hard-tissue) drilling, a challenge inherent to spine surgery simulation, is also addressed. Collaboration with simulation firms like SimQuest that possess the technical expertise to customize standard haptic interfaces and merge tissue deformation modalities is

Copyright © Congress of Neurological Surgeons. Unauthorized reproduction of this article is prohibited.

essential to the continued evolution of computer-based neurosurgery simulation.

Hani Malone
Omar Syed
Michael Kaiser
New York, New York

10.1227/NEU.0b013e3182127c00

Relationship Between Decompressive Craniectomy and Hydrocephalus

To the Editor:

We read with great interest the article by Rahme et al[1] in which the authors reviewed the records of 17 patients with stroke-related increased intracranial pressure who underwent decompressive craniectomy (DC). The authors described a 0% rate of shunting after DC and concluded that hydrocephalus does not frequently occur after DC. On the other hand, in the series of Waziri et al,[2] hydrocephalus developed in 15 of 17 patients after DC, and 5 required shunting after cranioplasty. Rahme et al[1] speculated that the explanation for this discrepancy might lie in the definition of hydrocephalus and the indications for shunting.

We completely agree with the viewpoint of Rahme et al[1]; however, we wish to provide further comment on this issue. Bogousslavsky and Regli[3] reported that, in 60 cases of internal carotid artery occlusion, the occurrence of ventricular dilation was related to the volume of infarction. Additionally, Barber et al[4] reported that hydrocephalus was present in 22% of patients who had a large middle cerebral artery infarction, and they received conventional medical therapy (without surgery).

Therefore, we believe that the possibility of hydrocephalus developing in the course of a large infarction should be considered. From this viewpoint, we consider that an additional explanation for the discrepancy between the results of Rahme et al[1] and Waziri et al[2] might be differences in the area and volume of the infarction. Indeed, in the Waziri et al series, all 4 patients with internal carotid artery infarction developed hydrocephalus after DC (half required shunting), and none of the 7 patients with middle cerebral artery infarction received shunting, whereas the Rahme et al series included no patients with internal carotid artery infarction.[1]

Satoru Takeuchi
Naoki Otani
Hiroshi Nawashiro
Tokorozawa, Saitama, Japan

1. Rahme R, Weil AG, Sabbagh M, Moumdjian R, Bouthillier A, Bojanowski MW. Decompressive craniectomy is not an independent risk factor for communicating hydrocephalus in patients with increased intracranial pressure. *Neurosurgery*. 2010;67(3):675-678.
2. Waziri A, Fusco D, Mayer SA, McKhann GM II, Connolly ES Jr. Postoperative hydrocephalus in patients undergoing decompressive hemicraniectomy for ischemic or hemorrhagic stroke. *Neurosurgery*. 2007;61(3):489-493.
3. Bogousslavsky J, Regli F. Obstruction of the internal carotid artery and cerebral malacias: tomodensitometric factors of the prognosis in 150 cases [in French]. *Schweiz Arch Neurol Neurochir Psychiatr*. 1984;134(1):13-28.
4. Barber PA, Demchuk AM, Zhang J, et al. Computed tomographic parameters predicting fatal outcome in large middle cerebral artery infarction. *Cerebrovasc Dis*. 2003;16(3):230-235.

10.1227/NEU.0b013e3182124403

In Reply:

We would like to thank Drs Takeuchi, Otani, and Nawashiro for their interest in our article.[1] However, we find that the 2 studies they are referring to do not really lend support to their hypothesis that the divergence between our results and those of Waziri et al[2] lies in the difference in patient characteristics, specifically the extent of infarction.

In the article of Bogousslavsky and Regli,[3] the authors analyzed the development of unilateral ipsilateral ventricular dilation and cortical atrophy in patients with large strokes secondary to internal carotid artery occlusion or stenosis. There was no mention of hydrocephalus in their report. It is important to distinguish between true hydrocephalus, that is, mismatch between CSF production and resorption, and ventricular dilation or hydrocephalus ex vacuo, which is merely a radiological finding caused by large areas of neuronal loss and encephalomalacia after a massive infarction.

In their publication, Barber et al[4] sought to determine early CT signs predictive of death after large middle cerebral artery (MCA) infarction in a large cohort of conservatively managed patients, none of which had undergone decompressive craniectomy. The authors found that moderate or severe hydrocephalus was predictive of death on univariate, but not multivariate analysis. It must be noted, however, that these authors were referring to acute obstructive hydrocephalus, a complication of cerebral edema-related mass effect in large ischemic strokes. Conversely, in our study[1] and that of Waziri et al,[2] patients were typically protected against obstructive hydrocephalus by the wide surgical decompression. Rather, the incidence of chronic communicating hydrocephalus in survivors of malignant MCA territory infarction and other types of stroke was assessed.

To the best of our knowledge, there is no direct relationship between communicating hydrocephalus and ischemic stroke. Additionally, in our experience, hydrocephalus is not a frequent complication of decompressive craniectomy.[1] Therefore, unless new scientific evidence comes to disprove these findings, we have no reason to believe that hydrocephalus should be a major concern in the management of patients with large MCA or internal carotid artery infarctions.

Ralph Rahme
Alexander G. Weil
Michel W. Bojanowski
Montreal, Quebec, Canada

Copyright © Congress of Neurological Surgeons. Unauthorized reproduction of this article is prohibited.

1. Rahme R, Weil AG, Sabbagh M, Moumdjian R, Bouthillier A, Bojanowski MW. Decompressive craniectomy is not an independent risk factor for communicating hydrocephalus in patients with increased intracranial pressure. *Neurosurgery*. 2010;67(3):675-678.
2. Waziri A, Fusco D, Mayer SA, McKhann GM II, Connolly ES Jr. Postoperative hydrocephalus in patients undergoing decompressive hemicraniectomy for ischemic or hemorrhagic stroke. *Neurosurgery*. 2007;61(3):489-494.
3. Bogousslavsky J, Regli F. Obstruction of the internal carotid artery and cerebral malacias. Tomodensitometric factors of the prognosis in 150 cases [French]. *Schweiz Arch Neurol Neurochir Psychiatr*. 1984;134(1):13-28.
4. Barber PA, Demchuk AM, Zhang J, et al. Computed tomographic parameters predicting fatal outcome in large middle cerebral artery infarction. *Cerebrovasc Dis*. 2003;16(3):230-235.

10.1227/NEU.0b013e3182127bdc

Copyright © Congress of Neurological Surgeons. Unauthorized reproduction of this article is prohibited.

Surgical Approaches to Tumors of the Gyrus Cinguli

To the Editor:

We read the article by Talacchi et al[1] entitled "Surgical Approaches to Tumors of the Anterior Gyrus Cinguli" with great interest. To their credit, the authors have successfully focused attention on a surgical site that rarely receives the attention it deserves, and we applaud them for this. In fact, we believe that it is safe to say that, apart from any functional considerations, tumors involving the cingulate gyrus are significant both because of their deep location and because they are supplied with a specific anatomic pathway like the interhemispheric fissure. In our opinion, however, based on more than 100 interhemispheric approaches performed over the course of 5 years (for a variety of lesions that lie deep in the interhemispheric fissure), there is another approach to reach this region that Talacchi et al might have considered. We are referring to the contralateral transfalcine interhemispheric approach. In 1984, Machado de Almeida et al[2] were the first to take an exclusively contralateral approach to removing a parasagittal arteriovenous malformation. In 1995, Goel[3] systematically elaborated on this specific approach as a means of reaching contralateral tumors involving the cingulate gyrus. He underscored the value of this approach in the treatment of deep-seated brain tumors, emphatically stressing that this approach, if correctly performed, is direct, safe, and helpful in the successful resection of such tumors. He further suggested that this approach also provides an exposure that obviates the need for traversing or retracting the homolateral edematous brain. In 1996, Lawton et al[4] further elaborated on this approach by introducing the concept of a gravity-aided contralateral approach. With the patient lying in a supine position and with the midline orientated horizontally, they were able to make their lesion on the upper aspect (see their Figure 1). They suggested that this position has the following 2 main advantages: Gravity alone will retract the lower hemisphere and, in so doing, open the interhemispheric fissure; and the lesion will naturally come into greater view as removal of the tumor progresses. Recently, Chi and Lawton[5] also stressed the benefits of a gravity retraction that allows a wider operative exposure, which has the additional benefit of reducing morbidity.

We have developed expertise in this approach as a result of time spent with Dr Spetzler in Phoenix in 2003. To date, we have had numerous opportunities to successfully use this approach to treat a variety of neoplastic and/or vascular lesions that were found in or around the cingulate gyrus. It is on the basis of these surgical opportunities that we fully appreciate the advantages that, we believe, are incomparable when it comes to cases of small lesions deep within a motor area that is swollen as a result of the underlying lesion.[6] Because the interhemispheric corridor is tempting but, it should also be noted, rich in dangerous snares, we offer the following strategies that we have found extremely helpful for avoiding these hazards during surgery: (1) use the Lawton-Spetzler position; (2) make a linear incision parallel to the midline; (3) perform magnetic resonance angiography– or image–guided craniotomy perfectly centered between the entry point of bridging veins in the superior sagittal sinus; (4) expose the superior sagittal sinus by ad hoc placed burr holes and craniotome only after full control and detachment of dura mater from the bone; (5) gently retract and release the brain with working instruments rather than with a fixed spatula; and (6) consider the use of indocyanine green videoangiography to evaluate the presence of collateral drainage pathways before sacrifice or putting a bridging vein at risk (Ferroli et al[7]).

Ferroli Paolo
Giovanni Tringali
Morgan Broggi
Francesco Acerbi
Edvin Zekaj
Angelo Franzini
Giovanni Broggi
Milan, Italy

1. Talacchi A, Corsini F, Gerosa M. Surgical approaches to tumors of the anterior gyrus cinguli. *Neurosurgery*. 2010;66(6)(suppl operative):245-251.
2. Machado de Almeida G, Shibata MK, Nakagawa EJ. Contralateral parafalcine approach for parasagittal and callosal arteriovenous malformations. *Neurosurgery*. 1984;14(6):744-746.
3. Goel A. Transfalcine approach to a contralateral hemispheric tumour. *Acta Neurosurg*. 1995;135(3-4):210-212.
4. Lawton MT, Golfinos JG, Spetzler RF. The contralateral transcallosal approach experience with 32 patients. *Neurosurgery*. 1996;39(4):729-734.
5. Chi JH, Lawton MT. Posterior interhemispheric approach: surgical technique, application to vascular lesion, and benefits of gravity retraction. *Neurosurgery (ONS suppl)*. 2006;59:41-49.
6. Ferroli P, Russo A, Albanese E, Tringali G, Broggi G. Gravity-aided trans-falcine removal of a contralateral subcortical ependymoma. *Acta Neurochir (Wien)*. 2007;149(11):1147-1150.
7. Ferroli P, Nakaji P, Acerbi F, Albanese E, Broggi G. ICG temporary clipping test to asses collateral circulation before venous sacrifice: technical note. *World Neurosurgery*. In press.

10.1227/NEU.0b013e31821243f1

In Reply:

Ferroli and colleagues note that anterior gyrus cinguli tumors may be approached contralaterally. In our series of anterior gyrus cinguli tumors, we used—among others—the interhemispheric bilateral approach in perigenual tumors extending contralaterally and the unilateral approach in perirolandic tumors, based on the finding that tumors never extend contralaterally at this level. From this observation and evidence for the absence of drawbacks to the ipsilateral interhemispheric approach in small lesions, we believe that the contralateral approach may not necessarily offer

Copyright © Congress of Neurological Surgeons. Unauthorized reproduction of this article is prohibited.

an additional advantage over the ipsilateral approach. Furthermore, maneuvers like falx transection with division of the inferior sagittal sinus and the falcine venous plexus, which can carry unpredictable consequences for venous drainage, are not justified in our opinion.[1] However, we were aware of this approach and mentioned it in the discussion, but, because of its limited indications and the scarce success reported in the literature, we decided not to discuss it further.

Andrea Talacchi
Massimo Gerosa
Verona, Italy

1. Tubbs RS, Loukas M, Louis RG Jr, et al. Anatomy of the falcine venous plexus. *J Neurosurg*. 2007;107(1):155-157.

10.1227/NEU.0b013e3182127bee

Spinal Cord Stimulation for Thalamic or Central Pain

To the Editor:

I have read with great interest the paper of Ali et al[1] regarding the usefulness of spinal cord stimulation (SCS) in the treatment of central pain after stroke (CPSP), also well known as thalamic pain.

Patients with focal CPSP instead of generalized pain were considered for treatment by Ali et al.[1] Two cases with complete hemibody pain had circumscribed areas of more severe pain.

Percutaneous tetrapolar epidural electrodes were implanted and held for a 2- to 7-day trial period in 30 patients. Then, the electrode was removed. The analgesic results of the trial period were discussed with the patient. Ten patients received a new tetrapolar electrode. After a second trial period (whose duration is not specified), the internal pulse generator was implanted.

In their discussion the authors claim to be the first to describe good results with the SCS for the treatment of CPSP. The work published by our group[2] shows that this statement is not true. Our series is shorter than the one by Ali et al.[1] Follow-up is longer. They have a 28-month follow-up (range, 6-62), while that ours is longer: 81.6 months (range, 36-149).

I assume with Ali et al[1] that SCS is a much less aggressive surgical method than deep brain stimulation or motor prefrontal cortex. I also agree that better results can be attained in cases of focal pain rather than generalized pain.

I disagree with Ali et al[1] on the appropriateness of a short trial period of 2 to 7 days. I disagree very much with the removal of the electrode test and the return to implant it in the case of the definite implant. It is possible that the second electrode failed to obtain the same paresthesia as did the first. In addition, the rate of local complications could be increased.

Congratulations to Ali et al[1] for his excellent work, which confirms the good results that were previously shown by our work.[2]

Jose Antonio Lopez Lopez
Cadiz, Spain

1. Ali M, Saitoh Y, Hosomi K, Oshino S, Kishima H, Yoshimiro T. Spinal cord stimulation for central poststroke pain. *Neurosurgery*. 2010;67(3): ONS206–ONS212.
2. Lopez JA, Torres LM, Gala F, Iglesias I. Spinal cord stimulation and thalamic pain: long-term results of eight cases. *Neuromodulation*. 2009;12(3):240-243.

10.1227/NEU.0b013e318210f024

In Reply:

We would like to thank Lopez and colleagues for their interest in our article.[1] Lope et al[2] reported on a small series of spinal cord stimulation (SCS) for thalamic pain; 6 of 8 patients (75%) achieved satisfactory pain relief in the long term. Lopez et al restricted their indication to patients with localized pain distribution that could be entirely covered by stimulation paraesthesia; and this may explain their relatively high success rate.[2] Unfortunately this work had not yet been published when we submitted our report for publication.

Lopez et al reported that our trial period (2–7 days) was short. Actually, within this time frame we were able to unequivocally evaluate the analgesic effect of SCS in all patients. In general, there is no consensus on the length of SCS trial period, and periods of one day to several weeks have been reported.[2,3] There is no doubt that long trial periods give a better opportunity to evaluate the exact response to SCS, but unfortunately this comes with the price of increasing the risk of infection.

In our series, we used to remove the trial electrodes, and discharge patients after the trial period. At the time of counseling the patients in the outpatient clinic, those who decided to proceed were scheduled for the second trial and permanent SCS implantation.[1] Lopez et al disagree with this approach because they think it may increase the rate of local complications and the second electrode may fail to provoke the same paresthesia. The rationale for our approach was that, during trial stimulation, patients tend to respond in an affirmative manner, and therefore overestimate the analgesic efficacy.[4] We believe that repeating trials before permanent implant of SCS electrodes will minimize this phenomenon. However, there is no evidence that our method can improve outcome. We did not have any added complications from the second trial, but it obviously increases the cost of treatment. Finally, it is interesting to find that our results of SCS for central poststroke pain (CPSP) could be reproduced at other institutes. Hopefully these reports will encourage other centers to use SCS for CPSP, particularly in the face of safety of SCS trials and limited therapeutic options for CPSP.

Mohamed M. Aly
Youichi Saitoh
Satoru Oshino
Koichi Hosomi
Haruhiko Kishima
Toshiki Yoshimine
Suita, Japan

Copyright © Congress of Neurological Surgeons. Unauthorized reproduction of this article is prohibited.

1. Aly MM, Saitoh Y, Hosomi K, Oshino S, Kishima H, Yoshimine T. Spinal cord stimulation for central poststroke pain. *Neurosurgery*. 2010;67(3): ONS206-ONS212.
2. Lopez JA, Torres LM, Gala F, Iglesias I. Spinal cord stimulation and thalamic pain: long term results of eight cases. *Neuromodulation*. 2009;12(3): 240-243.
3. Stojanovic M, Abdi S. Spinal cord stimulation. *Pain Phys*. 2002;5(2):156-166.
4. Coffey RJ, Lozano AM. Neurostimulation for chronic noncancer pain: an evaluation of the clinical evidence and recommendations for future trial designs. *J Neurosurg*. 2006;105(2):175-198.

10.1227/NEU.0b013e318210f04b

Neurosurgery Simulation

In their neurosurgery simulation technology review, Malone et al[1] address an important yet largely unaddressed surgical area that can significantly benefit from the availability of an effective simulation-based surgical training system. Further, they touch on a number of relevant aspects of developments that will underpin their work on a pedicle screw placement simulator. We would like to add some additional thoughts here, which are based our work over the past several years in developing both a hard-tissue (burr hole) drilling simulator prototype for the US Army as well as a generalized soft-tissue simulation and bleeding system for general surgical resident training.

The authors have correctly identified that the foundational step in developing a system that provides clinically useful surgical skills training is to isolate the subtasks that will benefit most from simulation. Minimizing effort devoted to already mastered or commonly acquired skills and, instead, focusing on critical skill areas that are not well addressed with currently available approaches is critical to producing a simulator that meets unmet needs. To build simulations for those subtasks, the movements and loads experienced by the surgeon during both expected and unexpected actions in the procedure need to form the basis for the mathematical modeling and haptic device interfaces that will be developed. We have also found that, as the authors note, these movements and loads are often not known/available, and we have had to obtain this information ourselves as well. Measuring how actions are done wrong is just as important, if not more so, as measuring when they are done correctly, because an effective simulator must provide learners with the complete range of possible interactions. Learning what happens when something is done right often occurs in the context of learning what happens when things are done wrong.

Also important at the earliest stage of planning a simulator is defining objective, quantitative metrics of performance that can be used to measure attainment of proficiency of the skills being learned. This enables the simulator to be designed to provide reliable, appropriate metrics of performance that can stand up to rigorous evaluation and professional scrutiny.

The authors mention the limitations of current haptic devices and illustrate with the results in their work on measuring the loads encountered in pedicle screw placement. Current, commercially available haptic devices typically provide about 1 lb of force, whereas approximately 15 lb of force are experienced during screw placement in the authors' work. Our research in drilling fresh frozen cadaver skulls showed that forces as high as 30 lb can be experienced. To approach the forces and torques we measured, however, we needed to develop a custom haptic device using augmented off-the-shelf haptic devices. We expect that the availability of haptic devices having sufficient force/torque capacity and adequate range of movement and orientation will remain a major challenge for simulators that focus on high-load situations such as bone drilling.

A final consideration is the mixture of soft-tissue-centric lower-force actions with bone-centric high-load actions in the same simulation. Typically, soft-tissue simulations are modeled with finite-element methods centered on deformation and transection, whereas bone-centric simulations are done with voxel-based techniques in which the goal is often to remove bone through an energy-based methodology that represents the action of drill or saw blades. These techniques are quite different from one another, as are the haptic interface requirements. To our knowledge, no simulator has been produced to date that supports interaction with both soft tissue and bone in the same user experience. This limitation calls for attention to how procedural subtasks are deconstructed if combined soft-tissue–bone actions are encountered, which is not uncommon in spinal procedures.

Malone and colleagues are to be congratulated for taking on an important and largely unaddressed area. Much work lies ahead in the years to come, however, before the potential of such simulators is realized.

Dwight Meglan
Howard R. Champion
Silver Spring, Maryland

1. Malone HR, Syed ON, Downes MS, D'Ambrosio AL, Quest DO, Kaiser MG. Simulation in neurosurgery: a review of computer-based simulation environments and their surgical applications. *Neurosurgery*. 2010;67(4):1105-1116.

10.1227/NEU.0b013e318210f038

In Reply:

We appreciate the remarks of Drs Meglan and Champion of SimQuest, LLC. They are right to emphasize the limitations of many available haptic interfaces in reproducing the torques and loads encountered in the operative theater. The difficulty of simultaneously modeling finite-element–based soft-tissue deformation and voxel-based bone (hard-tissue) drilling, a challenge inherent to spine surgery simulation, is also addressed. Collaboration with simulation firms like SimQuest that possess the technical expertise to customize standard haptic interfaces and merge tissue deformation modalities is

Copyright © Congress of Neurological Surgeons. Unauthorized reproduction of this article is prohibited.

essential to the continued evolution of computer-based neurosurgery simulation.

Hani Malone
Omar Syed
Michael Kaiser
New York, New York

10.1227/NEU.0b013e3182127c00

Relationship Between Decompressive Craniectomy and Hydrocephalus

To the Editor:

We read with great interest the article by Rahme et al[1] in which the authors reviewed the records of 17 patients with stroke-related increased intracranial pressure who underwent decompressive craniectomy (DC). The authors described a 0% rate of shunting after DC and concluded that hydrocephalus does not frequently occur after DC. On the other hand, in the series of Waziri et al,[2] hydrocephalus developed in 15 of 17 patients after DC, and 5 required shunting after cranioplasty. Rahme et al[1] speculated that the explanation for this discrepancy might lie in the definition of hydrocephalus and the indications for shunting.

We completely agree with the viewpoint of Rahme et al[1]; however, we wish to provide further comment on this issue. Bogousslavsky and Regli[3] reported that, in 60 cases of internal carotid artery occlusion, the occurrence of ventricular dilation was related to the volume of infarction. Additionally, Barber et al[4] reported that hydrocephalus was present in 22% of patients who had a large middle cerebral artery infarction, and they received conventional medical therapy (without surgery).

Therefore, we believe that the possibility of hydrocephalus developing in the course of a large infarction should be considered. From this viewpoint, we consider that an additional explanation for the discrepancy between the results of Rahme et al[1] and Waziri et al[2] might be differences in the area and volume of the infarction. Indeed, in the Waziri et al series, all 4 patients with internal carotid artery infarction developed hydrocephalus after DC (half required shunting), and none of the 7 patients with middle cerebral artery infarction received shunting, whereas the Rahme et al series included no patients with internal carotid artery infarction.[1]

Satoru Takeuchi
Naoki Otani
Hiroshi Nawashiro
Tokorozawa, Saitama, Japan

1. Rahme R, Weil AG, Sabbagh M, Moumdjian R, Bouthillier A, Bojanowski MW. Decompressive craniectomy is not an independent risk factor for communicating hydrocephalus in patients with increased intracranial pressure. *Neurosurgery*. 2010;67(3):675-678.
2. Waziri A, Fusco D, Mayer SA, McKhann GM II, Connolly ES Jr. Postoperative hydrocephalus in patients undergoing decompressive hemicraniectomy for ischemic or hemorrhagic stroke. *Neurosurgery*. 2007;61(3):489-493.
3. Bogousslavsky J, Regli F. Obstruction of the internal carotid artery and cerebral malacias: tomodensitometric factors of the prognosis in 150 cases [in French]. *Schweiz Arch Neurol Neurochir Psychiatr*. 1984;134(1):13-28.
4. Barber PA, Demchuk AM, Zhang J, et al. Computed tomographic parameters predicting fatal outcome in large middle cerebral artery infarction. *Cerebrovasc Dis*. 2003;16(3):230-235.

10.1227/NEU.0b013e3182124403

In Reply:

We would like to thank Drs Takeuchi, Otani, and Nawashiro for their interest in our article.[1] However, we find that the 2 studies they are referring to do not really lend support to their hypothesis that the divergence between our results and those of Waziri et al[2] lies in the difference in patient characteristics, specifically the extent of infarction.

In the article of Bogousslavsky and Regli,[3] the authors analyzed the development of unilateral ipsilateral ventricular dilation and cortical atrophy in patients with large strokes secondary to internal carotid artery occlusion or stenosis. There was no mention of hydrocephalus in their report. It is important to distinguish between true hydrocephalus, that is, mismatch between CSF production and resorption, and ventricular dilation or hydrocephalus ex vacuo, which is merely a radiological finding caused by large areas of neuronal loss and encephalomalacia after a massive infarction.

In their publication, Barber et al[4] sought to determine early CT signs predictive of death after large middle cerebral artery (MCA) infarction in a large cohort of conservatively managed patients, none of which had undergone decompressive craniectomy. The authors found that moderate or severe hydrocephalus was predictive of death on univariate, but not multivariate analysis. It must be noted, however, that these authors were referring to acute obstructive hydrocephalus, a complication of cerebral edema-related mass effect in large ischemic strokes. Conversely, in our study[1] and that of Waziri et al,[2] patients were typically protected against obstructive hydrocephalus by the wide surgical decompression. Rather, the incidence of chronic communicating hydrocephalus in survivors of malignant MCA territory infarction and other types of stroke was assessed.

To the best of our knowledge, there is no direct relationship between communicating hydrocephalus and ischemic stroke. Additionally, in our experience, hydrocephalus is not a frequent complication of decompressive craniectomy.[1] Therefore, unless new scientific evidence comes to disprove these findings, we have no reason to believe that hydrocephalus should be a major concern in the management of patients with large MCA or internal carotid artery infarctions.

Ralph Rahme
Alexander G. Weil
Michel W. Bojanowski
Montreal, Quebec, Canada

Copyright © Congress of Neurological Surgeons. Unauthorized reproduction of this article is prohibited.

1. Rahme R, Weil AG, Sabbagh M, Moumdjian R, Bouthillier A, Bojanowski MW. Decompressive craniectomy is not an independent risk factor for communicating hydrocephalus in patients with increased intracranial pressure. *Neurosurgery*. 2010;67(3):675-678.
2. Waziri A, Fusco D, Mayer SA, McKhann GM II, Connolly ES Jr. Postoperative hydrocephalus in patients undergoing decompressive hemicraniectomy for ischemic or hemorrhagic stroke. *Neurosurgery*. 2007;61(3):489-494.
3. Bogousslavsky J, Regli F. Obstruction of the internal carotid artery and cerebral malacias. Tomodensitometric factors of the prognosis in 150 cases [French]. *Schweiz Arch Neurol Neurochir Psychiatr*. 1984;134(1):13-28.
4. Barber PA, Demchuk AM, Zhang J, et al. Computed tomographic parameters predicting fatal outcome in large middle cerebral artery infarction. *Cerebrovasc Dis*. 2003;16(3):230-235.

10.1227/NEU.0b013e3182127bdc

Copyright © Congress of Neurological Surgeons. Unauthorized reproduction of this article is prohibited.

Surgical Approaches to Tumors of the Gyrus Cinguli

To the Editor:

We read the article by Talacchi et al[1] entitled "Surgical Approaches to Tumors of the Anterior Gyrus Cinguli" with great interest. To their credit, the authors have successfully focused attention on a surgical site that rarely receives the attention it deserves, and we applaud them for this. In fact, we believe that it is safe to say that, apart from any functional considerations, tumors involving the cingulate gyrus are significant both because of their deep location and because they are supplied with a specific anatomic pathway like the interhemispheric fissure. In our opinion, however, based on more than 100 interhemispheric approaches performed over the course of 5 years (for a variety of lesions that lie deep in the interhemispheric fissure), there is another approach to reach this region that Talacchi et al might have considered. We are referring to the contralateral transfalcine interhemispheric approach. In 1984, Machado de Almeida et al[2] were the first to take an exclusively contralateral approach to removing a parasagittal arteriovenous malformation. In 1995, Goel[3] systematically elaborated on this specific approach as a means of reaching contralateral tumors involving the cingulate gyrus. He underscored the value of this approach in the treatment of deep-seated brain tumors, emphatically stressing that this approach, if correctly performed, is direct, safe, and helpful in the successful resection of such tumors. He further suggested that this approach also provides an exposure that obviates the need for traversing or retracting the homolateral edematous brain. In 1996, Lawton et al[4] further elaborated on this approach by introducing the concept of a gravity-aided contralateral approach. With the patient lying in a supine position and with the midline orientated horizontally, they were able to make their lesion on the upper aspect (see their Figure 1). They suggested that this position has the following 2 main advantages: Gravity alone will retract the lower hemisphere and, in so doing, open the interhemispheric fissure; and the lesion will naturally come into greater view as removal of the tumor progresses. Recently, Chi and Lawton[5] also stressed the benefits of a gravity retraction that allows a wider operative exposure, which has the additional benefit of reducing morbidity.

We have developed expertise in this approach as a result of time spent with Dr Spetzler in Phoenix in 2003. To date, we have had numerous opportunities to successfully use this approach to treat a variety of neoplastic and/or vascular lesions that were found in or around the cingulate gyrus. It is on the basis of these surgical opportunities that we fully appreciate the advantages that, we believe, are incomparable when it comes to cases of small lesions deep within a motor area that is swollen as a result of the underlying lesion.[6] Because the interhemispheric corridor is tempting but, it should also be noted, rich in dangerous snares, we offer the following strategies that we have found extremely helpful for avoiding these hazards during surgery: (1) use the Lawton-Spetzler position; (2) make a linear incision parallel to the midline; (3) perform magnetic resonance angiography– or image–guided craniotomy perfectly centered between the entry point of bridging veins in the superior sagittal sinus; (4) expose the superior sagittal sinus by ad hoc placed burr holes and craniotome only after full control and detachment of dura mater from the bone; (5) gently retract and release the brain with working instruments rather than with a fixed spatula; and (6) consider the use of indocyanine green videoangiography to evaluate the presence of collateral drainage pathways before sacrifice or putting a bridging vein at risk (Ferroli et al[7]).

Ferroli Paolo
Giovanni Tringali
Morgan Broggi
Francesco Acerbi
Edvin Zekaj
Angelo Franzini
Giovanni Broggi
Milan, Italy

1. Talacchi A, Corsini F, Gerosa M. Surgical approaches to tumors of the anterior gyrus cinguli. *Neurosurgery*. 2010;66(6)(suppl operative):245-251.
2. Machado de Almeida G, Shibata MK, Nakagawa EJ. Contralateral parafalcine approach for parasagittal and callosal arteriovenous malformations. *Neurosurgery*. 1984;14(6):744-746.
3. Goel A. Transfalcine approach to a contralateral hemispheric tumour. *Acta Neurosurg*. 1995;135(3-4):210-212.
4. Lawton MT, Golfinos JG, Spetzler RF. The contralateral transcallosal approach experience with 32 patients. *Neurosurgery*. 1996;39(4):729-734.
5. Chi JH, Lawton MT. Posterior interhemispheric approach: surgical technique, application to vascular lesion, and benefits of gravity retraction. *Neurosurgery (ONS suppl)*. 2006;59:41-49.
6. Ferroli P, Russo A, Albanese E, Tringali G, Broggi G. Gravity-aided trans-falcine removal of a contralateral subcortical ependymoma. *Acta Neurochir (Wien)*. 2007;149(11):1147-1150.
7. Ferroli P, Nakaji P, Acerbi F, Albanese E, Broggi G. ICG temporary clipping test to asses collateral circulation before venous sacrifice: technical note. *World Neurosurgery*. In press.

10.1227/NEU.0b013e31821243f1

In Reply:

Ferroli and colleagues note that anterior gyrus cinguli tumors may be approached contralaterally. In our series of anterior gyrus cinguli tumors, we used—among others—the interhemispheric bilateral approach in perigenual tumors extending contralaterally and the unilateral approach in perirolandic tumors, based on the finding that tumors never extend contralaterally at this level. From this observation and evidence for the absence of drawbacks to the ipsilateral interhemispheric approach in small lesions, we believe that the contralateral approach may not necessarily offer

Copyright © Congress of Neurological Surgeons. Unauthorized reproduction of this article is prohibited.

an additional advantage over the ipsilateral approach. Furthermore, maneuvers like falx transection with division of the inferior sagittal sinus and the falcine venous plexus, which can carry unpredictable consequences for venous drainage, are not justified in our opinion.[1] However, we were aware of this approach and mentioned it in the discussion, but, because of its limited indications and the scarce success reported in the literature, we decided not to discuss it further.

Andrea Talacchi
Massimo Gerosa
Verona, Italy

1. Tubbs RS, Loukas M, Louis RG Jr, et al. Anatomy of the falcine venous plexus. *J Neurosurg*. 2007;107(1):155-157.

10.1227/NEU.0b013e3182127bee

Spinal Cord Stimulation for Thalamic or Central Pain

To the Editor:

I have read with great interest the paper of Ali et al[1] regarding the usefulness of spinal cord stimulation (SCS) in the treatment of central pain after stroke (CPSP), also well known as thalamic pain.

Patients with focal CPSP instead of generalized pain were considered for treatment by Ali et al.[1] Two cases with complete hemibody pain had circumscribed areas of more severe pain.

Percutaneous tetrapolar epidural electrodes were implanted and held for a 2- to 7-day trial period in 30 patients. Then, the electrode was removed. The analgesic results of the trial period were discussed with the patient. Ten patients received a new tetrapolar electrode. After a second trial period (whose duration is not specified), the internal pulse generator was implanted.

In their discussion the authors claim to be the first to describe good results with the SCS for the treatment of CPSP. The work published by our group[2] shows that this statement is not true. Our series is shorter than the one by Ali et al.[1] Follow-up is longer. They have a 28-month follow-up (range, 6-62), while that ours is longer: 81.6 months (range, 36-149).

I assume with Ali et al[1] that SCS is a much less aggressive surgical method than deep brain stimulation or motor prefrontal cortex. I also agree that better results can be attained in cases of focal pain rather than generalized pain.

I disagree with Ali et al[1] on the appropriateness of a short trial period of 2 to 7 days. I disagree very much with the removal of the electrode test and the return to implant it in the case of the definite implant. It is possible that the second electrode failed to obtain the same paresthesia as did the first. In addition, the rate of local complications could be increased.

Congratulations to Ali et al[1] for his excellent work, which confirms the good results that were previously shown by our work.[2]

Jose Antonio Lopez Lopez
Cadiz, Spain

1. Ali M, Saitoh Y, Hosomi K, Oshino S, Kishima H, Yoshimiro T. Spinal cord stimulation for central poststroke pain. *Neurosurgery*. 2010;67(3): ONS206–ONS212.
2. Lopez JA, Torres LM, Gala F, Iglesias I. Spinal cord stimulation and thalamic pain: long-term results of eight cases. *Neuromodulation*. 2009;12(3):240-243.

10.1227/NEU.0b013e318210f024

In Reply:

We would like to thank Lopez and colleagues for their interest in our article.[1] Lope et al[2] reported on a small series of spinal cord stimulation (SCS) for thalamic pain; 6 of 8 patients (75%) achieved satisfactory pain relief in the long term. Lopez et al restricted their indication to patients with localized pain distribution that could be entirely covered by stimulation paraesthesia; and this may explain their relatively high success rate.[2] Unfortunately this work had not yet been published when we submitted our report for publication.

Lopez et al reported that our trial period (2–7 days) was short. Actually, within this time frame we were able to unequivocally evaluate the analgesic effect of SCS in all patients. In general, there is no consensus on the length of SCS trial period, and periods of one day to several weeks have been reported.[2,3] There is no doubt that long trial periods give a better opportunity to evaluate the exact response to SCS, but unfortunately this comes with the price of increasing the risk of infection.

In our series, we used to remove the trial electrodes, and discharge patients after the trial period. At the time of counseling the patients in the outpatient clinic, those who decided to proceed were scheduled for the second trial and permanent SCS implantation.[1] Lopez et al disagree with this approach because they think it may increase the rate of local complications and the second electrode may fail to provoke the same paresthesia. The rationale for our approach was that, during trial stimulation, patients tend to respond in an affirmative manner, and therefore overestimate the analgesic efficacy.[4] We believe that repeating trials before permanent implant of SCS electrodes will minimize this phenomenon. However, there is no evidence that our method can improve outcome. We did not have any added complications from the second trial, but it obviously increases the cost of treatment. Finally, it is interesting to find that our results of SCS for central poststroke pain (CPSP) could be reproduced at other institutes. Hopefully these reports will encourage other centers to use SCS for CPSP, particularly in the face of safety of SCS trials and limited therapeutic options for CPSP.

Mohamed M. Aly
Youichi Saitoh
Satoru Oshino
Koichi Hosomi
Haruhiko Kishima
Toshiki Yoshimine
Suita, Japan

Copyright © Congress of Neurological Surgeons. Unauthorized reproduction of this article is prohibited.

1. Aly MM, Saitoh Y, Hosomi K, Oshino S, Kishima H, Yoshimine T. Spinal cord stimulation for central poststroke pain. *Neurosurgery*. 2010;67(3): ONS206-ONS212.
2. Lopez JA, Torres LM, Gala F, Iglesias I. Spinal cord stimulation and thalamic pain: long term results of eight cases. *Neuromodulation*. 2009;12(3): 240-243.
3. Stojanovic M, Abdi S. Spinal cord stimulation. *Pain Phys*. 2002;5(2):156-166.
4. Coffey RJ, Lozano AM. Neurostimulation for chronic noncancer pain: an evaluation of the clinical evidence and recommendations for future trial designs. *J Neurosurg*. 2006;105(2):175-198.

10.1227/NEU.0b013e318210f04b

Neurosurgery Simulation

In their neurosurgery simulation technology review, Malone et al[1] address an important yet largely unaddressed surgical area that can significantly benefit from the availability of an effective simulation-based surgical training system. Further, they touch on a number of relevant aspects of developments that will underpin their work on a pedicle screw placement simulator. We would like to add some additional thoughts here, which are based our work over the past several years in developing both a hard-tissue (burr hole) drilling simulator prototype for the US Army as well as a generalized soft-tissue simulation and bleeding system for general surgical resident training.

The authors have correctly identified that the foundational step in developing a system that provides clinically useful surgical skills training is to isolate the subtasks that will benefit most from simulation. Minimizing effort devoted to already mastered or commonly acquired skills and, instead, focusing on critical skill areas that are not well addressed with currently available approaches is critical to producing a simulator that meets unmet needs. To build simulations for those subtasks, the movements and loads experienced by the surgeon during both expected and unexpected actions in the procedure need to form the basis for the mathematical modeling and haptic device interfaces that will be developed. We have also found that, as the authors note, these movements and loads are often not known/available, and we have had to obtain this information ourselves as well. Measuring how actions are done wrong is just as important, if not more so, as measuring when they are done correctly, because an effective simulator must provide learners with the complete range of possible interactions. Learning what happens when something is done right often occurs in the context of learning what happens when things are done wrong.

Also important at the earliest stage of planning a simulator is defining objective, quantitative metrics of performance that can be used to measure attainment of proficiency of the skills being learned. This enables the simulator to be designed to provide reliable, appropriate metrics of performance that can stand up to rigorous evaluation and professional scrutiny.

The authors mention the limitations of current haptic devices and illustrate with the results in their work on measuring the loads encountered in pedicle screw placement. Current, commercially available haptic devices typically provide about 1 lb of force, whereas approximately 15 lb of force are experienced during screw placement in the authors' work. Our research in drilling fresh frozen cadaver skulls showed that forces as high as 30 lb can be experienced. To approach the forces and torques we measured, however, we needed to develop a custom haptic device using augmented off-the-shelf haptic devices. We expect that the availability of haptic devices having sufficient force/torque capacity and adequate range of movement and orientation will remain a major challenge for simulators that focus on high-load situations such as bone drilling.

A final consideration is the mixture of soft-tissue-centric lower-force actions with bone-centric high-load actions in the same simulation. Typically, soft-tissue simulations are modeled with finite-element methods centered on deformation and transection, whereas bone-centric simulations are done with voxel-based techniques in which the goal is often to remove bone through an energy-based methodology that represents the action of drill or saw blades. These techniques are quite different from one another, as are the haptic interface requirements. To our knowledge, no simulator has been produced to date that supports interaction with both soft tissue and bone in the same user experience. This limitation calls for attention to how procedural subtasks are deconstructed if combined soft-tissue–bone actions are encountered, which is not uncommon in spinal procedures.

Malone and colleagues are to be congratulated for taking on an important and largely unaddressed area. Much work lies ahead in the years to come, however, before the potential of such simulators is realized.

Dwight Meglan
Howard R. Champion
Silver Spring, Maryland

1. Malone HR, Syed ON, Downes MS, D'Ambrosio AL, Quest DO, Kaiser MG. Simulation in neurosurgery: a review of computer-based simulation environments and their surgical applications. *Neurosurgery*. 2010;67(4):1105-1116.

10.1227/NEU.0b013e318210f038

In Reply:

We appreciate the remarks of Drs Meglan and Champion of SimQuest, LLC. They are right to emphasize the limitations of many available haptic interfaces in reproducing the torques and loads encountered in the operative theater. The difficulty of simultaneously modeling finite-element–based soft-tissue deformation and voxel-based bone (hard-tissue) drilling, a challenge inherent to spine surgery simulation, is also addressed. Collaboration with simulation firms like SimQuest that possess the technical expertise to customize standard haptic interfaces and merge tissue deformation modalities is

Copyright © Congress of Neurological Surgeons. Unauthorized reproduction of this article is prohibited.

essential to the continued evolution of computer-based neurosurgery simulation.

Hani Malone
Omar Syed
Michael Kaiser
New York, New York

10.1227/NEU.0b013e3182127c00

Relationship Between Decompressive Craniectomy and Hydrocephalus

To the Editor:

We read with great interest the article by Rahme et al[1] in which the authors reviewed the records of 17 patients with stroke-related increased intracranial pressure who underwent decompressive craniectomy (DC). The authors described a 0% rate of shunting after DC and concluded that hydrocephalus does not frequently occur after DC. On the other hand, in the series of Waziri et al,[2] hydrocephalus developed in 15 of 17 patients after DC, and 5 required shunting after cranioplasty. Rahme et al[1] speculated that the explanation for this discrepancy might lie in the definition of hydrocephalus and the indications for shunting.

We completely agree with the viewpoint of Rahme et al[1]; however, we wish to provide further comment on this issue. Bogousslavsky and Regli[3] reported that, in 60 cases of internal carotid artery occlusion, the occurrence of ventricular dilation was related to the volume of infarction. Additionally, Barber et al[4] reported that hydrocephalus was present in 22% of patients who had a large middle cerebral artery infarction, and they received conventional medical therapy (without surgery).

Therefore, we believe that the possibility of hydrocephalus developing in the course of a large infarction should be considered. From this viewpoint, we consider that an additional explanation for the discrepancy between the results of Rahme et al[1] and Waziri et al[2] might be differences in the area and volume of the infarction. Indeed, in the Waziri et al series, all 4 patients with internal carotid artery infarction developed hydrocephalus after DC (half required shunting), and none of the 7 patients with middle cerebral artery infarction received shunting, whereas the Rahme et al series included no patients with internal carotid artery infarction.[1]

Satoru Takeuchi
Naoki Otani
Hiroshi Nawashiro
Tokorozawa, Saitama, Japan

1. Rahme R, Weil AG, Sabbagh M, Moumdjian R, Bouthillier A, Bojanowski MW. Decompressive craniectomy is not an independent risk factor for communicating hydrocephalus in patients with increased intracranial pressure. *Neurosurgery*. 2010;67(3):675-678.
2. Waziri A, Fusco D, Mayer SA, McKhann GM II, Connolly ES Jr. Postoperative hydrocephalus in patients undergoing decompressive hemicraniectomy for ischemic or hemorrhagic stroke. *Neurosurgery*. 2007;61(3):489-493.
3. Bogousslavsky J, Regli F. Obstruction of the internal carotid artery and cerebral malacias: tomodensitometric factors of the prognosis in 150 cases [in French]. *Schweiz Arch Neurol Neurochir Psychiatr*. 1984;134(1):13-28.
4. Barber PA, Demchuk AM, Zhang J, et al. Computed tomographic parameters predicting fatal outcome in large middle cerebral artery infarction. *Cerebrovasc Dis*. 2003;16(3):230-235.

10.1227/NEU.0b013e3182124403

In Reply:

We would like to thank Drs Takeuchi, Otani, and Nawashiro for their interest in our article.[1] However, we find that the 2 studies they are referring to do not really lend support to their hypothesis that the divergence between our results and those of Waziri et al[2] lies in the difference in patient characteristics, specifically the extent of infarction.

In the article of Bogousslavsky and Regli,[3] the authors analyzed the development of unilateral ipsilateral ventricular dilation and cortical atrophy in patients with large strokes secondary to internal carotid artery occlusion or stenosis. There was no mention of hydrocephalus in their report. It is important to distinguish between true hydrocephalus, that is, mismatch between CSF production and resorption, and ventricular dilation or hydrocephalus ex vacuo, which is merely a radiological finding caused by large areas of neuronal loss and encephalomalacia after a massive infarction.

In their publication, Barber et al[4] sought to determine early CT signs predictive of death after large middle cerebral artery (MCA) infarction in a large cohort of conservatively managed patients, none of which had undergone decompressive craniectomy. The authors found that moderate or severe hydrocephalus was predictive of death on univariate, but not multivariate analysis. It must be noted, however, that these authors were referring to acute obstructive hydrocephalus, a complication of cerebral edema-related mass effect in large ischemic strokes. Conversely, in our study[1] and that of Waziri et al,[2] patients were typically protected against obstructive hydrocephalus by the wide surgical decompression. Rather, the incidence of chronic communicating hydrocephalus in survivors of malignant MCA territory infarction and other types of stroke was assessed.

To the best of our knowledge, there is no direct relationship between communicating hydrocephalus and ischemic stroke. Additionally, in our experience, hydrocephalus is not a frequent complication of decompressive craniectomy.[1] Therefore, unless new scientific evidence comes to disprove these findings, we have no reason to believe that hydrocephalus should be a major concern in the management of patients with large MCA or internal carotid artery infarctions.

Ralph Rahme
Alexander G. Weil
Michel W. Bojanowski
Montreal, Quebec, Canada

Copyright © Congress of Neurological Surgeons. Unauthorized reproduction of this article is prohibited.

1. Rahme R, Weil AG, Sabbagh M, Moumdjian R, Bouthillier A, Bojanowski MW. Decompressive craniectomy is not an independent risk factor for communicating hydrocephalus in patients with increased intracranial pressure. *Neurosurgery*. 2010;67(3):675-678.
2. Waziri A, Fusco D, Mayer SA, McKhann GM II, Connolly ES Jr. Postoperative hydrocephalus in patients undergoing decompressive hemicraniectomy for ischemic or hemorrhagic stroke. *Neurosurgery*. 2007;61(3):489-494.
3. Bogousslavsky J, Regli F. Obstruction of the internal carotid artery and cerebral malacias. Tomodensitometric factors of the prognosis in 150 cases [French]. *Schweiz Arch Neurol Neurochir Psychiatr*. 1984;134(1):13-28.
4. Barber PA, Demchuk AM, Zhang J, et al. Computed tomographic parameters predicting fatal outcome in large middle cerebral artery infarction. *Cerebrovasc Dis*. 2003;16(3):230-235.

10.1227/NEU.0b013e3182127bdc

Copyright © Congress of Neurological Surgeons. Unauthorized reproduction of this article is prohibited.

Surgical Approaches to Tumors of the Gyrus Cinguli

To the Editor:

We read the article by Talacchi et al[1] entitled "Surgical Approaches to Tumors of the Anterior Gyrus Cinguli" with great interest. To their credit, the authors have successfully focused attention on a surgical site that rarely receives the attention it deserves, and we applaud them for this. In fact, we believe that it is safe to say that, apart from any functional considerations, tumors involving the cingulate gyrus are significant both because of their deep location and because they are supplied with a specific anatomic pathway like the interhemispheric fissure. In our opinion, however, based on more than 100 interhemispheric approaches performed over the course of 5 years (for a variety of lesions that lie deep in the interhemispheric fissure), there is another approach to reach this region that Talacchi et al might have considered. We are referring to the contralateral transfalcine interhemispheric approach. In 1984, Machado de Almeida et al[2] were the first to take an exclusively contralateral approach to removing a parasagittal arteriovenous malformation. In 1995, Goel[3] systematically elaborated on this specific approach as a means of reaching contralateral tumors involving the cingulate gyrus. He underscored the value of this approach in the treatment of deep-seated brain tumors, emphatically stressing that this approach, if correctly performed, is direct, safe, and helpful in the successful resection of such tumors. He further suggested that this approach also provides an exposure that obviates the need for traversing or retracting the homolateral edematous brain. In 1996, Lawton et al[4] further elaborated on this approach by introducing the concept of a gravity-aided contralateral approach. With the patient lying in a supine position and with the midline orientated horizontally, they were able to make their lesion on the upper aspect (see their Figure 1). They suggested that this position has the following 2 main advantages: Gravity alone will retract the lower hemisphere and, in so doing, open the interhemispheric fissure; and the lesion will naturally come into greater view as removal of the tumor progresses. Recently, Chi and Lawton[5] also stressed the benefits of a gravity retraction that allows a wider operative exposure, which has the additional benefit of reducing morbidity.

We have developed expertise in this approach as a result of time spent with Dr Spetzler in Phoenix in 2003. To date, we have had numerous opportunities to successfully use this approach to treat a variety of neoplastic and/or vascular lesions that were found in or around the cingulate gyrus. It is on the basis of these surgical opportunities that we fully appreciate the advantages that, we believe, are incomparable when it comes to cases of small lesions deep within a motor area that is swollen as a result of the underlying lesion.[6] Because the interhemispheric corridor is tempting but, it should also be noted, rich in dangerous snares, we offer the following strategies that we have found extremely helpful for avoiding these hazards during surgery: (1) use the Lawton-Spetzler position; (2) make a linear incision parallel to the midline; (3) perform magnetic resonance angiography– or image–guided craniotomy perfectly centered between the entry point of bridging veins in the superior sagittal sinus; (4) expose the superior sagittal sinus by ad hoc placed burr holes and craniotome only after full control and detachment of dura mater from the bone; (5) gently retract and release the brain with working instruments rather than with a fixed spatula; and (6) consider the use of indocyanine green videoangiography to evaluate the presence of collateral drainage pathways before sacrifice or putting a bridging vein at risk (Ferroli et al[7]).

Ferroli Paolo
Giovanni Tringali
Morgan Broggi
Francesco Acerbi
Edvin Zekaj
Angelo Franzini
Giovanni Broggi
Milan, Italy

1. Talacchi A, Corsini F, Gerosa M. Surgical approaches to tumors of the anterior gyrus cinguli. *Neurosurgery*. 2010;66(6)(suppl operative):245-251.
2. Machado de Almeida G, Shibata MK, Nakagawa EJ. Contralateral parafalcine approach for parasagittal and callosal arteriovenous malformations. *Neurosurgery*. 1984;14(6):744-746.
3. Goel A. Transfalcine approach to a contralateral hemispheric tumour. *Acta Neurosurg*. 1995;135(3-4):210-212.
4. Lawton MT, Golfinos JG, Spetzler RF. The contralateral transcallosal approach experience with 32 patients. *Neurosurgery*. 1996;39(4):729-734.
5. Chi JH, Lawton MT. Posterior interhemispheric approach: surgical technique, application to vascular lesion, and benefits of gravity retraction. *Neurosurgery (ONS suppl)*. 2006;59:41-49.
6. Ferroli P, Russo A, Albanese E, Tringali G, Broggi G. Gravity-aided trans-falcine removal of a contralateral subcortical ependymoma. *Acta Neurochir (Wien)*. 2007;149(11):1147-1150.
7. Ferroli P, Nakaji P, Acerbi F, Albanese E, Broggi G. ICG temporary clipping test to asses collateral circulation before venous sacrifice: technical note. *World Neurosurgery*. In press.

10.1227/NEU.0b013e31821243f1

In Reply:

Ferroli and colleagues note that anterior gyrus cinguli tumors may be approached contralaterally. In our series of anterior gyrus cinguli tumors, we used—among others—the interhemispheric bilateral approach in perigenual tumors extending contralaterally and the unilateral approach in perirolandic tumors, based on the finding that tumors never extend contralaterally at this level. From this observation and evidence for the absence of drawbacks to the ipsilateral interhemispheric approach in small lesions, we believe that the contralateral approach may not necessarily offer

Copyright © Congress of Neurological Surgeons. Unauthorized reproduction of this article is prohibited.

an additional advantage over the ipsilateral approach. Furthermore, maneuvers like falx transection with division of the inferior sagittal sinus and the falcine venous plexus, which can carry unpredictable consequences for venous drainage, are not justified in our opinion.[1] However, we were aware of this approach and mentioned it in the discussion, but, because of its limited indications and the scarce success reported in the literature, we decided not to discuss it further.

Andrea Talacchi
Massimo Gerosa
Verona, Italy

1. Tubbs RS, Loukas M, Louis RG Jr, et al. Anatomy of the falcine venous plexus. *J Neurosurg*. 2007;107(1):155-157.

10.1227/NEU.0b013e3182127bee

Spinal Cord Stimulation for Thalamic or Central Pain

To the Editor:

I have read with great interest the paper of Ali et al[1] regarding the usefulness of spinal cord stimulation (SCS) in the treatment of central pain after stroke (CPSP), also well known as thalamic pain.

Patients with focal CPSP instead of generalized pain were considered for treatment by Ali et al.[1] Two cases with complete hemibody pain had circumscribed areas of more severe pain.

Percutaneous tetrapolar epidural electrodes were implanted and held for a 2- to 7-day trial period in 30 patients. Then, the electrode was removed. The analgesic results of the trial period were discussed with the patient. Ten patients received a new tetrapolar electrode. After a second trial period (whose duration is not specified), the internal pulse generator was implanted.

In their discussion the authors claim to be the first to describe good results with the SCS for the treatment of CPSP. The work published by our group[2] shows that this statement is not true. Our series is shorter than the one by Ali et al.[1] Follow-up is longer. They have a 28-month follow-up (range, 6-62), while that ours is longer: 81.6 months (range, 36-149).

I assume with Ali et al[1] that SCS is a much less aggressive surgical method than deep brain stimulation or motor prefrontal cortex. I also agree that better results can be attained in cases of focal pain rather than generalized pain.

I disagree with Ali et al[1] on the appropriateness of a short trial period of 2 to 7 days. I disagree very much with the removal of the electrode test and the return to implant it in the case of the definite implant. It is possible that the second electrode failed to obtain the same paresthesia as did the first. In addition, the rate of local complications could be increased.

Congratulations to Ali et al[1] for his excellent work, which confirms the good results that were previously shown by our work.[2]

Jose Antonio Lopez Lopez
Cadiz, Spain

1. Ali M, Saitoh Y, Hosomi K, Oshino S, Kishima H, Yoshimiro T. Spinal cord stimulation for central poststroke pain. *Neurosurgery*. 2010;67(3): ONS206–ONS212.
2. Lopez JA, Torres LM, Gala F, Iglesias I. Spinal cord stimulation and thalamic pain: long-term results of eight cases. *Neuromodulation*. 2009;12(3):240-243.

10.1227/NEU.0b013e318210f024

In Reply:

We would like to thank Lopez and colleagues for their interest in our article.[1] Lope et al[2] reported on a small series of spinal cord stimulation (SCS) for thalamic pain; 6 of 8 patients (75%) achieved satisfactory pain relief in the long term. Lopez et al restricted their indication to patients with localized pain distribution that could be entirely covered by stimulation paraesthesia; and this may explain their relatively high success rate.[2] Unfortunately this work had not yet been published when we submitted our report for publication.

Lopez et al reported that our trial period (2–7 days) was short. Actually, within this time frame we were able to unequivocally evaluate the analgesic effect of SCS in all patients. In general, there is no consensus on the length of SCS trial period, and periods of one day to several weeks have been reported.[2,3] There is no doubt that long trial periods give a better opportunity to evaluate the exact response to SCS, but unfortunately this comes with the price of increasing the risk of infection.

In our series, we used to remove the trial electrodes, and discharge patients after the trial period. At the time of counseling the patients in the outpatient clinic, those who decided to proceed were scheduled for the second trial and permanent SCS implantation.[1] Lopez et al disagree with this approach because they think it may increase the rate of local complications and the second electrode may fail to provoke the same paresthesia. The rationale for our approach was that, during trial stimulation, patients tend to respond in an affirmative manner, and therefore overestimate the analgesic efficacy.[4] We believe that repeating trials before permanent implant of SCS electrodes will minimize this phenomenon. However, there is no evidence that our method can improve outcome. We did not have any added complications from the second trial, but it obviously increases the cost of treatment. Finally, it is interesting to find that our results of SCS for central poststroke pain (CPSP) could be reproduced at other institutes. Hopefully these reports will encourage other centers to use SCS for CPSP, particularly in the face of safety of SCS trials and limited therapeutic options for CPSP.

Mohamed M. Aly
Youichi Saitoh
Satoru Oshino
Koichi Hosomi
Haruhiko Kishima
Toshiki Yoshimine
Suita, Japan

Copyright © Congress of Neurological Surgeons. Unauthorized reproduction of this article is prohibited.

1. Aly MM, Saitoh Y, Hosomi K, Oshino S, Kishima H, Yoshimine T. Spinal cord stimulation for central poststroke pain. *Neurosurgery*. 2010;67(3): ONS206-ONS212.
2. Lopez JA, Torres LM, Gala F, Iglesias I. Spinal cord stimulation and thalamic pain: long term results of eight cases. *Neuromodulation*. 2009;12(3): 240-243.
3. Stojanovic M, Abdi S. Spinal cord stimulation. *Pain Phys*. 2002;5(2):156-166.
4. Coffey RJ, Lozano AM. Neurostimulation for chronic noncancer pain: an evaluation of the clinical evidence and recommendations for future trial designs. *J Neurosurg*. 2006;105(2):175-198.

10.1227/NEU.0b013e318210f04b

Neurosurgery Simulation

In their neurosurgery simulation technology review, Malone et al[1] address an important yet largely unaddressed surgical area that can significantly benefit from the availability of an effective simulation-based surgical training system. Further, they touch on a number of relevant aspects of developments that will underpin their work on a pedicle screw placement simulator. We would like to add some additional thoughts here, which are based our work over the past several years in developing both a hard-tissue (burr hole) drilling simulator prototype for the US Army as well as a generalized soft-tissue simulation and bleeding system for general surgical resident training.

The authors have correctly identified that the foundational step in developing a system that provides clinically useful surgical skills training is to isolate the subtasks that will benefit most from simulation. Minimizing effort devoted to already mastered or commonly acquired skills and, instead, focusing on critical skill areas that are not well addressed with currently available approaches is critical to producing a simulator that meets unmet needs. To build simulations for those subtasks, the movements and loads experienced by the surgeon during both expected and unexpected actions in the procedure need to form the basis for the mathematical modeling and haptic device interfaces that will be developed. We have also found that, as the authors note, these movements and loads are often not known/available, and we have had to obtain this information ourselves as well. Measuring how actions are done wrong is just as important, if not more so, as measuring when they are done correctly, because an effective simulator must provide learners with the complete range of possible interactions. Learning what happens when something is done right often occurs in the context of learning what happens when things are done wrong.

Also important at the earliest stage of planning a simulator is defining objective, quantitative metrics of performance that can be used to measure attainment of proficiency of the skills being learned. This enables the simulator to be designed to provide reliable, appropriate metrics of performance that can stand up to rigorous evaluation and professional scrutiny.

The authors mention the limitations of current haptic devices and illustrate with the results in their work on measuring the loads encountered in pedicle screw placement. Current, commercially available haptic devices typically provide about 1 lb of force, whereas approximately 15 lb of force are experienced during screw placement in the authors' work. Our research in drilling fresh frozen cadaver skulls showed that forces as high as 30 lb can be experienced. To approach the forces and torques we measured, however, we needed to develop a custom haptic device using augmented off-the-shelf haptic devices. We expect that the availability of haptic devices having sufficient force/torque capacity and adequate range of movement and orientation will remain a major challenge for simulators that focus on high-load situations such as bone drilling.

A final consideration is the mixture of soft-tissue-centric lower-force actions with bone-centric high-load actions in the same simulation. Typically, soft-tissue simulations are modeled with finite-element methods centered on deformation and transection, whereas bone-centric simulations are done with voxel-based techniques in which the goal is often to remove bone through an energy-based methodology that represents the action of drill or saw blades. These techniques are quite different from one another, as are the haptic interface requirements. To our knowledge, no simulator has been produced to date that supports interaction with both soft tissue and bone in the same user experience. This limitation calls for attention to how procedural subtasks are deconstructed if combined soft-tissue–bone actions are encountered, which is not uncommon in spinal procedures.

Malone and colleagues are to be congratulated for taking on an important and largely unaddressed area. Much work lies ahead in the years to come, however, before the potential of such simulators is realized.

Dwight Meglan
Howard R. Champion
Silver Spring, Maryland

1. Malone HR, Syed ON, Downes MS, D'Ambrosio AL, Quest DO, Kaiser MG. Simulation in neurosurgery: a review of computer-based simulation environments and their surgical applications. *Neurosurgery*. 2010;67(4):1105-1116.

10.1227/NEU.0b013e318210f038

In Reply:

We appreciate the remarks of Drs Meglan and Champion of SimQuest, LLC. They are right to emphasize the limitations of many available haptic interfaces in reproducing the torques and loads encountered in the operative theater. The difficulty of simultaneously modeling finite-element–based soft-tissue deformation and voxel-based bone (hard-tissue) drilling, a challenge inherent to spine surgery simulation, is also addressed. Collaboration with simulation firms like SimQuest that possess the technical expertise to customize standard haptic interfaces and merge tissue deformation modalities is

Copyright © Congress of Neurological Surgeons. Unauthorized reproduction of this article is prohibited.

essential to the continued evolution of computer-based neurosurgery simulation.

Hani Malone
Omar Syed
Michael Kaiser
New York, New York

10.1227/NEU.0b013e3182127c00

Relationship Between Decompressive Craniectomy and Hydrocephalus

To the Editor:

We read with great interest the article by Rahme et al[1] in which the authors reviewed the records of 17 patients with stroke-related increased intracranial pressure who underwent decompressive craniectomy (DC). The authors described a 0% rate of shunting after DC and concluded that hydrocephalus does not frequently occur after DC. On the other hand, in the series of Waziri et al,[2] hydrocephalus developed in 15 of 17 patients after DC, and 5 required shunting after cranioplasty. Rahme et al[1] speculated that the explanation for this discrepancy might lie in the definition of hydrocephalus and the indications for shunting.

We completely agree with the viewpoint of Rahme et al[1]; however, we wish to provide further comment on this issue. Bogousslavsky and Regli[3] reported that, in 60 cases of internal carotid artery occlusion, the occurrence of ventricular dilation was related to the volume of infarction. Additionally, Barber et al[4] reported that hydrocephalus was present in 22% of patients who had a large middle cerebral artery infarction, and they received conventional medical therapy (without surgery).

Therefore, we believe that the possibility of hydrocephalus developing in the course of a large infarction should be considered. From this viewpoint, we consider that an additional explanation for the discrepancy between the results of Rahme et al[1] and Waziri et al[2] might be differences in the area and volume of the infarction. Indeed, in the Waziri et al series, all 4 patients with internal carotid artery infarction developed hydrocephalus after DC (half required shunting), and none of the 7 patients with middle cerebral artery infarction received shunting, whereas the Rahme et al series included no patients with internal carotid artery infarction.[1]

Satoru Takeuchi
Naoki Otani
Hiroshi Nawashiro
Tokorozawa, Saitama, Japan

1. Rahme R, Weil AG, Sabbagh M, Moumdjian R, Bouthillier A, Bojanowski MW. Decompressive craniectomy is not an independent risk factor for communicating hydrocephalus in patients with increased intracranial pressure. *Neurosurgery*. 2010;67(3):675-678.
2. Waziri A, Fusco D, Mayer SA, McKhann GM II, Connolly ES Jr. Postoperative hydrocephalus in patients undergoing decompressive hemicraniectomy for ischemic or hemorrhagic stroke. *Neurosurgery*. 2007;61(3):489-493.
3. Bogousslavsky J, Regli F. Obstruction of the internal carotid artery and cerebral malacias: tomodensitometric factors of the prognosis in 150 cases [in French]. *Schweiz Arch Neurol Neurochir Psychiatr*. 1984;134(1):13-28.
4. Barber PA, Demchuk AM, Zhang J, et al. Computed tomographic parameters predicting fatal outcome in large middle cerebral artery infarction. *Cerebrovasc Dis*. 2003;16(3):230-235.

10.1227/NEU.0b013e3182124403

In Reply:

We would like to thank Drs Takeuchi, Otani, and Nawashiro for their interest in our article.[1] However, we find that the 2 studies they are referring to do not really lend support to their hypothesis that the divergence between our results and those of Waziri et al[2] lies in the difference in patient characteristics, specifically the extent of infarction.

In the article of Bogousslavsky and Regli,[3] the authors analyzed the development of unilateral ipsilateral ventricular dilation and cortical atrophy in patients with large strokes secondary to internal carotid artery occlusion or stenosis. There was no mention of hydrocephalus in their report. It is important to distinguish between true hydrocephalus, that is, mismatch between CSF production and resorption, and ventricular dilation or hydrocephalus ex vacuo, which is merely a radiological finding caused by large areas of neuronal loss and encephalomalacia after a massive infarction.

In their publication, Barber et al[4] sought to determine early CT signs predictive of death after large middle cerebral artery (MCA) infarction in a large cohort of conservatively managed patients, none of which had undergone decompressive craniectomy. The authors found that moderate or severe hydrocephalus was predictive of death on univariate, but not multivariate analysis. It must be noted, however, that these authors were referring to acute obstructive hydrocephalus, a complication of cerebral edema-related mass effect in large ischemic strokes. Conversely, in our study[1] and that of Waziri et al,[2] patients were typically protected against obstructive hydrocephalus by the wide surgical decompression. Rather, the incidence of chronic communicating hydrocephalus in survivors of malignant MCA territory infarction and other types of stroke was assessed.

To the best of our knowledge, there is no direct relationship between communicating hydrocephalus and ischemic stroke. Additionally, in our experience, hydrocephalus is not a frequent complication of decompressive craniectomy.[1] Therefore, unless new scientific evidence comes to disprove these findings, we have no reason to believe that hydrocephalus should be a major concern in the management of patients with large MCA or internal carotid artery infarctions.

Ralph Rahme
Alexander G. Weil
Michel W. Bojanowski
Montreal, Quebec, Canada

Copyright © Congress of Neurological Surgeons. Unauthorized reproduction of this article is prohibited.

1. Rahme R, Weil AG, Sabbagh M, Moumdjian R, Bouthillier A, Bojanowski MW. Decompressive craniectomy is not an independent risk factor for communicating hydrocephalus in patients with increased intracranial pressure. *Neurosurgery*. 2010;67(3):675-678.
2. Waziri A, Fusco D, Mayer SA, McKhann GM II, Connolly ES Jr. Postoperative hydrocephalus in patients undergoing decompressive hemicraniectomy for ischemic or hemorrhagic stroke. *Neurosurgery*. 2007;61(3):489-494.
3. Bogousslavsky J, Regli F. Obstruction of the internal carotid artery and cerebral malacias. Tomodensitometric factors of the prognosis in 150 cases [French]. *Schweiz Arch Neurol Neurochir Psychiatr*. 1984;134(1):13-28.
4. Barber PA, Demchuk AM, Zhang J, et al. Computed tomographic parameters predicting fatal outcome in large middle cerebral artery infarction. *Cerebrovasc Dis*. 2003;16(3):230-235.

10.1227/NEU.0b013e3182127bdc

Copyright © Congress of Neurological Surgeons. Unauthorized reproduction of this article is prohibited.

Surgical Approaches to Tumors of the Gyrus Cinguli

To the Editor:

We read the article by Talacchi et al[1] entitled "Surgical Approaches to Tumors of the Anterior Gyrus Cinguli" with great interest. To their credit, the authors have successfully focused attention on a surgical site that rarely receives the attention it deserves, and we applaud them for this. In fact, we believe that it is safe to say that, apart from any functional considerations, tumors involving the cingulate gyrus are significant both because of their deep location and because they are supplied with a specific anatomic pathway like the interhemispheric fissure. In our opinion, however, based on more than 100 interhemispheric approaches performed over the course of 5 years (for a variety of lesions that lie deep in the interhemispheric fissure), there is another approach to reach this region that Talacchi et al might have considered. We are referring to the contralateral transfalcine interhemispheric approach. In 1984, Machado de Almeida et al[2] were the first to take an exclusively contralateral approach to removing a parasagittal arteriovenous malformation. In 1995, Goel[3] systematically elaborated on this specific approach as a means of reaching contralateral tumors involving the cingulate gyrus. He underscored the value of this approach in the treatment of deep-seated brain tumors, emphatically stressing that this approach, if correctly performed, is direct, safe, and helpful in the successful resection of such tumors. He further suggested that this approach also provides an exposure that obviates the need for traversing or retracting the homolateral edematous brain. In 1996, Lawton et al[4] further elaborated on this approach by introducing the concept of a gravity-aided contralateral approach. With the patient lying in a supine position and with the midline orientated horizontally, they were able to make their lesion on the upper aspect (see their Figure 1). They suggested that this position has the following 2 main advantages: Gravity alone will retract the lower hemisphere and, in so doing, open the interhemispheric fissure; and the lesion will naturally come into greater view as removal of the tumor progresses. Recently, Chi and Lawton[5] also stressed the benefits of a gravity retraction that allows a wider operative exposure, which has the additional benefit of reducing morbidity.

We have developed expertise in this approach as a result of time spent with Dr Spetzler in Phoenix in 2003. To date, we have had numerous opportunities to successfully use this approach to treat a variety of neoplastic and/or vascular lesions that were found in or around the cingulate gyrus. It is on the basis of these surgical opportunities that we fully appreciate the advantages that, we believe, are incomparable when it comes to cases of small lesions deep within a motor area that is swollen as a result of the underlying lesion.[6] Because the interhemispheric corridor is tempting but, it should also be noted, rich in dangerous snares, we offer the following strategies that we have found extremely helpful for avoiding these hazards during surgery: (1) use the Lawton-Spetzler position; (2) make a linear incision parallel to the midline; (3) perform magnetic resonance angiography– or image–guided craniotomy perfectly centered between the entry point of bridging veins in the superior sagittal sinus; (4) expose the superior sagittal sinus by ad hoc placed burr holes and craniotome only after full control and detachment of dura mater from the bone; (5) gently retract and release the brain with working instruments rather than with a fixed spatula; and (6) consider the use of indocyanine green videoangiography to evaluate the presence of collateral drainage pathways before sacrifice or putting a bridging vein at risk (Ferroli et al[7]).

Ferroli Paolo
Giovanni Tringali
Morgan Broggi
Francesco Acerbi
Edvin Zekaj
Angelo Franzini
Giovanni Broggi
Milan, Italy

1. Talacchi A, Corsini F, Gerosa M. Surgical approaches to tumors of the anterior gyrus cinguli. *Neurosurgery*. 2010;66(6)(suppl operative):245-251.
2. Machado de Almeida G, Shibata MK, Nakagawa EJ. Contralateral parafalcine approach for parasagittal and callosal arteriovenous malformations. *Neurosurgery*. 1984;14(6):744-746.
3. Goel A. Transfalcine approach to a contralateral hemispheric tumour. *Acta Neurosurg*. 1995;135(3-4):210-212.
4. Lawton MT, Golfinos JG, Spetzler RF. The contralateral transcallosal approach experience with 32 patients. *Neurosurgery*. 1996;39(4):729-734.
5. Chi JH, Lawton MT. Posterior interhemispheric approach: surgical technique, application to vascular lesion, and benefits of gravity retraction. *Neurosurgery (ONS suppl)*. 2006;59:41-49.
6. Ferroli P, Russo A, Albanese E, Tringali G, Broggi G. Gravity-aided trans-falcine removal of a contralateral subcortical ependymoma. *Acta Neurochir (Wien)*. 2007;149(11):1147-1150.
7. Ferroli P, Nakaji P, Acerbi F, Albanese E, Broggi G. ICG temporary clipping test to asses collateral circulation before venous sacrifice: technical note. *World Neurosurgery*. In press.

10.1227/NEU.0b013e31821243f1

In Reply:

Ferroli and colleagues note that anterior gyrus cinguli tumors may be approached contralaterally. In our series of anterior gyrus cinguli tumors, we used—among others—the interhemispheric bilateral approach in perigenual tumors extending contralaterally and the unilateral approach in perirolandic tumors, based on the finding that tumors never extend contralaterally at this level. From this observation and evidence for the absence of drawbacks to the ipsilateral interhemispheric approach in small lesions, we believe that the contralateral approach may not necessarily offer

Copyright © Congress of Neurological Surgeons. Unauthorized reproduction of this article is prohibited.

an additional advantage over the ipsilateral approach. Furthermore, maneuvers like falx transection with division of the inferior sagittal sinus and the falcine venous plexus, which can carry unpredictable consequences for venous drainage, are not justified in our opinion.[1] However, we were aware of this approach and mentioned it in the discussion, but, because of its limited indications and the scarce success reported in the literature, we decided not to discuss it further.

Andrea Talacchi
Massimo Gerosa
Verona, Italy

1. Tubbs RS, Loukas M, Louis RG Jr, et al. Anatomy of the falcine venous plexus. *J Neurosurg*. 2007;107(1):155-157.

10.1227/NEU.0b013e3182127bee

Spinal Cord Stimulation for Thalamic or Central Pain

To the Editor:

I have read with great interest the paper of Ali et al[1] regarding the usefulness of spinal cord stimulation (SCS) in the treatment of central pain after stroke (CPSP), also well known as thalamic pain.

Patients with focal CPSP instead of generalized pain were considered for treatment by Ali et al.[1] Two cases with complete hemibody pain had circumscribed areas of more severe pain.

Percutaneous tetrapolar epidural electrodes were implanted and held for a 2- to 7-day trial period in 30 patients. Then, the electrode was removed. The analgesic results of the trial period were discussed with the patient. Ten patients received a new tetrapolar electrode. After a second trial period (whose duration is not specified), the internal pulse generator was implanted.

In their discussion the authors claim to be the first to describe good results with the SCS for the treatment of CPSP. The work published by our group[2] shows that this statement is not true. Our series is shorter than the one by Ali et al.[1] Follow-up is longer. They have a 28-month follow-up (range, 6-62), while that ours is longer: 81.6 months (range, 36-149).

I assume with Ali et al[1] that SCS is a much less aggressive surgical method than deep brain stimulation or motor prefrontal cortex. I also agree that better results can be attained in cases of focal pain rather than generalized pain.

I disagree with Ali et al[1] on the appropriateness of a short trial period of 2 to 7 days. I disagree very much with the removal of the electrode test and the return to implant it in the case of the definite implant. It is possible that the second electrode failed to obtain the same paresthesia as did the first. In addition, the rate of local complications could be increased.

Congratulations to Ali et al[1] for his excellent work, which confirms the good results that were previously shown by our work.[2]

Jose Antonio Lopez Lopez
Cadiz, Spain

1. Ali M, Saitoh Y, Hosomi K, Oshino S, Kishima H, Yoshimiro T. Spinal cord stimulation for central poststroke pain. *Neurosurgery*. 2010;67(3): ONS206–ONS212.
2. Lopez JA, Torres LM, Gala F, Iglesias I. Spinal cord stimulation and thalamic pain: long-term results of eight cases. *Neuromodulation*. 2009;12(3):240-243.

10.1227/NEU.0b013e318210f024

In Reply:

We would like to thank Lopez and colleagues for their interest in our article.[1] Lope et al[2] reported on a small series of spinal cord stimulation (SCS) for thalamic pain; 6 of 8 patients (75%) achieved satisfactory pain relief in the long term. Lopez et al restricted their indication to patients with localized pain distribution that could be entirely covered by stimulation paraesthesia; and this may explain their relatively high success rate.[2] Unfortunately this work had not yet been published when we submitted our report for publication.

Lopez et al reported that our trial period (2–7 days) was short. Actually, within this time frame we were able to unequivocally evaluate the analgesic effect of SCS in all patients. In general, there is no consensus on the length of SCS trial period, and periods of one day to several weeks have been reported.[2,3] There is no doubt that long trial periods give a better opportunity to evaluate the exact response to SCS, but unfortunately this comes with the price of increasing the risk of infection.

In our series, we used to remove the trial electrodes, and discharge patients after the trial period. At the time of counseling the patients in the outpatient clinic, those who decided to proceed were scheduled for the second trial and permanent SCS implantation.[1] Lopez et al disagree with this approach because they think it may increase the rate of local complications and the second electrode may fail to provoke the same paresthesia. The rationale for our approach was that, during trial stimulation, patients tend to respond in an affirmative manner, and therefore overestimate the analgesic efficacy.[4] We believe that repeating trials before permanent implant of SCS electrodes will minimize this phenomenon. However, there is no evidence that our method can improve outcome. We did not have any added complications from the second trial, but it obviously increases the cost of treatment. Finally, it is interesting to find that our results of SCS for central poststroke pain (CPSP) could be reproduced at other institutes. Hopefully these reports will encourage other centers to use SCS for CPSP, particularly in the face of safety of SCS trials and limited therapeutic options for CPSP.

Mohamed M. Aly
Youichi Saitoh
Satoru Oshino
Koichi Hosomi
Haruhiko Kishima
Toshiki Yoshimine
Suita, Japan

Copyright © Congress of Neurological Surgeons. Unauthorized reproduction of this article is prohibited.

1. Aly MM, Saitoh Y, Hosomi K, Oshino S, Kishima H, Yoshimine T. Spinal cord stimulation for central poststroke pain. *Neurosurgery*. 2010;67(3): ONS206-ONS212.
2. Lopez JA, Torres LM, Gala F, Iglesias I. Spinal cord stimulation and thalamic pain: long term results of eight cases. *Neuromodulation*. 2009;12(3): 240-243.
3. Stojanovic M, Abdi S. Spinal cord stimulation. *Pain Phys*. 2002;5(2):156-166.
4. Coffey RJ, Lozano AM. Neurostimulation for chronic noncancer pain: an evaluation of the clinical evidence and recommendations for future trial designs. *J Neurosurg*. 2006;105(2):175-198.

10.1227/NEU.0b013e318210f04b

Neurosurgery Simulation

In their neurosurgery simulation technology review, Malone et al[1] address an important yet largely unaddressed surgical area that can significantly benefit from the availability of an effective simulation-based surgical training system. Further, they touch on a number of relevant aspects of developments that will underpin their work on a pedicle screw placement simulator. We would like to add some additional thoughts here, which are based our work over the past several years in developing both a hard-tissue (burr hole) drilling simulator prototype for the US Army as well as a generalized soft-tissue simulation and bleeding system for general surgical resident training.

The authors have correctly identified that the foundational step in developing a system that provides clinically useful surgical skills training is to isolate the subtasks that will benefit most from simulation. Minimizing effort devoted to already mastered or commonly acquired skills and, instead, focusing on critical skill areas that are not well addressed with currently available approaches is critical to producing a simulator that meets unmet needs. To build simulations for those subtasks, the movements and loads experienced by the surgeon during both expected and unexpected actions in the procedure need to form the basis for the mathematical modeling and haptic device interfaces that will be developed. We have also found that, as the authors note, these movements and loads are often not known/available, and we have had to obtain this information ourselves as well. Measuring how actions are done wrong is just as important, if not more so, as measuring when they are done correctly, because an effective simulator must provide learners with the complete range of possible interactions. Learning what happens when something is done right often occurs in the context of learning what happens when things are done wrong.

Also important at the earliest stage of planning a simulator is defining objective, quantitative metrics of performance that can be used to measure attainment of proficiency of the skills being learned. This enables the simulator to be designed to provide reliable, appropriate metrics of performance that can stand up to rigorous evaluation and professional scrutiny.

The authors mention the limitations of current haptic devices and illustrate with the results in their work on measuring the loads encountered in pedicle screw placement. Current, commercially available haptic devices typically provide about 1 lb of force, whereas approximately 15 lb of force are experienced during screw placement in the authors' work. Our research in drilling fresh frozen cadaver skulls showed that forces as high as 30 lb can be experienced. To approach the forces and torques we measured, however, we needed to develop a custom haptic device using augmented off-the-shelf haptic devices. We expect that the availability of haptic devices having sufficient force/torque capacity and adequate range of movement and orientation will remain a major challenge for simulators that focus on high-load situations such as bone drilling.

A final consideration is the mixture of soft-tissue-centric lower-force actions with bone-centric high-load actions in the same simulation. Typically, soft-tissue simulations are modeled with finite-element methods centered on deformation and transection, whereas bone-centric simulations are done with voxel-based techniques in which the goal is often to remove bone through an energy-based methodology that represents the action of drill or saw blades. These techniques are quite different from one another, as are the haptic interface requirements. To our knowledge, no simulator has been produced to date that supports interaction with both soft tissue and bone in the same user experience. This limitation calls for attention to how procedural subtasks are deconstructed if combined soft-tissue–bone actions are encountered, which is not uncommon in spinal procedures.

Malone and colleagues are to be congratulated for taking on an important and largely unaddressed area. Much work lies ahead in the years to come, however, before the potential of such simulators is realized.

Dwight Meglan
Howard R. Champion
Silver Spring, Maryland

1. Malone HR, Syed ON, Downes MS, D'Ambrosio AL, Quest DO, Kaiser MG. Simulation in neurosurgery: a review of computer-based simulation environments and their surgical applications. *Neurosurgery*. 2010;67(4):1105-1116.

10.1227/NEU.0b013e318210f038

In Reply:

We appreciate the remarks of Drs Meglan and Champion of SimQuest, LLC. They are right to emphasize the limitations of many available haptic interfaces in reproducing the torques and loads encountered in the operative theater. The difficulty of simultaneously modeling finite-element–based soft-tissue deformation and voxel-based bone (hard-tissue) drilling, a challenge inherent to spine surgery simulation, is also addressed. Collaboration with simulation firms like SimQuest that possess the technical expertise to customize standard haptic interfaces and merge tissue deformation modalities is

Copyright © Congress of Neurological Surgeons. Unauthorized reproduction of this article is prohibited.

essential to the continued evolution of computer-based neurosurgery simulation.

Hani Malone
Omar Syed
Michael Kaiser
New York, New York

10.1227/NEU.0b013e3182127c00

Relationship Between Decompressive Craniectomy and Hydrocephalus

To the Editor:

We read with great interest the article by Rahme et al[1] in which the authors reviewed the records of 17 patients with stroke-related increased intracranial pressure who underwent decompressive craniectomy (DC). The authors described a 0% rate of shunting after DC and concluded that hydrocephalus does not frequently occur after DC. On the other hand, in the series of Waziri et al,[2] hydrocephalus developed in 15 of 17 patients after DC, and 5 required shunting after cranioplasty. Rahme et al[1] speculated that the explanation for this discrepancy might lie in the definition of hydrocephalus and the indications for shunting.

We completely agree with the viewpoint of Rahme et al[1]; however, we wish to provide further comment on this issue. Bogousslavsky and Regli[3] reported that, in 60 cases of internal carotid artery occlusion, the occurrence of ventricular dilation was related to the volume of infarction. Additionally, Barber et al[4] reported that hydrocephalus was present in 22% of patients who had a large middle cerebral artery infarction, and they received conventional medical therapy (without surgery).

Therefore, we believe that the possibility of hydrocephalus developing in the course of a large infarction should be considered. From this viewpoint, we consider that an additional explanation for the discrepancy between the results of Rahme et al[1] and Waziri et al[2] might be differences in the area and volume of the infarction. Indeed, in the Waziri et al series, all 4 patients with internal carotid artery infarction developed hydrocephalus after DC (half required shunting), and none of the 7 patients with middle cerebral artery infarction received shunting, whereas the Rahme et al series included no patients with internal carotid artery infarction.[1]

Satoru Takeuchi
Naoki Otani
Hiroshi Nawashiro
Tokorozawa, Saitama, Japan

1. Rahme R, Weil AG, Sabbagh M, Moumdjian R, Bouthillier A, Bojanowski MW. Decompressive craniectomy is not an independent risk factor for communicating hydrocephalus in patients with increased intracranial pressure. *Neurosurgery*. 2010;67(3):675-678.
2. Waziri A, Fusco D, Mayer SA, McKhann GM II, Connolly ES Jr. Postoperative hydrocephalus in patients undergoing decompressive hemicraniectomy for ischemic or hemorrhagic stroke. *Neurosurgery*. 2007;61(3):489-493.
3. Bogousslavsky J, Regli F. Obstruction of the internal carotid artery and cerebral malacias: tomodensitometric factors of the prognosis in 150 cases [in French]. *Schweiz Arch Neurol Neurochir Psychiatr*. 1984;134(1):13-28.
4. Barber PA, Demchuk AM, Zhang J, et al. Computed tomographic parameters predicting fatal outcome in large middle cerebral artery infarction. *Cerebrovasc Dis*. 2003;16(3):230-235.

10.1227/NEU.0b013e3182124403

In Reply:

We would like to thank Drs Takeuchi, Otani, and Nawashiro for their interest in our article.[1] However, we find that the 2 studies they are referring to do not really lend support to their hypothesis that the divergence between our results and those of Waziri et al[2] lies in the difference in patient characteristics, specifically the extent of infarction.

In the article of Bogousslavsky and Regli,[3] the authors analyzed the development of unilateral ipsilateral ventricular dilation and cortical atrophy in patients with large strokes secondary to internal carotid artery occlusion or stenosis. There was no mention of hydrocephalus in their report. It is important to distinguish between true hydrocephalus, that is, mismatch between CSF production and resorption, and ventricular dilation or hydrocephalus ex vacuo, which is merely a radiological finding caused by large areas of neuronal loss and encephalomalacia after a massive infarction.

In their publication, Barber et al[4] sought to determine early CT signs predictive of death after large middle cerebral artery (MCA) infarction in a large cohort of conservatively managed patients, none of which had undergone decompressive craniectomy. The authors found that moderate or severe hydrocephalus was predictive of death on univariate, but not multivariate analysis. It must be noted, however, that these authors were referring to acute obstructive hydrocephalus, a complication of cerebral edema-related mass effect in large ischemic strokes. Conversely, in our study[1] and that of Waziri et al,[2] patients were typically protected against obstructive hydrocephalus by the wide surgical decompression. Rather, the incidence of chronic communicating hydrocephalus in survivors of malignant MCA territory infarction and other types of stroke was assessed.

To the best of our knowledge, there is no direct relationship between communicating hydrocephalus and ischemic stroke. Additionally, in our experience, hydrocephalus is not a frequent complication of decompressive craniectomy.[1] Therefore, unless new scientific evidence comes to disprove these findings, we have no reason to believe that hydrocephalus should be a major concern in the management of patients with large MCA or internal carotid artery infarctions.

Ralph Rahme
Alexander G. Weil
Michel W. Bojanowski
Montreal, Quebec, Canada

Copyright © Congress of Neurological Surgeons. Unauthorized reproduction of this article is prohibited.

1. Rahme R, Weil AG, Sabbagh M, Moumdjian R, Bouthillier A, Bojanowski MW. Decompressive craniectomy is not an independent risk factor for communicating hydrocephalus in patients with increased intracranial pressure. *Neurosurgery*. 2010;67(3):675-678.
2. Waziri A, Fusco D, Mayer SA, McKhann GM II, Connolly ES Jr. Postoperative hydrocephalus in patients undergoing decompressive hemicraniectomy for ischemic or hemorrhagic stroke. *Neurosurgery*. 2007;61(3):489-494.
3. Bogousslavsky J, Regli F. Obstruction of the internal carotid artery and cerebral malacias. Tomodensitometric factors of the prognosis in 150 cases [French]. *Schweiz Arch Neurol Neurochir Psychiatr*. 1984;134(1):13-28.
4. Barber PA, Demchuk AM, Zhang J, et al. Computed tomographic parameters predicting fatal outcome in large middle cerebral artery infarction. *Cerebrovasc Dis*. 2003;16(3):230-235.

10.1227/NEU.0b013e3182127bdc

Copyright © Congress of Neurological Surgeons. Unauthorized reproduction of this article is prohibited.

Surgical Approaches to Tumors of the Gyrus Cinguli

To the Editor:

We read the article by Talacchi et al[1] entitled "Surgical Approaches to Tumors of the Anterior Gyrus Cinguli" with great interest. To their credit, the authors have successfully focused attention on a surgical site that rarely receives the attention it deserves, and we applaud them for this. In fact, we believe that it is safe to say that, apart from any functional considerations, tumors involving the cingulate gyrus are significant both because of their deep location and because they are supplied with a specific anatomic pathway like the interhemispheric fissure. In our opinion, however, based on more than 100 interhemispheric approaches performed over the course of 5 years (for a variety of lesions that lie deep in the interhemispheric fissure), there is another approach to reach this region that Talacchi et al might have considered. We are referring to the contralateral transfalcine interhemispheric approach. In 1984, Machado de Almeida et al[2] were the first to take an exclusively contralateral approach to removing a parasagittal arteriovenous malformation. In 1995, Goel[3] systematically elaborated on this specific approach as a means of reaching contralateral tumors involving the cingulate gyrus. He underscored the value of this approach in the treatment of deep-seated brain tumors, emphatically stressing that this approach, if correctly performed, is direct, safe, and helpful in the successful resection of such tumors. He further suggested that this approach also provides an exposure that obviates the need for traversing or retracting the homolateral edematous brain. In 1996, Lawton et al[4] further elaborated on this approach by introducing the concept of a gravity-aided contralateral approach. With the patient lying in a supine position and with the midline orientated horizontally, they were able to make their lesion on the upper aspect (see their Figure 1). They suggested that this position has the following 2 main advantages: Gravity alone will retract the lower hemisphere and, in so doing, open the interhemispheric fissure; and the lesion will naturally come into greater view as removal of the tumor progresses. Recently, Chi and Lawton[5] also stressed the benefits of a gravity retraction that allows a wider operative exposure, which has the additional benefit of reducing morbidity.

We have developed expertise in this approach as a result of time spent with Dr Spetzler in Phoenix in 2003. To date, we have had numerous opportunities to successfully use this approach to treat a variety of neoplastic and/or vascular lesions that were found in or around the cingulate gyrus. It is on the basis of these surgical opportunities that we fully appreciate the advantages that, we believe, are incomparable when it comes to cases of small lesions deep within a motor area that is swollen as a result of the underlying lesion.[6] Because the interhemispheric corridor is tempting but, it should also be noted, rich in dangerous snares, we offer the following strategies that we have found extremely helpful for avoiding these hazards during surgery: (1) use the Lawton-Spetzler position; (2) make a linear incision parallel to the midline; (3) perform magnetic resonance angiography– or image–guided craniotomy perfectly centered between the entry point of bridging veins in the superior sagittal sinus; (4) expose the superior sagittal sinus by ad hoc placed burr holes and craniotome only after full control and detachment of dura mater from the bone; (5) gently retract and release the brain with working instruments rather than with a fixed spatula; and (6) consider the use of indocyanine green videoangiography to evaluate the presence of collateral drainage pathways before sacrifice or putting a bridging vein at risk (Ferroli et al[7]).

Ferroli Paolo
Giovanni Tringali
Morgan Broggi
Francesco Acerbi
Edvin Zekaj
Angelo Franzini
Giovanni Broggi
Milan, Italy

1. Talacchi A, Corsini F, Gerosa M. Surgical approaches to tumors of the anterior gyrus cinguli. *Neurosurgery*. 2010;66(6)(suppl operative):245-251.
2. Machado de Almeida G, Shibata MK, Nakagawa EJ. Contralateral parafalcine approach for parasagittal and callosal arteriovenous malformations. *Neurosurgery*. 1984;14(6):744-746.
3. Goel A. Transfalcine approach to a contralateral hemispheric tumour. *Acta Neurosurg*. 1995;135(3-4):210-212.
4. Lawton MT, Golfinos JG, Spetzler RF. The contralateral transcallosal approach experience with 32 patients. *Neurosurgery*. 1996;39(4):729-734.
5. Chi JH, Lawton MT. Posterior interhemispheric approach: surgical technique, application to vascular lesion, and benefits of gravity retraction. *Neurosurgery (ONS suppl)*. 2006;59:41-49.
6. Ferroli P, Russo A, Albanese E, Tringali G, Broggi G. Gravity-aided trans-falcine removal of a contralateral subcortical ependymoma. *Acta Neurochir (Wien)*. 2007;149(11):1147-1150.
7. Ferroli P, Nakaji P, Acerbi F, Albanese E, Broggi G. ICG temporary clipping test to asses collateral circulation before venous sacrifice: technical note. *World Neurosurgery*. In press.

10.1227/NEU.0b013e31821243f1

In Reply:

Ferroli and colleagues note that anterior gyrus cinguli tumors may be approached contralaterally. In our series of anterior gyrus cinguli tumors, we used—among others—the interhemispheric bilateral approach in perigenual tumors extending contralaterally and the unilateral approach in perirolandic tumors, based on the finding that tumors never extend contralaterally at this level. From this observation and evidence for the absence of drawbacks to the ipsilateral interhemispheric approach in small lesions, we believe that the contralateral approach may not necessarily offer

Copyright © Congress of Neurological Surgeons. Unauthorized reproduction of this article is prohibited.

an additional advantage over the ipsilateral approach. Furthermore, maneuvers like falx transection with division of the inferior sagittal sinus and the falcine venous plexus, which can carry unpredictable consequences for venous drainage, are not justified in our opinion.[1] However, we were aware of this approach and mentioned it in the discussion, but, because of its limited indications and the scarce success reported in the literature, we decided not to discuss it further.

Andrea Talacchi
Massimo Gerosa
Verona, Italy

1. Tubbs RS, Loukas M, Louis RG Jr, et al. Anatomy of the falcine venous plexus. *J Neurosurg*. 2007;107(1):155-157.

10.1227/NEU.0b013e3182127bee

Spinal Cord Stimulation for Thalamic or Central Pain

To the Editor:

I have read with great interest the paper of Ali et al[1] regarding the usefulness of spinal cord stimulation (SCS) in the treatment of central pain after stroke (CPSP), also well known as thalamic pain.

Patients with focal CPSP instead of generalized pain were considered for treatment by Ali et al.[1] Two cases with complete hemibody pain had circumscribed areas of more severe pain.

Percutaneous tetrapolar epidural electrodes were implanted and held for a 2- to 7-day trial period in 30 patients. Then, the electrode was removed. The analgesic results of the trial period were discussed with the patient. Ten patients received a new tetrapolar electrode. After a second trial period (whose duration is not specified), the internal pulse generator was implanted.

In their discussion the authors claim to be the first to describe good results with the SCS for the treatment of CPSP. The work published by our group[2] shows that this statement is not true. Our series is shorter than the one by Ali et al.[1] Follow-up is longer. They have a 28-month follow-up (range, 6-62), while that ours is longer: 81.6 months (range, 36-149).

I assume with Ali et al[1] that SCS is a much less aggressive surgical method than deep brain stimulation or motor prefrontal cortex. I also agree that better results can be attained in cases of focal pain rather than generalized pain.

I disagree with Ali et al[1] on the appropriateness of a short trial period of 2 to 7 days. I disagree very much with the removal of the electrode test and the return to implant it in the case of the definite implant. It is possible that the second electrode failed to obtain the same paresthesia as did the first. In addition, the rate of local complications could be increased.

Congratulations to Ali et al[1] for his excellent work, which confirms the good results that were previously shown by our work.[2]

Jose Antonio Lopez Lopez
Cadiz, Spain

1. Ali M, Saitoh Y, Hosomi K, Oshino S, Kishima H, Yoshimiro T. Spinal cord stimulation for central poststroke pain. *Neurosurgery*. 2010;67(3): ONS206–ONS212.
2. Lopez JA, Torres LM, Gala F, Iglesias I. Spinal cord stimulation and thalamic pain: long-term results of eight cases. *Neuromodulation*. 2009;12(3):240-243.

10.1227/NEU.0b013e318210f024

In Reply:

We would like to thank Lopez and colleagues for their interest in our article.[1] Lope et al[2] reported on a small series of spinal cord stimulation (SCS) for thalamic pain; 6 of 8 patients (75%) achieved satisfactory pain relief in the long term. Lopez et al restricted their indication to patients with localized pain distribution that could be entirely covered by stimulation paraesthesia; and this may explain their relatively high success rate.[2] Unfortunately this work had not yet been published when we submitted our report for publication.

Lopez et al reported that our trial period (2–7 days) was short. Actually, within this time frame we were able to unequivocally evaluate the analgesic effect of SCS in all patients. In general, there is no consensus on the length of SCS trial period, and periods of one day to several weeks have been reported.[2,3] There is no doubt that long trial periods give a better opportunity to evaluate the exact response to SCS, but unfortunately this comes with the price of increasing the risk of infection.

In our series, we used to remove the trial electrodes, and discharge patients after the trial period. At the time of counseling the patients in the outpatient clinic, those who decided to proceed were scheduled for the second trial and permanent SCS implantation.[1] Lopez et al disagree with this approach because they think it may increase the rate of local complications and the second electrode may fail to provoke the same paresthesia. The rationale for our approach was that, during trial stimulation, patients tend to respond in an affirmative manner, and therefore overestimate the analgesic efficacy.[4] We believe that repeating trials before permanent implant of SCS electrodes will minimize this phenomenon. However, there is no evidence that our method can improve outcome. We did not have any added complications from the second trial, but it obviously increases the cost of treatment. Finally, it is interesting to find that our results of SCS for central poststroke pain (CPSP) could be reproduced at other institutes. Hopefully these reports will encourage other centers to use SCS for CPSP, particularly in the face of safety of SCS trials and limited therapeutic options for CPSP.

Mohamed M. Aly
Youichi Saitoh
Satoru Oshino
Koichi Hosomi
Haruhiko Kishima
Toshiki Yoshimine
Suita, Japan

Copyright © Congress of Neurological Surgeons. Unauthorized reproduction of this article is prohibited.

1. Aly MM, Saitoh Y, Hosomi K, Oshino S, Kishima H, Yoshimine T. Spinal cord stimulation for central poststroke pain. *Neurosurgery*. 2010;67(3): ONS206-ONS212.
2. Lopez JA, Torres LM, Gala F, Iglesias I. Spinal cord stimulation and thalamic pain: long term results of eight cases. *Neuromodulation*. 2009;12(3): 240-243.
3. Stojanovic M, Abdi S. Spinal cord stimulation. *Pain Phys*. 2002;5(2):156-166.
4. Coffey RJ, Lozano AM. Neurostimulation for chronic noncancer pain: an evaluation of the clinical evidence and recommendations for future trial designs. *J Neurosurg*. 2006;105(2):175-198.

10.1227/NEU.0b013e318210f04b

Neurosurgery Simulation

In their neurosurgery simulation technology review, Malone et al[1] address an important yet largely unaddressed surgical area that can significantly benefit from the availability of an effective simulation-based surgical training system. Further, they touch on a number of relevant aspects of developments that will underpin their work on a pedicle screw placement simulator. We would like to add some additional thoughts here, which are based our work over the past several years in developing both a hard-tissue (burr hole) drilling simulator prototype for the US Army as well as a generalized soft-tissue simulation and bleeding system for general surgical resident training.

The authors have correctly identified that the foundational step in developing a system that provides clinically useful surgical skills training is to isolate the subtasks that will benefit most from simulation. Minimizing effort devoted to already mastered or commonly acquired skills and, instead, focusing on critical skill areas that are not well addressed with currently available approaches is critical to producing a simulator that meets unmet needs. To build simulations for those subtasks, the movements and loads experienced by the surgeon during both expected and unexpected actions in the procedure need to form the basis for the mathematical modeling and haptic device interfaces that will be developed. We have also found that, as the authors note, these movements and loads are often not known/available, and we have had to obtain this information ourselves as well. Measuring how actions are done wrong is just as important, if not more so, as measuring when they are done correctly, because an effective simulator must provide learners with the complete range of possible interactions. Learning what happens when something is done right often occurs in the context of learning what happens when things are done wrong.

Also important at the earliest stage of planning a simulator is defining objective, quantitative metrics of performance that can be used to measure attainment of proficiency of the skills being learned. This enables the simulator to be designed to provide reliable, appropriate metrics of performance that can stand up to rigorous evaluation and professional scrutiny.

The authors mention the limitations of current haptic devices and illustrate with the results in their work on measuring the loads encountered in pedicle screw placement. Current, commercially available haptic devices typically provide about 1 lb of force, whereas approximately 15 lb of force are experienced during screw placement in the authors' work. Our research in drilling fresh frozen cadaver skulls showed that forces as high as 30 lb can be experienced. To approach the forces and torques we measured, however, we needed to develop a custom haptic device using augmented off-the-shelf haptic devices. We expect that the availability of haptic devices having sufficient force/torque capacity and adequate range of movement and orientation will remain a major challenge for simulators that focus on high-load situations such as bone drilling.

A final consideration is the mixture of soft-tissue-centric lower-force actions with bone-centric high-load actions in the same simulation. Typically, soft-tissue simulations are modeled with finite-element methods centered on deformation and transection, whereas bone-centric simulations are done with voxel-based techniques in which the goal is often to remove bone through an energy-based methodology that represents the action of drill or saw blades. These techniques are quite different from one another, as are the haptic interface requirements. To our knowledge, no simulator has been produced to date that supports interaction with both soft tissue and bone in the same user experience. This limitation calls for attention to how procedural subtasks are deconstructed if combined soft-tissue–bone actions are encountered, which is not uncommon in spinal procedures.

Malone and colleagues are to be congratulated for taking on an important and largely unaddressed area. Much work lies ahead in the years to come, however, before the potential of such simulators is realized.

Dwight Meglan
Howard R. Champion
Silver Spring, Maryland

1. Malone HR, Syed ON, Downes MS, D'Ambrosio AL, Quest DO, Kaiser MG. Simulation in neurosurgery: a review of computer-based simulation environments and their surgical applications. *Neurosurgery*. 2010;67(4):1105-1116.

10.1227/NEU.0b013e318210f038

In Reply:

We appreciate the remarks of Drs Meglan and Champion of SimQuest, LLC. They are right to emphasize the limitations of many available haptic interfaces in reproducing the torques and loads encountered in the operative theater. The difficulty of simultaneously modeling finite-element–based soft-tissue deformation and voxel-based bone (hard-tissue) drilling, a challenge inherent to spine surgery simulation, is also addressed. Collaboration with simulation firms like SimQuest that possess the technical expertise to customize standard haptic interfaces and merge tissue deformation modalities is

Copyright © Congress of Neurological Surgeons. Unauthorized reproduction of this article is prohibited.

essential to the continued evolution of computer-based neurosurgery simulation.

Hani Malone
Omar Syed
Michael Kaiser
New York, New York

10.1227/NEU.0b013e3182127c00

Relationship Between Decompressive Craniectomy and Hydrocephalus

To the Editor:

We read with great interest the article by Rahme et al[1] in which the authors reviewed the records of 17 patients with stroke-related increased intracranial pressure who underwent decompressive craniectomy (DC). The authors described a 0% rate of shunting after DC and concluded that hydrocephalus does not frequently occur after DC. On the other hand, in the series of Waziri et al,[2] hydrocephalus developed in 15 of 17 patients after DC, and 5 required shunting after cranioplasty. Rahme et al[1] speculated that the explanation for this discrepancy might lie in the definition of hydrocephalus and the indications for shunting.

We completely agree with the viewpoint of Rahme et al[1]; however, we wish to provide further comment on this issue. Bogousslavsky and Regli[3] reported that, in 60 cases of internal carotid artery occlusion, the occurrence of ventricular dilation was related to the volume of infarction. Additionally, Barber et al[4] reported that hydrocephalus was present in 22% of patients who had a large middle cerebral artery infarction, and they received conventional medical therapy (without surgery).

Therefore, we believe that the possibility of hydrocephalus developing in the course of a large infarction should be considered. From this viewpoint, we consider that an additional explanation for the discrepancy between the results of Rahme et al[1] and Waziri et al[2] might be differences in the area and volume of the infarction. Indeed, in the Waziri et al series, all 4 patients with internal carotid artery infarction developed hydrocephalus after DC (half required shunting), and none of the 7 patients with middle cerebral artery infarction received shunting, whereas the Rahme et al series included no patients with internal carotid artery infarction.[1]

Satoru Takeuchi
Naoki Otani
Hiroshi Nawashiro
Tokorozawa, Saitama, Japan

1. Rahme R, Weil AG, Sabbagh M, Moumdjian R, Bouthillier A, Bojanowski MW. Decompressive craniectomy is not an independent risk factor for communicating hydrocephalus in patients with increased intracranial pressure. *Neurosurgery*. 2010;67(3):675-678.
2. Waziri A, Fusco D, Mayer SA, McKhann GM II, Connolly ES Jr. Postoperative hydrocephalus in patients undergoing decompressive hemicraniectomy for ischemic or hemorrhagic stroke. *Neurosurgery*. 2007;61(3):489-493.
3. Bogousslavsky J, Regli F. Obstruction of the internal carotid artery and cerebral malacias: tomodensitometric factors of the prognosis in 150 cases [in French]. *Schweiz Arch Neurol Neurochir Psychiatr*. 1984;134(1):13-28.
4. Barber PA, Demchuk AM, Zhang J, et al. Computed tomographic parameters predicting fatal outcome in large middle cerebral artery infarction. *Cerebrovasc Dis*. 2003;16(3):230-235.

10.1227/NEU.0b013e3182124403

In Reply:

We would like to thank Drs Takeuchi, Otani, and Nawashiro for their interest in our article.[1] However, we find that the 2 studies they are referring to do not really lend support to their hypothesis that the divergence between our results and those of Waziri et al[2] lies in the difference in patient characteristics, specifically the extent of infarction.

In the article of Bogousslavsky and Regli,[3] the authors analyzed the development of unilateral ipsilateral ventricular dilation and cortical atrophy in patients with large strokes secondary to internal carotid artery occlusion or stenosis. There was no mention of hydrocephalus in their report. It is important to distinguish between true hydrocephalus, that is, mismatch between CSF production and resorption, and ventricular dilation or hydrocephalus ex vacuo, which is merely a radiological finding caused by large areas of neuronal loss and encephalomalacia after a massive infarction.

In their publication, Barber et al[4] sought to determine early CT signs predictive of death after large middle cerebral artery (MCA) infarction in a large cohort of conservatively managed patients, none of which had undergone decompressive craniectomy. The authors found that moderate or severe hydrocephalus was predictive of death on univariate, but not multivariate analysis. It must be noted, however, that these authors were referring to acute obstructive hydrocephalus, a complication of cerebral edema-related mass effect in large ischemic strokes. Conversely, in our study[1] and that of Waziri et al,[2] patients were typically protected against obstructive hydrocephalus by the wide surgical decompression. Rather, the incidence of chronic communicating hydrocephalus in survivors of malignant MCA territory infarction and other types of stroke was assessed.

To the best of our knowledge, there is no direct relationship between communicating hydrocephalus and ischemic stroke. Additionally, in our experience, hydrocephalus is not a frequent complication of decompressive craniectomy.[1] Therefore, unless new scientific evidence comes to disprove these findings, we have no reason to believe that hydrocephalus should be a major concern in the management of patients with large MCA or internal carotid artery infarctions.

Ralph Rahme
Alexander G. Weil
Michel W. Bojanowski
Montreal, Quebec, Canada

Copyright © Congress of Neurological Surgeons. Unauthorized reproduction of this article is prohibited.

1. Rahme R, Weil AG, Sabbagh M, Moumdjian R, Bouthillier A, Bojanowski MW. Decompressive craniectomy is not an independent risk factor for communicating hydrocephalus in patients with increased intracranial pressure. *Neurosurgery*. 2010;67(3):675-678.
2. Waziri A, Fusco D, Mayer SA, McKhann GM II, Connolly ES Jr. Postoperative hydrocephalus in patients undergoing decompressive hemicraniectomy for ischemic or hemorrhagic stroke. *Neurosurgery*. 2007;61(3):489-494.
3. Bogousslavsky J, Regli F. Obstruction of the internal carotid artery and cerebral malacias. Tomodensitometric factors of the prognosis in 150 cases [French]. *Schweiz Arch Neurol Neurochir Psychiatr*. 1984;134(1):13-28.
4. Barber PA, Demchuk AM, Zhang J, et al. Computed tomographic parameters predicting fatal outcome in large middle cerebral artery infarction. *Cerebrovasc Dis*. 2003;16(3):230-235.

10.1227/NEU.0b013e3182127bdc

Copyright © Congress of Neurological Surgeons. Unauthorized reproduction of this article is prohibited.

Surgical Approaches to Tumors of the Gyrus Cinguli

To the Editor:

We read the article by Talacchi et al[1] entitled "Surgical Approaches to Tumors of the Anterior Gyrus Cinguli" with great interest. To their credit, the authors have successfully focused attention on a surgical site that rarely receives the attention it deserves, and we applaud them for this. In fact, we believe that it is safe to say that, apart from any functional considerations, tumors involving the cingulate gyrus are significant both because of their deep location and because they are supplied with a specific anatomic pathway like the interhemispheric fissure. In our opinion, however, based on more than 100 interhemispheric approaches performed over the course of 5 years (for a variety of lesions that lie deep in the interhemispheric fissure), there is another approach to reach this region that Talacchi et al might have considered. We are referring to the contralateral transfalcine interhemispheric approach. In 1984, Machado de Almeida et al[2] were the first to take an exclusively contralateral approach to removing a parasagittal arteriovenous malformation. In 1995, Goel[3] systematically elaborated on this specific approach as a means of reaching contralateral tumors involving the cingulate gyrus. He underscored the value of this approach in the treatment of deep-seated brain tumors, emphatically stressing that this approach, if correctly performed, is direct, safe, and helpful in the successful resection of such tumors. He further suggested that this approach also provides an exposure that obviates the need for traversing or retracting the homolateral edematous brain. In 1996, Lawton et al[4] further elaborated on this approach by introducing the concept of a gravity-aided contralateral approach. With the patient lying in a supine position and with the midline orientated horizontally, they were able to make their lesion on the upper aspect (see their Figure 1). They suggested that this position has the following 2 main advantages: Gravity alone will retract the lower hemisphere and, in so doing, open the interhemispheric fissure; and the lesion will naturally come into greater view as removal of the tumor progresses. Recently, Chi and Lawton[5] also stressed the benefits of a gravity retraction that allows a wider operative exposure, which has the additional benefit of reducing morbidity.

We have developed expertise in this approach as a result of time spent with Dr Spetzler in Phoenix in 2003. To date, we have had numerous opportunities to successfully use this approach to treat a variety of neoplastic and/or vascular lesions that were found in or around the cingulate gyrus. It is on the basis of these surgical opportunities that we fully appreciate the advantages that, we believe, are incomparable when it comes to cases of small lesions deep within a motor area that is swollen as a result of the underlying lesion.[6] Because the interhemispheric corridor is tempting but, it should also be noted, rich in dangerous snares, we offer the following strategies that we have found extremely helpful for avoiding these hazards during surgery: (1) use the Lawton-Spetzler position; (2) make a linear incision parallel to the midline; (3) perform magnetic resonance angiography– or image–guided craniotomy perfectly centered between the entry point of bridging veins in the superior sagittal sinus; (4) expose the superior sagittal sinus by ad hoc placed burr holes and craniotome only after full control and detachment of dura mater from the bone; (5) gently retract and release the brain with working instruments rather than with a fixed spatula; and (6) consider the use of indocyanine green videoangiography to evaluate the presence of collateral drainage pathways before sacrifice or putting a bridging vein at risk (Ferroli et al[7]).

Ferroli Paolo
Giovanni Tringali
Morgan Broggi
Francesco Acerbi
Edvin Zekaj
Angelo Franzini
Giovanni Broggi
Milan, Italy

1. Talacchi A, Corsini F, Gerosa M. Surgical approaches to tumors of the anterior gyrus cinguli. *Neurosurgery*. 2010;66(6)(suppl operative):245-251.
2. Machado de Almeida G, Shibata MK, Nakagawa EJ. Contralateral parafalcine approach for parasagittal and callosal arteriovenous malformations. *Neurosurgery*. 1984;14(6):744-746.
3. Goel A. Transfalcine approach to a contralateral hemispheric tumour. *Acta Neurosurg*. 1995;135(3-4):210-212.
4. Lawton MT, Golfinos JG, Spetzler RF. The contralateral transcallosal approach experience with 32 patients. *Neurosurgery*. 1996;39(4):729-734.
5. Chi JH, Lawton MT. Posterior interhemispheric approach: surgical technique, application to vascular lesion, and benefits of gravity retraction. *Neurosurgery (ONS suppl)*. 2006;59:41-49.
6. Ferroli P, Russo A, Albanese E, Tringali G, Broggi G. Gravity-aided trans-falcine removal of a contralateral subcortical ependymoma. *Acta Neurochir (Wien)*. 2007;149(11):1147-1150.
7. Ferroli P, Nakaji P, Acerbi F, Albanese E, Broggi G. ICG temporary clipping test to asses collateral circulation before venous sacrifice: technical note. *World Neurosurgery*. In press.

10.1227/NEU.0b013e31821243f1

In Reply:

Ferroli and colleagues note that anterior gyrus cinguli tumors may be approached contralaterally. In our series of anterior gyrus cinguli tumors, we used—among others—the interhemispheric bilateral approach in perigenual tumors extending contralaterally and the unilateral approach in perirolandic tumors, based on the finding that tumors never extend contralaterally at this level. From this observation and evidence for the absence of drawbacks to the ipsilateral interhemispheric approach in small lesions, we believe that the contralateral approach may not necessarily offer

Copyright © Congress of Neurological Surgeons. Unauthorized reproduction of this article is prohibited.

an additional advantage over the ipsilateral approach. Furthermore, maneuvers like falx transection with division of the inferior sagittal sinus and the falcine venous plexus, which can carry unpredictable consequences for venous drainage, are not justified in our opinion.[1] However, we were aware of this approach and mentioned it in the discussion, but, because of its limited indications and the scarce success reported in the literature, we decided not to discuss it further.

Andrea Talacchi
Massimo Gerosa
Verona, Italy

1. Tubbs RS, Loukas M, Louis RG Jr, et al. Anatomy of the falcine venous plexus. *J Neurosurg*. 2007;107(1):155-157.

10.1227/NEU.0b013e3182127bee

Spinal Cord Stimulation for Thalamic or Central Pain

To the Editor:

I have read with great interest the paper of Ali et al[1] regarding the usefulness of spinal cord stimulation (SCS) in the treatment of central pain after stroke (CPSP), also well known as thalamic pain.

Patients with focal CPSP instead of generalized pain were considered for treatment by Ali et al.[1] Two cases with complete hemibody pain had circumscribed areas of more severe pain.

Percutaneous tetrapolar epidural electrodes were implanted and held for a 2- to 7-day trial period in 30 patients. Then, the electrode was removed. The analgesic results of the trial period were discussed with the patient. Ten patients received a new tetrapolar electrode. After a second trial period (whose duration is not specified), the internal pulse generator was implanted.

In their discussion the authors claim to be the first to describe good results with the SCS for the treatment of CPSP. The work published by our group[2] shows that this statement is not true. Our series is shorter than the one by Ali et al.[1] Follow-up is longer. They have a 28-month follow-up (range, 6-62), while that ours is longer: 81.6 months (range, 36-149).

I assume with Ali et al[1] that SCS is a much less aggressive surgical method than deep brain stimulation or motor prefrontal cortex. I also agree that better results can be attained in cases of focal pain rather than generalized pain.

I disagree with Ali et al[1] on the appropriateness of a short trial period of 2 to 7 days. I disagree very much with the removal of the electrode test and the return to implant it in the case of the definite implant. It is possible that the second electrode failed to obtain the same paresthesia as did the first. In addition, the rate of local complications could be increased.

Congratulations to Ali et al[1] for his excellent work, which confirms the good results that were previously shown by our work.[2]

Jose Antonio Lopez Lopez
Cadiz, Spain

1. Ali M, Saitoh Y, Hosomi K, Oshino S, Kishima H, Yoshimiro T. Spinal cord stimulation for central poststroke pain. *Neurosurgery*. 2010;67(3): ONS206–ONS212.
2. Lopez JA, Torres LM, Gala F, Iglesias I. Spinal cord stimulation and thalamic pain: long-term results of eight cases. *Neuromodulation*. 2009;12(3):240-243.

10.1227/NEU.0b013e318210f024

In Reply:

We would like to thank Lopez and colleagues for their interest in our article.[1] Lope et al[2] reported on a small series of spinal cord stimulation (SCS) for thalamic pain; 6 of 8 patients (75%) achieved satisfactory pain relief in the long term. Lopez et al restricted their indication to patients with localized pain distribution that could be entirely covered by stimulation paraesthesia; and this may explain their relatively high success rate.[2] Unfortunately this work had not yet been published when we submitted our report for publication.

Lopez et al reported that our trial period (2–7 days) was short. Actually, within this time frame we were able to unequivocally evaluate the analgesic effect of SCS in all patients. In general, there is no consensus on the length of SCS trial period, and periods of one day to several weeks have been reported.[2,3] There is no doubt that long trial periods give a better opportunity to evaluate the exact response to SCS, but unfortunately this comes with the price of increasing the risk of infection.

In our series, we used to remove the trial electrodes, and discharge patients after the trial period. At the time of counseling the patients in the outpatient clinic, those who decided to proceed were scheduled for the second trial and permanent SCS implantation.[1] Lopez et al disagree with this approach because they think it may increase the rate of local complications and the second electrode may fail to provoke the same paresthesia. The rationale for our approach was that, during trial stimulation, patients tend to respond in an affirmative manner, and therefore overestimate the analgesic efficacy.[4] We believe that repeating trials before permanent implant of SCS electrodes will minimize this phenomenon. However, there is no evidence that our method can improve outcome. We did not have any added complications from the second trial, but it obviously increases the cost of treatment. Finally, it is interesting to find that our results of SCS for central poststroke pain (CPSP) could be reproduced at other institutes. Hopefully these reports will encourage other centers to use SCS for CPSP, particularly in the face of safety of SCS trials and limited therapeutic options for CPSP.

Mohamed M. Aly
Youichi Saitoh
Satoru Oshino
Koichi Hosomi
Haruhiko Kishima
Toshiki Yoshimine
Suita, Japan

Copyright © Congress of Neurological Surgeons. Unauthorized reproduction of this article is prohibited.

1. Aly MM, Saitoh Y, Hosomi K, Oshino S, Kishima H, Yoshimine T. Spinal cord stimulation for central poststroke pain. *Neurosurgery*. 2010;67(3): ONS206-ONS212.
2. Lopez JA, Torres LM, Gala F, Iglesias I. Spinal cord stimulation and thalamic pain: long term results of eight cases. *Neuromodulation*. 2009;12(3): 240-243.
3. Stojanovic M, Abdi S. Spinal cord stimulation. *Pain Phys*. 2002;5(2):156-166.
4. Coffey RJ, Lozano AM. Neurostimulation for chronic noncancer pain: an evaluation of the clinical evidence and recommendations for future trial designs. *J Neurosurg*. 2006;105(2):175-198.

10.1227/NEU.0b013e318210f04b

Neurosurgery Simulation

In their neurosurgery simulation technology review, Malone et al[1] address an important yet largely unaddressed surgical area that can significantly benefit from the availability of an effective simulation-based surgical training system. Further, they touch on a number of relevant aspects of developments that will underpin their work on a pedicle screw placement simulator. We would like to add some additional thoughts here, which are based our work over the past several years in developing both a hard-tissue (burr hole) drilling simulator prototype for the US Army as well as a generalized soft-tissue simulation and bleeding system for general surgical resident training.

The authors have correctly identified that the foundational step in developing a system that provides clinically useful surgical skills training is to isolate the subtasks that will benefit most from simulation. Minimizing effort devoted to already mastered or commonly acquired skills and, instead, focusing on critical skill areas that are not well addressed with currently available approaches is critical to producing a simulator that meets unmet needs. To build simulations for those subtasks, the movements and loads experienced by the surgeon during both expected and unexpected actions in the procedure need to form the basis for the mathematical modeling and haptic device interfaces that will be developed. We have also found that, as the authors note, these movements and loads are often not known/available, and we have had to obtain this information ourselves as well. Measuring how actions are done wrong is just as important, if not more so, as measuring when they are done correctly, because an effective simulator must provide learners with the complete range of possible interactions. Learning what happens when something is done right often occurs in the context of learning what happens when things are done wrong.

Also important at the earliest stage of planning a simulator is defining objective, quantitative metrics of performance that can be used to measure attainment of proficiency of the skills being learned. This enables the simulator to be designed to provide reliable, appropriate metrics of performance that can stand up to rigorous evaluation and professional scrutiny.

The authors mention the limitations of current haptic devices and illustrate with the results in their work on measuring the loads encountered in pedicle screw placement. Current, commercially available haptic devices typically provide about 1 lb of force, whereas approximately 15 lb of force are experienced during screw placement in the authors' work. Our research in drilling fresh frozen cadaver skulls showed that forces as high as 30 lb can be experienced. To approach the forces and torques we measured, however, we needed to develop a custom haptic device using augmented off-the-shelf haptic devices. We expect that the availability of haptic devices having sufficient force/torque capacity and adequate range of movement and orientation will remain a major challenge for simulators that focus on high-load situations such as bone drilling.

A final consideration is the mixture of soft-tissue-centric lower-force actions with bone-centric high-load actions in the same simulation. Typically, soft-tissue simulations are modeled with finite-element methods centered on deformation and transection, whereas bone-centric simulations are done with voxel-based techniques in which the goal is often to remove bone through an energy-based methodology that represents the action of drill or saw blades. These techniques are quite different from one another, as are the haptic interface requirements. To our knowledge, no simulator has been produced to date that supports interaction with both soft tissue and bone in the same user experience. This limitation calls for attention to how procedural subtasks are deconstructed if combined soft-tissue–bone actions are encountered, which is not uncommon in spinal procedures.

Malone and colleagues are to be congratulated for taking on an important and largely unaddressed area. Much work lies ahead in the years to come, however, before the potential of such simulators is realized.

Dwight Meglan
Howard R. Champion
Silver Spring, Maryland

1. Malone HR, Syed ON, Downes MS, D'Ambrosio AL, Quest DO, Kaiser MG. Simulation in neurosurgery: a review of computer-based simulation environments and their surgical applications. *Neurosurgery*. 2010;67(4):1105-1116.

10.1227/NEU.0b013e318210f038

In Reply:

We appreciate the remarks of Drs Meglan and Champion of SimQuest, LLC. They are right to emphasize the limitations of many available haptic interfaces in reproducing the torques and loads encountered in the operative theater. The difficulty of simultaneously modeling finite-element–based soft-tissue deformation and voxel-based bone (hard-tissue) drilling, a challenge inherent to spine surgery simulation, is also addressed. Collaboration with simulation firms like SimQuest that possess the technical expertise to customize standard haptic interfaces and merge tissue deformation modalities is

Copyright © Congress of Neurological Surgeons. Unauthorized reproduction of this article is prohibited.

essential to the continued evolution of computer-based neurosurgery simulation.

Hani Malone
Omar Syed
Michael Kaiser
New York, New York

10.1227/NEU.0b013e3182127c00

Relationship Between Decompressive Craniectomy and Hydrocephalus

To the Editor:

We read with great interest the article by Rahme et al[1] in which the authors reviewed the records of 17 patients with stroke-related increased intracranial pressure who underwent decompressive craniectomy (DC). The authors described a 0% rate of shunting after DC and concluded that hydrocephalus does not frequently occur after DC. On the other hand, in the series of Waziri et al,[2] hydrocephalus developed in 15 of 17 patients after DC, and 5 required shunting after cranioplasty. Rahme et al[1] speculated that the explanation for this discrepancy might lie in the definition of hydrocephalus and the indications for shunting.

We completely agree with the viewpoint of Rahme et al[1]; however, we wish to provide further comment on this issue. Bogousslavsky and Regli[3] reported that, in 60 cases of internal carotid artery occlusion, the occurrence of ventricular dilation was related to the volume of infarction. Additionally, Barber et al[4] reported that hydrocephalus was present in 22% of patients who had a large middle cerebral artery infarction, and they received conventional medical therapy (without surgery).

Therefore, we believe that the possibility of hydrocephalus developing in the course of a large infarction should be considered. From this viewpoint, we consider that an additional explanation for the discrepancy between the results of Rahme et al[1] and Waziri et al[2] might be differences in the area and volume of the infarction. Indeed, in the Waziri et al series, all 4 patients with internal carotid artery infarction developed hydrocephalus after DC (half required shunting), and none of the 7 patients with middle cerebral artery infarction received shunting, whereas the Rahme et al series included no patients with internal carotid artery infarction.[1]

Satoru Takeuchi
Naoki Otani
Hiroshi Nawashiro
Tokorozawa, Saitama, Japan

1. Rahme R, Weil AG, Sabbagh M, Moumdjian R, Bouthillier A, Bojanowski MW. Decompressive craniectomy is not an independent risk factor for communicating hydrocephalus in patients with increased intracranial pressure. *Neurosurgery*. 2010;67(3):675-678.
2. Waziri A, Fusco D, Mayer SA, McKhann GM II, Connolly ES Jr. Postoperative hydrocephalus in patients undergoing decompressive hemicraniectomy for ischemic or hemorrhagic stroke. *Neurosurgery*. 2007;61(3):489-493.
3. Bogousslavsky J, Regli F. Obstruction of the internal carotid artery and cerebral malacias: tomodensitometric factors of the prognosis in 150 cases [in French]. *Schweiz Arch Neurol Neurochir Psychiatr*. 1984;134(1):13-28.
4. Barber PA, Demchuk AM, Zhang J, et al. Computed tomographic parameters predicting fatal outcome in large middle cerebral artery infarction. *Cerebrovasc Dis*. 2003;16(3):230-235.

10.1227/NEU.0b013e3182124403

In Reply:

We would like to thank Drs Takeuchi, Otani, and Nawashiro for their interest in our article.[1] However, we find that the 2 studies they are referring to do not really lend support to their hypothesis that the divergence between our results and those of Waziri et al[2] lies in the difference in patient characteristics, specifically the extent of infarction.

In the article of Bogousslavsky and Regli,[3] the authors analyzed the development of unilateral ipsilateral ventricular dilation and cortical atrophy in patients with large strokes secondary to internal carotid artery occlusion or stenosis. There was no mention of hydrocephalus in their report. It is important to distinguish between true hydrocephalus, that is, mismatch between CSF production and resorption, and ventricular dilation or hydrocephalus ex vacuo, which is merely a radiological finding caused by large areas of neuronal loss and encephalomalacia after a massive infarction.

In their publication, Barber et al[4] sought to determine early CT signs predictive of death after large middle cerebral artery (MCA) infarction in a large cohort of conservatively managed patients, none of which had undergone decompressive craniectomy. The authors found that moderate or severe hydrocephalus was predictive of death on univariate, but not multivariate analysis. It must be noted, however, that these authors were referring to acute obstructive hydrocephalus, a complication of cerebral edema-related mass effect in large ischemic strokes. Conversely, in our study[1] and that of Waziri et al,[2] patients were typically protected against obstructive hydrocephalus by the wide surgical decompression. Rather, the incidence of chronic communicating hydrocephalus in survivors of malignant MCA territory infarction and other types of stroke was assessed.

To the best of our knowledge, there is no direct relationship between communicating hydrocephalus and ischemic stroke. Additionally, in our experience, hydrocephalus is not a frequent complication of decompressive craniectomy.[1] Therefore, unless new scientific evidence comes to disprove these findings, we have no reason to believe that hydrocephalus should be a major concern in the management of patients with large MCA or internal carotid artery infarctions.

Ralph Rahme
Alexander G. Weil
Michel W. Bojanowski
Montreal, Quebec, Canada

Copyright © Congress of Neurological Surgeons. Unauthorized reproduction of this article is prohibited.

1. Rahme R, Weil AG, Sabbagh M, Moumdjian R, Bouthillier A, Bojanowski MW. Decompressive craniectomy is not an independent risk factor for communicating hydrocephalus in patients with increased intracranial pressure. *Neurosurgery*. 2010;67(3):675-678.
2. Waziri A, Fusco D, Mayer SA, McKhann GM II, Connolly ES Jr. Postoperative hydrocephalus in patients undergoing decompressive hemicraniectomy for ischemic or hemorrhagic stroke. *Neurosurgery*. 2007;61(3):489-494.
3. Bogousslavsky J, Regli F. Obstruction of the internal carotid artery and cerebral malacias. Tomodensitometric factors of the prognosis in 150 cases [French]. *Schweiz Arch Neurol Neurochir Psychiatr*. 1984;134(1):13-28.
4. Barber PA, Demchuk AM, Zhang J, et al. Computed tomographic parameters predicting fatal outcome in large middle cerebral artery infarction. *Cerebrovasc Dis*. 2003;16(3):230-235.

10.1227/NEU.0b013e3182127bdc

Copyright © Congress of Neurological Surgeons. Unauthorized reproduction of this article is prohibited.

Erratum

In the article "A Novel Technique of Odontoidoplasty and C1 Arch Reconstruction: Anatomical and Biomechanical Basis" by Agrawal et al (*Neurosurgery*. 2011;68(S1):ons103-ons113.), two incorrect editorial comments appeared at the end of the article. Additionally, the first author is Abhishek Agrawal, MD.

10.1227/NEU.0b013e318219d82d

Copyright © Congress of Neurological Surgeons. Unauthorized reproduction of this article is prohibited.

Calendar of Events

Full contact information is available online only

Listings for this section must be submitted at least 3 months in advance. Please include a telephone number and/or a fax number.

Submit Listings to:
Russell R. Lonser, MD
National Institutes of Neurological Disorders and Stroke
National Institutes of Health
10 Center Drive
Building 10, Room 5D37
Bethesda, MD 20892-1414.
Tel: (301) 496 5728
Fax: (301) 402 0380
E-mail:lonserr@ninds.nih.gov

NATIONAL AND REGIONAL MEETINGS

MAY 2-5, 2011	**Joint EANS Annual Meeting-4th World ICH Conference 2011**	Newcastle-Gateshead, United Kingdom	**Contact:** Congress Organizer **Tel:** +41 22 908 0488 **Fax:** +41 22 906 9140 **E-mail:** wcn@kenes.com **Web Site:** www2.kenes.com/eans-ich
SEPTEMBER 12-17, 2011	**7th Congress of the European Federation of IASP Chapters (EFIC)**	Hamburg, Germany	**Contact:** Congress Organizer **Tel:** +41 22 908 0488 **Fax:** +41 22 906 9140 **E-mail:** eans-ich@kenes.com **Web Site:** www2.kenes.com/efic
NOVEMBER 12-17, 2011	**World Congress of Neurology**	Marrakesh, Morocco	**Contact:** Congress Organizer **Tel:** +41 22 908 0488 **Fax:** +41 22 906 9140 **E-mail:** efic2011@kenes.com **Web Site:** www2.kenes.com/wcn/Pages/Home.aspx

INTERNATIONAL/GENERAL NEUROSURGERY

MAY 2-5, 2011	**Joint EANS Annual Meeting - 4th World ICH Conference**	Newcastle-Gateshead, UK	**Contact:** Kenes International **Tel:** +41-22-908-0488 **Fax:** +41-22-906-9140 **E-mail:** eans@kenes.com **Web Site:** www.kenes.com/eans-ich
MAY 8-12, 2011	**International Stereotactic Radiosurgery Society**	Paris, France	**Contact:** Colloquium Brussels **Tel:** +32-02-777-01-47 **Fax:** +32-02-779-59-60 **E-mail:** isrs2011@clq-group.com **Web Site:** isrscongress.org
MAY 24-28, 2011	**XXVth International Symposium on Cerebral Blood Flow, Metabolism, and Function & Xth International Conference on Quantification of Brain Function With PET**	Barcelona, Spain	**Contact:** Kenes International **Tel:** +41-22-908-0488 **Fax:** +41-22-906-9140 **E-mail:** brain@kenes.com **Web Site:** www.kenes.com/brain2011/
JUNE 16-18, 2011	**International Hands-on Course on Full HD Endoscopic Neurosurgery**	Greifswald, Germany	**Contact:** Elke Rösel **Fax:** +49-3834 86-6164 **E-mail:** elke.roesel@uni-greifswald.de **Web Site:** www.medizin.uni-greifswald.de/neuro_ch
SEPTEMBER 14-17, 2011	**14th Interim Meeting of the World Federation of Neurosurgical Societies (WFNS) (simultaneously with) 15th Brazilian Congress of Continuous Education**	Recife (Porto de Galinhas), Brazil	**Contact:** Hildo Azevedo-Filho **Tel:** +55-81-32221354 **Fax:** +55-81-32212899 **E-mail:** azevedoh@uol.com.br **Web Site:** www.wfnsinterimmeeting2011.com.br
SEPTEMBER 8-13, 2013	**15th Word Federation of Neurosurgical Societies (WFNS) World Congress of Neurosurgery**	Seoul, South Korea	**Contact:** Hee-Won Jung **Tel:** +82-11-391-2339 **Fax:** +82-2-744-2339 **E-mail:** hwnjung@snu.ac.lcr **Web Site:** www.wfns2013.org

Copyright © Congress of Neurological Surgeons. Unauthorized reproduction of this article is prohibited.

CEREBROVASCULAR

AUGUST 24-28, 2011	**Zurich Course on Interventional Neuroradiology**	Zurich, Switzerland	**CONTACT:** University Hospital of Zurich **TEL:** +41 44 255 56 00 **FAX:** +41 44 255 45 04 **E-MAIL:** neuroradiologie@usz.ch **WEB SITE:** www.cinr-zurich.ch

CRANIAL BASE

APRIL 18-19, 2011	**Endoscopic Transsphenoidal Surgery: From Pituitary to Skull Base**	Bologna, Italy	**CONTACT:** CSR Congressi SRI **TEL:** +39 051765357 **FAX:** +39 051 765195 **E-MAIL:** info@csrcongressi.com **WEB SITE:** www.csrcongressi.com
MAY 30-31, 2011	**Endoscopic Endonasal Skull Base Surgery Training and Surgical Education**	Naples, Italy	**CONTACT:** Prof. Paolo Cappabianca **TEL:** +39 081 7462559 **FAX:** +39 081 7462497 **E-MAIL:** info.neurochirurgia@unina.it **WEB SITE:** www.neurochirurgia.unina.it
JUNE 10-11, 2011	**Advanced Endoscopic Skull Base and Pituitary Surgery, Hands-on Symposium**	New York, NY	**CONTACT:** Jessica Grajales **TEL:** (212) 585 6800 **FAX:** (212) 297 5569 **E-MAIL:** jeg9059@nyp.org **WEB SITE:** www.cornellneurosurgery.org
NEW SEPTEMBER 9-10, 2011	**From Cranial to Spine: A Comprehensive Overview of Neurosurgical Topics for the Mid-Level Practictioner**	Chicago, IL	**CONTACT:** Heather Hodge **TEL:** (847) 387-0500 **E-MAIL:** epm@aans.org **WEB SITE:** www.AANS.org

MINIMALLY INVASIVE NEUROSURGERY

DECEMBER 1-3, 2011	**Indications and Controversies: Minimally Invasive Spinal Surgery and Navigation-Hands-on Symposium**	New York, NY	**CONTACT:** Jessica Grajales **TEL:** (212) 585 6800 **FAX:** (212) 297 5569 **E-MAIL:** jeg9059@nyp.org **WEB SITE:** www.cornellneurosurgery.org

SPINE/PERIPHERAL NERVE

JULY 13-19, 2011	**Cleveland Spine Review Hands-on Course**	Cleveland, OH	**CONTACT:** Monét Redrick-Smith **TEL:** (216) 444 9380 **FAX:** (213) 445 9999 **E-MAIL:** smithm8@ccf.org **WEB SITE:** www.ccfcme.org/spinereview11

PEDIATRICS

SEPTEMBER 4-7, 2011	**ISHCSF Hydrocephalus 2011**	Malmo, Sweden	**CONTACT:** Mrs. Lotta Ahlbertz **TEL:** +46-40-258558 **FAX:** +46-40-258559 **E-MAIL:** lotta@malmokongressbyra.se **WEB SITE:** www.ishcsf.com/copenhagen.htm
NEW NOVEMBER 29-DECEMBER 2, 2011	**AANS/CNS Section of Pediatric Neurological Surgery**	Austin, TX	**CONTACT:** Jennifer Healy **TEL:** (847) 387-0500 **E-MAIL:** meetings@aans.org **WEB SITE:** www.AANS.org

Copyright © Congress of Neurological Surgeons. Unauthorized reproduction of this article is prohibited.

STEREOTACTIC/FUNCTIONAL

SEPTEMBER 16-18, 2011	**12th Biennial Conference of the Indian Society of Stereotaxy and Functional Neurosurgery (ISSFN)**	Chennai, Tamil Nadu, India	**Contact:** Dr M. Balamurugan **E-mail:** info@issfn2011.co.in **Web Site:** www.issfn2011.co.in/

SPECIAL TOPICS

MARCH 21-25, 2011	**Principles and Practice of Gamma Knife Radiosurgery 4C and Perfexion Training Course**	Pittsburgh, PA	**Contact:** Charlene H. Baker **Tel:** (412) 881-0602 **Fax:** (412) 881-2450 **E-mail:** bakerch@comcast.net **Web Site:** neurosurgery.pitt.edu
MAY 1-3, 2011	**Goodman Oral Board Preparation Neurosurgery Review by Case Management**	Houston, TX	**Contact:** Vanessa Spinnato **Tel:** 847-378-0500 **E-mail:** meetings@aans.org **Web Site:** www.aans.org
MAY 2-6, 2011	**Principles and Practice of Gamma Knife Radiosurgery 4C and Perfexion Training Course**	Pittsburgh, PA	**Contact:** Charlene H. Baker **Tel:** (412) 881-0602 **Fax:** (412) 881-2450 **E-mail:** bakerch@comcast.net **Web Site:** neurosurgery.pitt.edu
MAY 16-20, 2011	**Gamma Knife Radiosurgery Course**	Cleveland, OH	**Contact:** Monét Redrick-Smith **Tel:** (216) 444 9380 **Fax:** (213) 445 9999 **E-mail:** smithm8@ccf.org **Web Site:** my.clevelandclinic.org/brain_tumor/education/gamma_knife_radiosurgery/default.aspx
JUNE 6-10, 2011	**Principles and Practice of Gamma Knife Radiosurgery 4C and Perfexion Training Course**	Pittsburgh, PA	**Contact:** Charlene H. Baker **Tel:** (412) 881-0602 **Fax:** (412) 881-2450 **E-mail:** bakerch@comcast.net **Web Site:** neurosurgery.pitt.edu
NEW JUNE 11-19, 2011	**Chicago Review Course in Neurological Dissection**	Chicago, IL	**Contact:** Maria Peña **Tel:** (773) 348-4333 **Fax:** (773) 348-2434 **E-mail:** mpena@chicagoreviewcourse.com **Web Site:** www.chicagoreviewcourse.com
JULY 11-15, 2011	**Principles and Practice of Gamma Knife Radiosurgery 4C and Perfexion Training Course**	Pittsburgh, PA	**Contact:** Charlene H. Baker **Tel:** (412) 881-0602 **Fax:** (412) 881-2450 **E-mail:** bakerch@comcast.net **Web Site:** neurosurgery.pitt.edu
JULY 21-23, 2011	**Vasospasm 2011: The 11th International Conference on Neurovascular Events after Subarachnoid Hemorrhage**	Cincinnati, OH	**Contact:** Joanie Pope **Tel:** (513) 558 3556 **Fax:** (513) 558 3361 **E-mail:** joan.pope@uc.edu **Web Site:** www.vasospasm11.com
JULY 28-29, 2011	**Managing Coding & Reimbursement Challenges in Neurosurgery**	Boston, MA	**Contact:** Heather Hodge **Tel:** (847) 378-0500 **E-mail:** epm@aans.org **Web Site:** www.aans.org
JULY 29-30, 2011	**Brain Endoscopy Course**	Buffalo, NY	**Contact:** Caitlin Hartney **Tel:** (716) 887-5200 ext. 2216 **E-mail:** cpeekstok@ubns.com **Web Site:** www.ubneurosurgery.com

Copyright © Congress of Neurological Surgeons. Unauthorized reproduction of this article is prohibited.

JULY 30-31, 2011	**Neurosurgeon as CEO, The Business of Neurosurgery**	Boston, MA	**CONTACT:** Heather Hodge **TEL:** (847) 378-0500 **E-MAIL:** epm@aans.org **WEB SITE:** www.aans.org
AUGUST 8-12, 2011	**Gamma Knife Radiosurgery Course**	Cleveland, OH	**CONTACT:** Monét Redrick-Smith **TEL:** (216) 444 9380 **FAX:** 213) 445 9999 **E-MAIL:** smithm8@ccf.org **WEB SITE:** my.clevelandclinic.org/brain_tumor/education/gamma_knife_radiosurgery/default.aspx
SEPTEMBER 7-9, 2011	**University of Virginia Gamma Knife Advanced Course Gamma Knife Perfexion Course**	Charlottesville, VA	**CONTACT:** Sophie L. Yu **TEL:** (434) 924-2336 **FAX:** (434) 977-6279 **E-MAIL:** sly9p@virginia.edu **WEB SITE:** http://www.medicine.virginia.edu/clinical/departments/neurosurgery/gammaknife/conference/advanced_course-page/
SEPTEMBER 9-10, 2011	**Managing Coding & Reimbursement Challenges in Neurosurgery**	Nashville, TN	**CONTACT:** Heather Hodge **TEL:** (847) 378-0500 **E-MAIL:** epm@aans.org **WEB SITE:** www.aans.org
SEPTEMBER 17-18, 2011	**2011 Gamma Knife Radiosurgery in the Americas**	Pittsburgh, PA	**CONTACT:** Sharon DeCesare **TEL:** (412) 647 4994 **FAX:** (412) 647 8445 **E-MAIL:** decesares@upmc.edu **WEB SITE:** www.nagkc.pitt.edu
SEPTEMBER 26-30, 2011	**Principles and Practice of Gamma Knife Radiosurgery 4C and Perfexion Training Course**	Pittsburgh, PA	**CONTACT:** Charlene H. Baker **TEL:** (412) 881-0602 **FAX:** (412) 881-2450 **E-MAIL:** bakerch@comcast.net **WEB SITE:** neurosurgery.pitt.edu
OCTOBER 24-25, 2011	**Gamma Knife Radiosurgery Course**	Cleveland, OH	**CONTACT:** Monét Redrick-Smith **TEL:** (216) 444 9380 **FAX:** (213) 445 9999 **E-MAIL:** smithm8@ccf.org **WEB SITE:** my.clevelandclinic.org/brain_tumor/education/gamma_knife_radiosurgery/default.aspx
OCTOBER 24-28, 2011	**Principles and Practice of Gamma Knife Radiosurgery 4C and Perfexion Training Course**	Pittsburgh, PA	**CONTACT:** Charlene H. Baker **TEL:** (412) 881-0602 **FAX:** (412) 881-2450 **E-MAIL:** bakerch@comcast.net **WEB SITE:** neurosurgery.pitt.edu
NOVEMBER 6-8, 2011	**Goodman Oral Board Preparation Neurosurgery Review by Case Management**	Houston, TX	**CONTACT:** Vanessa Spinnato **TEL:** 847-378-0500 **FAX:** (412) 881-2450 **E-MAIL:** meetings@aans.org **WEB SITE:** www.aans.org
NOVEMBER 28-DECEMBER 2, 2011	**Gamma Knife Radiosurgery Course**	Cleveland, OH	**CONTACT:** Monét Redrick-Smith **TEL:** (216) 444 9380 **FAX:** (213) 445 9999 **E-MAIL:** smithm8@ccf.org **WEB SITE:** my.clevelandclinic.org/brain_tumor/education/gamma_knife_radiosurgery/default.aspx

Copyright © Congress of Neurological Surgeons. Unauthorized reproduction of this article is prohibited.

DECEMBER 11-14, 2011	**World Federation of Neurology World Congress on Parkinson's Disease and Related Disorders**	Shanghai, China	**CONTACT:** Kenes International **TEL:** +41 22 908 0488 **FAX:** +41 22 906 9140 **E-MAIL:** parkinson2011@kenes.com **WEB SITE:** www2.kenes.com/parkinson/Pages/Home.aspx
NEW JANUARY 26-FEBRUARY 5, 2012	**Chicago Review Course in Neurosurgery**	Chicago, IL	**CONTACT:** Maria Peña/Lucy Salgado **TEL:** (773) 348-4333 or (773) 296-6666 **FAX:** (773) 348-2434 **E-MAIL:** lsalgado@chicagoreviewcourse.com **WEB SITE:** www.chicagoreviewcourse.com

TRAUMA/CRITICAL CARE

SEPTEMBER 16, 2011	**Practical Management of Acute Stroke Conference**	Cleveland, OH	**CONTACT:** Monét Redrick-Smith **TEL:** (216) 444 9380 **FAX:** (213) 445 9999 **E-MAIL:** smithm8@ccf.org **WEB SITE:** www.ccfcme.org/acutestroke11

Copyright © Congress of Neurological Surgeons. Unauthorized reproduction of this article is prohibited.

NEUROSURGERY
THE REGISTER OF THE NEUROSURGICAL MEME

Table of Contents by Topic

May 2011 Volume 68 | Number 5 Pages 1161–1482

Articles are grouped by categories, complete author listings can be found on preceding Table of Contents

CEREBROVASCULAR

1164 **Relationship of Growth to Aneurysm Rupture in Asymptomatic Aneurysms ≤ 7 mm: A Systematic Analysis of the Literature:** *Mohamad Chmayssani*

1172 **A Review of Laboratory and Clinical Data Supporting the Safety and Efficacy of Cyclosporin A in Traumatic Brain Injury:** *Dzenan Lulic*

1187 **Early Recognition of Lumbar Overdrainage by Lumboventricular Pressure Gradient:** *Dimitre Staykov*

1227 **Epilepsy After Bypass Surgery in Adult Moyamoya Disease:** *Sung-Chul Jin*

1270 **Geometry of the Internal Carotid Artery and Recurrent Patterns in Location, Orientation, and Rupture Status of Lateral Aneurysms: An Image-Based Computational Study:** *Marina Piccinelli*

1286 **Packed Red Blood Cell Transfusion and Decreased Mortality in Intracerebral Hemorrhage:** *Kevin N. Sheth*

1334 **Neuroprotection With Intraventricular Brain-Derived Neurotrophic Factor in Rat Venous Occlusion Model:** *Yasuhiro Takeshima*

1342 **Thrombospondin-1 Modulates the Angiogenic Phenotype of Human Cerebral Arteriovenous Malformation Endothelial Cells:** *Christopher J. Stapleton*

1372 **Granulocyte Colony-Stimulating Factor Enhances the Angiogenetic Effect of Indirect Bypass Surgery for Chronic Cerebral Hypoperfusion in a Rat Model:** *Yuki Ohmori*

1388 **Magnetic Microparticles for Endovascular Aneurysm Treatment: In Vitro and In Vivo Experimental Results:** *Johanna Oechtering*

1418 **Newly Synthesized Radical-Containing Nanoparticles Enhance Neuroprotection After Cerebral Ischemia-Reperfusion Injury:** *Aiki Marushima*

1427 **Robotic Digital Subtraction Angiography Systems Within the Hybrid Operating Room:** *Yuichi Murayama*

1434 **Open and Endovascular Treatment of Unruptured Carotid-Ophthalmic Aneurysms: Clinical and Radiographic Outcomes:** *Sanjay Yadla*

1465 **Reactive Expansive Intracerebral Process as a Complication of Endovascular Coil Treatment of an Unruptured Intracranial Aneurysm: Case Report:** *Marton König*

1473 **"Double-Barrel" Stent Reconstruction of a Symptomatic Fusiform Basilar Artery Aneurysm: Case Report:** *Mark Bain*

1475 **Onyx Pulmonary Artery Embolization After Treatment of a Low-Flow Dural Arteriovenous Fistula: Case Report:** *Bryan A. Pukenas*

CLINICAL TRIAL

1172 **A Review of Laboratory and Clinical Data Supporting the Safety and Efficacy of Cyclosporin A in Traumatic Brain Injury:** *Dzenan Lulic*

1233 **Weight Changes in Subthalamic Nucleus vs Globus Pallidus Internus Deep Brain Stimulation: Results From the COMPARE Parkinson Disease Deep Brain Stimulation Cohort:** *Maren C. Locke*

1286 **Packed Red Blood Cell Transfusion and Decreased Mortality in Intracerebral Hemorrhage:** *Kevin N. Sheth*

1309 **Prospective, Randomized, Double-Blind Clinical Study Evaluating the Correlation of Clinical Outcomes and Cervical Sagittal Alignment:** *Alan T. Villavicencio*

CRANIAL BASE

1200 **Stereotactic Radiosurgery of Cranial Nonvestibular Schwannomas: Results of Single- and Multisession Radiosurgery:** *Clara Y.H. Choi*

1465 **Reactive Expansive Intracerebral Process as a Complication of Endovascular Coil Treatment of an Unruptured Intracranial Aneurysm: Case Report:** *Marton König*

ENDOVASCULAR

1164 **Relationship of Growth to Aneurysm Rupture in Asymptomatic Aneurysms ≤ 7 mm: A Systematic Analysis of the Literature:** *Mohamad Chmayssani*

1388 **Magnetic Microparticles for Endovascular Aneurysm Treatment: In Vitro and In Vivo Experimental Results:** *Johanna Oechtering*

1418 **Newly Synthesized Radical-Containing Nanoparticles Enhance Neuroprotection After Cerebral Ischemia-Reperfusion Injury:** *Aiki Marushima*

1427 **Robotic Digital Subtraction Angiography Systems Within the Hybrid Operating Room:** *Yuichi Murayama*

1434 **Open and Endovascular Treatment of Unruptured Carotid-Ophthalmic Aneurysms: Clinical and Radiographic Outcomes:** *Sanjay Yadla*

1465 **Reactive Expansive Intracerebral Process as a Complication of Endovascular Coil Treatment of an Unruptured Intracranial Aneurysm: Case Report:** *Marton König*

1473 **"Double-Barrel" Stent Reconstruction of a Symptomatic Fusiform Basilar Artery Aneurysm: Case Report:** *Mark Bain*

1475 **Onyx Pulmonary Artery Embolization After Treatment of a Low-Flow Dural Arteriovenous Fistula: Case Report:** *Bryan A. Pukenas*

EPILEPSY

1227 **Epilepsy After Bypass Surgery in Adult Moyamoya Disease:** *Sung-Chul Jin*

1326 **Seizures and the Natural History of World Health Organization Grade II Gliomas: A Review:** *Anja Smits*

EVIDENCE-BASED MEDICINE

1164 **Relationship of Growth to Aneurysm Rupture in Asymptomatic Aneurysms ≤ 7 mm: A Systematic Analysis of the Literature:** *Mohamad Chmayssani*

1286 **Packed Red Blood Cell Transfusion and Decreased Mortality in Intracerebral Hemorrhage:** *Kevin N. Sheth*

FUNCTIONAL NEUROSURGERY

1233 **Weight Changes in Subthalamic Nucleus vs Globus Pallidus Internus Deep Brain Stimulation: Results From the COMPARE Parkinson Disease Deep Brain Stimulation Cohort:** *Maren C. Locke*

1252 **Differential Efficacy of Electric Motor Cortex Stimulation and Lesioning of the Dorsal Root Entry Zone for Continuous vs Paroxysmal Pain After Brachial Plexus Avulsion:** *Mohamed Ali*

1300 **Treatment of Severe Trigeminal Headache in Patients With Pituitary Adenomas:** *Tiago da Silva Freitas*

1405 **Autologous Adult Cortical Cell Transplantation Enhances Functional Recovery Following Unilateral Lesion of Motor Cortex in Primates: A Pilot Study:** *Mélanie Kaeser*

1452 **The Effect of Pulse Width and Contact Configuration on Paresthesia Coverage in Spinal Cord Stimulation:** *Jan Holsheimer*

1464 **Ventral Intermediate Thalamic Stimulation for Monoclonal Gammopathy-Associated Tremor: Case Report:** *Donald C. Shields*

1477 **High-Frequency Pallidal Stimulation for Camptocormia in Parkinson Disease: Case Report:** *Nova B. Thani*

GENERAL NEUROSURGERY

1164 **Relationship of Growth to Aneurysm Rupture in Asymptomatic Aneurysms ≤ 7 mm: A Systematic Analysis of the Literature:** *Mohamad Chmayssani*

1259 **Surgical Mortality at 30 Days and Complications Leading to Recraniotomy in 2630 Consecutive Craniotomies for Intracranial Tumors:** *Benjamin Lassen*

1317 **Navigated Transcranial Magnetic Stimulation and Functional Magnetic Resonance Imaging: Advanced Adjuncts in Preoperative Planning for Central Region Tumors:** *Marie-Thérèse Forster*

1418 **Newly Synthesized Radical-Containing Nanoparticles Enhance Neuroprotection After Cerebral Ischemia-Reperfusion Injury:** *Aiki Marushima*

1467 **Navigated Brain Stimulation for Preoperative Cortical Mapping in Paretic Patients: Case Report of a Hemiplegic Patient:** *Thomas Picht*

HYDROCEPHALUS

1187 **Early Recognition of Lumbar Overdrainage by Lumboventricular Pressure Gradient:** *Dimitre Staykov*

IMAGING

1239 **Optic Radiation Fiber Tracking Using Anteriorly Angulated Diffusion Tensor Imaging: A Tested Algorithm for Quick Application:** *Lennart H. Stieglitz*

1270 **Geometry of the Internal Carotid Artery and Recurrent Patterns in Location, Orientation, and Rupture Status of Lateral Aneurysms: An Image-Based Computational Study:** *Marina Piccinelli*

1317 **Navigated Transcranial Magnetic Stimulation and Functional Magnetic Resonance Imaging: Advanced Adjuncts in Preoperative Planning for Central Region Tumors:** *Marie-Thérèse Forster*

1380 **Computed Tomography Imaging of Transferrin Targeting Liposomes Encapsulating Both Boron and Iodine Contrast Agents by Convection-Enhanced Delivery to F98 Rat Glioma for Boron Neutron Capture Therapy:** *Shiro Miyata*

1427 **Robotic Digital Subtraction Angiography Systems Within the Hybrid Operating Room:** *Yuichi Murayama*

1467 **Navigated Brain Stimulation for Preoperative Cortical Mapping in Paretic Patients: Case Report of a Hemiplegic Patient:** *Thomas Picht*

1475 **Onyx Pulmonary Artery Embolization After Treatment of a Low-Flow Dural Arteriovenous Fistula: Case Report:** *Bryan A. Pukenas*

Copyright © Congress of Neurological Surgeons. Unauthorized reproduction of this article is prohibited.

Table of Contents by Topic

INFECTION

1259 Surgical Mortality at 30 Days and Complications Leading to Recraniotomy in 2630 Consecutive Craniotomies for Intracranial Tumors: *Benjamin Lassen*

1469 Community-Associated Methicillin-Resistant *Staphylococcus Aureus*–Infected Chronic Scalp Wound With Exposed Dura in a 10-Year-Old Boy: Vacuum-Assisted Closure Is a Feasible Option: Case Report: *Ulrike Subotic*

1471 Pott Disease in a 13-Month-Old: Case Report: *Giac Consigilieri*

INTENSIVE CARE

1286 Packed Red Blood Cell Transfusion and Decreased Mortality in Intracerebral Hemorrhage: *Kevin N. Sheth*

1363 Induction of Angiogenesis and Modulation of Vascular Endothelial Growth Factor Receptor-2 by Simvastatin After Traumatic Brain Injury: *Hongtao Wu*

MOLECULAR AND CELLULAR NEUROSURGERY

1172 A Review of Laboratory and Clinical Data Supporting the Safety and Efficacy of Cyclosporin A in Traumatic Brain Injury: *Dzenan Lulic*

1334 Neuroprotection With Intraventricular Brain-Derived Neurotrophic Factor in Rat Venous Occlusion Model: *Yasuhiro Takeshima*

1342 Thrombospondin-1 Modulates the Angiogenic Phenotype of Human Cerebral Arteriovenous Malformation Endothelial Cells: *Christopher J. Stapleton*

1363 Induction of Angiogenesis and Modulation of Vascular Endothelial Growth Factor Receptor-2 by Simvastatin After Traumatic Brain Injury: *Hongtao Wu*

1372 Granulocyte Colony-Stimulating Factor Enhances the Angiogenetic Effect of Indirect Bypass Surgery for Chronic Cerebral Hypoperfusion in a Rat Model: *Yuki Ohmori*

1380 Computed Tomography Imaging of Transferrin Targeting Liposomes Encapsulating Both Boron and Iodine Contrast Agents by Convection-Enhanced Delivery to F98 Rat Glioma for Boron Neutron Capture Therapy: *Shiro Miyata*

1405 Autologous Adult Cortical Cell Transplantation Enhances Functional Recovery Following Unilateral Lesion of Motor Cortex in Primates: A Pilot Study: *Mélanie Kaeser*

1418 Newly Synthesized Radical-Containing Nanoparticles Enhance Neuroprotection After Cerebral Ischemia-Reperfusion Injury: *Aiki Marushima*

NEUROTRAUMA

1172 A Review of Laboratory and Clinical Data Supporting the Safety and Efficacy of Cyclosporin A in Traumatic Brain Injury: *Dzenan Lulic*

PEDIATRICS

1469 Community-Associated Methicillin-Resistant *Staphylococcus Aureus*–Infected Chronic Scalp Wound With Exposed Dura in a 10-Year-Old Boy: Vacuum-Assisted Closure Is a Feasible Option: Case Report: *Ulrike Subotic*

1471 Pott Disease in a 13-Month-Old: Case Report: *Giac Consigilieri*

PERIPHERAL NERVE

1252 Differential Efficacy of Electric Motor Cortex Stimulation and Lesioning of the Dorsal Root Entry Zone for Continuous vs Paroxysmal Pain After Brachial Plexus Avulsion: *Mohamed Ali*

1354 A Long Peripheral Nerve Autograft Model in the Sheep Forelimb: *Joanne Forden*

1399 Application of 2 Different Hemostatic Procedures During Microsurgical Median Nerve Reconstruction in the Rat Does Not Hinder Axonal Regeneration: *Nektarios Sinis*

1462 Review of: Focal Peripheral Neuropathies (Fourth Edition): *Boon Pang*

RADIOSURGERY

1200 Stereotactic Radiosurgery of Cranial Nonvestibular Schwannomas: Results of Single- and Multisession Radiosurgery: *Clara Y.H. Choi*

SPINE

1220 Anterior Thoracolumbar Corpectomies: Approach Morbidity With and Without an Access Surgeon: *Seunggu J. Han*

1252 Differential Efficacy of Electric Motor Cortex Stimulation and Lesioning of the Dorsal Root Entry Zone for Continuous vs Paroxysmal Pain After Brachial Plexus Avulsion: *Mohamed Ali*

1309 Prospective, Randomized, Double-Blind Clinical Study Evaluating the Correlation of Clinical Outcomes and Cervical Sagittal Alignment: *Alan T. Villavicencio*

1427 Robotic Digital Subtraction Angiography Systems Within the Hybrid Operating Room: *Yuichi Murayama*

1452 The Effect of Pulse Width and Contact Configuration on Paresthesia Coverage in Spinal Cord Stimulation: *Jan Holsheimer*

1462 Review of: Focal Peripheral Neuropathies (Fourth Edition): *Boon Pang*

1471 Pott Disease in a 13-Month-Old: Case Report: *Giac Consigilieri*

STEREOTAXIS

1200 Stereotactic Radiosurgery of Cranial Nonvestibular Schwannomas: Results of Single- and Multisession Radiosurgery: *Clara Y.H. Choi*

1209 Stereotactic ^{125}Iodine Brachytherapy for the Treatment of Singular Brain Metastases: Closing a Gap?: *Maximilian I. Ruge*

1233 Weight Changes in Subthalamic Nucleus vs Globus Pallidus Internus Deep Brain Stimulation: Results From the COMPARE Parkinson Disease Deep Brain Stimulation Cohort: *Maren C. Locke*

1239 Optic Radiation Fiber Tracking Using Anteriorly Angulated Diffusion Tensor Imaging: A Tested Algorithm for Quick Application: *Lennart H. Stieglitz*

1464 Ventral Intermediate Thalamic Stimulation for Monoclonal Gammopathy-Associated Tremor: Case Report: *Donald C. Shields*

1477 High-Frequency Pallidal Stimulation for Camptocormia in Parkinson Disease: Case Report: *Nova B. Thani*

SURGICAL ANATOMY

1444 Endoscopic Port Surgery for Resection of Lesions of the Cerebellar Peduncles: Technical Note: *Pawel G. Ochalski*

SURGICAL STRATEGY

1192 Awake Craniotomy vs Surgery Under General Anesthesia for Resection of Supratentorial Lesions: *Oumar Sacko*

1209 Stereotactic ^{125}Iodine Brachytherapy for the Treatment of Singular Brain Metastases: Closing a Gap?: *Maximilian I. Ruge*

1220 Anterior Thoracolumbar Corpectomies: Approach Morbidity With and Without an Access Surgeon: *Seunggu J. Han*

1227 Epilepsy After Bypass Surgery in Adult Moyamoya Disease: *Sung-Chul Jin*

1252 Differential Efficacy of Electric Motor Cortex Stimulation and Lesioning of the Dorsal Root Entry Zone for Continuous vs Paroxysmal Pain After Brachial Plexus Avulsion: *Mohamed Ali*

1300 Treatment of Severe Trigeminal Headache in Patients With Pituitary Adenomas: *Tiago da Silva Freitas*

1399 Application of 2 Different Hemostatic Procedures During Microsurgical Median Nerve Reconstruction in the Rat Does Not Hinder Axonal Regeneration: *Nektarios Sinis*

1405 Autologous Adult Cortical Cell Transplantation Enhances Functional Recovery Following Unilateral Lesion of Motor Cortex in Primates: A Pilot Study: *Mélanie Kaeser*

1462 Review of: Focal Peripheral Neuropathies (Fourth Edition): *Boon Pang*

1477 High-Frequency Pallidal Stimulation for Camptocormia in Parkinson Disease: Case Report: *Nova B. Thani*

SURGICAL TECHNIQUE

1220 Anterior Thoracolumbar Corpectomies: Approach Morbidity With and Without an Access Surgeon: *Seunggu J. Han*

1239 Optic Radiation Fiber Tracking Using Anteriorly Angulated Diffusion Tensor Imaging: A Tested Algorithm for Quick Application: *Lennart H. Stieglitz*

1354 A Long Peripheral Nerve Autograft Model in the Sheep Forelimb: *Joanne Forden*

1399 Application of 2 Different Hemostatic Procedures During Microsurgical Median Nerve Reconstruction in the Rat Does Not Hinder Axonal Regeneration: *Nektarios Sinis*

1434 Open and Endovascular Treatment of Unruptured Carotid-Ophthalmic Aneurysms: Clinical and Radiographic Outcomes: *Sanjay Yadla*

1444 Endoscopic Port Surgery for Resection of Lesions of the Cerebellar Peduncles: Technical Note: *Pawel G. Ochalski*

1462 Review of: Focal Peripheral Neuropathies (Fourth Edition): *Boon Pang*

1465 Reactive Expansive Intracerebral Process as a Complication of Endovascular Coil Treatment of an Unruptured Intracranial Aneurysm: Case Report: *Marton König*

1469 Community-Associated Methicillin-Resistant *Staphylococcus Aureus*–Infected Chronic Scalp Wound With Exposed Dura in a 10-Year-Old Boy: Vacuum-Assisted Closure Is a Feasible Option: Case Report: *Ulrike Subotic*

1471 Pott Disease in a 13-Month-Old: Case Report: *Giac Consigilieri*

TECHNIQUE ASSESSMENT

1187 Early Recognition of Lumbar Overdrainage by Lumboventricular Pressure Gradient: *Dimitre Staykov*

1220 Anterior Thoracolumbar Corpectomies: Approach Morbidity With and Without an Access Surgeon: *Seunggu J. Han*

1300 Treatment of Severe Trigeminal Headache in Patients With Pituitary Adenomas: *Tiago da Silva Freitas*

1388 Magnetic Microparticles for Endovascular Aneurysm Treatment: In Vitro and In Vivo Experimental Results: *Johanna Oechtering*

1434 Open and Endovascular Treatment of Unruptured Carotid-Ophthalmic Aneurysms: Clinical and Radiographic Outcomes: *Sanjay Yadla*

Copyright © Congress of Neurological Surgeons. Unauthorized reproduction of this article is prohibited.

1464 **Ventral Intermediate Thalamic Stimulation for Monoclonal Gammopathy-Associated Tremor: Case Report:** *Donald C. Shields*

1467 **Navigated Brain Stimulation for Preoperative Cortical Mapping in Paretic Patients: Case Report of a Hemiplegic Patient:** *Thomas Picht*

1475 **Onyx Pulmonary Artery Embolization After Treatment of a Low-Flow Dural Arteriovenous Fistula: Case Report:** *Bryan A. Pukenas*

TRAUMA

1363 **Induction of Angiogenesis and Modulation of Vascular Endothelial Growth Factor Receptor-2 by Simvastatin After Traumatic Brain Injury:** *Hongtao Wu*

1399 **Application of 2 Different Hemostatic Procedures During Microsurgical Median Nerve Reconstruction in the Rat Does Not Hinder Axonal Regeneration:** *Nektarios Sinis*

1405 **Autologous Adult Cortical Cell Transplantation Enhances Functional Recovery Following Unilateral Lesion of Motor Cortex in Primates: A Pilot Study:** *Mélanie Kaeser*

TUMOR

1192 **Awake Craniotomy vs Surgery Under General Anesthesia for Resection of Supratentorial Lesions:** *Oumar Sacko*

1200 **Stereotactic Radiosurgery of Cranial Nonvestibular Schwannomas: Results of Single- and Multisession Radiosurgery:** *Clara Y.H. Choi*

1209 **Stereotactic ^{125}Iodine Brachytherapy for the Treatment of Singular Brain Metastases: Closing a Gap?:** *Maximilian I. Ruge*

1239 **Optic Radiation Fiber Tracking Using Anteriorly Angulated Diffusion Tensor Imaging: A Tested Algorithm for Quick Application:** *Lennart H. Stieglitz*

1259 **Surgical Mortality at 30 Days and Complications Leading to Recraniotomy in 2630 Consecutive Craniotomies for Intracranial Tumors:** *Benjamin Lassen*

1293 **World Health Organization Grade II Gliomas and Subventricular Zone: Anatomic, Genetic, and Clinical Considerations:** *Francesco Vergani*

1300 **Treatment of Severe Trigeminal Headache in Patients With Pituitary Adenomas:** *Tiago da Silva Freitas*

1317 **Navigated Transcranial Magnetic Stimulation and Functional Magnetic Resonance Imaging: Advanced Adjuncts in Preoperative Planning for Central Region Tumors:** *Marie-Thérèse Forster*

1326 **Seizures and the Natural History of World Health Organization Grade II Gliomas: A Review:** *Anja Smits*

1380 **Computed Tomography Imaging of Transferrin Targeting Liposomes Encapsulating Both Boron and Iodine Contrast Agents by Convection-Enhanced Delivery to F98 Rat Glioma for Boron Neutron Capture Therapy:** *Shiro Miyata*

1444 **Endoscopic Port Surgery for Resection of Lesions of the Cerebellar Peduncles: Technical Note:** *Pawel G. Ochalski*

1467 **Navigated Brain Stimulation for Preoperative Cortical Mapping in Paretic Patients: Case Report of a Hemiplegic Patient:** *Thomas Picht*

Copyright © Congress of Neurological Surgeons. Unauthorized reproduction of this article is prohibited.